



Government
of Canada

Gouvernement
du Canada



CANADIAN **SMOG** SCIENCE ASSESSMENT

Volume 1
Atmospheric Science and Environmental/Economic Impacts

Canada 

CANADIAN SMOG SCIENCE ASSESSMENT

VOLUME 1: ATMOSPHERIC SCIENCE AND
ENVIRONMENTAL/ ECONOMIC IMPACTS

Printed Version

Cat. no.: EN88-5/1-2012E

ISBN 978-1-100-21310-1

PDF Version

Cat. no.: EN88-5/1-2012E-PDF

ISBN 978-1-100-21311-8

Information contained in this publication or product may be reproduced, in part or in whole, and by any means, for personal or public non-commercial purposes, without charge or further permission, unless otherwise specified.

You are asked to:

- Exercise due diligence in ensuring the accuracy of the materials reproduced;
- Indicate both the complete title of the materials reproduced, as well as the author organization; and
- Indicate that the reproduction is a copy of an official work that is published by the Government of Canada and that the reproduction has not been produced in affiliation with or with the endorsement of the Government of Canada.

Commercial reproduction and distribution is prohibited except with written permission from the author.

For more information, please contact Environment Canada's Inquiry Centre at 1-800-668-6767 (in Canada only) or 819-997-2800 or email to enviroinfo@ec.gc.ca.

Photos: © Photos.com – 2011, Environment Canada.

© Her Majesty the Queen in Right of Canada, represented by the Minister of the Environment, 2013

Aussi disponible en français

Preamble

The Canadian Smog Science Assessment was co-authored by Environment Canada and Health Canada. This initiative is the most recent effort¹ by the Government of Canada to assess the adverse effects of smog on Canadians and their environment, quantify emissions of smog-forming pollutants, describe their behaviour in the atmosphere at a regional scale, and report on recent and projected levels of smog in the air we breathe. It represents the first time all the scientific material related to smog in Canada has been addressed together, combining characterization of both particulate matter and ground-level ozone in a single document.

¹ Previous assessments include:

Federal-Provincial Working Group on Air Quality Objectives and Guidelines, 1999. *National ambient air quality objectives for ground-level ozone: Science assessment document*. The Working Group, Ottawa.

Federal-Provincial Working Group on Air Quality Objectives and Guidelines, 1999. *National ambient air quality objectives for particulate matter, Part 1: Science assessment document*. Health Canada and Environment Canada, Ottawa.

Joint Action Implementation Coordinating Committee, 2005. *An Update in Support of the Canada-wide Standards for Particulate Matter and Ozone: Part A – 2003 science review*. Report to the Canadian Council of Ministers of the Environment [Available at www.ccme.ca].

Acknowledgements

AUTHORS

Canadian Smog Science Assessment Highlights and Key Messages

Barry Jessiman, Health Canada
Silvina Carou, Environment Canada
Rosa Wu, Environment Canada
Lead authors of Canadian Smog Science Assessment (listed below)
Joanne Egan, Environment Canada (technical editor)

Volume 1: Atmospheric Science and Environmental/ Economic Impacts

Chapter 1 – Introduction

Carrie Taylor, Environment Canada
Barry Jessiman, Health Canada
Jeffrey R. Brook, Environment Canada
Silvina Carou, Environment Canada
Ron Newhook, Health Canada
Vanessa Beaulac, Health Canada

Chapter 2 – Atmospheric Processes

Craig Stroud, Environment Canada
Jonathan Abbatt, University of Toronto
Leiming Zhang, Environment Canada
David Flagg, York University, now University of Hamburg
Paul A. Makar, Environment Canada

Chapter 3 – Ambient Measurements and Observations

Tom Dann, Environment Canada
Bob Vet, Environment Canada
Jeffrey R. Brook, Environment Canada
Roxanne Vingarzan, Environment Canada
Elton Chan, Environment Canada
Mike Shaw, Environment Canada
Jason O'Brien, Environment Canada
Dennis Herod, Environment Canada
Ewa Dabek, Environment Canada
Daniel Wang, Environment Canada

Domenic Mignacca, Environment Canada
Kurt Anlauf, Environment Canada
Kalyani Martinelango, Environment Canada

Chapter 4 – Emissions and Sources of Smog Precursors

David Niemi, Environment Canada
Patrick George, Environment Canada

Chapter 5 – Chemical Transport Models: Model Description and Evaluation

Wanmin Gong, Environment Canada
Colleen Farrell, Environment Canada
Paul A. Makar, Environment Canada
Richard Ménard, Environment Canada
Michael D. Moran, Environment Canada
Gilles Morneau, Environment Canada
Craig Stroud, Environment Canada
Véronique Bouchet, Environment Canada
Colin di Cenzo, Environment Canada
Dave Fox, Environment Canada
Weimin Jiang, National Research Council of Canada
Steve Smyth, Environment Canada
Junhua Zhang, Environment Canada
Qiong Zheng, Environment Canada

Chapter 6 – Model Scenarios and Applications

Véronique Bouchet, Environment Canada
Kathleen Buset, Health Canada
Robert Bloxam, Ontario Ministry of the Environment
Silvina Carou, Environment Canada
Sophie Cousineau, Environment Canada
Colin di Cenzo, Environment Canada
Didier Davignon, Environment Canada
Colleen Farrell, Environment Canada
Weimin Jiang, National Research Council of Canada
Markus Kellerhals, B.C. Ministry of Environment
Paul A. Makar, Environment Canada
Gilles Morneau, Environment Canada
Simon Pelletier, Environment Canada
Steve Smyth, Environment Canada
Roxanne Vingarzan, Environment Canada

Chapter 7 – Air Quality at the Regional and Local Scales: The What, Where, Why and How of Concentration Variations

Jeffrey R. Brook, Environment Canada
Julie Dion, Private Consultant
Colleen Farrell, Environment Canada
Kristina Friesen
Lisa Phinney Langley, Environment Canada
Markus Kellerhals, B.C. Ministry of Environment
Gilles Morneau, Environment Canada
Neville Reid, Private Consultant
Roxanne Vingarzan, Environment Canada
David Waugh, Environment Canada
Brian Wiens, Environment Canada
Mario Benjamin, Environment Canada
Claude Gagnon, Ville de Montréal
Jacques Rousseau, Environment Canada

Chapter 8 – New Directions in Smog Science

Paul A. Makar, Environment Canada
David Flagg, York University, now University of Hamburg
Janya Kelly, Environment Canada
David Plummer, Environment Canada
Randall Martin, Dalhousie University

Chapter 9 – Air Pollution from Intercontinental Transport and Natural Sources

Sunling Gong, Environment Canada
Anne-Marie Macdonald, Environment Canada
Richard Leitch, Environment Canada

Chapter 10 – Impact of Smog on Vegetation and Materials

Beverly Hale, University of Guelph
Barbara Dowsley, Stantec Consulting Ltd., now Canadian Nuclear Safety Commission
Tom Dann, Environment Canada
Markus Kellerhals, B.C. Ministry of Environment

Chapter 11 – Impact of Smog on Visibility in Developed Regions of Canada

Karen McDonald, Concordia University College of Alberta

Chapter 12 – Quantification of Social and Economic Impacts of Smog

Timothy Folkins, Environment Canada
Yves Bourassa, Environment Canada
Michael Donohue, Health Canada

Jean-Sébastien Landry, Environment Canada
Robyn Rittmaster, Health Canada
Dave Stieb, Health Canada

Volume 2: Health Effects Chapter 13 – Introduction to Volume 2 of the Canadian Smog Science Assessment

Barry Jessiman, Health Canada
Ron Newhook, Health Canada

Chapter 14 – Health Effects of Ambient Fine Particulate Matter

Jacques-Francois Cartier, Health Canada
Guillaume Colas, Health Canada
Tatiana Dinu, Health Canada
Katherine Guindon-Kezis, Health Canada
Barry Jessiman, Health Canada
Vanessa Beaulac, Health Canada
Jill Kearney, Health Canada
Cheryl Khoury, Health Canada
Ninon Lyrette, Health Canada
Ron Newhook, Health Canada
Pierre Raymond, Health Canada
Jeff Willey, Health Canada

Chapter 15 – Health Effects of Ground-level Ozone

Guillaume Colas, Health Canada
Tatiana Dinu, Health Canada
Katherine Guindon-Kezis, Health Canada
Barry Jessiman, Health Canada
Cheryl Khoury, Health Canada
Ninon Lyrette, Health Canada
Ron Newhook, Health Canada
Jeff Willey, Health Canada

Parts of Volume 2 of the Canadian Smog Science Assessment document are based on background information prepared by the following individuals who are not employees of Health Canada:

Mark Goldberg, McGill University (epidemiology)
Colleen Purtill, Toxico-Logic Consulting Inc., with assistance from Rhonda Taylor (toxicology studies of ozone in animals and humans)
Tim Ramsay, University of Ottawa (measurement error issues for PM)
Lance Wallace, retired from US EPA (input to drafts of Exposure Assessment section for PM)
Scott Weichenthal, McGill University (chemical composition of PM)

REVIEWERS

Volume 1 chapters were reviewed by the following scientific experts:

Chapter 2 – Atmospheric Processes

Peter Buijijtes, TNO-MEL
John Orlando, National Center for Atmospheric Research
James Sloan, University of Waterloo

Chapter 3 – Ambient Measurements and Observations

George Allen, Northeast States for Coordinated Air Use Management (NESCAUM)
Judith Chow, Desert Research Institute
Douw Steyn, University of British Columbia

Chapter 4 – Emissions and Sources of Smog Precursors

Eric Fujita, Desert Research Institute
Marc Houyoux, US EPA
Gregory Stella, Alpine Geophysics

Chapter 5 – Chemical Transport Models: Model Description and Evaluation

Amir Hakami, Carleton University
Prakash Karamchandani, Atmospheric and Environmental Research, Inc.
Spyros Pandis, Carnegie Mellon University

Chapter 6 – Model Scenarios and Applications

Amir Hakami, Carleton University
Prakash Karamchandani, Atmospheric and Environmental Research, Inc.
Spyros Pandis, Carnegie Mellon University

Chapter 7 – Air Quality at the Regional and Local Scales: The What, Where, Why and How of Concentration Variations

George Allen, Northeast States for Coordinated Air Use Management (NESCAUM)
Judith Chow, Desert Research Institute
Douw Steyn, University of British Columbia

Chapter 8 – New Directions in Smog Science

Ray Hoff, University of Maryland
Daniel Jacob, Harvard University
Tim Oke, University of British Columbia

Chapter 9 – Air Pollution from Intercontinental Transport and Natural Sources

Hajime Akimoto, Asia Center for Air Pollution Research
Daniel Jacob, Harvard University
Dan Jaffe, University of Washington-Bothell
Sophie Szopa, Institut Pierre Simon Laplace LSCE-Orme

Chapter 10 – Impact of Smog on Vegetation and Materials

Mike Ashmore, University of York
Elena Paoletti, Istituto per la Protezione delle Piante
Kevin Percy, Air Quality Effects Consulting Ltd.

Chapter 11 – Impact of Smog on Visibility in Developed Regions of Canada

Richard Poirot, State of Vermont
Gregory Stella, Alpine Geophysics
Ivar Tombach, Independent Consultant

Chapter 12 – Quantification of Social and Economic Impacts of Smog

Alan Krupnick, Center for Energy Economics and Policy Resources for the Future
Suren Kulshreshtha, University of Saskatchewan
Van Lantz, University of New Brunswick

Volume 2 chapters on the health effects of the fine PM and ground-level ozone were reviewed by the following scientific experts:

Mark Frampton, M.D., University of Rochester Medical Center
Alison Geyh, Ph.D., Johns Hopkins Bloomberg School of Public Health
Bernard Goldstein, M.D., University of Pittsburgh Graduate School of Public Health
Terry Gordon, Ph.D., New York University
Gerard Hoek, Ph.D., Utrecht University
Paul Lioy, Ph. D., University of Medicine and Dentistry of New Jersey
Jonathan Samet, M.D., University of Southern California
Frank Speizer, M.D., Harvard Medical School
Ira Tager, M.D., University of California, Berkeley
John Vandenberg, Ph.D., U.S. Environmental Protection Agency

Table of Contents

Preamble	1
Acknowledgements	2
Authors	2
Reviewers	6
Chapter 1: Introduction to the Canadian Smog Science Assessment	50
1.1 Canadian Air Quality Policy Framework	58
1.2 Air Quality Risk Assessment Framework.....	60
1.3 Brief History Of Past Assessments In Canada And The U.S.	62
1.4 Evolution of Smog Science	63
1.5 Content of the Report	66
1.6 Highlights and Key Messages	68
CHAPTER 2: Atmospheric Processes	69
Key Messages and Implications	69
2.1 Introduction.....	70
2.2 Smog Production Mechanisms.....	71
2.3 Hygroscopic Growth and Cloud Nucleation.....	96
2.4 Deposition of Gases and Particles.....	101
2.5 Meteorological Influences on Air Quality	108
2.6 Conclusions.....	114
2.7 Future Research Directions	116
Acknowledgements.....	117
References.....	117

CHAPTER 3: Ambient Measurements and Observations.....	130
Key Messages and Implications	130
3.1 Topic Introduction and Organization of Chapter	132
3.2 Canadian Monitoring Networks and Monitoring Methods for Ozone, PM _{2.5} and Precursors.....	133
3.3 Ozone.....	142
3.4 Ozone Precursors	184
3.5 PM _{2.5} Mass, Composition and Precursors	207
3.6 PM _{10-2.5} Mass and Trends	251
3.7 Summary and Conclusions	255
3.8 Recommendations for Changes to the Monitoring Networks and for Additional Monitoring and Special Studies	257
References.....	259
CHAPTER 4: Emissions and Sources of Smog Precursors	270
Key Messages and Implications	270
4.1 Introduction.....	270
4.2 Conclusions from previous assessments	272
4.3 Smog Precursor Pollutants	275
4.4 NPRI Reporting & CAC Emissions Inventory Process	276
4.5 Inventory Updates and Improvements	285
4.6 Canadian Smog Precursor Emissions	287
4.7 Trends and Projections.....	298
4.8 Summary and Conclusions	323

References.....	324
CHAPTER 5: Chemical Transport Models: Model Description and Evaluation ..	329
Key Messages and Implications	329
5.1 Introduction.....	330
5.2 Recent major advances in CTM development and capabilities	331
5.3 Description of the CTMs used in this assessment	333
5.4 Model evaluation	338
5.5 Uncertainties	396
5.6 Summary and Conclusions	398
5.7 Recommendations for Future Research	401
References.....	403
Appendix	423
CHAPTER 6: Model Scenarios and Applications	425
Key Messages and Implications	425
6.1 Introduction.....	426
6.2 Use and limitations of modelling scenarios	430
6.3 Sensitivity of PM _{2.5} and O ₃ to changes in smog precursors – Sector-based analysis.....	431
6.4 Projected levels of PM _{2.5} and O ₃ in Canada based on implementation of current legislation	460
6.5 Projected levels of PM _{2.5} and O ₃ in Canada from emission reductions above and beyond current legislation	485
6.6 Transboundary influences on PM _{2.5} , O ₃ and smog precursors.....	495
6.7 Assessments of Uncertainties	511

6.8 Summary and conclusions	516
6.9 Recommendations for future research	522
References.....	524
Appendix – Table of model versions used in the modelling scenarios presented in Chapter 6.....	530
CHAPTER 7: Air Quality at the Regional and Local Scale: The What, Where, Why and How of Concentration Variations	538
Key Messages and Implications	538
7.1 Introduction.....	539
7.2 Overview of Air Pollutant Behaviour and Issues Across Canada - Regional Conceptual Models	540
7.3 Regional Air Pollutant Emissions and Areas of Concern	560
7.4 Meteorological Influences on Air Quality	588
7.5 Regional Characteristics of Air Quality.....	605
7.6 Long-Range Transport of Air Pollutants.....	689
7.7 Case Studies of Local, Regional and/or National Significance	708
7.8 Summary and Needs for Further Research	749
References.....	756
CHAPTER 8: New Directions in Smog Science	778
Key Messages and Implications	778
8.1 Topic Introduction and Organization of Chapter	779
8.2 Climate Change and Air Quality.....	780
8.3 Pollutant Transport in the Atmospheric Boundary Layer	796
8.4 Satellite remote sensing of smog.....	814

References.....	824
Chapter 9: Air Pollution from Intercontinental Transport (ICP) and Natural Sources	852
Key Messages and Implications	852
9.1 Topic Introduction.....	852
9.2 Organization of the Chapter.....	853
9.3 Features of ICT.....	854
9.4 Observational Evidence	857
9.5 Modelling the Contributions of Anthropogenic Pollutants to ICT.....	866
9.6 Modelling the Contributions from Natural PM Components.....	872
9.7 Uncertainties	876
9.8 Summary and conclusions.....	877
9.9 Recommendations for future research.....	877
References.....	878
CHAPTER 10: Impact of Smog on Vegetation and Materials	885
Key Messages and Implications	885
10.1 Introduction	886
10.2 Characterization of Vegetation Exposure to Ozone.....	889
10.3 Summary of Previous Assessments.....	896
10.4 Recent literature on ozone effects.....	902
10.5 Recent Literature on Particulate Matter Effects.....	935
10.6 Uncertainties	937
10.7 Summary and Conclusions.....	939

10.8 Effects of Ozone and PM on Wildlife – an emerging issue.....	943
10.9 Recommendations for Future Research.....	944
References.....	946
CHAPTER 11: Impact of Smog on Visibility in Developed Regions of Canada ..	964
Key Messages and Implications	964
11.1 Context and Issue	964
11.2 Relationship between Ambient PM and Visibility	965
11.3 Literature Review of Visibility Research Post-2003	967
11.4 Reconstructed Particulate Matter Levels and Visibility in Canada	971
11.5 Predicted Visibility from Air Quality Modelling Applications	984
11.6 Conclusions and Recommendations for Future Research	989
References.....	991
CHAPTER 12: Quantification of Social and Economic Impacts of Smog	996
Key Messages and Implications	996
12.1 Introduction	996
12.2 Overview of Economic Valuation	998
12.3 Valuation of Environmental Smog Impacts on the Welfare of Canadians	1008
12.4 Valuation of the Impacts of Smog on Health.....	1018
12.5 Conclusion.....	1026
References.....	1030

Table of Figures

Figure 1.1 Theoretical Air Quality Risk Assessment Framework.....	60
Figure 2.1 Schematic illustrating the initiation and propagation reactions for radical and NO _x reactions involved in O ₃ formation (panel a), degradation of volatile organic compounds (VOCs) under low NO _x (panel b) and high NO _x (panel c) conditions. Reactions in grey font are inefficient under different scenarios.	73
Figure 2.2 Night-time chemistry illustrating the oxidation of VOCs by NO ₃ , O ₃ and OH, the cycling of NO _x and RO _x species, and the production of stable intermediates (N ₂ O ₅ , RC(O)OONO ₂ , RONO ₂ , HNO ₃ , RCHO, RC(O)OH, H ₂ O ₂ , ROOH). Species in smaller font alongside arrows are co-reactants in the chemical reaction.	75
Figure 2.3 Number (N), surface area (S) and mass size (M) distribution for a typical urban aerosol (Seinfeld and Pandis, 1998).....	76
Figure 2.4 Particle-phase composition and chemical transformation processes. Species in red are primary gaseous and particulate components. Species in green are secondary gaseous components. Species in purple are involved in particle-phase production of secondary components.	78
Figure 2.5 Composition-resolved mass size distributions for two samples collected in downtown Toronto, Ontario (Broekhuizen <i>et al.</i> , 2006). In panel (a), the sample is dominated by the organic fraction for all submicron particle sizes. The organic fraction is a combination of primary and secondary components as characterized by similar magnitude m/z = 43,44 and m/z = 57 ratios. In panel (b), the sample has a large secondary aerosol component at particle diameters 200-600 nm characterized by SO ₄ , NH ₄ , NO ₃ and secondary organics (m/z = 43,44).....	79
Figure 2.6 Composition-resolved mass size distributions for two samples collected at Egbert, Ontario (Rupekheti <i>et al.</i> , 2005). The top panels are from a sample collected in the processed Toronto plume. The bottom panels are from a sample collected from an aged air mass originating on the mid-western United States several days earlier.....	80
Figure 2.7 Aging processes for organic aerosol components: Condensational aging (gas-phase diffusion, surface accommodation, NVOC = non-volatile organic compound), heterogeneous aging (surface oxidation), and homogeneous aging (bulk-phase oligomer and oxidation chemistry, HULIS = humic like substances).....	91
Figure 2.8 Hygroscopic growth curves for selected single-component particles and particles generated from single precursor VOC oxidation chamber experiments (termed “Biogenic SOA” and “Aromatic SOA”).....	97

Figure 2.9 Particle deposition velocities to forest and agricultural canopies (compiled in Zhang and Vet, 2006; original data and symbol coding from Gallagher <i>et al.</i> , 1997).....	104
Figure 2.10 The convective mixed layer can be divided into a surface layer and an Ekman layer. The surface layer can be further sub-divided into an inertial sublayer and a roughness sublayer. The surface layer is typically 0.1 of the boundary layer height.....	109
Figure 2.11 Diurnal time series of the vertical stability of the atmosphere.	110
Figure 2.12 Plume structures in the atmosphere for different vertical profiles of virtual potential temperature (θ_v).....	110
Figure 3.1 Location of NAPS Ozone and PM _{2.5} monitoring sites in Eastern Canada – 2006. ..	134
Figure 3.2 Location of NAPS Ozone and PM _{2.5} monitoring sites in Western Canada – 2006. .	135
Figure 3.3 Location of CAPMoN Monitoring Sites and Parameters Measured (Note: PM sampling (brown) is temporally on hiatus at all sites except Egbert).....	136
Figure 3.4 Probability densities of air parcel trajectory clusters (cleanest background air) associated with the lowest May – September 95th percentile ozone mixing ratios for 14 statistically representative sites (out of 97 in total) for the years 1997–2006 combined. The total number of trajectories for the cluster and the transport frequency (in bracket, %) is shown above the horizontal bar. The relative seasonal transport frequencies (relative to other five clusters) are shown below the bar (other five clusters not shown). The gridded population shown in the centre was obtained from the Centre for International Earth Science Information Network (CIESIN), Columbia University; and Centro Internacional de Agricultural Tropical (CIAT), Gridded Population of the World (GPW), Version 3, for the year 2005. Palisades, NY: CIESIN, Columbia University. Available at: http://sedac.ciesin.columbia.edu/gpw	146
Figure 3.5 Seasonal ozone variations generated by LOWESS associated with the cleanest air trajectory clusters for all 97 sites. The error bars show the monthly ensemble site 5 th to 95 th percentiles for the region. The regional groupings are based on rotated PCA for JJA months. Elevations (above sea level, metres) are shown in gray scale from dark to light to represent low to high elevations. Elevations have been normalized to have a minimum of zero metre.	148
Figure 3.6 Daily maximum 8-h ozone concentration in ppb (median, 25 th and 75 th percentiles and minimum/maximum) for active stations (May to September of 2004-2006).	153
Figure 3.7 Spatial distribution of the 3-year-average 4 th highest daily maximum 8-hr ozone concentration in ppb (2004-2006).	154

Figure 3.8 Annual average number of days with daily maximum 8-hr ozone above 65 ppb in the 3-year period of 2004 – 2006.....	154
Figure 3.9 Mean (○) and mean daily maximum (●) ozone (ppb) by month averaged for the years 2001 to 2005. (Note: mean ozone concentration in ppb shown on y-axis).....	159
Figure 3.10 Average hours per month with ozone above 50 and 60 ppb averaged for the years 2001 to 2005.(Note: average hours per month shown on y-axis)	160
Figure 3.11 Average days per month with ozone greater than 65 ppb for the years 2001 to 2005. (Only sites averaging at least one day per year > 65 ppb are included in the plot).....	161
Figure 3.12 Diurnal variation in ozone concentration (ppb) – summer (May-Sep) (●) and winter (Nov-Mar) (○) averaged for years 2001 to 2005. (Note: Mean ozone concentration in ppb shown on y-axis).....	162
Figure 3.13 Diurnal variation in ozone concentration (ppb) – weekday (●) and weekend (○) for summertime (May to September) averaged for years 2001 – 2005. (Note: mean ozone concentration in ppb shown on y-axis).....	163
Figure 3.14 Diurnal variation in summertime (May to September) ozone (ppb) for 1991-1995 (○) vs. 2001-2005 (●). (Note: mean ozone concentration in ppb shown on y-axis).....	164
Figure 3.15 Average hours per month with ozone above 50 and 60 (ppb) at high-elevation sites averaged for the years 2001 to 2005. (Note: average hours per month shown on y-axis).....	165
Figure 3.16 Comparison of the summertime diurnal ozone profile (ppb) for Toronto CN Tower (●) - Brampton (○) and Mont Sutton (●) - L'Acadie (○) in 2005.	166
Figure 3.17 Ozone site locations and PCA-derived regions based on daily maximum 8-hr mixing ratios (97 Non-urban sites were used in the study).....	168
Figure 3.18 Average month-to-month cycles in PC1, PC2, PC3, PC4, PC5, PC7 and PC9 based on daily O ₃ maximum 8-hr average values (in ppb) from 1997 to 2006.	169
Figure 3.19 Top row: anomalies in the seasonal average (subtracted by the overall mean) meteorological-adjusted trends modelled by GLMM (red) and observed ozone (blue) based on daily maximum 8-hr values (in ppb) for 1997 to 2006 during May – September for five PCA-derived regions. Bottom row: anomalies in seasonal average relative humidity in % (red), temperature in °C (blue) and wind speed in m s ⁻¹ (green) for the same regions.	172
Figure 3.20 Six trajectory clusters used in GLMM for PC1.	174

Figure 3.21 Three-year average during May – September differences from 1997 – 2000 to 2003 – 2006 of the meteorological-adjusted ozone trends modelled by GLMM based on daily maximum 8-hr values..... 178

Figure 3.22 The 3-year running average of the 4th highest daily maximum 8-h ozone concentration for 1990 to 2006 (all Canadian sites and all sites greater than 65 ppb for 2004-2006)..... 179

Figure 3.23 The 3-year running average of the seasonal mean of daily maximum 8-h ozone concentrations for 1990 to 2006 (urban and rural sites)..... 180

Figure 3.24 Trend in Daily Maximum 8h Ozone 10th, 25th, 50th, 75th, 90th, 95th percentiles and maximum for Canadian urban sites for 1990 - 2006. Regression lines marked with ** are statistically significant at the 95th percentile confidence level..... 181

Figure 3.25 Trend in Daily Maximum 8h Ozone 10th, 25th, 50th, 75th, 90th, 95th percentiles and maximum for Canadian rural sites for 1990-2006. Regression lines marked with ** are statistically significant at the 95th percentile confidence level..... 182

Figure 3.26 Relationship between days with daily maximum temperatures above 27°C and average hours above 82 ppb ozone (1994-2002 and 2004, 2005, 2006). 183

Figure 3.27 Mean monthly concentrations of NO, NO₂, NO_y and PAN (logarithmic scale) for Kejimikujik (top) and Egbert (bottom) during 2003..... 185

Figure 3.28 Relative abundance of several NO_y species as a fraction of the total measured NO_y concentration at Kejimikujik (top) and Egbert (bottom) during 2003. 186

Figure 3.29 The monthly estimated percentage of an NO₂ measurement that could potentially be falsely identified as NO₂ due to interfering species if the conventional NO_x instrumentation were deployed at the Egbert station in 2003..... 187

Figure 3.30 Mean, 10th and 98th percentile of NO and NO₂ concentrations at selected urban sites (2005). 188

Figure 3.31 Mean NO (●) and NO₂ (○) by month (ppb) averaged over the years 2003 to 2005. (Note: Mean NO and NO₂ concentration (ppb) shown on y-axis)..... 189

Figure 3.32 Diurnal variation in NO (●) and NO₂ (○) concentrations (ppb) for all days of the week averaged over the years 2003 – 2005. (Note: Mean NO and NO₂ concentration (ppb) shown on y-axis)..... 190

Figure 3.33 Comparison of composite weekday vs. weekend diurnal profiles for NO and NO ₂ (2003 – 2005) for 45 urban sites.....	191
Figure 3.34 Mean, 10 th and 90 th percentile non-methane hydrocarbons (NMHC) concentrations (ppbC) May to September (2004 to 2006).	196
Figure 3.35 Seasonal variation in non-methane hydrocarbons (NMHC) concentrations for site groups.....	197
Figure 3.36 Day of week variation in NMHC concentrations for site groups.	198
Figure 3.37 Biogenic hydrocarbon fraction of total C ₂ to C ₁₂ HC - MIR _{prop} weighted (ppbC) – summer only.....	201
Figure 3.38 Seasonal variation in isoprene and α -pinene (ppbv) for selected rural sites and for the average of all rural sites.....	201
Figure 3.39 Relationship between total C ₂ to C ₁₂ HC (biogenics excluded) and daily maximum temperature – June, July, August (2001-2006).	203
Figure 3.40 Trend in annual mean NO _x (ppb) and VOC (ppbC) at Canadian urban sites.	204
Figure 3.41 Trend in annual and summer mean NO and NO ₂ (ppb) at Canadian urban sites.	204
Figure 3.42 Trend in non-biogenic C ₂ to C ₁₂ HC at urban and rural sites (May to September only).....	205
Figure 3.43 Trend in selected major NMHC species (ppbC).....	205
Figure 3.44 Trend in NMHC to NO _x ratios at selected sites (May to September) (median, 25 th and 75 th percentiles, non-outlier maximum and minimum).....	206
Figure 3.45 Probability densities of air parcel trajectory clusters associated with the lowest PM _{2.5} concentrations at the 95th percentile for seven rural sites for time periods with available PM _{2.5} data between 1996 and 2005. The inset box at the bottom of the figure shows, for each site, the percentile values (in red) and box-and-whisker plots (in black) of all 6-hour- average PM _{2.5} concentrations associated with the baseline trajectory cluster. The box-and-whisker plot shows the overall annual statistics including the 5 th , 25 th , median (50 th), mean, 75 th and 95 th percentiles for each selected site. The dashed line shows the overall median of 3.2 $\mu\text{g m}^{-3}$ of the medians from all sites.	208

Figure 3.46 Comparison of PM _{2.5} 24-h mass concentrations from filter-based samplers measured from 2004 to 2006 (median, 25 th and 75 th percentile, 2 nd and 98 th percentile, outliers and extremes).....	210
Figure 3.47 Comparison of PM _{2.5} 24-h mass concentrations from TEOM samplers for the period of 2004 to 2006 (median, 25 th and 75 th percentile, 2 nd and 98 th percentile, outliers and extremes).....	211
Figure 3.48 98th Percentile PM _{2.5} Concentrations (µg m ⁻³) – 2004 -2006.....	211
Figure 3.49 Annual Mean PM _{2.5} Concentrations (µg m ⁻³) – 2004 -2006.....	212
Figure 3.50 Adjusted and unadjusted annual mean and 98 th percentile PM _{2.5} for TEOM sites that would exceed 30 µg m ⁻³ averaged over 2004-2006.....	214
Figure 3.51 Seasonal variability of PM _{2.5} mass from the filter-based samplers (median, 25 th and 75 th percentile, non-outlier maximum and minimum).....	215
Figure 3.52 Winter vs. summer concentrations of PM _{2.5} mass from the filter-based samplers for selected Sites (median, 25 th and 75 th percentile, non-outlier maximum and minimum).....	216
Figure 3.53 Average days per month with PM _{2.5} concentrations greater than 30 µg m ⁻³ ppb for the years 2001 to 2005. (Only sites averaging at least one day per year > 30 µg m ⁻³ are included in the plot).....	216
Figure 3.54 Diurnal variation in PM _{2.5} mass, weekday vs. weekend, from TEOM samplers (2003 – 2005).....	217
Figure 3.55 Comparison of ammonium sulphate concentrations (µg m ⁻³) by site and month (median, 25 th and 75 th percentile, non-outlier maximum and minimum).....	218
Figure 3.56 Comparison of ammonium nitrate concentrations (µg m ⁻³) by site and month (median, 25 th and 75 th percentile, non-outlier maximum and minimum).....	219
Figure 3.57 Comparison of organic matter (µg m ⁻³) by site and month (median, 25 th and 75 th percentile, non-outlier maximum and minimum).....	220
Figure 3.58 Comparison of elemental carbon (µg m ⁻³) by site and month (median, 25 th and 75 th percentile, non-outlier maximum and minimum).....	220
Figure 3.59 Comparison of potassium ion concentrations (µg m ⁻³) by site and month (median, 25 th and 75 th percentile, non-outlier maximum and minimum).....	221

Figure 3.60 Comparison of oxalate ion concentrations ($\mu\text{g m}^{-3}$) by site and month (median, 25 th and 75 th percentile, non-outlier maximum and minimum).	222
Figure 3.61 Results for five major metal species (arsenic, vanadium, nickel, selenium, lead) by site (2003 – 2006).	222
Figure 3.62 Reconstruction of total $\text{PM}_{2.5}$ mass for all sampling days in the warm season (2003 – 2006).	223
Figure 3.63 Reconstruction of total $\text{PM}_{2.5}$ mass for all sampling days in the cold season (2003 – 2006).	224
Figure 3.64 Reconstruction of total $\text{PM}_{2.5}$ mass for 10 highest days in warm season (2003 – 2006).	224
Figure 3.65 Reconstruction of total $\text{PM}_{2.5}$ mass for 10 highest days in cold season (2003 – 2006).	224
Figure 3.66 Mean, 10 th and 98 th percentile of daily-average SO_2 concentrations for all sites reporting valid annual means in 2006.	226
Figure 3.67 Monthly mean and monthly mean daily maximum SO_2 concentrations (ppb) for urban sites with no local point sources.	226
Figure 3.68 Ammonia concentrations (ppb) by month from the NAPS speciation network (median, 25 th and 75 th percentile, non-outlier maximum and minimum).	227
Figure 3.69 Nitric acid concentrations ($\mu\text{g m}^{-3}$) by month from the NAPS speciation network (median, 25 th and 75 th percentile, non-outlier maximum and minimum).	228
Figure 3.70 Long-term trend in composite annual mean and 98 th percentile $\text{PM}_{2.5}$ mass from dichotomous sampler urban sites for the period 1985 to 2006.	232
Figure 3.71 Relationship between annual mean and 98 th percentile $\text{PM}_{2.5}$ mass from dichotomous sampler urban sites (1985-1994 vs. 1995-2007).	233
Figure 3.72 Trend in 98 th percentile $\text{PM}_{2.5}$ mass from TEOM sites.	234
Figure 3.73 Trend in composite annual mean $\text{PM}_{2.5}$ mass and p-sulphate concentrations from dichotomous sampler sites.	235
Figure 3.74 Trend in composite annual mean SO_2 concentrations (ppb) at urban and industrial-influence sites.	236

Figure 3.75 (a) Annual SO₂ emissions (MT yr⁻¹) for the Southeast Canada Sulphur Oxide Management Area (EC/SOMA) and the eastern US Pollutant Emission Management Area (EUS/PEMA) and (b) Annual NO_x emissions (MT NO₂ yr⁻¹) for the Eastern Canadian Pollutant Emission Management Area (EC/PEMA) and the EUS/PEMA.237

Figure 3.76 Long-term trends of SO₂ and p-SO₄⁻² at CAPMoN and CASTNET sites (in µg m⁻³ at 0°C and 1 atmosphere).238

Figure 3.77 Changing SO₂ concentrations with time. The map insert shows the percent difference in 3-year-mean concentrations between two periods: 1991-1993 and 2004-2006. The downward facing triangles denote decreasing concentrations between the two periods for the corresponding numbered site. Asterisks indicate that the differences in 3-year-mean concentrations were not statistically significant. The three multiple-trends plots show the superimposed time trends for all sites in three different regions normalized to the year 1995. The vertical shaded bars in the years 1995 and 1999 show the years when largest SO₂ and NO_x emission reductions occurred in the EUS PEMA. The horizontal red bars along the x-axis illustrate the two averaging periods used for the map.239

Figure 3.78 Changing p-SO₄⁻² concentrations with time. The map insert shows the percent difference in 3-year-mean concentrations between two periods: 1991-1993 and 2004-2006. The downward facing triangles denote decreasing concentrations between the two periods for the corresponding numbered site. Asterisks indicate that the differences in 3-year-mean concentrations were not statistically significant. The three multiple-trends plots show the superimposed time trends for all sites in three different regions normalized to the year 1995. The vertical shaded bars in the years 1995 and 1999 show the years when largest SO₂ and NO_x emission reductions occurred in the EUS PEMA. The horizontal red bars along the x-axis illustrate the two averaging periods used for the map.240

Figure 3.79 Long-term trends of HNO₃, p-NO₃⁻ and p-NH₄⁺ at CAPMoN and CASTNET sites (in µg m⁻³ at 0°C and 1 atmosphere).243

Figure 3.80 Changing HNO₃ concentrations with time. The map insert shows the percent difference in 3-year-mean concentrations between two periods: 1991-1993 and 2004-2006. The downward facing triangles denote decreasing concentrations between the two periods for the corresponding numbered site. Asterisks indicate that the differences in 3-year-mean concentrations were not statistically significant. The three multiple-trends plots show the superimposed time trends for all sites in three different regions normalized to the year 1995. The vertical shaded bars in the years 1995 and 1999 show the years when largest SO₂ and NO_x emission reductions occurred in the EUS PEMA. The horizontal red bars along the x-axis illustrate the two averaging periods used for the map.244

- Figure 3.81 Changing p-NO₃⁻ concentrations with time. The map insert shows the percent difference in 3-year-mean concentrations between two periods: 1991-1993 and 2004-2006. The downward facing triangles denote decreasing concentrations between the two periods for the corresponding numbered site. Asterisks indicate that the differences in 3-year-mean concentrations were not statistically significant. The three multiple-trends plots show the superimposed time trends for all sites in three different regions normalized to the year 1995. The vertical shaded bars in the years 1995 and 1999 show the years when largest SO₂ and NO_x emission reductions occurred in the EUS PEMA. The horizontal red bars along the x-axis illustrate the two averaging periods used for the map.245
- Figure 3.82 Changing p-NH₄⁺ concentrations with time. The map insert shows the percent difference in 3-year-mean concentrations between two periods: 1991-1993 and 2004-2006. The downward facing triangles denote decreasing concentrations between the two periods for the corresponding numbered site. Asterisks indicate that the differences in 3-year-mean concentrations were not statistically significant. The three multiple-trends plots show the superimposed time trends for all sites in three different regions normalized to the year 1995. The vertical shaded bars in the years 1995 and 1999 show the years when largest SO₂ and NO_x emission reductions occurred in the EUS PEMA. The horizontal red bars along the x-axis illustrate the two averaging periods used for the map.246
- Figure 3.83 Comparison of PM_{10-2.5} 24-h mass concentrations (µg/m³) from filter-based samplers: 2004 to 2006. (median, 25th and 75th percentile, 2nd and 98th percentile, outliers and extremes).251
- Figure 3.84 March/April vs. other season concentrations of PM_{10-2.5} mass – filter-based samplers for selected sites (median, 25th and 75th percentile, non-outlier max and min).252
- Figure 3.85 Diurnal Variation in PM_{2.5} (–) and PM_{10-2.5} (–) mass concentration (µg m⁻³) from sites with co-located PM₁₀ and PM_{2.5} TEOMs (Note: PM mass concentration shown on y-axis).253
- Figure 3.86 Diurnal Variation in PM_{10-2.5} Mass for March/April (–), Summer (–) and Winter (–) for sites with co-located PM₁₀ and PM_{2.5} TEOMs. (Note: PM mass concentration shown on y-axis).253
- Figure 3.87 Trend in composite annual mean and 98th percentile PM_{10-2.5} mass (µg/m³) from dichotomous sampler sites.254
- Figure 4.1 Relative Provincial Contributions to the 2006 National Emissions of PM_{2.5} (Environment Canada, 2010b).289

Figure 4.2 Relative Provincial Contributions to the 2006 National Emissions of SO _x (Environment Canada, 2010b).....	290
Figure 4.3 Relative Provincial Contributions to the 2006 National Emissions of NO _x (Environment Canada, 2010b).....	290
Figure 4.4 Relative Provincial Contributions to the 2006 National Emissions of VOCs (Environment Canada, 2010b).....	291
Figure 4.5 Relative Provincial Contributions to the 2006 National Emissions of NH ₃ (Environment Canada, 2010b).....	291
Figure 4.6 Emissions Density Map of the 2006 North American PM _{2.5} Emissions (Environment Canada, 2009b).....	292
Figure 4.7 Emissions Density Map of the 2006 North American SO _x Emissions (Environment Canada, 2009b).....	293
Figure 4.8 Emissions Density Map of the 2006 North American NO _x Emissions (Environment Canada, 2009b).....	293
Figure 4.9 Emissions Density Map of the 2006 North American VOC Emissions (Environment Canada, 2009b).....	293
Figure 4.10 Emissions Density Map of the 2006 North American NH ₃ Emissions (Environment Canada, 2009b).....	294
Figure 4.11 Canadian National Emissions Trends and Projections (Environment Canada, 2006; 2010b).....	299
Figure 4.12 Sectors contributing to PM ₁₀ Emissions without Open Sources (Environment Canada, 2010b).....	300
Figure 4.13 Sectors contributing to PM ₁₀ Emissions with Open Sources (Environment Canada, 2010b).....	301
Figure 4.14 Sectors contributing to PM _{2.5} Emissions without Open Sources (Environment Canada, 2010b).....	302
Figure 4.15 Sectors contributing to SO _x Emissions without Open Sources (Environment Canada, 2010b).....	303

Figure 4.16 Sectors contributing to NO _x Emissions without Open Sources (Environment Canada, 2010b)	304
Figure 4.17 Breakdown of the Transportation Sectors NO _x Emissions Sources (Environment Canada, 2010b)	304
Figure 4.18 Sectors Contributing to VOC Emissions without Open Sources (Environment Canada, 2010b)	305
Figure 4.19 Breakdown of the Transportation Sectors VOC Emissions Sources (Environment Canada, 2010b)	305
Figure 4.20 Sectors Contributing to NH ₃ Emissions with Open Sources (Environment Canada, 2010b).....	306
Figure 4.21 Sectors Contributing to NH ₃ Emissions without Open Sources (Environment Canada, 2010b)	307
Figure 4.22 National U.S. Emissions Trend (US EPA, 2010f)	309
Figure 4.23 U.S. PM _{2.5} Emissions by Category (US EPA, 2010f).....	310
Figure 4.24 U.S. SO _x Emissions by Category (US EPA, 2010f).....	311
Figure 4.25 U.S. NO _x Emissions by Category (US EPA, 2010f)	312
Figure 4.26 U.S. VOC Emissions by Category (US EPA, 2010f)	313
Figure 4.27 U.S. NH ₃ Emissions by Category (US EPA, 2010f).....	313
Figure 4.28 U.S. PEMA (IJC, 2008)	314
Figure 4.29 U.S. PEMA Emissions Trend (US EPA, 2010a,b,c,d,e).....	315
Figure 4.30 U.S. PEMA PM _{2.5} Emissions Trend (US EPA, 2010a,b,c,d,e)	315
Figure 4.31 U.S. PEMA SO _x Emissions Trend (US EPA, 2010a,b,c,d,e)	316
Figure 4.32 U.S. PEMA NO _x Emissions Trend (US EPA, 2010a,b,c,d,e)	317
Figure 4.33 U.S. PEMA VOC Emissions Trend (US EPA, 2010a,b,c,d,e).....	318
Figure 4.34 U.S. PEMA NH ₃ Emissions Trend (US EPA, 2010a,b,c,d,e)	318

Figure 4.35 Schematic of the E3MC Interactions (Macaluso, 2009)	320
Figure 4.36 North American 2002 SO _x Emissions Density Map. (Environment Canada, 2009b)	322
Figure 4.37 North American 2015 SO _x Emissions Density Map. (Environment Canada, 2009b)	322
Figure 5.1 AURAMS predicted (left panel) 3rd quarter (July, August, and September, 2002) average ozone concentration (ppbv) compared to the observations (right panel).	341
Figure 5.2 Comparison between AURAMS predicted (left panel) and observed (right panel) annual (2002) ground-level PM _{2.5} mass concentration (µg m ⁻³).	343
Figure 5.3 Spatial distribution of the correlation coefficient (r) and the mean bias (MB) for daily 1-hour maximum ozone (top panels) and daily average PM _{2.5} (bottom panels) for the AURAMS simulation of the ICARTT 2004 field study period.	344
Figure 5.4 Model-observation comparisons of averaged diurnal (a) ozone and (b) PM _{2.5} over the AIRNOW sites for the ICARTT 2004 field study period. Modelled averaged diurnal speciated PM _{2.5} components are also shown in (b).	345
Figure 5.5 (a) Selected sites from the GVRD (Greater Vancouver Regional District) monitoring network and from Washington state used for evaluating RWDI CMAQ/MC2 Pacific 2001 simulation; (b) the nested 4-km NRC CMAQ/MM5 domain and locations of GVRD and Pacific 2001 measurement sites.	347
Figure 5.6 Time series comparison between the CMAQ/MC2 simulation and observed (a) O ₃ and (c) PM _{2.5} averaged over the sites for the period between August 9 and 31, 2001. Time series of root-mean-square-errors (RMSE), including the systematic RMSE (RMSE-S) and unsystematic RMSE (RMSE-U), are shown in (b) for O ₃ and (d) for PM _{2.5}	348
Figure 5.7 The model domain for PNR CMAQ simulation of 2002 summer season and Alberta ozone monitoring sites. Stations in red were operating in 2002. Additional stations shown in blue were also measuring ozone in 2006.	350
Figure 5.8 Normalized mean bias (a) and normalized mean error (b) of CMAQ-predicted ozone compared to observations at Alberta ozone monitoring sites for summer 2002.	351
Figure 5.9 Comparison between AURAMS predicted (left panel) and observed (right panel) annual (2002) ground-level speciated PM _{2.5} mass concentration (µg m ⁻³): sulphate – top panels, nitrate – middle panels, and ammonium – bottom panels.	352

- Figure 5.10 Model vs. observation scatter-plots of (a) sulphate_{2.5}, (b) nitrate_{2.5}, (c) organic matter, OM_{2.5}, and (d) sulphate fraction. Both model (AURAMS) results and observations are averaged over the ICARTT simulation period.355
- Figure 5.11 Comparison of AURAMS predicted PM_{2.5} (a) and its components, (b) sulphate, (c) nitrate, and (d) organic matter, with observations at IMPROVE sites over the ICARTT simulation period. The sites on the x-axis are arranged to move from the U.S. Midwest and Ohio Valley source regions to northeast coastal areas.356
- Figure 5.12 Time series comparison at two sites, Slocan Park (urban; upper panels) and Langley (rural; lower panels), from the CMAQ/MC2 simulation for sulphate (left), nitrate (centre), and organic component (right), all in $\mu\text{g m}^{-3}$357
- Figure 5.13 Comparison of model-predicted and measurement-based average OH-reactivity for lumped VOC species: AROM, ISOP, ALKE, and ALKA, as well as total VOC, at sites across Canada. Two model runs are included: base case and a sensitivity run with new vegetation data.360
- Figure 5.14 Comparison between AURAMS predicted (left panel) and observed (right panel) annual (2002) ground-level NO₂ concentration (top panels), SO₂ (middle panels), and HNO₃ (bottom panels), all in ppbv.363
- Figure 5.15 In-situ comparison of observed (in black) and AURAMS modelled (in blue) gaseous and particle species (from the top row down: CO, NO₂, O₃, SO₂, SO₄⁻², HNO₃, and NO₃⁻) for selected Convair 580 flights during ICARTT 2004 field campaign. Measurements of the gaseous species (SO₂, NO₂, CO, and O₃) are at 1-s frequency; HNO₃ measurements are 5-minute averages; measurements of inorganic ions are from the 10-minute integrated PILS; also included is air equivalent cloud-water sulphate (black diamonds) from bulk cloud water samples (varying in sampling duration).367
- Figure 5.16 (a) ground-based measurements of PM_{2.5}, PM_{1.0} sulphate, and SO₂ 80 km east of Edmonton; (b) AURAMS prediction at the grid containing the site at 21 km resolution; (c) AURAMS predictions at 3-km resolution.370
- Figure 5.17 An example of model-observation comparison along a flight track for PM_{1.0}-sulphate: 3-D plots of SO₄ along flight track shown on the left with corresponding plan view shown on the right, (top – observation; bottom – model).372
- Figure 5.18 (a) Modelled isoprene concentration at the lowest model level from the base run for 1800 UTC, August 2, 2001, and (b) difference in isoprene concentration between the base-case run and the sensitivity run with new vegetation data and revised isoprene emission factors, positive values corresponding to decreases from the base run.374

Figure 5.19 The model predicted maximum one-hour ozone concentrations for August 2, 2001: (a) base-case run and (b) sensitivity run with new vegetation data and revised isoprene emission factors, with the difference field (base run – sensitivity run) shown in (c), all in ppbv.375

Figure 5.20 Comparison of modelled and measured NO at Edmonton Central from the PrAIRie2005 simulations (Original denotes the current operation GEM, while TKE_NEW_R includes new parameterizations for urban heat islands, boundary layer height, and turbulent kinetic energy and NEWLM includes an additional observation-based lower limit in TKE).376

Figure 5.21 Comparison of 24-hour average modelled and measured organic aerosol concentrations at the Pitts Meadows site in the Lower Fraser Valley during the PACIFIC 2001 study.379

Figure 5.22 (a) Model-observation comparison of sulphate_{2.5} at the IMPROVE sites (arranged by locations from Midwest source region to eastern seaboard along the x-axis, left to right); (b) relative difference of the two sensitivity runs with respect to the base-case run.382

Figure 5.23 Comparison of Sea-salt fluxes at $u_{10} = 20 \text{ ms}^{-1}$ for four different parameterizations.383

Figure 5.24 AURAMS predicted surface fine particulate mass concentration (PM_{2.5}) using various sea-salt generation parameterizations versus measured PM_{2.5} at Sable Island 5-8 Feb 2005.....384

Figure 5.25 AURAMS predicted surface fine sea salt aerosol (SE25) versus hourly wind speed at Sable Island, NS, 5-8 February 2005.....385

Figure 5.26 (a) Comparison of modelled and measured NO 80 km downwind of Edmonton and; (b) Comparison of modelled and measured NO at Edmonton Central.....387

Figure 5.27 Domain-averaged ozone time series for the month of September 2002 from two AURAMS runs, one starting on May 1, 2002 (denoted as “200209”) and the other starting on September 1, 2002 (denoted as “200209_spinup”), both from the same initial conditions and with zero-gradient boundary conditions.388

Figure 5.28 Same runs as in Figure 5.27 but with time-independent first-order boundary conditions.....388

- Figure 5.29 The difference (ppbv) in modelled daily maximum 8-hour ozone concentrations averaged over the ICARTT period between the base case (i.e., without the NO_x emission adjustment) and the sensitivity run (i.e., with the emission adjustment). Positive values correspond to a decrease in ozone concentration due to the adjustment to NO_x emission. A statistical comparison with observation was done over the boxed area.395
- Figure 6.1 Average seasonal changes in PM_{2.5} mass associated with a 30% Canada and U.S. ammonia emission reduction for March, April May (top) and June, July and August (bottom). Positive values indicate decreases in PM_{2.5} mass associated with a 30% reduction in ammonia emissions. [S1]432
- Figure 6.2 Changes in the annual number of exceedance days in which the 24-hour average PM_{2.5} mass exceeds 30 µg m⁻³ associated with a 30% reduction in ammonia emissions [S1]. Positive values indicate areas where the PM CWS exceedance days have decreased in response to decreasing ammonia emissions.433
- Figure 6.3 Changes in total sulphur deposition (kg S /ha per season) associated with a 30% reduction in NH₃ emissions for December, January, February(top) and June, July, August (bottom). Positive values indicate decreases in sulphur deposition resulting from decreasing NH₃ emissions; negative values indicate increases. [S1].....435
- Figure 6.4 Changes in total nitrogen deposition (kg N/ha per season) associated with a 30% reduction in NH₃ emissions for December, January, February (top) and June, July, August (bottom). Positive values indicate decreases in N deposition resulting from decreasing NH₃ emissions; negative values indicate increases. [S1]436
- Figure 6.5 Canadian (S + N) critical load exceedances (eq/ha/y) for 2002 for the reference case simulation.....437
- Figure 6.6 Changes in the magnitude of (S + N) critical load exceedances for 2002 associated with a 30% reduction in NH₃ emissions. Positive values indicate areas where critical load exceedances have decreased in response to decreasing ammonia emissions. [S1].437
- Figure 6.7 The CMAQ model domains for the Lower Fraser Valley scenarios: (a) S2 and (b) S3; (c) Major geographic references within the Lower Fraser Valley model domains.439
- Figure 6.8 Predicted changes in ground-level ozone concentration at 18:00 PDT on August 12, 2001 associated with the no-marine emission case. [S4]443
- Figure 6.9 CMAQ model domain showing the coarse (36km by 36km) and fine (12 km by 12km) grid domains used in the S5, S6, S7 and S8 scenarios.445

Figure 6.10 Sectoral contributions to Alberta total emission inventory of NO_x and VOC used in the reference case for S5, S6, S7 and S8. “EPG” stands for “electric power generation”.....445

Figure 6.11 (a) Predicted mean daily 8-hour O₃ maximum with in the reference case for the 12-km grid; (b) difference in the mean daily 8-hour O₃ maximum (no-upstream oil and gas-emissions scenario minus reference case). [S5].....447

Figure 6.12 (a) Predicted number of days with 8-hour average ozone > 65 ppbv in the reference case for the 12-km grid; (b) difference in the number of days with 8-hour average ozone > 65 ppbv (no upstream oil and gas emissions scenario minus reference case) (b). [S5]449

Figure 6.13 (a) Difference in the number of days with 8-hour average ozone > 65 ppb (no-oil sands emission scenario minus reference case); (b) difference in the mean daily 8-hour O₃ maximum (no-oil sands-emissions scenario minus reference case). [S6].....451

Figure 6.14 Difference in (a) the mean daily 8-hour O₃ maximum (no-refinery-and-chemical-sector emission scenario minus reference case); (b) the number of days with 8-hour average O₃ > 65 ppbv (no-refinery-and-chemical-sector emissions scenario minus reference case). [S7] 453

Figure 6.15 Difference in (a) the mean daily 8-hour O₃ maximum (no-electricity-sector emission scenario minus reference case); (b) the number of days with 8-hour average O₃ > 65 ppbv (no electricity sector emissions scenario minus reference case). [S8]455

Figure 6.16 Reduction in hourly ambient PM_{2.5} concentrations resulting from the conversion of non-certified wood-burning appliances to EPA-certified products for the Nov. 20-26, 2006 period. The results are averaged over Montreal Island. The modelled wind speed is also plotted to show the relationship between reduction in PM_{2.5} concentration and local meteorological conditions. [S9]457

Figure 6.17 Relative difference in time averaged PM_{2.5} concentrations as a percentage between the base case and (a) the 25% conversion scenario and (b) the 50% conversion for the Nov. 20-26, 2006 period. Please note that the colour scale is different in (a) and (b). [S9].....458

Figure 6.18 Averaged daily 8-hour maximum background O₃ concentration (ppbv) for May-September 2005. [S10]459

Figure 6.19 Map of U.S. states covered by the CAIR rule (U.S. EPA, 2009)461

Figure 6.20 Absolute difference in the average O₃ summertime (June-July-August) 8-hour daily maximum between the 2015 BAU simulation and the 2002 reference case. [S11]463

Figure 6.21 Differences in monthly averaged VOC emission levels between the 2015 and 2002 inventories. [S11]463

Figure 6.22 Differences in monthly averaged NO _x emission levels between the 2015 and 2002 inventories. [S11]	464
Figure 6.23 Absolute difference in the annual PM _{2.5} 24hr average between the 2015 BAU simulation and the 2002 reference case. [S11]	466
Figure 6.24 Differences in monthly averaged primary PM _{2.5} emission levels between the 2015 and 2002 inventories. [S11]	467
Figure 6.25 Differences in monthly averaged SO _x emission levels between the 2015 and 2002 inventories. [S11]	467
Figure 6.26 Differences in annual 24-hour average PM _{2.5} -ammonium levels between the 2015 BAU simulation and the 2002 reference case. [S11]	468
Figure 6.27 Differences in annual 24-hour average PM _{2.5} -nitrate levels between the 2015 BAU simulation and the 2002 reference case. [S11]	468
Figure 6.28 Differences in annual 24-hour average PM _{2.5} -sulphate levels between the 2015 BAU simulation and the 2002 reference case. [S11]	469
Figure 6.29 Differences in annual 24-hour average PM _{2.5} -crustal material levels between the 2015 BAU simulation and the 2002 reference case. [S11]	469
Figure 6.30 Differences in summer (June-July-August) 24-hour average PM _{2.5} -sulphate levels between the 2015 BAU simulation and the 2002 reference case. [S11]	470
Figure 6.31 Differences in summer (June-July-August) 24-hour average PM _{2.5} -nitrate levels between the 2015 BAU simulation and the 2002 reference case. [S11]	471
Figure 6.32 Differences in winter (January-February-March) 24-hour average PM _{2.5} -sulphate levels between the 2015 BAU simulation and the 2002 reference case. [S11]	471
Figure 6.33 Differences in winter (January-February-March) 24-hour average PM _{2.5} -nitrate levels between the 2015 BAU simulation and the 2002 reference case. [S11]	472
Figure 6.34 Differences in the number of CWS exceedance days for O ₃ between the 2015 BAU simulation and the 2002 reference case. [S11]	473
Figure 6.35 Number of O ₃ CWS exceedance days for the 2015 BAU simulation. [S11]	473
Figure 6.36 Differences in the number of CWS exceedance days for PM _{2.5} between the 2015 BAU simulation and the 2002 reference case. [S11]	474

Figure 6.37 Difference in annual total sulphur deposition between the 2015 BAU simulation and the 2002 reference case. [S11]	475
Figure 6.38 Difference in annual total nitrogen deposition between the 2015 BAU simulation and the 2002 reference case. [S11]	475
Figure 6.39 Combined aquatic and terrestrial critical load map for Canada. White regions on the map represent areas where no data is available. (Wong <i>et al.</i> , 2008). [S11]	476
Figure 6.40 Difference in annual critical load exceedances for sulphur+nitrogen between the 2015 BAU simulation and the 2002 reference case based on critical load map from Wong and Dennis (2008). [S11]	476
Figure 6.41 Modelling domains of the S13 scenario: (a) 15 km domain; (b) nested 5 km domain.[S13].....	478
Figure 6.42 Difference over Alberta in (a) mean daily 8-hour O ₃ maximum between the 2015 future case and the 2002 reference case; and (b) the number of days with 8-hour average O ₃ > 65 ppb between the 2015 future case and the 2002 reference case. [S14]	484
Figure 6.43 Difference in the spatial distribution of NO _x emissions between the S15 scenario and the 2015 BAU case for a typical month (in tons/month/cell). (S15 scenario minus 2015 BAU). [S15].....	487
Figure 6.44 Change in average summertime daily 8-hour O ₃ maximum (in ppb) between the S15 scenario and the BAU case (S15 scenario minus 2015 BAU). [S15].....	488
Figure 6.45 Change in annual PM _{2.5} levels (in µg m ⁻³) between the S15 scenario and the BAU case (S15 scenario minus 2015 BAU). [S15].....	488
Figure 6.46 Change in average summer fine particle sulphate level (in µg m ⁻³) between the scenario and the BAU (S15 scenario minus 2015 BAU). [S15].....	489
Figure 6.47 Change in annual PM _{2.5} levels (in µg m ⁻³) between S15 scenario and the no-oil-and-gas emission reduction scenario (S15 scenario minus S15 scenario with no oil and gas reduction). [S15].....	490
Figure 6.48 Change in annual PM _{2.5} levels (in µg m ⁻³) between the S15 scenario and the no-smelting-and-electricity generation industries emission reduction scenario (S15 scenario minus S15 scenario with no smelting-and-electricity generation reduction). [S15].....	490

Figure 6.49 Change in annual PM _{2.5} levels (in $\mu\text{g m}^{-3}$) between the S15 scenario and the no 'other sectors' emission reduction scenario (S15 scenario minus S15 scenario with no 'other sectors' reduction). [S15]	490
Figure 6.50 Difference in the number of CWS exceedance days for O ₃ (S15 scenario minus 2015 BAU). [S15].....	491
Figure 6.51 Difference in the number of CWS exceedance days for PM _{2.5} (S15 scenario minus 2015 BAU). [S15].....	491
Figure 6.52 Changes in total sulphur deposition in eq/ha/yr (S15 scenario minus 2015 BAU). [S15]	492
Figure 6.53 Changes in total sulphur critical load exceedances between (S15 scenario minus 2015 BAU), based on critical load map from Wong and Dennis (2008). [S15].....	493
Figure 6.54 Changes in total sulphur + nitrogen critical load exceedances (S15 scenario minus 2015 BAU), based on critical load map from Wong and Dennis (2008). [S15].....	493
Figure 6.55 Composite map of the influence of Canadian emissions on PM _{2.5} levels in the U.S. for summer 2003 (expressed as relative sensitivity of PM _{2.5} levels in $\mu\text{g m}^{-3}$). [S18]	496
Figure 6.56 Composite map of the influence of Canadian emissions on PM _{2.5} levels in the U.S. for summer 2004 (expressed as relative sensitivity of PM _{2.5} levels in $\mu\text{g m}^{-3}$). [S19]	497
Figure 6.57 Composite map of the projected influence of Canadian emissions on PM _{2.5} levels in the U.S. in 2015 during summertime (expressed as relative sensitivity of PM _{2.5} levels in $\mu\text{g m}^{-3}$). [S20]	498
Figure 6.58 Map of influence of U.S. emissions on Canadian PM _{2.5} levels in Canada for summer 2004 (expressed as relative sensitivity of PM _{2.5} levels in $\mu\text{g m}^{-3}$). [S19].....	499
Figure 6.59 Map of influence of 2015 projected U.S. emissions on Canadian PM _{2.5} levels during summer (expressed as relative sensitivity of PM _{2.5} levels in $\mu\text{g m}^{-3}$). [S20].....	500
Figure 6.60 Averaged change in the daily 8-hour O ₃ maximum levels (ppb) between the 2002 reference case and the 2005 emission scenario for the May to September 2005 period (2002 reference case minus 2005 scenario). Sub-domains are depicted by the red boxes. [S21].....	502
Figure 6.61 Map of influence of British Columbia emissions on ambient PM _{2.5} levels in rest of Canada and the U.S. for summer 2004 (expressed as relative sensitivity of PM _{2.5} levels in $\mu\text{g m}^{-3}$). [S19].....	505

Figure 6.62 Map of influence of emissions from the Prairies on ambient PM _{2.5} levels in the rest of Canada and the U.S. for summer 2004 (expressed as relative sensitivity of PM _{2.5} levels in µg m ⁻³). [S19]	505
Figure 6.63 Map of influence of Ontario emissions on ambient PM _{2.5} levels in the rest of Canada and the U.S. for summer 2004 (expressed as relative sensitivity of PM _{2.5} levels in µg m ⁻³). [S19]	506
Figure 6.64 Map of influence of Québec emissions on ambient PM _{2.5} levels in the rest of Canada and the U.S. for summer 2004 (expressed as relative sensitivity of PM _{2.5} levels in µg m ⁻³). [S19]	507
Figure 6.65 Map of influence of emissions from Maritime provinces on ambient PM _{2.5} levels in the rest of Canada and the U.S. for summer 2004 (expressed as relative sensitivity of PM _{2.5} levels in µg m ⁻³). [S19]	508
Figure 6.66 Daily (a) PM _{2.5} (b) 8-hour O ₃ maximum measured and modelled for four locations along the St. Lawrence valley from west to east. Also shown are computed estimates of the local and transboundary contributions. [S23]	509
Figure 6.67 S25 modelling domain with locations of selected major cities. [S25]	513
Figure 7.1 A conceptual model represents initial hypotheses of how emissions, chemistry and meteorology interact to produce the observed pollutant concentrations. Observations, source apportionment analyses with this observations and applications of models are the tools used to develop and test the conceptual model.	541
Figure 7.2 Map of Southern Atlantic Region with locations of main sites, cities and geographic regions discussed in this chapter.	542
Figure 7.3 Southern Atlantic Canada Conceptual Model.	544
Figure 7.4 Map of the Southern Québec and Eastern Ontario region with locations of main sites, cities and geographic regions discussed in this chapter.	546
Figure 7.5 Southern Québec and Eastern Ontario Conceptual Model.	547
Figure 7.6 Map of the Southern Great Lakes Region with locations of the main sites, cities and geographic regions discussed in this chapter.	549
Figure 7.7 Southern Great Lakes Region Conceptual Model.	550

Figure 7.8 Map of the Alberta and the Prairie Region showing locations of the main sites, cities and geographic features discussed in this chapter.	552
Figure 7.9 Alberta and the Prairie Region Conceptual Model.	553
Figure 7.10 Map of the Lower Fraser Valley region with locations of the main sites, cities and geographic features discussed in this chapter.	555
Figure 7.11 Lower Fraser Valley Conceptual Model.	556
Figure 7.12 Map of the Interior BC region with locations of the main sites, cities and geographic features discussed in this chapter.	558
Figure 7.13 Interior British Columbia Conceptual Model.	559
Figure 7.14 2005 Atlantic Provinces Criteria Air Contaminants (CAC) inventory by sector contribution for a) NO _x , b) SO _x , c) VOCs, and d) PM _{2.5} . Electrical Power Generation dominates NO _x and SO _x emissions while Residential Fuel Wood Combustion dominates VOC emissions and Dust from Paved and Unpaved Roads are the major contributors PM _{2.5} emissions. Environment Canada, 2007a.	562
Figure 7.15 Quebec's anthropogenic criteria air contaminants emissions by sector contribution for a) NO _x , b) SO _x , c) VOCs, and d) PM _{2.5} . The transportation sector (which can be broken into on-road emissions (37%) and off-road emissions (19%)) dominates NO _x emissions while industrial activity is the major source of SO _x emissions. Transportation and residential fuel wood combustion dominate VOC emissions while road dust contributes to almost one half of regional PM _{2.5} emissions.	567
Figure 7.16 Ontario's anthropogenic criteria air contaminants emissions by sector. a) NO _x , b) SO _x , c) VOCs, and d) PM _{2.5} . (Pollution Data Branch, 2007). Environment Canada, 2007a.	572
Figure 7.17 Alberta, Saskatchewan and Manitoba anthropogenic criteria air contaminants emissions by sector. a) NO _x , b) SO _x , c) VOCs, and d) PM _{2.5} . Environment Canada, 2007a.	578
Figure 7.18 British Columbia's anthropogenic criteria air contaminants emissions by sector. a) NO _x , b) SO _x , c) VOCs, and d) PM _{2.5} . Environment Canada, 2007a.	584
Figure 7.19 Forecast of smog forming pollutant sources for the LFV based on the 2005 emission inventory (Metro Vancouver, 2007).	585
Figure 7.20 Emission forecasts of smog forming pollutants for the LFV based on the 2005 emission inventory (Metro Vancouver, 2007).	586

Figure 7.21 Example of a synoptic weather pattern typically associated with regional air pollution events affecting eastern Canada from southern Ontario to the southern Atlantic region. Common features are the high pressure system (H) to the south and lower pressures (L) toward the northwest and north. This pattern places eastern Canada in the warm sector of the low pressure system with southerly to southwesterly wind flow. On days prior to this pattern the 'Bermuda' high and ridge often lay over the eastern U.S. and southern Canada promoting stagnation, light winds and sunny weather over the emission areas. With the low pressure system moving into northern Ontario and then into Québec the wind flow transports pollutants northeastward in the warm sector or 'back of the high'. Depending upon the track of the low and the high this can lead to build up and transport into Ontario, Québec and Atlantic Canada. The black lines are isobars. The heavy red and blue lines indicate warm and cold fronts, respectively.590

Figure 7.22 Median airshed contours for Kejimikujik, Nova Scotia based on 925 hPa back-trajectories for the period 1999-2001 (Ketch *et al.*, 2005). The 3-day median airshed encompasses the eastern half of Ontario, all of Québec, Atlantic Canada and the northeastern U.S. including the states of Ohio, West Virginia and Virginia where significant precursor emissions occur.592

Figure 7.23 Typical pressure pattern leading to high winter PM_{2.5} levels (1000 hPa pressure surface in decameters above sea-level) shows a high pressure centre lying to the southwest of the Lower Great Lakes with a ridge extending across Ontario and Québec. This pattern can push air from high emissions areas into southern Ontario, the St. Lawrence River Valley and potentially Atlantic Canada.593

Figure 7.24 Vertical profiles of concentrations of a) CO, b) total number concentration (PCASP), and c) O₃, showing layering of pollutants during ICARTT – TIMs Flight 3, 16:18 – 18:12 UTC, July 22, 2004 (Vaugh *et al.*, 2007). Colours indicate concentrations (red = high, blue = low), and the x-axis represents the location of the aircraft profiles (McAdam, NB, Grand Manan, NB, Brier Island, NS, and Port Maitland, NS) in relation to McAdam. Each plot can be considered as an interrupted view of a vertical cross section along the transect from McAdam to Port Maitland, across the Bay of Fundy. CO, particles, and O₃ all tend to be highest at an elevation of 500 m above Grand Manan Island, but in general the CO and O₃ plumes appear to ride over top of the marine boundary layer over Brier Island and Port Maitland.595

Figure 7.25 Typical relationship between evening wind speed and PM_{2.5} levels in East Montréal (Rivière-des-Prairies) in winter where local primary PM_{2.5} sources prevail (adapted from Carter *et al.*, 2004).597

Figure 7.26 Geographical distribution of number of 1-hour O₃ exceedences across Ontario in 2005 (MOE, 2006).598

Figure 7.27 Mean and maximum mixing heights by month derived from measurements at Stony Plain, Alberta.....600

Figure 7.28 Trajectory cluster mean vectors at 10 O₃ sites. Six trajectory clusters were sorted by the k-means clustering technique similar to Dorling *et al.* (1992a,b) using Euclidean distance as the dissimilarity measure on CMC 3-day air parcel backward trajectories from 1994 through 2005 for all sites. This method primarily used here is to define synoptic flow patterns associated with these sites. The endpoint for the vectors shown represents the mean upwind distance three days back in time. Shorter vectors thus indicate slow travel speed and possible stagnation along the path while longer vectors are related to strong wind speeds. See Section 7.6.1 for more discussion on this figure.601

Figure 7.29 Seasonal box-and-whisker O₃ plots by trajectory clusters at 10 O₃ sites. The time period of the O₃ data record at any given site used in the analysis is shown below the site name in each panel. Seasonal breakdowns are as follows: March – April – May (MAM), June – July – August (JJA), September – October – November (SON) and December – January – February (DJF). Note that different vertical scales, which are in ppb, are used across sites to highlight location-specific differences in O₃ by transport direction. See Section 7.6.1 for more discussion on this figure.602

Figure 7.30 Mean Ozone diurnal cycles for a) All Days (Mon-Sun), b) Weekdays (Mon-Fri) and c) Weekends (Sat-Sun), for the years 1997-2005 at Point Lepreau, Saint John Customs, Forest Hills, and Norton, New Brunswick. Median values for each hour are shown as a short horizontal line, the shaded boxes indicate values that lie between the 25th and 75th percentile of all values, and the whiskers indicate the 10th and 90th percentiles. The rural site of Norton has the greatest daily range of ozone concentrations (10.4 ppb) while the urban site at Forest Hills and the coastal site (Point Lepreau) have the least daily variability (~6 ppb). The absolute levels are lower at the urban site due to O₃ titration by NO. The rural sites of Norton and Point Lepreau ozone values exhibit a characteristic rural diurnal pattern, rising throughout the morning and early afternoon due to photochemistry, peaking at approximately 5pm, and decreasing through the dark evening and early morning hours to a minimum at about 7am. In contrast, Saint John Customs and Forest Hills indicate a strong O₃ titration by NO in the morning (8 am minimum due to urban traffic patterns), and a suppressed afternoon peak owing to continued titration which is enhanced by the shallow mixed-layer due to cool marine air.....608

Figure 7.31 Trend plots of the 10, 25, 50, 75, 90, 95th and maximum percentiles for five Atlantic region sites: (a) St. John's, NL, (b) Saint John Forest Hills, NB, (c) Kejimikujik, NS, (d) Blissville and (e) Norton, NB. The blue line indicates a non-statistically significant trend and the red line a statistically significant trend at the 95% confidence limit based upon the T-test.613

Figure 7.32 Probability density for the trajectories that result in 90th percentile values of $PM_{2.5}$ for two sites in the Atlantic region (Kejimikujik, NS; Forest Hills, NB) and two sites in the northeastern US near the Canadian border (Acadia National Park, ME; Moosehorn National Wildlife Refuge, ME). Mass contributions to annual 90th percentile are shown; at all stations the summer months (JJA) show the greatest contribution to 90th percentile values (51%, 65%, 71% and 62% for Forest Hills, Kejimikujik, Acadia and Moosehorn, respectively). Probability densities show the most influential trajectory at all stations to be that from the west-southwest.....616

Figure 7.33 Summer (May to September) diurnal variation of ozone for a rural site (Saint-Anicet), an urban site (Ontario Street, downtown Montréal) and a suburban site (Rivière-des-Prairies) from 2003-2006.620

Figure 7.34 NO_2 mean diurnal cycle for all days (annual) and for weekends vs. weekdays averaged across six stations located in Montréal (Saint-Anne-de-Bellevue, Aéroport de Montréal, Parc Pilon, Jardin Botanique, St-Jean-Batiste and Verdun) for 2005 to 2006.621

Figure 7.35 Trends in warm season daily 8 hour maximum ozone for five sites in southern Québec and one in eastern Ontario from 1991 to 2008. Background site: Ferme-Neuve (located 180 km northwest of Montréal). Urban sites: Saint Jean Baptiste, Parc Pilon (both on Montréal Island) and Ottawa. Rural sites: Saint Zéphirin, La Patrie. Trend lines shown in red are significant at the 95% confidence level based upon the T-test.....624

Figure 7.36 Mean monthly $PM_{2.5}$ concentrations based upon TEOM measurements for Montréal (Drummond site), Québec, Trois-Rivières, Saint-Anicet, L'Assomption and L'Acadie from 1999 to 2002.....626

Figure 7.37 $PM_{2.5}$ diurnal cycles based on TEOM measurements at a suburban (Rivière-des-Prairies, referred to as RDP) and urban (Maisonneuve, downtown Montréal, referred to as DRU) site over three summers and winters (2004-2006) compared to the annual average diurnal cycle at the rural site of Saint-Anicet (WBZ) site.626

Figure 7.38 Spatial distribution of ozone in Ontario expressed as the CWS metric. Warm seasons of 2004–2006, fourth highest daily maximum 8-hour average ozone. The black dots show the locations of all the available monitoring sites used for the interpolation based upon an inverse distance weighting scheme.630

Figure 7.39 Spatial distribution of ozone in Ontario expressed as the CWS metric. Warm seasons of 2004–2006, fourth highest daily maximum 8-hour average ozone derived from an optimal interpolation of the monitoring site data typically available as of 2003 and output from the O_3 forecast model, CHRONOS.631

- Figure 7.40 Geographical distribution across Ontario of PM_{2.5} concentrations expressed in terms of the Canada-wide standard metric (ending years of 2005, 2006 and 2007). 633
- Figure 7.41 a) May 10, 2006 – a high SO₂ and PM_{2.5} concentration episode in Hamilton, Ontario. The gases have units of ppb while PM_{2.5} is in µg/m³. b) June 15, 2006 – a high SO₂ (ppb) and PM_{2.5} (µg/m³) concentration episode in Sault Ste. Marie, Ontario. 635
- Figure 7.42 Median 6 hr PM_{2.5} concentrations for the warm seasons (May-September) of 1998-2001 (non-precipitating days). “All” represents all measurements in the period when each of the four sites were reporting simultaneously. The sites shown represent a southwest to northeast transect from a rural location (Simcoe) to the outskirts of Hamilton (Hamilton Mtn.) and two sites in Toronto. Etobicoke is in the southwestern part of Toronto and is impacted by traffic. 636
- Figure 7.43 Inter-annual O₃ trend plots by trajectory cluster at 10 sites. The time period of the O₃ data record at any given site used in the analysis is shown below the site name in each panel. The curves associated with each cluster were generated using LOWESS (Cleveland *et al.*, 1988), a non-parametric smoothing technique. See Section 7.6.1 for more discussion on this figure. 639
- Figure 7.44 Southern Ontario trends in warm season (May-September) daily 8 hour maximum ozone concentrations for 1991-2008. Trend lines shown in red are statistically significant with 95% confidence based upon the T Test. 642
- Figure 7.45 Seasonal O₃ trend plots by trajectory clusters at 10 O₃ sites. The time period of the O₃ data record at any given site used in the analysis is shown below the site name in each panel. The O₃ trends were generated using LOWESS (Cleveland *et al.*, 1988), a non-parametric smoothing technique, associated with these cluster. Note that different scales are used across sites. See Section 7.6.1 for more discussion on this figure. 645
- Figure 7.46 The daily average and maximum ozone concentrations at two Ontario sites: (a) Toronto West and; (b) Dorset. The solid line is the 10-point running mean. Note that data for other years, not shown here, exhibit essentially identical patterns. 646
- Figure 7.47 Diurnal pattern in ozone concentration for sites in Ontario for 2006. 647
- Figure 7.48 Diurnal patterns of PM_{2.5} (all year and summer only) for Dorset, Port Stanley, and Toronto West. 649
- Figure 7.49 Annual average estimated fine nitrate from CAPMoN sites in southern Ontario and Québec. 650

Figure 7.50 Seasonal cycle of O₃, PM_{2.5}, NO₂ and NO at Edmonton East monitoring site Box plots display: the 95th percentile (highest circle), 90th percentile (upper whisker), 75th percentile (upper boundary of box), median (horizontal line through box), 25th percentile (lower boundary of box), 10th percentile (lower whisker) and 5th percentile (lower circle) of all observations for each category.657

Figure 7.51 Percent exceedances of the CWS for O₃ in Alberta – comparison of urban and non-urban sites. (Percentage of days with 8 hour ozone >65 ppb at a selection of Alberta sites) ..659

Figure 7.52 95th percentile NO₂ (top), O₃ (middle), and PM_{2.5} (bottom) concentrations in summer and winter (2000-2005) at sites across the Prairies.661

Figure 7.53 PM_{2.5} concentration (heavy grey line) and NO (green line) mixing ratio along with wind speed and mixing heights during a winter episode in Edmonton. Pollutants and wind speed were measured at Edmonton East monitoring station, estimated mixing height was determined from Stony Plain radiosonde launches, 20km west of Edmonton. The blue box and whisker plots indicate the observed wind speeds on each day while the red line shows the long term average wind speed at the site. Note the observed wind speeds were much lower than average during the highest NO and PM_{2.5} periods on Dec. 10 and 11.662

Figure 7.54 Mean frequency of days with 8-hour ozone above 65 ppb at five sites near Edmonton (1996-2005). The five Edmonton area sites are Edmonton Northwest, Edmonton Central, Edmonton East, Fort Saskatchewan and Tomahawk (80 km WSW of Edmonton) monthly frequency of ozone episodes in Edmonton 1989-2003. An ozone episode is defined as a day with one or more of the four Edmonton area sites (Northwest, Central, East and Fort Saskatchewan) reporting 8-hour O₃ above 65 ppb.663

Figure 7.55 Trends in warm season (May-September) daily 8 hour maximum ozone concentrations for 1991-2008 in three Prairie cities. Trend lines shown in red are statistically significant with 95% confidence based upon the T Test.667

Figure 7.56 Ozone production and NO_y loss during a plume tracking sampling flight, August 10, 2001. The blue line represents NO_x concentrations observed during the flight, with concentrations increasing along the z-axis (not shown for simplicity) Ozone concentrations measured on the same flight are shown as a colored surface. Note the higher NO_x concentrations associated with lower ozone concentrations. Figure reproduced from AMEC. 2003. Ozone production and NO_y loss during a plume tracking sampling flight, August 10, 2001. Reproduced from AMEC (2003).672

Figure 7.57 Oilsands sector scenario: (a) fourth highest daily maximum ozone (b) emissions from the oilsands sector excluded (c) maximum percent difference between (a) and (b).673

Figure 7.58 Interpolated ozone plumes for the LFV for August 3 1988 and July 29, 2003. From Steyn and Ainslie (2007).	674
Figure 7.59 a) Diurnal pattern of NO concentrations at Robson, Vancouver (1995-2006). b) Diurnal pattern of NO ₂ concentrations at Robson, Vancouver (1995-2006). c) Diurnal pattern of NO concentrations at Hope (1996-2006). d) Diurnal pattern of O ₃ concentrations at Robson, Vancouver (1995-2006). e) Diurnal pattern of O ₃ concentrations at Hope (1996-2006).....	676
Figure 7.60 VOC:NO _x ratios, NO _x and total VOCs at NAPS stations in the LFV (May – September 1990-2006). Stations arranged in decreasing order of VOC/NO _x ratios.	677
Figure 7.61 a) Diurnal pattern of PM _{2.5} concentrations at Vancouver, West 10th (2006). b) Diurnal pattern of PM _{2.5} concentrations at Hope (2005-2006).	678
Figure 7.62 a) Seasonal pattern of O ₃ concentrations at Vancouver Airport (1996-2006). b) Seasonal pattern of O ₃ concentrations at Chilliwack (1995-2006). c) Seasonal pattern of PM _{2.5} concentrations at Chilliwack (1995-2006).	679
Figure 7.63 Ozone trends for sites in the western (a) and eastern (b) LFV for different percentiles in the statistical distribution. Statistically significant trends at p<0.05 shown in red. For the western LFV data were averaged for the following sites: Hastings and Kensington, Rocky Point, Vancouver West 10th, Delta, Burnaby Ring Road, Richmond South, Mahon Park. For the eastern LFV, data were averaged for the sites: Surrey East, Abbotsford S. Fraser Hwy., Chilliwack Airport.....	680
Figure 7.64 Statistical distributions for (a) reconstructed light extinction and (b) visual range at Burnaby South and Abbotsford Airport for the period 2003-2008.....	683
Figure 7.65 Seasonal pattern of reconstructed light extinction at Burnaby South and Abbotsford Airport for the period 2003-2008.	683
Figure 7.66 Seasonal pattern of PM _{2.5} concentrations at Prince George, Plaza 400 (1998-2006).	685
Figure 7.67 Daily average PM ₁₀ in Yellowknife for April and May 2007.....	687
Figure 7.68 Hourly average PM ₁₀ in Yellowknife during April and May 2007.....	687

Figure 7.69 Trajectory cluster mean vectors derived from the time period (ranging from 1994 to 2005) of available PM_{2.5} data at 8 selected sites. Note that although the time period used to derive these clusters and those in Figure 7.34 were considerably different very similar transport patterns were identified when the same sites were examined (i.e., Kejimikujik and Forest Hills (Saint John)). Also note that the identified prevailing transport pathways at nearby sites (e.g., Kejimikujik and Forest Hills; Saint Anicet and Roundtop Ridge; Edmonton NW and Ester) are similar. This highlights the fact that, due to the input data used and the meteorological factors that are most influential, trajectories only resolve regional and larger scale phenomena as opposed to local scale features.691

Figure 7.70 Seasonal box-and-whisker PM_{2.5} plots by trajectory clusters at 8 PM_{2.5} sites. The time period of the PM_{2.5} data record at any given site used in the analysis is shown below the site name in each panel. Seasonal breakdowns are as follows: March – April – May (MAM), June – July – August (JJA), September – October – November (SON) and December – January – February (DJF). Note that different scales are used across sites.694

Figure 7.71 Source Sector geographic boundary definition (Ketch *et al.*, 2005) for St. Andrews, NB and Kejimikujik, NS. Trajectories (3-day, 925 hPa) arriving at each site were sorted according to three upwind regions or sectors: U.S., Canada and Ocean. A fourth grouping, “multi-sector”, was defined for any trajectory that did not have at least 10 of its 12 segments solely in one of these three regions. (Ketch *et al.*, 2005).695

Figure 7.72 QTBA results showing the relative contribution to ozone concentrations during periods with widespread CWS metric exceedances of ozone (left panel) and PM_{2.5} (right panel) for Kejimikujik (Johnson, 2004). Both panels illustrate that the trajectories contributing to the higher concentrations of these pollutants are generally from the west. Ozone data are based on the period 1990-2002 and PM_{2.5} from 1998-2002. The transport path for elevated ozone is more westerly than the path for PM_{2.5}. The legend indicates the relative contribution of parcels passing over a grid square to the concentrations at Kejimikujik where the green colour represents a factor of 1 and the darkest red colour a factor of 3 above the average concentration.695

Figure 7.73 Clustered one day mesoscale back trajectories for O₃ at Saturna CAPMoN (December 2003-March 2005).702

Figure 7.74 Clustered one day mesoscale back trajectories for O₃ at Chilliwack Airport (December 2003-March 2005).703

Figure 7.75 Clustered one day mesoscale back trajectories for O₃ at Kelowna College (December 2003-March 2005).704

Figure 7.76 Trajectory probability density map of maximum summer O₃ at Saturna CAPMoN, based on three day CMC back trajectories.705

Figure 7.77 Trajectory probability density map of maximum summer O ₃ at Saturna CAPMoN, based on one day mesoscale back trajectories.	705
Figure 7.78 Wind sector analysis showing percentage contributions by each sector to pollutants measured at Christopher Point. Canadian contributions are shown as both local and transported.....	707
Figure 7.79 Weather maps associated with the February, 2005, PM _{2.5} event in Ontario and Quebec. Map time stamps are EST with surface synoptic charts for February 1 – February 6 on the top two rows and 500 mb charts for February 1, 3, 4, 5 on the bottom row. The surface charts illustrate a ridge of high pressure (wavy line) lying nearly stationary over southern Ontario, the lower Great Lakes and southern Quebec during the period to February 6th.	710
Figure 7.80 a) Time series of unadjusted TEOM (SES) 6 hour average PM _{2.5} concentrations for site group averages in the Windsor, Toronto, eastern Ontario and Montréal areas for the period 29 January to 10 February 2005. Although Montréal sites had the highest values and were elevated prior to the other areas the graph illustrates the rapid return to low concentrations as the cold front and attendant weather approached on February 8th. b) Beta Attenuation Monitor (BAM) 6 hour average PM _{2.5} concentrations for selected sites in each region. This instrument is much less sensitive to loss of ammonium nitrate (especially in winter) and thus the concentrations shown tend to be larger than those in Figure 7.66a.....	711
Figure 7.81 Filter-based PM _{2.5} mass, nitrate and sulphate concentrations (24 hr averages) for the areas of Windsor, Toronto, East Ontario and New Brunswick during the February 2005 winter PM episode. Concentrations were averaged among the available sites in the four selected regions. The 24 hr mass measurements shown in the top panel are the best estimate of the true values.	713
Figure 7.82 PM _{2.5} concentrations (24 hour average) on February 6, 2005, the day with the highest levels in southern Quebec, which were the highest PM _{2.5} (24 hour, filter-based samples) levels observed in Canada during the past 10 years.	715
Figure 7.83 Average 2000-2004 forest fire PM _{2.5} emissions and area burned by Province (Lavoué <i>et al.</i> , 2007).....	716
Figure 7.84 View of downtown Calgary looking west at 7:30 PM August 13, 2003. Forest fire smoke from fires in southeastern B.C. Fine particulate matter levels = 125 μ g m ⁻³ (average of three Calgary monitoring stations).	717

Figure 7.85 Hourly and daily PM _{2.5} at Calgary Northwest monitoring station during the August 2003 forest fire smoke episode. The green line shows August median hourly PM _{2.5} at this site, the light blue line shows the August 95th percentile hourly PM _{2.5} at this site and the red line shows the CWS for PM.....	718
Figure 7.86 Results from the 2002 Québec case study for July 6, 2002. Left: Terra MODIS image at 15:50 UTC; Right: GEM/CHRONOS PM _{2.5} output at 16UTC with (bottom) and without (top) wildfire emissions. Without the inclusion of emissions from the forest fires the model is unable to forecast the elevated PM observed.	719
Figure 7.87 Concentration of NO ₂ and particulate matter as a function of distance from a major highway (Beckerman <i>et al.</i> , 2007).....	721
Figure 7.88 Map of NO ₂ concentrations from a) Toronto (Jerrett <i>et al.</i> , 2007), and b) Windsor (Wheeler <i>et al.</i> , 2007), generated using a land-use regression (LUR) model.	724
Figure 7.89 Seasonal variations in the contributions of the PMF modelled factors at Burnaby South (Dec 2003 – Dec 2008).	726
Figure 7.90 Seasonal variations in the contributions of the PMF modelled factors at Abbotsford (Dec 2003 – Dec 2008).....	727
Figure 7.91 Seasonal PMF and CMB factor contributions to PM _{2.5} mass at Prince George, Plaza 400 (2004-2006). Courtesy of BC Environment.	728
Figure 7.92 Seasonal factor contributions to PM _{2.5} mass at Golden (2004-2006). Courtesy of BC Environment.....	728
Figure 7.93 Source contributions to PM _{2.5} mass at five Canadian cities (2006-2007). SOA corresponds to secondary organic aerosols (Jeong <i>et al.</i> , 2009).....	729
Figure 7.94 Backscatter ratio measurement obtained with the Dalhousie Raman Lidar on 14 July 2007. Aerosols are revealed by ratios greater than 1 (i.e. light blue to red on the colour scale). A separate low-altitude receiver is used for measurements between the ground and 1 km altitude. The particles were first detected between 1 and 2 km aloft and gradually descended toward the ground level. Elevated surface concentrations of O ₃ and PM _{2.5} were measured when this layer reached the ground.	731
Figure 7.95 72-h back trajectory for air arriving at 1, 2 and 3 km altitude above Halifax at 2000 UTC on 14 July 2007 associated with the plume detected in Figure 7.85.....	731

- Figure 7.96 Dalhousie Raman Lidar measurement of a biomass burning plume originating from the state of Montana on 15 August 2007 where the plume shows a layer extending from 2.5 to 5.5 km in altitude.....732
- Figure 7.97 Median ozone concentration with SW winds and <50% cloud cover at each site near Saint John, NB, during daylight hours selected for optimal conditions for photochemistry, May-September, 1997-2005. Box represents values between the 25th and 75th percentiles; whiskers represent the 10th and 90th percentiles. “UW” refers to upwind, “DW” to downwind. Evidence of titration of O₃ by NO_x is indicated by the lower O₃ values at the Saint John customs site, which persist to the downwind suburban site of Forest Hills. The downwind rural site of Norton exhibits the highest O₃ concentrations during the selected hours, higher than the upwind rural site of Point Lepreau, indicating photochemical production from precursors released in the urban core.....734
- Figure 7.98 Average PM_{2.5} concentrations, hour by hour, in 2006 during winter months (November to March). The traffic site, Montreal downtown, is affected by the afternoon rush hour but concentration return to average values later in the evening. In contrast, communities affected by wood combustion are subject to an increase in PM_{2.5} concentrations later in the evening and return to average values well after midnight. The star (*) in the legend indicates that PM is measured by a BAMM instrument whose values are known to be higher than the TEOM with dryer instrument (sites without the star).736
- Figure 7.99 Comparison between PM_{2.5} from forest fires and fireworks in 2002 reported at Hochelaga (1.8 km north of the fireworks site) and Rivière-des-Prairies (RDP, 14 km north of the fireworks site) (Gagnon *et al.* 2003).737
- Figure 7.100 Transboundary and Ontario contributions to ozone on high concentration days for May – October (MOE, 2005).740
- Figure 7.101 Transboundary and Ontario contributions to PM_{2.5} on high concentration days for May – October (MOE, 2005).741
- Figure 7.102 Transboundary and Ontario contributions to PM_{2.5} on all days for May – October (MOE, 2005)742
- Figure 7.103 (a) AURAMS forecast for surface ozone for August 28th, 12:24 local daylight time during the PRAIRIE 2005 study; (b) vertical cross section of transect from A to B showing ozone depletion at the surface and two regions of high ozone aloft, from down mixing from the middle troposphere and local chemical enhancement at the 700 m level.743

Figure 7.104 Model predicted daily mean of maximum 8 hour ozone for a three month simulation (JJA) for (a) the base case, (b) pollution sources outside Alberta set to zero (clean air boundary condition). Note that trans-boundary sources are more important to high ozone levels in Calgary than in Edmonton. (Model predicted daily mean of maximum 8 hour ozone for a three month simulation (JJA) for (a) the base case, (b) pollution sources outside Alberta set to zero (clean air boundary condition) (Fox and Kellerhals, 2007).....745

Figure 7.105 LFV station locations during the Pacific 2001 Study (Vingarzan and Li, 2006). ..747

Figure 8.1 Representation of the links between climate change and air quality. Changes to the energy balance of the climate system can impact meteorological parameters, which can impact the formation and distribution of atmospheric species, changing air quality. Changes to the distribution and formation of atmospheric species can feedback and change the energy balance of the climate system.780

Figure 8.2 General off-line GCM-CTM set up for investigating the effect of climate change on air quality from Jacob and Winner (2009). GCM = general circulation model, RCM = regional climate model and CTM = chemical transport model.784

Figure 8.3 Surface PM_{2.5} concentrations inferred from satellite observations of aerosol optical depth. The top panels show PM_{2.5} for June – August from the MISR satellite instrument and from surface monitors. The bottom panel shows the temporal relationship of two satellite observations with a collocated ground-based monitor in Toronto. (Adapted from van Donkelaar *et al.*, 2006.).....818

Figure 8.4 Monthly mean tropospheric HCHO/NO₂ column ratio retrieved from the GOME satellite instrument for East Asia and North America. Areas with ratios > 1 tend to be NO_x-limited while areas with ratios < 1 tend to be VOC-limited. White areas: less polluted regions (observed tropospheric NO₂ columns less than 2.5 x10¹⁵ molecules cm⁻²) or below the HCHO column detection limit of 4x10¹⁵ molecules cm⁻². (After Martin *et al.*, 2004.).....819

Figure 8.5 (Left) Tropospheric NO₂ columns for 2004-2005 determined from the SCIAMACHY satellite instrument. (Right) Surface NO_x emissions for 2004-2005 determined through inverse modelling of the SCIAMACHY observations using GEOS-Chem. The largest differences with bottom-up inventories occur over rapidly developing regions where the bottom-up inventory is out-of-date. Aircraft measurements were taken as part of the ICARTT aircraft campaign in support of the SCIAMACHY inventory program (Martin *et al.*, 2006).821

Figure 8.6 (Left) Formaldehyde (HCHO) columns over the United States determined from the OMI satellite instrument for summer 2006. (Right) Isoprene emissions determined through inverse modelling of the OMI observations using a chemical transport model (GEOS-Chem) (*Millet et al.*, 2008). Aircraft measurements show that isoprene is the dominant source of variability in column formaldehyde over North America (*Millet et al.*, 2006).....821

Figure 8.7 The left panel shows the seasonal average GOME tropospheric O₃ columns (Dobson units) for June – August 1997 (*Liu et al.*, 2006b). The right panel indicates the MOPITT 700 hPa CO mixing ratio (ppbv) for 15-23 July 2004 (*Pfister et al.*, 2006).823

Figure 9.1 Chemical and transport processes related to atmospheric composition. These processes link the atmosphere with other components of the Earth system, including the oceans, land, and terrestrial and marine plants and animals. Credit: Climate Change Science Program Strategic Plan, 2005 (illustrated by P. Rekacewicz).854

Figure 9.2 Satellite observation of (a) the Trans-Pacific Transport of Asian CO and (b) sand and dust storms.855

Figure 9.3 The zonal transport fluxes ($\text{mg m}^{-2} \text{s}^{-1}$) of Asian dust in spring of (a) 8 El Niño years (1966, 73, 83, 87, 87, 92, 98 and 2003) and (b) 8 La Niña years (1965, 71, 74, 76, 86, 89, 99 and 2000). The contour lines are for the anomalies relative to the 44-year mean of Asian dust aerosol in spring (*Zhao et al.*, 2006). The red dark arrow lines indicate the dominant pathways of intercontinental transport.856

Figure 9.4 (a) Time series of spring mean PM₁₀ concentrations at 15 sites in the western U.S and the total SDS process numbers in China from spring 2000 to 2006. The 15 sites are Bliss State Park, CA; Bridger Wilderness, WY; Columbia River, WA; Crater Lake, OR; Craters of the Moon, ID; Lassen, CA; Mt. Rainier, WA; Pinnacles, CA; Redwood NP, CA; Sawtooth NF, ID; Snoqualmie Pass, WA; Sula Peak, MT; Three Sisters, OR; Yellowstone, WY; and Yosemite, CA. (b) Same as in Figure 9.4(a) but for spring mean Ca concentrations contained in aerosols collected at Saturna Island, Canada, from 2001 to 2006.858

Figure 9.5 Monthly averages of (a) calcium and (b) sulphate less than 2.5 μm , collected at Whistler from 2002-2006.....860

Figure 9.6 Monthly averages of (a) carbon monoxide and (b) ozone during nighttime at the Whistler high elevation site from March 2002 to November 2006.....861

Figure 9.7 Frequency distributions of night-time (a) CO and (b) O₃ at Whistler, BC during summertime periods (May-August) during 2002-2005.....862

Figure 9.8 Time series of particle measurements at the Whistler, BC high elevation site during the Intex-B spring 2006 period, (a) Particle volume distributions ($dV/d\log D$), major transport events are identified by increase in coarse particle volume. (b) Fine fraction sulphate and coarse fraction calcium from impactor samples.863

Figure 9.9 Average profiles of the mass concentrations (in $\mu\text{g m}^{-3}$) of nitrate, sulphate and total organics measured with the AMS. Also, the average profile of coarse particle number concentration profiles (in cm^{-2}) from 19 flights from April 22 to May 15, 2006 are used in the averages.865

Figure 9.10 Annual averaged PM surface concentrations (colour filled contours) and the reduction (dashed contour lines) due to the elimination of the East Asian anthropogenic sources (sulphate, BC and OC). PM includes sulphate, BC, OC, dust and sea-salt in this figure.867

Figure 9.11 Simulated sulphate (top panels) over April and May 2006 from two models (a) GEM-AQ/EC and (b) GEOS-CHEM vertically averaged from 0 to 2 km (note the differences between colour scales). The middle panels show the average vertical profile between the red (blue) lines, and the bottom panels show the percent of sulphate that is of Asian origin from both models. This suggests that for much of Canada, East Asian sulphur emissions have little influence on the surface. A notable exception to this is the west coast, where Asian emissions account for 20-30% of the surface sulphate. At higher altitudes, Asian sulphate appears significant across the country.868

Figure 9.12 (a) Model ensemble surface O_3 response (ppb) over North America (NA, in red) to 20% reductions in anthropogenic O_3 precursor emissions individually (NO_x , NMVOC, and CO), combined (ALL), and to CH_4 originating from three foreign source regions (where EU is Europe, EA is East Asia and SA is South Asia). (b) Annual and seasonal mean contribution to total surface O_3 from foreign source regions to North America (Europe only, EU in green; East Asia only, EA in blue; combination of both Europe and East Asia, EU + EA in grey) as estimated from the individual model results of HTAP and from studies in the published literature (thin vertical bars for ranges across studies and regions; squares indicating where only one value is reported). The white circles represent the multimodel median value. (Fiore *et al.*, 2009).....870

Figure 9.13 O_3 concentrations and reductions due to (a) 100% and (b) 20% reductions in NO_x and VOC in Asia (annual average), showing the non-linear response of ambient concentrations to emissions reductions. The coloured filled contours are the ozone surface concentrations and the dashed contour lines are the reductions (ppbv).871

Figure 9.14 (a) The annual average concentration ($\mu\text{g m}^{-3}$) of PM from 1998-2004 simulations in North America. (b) Percentage of PM from natural contributions in North America. The coloured filled contours are the percentages and the contour lines are the standard deviations.872

Figure 9.15 Percentage of PM from natural contributions in Canadian coastal areas (a) east and (b) west. The coloured filled contours are the percentages and the contour lines are for the standard deviations.....	874
Figure 9.16 Ambient dust and carbonaceous aerosol concentrations from natural sources in (a) Spring and (b) Summer.....	875
Figure 9.17 Averaged Import and export fluxes from East Asia and North America for total PM and standard deviations from 10 year simulations. The background contour illustrates the averaged spring transport fluxes ($\text{mg m}^{-2} \text{s}^{-1}$) vertically integrated from 3-10 km while the numbers with arrows show the 10 year averaged transported fluxes (Tg day^{-1}) and deviations crossing each boundary of the two HTAP defined regions (East Asia and North America) from surface to the model upper boundary.....	876
Figure 10.1 Spatial pattern of vegetation exposure to O_3 concentrations (2005) in North America based on the W126 Exposure Index (ppm-hours). The dots represent the locations of monitoring sites used in the analysis	890
Figure 10.2 Spatial pattern of vegetation exposure to O_3 concentrations (2005) in North America based on the SUM06 Exposure Index (ppm-hours). The dots represent the locations of monitoring sites used in the analysis.	891
Figure 10.3 Interannual relationship between SUM06 (top left), W126 (top right), and AOT40 (bottom) and annual values of the 4 th highest daily maximum 8-hour O_3 concentration calculated for all National Air Pollution Surveillance (NAPS) network sites for 1990-2006.	893
Figure 10.4 Model predicted SUM60 in Alberta for the 2002 base-case (left) and a future scenario (right).....	894
Figure 10.5 Model predicted AOT40 levels in Alberta for the 2002 base-case (left) and a future scenario (right).....	895
Figure 11.1 Summary of NAPS monitoring stations and data availability used in the assessment of visibility over the period 2003-2007.....	973
Figure 11.2 Comparison of means of measured and reconstructed fine mass at NAPS speciation sampling sites. Note that the SNC Reconstructed mass includes only ammonium sulphate, ammonium nitrate, and carbon species. The Total Reconstructed mass includes soils and sea salt where available.....	975

Figure 11.3 Statistical representation of reconstructed fine mass ($\mu\text{g m}^{-3}$) with ammonium sulphate, ammonium nitrate, and carbon species only at NAPS speciation stations. Tops of the blue bars represent the mean values. The outlined box represents the 20th to 80th percentile range. Whiskers represent the 2nd to 98th percentile range.....976

Figure 11.4 Reconstructed extinction coefficient (Mm^{-1}) statistical ranges for PM species and $\text{NO}_2(\text{g})$ at NAPS speciation sites where available. Tops of the blue bars represent the mean values. The outlined box represents the 20th to 80th percentile range. Whiskers represent the 2nd to 98th percentile range.....978

Figure 11.5 Reconstructed visual range (km) statistical ranges for PM species and $\text{NO}_2(\text{g})$ at NAPS speciation sites where available. Tops of the blue bars represent the mean values. The outlined box represents the 20th to 80th percentile range. Whiskers represent the 2nd to 98th percentile range.979

Figure 11.6 a) Proportion of mean particle extinction contributions at Western Canada NAPS sites. b) Proportion of mean particle extinction contributions at Ontario NAPS sites. c) Proportion of mean particle extinction contributions at Eastern Canada NAPS sites.....981

Figure 11.7 Five-year average (2000–2004) deciview (DV) using only IMPROVE data from IMPROVE (2006)983

Figure 11.8 Comparison of AURAMS modelled visibility calculations (top) and measurement data collected from the IMPROVE network (bottom) for July 16th, 2006 produced using the same extinction reconstruction algorithm.....985

Figure 11.9 Comparison of AURAMS predicted visibility calculations (y-axis) against IMPROVE measurement site data (x-axis) for July 2002.986

Figure 11.10 Projected annual average levels of visibility in 2015 BAU modelling scenario (top), and the difference in annual average visibility between the 2015 BAU and the 2002 base-case scenarios (bottom).987

Figure 11.11 Projected difference in the annual average visibility between the 2015 CARA and 2015 BAU emissions scenarios.988

Figure 11.12 Photographs of Toronto featuring a day with $6 \mu\text{g m}^{-3}$ (top panel) and $33 \mu\text{g m}^{-3}$ (bottom panel) (TEOM measurement).990

Figure 12.1 Values that comprise the total economic value, or TEV, of the environment.1000

Figure 12.2 Steps in the damage function approach to policy analysis.....1005

Table of Tables

Table 2.1 Sources of organic aerosol.....	78
Table 2.2 Overall aerosol yields (SOA formed per amount of precursor reacted) at a typical organic aerosol mass concentration of $5 \mu\text{g m}^{-3}$ from selected precursors under different light, NO_x , humidity, temperature and seed conditions.	81
Table 2.3 Aging time defined as the lifetime to convert hydrophobic aerosol to hydrophilic aerosol.	95
Table 2.4 Relationship between emission reduction and pollutant concentration.	114
Table 3.1 PM Speciation Sampling Modules and Target Analyte Groups.....	140
Table 3.2 Linear Regression Results for 24-hr Cold Season Data for TEOM-SES Instruments vs. Filter Based Instruments.	141
Table 3.3 Range of monthly (January-December) 8-hour median and maximum ozone concentrations and 4 th highest daily max 8h (ppb) at Canadian background stations, (2006).	145
Table 3.4 Meteorologically and easonally adjusted trends at CAPMoN sites using GLMM analysis. Values in bold are statistically significant at $p < 0.05$. Daytime averages: 10:00-18:00hrs; nighttime averages: 20:00-4:00 hrs. (1990 – 2006)	150
Table 3.5 Summary of Regional Scale Ozone Episodes by Region for the Period 2001-2005 (NOTE: Episodes defined as days where 33% of monitoring sites in a region record maximum daily 8h ozone greater than 65 ppb)	156
Table 3.6 Available High-elevation monitoring sites	166
Table 3.7 Overview of ozone trends based on various daily ozone averaged values from 1997 – 2006 during January – December months in selected PCA-derived regions with Meteorological Adjustment. Trends that are significant at 0.05 are in bold.	170
Table 3.8 Percentage differences in the 3-year-average meteorological adjusted trends of daily maximum 8-hr ozone average from May-Sep 1997–2000 to May-Sep 2003–2006 based on GLMM shown in Figure 3.20. The differences represent the 2003–2006 average concentration minus the 1997–2000 average concentration divided by the 1997–2000 average concentration.	177
Table 3.9 Nitrogen Oxides - Species and Terminology.....	184

Table 3.10 Correlations between ambient concentrations of selected VOCs and carbonyls and NO ₂ , NO and PM _{2.5}	192
Table 3.11 Definition of Terms to Describe Reactivity of VOC.....	195
Table 3.12 Ten most abundant NMHC Species as a percentage of total carbon and as a percent of NMHC _{prop} – Urban, Refinery Impact and Rural Sites (Summer Only) 2002 – 2006.....	199
Table 3.13 Contribution of Carbonyls to VOC _{prop} at Urban and Rural Sites (Summer Only) 2002-2006.....	202
Table 4.1 Proportions of NPRI reported emissions by estimate method (Environment Canada, 2010a).....	283
Table 4.2 2006 smog Precursor Emissions by Category (Environment Canada, 2010b).....	287
Table 4.3 Major Sectors Contributing to the 2006 National Emissions Inventory (Environment Canada, 2010b).....	288
Table 4.4 Speciated Particulate from the 2002 Emissions Inventory (Environment Canada, 2005).....	295
Table 5.1 Comparison of key characteristics of AURAMS, CHRONOS, and CMAQ circa 2008.	333
Table 5.2 Model simulations included in this evaluation.....	340
Table 5.3 Ozone evaluation statistics, i.e., mean bias (MB), normalised mean bias (NMB), and linear correlation coefficient (r), from the AURAMS annual simulation of 2002.....	342
Table 5.4 PM _{2.5} evaluation statistics from the AURAMS annual simulation of 2002	343
Table 5.5 Ambient ozone and PM _{2.5} evaluation statistics from the AURAMS ICARTT simulation against AIRNow observations.	345
Table 5.6 Ambient ozone and PM _{2.5} evaluation statistics from the NRC CMAQ/MM5 simulation for the Pacific 2001 period.	349
Table 5.7 Sulphate _{2.5} evaluation statistics from the AURAMS annual simulation of 2002	353
Table 5.8 Nitrate _{2.5} evaluation statistics from the AURAMS annual simulation of 2002.....	353
Table 5.9 Ammonium _{2.5} evaluation statistics from the AURAMS annual simulation of 2002.....	354

Table 5.10 Ambient speciated PM _{2.5} evaluation statistics from the NRC CMAQ/MM5 simulation for the Pacific 2001 period.	357
Table 5.11 Evaluation statistics for NO ₂ , HNO ₃ , and SO ₂ from the AURAMS annual simulation of 2002.....	364
Table 5.12 Ozone and PM statistics for PrAIRie2005 flights.....	371
Table 5.13 AURAMS statistics for SOA comparison with observations from the IMPROVE and NAPS networks (20 sites in the northeastern US and eastern Canada, number of points = 235, 24-hr samples every 3 days).....	379
Table 5.14 AURAMS statistics for POA and EC comparison with observations from the IMPROVE and NAPS networks (20 sites in the northeastern US and eastern Canada, number of points = 235, 24-hr samples every 3 days).....	380
Table 5.15 Ambient ozone and PM _{2.5} evaluation statistics from the NRC AURAMS-CMAQ comparative evaluation for July 2002.....	392
Table 5.16 Speciated PM _{2.5} (sulphate, nitrate, ammonium, and organic components) evaluation statistics from the NRC AURAMS-CMAQ comparative evaluation for July 2002.	393
Table 6.1 Comparison of daily maximums of 24-hour rolling average PM _{2.5} concentrations averaged over entire modelling domain for base case and NH ₃ sensitivity simulations over the entire simulation period. [S2]	440
Table 6.2 Summary of exceedances over Canada-Wide Standard of 30 µg m ⁻³ for PM _{2.5} for reference case and three NH ₃ sensitivity cases. [S2]	440
Table 6.3 Summary of exceedances over Canada-Wide Standard of µg m ⁻³ for PM _{2.5} for the reference case and the summer-time 60% NH ₃ reduction scenario. [S3]	442
Table 6.4 Emissions (Tonnes/Year) and overall changes in NO _x , SO ₂ , VOC and PM _{2.5} emissions between the 2002 and 2015 Canada + United States combined inventory. [S11].....	461
Table 6.5 Total emissions and emission changes for the 1993 reference case (BA), 2020 business as usual scenario (FBA), implementation of mobile emission standard 2020 scenario (ES) and 2020 no-mobile scenarios (FNM). [S13]	479
Table 6.6 Comparison of daily maximums of 24-hour rolling average PM _{2.5} concentrations averaged over entire modelling domain and simulation period for base case (BA), future base case (FBA), future no-mobile case (FNM), and future emission scenario (ES). [S13]	480

Table 6.7 Summary of exceedances over Canada-Wide Standard of $30 \mu\text{g m}^{-3}$ for $\text{PM}_{2.5}$ for reference case (BA), future base case (FBA), future no-mobile case (FNM), and future emission scenario (ES). [S13].....480

Table 6.8 Percentage reductions in the 2015 S15 emission levels in each of the 16 sectors compared to their 2015 BAU case levels ($\text{PM}_{2.5}$ refers to primary $\text{PM}_{2.5}$ emissions).[S15].....486

Table 6.9 Change in the daily 8-hour O_3 maximum levels (ppb) between a 2002 reference case and a 2005 emission case for May-September 2005 across model sub-domains as referenced in Figure 6.60 (2002 reference case minus 2005 scenario). [S21].....502

Table 6.10 Average percent contribution to CHRONOS modelled O_3 at New Brunswick and Nova Scotia monitoring sites on days when the Canada-Wide Standard was exceeded [S24]511

Table 6.11 Average percent contribution to CHRONOS modelled $\text{PM}_{2.5}$ at New Brunswick and Nova Scotia monitoring sites on days when the Canada-Wide Standard was exceeded [S24]511

Table 6.12 Schematic summary of O_3 and $\text{PM}_{2.5}$ changes, with qualitative estimates of confidence level, as a result of a change in a given precursors or set of precursors based on the studies reviewed in this chapter.519

Table 7.1 Comparison of emissions from Windsor, Sarnia, Hamilton, Toronto and Ottawa, 2006 values in kilotonnes (NPRI, 2007b).....573

Table 7.2 10 largest point source emitters of NO_x and SO_x in Ontario.574

Table 7.3 Seasonal mean and peak concentrations of O_3 , $\text{PM}_{2.5}$ and NO_2 at urban and rural NAPS sites in the Atlantic region for years 2002-2006. Seasonal mean values refer to the mean of all hourly values in each season over these 5 years. Seasonal peak values are calculated as the average over these 5 years of the seasonal mean of the 98th percentile hourly values each day. Seasons that do not fulfill the completeness criteria are not included. Uncertainty is expressed as one standard deviation of the yearly seasonal mean values; where no uncertainty is given there is only one seasonal mean within the 5-year period that meets the completeness criteria. $\text{PM}_{2.5}$ measurements are from the BAM instrument at each site, which is why the values differ from the seasonal $\text{PM}_{2.5}$ values shown in Figures 3.62-3.65.....614

Table 7.4 Frequency of exceedances of the CWS daily metric for ozone and $\text{PM}_{2.5}$ in Quebec. Exceedance frequency is the frequency when at least one site in the region is in exceedance and WS33 is the frequency when at least 33% of the sites in the region are in exceedance.

Ozone statistics are based on data from 15 monitoring sites during 1990 to 2002 while PM _{2.5} statistics use data from 6 sites from 1998 to 2002 (source: Johnson, 2004).	619
Table 7.5 Average mass concentration and percent fractional chemical composition for Saint-Anicet and Montréal (Ontario Street) based on 24-hour mean PM _{2.5} reconstructed mass. All days with concurrent measurements at both sites from 2003 to 2007 (N=386) are included in the All Year columns. The last four columns are based upon the concurrent measurements but when PM _{2.5} ≥ 30. There were 13 days in Montréal (6 winter) and 8 days at Saint-Anicet (3 winter). Total mass corresponds to the reconstructed mass summed from the chemical fractions. Organic matter is estimated as 1.8xOC for Saint-Anicet and 1.6xOC for Montréal. Estimated water is determined from 0.32x(sulphate+ammonium).	628
Table 7.6 Percent Change in mean CAPMoN cold season concentrations of HNO ₃ , NH ₄ , NO ₃ , SO ₂ , SO ₄ , estimated fine nitrate (fNO ₃), estimated coarse nitrate (cNO ₃) and total nitrate (tNO ₃) between the periods of 1988 – 1993 and 1996 – 2001.	651
Table 7.7 Edmonton mass reconstruction using speciation sampling results and formulae as described in Section 3.5.2 (Chapter 3). Concentration measurements to compute the contributions from Soil and TOE (total other elements) are not available for this period.	658
Table 7.8 Meteorologically and seasonally adjusted ozone (ppb yr ⁻¹) and PM _{2.5} (µg m ⁻³ yr ⁻¹) trends at PYR sites. All trends are statistically significant at p<0.05	681
Table 7.9 Percentage of trajectories from each sector for the data period 1999-2002 for St. Andrews, NB and Kejimikujik, NS. as well as the average ozone and PM _{2.5} concentrations attributed to each of these sectors.	696
Table 7.10 Seasonal mean O ₃ concentrations at the 17 sites monitored during the Annapolis Valley, NS O ₃ study.	733
Table 8.1 Future ozone projections for North America. Values given are for mean daily maximum 8-hour ozone and continental U.S. unless otherwise noted (table modified from Jacob and Winner, 2009).	788
Table 8.2 Future ozone projections for Europe and globally. Values given are for mean daily maximum 8-hour ozone unless otherwise noted.	789
Table 8.3 Future air quality projections for particulate matter (PM). Values shown are mean 24-hour concentrations unless otherwise noted.	792
Table 8.4 Satellite remote sensing of surface air quality	816

Table 10.1 Vegetation exposure indices calculated for rural Canadian sites in 2005. Right column presents the 4 th highest daily maximum O ₃ concentration (ppb) as measured at each site. Sites were selected to provide a cross-section of results across Canada	892
Table 10.2 Recent studies that contributed to the advancement of understanding of the impact of O ₃ on individual plant species	903
Table 10.3 Recent studies on the impact of O ₃ on individual species that included dose response relationships	904
Table 10.4 Recent studies on the impact of O ₃ on individual species that confirmed previous results	906
Table 10.5 Recent studies that contributed to the advancement of understanding of the impact of O ₃ on ecosystems	914
Table 10.6 Recent studies on the impact of O ₃ on ecosystems that confirmed previous results	914
Table 10.7 Recent studies that contributed to the advancement of understanding on the impact of O ₃ combined with other stressors or mixtures on vegetation	917
Table 10.8 Recent studies on the impact of O ₃ combined with other stressors or in mixtures that included dose response relationships	919
Table 10.9 Recent studies on the impact of O ₃ combined with other stressors or in mixtures that confirmed previous results	919
Table 10.10 Recent studies contributing to the advancement of understanding of O ₃ dose expression.	927
Table 10.11 Recent studies summarizing O ₃ dose expression issues	931
Table 10.12 Recent studies on the impact of PM on vegetation that confirmed previous results	936
Table 11.1 Site specific Rayleigh scattering values for Canadian NAPS particle speciation monitoring locations	972
Table 11.2 Canadian total reconstructed fine particle mass statistics for the period 2003-2007 as available. Note that these values are determined by applying the IMPROVE reconstruction procedure to mass and chemical concentration measurements taken at the NAPS stations.	977

Table 11.3 Total reconstructed fine particle mass statistics for the period 2003-2007 as available. Note that these values are determined by applying the IMPROVE reconstruction procedure to mass and chemical concentration measurements taken at the NAPS stations. Correlation with measured fine mass is shown.	979
Table 11.4 Mean scattering contributions by chemical component for NAPS sites across Canada for the period 2003-2007. Note that the Best columns include the site specific Rayleigh scattering term.	982
Table 11.5 Mean deciview visibility at Canadian NAPS stations (2003-2007).	984
Table 12.1 Examples of values that comprise the total economic value, or TEV, of trees in forest ecosystems.	1012
Table 12.2 Valuation estimates ^a (in 1997 dollars) and ratio of total value to cost of illness, by endpoint and component.	1024

CHAPTER 1: Introduction to the Canadian Smog Science Assessment

Carrie Lillyman, Barry Jessiman, Jeffrey R. Brook, Silvina Carou and Ron Newhook

The Canadian Smog Science Assessment is a comprehensive review of the state of smog science in Canada, considering the atmospheric, human health and ecosystem health perspectives. The review was initiated in 2005 in response to a rapidly evolving scientific body of knowledge and was designed to feed into the next round of decision making as Canada moves forward in the evolution of its air quality policies.

This Assessment addresses the science of particulate matter and ground-level ozone within one document. These pollutants are generally considered to be the main ingredients in ‘smog’, a mixture that has a significant negative impact on both human and ecosystem health. The decision to combine both particulate matter and ozone throughout the contents of this Assessment is in response to an evolution in thinking, both in the scientific and policy communities, where the atmosphere is considered as a single entity composed of a complex mixture of pollutants that are intricately linked. Future iterations using this approach will likely continue with a focus on these substances but may add other major air pollutants as our understanding of linkages and effects evolves.

The primary objective of this Assessment is to provide a comprehensive and reliable scientific synthesis of available information on particulate matter and ozone in Canada, including the impacts of smog on ecosystems and human health, as well as to;

- Describe the relevance of recent scientific research on smog within the context of the Canadian policy framework;
- Identify gaps and areas for further research on particulate matter and ozone; and
- Determine if emission reductions aimed at targeting smog have had or will have beneficial impacts on smog levels in Canada as well as ecosystem and human health.

Within this Assessment, consideration is given to ground-level ozone (O_3), fine and coarse particulate matter ($PM_{2.5}$ and $PM_{2.5-10}$), and the precursor gases that lead to the formation of these pollutants. Where needed, consideration is also given to the constituents of PM in order to understand atmospheric and environmental sources, fate and behaviour. The health effects components focus on ground-level ozone and fine particulate matter, with a separate document available on the health impacts of coarse PM.

This chapter provides the context for the development of this comprehensive review, as well as a description of the process behind it and how the content is organized.

What is Smog?

Smog is a term that was originally used to describe the combination of “smoke and fog”, as was experienced in an era of high sulphur emissions impacting populations in European cities (e.g., London, UK). Subsequently, smog was further defined to be sulphurous smog or photochemical smog of the type troubling Los Angeles, particularly in decades past. Oxidant gases, such as ozone, were identified as the chief ingredient in the smog over L.A.. Today smog is a general term for poor air quality, often with reduced visibility, and represents a mixture or ‘soup’ of atmospheric pollutants. Two of the main components in smog are particulate matter (PM) and ground-level ozone (O₃). As these pollutants build-up over Canadian and U.S. cities and spread into rural areas crossing international borders, other pollutants tend to increase, most importantly nitrogen dioxide (NO₂), which is strongly linked to fuel combustion.

Particulate matter refers to a complex mixture of organic and inorganic airborne liquid and solid particles that are microscopic in size (ranging from as large as 100 µm in diameter and as small as 0.005 µm). The more respirable particles are classified as coarse PM (between 10µm and 2.5 µm in diameter), fine PM (less than 2.5 µm) and ultrafine PM (less than 0.1µm).

When PM is emitted directly into the atmosphere from the source, including those emitted from physical processes such as erosion, it is termed ‘primary’ PM. Primary PM and the gas precursors to smog formation originate from both natural (windblown soil, sea salt spray, volcanic dust) and anthropogenic sources (fossil fuel burning, various industrial processes, farmlands, roads, etc). Secondary PM forms in the atmosphere through a series of chemical reactions involving precursor gases (NO_x, SO₂, NH₃ and VOCs). The composition of secondary PM varies considerably by location but generally they are made up of organic (carbon) and inorganic (sulphates, nitrates, ammonium, metals) compounds. Ground-level ozone is a gas that forms in the atmosphere through reactions between nitrogen oxides (NO_x) and volatile organic compounds (VOCs) in the presence of sunlight.

PM and O₃ have deleterious effects on the respiratory and cardio-vascular systems, are toxic to vegetation, damage materials and, in the case of PM, reduce visibility. Because of the near ubiquitous exposure of Canadians to smog, and the large scale of resulting effects, smog exerts significant public health and environmental impacts.

1.1 Canadian Air Quality Policy Framework

Ambient air quality management in Canada is a shared responsibility among provincial, territorial, federal, international and in some cases municipal governments, made possible through an array of commitments and initiatives that have evolved over many decades.

Federal, provincial and territorial governments work together in partnership under the framework of the Canadian Council of Ministers of the Environment (CCME) through the 1998 Canada-wide Accord on Environmental Harmonization and the Canada-wide Standards (CWSs) Sub Agreement. Canada-wide Standards for PM_{2.5} and O₃ were established in June 2000 in order to establish a comprehensive risk management strategy for these pollutants, and to minimize the risk associated with these pollutants to human health and the environment, by 2010. The PM_{2.5} and O₃ CWSs were based on science assessments published in 1999 for these two substances. An interim review of the Standards was completed in 2005, which determined that no changes to the existing numerical targets were required, reported on the progress made towards creating the infrastructure required to report on achievement of the Standards (e.g. expansion and upgrade of air quality monitoring networks) and the implementation of a variety of initiatives by jurisdictions. At the time this Assessment was written, the next review of the Standards was planned for 2010/2011 to assess attainment of all provisions of the CWSs and if appropriate, revise the numeric targets for PM_{2.5} and ozone for years beyond 2015 to reflect new scientific understanding. This Assessment was developed in order to provide the scientific basis for the 2010/11 CWS review.

The Canadian Environmental Protection Act (CEPA) provides the federal government with broad authority to address emissions into the atmosphere of substances that have negative impacts on the health and environment throughout their life cycle. CEPA was first promulgated in 1988, and was revised and renewed as a new Act in 1999 after a five-year review process. The focus of CEPA (1999) is pollution prevention and the protection of the environment and human health as a means to promote sustainable development. The Departments of Environment and Health share responsibility under CEPA to assess and manage the threats that pollutants may pose; Health Canada focuses on risks to human health, while Environment Canada focuses on risks to the environment. Ground-level ozone, PM₁₀ and gaseous precursors (sulphur dioxide, nitrogen oxides, ammonia and VOCs) have all been declared “toxic” under CEPA meaning that they are “entering or may enter the environment in a quantity or concentration or under conditions that: have or may have an immediate long-term harmful effect on the environment or its biological diversity (a) and constitute or may constitute a danger in Canada to human life or health (c)”.

Internationally, Canada is a signatory to the 1999 Gothenburg Protocol to Abate Acidification, Eutrophication and Ground-level Ozone (under the Convention on Long-Range Transport of Air Pollution) and the Canada-U.S. Air Quality Agreement, both of which contain measures for the reduction of smog precursors. Canada continues to actively participate in the development of additional measures under these international agreements, including the exploration of a possible annex to the Canada-U.S. Agreement to specifically address PM.

One of the most significant influences on air quality in Canada is the United States. The two countries are in such close proximity that measures to reduce emissions in the United States will likely have a positive impact on parts of Canada. This Assessment is the first to evaluate the impact of significant NO_x emission reductions from coal-fired electricity generation in the northern states on ambient air quality in Canada.

The information and conclusions from this Assessment are primarily intended to provide scientific guidance to decision-makers in the review and/or development of air quality policies, including ambient air quality objectives and standards designed to risk manage particulate matter and ozone in order to reduce the risk of these pollutants to the health of Canadians and their environment. The information will also provide context for international negotiations targeted to further reducing the transboundary and transcontinental flow of air pollutants. The knowledge gaps identified in this assessment are intended to provide direction for future scientific research so that Canadian information improves to better support future policy requirements.

1.2 Air Quality Risk Assessment Framework

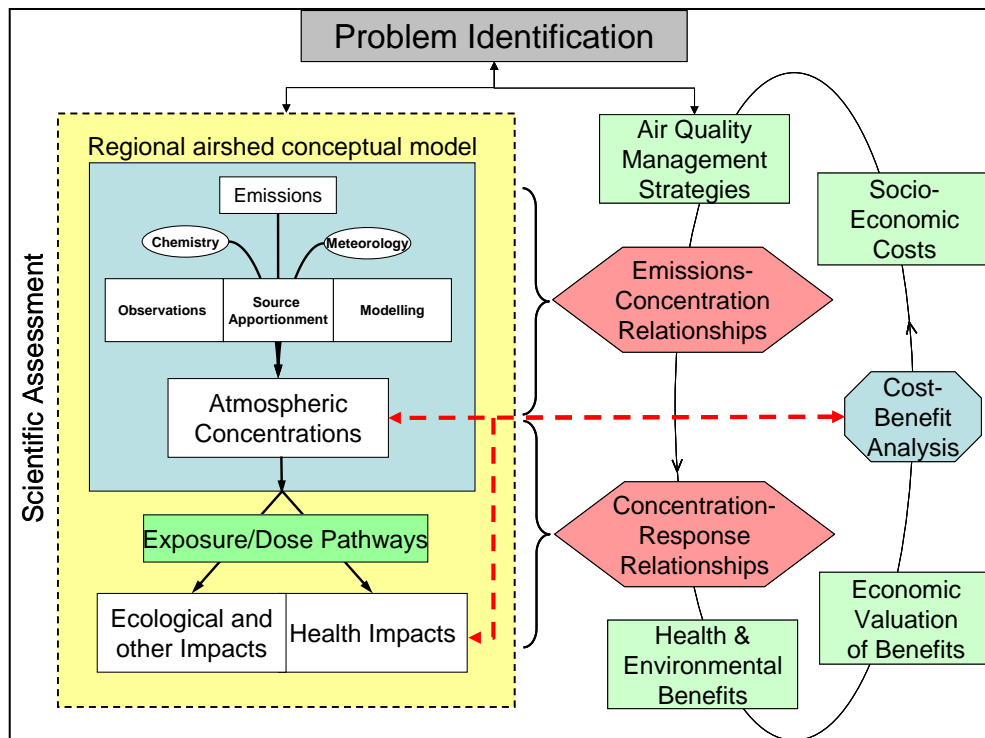


Figure 1.1 Theoretical Air Quality Risk Assessment Framework

A framework developed for providing a clearer sense of how scientific tools fit together to support air quality management, and for providing structure to the Assessment, is illustrated in Figure 1.1.

Given an identified problem (e.g., smog in cities) there is a role for atmospheric, exposure, health and environmental science in understanding the problem, its causes and impacts. The main steps in this science are shown on the left side of the figure. The main goal is to link emissions to atmospheric concentrations to impacts in a quantitative and predictive fashion. A key outcome of this linkage is the development of emissions to concentration and concentration to response relationships (seen as red hexagons in Figure 1.1).

Developing emissions to concentration (E-C) relationships typically implies the application of regional air quality models with current, accurate emissions and meteorology as their input and predictions of concentrations over episodic (i.e., hourly to daily) to multi-year time scales as their output. Actual observations can then be used to validate these predictions. In a broader, one atmospheric context such predictions would also be of acidic and toxic deposition amounts as well as bi-directional linkages to climate change. Concentration-response (C-R) relationships for health impacts are derived from analyses of epidemiological studies with the goal to directly relate air concentrations to population level responses. Concentrations or deposition amounts are also quantitatively linked to a range of other effects from ecological, to materials to visibility and climate. The components within the framework's yellow box are largely in the realm of scientific research and applications and make up the contents of this assessment.

The right side of the figure depicts the steps and cyclic nature of air quality management. Current evidence indicates that there are population health risks related to present air pollutant levels and that there is no level below which the risk becomes zero. This implies that any improvement in air quality would result in benefits to human health and the environment. In order to determine the appropriate amount of reduction in emissions or ambient concentrations, decision-makers need to consider both the socioeconomic costs and the health and environmental benefits of selected air quality management strategies. E-C and C-R relationships derived from the science (yellow box) are necessary to conduct a cost-benefit analysis.

Ultimately, the process as depicted in Figure 1.1 leads to the identification of the optimal approach(es) for managing air pollution, given current scientific and economic knowledge and societal factors. However, these can change and thus, the process needs to be one of continual re-assessment (i.e., cyclic). Furthermore, there remains considerable uncertainty throughout the framework. Thus, the bottom line is to carefully assess, through monitoring and other quantitative measures, if the expected air concentrations or deposition changes due to a given policy occur or ideally, if the impacts are reduced as desired (i.e. the benefits are realized). This last step, indicated by the red dashed line in the figure is generally referred to as accountability. It is crucial, given the costs involved in air quality management to verify that the expected benefits occur, which necessitates ongoing atmospheric and environmental monitoring, and to have measures in place to ensure that if the anticipated changes do not occur that the current management strategies are revisited. Clearly, for accountability it is best

to monitor the impacts, as assessing accountability based upon whether or not $PM_{2.5}$ (mass) decreased, for example, does not mean that the desired health benefits have been realized, particularly if the decrease is due to a non-toxic PM constituent. The framework can also be used to ensure a more systematic assessment of past progress and future needs in the development of scientific tools.

1.3 Brief History of Past Assessments in Canada and the U.S.

The health and environmental effects of ambient PM and O_3 have been recognized since the 1970s, and have previously been the subject of extensive assessments in Canada and the US, as well as other countries and organizations around the world. In 1999, Health Canada and Environment Canada completed science assessment documents (SADs) containing a detailed review and critical analysis of information about the effects of PM and O_3 on human health, animals, vegetation and materials, drawing on studies published up to 1997 (Health Canada and Environment Canada, 1999a, 1999b). These were updated as part of the Canada-wide Standards process in 2004. At about this time, the US Environmental Protection Agency (EPA) published updated air quality criteria documents (AQCD) for their 1990s-era assessments. The Air Quality Criteria for Particulate Matter (US EPA, 2004) was a multi-volume review and assessment of the evidence for health and environmental effects from exposure to ambient PM, and was followed in 2006 with an extensive assessment of ozone: Air Quality Criteria for Ozone and Related Photochemical Oxidants (US EPA, 2006)².

The findings presented in the above peer-reviewed reports and in more recent ones focused on the atmospheric aspect of particulate matter – including the 2001 Precursors to Ambient $PM_{2.5}$ Assessment (Environment Canada, 2001) and the 2004 Canada-U.S. Transboundary PM Science Assessment (Canada-U.S., 2004), emphasized the need for reductions in emissions of precursor pollutants as well as primary PM in order to achieve emission targets and to meet the Canada-wide Standards for PM and ozone. The 2004 Canada-U.S. Transboundary PM Science Assessment also demonstrated the transport of PM and its precursors across jurisdictional boundaries, highlighting the need for a multi-jurisdictional approach to air quality management.

²The U.S. EPA has since completed additional analyses, most notably the 2009 Integrated Science Assessment for PM. This document was completed and available too recently for inclusion here.

The above peer-reviewed documents provided extensive evidence of a wide range of air-pollution-related effects on the environment and human health, such as increases in cardiac and/or pulmonary mortality, hospital admissions, and emergency department visits. They also point out significant areas of uncertainty in the science and highlight the need for continued evaluation of the atmospheric, environmental and health science in order to provide the most relevant basis for risk management strategies.

1.4 Evolution of Smog Science

Atmospheric Science

While there has been considerable progress on many fronts with respect to atmospheric science, one of the most notable advancements has been the development of regional chemical transport or air quality models. Over a span of 10 years, our ability to credibly simulate the processes that relate emission changes to ambient concentrations of multiple pollutants and to wet and dry deposition has evolved dramatically. In the last half of the 1990s the state-of-the-art was single issue models for acid deposition, which was generally only trusted for assessing the impacts of sulphur emission changes, and for ozone. Furthermore, the spatial resolution of these models was very coarse with grid sizes of >100 km and they could only be applied to a limited number of scenarios. In terms of PM, sulphate could be predicted by the acid deposition models, but to treat the other ~60% of the PM mass, only simple conceptual models (such as those used to establish sulphur-content regulations for motor vehicle fuel in the 1990s) were available. Today's comprehensive multi-pollutant models consider all the important processes that govern the fate of pollutants and oxidants in the atmosphere, are run for year long periods and are quickly approaching the resolution that permits evaluation of urban scale patterns of smog. For example, Canadian models have evolved from the Acid Deposition and Oxidant (ADOM) model with an eastern Canada domain and a 127 km grid resolution, to A Unified Regional Air quality Modelling System (AURAMS) that couples a regional emissions processing system, a regional air quality model, and is driven by the Global Environmental Multiscale meteorological model. The AURAMS domain includes almost all of Canada and the U.S., with a resolution of 15 km and as high as 2.5 km for smaller windows. Air quality models coupled with observations provide our best means of connecting, quantitatively, the magnitude and geographic distribution of pollutant emissions to resulting ambient air concentrations and deposition rates. They also provide the means to predict future pollutant concentrations based on estimated future emission levels; thus, they can be (and have been) used to guide decisions with respect to air pollutant management strategies and for air quality forecasting.

Over the last decade, a number of intensive field studies (PACIFIC 2001, ICARTT 2004, PRAIRIE 2005 and BAQSMET 2007) have generated measurements of PM levels, size and composition as well as O₃ levels at high time-resolutions (hours to minutes), providing

valuable insights on complex atmospheric processes. Large investments in long-term monitoring networks and measurement technologies have resulted in better national coverage and more accurate continuous PM_{2.5} and real-time O₃ data available for analysis. Also, a wealth of new data on the chemical composition of PM_{2.5} and VOC speciation are now available for improving source-attribution and emissions information.

Although emissions have decreased significantly over the last ten years as have ambient levels of NO_x, VOC and SO₂, reductions in ozone have not been dramatic and have even increased in some urban areas due to complex chemistry. While an impact on the currently observed trends has not been demonstrated, there is now increased recognition that trans-Pacific (or intercontinental) transport of ozone and its precursors contributes to ozone levels in Canada, and PM from very distant areas (e.g. Asia, Africa) has been periodically detected over Canada. New methodologies are being introduced to study atmospheric composition and to describe air quality, such as use of satellite data to measure spatial and temporal patterns in certain air pollutants, combining surface and satellite measurements with output from models to give a better picture of the state of the atmosphere, and the coupling of regional air quality and climate models with global climate models to study how air quality could change under different climate scenarios.

Ecosystem and Environmental Effects Science

Most past research on the ecosystem impacts of smog has focused on quantifying the concentration-response relationship for vegetation effects resulting from chronic O₃ exposure. A number of indices have been used to quantify cumulative exposure (e.g. SUM60, W126, AOT40) with SUM60 being the preferred one in Canada. Over the last decade studies have pointed to the need to improve how the SUM60 ascertains the exposure-response relationship for Canadian species; however, the means by which to do so have not become clear. Meanwhile, a large number of studies in Europe over the last decade have increased recognition that accounting for the O₃ that enters the plant (flux) is a more realistic metric of plant effects. Regardless, further work is required to better understand the complexity of biological responses before the concept of flux can be used to refine air quality standards; thus, exposure based metrics are still the approach used for setting secondary standards to protect vegetation.

Health Science

The relationship between air pollution and adverse health effects has been known since the mid 1900's. Over the last 60 years, much scientific inquiry has occurred into the effects of air pollution and human health. The 1999 Science Assessment Documents (SADs) for Particulate Matter and Ozone were the first comprehensive treatment of the subject in Canada. The health chapters of these documents were based upon a relatively large body of epidemiological evidence for the adverse effects of exposures to both PM and Ozone, and included a range of

adverse endpoints up to and including premature death. More recent assessments continue to highlight the importance of epidemiological relationships but also highlight a series of advances in our understanding of the mechanisms and impacts of air pollution on human health. The following paragraphs summarize what we knew then and some of the novel scientific developments that have happened over the last decade.

The SAD for PM noted a relative lack of mechanistic and toxicological evidence to provide support for the epidemiological findings on which conclusions in that document were based. Despite this lack, the SAD concluded that the volume, quality, coherence and consistency of the epidemiologic findings were sufficient to support significant risk management actions to reduce PM_{2.5}. Since that time, an enormous new and complex database on toxicological outcomes (in human, animal and other experimental settings) has emerged that provides a mechanistic basis for the outcomes seen in epidemiologic studies. These studies also indicate the potential to reach beyond the respiratory and cardiovascular systems to exert effects and preliminary findings of interactions with the Central Nervous System and reproductive systems are coming to light. However, the overall database provides indications that the predominant effect of PM is on the cardiovascular system. The SAD noted that chronic exposure mortality appeared to be the outcome of most importance from a public health perspective, but noted the reliance on a small number of datasets (especially the American Cancer Society and the Harvard Six-city cohorts). While new cohorts have become available and buttress the previous findings, the most important contributions have resulted from reanalysis and extension of the ACS and Six-city work. Findings support the original analyses but demonstrate specific impact on large susceptible subgroups (e.g. COPD patients), the dominance of PM metrics (versus gaseous) in the effects, and the ability to account for a large number of potential confounders in the associations seen.

The original SAD for ozone found a relative wealth of evidence from epidemiological studies of acute exposure effects up to and including premature mortality. Since that time, research has provided additional support for these findings. Areas of concern identified in the SAD included uncertainty in exposure from the use of fixed ambient monitors for epidemiological findings, the potential confounding effects of temperature, the importance of spirometric endpoints to denote adverse outcomes, and only weak indications of chronic-exposure effects. The issue of the use of fixed ambient monitors in epidemiology has received considerable attention and results indicate that these monitors adequately represent population exposure in such studies. Temperature continues to need close attention in the understanding of ozone epidemiologic studies, however the use of various modelling approaches indicates that the temperature effect on adverse outcomes is adequately addressed in such studies. Considerable new work indicates that the effects of ozone on spirometric outcomes (i.e. lung function) may be separate from inflammation and airway hyper-reactivity and each should be treated as relatively independent adverse outcomes. Work on the effect of chronic exposure to ozone (and other pollutants) benefited greatly from the California Children's Health Study and clearly suggests independent effects of ozone on some adverse outcomes.

For both PM_{2.5} and ozone, significant new work has provided a more robust basis for the use of ambient fixed site monitors to provide exposure indices in epidemiology studies. Exposure studies have been especially good at indicating the utility of these monitors in providing estimates of exposure to ozone and ambient-source PM. Work on particle components and metrics such as particle number and the ultrafine component of PM has been extensive, but to date does not provide a more specific scope for risk management.

1.5 Content of the Report

The report consists of two volumes. Volume 1 presents the state of the science on the environmental (atmospheric and ecosystem impacts) and socio-economic aspects of particulate matter and ozone. Volume 2 reviews the information related to the impacts of these pollutants on human health.

This report is intended as a document which reviews, evaluates and places in context the scientific perspectives on smog. In turn it is expected that it will also serve as a foundation for subsequent policy development on national, regional and local scales, including the development of ambient air standards and associated risk management actions. In this light, a summary of key results prepared from this document highlights, for policy makers and interested parties, issues of particular relevance from both scientific and practical points of view. Risk managers, stakeholders and other interested parties should be able to reference specific aspects of both the summary and full assessment documents in developing policies and measures.

Volume 1: Atmospheric Science and Environmental/Economic Impacts (Chapters 2 – 12)

The chapters in this volume were prepared by Environment Canada in collaboration with several academic and provincial partners. The information within the chapters reflects current knowledge pertaining to the scientific areas inside the yellow box in Figure 1.1 and builds from previous Canadian science assessments. Many of the chapters in this volume cover the recent literature for the period 2003 to 2007 (and beyond in special cases) and some report on results of new analyses carried out specifically for this assessment or in support of recent policy requirements.

Chapter 2 describes the physical and chemical mechanisms behind smog production, transformation, and removal from the atmosphere as well as how these are influenced by meteorology. Knowledge has evolved considerably in the last 5 years and this chapter provides an up-to-date assessment of what is understood. Chapter 3 focuses on monitoring networks and methods, ambient concentrations and trends for ozone and PM (fine and coarse), including PM composition, and their precursors in Canada. Chapter 4 describes emissions reporting and

inventories and also discusses sources, spatial distribution and trends and projections of emissions of smog precursors in Canada and to some extent in the U.S. Chapter 5 provides the status of and confidence in Canadian chemical transport models (CTMs), which represent the science behind E-C relationships (Figure 1.1). Chapter 6 provides a review of recent air quality modelling studies performed with current CTMs to calculate ozone, PM and deposition in Canada based on emission reduction scenarios.

Canada is a large country with diverse landscapes, climates, weather patterns and sources of pollution. For this reason, Chapter 7 provides a region-by-region perspective of emissions, physical features, meteorology, and long-range transport that give rise to air quality conditions over distinct areas of Canada. On the opposite side of the scale, Chapter 9 reviews the features of transcontinental transport of pollutants across the Pacific to North America and how these enhance smog levels in Canada. The atmospheric science portion of the volume is complemented by a review of new scientific research discoveries that are or have the potential to modify our understanding of air pollution formation and transport (Chapter 8). These include the effects of climate change on air pollution, the atmospheric boundary layer and its relationship to air pollution, and satellite observations of air quality constituents from space.

Chapters 10 and 11 review recent literature on the effects of smog on vegetation and materials, and visibility, respectively. The latter chapter also presents results from the application of recent advances to investigate the relationship of PM_{2.5} to visibility in selected regions of Canada for which there are data available. As can be seen in Figure 1.1, these chapters pertain to the bottom left side of the framework. Lastly, an overview of the role of economic valuation and recent progress in evaluating the impacts of smog on the environment and human health are presented in Chapter 12, thereby providing an assessment of the science behind some of the processes depicted on the right side of Figure 1.1.

Volume 2: Health Effects (Chapters 13 – 15)

This volume, prepared by Health Canada with input from several external contributors, builds upon the most recent previous Canadian and US assessments and critically evaluates relevant information that has become available since the earlier assessments up to 2007. The assessment of this information is critical for supporting the use of C-R relationships (Figure 1.1) to estimate the health impacts of current air quality or the benefits from future ambient concentration changes.

Chapter 14 presents a scientific review and assessment of the health-related information on ambient PM. Exposure of the general population to ambient PM is covered in Section 14.1. Section 14.2 discusses the dosimetry of inhaled particles in the respiratory tract. Sections 14.3 and 14.4 examine the results of toxicological studies of various types of PM in animals and humans, respectively. Section 14.5 reviews the epidemiological literature—studies of the association between acute exposure to fine ambient PM and health effects. Sections 14.6, 14.7

and 14.8 assess epidemiological studies of reproductive and developmental endpoints, of genetics, and of health effects associated with chronic exposure to fine ambient PM, respectively. A risk characterization integrating key information from the prior chapters on exposure, dosimetry, and health effects of fine PM is presented in Section 14.9.

Chapter 15 presents the corresponding scientific review and assessment of the health-related information on ground-level ozone, including exposure assessment (Section 15.1), dosimetry (15.2), toxicological studies in animals (15.3) and humans (15.4), acute exposure epidemiology (15.5), epidemiology of reproductive and developmental endpoints (15.6), genetics (15.7), and chronic exposure (15.8), followed by a risk characterization (15.9).

Chapters 1 and 13 set the context for each volume. The chapters in both volumes have been peer reviewed internally and externally by experts on the key subject areas assessed in the report. The external peer review, managed by an independent non-profit organization (TERA: Toxicological Excellence for Risk Assessment), focused on the validity of the selection of pertinent studies included in the chapters, the potential need for additional information to be included, and the quality of the analysis, summarization and interpretation of the literature.

1.6 Highlights and Key Messages

The information contained within the Assessment was tailored to be focused on policy-relevant issues as collectively identified by the scientific and policy communities at the onset of this review. A summary of the most important results, focused on certain specific aspects of the science and related risk management issues, are contained in a separate piece entitled the Canadian Smog Science Assessment Highlights and Key Messages.

CHAPTER 2: Atmospheric Processes

Craig Stroud, Jonathan Abbatt, Leiming Zhang, David Flagg, Paul Makar

KEY MESSAGES AND IMPLICATIONS

- Ozone (O_3) production is a complex function of oxides of nitrogen (NO_x defined as the sum of NO and NO_2) concentrations, volatile organic compound (VOC) reactivity/composition and radical production rates. There are key uncertainties in our understanding of O_3 production under VOC-limited conditions.
- The relationship between precursor emissions and ambient concentrations of ozone and particulate is non-linear in nature. Processes that influence ambient levels are all inter-related and interact with each other resulting in a disproportionate relationship between change in precursor emission and change in concentration. A better understanding of all these processes will allow for better evaluation of emissions reduction strategies.
- Advances have been made in understanding how particle composition can feedback and impact gas-phase chemistry and future particle growth. These advances further complicate the non-linear relationship between precursor emissions reductions and benefits.
- The non-linear dependence of secondary organic aerosol (SOA) formation under a wide array of conditions suggests experiments need to be performed with representative atmospheric concentrations, rates of oxidation, temperature, humidity and seed particle compositions. The complex dependence of SOA yields suggests more detailed parameterizations are needed in air quality models.
- Secondary organic aerosols can form very rapidly from precursor emissions (either through evaporation and oxidation of primary organic aerosols or via intermediate volatile organic compounds), exceeding what is being predicted by models.
- Measurements and modelling have both identified important underestimates in our inventories of biogenic and anthropogenic VOC emissions.
- Due to the non-linear interactions between gas, aerosol and cloud components, air quality is unlikely to be improved by reducing a single pollutant but will require concurrent reductions in ammonia (NH_3), sulphur dioxide (SO_2), NO_x and VOCs.
- The development of air quality models that can account for the non-linear behaviour in the chemical, microphysical and meteorological processes will be fundamental to developing effective emission reduction strategies in the future.

2.1 Introduction

2.1.1 Research on Atmospheric Processes

Air quality research over the past several decades has focused on understanding the physical and chemical processes that define the non-linear relationship between emissions and ambient pollutant concentrations. Environment Canada published the assessment Precursor Contributions to Ambient Fine Particulate Matter in Canada in 2001 (Environment Canada, 2001). The major conclusions from the assessment were:

- While the contribution of SO₂, NO_x and NH₃ to PM formation is better understood, the extent of primary and secondary VOC contributions to PM requires investigation.
- Meteorology plays an important role in large-scale PM_{2.5} mass episodes.
- Particle sulphate (p-SO₄²⁻) dominates PM_{2.5} mass in eastern Canada in summer episodes while winter episodes are dominated by particle nitrate (p-NO₃⁻).
- The long-term trend in p-SO₄²⁻ mass is decreasing; however, this trend does not necessarily translate into lower PM_{2.5} mass, as particle composition shifts from ammonium sulphate to ammonium nitrate. Increasing NO_x emissions and decreasing SO₄²⁻ mass leaves more ammonia free for the formation of ammonium nitrate.
- There was insufficient information to link specific source types quantitatively to local ambient PM_{2.5} concentrations.

In 2003, the Particulate Matter Science for Policy Makers assessment was published by NARSTO (NARSTO, 2003). Its main conclusions were:

- Existing management strategies in North America based on reductions in SO₂ emissions will reduce PM_{2.5} mass but the benefits from emissions reductions in NO_x and VOCs are uncertain.
- PM_{2.5} strategies need to include both local and transported sources of direct and precursor emissions in the context of prevailing meteorology and seasonal variability, which may necessitate differing strategies from one region or airshed to another.
- PM_{2.5} is related to acid rain and other atmospheric processes, requiring an integrated management strategy.

The goal of this chapter is to draw from the recent research findings to assess our current understanding of the chemical and meteorological factors which contribute to poor air quality. The focus will be on describing the key inter-related processes which transform urban and industrial emissions into oxidants, such as O₃, and particulate matter (PM).

The ozone (O₃) research community is currently involved in 1) analysis of intensive, focused, process-level airborne and ground-based field programs, 2) trend analysis of long-term measurements from ground-based networks, and 3) air quality model development, evaluation and sensitivity studies. The O₃ research community is piecing the puzzle together for an integrated understanding of the processes affecting short-term O₃ episodes and longer-term O₃ trends. The aerosol research community is in the early stages of understanding aerosol processes. The aerosol research community is identifying the individual pieces of the puzzle through laboratory studies, box modelling and process-level field programs.

2.1.2 Chapter Outline

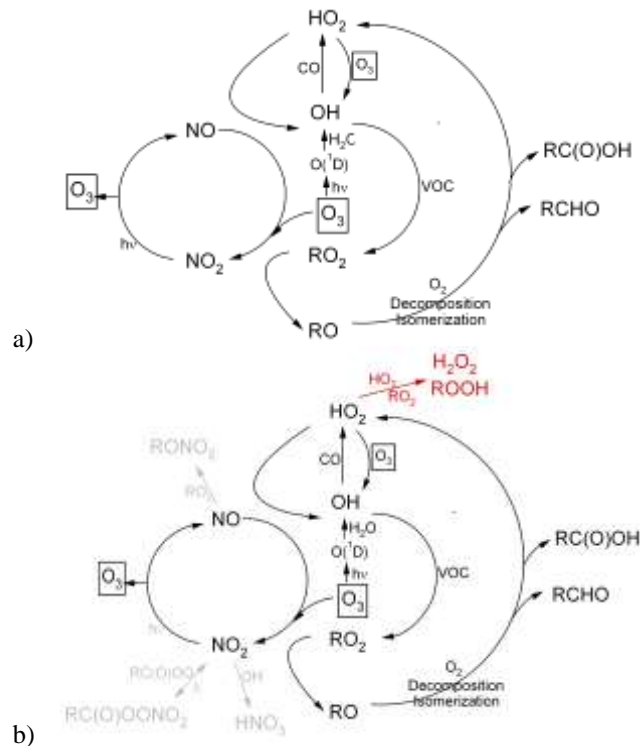
Section 2.2 of this chapter describes smog production mechanisms for urban, power-plant, industrial and regional plumes. The attempt is to discuss smog production for each plume in a “unified” manner describing both O₃ and PM formation concurrently and the non-linear feedbacks between processes. Section 2.3 describes key processes that transform aged aerosol, namely aerosol water uptake and cloud nucleation studies. Section 2.4 describes processes that remove pollutants from the atmosphere, such as wet and dry deposition. Section 2.5 describes meteorological influences on air quality. Section 2.6 and 2.7 summarizes conclusions and identifies knowledge gaps.

2.2 Smog Production Mechanisms

2.2.1 Chemistry of Ozone Formation: General Concepts

Reduced carbon, nitrogen and sulphur gases are emitted into the atmosphere from mobile, point, area and biogenic sources. Some of these gases, such as sulphur dioxide (SO₂), nitric oxide (NO) and methane (CH₄), react chemically in the atmosphere due to the atmosphere’s oxidizing (adding oxygen atoms) nature. As emitted gases are transformed and become more oxidized, they also generally become more soluble; thus, the oxidizing capacity of the atmosphere promotes the cleansing of species through wet and dry deposition. The oxidizing

nature of the atmosphere is driven by the production of the hydroxyl radical³ (OH) during the daytime and the nitrate radical (NO₃) during the night-time. O₃ is also an oxidant for several classes of emitted species. More importantly, the photolysis (the breakdown of molecules through the absorption of light – represented by hv) of O₃ results in the formation of OH. Thus, O₃ is a key species in determining the oxidizing capacity of the atmosphere. However, O₃ is also itself a key product of photochemical reactions involving the oxidation of VOCs catalyzed by nitrogen oxides (NO_x). Thus, O₃ plays a central role in air quality as an initiator and product of photochemistry. The oxidation of reduced carbon, nitrogen and sulphur gases to form multi-functional organic species, nitric acid, and sulphuric acid also results in the in situ production of aerosol (termed secondary aerosol). O₃ and precursors to secondary particle formation are formed from atmospheric reactions involving four main classes of emissions: VOCs, NO_x, ammonia (NH₃) and SO₂.



³ Radicals are atoms, molecules or ions with unpaired electrons, which can take part in chemical reactions because they tend to be reactive.

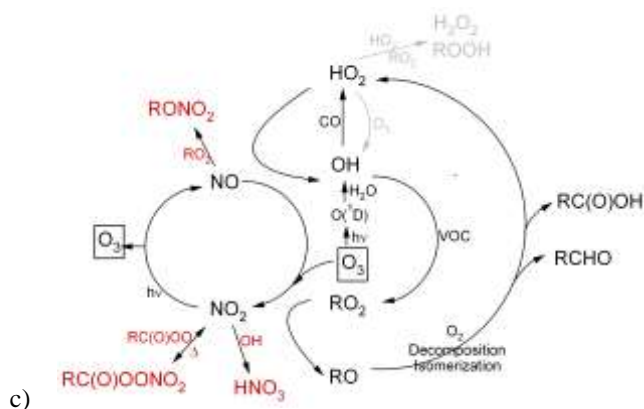


Figure 2.1 Schematic illustrating the initiation and propagation reactions for radical and NO_x reactions involved in O₃ formation (panel a), degradation of volatile organic compounds (VOCs) under low NO_x (panel b) and high NO_x (panel c) conditions. Reactions in grey font are inefficient under different scenarios.

Classes of VOCs important in O₃ formation include alkanes, alkenes, aromatics, carbonyls, alcohols and organic peroxides. In urban areas, the most reactive VOC classes (alkenes, aromatics, higher chain alkanes) and carbon monoxide (CO) are important precursors to O₃ formation. In forested areas, biogenic VOC emissions can mix with long-lived anthropogenic gases to produce O₃. In the remote troposphere, CO and CH₄ are the critical carbon containing species in forming O₃. Organic radicals undergo cyclic reaction mechanism with initiation reactions, propagation reactions and termination reactions. Figure 2.1a illustrates the key daytime processes involved in the 1) oxidation of VOCs, 2) production of organic radicals (RO_x), 3) propagation of reaction chains involving RO_x and NO_x species and 4) production of O₃. VOCs react largely with OH during sunlight hours leading to peroxy radical production (RO₂). The RO₂ radicals play a critical role in oxidizing NO to NO₂, a step that is rate limiting for O₃ formation. The photolysis of NO₂ regenerates NO and also produces an oxygen atom which combines with molecular oxygen to produce O₃. The alkoxy radical product (RO) produced from the reaction of RO₂ with NO can react rapidly to form HO₂ and a carbonyl species⁴ [RC(O)R']. The HO₂ can oxidize NO regenerating OH and producing a second NO₂ molecule. In most cases, the carbonyl product reacts further in a similar manner resulting in more than two O₃ molecules per VOC emitted. The carbonyl species may also be more reactive than the precursor VOC (e.g. the precursor toluene and its reactive by-product

⁴ Carbonyl species –oxygenated volatile organic compounds with a carbon to oxygen double bond

muconaldehyde). In this way, the NO_x and RO_x ($\text{OH} + \text{HO}_2 + \text{RO}_2 + \text{RO}$) cycles propagate and O_3 production is a complex function of 1) NO_x and RO_x abundances (as well as partitioning within NO_x and RO_x species), 2) VOC reactivity and 3) radical production rates.

As shown in Figure 2.1b, under conditions of low NO_x , RO_x chain termination is dominated by hydrogen and organic peroxide formation (H_2O_2 , ROOH). RO_2 mixing ratios are insensitive to NO_x mixing ratios. O_3 production at low NO_x increases linearly with NO_x (chemical regime is termed NO_x limited). The reaction between HO_2 and O_3 is also efficient at chemically removing O_3 . Consequently, under condition of low NO_x , O_3 levels are also low.

As NO_x increases, propagation reactions increase, O_3 production is very efficient, and the $\text{RO}_x + \text{NO}_x$ termination reactions become faster than the $\text{RO}_x + \text{RO}_x$ termination reactions. Figure 2.1c illustrates the key chain termination reactions for RO_x and NO_x species under high NO_x conditions; namely, the formation of nitric acid, HNO_3 ($\text{OH} + \text{NO}_2 + \text{M} \rightarrow \text{HNO}_3 + \text{M}$) and the formation of organic nitrates (alkyl nitrates, $\text{RO}_2 + \text{NO} + \text{M} \rightarrow \text{RONO}_2 + \text{M}$ and peroxyacetyl nitrates, $\text{RC(O)OO} + \text{NO}_2 + \text{M} \rightarrow \text{RC(O)OONO}_2 + \text{M}$). Under conditions of high NO_x , the O_3 production rate slows and begins to decrease as the NO_x mixing ratio increases (termed the VOC limited regime). In this regime, the reaction forming HNO_3 is very efficient at removing both RO_x and NO_x species. HNO_3 contributes to particle formation in the presence of ammonia or other base cations in particles.

O_3 production is also affected by the rate of RO_x production which in turn is impacted by the photolysis of precursor species (O_3 , carbonyls, and nitrous acid). An increase in RO_x concentrations, for a given NO_x concentration, enhances the relative importance of $\text{RO}_x + \text{RO}_x$ termination reactions compared to $\text{RO}_x + \text{NO}_x$ termination reactions because the rate of $\text{RO}_x + \text{RO}_x$ reactions increase as the square of the RO_x concentration. The peak O_3 production rate is defined at the cross-over point between NO_x limited and VOC limited conditions. Research results have shown that increases in RO_x production shift the peak O_3 production rate to higher NO_x levels (Thornton *et al.*, 2002). The cross-over point remains an important issue from both an emissions regulatory standpoint and as a test of our understanding of photochemistry in numerical models.

Very low O_3 mixing ratios are often observed over urban airsheds and in high NO_x plumes. In part, this is a result of a decrease in the O_3 production rate under high NO_x conditions, but even more so the low O_3 mixing ratios are the result of the direct reaction between O_3 and NO . This reaction shifts odd oxygen (sum of the concentrations of $\text{O}_3 + \text{O} + \text{NO}_2 + \text{NO}_2$) from O_3 to NO_2 (so called “NO titration of O_3 ”). As the high NO_x plume dilutes with clean background air, the odd oxygen is rapidly shifted back from NO_2 to O_3 and the O_3 mixing ratio recovers. As a result, it is more informative to examine the sum of the odd oxygen species, as odd oxygen is a more conserved quantity and changes more gradually in response to O_3 production and loss processes.

Figure 2.2 illustrates the night-time oxidation of VOCs and NO_x. At night, the photolysis of NO₂ ceases and the reaction between NO₂ and O₃ results in the formation of the NO₃ radical. The NO₃ radical can further react with NO₂ forming N₂O₅. The NO₃ radical can also react with NO reforming NO₂ molecules. Thus, the NO₂/NO ratio plays a key role in determining the potential for N₂O₅ formation. In an airshed with high NO emissions at night, it is possible to chemically destroy the available O₃ which decreases the rate of production of NO₃. Also, a low NO₂/NO ratio due to high NO emissions (e.g. from combustion) favours the destruction of NO₃ via the NO₃ + NO → 2NO₂ reaction. N₂O₅ plays a key role in heterogeneous and multi-phase chemistry. Furthermore, the NO₃ radical plays a central role in night-time chemistry as an oxidant for certain VOCs (e.g. alkenes). O₃ is also still available at night for reaction with alkenes.

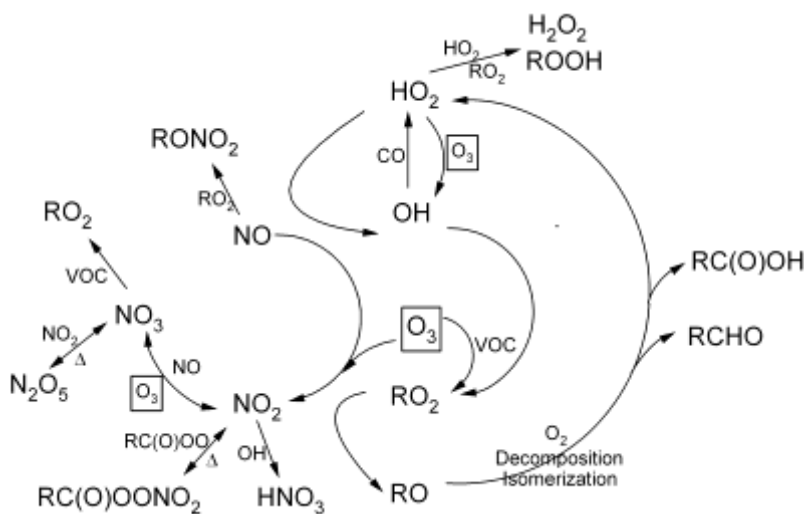


Figure 2.2 Night-time chemistry illustrating the oxidation of VOCs by NO₃, O₃ and OH, the cycling of NO_x and RO_x species, and the production of stable intermediates (N₂O₅, RC(O)OONO₂, RONO₂, HNO₃, RCHO, RC(O)OH, H₂O₂, ROOH). Species in smaller font alongside arrows are co-reactants in the chemical reaction.

The total OH reactivity is defined as the inverse of the OH lifetime⁵. It can also be thought of as the sum of all the VOC mixing ratios weighted by their OH-rate coefficient ($\sum k_{OH}[VOC]$). Recent measurement studies have observed greater than expected OH reactivities (Kovacs *et al.*, 2003; Sadanaga *et al.*, 2005). At a forested site in Michigan, Di Carlo *et al.* (2004) showed

⁵ Lifetime – the time needed to remove a chemical species to 37% (i.e. 1/e) of its initial concentration

that the difference between measured and modelled OH reactivity, called the missing OH reactivity, increased with temperature, as did emission rates for terpenes and other biogenic VOCs. One hypothesis is that unknown reactive biogenic VOCs provide the missing OH reactivity (in addition to the typically measured anthropogenic and biogenic VOCs during intensive or routine monitoring). Alternatively, inaccuracies in the measurement of biogenic VOCs could explain the differences. Generally, missing OH reactivity within models will result in less modelled O_3 and SOA production.

2.2.2 Chemistry of Secondary Particle Formation: General Concepts

Unlike gaseous pollutants, aerosol particles in the atmosphere are not specific chemical entities. They are present in many different sizes and are composed of different chemical species resulting from many sources and processes. Figure 2.3 shows an example of a modal particle size distribution by number, surface area and volume for an urban location. Fine particles are defined as particles with diameter less than $2.5 \mu\text{m}$. Fine particles are composed of nucleation, Aiken and accumulation mode particles.

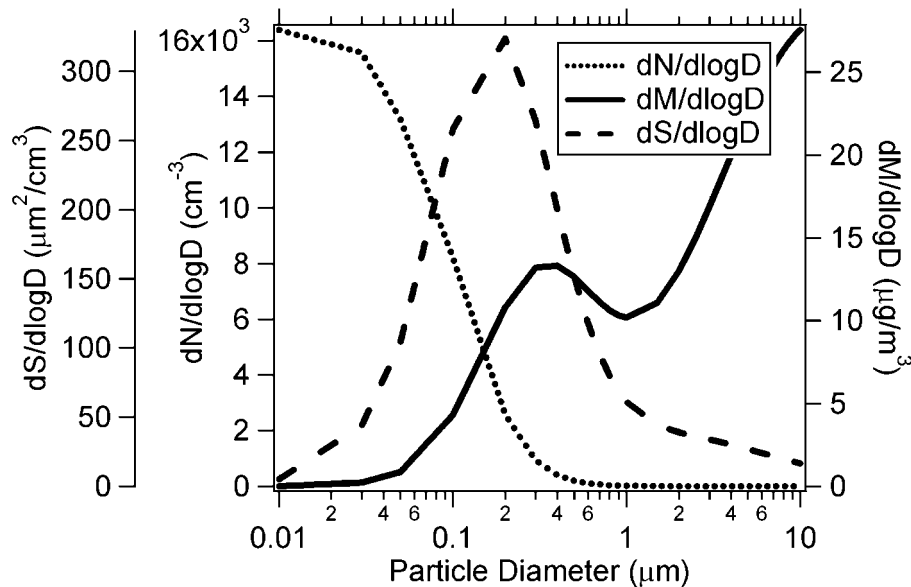


Figure 2.3 Number (N), surface area (S) and mass size (M) distribution for a typical urban aerosol (Seinfeld and Pandis, 1998).

The nucleation mode is formed from freshly nucleated particles (clustering of gas-phase species until a critical size is reached and a particle is formed) and encompasses particles with diameters less than 10 nm. The Aiken mode is composed of particle diameters between 10-100 nm and result from direct emission, the coagulation of nucleation mode particles, and the

condensation of oxidized material from the gas phase onto nucleation mode particles. The linear growth rate by coagulation and condensation decreases as particle size increases and the particles “accumulate” in the accumulation mode (0.1-2.5 μm). If there has been cloud processing of aerosol, the accumulation mode may split into a larger droplet size mode and a smaller condensation mode.

Aerosol particles can be externally or internally mixed. Externally mixed aerosols have particles of a given size with different compositions. For the internally mixed assumption, particles of a given size all have the same composition.

Particle composition is a function of particle size, source and chemical processing. Fine particles are composed of metals, soot, organic material, crustal material, marine spray, sulphate (SO_4), nitrate (NO_3), ammonium (NH_4) and hydrogen ions. Some fine particles are hygroscopic⁶ and contain particle bound water. Figure 2.4 summarizes the primary emitted components of atmospheric particles and the key chemical pathways leading to secondary particle formation. The organic fraction is especially complex and can contain thousands of individual organic species. Table 2.1 lists sources of organic aerosol found in the atmosphere. The largest sources include fossil-fuel combustion, bio-fuel combustion, biomass burning, biological, and solvent usage.

⁶ Hygroscopic – having the ability to attract water molecules

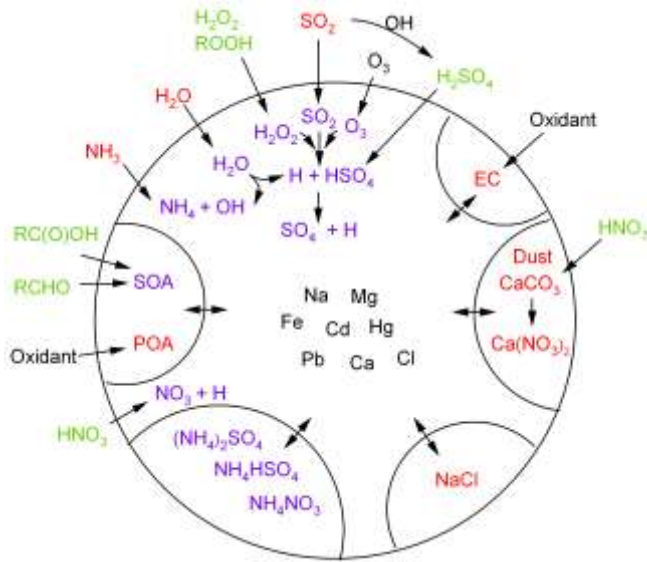


Figure 2.4 Particle-phase composition and chemical transformation processes. Species in red are primary gaseous and particulate components. Species in green are secondary gaseous components. Species in purple are involved in particle-phase production of secondary components.

Table 2.1 Sources of organic aerosol

Sources	Formation Pathway and Composition
Biogenic POA	Bacteria, Pollens, Spores, Plant Waxes, Decaying Biomass
Biogenic SOA	Oxidation of VOCs of biogenic origin (e.g. isoprene, α -pinene) and condensation of products; Direct condensation of VOCs on acidic aerosol (e.g. α -pinene)
Fossil Fuel Combustion POA	Organic particles or gases (which condense on cooling to ambient temperature) from fossil fuel combustion
Fossil Fuel Combustion SOA	Oxidation of VOCs from fossil fuel combustion (e.g. toluene, xylenes) and condensation of products
Bio-Fuel Combustion POA	Organic particles or gases (which condense on cooling to ambient temperature) from bio-fuel combustion
Bio-Fuel Combustion SOA	Oxidation of VOCs from bio-fuel combustion and condensation of products
Anthropogenic Non-combustion POA	Organic particles from anthropogenic non-combustion emissions (chemical solvents, base metal smelters, iron and steel, cement, petroleum refineries)
Anthropogenic Non-Combustion SOA	Oxidation of VOCs from anthropogenic non-combustion emissions and condensation of products
Biomass Burning POA	Organic particles or gases (which condense on cooling to ambient temperature) from natural forest fires and deforestation practices
Biomass Burning SOA	Oxidation of VOCs from biomass burning emissions and condensation of products

The coarse mode refers to particles formed largely by the mechanical breakdown of crustal material and organic debris. In addition to minerals and organic material, the coarse mode may include sea salt (from evaporated sea spray) and nitrate formed from the reaction of HNO_3 with calcium carbonate (Anlauf *et al.*, 2006).

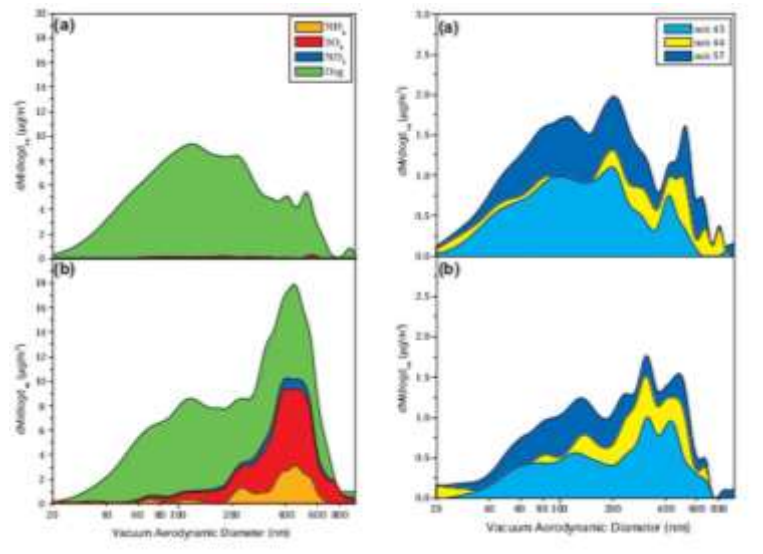


Figure 2.5 Composition-resolved mass size distributions for two samples collected in downtown Toronto, Ontario (Broekhuizen *et al.*, 2006). In panel (a), the sample is dominated by the organic fraction for all submicron particle sizes. The organic fraction is a combination of primary and secondary components as characterized by similar magnitude $m/z = 43,44$ and $m/z = 57$ ratios. In panel (b), the sample has a large secondary aerosol component at particle diameters 200-600 nm characterized by SO_4 , NH_4 , NO_3 and secondary organics ($m/z = 43,44$).

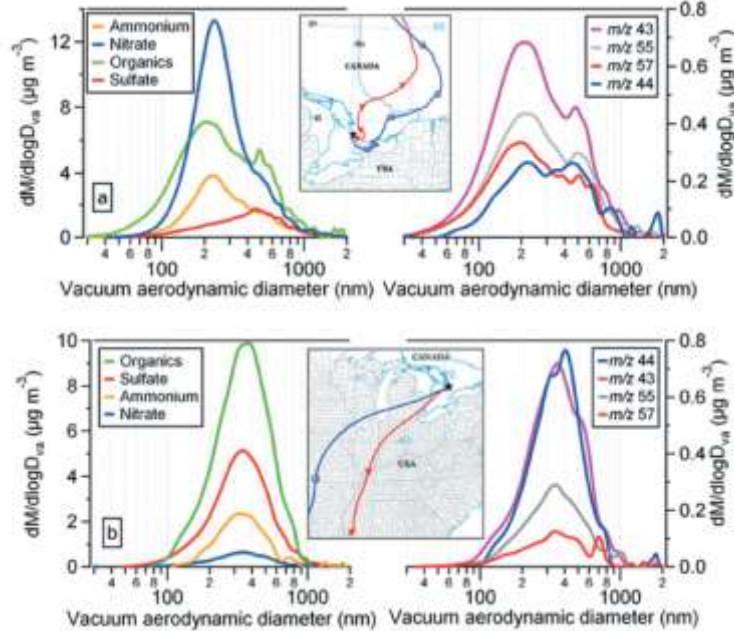


Figure 2.6 Composition-resolved mass size distributions for two samples collected at Egbert, Ontario (Rupakheti *et al.*, 2005). The top panels are from a sample collected in the processed Toronto plume. The bottom panels are from a sample collected from an aged air mass originating on the mid-western United States several days earlier.

Figures 2.5 and 2.6 illustrate examples of compositionally-resolved mass size distributions measured with an aerosol mass spectrometer for 1) a downtown location with large organic aerosol emissions (Figure 2.5 a), 2) a downtown location with a secondary particle production event (Figure 2.5 b), 3) a processed urban plume (Figure 2.6a) with high nitrate to sulphate aerosol ratios and 4) an aged regional air mass (Figure 2.6b) with low nitrate to sulphate aerosol ratios and low nitrate to organic aerosol ratios (Rupakheti *et al.*, 2005; Broekhuizen *et al.*, 2006). In the downtown urban sample (Figure 2.5 a), the organic fraction dominates for all submicron particle sizes. The organic fraction is a combination of primary and secondary components as characterized by similar magnitude aerosol mass spectrometer (AMS) fragments with mass to charge ratios of $m/z = 43$ (marker for SOA), $m/z = 44$ (marker for SOA) and $m/z = 57$ (marker for POA). In the downtown urban sample with a secondary particle production event (Figure 2.5 b), the sample has large secondary aerosol components characterized by sulphate, ammonium and SOA ($m/z = 43, 44$). The maximum in the aerosol sulphate mass distribution at diameters of typically 200-600 nm is consistent with possible cloud processing of SO_2 . In the processed urban plume (Figure 2.6a), the aerosol nitrate peaks in the mass size distribution at particle diameters where the surface area distribution maximizes (100-400 nm) due to the nitrate aerosol formation from N_2O_5 and HNO_3 condensation. In the aged plume (Figure 2.6b), all $\text{PM}_{2.5}$ aerosol components are internally mixed and maximize at larger particle diameters in the accumulation mode due to a

combination of condensation and cloud processing. The mass to charge ratios of aerosol in the aged plume (high $m/z = 44$ relative to $m/z = 57$) are a good example of a highly oxidized organic aerosol, likely SOA.

Table 2.2 Overall aerosol yields (SOA formed per amount of precursor reacted) at a typical organic aerosol mass concentration of $5 \mu\text{g m}^{-3}$ from selected precursors under different light, NO_x , humidity, temperature and seed conditions.

Precursor	Light	NO_x/VOC	Relative Humidity	Seed	Temp ($^{\circ}\text{C}$)	Yield at $5 \mu\text{g m}^{-3}$
α -Pinene + O_3^{a}	Dark	Low NO_x	Low	$(\text{NH}_4)_2\text{SO}_4$	25	0.079
α -Pinene + O_3^{a}	Dark	High NO_x	Low	$(\text{NH}_4)_2\text{SO}_4$	25	0.032
α -Pinene + O_3^{a}	UV	High NO_x	Low	$(\text{NH}_4)_2\text{SO}_4$	25	0.027
α -Pinene + O_3^{a}	Dark	Low NO_x	High	$(\text{NH}_4)_2\text{SO}_4$	25	0.079
α -Pinene + O_3^{a}	UV	Low NO_x	Low	$(\text{NH}_4)_2\text{SO}_4$	25	0.050
α -Pinene + O_3^{b}	Dark	Low NO_x	Low	$(\text{NH}_4)_2\text{SO}_4$	25 ¹	0.067
m-Xylene + OH^{c}	UV	Low NO_x	Low	$(\text{NH}_4)_2\text{SO}_4$	25	0.30
m-Xylene + OH^{c}	UV	High NO_x	Low	$(\text{NH}_4)_2\text{SO}_4$	25	0.036
m-Xylene + OH^{d}	UV	Low NO_x	Low	No seed	25	0.036
m-Xylene + OH^{d}	UV	High NO_x	Low	No seed	25	0.016
m-Xylene + OH^{e}	UV	High NO_x	Low	$(\text{NH}_4)_2\text{SO}_4$	25 ²	0.010
Toluene + OH^{f}	UV	High NO_x	Low	$(\text{NH}_4)_2\text{SO}_4$	25	0.013
Toluene + OH^{c}	UV	High NO_x	Low	$(\text{NH}_4)_2\text{SO}_4$	25	0.061
Toluene + OH^{c}	UV	Low NO_x	Low	$(\text{NH}_4)_2\text{SO}_4$	25	0.36
Toluene + OH^{e}	UV	High NO_x	Low	$(\text{NH}_4)_2\text{SO}_4$	25 ²	0.024
Limonene + O_3^{g}	Dark	Low NO_x	Low	No seed	25	0.40
Limonene + O_3^{g}	UV	Low NO_x	Low	No seed	25	0.30
Limonene + O_3^{g}	Dark	High NO_x	Low	No seed	25	0.40
Limonene + OH^{b}	UV	High NO_x	Low	$(\text{NH}_4)_2\text{SO}_4$	25	0.10
Isoprene + OH^{h}	UV	High NO_x	Low	$(\text{NH}_4)_2\text{SO}_4$	25	0.025
Isoprene + OH^{h}	UV	Low NO_x	Low	$(\text{NH}_4)_2\text{SO}_4$	25	0.035

^a Pathak *et al.* (2007), ^b Griffin *et al.* (1999), ^c Ng *et al.* (2007), ^d Song *et al.* (2005)
^e Odum *et al.* (1996), ^f Stroud *et al.* (2004), ^g Zhang *et al.* (2006), ^h Kroll *et al.* (2006)
¹ adjusted to 25 $^{\circ}\text{C}$ using $\Delta H_v = 30\text{kJ mol}^{-1}$, ² adjusted to 25 $^{\circ}\text{C}$ using $\Delta H_v = 40\text{kJ mol}^{-1}$

The rate of secondary aerosol formation (including SOA, nitrate and sulphate) is impacted by the relative abundance of NO_x and RO_x , which impacts OH mixing ratios and the rate of VOC, NO_x and SO_2 oxidation. Recent smog chamber studies of SOA formation show SOA yields have a complex dependence on initial VOC to NO_x ratios (see Table 2.2) (Presto and Donahue, 2006; Zhang *et al.*, 2006; Chan *et al.*, 2007; Ng *et al.*, 2007). SOA production is a two-step

process involving gas-phase production of condensable products followed by gas-to-particle partitioning. The gas-phase production of condensable products depends on precursor VOC mixing ratio and their reactivity, as well as OH mixing ratio which depends on the relative abundance of NO_x and RO_x . Gas-to-particle partitioning depends on the saturation vapour pressure and solubility of condensable products and the amount of available absorbing liquid. Organic nitrate products (which are favoured under high NO_x conditions) have higher saturation vapour pressures and lower solubilities than organic peroxides and organic acids (which are condensable products favored under low NO_x conditions) (Stroud *et al.*, 2004).

Recently, the volatility of primary organic aerosol (POA) emissions has been measured with dilution flow tube experiments and thermal denuders. Robinson *et al.* (2007) showed that POA emissions can evaporate in the gas-phase and subsequently oxidize to form SOA. This process will add mass to the organic aerosol in terms of functional groups (-OH, -C(O)-, -ONO₂) and will shift the burden of organic aerosol from urban to regional scales.

Gas-phase HNO_3 is formed directly from the reaction between OH and NO_2 . Thus, HNO_3 production is a non-linear function of NO_x and RO_x and reaches a maximum plateau at high NO_x conditions. Gas-phase sulphuric acid (H_2SO_4) is formed from SO_2 oxidation which, except for fresh plume conditions, does not impact the RO_x and NO_x budgets. Thus, gas-phase H_2SO_4 production depends on background NO_x and RO_x conditions which govern OH mixing ratios. Particle- and cloud-phase production of sulphate aerosol from dissolved SO_2 , H_2O_2 and O_3 also depend in a complex manner on RO_x and NO_x conditions; H_2O_2 -initiated SO_2 oxidation being favoured under high VOC to NO_x ratios (i.e. NO_x limiting regime).

2.2.3 Urban Plumes

Urban-scale pollution has important implications on visibility reduction and associated health problems (respiratory and cardiovascular function and spread of micro-organics, allergic and infectious diseases). These related costs are becoming increasingly more important because a large and increasing fraction of the human population live in urban locations. Urban plumes are characterized by emissions from mobile, industrial and residential sources which produce substantial quantities of CO, VOCs and NO_x , but generally little SO_2 . Processes at the urban scale are rapid with time scales from minutes to a few hours. In this section, the discussion is focused on key uncertainties in our understanding of O_3 photochemistry, especially at low VOC to NO_x ratio, and advances in our understanding of secondary aerosol formation in urban plumes.

2.2.3.1 Free Radical Closure Studies

Over the past decade, with the advancement of spectroscopic and spectrometric techniques to measure radical mixing ratios (OH, HO₂, RO_x), there have been a number of field studies focusing on the comparison between measured and modelled free radical mixing ratios in urban airsheds. These closure studies are elegant because they isolate chemical processes from other processes. Radicals are sufficiently short lived that the relevant chemical timescales can be isolated from transport. Radical mixing ratios are calculated using chemical box models. Measurements of longer-lived species, such as O₃, H₂O, CO, NO_x and VOCs, are used to constrain box model species. These longer-lived species play a key role as sources of radicals (photolysis of O₃, H₂O₂, formaldehyde and nitrous oxide) and sinks for radicals (NO_x + RO_x reactions). Studies show that in some cases box models can predict RO_x behaviour quite well, while in others the discrepancy is as large as a factor of 6 due to the complexity of the urban atmosphere. Here, the urban closure studies are summarized for 1) summertime, 2) wintertime and 3) night-time conditions.

2.2.3.1.1 Summertime Conditions

Martinez *et al.* (2003) measured OH and HO₂ in Nashville, Tennessee and found that overall daytime-observed OH and HO₂ were a factor of 1.33 and 1.56 greater than modelled values. However, Martinez *et al.* found that observed HO₂ was significantly greater than expected when NO mixing ratios were greater than 2 ppbv; thus, O₃ production did not decrease as much as expected at high NO_x mixing ratios. Ren *et al.* (2003) found a similar result for observations in New York City. O₃ production rates derived from observed peroxy radicals were greater than O₃ production rates derived from modelled peroxy radicals at higher values of NO_x. In fact, average daily cumulative O₃ production derived from observations was a factor of 1.5 greater than from model calculations. In New York City, the budgets for HO_x show that during the daytime the photolysis of HONO accounted for the largest fraction of HO_x production. For the Birmingham, England airshed, Emmerson *et al.* (2005) found an average daytime HO_x measured to modelled ratio of 1.7 with modelled OH concentrations in better agreement than HO₂. The predicted radical concentrations were more sensitive to NO_x than observations, especially at higher NO_x mixing ratios. Collectively, these studies suggest a gap in our understanding of radical photochemistry at high NO_x levels typical of polluted conditions (>2 ppbv) resulting in a summertime model underprediction of RO_x.

2.2.3.1.2 Wintertime Conditions

HO_x has only been measured during a few wintertime urban field studies. HO_x observations in Birmingham, England showed that daytime OH levels in winter were only a factor of 2 less than in summer (Emmerson *et al.*, 2005). Noontime HO₂ were similar for summer and winter despite a reduction in OH production from the photolysis of O₃ between summer and winter by a factor of 15. The calculated wintertime OH source was largely the ozonolysis of alkenes. Ren *et al.* (2006) measured HO_x in the wintertime in New York City and found that modelled OH

was well reproduced by model calculations with a median measured to modelled ratio of 0.98. However, HO₂ was significantly underpredicted with a median measured to modelled ratio of 6.0. The discrepancy was also more pronounced at higher NO_x. Additional HO₂ production of up to 3 times the calculated HO₂ production was needed for model agreement with measured values. This HO₂ production could come from new HO₂ production terms or from unknown HO₂ recycling that does not go through OH. Photolysis of HONO was the dominant calculated HO_x source during daylight hours. Collectively, the wintertime studies show a similar trend to the summertime studies with uncertainties in the HO_x closure at higher NO_x mixing ratios.

2.2.3.1.3 Night-time Conditions

Measurement and modelling studies of night-time HO_x are very limited. In urban Nashville, Martinez *et al.* (2003) found frequent periods of high OH and HO₂ mixing ratios at night and provided evidence for a source from the ozonolysis of alkenes; however, even when considering all the ozonolysis reactions involving alkenes, the night-time OH could not be accounted for in model studies. In urban New York City, Ren *et al.* (2003) found that model calculations significantly underestimated OH during the night-time. The underestimation of OH was attributed to a combination of a missing propagation route from HO₂ to OH and to missing sources for OH. In the model results, the production of HO_x at night was dominated by the ozonolysis of alkenes. In Birmingham, England, Emmerson *et al.* (2005) reached the same conclusion with measurements of HO_x. The night-time measured to modelled ratio for OH and HO₂ were both 2.0. Their results also demonstrated the importance of ozonolysis reactions for alkenes in an urban atmosphere, particularly at night. Collectively, these studies suggest a significant unaccounted for night-time source for OH in current chemical box models.

2.2.3.2 Ozone Production in Urban Plumes

In Vancouver during the PACIFIC 2001 intensive study, O₃ production in the Lower Fraser Valley was VOC limited (Vingarzan and Li, 2006). The ranking of VOC species in terms of OH-reactivity illustrated that a mixture of biogenic and anthropogenic gases were important in O₃ production. At the urban Slocan Park location, limonene, xylenes, α -pinene, toluene and propene were the most important VOC precursors to O₃ production. At the suburban Langley location, isoprene, butenes, propene, ethene, and α -pinene were the dominant VOC precursors to O₃ production (Wang *et al.*, 2005). Stroud *et al.* (2008) compared summertime model predictions with measurement-derived OH-reactivities for VOCs at 18 sites across Canada. Significant variability from site to site was observed in VOC speciation contributing to total OH-reactivity. For example, alkanes were the dominant contributor to OH-reactivity in Edmonton whereas in Toronto and Montreal alkenes (e.g. styrene, propene, 1-butene) contributed the largest fraction to OH-reactivity. Given the importance of alkene oxidation, improving uncertainties associated with anthropogenic alkene emissions and alkene oxidation chemistry should be a priority.

2.2.3.3 Aerosol Characterization in Urban Plumes

Measurements of aerosol composition in urban airsheds reveal a great deal of heterogeneity both within a city and between cities. Within a city, variability is observed at fine spatial scale due to the various emission sources (traffic combustion, wood combustion, oil and natural gas combustion, industrial releases). Collectively, studies suggest that the organic aerosol fraction is ubiquitous to fine PM in urban airsheds. Sulphate aerosol is produced downwind of power plants and petrochemical facilities and is regional in nature. Nitrate aerosol is produced in recently processed urban plumes with available NH_3 emissions.

Zhang *et al.* (2005a) measured particle composition in Pittsburgh, Pennsylvania and found that organic aerosol in the fine mode was the dominant chemical component. The organic aerosol was composed of an oxygenated and hydrocarbon-like fraction with the oxygenated fraction, on average, contributing 66%, by mass, to organic aerosol. The accumulation mode was dominated by sulphate aerosol and oxygenated organic aerosol while the ultra-fine mode contained the hydrocarbon-like organic aerosol. During nucleation events, sulphate was the species observed in the smallest particles. Organic condensed onto the nucleation mode causing growth to Aiken and accumulation modes, but only during daytime photochemically active periods.

Rapid SOA growth has been observed downwind of Mexico City. SOA growth rates resulted in SOA loadings quickly surpassing the primary organic aerosol (POA) loadings (Volkamer *et al.*, 2006; Kleinman *et al.*, 2007a). Volkamer *et al.* (2006) showed that a significant amount of SOA can be produced in Mexico City from anthropogenic precursors including intermediate volatile organic compounds (IVOCs, e.g. long chain alkanes) and water-soluble aromatic oxidation products (e.g. glyoxal). The amount of SOA produced from these anthropogenic precursors greatly exceeds what is currently predicted from traditional SOA models. The aerosol oxygen/carbon ratio was observed to increase with photochemical age in the Mexico City plume consistent with condensation of oxygenated organic species. Interestingly, nitrate aerosol was enhanced in the urban area and immediate outflow; however, nitrate decreased quickly with distance downwind, likely due to evaporation. In fact, the nitrate aerosol to gaseous CO ratio levelled off in the aging plume while the organic aerosol to gaseous CO ratio kept increasing.

Kleinman *et al.* (2007b) found a similar result downwind of the east-coast during the New England Air Quality Study. The ratio of the organic aerosol to CO quadrupled as the plume aged (while NO_x/NO_y ratio dropped from 100 to 10%). This suggests that in the aged plume the organic aerosol was >75% secondary in nature.

Weber *et al.* (2007) measured water-soluble organic carbon (WSOC) aerosol downwind of Atlanta and New York City. WSOC was observed to correlate with CO which is a good tracer for vehicular emissions; however, WSOC is not directly emitted from vehicular emissions.

This suggests the WSOC must be produced downwind of vehicular emission sources. WSOC was also found in similar proportion to anthropogenic tracers in both Atlanta and NYC, even though Atlanta has a larger background of biogenic VOCs. Interestingly, radiocarbon analysis estimates that 70-80% of the aerosol carbon in the Atlanta plume was biogenic. Collectively, these observations suggest that in the Atlanta plume the biogenic VOCs are precursors; however, there is an anthropogenic component to the SOA formation processes which is limiting (possibly NO_x or primary aerosol components).

Nitrate aerosol has been observed in recently processed urban plumes which are also influenced by NH_3 emissions. In the Los Angeles plume downwind of NH_3 emissions, measurements of accumulation mode aerosol illustrate the importance of the ammonium nitrate fraction. Neuman *et al.* (2003) demonstrated that there exists an important vertical component to the spatial variability of ammonium nitrate aerosol. In altitude profiles, CO and O_3 mixing ratios were nearly constant within the boundary layer, whereas HNO_3 was depleted and fine particle mass enhanced near the top of the boundary layer. The vertical gradients in the boundary layer were indicative that the equilibration time of ammonium nitrate formation was faster than boundary layer mixing times.

During PACIFIC 2001, in the western part of the Lower Fraser Valley, the aerosol was dominated by combustion-related species, sea salt and organics (biogenic and anthropogenic). In the eastern part of the Lower Fraser Valley, the airshed was dominated by $\text{NH}_4\text{-SO}_4\text{-NO}_3$ chemistry and biogenic SOA (Vingarzan and Li, 2006).

In Toronto, Ontario, multi-variate receptor modelling uncovered that the main sources of $\text{PM}_{2.5}$ were local motor-vehicle emissions (20%), coal-fired power plants (20-25%), secondary organic aerosol (15%) and secondary nitrate formation (35%) likely related to vehicular emissions (Brook *et al.*, 2007). On average, it was estimated that 30-45% of the $\text{PM}_{2.5}$ in Toronto was associated with local sources and 55-70% with regional transport. It is likely that, at any time, the PM in Toronto is dominated by local or regional sources and there are probably a few regional events that influence mean values.

2.2.4 Power Plant Plumes

Power plants are responsible for the majority of the SO_2 emissions in North America. A single power plant can also have significant mass emissions of NO_x , comparable to a mid-sized city. Power plant plume studies over the past decade have focused on determining the formation rate of sulphate aerosol, the evolution of particle size distributions, the oxidation rate of NO_x , and the efficiency of O_3 production. In this section, the focus is on processes that affect SO_2 and NO_x oxidation in plumes, particularly with respect to what processes influence the concentrations of SO_2 and NO_x and their oxidation products in the near field at receptor sites within tens of kilometers from the source.

Sulphate aerosol forms during the daytime when sufficient oxidant is available in the plume. Close to the source, oxidant depletion occurs rapidly within the plume by reaction of O_3 with emitted NO. If sufficient mixing with background air occurs, O_3 concentrations will recover by mixing of O_3 itself and VOCs, which can in turn form RO_2 radicals. RO_2 radicals rapidly convert NO to NO_2 without consumption of O_3 .

The SO_2 oxidation rates seen in plumes from point sources vary from nearly zero to more than $16\% \text{ hr}^{-1}$. In non-cloudy conditions, SO_2 removal in power plant plumes occurs primarily during the daytime by reaction with OH. NO_x removal occurs during the daytime by fast reactions with OH and at night-time by the NO_3/N_2O_5 pathway. In non-cloudy conditions, NO_x removal will occur much more rapidly than SO_2 oxidation (factor of 10 times). An important consideration in a plume is the competition between NO_x and SO_2 for the available oxidants. The oxidation of NO_2 by OH is faster than SO_2 , hence the presence of NO_x in a plume will inhibit SO_2 oxidation rates relative to background air. In cloudy conditions, SO_2 will be removed rapidly by reactions in the aqueous phase. Due to the SO_2 oxidation rates being non-linear and strong functions of cloud liquid water content, measurements have shown considerable variability in derived SO_2 oxidation rates. The cloud uptake of N_2O_5 is rapid; thus, if N_2O_5 can be produced in cloud interstitial air then NO_x loss will also be rapid (Leitch *et al.*, 1988; Hayden *et al.*, 2008). The Cumberland Valley plume was sampled during the 1995 Southern Oxidant Study. Gillani *et al.* (1998) found high nitrate formation rates of $10\text{-}15\% \text{ hr}^{-1}$ and a higher loss rate of nitrogen compared to sulphur by a factor of 8.

Daytime power plant studies under cloud-free conditions can give estimates of OH from either the oxidation of SO_2 or from the oxidation of NO_x ; however, the two measures often give different estimates of OH concentration. Recently, Springston *et al.* (2005) studied an isolated lignite fired power plant plume over a plume lifetime of 4.6 hr centered near local noon. The appearance of sulphate aerosol and the conversion of NO_x to oxidation products as a function of atmospheric processing time yielded average OH concentrations of 8.0×10^6 and 11×10^6 molecules per cm^3 , respectively. Unlike prior studies, these estimates agreed with each other within uncertainty limits. As the plume ages, particle size spectra were consistent with the addition of sulphate mass by condensation onto Aitken and accumulation mode size particles. Aerosol size distributions adjusted for dilution showed constant number concentration and a marked increase in accumulation mode particles ($D > 0.1 \mu\text{m}$). Primary emissions of fly ash particles ($D = 6\text{-}8 \mu\text{m}$) were also observed. O_3 production efficiencies varied from near zero at the stack to 5-6 (O_3 molecules produced per NO_x molecule lost) on downwind traverses.

Brock *et al.* (2003) measured particle size distributions in plumes downwind from coal-fired power plants in the vicinity of Houston, TX. In SO_2 -rich plumes that did not contain elevated concentrations of VOCs, particle volume increased with increasing plume age at a rate consistent with condensation and neutralization of the gas-phase oxidation products of SO_2 . In plumes that were enhanced in both SO_2 and VOCs, observed particle growth exceeded that expected from SO_2 oxidation, indicating the formation of organic or nitrate PM. Ground-based

particle composition observations a few km south of the Houston ship channel support this explanation. Organic matter was positively correlated with ammonium and sulphate during photochemically active periods and accounted for greater than 30% of total particle volume. Brock *et al.* concluded that photochemical oxidation of SO₂ is the key process regulating particle growth in plumes rich in SO₂, but little VOC. Uptake of organic matter contributes a substantial mass to plumes rich in both SO₂ and VOCs. Lab studies of particle growth are recommended with precursor concentrations of NO_x, VOCs and SO₂ representative of ambient plume conditions.

Cho *et al.* (2008) used a high-resolution regional air quality model to assess the impact of coal-fired power plants on PM_{2.5} levels in Edmonton, Alberta during the PrAIRie 2005 field study. Emission data for three coal-fired power plants located west of Edmonton were improved by using mass emission rates from the Continuous Emissions Monitoring System (CEMS) combined with measured particle size distribution and chemical speciation from stack sampling. The revised emissions data greatly improved the model-measurement comparisons for sulphate aerosol. The modified emissions also increased the coarse mode particle concentrations close to power plants relative to the base case simulation.

2.2.5 Industrial Plumes

The chemistry and dispersion of SO₂ and NO_x in plumes from oil-fired stations, petroleum refineries, and metal smelters have been studied, but not as extensively as from coal-fired power generation. Cheng *et al.* (1987) studied the plume from an oil sands extraction plant in Alberta. The oil sands plume contained high aerosol concentrations near the source and the aerosol in the plume was characterized as hygroscopic. SO₂ conversion rates of 0-2.8% hr⁻¹ in winter and 0-6% hr⁻¹ in summer were found. Heterogeneous processes were believed to be appreciable on the wet surfaces close to the point of emission. Given the growing Canadian emissions from the oil sands extraction and Upstream Oil and Gas sector, further studies should be performed on these sectors to improve their emission inventories (magnitude and speciation, see conclusions of Chapter 4) and oxidation chemistry. Plumes from metal smelters have high concentrations of trace metals (Banic *et al.*, 2006). It is postulated that plumes rich in trace metals might have elevated SO₂ conversion rates, due to catalytic effects, but this has not been borne out in field experiments.

Cho (2005) compared modelled and observed particle size distributions in a coal-fired power plant and copper smelter plume. The modelled results for downwind particle size distribution were also highly dependent on having available stack initial particle size distributions. Cho (2005) concluded that binary particle nucleation⁷ was shown to be responsible for the formation of nano-sized particles in the plumes. A competition between the condensational growth of particles to Aiken mode sizes and their removal by coagulation was often observed.

Brock *et al.* (2003) observed that most of the particle mass flux advected downwind of Houston, TX came from the petrochemical industries at the periphery of the city rather than downwind of the urban core. Particle growth within the VOC-rich petrochemical plumes along the ship channel district exceeded that expected solely from SO₂ oxidation, indicating the formation of organic PM in the presence of sulphate aerosol. Particle volume enhancements exceeding 12 µm³ cm⁻³ above background were found for >45 km along a flight track in the furthest transect >90 km downwind of the ship channel. This substantial horizontal dispersion of enhanced particulate concentration illustrates the potential influence of the Houston-area petrochemical industries on regional air quality. Two other geographically isolated industrial plumes were sampled during Texas Air Quality Study 2000. The Gulf plant, a catalyst manufacturing facility, was richer in SO₂ emissions than the Dow plant, a plastics, epoxy and hydrocarbon processing facility. Oxidation and condensation of organic matter in the SO₂-poor Dow plume was insufficient to produce detectable enhancements in particle volume above background. However, particle volume growth well above background levels was observed in the Gulf plume. VOC measurements in both plumes showed similar levels of aromatic and other VOC particle precursors. Indeed, the Brock *et al.* (2003) study suggests maximum particle growth rates for plumes rich in both SO₂ and VOCs. There are few laboratory data available on particle formation in VOC-rich and SO₂-rich mixtures at concentrations representative of the ambient atmosphere. Jang and Kamens (2001) hypothesized heterogeneous mechanisms for the formation of organic particle mass, such as acid-catalyzed reactions. This mechanism may have contributed to SOA formation within the petrochemical refinery plumes and might explain the observed association of SOA growth with enhanced SO₂ concentrations.

In terms of O₃ production, O₃ is formed very rapidly and very efficiently downwind of areas dominated by industrial VOC and NO_x emissions. During the Texas Air Quality Study 2000, the calculated rate of O₃ production downwind of industrial sources ranged from 50 ppbv hr⁻¹

⁷ Binary particle nucleation is the clustering of H₂SO₄ and H₂O molecules to a critical size to form a particle

to 150 ppbv hr⁻¹ (Ryerson *et al.*, 2003). In addition, the high ozone production rate is consistent with a high O₃ production efficiency ranging from 10-20 molecules of O₃ formed per molecule of NO_x reacted. These efficiencies of O₃ formation are much higher than those observed in other urban areas (typically 3-5) or those observed in the plumes from isolated power plants (typically 1-3). Ryerson *et al.* concluded that O₃ is produced very efficiently in industrial plumes due to the combination of high VOC and NO_x mixing ratios. In the industrial plumes downwind of the Ship Channel region in Houston, the samples with the highest O₃ production rates had high mixing ratios of ethene, propene, butenes, butanes and aromatic VOCs. In the industrial plumes, models predicted lower mixing ratios of alkenes compared to measurements. The balance of evidence from the Texas Air Quality Study suggested an underestimate of refinery alkene emissions from the emission inventory.

2.2.6 Chemical Processing in Regional Plumes

As plumes dilute from the urban to the regional environment, there is a general transition from VOC-limited to NO_x-limited chemistry. This transition affects the rate of oxidant and particle formation and the chemical composition of the additional product formation.

2.2.6.1 Condensation onto pre-existing particles

As plumes dilute and chemically age, the composition of the background atmosphere becomes important in the nature of further chemical processing. In particular, reactive biogenic VOCs in the background atmosphere can add significantly to a regional plume's OH reactivity. It is now well known that gas-phase oxidation of biogenic hydrocarbons, such as a variety of terpenes and sesquiterpenes, gives rise to SOA formation (Lee *et al.*, 2006). It is thought that a small number of the oxidation products of these compounds have sufficiently low volatility that they condense onto pre-existing aerosol giving rise to aerosol growth (Seinfeld and Pankow, 2003). In parts of the atmosphere that are heavily biogenically impacted these products may be involved in nucleation events themselves (Leaich *et al.*, 1999), whereas in more polluted regions they will contribute to growth of the accumulation mode particles. On a per molecule basis, higher aerosol yields are generally obtained from oxidation of these biogenic precursors than from oxidation of anthropogenic molecules that are also known to give rise to SOA, e.g. xylenes from gasoline emissions (Seinfeld and Pankow, 2003).

There are indications that conventional modelling of SOA formation from biogenics underestimates the level of secondary organic carbon in the atmosphere (Heald *et al.*, 2006). Recent findings in the field and laboratory are that isoprene photo-oxidation can also give rise to SOA (Claeys *et al.*, 2004; Kroll *et al.*, 2006). Given that isoprene emissions are very much higher than other biogenics (aside from methane), even a small aerosol yield from its oxidation could have significant impact on levels of secondary organics. Products likely to arise from isoprene OH oxidation, such as 2-methyltetrols, have been identified in aerosol formed in

biogenically rich regions (Claeys *et al.*, 2004). Smog chamber experiments indicate that aerosol yields, relative to loss of isoprene mass, are a few percent, being dependent on NO_x levels (Kroll *et al.*, 2006). Inclusion of this small fraction of isoprene oxidation into models of secondary organic aerosol formation is only now being performed (Henze and Seinfeld, 2006), and results show that the isoprene source of SOA can be at least as large as from the oxidation of terpenes and sesquiterpenes. Table 2.2 lists overall SOA yields (defined as amount of organic aerosol formed per amount of precursor reacted) for a series of selected precursors at a typical ambient organic aerosol mass concentration of $5 \mu\text{g m}^{-3}$. Even at a given organic aerosol mass concentration, there is considerable variability in yields depending on NO_x/VOC ratios, radiation levels, temperature, relative humidity and existing particle composition (e.g. acidic versus non-acidic conditions).

2.2.6.2 Oligomer Formation

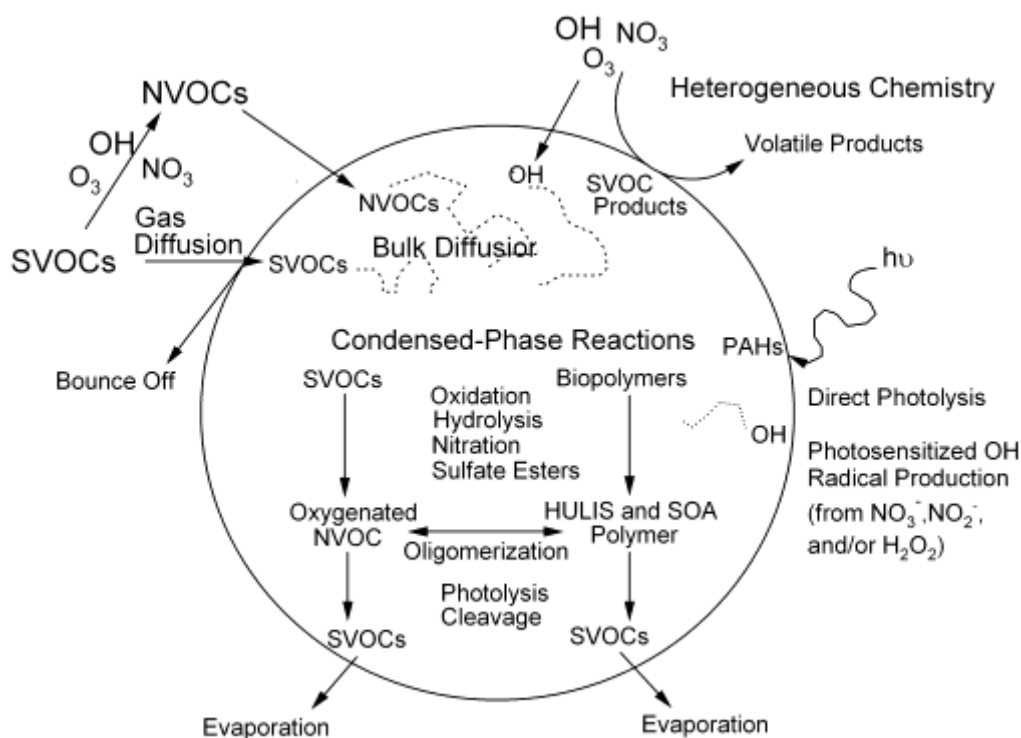


Figure 2.7 Aging processes for organic aerosol components: Condensational aging (gas-phase diffusion, surface accommodation, NVOC = non-volatile organic compound), heterogeneous aging (surface oxidation), and homogeneous aging (bulk-phase oligomer and oxidation chemistry, HULIS = humic like substances).

Figure 2.7 illustrates processes that transform organic aerosol including heterogeneous aging (uptake of oxidants and aerosol surface reactions) and condensed-phase reactions. These interactions give rise to additional particle growth beyond that produced by the condensation of products from photo-oxidation of biogenic and aromatic precursors. These processes also chemically transform the aerosol constituents.

From smog chamber experiments, there is evidence that small carbonyls which partition to the aerosol can react with each other in oligomerization⁸ processes (Jang and Kamens, 2001; Liggio *et al.*, 2004; Kalberer *et al.*, 2004). These reactions lead to the formation of higher molecular weight products that are less volatile than the precursors. Conventional models for SOA formation (based on Odum *et al.*, 1996; Griffin *et al.*, 1999) that do not include this process will under-predict the growth rates of accumulation mode particles. Several laboratory studies indicate that the rate of this chemistry is enhanced with higher aerosol acidity. In particular, one laboratory study focused on the uptake of glyoxal (a product of aromatic hydrocarbon oxidation) on PM of acidic and non-acidic nature (Liggio *et al.*, 2005; Liggio *et al.*, 2004). These experiments were the first to report evidence of sulphuric acid seed particles reacting with carbonyls to form sulphate-ester products, and essentially transforming a portion of the particulate inorganic mass to organic mass. Uptake coefficients for glyoxal were indeed large enough ($\sim 2.9 \times 10^{-3}$) to be of significant consequence in the ambient atmosphere, resulting in a heterogeneous lifetime comparable to that of other gas-phase glyoxal loss mechanisms (photolysis, reaction with OH).

Similar experiments utilizing pinonaldehyde (a terpene oxidation product) were also performed (Liggio and Li, 2006a; Liggio and Li, 2006b). Oligomer products in the uptake of pinonaldehyde were also observed from the particle mass spectrum yet occurred via completely different mechanisms than glyoxal, specifically via aldol condensation reactions. An observation of particular interest was the formation of a significant amount of sulphate-ester products from the reaction of sulphuric acid (or sulphate) with available carbonyl functional groups. Approximately 6 – 51% of the initial sulphate mass was converted to sulphate-ester. This implies that inorganic sulphate in the ambient atmosphere may in part be masked as an organic species, the properties of which are completely unknown. Such a sink for inorganic sulphate suggests that current measurements have underestimated ambient sulphate levels, and implies that a link exists between inorganic and organic species in aerosols which has not been taken into account in atmospheric models. Some organosulphates have been observed in ambient samples (Surratt *et al.*, 2006).

Recent experiments utilizing unsaturated compounds (alkenes) of biogenic origin such as isoprene, and α -pinene have suggested that the direct polymerization⁹ of these species on acidic aerosols can also occur without the need for a prior oxidation step (Liggio and Li,

⁸ Oligomerization – reaction of a chemical species in the liquid phase to form a network structure with a finite number of units

⁹ Polymerization – reaction of chemical species to form a large unbounded network structure in the liquid or solid phase

2006b). This novel finding illustrates another route for SOA formation, which is of potential importance to the atmosphere given the large number of unsaturated species present. Clearly, heterogeneous reactions of organic gases will play a major role in our movement towards a full understanding of SOA formation and its implications. Inclusion of both oligomerization reactions and organosulphate chemistry in air quality models should be undertaken cautiously given the large uncertainties in the rates and mechanisms of such processes under atmospheric conditions. It is an open area of debate about whether bimolecular condensed-phase reactions may occur at a higher rate in chamber experiments than the atmosphere because SOA concentrations will be diluted in ambient aerosol due to pre-existing aerosol (Chan *et al.*, 2007).

2.2.6.3 Heterogeneous oxidation

A second process that may also affect organic aerosol is oxidation by gas-surface interactions (heterogeneous aging). In a number of studies, it has been shown that O₃ can readily oxidize alkenes that sit near the particle surface (Rudich, 2003), however indications are that this chemistry is much slower when the alkene is part of mixed composition particles (Knopf *et al.*, 2005). Particle phase also has a strong effect on the kinetics with reactions proceeding faster in liquids than in solids (Rudich, 2003). Oxidation may also occur with gas-phase radicals such as OH and NO₃ (Bertram *et al.*, 2001; Moise *et al.*, 2002; Molina *et al.*, 2004). The aerosol matrix can significantly affect the rates of heterogeneous reactions when reactions involve a surface process (Kwamena *et al.*, 2007; Rudich *et al.*, 2007). Laboratory results show reduced O₃ uptake in mixtures designed to mimic ambient particles compared to single component particles. Evidence suggests that biomarkers, such as hopanes and oleic acid, are subject to some oxidative loss during photochemically active times (Robinson *et al.*, 2006). There is currently scientific debate, however, about whether sufficient reductions in O₃ uptake have been observed on mixed laboratory particles to explain the observationally-derived lifetimes of organic aerosol tracers (e.g. oleic acid). Oxidation is expected to make the aerosol more oxygenated, less volatile, and more hygroscopic (Broekhuizen *et al.*, 2004). As with the oligomerization and organosulphate chemistry, care should be taken when incorporating these processes into air quality models as many uncertainties in the kinetics and mechanisms remain.

Field observations indicate that there is an increase in the degree of oxidation of the organic aerosol component of regional plumes with the age of the air (de Gouw *et al.*, 2005). In particular, the development of in situ characterization of aerosol composition using on-line mass spectrometry has illustrated that within urban regions the organic aerosol is best characterized by a hydrocarbon-like component (HOA), likely arising from some components of unburnt fuel oil and lubricating oil, whereas in regions downwind from cities a more highly oxygenated organic aerosol (OOA), characteristic of the regional background, is more prevalent. Factor analysis techniques that deconvolute the less and more oxidized components of the aerosol are being used to quantify this transformation in the field (Zhang *et al.*, 2005b). There is no doubt that the OOA factor is associated with aerosol aging. The increase in OOA is

highly correlated with increasing photochemical age and increasing hygroscopic growth. The size distribution of the HOA factor tends to favour the smallest particles whereas the OOA factor typically dominates the 200-300 nm diameter size range (where the surface area distribution and condensation rates maximize). The sources of the compounds composing the OOA factor remains under debate.

There is emerging experimental evidence that heterogeneous chemistry on the surface of particles can feedback and have implications on gas-phase chemistry (NO_x processing, VOC oxidation and thus O_3). Brown *et al.* (2006) studied the efficiency of N_2O_5 hydrolysis¹⁰ on aerosol in the nocturnal atmosphere over the northeastern United States. They were able to experimentally determine N_2O_5 uptake coefficients based on measurements of N_2O_5 and NO_3 in regionally processed plumes downwind of urban centres and coal-fired power-plant sources. Brown *et al.* showed that there is considerable processing of NO_x at night via N_2O_5 hydrolysis. The rate of N_2O_5 hydrolysis was highly variable depending on aerosol composition, particularly the sulphate content. These results have important implications on regional O_3 production and suggest a stronger interaction between anthropogenic SO_2 and NO emissions than previously recognized. Section 2.6 will assess the potential impacts of N_2O_5 hydrolysis on emission reduction strategies.

Recent boundary layer measurements have revealed a strongly enhanced formation of nitrous acid (HONO) during the daytime which cannot be accounted for in current air quality models. HONO is a significant photochemical precursor to OH. Field studies have indicated an unaccounted for photolytic source of HONO in forests, on rural mountain sites, and above arctic snow packs. Stemmler *et al.* (2006) exposed humic acid films to NO_2 in an irradiated gas flow tube and found that the reduction of NO_2 was an important source of HONO. Their findings indicate that soil and other surfaces containing humic acid exhibit an organic surface photochemistry that produces reductive species which can react with NO_2 . The observed rate of HONO formation may explain the recently observed high daytime HONO mixing ratios in the boundary layer, the photolysis of which accounts for significant OH production, as discussed in Section 2.2.3.1.

An unidentified diffuse source of VOCs in the free troposphere may arise from the heterogeneous oxidation of organic aerosol. Researchers studying the OH-initiated oxidation of organic aerosol have found evidence for substantial carbon-carbon bond breakage occurring

¹⁰ Hydrolysis – chemical reaction where one of the reactants is water

in saturated alkyl chains, giving rise to small volatile carbonyls and acids (Molina *et al.*, 2004). Compared with gas-phase reactions, the surface reactions are faster (Molina *et al.*, 2004; Wadia *et al.*, 2000). This could represent a significant source of small VOCs to the troposphere (Kwan *et al.*, 2006).

2.2.6.4 Cloud processing

Clouds provide a medium to concentrate soluble species and increase the rates of photolytic processes. It was discussed earlier in Section 2.2.3 that in-cloud sulphur oxidation contributes extensively to aerosol mass production in coal-fired power plant plumes (Gong *et al.*, 2006). However, on regional and remote scales when the gas-phase mixing ratio of SO₂ decreases, it is postulated that in-cloud production of organics might be an important source of particle growth. For example, it has been shown that aqueous phase reactions are a source of oxalic acid which is a ubiquitous particle phase component. Maria *et al.* (2004) provide experimental evidence for in-cloud production of organic aerosol. Different aging scenarios (surface-limited oxidation, volume-limited oxidation and condensation) were identified to have different sensitivities to ratios of the measured aerosol carbonyl content, total carbon content and total mass. Evidence for organic condensation and volume-limited organic oxidation was observed during fog events when the aerosol contained significant particle-bound water.

2.2.6.5 Summary of Organic Aerosol Aging

Table 2.3 Aging time defined as the lifetime to convert hydrophobic aerosol to hydrophylic aerosol.

Aerosol Type and Conditions	Aging Lifetime	Reference
Soot	39 hr	Cooke and Wilson (1996)
Organic carbon	1 week	Maria <i>et al.</i> (2004)
Hoptane in ambient aerosol Oleic acid in ambient aerosol	1 day (summer) several days (winter)	Robinson <i>et al.</i> (2006)

Table 2.3 lists aging lifetimes for conversion of hydrophobic carbonaceous aerosol. Current estimates span 1 day to 1 week suggesting that considerable processing of primary carbonaceous aerosol occurs given that best estimates of mean particle age are 4-7 days. As plumes age from urban to regional scales, SOA evolves by the condensation of semi-volatile species onto pre-existing particles, by reactions that lead to oligomer formation in the particle phase, by heterogeneous oxidation of the particle surface and possibly by cloud processing. The degree to which each of the above mechanisms dominate the evolution of aerosol composition within regional plumes remains uncertain and a subject of current research.

2.3 Hygroscopic Growth and Cloud Nucleation

The extent to which aerosol particles adsorb and lose liquid water as the ambient relative humidity (RH) changes affects visibility in polluted environments, the aerosol direct radiative forcing on climate, reactive aerosol chemistry, the removal rates of aerosols by wet deposition, and the ability of particles to penetrate deep into the human respiratory system. As described earlier, it is now apparent that aged or processed tropospheric aerosol has a high degree of internal mixing between different aerosol components whereas fresh emissions are more chemically distinct. Recent research has focused upon characterization of the hygroscopic behaviour of mixed composition particles, with a focus on particulate organics. A related issue is the phase, i.e. solid or liquid, in which particles exist in the atmosphere. General concepts associated with aerosol hygroscopic growth will be described first. Research results will then be summarized for pure aerosol types – soluble inorganics, organics, mineral dust, soot – and for internally mixed particles. Cloud nucleation studies have important implications on aerosol indirect radiative forcing mechanisms, precipitation and acid deposition.

2.3.1 General Behaviour

Water-soluble, single-component particles exhibit distinct phase transitions from solid-to-aqueous (deliquescence¹¹) and from aqueous-to-solid (efflorescence¹²) forms (Martin, 2000). These transitions occur at well-defined RHs, with the efflorescence RH lower than the deliquescence value because of kinetic limits to the rate of crystallization. An implication of this hysteresis¹³ is that the prediction of a particle's phase requires not only the current RH but also the history of RH conditions experienced by the particle over its lifetime. The lowest efflorescence RHs occur when the phase transition occurs homogeneously, involving a direct conversion of supersaturated solution to solid. The presence of insoluble inclusions within the particle may give rise to heterogeneous nucleation instead, where the inclusion facilitates the formation of solid. In this case the efflorescence RH is higher than the homogeneous value.

¹¹ Deliquescence - relative humidity where dissolution of solute occurs to form a wet particle

¹² Efflorescence – relative humidity where crystallization of solute occurs to form a dry particle

¹³ Hysteresis – particle can be either in a meta-stable liquid phase or a stable dry phase depending on the history of RH conditions experienced by the particle

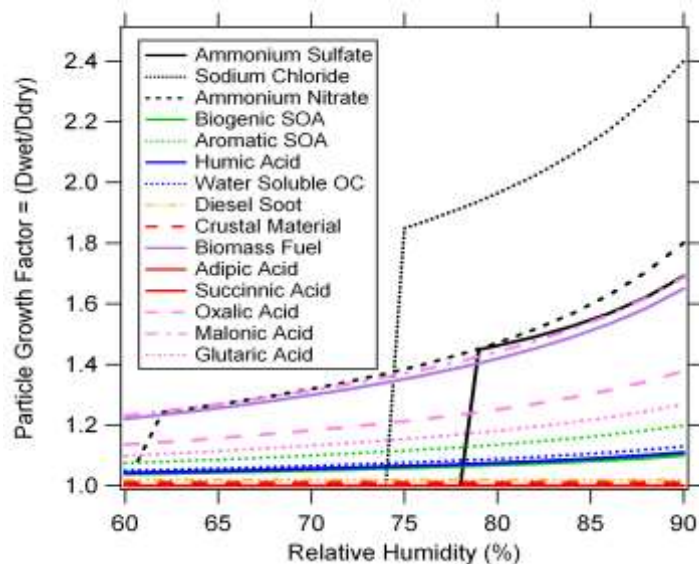


Figure 2.8 Hygroscopic growth curves for selected single-component particles and particles generated from single precursor VOC oxidation chamber experiments (termed “Biogenic SOA” and “Aromatic SOA”).

The hygroscopic growth factor (GF) describes the change in particle diameter, D , that occurs when the RH is raised from low (typically 20% or less) to high values (80% or higher) ($GF = D \text{ (at high RH)} / D \text{ (at low RH)}$). Discrete changes in the growth factor as a function of RH are indicative of phase transitions whereas continuous changes are indicative of a particle with aqueous components continually taking up water and growing. Atmospherically significant growth factors involve more uptake of water than occurs when a single layer of water binds to a particle’s surface; instead, a significant fraction of the particle volume is involved. Figure 2.8 presents hygroscopic growth factors for single component particles and particles produced during single VOC oxidation experiments.

Particle hygroscopic growth at RHs above 100% leads to cloud formation. If the RH is saturated with respect to liquid water, then liquid water cloud droplets can form. Processes that give rise to efficient droplet formation are the presence of highly soluble species that lower the vapour pressure of the growing droplet and surface species that lower its surface tension. At low temperatures, the RH can become saturated with respect to ice, and ice crystals can form directly. Particles that promote ice formation are usually solids, including mineral dust and some solid organics and inorganics.

2.3.2 Soluble Inorganics

The efflorescence and deliquescence behaviour of single component soluble species, such as ammonium sulphate or sodium chloride, is well documented with deliquescence occurring at the thermodynamic value and efflorescence at much lower values (Seinfeld and Pandis, 1998).

It is now known that other simple inorganics, such as ammonium nitrate, ammonium bisulphate and sulphuric acid, do not homogeneously effloresce under atmospherically relevant conditions (Martin, 2000). If impurities are not available for heterogeneous efflorescence then these species once in solution will not crystallize back in the troposphere. Also, simple mixtures of inorganic systems initially deliquesce at lower RHs than do their individual components (Tang and Munkelwitz, 1993). On the other hand, the presence of insoluble inclusions, such as a variety of metal oxides, increases the likelihood of crystallization which will be dependent upon the surface properties and size of the solid (Pant *et al.*, 2006). The presence of soot inclusions appears to not affect crystallization rates to a significant degree (Pant *et al.*, 2006).

2.3.3 Organics

The organic composition of aerosols is highly complex and can include highly soluble species (such as low molecular weight dicarboxylic acids), larger soluble species (such as levoglucosan), higher molecular weight, polyfunctional oxygenated species (as might be formed by oligomerization or by gas-to-particle conversion of oxidized biogenics), and insoluble species (such as long-chain fatty acids). It has been shown that the soluble species behave as do soluble inorganics, exhibiting distinct phase transitions (Peng *et al.*, 2001; Braban *et al.*, 2003). The higher molecular weight species are significantly less soluble and tend to show no distinct phase transitions in hygroscopic growth experiments, perhaps indicating that they exist in supersaturated states that more readily absorb water than would be the case had they crystallized at low relative humidity (Brooks *et al.*, 2004; Badger *et al.*, 2006). In general, the overall growth factors of these low solubility species are considerably lower than those of pure, soluble inorganics, such as ammonium sulphate.

2.3.4 Mineral Dust

The growth factors of mineral dust particles are small compared to those of soluble inorganics and many organics. This is consistent with water uptake being confined to the surface of the particles. One exception arises in the case of carbonate-containing particles. In this case, gas-phase nitric acid can react with the particle to form calcium nitrate, giving rise to considerably higher hygroscopic growth factors than exhibited by fresh, unprocessed mineral dusts.

2.3.5 Soot

The growth factors of freshly emitted soot particles are also small, indicative of little interaction of atmospheric water beyond surface adsorption. This is consistent with our understanding that diesel soot, for example, is primarily composed of both elemental carbon and large hydrocarbons that come from lubricating oil used in the engine. Both of these components are highly hydrophobic.

2.3.6 Internally Mixed Particles

Mixtures of more than one soluble component generally exhibit reduced deliquescence and efflorescence RHs relative to behaviour exhibited by the corresponding single component particles (Brooks *et al.*, 2003; Parsons *et al.*, 2004; Braban and Abbatt, 2004; Marcolli *et al.*, 2004). If one component remains a major fraction of the aerosol, then the effects may not be substantial. This would be the case for a particle that is primarily ammonium sulphate with a small amount of organic present, or a marine particle where sodium chloride dominates. However, if comparable amounts of two components are mixed (for example, of ammonium sulphate and a soluble diacid) then the resulting particles do not readily homogeneously effloresce (Parsons *et al.*, 2004; Braban and Abbatt, 2004). For the situation frequently encountered in the boundary layer where many organic and inorganic constituents are internally mixed within accumulation mode particles, it is possible that little crystallization of the soluble constituents will occur. As described above, this will be especially true if the particles are not fully neutralized by ammonia (NH₃). If insoluble species are also present, a mixed phase particle may result.

A second general finding is that the hygroscopic growth factor increases as soluble constituents are added to a low solubility particle (Hameri *et al.*, 2002; Brooks *et al.*, 2004; Badger *et al.*, 2006). Examples include the condensation of sulphates or secondary organics onto either soot or mineral dust particles. This occurs with aged, accumulation mode particles in polluted environments that frequently contain a number of much smaller soot inclusions. The hygroscopic growth of these particles is dominated by the soluble component.

A major uncertainty arises from there being few measurements of particle phase in the atmosphere. With knowledge of phase, composition and mixing state, there is confidence that the sub-saturated hygroscopic growth factors could be predicted with some accuracy given that simple linear mixing models appear to describe hygroscopic growth accurately (Aklilu *et al.*, 2006).

Hygroscopic growth factor measurements in the field indicate that continuous water uptake is common (Aklilu and Mozurkewich, 2004). There are few examples of discrete changes of the growth factor as a function of RH that would be indicative of phase transitions. This implies

that a sizable component of accumulation mode, mixed organic-sulphate particles exist in a thermodynamically metastable aqueous state, in accord with the laboratory studies described above on mixed particles. The degree to which solid inclusions promote crystallization of a subset of these particles is not known.

2.3.7 Cloud Nucleation

Cloud processing of pollutants can be a source for aerosol growth if the cloud droplets evaporate; however, the incorporation of aerosol particles into cloud droplets represents a major loss mechanism for aerosols when the droplets precipitate (see Section 2.4, Wet Deposition). Cloud processing of pollutants is also a source of acid precipitation.

Our understanding of the cloud-activating properties of pure soluble inorganics, mineral dust and soot is quantitatively well advanced, i.e. soluble species actively promote droplet activation¹⁴ whereas insoluble species do not. On the other hand, the organic component is harder to characterize, with lab experiments indicating that solubility is usually also the key factor (Broekhuizen *et al.*, 2006). In closure experiments from the field where the number of cloud condensation nuclei (CCN) are both measured and calculated from measured aerosol composition and size distributions, there are uncertainties as to how to simulate the organic mode accurately, whereas particles that are largely inorganic are modelled well (Roberts *et al.*, 2002; Broekhuizen *et al.*, 2006).

For the organics, the degree of WSOC is variable from location to location, its average molecular weight is not well known, and the degree of surface tension reduction by the organics is very poorly characterized. In a study in downtown Toronto, best closure between predicted and measured CCN levels was obtained when the organics were modelled as being fully insoluble, as expected if they arise largely from combustion exhaust (Broekhuizen *et al.*, 2006). At semi-rural sites and those impacted by biogenics (Roberts *et al.*, 2002; Stroud *et al.*, 2007; Chang *et al.*, 2007), the organics exhibit some activity towards droplet activation although it is unclear whether it arises from surface tension reduction or through water solubility.

¹⁴ Activation – critical droplet size where further water uptake reduces the water vapour equilibrium with the droplet surface (due to flatter droplet surface) promoting further water uptake

For cloud droplet formation, the water uptake properties of particles with mixed compositions consisting of appreciable amounts of soluble material can be accurately modelled if their composition and size distributions are known. For these situations, the uncertainties associated with the organics are not nearly as important as they are when the particles are largely organic. Research needs to be focused on this latter case, where particles are formed in biogenically-rich environments or are emitted directly from combustion sources.

The kinetics of water uptake within a cloud updraft can also have an impact on the maximum supersaturation¹⁵ achieved and the overall number of cloud droplets activated. Organic compounds in aerosol can take a finite time to dissolve resulting in a slower rate of water vapour uptake which can promote higher maximum supersaturation in cloud updrafts. Organic films on aerosol can also slow the kinetic process of water uptake. The role of bio-aerosol (pollens, spores, bacteria, fungi) to act as giant CCN is another emerging area of research. Studies suggest giant CCN can reduce cloud number, reduce cloud albedo, and promote initiation of rainfall.

Formation of ice particles under the low temperature conditions frequently encountered in Canada is not as important for aerosol removal as is formation of liquid water droplets. For one, the fraction of the background aerosol that forms ice is much smaller than that which forms liquid water droplets, under saturated conditions. Second, the temperature has to be quite cold for ice formation to prevail over liquid water formation, in particular for mixed sulphate-organic particles.

2.4 Deposition of Gases and Particles

2.4.1 Dry Deposition of Gases

In the absence of precipitation, dry deposition is the main process that removes chemical species from the atmosphere. Dry deposition of gaseous species is influenced by a number of factors including meteorological conditions, characteristics of underlying surfaces and the species' physical and chemical properties. There are many field measurements of dry

¹⁵ Supersaturation – an environment where the water vapour pressure exceeds saturation vapour pressure

deposition fluxes for O₃, SO₂, HNO₃, NO₂ and NH₃ and some limited measurements for several other species such as peroxyacetyl nitrate (PAN), H₂O₂, nitrous acid (HONO), formaldehyde (HCHO), formic acid, and organic peroxides (Wesely and Hicks, 2000; Zhang *et al.*, 2002).

Stomatal¹⁶ fluxes contribute much more than non-stomatal¹⁷ fluxes to total O₃ depositional fluxes during dry daytime conditions over vegetated surfaces. Non-stomatal fluxes are more important under dark and wet conditions. On an annual basis, non-stomatal uptake of O₃ contributes at least 40-60% to total fluxes depending on canopy type. Wetness generally increases the non-stomatal uptake of O₃, though it may decrease stomatal uptake due to stomatal blocking by water drops (or films) (Zhang *et al.*, 2003). Non-stomatal uptake pathways are less important for species with very low solubility (e.g. NO₂, PAN) but can be much more important for species with high solubility (HNO₃, NH₃).

The resistance-analogy approach has been commonly used for studying dry deposition processes (Wesely, 1989; Zhang *et al.*, 2003). The concept of a dry deposition velocity has been developed to describe an equivalent velocity for the flux of mass loss through the ground. The dry deposition velocity (V_d) to vegetation and other surfaces is defined by Equation (1).

$$V_d = \frac{1}{R_t} = \frac{1}{R_a + R_b + R_c} \quad (1)$$

where R_t is the total resistance which is the sum of aerodynamic resistance, R_a, quasi-laminar sublayer resistance, R_b, and surface or canopy resistance, R_c. R_a is only a function of micrometeorological conditions and the roughness characteristics of the underlying surface, so it is independent of chemical species. R_b is a function of friction velocity and the molecular diffusivity of each chemical species. R_c is the most complex term depending on meteorological conditions, biological information and gaseous species' properties.

Most R_c parameterizations include stomatal and non-stomatal portions. Models for stomatal resistance range from simple parameterizations as functions of solar radiation and time of day to one- or two-big-leaf approaches which include the effect of photosynthetically active

¹⁶ Stomatal – tiny pore on a leaf used for gas exchange

¹⁷ Non-stomatal – deposition occurs to the leaf surface, barks, soil, water, snow, etc.

radiation, air temperature, water vapour pressure deficit and water stress (leaf water potential). For non-stomatal resistance, earlier studies used a constant typically chosen for a particular season and land type (e.g., Wesely, 1989), thereby ignoring many processes that can affect this deposition pathway. Based on the data analysis of O₃ and SO₂ deposition fluxes measured over five different canopies (mixed forest, deciduous forest, corn, soybean and pasture) in the eastern United States, a new non-stomatal resistance was developed as a function of friction velocity, relative humidity and leaf wetness. As a consequence, an updated big-leaf model with the newly developed non-stomatal resistance parameterization and a sunlit/shade (or two-big leaf) stomatal resistance sub-module was developed by Zhang *et al.* (2003). In this model, O₃ and SO₂ were taken as two base species similar to the approach used in Wesely (1989). Non-stomatal resistance for other gaseous species were calculated by scaling to O₃ and SO₂. Thirty gaseous species and 26 different land use categories were considered in this model. Deposition velocities for most gaseous species are in the range 0.1-1 cm s⁻¹.

For those species that are also emitted from the surface (e.g., NH₃, NO₂), bi-directional exchange models are needed to quantify their dry deposition (e.g., Sutton *et al.*, 1998). However, validation of such models over different land types and under different meteorological conditions has yet to be done in order to generalize these models for applications in large-scale models.

2.4.2 Dry Deposition of Particles

Particle dry deposition is a slower process compared to particle wet deposition; however, it is a continuous process that occurs at all times over all surfaces, as opposed to wet deposition, which is more episodic. At some times of the year and in some regions, the accumulated removal by dry deposition can be more important than wet removal. Besides meteorological conditions and the characteristics of underlying surfaces, particle size is another important factor that affects its deposition rate.

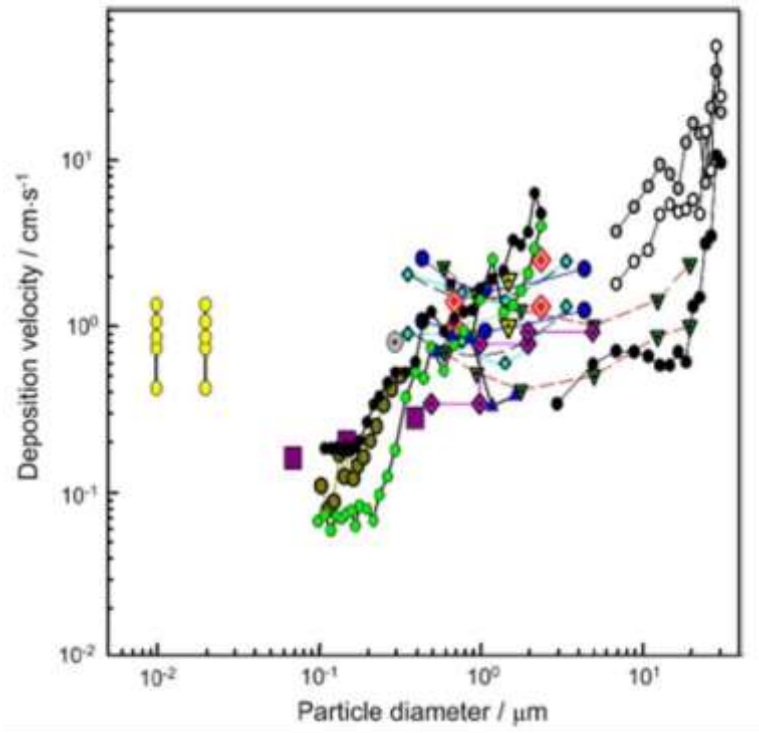


Figure 2.9 Particle deposition velocities to forest and agricultural canopies (compiled in Zhang and Vet, 2006; original data and symbol coding from Gallagher *et al.*, 1997)

Most measurements on particle dry deposition fluxes made between 1970 and 1990 did not discriminate for particle size due to the limitations in particle measurement techniques. The development of more sophisticated measurement techniques in the 1990's made it possible to measure size-resolved particle physical and chemical properties. V_d generally increases with particle size for particles larger than $2 \mu\text{m}$ because the collection efficiency¹⁸ by interception and impaction increases with particle size. Particles larger than $2 \mu\text{m}$ tend to have a deposition velocity as high as a few cm s^{-1} over rough forests. V_d also increases with the decrease of particle size for particles smaller than $0.1 \mu\text{m}$ since the collection efficiency by Brownian diffusion¹⁹ is larger for smaller particles. Figure 2.9 summarizes dry deposition velocities as a function of particle size. Available measurements show that V_d of ultra-fine particles (< 0.01

¹⁸ a parameter defined as the ratio of the total number of aerosols collected by falling drops to the total number of aerosols within the swept volume of falling drops

¹⁹ Brownian diffusion – random movement of particles in the air

μm) at field conditions can be higher than 5 cm s^{-1} . V_d for particles in the size range of 0.1-2 μm is lowest and can vary by several orders of magnitude. Many earlier laboratory experiments over smooth surfaces, such as grass, suggest that the deposition velocity for this size range of particles should be of the order of 0.01 cm s^{-1} or less. Higher values have been obtained in many recent field studies over smooth and rough surfaces (Zhang and Vet, 2006; Pryor *et al.*, 2008).

The resistance analogy is also used for the parameterization of particle deposition velocity. Recently developed models now calculate particle dry deposition velocity as a function of particle size (see a review in Zhang and Vet, 2006). Current estimates compared to earlier models (Ruijgrok *et al.*, 1995) reveal the largest differences in calculated dry deposition velocity are for the 0.1-1.0 μm particle size range. Zhang *et al.* (2001) developed a size-resolved deposition model which produces higher V_d values for submicron particles than most earlier models ($0.1\text{-}1 \text{ cm s}^{-1}$ over vegetated surfaces). The model also produces slightly higher V_d over coniferous trees than over broadleaf trees. A similar model was also used by Nho-Kim *et al.* (2004). Although the models in Zhang *et al.* (2001) and Nho-Kim *et al.* (2004) seem to be able to produce higher V_d values for submicron particles compared to many earlier dry deposition models, the minimum V_d produced by these models is shifted to larger particle sizes (e.g., 1-2 μm). The minimum V_d in Slinn's (1982) model, in contrast, appears at particle sizes of 0.2-0.4 μm . Further studies are needed to parameterize particle dry deposition over different surface types and meteorological conditions.

2.4.3 Wet Deposition of Gaseous Species

Wet deposition of gaseous species includes 1) mass transfer from air to cloud droplets which can grow into rain drops (often referred to as rain out) and 2) the direct scavenging of gaseous species by falling rain drops (referred to as below-cloud scavenging or wash out). Current wet deposition parameterizations used in large-scale chemical transport models vary substantially and have large uncertainties. A comparison of results of 15 global models shows that the largest uncertainties exist in the upper troposphere for species undergoing wet scavenging processes (Rasch *et al.*, 2000). Several identified causes of uncertainties for soluble gas removal in large scale models include (1) unrealistic treatment of subgrid cloud scales, (2) using bulk droplet rather than size-resolved droplet aqueous-phase chemistry, and (3) using Henry's law equilibrium rather than a kinetic limitation approach.

Cloud processes are subgrid scale in global models since clouds and precipitation usually only occupy part of a grid volume. The spatial distribution of the clouds within a column and the ways they overlap each other further complicate the issue. The simplest approach for handling this situation was to scale the wet deposition using the cloud fraction within a model grid.

More recent studies have tried to distinguish large-scale and convective clouds by treating the wet deposition in convective clouds differently from the large-scale clouds, e.g. using the mass flux calculated from a convective cloud scheme (Barth *et al.*, 2000).

Due to the high computational cost of size-resolved aqueous-phase chemistry, a bulk description of this process is typically used in three-dimensional chemical transport models. One example of errors caused by using bulk rather than size-resolved aqueous-phase chemistry is the significant under-prediction of sulphate production in cloud water. A comparison of several bulk and size-resolved parcel models confirms previous studies, i.e., the size-resolved models consistently calculate 2–3 times more oxidation via the $\text{SO}_2 + \text{O}_3$ pathway due to the calculated cloud water pH variability among cloud droplets (Barth *et al.*, 2003).

The Henry's law equilibrium approach is often used to determine the mass transfer of a chemical species from the gas phase into hydrometeors²⁰. However, a chemical species may not attain equilibrium on the timescales of the cloud model's time step because of slow mass transfer between phases (Herrmann *et al.*, 2000). A field study by Sellegri *et al.* (2003) showed that nitric and hydrochloric acids can be considered close to Henry's law equilibrium while the dissolution of NH_3 and carboxylic acids from the gas phase into cloud droplets is kinetically limited. Using the gas-liquid equilibrium in chemistry models can lead to overestimation of scavenging of soluble gases by raindrops (Barth *et al.*, 2001).

The simplest approach for below-cloud scavenging in large-scale models is to parameterize this process as a first order loss rate using a scavenging coefficient, S_c . S_c is commonly parameterized as a simple function of the precipitation rate, mean raindrop size and species' physical and chemical properties (e.g., Mircea *et al.*, 2004; Gong *et al.*, 2006). Only a few gases (e.g., H_2SO_4 , HNO_3 , NH_3) are considered in large-scale models and their scavenging rates are based on analogy to water vapour deposition rate on snow and ice (Gong *et al.*, 2006). Further studies are needed in developing better parameterizations for below-cloud scavenging of gaseous species.

²⁰ Hydrometeor – any water or ice particle that has formed in the atmosphere due to sublimation or condensation.

2.4.4 Wet Deposition of Particles

Atmospheric particles can be incorporated into hydrometeors through nucleation scavenging (serving as CCN or ice nuclei) or impaction scavenging (being collected by falling hydrometeors, including cloud droplets, raindrops, and snow crystals). In-cloud scavenging of particles includes contributions from both nucleation and impaction scavenging while below-cloud scavenging only includes contributions from impaction scavenging. Nucleation scavenging was discussed in Section 2.3.7. In this section, only below-cloud scavenging is discussed.

For practical considerations, below-cloud scavenging of particles is also represented by a scavenging coefficient (S_c), as is done for gaseous species, in the aerosol mass continuity equations in large-scale atmospheric chemistry models. Particles ranging from 0.01 to 20 μm must be included in these models and S_c values for this size range differ over three to five orders of magnitude. S_c is a function of the collection efficiency (E_c). Usually, E_c is much smaller than 1 because particles can follow the streamlines around the drop. It can however be larger than 1 under certain conditions, e.g., for charged particles.

Brownian diffusion is important for smaller aerosol particles with little inertia and can bring them into contact with the drop, thus increasing their collection efficiency. The Brownian diffusion of particles decreases rapidly as particle size increases and this mechanism will be most important for particles having a diameter smaller than 0.1 μm . Larger sized particles tend to experience inertial impaction because their inertia prevents them from following the rapidly curving streamlines around the falling droplets. Inertial impaction increases with particle size and is important for particles larger than 2 μm . For particles within the size range of 0.1-2 μm , commonly referred to as the ‘Greenfield gap’ in the literature, neither the Brownian diffusion nor the inertial impaction plays an effective role. Thus the collection efficiency is smallest in this size range. For this size range of particles, other collection mechanisms (e.g., charge, diffusiophoresis, thermophoresis) play equivalent roles as Brownian diffusion and inertial impaction.

Some experimental studies have been dedicated to estimating S_c and E_c values under a variety of conditions (see a review in Zhang and Vet, 2006). Jylhä (1999) also derived scavenging coefficients from radar reflectivity based on the fact that both are functions of the hydrometeor size distribution. Parameterizations of bulk S_c currently used in large-scale models are treated as a simple function of known precipitation properties (e.g., $S_c = a\text{PR}^b$, with PR being the precipitation rate and a and b are empirical constants). Size-resolved S_c parameterizations either calculate S_c based on analytical formulas of raindrop-particle collection efficiency, raindrop size distribution, and raindrop terminal velocity, or uses an empirical fit to S_c values derived from field measurements (see a review in Wang *et al.*, 2010).

All of the current theoretical S_c parameterizations under liquid precipitation condition underpredict the S_c values by one to two orders of magnitude for particles smaller than 3 μm compared with most available field measurements or with empirical formulas generated from field observations. The combined uncertainties from known sources are not enough to explain the large discrepancies between the theoretical and experiment studies. The predicted bulk concentrations (integrated over the particle size distribution) from using different theoretical and empirical Λ parameterizations can differ by up to 50% for particle number and by up to 25% for particle mass after just 2-5 mm of rain (Wang *et al.*, 2010).

The stronger dependence of S_c on total droplet surface area than on precipitation intensity (Zhang *et al.*, 2004) suggests that future bulk S_c parameterizations need to include more precipitation properties. The large discrepancies between theoretical and empirical size-resolved S_c values suggest that new collection mechanisms need to be identified in the current theoretical framework through field, laboratory, and numerical studies. Knowledge on impaction scavenging by solid precipitation is more limited and thus more studies are also needed on this topic. Newly developed S_c parameterizations should be evaluated against detailed cloud microphysics models and size-resolved field measurements under different precipitation intensities.

2.5 Meteorological Influences on Air Quality

Air quality is influenced by the vertical mixing and horizontal advection of gases and aerosol during transport away from pollution sources. In this section, the discussion is limited to a general description of the vertical structure of the boundary layer. Chapter 8 includes a summary of recent research studies related to local and regional circulation patterns. Chapter 9 includes a discussion of long range transport with a summary of recent research studies related to Asian influences on North America.

2.5.1 Vertical Mixing and Plume Dispersion

Gases and particles are emitted into the boundary layer, defined as a relatively thin layer of air near the ground that responds to surface forcings with a timescale of up to an hour. These forcings include frictional drag, evaporation, transpiration, heat transfer and terrain induced mixing. The daytime boundary layer is highly turbulent, implying a nearly ubiquitous presence of random, three dimensional rotational motion that can mix air pollutants rapidly. Convection is driven by heat transfer from a warm surface which creates thermals of rising air. Radiative cooling from the top of a cloud layer can create downdrafts sinking from cloud top. Boundary layers driven by convective turbulence are often called mixed layers because the layer is well mixed vertically. In addition to convective turbulence, there are sources of mechanical

turbulence generated by surface elements (e.g., trees, buildings) and topography which exert drag forces on the boundary layer. Wind shear across the top of the mixed layer can also generate mechanical turbulence.

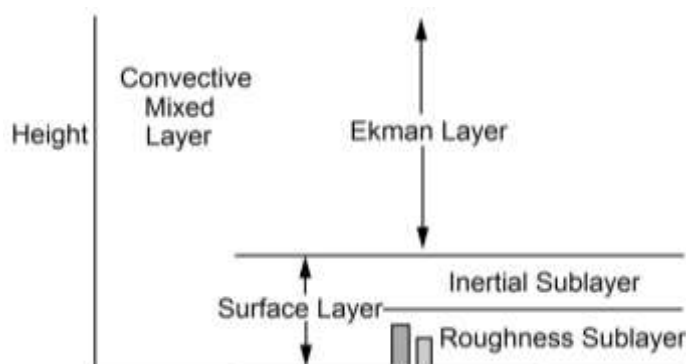


Figure 2.10 The convective mixed layer can be divided into a surface layer and an Ekman layer. The surface layer can be further sub-divided into an inertial sublayer and a roughness sublayer. The surface layer is typically 0.1 of the boundary layer height.

As illustrated in Figure 2.10, the boundary layer (or convective mixed layer) can be divided into an outer layer (often termed Ekman layer) and a surface layer. The Ekman layer is largely sheltered from the surface forcings; its characteristics derive, in part, from the Earth's rotation. The surface layer is generally defined as a mixed layer near the ground where turbulent stresses vary by less than 10% (Stull, 1988). During the daytime over land surfaces, the surface layer often forms the lowest hundred meters of a convectively mixed layer. The surface layer is further subdivided into inertial and roughness sublayers. The inertial sublayer functions as a matching layer where the description of motions from both the surface layer and Ekman layer are valid and has a constant vertical transport of atmospheric properties (heat, momentum, pollutants). The roughness sublayer is mostly driven by surface forcings.

Virtual potential temperature, θ_v , profiles are useful in diagnosing the stability of the boundary layer. θ_v is the temperature an air parcel would have if all the water vapour were removed and the corresponding specific energy were added to the parcel then displaced vertically to an air pressure of 1000 hPa without any energy exchange with the surrounding air. In the surface layer, one often finds a superadiabatic layer (decrease in θ_v with height) adjacent to the ground. θ_v profiles are nearly adiabatic (no change in θ_v with height) in the middle portion of the mixed

layer. An increase in θ_v with altitude is characteristic of the entrainment²¹ zone at the interface between the boundary layer and free troposphere and is thus termed the inversion height or boundary layer height. An accurate model calculation of meteorological parameters that affect the mixing of chemical species (such as boundary layer height, friction velocity and eddy diffusivity) is extremely important for accurate predictions of air quality. Further details on the importance of boundary layer parameterizations for dispersing air pollutants can be found in Section 8.3.

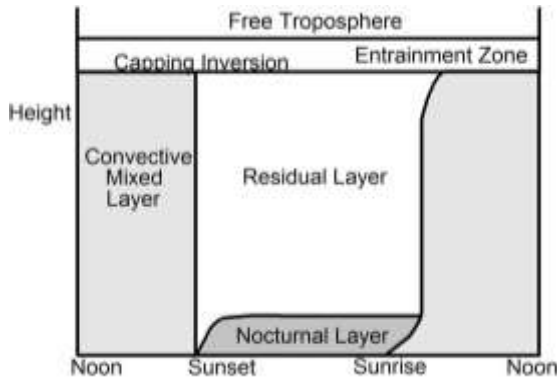


Figure 2.11 Diurnal time series of the vertical stability of the atmosphere.

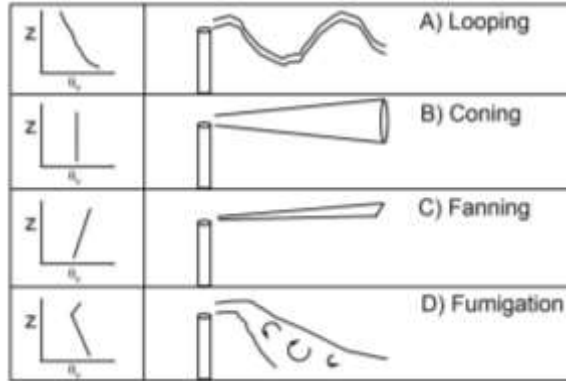


Figure 2.12 Plume structures in the atmosphere for different vertical profiles of virtual potential temperature (θ_v).

²¹ Entrainment – mixing of air across the interface between two air masses (e.g. boundary layer and free troposphere)

As shown in Figure 2.11, over land surfaces in high pressure regions, the boundary layer has a well-defined structure that evolves with the diurnal cycle. Mobile, area, biogenic and lower elevation point sources are emitted into the surface layer. Starting about a half an hour after sunrise, a turbulent mixed layer begins to grow in depth. It grows by entraining less turbulent air from above. The mixed layer reaches its maximum height in the late afternoon. Pollutants emitted into a convectively well mixed layer often exhibit a looping structure with distance from the surface source (Figure 2.12a). A stable entrainment layer at the top of the mixed layer acts as a lid to rising thermals. A mixing down of air from the overlying free troposphere is an important characteristic of the entrainment layer. Mixing ratios of pollutants tend to decrease with altitude even within the center portion of the mixed layer. This reflects the emission of pollutants from the surface and entrainment of cleaner air from the free troposphere.

About a half hour before sunset, surface cooling decouples the flow in the upper part of the prior afternoon's mixed layer from the surface layer. The resulting layer of air is called the residual layer because the chemical compounds previously resided in the afternoon mixed layer. The residual layer is often neutrally stratified, driven by weak mechanical turbulence that is nearly of equal intensity in all directions. As a result, pollution plumes in the residual layer tend to disperse at equal rates in all directions creating a cone-shaped plume (Figure 2.12b). A shear-based surface layer remains in place during the nocturnal period, so the residual layer does not have direct contact with the surface.

As the night progresses, the bottom portion of the surface layer is transformed by its contact with the ground into a statically stable boundary layer with weak and sporadic turbulence. Such decoupling of the flow between the residual layer and stable boundary layer leads to a night-time acceleration of the winds at the interface in a phenomenon termed the low-level jet. The developing low-level jet can sporadically enhance wind shears that will generate turbulence. As a result, turbulence sometimes occurs in short bursts that mix pollutants throughout the stable boundary layer. During the non-turbulent times, the flow becomes decoupled from the surface. These nocturnal accelerations of the flow aloft can carry pollution hundreds of kilometres from the source region overnight and thus becomes an important mechanism for regional transport of pollution. Pollutants emitted into the stable boundary layer disperse relatively little in the vertical. They disperse more rapidly in the horizontal resulting in a fanning out of the plume (Figure 2.12c).

After sunrise a new mixed layer begins to grow, eventually reaching the height of the elevated plume from the previous night. At this time, the elevated pollutants are mixed down to the surface in a process called fumigation (Figure 2.12d). In the early morning when the top of the growing mixed layer reaches the base of the residual layer, the mixed layer growth becomes very rapid. During the PACIFIC 2001 field program, lidar scans of the boundary layer over time showed clear evidence of the entrainment of elevated aerosol layers into the growing mixed layer (Strawbridge and Snyder, 2004).

Water vapour often behaves as an excellent passive tracer for diagnosing the evolution of the boundary layer. Water vapour often increases in the surface layer at sunrise due to evaporation. When the top of the mixed layer reaches the bottom of the residual layer, it is common for the water vapour to drop abruptly due to the sinking of drier air from the residual layer. Rapid fluctuations in the water vapour concentration time series is also observed at this point as larger scale eddies are formed.

2.5.2 Mesoscale Circulations and Applications

2.5.2.1 Surface and Topographic Forcing

Boundary layer development can be especially sensitive to local topography. In a valley at sunset, a residual layer occupies the depth of the valley up to and above the surrounding mountains to the capping inversion. However, because the valley surfaces cool first, shallow, downsloping (a.k.a. ‘katabatic’) winds pool cold air at the valley floor, creating a stably stratified layer at the surface, also called a “valley inversion,” and effectively lifting the residual layer aloft. Along with the cold air, downsloping winds pool pollutant aerosol and gases to potentially very high concentrations at the valley floor. During the morning, valley wall and floor heating induces upsloping (a.k.a. ‘anabatic’) winds. The anabatic winds help build a mixed layer upward from the valley floor, gradually replacing the nocturnal valley inversion with a full, turbulent mixed layer extending to the capping inversion aloft (Zoumakis and Efstathiou, 2006).

2.5.2.2 Urban Boundary Layers

An urban surface provides increased height and spatial variation of roughness elements, a heating source due to human activities, and physical surface characteristics that can differ greatly from surrounding vegetated or water surfaces. At night, normal nocturnal boundary layer development may be disrupted due to artificial surface heating and reduced low level stability. Under weak synoptic-scale flow, enhanced sensible heat flux in the urban boundary layer can induce a two-dimensional circulation with a dome of rising air over the urban core supplemented by subsidence in the surrounding rural areas with near surface flow back to the urban core. This mesoscale pattern is called the urban heat island (UHI) circulation. Recent research results suggest that UHIs can display different spatial scales, have different magnitudes and show different diurnal patterns. Arnfield (2003) list the key factors that determine the UHI magnitude:

- UHI intensity decreases with increasing wind speed
- UHI intensity decreases with increasing cloud cover
- UHI intensity is greatest during anti-cyclonic conditions

- UHI intensity is best developed in the summer season
- UHI intensity tends to increase with city size and/or population
- UHI intensity is greatest at night
- UHI may disappear by day

One of the distinguishing characteristics of the urban boundary layer is its roughness sublayer. Anthropogenic structures at the surface can apply significant drag on the boundary layer, impeding the advance of sea-breeze fronts, creating local internal boundary layers and thermal internal boundary layers and modifying the typical pattern of increase in wind speed with increasing height (e.g. wind speed decreasing exponentially rather than logarithmically with height). Simple methods are still needed to estimate UHI intensity within urban areas, as a function of time, weather conditions and structural attributes, for practical applications such as numerical air quality predictions.

2.5.2.3 Marine Boundary Layers and the Sea Breeze

Over large water bodies, the surface is more uniform and lacks the sensitivity of land to daily variations in input of solar energy; the daily variation in surface-emitted heat is low and, hence, has little effect on boundary layer structure. Frequently cloud topped and often neutrally stratified, the marine boundary layer is generally not well mixed (especially outside tropical waters). Assessment of the marine boundary layer height is ambiguous and can correspond to cloud base or cloud top height depending on the location of any sharp change in vertical turbulent transfer. In some near-neutral or slightly unstable cases, a shallow mixed layer may develop, but tends to be much lower in height than that of the ambient temperature inversion.

After sunrise, the land heats faster than the adjacent water, sparking a local circulation above the surface where dense ocean air replaces air at the shore, better known as a sea-breeze or, for suitably large lakes, a lake-breeze. The air heated over the land rises to heights just below about 1 km and spreads out (diverges) promoting sinking of the air over the water, thus completing a two-dimensional circulation (air rising over the land and sinking over water, with a surface wind from water-to-land, and a wind aloft from over land to over water). When this circulation occurs along the length of a coastline, it defines the sea-breeze front (SBF), which advances inland, reducing temperature by several degrees and increasing humidity. The distance the front travels inland is largely dependent on the synoptic scale flow and local geography. At night, the land cools more quickly than the ocean, reversing the direction of circulation, thus creating a land-breeze.

2.6 Conclusions

Table 2.4 Relationship between emission reduction and pollutant concentration.

Emission Reduction	Ozone Response	Sulphate Response	Nitrate Response	Organic Aerosol Response	PM _{2.5} Response
SO ₂ ↓	↑ a	↓	↑ b ↓ a	↑ a ↓ c	↓
NO _x ↓	↑ d ↓ e	↑ f ↓ f	↓	↑ d ↓ e	↓
VOC ↓	↓ g	↓ d ↓ e	↑ d ↓ e	↓	↓
NH ₃ ↓		↓ h	↓	↑ c ↓ i	↓

^a SO₄ – N₂O₅ – NO_x – oxidant feedback (Brown *et al.*, 2006)

^b NH₄ limited conditions

^c aerosol pH – oligomer SOA formation feedback

^d urban - VOC limited conditions – impact on HO_x

^e rural - NO_x limited conditions

^f NO_x impact on O₃ and H₂O₂ with feedback to aqueous SO₂ oxidation rate

^g VOC impact on RO_x production rate

^h cloud water pH impacts SO₂ oxidation rate

ⁱ NH₃ impacts organic acid salt formation

One of the difficulties in predicting the impact of emissions reductions is the uncertain nature of the mechanisms and rates included in current air quality models. In particular, many processes interact non-linearly to result in a disproportionate relationship between change in precursor emission and change in concentration (Table 2.4). Prior assessments focused on the impacts of gas-phase chemistry on secondary particle formation through the formation of semi-volatile products, which can partition to the aerosol phase. Over the past decade, research has continued to elucidate the gas-phase precursors and gas-phase processes forming semi-volatile products; however, the most novel advances have been made in understanding how particle composition can feedback and impact gas-phase chemistry and future particle growth. These advances further complicate the non-linear relationship between precursor emission reduction and benefit. The dependence of N₂O₅ hydrolysis on particle sulphate can play a key role in determining the lifetime of gas-phase NO_x and suggest a stronger interaction between SO₂ and NO_x emissions than previously believed.

Applying an SO₂ emission reduction will result in a sulphate aerosol reduction; however, the accompanying increase in gas-phase NO_x may increase O₃ production, OH production and thus gas-phase organic oxidation rates on regional scales. Similarly, the dependence of particle-phase organic oligomer formation on particle acidity suggests a stronger link between organic aerosol growth and SO₂ emissions than previously identified. Applying an SO₂ emission

reduction could also result in a reduction in secondary organic aerosol from decreased particle-phase oligomer formation. Reductions in SO₂ emissions may also reduce the formation rate of new particles via nucleation. Since these particles act as seeds for condensational growth, an SO₂ emission reduction may further reduce the condensation rate of semi-volatile organics and inorganics. An SO₂ emission reduction may not have a beneficial effect on all particle components. For example, reductions in aerosol acidity due to sulphate decreases will allow more of the available NH₃ to be used in particle nitrate formation. In regions with abundant gas-phase NH₃, an SO₂ reduction results in a change in particle composition from sulphate to nitrate.

Reductions in NO_x emissions can reduce O₃ mixing ratios in NO_x-limited environments (rural areas). Reductions in NO_x can also reduce particle nitrate by decreasing the nitric acid formation rate from the NO₂ reaction with OH. In addition, accompanying decreases in O₃, OH and NO₃ may decrease gas-phase organic oxidation rates and SOA formation. However, under VOC-limited conditions (near combustion sources such as urban centers or power-plant plumes) reductions in NO_x may lead to higher O₃, OH and thus SOA formation and negligible changes in particulate nitrate formation. The limiting reaction in determining the rate of O₃ formation is the RO₂ reaction with NO. A decrease in NO_x and no change in RO₂ levels will result in a decrease in O₃ production. However, if a decrease in NO_x is accompanied by a disproportional increase in RO₂ concentration (due to non-linear chemistry in the VOC limited regime) then O₃ production rates will increase with decreases in NO_x. Over the past decade, studies have shown that under VOC-limited conditions our ability to predict RO₂ levels needs improvement suggesting we are missing some fundamental processes (e.g. RO₂ under-predictions will translate into O₃ under-predictions). Also, O₃ and SOA production is particularly sensitive to the accuracy of the VOC emissions inventory under VOC-limited conditions both in terms of mass emission and emission chemical speciation. Field studies over the past decade have highlighted examples such as the discovery of an underestimate in the emission inventories for olefins in refineries in Houston and Edmonton and biogenic VOCs in forested environments. In particular cases, where NO_x plumes traverse forested environments, the VOC emissions inventory for biogenics becomes critical for determining O₃ and secondary particle production rates. Recent research results suggest there is a significant difference between measured VOC reactivity and calculated VOC reactivity over forested areas due to unaccounted for VOC emissions hypothesized to be sesquiterpenes.

Reductions in NH₃ gas emissions will decrease particle mass directly by decreasing the ammonium concentration (as ion or crystalline solid). Reductions of NH₃ may also 1) decrease nitrate aerosol due to the volatility of HNO₃ in the absence of ammonium aerosol and 2) decrease sulphate aerosol production due to cloud processing and evaporation. However, due to the buffering capacity of NH₃, large reductions in NH₃ will increase the acidity of aerosol, cloud and rainfall. Given the direct environmental effects of acidified precipitation and the non-linearities identified above which accompany an acidified aerosol (enhanced oligomer formation, enhanced N₂O₅ hydrolysis) it is unwise to devise an emission reduction strategy

based solely on reducing NH_3 emissions. Because of the complex factors briefly discussed above, air quality is unlikely to be improved by reducing a single pollutant but will require concurrent reductions in NH_3 , SO_2 , NO_x and VOCs. The continued development of air quality models that can account for the non-linearities in the chemical, microphysical and meteorological processes will be fundamental to improving the reliability of emission reduction strategies in the future.

2.7 Future Research Directions

Emission-based air quality models are only as good as our understanding of the emissions and processes formulated in the modelling systems. Below is a summary of key processes which need improved understanding from a combination of laboratory experiments and process-level field studies so that their potential impact on air quality can be assessed within the framework of an air quality model:

- Improvement in emissions information for NH_3 and amines
- Targeted studies addressing our understanding of ozone photochemistry at high NO_x (e.g. role of HONO photolysis and alkene ozonolysis)
- Identify sources and speciation of missing biogenic and anthropogenic VOC emissions not included in OH-reactivity closure studies. What are the implications on O_3 production and SOA production?
- Determine SOA production from VOC precursors under a range of conditions representative of the ambient atmosphere (VOC/ NO_x ratios, SO_2 , RH, oxidation rates, extent of reaction, temperature, ambient particle compositions and loadings)
- Characterize particle phase chemistry including bulk transformation rates for oxidation and oligomer formation
- Characterize heterogeneous chemistry on particle surfaces and impacts on gas-phase HO_x and NO_x budgets (e.g. N_2O_5 hydrolysis, NO_2 reduction to HONO)
- Characterize cloud processing of aerosol components
- Perform field studies to uncover the phase and mixing state of aerosol
- Perform speciated gaseous and particle depositional flux measurements and include their parameterization into air quality models
- Resolve mesoscale circulations, such as land-sea breezes, dry line convergence and urban heat islands and determine their impact on mixing of pollutants and photochemistry

Acknowledgements

The authors would like to thank Jennifer Murphy, Richard Leitch and A. Petroff for reviewing the chapter and providing constructive comments. The authors are also appreciative of the editing performed by Peter Taylor on early drafts of the meteorology section; unfortunately, the meteorology section had to be significantly scaled back due to page restrictions.

References

- Aklilu, Y. -A, and M. Mozurkewich. 2004. Determination of external and internal mixing of organic and inorganic aerosol components from hygroscopic properties of submicrometer particles during a field study in the Lower Fraser Valley. *Aerosol Science and Technology* 38, (2): 140-154.
- Aklilu, Y., M. Mozurkewich, A. J. Prenni, S. M. Kreidenweis, M. R. Alfarra, J. D. Allan, and K. Anlauf, J. Brook, W.R. Leitch, S. Sharma, H. Boudries, D.R. Worsnop. 2006. Hygroscopicity of particles at two rural, urban influenced sites during pacific 2001: Comparison with estimates of water uptake from particle composition. *Atmospheric Environment* 40, (15): 2650-2661.
- Anlauf, K., S. -M Li, R. Leitch, J. Brook, K. Hayden, D. Toom-Sauntry, and A. Wiebe. 2006. Ionic composition and size characteristics of particles in the Lower Fraser Valley: Pacific 2001 field study. *Atmospheric Environment* 40, (15): 2662-2675.
- Armfield, A. J. 2003. Two decades of urban climate research: a review of turbulence, exchanges of energy and water, and the urban heat island, *International Journal of Climatology* 23: 1-26.
- Badger, C. L., I. George, P. T. Griffiths, C. F. Braban, R. A. Cox, and J. P. D. Abbatt. 2006. Phase transitions and hygroscopic growth of aerosol particles containing humic acid and mixtures of humic acid and ammonium sulphate. *Atmospheric Chemistry and Physics* 6, (3): 755-768.
- Banic, C., W. R. Leitch, K. Strawbridge, R. Tanabe, H. Wong, C. Gariépy, A. Simonetti, Z. Nejedly, J. L. Campbell, J. Lu, J. Skeaff, D. Paktunc, J. I. MacPherson, S. Daggupaty, H. Geonac'h, A. Chatt, and M. Lamoureaux. 2006. The physical and chemical evolution of aerosols in smelter and power plant plumes: An airborne study. *Geochemistry: Exploration, Environment, Analysis* 6, (2-3): 111-120.

Barth, M. C., P. J. Rasch, J. T. Kiehl, C. M. Benkovitz, and S. E. Schwartz. 2000. Sulphur chemistry in the national center for atmospheric research community climate model: Description, evaluation, features, and sensitivity to aqueous chemistry. *Journal of Geophysical Research D: Atmospheres* 105, (D1): 1387-1415.

Barth, M. C., A. L. Stuart, and W. C. Skamarock. 2001. Numerical simulations of the July 10, 1996, stratospheric-tropospheric experiment: Radiation, aerosols, and ozone (STERAO)-deep convection experiment storm: Redistribution of soluble tracers. *Journal of Geophysical Research D: Atmospheres* 106, (D12): 12381-12400.

Barth, M. C., S. Sillman, R. Hudman, M. Z. Jacobson, C. -H Kim, A. Monod, and J. Liang. 2003. Summary of the cloud chemistry modelling intercomparison: Photochemical box model simulation. *Journal of Geophysical Research D: Atmospheres* 108, (7): AAC 5-1 AAC 5-19,

Bertram, A. K., A. V. Ivanov, M. Hunter, L. T. Molina, and M. J. Molina. 2001. The reaction probability of OH on organic surfaces of tropospheric interest. *Journal of Physical Chemistry A* 105, (41): 9415-9421.

Braban, C. F., M. F. Carroll, S. A. Styler, and J. P. D. Abbatt. 2003. Phase transitions of malonic and oxalic acid aerosols. *Journal of Physical Chemistry A* 107, (34): 6594-6602.

Braban, C. F., and J. P. D. Abbatt. 2004. A study of the phase transition behavior of internally mixed ammonium sulphate - malonic acid aerosols. *Atmospheric Chemistry and Physics* 4, (5): 1451-1459.

Brock, C. A., M. Trainer, T. B. Ryerson, J. A. Neuman, D. D. Parrish, J. S. Holloway, D. K. Nicks Jr, G. J. Frost, G. Hubler, F. C. Fehsenfeld, J. C. Wilson, J. Michael Reeves, B. G. Lafleur, H. Hilbert, E. L. Atlas, S. G. Donnelly, S. M. Schauffler, V. R. Stroud, and C. Wiedinmyer. 2003. Particle growth in urban and industrial plumes in Texas. *Journal of Geophysical Research D: Atmospheres* 108, (3): ACH 11-1 - ACH 11-12.

Broekhuizen, K., P. P. Kumar, and J. P. D. Abbatt. 2004. Partially soluble organics as cloud condensation nuclei: Role of trace soluble and surface active species. *Geophysical Research Letters* 31, (1): L01107 1-5.

Broekhuizen, K., R. Y. -W Chang, W. R. Leaitch, S. -M Li, and J. P. D. Abbatt. 2006. Closure between measured and modelled cloud condensation nuclei (CCN) using size-resolved aerosol compositions in downtown Toronto. *Atmospheric Chemistry and Physics* 6, (9): 2513-2524.

Brook, J. R., R. L. Poirot, T. F. Dann, P. K. H. Lee, C. D. Lillyman, and T. Ip. 2007. Assessing sources of PM_{2.5} in cities influenced by regional transport. *Journal of Toxicology and Environmental Health - Part A: Current Issues* 70, (3-4): 191-199.

Brooks, S. D., R. M. Garland, M. E. Wise, A. J. Prenni, M. Cushing, E. Hewitt, and M. A. Tolbert. 2003. Phase changes in internally mixed maleic acid/ammonium sulfate aerosols. *Journal of Geophysical Research D: Atmospheres* 108, (15): ACH 23-1 - ACH 23-10.

Brooks, S. D., P. J. DeMott, and S. M. Kreidenweis. 2004. Water uptake by particles containing humic materials and mixtures of humic materials with ammonium sulphate. *Atmospheric Environment* 38, (13): 1859-1868.

Brown, S. S., T. B. Ryerson, A. G. Wollny, C. A. Brock, R. Peltier, A. P. Sullivan, R. J. Weber, W. P. Dubé, M. Trainer, J. F. Meagher, F. C. Fehsenfeld, and A. R. Ravishankara. 2006. Variability in nocturnal nitrogen oxide processing and its role in regional air quality. *Science* 311, (5757): 67-70.

Chan, A. W. H., J. H. Kroll, N. L. Ng, and J. H. Seinfeld. 2007. Kinetic modelling of secondary organic aerosol formation: Effects of particle- and gas-phase reactions of semivolatile products. *Atmospheric Chemistry and Physics Discussions* 7, (3): 7051-7085.

Chang, R. Y. -W, P. S. K. Liu, W. R. Leitch, and J. P. D. Abbatt. 2007. Comparison between measured and predicted CCN concentrations at Egbert, Ontario: Focus on the organic aerosol fraction at a semi-rural site. *Atmospheric Environment* 41, (37): 8172-8182.

Cheng, L., E. Peake, and A. Davis. 1987. The rate of SO₂ to sulphate particle formation in an air parcel from an oil sands extraction plant plume. *Journal of the Air Pollution Control Association* 37, (2): 163-167.

Cho, S. 2005. Detailed microphysical modelling study of particle size distributions in an industrial plume, Ph.D. dissertation, Earth and Space Science, York University.

Cho, S., P.A. Makar, T. Herage, W.S. Lee, J. Liggio, S.M. Li, B. Wiens, L. Graham. 2008. Evaluation of A Unified Regional Air-Quality Modelling System (AURAMS) using PrAIRie 2005 field study data: the effects of emissions data accuracy on particle sulphate predictions, submitted to *Atmospheric Environment*.

Claeys, M., B. Graham, G. Vas, W. Wang, R. Vermeylen, V. Pashynska, and J. Cafmeyer P. Guyon, M. O. Andreae, P. Artaxo, and W. Maenhaut. 2004. Formation of secondary organic aerosols through photooxidation of isoprene. *Science* 303, (5661): 1173-1176.

Cooke, W. F., and J. J. N. Wilson. 1996. A global black carbon aerosol model. *Journal of Geophysical Research D: Atmospheres* 101, (14): 19395-19409.

de Gouw, J. A., A. M. Middlebrook, C. Warneke, P. D. Goldan, W. C. Kuster,

- J. M. Roberts, F. C. Fehsenfeld, D. R. Worsnop, M. R. Canagaratna, A. A. P. Pszenny, W. C. Keene, M. Marchewka, S. B. Bertman, and T. S. Bates. 2005. Budget of organic carbon in a polluted atmosphere: Results from the New England air quality study in 2002. *Journal of Geophysical Research D: Atmospheres* 110, (16): 1-22.
- Di Carlo, P., W. H. Brune, M. Martinez, H. Harder, R. Leshner, X. Ren, T. Thornberry, M. A. Carroll, V. Young, P. B. Shepson, D. Riemer, E. Apel, and C. Campbell. 2004. Missing OH reactivity in a forest: Evidence for unknown reactive biogenic VOCs. *Science* 304, (5671): 722-725.
- Emmerson, K. M., N. Carslaw, L. J. Carpenter, D. E. Heard, J. D. Lee, and M. J. Pilling. 2005. Urban atmospheric chemistry during the PUMA campaign 1: Comparison of modelled OH and HO₂ concentrations with measurements. *Journal of Atmospheric Chemistry* 52, (2): 143-164.
- Environment Canada, 2001. Precursor contributions to ambient fine particulate matter in Canada, a report by the Meteorological Service of Canada, May 2001. Report available online at: www.msc-smc.ec.gc.ca/saib
- Gallagher, M. W., K. M. Beswick, J. Duyzer, H. Westrate, T. W. Choularton, and P. Hummelshøj. 1997. Measurements of aerosol fluxes to speulderforest using a micrometeorological technique. *Atmospheric Environment* 31, (3): 359-373.
- Gillani, N. V., M. Luria, R. J. Valente, R. L. Tanner, R. E. Imhoff, and J. F. Meagher. 1998. Loss rate of NO_y from a power plant plume based on aircraft measurements. *Journal of Geophysical Research D: Atmospheres* 103, (D17): 22585-22592.
- Gong, W., A. P. Dastoor, V. S. Bouchet, S. Gong, P. A. Makar, M. D. Moran, B. Pabla, S. Ménard, L.-P. Crevier, S. Cousineau, S. Venkatesh. 2006. Cloud processing of gases and aerosols in a regional air quality model (AURAMS). *Atmospheric Research* 82, (1-2): 248-275.
- Griffin, R. J., D. R. Cocker III, R. C. Flagan, and J. H. Seinfeld. 1999. Organic aerosol formation from the oxidation of biogenic hydrocarbons. *Journal of Geophysical Research D: Atmospheres* 104, (D3): 3555-3567.
- Hämeri, K., R. Charlson, and H. -C Hansson. 2002. Hygroscopic properties of mixed ammonium sulfate and carboxylic acids particles. *AIChE Journal* 48, (6): 1309-1316.
- Hayden, K. L., A. M. MacDonald, W. Gong, D. Toom-Sauntry, K. G. Anlauf, A. Leithead, S. – M. Li, W. R. Leaitch, K. Noone. 2008. Cloud processing of nitrate, submitted to *Journal of Geophysical Research D: Atmospheres* 113, D18210, doi: 10.1029/2007JD00973.

Heald, C. L., D. J. Jacob, R. J. Park, L. M. Russell, B. J. Huebert, J. H. Seinfeld, H. Liao, and R. J. Weber. 2005. A large organic aerosol source in the free troposphere missing from current models. *Geophysical Research Letters* 32, (18): 1-4.

Henze, D. K., and J. H. Seinfeld. 2006. Global secondary organic aerosol from isoprene oxidation. *Geophysical Research Letters* 33, (9).

Herrmann, H., B. Ervens, H. -W Jacobi, R. Wolke, P. Nowacki, and R. Zellner. 2000. CAPRAM2.3: A chemical aqueous phase radical mechanism for tropospheric chemistry. *Journal of Atmospheric Chemistry* 36, (3): 231-284.

Jang, M., and R. M. Kamens. 2001. Atmospheric secondary aerosol formation by heterogeneous reactions of aldehydes in the presence of a sulphuric acid aerosol catalyst. *Environmental Science and Technology* 35, (24): 4758-4766.

Jylhä K. 1999. Relationship between the scavenging coefficient for pollutants in precipitation and the radar reflectivity factor. part I: Derivation. *Journal of Applied Meteorology* 38, (10): 1421-1434.

Kalberer, M., D. Paulsen, M. Sax, M. Steinbader, J. Dommen, A. S. H. Prevot, R. Fisseha, E. Weingartner, V. Frankevich, R. Zenobi, and U. Baltensperger. 2004. Identification of polymers as major components of atmospheric organic aerosols. *Science* 303, (5664): 1659-1662.

Kleinman, L. I., P. H. Daum, Y. -N Lee, G. I. Senum, S. R. Springston, J. Wang, C. Berkowitz, J. Hubbe, R. A. Zaveri, F. J. Brechtel, J. Jayne, T. B. Onasch, and D. Worsnop. 2007a. Aircraft observations of aerosol composition and ageing in New England and mid-Atlantic states during the summer 2002 New England air quality study field campaign. *Journal of Geophysical Research D: Atmospheres* 112, (9).

Kleinman, L. I., S. R. Springston, P. H. Daum, Y. -N Lee, L. J. Nunnermacker, G. I. Senum, J. Wang, Weinstein-Lloyd, M. L. Alexander, J. Hubbe, J. Ortega, M. R. Canagaratna, and J. Jayne. 2007b. The time evolution of aerosol composition over the Mexico City plateau. *Atmospheric Chemistry and Physics Discussions* 7, (5): 14461-14509.

Knopf, D. A., L. M. Anthony, and A. K. Bertram. 2005. Reactive uptake of O₃ by multi-component and multiphase mixtures containing oleic acid. *Journal of Physical Chemistry A* 109, (25): 5579-5589.

Kovacs, T. A., W. H. Brune, H. Harder, M. Martinez, J. B. Simpas, G. J. Frost, E. Williams, T. Jobson, C. Stroud, V. Young, A. Fried and B. Wert. 2003. Direct measurements of urban OH reactivity during Nashville SOS in summer 1999. *Journal of Environmental Monitoring* 5, (1): 68-74.

- Kroll, J. H., N. L. Ng, S. M. Murphy, R. C. Flagan, and J. H. Seinfeld. 2006. Secondary organic aerosol formation from isoprene photooxidation. *Environmental Science and Technology* 40, (6): 1869-1877.
- Kwamena, N. -O A., J. P. Clarke, T. F. Kahan, M. L. Diamond, and D. J. Donaldson. 2007. Assessing the importance of heterogeneous reactions of polycyclic aromatic hydrocarbons in the urban atmosphere using the multimedia urban model. *Atmospheric Environment* 41, (1): 37-50.
- Kwan, A. J., J. D. Crouse, A. D. Clarke, Y. Shinozuka, B. E. Anderson, J. H. Crawford, M. A. Avery, C. S. McNaughton, W. H. Brune, H. B. Singh, and P. O. Wennberg. 2006. On the flux of oxygenated volatile organic compounds from organic aerosol oxidation. *Geophysical Research Letters* 33, (15).
- Leaith, W. R., J. W. Bottenheim, and J. W. Strapp. 1988. Possible contribution of N₂O₅ scavenging to HNO₃ observed in winter stratiform cloud. *Journal of Geophysical Research* 93, (D10): 12,569-12,584.
- Leaith, W. R., J. W. Bottenheim, T. A. Biesenthal, S. -M Li, P. S. K. Liu, K. Asalian, H. Dryfhout-Clark, F. Hopper, and F. Brechtel. 1999. A case study of gas-to-particle conversion in an eastern Canadian forest. *Journal of Geophysical Research D: Atmospheres* 104, (D7): 8095-8111.
- Lee, A., A. H. Goldstein, M. D. Keywood, S. Gao, V. Varutbangkul, R. Bahreini, N. L. Ng, R. C. Flagan, and J. H. Seinfeld. 2006. Gas-phase products and secondary aerosol yields from the ozonolysis of ten different terpenes. *Journal of Geophysical Research D: Atmospheres* 111, (7).
- Liggio, J., S. -M Li, and R. McLaren. 2004. Reactive uptake of glyoxal by particulate matter. *Journal of Geophysical Research D: Atmospheres* 110, (10): 1-13.
- Liggio, J., S. -M Li, and R. McLaren. 2005. Heterogeneous reactions of glyoxal on particulate matter: Identification of acetals and sulphate esters. *Environmental Science and Technology* 39, (6): 1532-1541.
- Liggio, J., and S. -M Li. 2006a. Organosulphate formation during the uptake of pinonaldehyde on acidic sulphate aerosols. *Geophysical Research Letters* 33, (13).
- Liggio, J., and S. -M Li. 2006b. Reactive uptake of pinonaldehyde on acidic aerosols. *Journal of Geophysical Research D: Atmospheres* 111, (24).
- Marculli, C., B. Luo, and T. Peter. 2004. Mixing of the organic aerosol fractions: Liquids as the thermodynamically stable phases. *Journal of Physical Chemistry A* 108, (12): 2216-2224.

- Maria, S. F., L. M. Russell, M. K. Gilles, and S. C. B. Myneni. 2004. Organic aerosol growth mechanisms and their climate-forcing implications. *Science* 306, (5703): 1921-1924.
- Martin, S. T. 2000. Phase transitions of aqueous atmospheric particles. *Chemical Reviews* 100, (9): 3403-3453.
- Martinez, M., H. Harder, T. A. Kovacs, J. B. Simpas, J. Bassis, R. Leshner, W. H. Brune, G. J. Frost, E. J. Williams, C. A. Stroud, B. T. Jobson, J. M. Roberts, S. R. Hall, R. E. Shetter, B. Wert, A. Fried, B. Alicke, J. Stutz, V. L. Young, A. B. White, and R. J. Zamora. 2003. OH and HO₂ concentrations, sources, and loss rates during the southern oxidants study in Nashville, Tennessee, summer 1999. *Journal of Geophysical Research D: Atmospheres* 108, (19): ACH 8-1 - 8-17.
- Mircea, M., S. Stefan, M. C. Facchini, and S. Fuzzi. 2004. Analytical formulas for the below-cloud scavenging coefficient of an irreversibly soluble gas: A quantitative evaluation for HNO₃. *International Journal of Environment and Pollution* 21, (6): 547-565.
- Moise, T., R. K. Talukdar, G. J. Frost, R. W. Fox, and Y. Rudich. 2002. Reactive uptake of NO_x by liquid and frozen organics. *Journal of Geophysical Research D: Atmospheres* 107, (1-2): AAC 6-1 - AAC 6-9.
- Molina, M. J., A. V. Ivanov, S. Trakhtenberg, and L. T. Molina. 2004. Atmospheric evolution of organic aerosol. *Geophysical Research Letters* 31, (22): 1-5.
- NARSTO, 2003. Particulate matter science for policy makers: a NARSTO assessment, February 2003.
- Neuman, J. A. J. B. Nowak, C. A. Brock, M. Trainer, F. C. Fehsenfeld, J. S. Holloway, G. Hübler, P. K. Hudson, D. M. Murphy, D. K. Nicks Jr., D. Orsini, D. D. Parrish, T. B. Ryerson, D. T. Sueper, A. Sullivan, and R. Weber. 2003. Variability in ammonium nitrate formation and nitric acid depletion with altitude and location over California. *Journal of Geophysical Research D: Atmospheres* 108, (17): AAC 6-1 - AAC 6-12.
- Ng, N.L., P. S. Chhabra, A. W. H. Chan, J. D. Surratt, J. H. Kroll, A. J. Kwan, D. C. McCabe, P. O. Wennberg, A. Sorooshian, S. M. Murphy, N. F. Dalleska, R. C. Flagan, and J. H. Seinfeld. 2007. Effect of NO_x level on secondary organic aerosol (SOA) formation from the photooxidation of terpenes. *Atmospheric Chemistry and Physics Discussions* 7, (4): 10131-10177.
- Nho-Kim, E. -Y, M. Michou, and V. -H Peuch. 2004. Parameterization of size-dependent particle dry deposition velocities for global modelling. *Atmospheric Environment* 38, (13): 1933-1942.

- Odum, J. R., T. Hoffmann, F. Bowman, D. Collins, R. C. Flagan, and J. H. Seinfeld. 1996. Gas/particle partitioning and secondary organic aerosol yields. *Environmental Science and Technology* 30, (8): 2580-2585.
- Pant, P., P. Hegde, U. C. Dumka, R. Sagar, S. K. Satheesh, K. K. Moorthy, A. Saha, and M. K. Srivastava. 2006. Aerosol characteristics at a high-altitude location in central Himalayas: Optical properties and radiative forcing. *Journal of Geophysical Research D: Atmospheres* 111, (17).
- Parsons, M. T., D. A. Knopf, and A. K. Bertram. 2004. Deliquescence and crystallization of ammonium sulphate particles internally mixed with water-soluble organic compounds. *Journal of Physical Chemistry A* 108, (52): 11600-11608.
- Pathak, R. K., A. A. Presto, T. E. Lane, C. O. Stanier, N. M. Donahue, and S. N. Pandis. 2007. Ozonolysis of α -pinene: Parameterization of secondary organic aerosol mass fraction. *Atmospheric Chemistry and Physics* 7, (14): 3811-3821.
- Peng, C., M. N. Chan, and C. K. Chan. 2001. The hygroscopic properties of dicarboxylic and multifunctional acids: Measurements and UNIFAC predictions. *Environmental Science and Technology* 35, (22): 4495-4501.
- Presto, A. A., and N. M. Donahue. 2006. Investigation of α -pinene + ozone secondary organic aerosol formation at low total aerosol mass. *Environmental Science and Technology* 40, (11): 3536-3543.
- Pryor, S. C., M. Gallagher, H. Sievering, S. E. Larsen, R. J., Barthelme, F. Birsan, E., Nemitz, J. Rinne, M. Kulmala, T. Groenholm, R. Taipale, T. Vesala, 2008. A review of measurement and modelling results of particle atmosphere-surface exchange. *Tellus B.* 60, (1), 42-75.
- Rasch, P. J, J. Feichter, K. Law, N. Mahowald, J. Penners, C. Benkovitz, C. Genthon, C. Giannakopoulos, P. Kasibhatla, D. Koch, H. Levy, T. Maki, M. Prather, D. L. Roberts, G.-J. Roelofs, D. Stevenson, Z. Stockwell, S. Taguchi, M. Kritz, M. Chipperfield, D. Baldocchi, P. McMurry, L. Barrie, Y. Balkanski, R. Chatfield, E. Kjellstrom, M. Lawrence, H. N. Lee, J. Leliveld, K. J. Noone, J. Seinfeld, G. Stenchikov, S. Schwartz, C. Walcek, D. Williamson. 2000. A comparison of scavenging and deposition processes in global models: Results from the WCRP Cambridge workshop of 1995. *Tellus, Series B: Chemical and Physical Meteorology* 52, (4): 1025-1056.
- Ren, X., H. Harder, M. Martinez, R. L. Lesher, A. Oligier, J. B. Simpas, W. H. Brune, J. J. Schwab, K. L. Demerjian, Y. He, X. Zhou, H. Gao. 2003. OH and HO₂ chemistry in the urban atmosphere of New York City. *Atmospheric Environment* 37, (26): 3639-3651.

- Ren, X., W. H. Brune, J. Mao, M. J. Mitchell, R. L. Lesher, J. B. Simpas, A. R. Metcalf, J. J. Schwab, C. Cai, Y. Li, K. L. Demerjian, H. D. Felton, G. Boynton, A. Adams, J. Perry, Y. He, X. Zhou, J. Hou. 2006. Behavior of OH and HO₂ in the winter atmosphere in New York City. *Atmospheric Environment* 40, (SUPPL. 2): 252-263.
- Roberts, G. C., P. Artaxo, J. Zhou, E. Swietlicki, and M. O. Andreae. 2002. Sensitivity of CCN spectra on chemical and physical properties of aerosol: A case study from the Amazon basin. *Journal of Geophysical Research D: Atmospheres* 107, (20): 37-1-37-18.
- Robinson, A. L., N. M. Donahue, and W. F. Rogge. 2006. Photochemical oxidation and changes in molecular composition of organic aerosol in the regional context. *Journal of Geophysical Research D: Atmospheres* 111, (3).
- Robinson, A.L., N.M. Donahue, M.K. Shrivastava, E.A. Weitkamp, A.M. Sage, A.P. Grieshop, T.E. Lane, J.R. Pierce and S.N. Pandis, 2007. Rethinking organic aerosols: semivolatile emissions and photochemical aging. *Science* 315, (5816): 1259-1262.
- Rudich, Y. 2003. Laboratory perspectives on the chemical transformations of organic matter in atmospheric particles. *Chemical Reviews* 103, (12): 5097-5124.
- Rudich, Y., Donahue, N. M., and Mentel, T. F. 2007. Aging of organic aerosol: Bridging the gap between laboratory and field studies, *Ann. Rev. Phys. Chem.*, 58, 321-352.
- Ruijgrok, W., C. I. Davidson, and K. W. Nicholson. 1995. Dry deposition of particles: Implications and recommendations for mapping of deposition over Europe. *Tellus, Series B* 47 B, (5): 587-601.
- Rupakheti, M., W. R. Leitch, U. Lohmann; K. Hayden, P. Brickell, G. Lu; S.-M. Li, D. Toom-Saunty, J. W. Bottenheim, J. R. Brook, R. Vet, J. T. Jayne, D. R. Worsnop. 2005. An intensive study of the size and composition of submicron atmospheric aerosols at a rural site in Ontario, Canada. *Aerosol Science and Technology* 39, (8): 722-736.
- Ryerson, T.B., M. Trainer, W. M. Angevine, C. A. Brock, R. W. Dissly, F. C. Fehsenfeld, G. J. Frost, P. D. Goldan, J. S. Holloway, G. Hübler, R. O. Jakoubek, W. C. Kuster, J. A. Neuman, D. K. Nicks Jr., D. D. Parrish, J. M. Roberts, D. T. Sueper, E. L. Atlas, S. G. Donnelly, F. Flocke, A. Fried, W. T. Potter, S. Schauffler, V. Stroud, A. J. Weinheimer, B. P. Wert, and C. Wiedinmyer, R. J. Alvarez, R. M. Banta, L. S. Darby, and C. J. Senff 2003. Effect of petrochemical industrial emissions of reactive alkenes and NO_x on tropospheric ozone formation in Houston, Texas. *Journal of Geophysical Research D: Atmospheres* 108, (8): ACH 8-1 - ACH 8-24.

- Sadanaga, Y., A. Yoshino, S. Kato, and Y. Kajii. 2005. Measurements of OH reactivity and photochemical ozone production in the urban atmosphere. *Environmental Science and Technology* 39, (22): 8847-8852.
- Seinfeld, J. H. and S. N. Pandis. 1998. *Atmospheric Chemistry & Physics: From Air Pollution to Climate Change*, John Wiley & Sons.
- Seinfeld, J. H., and J. F. Pankow. 2003. Organic atmospheric particulate material. *Annual Review of Physical Chemistry*, 54, 121-140.
- Sellegri, K., P. Laj, R. Dupuy, M. Legrand, S. Preunkert, and J. -P Putaud. 2003. Size-dependent scavenging efficiencies of multicomponent atmospheric aerosols in clouds. *Journal of Geophysical Research D: Atmospheres* 108, (11): AAC 3-1 - AAC 3-15.
- Slinn, W. G. N. 1982. Predictions for particle deposition to vegetative canopies. *Atmospheric Environment* 16, (7): 1785-1794.
- Song, C., K. Na, and D. R. Cocker III. 2005. Impact of the hydrocarbon to NO_x ratio on secondary organic aerosol formation. *Environmental Science and Technology* 39, (9): 3143-3149.
- Springston, S. R., L. I. Kleinman, F. Brechtel, Y. -N Lee, L. J. Nunnermacker, and J. Wang. 2005. Chemical evolution of an isolated power plant plume during the TexAQS 2000 study. *Atmospheric Environment* 39, (19): 3431-3443.
- Stemmler, K., M. Ammann, C. Donders, J. Kleffmann, and C. George. 2006. Photosensitized reduction of nitrogen dioxide on humic acid as a source of nitrous acid. *Nature* 440, (7081): 195-198.
- Strawbridge, K. B., and B. J. Snyder. 2004. Daytime and night-time aircraft lidar measurements showing evidence of particulate matter transport into the northeastern valleys of the Lower Fraser Valley, BC. *Atmospheric Environment* 38, (34): 5873-5886.
- Stroud, C. A., P. A. Makar, D. V. Michelangeli, M. Mozurkewich, D. R. Hastie, A. Barbu, and J. Humble. 2004. Simulating organic aerosol formation during the photooxidation of toluene/NO_x mixtures: Comparing the equilibrium and kinetic assumption. *Environmental Science and Technology* 38, (5): 1471-1479.
- Stroud, C. A., A. Nenes, J. L. Jimenez, P. F. DeCarlo, J. A. Huffman, R. Bruintjies, E. Nemitz, A. E. Delia, D. W. Toohey, A. B. Guenther, and S. Nandi. 2007. Cloud activating properties of aerosol observed during CELTIC. *Journal of the Atmospheric Sciences* 64, (2): 441-459.

- Stroud, C. A., G. Morneau, P. A. Makar, M. D. Moran, W. Gong, B. Pabla, J. Zhang, *et al.* 2008. OH-reactivity of volatile organic compounds at urban and rural sites across Canada. Evaluation of air quality model predictions using speciated VOC measurements. *Atmospheric Environment* 42, (33): 7746-7756.
- Stull, R.B. 1988. An introduction to boundary layer meteorology, first edition. Dordrecht: Kluwer Academic Publishers.
- Surratt, J. D., S. M. Murphy, J. H. Kroll, N. L. Ng, L. Hildebrandt, A. Sorooshian, R. Szmigielski, R. Vermeylen, W. Maenhaut, M. Claeys, R. C. Flagan, and J. H. Seinfeld. 2006. Chemical composition of secondary organic aerosol formed from the photooxidation of isoprene. *Journal of Physical Chemistry A* 110, (31): 9665-9690.
- Sutton M. A., J. K. Burkhardt., D. Guerin, E. Nemitz and D. Fowler D., 1998. Development of resistance models to describe measurements of bi-directional ammonia surface atmospheric exchange, *Atmospheric Environment* 32, 473-480, 1998.
- Tang, I. N., and H. R. Munkelwitz. 1993. Composition and temperature dependence of the deliquescence properties of hygroscopic aerosols. *Atmospheric Environment - Part A General Topics* 27 A, (4): 467-473.
- Thornton, J. A., P. J. Wooldridge, R. C. Cohen, M. Martinez, H. Harder, W. H. Brune, E. J. Williams, J. M. Roberts, F. C. Fehsenfeld, S. R. Hall, R. E. Shetter, B. P. Wert, and A. Fried. 2002. Ozone production rates as a function of NO_x abundances and HO_x production rates in the Nashville urban plume. *Journal of Geophysical Research D: Atmospheres* 107, (12): ACH 7-1 - ACH 7-17.
- Vingarzan, R., and S. -M Li. 2006. The Pacific 2001 air quality study-synthesis of findings and policy implications. *Atmospheric Environment* 40, (15): 2637-2649.
- Volkamer, R., J. L. Jimenez, F. San Martini, K. Dzepina, Q. Zhang, D. Salcedo, L. T. Molina, D. R. Worsnop, and M. J. Molina. 2006. Secondary organic aerosol formation from anthropogenic air pollution: Rapid and higher than expected. *Geophysical Research Letters* 33, (17).
- Wadia, Y., D. J. Tobias, R. Stafford, and B. J. Finlayson-Pitts. 2000. Real-time monitoring of the kinetics and gas-phase products of the reaction of ozone with an unsaturated phospholipid at the air-water interface. *Langmuir* 16, (24): 9321-9330.
- Wang, D., J. D. Fuentes, D. Travers, T. Dann, and T. Connolly. 2005. Non-methane hydrocarbons and carbonyls in the Lower Fraser Valley during PACIFIC 2001. *Atmospheric Environment* 39, (29): 5261-5272.

- Wang, X., L. Zhang and M. Moran, 2009. Uncertainty assessment of current size-resolved parameterizations for below-cloud aerosol scavenging by rain. *Atmospheric Chemistry and Physics Discussion*, in press.
- Weber, J. P., A. P. Sullivan, R. E. Peltier, A. Russell, B. Yan, M. Zheng, J. de Gouw, C. Warneke, C. Brock, J. S. Holloway, E. L. Atlas, and E. Edgerton. 2007. A study of secondary organic aerosol formation in the anthropogenic-influenced southeastern United States. *Journal of Geophysical Research D: Atmospheres* 112, (13).
- Wesely, M. L. 1989. Parameterization of surface resistances to gaseous dry deposition in regional-scale numerical models. *Atmospheric Environment* 23, (6): 1293-1304.
- Wesely, M. L., and B. B. Hicks. 2000. A review of the current status of knowledge on dry deposition. *Atmospheric Environment* 34, (12-14): 2261-2282.
- Zhang, J., K. E. Huff Hartz, S. N. Pandis, and N. M. Donahue. 2006. Secondary organic aerosol formation from limonene ozonolysis: Homogeneous and heterogeneous influences as a function of NO_x . *Journal of Physical Chemistry A* 110, (38): 11053-11063.
- Zhang, L., S. Gong, J. Padro, and L. Barrie. 2001. A size-segregated particle dry deposition scheme for an atmospheric aerosol module. *Atmospheric Environment* 35, (3): 549-560.
- Zhang, L., M. D. Moran, P. A. Makar, J. R. Brook, and S. Gong. 2002. Modelling gaseous dry deposition in AURAMS: A unified regional air-quality modelling system. *Atmospheric Environment* 36, (3): 537-560.
- Zhang, L., J. R. Brook, and R. Vet. 2003. A revised parameterization for gaseous dry deposition in air-quality models. *Atmospheric Chemistry and Physics* 3, 2067-2082.
- Zhang, L., D. V. Michelangeli, and P. A. Taylor. 2004. Numerical studies of aerosol scavenging by low-level, warm stratiform clouds and precipitation. *Atmospheric Environment* 38, (28): 4653-4665.
- Zhang, L. and R. Vet, 2006. A review of current knowledge concerning size-dependent aerosol removal, *China Particuology*, Vol. 4, No. 6, 272-282.
- Zhang, Q., M. R. Canagaratna, J. T. Jayne, D. R. Worsnop, and J. -L Jimenez. 2005a. Time- and size-resolved chemical composition of submicron particles in Pittsburgh: Implications for aerosol sources and processes. *Journal of Geophysical Research D: Atmospheres* 110, (7): 1-19.

Zhang, Q., D. R. Worsnop, M. R. Canagaratna, and J. L. Jimenez. 2005b. Hydrocarbon-like and oxygenated organic aerosols in Pittsburgh: Insights into sources and processes of organic aerosols. *Atmospheric Chemistry and Physics* 5, (12): 3289-3311.

Zoumakis, N. M., and G. A. Efstathiou. 2006. Parameterization of inversion breakup in idealized valleys. part II: Thermodynamic model. *Journal of Applied Meteorology and Climatology* 45, (4): 609-621.

CHAPTER 3: Ambient Measurements and Observations

Tom Dann, Bob Vet, Jeff Brook, Roxanne Vingarzan, Elton Chan, Mike Shaw, Jason O'Brien, Dennis Herod, Ewa Dabek, Daniel Wang, Domenic Mignacca, Kurt Anlauf, Kalyani Martinelango

KEY MESSAGES AND IMPLICATIONS

- Fine particulate matter (PM_{2.5}) and ground-level ozone (O₃) levels vary considerably across the country by region in time, space and chemical composition.
- Ontario and southern Quebec continue to record the highest O₃ levels (in the form of the Canada-wide Standard (CWS), the 3 year average of the 4th highest daily maximum ozone concentration, ranging from 70 to 87 ppb) and most frequent number of days above the CWS (30 to 50 days per year). Almost all sites over the CWS 2010 target are located in these areas.
- Outside of Ontario and Quebec almost all sites record higher spring-time O₃ than summer O₃ and photochemical episodes are rare despite high emission densities in some regions.
- Trend results for ozone for urban sites across Canada for 1990-2006 show a statistically significant positive trend for lower percentiles and the median concentrations. Rural sites in Ontario and Quebec, however, showed statistically significant decreases in maximum and upper percentiles of maximum daily 8-hour ozone levels. The urban results illustrate the effect of decreasing NO levels in reducing ozone scavenging and thus resulting in a net apparent upward trend in average ozone concentrations.
- A detailed trend analysis for regionally representative sites indicates that May-September daily maximum 8-hour average ozone concentrations decreased from the 3-year averaging periods 1997-2000 to 2003-2006 by 4.1% for sites in southern Ontario/Great Lakes/Upper Ohio and by 3.2% for the sites in Southern Quebec, but remained constant at sites in Alberta and increased by 5.2% at sites in the Georgia Basin area of the Pacific coast and by 2.1% in Atlantic Canada.
- Baseline ozone levels are increasing in a number of areas of Canada, namely: the Georgia Basin area of the Pacific coast, the Atlantic coast, and continental western Canada, but are decreasing in Ontario and Quebec where the signal is affected by within-region sources and by transboundary transport from the United States.

- Transportation sources dominate urban VOCs and NO_x, and they strongly influence urban PM_{2.5} and PM_{10-2.5} concentrations. Between 1990 and 2006 annual mean NO decreased by 55%, NO₂ by 34% and VOCs by 46% at Canadian urban sites. The trends were very consistent on a site by site basis with essentially all urban sites (56 sites for NO_x and 25 for VOC) in Canada recording similar decreases in ambient levels. As noted above the NO_x emission decreases served to decrease peak ozone levels in several non-urban areas of the country but increase average ozone in almost all urban areas.
- Ozone concentrations in eastern Canada appear to have decreased in the period 2004 to 2007 at a much faster rate than in previous years possibly due to a large reduction in U.S. NO_x emissions from coal-fired power plants (NO_x SIP Call) over this time period.
- The highest PM_{2.5} levels and frequency of episodes and days greater than 30 µg m⁻³ are also recorded in Ontario and southern Quebec although the sites with the highest 3-year average of 98th percentile concentrations are much closer to achieving the CWS 2010 target level than is the case for ozone.
- The major components of PM_{2.5} at speciation measurement sites across the country are ammonium sulphate, organic material and ammonium nitrate. In the east, ammonium sulphate reaches its maximum in the summer months when photochemistry and transport from Canadian and US emission sources are greatest. Ammonium nitrate peaks during the winter months at sites in the east and in Edmonton.
- Since 2001, emission reductions of SO₂ and NO_x in eastern Canada and the northeastern U.S. have resulted in declines in ambient ammonium sulphate and ammonium nitrate particles as well as ambient SO₂ and HNO₃ precursor gases.
- There was a large reduction in urban PM_{2.5} and PM_{10-2.5} between 1985 to 1998 and little change in PM_{2.5} since then, but PM_{10-2.5} continues to decline. The limited data on compositional change restricts conclusions on its trends.
- In the east, the highest PM_{2.5} days during the warm season are dominated by (NH₄)₂SO₄ and the highest in the cold season are dominated by NH₄NO₃ (except at sites in Atlantic Canada where (NH₄)₂SO₄ is dominant in both seasons). In the west, the highest PM_{2.5} days during both the warm and cold seasons are dominated by organic material.
- Agriculture is the dominant source of ambient NH₃, a precursor of particle ammonium sulphate and ammonium nitrate. In light of decreasing SO_x and NO_x emissions in various areas of North America, NH₃ emissions and ambient concentrations are expected to become more important in establishing ambient levels of total PM_{2.5}. In five agriculturally-intense areas of Canada (viz., the Lower Fraser Valley of BC, southern Alberta, southern Manitoba, south-western Quebec and the Maritime provinces), PM_{2.5} levels are thought to be relatively insensitive to a major reduction in NH₃ emissions, say of 30%. This means that very large reductions of NH₃ emissions (>30%) would be needed in these areas to arrive at the point at which ambient p-NH₄⁺ levels would be sensitive to further NH₃ emission reductions.

- The available data suggest that the consistently strong association between NO₂ and mortality in Canadian cities is because NO₂ is a good indicator of local combustion emissions (likely motor vehicles) along with being indicative of the local build up of photochemically processed urban air pollution

3.1 Topic Introduction and Organization of Chapter

Ambient air quality measurements provide crucial information to policy makers and scientists. In Canada they have provided the scientific basis for assessing the effects of air pollutants on the environment and human health, for establishing Canada-wide Standards for ozone and particulate matter (CCME, 2007) and for analyzing ambient ozone and PM levels relative to the Canada-wide Standards (Government of Canada, 2007).

The information presented in this chapter updates and expands upon our earlier knowledge of ozone and PM air quality in Canada, as has been documented in previous assessments and publications (Health Canada and Environment Canada, 1999a, b; Environment Canada, 1997, 2001, 2004). These publications describe the levels and characteristics of ambient ozone and PM across the country during the 1990s and early 2000s and, therein, provide a context for the new and updated knowledge presented in this chapter.

In this context, the balance of this chapter improves upon our understanding and knowledge of ozone and PM in Canada by taking advantage of new and increased monitoring results and new data analysis techniques. Much of the chapter is devoted to the overarching theme of understanding the response of ozone and PM in Canada to the major NO_x, VOC and SO₂ emission reductions that took place in Canada and the United States in the 2000s.

Section 3.2 summarizes the available data from Canadian air quality monitoring sites and describes the methods of monitoring ozone, PM, precursor gases and chemical constituents of PM. Section 3.3 discusses ozone background and baseline levels, climatology, and spatial and temporal trends. Section 3.4 describes measurement techniques and trends related to ozone precursors and Section 3.5 discusses background and baseline levels and composition of PM_{2.5}, as well as overall trends in ambient levels of PM_{2.5} mass, its constituents and precursors. Section 3.6 covers ambient levels and trends of coarse PM. The chapter ends with a Summary and Conclusions (Section 3.7), and a set of recommendations (Section 3.8), for future work related to monitoring networks and special studies.

3.2 Canadian Monitoring Networks and Monitoring Methods for Ozone, PM_{2.5} and Precursors

3.2.1 Networks and Monitoring Site Locations

Routine ambient air quality monitoring across Canada is conducted by government, industry, and in some provinces, non-government organizations (NGOs). Many of the industrial monitoring sites are established in close proximity to their facilities and are usually required as part of a provincial permit to operate. In some jurisdictions, industry also collaborates with government (and NGOs) to operate regional monitoring networks.

All three levels of government (federal, provincial/territorial, regional/municipal) have established monitoring programs. Most of the air quality measurement data presented in this assessment comes from two monitoring networks, the National Air Pollution Surveillance (NAPS) network and the Canadian Air and Precipitation Monitoring Network (CAPMoN).

The National Air Pollution Surveillance (NAPS) Program is a joint federal, provincial, territorial and municipal initiative. The purpose of this Program is to coordinate the collection of air quality data from existing provincial, territorial and municipal air quality monitoring networks and provide a unified Canada-wide air quality data base. Through the NAPS program, accurate and long-term air quality data of a uniform standard throughout Canada are made publicly available through the Canada-wide air quality database and publication in annual air quality data summary reports

(http://www.etc-ct e.ec.gc.ca/publications/napsreports_e.html).

Although initially begun as a cooperative agreement among monitoring agencies, NAPS evolved into a formal partnership in 2004 with the endorsement of a Memorandum of Understanding (MOU) between the federal, provincial territorial and regional governments (Supplement Canada Gazette, Part I January 31, 2004). This agreement outlines the general terms and conditions of cooperation in the overall management and support of the NAPS air quality monitoring program for designated NAPS sites. These sites are selected for inclusion in the NAPS network by Environment Canada and the province or territory in which the site is located, primarily to support national air quality programs like the CWS. Several provinces, territories and regional governments operate additional monitoring stations to meet the requirements of their own ambient monitoring programs. Ambient air pollution data from most of these sites are also submitted to the NAPS Canada-wide database at the discretion of each monitoring agency.

As of 2006, the associated provincial/territorial/regional monitoring networks reporting data to the Canada-wide air quality database consisted of approximately 325 monitoring stations in over 215 communities in Canada. Although NAPS is considered primarily an urban

monitoring network, 82 of the monitoring stations were located in rural areas. Essentially all available monitoring data in the country (excluding industrial self-monitoring) was available for this report through the database. This included approximately 820 continuous monitors measuring sulphur dioxide (SO₂), carbon monoxide (CO), nitrogen dioxide (NO₂), ozone (O₃), and particulate matter (PM), and over 150 air samplers measuring components of PM and volatile organic compounds (VOCs). The Analysis and Air Quality Division of Environment Canada coordinates operation of the NAPS program, provides air monitoring instrumentation and reference standards, operates a laboratory for the chemical speciation of NAPS samples, directs a national quality assurance program, coordinates the development of equipment specifications for the monitoring network as a whole and maintains the Canada-wide air quality database. The provincial, territorial and regional governments share in overall management of the NAPS Program, support the development of standardized methods, and assume the responsibility for ongoing operation and maintenance of monitoring sites and instrumentation, data acquisition and validation, and reporting within their jurisdictions. Maps showing NAPS PM_{2.5} and ozone monitoring sites are provided in Figures 3.1 and 3.2. More detailed maps on a regional basis (with additional place names) are provided in Chapter 7 and a complete listing of observations by NAPS site code can be found at the NAPS web site: www.etc-cte.ec.gc.ca/NapsData/Web-Information.

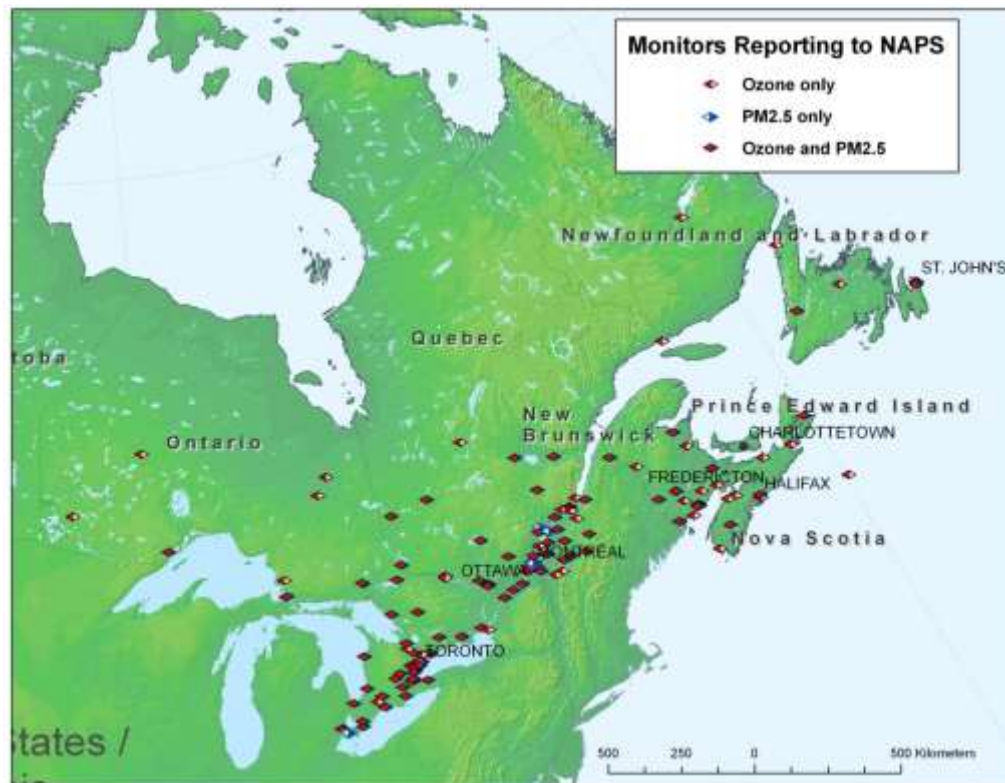


Figure 3.1 Location of NAPS Ozone and PM_{2.5} monitoring sites in Eastern Canada – 2006.

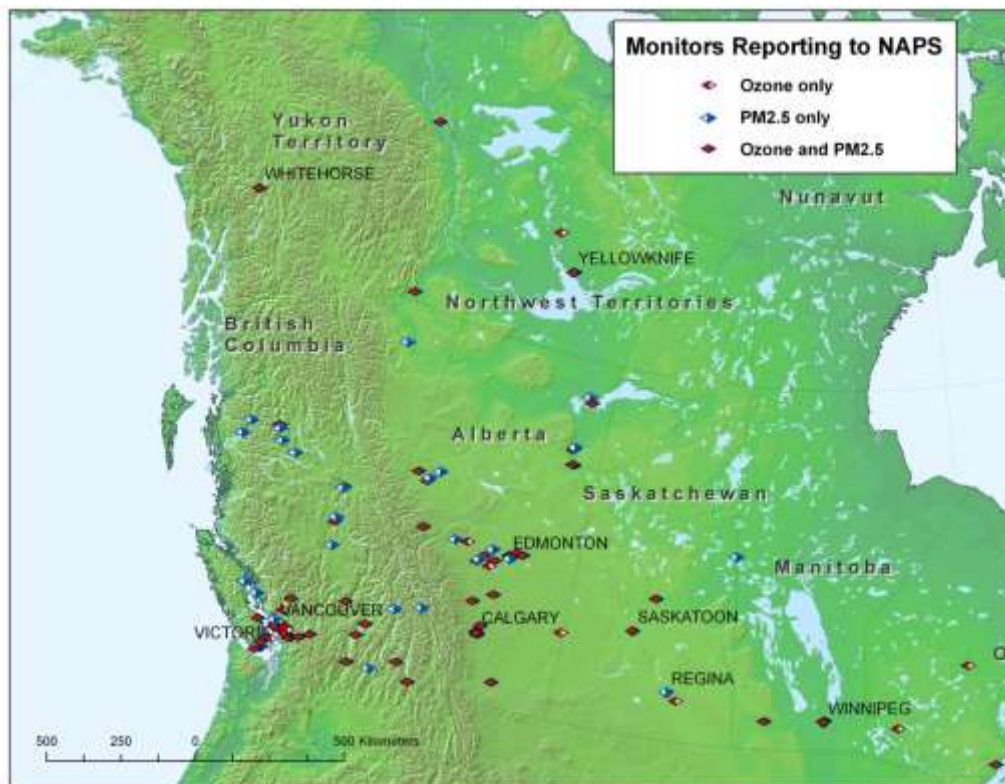


Figure 3.2 Location of NAPS Ozone and PM_{2.5} monitoring sites in Western Canada – 2006.

In the past ten years numerous enhancements have been made to the NAPS network to better characterize ambient air quality in Canada. Some of the most significant changes include a multi-million dollar investment that has reduced the average age of NAPS instruments from over 10 years to 5 years, increased the number of continuous PM_{2.5} monitoring sites from 60 to over 200 and increased the number of ozone monitoring sites from 160 to 200. The provincial and municipal data logging and data reporting systems were also modernized to allow more timely reporting of data and improve quality of real time data. Most agencies are now reporting real time data to AIRNow (US portal to provide public with easy access to national air quality information, www.airnow.gov) and to the Air Quality Health Index (AQHI). A new program to provide complete characterization of PM components was initiated in 2003 (see Section 3.2.6.1) and existing measurement programs for volatile organic compounds (VOC) were also enhanced. These latter programs required a large investment in new laboratory analytical equipment.

The Canada-wide standards (CWS) for particulate matter and ozone specify that communities (census metropolitan areas – CMAs and census agglomerations – CAs) with a population over 100,000 are required to report on compliance with the 2010 CWS target levels. In Canada, there are 36 CMA/CAs that meet this criterion, however, provinces/territories may also report on smaller communities based on considerations such as regional population density,

proximity to sources and local air quality. Provinces may choose to subdivide large CMA's into reporting sub-areas (RSAs) to better represent variations in ambient levels across the community or to delineate urban centres within the larger metropolitan area. For the three-year period ending in 2005, provinces and territories reporting progress on compliance with the ambient $PM_{2.5}$ and ozone 2010 CWS target levels, reported data for a total of 70 communities (CMA, CA and RSA) representing more than 70% of the Canadian population.



Figure 3.3 Location of CAPMoN Monitoring Sites and Parameters Measured (Note: PM sampling (brown) is temporally on hiatus at all sites except Egbert).

The Canadian Air and Precipitation Monitoring Network (CAPMoN) is operated by the Air Quality Research Division of the Science and Technology Branch of Environment Canada. CAPMoN site locations are shown in Figure 3.3. The objectives of CAPMoN differ from those of NAPS in that CAPMoN measurements provide data for research into: (1) regional-scale spatial and temporal variations of air pollutants and deposition, (2) long range transport of air pollutants (including transboundary transport), (3) atmospheric processes, and chemical transport model evaluation. In contrast to most (but not all) NAPS sites, which are generally located in urban, suburban and industrial areas, CAPMoN sites are located in rural and remote areas.

Four types of measurements are made in CAPMoN, namely: the chemical composition of precipitation (major ions and cations), the chemical composition of atmospheric particles (both acidic and basic), particle mass ($PM_{2.5}$ and PM_{10}), and the concentration of selected gases

including O₃, SO₂, nitric acid (HNO₃), NO/NO₂/NO_y²², peroxyacetyl nitrate (PAN), mercury (Hg) and ammonia (NH₃). CAPMoN measurement methods include both size-selective and non-size-selective filter methods for particle composition and mass, specialized denuders, impregnated filters and continuous monitors for gases, and wet-only deposition collectors for precipitation chemistry. The CAPMoN Laboratory is responsible for all PM_{2.5}, PM₁₀ and wet chemical measurements. Ozone monitoring data from CAPMoN are included in the Canada-wide database and the sites are included in the totals listed for NAPS.

Over the past ten years the CAPMoN network has expanded its rural/remote monitoring. The number of CAPMoN ozone monitoring sites was increased from six to fourteen in order to provide national coverage. At the same time, the monitoring methods were upgraded such that each CAPMoN ozone monitor now collects real-time ozone data on an hourly basis and is calibrated monthly to an internationally-accepted primary standard. The raw data are automatically submitted to the Canadian Air Quality Forecast system at the Canadian Meteorological Centre and to the US-Canada AIRNOW database, and the finalized data are archived annually in the NAPS ozone database and World Meteorological Organization Data Centre for Greenhouse Gases. In addition, rural/remote measurements of NO_y, NO, NO_x and true-NO₂ are made at three CAPMoN sites. These measurements provide hourly data at the low concentrations characteristic of rural/remote areas of Canada. To complement the nitrogen oxide measurements, continuous measurements of ammonia and C₂-C₈ non-methane hydrocarbons are made at one of the CAPMoN sites (although these measurements are not part of the routine suite of CAPMoN measurements).

Data from the United States Environmental Protection Agency (U.S. EPA) Air Quality System (AQS) database (<http://www.epa.gov/ttn/airs/airsaqs>) has also been used in some sections of the chapter. The locations of U.S. sites are shown in the appropriate figures.

²² NO_y= NO₂+ NO_x and

NO₂= HNO₃+ HONO+2N₂O₅+HO₂NO₂+PAN+NO₃+ organic nitrates (not NH₃)

3.2.2 Ozone (O₃)

Ozone measurements are carried out using gas analyzers that operate on the UV light absorption principle. All ozone measurements in Canada are ultimately referenced to a National Institute of Standards and Technology (NIST) primary UV calibration device. As of 2006, there were 213 O₃ monitoring sites reporting data to the Canada-wide data base including 14 CAPMoN regional-scale O₃ sites. Measurements are made year-round.

3.2.3 Nitrogen Oxides (NO_x)

There are 142 sites in the NAPS database reporting nitrogen dioxide (NO₂), nitric oxide (NO) and NO_x data. Many sites reported only NO₂ data prior to 1986. All measurements are made with analyzers operating on the principle of chemiluminescence involving the gas phase reaction of NO with O₃. Since these analyzers only measure NO directly, NO₂ is measured by reducing it to NO using a catalytic converter. Converters used in conventional instruments convert some portion of other nitrogen species to NO, as well as converting NO₂. The amount of interference caused by this conversion is more important at rural sites, as discussed in Section 3.4.1.

Conventional NO_x analyzers do not have the required sensitivity to be used at rural and remote sites, where many of the observations would be expected to be at low concentration levels. High-sensitivity NO_y instruments have been deployed at a number of rural CAPMoN sites in recent years (see Section 3.4.1 for details).

3.2.4 Volatile Organic Compounds (VOCs)

A routine VOC sampling program is operated under NAPS at 37 urban monitoring sites. Samples are usually collected over 24-hr periods once every six days and analyzed for more than 100 different C₂ to C₁₂ hydrocarbon species. VOC measurements are also made at 14 rural sites and at these sites samples are collected over 4-h sampling periods (12:00-16:00) to capture the well mixed atmosphere and avoid local site influences during night-time.

Ambient air samples are collected in 6 L or 3.2 L stainless steel Summa™ polished canisters (Scientific Instrumental Specialists, Inc. or BRC Rasmussen). The canisters were cleaned and evacuated before shipment to the sampling sites according to the procedures described in EPA Method TO 14/15 (U.S. EPA, 1999; Wang 2006a, b). In the field, samples are collected using whole air samplers (Xontech, Inc. Model 910A).

A combined gas chromatography/flame ionization detector (GC/FID) system (Agilent model 6890, Palo Alto, CA) was used for quantification of C₂ hydrocarbons, while a combined gas chromatography/mass selective detector (GC/MSD) system (Agilent model 6890/5973) was used for quantification of C₃ to C₁₂ hydrocarbons. Additional details on the hydrocarbon analytical methods are presented in Wang and Austin (2006a), Dann and Wang (1992a, b) and Fuentes et al (1996). Approximately 150 VOCs are routinely quantified in the samples. Beginning in 2003 a number of polar species including α -pinene, β -pinene, δ -limonene and camphene began to be quantified in the canister samples.

Carbonyl measurements are also made at a number of sites using DNPH coated silica gel cartridges with subsequent analysis by high pressure liquid chromatography (HPLC) as described in EPA Method TO-11A (U.S. EPA, 1999).

3.2.5 Sulphur Dioxide (SO₂)

Continuous SO₂ measurements are made at 133 urban sites in the NAPS network using pulse-fluorescence ultraviolet (UV) adsorption instruments. The CAPMoN network measures 24-h integrated SO₂ concentrations using an impregnated filter mounted in a multi-stage filter pack (that simultaneously measures particle sulphate, nitrate and ammonium and gaseous nitric acid). In 2008, there were 13 CAPMoN sites making these measurements at rural/remote locations across Canada.

3.2.6 PM_{2.5} Mass and Components

3.2.6.1 Manual Sampling Methods

Since 1984 both fine (< 2.5 μm – PM_{2.5}) and coarse (2.5 to 10 μm – PM_{10-2.5}) particle mass measurements have been made at NAPS network sites using dichotomous filter-based samplers. As of 2006, there were 27 dichotomous samplers operating at NAPS sites supplemented by an additional 13 U.S. EPA federal reference method (FRM) (U.S. EPA, 1998) samplers measuring only PM_{2.5}. The Teflon filters from the dichotomous and FRM samplers are routinely analyzed for elements using energy dispersive X-ray fluorescence (EDXRF) and for anions and cations using ion chromatography (IC) (Brook *et al.*, 1997). The coarse fraction filters from the samplers have also been submitted to the same analytical protocols.

Although this program has generated valuable data on PM_{2.5} mass, metals and some ions, a complete accounting of PM components could not be made since organic and elemental carbon were not being measured and ammonium nitrate was being lost from the samples during EDXRF analysis (Brook and Dann, 1998). In 2002, a new particle speciation program was

designed to allow accurate measurement of all the important components of PM_{2.5}. New sampling equipment was tendered and purchased, and program implementation began at both NAPS and CAPMoN stations in 2003.

Speciation sampling sites are equipped with R&P Partisol-Plus 2025-D sequential dichotomous particulate samplers along with R&P Partisol Model 2300 Speciation samplers. These units share common software and data storage systems. The speciation sampler uses Harvard designed Chemcomb® cartridges which employ honeycomb glass denuders and filter packs with Teflon and Nylon media.

Table 3.1 PM Speciation Sampling Modules and Target Analyte Groups

Unit	Module Description	Media	Function/Analytes
Dichot Partisol	Fine Fraction Filter	47 mm Teflon	Mass, Metals (XRF, ICPMS)
	Coarse Fraction Filter	47 mm Teflon	Mass, Metals (XRF)
Speciation Sampler	Cartridge C (4 components)	Sodium Carbonate Denuder	SO ₂ & HNO ₃
		Citric Acid Denuder	Ammonia
		Teflon Filter	Sulphate and other major Inorganic and Organic Ions Metals (ICPMS)
		Nylon Filter	Nitrate, Sulphate
	Cartridge A	Pre-fired Quartz Filter	Black carbon, Organic carbon
	Cartridge B (2 components)	Teflon Filter	Mass, Metals (QA Check)
Pre-fired Quartz Filter		Organic carbon artifact	

The samplers are operated once every three days and samples are collected over 24 hours. One fine and one coarse filter sample are collected on the dichotomous sampler and three Chemcomb cartridge samples are collected with the speciation sampler as shown in Table 3.1. The Chemcomb cartridges are shipped to the field completely assembled and sealed and they require only mounting and leak-checking. A complete description of analytical protocols can be found in Environment Canada (2005a). Organic carbon (OC) and elemental carbon (EC) are determined on quartz filters using a DRI Model 2001 thermal/dual-optical carbon analyzer (Atmoslytic Inc Calabasas, CA) and the IMPROVE (Interagency Monitoring of Protected Visual Environments) analysis protocol. All collected samples are analyzed in Ottawa. Through the NAPS program a total of 14 (4 rural and 10 urban) sites are now in operation across Canada. In addition a complementary program was initiated at 5 CAPMoN sites using the same monitoring equipment and analytical methods. Sites have been chosen in both programs to allow urban-rural pairing of sites.

3.2.6.2 Continuous Sampling Methods for PM_{2.5}

Real-time particle monitoring began in the NAPS network in 1995, and the number of instruments grew rapidly with over 185 instruments reporting to the network in 2006. The majority of the instruments (155) are THERMO Tapered Element Oscillating Microbalance (TEOM) instruments that measure and report hourly values of PM_{2.5} mass. Beginning in 2002 many TEOM instruments in the NAPS PM_{2.5} network were fitted with a sample equilibration system (SES). The SES incorporates a special low-particle-loss Nafion dryer allowing for conditioning of the PM sample stream to a lower humidity and temperature level. Unless indicated otherwise, all PM_{2.5} mass data in this chapter are from TEOM-SES instruments operated at 30 °C or TEOMs operating at 40 °C.

The addition of real-time PM monitoring to NAPS has greatly increased the spatial and temporal resolution of the network. However, as with all methods for measuring the mass of particles or aerosols suspended in air, there are uncertainties with the TEOM measurements associated with the loss of semi-volatile chemical constituents. Due to the heterogeneous physical and chemical makeup of PM_{2.5} concentration measurements in air, no suitable reference standard exists for calibrating PM_{2.5} instruments. Therefore, PM_{2.5} can only be defined operationally according to the sampling and mass determination method utilized. The U.S. EPA has defined a Federal Reference Method (FRM) for sampling PM_{2.5}, which includes a combination of design and performance based criteria for both the sampler and subsequent laboratory treatment of the sample filter. The calibration of PM samplers for accuracy is estimated by comparison with the designated “reference” method instrument. Performance specification limits are used to control the overall PM sampling accuracy.

In Canada, the manual, 24-hour, filter-based, gravimetric method (Method No.: 8.06/1.0/M) has been adopted as the NAPS Reference Method (RM) for PM_{2.5} measurements. Interim data quality objectives (DQOs) have also been established for comparison of continuous PM_{2.5} instruments with the reference method monitors.

Table 3.2 Linear Regression Results for 24-hr Cold Season Data for TEOM-SES Instruments vs. Filter Based Instruments.

City	Years	Slope	Intercept	Adjusted TEOM value of 30 µg m ⁻³
Ontario/Quebec	2004-2005	1.30	1.8	40.8
Ottawa	2004-2006	1.39	0.3	42.0
Toronto	2004-2005	1.45	1.6	45.1
Edmonton	2004-2005	1.08	2.0	34.4
Golden	2004-2005	1.66	0.1	49.9
Abbotsford	2004-2006	1.20	2.0	38.0

At a number of locations in Canada, TEOMs, BAMs and TEOM-FDMS units (along with a number of other commercially available units) have been co-located with reference method filter-based samplers and numerous comparisons of continuous and manual PM_{2.5} measurement methods have been conducted. Preliminary data confirm the results of similar studies in Europe, the USA and western Canada, namely, that TEOM mass measurements in the cold season are generally lower than mass measured by the manual gravimetric methods (NAPS reference method) due largely to the volatilization of semi-volatile compounds from the TEOMs (Allen *et al.*, 1997; Environment Canada, 2004, Dann *et al.*, 2006). The relationship between the TEOMs and the reference method in the cold season is quite consistent across Canada and some results are summarized in Table 3.2. Agreement between the TEOM and filter-based methods during the warm season is generally excellent (Environment Canada, 2004). In some figures in this Chapter TEOM data have been adjusted to account for the cold season underestimation of PM_{2.5} mass. Since there is no ‘official’ method of adjusting TEOM data, this is done for illustration purposes only.

3.3 Ozone

3.3.1 Background and Baseline Levels of Ozone

3.3.1.1 Introduction

There is considerable interest in quantifying surface background O₃ concentrations and associated trends, as they serve to define the lower limit that can be achieved by reductions in emissions of anthropogenic precursors. Background O₃ is defined as the ambient level resulting from anthropogenic and natural emissions outside North America and natural sources within North America, and is typically a model-derived value (CCME, 2006; Fiore *et al.*, 2003). In contrast, hemispheric background has been defined as the model-based estimate of the O₃ atmospheric mixing ratio due to natural emissions only (TF HTAP, 2010). Background O₃ concentrations are variable, with variability due to geographic location, elevation, time of year, meteorology and long-range transport influences. Geographically, background O₃ levels are higher in the Northern Hemisphere, with notably large enhancements observed during the spring season. Elevation is particularly important, especially at sites with exposure to the free troposphere.

Background O₃ can exert a significant influence on ambient O₃ levels. The portion attributable to background can not only contribute to exceedances of air quality standards and objectives but also to overall exposure, thus increasing the risk to human health. As such, understanding the magnitude of background O₃ in an airshed and how it changes over time is critically important in air quality management.

However, background levels are not directly observable so the term baseline level has been defined to describe measured levels that correspond to ozone concentrations least affected by local anthropogenic precursor emissions (Chan and Vet, 2010). While this section describes both background and baseline levels, in many instances the discussion of literature-reported background levels actually refers to baseline concentrations as defined above. The original term, as published, has been retained in the discussion below.

3.3.1.2 Sources of Background Ozone

There are three sources which contribute to background O₃ in Canada: 1) downward mixing from the stratosphere to the troposphere 2) transport of O₃ from outside North America and 3) in-situ photochemical production from natural (biogenic methane, NO_x, VOC) and intercontinental transport of O₃ precursors. Although background O₃ sources are relatively well understood, there is less certainty regarding the fractional contribution of each of these sources at any given location. An example of a significant impact by background O₃ occurs during the period referred to as the spring maximum, occurring between the months of March and May.

Much of the background O₃ affecting surface levels resides in the free troposphere. Downward transfer from the free troposphere to the surface occurs relatively frequently and is facilitated by vertical motion caused by convective and frontal activity. A combination of processes appears to contribute to this dynamic repository, including in situ O₃ production, downward fluxes from the stratosphere and intercontinental transport. There is some controversy around the magnitude of the influence of stratospheric O₃ on surface background levels. While Lefohn *et al.* (2001) maintain that the influence of stratospheric O₃ is a significant component of the background concentration, modelling by Fiore *et al.* (2003) suggests that the stratospheric influence is low (<20 ppb) and that regional and hemispheric influences are the principal contributors to background O₃.

The influence of stratospheric O₃ intrusions over the Lower Fraser Valley of British Columbia was studied by Bovis (2003) using a beryllium radioisotope (⁷Be), a tracer for stratospheric O₃. The study found that although stratospheric intrusions contribute to background O₃, the episodic impact on background concentrations at ground level is relatively small. Moreover, the study did not find an increased frequency of stratospheric-tropospheric exchange (STE) events during the spring, when median O₃ concentrations are highest. Stratospheric intrusion events are typically more important at high elevation sites. ⁷Be measurements coupled with modelling studies confirmed the occurrence of STE events at two high elevation sites in Alberta (Hessel, 2003; Raven, 2004); however the contribution from STE to surface O₃ at these sites was not quantitatively determined. For more information on high elevation ozone measurements see Chapter 7, Section 7.5.5 (Stratospheric Ozone Influence in Alberta). On the south coast of BC, elevated winter O₃ levels of up to 77 ppb were associated with vertical motion coincident with the passage of a cold front (Vingarzan *et al.*, 2007).

3.3.1.3 Annual Cycles

The spring O₃ maximum is a Northern Hemisphere phenomenon and a defining feature of the annual cycle at remote and rural sites (Monks, 2000). The peak is maximal between 10-60° latitude and increases in concentration in a south to north direction (Winkler, 1988).

Latitudinal gradients in the annual cycle are the result of regional variability acting on photochemistry, deposition and transport. There is evidence that the magnitude of the spring maximum has increased over the last century (Monks, 2000). There appear to be several mechanisms responsible for the spring maximum, including UV-enhanced photochemistry in the free troposphere (Dibb *et al.*, 2003), stratospheric-tropospheric exchange (Diem, 2004; Tarasick *et al.*, 2005) and enhanced hemispheric transport (Jaffe *et al.*, 2003).

The spring maximum is a major feature of the annual cycle at all Canadian CAPMoN stations. Typically sites which are affected by significant ground level O₃ production exhibit an additional broad summer maximum. This is seen at all CAPMoN sites with the exception of Experimental Lakes Area (ELA) where the annual maximum occurs in late spring - early summer. The highest O₃ maximum values occur at Kejimikujik, Nova Scotia, Algoma, Ontario, and Egbert, Ontario, which are stations impacted by long-range transport. At Alert, in the Canadian Arctic, the spring peak is also observed between March-May; however the mean concentration for these months is reduced due to the influence of O₃ depletion events sustained by bromine reactions on aerosols (Helmig *et al.*, 2007). These depletion events can last for up to 5-10 days, during which time O₃ is completely destroyed from the boundary layer. As a result of these events, median concentrations at Alert peak between December and May. In contrast to mid-latitude sites, the lowest mean concentrations occur in the summer, a pattern typical of Arctic sites in the Northern Hemisphere (Helmig *et al.*, 2007).

3.3.1.4 Baseline and Background Concentrations and Trends

Table 3.3 Range of monthly (January-December) 8-hour median and maximum ozone concentrations and 4th highest daily max 8h (ppb) at Canadian background stations, (2006).

Location	Period of Record	Range of 8-hr Monthly Medians	Range of 8-hr Monthly Maxima	4 th Highest Daily Max 8h	Peak Month for Hours > 50 ppb (Count)
Goose Bay, Nfld.	2006	22-46	40-68	53	March (119)
Mingan, Que.	2006	25-42	40-77	52	May (28)
Fraserdale, Ont.	2006	20-39	36-72	67	May (126)
E.L.A., Ont.	2006	27-45	37-67	61	April (210)
Pickle Lake, Ont.	2006	25-44	39-71	62	April (168)
Bratt's Lake, Sask.	2006	20-39	37-65	57	August (84)
Ft. Chipewyan, Al.	2006	22-37	30-66	53	June (43)
Saturna Island, BC	2006	25-39	42-72	60	May (106)
Norman Wells, NWT	2006	21-34	33-51	46	May (6)
Inuvik, NWT	2006	17-31	29-53	44	May (5)
Snare Rapids, NWT	2006	21-39	35-54	51	March (80)

In 2006, monthly median 8-hr O₃ measurements at Canadian CAPMoN stations ranged between 17 and 46 ppb and monthly 8-hr daily maxima between 29 and 77 ppb (Table 3.3). Most sites experience winter monthly 8-hr maxima in the range of 40-45 ppb and show a spring peak in the number of hours greater than 50 ppb. The 4th highest daily maximum 8h ozone concentrations at these sites are shown in the Table and ranged from 44 to 67 ppb in 2006. Note, however, that a number of these stations are at times influenced by anthropogenic sources and, as such, the O₃ concentrations more accurately reflect baseline levels rather than actual background levels, as the two terms are defined in Section 3.3.1.1.

A recent investigation of baseline O₃ for different regions at 97 non-urban sites in Canada and the U.S. (Chan and Vet, 2010), showed that in Canada, annually-averaged baseline levels are 19 ± 10 ppb in Pacific Canada, 28 ± 10 ppb in continental western Canada, 30 ± 9 ppb in continental Eastern Canada, and 27 ± 9 ppb in Atlantic Canada. These estimates were based on six-hour averages of hourly O₃ values measured at sites from four major North American networks over the period 1997-2006. This analysis concluded that baseline O₃ levels vary seasonally (and diurnally) in all regions of the country and that baseline concentrations in Canada are 37 ± 7 ppb in the spring (32 ± 5 ppb in the winter) in continental Eastern Canada, 34 ± 7 ppb (31 ± 6 ppb) in Atlantic Canada, 25 ± 11 ppb (18 ± 9) in Pacific Canada, and 36 ± 8 ppb (29 ± 6 ppb) in continental Western Canada.

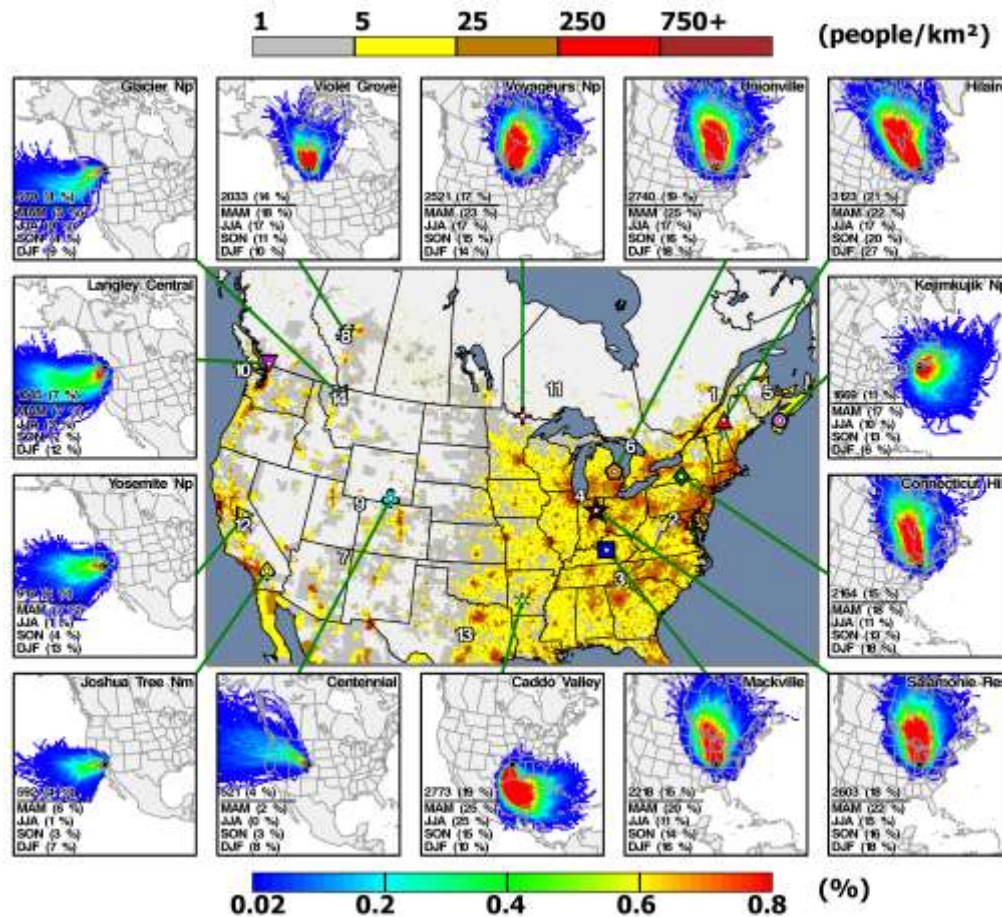


Figure 3.4 Probability densities of air parcel trajectory clusters (cleanest background air) associated with the lowest May – September 95th percentile ozone mixing ratios for 14 statistically representative sites (out of 97 in total) for the years 1997–2006 combined. The total number of trajectories for the cluster and the transport frequency (in bracket, %) is shown above the horizontal bar. The relative seasonal transport frequencies (relative to other five clusters) are shown below the bar (other five clusters not shown). The gridded population shown in the centre was obtained from the Centre for International Earth Science Information Network (CIESIN), Columbia University; and Centro Internacional de Agricultural Tropical (CIAT), Gridded Population of the World (GPW), Version 3, for the year 2005. Palisades, NY: CIESIN, Columbia University. Available at: <http://sedac.ciesin.columbia.edu/gpw>

¹The trajectory probability value associated with each grid square was calculated by summing all trajectories that had traversed over a given grid divided by the total number of trajectories for the entire time period included in the cluster analysis. The endpoint of the upper whisker, upper edge, line inside, dot inside, lower edge of the box and endpoint of the lower whisker show the overall (Jan - Dec) 95th, 75th, median, mean, 25th and 5th percentiles respectively. The dashed line shows the overall median of 29 ppb of the medians from all sites. The bottom panels on the left shows the long-term trends of ozone (ppb) generated by the LOWESS technique and on the right shows the intra-annual cycles associated with these trajectory clusters.

The following text provides a brief description of the methods used by Chan and Vet (2010) to estimate the aforementioned baseline O₃ levels. To begin, Figure 3.4 shows the probability densities of air parcel trajectory clusters (cleanest background air) associated with the lowest May – September 95th percentile ozone mixing ratios for 14 statistically representative sites (out of 97 in total) for the years 1997–2006 combined. The Canadian Meteorological Centre’s (CMC) 3-day backward trajectories at the 925 mbar arrival pressure level were used. The total number of trajectories for the cluster and the transport frequency (in brackets, %) is shown above the horizontal bar. The relative seasonal transport frequencies (relative to other five clusters) are shown below the bar (other five clusters not shown). The trajectory clusters chosen are associated with the lowest 95th percentile O₃ concentration at all sites during May to September. This was selected to represent baseline air flow in the hope of minimizing the influence of local photochemically-produced and long-range transported O₃, which generally contributes to peak levels. Thus, the least anthropogenic influence should be expected from these baseline clusters. Generally, the lowest concentrations for inland sites are associated with northerly arctic flows whereas, for coastal sites, they are associated with oceanic flows. For the most part, this set of air mass clusters traverses areas with minimal known precursor sources. However, it is important to note that the estimated baseline value for each site may be affected by various O₃ removal processes such as local dry deposition and NO scavenging.

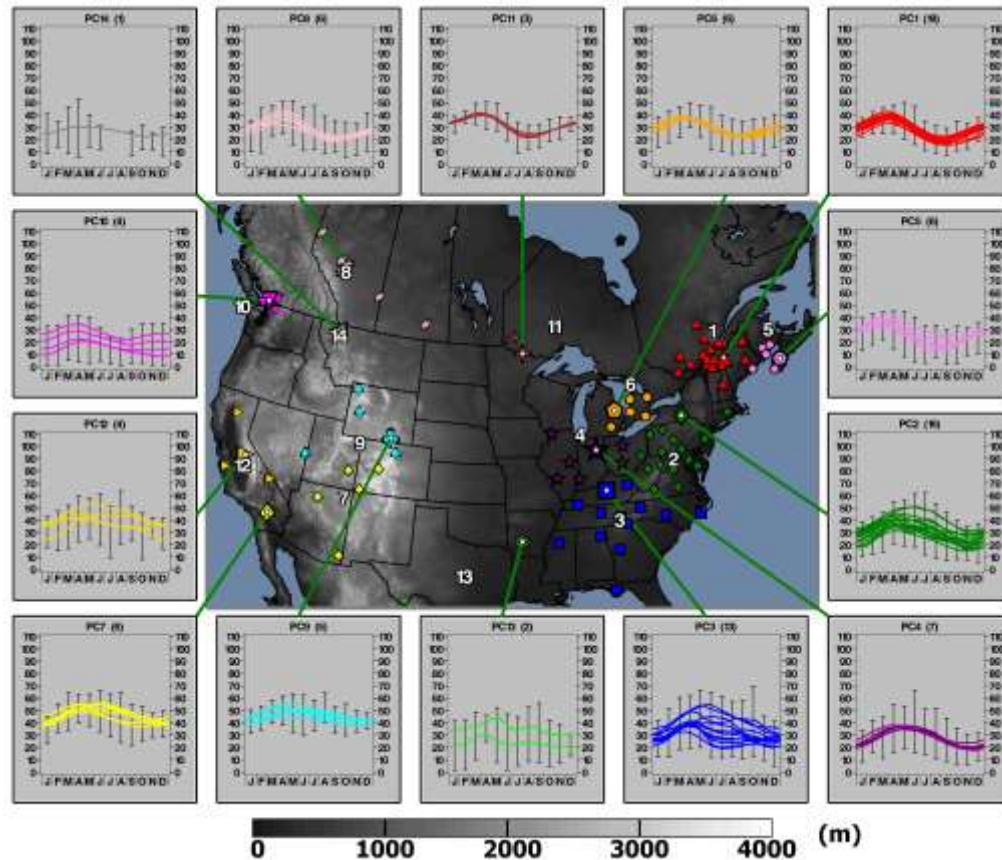


Figure 3.5 Seasonal ozone variations generated by LOWESS associated with the cleanest air trajectory clusters for all 97 sites. The error bars show the monthly ensemble site 5th to 95th percentiles for the region. The regional groupings are based on rotated PCA for JJA months. Elevations (above sea level, metres) are shown in gray scale from dark to light to represent low to high elevations. Elevations have been normalized to have a minimum of zero metre.

Figure 3.5 shows seasonal O₃ variations generated by LOWESS (Chan and Vet, 2010) associated with the cleanest air trajectory clusters for all 97 sites. The error bars show the monthly 5th to 95th percentiles for all sites in the region. Elevations (above sea level, meters) are shown in gray scale from dark to light to represent low to high elevations. For the cleanest air clusters in Figure 3.4, the high springtime ozone peak and the lack of high summertime values in all regions except PC2, PC3 and PC4 (eastern, southeastern and Midwest US) suggest a lack of active local or regional photochemical ozone production (Goldstein *et al.*, 2004), and the influence of long-range transport to the sites with air descending from either the Pacific, Arctic or Atlantic Oceans, as seen in Figure 3.4. In contrast, precursor-source-influenced air in Canada and the US appears to strongly affect regions PC2, PC3 and PC4 because of the presence of high summertime values. Not surprisingly, this suggests that, even for these non-urban sites, the baseline level is influenced by proximity to high density precursor emission sources and by high frequencies of subsidence inversions (Fiore *et al.*, 2002, 2003; Chan and Vet, 2010). Because of the similarity of the within-region seasonal

profiles and the narrow range of variability over such large spatial scales, the statistical method used is effective at selecting baseline air in most of the regions. These seasonal profiles (which exhibit spring maxima and summer minima) are consistent with typical ozone seasonal variations at remote locations in the Northern Hemisphere (Singh *et al.*, 1978).

Annual average O₃ levels at CAPMON stations fall within the range reported for most US national parks (based on CASTNet data at <http://java.epa.gov/castnet>) and some northern hemisphere remote sites (based on data from US NOAA Earth System Research Laboratory at <http://www.esrl.noaa.gov/gmd/>). In addition they are in the range of estimates of annual average northern hemisphere background levels of between 25 and 40 ppb (Jaffe *et al.*, 2003; Lindskog and Kindbom, 2001; ACCENT, 2006; Fiore *et al.*, 2003). The annual range is higher at the Arctic station of Alert, with medians ranging between 30-34 ppb. The higher levels observed at Alert are typical of arctic sites which are subject to a significant amount of long-range transport from the mid-latitudes during the spring and summer (Helmig *et al.*, 2007).

O₃ levels at background sites over the mid-latitudes of the Northern Hemisphere have approximately doubled from those measured over a century ago, with the greatest increase having occurred since the 1950s (Vingarzan, 2004). Recent trend analyses suggest that this trend continues at remote or high altitude locations (Simmonds *et al.*, 2004; Lelieveld *et al.*, 2004; Oltmans *et al.*, 2006) and in incoming air on the west coast of North America.

This increase has occurred while peak O₃ concentrations have declined in many of the more densely populated areas of the United States due to reductions in local emissions of NO_x and non-methane hydrocarbons (NMHCs) precursors (U.S. Environmental Protection Agency, 2003).

Table 3.4 Meteorologically and seasonally adjusted trends at CAPMoN sites using GLMM analysis. Values in bold are statistically significant at $p < 0.05$. Daytime averages: 10:00-18:00hrs; nighttime averages: 20:00-4:00 hrs. (1990 – 2006)

Location	Parameter	Elevation (m)	Adjusted Trend (ppb yr ⁻¹)
Kejimikujik, NS	O ₃ daily avg.	127	0.91
Kejimikujik, NS	O ₃ daytime avg.	127	0.79
Kejimikujik, NS	O ₃ nighttime avg.	127	0.79
Algoma, Ontario	O ₃ daily avg.	411	-0.54
Algoma, Ontario	O ₃ daytime avg.	411	-0.41
Algoma, Ontario	O ₃ nighttime avg.	411	-0.48
Egbert, Ontario	O ₃ daily avg.	253	-0.31
Egbert, Ontario	O ₃ daytime avg.	253	-0.21
Egbert, Ontario	O ₃ nighttime avg.	253	-0.37
Bratt's Lake, Sask.	O ₃ daily avg.	588	0.09
Bratt's Lake, Sask.	O ₃ daytime avg.	588	0.05
Bratt's Lake, Sask.	O ₃ nighttime avg.	588	-0.03
Esther, Alberta	O ₃ daily avg.	707	0.22
Esther, Alberta	O ₃ daytime avg.	707	0.26
Esther, Alberta	O ₃ nighttime avg.	707	0.23
Saturna Island, BC	O ₃ daily avg.	178	0.56
Saturna Island, BC	O ₃ daytime avg.	178	0.74
Saturna Island, BC	O ₃ nighttime avg.	178	0.49

There is evidence that O₃ entering North America above the boundary layer in spring has increased significantly over 20 years (Cooper et al, 2010), with the largest increase in air parcels that originate over major Asian emission regions. To investigate changes in baseline O₃ at Canadian locations, meteorologically and seasonally adjusted trends were calculated for Canadian sites which experience the least anthropogenic influence, as shown in Table 3.4. In order to minimize the effect of anthropogenic influences, trends in the daily average, daytime average and night-time average (rather than the maxima) were evaluated for each site. The results indicate a spatial pattern of positive trends in maritime Canada, negative trends in Ontario and positive trends in western Canada. There is no overall daytime or night-time pattern in the trends, as these were influenced more by location than time of day. Note that Kejimikujik, Egbert and Saturna are subject to regional and or transported pollution which influences the trends. In particular, the negative trends at the Ontario sites are likely influenced by reductions in precursor emissions in the U.S. For more detailed regional information on ozone trends and further region-specific discussion please refer to Chapter 7.

In the Canadian Arctic, at Alert, there is a positive trend of 0.19 ppb yr^{-1} for the period 1992-2004, in addition to an above average increase in O_3 during the spring period (Helmig *et al.*, 2007). Positive trends of approximately 0.4 ppb were also reported from measurements in the lower troposphere over Alert (Tarrasick *et al.*, 2005). Recent analysis of Canadian ozonesonde data indicates that trends in the Canadian Arctic have reversed from the 1990s and are now positive in both the lower stratosphere and upper troposphere (Tarrasick *et al.*, 2005). This rebound was attributed to small changes in atmospheric circulation, rather than a recovery of the ozone layer from halocarbon-induced depletion.

Previous studies at background sites outside of North America have also seen increasing trends in overall O_3 mixing ratios, e.g. Greenland (Helmig *et al.*, 2007), the North Atlantic (Lelieveld *et al.*, 2004), Ireland (Simmonds *et al.*, 2004), continental Europe (EMEP, 2005), Japan (Tanimoto, 2007), China (Chan *et al.*, 2003) and Antarctica (Helmig *et al.*, 2007). Rising trends have not been uniform, however, as the relatively steep trends of the 1970s and 1980s have in some cases given way to more modest trends post 1990. At mid-latitudes in the Northern Hemisphere, continental Europe and Japan, significant increases in the 1970s and 1980s appear to have leveled off or in some cases declined in the more recent decades. Time series, beginning in the 1980s at sites located in the mid latitudes of North America, generally confirm the modest changes in the most recent two decades. (Oltmans *et al.*, 2006). The slower rate of increase, or in some cases lack of an increase, over the past decade is believed to reflect recent declines in O_3 precursor emissions in North America and Europe. Reductions in precursor emissions have also resulted in decreasing peak O_3 concentrations in a number of urban and rural-impacted areas of Canada, United States and Europe (Vingarzan and Taylor, 2003; US EPA, 2003; EMEP, 2005).

Modelling studies by Fusco and Logan (2003) have provided insight into possible reasons for the observed rising O_3 trends. Results indicate that since the 1970s, rising NO_x emissions account for a 10-20% increase in O_3 , and rising methane emissions account for a 3-4% increase in background O_3 . Although NO_x has been declining in North America and Europe, it continues to rise globally due to emissions from East Asia, which have been increasing at a rate of 4-6% per year over the past two decades (Streets *et al.*, 2001). Although recent statistics on energy use in China suggest a slight decline in emissions since 1996 (Carmichael *et al.*, 2002), the continuing rapid pace of industrialization in Asia is expected to result in a continuing rise in global NO_x emissions, at least for the first part of the 21st century (Amann *et al.*, 2006; Hudman *et al.*, 2004).

Some of the most compelling evidence for increasing hemispheric background levels relates to trans-continental transport. Measurements from background sites on the west coast of the United States have repeatedly detected episodic enhancements of surface O_3 related to trans-Pacific transport. A particularly large O_3 enhancement occurred during the summer of 2003 as a result of large-scale fires in Siberia, resulting in exceedances of the air quality standard in Washington State (Jaffe *et al.*, 2004). Modelling studies using global chemical transport

models lend further evidence to the impact of continental transport. Results indicate that Asian pollution contributes about 3-10 ppb to average background O₃ levels in the western United States during the spring (Jacob *et al.*, 1999; Yienger *et al.*, 2000), when storm and frontal activity in Asia is most prevalent and westerly transport of Asian air across the North Pacific is strongest (Merrill, 1989; Savoie *et al.*, 1989). The influence of hemispheric background O₃ is not limited to the spring season. Fiore *et al.* (2002) estimated that during the summer of 1995, background O₃ produced outside of the North American boundary layer contributed an average of 25-35 ppb to afternoon surface O₃ concentrations in the western United States and 15-30 ppb in the eastern United States. Local meteorology was also found to affect the influence of background O₃. While the background influence was least during acute high O₃ episodes associated with regional stagnation, it was greatest (up to 14 ppb) under moderately polluted conditions (50-70 ppb O₃), when subsidence from the free troposphere associated with convective events combines with subsequent in situ O₃ production in the boundary layer (Fiore *et al.*, 2002).

Not all O₃ attributed to upstream continental sources is transported as molecular O₃. There is evidence of in situ O₃ formation during trans-Pacific transport (Nowak *et al.*, 2004), and formation in subsiding plumes reaching North America (Roberts *et al.*, 2004). The latter is based on measurements of PAN, a non-soluble, efficiently transported NO_y species, which, upon decomposition, releases NO_x and contributes to O₃ formation.

Models also suggest that North American emissions have substantial effects on Europe. It has been reported that 20% of the exceedances of the European Community ozone standard in the summer of 1997 over Europe would not have occurred in the absence of anthropogenic emissions from North America (Li *et al.*, 2002). Asia is a significant source of O₃ precursors and the circulation patterns result in trans-Pacific long range transport. It is estimated that precursors from North America and Europe contribute as much to surface O₃ in Asia, as Asian sources contribute to each other (HTAP, 2010). Note that model projections should be interpreted with caution; however, as there is still a significant amount of uncertainty associated with projections of background levels and intercontinental transport.

3.3.2 Ozone Climatology

3.3.2.1 Introduction and Current Ozone Concentrations

There were 240 Canadian O₃ monitoring stations reporting at least one year of data in the time period of 1990 to 2006. Of these sites, 89 had a long enough period of record (at least 14 out of 17 years) to be included in the trend analysis. Fifty-eight of these trend sites were located in urban or suburban areas and 31 were at rural locales. Data from an additional 1,000 U.S. urban and rural sites are used in some figures in order to extend the spatial analysis to include most of North America. O₃ data have been analyzed to illustrate seasonal, diurnal and day-of-the-

Daily maximum 8-hr O₃ concentrations (mean, 25th and 75th percentiles, minimum/maximum and outliers/extremes) for active stations arranged west to east are shown in Figure 3.6. These O₃ statistics are provided for May to September for the years 2004 to 2006. For the Canadian sites, median 8-hr O₃ concentrations ranged from 18 (Vancouver-Robson and Hornby) to 51 ppb (Port Stanley and Chatham). As shown in many studies, mean and median O₃ concentrations are highest at rural sites and lowest at downtown urban sites (McKendry, 1993). The highest 8-hr daily maximum O₃ concentration for 2004 to 2006 was 104 ppb, recorded at the Grand Bend site in 2005. The highest 1-hr O₃ concentration for 2004 to 2006 was 131 ppb also recorded at the Grand Bend site in 2005. The highest 75th percentile 8-hr O₃ value of 61 ppb was recorded at the Port Stanley site. It is clear from Figure 3.6 that 8-hr values over 65 ppb are infrequent at most sites outside of southern Ontario and Quebec. The most notable exceptions are Chilliwack and Hope B.C., and Kejimikujik National Park, N.S. The lowest peak O₃ concentrations are found in the Yukon, North West Territories, eastern Nova Scotia and in Newfoundland and Labrador.

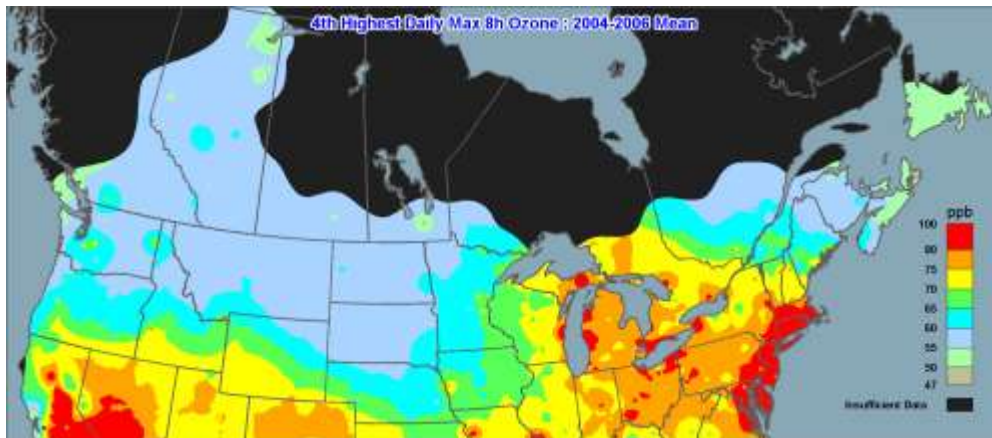


Figure 3.7 Spatial distribution of the 3-year-average 4th highest daily maximum 8-hr ozone concentration in ppb (2004-2006).

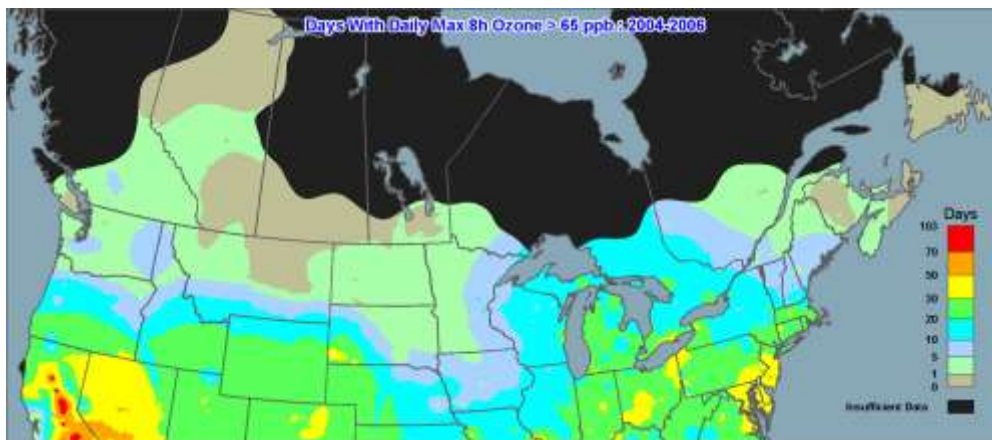


Figure 3.8 Annual average number of days with daily maximum 8-hr ozone above 65 ppb in the 3-year period of 2004 – 2006.

The spatial pattern of peak O₃ concentrations as defined by the CWS metric (4th highest daily maximum 8-hr ozone) for 2004 to 2006 is provided in Figure 3.7, and the number of days with daily maximum 8-hr O₃ greater than 65 ppb is given in Figure 3.8. Both these figures include data from approximately 1,100 U.S. monitoring sites using data extracted from the AQS database (see Section 3.2.1). Annual statistics for these sites for the 2004-2006 period were spatially interpolated using ordinary kriging. To minimize interpolation error, the data were divided into two populations: regions where the site density was high (California, the Northeast US, Southern Ontario and Quebec) and regions where the site density was lower (all the remaining sites). The two populations were interpolated separately and the results were combined to produce the final maps. The interpolation uncertainty in Figure 3.7 is generally under 15% and as high as 25% in some areas, particularly in regions with low site density like portions of western Canada.

On the assumption that local uncertainties are high but the general spatial pattern is reasonable, the map of the 3-year 4th highest 8-hour daily maximum values for the period 2004-2006 (Figure 3.7) shows that southern Ontario is part of a large high concentration area (>65 ppb) that encompasses the entire northeastern U.S., with highest values (75-100 ppb) occurring in southern Ontario, the Great Lakes states and the US eastern seaboard. As discussed later in Chapter 7, the high O₃ levels that occur in southern Ontario are due, in part, to Ontario emissions and in part to transboundary transport of O₃ and O₃ precursors from the United States. By comparison, western Canada shows low levels of O₃ (40-60 ppb) except around Edmonton, Alberta and the Lower Fraser Valley, BC. It is important to point out that, with respect to temporal representativeness, the 2004-2006 period exhibited the lowest 3-year ozone concentrations of any 3-year period between 2000 and 2007 (both in the east and the west). The period with the highest concentrations was 2001-2003.

Figure 3.8 shows that southern Ontario, along the north shore of Lake Erie, had the highest number of days (30-50) that exceeded 65 ppb in Canada in the 2004-2006 period, and that the rest of southern Ontario and parts of southern Quebec exceeded that value between 5 and 30 days. In contrast, almost all of western Canada and the Atlantic provinces exceeded 65 ppb from only 0 to 5 days. Figures 3.7 and 3.8 confirm, in a spatial sense, the information in Figure 3.6 that southern Ontario is part of a large eastern US - southeastern Canada airshed that has high levels (i.e., >65 ppb) of O₃ with relatively high frequency, while western Canada and Atlantic Canada seldom have such high levels.

Table 3.5 Summary of Regional Scale Ozone Episodes by Region for the Period 2001-2005 (NOTE: Episodes defined as days where 33% of monitoring sites in a region record maximum daily 8h ozone greater than 65 ppb)

Region	Regional Episode Criteria	Total No. of Regional Scale Episodes	Notable Episode Dates	No. of Sites Recording Daily Max 8h Ozone > 65 ppb	Max. 8h Ozone (ppb)	Sites with PM _{2.5} > 30 µg m ⁻³	Max 24h PM _{2.5} Conc. (µg m ⁻³)
Southern Atlantic	6 or more Sites > 65 ppb (Total Sites 21)	20	20-Jun-2001	13	104	0	-
			03-Aug-2001	12	90	0	-
			10-Aug-2001	10	104	3	35
			27-Jun-2003	12	87	2	31
			25-Jun-2005	10	79	0	-
S. Quebec/ Eastern Ontario	15 or more Sites > 65 ppb (Total Sites 46)	49	02-May-2001	38	95	0	-
			11-May-2001	32	82	0	-
			15-Jun-2001	34	89	2	44
			19-Jun-2001	36	102	0	-
			20-Jun-2001	32	94	0	-
			21-Jun-2002	34	84	0	-
			11-Aug-2002	35	96	0	-
			12-Aug-2002	33	84	12	49
			13-Aug-2002	31	89	12	47
			14-Aug-2002	34	86	12	42
			09-Sep-2002	33	95	5	34
			10-Sep-2002	34	92	11	54
			25-Jun-2003	32	102	11	44
			26-Jun-2003	37	103	16	54
			27-Jun-2003	37	97	0	-
21-Aug-2003	31	86	11	40			
30-Apr-2004	32	80	0	-			
08-Jun-2004	33	84	13	39			
Southern Ontario	18 or more Sites > 65 ppb (Total Sites 56)	118	03-May-2001	34	91	5	33
			13-Jun-2001	29	94	6	40
			14-Jun-2001	36	105	13	53
			15-Jun-2001	37	108	20	54
			19-Jun-2001	33	117	0	-
			27-Jun-2001	36	106	20	45
			28-Jun-2001	32	95	16	44

Region	Regional Episode Criteria	Total No. of Regional Scale Episodes	Notable Episode Dates	No. of Sites Recording Daily Max 8h Ozone > 65 ppb	Max. 8h Ozone (ppb)	Sites with PM _{2.5} > 30 µg m ⁻³	Max 24h PM _{2.5} Conc. (µg m ⁻³)
			29-Jun-2001	36	128	10	39
			30-Jun-2001	37	109	12	39
Southern Ontario			30-Jun-2002	34	107	14	35
			01-Jul-2002	32	100	14	48
			10-Aug-2002	35	92	0	-
			11-Aug-2002	36	108	21	47
			12-Aug-2002	33	103	19	50
			13-Aug-2002	33	99	14	38
			14-Aug-2002	18	101	9	43
			08-Sep-2002	37	113	4	41
			09-Sep-2002	35	109	20	49
			10-Sep-2002	28	94	10	40
			23-Jun-2003	31	107	0	-
			24-Jun-2003	36	112	8	33
			25-Jun-2003	36	123	28	46
			26-Jun-2003	35	108	28	55
			02-Jul-2003	30	110	11	36
			03-Jul-2003	33	108	19	46
			04-Jul-2003	29	101	5	33
			24-Jun-2005	39	104	5	38
			25-Jun-2005	37	98	9	35
Southern Ontario			26-Jun-2005	14	81	0	-
			27-Jun-2005	31	98	8	52
			28-Jun-2005	37	101	30	53
			12-Sep-2005	33	82	23	46
			13-Sep-2005	37	93	36	48
			14-Sep-2005	18	89	26	41
Prairies	7 or more Sites > 65 ppb	3	12-Jul-2002	7	84	0	-
	(Total Sites 23)		09-Aug-2003	6	71	0	-
			15-Aug-2003	10	80	7	95
			16-Aug-2003	6	80	6	54
			04-Jun-2004	9	71	0	-
LFV	4 or more Sites > 65 ppb	2	20-Jun-2004	9	70	0	-
	(Total Sites 12)		14-Aug-2005	4	71	0	-

Following on from the spatial analysis, the frequency of regional scale episodes (defined as days where 33% of monitoring sites in a region record maximum daily 8h ozone greater than 65 ppb) has been calculated for the period 2000 to 2005 and results are shown in Table 3.5. Dates of occurrence of notable episodes (in terms of spatial extent and maximum ozone levels) are also provided in the table along with an indication of whether high PM levels were also recorded during the episode. The greatest frequency of regional-scale episodes occurred in Ontario followed by Quebec and for both these regions high ozone values often persisted for several days and were highly likely to be associated with PM_{2.5} values greater than the CWS metric of 30 µg/m³ (see Section 3.5). Regional scale episodes of ozone were almost non-existent in the Prairies and in the Lower Fraser Valley with one or two exceptions. The most notable regional scale ozone event in the Prairies was actually associated with the August 2003 forest fires in the southern B.C. interior.

A complete analysis of ozone in terms of the Canada-wide Standard can be found in the Government of Canada Five-year Progress Report on Canada-wide Standards for Particulate Matter and Ozone (Government of Canada, 2007). For the period 2003 to 2005, at least 40% of the Canadian population (approximately 13 million) lived in communities with levels above the CWS. Most of these were located in Ontario and Quebec. Outside these two provinces, only one community in British Columbia and one non-urban area in Atlantic Canada had levels above the CWS. With the exception of Saskatchewan, Manitoba and the territories, all other regions had at least one location with levels within 10% of the CWS. Provinces and territories reported data for a total of 70 communities (CMA, CA and RSA) representing more than 70% of the Canadian population.

3.3.2.2 Monthly Variation in Daily Mean and Maximum Ozone Concentrations

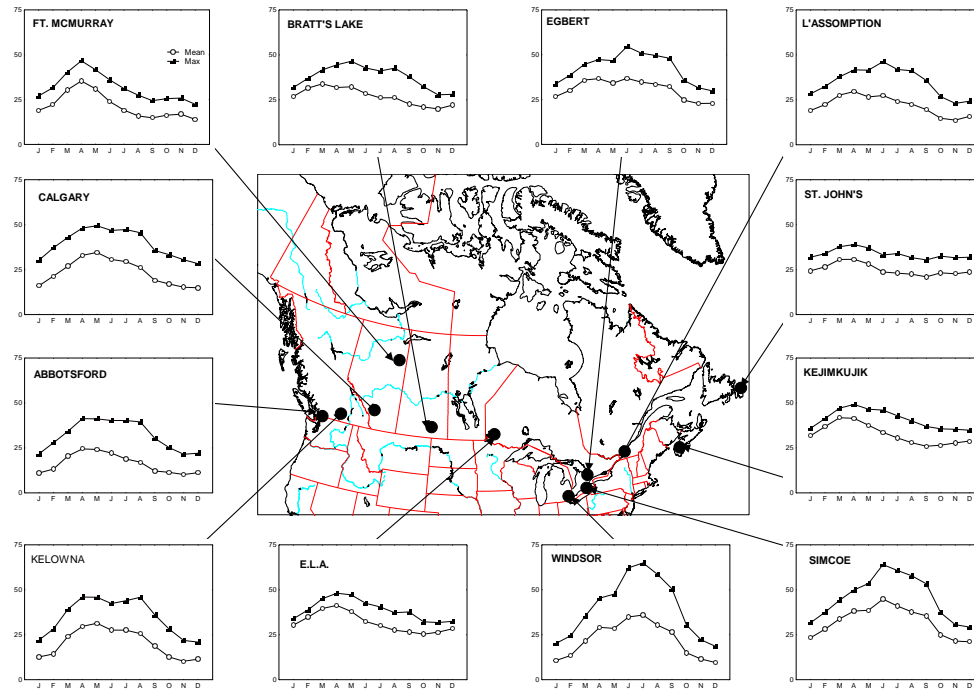


Figure 3.9 Mean (○) and mean daily maximum (●) ozone (ppb) by month averaged for the years 2001 to 2005. (Note: mean ozone concentration in ppb shown on y-axis).

Averages of daily mean and daily maximum O_3 concentrations were calculated for each month to examine seasonal variations in the data. These monthly averages revealed pronounced seasonal variations of O_3 at individual stations and regions throughout Canada (Figure 3.9). As discussed in Section 3.3.1, springtime maxima in O_3 concentrations are often a feature of remote rural and baseline sites. This observation of springtime O_3 maxima is contrary to the notion of experiencing greatest O_3 formation during the summer, when local photochemistry is usually greatest. As shown in Figure 3.9, many sites in Canada experience March to May peaks in mean and mean daily maximum O_3 . Out of 125 sites examined for the 2001 to 2005 time period only 46 experienced the highest mean daily maximum O_3 in the months of June, July or August. All of these sites except Hope, BC, were located in southern Ontario and southern Quebec. In these areas, regional-scale photochemical O_3 production and the long-range transport of pollutants can contribute significantly to enhanced O_3 levels measured from June to August, and summer-time maximum O_3 concentrations are significantly higher than those in other areas of the country (Figures 3.6 and 3.7).

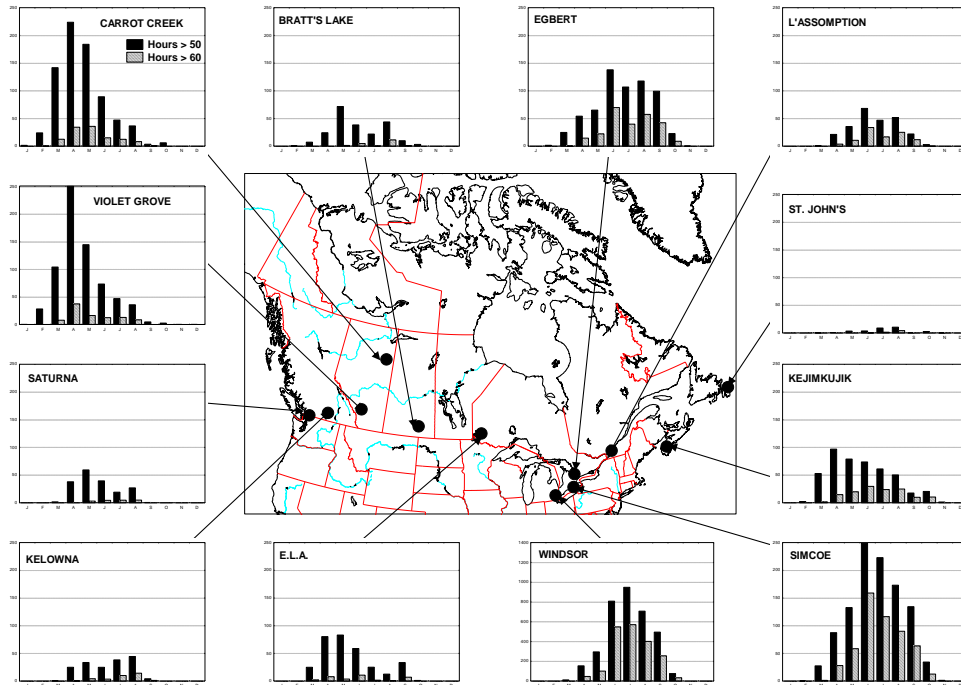


Figure 3.10 Average hours per month with ozone above 50 and 60 ppb averaged for the years 2001 to 2005. (Note: average hours per month shown on y-axis)

A similar seasonal effect is found for total hours of O_3 levels > 50 and 60 ppb by month as shown in Figure 3.10. Many western sites experience the greatest frequency of hours with O_3 levels > 50 and 60 ppb in the month of April. This high frequency of hours is driven by the processes described in Section 3.3.1 and is not associated with classical photochemical O_3 production.

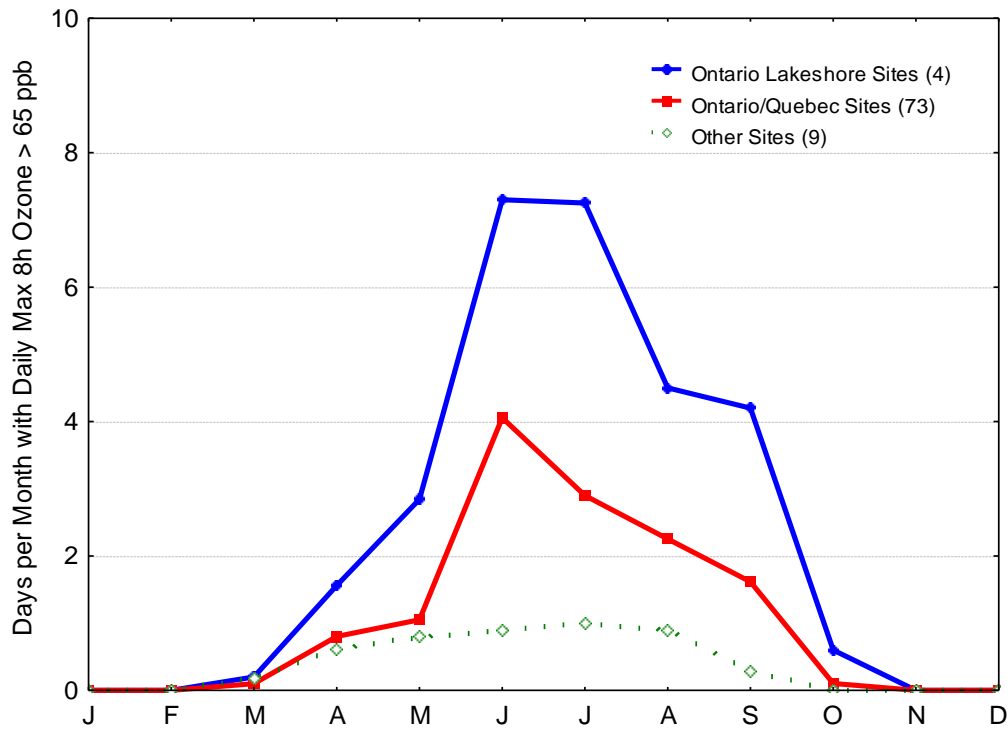


Figure 3.11 Average days per month with ozone greater than 65 ppb for the years 2001 to 2005. (Only sites averaging at least one day per year > 65 ppb are included in the plot).

The relative frequency of days per month greater than 65 ppb is shown in Figure 3.11 for the 5-year period 2001 to 2005. Only sites that averaged at least 1 day per year greater than 65 ppb were used to create the plot. The Ontario lake shore sites (Port Stanley, Tiverton, Grand Bend and Parry Sound) that experience the highest frequency of days greater than 65 ppb are shown separately. Only 8 sites outside of Ontario and Quebec met the criteria to be included. From the Figure it can be seen that ozone concentrations greater than 65 ppb can be experienced in any of the months March through October but the greatest frequencies occur for June through September with June being the peak month during the 2001 – 2005 time period.

3.3.2.3 Diurnal Variation in Ozone Concentrations - Summer and Winter

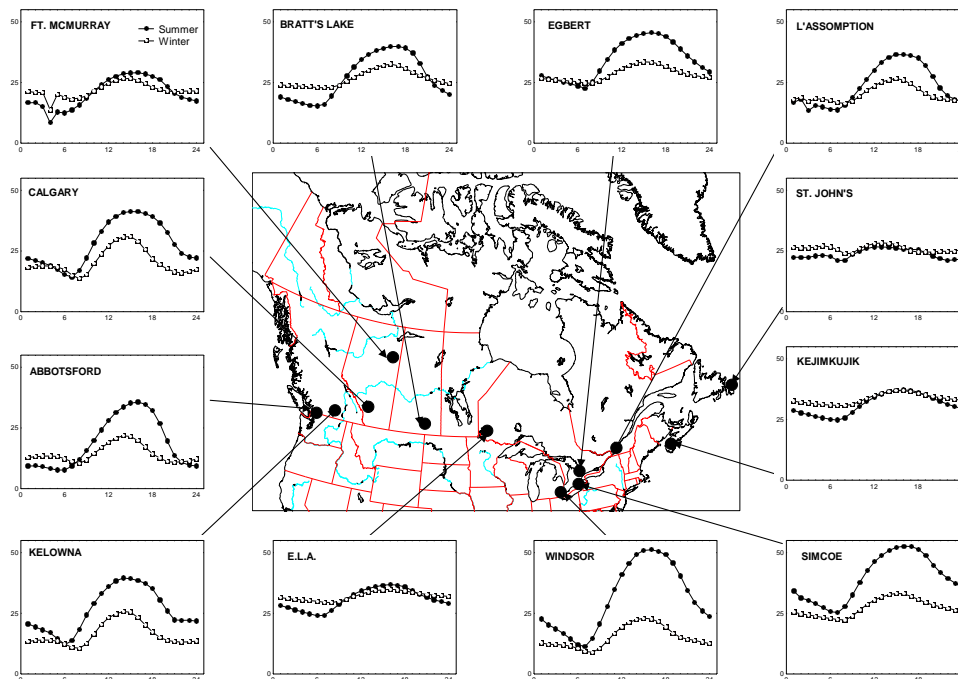


Figure 3.12 Diurnal variation in ozone concentration (ppb) – summer (May-Sep) (●) and winter (Nov-Mar) (○) averaged for years 2001 to 2005. (Note: Mean ozone concentration in ppb shown on y-axis)

Hourly O_3 data for winter and summer time were aggregated separately to compute ensemble averages. Winter months in this analysis comprised November to March, while summer months included May to September. As expected, large differences exist in the amplitude of diurnal O_3 concentration cycles for winter and summer-time (see Figure 3.12). Ozone levels during winter remain low due to limited photochemistry and exhibit smaller diurnal variations. Most urban sites record mean winter O_3 concentrations in the range of 15 to 20 ppb. The rural remote sites of ELA and Kejimikujik had mean winter O_3 concentrations of 25 to 30 ppb. The St. John's and Kejimikujik sites showed the smallest variation between summer and winter diurnal profiles with mean winter O_3 being slightly higher than summer. Sites in southern Ontario, Toronto and Vancouver showed the greatest divergence between the summer and winter profiles.

Most urban sites recorded comparable summer and winter nighttime O_3 concentrations. At urban sites, O_3 concentrations were much lower during nighttime than daytime. Overall daily mean O_3 concentrations in rural locations were greater than those recorded in nearby urban sites and diurnal profiles were much smoother, with higher nighttime O_3 concentrations. As described in the next section the shape and amplitude of diurnal O_3 concentration cycles are strongly influenced by atmospheric conditions, site location and prevailing NO_x levels.

3.3.2.4 Diurnal Variation in Ozone Concentrations - Weekdays and Weekends and 1991 to 1995 versus 2001 to 2005

It is known that the O₃ precursor emissions have strong temporal variations on several time scales. For example, the main source of NO in urban areas - traffic - shows a very strong diurnal cycle with a maximum generally in the daylight hours (see Section 3.4.2). Superimposed on this is a further modulation, especially in urban areas, related to the maximum traffic flow in the morning and evening rush hours. In addition, the diurnal variation of emissions is different on weekends to that occurring on weekdays. Fewer people go to work on Saturdays, making the morning rush hour weaker, but shopping trips increase automobile traffic during the day. On Sunday, the pattern is very different again, with little early morning traffic and a steadier flow during the rest of the day. The number of heavy duty diesel vehicles is also substantially reduced on Saturdays and even further again on Sundays. These changes in the precursor emission patterns suggest that especially during the daylight hours O₃ concentrations might show significant differences in weekend versus weekday behaviour. Previous studies (Environment Canada, 1997; Fuentes and Dann, 1993; Pryor *et al.*, 1995) have shown substantial differences between weekdays and weekends in urban diurnal O₃ profiles.

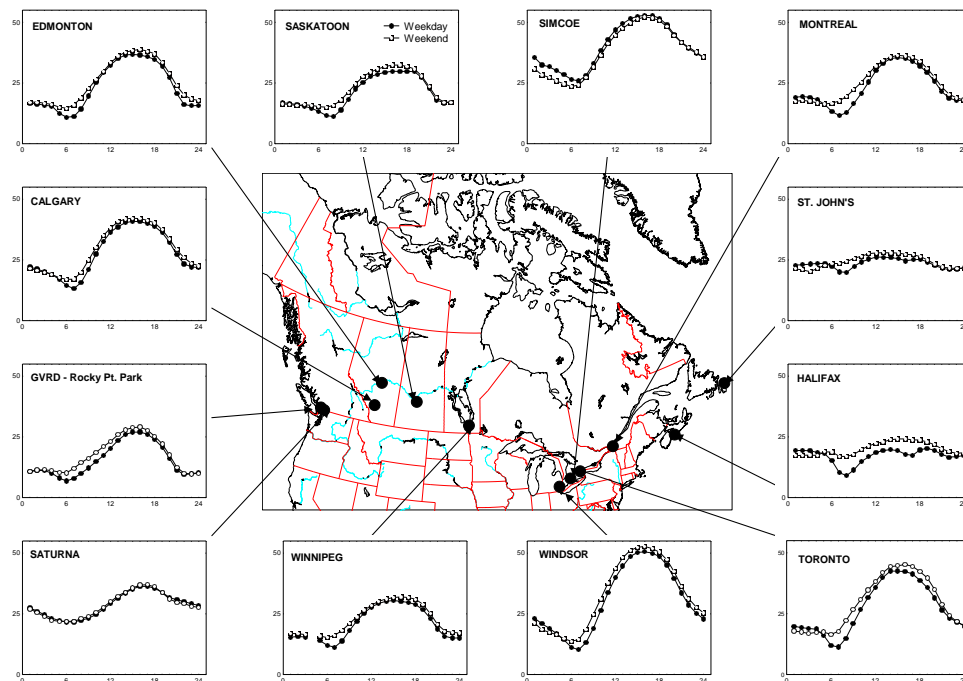


Figure 3.13 Diurnal variation in ozone concentration (ppb) – weekday (●) and weekend (○) for summertime (May to September) averaged for years 2001 – 2005. (Note: mean ozone concentration in ppb shown on y-axis).

O₃ data for urban and rural sites were aggregated to represent diurnal variations during weekdays (Monday through Friday) and weekends (Saturdays and Sundays) for the summer months and the results are shown in Figure 3.13. Reduced NO concentrations on weekends are the primary reason for the different profiles. When weekends are compared to weekdays, sites with the highest NO levels typically experience the largest increase in afternoon maximum O₃. At these sites, the increase in O₃ is observed during all daylight hours on weekends. This is attributed to the lower NO emissions and hence less titration of O₃. For the 2001 to 2005 time period 65 out of 72 urban sites showed a “weekend effect” while 32 out of 44 rural sites showed lower O₃ or no difference on weekends – this included all rural sites in southern Ontario.

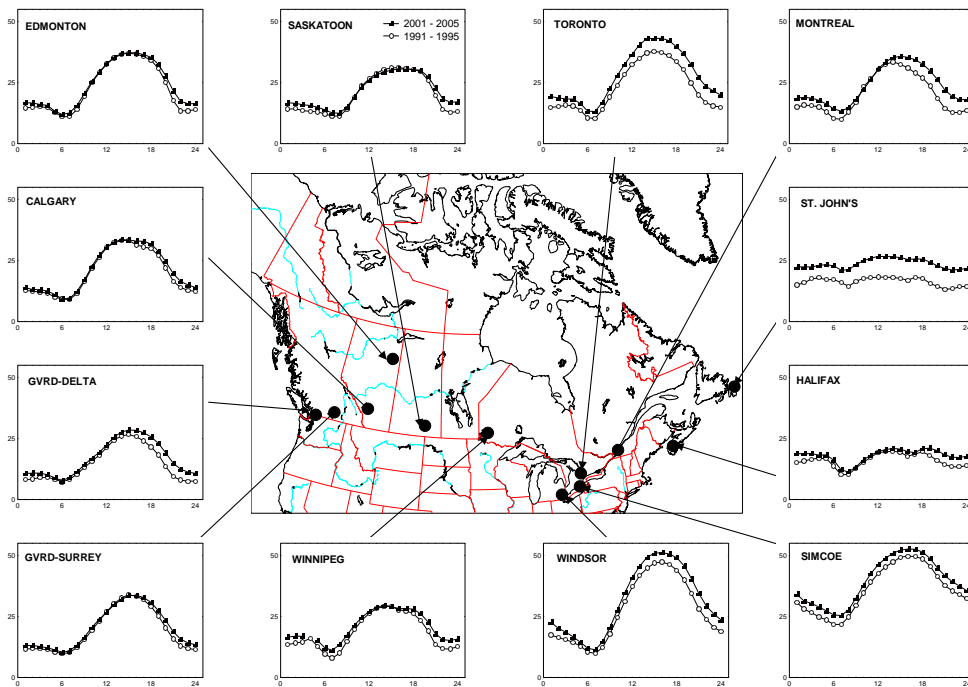


Figure 3.14 Diurnal variation in summertime (May to September) ozone (ppb) for 1991-1995 (O) vs. 2001-2005 (●). (Note: mean ozone concentration in ppb shown on y-axis).

This same effect can be seen if diurnal O₃ profiles for the time periods 1991 to 1995 and 2001 to 2005 are compared (see Figure 3.14). As will be discussed in Section 3.4.4, there have been large reductions in ambient NO and NO_x at urban sites in the period 1991 to 2005. This NO reduction has the same effect as the weekend NO reduction and is revealed as a “disbenefit” in terms of mean O₃ concentrations. Almost all urban sites in the country have seen an increase in mean diurnal O₃ as a result of NO reductions. This has had a noticeable effect on O₃ trends that are based on average levels as will be discussed in Section 3.3.4.2.

3.3.3 High-elevation Sites

Sites above 2000 m are often claimed to be “above the boundary layer” or “representative of the free troposphere” by sole consideration of their elevation (Chevalier *et al.*, 2007). However, mountains considerably enhance atmospheric turbulence and affect circulation for many reasons and it cannot be certain that all high-elevation sites are always free from the influence of the surface without further investigation (Chevalier *et al.*, 2007). It is also known that background O₃ level increases with height in the lower troposphere (Zbinden *et al.*, 2006, Vingarzan, 2004).

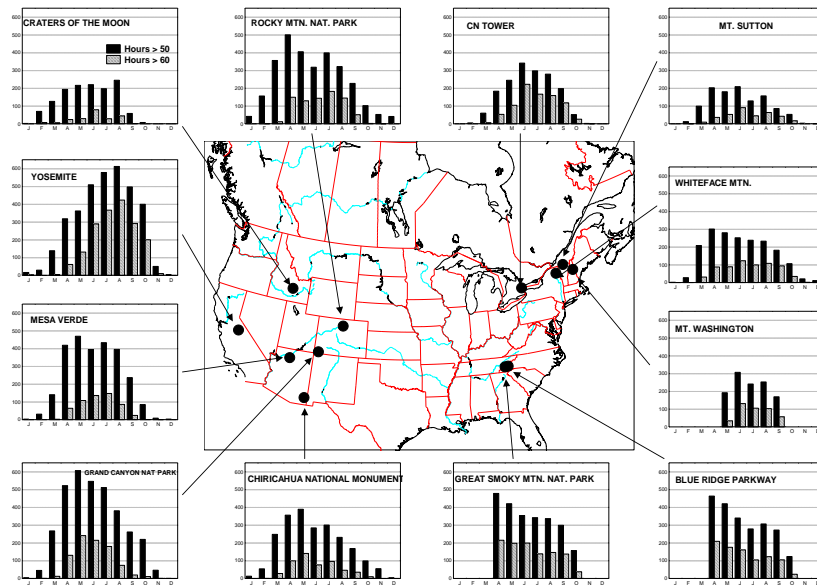
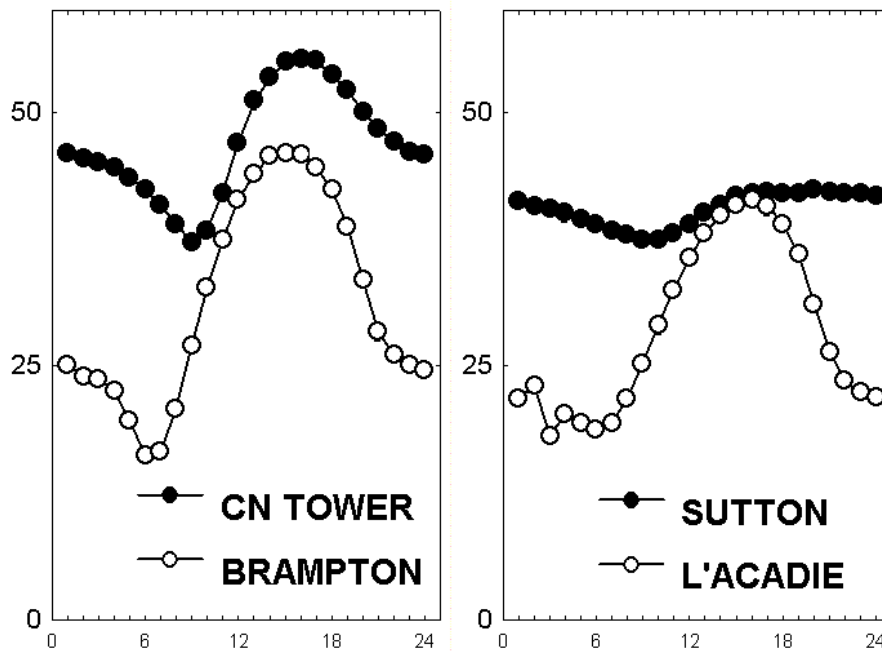


Figure 3.15 Average hours per month with ozone above 50 and 60 (ppb) at high-elevation sites averaged for the years 2001 to 2005. (Note: average hours per month shown on y-axis).

High-elevation sites are generally above the planetary boundary layer and hence should intercept pollutants transported over long distances. Furthermore, long-term continuous measurements of O₃ at these types of sites should indicate trends in ambient O₃, whether of global significance or of importance only to northeastern America. A number of elevated sites (actual elevations varied considerably) with long term data records were identified for North America as shown in Table 3.6. Two of the sites, Mount Sutton - Round Top Ridge and CN Tower are located in Canada. The average hours per month with O₃ levels > 50 and 60 ppb for the sites are shown in Figure 3.15. The number of hours over these thresholds is typically much higher than for surface sites (see Figure 3.10). For example the Yosemite Park site recorded on average 87% of total hours in August with O₃ levels > 50 ppb and 57% of hours with O₃ levels > 60 ppb. A number of the high-elevation sites experienced a significant number of hours with O₃ levels > 50 and 60 ppb in the months of January, February and March.

Table 3.6 Available High-elevation monitoring sites

NAPS ID	PROV/STATE	LOCATION	LAT	LONG	ELEV (m)
54102	QUEBEC	MONT SUTTON, ROUND TOP RIDGE	45.09	72.55	856
60419	ONTARIO	CN TOWER	43.64	79.39	480
160101	IDAHO	CRATERS OF THE MOON	43.46	113.56	1815
330701	NEW HAMPSHIRE	MT. WASHINGTON	44.28	71.30	1917
360301	NEW YORK	WHITEFACE MTM, SUMMIT	44.36	73.90	1480
372103	NORTH CAROLINA	GREAT SMOKY MOUNTAIN NATIONAL PARK	35.59	83.08	1550
471702	TENNESSEE	CLINGSMANS DOME, GREAT SMOKY MTNS. NP	35.56	83.50	2021
640101	ARIZONA	CHIRICAHUA NATIONAL MOUMENT	32.12	109.47	1570
640201	ARIZONA	GRAND CANYON NATIONAL PARK, W RIM DRIVE	36.07	112.15	2152
661801	CALIFORNIA	TURTLEBACK DOME, YOSEMITE NATL' PK 95389	37.71	119.70	1600
680901	COLORADO	ROCKY MOUNTAIN NP	40.28	105.55	2743
681001	COLORADO	MESA VERDE NATIONAL PARK, COLORADO	37.20	108.49	2165

**Figure 3.16 Comparison of the summertime diurnal ozone profile (ppb) for Toronto CN Tower (●) - Brampton (○) and Mont Sutton (●) - L'Acadie (○) in 2005.**

Other characteristics of elevated sites include high mean O₃ concentrations and very limited diurnal variation in concentration (see Figure 3.16). The l'Acadie site is a surface level rural site located within 50 km of Mount Sutton and the Brampton site is in a urban residential location within 25 km of the CN Tower. The Mount Sutton site has a more representative elevated-site diurnal profile than the CN Tower since the CN Tower is at a lower elevation and in an urban environment. Trends in O₃ at high elevation sites are discussed in Section 3.3.4.2.

3.3.4 Trends in Ozone

3.3.4.1 Principal Component Analysis (PCA) and Generalized Linear Mixed Model (GLMM) Trend Analysis

This section describes an analysis of ground level ozone trends in Canada and the United States for the period 1997 to 2006. The method involves a Principal Component Analysis and a Generalized Linear Mixed Model (GLMM) trend analysis. The use of the GLMM reduces the subjectivity associated with single site trend estimates by instead, combining data from multiple sites. The work and results have been published in Chan (2009) and are described in brief below.

3.3.4.1.1 PCA Analysis of North American Sites and Trend Estimation

In the past, single site trend studies have been questioned as to the validity of the data used (why a site was chosen over the other) and the statistical techniques applied to them. Inconsistencies in findings were noted among studies and even in the same region/city upon independent reanalysis. The choice of particular regions/cities/sites was questioned and it was not clear whether models had been selected that gave estimates of effect that were unbiased. These criticisms have since been addressed by the use of multi-site studies in which site-specific data on air pollution are assembled under a common framework. Hierarchical or random coefficient models provide a statistical approach for summarizing and integrating the findings of research studies in a particular area with such areas firstly defined by principal component analysis (PCA) (Eder *et al.*, 1993; Lehman *et al.*, 2004) and by positive matrix factorization (PMF) (Rizzo and Scheff, 2004). For this PCA analysis (Chan, 2009), O₃ sites were selected based on the physical reasoning of “minimal” local influence potentially caused by dry deposition and NO scavenging. In other words, the selected sites should be regionally-representative and represent well-mixed air. PCA was first performed on the correlation matrix for 97 non-urban sites from CAPMoN, NAPS, and the U.S. Clean Air Status and Trends Network (CASTNet) for the period of 1997 to 2006 during May – September using daily maximum 8-hr average O₃ values with the purpose of grouping sites that have similar O₃ characteristics.

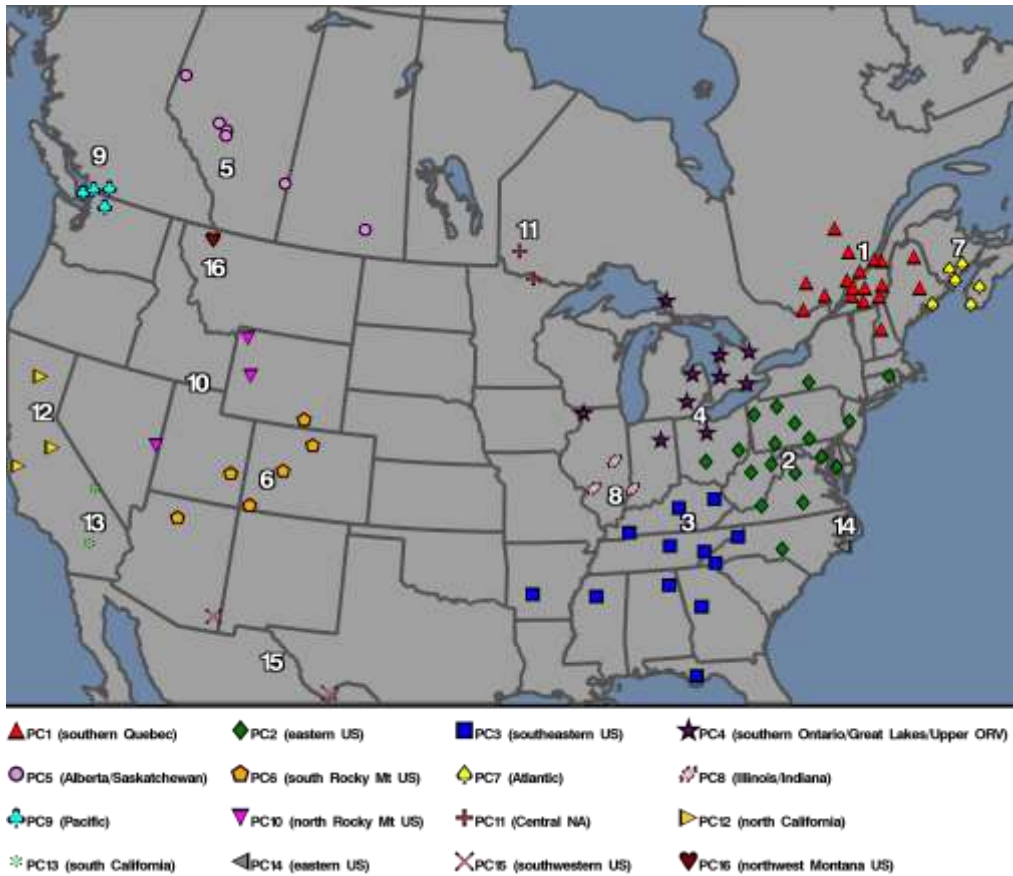


Figure 3.17 Ozone site locations and PCA-derived regions based on daily maximum 8-hr mixing ratios (97 Non-urban sites were used in the study).

The varimax orthogonal rotation led to 16 regions that together accounted for about 75% of the total variance. The PCA-derived regions or principal components were ordered by the percentage of the total variance explained from the largest to the least. Sites that were grouped together had the largest loadings associated with that particular principal component. Results of the PCA analysis are shown in Figure 3.17. The selected PCA-derived regions for subsequent trend analysis are defined as follows: PC1 – Quebec (18 sites), PC2 – northeastern U.S. (18 sites), PC3 –southeastern U.S. (12 sites), PC4 – southern Ontario/Great Lakes/Upper Ohio River Valley (10 sites), PC5 – Saskatchewan/Alberta (6 sites), PC7– Atlantic (6 sites) and PC9 – Pacific (4 sites). LOcally WEighted Scatter plot Smoothing (LOWESS) (Cleveland, 1979), a non-parametric technique was used as an exploratory analysis to display seasonal cycles and temporal trends for each PCA-derived region.

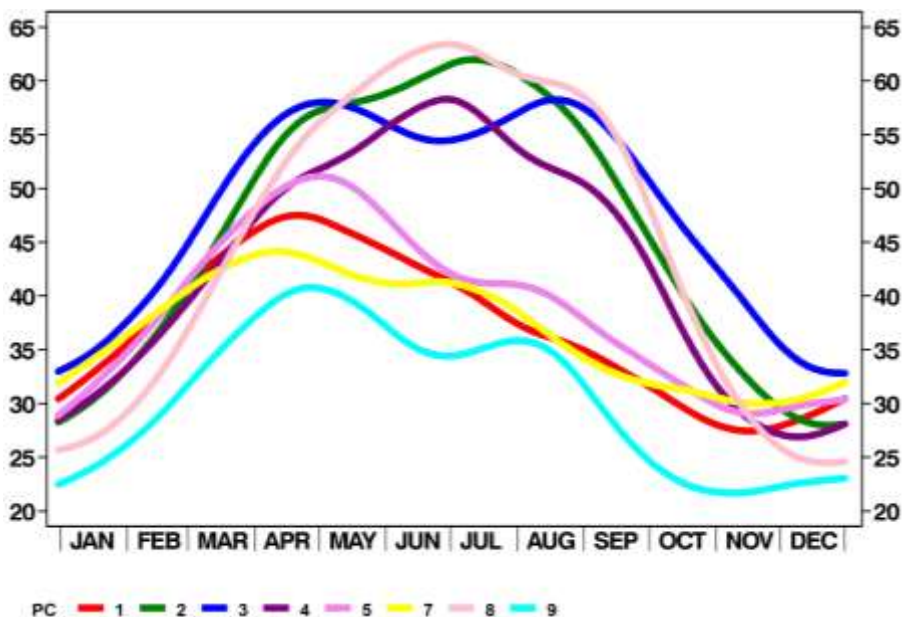


Figure 3.18 Average month-to-month cycles in PC1, PC2, PC3, PC4, PC5, PC7 and PC9 based on daily O₃ maximum 8-hr average values (in ppb) from 1997 to 2006.

The seasonal cycles are shown in Figure 3.18. As previously discussed the spring (March-May) O₃ maxima are a Northern Hemisphere phenomenon and appear in every region. The additional summer maxima are typical for locations that are affected by regional photochemical O₃ production as shown in Figure 3.18 for PC2, PC3, and PC4 which are located in the highest O₃ precursor emission source areas in the continent.

3.3.4.1.2 Meteorological Adjustment of Trends

As was done in past science assessments (Environment Canada, 1997) and published papers (Vingarzan and Taylor, 2003; Oltmans *et al.*, 2006; Thompson *et al.*, 2001), the effects of meteorological variability on O₃ trends are estimated herein by analyzing trends both with and without a meteorological adjustment. The inclusion of the meteorological adjustment in the GLMM analysis eliminates (or at least minimizes) the O₃ variability due to meteorological influences, thereby focusing the results on long term trends related to changes in precursor emissions

O₃ levels are a function of a large number of variables such as geographical location, elevation and distance from precursor sources. There are meteorologically-related factors that have been shown by various studies to be very important to O₃ formation including global solar radiation, wind speed (or stagnation), horizontal transport (advection), temperature, cloud opacity, precipitation (which affects relative humidity), transport from the lower stratosphere (convection) and vertical mixing (mixing height). On the other hand, O₃ is very reactive such that dry deposition and NO scavenging become the dominant processes that reduce O₃ in the troposphere, particularly during night-time.

The meteorological observations for the GLMM analysis were obtained from the Canadian Climate Archive to match with O₃ monitoring sites in Canada and CASTNet meteorological observations for the sites located in the U.S. Meteorological variables used in GLMM included daily maximum 1-hr temperature, daily average relative humidity, daily average wind speed and daily total precipitation. Canadian Meteorological Centre's (CMC) 3-day backward trajectories at 925 mbar arrival pressure level were used to segregate origins of air mass in order to provide a contrast to the O₃ seasonally adjusted model and the observed O₃ data for the evaluation of the meteorological effects. All-year combined data were used in the development of the trend analysis by GLMM and were modelled separately for each PCA-derived region. This is an improvement to the trend analysis technique used in previous analyses (Environment Canada, 1997). Only sites with 75% or more data capture for both O₃ and temperature (but no restrictions on other meteorological variables) in each of the four seasons during 1997 to 2006 were included for the PCA/GLMM trend analysis.

Table 3.7 Overview of ozone trends based on various daily ozone averaged values from 1997 – 2006 during January – December months in selected PCA-derived regions with Meteorological Adjustment. Trends that are significant at 0.05 are in bold.

PC	Metric	P Value	Met-adjusted Trend (% yr ⁻¹)	Met-adjusted Trend (ppb yr ⁻¹)	Non-adjusted Trend Minus Met-adjusted Trend (% yr ⁻¹)	Non-adjusted Trend Minus Met-adjusted Trend (ppb yr ⁻¹)
1	Max 1hr	<.0001	-0.46±0.18	-0.17±0.07	-0.2	-0.07
	Max 8hr	<.0001	-0.53±0.2	-0.19±0.07	-0.24	-0.09
	Dt avg	0.0002	-0.47±0.22	-0.15±0.07	-0.36	-0.11
	Dly avg	0.0789	-0.32±0.38	-0.09±0.11	-0.59	-0.16
	Nt avg	0.7176	-0.11±0.66	-0.03±0.17	-0.93	-0.24
2	Max 1hr	<.0001	-2.03±0.63	-0.95±0.29	-0.44	-0.2
	Max 8hr	<.0001	-2.09±0.67	-0.93±0.3	-0.36	-0.16
	Dt avg	<.0001	-2.09±0.68	-0.81±0.26	-0.52	-0.21
	Dly avg	<.0001	-2.08±0.81	-0.67±0.26	-0.28	-0.09
	Nt avg	<.0001	-2.59±1.14	-0.72±0.32	0.09	0.02
3	Max 1hr	<.0001	-2.63±0.76	-1.32±0.38	-0.87	-0.43
	Max 8hr	<.0001	-2.7±0.86	-1.28±0.41	-0.83	-0.39
	Dt avg	<.0001	-2.5±0.98	-1.05±0.41	-1.14	-0.47
	Dly avg	0.0002	-2.61±1.32	-0.89±0.45	-0.99	-0.34
	Nt avg	0.0016	-3.07±2.14	-0.92±0.64	-0.8	-0.24
4	Max 1hr	0.0030	-1.43±0.91	-0.6±0.38	-0.31	-0.13
	Max 8hr	0.0049	-1.39±0.96	-0.56±0.39	-0.22	-0.09
	Dt avg	0.0150	-1.24±1.06	-0.44±0.38	-0.29	-0.11
	Dly avg	0.0667	-1.01±1.23	-0.31±0.38	-0.04	-0.01
	Nt avg	0.2460	-0.68±1.35	-0.19±0.37	0.21	0.06

PC	Metric	P Value	Met-adjusted Trend (% yr ⁻¹)	Met-adjusted Trend (ppb yr ⁻¹)	Non-adjusted Trend Minus Met-adjusted Trend (% yr ⁻¹)	Non-adjusted Trend Minus Met-adjusted Trend (ppb yr ⁻¹)
5	Max 1hr	0.8561	0.05±0.76	0.02±0.31	-0.13	-0.05
	Max 8hr	0.9146	0.03±0.85	0.01±0.33	-0.17	-0.06
	Dt avg	0.7805	-0.11±1.06	-0.04±0.37	-0.12	-0.04
	Dly avg	0.9119	-0.06±1.34	-0.02±0.39	-0.2	-0.06
	Nt avg	0.8073	-0.16±1.87	-0.04±0.49	-0.18	-0.05
7	Max 1hr	0.0216	0.43±0.32	0.16±0.12	-0.24	-0.09
	Max 8hr	0.0304	0.44±0.37	0.16±0.13	-0.27	-0.1
	Dt avg	0.0165	0.81±0.56	0.26±0.18	-0.41	-0.13
	Dly avg	0.0834	0.76±0.92	0.22±0.27	-0.44	-0.13
	Nt avg	0.5169	0.47±1.98	0.13±0.54	-0.52	-0.14
9	Max 1hr	0.0154	0.77±0.5	0.27±0.18	-0.33	-0.12
	Max 8hr	0.0259	0.98±0.76	0.3±0.24	-0.43	-0.13
	Dt avg	0.0405	1.35±1.23	0.36±0.33	-0.58	-0.15
	Dly avg	0.0944	1.56±2.1	0.32±0.43	-0.76	-0.16
	Nt avg	0.2223	2.08±4.81	0.3±0.69	-1.23	-0.18

As noted, five averaging metrics for O₃ including daily maximum 1-hr, daily maximum 8-hr average, daytime (10:00 – 18:00) average, daily average, and nighttime (20:00 – 04:00) average are presented in Table 3.7 with meteorological adjustment (including all meteorological variables mentioned previously) and without meteorological adjustment. These values were used for testing the sensitivity of the regression coefficient, for estimating the meteorological effects of the long-term linear time component (slope term with O₃) calculated by this mixed model, and most importantly, for understanding the link between levels of O₃ in the frequency distribution and changes in precursor emissions.

Meteorologically adjusted trend results, presented in Table 3.7, derived from the daily maximum 8-hr values representing the peak levels are summarized as follows: statistically significant decreasing trends are found in the PCA-derived regions in eastern North America (PC1, PC2, PC3 and PC4). The Prairie Provinces, represented by PC5, show non-significant increasing trends. The east and west regions represented by PC7 and PC9 show significant increasing trends. The trends for the daily maximum 1-hr O₃ values are similar to those for the 8-hr values. These results highlight a large heterogeneity in O₃ chemistry regimes across the continent potentially resulting from different precursor spatial distributions, meteorological influences and topography.

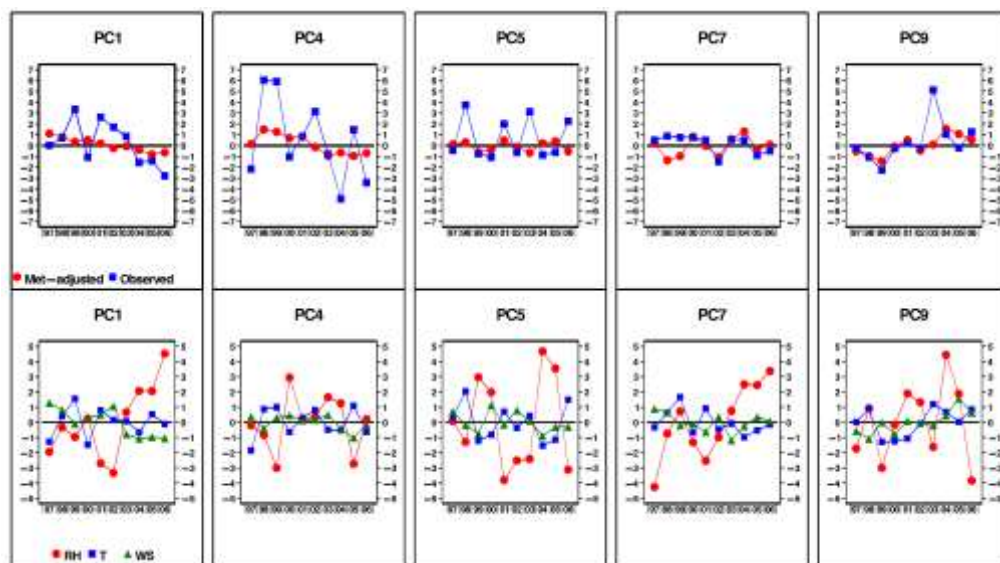


Figure 3.19 Top row: anomalies in the seasonal average (subtracted by the overall mean) meteorological-adjusted trends modelled by GLMM (red) and observed ozone (blue) based on daily maximum 8-hr values (in ppb) for 1997 to 2006 during May – September for five PCA-derived regions. Bottom row: anomalies in seasonal average relative humidity in % (red), temperature in °C (blue) and wind speed in m s^{-1} (green) for the same regions.

As shown in Table 3.7 (the 2 right most columns), meteorological adjustment, on the daily maximum 8-hr average O_3 values resulted in a decrease in slopes for PC1 of 0.24 \% yr^{-1} (0.09 ppb yr^{-1}), PC2 of 0.36 \% yr^{-1} (0.16 ppb yr^{-1}), PC3 of 0.83 \% yr^{-1} (0.39 ppb yr^{-1}), PC4 of 0.22 \% yr^{-1} (0.09 ppb yr^{-1}), PC5 of 0.17 \% yr^{-1} (0.06 ppb yr^{-1}), PC7 of 0.27 \% yr^{-1} (0.1 ppb yr^{-1}) and PC9 of 0.43 \% yr^{-1} (0.13 ppb yr^{-1}). As shown in Figure 3.19, the inter-annual variability that is due to meteorological changes has been substantially reduced in the long-term trends. Most meteorological variables used were found to be statistically significant in the model in all regions except daily total precipitation, which did not show a significant relationship with O_3 in PC3, PC4 and PC7; and temperature and wind speed ($T \times WS$), which did not show a significant relationship with O_3 in PC4. All the quadratic and cubic terms in temperature were significant for all PC groupings.

The averaging metrics of the daily maximum 1-hr and daily maximum 8-hr O_3 values representing the higher end (peak level of the O_3 distribution) show greater decrease than the daily and nighttime (20:00 – 04:00) averages that represent the lower end of the distribution. The trend results based on the daily maximum 1-hr versus the daily average are as follows: PC1 -0.17 vs. $-0.09 \text{ ppb yr}^{-1}$, PC2 -0.95 vs. $-0.67 \text{ ppb yr}^{-1}$, PC3 -1.32 vs. $-0.89 \text{ ppb yr}^{-1}$ and PC4 -0.6 vs. $-0.31 \text{ ppb yr}^{-1}$ (Table 3.7). As discussed by Lelieveld *et al.*, 2004, the higher end of the O_3 distributions represents the precursor emissions at closer distance and the average or lower values represent the background O_3 . A modelling study (Fiore *et al.*, 2002) using the GEOS-CHEM model relates the decrease in the high end of the O_3 distribution in surface air over the United States (reflecting reduction of domestic hydrocarbon and nitrogen oxides

emissions) and the increase in the low end (reflecting rising Asian emissions). This explanation corresponds reasonably well with decreasing higher O₃ levels in this study potentially related to the reduced NO_x emissions observed in the recent years (2003 and onwards) due to the EPA's NO_x Budget trading Program (or the NO_x State Implementation Plan (SIP) Call) across the eastern U.S. (U.S. EPA, 2006a). The results for the PC5 region show a non-significant increasing trend in the higher O₃ values (0.02 ppb yr⁻¹), which may relate to the increase in industrial activities in Alberta and Saskatchewan in recent years. In PC7 and PC9, increasing trends are observed at all levels of O₃, consistent with results published by Lelieveld *et al.* (2004) reporting an increasing trend over the Atlantic Ocean, and by Jaffe *et al.* (2003) and Vingarzan and Taylor (2003), who reported an increasing trend on the west coast of North America. However, similar to the results and explanations for the PC1, PC2, PC3 and PC4 regions, the relative magnitude in the increase in the daily maximum 1-hr O₃ values is slightly smaller than the daily average values with 0.16 vs. 0.22 ppb yr⁻¹ and 0.27 vs. 0.32 ppb yr⁻¹ for PC7 and PC9 respectively. To summarize, in the context of this study, the relatively slow rate of decrease from the daily average values compared with the daily maximum 1-hr values for PC1, PC2, PC3 and PC4, and the relatively fast rate of increase for PC5, PC7 and PC9 may once again confirm a wide-spread O₃ increase in the North Hemispheric baseline level. To keep in mind, there are relatively fewer sites in PC5, PC7 and PC9 compared to other PCA-derived regions. Therefore, there is higher uncertainty in the results in these three regions.

3.3.4.1.3 Ozone Changes in Relation to Changes in Meteorology

To understand the potential causes for the O₃ inter-annual variability, the seasonal averages during May to September of the meteorologically-adjusted trends (seasonality has also been accounted for in the model by sinusoidal functions varying from 3 months to 1 year periodicities - see model definitions), are compared against the daily maximum 1-hr temperature, daily average relative humidity and daily average wind speed anomalies shown in Figure 3.19. It is known that increasing temperature leads to a faster photochemical reaction rate for O₃ formation, while increasing wind speeds relate to long-range transport from precursor source areas upwind are usually associated with increasing O₃ for non-urban sites (for sites that are closer to the precursor sources, increasing wind speed is related to decreasing O₃ levels due to the dilution effect.) On the other hand, higher humidity levels are usually associated with greater cloud abundance and atmospheric instability, and thus photochemical processes are slowed and ground level O₃ is depleted (Camalier *et al.*, 2007).

It is, however, important to point out that the above mentioned meteorological variables only serve as simple surrogates for the complex meteorological processes and synoptic weather patterns acting upon the precursors that affect O₃ levels. The 1st row in Figure 3.19 shows seasonal average O₃ with meteorological adjustment (red circles) and the observed data (blue squares) for each of the PCA-derived regions during May to September. The 2nd row corresponds to seasonal average temperature, relative humidity and wind speed anomalies during May to September. A noticeable association appears in all 5 selected PCA-derived

regions that the inter-annual variations of the observed O₃ and temperature values are tracking each other very closely. For instance, typically a year with positive temperature anomaly is associated with positive O₃ anomaly and vice versa during May to September. Taking PC4 as an example, in 1999 the seasonal average O₃ was adjusted downward because the corresponding positive temperature (blue squares), negative relative humidity (red circles) anomalies and wind speed (green triangles) close to the ten-year average, created a relatively favorable meteorological condition for O₃ formation. This downward adjustment in 1999 also occurs in most other regions in eastern North America. The upward adjustment in 2000 for example, was needed to compensate for the unfavorable O₃ formation condition potentially caused by the negative temperature and positive relative humidity anomalies. As for 2003, the meteorologically-adjusted values are more or less the same as the observed values, which is a result of the unfavorable conditions created by negative temperature and positive relative humidity anomalies acting in opposition to the favorable condition created by positive wind speed anomaly. It is re-emphasized here that because of the non-linear nature of O₃ chemistry and the synergistic (or antagonistic for temperature and relative humidity) effects of different meteorological variables, this rather simple explanation may fail in other cases.

Despite this caveat, the meteorological-adjusted trends seem to follow this logic reasonably well in this particular set of PCA-derived regions even for the remaining years

3.3.4.1.4 Average Ozone Concentrations in Different Air Mass Types

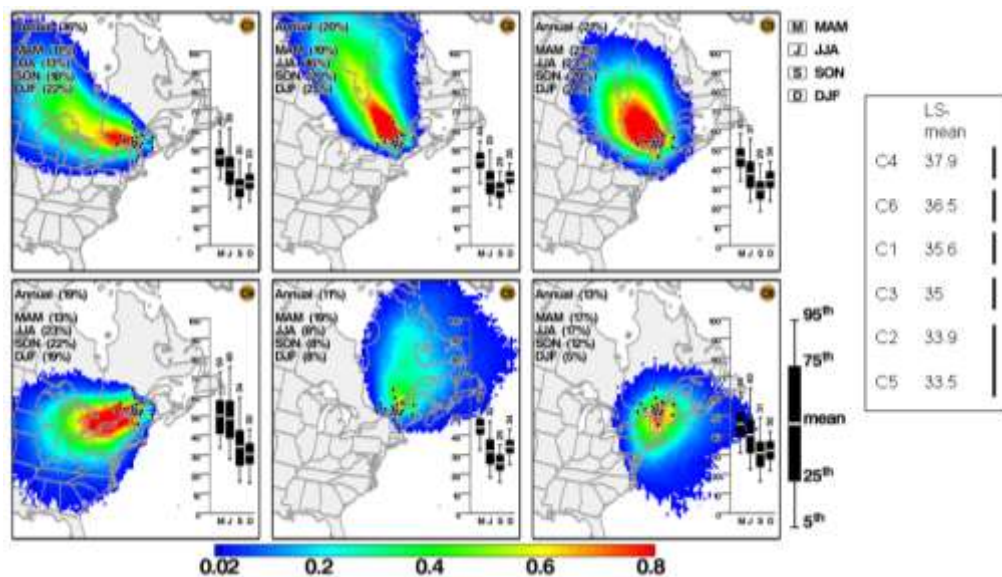


Figure 3.20 Six trajectory clusters used in GLMM for PC1.²

² Each cluster's seasonal and annual transport frequencies are shown in the top left corner of the box. Seasonal box plots based on daily maximum 8-hr average ozone values (in ppb) for each cluster are shown on the right. The endpoint of the upper whisker, upper edge, line inside, lower edge of the box and endpoint of the lower whisker show the 95th, 75th, mean, 25th and 5th percentiles respectively. The numerical

values of the seasonal means are shown immediately above the upper whisker. The Step-down Bonferroni significance test (at a family-wise 95% confidence level) results are shown to the right of the figure, ordered from the highest to lowest least square (LS) means ozone levels associated with air mass clusters for PC1 (Southern Quebec) based on 1997 to 2006 data during January to December. Significant differences do not exist when different clusters are joined by the vertical bars.

As described in Chan (2009), air mass trajectories were first sorted by a trajectory clustering method (Dorling *et al.*, 1992) to be used as an air mass type classification variable in the GLMM. Thus, a multiple comparison of the least-squares means of the O₃ concentrations associated with different air mass types were made and results are presented to the right in Figure 3.20 using data for the entire year (not limited to the O₃ season). Least-squares means calculated from GLMM represent the annual O₃ averages that have been adjusted for the within-site and between-site variations. These results provide an overview of the air mass types and transport patterns associated with high- and low-O₃ values across the regions. Taking PC1 (southern Quebec) shown in Figure 3.20 as an example, the highest least square (LS)-mean O₃ concentration (38 ppb) from all 18 sites within this region were associated with trajectory Cluster 4 (C4) which corresponds to air flows passing over the Ohio River Valley (ORV) and Midwest US areas traversing southeastern Ontario and affecting the region. The box plot for this cluster shows the highest means as well as variations of the O₃ concentrations in the spring (MAM), summer (JJA) and the fall (SON). This may suggest that O₃ levels in the spring not only consist of the hemispheric background and stratospheric inputs but also the additional photochemical O₃ produced in polluted areas and forming along the transport path. This is not surprising given the fact that solar radiation starts to rise as early as March in mid-latitudes in Northern Hemisphere. Comparing the seasonal trajectory frequencies for the cluster shown in the top left corner, relatively high percentages of this transport pattern occur in JJA (23%) and SON (22%). This transport pattern has been discussed elsewhere as frontal passages and the clockwise air flow coming around the back side of a stagnant high pressure system bringing polluted air masses across the border (Lyons and Cole, 1976; Wolff and Liroy, 1980).

The second highest LS-mean O₃ is associated with Cluster 6 (C6), where air masses originate in the northeastern US (LS-mean of 36.5 ppb). This transport pattern has been associated with stagnation caused by slow-moving, high-pressure weather systems from the Atlantic as discussed in many studies (Wolff *et al.*, 1977; Altshuller 1978; Vukovich and Fishman 1986). This pattern was confirmed with average transport height and distance (not shown) that showed the shortest transport range and minimal lifting particularly during JJA months compared to the other five clusters.

The lowest O₃ LS-mean concentration of 33.5 ppb is associated with Cluster 5 (C5), which has the highest percentage of transport during MAM, with air mass coming from the North Atlantic Ocean. The second lowest LS-mean concentration of 34 ppb is associated with Cluster 2 (C2), which is not significantly different from C5 (joined by the vertical bar at the extreme

right of Figure 3.20). This cluster experiences long range transport from northern Canada with relatively high transport height (not shown) and is the most frequent during DJF. However, the average O₃ concentration shown in the box-and-whisker plot is the highest for this particular cluster during DJF in comparison other clusters during the same months. Although data for the entire year were used for the LS-mean comparisons, these results are consistent with our current knowledge that higher O₃ values are formed in high anthropogenic NO_x and VOC source areas while lower O₃ values originate in the more pristine and remote area from the cold North (Schichtel and Husar, 2001; Brankov *et al.*, 2003) and the oceans. There are many possible reasons for the reverse behaviour in the LS-mean O₃ levels associated with flows originating in the north and the south of the region during the colder months. One obvious reason is that the air mass being transported from the north is on average travelling at relatively high altitude in the troposphere compared with the air mass being transported from the south side of the region. Thus, relatively low dry depositions would occur. The second possible reason is that the relatively low O₃ levels from the south during the colder months may be a result of NO scavenging taking place along the transport path.

Singh *et al.* (1978) showed idealized variations in O₃ at remote locations and that O₃ during JJA comprises mainly three components, namely, the natural O₃ (background O₃), the regional photochemical O₃ and the long-range transported O₃. It may be possible to estimate sub-regional and/or long-range transported O₃ contributions using a similar idea by simply separating air mass origins through air parcel backward trajectory clustering. Comparison can be made by taking the difference between the mean O₃ concentrations associated with any selected air mass origin and that of the cleanest air mass having minimal anthropogenic impacts. Also, any O₃ losses such as those caused by dry deposition or NO scavenging should be minimized by the use of daily maximum 8-hr average O₃ values. For instance, during JJA, a mean of 32 ppb is associated with Cluster 5 corresponding to the oceanic flows which bring on average the lowest O₃ levels among other clusters in the same season. On the other hand, a mean of 49 ppb is associated with Cluster 4 corresponding to additional O₃ contributed by precursor emission sources located along Windsor-Quebec corridor and the major point sources near the Ohio River Valley located further upwind. Thus, the average sub-regional contribution from these areas can be estimated to be about 17 ppb.

3.3.4.1.5 Four-year Average comparison from 1997 to 2000 vs. 2003 to 2006

Table 3.8 Percentage differences in the 3-year-average meteorological adjusted trends of daily maximum 8-hr ozone average from May-Sep 1997–2000 to May-Sep 2003–2006 based on GLMM shown in Figure 3.20. The differences represent the 2003–2006 average concentration minus the 1997–2000 average concentration divided by the 1997–2000 average concentration.

PC	Averaging Period	Mean	Percent Change
1	2003 to 2006 (T1)	35.2	-3.2
	1997 to 2000 (T2)	36.4	
	Diff (T1-T2)	-1.2	
2	2003 to 2006 (T1)	42.3	-7.9
	1997 to 2000 (T2)	46.0	
	Diff (T1-T2)	-3.6	
3	2003 to 2006 (T1)	45.2	-8.6
	1997 to 2000 (T2)	49.4	
	Diff (T1-T2)	-4.3	
4	2003 to 2006 (T1)	39.5	-4.1
	1997 to 2000 (T2)	41.2	
	Diff (T1-T2)	-1.7	
5	2003 to 2006 (T1)	38.5	0.0
	1997 to 2000 (T2)	38.5	
	Diff (T1-T2)	0.0	
7	2003 to 2006 (T1)	36.5	2.1
	1997 to 2000 (T2)	35.7	
	Diff (T1-T2)	0.8	
9	2003 to 2006 (T1)	31.8	5.2
	1997 to 2000 (T2)	30.2	
	Diff (T1-T2)	1.6	

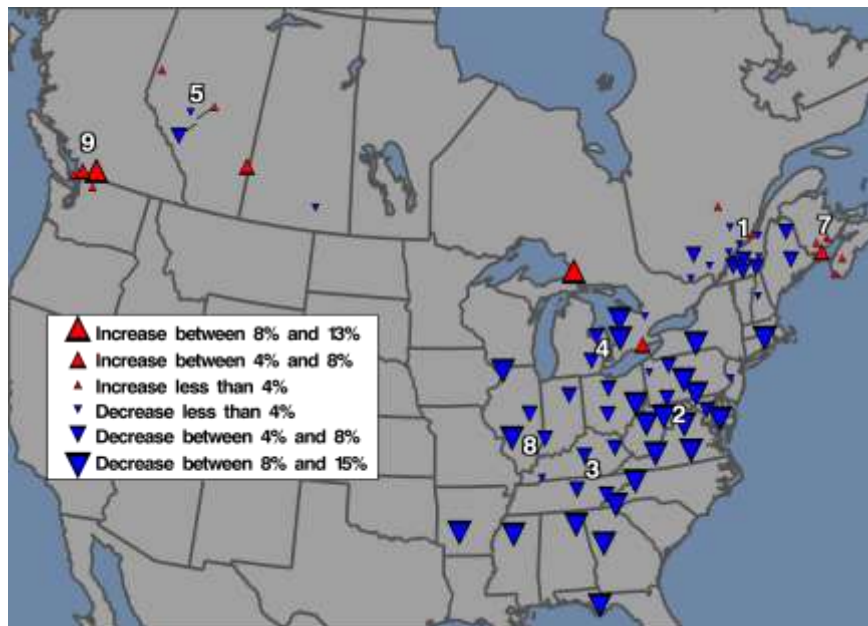


Figure 3.21 Three-year average during May – September differences from 1997 – 2000 to 2003 – 2006 of the meteorological-adjusted ozone trends modelled by GLMM based on daily maximum 8-hr values.

United States emissions of NO_x decreased continuously from 1997 to 2006 as a result of reductions from on-road mobile sources, electric power generation sources and industrial sources (Canada-US, 2008). To evaluate whether these reductions produced lower concentrations of O_3 at non-urban measurement sites, a comparison was made between the 4-year mean O_3 concentrations in 1997-2002 versus 2003-2006. A 4-year averaging period was chosen to minimize the effects of inter-annual meteorological variability and the 1997-2000 and 2003-2006 periods were chosen to maximize the potential concentration differences between the earliest part of the period (i.e., the period of highest NO_x emissions) and the latest part of the data period (i.e., the period of lowest emissions). The intervening years, 2001 and 2002, were omitted to maximize the differences. The differences between the 4-year averages for the 1997-2000 and 2003-2006 periods during May to September from the meteorological-adjusted trends based on daily maximum 8-hr average values modelled by PCA/GLMM trend analysis for each analyzed PCA-derived region are summarized in Table 3.8. Differences between the two periods are all statistically significant. There is a 3.2% decrease in PC1 (Quebec), a 7.9% decrease in PC2 (northeastern US), an 8.6% decrease in PC3 (southeastern US), a 4.1% decrease in PC4 (southern Ontario/Great Lakes/Upper Ohio), a 0.0% change in PC5 (Alberta), a 2.1% increase in PC7 (Atlantic), and a 5.2% increase in PC9 (Pacific). A regional perspective of O_3 changes has been shown earlier in Figure 3.17. Results of the changes in individual sites are also provided in Figure 3.21, showing large decreases in the southeastern to northeastern U.S. areas and a number of locations in southern Ontario and Quebec. Consistent and comparable results can be found in the NBP 2007 Progress Report (U.S. EPA, 2008) and in G ego *et al.* (2007). On the other hand, the sites included in this study

that are located in the Pacific (Georgia Basin) and Atlantic regions show moderate increases over the two averaging periods. Mixed results are found at sites in Alberta/Saskatchewan. In Gégó *et al.* (2007), the May to September O₃ concentrations from 2003-2004 in the eastern U.S. showed an average improvement of 13% from the 1997-1998 concentrations, based on daily maximum 8-hr average O₃.

3.3.4.2 Other Reported Ozone Trends

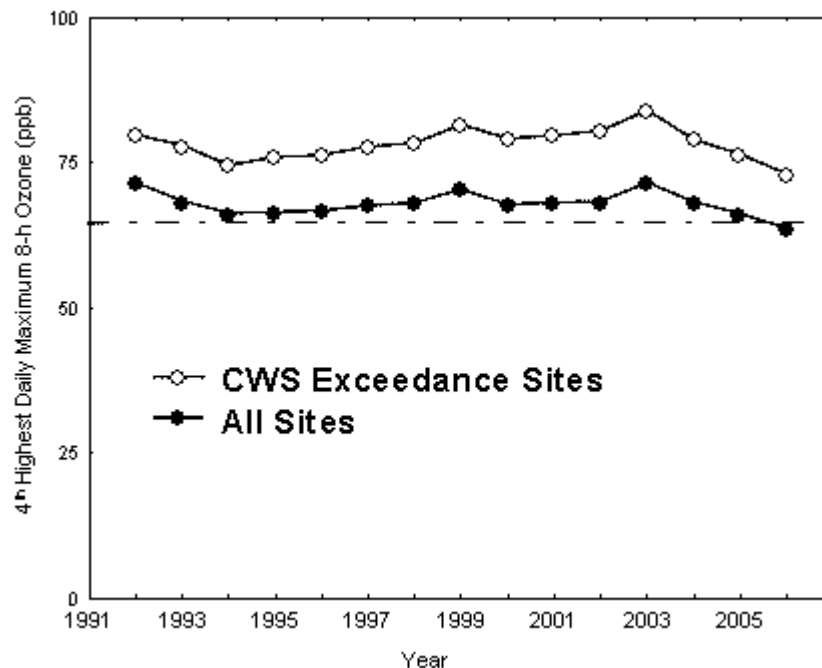


Figure 3.22 The 3-year running average of the 4th highest daily maximum 8-h ozone concentration for 1990 to 2006 (all Canadian sites and all sites greater than 65 ppb for 2004-2006).

The 3-year running averages of the 4th highest daily maximum 8-hr O₃ concentration from 1990 to 2006 for all Canadian sites are presented in Figure 3.22. The 3-year average of the 4th highest daily maximum 8-hr O₃ concentration is the metric used for the O₃ CWS. Only sites with at least 75% of the years were included in the plot (88 sites in total). Also included in the graph is the subset of trend sites that exceeded the value of 65 ppb for the years 2004 to 2006. There were a total of 37 sites in this group and all were located in Ontario and Quebec except for the Kejimikujik National Park site. As reported in the Five-Year Progress Report for the CWS (Government of Canada, 2007) there was no trend in national O₃ levels in the form of the CWS for the period 2001-2005. It is evident in Figure 3.22, however, that the current plot shows an inflection point in 2003 with a downward slope from 2003 to 2006.

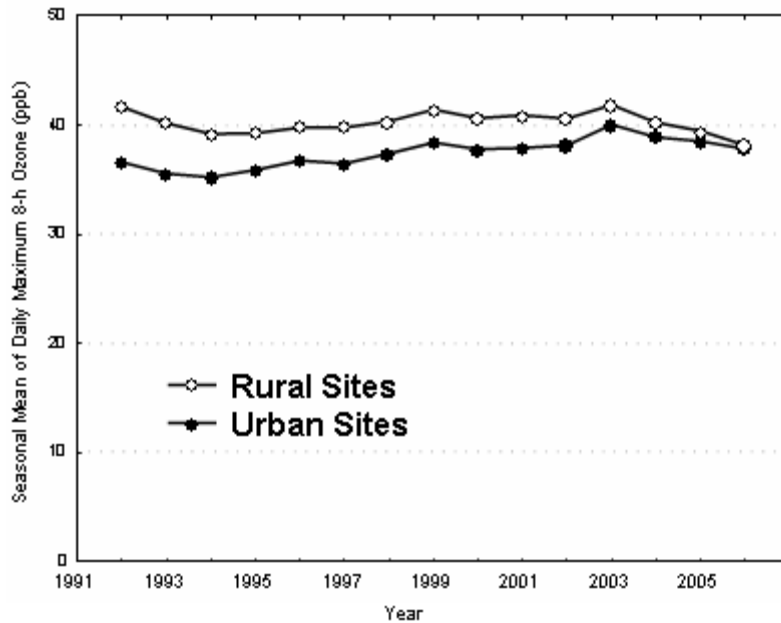


Figure 3.23 The 3-year running average of the seasonal mean of daily maximum 8-h ozone concentrations for 1990 to 2006 (urban and rural sites).

The Canadian Environmental Sustainability indicator (CESI) for O_3 is based on the seasonal mean of daily maximum 8-hr O_3 . The 3-year running average of seasonal mean daily maximum 8-hr O_3 concentrations for 1990 to 2006 is shown separately for urban and rural sites (at least 75% data completeness) in Figure 3.23. As noted previously urban sites have lower seasonal mean O_3 than rural sites. From Figure 3.23 it can be seen that urban site means are approaching rural means as NO scavenging is reduced due to decreasing NO. This has resulted in an apparent upward trend in this O_3 indicator since it is driven largely by results from urban sites. An inflection point in both lines is seen in 2003 with a downward slope from 2003 to 2006. Urban and rural differences are discussed further below.

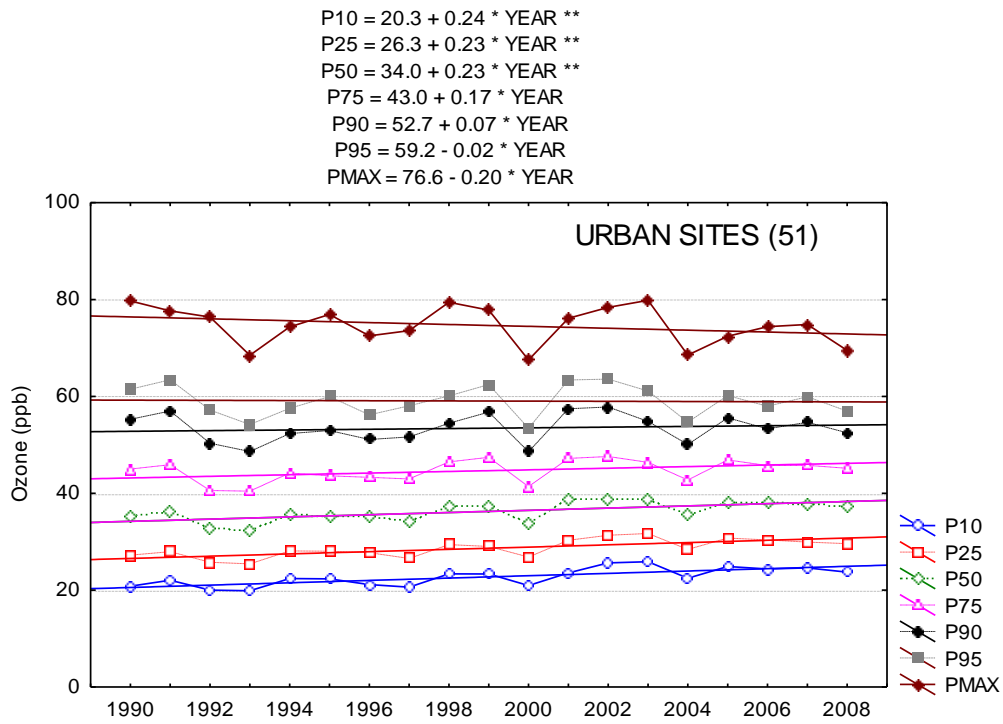


Figure 3.24 Trend in Daily Maximum 8h Ozone 10th, 25th, 50th, 75th, 90th, 95th percentiles and maximum for Canadian urban sites for 1990 - 2006. Regression lines marked with ** are statistically significant at the 95th percentile confidence level.

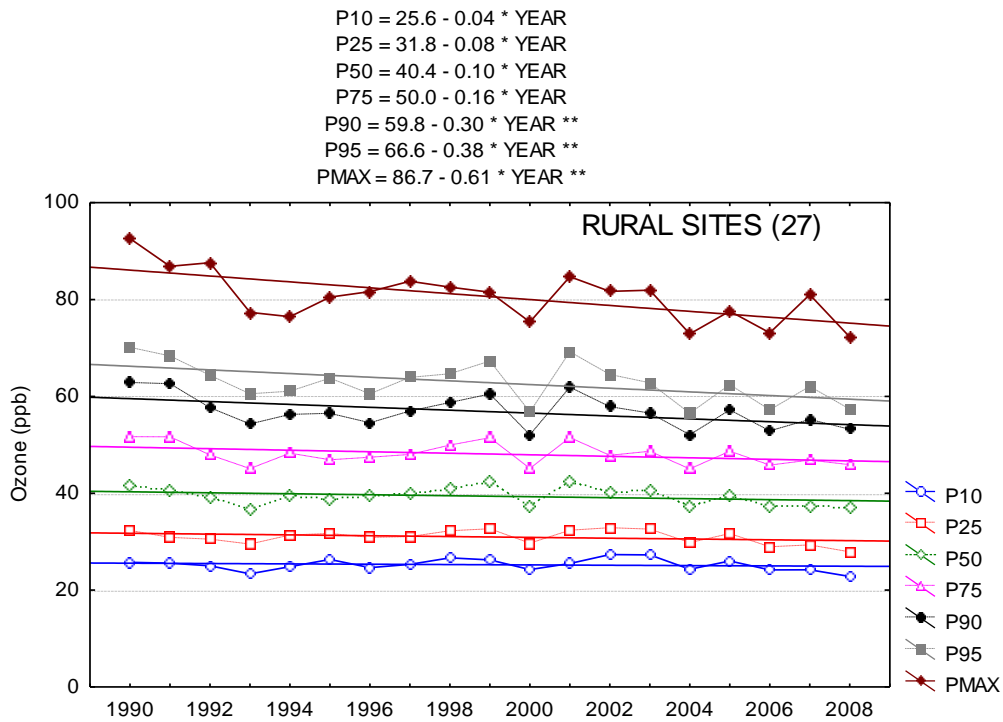


Figure 3.25 Trend in Daily Maximum 8h Ozone 10th, 25th, 50th, 75th, 90th, 95th percentiles and maximum for Canadian rural sites for 1990-2006. Regression lines marked with ** are statistically significant at the 95th percentile confidence level.

As discussed by Jenkin (2008) and Ainslie and Steyn (2007) and as shown in the preceding sections, trends in O₃ can vary markedly depending on site location (urban, rural, background) and on which statistic is being examined. An analysis of trends in daily maximum 8h ozone (April to September only) at different percentile levels (10th, 25th, 50th, 75th, 95th and maximum) was carried out for a group of urban and rural sites for the period 1990 to 2006. Fifty-one urban sites and 27 rural sites met data completeness requirements. The urban sites were distributed across Canada but the rural sites were primarily located in Ontario and Quebec with 3 sites in Atlantic Canada and 2 sites in British Columbia. Figure 3.24 shows trend results for the urban sites with a statistically significant (at the 95th confidence level) positive trends for the 10th, 25th and 50th percentiles. Although the slopes were negative for the higher percentile plots they were not statistically significant. As shown in Figure 3.25 the rural sites showed negative slopes for all percentiles with statistically significant decreases in maximum, 95th and 75th percentile 8h ozone. The urban results illustrate the effect of NO reductions in reducing ozone scavenging and resulting in a net apparent upward trend in lower percentile and average ozone concentrations. Higher percentile ozone concentrations in urban areas show a negative trend but not a statistically significant one. The rural sites show that on a regional scale ozone has responded to emission reductions and upper percentile 8h ozone concentrations show a statistically significant decrease. There is also no evidence for this group of rural sites (predominantly in Ontario and Quebec) that there has been any increase in median ozone levels due to increasing background ozone.

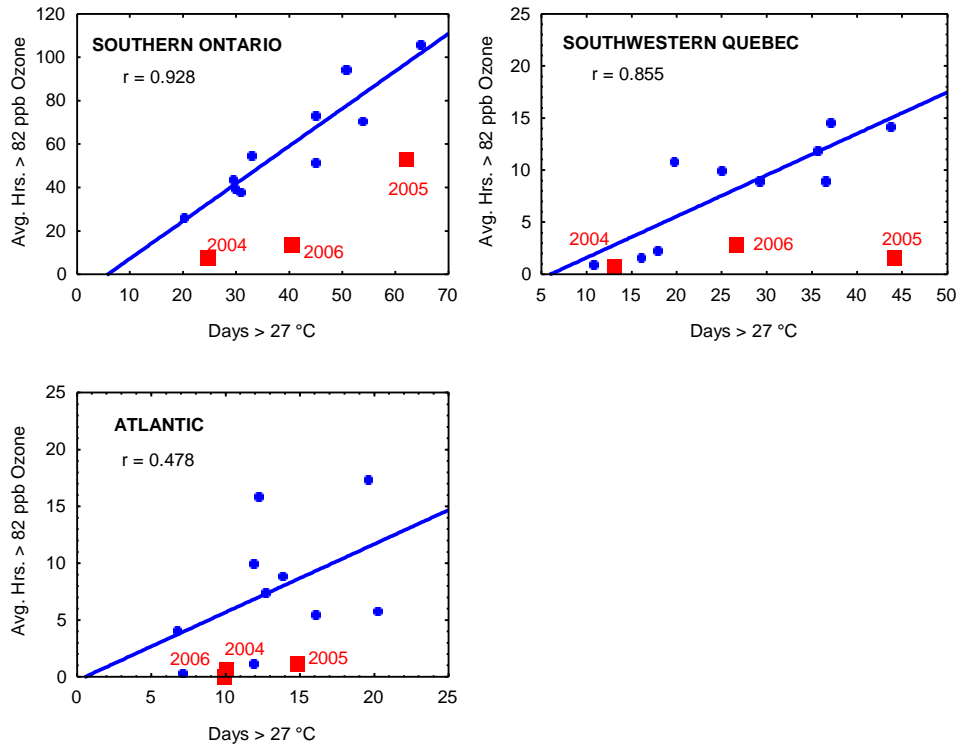


Figure 3.26 Relationship between days with daily maximum temperatures above 27°C and average hours above 82 ppb ozone (1994-2002 and 2004, 2005, 2006).

As previously discussed, daily maximum temperature is an important predictor of elevated O₃ concentrations. In the east it has been shown that the number of days with daily maximum temperatures greater than 27 °C is well correlated with days with daily maximum O₃ > 65 ppb and with hours with maximum O₃ greater than 82 ppb (the previous national air quality objective for O₃) (Environment Canada, 2005b). In Figure 3.26 the relationship between days with daily maximum temperature > 27°C and the average hours with O₃ > 82 ppb is plotted for three regions (using only sites with complete data) for the period 1994-2002. The correlation was highest for southern Ontario. The results for the years 2004, 2005 and 2006 were treated separately and the graphs clearly show that peak ozone levels in the 2004-2006 period were considerably lower on high temperature days than in the past (1994-2002). This same result has been shown for sites in the U.S. northeast and is a result of significant reductions in NO_x emissions in the U.S. between 2002 and 2006 (U.S. EPA, 2007).

3.4 Ozone Precursors

3.4.1 Rural NO_x and NO_y

3.4.1.1 Introduction

Table 3.9 Nitrogen Oxides - Species and Terminology

Formula/ Abbreviation	Compound/ Definition
NO	Nitric Oxide
NO ₂	Nitrogen Dioxide
NO _x	= NO + NO ₂
PAN	Peroxyacetyl Nitrate
HNO ₃	Nitric Acid
p-NO ₃ ⁻	Particulate Nitrate
RONO ₂	Organic Nitrates
HONO	Nitrous Acid
NO _z	= PAN + HNO ₃ + p-NO ₃ ⁻ + HONO + RONO ₂ + additional oxidized nitrogen species
NO _y	= NO _x + NO _z

Several chemical symbols (NO_x, NO_y and NO_z) are used to represent the different groups of oxidized nitrogen species that are important in rural atmospheres (Olszyna *et al.*, 1994). The common names and abbreviations of such species are outlined in Table 3.9. The family of tropospheric reactive oxidized nitrogen species, generically referred to here as NO_y, is primarily composed of NO, NO₂, peroxyacetyl nitrate (PAN), HNO₃ and particulate nitrate (p-NO₃⁻). Other inorganic and organic species may make additional contributions to the total family concentration. These species play several significant roles in tropospheric photochemistry, O₃ production and acid deposition. Organic peroxy and hydroperoxy radicals are responsible for much of the oxidation of NO to NO₂; hydroxyl radicals oxidize NO₂ to HNO₃ and peroxyacetyl radicals combine with NO₂ to form PAN (see chemistry discussion in Chapter 2). These reactions exert a controlling influence on the radical balance in the troposphere.

3.4.1.2 Measurement Technique Differences for NO and NO₂

There are four significant differences in the measurement techniques of NO and NO₂ between the CAPMoN network (rural/ remote sites) and the NAPS network (primarily urban sites) previously discussed in Section 3.2.3. The CAPMoN method has been developed specifically for rural/remote measurements. It minimizes sample line losses of NO_y species by locating the

molybdenum converter at the inlet. The sample inlet filter is placed after the molybdenum converter allowing $p\text{-NO}_3^-$ to be converted to NO and an additional instrument specifically converts NO_2 to NO (in NAPS instrumentation all NO_y species are converted), and trace level highly sensitive analyzers are used. The impact of these instrumentation differences on the reported NO_2 concentrations of the two measurement programs is described in section 3.4.1.4

3.4.1.3 Rural Nitrogen Species Concentrations

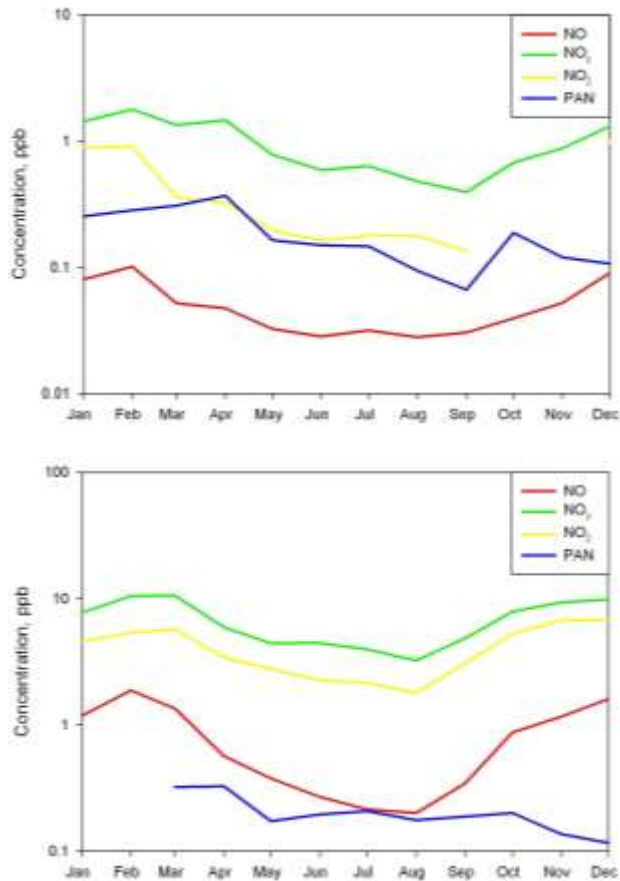


Figure 3.27 Mean monthly concentrations of NO, NO₂, NO_y and PAN (logarithmic scale) for Kejimikujik (top) and Egbert (bottom) during 2003.

CAPMoN has been conducting measurements of nitrogen species at three rural/remote sites: Egbert, ON and Kejimikujik National Park, NS (from August 2002-present); and Saturna Island, B.C. (from July 2004-present). Unfortunately, the Saturna Island data were not finalized at the time of writing so the analysis and discussion that follows is based solely on the data from the other two sites. The monthly mean concentrations of NO, NO₂, NO_y and PAN (PAN measured by gas chromatograph with a pulse discharge detector) at Egbert and Kejimikujik are depicted in Figure 3.27. Each of these sites shows a seasonal variation in the measured NO and NO₂ with the highest concentrations found during the winter months (note

log scale). At the Kejimikujik site, monthly means for NO ranged from 0.025-0.10 ppb and from 0.13-1.0 ppb for NO₂. As the Egbert site is less removed from emission sources, the concentration of NO and NO₂ are approximately an order of magnitude higher with ranges of 0.2-1.9 ppb and 1.8-6.7 ppb, respectively. In comparison, monthly means of NO and NO₂ levels at urban sites have been found to be in excess of 80 ppb and 30 ppb, respectively (Section 3.4.2).

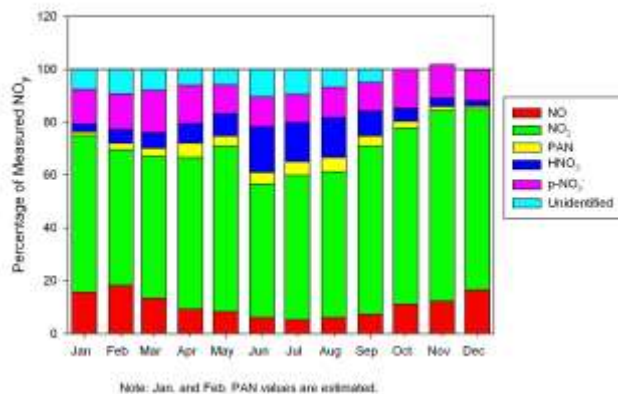
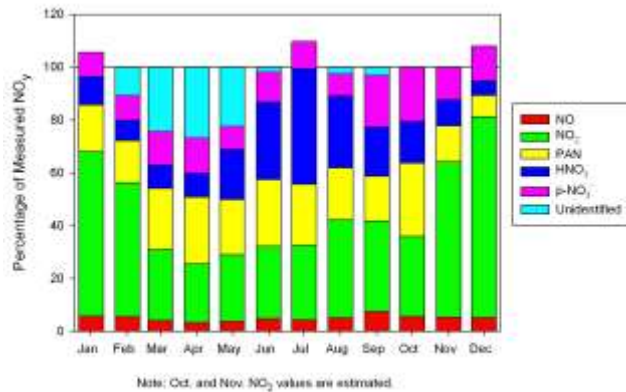


Figure 3.28 Relative abundance of several NO_y species as a fraction of the total measured NO_y concentration at Kejimikujik (top) and Egbert (bottom) during 2003.

As was the case with the NO_x concentrations, the NO_y levels at the Kejimikujik site are substantially lower than the Egbert site with monthly means ranging from 0.39-1.8 and 3.2-10 ppb respectively. In contrast, PAN levels were found to be very similar at both sites and ranged from 0.07 to 0.37 ppb with the maximum occurring in the spring. By supplementing these measurements with HNO₃ and p-NO₃⁻ data measured by CAPMoN, one can look at the relative abundance (on a mole/mole basis) of each species as it contributes to the total NO_y budget. Any shortfall between the sum of the individually measured species and the total measured NO_y concentration is reported as “Unidentified NO_y”. Due to the fact that there is some uncertainty in the reported measurements it is possible that the sum of the individual measurements of the components of NO_y could exceed that of the specifically determined total

NO_y measurement. Figure 3.28 shows the fraction of each nitrogen species as a percentage of the total measured NO_y concentration during 2003 at both the Egbert and Kejimikujik sites. For Egbert, NO₂ represented 51-72% of the total NO_y budget, followed by p-NO₃⁻ (11-16%), NO (5-18%), HNO₃ (2-17%), Unidentified NO_y (up to 10%) and PAN (1-6%). However at the Kejimikujik site, the distribution shifts more towards the products of photochemistry with NO₂ representing 22-76% of the budget followed by PAN (8-28%), HNO₃ (5-44%), p-NO₃⁻ (8-21%), Unidentified NO_y (up to 27%) and NO (3-7%). At the Kejimikujik site maximum contributions of NO and NO₂ are seen in the winter, HNO₃ in the summer, and PAN and Unidentified NO_y during the spring. The unidentified NO_y fraction is in agreement with the findings of Buhr *et al.* (1990) who found that that the known component concentrations of NO_y (NO, NO₂, HNO₃, PAN, organic nitrates and particulate nitrates) are typically less than the measured total NO_y and that this Unidentified NO_y is correlated with the degree of photochemical processing an air mass has undergone.

3.4.1.4 Differences in the Reported NO₂ Measurements

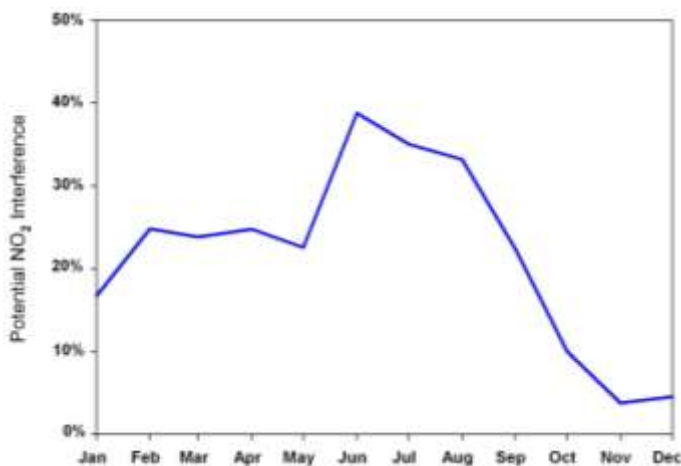


Figure 3.29 The monthly estimated percentage of an NO₂ measurement that could potentially be falsely identified as NO₂ due to interfering species if the conventional NO_x instrumentation were deployed at the Egbert station in 2003.

As mentioned in section 3.4.1.2, there are measurement-derived differences in the NO₂ concentrations reported by the CAPMoN and NAPS networks, i.e., the CAPMoN values are considered to be NO₂-specific (see Section 3.4.1.2) while the NAPS measurements are not. This is because the NAPS network NO₂ values are based on the assumption that the additional NO that is produced over the molybdenum converter is solely due to NO₂. However, other nitrogen species that may survive the sample inlet (HNO₃, PAN, organic nitrates, and unidentified components) are also converted to NO and therefore may cause an overestimation of NO₂ (and NO_x). The magnitude of the overestimation is dependent on the extent of photochemical processing of these other nitrogen species during the course of atmospheric transport to the measurement site. If we consider the CAPMoN Egbert site to be representative

of a typical suburban NAPS site, one can make a conservative estimate of the fraction of the NO_2 measured by the NAPS network suburban sites that could be attributed to other species. Figure 3.29 depicts the monthly percentage of an NO_2 measurement that could potentially be falsely identified as NO_2 if the conventional NO_x instrumentation were deployed at the Egbert station. The positive interference ranges from approximately 4% in the winter to 39% during the summer periods of elevated photochemical activity.

It should be noted that, when considering the impact of the foregoing on the NAPS NO_2 determinations, the foregoing is close to the worst case scenario. Most NO_x measurement sites in NAPS are located in urban environments which are impacted by local emissions and thus reduce the positive interference due to other nitrogen species. The over-prediction of NO_2 however, should increase as the distance from emission sources increases. Quantifying the positive interference in Canadian urban environments is a topic for future study.

3.4.2 Urban NO_2 , NO and NO_x

3.4.2.1 Current NO and NO_2 Concentrations

As discussed in Section 3.2.3, converters used in conventional NO_x analyzers convert some portion of other nitrogen species to NO as well as converting NO_2 . Consequently, reported NO_2 concentrations may not be strictly NO_2 , but may include other nitrogen species.

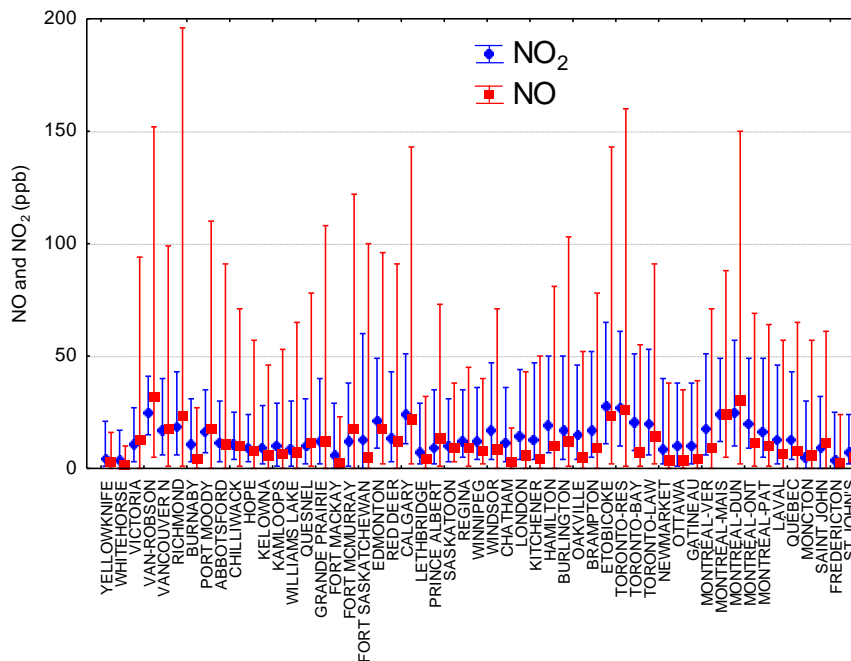


Figure 3.30 Mean, 10th and 98th percentile of NO and NO_2 concentrations at selected urban sites (2005).

Figure 3.30 provides mean, 10th and 98th percentile of NO and NO₂ concentrations at selected urban sites for the year 2005. The highest annual mean NO concentrations ranging from 22 to 32 ppb are found at city centres or roadway sites in the larger metropolitan areas. These sites also record the highest 98th percentile values (150 to 200 ppb). At these sites, NO₂-to-NO ratios range from 0.8 to 1, with NO typically accounting for 50 to 70% of measured NO_x. At suburban sites and commercial sites in smaller urban centres, annual mean NO concentrations are typically in the range of 10 to 20 ppb while NO₂-to-NO ratios are in the range of 1 to 4. Mean NO₂ concentrations ranged from 4 to 28 ppb at the urban sites with most sites in the range of 10 to 20 ppb. The highest 98th percentile NO₂ concentrations were measured in Toronto, Montreal, Calgary, Edmonton and Fort Saskatchewan (50 to 70 ppb).

3.4.2.2 Seasonal and Diurnal Profiles

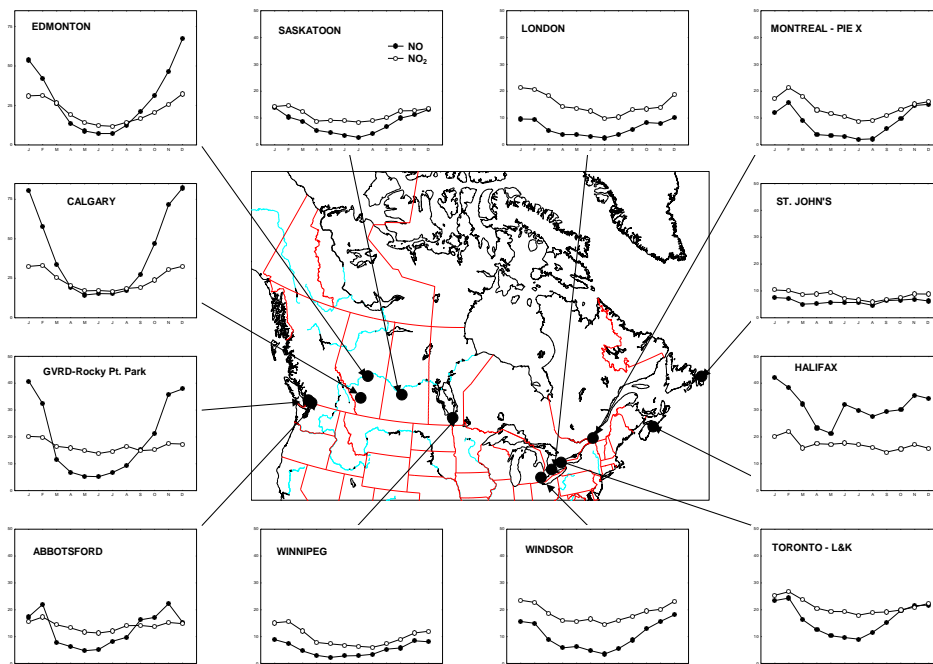


Figure 3.31 Mean NO (●) and NO₂ (○) by month (ppb) averaged over the years 2003 to 2005. (Note: Mean NO and NO₂ concentration (ppb) shown on y-axis)

Monthly mean NO and NO₂ concentrations for selected sites are presented in Figure 3.31 averaged over the years 2003 to 2005. Both NO and NO₂ concentrations are lower in the summer months and NO₂/NO ratios are higher. All urban sites show a strong seasonal cycle in NO, with maximum concentrations experienced in the winter months. The winter maximum is a result of three factors: increased emissions in the winter (primarily from fuel combustion); reduced atmospheric dispersion and a shallower mixed layer in winter; and less photochemical activity, resulting in slower destruction of NO. The western sites showed the largest seasonal variability in NO concentrations.

The NO₂ seasonal cycle is of smaller amplitude with a minimum generally recorded in midsummer, presumably due to faster conversion of NO₂ to NO_x. At most sites NO₂ to NO ratios increase during the months of May to July. At the Calgary and Edmonton sites mean monthly NO and NO₂ concentrations converged during the summer months.

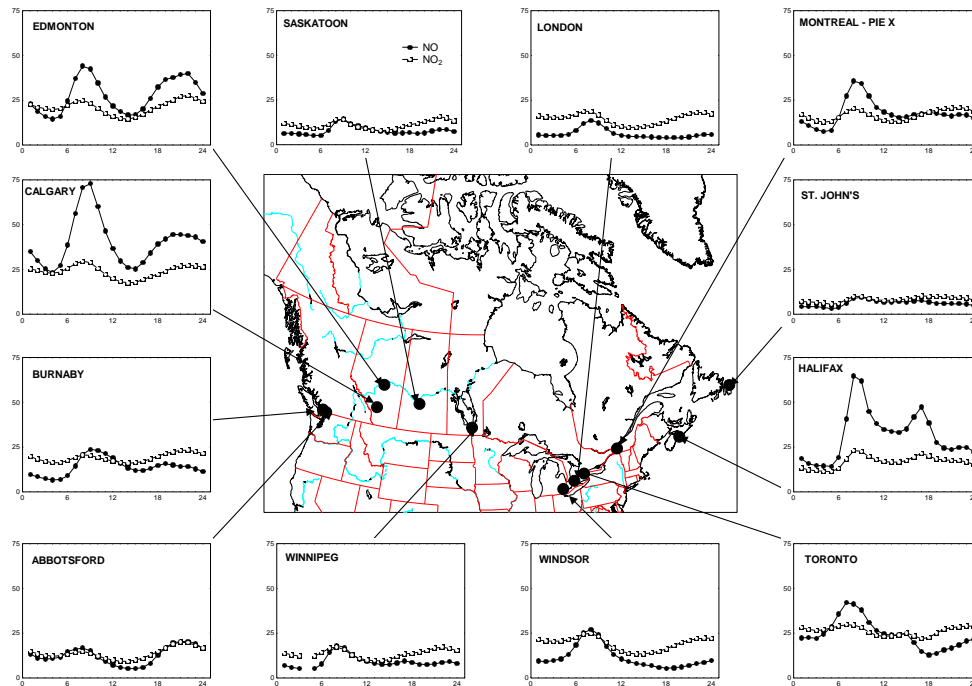


Figure 3.32 Diurnal variation in NO (●) and NO₂ (○) concentrations (ppb) for all days of the week averaged over the years 2003 – 2005. (Note: Mean NO and NO₂ concentration (ppb) shown on y-axis)

At urban sites, NO concentrations also exhibit a strong diurnal variation, as shown in Figure 3.32. At city-centre sites, such as Calgary and Edmonton, NO concentrations reach an overnight minimum at 04:00, increase sharply between 05:00-09:00 and then decline rapidly to reach values similar to the 04:00 minimum by 12:00. Concentrations typically climb after sunset to reach a secondary peak at approximately 22:00.

This ‘typical’ diurnal variation is a result of high emissions from automobiles during the morning rush-hour, coupled with a shallow mixed morning layer and limited photochemistry. Once sunlight intensity increases and O₃-rich air is mixed down from aloft, NO is rapidly destroyed. After sunset, the lower levels of the atmosphere again become stable and continuing emissions of NO lead to increasing concentrations. At the Halifax site, high NO concentrations persist throughout the afternoon hours. This site is located in a street canyon, so that limited mixing and high traffic volumes maintain the high NO concentrations.

NO₂ shows a smaller diurnal variation (see Figure 3.32). Almost all sites show an increase corresponding to the morning NO peak. Mixing ratios decline during the mid-afternoon, with an increase after sunset. Most of the suburban sites show a crossover at approximately noon, with NO₂ concentrations becoming greater than NO concentrations. Although ‘typical’ profiles have been discussed, it is clear from Figure 3.32 that each site has a unique diurnal profile which depends on the characteristics of nearby emission sources and local meteorology.

3.4.2.3 Day-of-Week Variations in NO₂ and NO Concentrations

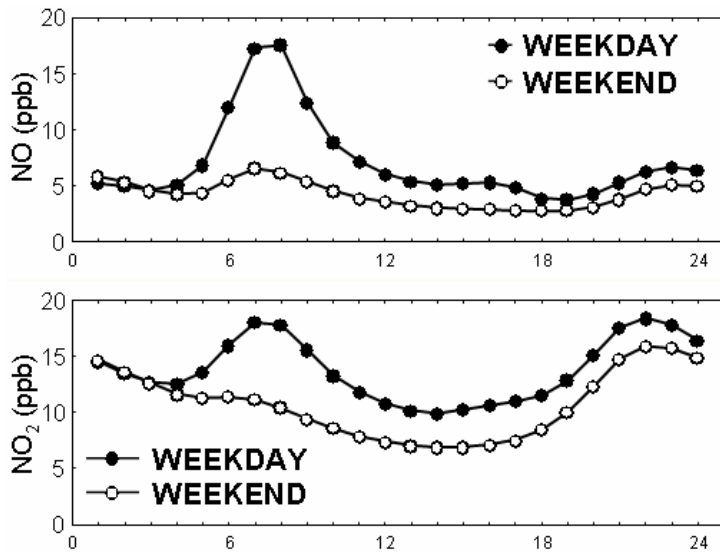


Figure 3.33 Comparison of composite weekday vs. weekend diurnal profiles for NO and NO₂ (2003 – 2005) for 45 urban sites.

As discussed previously, there are substantial differences between weekday and weekend NO and NO₂ concentrations driven by changes in automobile and truck travel patterns, which, in turn, cause differences in weekday/weekend concentrations of O₃. In Figure 3.33, composite weekday (Monday through Friday) NO and NO₂ diurnal concentrations for 45 urban sites are compared with weekend (Saturday and Sunday) ratios. On weekends composite peak morning NO is reduced from 17 to 6 ppb and daily mean NO from 7.1 to 4.3 ppb; composite peak NO₂ is reduced from 18 to 11 ppb and daily mean NO₂ from 14 to 11 ppb. Transportation sources clearly have a large impact on NO, NO₂ and O₃ and weekends in major urban centres may be regarded as a real-world example of an emission reduction effect.

3.4.2.4 NO₂ as an Indicator of Other Species**Table 3.10 Correlations between ambient concentrations of selected VOCs and carbonyls and NO₂, NO and PM_{2.5}.**

Pollutant	City	N	Benz-ene	Toluene	Ethylbenzene	<i>m,p</i> -Xylene	Acetylene	Acetaldehyde	Acetone	<i>o</i> -Xylene	Isoprene	1,3-Butadiene
NO ₂	Montreal	300	0.75	0.51	0.54	0.52	0.69	0.21	0.33	0.57	-0.02	0.67
NO		300	0.86	0.69	0.73	0.70	0.75	0.21	0.39	0.76	0.16	0.83
PM _{2.5}		272	0.65	0.34	0.41	0.42	0.51	0.49	0.41	0.43	0.22	0.47
NO ₂	Ottawa	292	0.86	0.52	0.68	0.59	0.75			0.69	-0.21	0.75
NO		292	0.84	0.56	0.80	0.68	0.82			0.80	-0.08	0.91
PM _{2.5}		262	0.58	0.43	0.45	0.36	0.34			0.47	0.21	0.39
NO ₂	Toronto	219	0.60	0.51	0.57	0.56	0.37			0.57	0.10	0.40
NO		219	0.71	0.52	0.64	0.65	0.47			0.65	0.03	0.62
PM _{2.5}		180	0.39	0.24	0.27	0.24	0.15			0.24	0.11	0.08
NO ₂	Hamilton	319	0.59	0.32	0.61	0.61	0.67			0.63	0.09	0.70
NO		319	0.54	0.43	0.77	0.76	0.70			0.79	0.16	0.84
PM _{2.5}		232	0.53	0.38	0.39	0.39	0.34			0.39	0.21	0.34
NO ₂	Windsor	174	0.47	0.36	0.24	0.19	0.68	0.32	0.11	0.16	0.01	0.56
NO		174	0.45	0.53	0.21	0.14	0.63	0.23	0.25	0.11	0.10	0.78
PM _{2.5}		125	0.31	0.11	0.25	0.23	0.27	0.46	0.21	0.23	0.29	0.20
NO ₂	Edmonton	348	0.78	0.49	0.43	0.48	0.65			0.49	-0.13	0.67
NO		348	0.83	0.55	0.56	0.60	0.69			0.61	-0.10	0.81
PM _{2.5}		302	0.60	0.41	0.32	0.35	0.50			0.35	0.07	0.52
NO ₂	Calgary	333	0.70	0.49	0.62	0.63	0.69			0.64	-0.10	0.72

Pollutant	City	N	Benz-ene	Toluene	Ethylbenzene	<i>m,p</i> -Xylene	Acetylene	Acetaldehyde	Acetone	<i>o</i> -Xylene	Isoprene	1,3-Butadiene
NO		333	0.81	0.65	0.78	0.80	0.72			0.79	0.00	0.87
PM _{2.5}		320	0.38	0.25	0.36	0.35	0.31			0.34	0.44	0.30
NO ₂	Vancouver	302	0.63	0.53	0.56	0.57	0.55	0.32	0.64	0.56	0.36	0.52
NO		302	0.78	0.69	0.70	0.70	0.74	0.16	0.63	0.70	0.24	0.80
PM _{2.5}		246	0.59	0.55	0.53	0.52	0.38	0.35	0.61	0.51	0.48	0.45
NO ₂	Average		0.67	0.47	0.53	0.52	0.63	0.28	0.36	0.54	0.01	0.62
NO			0.73	0.58	0.65	0.63	0.69	0.20	0.43	0.65	0.07	0.81
PM _{2.5}			0.50	0.34	0.37	0.36	0.35	0.43	0.41	0.37	0.26	0.34

Recent work examining NO₂ data (Brook *et al.*, 2007) reaffirms that NO₂ has the strongest association with mortality, particularly in the warm season. Although attributing such effects to NO₂ cannot be ruled out, it is plausible that NO₂ is acting as an indicator for some other exposure affecting the population. This could include PM_{2.5}, or a more specific type of PM_{2.5}, such as traffic-related particles, given that in cities the main source of NO₂ is motor vehicle exhaust. NO₂ could also be acting as a surrogate for other pollutant(s) originating from motor vehicles or high temperature combustion, such as VOCs or PAHs. Another possibility is other oxidized nitrogen species ('NO_Z') or photochemically produced pollutants that can co-vary with NO₂. Data to test these different possibilities across several Canadian cities were examined. The focus was on correlations in time or space between NO₂ and other pollutants that are more strongly linked to vehicle emissions. The results shown in Table 3.10 support the hypothesis that compared to PM_{2.5}, NO₂ is a better indicator of a range of other toxic pollutants. This includes VOCs, aldehydes, NO_Z and particle-bound organics in motor vehicle exhaust.

Furthermore, the fact that the mortality associations are largely driven by a warm season effect and that NO₂ tends to remain elevated throughout the afternoon and evening (see Figure 3.33), may explain why NO₂ has a stronger effect than NO. Nitrogen dioxide's diurnal behavior increases the potential for exposure and during warm season afternoons, the potential for secondary pollutants (such as NO_Z), secondary VOCs and secondary PAHs to co-vary with NO₂ is also expected to be greater. The available data suggest that the consistently strong association between NO₂ and mortality in Canadian cities is because NO₂ is a good indicator of local combustion emissions (likely motor vehicles) along with being indicative of the local build up of photochemically processed urban air pollution. However, the urban mix of air

pollutants is complex as are the biological mechanisms leading to serious outcomes such as mortality. Thus, more careful study is needed to learn more about what aspects of this mix are most harmful to human health.

3.4.3 Volatile Organic Compounds (VOCs)

3.4.3.1 Reactivity of Volatile Organic Compounds

Volatile organic compounds, or VOCs, are generally defined as compounds containing at least one carbon atom (excluding carbon dioxide and carbon monoxide) and with a vapour pressure of 0.01 kPa or greater at 25°C. Although there are many thousands of organic compounds in the natural and polluted troposphere that meet the definition of a VOC, most measurement programs have concentrated on the 50 to 150 most abundant C₂ to C₁₂ hydrocarbons consisting of the general formula C_xH_y and on C₂ to C₆ carbonyls (compounds that, in addition, contain the structural element R₂C=O). For this report, total non-methane hydrocarbons (total NMHC) are defined as the sum of all identified C₂ to C₁₂ hydrocarbons. Total VOC are defined as total NMHC plus carbonyls and other polar species. Monitoring data for other categories of VOCs, such as halogenated hydrocarbons and methane, are not included in this chapter. NMHC also includes a number of species emitted from biogenic sources including isoprene, α-pinene, β-pinene, δ-limonene and camphene.

As discussed in Chapter 2, O₃ formation includes a complex array of reactions involving the atmospheric oxidation of VOCs. In this process, individual VOCs differ in their efficiency towards O₃ formation. Therefore, a scale in which each compound is ranked according to its potential to form O₃ has long been considered for selective regulation of emissions rather than an approach that treats all VOCs equally. Depending on the ranking procedure, different terms have been used to denote the ability of an organic compound to contribute to the formation of O₃. Examples include photochemical O₃-forming potential, incremental reactivity or, simply reactivity (Paraskevopoulos *et al.*, 1995).

One ranking procedure developed in California is based on the concept of maximum incremental reactivity (MIR). MIR is defined as the increase in the peak O₃ concentration caused by the addition of small amounts of a test compound, VOC_i, into a base case mixture representing a typical urban air mass, $IR_i = \Delta[O_3] / \Delta[VOC_i]$. The MIR scale was developed by Carter (1994) and is based on modelling simulations of a number of urban-emissions scenarios. For each scenario, a base case is developed in which the NO_x emissions are adjusted to maximize the IR. In other words, the base case represents the NO_x condition that maximizes the change in peak O₃ for an incremental addition of total VOC. For the base case, the MIR value of each individual VOC is obtained as the change in peak O₃ for an incremental addition of the individual VOC.

The use of the rate coefficient for the reaction of OH + VOC (k_{OH}) as a measure of the reactivity of a VOC has been proposed much earlier. Although an attractive measure as it is an intrinsic property of an individual VOC, it does not take into account the intricacies of the complex chemical reactions that follow the initial reaction between the VOC and OH. Nevertheless, it is useful to consider the k_{OH} reactivity scale under conditions where the production of O_3 is largely limited by the supply of NO_x rather than VOCs. Such conditions prevail at locations removed from major source areas of VOCs, e.g., in rural and remote areas. Chameides *et al.* (1992) introduced a convenient procedure for scaling VOC-based k_{OH} . It involves scaling a VOC by multiplying its concentration (in ppbC) by the ratio of its rate coefficient with OH and the rate coefficient of the reaction between propylene and OH. The adjusted VOC concentration is called its Propyl-Equivalent concentration.

Table 3.11 Definition of Terms to Describe Reactivity of VOC.

Term	Definition	Description	Units
MIR_i	$\text{Max}\{\Delta[O_3] / \Delta[VOC_i]\} / NO_x$	Incremental Reactivity, maximized as function of NO_x	mole O_3 / mole C
$MIRP_i$	MIR_i / MIR_{prop}	Propylene equivalent MIR, the ratio of MIR for VOC_i and MIR of propylene	-
NMHC	$\sum [NMHC_i]$	Sum of C_2 to C_{12} hydrocarbons	ppb C
$NMHC_{prop}$	$\sum \{MIRP_i * [NMHC_i]\}$	Sum of all C_2 to C_{12} hydrocarbons, each scaled by propylene equivalent MIR	ppb C
$MIRP_{Avg}$	$NMHC_{prop} / NMHC$	Average reactivity of the NMHC mixture	-
FR_i	$\{MIRP_i * [NMHC_i]\} / NMHC_{prop}$	Fractional contribution of $NMHC_i$ to $NMHC_{prop}$	-
$k_{OH}P$	$k_{OH, VOC_i} / k_{OH, prop}$	Propylene equivalent OH rate coefficient	$ppm^{-1} \text{ min}^{-1}$
<i>Propyl-Equiv.</i>	$k_{OH}P * [NMHC_i]$	Sum of all C_2 to C_{12} hydrocarbons, each scaled by relative rate coefficient of reaction with OH	ppb C
$k_{OH}P_{Avg}$	<i>Propyl-Equiv.</i> / NMHC	Average propylene equivalent OH rate coefficient for NMHC mixture	-

In some figures and tables in this section the urban VOC data are scaled using the MIR factors. Rural data are analyzed using both the MIR and OH reactivity factors. Table 3.11 summarizes the different scaling factors and associated terms used later in this section.

3.4.3.2 Urban and Rural VOC Data

As noted previously VOC samples are routinely collected at 37 urban and 14 rural sites across Canada. Six of the urban sites are located near refineries.

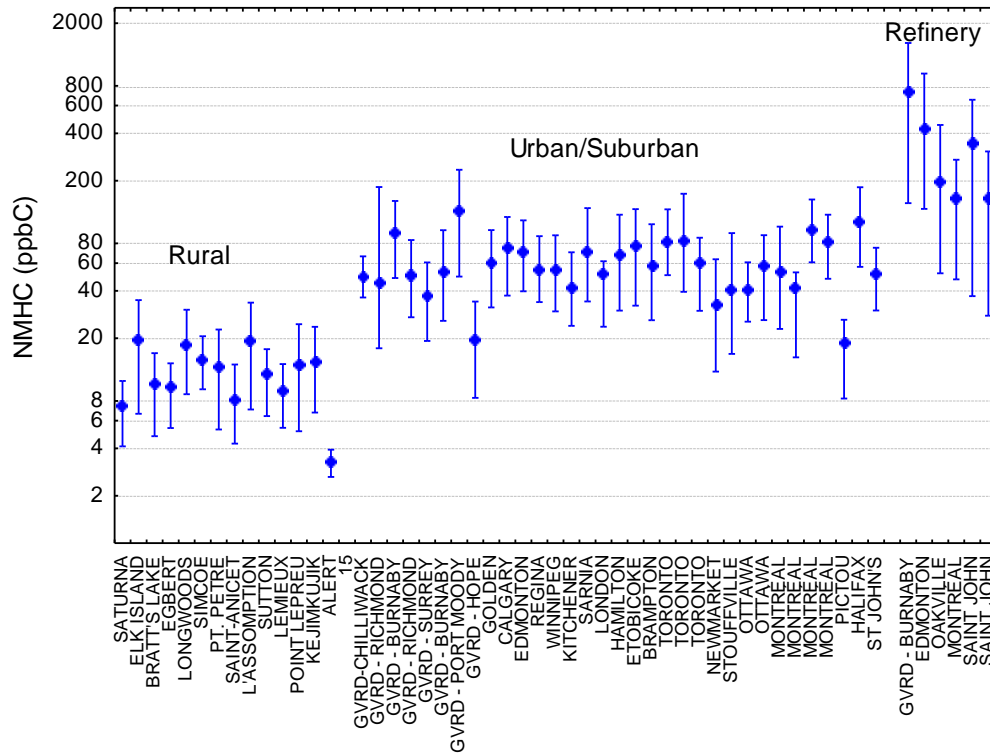


Figure 3.34 Mean, 10th and 90th percentile non-methane hydrocarbons (NMHC) concentrations (ppbC) May to September (2004 to 2006).

In Figure 3.34, different sites and site categories are compared using mean, 10th and 90th percentile NMHC concentrations for the O₃ season (May to September) based on measurements for the years 2004 through 2006. A log-scale has been used since mean concentrations vary by almost three orders of magnitude from the lowest site (Alert – 3.3 ppbC) to the highest site (Burnaby-Eton/Madison – 723 ppbC). The Burnaby site is located approximately 1 km from a Chevron refinery. The NMHC data indicate much lower concentrations at the regionally representative and remote sites than at the rural-urban impacted sites. However, this decrease is not uniform for all individual compounds. Some of the NMHC species with relatively long atmospheric lifetimes such as ethane are found in similar concentrations at urban and rural sites. As discussed later, biogenic species are usually more abundant at rural sites. For the rural sites the proximity of large source regions plays a role; for example, larger NMHC concentrations are observed at such sites as Simcoe, Longwoods, and l'Assomption which are relatively close to large urban areas.

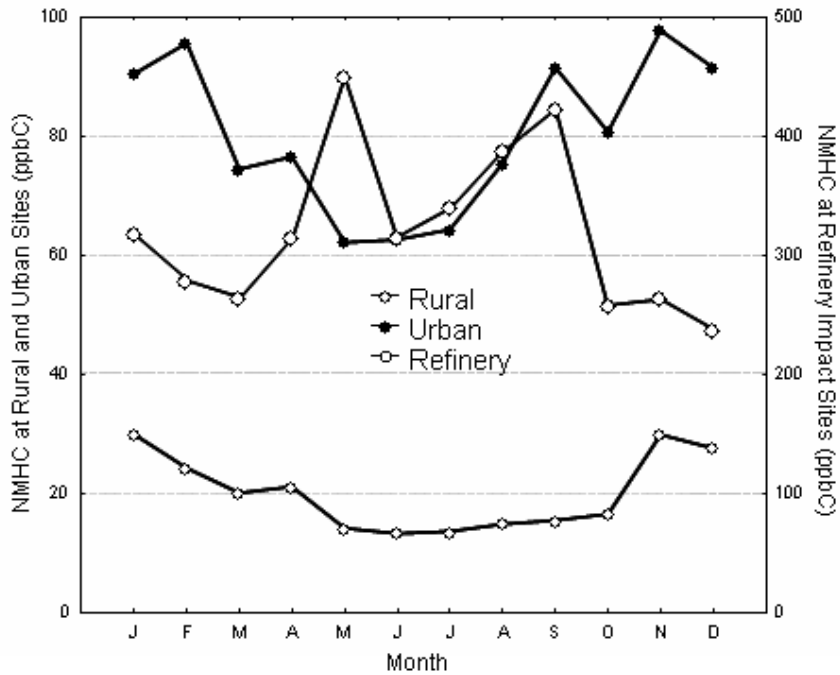


Figure 3.35 Seasonal variation in non-methane hydrocarbons (NMHC) concentrations for site groups.

The composite seasonal variation in NMHC concentrations for three groups of sites is provided in Figure 3.35. The seasonal changes in C₂ to C₁₂ hydrocarbon concentrations would be expected to be influenced by three factors: seasonal abundance of OH radical, changes in hydrocarbon source strengths and changes in meteorology, such as increased vertical mixing in the spring and summer (Jobson *et al.*, 1994). The seasonal variation of most hydrocarbons is largely driven by OH chemistry (Bottenheim and Shepherd, 1995). The greater abundance of OH radicals in the summertime and the increase in OH reaction rates with temperature result in summertime NMHC minima. For example, as shown in Figure 3.35, the NMHC concentrations at rural and urban sites reached a minimum in the May-to-September period. Refinery sites showed a much different pattern with highest concentrations measured during the summer months. This is very likely due to increased evaporative losses from storage tanks as temperatures increase (U.S. EPA, 2006b).

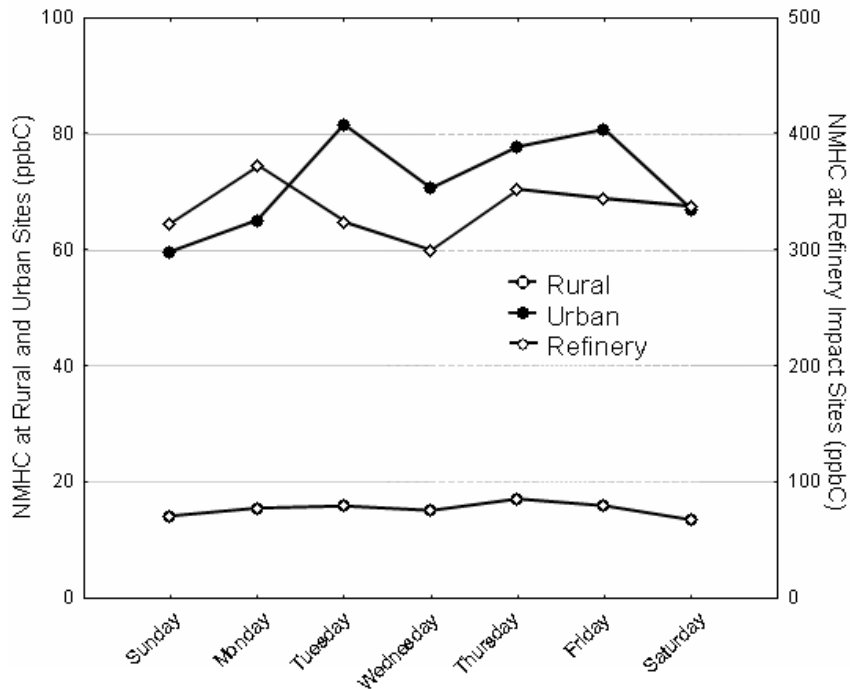


Figure 3.36 Day of week variation in NMHC concentrations for site groups.

Composite day-of-week variations in NMHC concentrations are illustrated in Figure 3.36. All urban sites show significantly lower median concentrations on Saturday and Sunday. The highest concentrations are usually recorded during mid-week (Tuesday to Friday). Using results for all sites, Tuesday-to-Thursday mean NMHC concentrations were 1.6 times higher than Sunday mean concentrations. The sites influenced by industrial sources are mainly located in suburban areas and show less day-of-week variation in NMHC concentrations.

Typically more than 100 NMHC species are routinely measured at each site. At some sites, carbonyl species are measured at the same time. The abundance, variation and O_3 -forming potential of the most important VOC species is summarized next. The O_3 -forming potential is estimated using the MIR scaling procedure. As was discussed before, the MIR factors from Carter (1994) were used for these calculations.

Table 3.12 Ten most abundant NMHC Species as a percentage of total carbon and as a percent of NMHC_{prop} – Urban, Refinery Impact and Rural Sites (Summer Only) 2002 – 2006.

Urban -Sorted by Concentration				Urban - Sorted by NMHC _{prop}		
Rank	Compound	Mean (ppbC)	% of Total	Compound	Mean (ppbC)	% of Total
1	Toluene	8.0	10.7%	<i>m</i> and <i>p</i> -Xylene	3.6	15.3%
2	Isopentane	6.6	8.8%	Toluene	2.7	11.6%
3	Propane	5.7	7.6%	Ethylene	2.5	10.4%
4	Butane	4.7	6.2%	Propylene	1.3	5.3%
5	<i>m</i> and <i>p</i> -Xylene	4.0	5.3%	Isopentane	1.0	4.0%
6	Ethane	3.7	4.9%	Isoprene	0.8	3.5%
7	Ethylene	3.2	4.2%	<i>o</i> -Xylene	0.8	3.3%
8	Pentane	2.8	3.7%	1,2,4-Trimethylbenzene	0.7	2.9%
9	Isobutane	2.8	3.7%	Butane	0.5	2.2%
10	2-Methylpentane	1.9	2.6%	3-Ethyltoluene	0.5	2.2%
ALL SPECIES		75.1			23.7	
Average Reactivity(MIRP _{avg})		0.32				
Refinery -Sorted by Concentration				Refinery - Sorted by NMHC _{prop}		
Rank	Compound	Mean (ppbC)	% of Total	Compound	Mean (ppbC)	% of Total
1	Isopentane	61.3	18.5%	Propylene	11.4	13.5%
2	Butane	33.1	10.0%	Isopentane	8.8	10.4%
3	Pentane	27.7	8.4%	<i>m</i> and <i>p</i> -Xylene	6.6	7.8%
4	Propane	18.7	5.6%	2-Methyl-2-butene	4.5	5.3%
5	Isobutane	15.5	4.7%	Butane	3.8	4.4%
6	2-Methylpentane	12.2	3.7%	Toluene	3.7	4.4%
7	Propylene	11.5	3.5%	Pentane	3.6	4.3%
8	Toluene	10.8	3.3%	trans-2-Pentene	2.7	3.2%
9	Hexane	7.9	2.4%	trans-2-Butene	2.6	3.0%
10	2,2,4-Trimethylpentane	7.5	2.3%	cis-2-Butene	2.2	2.6%
ALL SPECIES		330.8			84.6	
Average Reactivity(MIRP _{avg})		0.26				
Rural -Sorted by Concentration				Rural - Sorted by NMHC _{prop}		
Rank	Compound	Mean (ppbC)	% of Total	Compound	Mean (ppbC)	% of Total
1	Ethane	2.2	13.7%	Isoprene	1.2	22.8%
2	α -Pinene	1.5	9.3%	α -Pinene	0.6	10.6%

Urban - Sorted by Concentration				Urban - Sorted by NMHC _{prop}		
Rank	Compound	Mean (ppbC)	% of Total	Compound	Mean (ppbC)	% of Total
3	Isoprene	1.3	8.0%	Ethylene	0.4	7.0%
4	Propane	1.2	7.4%	Toluene	0.3	6.3%
5	Toluene	0.9	5.9%	<i>m</i> and <i>p</i> -Xylene	0.2	4.3%
6	Butane	0.7	4.4%	Propylene	0.2	3.6%
7	Isopentane	0.6	3.7%	δ-Limonene	0.1	2.2%
8	Ethylene	0.5	2.9%	1-Butene/Isobutene	0.1	1.9%
9	Isobutane	0.4	2.6%	β-Pinene	0.1	1.9%
10	Acetylene	0.4	2.4%	Camphene	0.1	1.8%
ALL SPECIES		16.0			5.2	
Average Reactivity(MIRP _{avg})		0.32				

Table 3.12 provides a list of the 10 most abundant NMHC species as a percent of total carbon and as a percent of NMHC_{prop} (NMHC expressed as propene equivalency) for the urban and refinery impact sites. The species *m* and *p*-xylene, toluene, ethylene, propylene and isopentane are the most important contributors to NMHC_{prop}. The most abundant species on a percent of carbon basis are toluene, isopentane, propane, butane and *m* and *p*-xylene. The urban sites show great uniformity in species profiles, which indicates that hydrocarbon concentrations are dominated by transportation source emissions.

Results for the refinery impact sites are similar to urban sites except for a greater abundance of C₃-C₅ alkanes (propane, butanes and pentanes). The individual site profiles are quite distinctive, reflecting the impact of the different refineries located nearby. The Saint John sites record high levels of methyl tertiary-butyl ether (MTBE) and propylene while the Burnaby site shows high levels of 2,2-dimethylbutane.

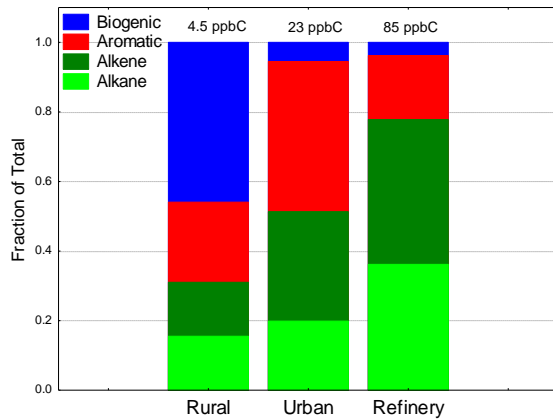


Figure 3.37 Biogenic hydrocarbon fraction of total C₂ to C₁₂ HC - MIR_{prop} weighted (ppbC) – summer only.

For the purpose of comparison with the urban data, Table 3.12 also lists the 10 most important NMHC species observed at regional sites. The results represent an average of all sites for the months of June, July and August. The most abundant compounds on a percent carbon basis were ethane, α -pinene, isoprene, propane and toluene. On a NMHC_{prop} basis, isoprene was the most important compound, accounting for an average of 23% of NMHC_{prop}. An overall comparison of the site groups in terms of VOC category (biogenic, aromatic, alkene, alkane) is provided in Figure 3.37 on an NMHC_{prop} basis.

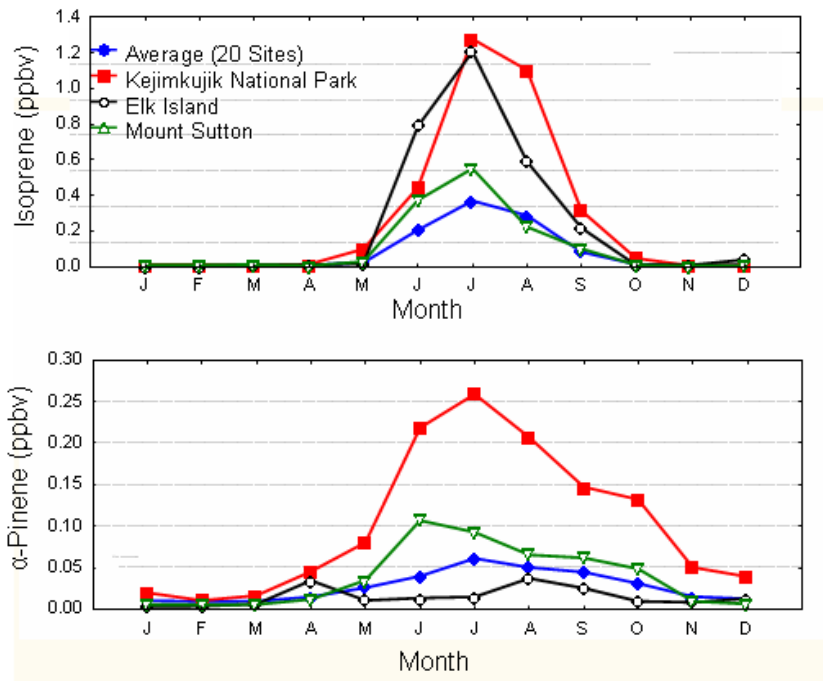


Figure 3.38 Seasonal variation in isoprene and α -pinene (ppbv) for selected rural sites and for the average of all rural sites.

Isoprene and other species emitted by plants are at a minimum in the winter. In other seasons, their abundance in air is controlled not only by reaction with OH but with changes in emission flux. The latter can vary in a given location on a given day by orders of magnitude, depending on the type and density of vegetation, the maturity of leaves, the temperature and the intensity of light (Fuentes *et al.*, 1999). As shown in Figure 3.38 isoprene and the terpenes are quite variable between the rural sites but are very important contributors to NMHC concentrations at many regional sites. Isoprene shows a defined seasonal cycle and is only present during May to September coinciding with leaf emergence. Maximum concentrations were found at the Kejimikujik and Elk Island sites with peak monthly averages in July. Monoterpenes (e.g., α -pinene) are emitted primarily by coniferous tree species (Fuentes *et al.*, 2007) and even though monoterpene levels still peak in July they are also found in measurable quantities throughout the year.

Table 3.13 Contribution of Carbonyls to VOC_{prop} at Urban and Rural Sites (Summer Only) 2002-2006.

Urban - Sorted by VOC _{prop}		
Compound	Mean (ppbC)	% of Total
Formaldehyde	2.2	6.8%
Acetaldehyde	1.2	3.9%
Propionaldehyde	0.4	1.2%
Acetone	0.3	1.1%
MEK	0.3	0.8%
Total Carbonyl	5.2	16.3%
Total C₂-C₁₂ HC	26.5	

Rural - Sorted by VOC _{prop}		
Compound	Mean (ppbC)	% of Total
Formaldehyde	1.5	19.0%
Acetaldehyde	0.7	9.2%
Acetone	0.5	6.8%
MEK	0.4	5.5%
Propionaldehyde	0.2	2.2%
Total Carbonyl	3.3	42.7%
Total C₂-C₁₂ HC	4.5	

The results above are limited to C₂ to C₁₂ hydrocarbon data. Other VOC categories, including carbonyls and alcohols, have been shown to be important at urban and rural sites (Fehsenfeld *et al.*,1992). Carbonyl results (six most abundant species) from seven urban and six rural Canadian sites are summarized in Table 3.13 in terms using MIRP weighting factors. Formaldehyde, acetaldehyde, propionaldehyde, methyl ethyl ketone (MEK) and acetone are the most important carbonyls at both sets of sites. As shown in the table, total carbonyls account for 16% of VOC_{prop} at the urban sites and 43% at rural sites. Only limited measurements of other polar species (alcohols, ethers, acetates, etc.) have been made and results from three sites are summarized in Table 3.14. At these three sites the total polar contribution (excluding terpenes and formaldehyde) of the total VOC concentration in ppbC ranged from 35 to 48%. Clearly measuring only C₂ to C₁₂ hydrocarbons can underestimate total VOC concentrations and overall VOC mixture reactivity.

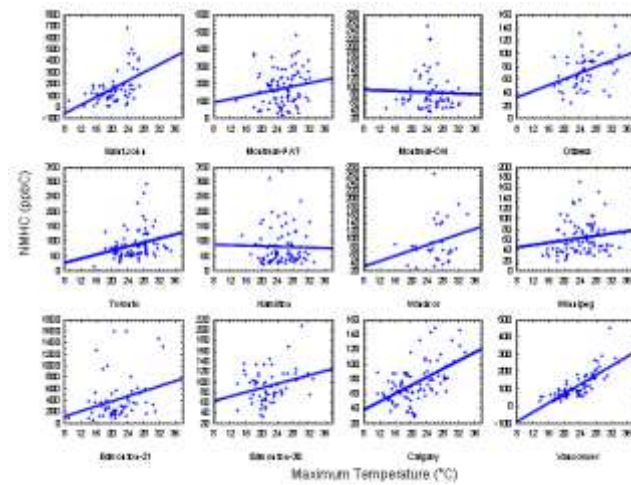


Figure 3.39 Relationship between total C₂ to C₁₂ HC (biogenics excluded) and daily maximum temperature – June, July, August (2001-2006).

As discussed in Section 3.3.4.1, temperature is an important variable when predicting maximum O₃ concentrations. Temperature also increases the emission flux of VOC sources. Evaporative emissions from vehicles, fuel storage and solvents would be expected to increase significantly with increasing temperature. As shown in Figure 3.39, summertime (June, July and August) weekday NMHC concentrations (biogenics excluded) show an increase with increasing daily maximum temperatures at most sites, although the relationship is weak. Similar results were recorded for sites with nearby industries with the strongest association recorded at the Saint John and Vancouver-Rocky Point Park sites.

3.4.4 Trends in Ozone Precursor Ambient Concentrations

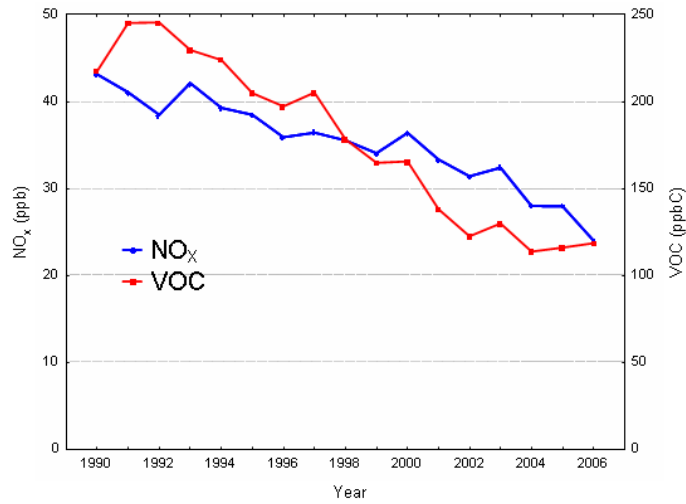


Figure 3.40 Trend in annual mean NO_x (ppb) and VOC (ppbC) at Canadian urban sites.

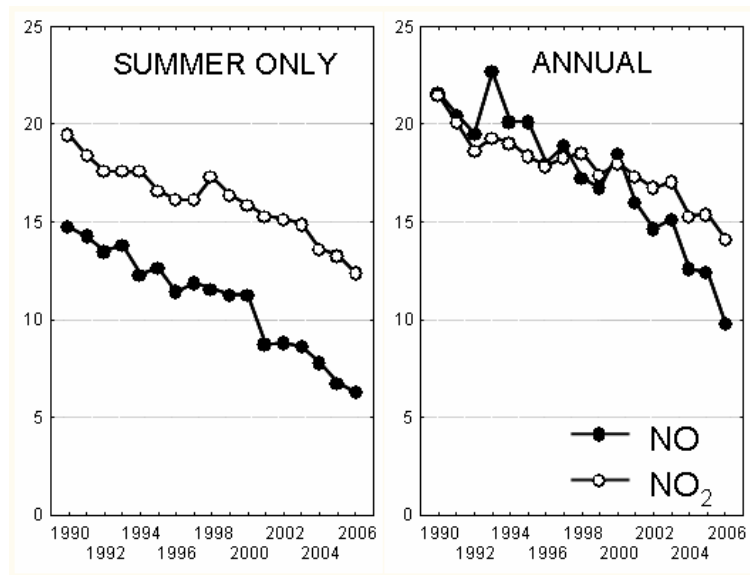


Figure 3.41 Trend in annual and summer mean NO and NO₂ (ppb) at Canadian urban sites.

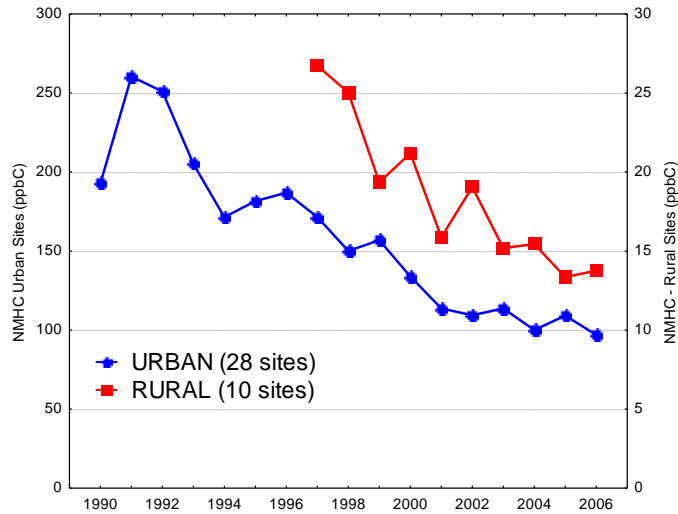


Figure 3.42 Trend in non-biogenic C₂ to C₁₂ HC at urban and rural sites (May to September only).

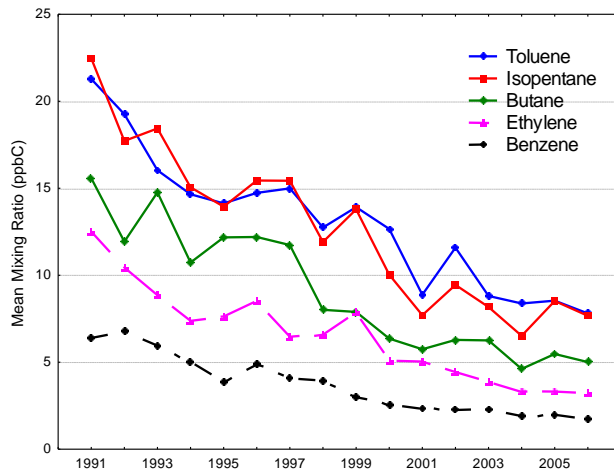


Figure 3.43 Trend in selected major NMHC species (ppbC).

Trends in total annual mean VOC and NO_x are shown in Figure 3.40 for Canadian urban sites with a complete data record (12 out of 17 years of data). A total of 56 sites located in 25 urban areas had complete NO_x data and a total of 28 sites located in 15 urban areas met data completeness requirements for VOC. Isoprene and terpenes are not included in the VOC trend. Trends in annual mean and summer mean NO and NO₂ are shown in Figure 3.41 and trends in summertime VOCs at urban and rural sites are provided in Figure 3.42. Between 1990 and 2006 annual mean NO decreased by 55%, NO₂ by 34% and VOCs by 46% at these Canadian urban sites. The trends were very consistent on a site by site basis with essentially all urban sites in Canada recording similar decreases in ambient levels. The ratio of composite annual mean NO₂ to NO increased from 1.0 to 1.4 during the time period. The ratio of composite summer mean NO₂ to NO increased from 1.3 to 2.0. Rural sites experienced a decline in

anthropogenic VOCs similar to the urban sites with a 49% decrease in mean summer concentration between 1997 and 2006. Trends in some of the major VOC species are provided in Figure 3.43. Mean concentrations of these five major VOC species have declined at a similar rate (range from 63 to 75%) between 1991 and 2006. The ranking of major species measured in NMHC mixtures in 2002-2006 as shown in Table 3.12 are essentially identical to those measured in 1989-1993 (Environment Canada, 1997). This very much reflects the fact that transportation sources dominate VOC emissions in urban areas. The reductions in ambient air NO_x and NMHC also matches the reduction in transportation sector emissions (Government of Canada, 2007).

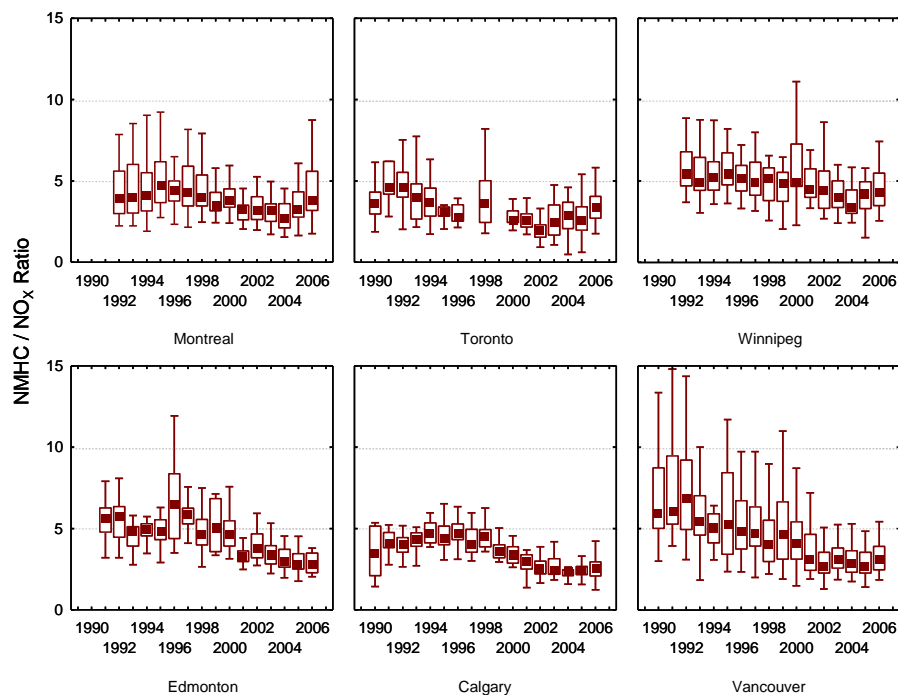


Figure 3.44 Trend in NMHC to NO_x ratios at selected sites (May to September) (median, 25th and 75th percentiles, non-outlier maximum and minimum).

As discussed in Chapter 2, O_3 concentrations can be VOC or NO_x -limited. At high VOC/ NO_x ratios (> 8), O_3 formation is said to be NO_x -limited, and reducing VOCs will not lead to a reduction in O_3 . Conversely, at low VOC/ NO_x ratios, O_3 formation is VOC-limited and reductions in NO_x will result in no change in O_3 or even increases in O_3 . Most eastern urban areas of Canada experience median summer-time NMHC-to- NO_x ratios (24-hr) in the range of 3 to 5 (ppbC/ppb), with sites near industrial sources of VOCs recording much higher ratios. Sites with the highest NO_x concentrations typically recorded the lowest NMHC-to- NO_x ratios. Trends in NMHC to NO_x ratios for selected cities are provided in Figure 3.44. There has been a trend to lower NMHC to NO_x ratios over the measurement period but a reversal of the trend begins at most sites in 2003.

As discussed, NMHC represent a variable fraction of total VOC, depending on site location. At urban sites, VOC-to-NO_x ratios could be expected to be 1.2 to 1.5 times higher than NMHC-to-NO_x ratios if unidentified hydrocarbons, carbonyls, alcohols and other polar species were included. At rural sites, VOC-to-NO_x ratios could be 1.5 to 3 times higher than NMHC-to-NO_x ratios, depending on carbonyl and alcohol abundance (Fehsenfeld *et al.*, 1992; Fuentes *et al.*, 2007).

3.5 PM_{2.5} Mass, Composition and Precursors

3.5.1 PM_{2.5} Mass

3.5.1.1 Estimates of Baseline and Background PM_{2.5}

“Background” and “baseline” particulate matter (PM) as defined here are similar to the definitions for “background” and “baseline” ozone (see Section 3.3.1.4). Background PM is that arising from local natural (non-anthropogenic) emissions of PM and PM precursors as well as PM and precursors transported into an airshed from afar, where the latter may be both natural and anthropogenic in origin (McKendry, 2006). Examples of relevant natural emissions of PM and its precursors include wind-blown dust, sea spray, volcanic eruptions, lightning, forest fires, wild animals and plants. Thus, background PM is the PM measured at a given site due to non-local and non-airshed anthropogenic sources. As with O₃, baseline PM_{2.5} is a measurement-based value at a given site in the absence of strong local influences. Note that discussion of background in this section as follows is often the term used in the published literature being referenced and in some instances, may actually be a description of baseline concentrations as defined above. The original term, as published, has been retained in the discussion below.

Baseline PM, in this case PM_{2.5}, was estimated for Canada using a two step process somewhat similar to the method used in Section 3.3.1.4 to estimate background ozone. In this case however, the lack of non-urban PM_{2.5} measurement sites limited the analysis to just a few regionally-representative rural sites. Step one involved selecting seven regionally representative measurement sites across the country, i.e., sites with minimal local emissions. Step two involved identifying a subset of the PM_{2.5} concentration data at those sites associated with air that travelled to the site over areas least affected by anthropogenic emissions. This approach was designed to minimize (but not totally eliminate) anthropogenic influences as much as possible.

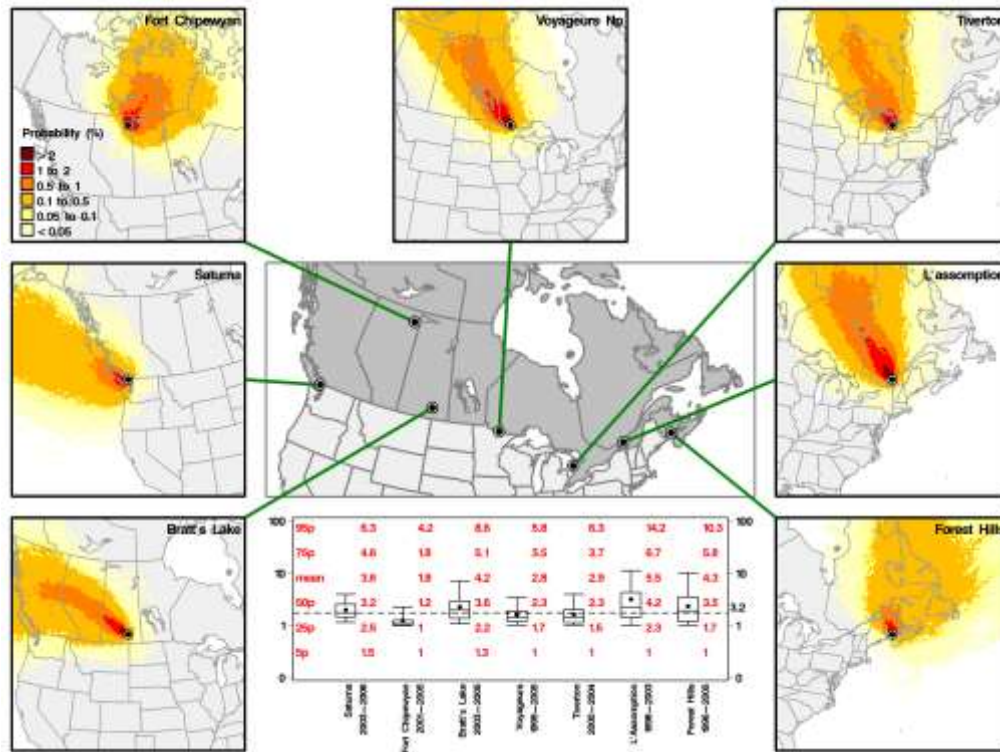


Figure 3.45 Probability densities of air parcel trajectory clusters associated with the lowest $PM_{2.5}$ concentrations at the 95th percentile for seven rural sites for time periods with available $PM_{2.5}$ data between 1996 and 2005. The inset box at the bottom of the figure shows, for each site, the percentile values (in red) and box-and-whisker plots (in black) of all 6-hour- average $PM_{2.5}$ concentrations associated with the baseline trajectory cluster. The box-and-whisker plot shows the overall annual statistics including the 5th, 25th, median (50th), mean, 75th and 95th percentiles for each selected site. The dashed line shows the overall median of $3.2 \mu g m^{-3}$ of the medians from all sites.

For the seven rural sites selected, Figure 3.45 shows probability densities of air parcel trajectory clusters associated with the lowest $PM_{2.5}$ concentrations at the 95th percentile for seven rural sites for time periods with available $PM_{2.5}$ data between 1996 and 2005. The trajectory probability value associated with each grid square was calculated by summing all trajectories that had traversed over a given grid divided by the total number of trajectories for the entire time period included in the cluster analysis.

The inset diagram at the bottom of Figure 3.45 shows, for each site, the percentile values (in red) and box-and-whisker plots (in black) of all 6-hour- average $PM_{2.5}$ concentrations associated with the baseline trajectory cluster. The box-and-whisker plot shows the overall annual statistics including the 5th, 25th, median (50th), mean, 75th and 95th percentiles for each selected site. The dashed line shows the overall median of $3.2 \mu g m^{-3}$ of the medians from all sites. The figure confirms that concentrations associated with the baseline clusters are indeed variable in space and time, as shown, respectively, by the between-site differences and the intra-site box plots, presumably due in some measure to anthropogenic sources of $PM_{2.5}$ and/or

its precursors. In light of this, the metric chosen to represent the baseline concentration at each site was the median (50th percentile) concentration shown in Figure 3.45. This metric varies from a low of 1.2 $\mu\text{g m}^{-3}$ at the remote Fort Chipewyan site in northern Alberta to a high of 4.2 $\mu\text{g m}^{-3}$ at the agricultural L'Assomption site northeast of Montreal, Quebec. The median was chosen to represent the central tendency of the baseline cluster data distribution.

Concentrations below the median are likely associated with air masses that travelled over low emission areas and experienced particle and/or precursor losses due to wet deposition, dry deposition and decoupling of elevated layers. Conversely, concentrations higher than the median are likely associated with air masses that travelled either over slightly higher emission baseline areas and/or experienced lower losses of particles and precursors.

In summary, baseline annual median $\text{PM}_{2.5}$ concentrations in Canada are both location- and time-dependent and range from 1.2 $\mu\text{g m}^{-3}$ at a continental site in northern Alberta to 4.2 $\mu\text{g m}^{-3}$ at an agricultural site near Montreal, QC. These values undoubtedly reflect some influence of local emission sources, such as at the L'Assomption, QC and Forest Hills, NB sites. This suggests that the foregoing baseline median values may be somewhat higher at these sites than they would be at nearby regionally-representative sites. This is an issue for future investigation (ideally, using the same methodology used in the baseline ozone analysis) when more regionally-representative data sets are available. Until such time, the current estimate of annual median baseline $\text{PM}_{2.5}$ concentration is between 1 and 4 $\mu\text{g m}^{-3}$, with an overall seven-site median of 3.2 $\mu\text{g m}^{-3}$. Using the 98th percentile statistic as defined in the CWS would result in a significantly higher estimate of baseline $\text{PM}_{2.5}$ as shown in the next Sections.

Unfortunately, only a few published values of background $\text{PM}_{2.5}$ are available in the scientific literature for comparison. For example, McKendry (2006) estimated a mean background concentration in air masses arriving in British Columbia from north Pacific trajectories to be 1.5 - 2 $\mu\text{g m}^{-3}$ (compared to the Saturna mean and median values of 3.6 and 3.2 $\mu\text{g m}^{-3}$ in Figure 3.45). Also on the Pacific west coast, Jaffe *et al.* (2005) estimates a combined marine/Asian $\text{PM}_{2.5}$ background of 1.5 $\mu\text{g m}^{-3}$ (mean = 2.1 $\mu\text{g m}^{-3}$) at Crater Lake, Oregon. Vingarzan (2004) estimates a western North America background range of 1-4 $\mu\text{g m}^{-3}$. With so few numbers for comparison, one can only generalize that the baseline levels of 1 to 4 $\mu\text{g m}^{-3}$ presented here are consistent with previously published values.

Unfortunately, the lack of long-term $\text{PM}_{2.5}$ measurement data at regionally-representative sites made it impossible to assess the long-term temporal trends of baseline $\text{PM}_{2.5}$ (as was done for baseline ozone in Section 3.3.1.4). Such analyses are recommended when sufficient data sets are available.

3.5.1.2 PM Climatology

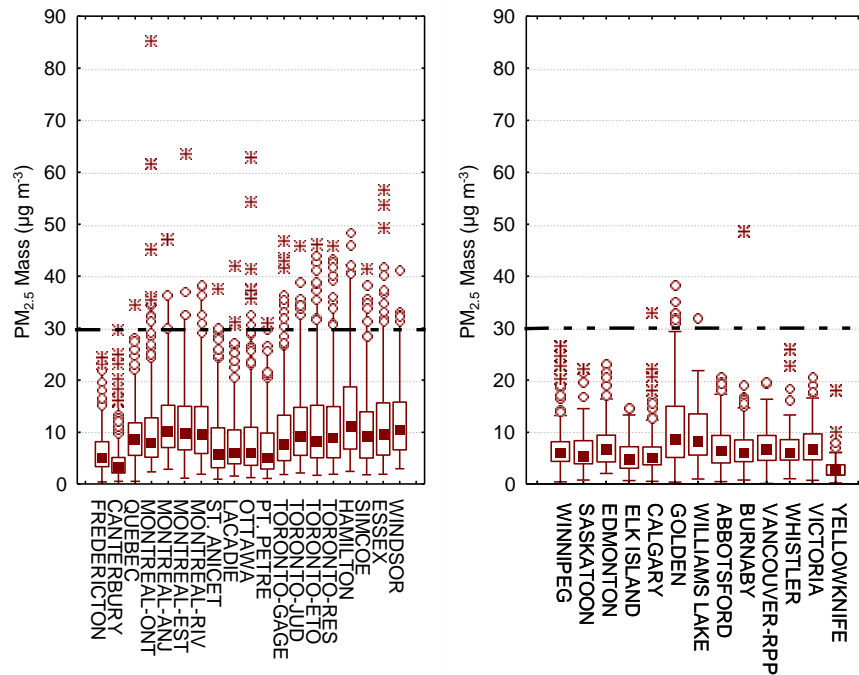


Figure 3.46 Comparison of PM_{2.5} 24-h mass concentrations from filter-based samplers measured from 2004 to 2006 (median, 25th and 75th percentile, 2nd and 98th percentile, outliers and extremes).

As noted in section 3.2.6.1, NAPS network sites have been measuring both fine ($< 2.5 \mu\text{m}$ – PM_{2.5}) and coarse (2.5 to $10\mu\text{m}$ – PM_{10-2.5}) particle mass since 1984 using dichotomous samplers. As of 2006, there were 27 dichotomous samplers operating at NAPS sites supplemented by an additional 13 U.S. EPA federal reference method (FRM) samplers measuring only PM_{2.5}. The Canada-wide standard for PM_{2.5} of $30 \mu\text{g m}^{-3}$ is based on a three year average of the 98th percentile of 24-hr measurements and requires daily sampling. Most of the filter-based samplers operate on a 1-in-6 or 1-in-3 day schedule and do not meet the requirements for CWS reporting. On the other hand, the filter-based samplers are by definition the reference method and are not subject to cold season losses of semi-volatile particulate matter and thus currently represent the most accurate estimate of year round PM_{2.5} mass (see Section 3.2.6.2). Figure 3.46 provides a box-plot comparison of PM_{2.5} 24-hr concentrations across the country as made by these filter-based samplers for the years 2004 through 2006. The statistics provided are the median, 2nd, 25th, 75th and 98th percentiles and outliers and extremes. Only sites with a minimum of 100 samples collected over this period are included and the sites are arranged east to west. It is clear from the figure that the majority of sites with 24-hr observations greater than $30 \mu\text{g m}^{-3}$ are located in eastern Canada with the Golden site a notable exception in the west.

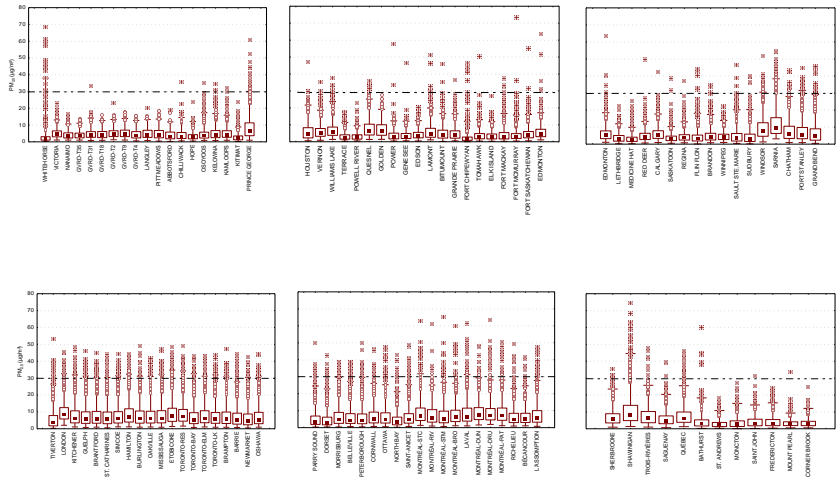


Figure 3.47 Comparison of PM_{2.5} 24-h mass concentrations from TEOM samplers for the period of 2004 to 2006 (median, 25th and 75th percentile, 2nd and 98th percentile, outliers and extremes).

A summary of 24-hr PM_{2.5} concentrations for the much larger TEOM network of PM_{2.5} monitors for the year 2006 is provided in Figure 3.47. As described in Section 3.2.6.2, the TEOM instruments lose volatile mass in the winter months and read low when compared to filter-based samplers. The same statistics as used in Figure 3.46 are displayed and because of the larger selection of sites and the daily frequency of sampling it can be seen that a large number of sites see at least occasional 24-hr PM_{2.5} concentrations greater than 30 µg m⁻³. The Ontario and Quebec sites still have much higher 98th percentile values than most western or Atlantic sites. The lowest observed 98th percentile PM_{2.5} values from both the filter-based and TEOM networks were in the range of 10 to 12 µg m⁻³.

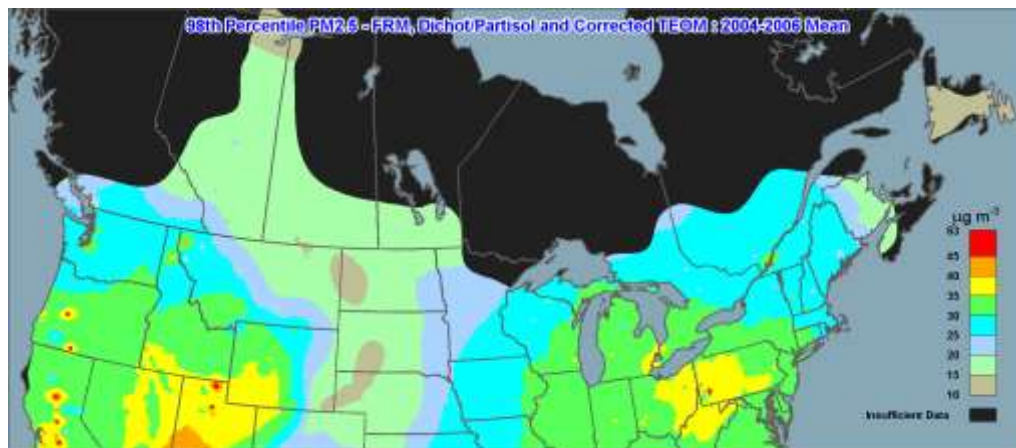


Figure 3.48 98th Percentile PM_{2.5} Concentrations (µg m⁻³) – 2004 -2006.

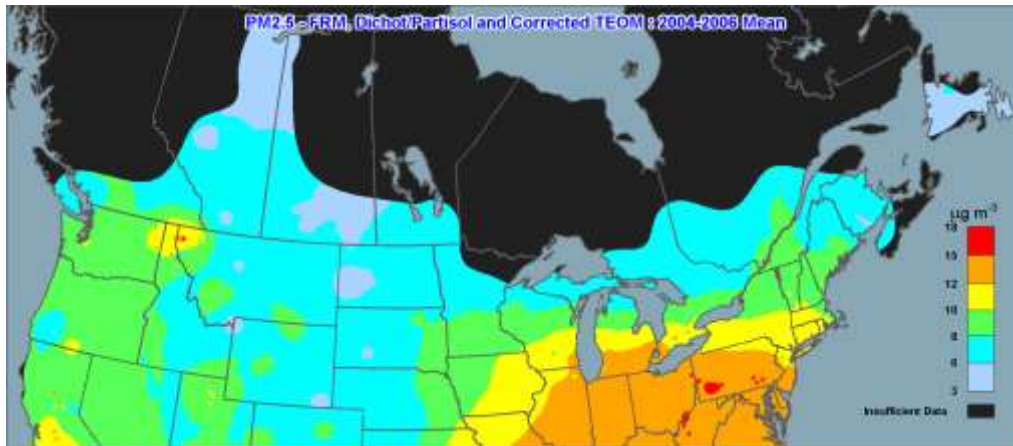


Figure 3.49 Annual Mean PM_{2.5} Concentrations ($\mu\text{g m}^{-3}$) – 2004 -2006.

Spatial maps of the 3-year mean of the annual 98th percentile PM_{2.5} values and 3-year average annual mean concentrations for the period 2004 to 2006 are shown in Figure 3.48 and 3.49, respectively. In order to create these maps, three sets of data were combined for a total of approximately 600 sites, namely: the NAPS filter-based sampler data, the U.S. FRM data as reported to AQS and adjusted Canadian TEOM data corrected for cold season losses, as described previously in Section 3.2. In the same way as for spatial maps of O₃ (Section 3.3.2.1), annual mean statistics for these sites were calculated and the 3-year averages of these annual values for the 2004-2006 period were spatially interpolated using ordinary kriging. To minimize interpolation error, the data were divided into two populations: sites in areas where the site density was high and sites in areas where the site density was lower. The two populations were interpolated separately and the results were combined to produce the final maps. The interpolation uncertainty in the two PM_{2.5} maps is higher than in the ozone maps (Figures 3.7 and 3.8) because of the lower density of PM measurement sites. In areas where site density is high such as in eastern Canada, the interpolation uncertainty is generally between 15 and 30% but it can be as high as 40% in parts of western Canada where single measurement sites drive the interpolation results.

On the assumption that local uncertainty is high but the spatial pattern is reasonable, the map of the 3-year average 98th percentile values for the period 2004-2006 (Figure 3.48) and the map of the 3-year annual mean concentration (Figure 3.49) indicate that southern Ontario and southern Quebec are part of a high concentration Canada-US airshed (98th percentile $>25 \mu\text{g m}^{-3}$ and annual mean $>8 \mu\text{g m}^{-3}$) that encompasses all of the eastern U.S. Central British Columbia is also an area of high concentrations due to measurements in Prince George and Quesnel, but is not shown as such in Figure 3.48 because the interpolation in that area is strongly influenced by those two measurement sites and thus the size and extent of the high concentration area are uncertain. It is worth noting that the annual PM_{2.5} maps from 2000 to 2007 (not shown) suggest a continual decrease in the 3-year 98th percentile concentrations

across the country during that period. As a result, the 3-year maps shown in Figures 3.48 and 3.49 are low compared to the earlier 3-year periods and the 2000-2002 map (not shown) would represent the highest concentration or worst case situation during that period.

A detailed discussion of the factors responsible for the different levels of PM_{2.5} is given on a region-by-region basis in Chapter 7. The chapter makes the point that PM_{2.5} episodes in southern Ontario and southern Quebec are affected not only by local PM and precursor emissions but also by the transboundary transport of PM and its precursors from the United States.

As carried out for O₃, the frequency of regional scale PM_{2.5} episodes (defined as days where 33% of monitoring sites in a region recorded 24-h PM_{2.5} concentrations greater than 30 µg m⁻³) has been calculated for the period 2001 to 2005 and results are shown in Table 3.15. Because of losses of semi-volatile PM by the TEOM instruments during the winter the winter time data were adjusted as described previously. Dates of occurrence of notable episodes (in terms of special extent and maximum PM_{2.5} levels) are also provided in the table along with an indication of whether high O₃ levels were also recorded during the episode. The greatest frequency of regional-scale episodes occurred in Ontario followed by Quebec and for both these regions high PM_{2.5} values often persisted for several days. Unlike for O₃, regional scale episodes of PM_{2.5} occurred in both winter and summer. As discussed previously, summer time PM_{2.5} episodes in Ontario and Quebec were highly likely to be associated with O₃ values greater than the CWS metric of 65 ppb. Regional scale episodes of PM_{2.5} were infrequent in the Prairies with the most notable regional scale PM_{2.5} event associated with the August 2003 forest fires in the southern B.C. interior. The only regional scale episode recorded in the Lower Fraser Valley was associated with the Burns Bog fire on September 13, 2005. Most other B.C. sites are separated by large distances and regional transport is constrained by topography but there were occasions when a number of interior B.C. communities simultaneously recorded elevated PM_{2.5} concentrations. These primarily occurred in October and November and are presumably due to similar meteorological conditions occurring over the interior. More details on selected PM episodes are found in Chapter 7.

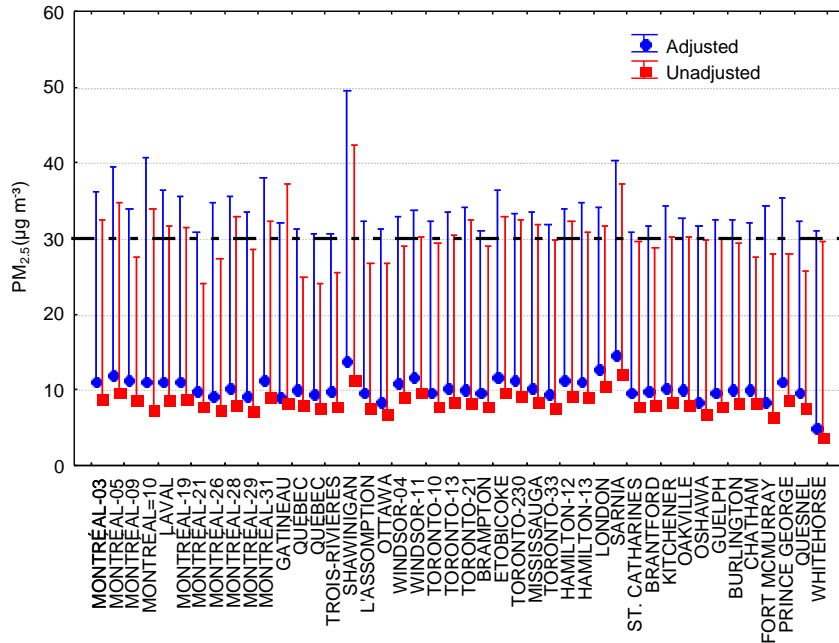


Figure 3.50 Adjusted and unadjusted annual mean and 98th percentile $PM_{2.5}$ for TEOM sites that would exceed $30 \mu g m^{-3}$ averaged over 2004-2006.

Figure 3.50 provides the annual mean and 98th percentile values for Canadian sites that would exceed the CWS value of $30 \mu g m^{-3}$ (2004 to 2006) with and/or without adjustment of the TEOM cold season results. There were a total of 17 TEOM sites (out of 137 with complete data) that exceeded a three-year average concentration of $30 \mu g m^{-3}$ in 2004 to 2006 with all of these sites located in Ontario and Quebec. Use of a cold season adjustment factor would increase the number of sites to 44 with 4 located outside of Ontario and Quebec (Fort McMurray, Quesnel, Prince George and Whitehorse).

A complete analysis of $PM_{2.5}$ in terms of the Canada-wide standard can be found in the Government of Canada Five-year Progress Report on Canada-wide Standards for Particulate Matter and Ozone (Government of Canada, 2007).

For the period 2003 to 2005, at least 30% of the Canadian population (approximately 10 million) lived in communities with levels above the CWS. Most of these were located in Ontario and Quebec. Outside these two provinces, only two communities in the interior of British Columbia reported levels above the CWS. Communities within 10% of the standard were also primarily located in Ontario and Quebec.

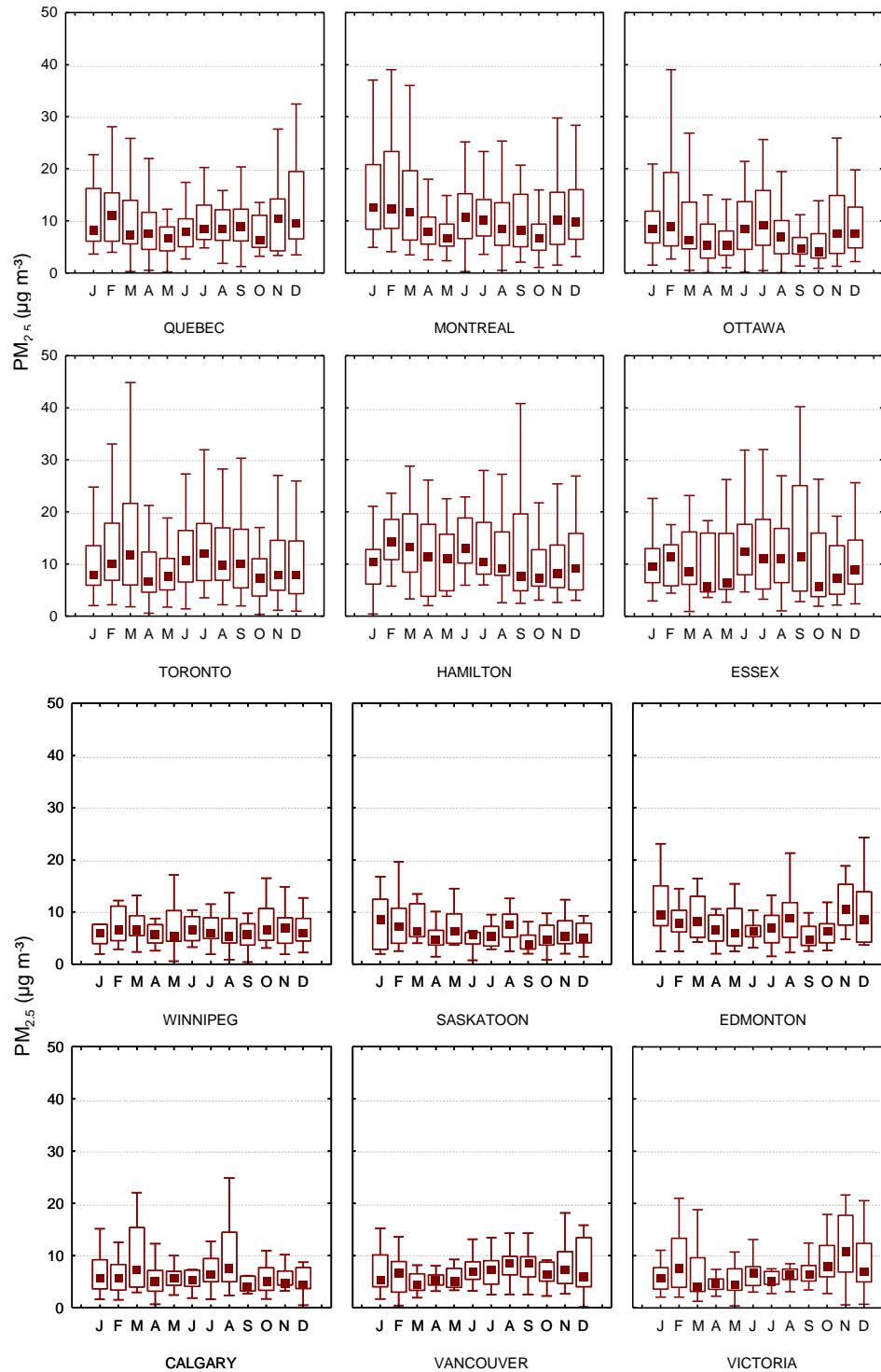


Figure 3.51 Seasonal variability of PM_{2.5} mass from the filter-based samplers (median, 25th and 75th percentile, non-outlier maximum and minimum).

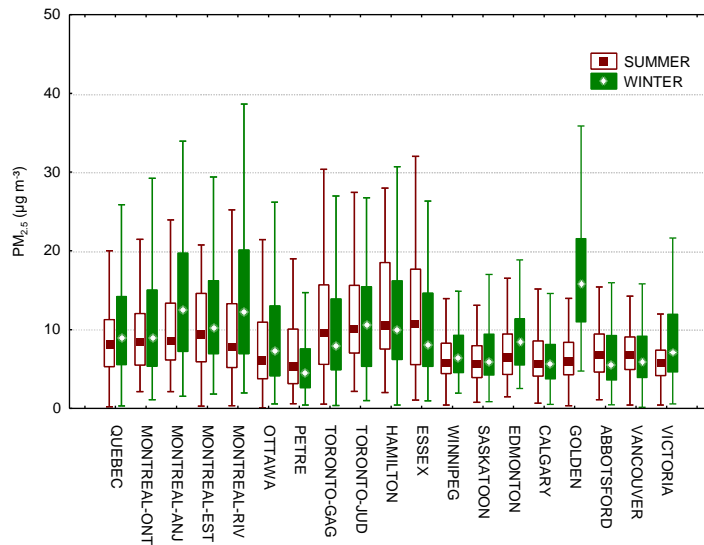


Figure 3.52 Winter vs. summer concentrations of $PM_{2.5}$ mass from the filter-based samplers for selected Sites (median, 25th and 75th percentile, non-outlier maximum and minimum).

Seasonal variability of $PM_{2.5}$ mass from the filter-based network is shown in Figure 3.51 and winter and summer differences in $PM_{2.5}$ mass are shown in Figure 3.52. Most of the eastern sites show spring and fall minima in $PM_{2.5}$ monthly means. Both winter and summer episodes of $PM_{2.5}$ do occur as discussed in the Chapter 7. Overall most sites see a similar distribution of values in winter and summer with some notable exceptions such as Golden.

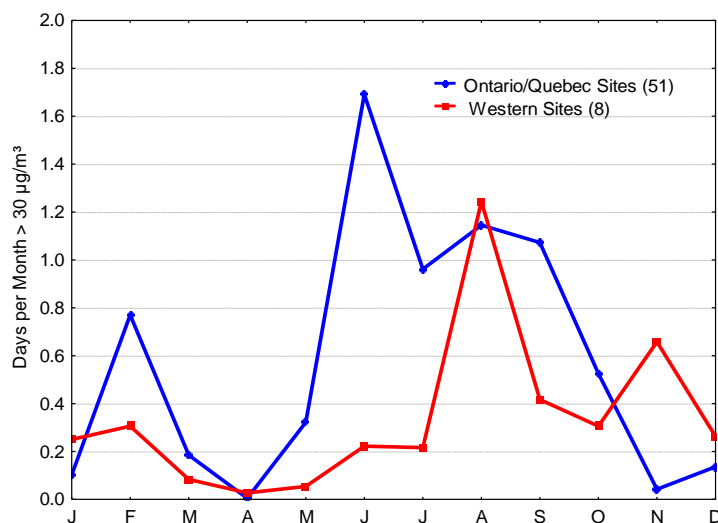


Figure 3.53 Average days per month with $PM_{2.5}$ concentrations greater than $30 \mu g m^{-3}$ for the years 2001 to 2005. (Only sites averaging at least one day per year $> 30 \mu g m^{-3}$ are included in the plot).

The relative frequency of days per month with $PM_{2.5}$ concentrations greater than $30 \mu g m^{-3}$ is shown in Figure 3.53 for the 5-year period 2001 to 2005. Only sites that averaged at least 1 day per year greater than $30 \mu g m^{-3}$ were used to create the plot. Only 8 sites outside of Ontario and Quebec met the criteria to be included. From the Figure it can be seen that $PM_{2.5}$ concentrations greater than $30 \mu g m^{-3}$ can be experienced in any month of the year but during the 2001 – 2005 time period the Ontario/Quebec sites experienced the greatest frequency of days $> 30 \mu g m^{-3}$ in June, July and August followed by February. The western sites showed a peak in August due to the occurrence of forest fires in B.C. in August, 2003 as discussed previously.

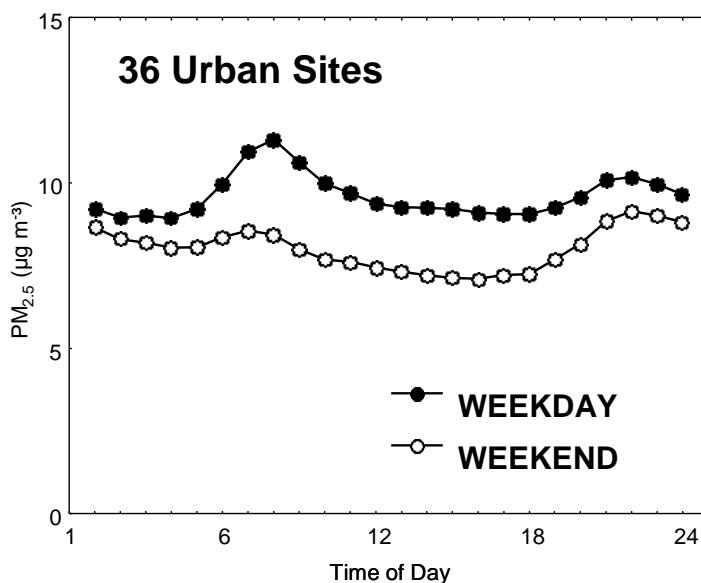


Figure 3.54 Diurnal variation in $PM_{2.5}$ mass, weekday vs. weekend, from TEOM samplers (2003 – 2005).

Using composite hourly data from the TEOM network the diurnal variability of $PM_{2.5}$ mass for weekdays versus weekends is illustrated in Figure 3.54. This figure clearly shows the impact of transportation sources on $PM_{2.5}$ concentrations with an approximate 25% decrease in the morning peak and a 17% decrease in the daily mean on weekends as compared to weekdays. As discussed in the following sections, the majority of $PM_{2.5}$ is of secondary origin so the transportation sector is making a very large contribution to primary emissions.

3.5.2 Chemical Composition of $PM_{2.5}$

As discussed previously, partial speciation (sulphate and major elements) of $PM_{2.5}$ mass from the dichotomous sampler network has been made since 1986. With the inception of the fine particle speciation network in 2003 all major components of $PM_{2.5}$ including ammonium nitrate, ammonium sulphate and organic and elemental carbon are now quantified and

reported. A listing of the NAPS speciation sites and available length of data record are provided in Table 3.16. Only sites with at least 50 days of results for both the warm and cold seasons are featured in the subsequent plots. Table 3.16 also contains a listing of the CAPMoN speciation sites and associated length of data record.

3.5.2.1 Major PM_{2.5} Components and Seasonal Cycle

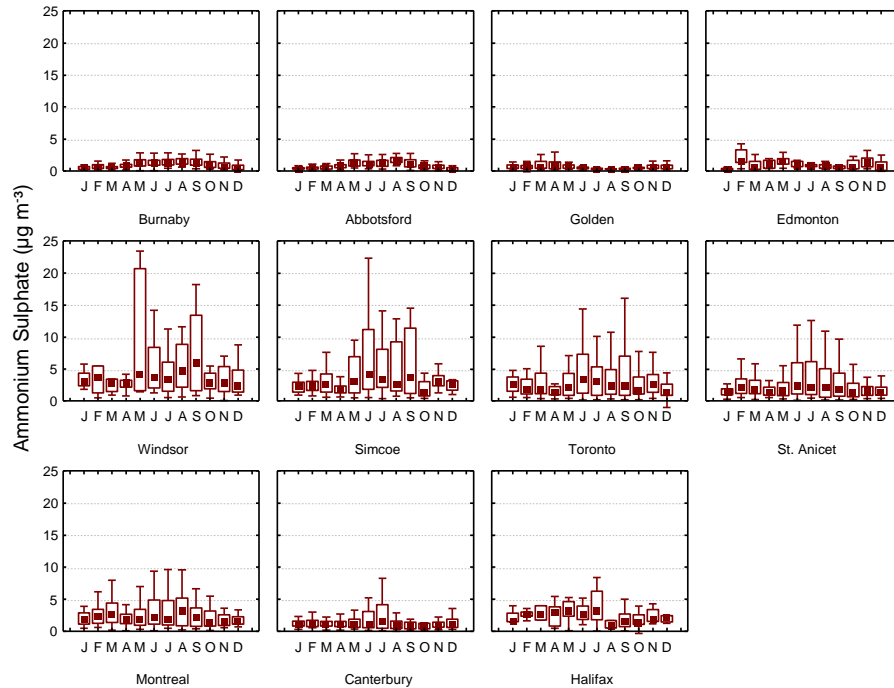


Figure 3.55 Comparison of ammonium sulphate concentrations ($\mu\text{g m}^{-3}$) by site and month (median, 25th and 75th percentile, non-outlier maximum and minimum).

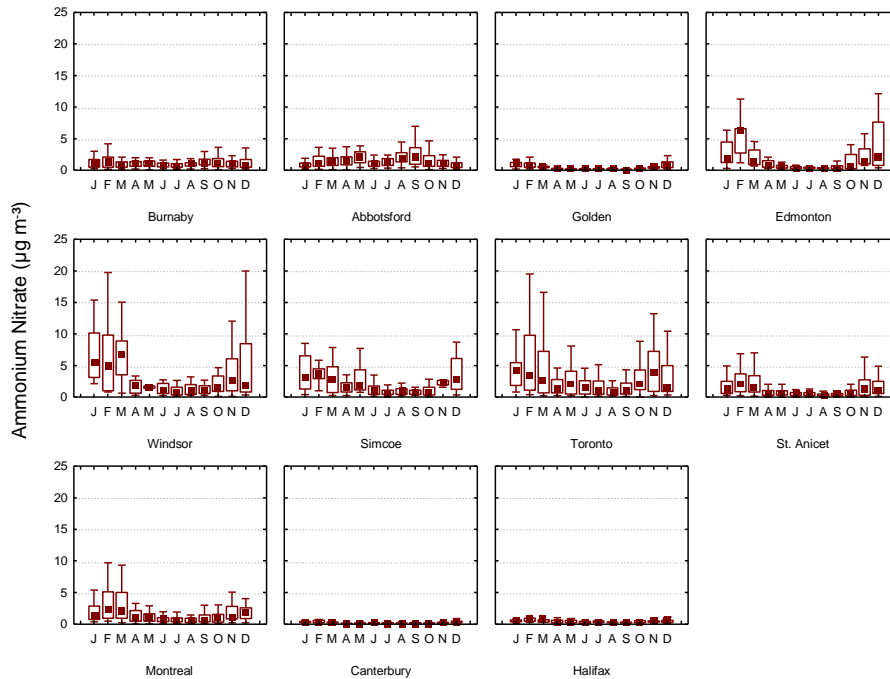


Figure 3.56 Comparison of ammonium nitrate concentrations ($\mu\text{g m}^{-3}$) by site and month (median, 25th and 75th percentile, non-outlier maximum and minimum).

Figures 3.55 and 3.56 respectively show monthly variations in ammonium sulphate ($(\text{NH}_4)_2\text{SO}_4$) and ammonium nitrate (NH_4NO_3) at the sites (median, 25th and 75th percentiles and non-outlier maximum and minimum). The measured ammonium (NH_4) was apportioned to SO_4 and NO_3 to compute $(\text{NH}_4)_2\text{SO}_4$ and NH_4NO_3 using the following steps:

$$[\text{NH}_4\text{NO}_3] = 1.29 \times [\text{NO}_3]$$

$$[(\text{NH}_4)_2\text{SO}_4] = [\text{SO}_4] + [\text{NH}_4] - 0.29 \times [\text{NO}_3]$$

Summertime median $(\text{NH}_4)_2\text{SO}_4$ concentrations were much higher at the Ontario sites ranging from 2.6 to 4.0 $\mu\text{g m}^{-3}$ with maxima in the range of 20 to 27 $\mu\text{g m}^{-3}$. The other eastern sites recorded summer medians ranging from 1.8 to 2.2 $\mu\text{g m}^{-3}$ and medians at the western sites ranged from 0.5 $\mu\text{g m}^{-3}$ (Golden) to 1.9 $\mu\text{g m}^{-3}$ (Abbotsford). All sites except Golden and Edmonton showed a strong seasonal cycle in $(\text{NH}_4)_2\text{SO}_4$ with highest median and peak concentrations in the summer months. NH_4NO_3 showed an opposite seasonal cycle with highest concentrations in the winter months at all sites except Abbotsford. The Abbotsford site recorded its highest NH_4NO_3 values in spring and fall. Edmonton and the Ontario and Quebec sites recorded the highest winter median NH_4NO_3 concentrations (1.3 to 2.7 $\mu\text{g m}^{-3}$) and Canterbury and Halifax the lowest (0.2 to 0.4 $\mu\text{g m}^{-3}$). The highest 24-hr NH_4NO_3 values were measured at Windsor and St. Anicet with a value of 34 $\mu\text{g m}^{-3}$.

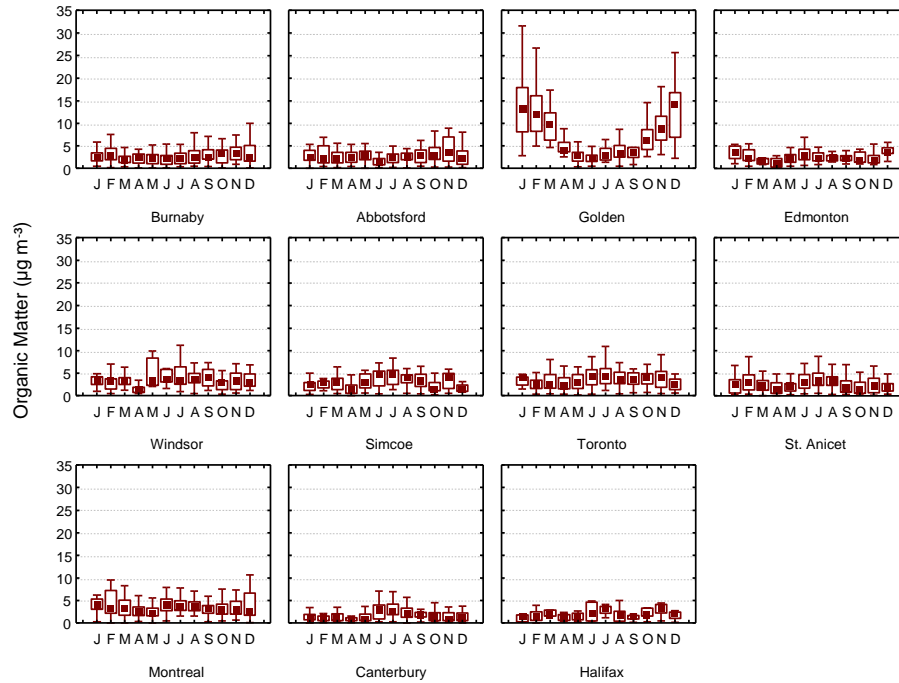


Figure 3.57 Comparison of organic matter ($\mu\text{g m}^{-3}$) by site and month (median, 25th and 75th percentile, non-outlier maximum and minimum).

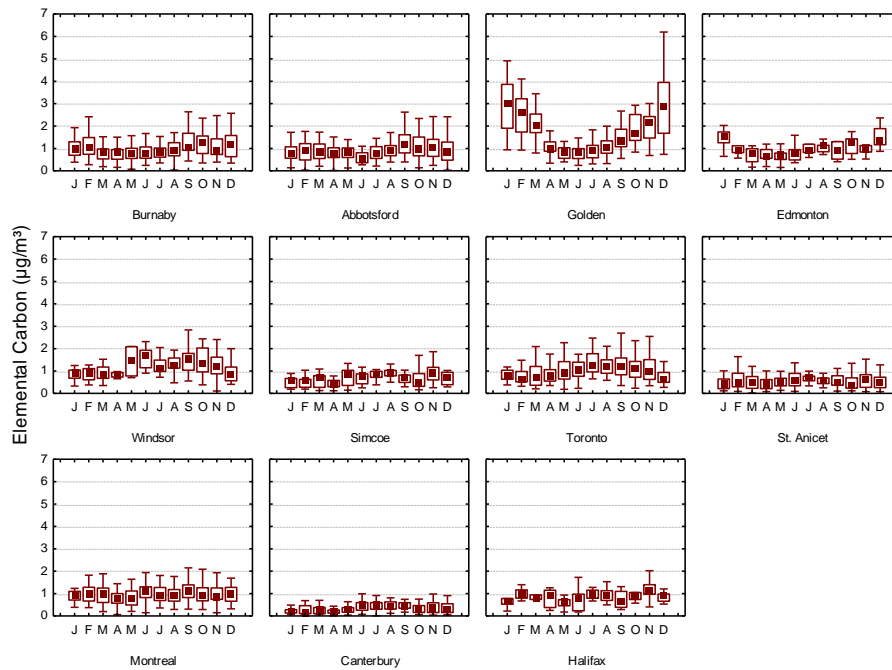


Figure 3.58 Comparison of elemental carbon ($\mu\text{g m}^{-3}$) by site and month (median, 25th and 75th percentile, non-outlier maximum and minimum).

In Figures 3.57 and 3.58 organic matter (OM) and elemental carbon (EC) results are shown by month and site. OM was calculated from blank corrected OC data by multiplying by a factor of 1.6 for urban sites and 1.8 at rural sites to adjust for the molecular form of the carbon species. The highest median OM concentration of $6 \mu\text{g m}^{-3}$ was measured at Golden and the lowest at Canterbury ($1.4 \mu\text{g m}^{-3}$). The other urban sites had median OM concentrations in the range of 2.4 to $3.3 \mu\text{g m}^{-3}$ and 75th percentile values in the range of 3.5 to $4.8 \mu\text{g m}^{-3}$. OM showed the largest seasonal cycle in Golden with winter-time maxima due to wood combustion influences. The other western sites also experienced higher mean values in winter while many of the eastern sites showed higher mid-summer values which may be associated with secondary production of organic carbon. The measured median EC concentration was also highest in Golden with a value of $1.4 \mu\text{g m}^{-3}$. Medians at the other urban sites ranged from 0.8 to $1.1 \mu\text{g m}^{-3}$ and medians at the rural sites ranged from 0.3 to $0.7 \mu\text{g m}^{-3}$. The seasonal patterns in EC were similar to those for OM with the western sites showing higher winter monthly medians and most of the eastern sites higher summertime values.

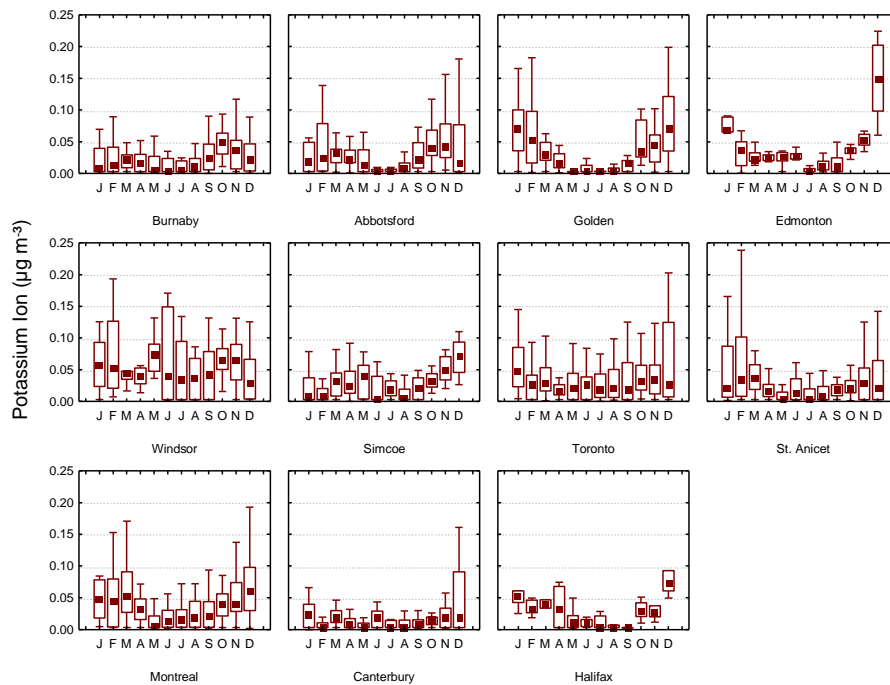


Figure 3.59 Comparison of potassium ion concentrations ($\mu\text{g m}^{-3}$) by site and month (median, 25th and 75th percentile, non-outlier maximum and minimum).

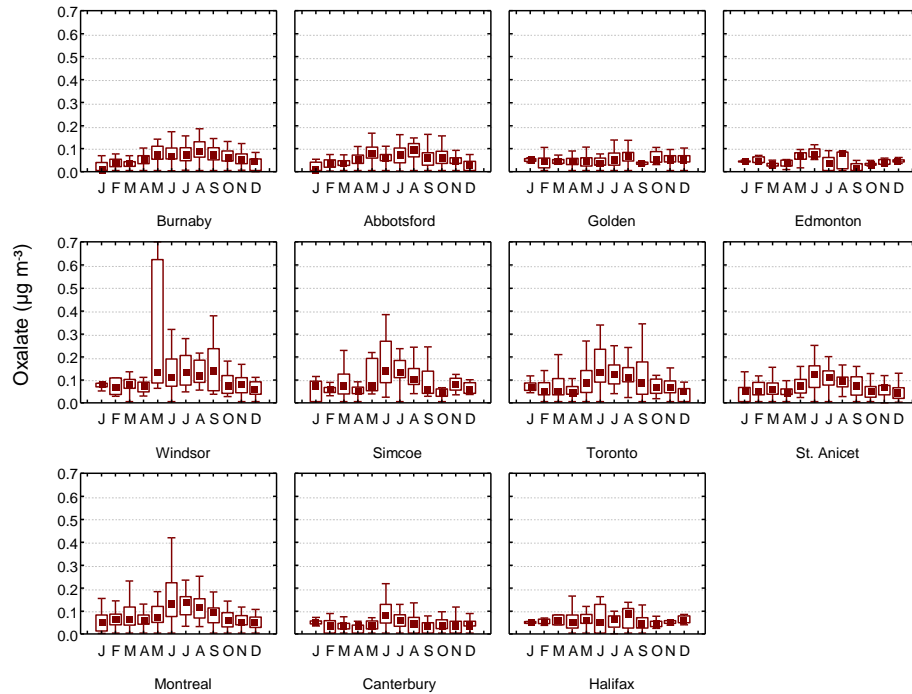


Figure 3.60 Comparison of oxalate ion concentrations ($\mu\text{g m}^{-3}$) by site and month (median, 25th and 75th percentile, non-outlier maximum and minimum).

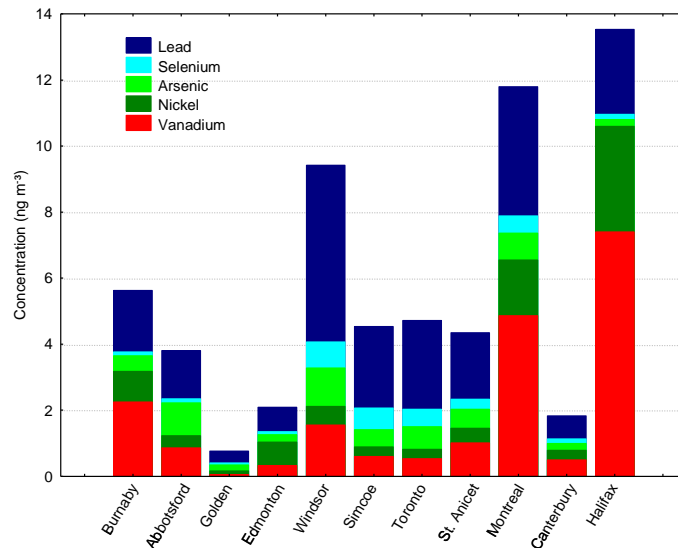


Figure 3.61 Results for five major metal species (arsenic, vanadium, nickel, selenium, lead) by site (2003 – 2006).

Besides sulphate, nitrate and ammonium, an additional 18 organic and inorganic ions are measured on the Teflon filter from Module C. Results for potassium ion are shown in Figure 3.59 and results for oxalate are shown in Figure 3.60. Potassium ion is a useful tracer of wood smoke and oxalate is associated with secondary aerosol formation in aged air masses. Over 17

water-soluble metals are available at very low detection levels by ICP-MS. Results for 5 major metal species (arsenic, vanadium, nickel, selenium) results by site are shown in Figure 3.61. Vanadium was highly correlated with nickel at all the sites ($r = 0.957$) and either element is a good indicator of emissions from heavy fuel oil combustion. Halifax recorded the highest levels of nickel and vanadium with higher than average values also measured in Montreal, Windsor and Burnaby. Total metal levels at the Toronto site were very similar to those measured at the two eastern rural sites of Simcoe and St. Anicet.

3.5.2.2 Mass Reconstruction

Mass reconstruction refers to the process of estimating the major components of PM mass (i.e., salt, soil, elemental carbon, organic carbon, NH_4NO_3 and $(\text{NH}_4)_2\text{SO}_4$), from the measured individual chemical species and estimating the total mass of the reconstructed components for comparison against the actual measured PM mass values. In theory, reconstructed mass will equal measured mass when all possible aerosol species are measured (i.e., none are missing) and all individual species measurements are highly accurate. In practice, reconstructed mass is often less than the measured mass as a result of: (1) some species not being analyzed, (2) volatilization of labile species (e.g., organics and NH_4NO_3), and (3) measurement inaccuracies. A similar process can be used to estimate light extinction and hence visibility from the particle speciation data as discussed in Chapter 10.

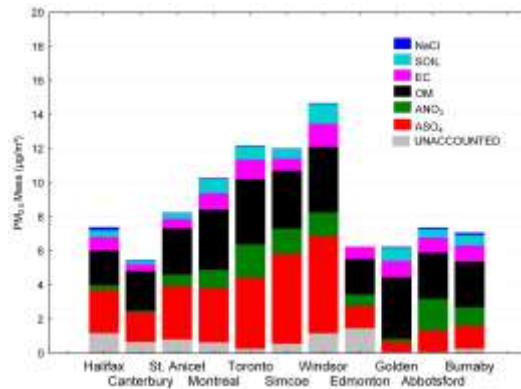


Figure 3.62 Reconstruction of total PM_{2.5} mass for all sampling days in the warm season (2003 – 2006).

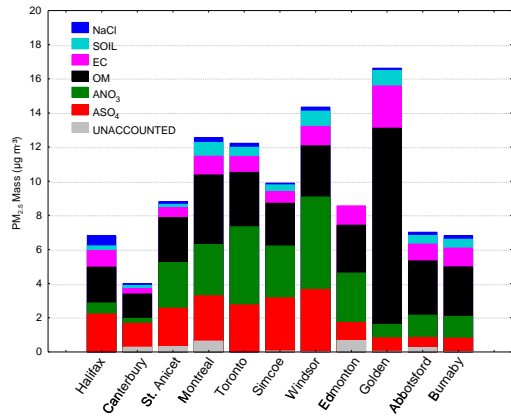


Figure 3.63 Reconstruction of total PM_{2.5} mass for all sampling days in the cold season (2003 – 2006).

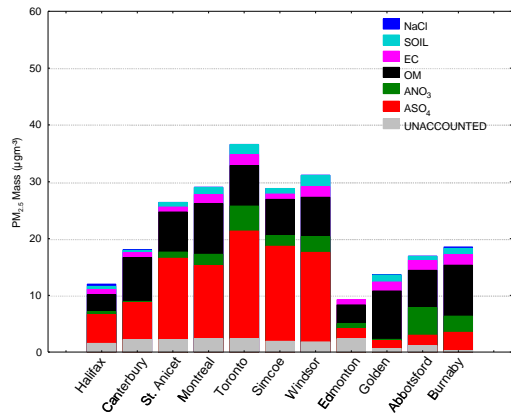


Figure 3.64 Reconstruction of total PM_{2.5} mass for 10 highest days in warm season (2003 – 2006).

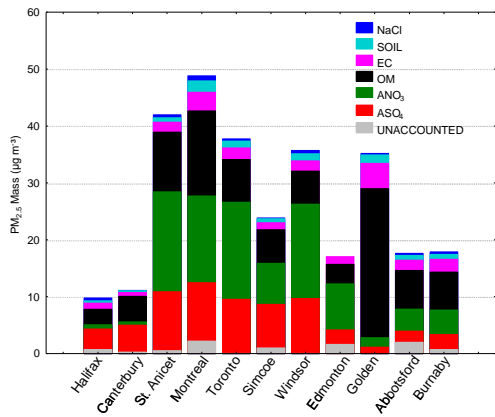


Figure 3.65 Reconstruction of total PM_{2.5} mass for 10 highest days in cold season (2003 – 2006).

Reconstruction of $PM_{2.5}$ mass was attempted for all the NAPS sites using standard procedures (Environment Canada, 2005a). Results are provided in Figures 3.62 to 3.65 for the warm (April to September) and cold (October to March) season for all samples and for the 10 days with the highest measured $PM_{2.5}$ mass in each season. On average the mass reconstruction method accounted for the majority of mass but there were significant day to day variations in mass closure. The number of days of data available for each site that were used in the charts is provided in Table 3.16. The calculated contributions were based on ammonium sulphate ($(NH_4)_2SO_4$), ammonium nitrate (NH_4NO_3), organic material (OM), elemental carbon (EC), crustal material and other oxidized metals (SOIL) and sodium chloride (NaCl). Combined secondary $(NH_4)_2SO_4$ and NH_4NO_3 on average accounted for 38 to 50% of total $PM_{2.5}$ mass at the eastern sites during the summer and 42 to 63% in the winter. For the western sites (excluding Golden) $(NH_4)_2SO_4$ and NH_4NO_3 accounted for 31 to 42% of mass in summer and 27 to 44% in winter. For the Golden site, $(NH_4)_2SO_4$ and NH_4NO_3 accounted for 12% and 10% of mass in summer and winter, respectively. Organic matter was the next most important contributor to mass. Excluding Golden, OM contributions to $PM_{2.5}$ mass for urban and rural sites ranged from 26 to 42% in summer and 21 to 45% in winter. For Golden OM accounted for 70% of mass in winter and 60% in summer. For the highest days in summer, $PM_{2.5}$ mass at eastern sites was primarily composed of $(NH_4)_2SO_4$ and OM (70 to 80%) while at the western sites other than Golden NH_4NO_3 was also an important contributor. For the highest concentration days in winter NH_4NO_3 and OM were the primary contributors to mass at almost all the sites but $(NH_4)_2SO_4$ was also an important contributor at the eastern sites and in particular in Halifax.

3.5.3 PM_{2.5} Precursors

3.5.3.1 Sulphur Dioxide and Ammonia

3.5.3.1.1 Concentrations and Seasonal Variation

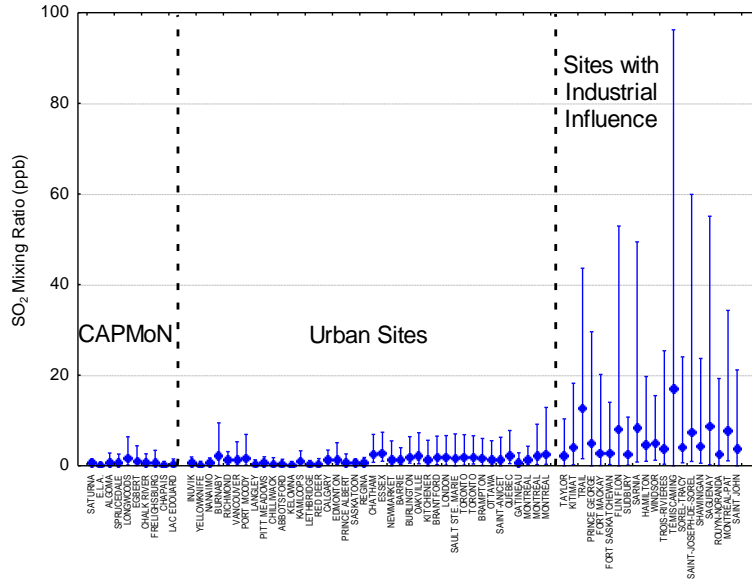


Figure 3.66 Mean, 10th and 98th percentile of daily-average SO₂ concentrations for all sites reporting valid annual means in 2006.

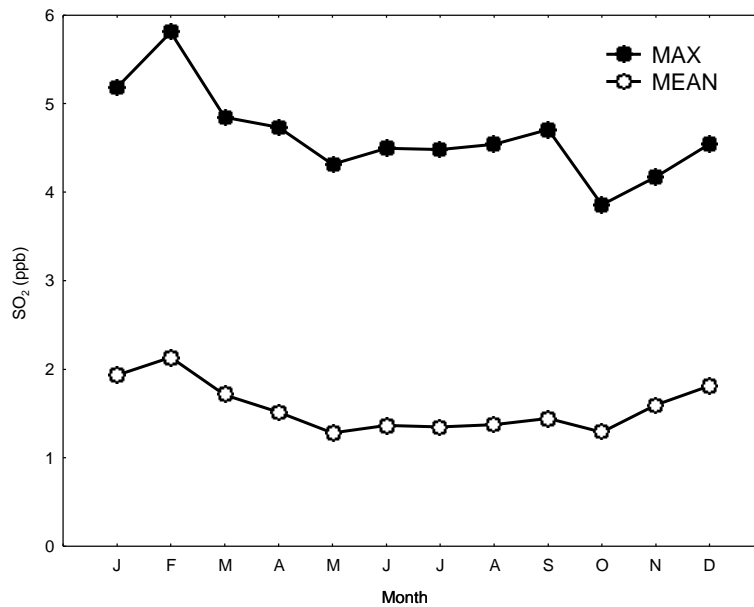


Figure 3.67 Monthly mean and monthly mean daily maximum SO₂ concentrations (ppb) for urban sites with no local point sources.

The major PM_{2.5} precursors include NO_x, VOCs (both covered in Section 3.4), sulphur dioxide (SO₂) and ammonia (NH₃). Figure 3.66 shows mean, 10th and 98th percentile of 24-hr SO₂ concentrations for all NAPS and CAPMoN sites reporting valid annual means in 2006. From the diagram, it can be seen that the highest average and 98th percentile SO₂ concentrations were generally measured at sites with nearby point sources (usually non-ferrous smelters), with the highest mean concentration being approximately 18 ppb at Temiscaming, Quebec. The lowest mean and 98th percentile concentrations were found at western and northern sites with no nearby industrial emissions. The Egbert and Longwoods CAPMoN sites located in Ontario had higher mean and 98th percentile SO₂ levels than a number of the western urban sites. As will be discussed in Section 3.5.4.2, rural sites in south-western Ontario exhibit higher SO₂ concentrations than some of the urban centres in western Canada. This is undoubtedly due to the higher emissions of SO₂ in the general area of those sites. Western sites with relatively high concentrations include Trail, Fort Mackay and Flin Flon. Figure 3.67 shows monthly mean and monthly mean daily maximum SO₂ concentrations for urban sites with no local point sources. Ambient SO₂ concentrations across Canada exhibit a seasonal cycle with higher urban SO₂ concentrations in the winter than in the summer.

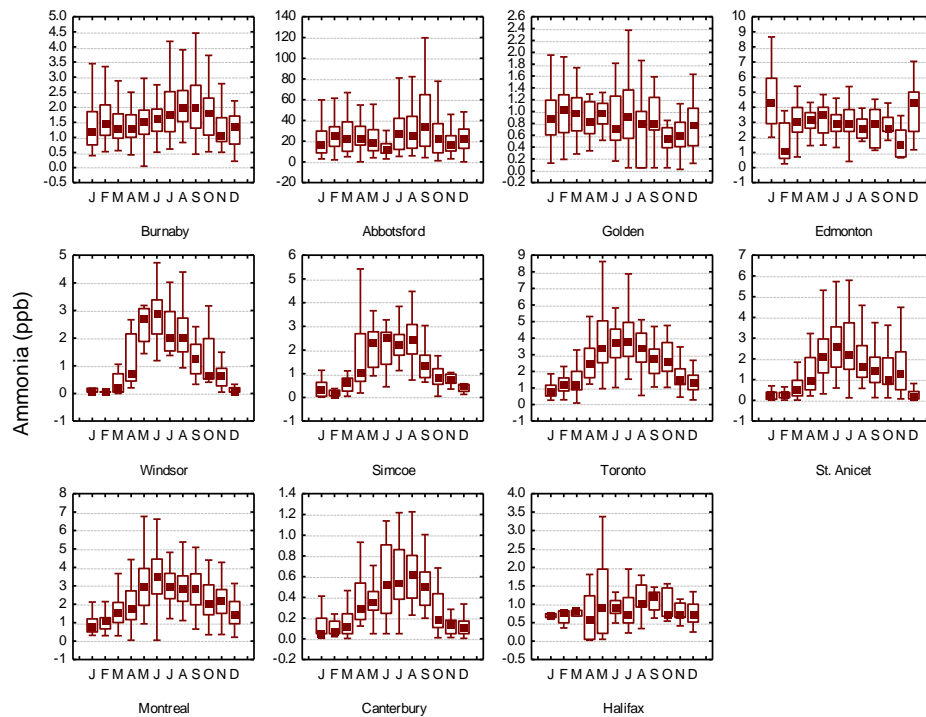


Figure 3.68 Ammonia concentrations (ppb) by month from the NAPS speciation network (median, 25th and 75th percentile, non-outlier maximum and minimum).

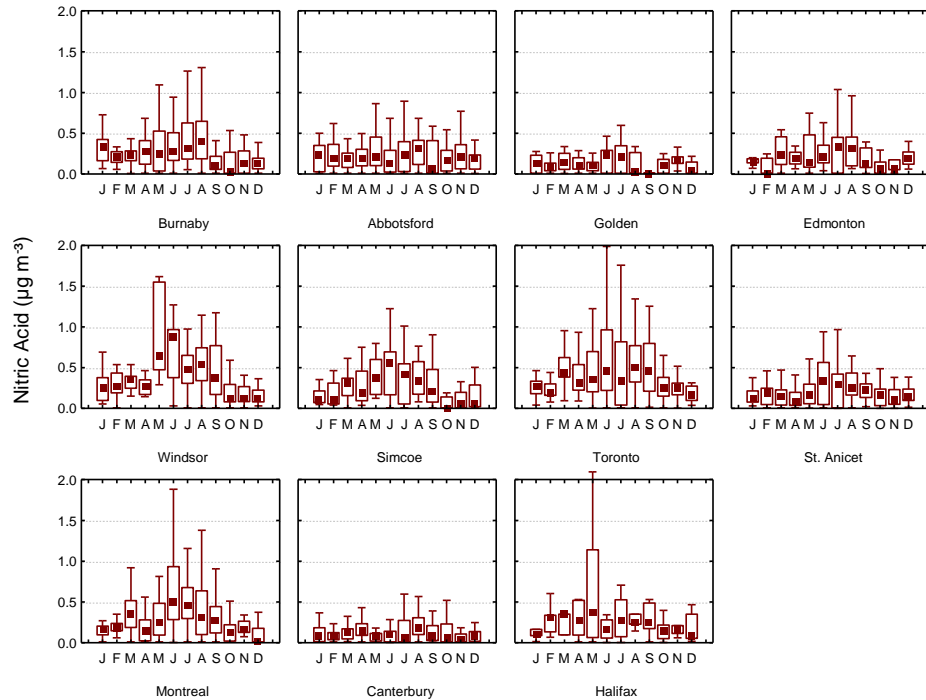


Figure 3.69 Nitric acid concentrations ($\mu\text{g m}^{-3}$) by month from the NAPS speciation network (median, 25th and 75th percentile, non-outlier maximum and minimum).

NH_3 concentrations (ppb) by month from the speciation network are shown in Figure 3.68. The graph uses independent scales since values at the Abbotsford site are much higher than any of the other locations. Median NH_3 levels at Abbotsford were 20 ppb with other sites ranging between 0.3 ppb (Canterbury) and 2.9 ppb (Edmonton). The eastern sites show a strong seasonal cycle in NH_3 with maxima in the summer months and very low values in the winter. The western sites show much less variability between months. Nitric acid concentrations from the speciation sites are shown in Figure 3.69. Summer median nitric acid concentrations were low at all sites ranging from $0.1 \mu\text{g m}^{-3}$ at Canterbury and Golden to $0.5 \mu\text{g m}^{-3}$ at Toronto and Windsor. At the sites with the highest concentrations a seasonal cycle with maxima in June and July is apparent.

3.5.3.1.2 Linear and Non-linear Interactions of Ammonia, Nitrate and Sulphate

The interactions between ammonia, nitrate and sulphate play an important role in determining the mass of $\text{PM}_{2.5}$ in the atmosphere. This section explores the potential sensitivity of $\text{PM}_{2.5}$ mass to reductions in ambient sulphate, nitrate and ammonia levels in various parts of the country using the gas ratio (GR) method (Ansari and Pandis, 1998).

In addition to NO_x emissions, formation of particulate nitrate (p-NO_3^-) requires NH_3 . While lower NH_3 levels can potentially reduce p-NO_3^- , changes in p-NO_3^- will also depend upon the ambient levels of NH_3 and sulphate (SO_4^{2-}). In areas or specific situations where p-NO_3^- is

present and there is very little NH_3 available, reduced concentrations of NH_3 could potentially lead to less p-NO_3^- . Conversely, if the NH_3 concentrations are high and in excess of the amount of SO_4^{2-} and HNO_3 in the ambient air, then reductions in NH_3 may have no effect on the p-NO_3^- present. Interestingly, the amount of sulphate in the ambient air can also influence the concentration of p-NO_3^- .

The interactions between the different precursors imply that $\text{PM}_{2.5}$ mass can respond non-linearly and even negatively (i.e. $\text{PM}_{2.5}$ increases when SO_4^{2-} is decreased) to changes in SO_4^{2-} and/or NH_3 . The gas ratio, GR, of total “free ammonia” to total nitrate (HNO_3T) (Ansari and Pandis, 1998) can be used to estimate the potential inorganic $\text{PM}_{2.5}$ response to SO_4^{2-} and NH_3 changes.

$$\text{GR} = \text{NH}_3^{\text{F}} / \text{HNO}_3^{\text{T}}$$

where,

$$\text{Free ammonia: } \text{NH}_3^{\text{F}} = \text{NH}_3(\text{g}) + \text{NH}_4^+ - (2 \times [\text{SO}_4^{2-}])$$

$$\text{Total nitrate: } \text{HNO}_3^{\text{T}} = \text{HNO}_3(\text{g}) + \text{p-NO}_3^-$$

The measurements of HNO_3 , p-NO_3^- , NH_3 , SO_4^{2-} and NH_4^+ needed to calculate GR are all available from the NAPS and CAPMoN speciation sampling sites (see Table 3.16). Weekly samples were also obtained at the two rural sites of Chalk River and Longwoods as part of the Southern Ontario Ammonia Passive Sampler Survey (SOAPSS). Criteria for classifying GR values were developed from figures in Ansari and Pandis (1998) and adapted in the Precursor Contributions to Ambient Fine Particulate Matter in Canada report (Environment Canada, 2001). Shown in Table 3.17 and 3.18 are the classification criteria used for analyzing the $\text{PM}_{2.5}$ response to SO_4^{2-} and NH_3 , respectively.

Results were classified by site and season as shown in Table 3.19. In general, large GR values indicate that $\text{PM}_{2.5}$ will respond linearly and as expected to decreases in SO_4^{2-} . The results in Table 3.19 show that during the warm months (April 15 – October 14), $\text{PM}_{2.5}$ mass response to changes in SO_4^{2-} at sites across Canada, regardless of the type of site, will be linear and positive with a small percentage of sampling days corresponding to acidic conditions (i.e., when $\text{GR} < 0$ indicating that PM contains more SO_4^{2-} than $\text{NH}_3(\text{g}) + \text{NH}_4^+$). Exceptions are the two rural coastal locations of Saturna (BC) and Kejimikujik (NS) which exhibit linear positive responses and a high percentage of sampling days with acidic PM, i.e., over 40% of the sampling days. The situation is considerably different in the colder months (October 15 – April 14). The greatest potential for non-linear, and in some cases negatively linear, responses to SO_4^{2-} changes occurred for 25 to 75% of the days at the eastern sites, southern Ontario in particular. The greatest potential for conditions conducive to a negative linear response was found in three locations. Two sites are located in southern Ontario: Simcoe (rural) and Windsor (urban) and the other in Alberta: Edmonton (urban). For about 2% of the cold season sampling days these sites fall into the negative linear response category, which means that there could

actually be increases in $PM_{2.5}$ through reductions in SO_4^{2-} . Thus, strategies to reduce $PM_{2.5}$ may need to be different depending upon season and careful examination of the situation through more ambient measurements and detailed modelling studies.

The GR value can also be used to estimate how $PM_{2.5}$ may respond to changes in NH_3 concentrations. A large GR value ($GR \gg 1$) implies that there is excess NH_3 and $p-NO_3^-$ formation that is not limited by NH_3 availability. Thus, a change in NH_3 emissions will have limited impact on the $PM_{2.5}$ mass concentration (not sensitive). When the GR value is small, there is a shortage of NH_3 and further reductions in NH_3 will strongly affect the potential for $p-NO_3^-$ to form (linear and very sensitive). The sensitivity of NH_4NO_3 formation to NH_3 is shown in Table 3.20. As shown in the Table and in contrast to $PM_{2.5}$ mass sensitivity to SO_4^{2-} changes, there is less consistency among sites for NH_3 potentially due to its localized nature. During the warm months (April 15 – October 14), there were no days, regardless of site, that were very sensitive to NH_3 changes. In general, more eastern sites and urban sites tended to be non-sensitive to NH_3 concentrations, likely due to higher ambient NH_3 concentrations. In fact, the $PM_{2.5}$ concentrations would be expected to be more sensitive to sulphate and/or nitrate concentrations in urban areas or downwind of emission sources (Table 3.19). In the colder months (October 15 – April 14), Simcoe and Windsor were the two urban locations with the greatest potential for $PM_{2.5}$ to show some response to NH_3 changes. One point of interest from Table 3.20 is that in most urban areas and throughout the year there is high probability that NH_3 changes may not affect $PM_{2.5}$ mass concentration.

It is important to point out the assumptions and potential problems (Ansari and Pandis, 1998) with the GR classification criteria before complete interpretations can be made. At equilibrium, the reaction of NH_3 and H_2SO_4 favours the formation of $(NH_4)_2SO_4$ which is largely irreversible. However, there are reasons to believe that the gas-aerosol system at any given site is not in equilibrium, particularly when there are NH_3 emissions at the site. It is difficult to test the assumption that gas phase NH_3 is in equilibrium with sulphate aerosol; however, as pointed out by Meng and Seinfeld (1996), local gas-aerosol equilibrium requires that the equilibrium time scale be short relative to the time scale on which volatile species and aerosol concentrations are changing within an air mass. Further details on the relationship between reaction rate and degree of neutralization can be found in the study by Walker *et al.* (2004).

To summarize, there are two important factors determining the sensitivity of the inorganic $PM_{2.5}$ mass to NH_3 concentrations: 1) whether NH_3 is the limiting species in the equilibrium with HNO_3 and 2) the relative percent mass contribution of NH_3 to the total inorganic $PM_{2.5}$ mass. A preliminary conclusion is that the greatest $PM_{2.5}$ reductions could be achieved by: (1) reducing SO_2 emissions during the warm season, (2) reducing NO_x emissions during the cold season and (3) reducing NH_3 emissions in the cold season in areas where SO_4^{2-} concentrations are low and PM sensitivity to changing NH_3 levels can be demonstrated.

A further assessment of the sensitivity of Canadian PM levels to agricultural ammonia emissions was published by Environment Canada as part of the National Agri-Environmental Standards Initiative (Environment Canada, 2009). The major results taken directly from the 2008 Canadian Atmospheric Assessment of Agricultural Ammonia (Environment Canada, 2009) are presented below. The Assessment focused on six agriculturally intensive areas of Canada: the Lower Fraser Valley (LFV) of British Columbia, southern Alberta, southern Manitoba, south-western Ontario, south-western Quebec and the Maritimes. Short-term monitoring studies were set up in southern Ontario, the southern Prairies and the LFV to monitor NH_3 emissions. The results showed that areas of high NH_3 emissions and ambient NH_3 concentrations do not necessarily always correspond to the areas of highest PM concentrations. For example, highest NH_3 levels are found in British Columbia, but areas of highest $\text{PM}_{2.5}$ concentrations are in south-western Ontario and southern Quebec. This suggests that PM levels are, in part, influenced by the long-range transport of ambient NH_3 and NH_4^+ particles, especially in the low ammonia emission areas of eastern Canada. Long-range transport appears to be less important in western Canada where modelling studies showed that much of the ammonia-related PM can be traced to local area sources.

Modelling was also used to assess the sensitivity of ambient PM levels to changes in NH_3 emissions. The major findings are summarized as follows:

- Agriculture is the major source of NH_3 emissions in the Lower Fraser Valley, southern Alberta, southern Manitoba, south-western Ontario, south-western Quebec and the Maritimes
- Areas of highest NH_3 emissions are not necessarily areas of highest ambient particle- NH_4^+ concentrations and vice versa. This means that particle- NH_4^+ can be advected by long-range transport to areas of low ammonia emissions, particularly in eastern Canada.
- Of the six agriculturally-intensive areas identified for intensive study, ambient PM levels in five are not sensitive to a 30% reduction in NH_3 emissions (median hourly PM concentration decrease of 0 to 4%)
- Ambient PM levels in the remaining region (south-western Ontario) are only slightly sensitive to a 30% reduction in NH_3 emissions (median hourly PM concentration decrease of 7.5%)
- Very large reductions in NH_3 emissions (>30%) would be needed in the five insensitive, NH_3 -saturated regions to arrive at a point where p- NH_4^+ levels would be sensitive to further emission reductions.
- The NH_3 -poor region of the Maritimes is generally insensitive to reductions in ambient NH_3 emissions
- Areas located downwind of the agriculturally-intense areas are more sensitive to NH_3 emission reductions, but these are generally areas with large monitoring gaps and lower population density.

In light of decreasing SO_x and NO_x emissions in various areas of North America, NH_3 concentration will become more important to total $\text{PM}_{2.5}$, raising a series of questions: Will emission reductions for NH_3 be effective in reducing $\text{PM}_{2.5}$ concentration? If so, starting from which areas and which season will give the most effective result? Knowing different sensitivity regimes across the continent is an important first step to understanding $\text{PM}_{2.5}$ response, but the temporal changes of these regimes will play an important role in the effectiveness of NH_3 reduction as a result of best agricultural practices. Use of modelling results will provide the spatial extent of different sensitivity regimes as well as an understanding of the interrelationship among the many PM constituents that are not being measured. Therefore, conducting more detailed analysis of model performance is of primary importance.

3.5.4 Trends in $\text{PM}_{2.5}$, Constituents and Precursors

3.5.4.1 Urban Sites

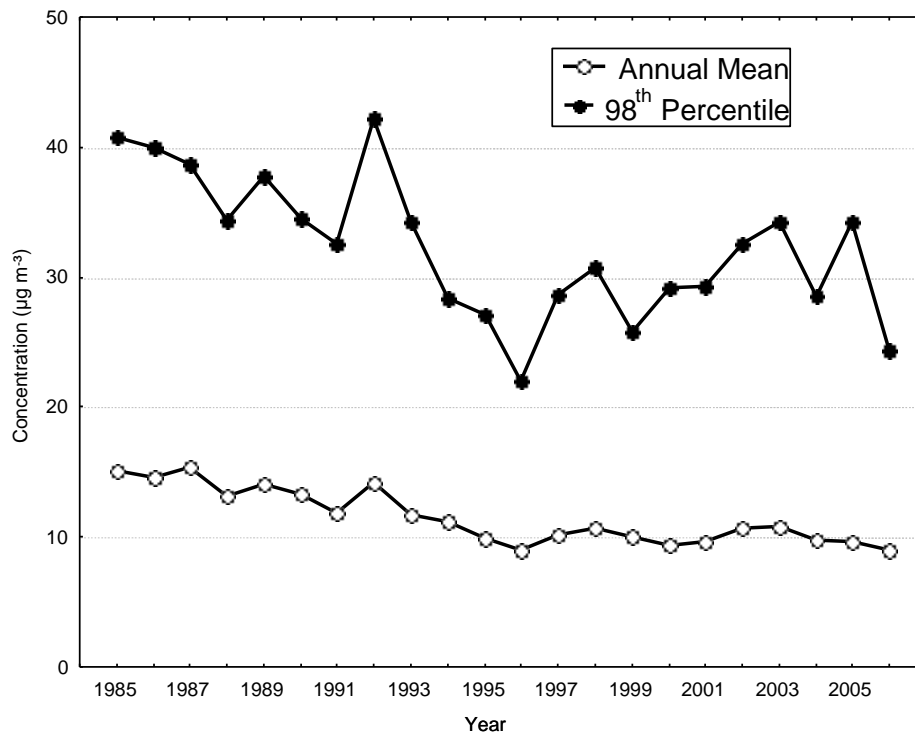


Figure 3.70 Long-term trend in composite annual mean and 98th percentile $\text{PM}_{2.5}$ mass from dichotomous sampler urban sites for the period 1985 to 2006.

The long term trend in annual mean and 98th percentile $\text{PM}_{2.5}$ mass from the dichotomous sampler sites is presented in Figure 3.70. Only cities with operational sites in at least 75% of the years were included. This amounted to an average of 14 sites in 11 cities. Composite

annual mean $PM_{2.5}$ concentrations decreased by 40% from 1985 to 1996, increased from 1996 to 2003 and have shown a downward trend since. Composite 98th percentile values show much more year-to-year variability but have also followed a similar pattern. The overall decrease in composite annual mean and 98th percentile $PM_{2.5}$ concentrations was 40%.

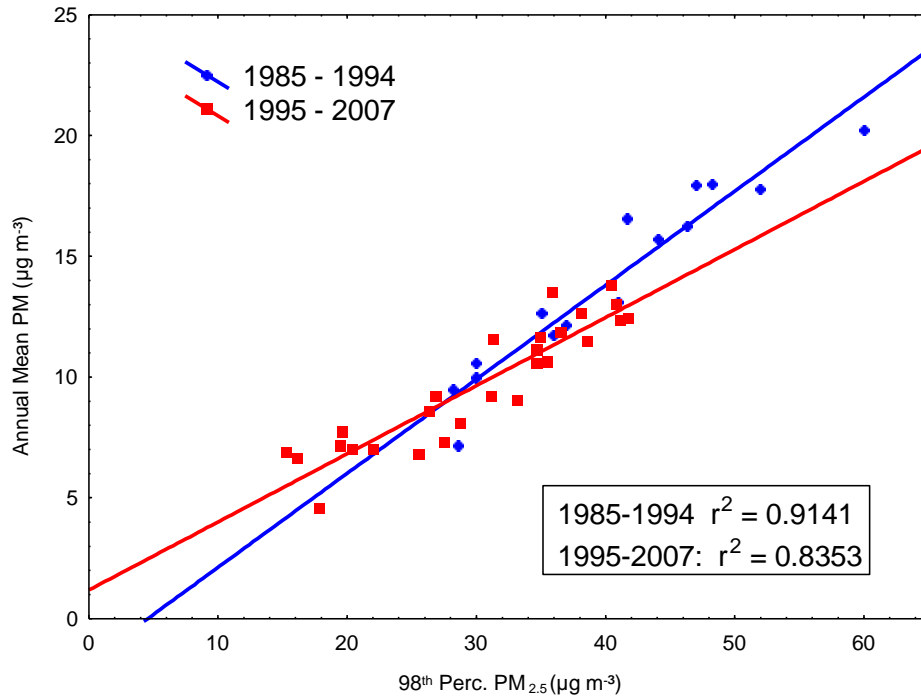


Figure 3.71 Relationship between annual mean and 98th percentile $PM_{2.5}$ mass from dichotomous sampler urban sites (1985-1994 vs. 1995-2007).

Unlike the United States, Canada does not have an air quality standard for $PM_{2.5}$ based on an annual mean. However, there is generally good correspondence between standards based on different averaging times as shown in Figure 3.71, in which the relationship between annual mean and 98th percentile $PM_{2.5}$ mass is compared for two time periods, 1985 to 1994 and 1995 to 2007. Although the two measures are highly correlated in both time periods, it is clear that the slope of the relationship has become smaller suggesting that peaks are being reduced more quickly than the mean.

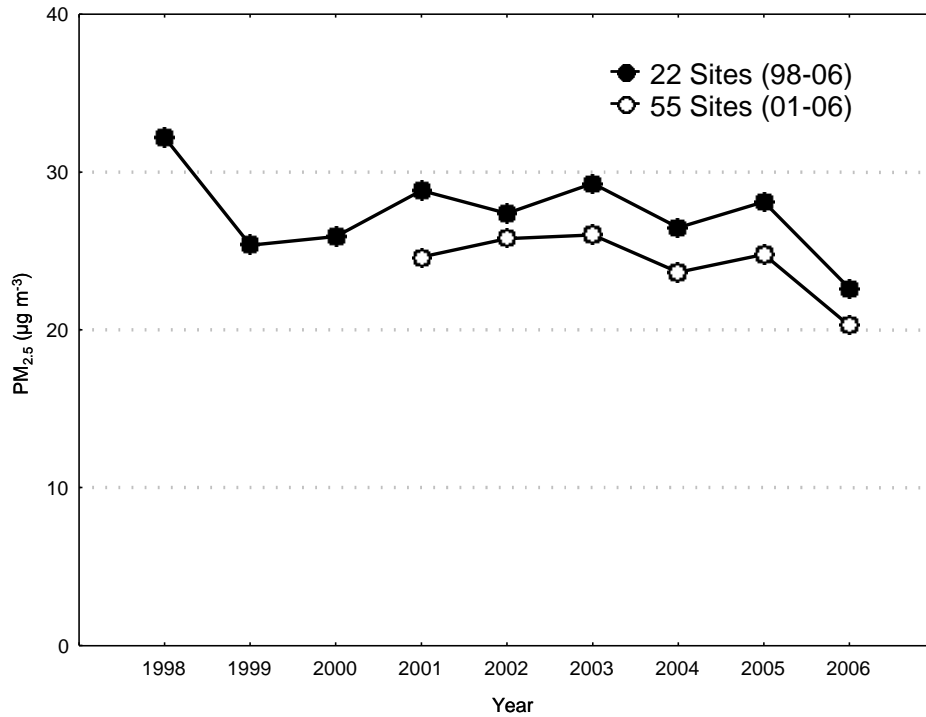


Figure 3.72 Trend in 98th percentile PM_{2.5} mass from TEOM sites.

The length of the PM_{2.5} mass data record from the TEOM sites is much more limited, but for the 1998 to 2006 period, 22 sites had 75% data completeness and for the 2001 to 2006 period, a total of 55 sites had complete data. The composite 98th percentile values are shown in Figure 3.72 for the two groups of sites. Values showed little change over the 1999 to 2005 time period but a reduction in concentration was seen in 2006 vs. the other years.

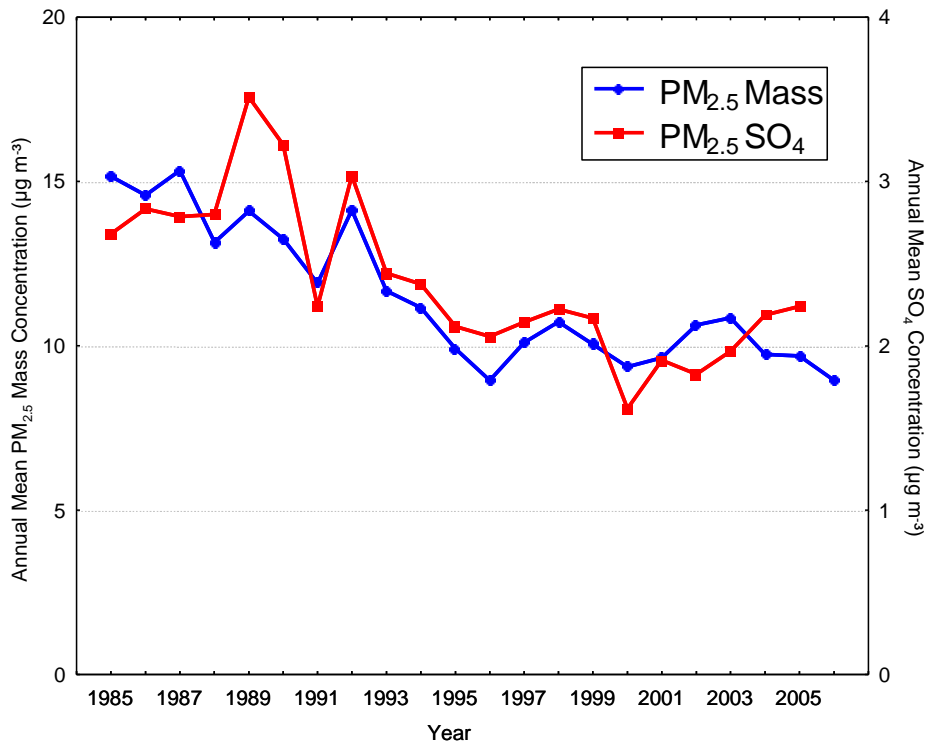


Figure 3.73 Trend in composite annual mean PM_{2.5} mass and p-sulphate concentrations from dichotomous sampler sites.

In Figure 3.73 annual mean p-SO₄²⁻ concentrations are compared with annual mean PM_{2.5} mass concentrations for the period 1986 to 2005. The two values track each other very well. Sulphate comprised on average 20% of PM_{2.5} mass and its proportion did not change over the time period.

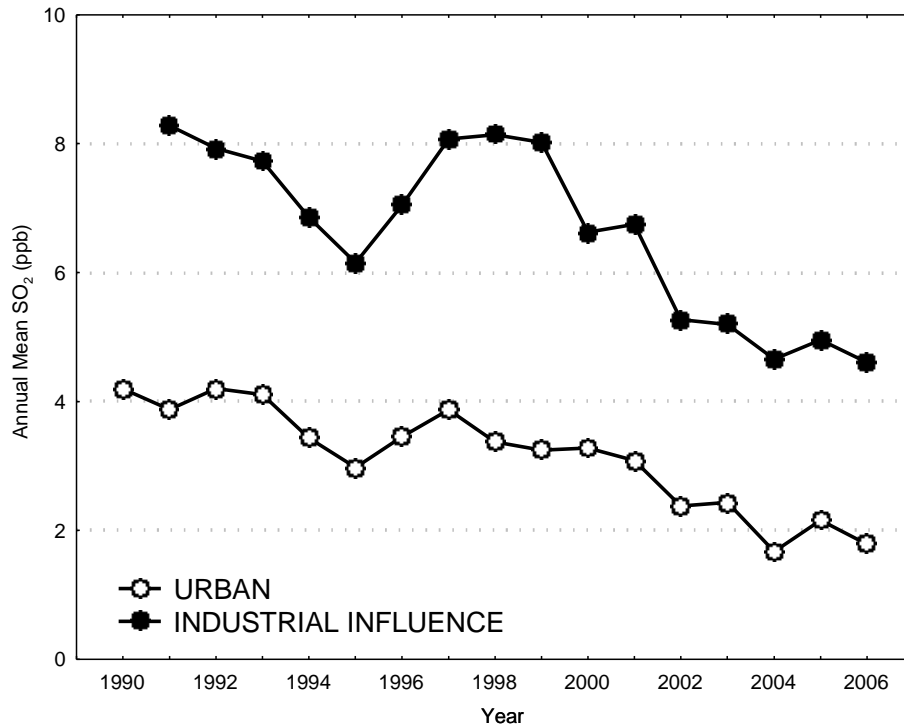


Figure 3.74 Trend in composite annual mean SO₂ concentrations (ppb) at urban and industrial-influence sites.

In Figure 3.74 annual mean SO₂ trends are shown for 12 urban and 9 industrial influence sites (with complete data records for the period) for the 1990 to 2006 time period. Composite annual mean SO₂ concentrations decreased by approximately 60% at both groups of sites.

3.5.4.2 Rural/Remote Sites

The lack of long-term PM_{2.5} mass data at rural/remote monitoring sites in Canada precludes any analyses of long-term trends for PM_{2.5} mass. However, long-term filter pack data collected at rural/remote of the CAPMoN network has made it possible to investigate long term trends of selected PM_{2.5} precursors, namely, SO₂ and HNO₃, and several major constituents of PM_{2.5}, namely, p-SO₄²⁻, p-NO₃⁻ and p-NH₄⁺. As shown in Figures 3.62 and 3.63, p-NH₄⁺, p-SO₄²⁻ and p-NO₃⁻ contribute, on average, about 50% of fine PM mass in eastern Canada and about 30% in western Canada. Since: (1) ammonium sulphate ((NH₄)₂SO₄) and ammonium nitrate (NH₄NO₃) are secondary aerosol products of SO₂ and NO_x emissions and (2) SO₂ and NO_x emissions have decreased in eastern North America over the past 15 years, we investigate in this section whether ambient concentrations of p-NH₄⁺, p-SO₄²⁻ and p-NO₃⁻ have decreased in concert with decreasing emissions. This is done by assessing the long term trends of these species as well as SO₂ and HNO₃. Unfortunately, the analysis could only be done for eastern

Canada (EC) and the northern portion of the eastern USA (EUS) since these are the only areas with sufficient numbers of long-term monitoring sites to draw regionally representative conclusions.

It is important to note that ambient PM_{2.5} concentrations in eastern Canada are attributable both to eastern Canadian emissions and the long range transport of precursor gases (SO₂ and NO_x) and their associated secondary aerosols (H₂SO₄, (NH₄)₂SO₄ and NH₄NO₃) from eastern U.S. (Dennis *et al.*, 1990; Olson *et al.*, 1983; Olson and Oikawa, 1989; Fay *et al.*, 1986; Vet and Ro, 2008). In light of this, trends in concentrations of PM_{2.5} and its constituents must be considered in the context of changing precursor emissions in EC and the EUS. Since annual SO₂ and NO_x emissions data for EC and EUS from the early 1990s to the mid-2000s were difficult to acquire, we found it necessary to use and present only the emissions data that were available and suitable for this analysis, specifically for two regions of EC and one region of the EUS. As will be seen in the following discussion, this had the effect of limiting the analysis to the emission-defined regions.

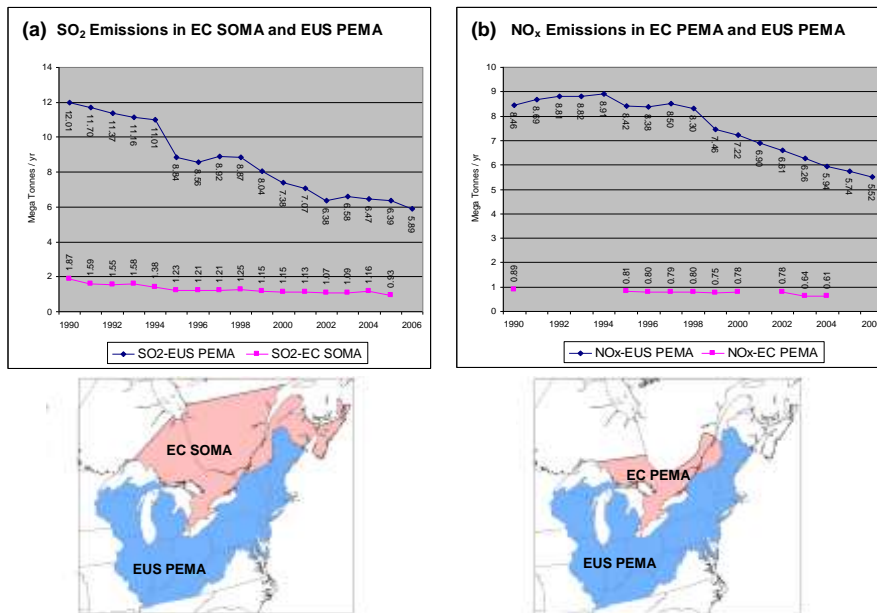


Figure 3.75 (a) Annual SO₂ emissions (MT yr⁻¹) for the Southeast Canada Sulphur Oxide Management Area (EC/SOMA) and the eastern US Pollutant Emission Management Area (EUS/PEMA) and (b) Annual NO_x emissions (MT yr⁻¹) for the Eastern Canadian Pollutant Emission Management Area (EC/PEMA) and the EUS/PEMA.

For SO₂ emissions, Figure 3.75(a) shows a time series of annual emissions for the period 1990 to 2006 for an area in the EUS known as the United States Pollution Emission Management Area or EUS PEMA (U.S. EPA, 2007) and for a region of EC called the Southeast Canada Sulphur Oxide Management Area or EC SOMA (Environment Canada, 2007). For NO_x emissions, Figure 3.75(b) shows annual emissions for the EUS PEMA (U.S. EPA, 2006a) plus a different region of EC called the Eastern Canada Pollution Emission Management Area or

EC PEMA (Environment Canada, 2007). Figure 3.75(a) shows that SO₂ emissions in the EUS PEMA decreased steadily from 1990 to 1995 (with a major drop in 1995), remained roughly unchanged from 1995 to 1998, again decreased steadily from 1999 to 2002, and remained roughly constant again from 2002 to 2006. In the EC SOMA, SO₂ emissions decreased steadily from 1990 to 1996 and remained roughly constant thereafter. Figure 3.75(b) shows that NO_x emissions in the EUS PEMA increased slightly from 1990-1994, dropped in 1995 (when SO₂ emissions also dropped dramatically), stayed roughly constant from 1995 to 1998 (similar to SO₂), and again dropped steadily from 1999 to 2006. In EC, NO_x emissions appeared to stay roughly constant from 1995 to 2002 and then decreased slightly in 2003 and 2004. No EC emissions data were available for 2001, 2005 and 2006. All emissions data were obtained from Environment Canada and the United States Environmental Protection Agency.

3.5.4.3 Long Term Regional Trends of SO₂ and p-SO₄²⁻

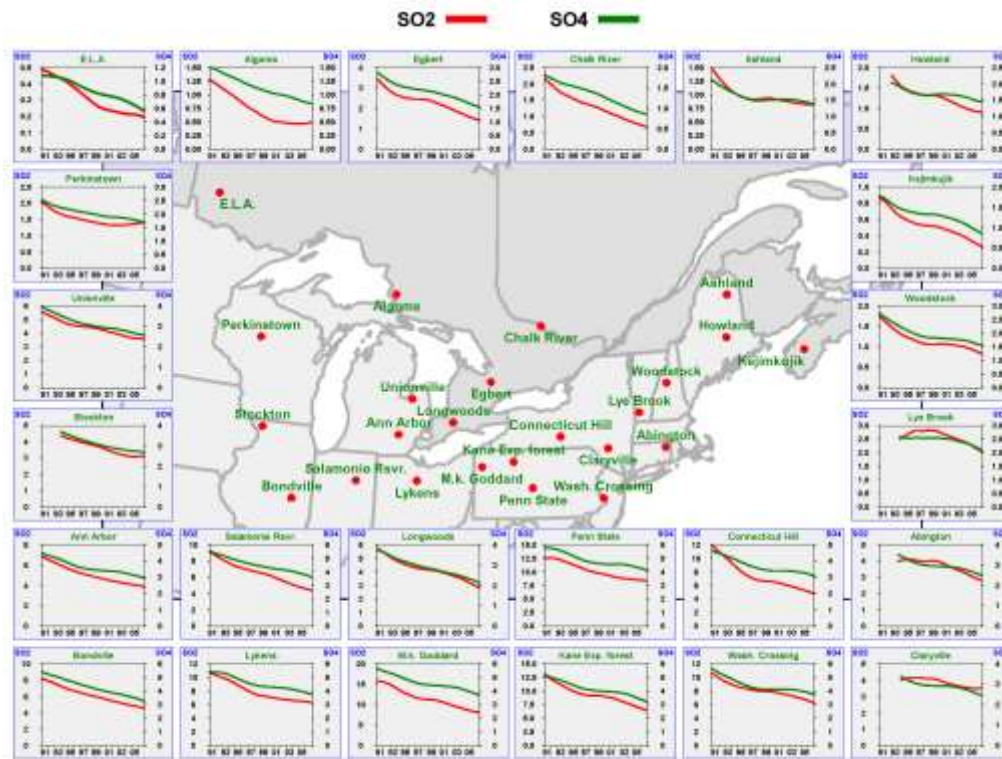


Figure 3.76 Long-term trends of SO₂ and p-SO₄²⁻ at CAPMoN and CASTNET sites (in µg m⁻³ at 0°C and 1 atmosphere).

Regionally-representative long-term trends of ambient SO₂ and p-SO₄²⁻ were assessed from data collected at rural/remote sites of the Canadian Air and Precipitation Monitoring Network (CAPMoN) and the United States Clean Air Status and Trends Network (CASTNET). The use of rural/remote sites, as opposed to urban sites, served to minimize the influence of local SO₂ sources, thereby allowing a focus on regional-scale PM. It is important to note that, although both networks measure p-SO₄²⁻ using a non-size-selective filtration technique, most p-SO₄²⁻ in

eastern North America is in the fine mode. It is therefore reasonable to assume that the $p\text{-SO}_4^{2-}$ trends presented herein represent $\text{PM}_{2.5}$ sulphate. Figure 3.76 shows the SO_2 , $p\text{-SO}_4^{2-}$, and $p\text{-NH}_4^+$ time trends at selected CAPMoN and CASTNET sites in eastern North America over the period 1991- 2006. The trend lines were created using a Kernel smoothing technique described in Sirois (1998). Although Kernel smoothing does not test for the statistical significance of trends, it is useful for illustrating long-term trends.

The trend lines in Figure 3.76 clearly show that regional-scale SO_2 and $p\text{-SO}_4^{2-}$ concentrations decreased from the early 1990s to the mid-2000s at most sites in eastern Canada and the eastern U.S. This is a reasonable indication that SO_2 emission reductions in eastern Canada and the eastern U.S. from the early 1990s to the mid-2000s were quite effective at decreasing ambient concentrations of SO_2 and $p\text{-SO}_4^{2-}$, especially in the high concentration areas of southern Ontario, southern Quebec and the northeast U.S.

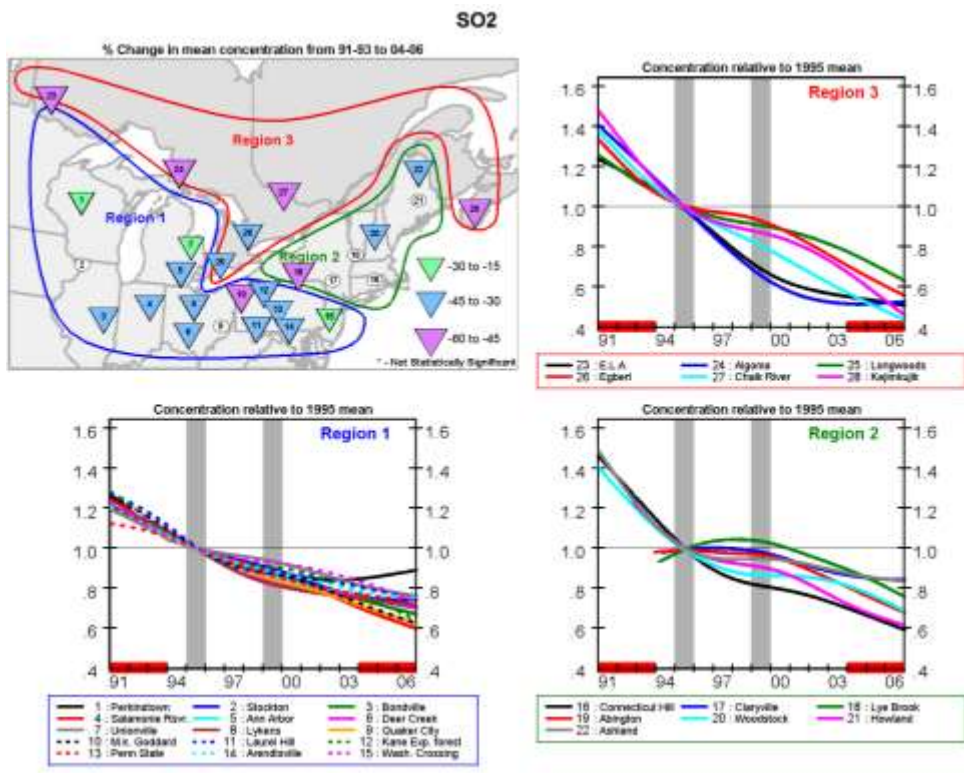


Figure 3.77 Changing SO_2 concentrations with time. The map insert shows the percent difference in 3-year-mean concentrations between two periods: 1991-1993 and 2004-2006. The downward facing triangles denote decreasing concentrations between the two periods for the corresponding numbered site. Asterisks indicate that the differences in 3-year-mean concentrations were not statistically significant. The three multiple-trends plots show the superimposed time trends for all sites in three different regions normalized to the year 1995. The vertical shaded bars in the years 1995 and 1999 show the years when largest SO_2 and NO_x emission reductions occurred in the EUS PEMA. The horizontal red bars along the x-axis illustrate the two averaging periods used for the map.

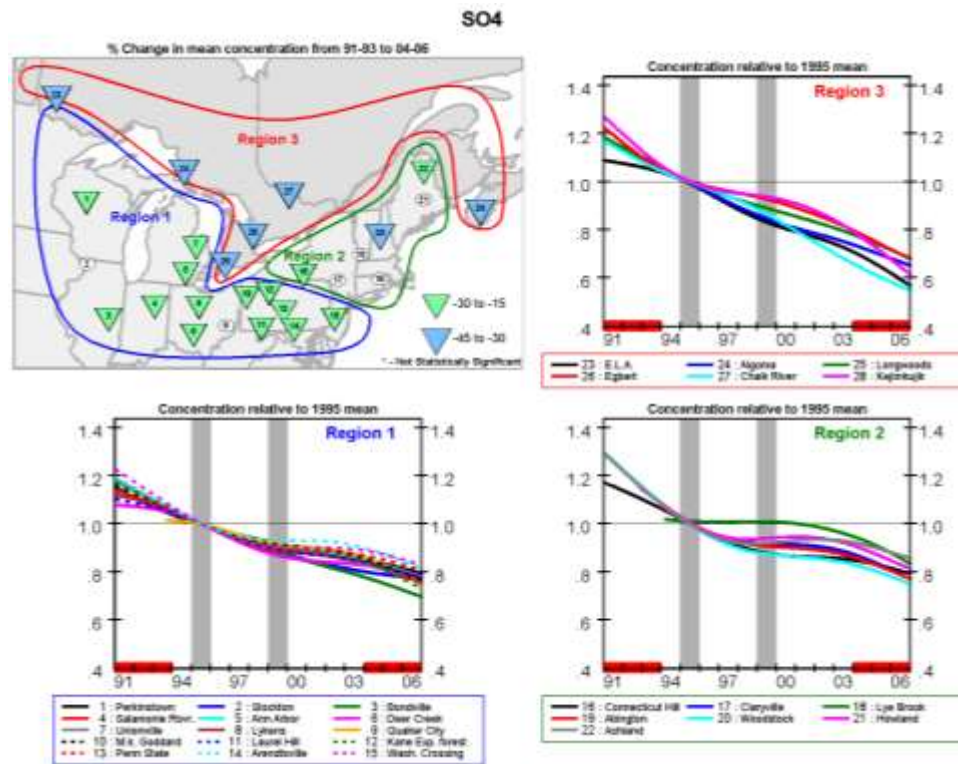


Figure 3.78 Changing $p\text{-SO}_4^{2-}$ concentrations with time. The map insert shows the percent difference in 3-year-mean concentrations between two periods: 1991-1993 and 2004-2006. The downward facing triangles denote decreasing concentrations between the two periods for the corresponding numbered site. Asterisks indicate that the differences in 3-year-mean concentrations were not statistically significant. The three multiple-trends plots show the superimposed time trends for all sites in three different regions normalized to the year 1995. The vertical shaded bars in the years 1995 and 1999 show the years when largest SO_2 and NO_x emission reductions occurred in the EUS PEMA. The horizontal red bars along the x-axis illustrate the two averaging periods used for the map.

Figures 3.77 and 3.78, respectively, provide a quantitative assessment of the downward SO_2 and $p\text{-SO}_4^{2-}$ trends at CAPMoN and CASTNET sites. Here, the inset map shows the locations of the CAPMoN and CASTNET sites and the downward triangles present the percentage decrease of 3-year average concentrations between two periods: 1991-1993 and 2004-2006. In this case, 3-year averages were chosen specifically to smooth out inter-annual meteorological variability and reduce the effect of years with unusual or extreme meteorology. For the trends, a time series model was not deemed necessary because the concentration changes were clear and consistent throughout the region (making it less important to remove imbedded sources of variability as is done in a comprehensive time series model). Statistical significance of the concentration differences ($\text{Pr} < 0.05$) was determined from a t-test of the 3-year mean log-transformed concentrations.

To gain an understanding of the year to year behaviour of the time trends, the remaining insets in Figures 3.77 and 3.78 show the superimposed normalized trends at all sites in the three different regions of the map domain. Region I (referred to hereafter as the Great Lakes Region) consists of CASTNET sites located in the Great Lakes states from Minnesota to Pennsylvania (but not including New York); Region 2 (referred to as the US Eastern Seaboard Region) comprises CASTNET sites located along the Eastern Seaboard of the US, including New York and the New England states; and Region 3 (referred to as Eastern Canada) includes CAPMoN sites in the region from the Manitoba-Ontario border eastward. The superimposed trend lines for the regions differ from the trends lines in Figure 3.76 in that they have been normalized to the year 1995 in order to compare all trends on the same scale. The year 1995 was chosen because it was the year that EUS PEMA SO₂ and NO_x emissions decreased dramatically as a result of the implementation of Title IV of the US Clean Air Act Amendments.

Figures 3.77 and 3.78 illustrate a number of important points about the trends and how they relate to changing SO₂ emissions:

SO₂:

The 3-year mean concentrations of ambient SO₂ at all EC and EUS sites decreased substantially and significantly (15 to 60%) from 1991-1993 to 2004-2006 (per inset map in Figure 3.77). These decreases were coincident with major SO₂ emission reductions in both Canada and the USA.

All six Canadian sites showed downward SO₂ trends that began before 1995 and continued until 2006 (see Region 3 trend lines in Figure 3.77). In fact, the Canadian trends generally dropped faster than the US Region 1 and Region 2 trends in relative terms. The two westernmost CAPMoN sites, ELA and Algoma, exhibited the most unusual SO₂ trends whereby the SO₂ concentrations stopped decreasing and levelled off after 2002. Both sites are located close to the US-Canada border and have no major Canadian SO₂ sources in the vicinity, so both are strongly affected by emissions from adjacent US states (Vet *et al.*, 2005). The levelling off of the trends after 2002 is consistent with relatively small changes in emissions in the adjacent states of Minnesota, Wisconsin and Michigan from 2002 to 2005 (U.S. EPA, 2007).

All CASTNET sites in the Great Lakes Region exhibited downward trends of SO₂ from 1991 to 2006 (see Region 1 trend lines in Figure 3.77). The consistency of the trends across all sites reflects the decrease in SO₂ emissions over most of the Region 1 states from 1991 to 2006. One site, Perkinstown, WI, located at the western edge of the domain, showed an unusual upward swing beginning in 2001. This is similar to the trends shown at the two westernmost CAPMoN sites discussed above and, similarly, is consistent with unchanging emissions in Minnesota, Wisconsin and Michigan emissions from 2002 to 2005.

The CASTNET sites in the US Eastern Seaboard Region, as with the other regions, showed overall downward trends from 1991 to 2006 (see Region 2 trend lines in Figure 3.77). However, unlike the other regions, the SO₂ trends at most sites levelled off for several years in the period from 1996 to 2002, then decreased again from 2003 to 2006.

p-SO₄²⁻:

As in the case with ambient SO₂, the 3-year mean concentrations of p-SO₄²⁻ decreased substantially and significantly from 1991-1993 to 2004-2006 at all EC and EUS sites (see the map inset in Figure 3.78). However, the maximum decreases in p-SO₄²⁻ concentrations (45%) were less than those for SO₂ (60%) which suggests there was a non-linear response of p-SO₄²⁻ to decreasing SO₂ emissions.

As with SO₂, the six Canadian sites showed downward p-SO₄²⁻ trends that began before 1995 and continued until 2006 (see the Region 3 trend lines in Figure 3.78). The two westernmost CAPMoN sites, ELA and Algoma, which exhibited a levelling off of their SO₂ concentration lines after 2002, showed continually decreasing trends of p-SO₄²⁻ concentrations. This could perhaps reflect the influence of decreased amounts of p-SO₄²⁻ being transported long distances from different source areas of the continent.

The CASTNET sites in the Great Lakes Region and the US Eastern Seaboard Region exhibited downward p-SO₄²⁻ trends from 1991 to 2006 (see the trend lines in Regions 1 and 2 of Figure 3.78). However, in both regions, most of the CASTNET sites showed a leveling of the trend from 1999 to 2003, followed by a decrease to 2006. The reason for this response is unclear, especially in light of the decrease of SO₂ emissions during this period.

In summary, the foregoing trends clearly indicate that SO₂ and p-SO₄²⁻ concentrations across most of EC and the EUS declined significantly from the early-1990s to the mid-2000s. These declining trends are coincident with declining SO₂ emissions in both EC and the EUS, suggesting that the emission reduction programs in Canada and the U.S. were very effective at reducing ambient SO₂ and p-SO₄²⁻ in eastern Canada and the eastern US.

3.5.4.2.2 Long Term Trends of HNO₃, p-NO₃⁻ and p-NH₄⁺

As discussed in Chapter 2, HNO₃ and p-NO₃⁻ are two of the main oxidation products of NO emissions to the atmosphere. These species, as well as p-NH₄⁺, are also measured routinely at rural/remote sites of CAPMoN and CASTNET in the US. As with SO₂ and p-SO₄²⁻, data from CASTNET and CAPMoN were used to investigate the long term trends of ambient HNO₃, p-NO₃⁻ and p-NH₄⁺ and their relationship to changing NO_x emissions (note that NH₃ emission changes are not discussed here because long-term NH₃ emission data were not available).

It is useful to point out two important factors related to the HNO_3 and p-NO_3^- measurement data: (1) the HNO_3 concentrations are likely overestimated and the p-NO_3^- measurements are likely underestimated because of volatilization of NH_4NO_3 , which is inherent to the measurement method (Yu *et al.*, 2006), and (2) the p-NO_3^- measurements likely represent both fine mode NH_4NO_3 and some unknown portion of coarse mode NO_3 (Zhang *et al.*, 2008), i.e., they are not truly representative of $\text{PM}_{2.5}\text{NO}_3^-$. Nevertheless, for the purpose of this trend analysis, the effects of volatilization and coarse particle collection are assumed to be consistent from year to year and are therefore considered to have no effect on the long-term trends. Note that the p-NH_4^+ trends shown here, like p-SO_4^{2-} , are thought to represent fine-mode- NH_4 because p-NH_4^+ exists in the atmosphere predominantly as $\text{PM}_{2.5}$.

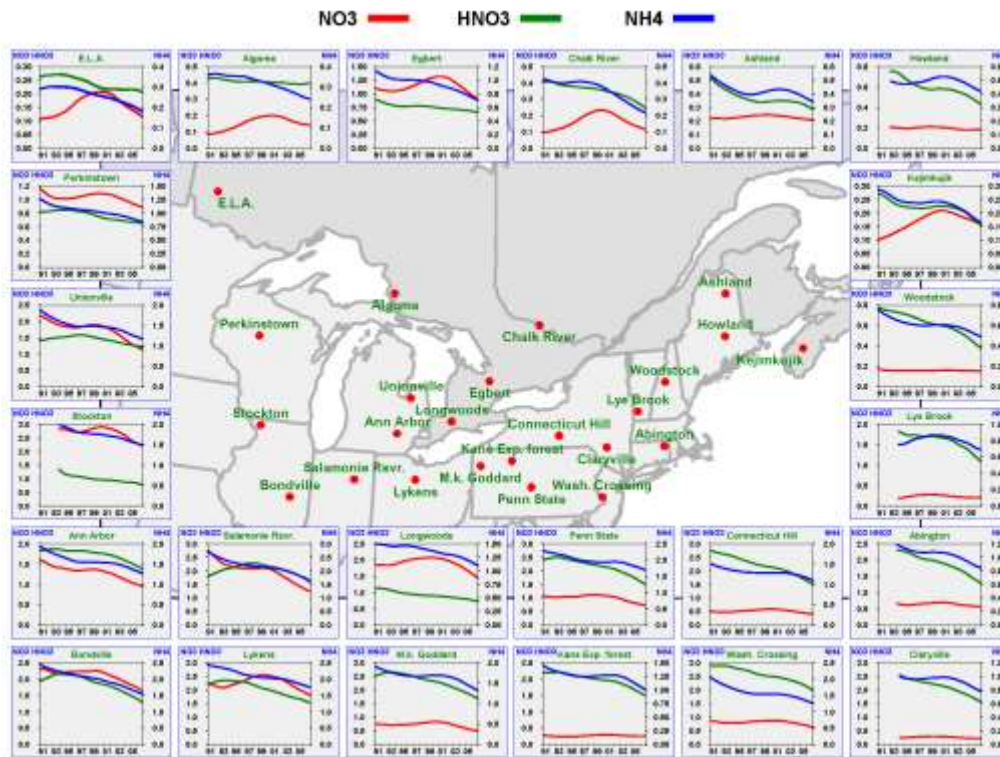


Figure 3.79 Long-term trends of HNO_3 , p-NO_3^- and p-NH_4^+ at CAPMoN and CASTNET sites (in $\mu\text{g m}^{-3}$ at 0°C and 1 atmosphere).

As was the case with SO_2 emissions and ambient SO_2 and p-SO_4^{2-} trends, one would expect to find a relationship between NO_x emission changes and concentration trends of HNO_3 and p-NO_3^- trends in EC and the EUS. Figure 3.79 shows the Kernel smoothing time trends (not normalized) for ambient HNO_3 , p-NO_3^- and p-NH_4^+ at the CAPMoN and CASTNET sites.

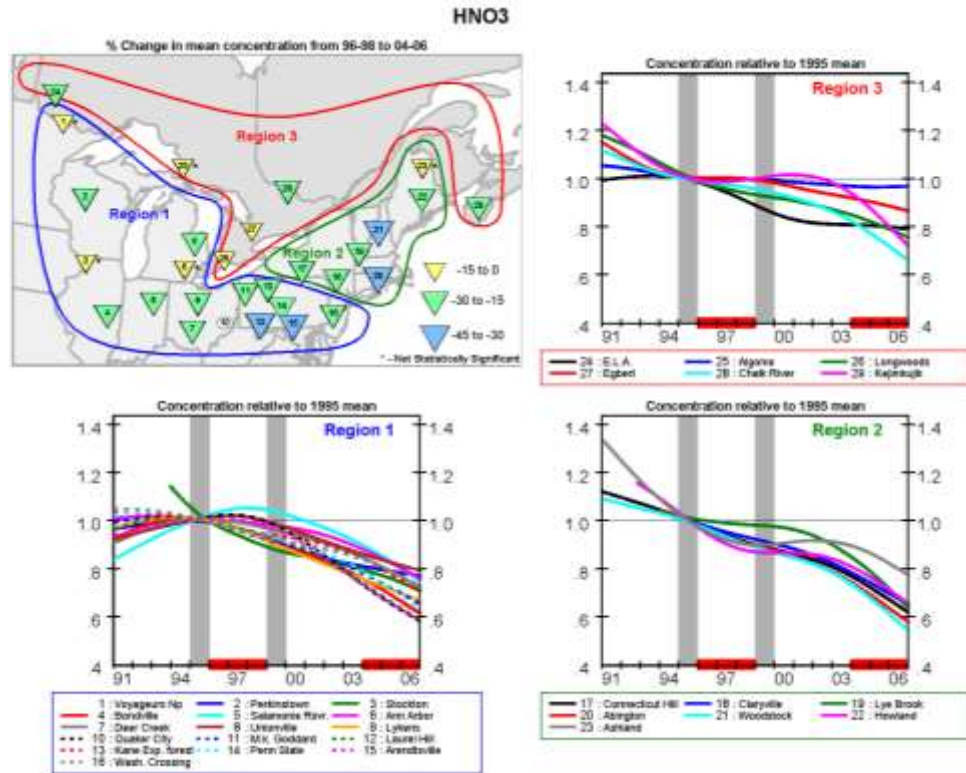


Figure 3.80 Changing HNO₃ concentrations with time. The map insert shows the percent difference in 3-year-mean concentrations between two periods: 1991-1993 and 2004-2006. The downward facing triangles denote decreasing concentrations between the two periods for the corresponding numbered site. Asterisks indicate that the differences in 3-year-mean concentrations were not statistically significant. The three multiple-trends plots show the superimposed time trends for all sites in three different regions normalized to the year 1995. The vertical shaded bars in the years 1995 and 1999 show the years when largest SO₂ and NO_x emission reductions occurred in the EUS PEMA. The horizontal red bars along the x-axis illustrate the two averaging periods used for the map.

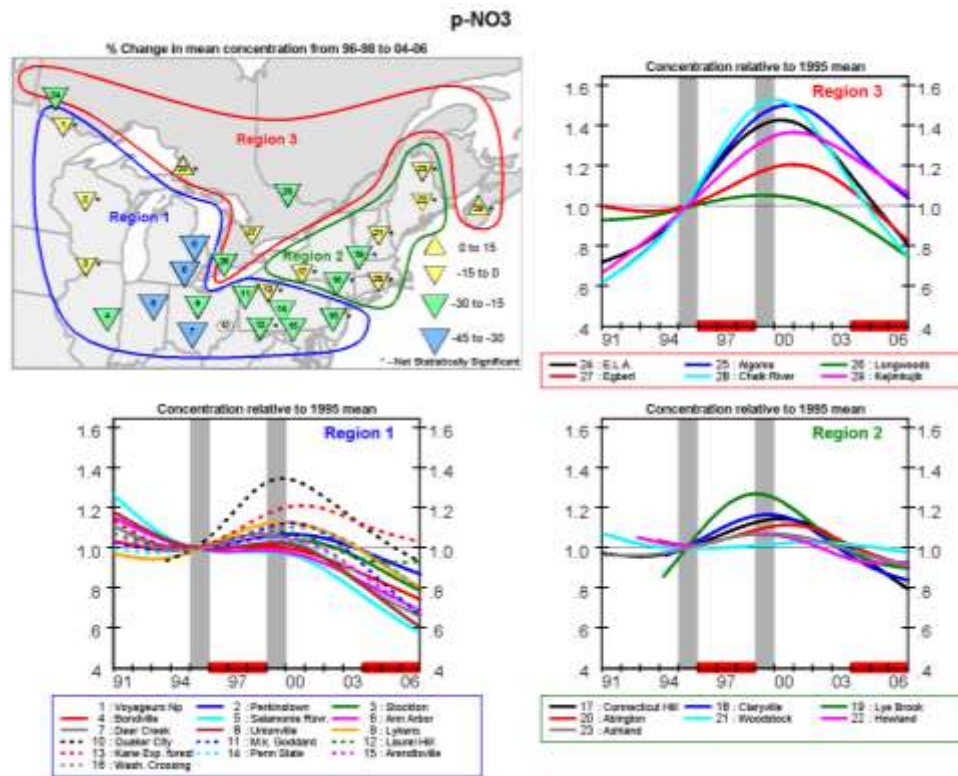


Figure 3.81 Changing $p\text{-NO}_3^-$ concentrations with time. The map insert shows the percent difference in 3-year-mean concentrations between two periods: 1991-1993 and 2004-2006. The downward facing triangles denote decreasing concentrations between the two periods for the corresponding numbered site. Asterisks indicate that the differences in 3-year-mean concentrations were not statistically significant. The three multiple-trends plots show the superimposed time trends for all sites in three different regions normalized to the year 1995. The vertical shaded bars in the years 1995 and 1999 show the years when largest SO_2 and NO_x emission reductions occurred in the EUS PEMA. The horizontal red bars along the x-axis illustrate the two averaging periods for the map.

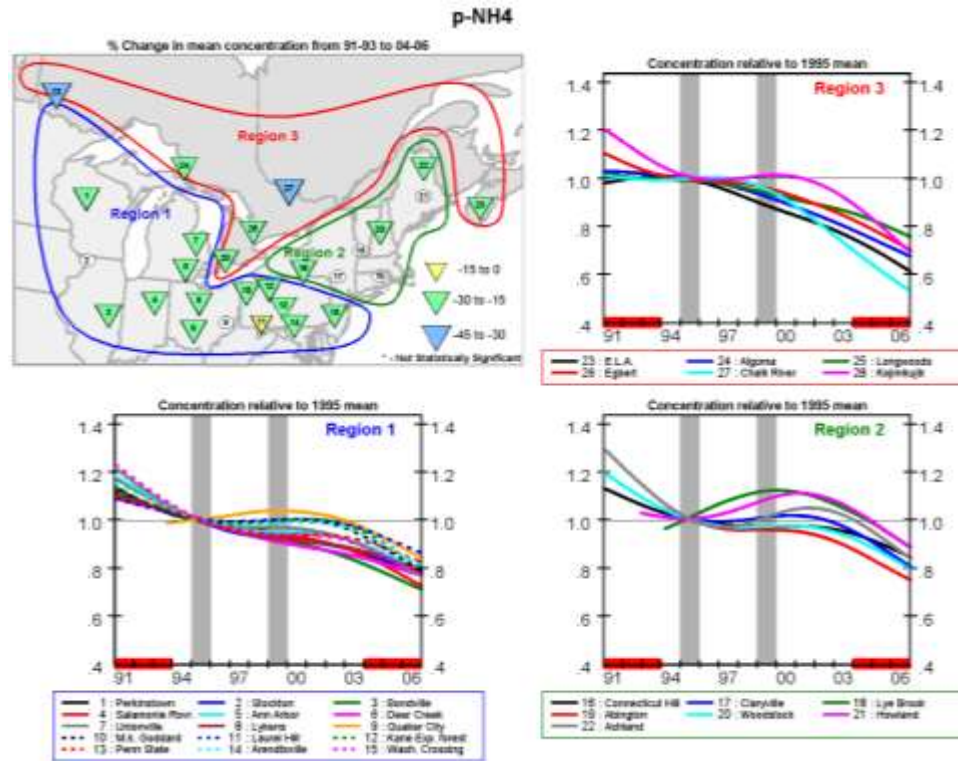


Figure 3.82 Changing $p\text{-NH}_4^+$ concentrations with time. The map insert shows the percent difference in 3-year-mean concentrations between two periods: 1991-1993 and 2004-2006. The downward facing triangles denote decreasing concentrations between the two periods for the corresponding numbered site. Asterisks indicate that the differences in 3-year-mean concentrations were not statistically significant. The three multiple-trends plots show the superimposed time trends for all sites in three different regions normalized to the year 1995. The vertical shaded bars in the years 1995 and 1999 show the years when largest SO_2 and NO_x emission reductions occurred in the EUS PEMA. The horizontal red bars along the x-axis illustrate the two averaging periods used for the map.

Figures 3.80, 3.81 and 3.82 show changing HNO_3 , $p\text{-NO}_3^-$ and $p\text{-NH}_4^+$ concentrations in Regions 1, 2 and 3 (as defined earlier). Each figure includes a map of the percent difference of 3-year-average concentrations between 1991-93 and 2004-06, and the normalized trend lines (normalized to 1995). Again, the downward facing triangles on the maps denote decreasing concentrations between the two periods. The results shown in Figures 3.80, 3.81 and 3.82 are discussed below by species.

HNO_3 :

The map of 3-year-average HNO_3 concentration changes in Figure 3.80 indicates that 3-year average concentrations declined between the periods 1996-98 and 2004-06 at all 26 sites. Note that 1996-1998 was chosen for this analysis because it had relatively constant emissions and good data coverage. The magnitude of the concentration decreases shown on the map varied from site to site, with 7 sites showing declines of 0% to 15% (5 not statistically significant at

Pr<0.05), 15 showing declines of 15% to 30% and 4 showing declines of 30% to 45%. This general decline is consistent with EUS NO_x emissions (Figure 3.75), which were relatively constant in the 1996-1998 period but dropped continuously starting in 1999.

The normalized trends in Figure 3.80 show that HNO₃ concentrations at all sites in the Great Lakes Region (Region 1) declined steadily from 1999 to 2006. In fact, all but three sites had decreasing trends from 1995 to 1999. In Region 2, the US Eastern Seaboard, all sites experienced downward trends from 1990 to 2006, although the two easternmost sites (Howland and Ashland, Maine) actually experienced increasing concentrations from 1999 to 2003 before declining again to 2006. All of the Eastern Canadian sites also showed downward trends from the early-1990s to 2006 but with differing slopes and shapes at the sites. Like the US Eastern Seaboard sites, but unlike the US Great Lakes sites, most of the Eastern Canadian sites showed decreasing trends from 1990 to 1995.

To summarize, HNO₃ concentrations at all but 2 sites in the northeast US decreased steadily after 1999 in concert with declining EUS NO_x emissions. In eastern Canada, HNO₃ concentrations did not decrease as consistently as in the EUS but, in general, were lower in the mid-2000s than in the early 1990s.

p-NO₃⁻:

Figure 3.81 shows that 3-year average p-NO₃⁻ concentrations decreased at all sites in all regions from 1996-1998 to 2004-2006. In the Great Lakes Region, 4 sites decreased between 30 and 45%, 7 between 15 and 30% (2 were not significant at Pr<0.05) and 4 sites between 0 and 15% (all not significant at Pr<0.05). In Region 2, the US Eastern Seaboard, all 7 sites had slightly lower concentrations in 2004-2006 than in 1996-1998 but the changes were not statistically significant. In Eastern Canada, 3 of the 6 sites had lower concentrations in 2004-2006, of which 3 decreased between 15% and 30% and 3 between 0 and 15% (only 1 being statistically significant). Overall, the 3-year-mean concentrations decreased from 1996-1998 to 2004-2006 but the largest and most significant changes occurred in southwestern Ontario and the eastern part of the Great Lakes Region, both of which are the highest emission areas in eastern Canada and the eastern U.S.

The normalized trends in Figure 3.81 show that, in contrast to the consistent downward trends of HNO₃, the concentrations of p-NO₃⁻ at most sites in the three regions increased from 1995 and peaked between 1998 and 2002 (with the peak year dependent on the site), followed by a steady decrease thereafter. Note that the increasing concentrations occurred during a period when the NO_x emissions in the US PEMA were relatively constant but lower than in the pre-1995 period. In the Great Lakes Region, the trends generally peaked within the years 1999 to 2000 while, in the U.S. Eastern Seaboard and the Eastern Canada Region, they peaked within a slightly longer period between 1998 and 2001. By 2000-2001, almost every site showed a downward trend, concomitant with constantly decreasing NO_x emissions in the EUS PEMA.

Since $p\text{-NO}_3^-$ concentrations are strongly seasonally-dependent (with winter concentrations being 3 to 4 times higher than summer concentrations), the foregoing trends are undoubtedly driven mainly by wintertime concentration changes.

p-NH₄⁺:

Figure 3.82 shows that the 3-year-average $p\text{-NH}_4^+$ concentrations decreased significantly ($Pr < 0.05$) at all sites in the three regions between the two periods of 1991-1993 and 2004-2006. Most of the decreases ranged between 15 and 30%, with only one site (in western Pennsylvania) showing a decrease of 0-15% and 2 sites (in Ontario) showing decreases between 30% and 45%. Note that the early period, 1991-1993, was chosen to correspond to the same period used for SO_2 and $p\text{-SO}_4^{2-}$ trends since $(\text{NH}_4)_2\text{SO}_4$ is the major constituent of $\text{PM}_{2.5}$ in Eastern Canada and the Eastern U.S.

For the Great Lakes States, the normalized trends in Figure 3.82 show that $p\text{-NH}_4^+$ concentrations decreased steadily at all sites from 1991 to 1995-1996. This is the same period that SO_2 emissions and ambient SO_2 and $p\text{-SO}_4^{2-}$ concentrations decreased in the EC SOMA and the EUS PEMA, reinforcing the strong relationship between $p\text{-NH}_4^+$ and $p\text{-SO}_4^{2-}$. After 1996, the $p\text{-NH}_4^+$ concentrations stayed roughly constant until 2002. This is the period that $p\text{-SO}_4^{2-}$ concentrations changed little while $p\text{-NO}_3^-$ concentrations increased rapidly. From 2003 to 2006, all sites experienced decreasing concentrations.

The trends at the US Eastern Seaboard sites differed from the trends in the Great Lakes Region in the period 1995 to 2002 when many sites showed increasing trends that peaked sometime between 1999 and 2002. This period of increasing trends coincides with the period of increasing $p\text{-NO}_3^-$ concentrations (Figure 3.81) and level $p\text{-SO}_4^{2-}$ concentrations (Figure 3.78), suggesting that NH_4NO_3 was increasing while $(\text{NH}_4)_2\text{SO}_4$ was decreasing. As with all of the other species, the $p\text{-NH}_4^+$ concentrations in the period 2003 to 2006 trended downward. In Eastern Canada, the trends at all sites changed little from 1991 to 1996 and then decreased systematically to 2006. The one exception to this was the Kejimikujik site in Nova Scotia which showed a trend similar to the trends in the US Eastern Seaboard Region.

3.5.4.2.3 Interpretation of SO_2 , $p\text{-SO}_4^{2-}$, HNO_3 , $p\text{-NO}_3^{2-}$ and $p\text{-NH}_4^+$ Trends

The foregoing trends provide some interesting insights into the relationship between $p\text{-SO}_4^{2-}$, $p\text{-NO}_3^-$ and $p\text{-NH}_4^+$ and their response to SO_2 and NO_x emission reductions in the Eastern Canada and Eastern U.S. areas. The major points are summarized below by relevant emission periods:

- 1990-1994: Based on Figure 3.75, 1990-1994 was characterized by steadily declining SO₂ emissions in the EC SOMA and the EUS PEMA, and slightly increasing NO_x emissions in the EUS PEMA (no data available for the EC PEMA). During this period, ambient SO₂, p-SO₄²⁻, p-NH₄⁺, p-NO₃⁻ and HNO₃ trends generally decreased, with the exception of increasing p-NO₃⁻ trends (in general) in the Eastern Canada Region and increasing HNO₃ trends (in general) in the US Great Lakes Region. In light of the declining SO₂ emissions, the decreasing trends of SO₂, p-SO₄²⁻ and p-NH₄⁺ seem reasonable but the increasing p-NO₃⁻ and HNO₃ trends are difficult to explain.
- 1995-1998: SO₂ and NO_x emissions in the EUS PEMA dropped dramatically in 1995 and then stayed roughly constant until 1998 (the 1995 drop being due Title IV requirements of the US Clean Air Act Amendments). Similarly, SO₂ emissions in the EC SOMA dropped in 1995 and then remained roughly constant until 1998. In the EC PEMA, NO_x emissions were roughly constant from 1995-1998 but no data were available from 1991 to 1994 to indicate whether a drop similar to the EUS PEMA occurred in 1995. While SO₂ emissions in both countries remained relatively constant from 1995 to 1998, the ambient SO₂ trends at almost all sites continued to decrease, more so at some sites than others. The exceptions to this were three sites in New York, Connecticut and Vermont where the trends remained constant or increased slightly (likely a reflection of the emission changes at specific sources upwind of these sites). P-SO₄²⁻ trends in all three regions decreased (with the exception of one site in Vermont) while p-NH₄⁺ concentrations either decreased slightly, remained relatively constant, or increased slightly depending on the site and p-NO₃⁻ concentrations actually increased at most sites. The combined trends suggest that lower SO₂ emissions (relative to the earlier years) led to lower atmospheric production of (NH₄)₂SO₄ and higher production of NH₄NO₃. A possible explanation of this is that the lower levels of emitted SO₂ led to lower levels of particle (NH₄)₂SO₄, which left the unused NH₃ to form two particles of NH₄NO₃ instead of one particle of (NH₄)₂SO₄. This would also explain why p-NH₄⁺ concentrations did not decrease in concert with p-SO₄²⁻ concentrations.
- 1999-2006: This period was characterized by steadily decreasing SO₂ and NO_x emissions in the EUS PEMA and the EC SOMA/PEMA. For example, SO₂ emissions in the EUS PEMA decreased by one third from the 1998 level of 8.87 MT to 5.89 MT in 2006, and the EC SOMA emissions dropped one quarter from the 1998 level of 1.25 MT to 0.93 MT in 2005 (2006 data not available). At the same time, NO_x emissions in the EUS PEMA also dropped one third from 8.30 MT in 1998 to 5.52 MT in 2006, and EC PEMA emissions also dropped one quarter from 0.80 MT in 1998 to 0.61 MT in 2004 (2005 and 2006 emissions data not available). In the first part of this period, 1999 to 2001, most of the sites in the 3 regions showed minor p-SO₄²⁻ changes but major increases and/or peaking of p-NO₃⁻ trends. At the same time, p-NH₄⁺ trends remained roughly constant in the US Great Lakes region, continued to decrease in EC (except in Nova Scotia) and stayed roughly constant or increased in the US northeast.

In the second part of this period (i.e., 2002-2006), SO₂ emissions decreased slowly and NO_x emissions dropped quickly; however, almost every site in the three regions exhibited strong downward trends of SO₂, HNO₃, p-SO₄²⁻, p-NO₃⁻ and p-NH₄⁺. This was presumably due to lower atmospheric production of both (NH₄)₂SO₄ and NH₄NO₃.

3.5.4.2.4 Summary

In summary, between 1999 and 2006, the SO₂ and NO_x emission reductions in Eastern Canada and Eastern U.S. were highly effective at reducing the ambient concentrations of SO₂, HNO₃, p-SO₄²⁻, p-NH₄⁺ and p-NO₃⁻. This was especially so in the period from 2002 to 2006 when all five species rapidly declined in all 3 regions. In the period 1995 to 1999, as SO₂ and NO_x emissions stayed roughly constant but at lower levels than 1990 to 1994, ambient NH₄NO₃ concentrations actually increased while (NH₄)₂SO₄ decreased. Although this suggests a possible disbenefit associated with the SO₂ emission reductions in that period, such a disbenefit cannot be proven with the available data. Further discussion on the topic is given in Section 7.5.4.1 of Chapter 7. Future work on the subject is merited. Unfortunately, too little measurement data is available in western Canada to make any conclusions about trends in that part of Canada.

3.6 PM_{10-2.5} Mass and Trends

3.6.1 Current levels of PM_{10-2.5}

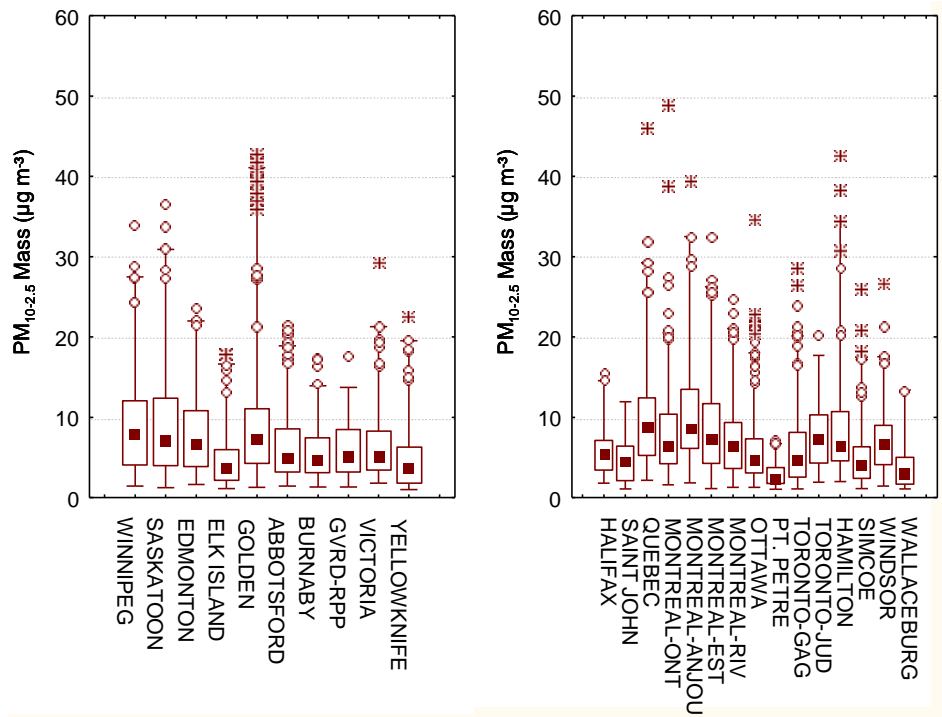


Figure 3.83 Comparison of PM_{10-2.5} 24-h mass concentrations (µg/m³) from filter-based samplers: 2004 to 2006. (median, 25th and 75th percentile, 2nd and 98th percentile, outliers and extremes).

Figure 3.83 provides a comparison of PM_{10-2.5} 24-hr concentrations across the country for the dichotomous sampler network for the years 2004 through 2006. Only sites with a minimum of 100 samples collected over this period are included. Most sites show 98th percentile values less than 30 µg m⁻³ with the highest values measured at the Golden, Saskatoon, Hamilton and Montreal-Anjou sites.

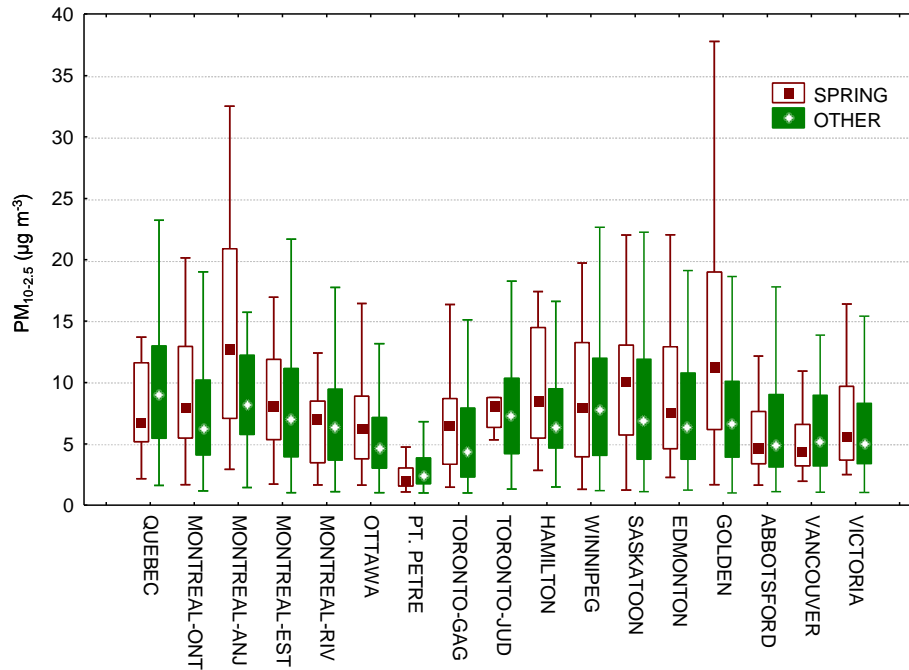


Figure 3.84 March/April vs. other season concentrations of PM_{10-2.5} mass – filter-based samplers for selected sites (median, 25th and 75th percentile, non-outlier max and min).

The differences in PM_{10-2.5} mass between the March/April versus other months are shown in Figure 3.84. Most sites record higher median and maximum concentrations in March/April as compared to the other seasons. This has been associated with road debris left over from winter road salting and sanding operations and with higher winds speeds often measured in these two months. The Golden and Montreal-Anjou sites showed the largest seasonal differences.

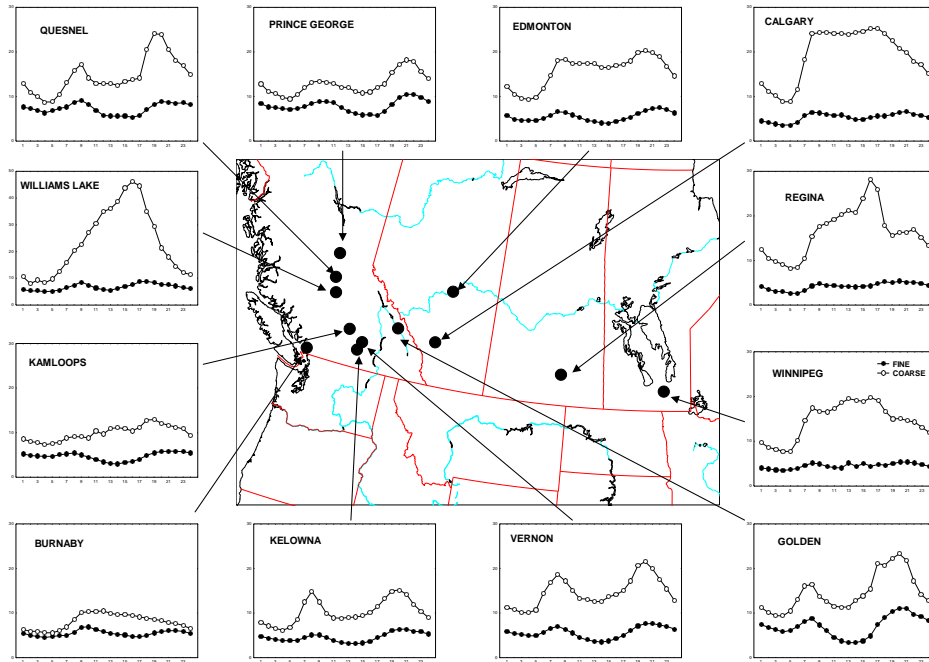


Figure 3.85 Diurnal Variation in $PM_{2.5}$ (●) and $PM_{10-2.5}$ (○) mass concentration ($\mu\text{g}/\text{m}^3$) from sites with co-located PM_{10} and $PM_{2.5}$ TEOMs (Note: PM mass concentration shown on y-axis).

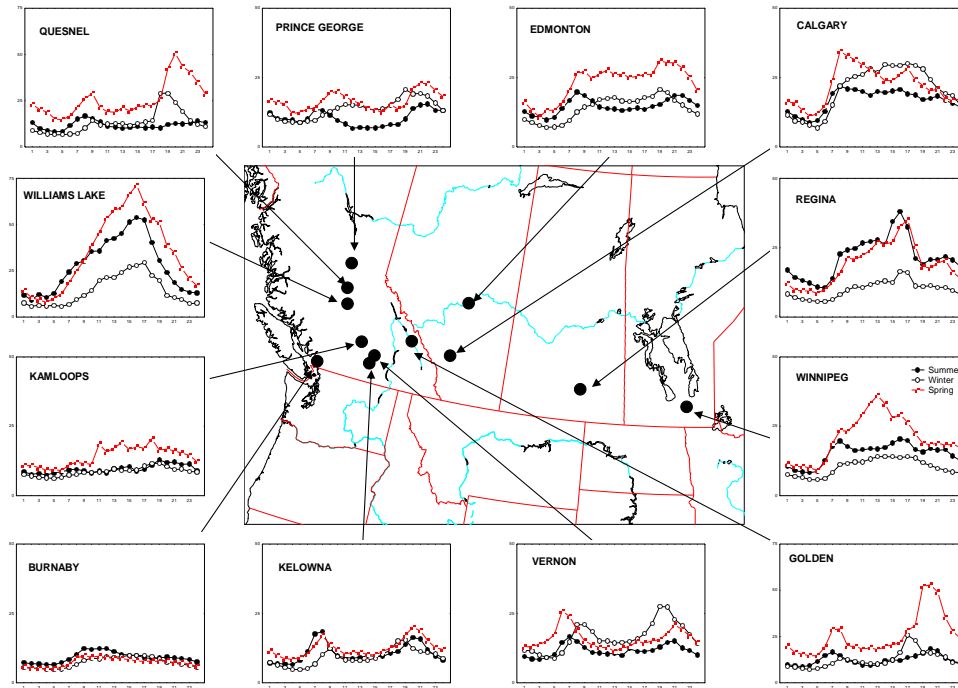


Figure 3.86 Diurnal Variation in $PM_{10-2.5}$ Mass for March/April (◇), Summer (●) and Winter (○) for sites with co-located PM_{10} and $PM_{2.5}$ TEOMs. (Note: PM mass concentration shown on y-axis).

In order to expand the number of sites with available data, coarse concentrations were also inferred using hourly data from sites with co-located PM_{10} and $PM_{2.5}$ TEOMs by subtracting the two values. In Figure 3.85 the diurnal variability of inferred $PM_{10-2.5}$ mass is compared with that of $PM_{2.5}$ mass. The amplitude of the coarse diurnal cycle is generally much larger than the $PM_{2.5}$ diurnal cycle, and there is evidence of both a morning and evening rush hour peak in concentrations at many sites. Seasonal (March/April, Summer – June, July, August and Winter – December, January, February) differences in diurnal inferred $PM_{10-2.5}$ mass are illustrated in Figure 3.86. Although the diurnal profiles are similar at most sites by season the concentration values do increase in the winter and March/April at the sites measuring the highest concentrations.

3.6.2 Trends in $PM_{10-2.5}$

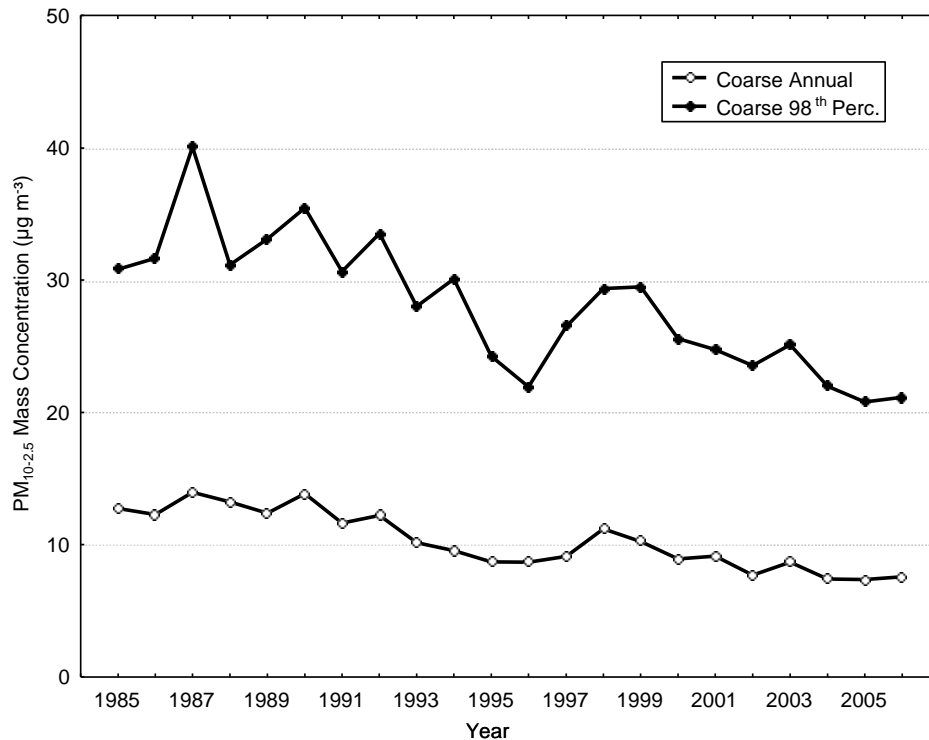


Figure 3.87 Trend in composite annual mean and 98th percentile $PM_{10-2.5}$ mass ($\mu\text{g}/\text{m}^3$) from dichotomous sampler sites.

In Figure 3.87 the long term trend in annual mean and 98th percentile $PM_{10-2.5}$ mass from the dichotomous sampler sites is presented. Only cities with operational sites in at least 75% of the years were included. This amounted to an average of 14 sites in 11 cities. The trend in coarse mass is very similar to the trend in fine mass shown in Figure 3.70. Between 1985 and 2006 composite annual mean $PM_{10-2.5}$ mass decreased by 40% and composite annual mean 98th percentile decreased by 30%. The exact reason for the decreasing trend in $PM_{10-2.5}$ is not

known since emission inventory estimates suggest there should have been an increase during this time period. Studies to reconcile the emission inventories with ambient observations are recommended for the future.

3.7 Summary and Conclusions

Spatial and Temporal Distribution of Ozone and PM in Canada:

- There is evidence that the concentrations of ozone entering North America above the boundary layer in spring have increased significantly over 20 years, with the largest increase in air parcels that originate over major Asian emission regions. Asian pollution is estimated to contribute about 3-10 ppb to average background O₃ levels in the western United States during the spring and is likely to contribute similarly in western Canada.
- Annual mean baseline levels of ozone in Canada have been estimated using the 5th percentile of daily maximum 6-hour average ozone concentrations. Estimates of annually-averaged baseline ozone are 19 ± 10 ppb in Pacific Canada, 28 ± 10 ppb in continental western Canada, 10 ± 9 ppb in continental Eastern Canada, and 27 ± 9 ppb in Atlantic Canada. The values are thought to represent a combined hemispheric and within-region signal. A calculation of baseline levels in the form of the CWS metric was not attempted but 4th highest daily maximum 8h ozone concentrations at the most remote sites in Canada ranged from 44 to 53 ppb in 2006.
- Baseline ozone levels are increasing in the Georgia Basin area of the Pacific coast as well as in continental western Canada and Atlantic Canada (Chan and Vet, 2010). In contrast, baseline levels appear to be decreasing in Ontario (and the eastern U.S.). These trends are consistent with increasing hemispheric background levels and decreasing precursor emissions in eastern Canada and the eastern US.
- Ontario and southern Quebec continue to record the highest O₃ levels (in the form of the CWS - 3 year average of the 4th highest daily maximum ozone concentration) ranging from 70 to 87 ppb) and most frequent number of days above the CWS (30 to 50 days per year). Almost all sites over the CWS 2010 target are located in these areas.
- Outside of Ontario and Quebec almost all sites record higher spring-time O₃ than summer O₃ and regional scale photochemical episodes are very rare despite high emission densities in some regions.
- The available data suggest that the consistently strong association between NO₂ and mortality in Canadian cities is because NO₂ is a good indicator of local combustion emissions (likely motor vehicles) along with being indicative of the local build up of photochemically processed urban air pollution

- The highest PM_{2.5} levels and frequency of episodes and days greater than 30 µg m⁻³ are also recorded in Ontario and southern Quebec although the sites with the highest 3-year average of 98th percentile concentrations are much closer to the CWS 2010 target value than is the case for ozone.
- The major components of PM_{2.5} at speciation measurement sites across the country are ammonium sulphate, organic material and ammonium nitrate. In the east, ammonium sulphate reaches its maximum in the summer months when photochemistry and transport from Canadian and US emission sources are greatest. Ammonium nitrate peaks during the winter months at sites in the east and in Edmonton. In the east, the highest PM_{2.5} days during the warm season are dominated by (NH₄)₂SO₄ and the highest in the cold season are dominated by NH₄NO₃ (except at sites in Atlantic Canada where (NH₄)₂SO₄ is dominant in both seasons).
- In the west, the highest PM_{2.5} days during both the warm and cold seasons are dominated by organic material

Changes Observed in Air Quality with Implementation of Emission Reduction Strategies:

- Transportation sources dominate urban VOC and NO_x ambient concentrations and they strongly influence observed PM_{2.5} and PM_{10-2.5} levels. The ‘weekend’ effect clearly shows the impact of transportation emission reductions and should be examined as to potential varying health impacts on weekends.
- Between 1990 and 2006 annual mean NO decreased by 55%, NO₂ by 34% and VOCs by 46% at Canadian urban sites. The trends were very consistent on a site by site basis with essentially all urban sites (56 sites for NO_x and 25 for VOC) in Canada recording similar decreases in ambient levels.
- Trend results for ozone for urban sites for 1990-2006 show a statistically significant positive trend for the 10th, 25th and 50th percentiles. Although the slopes were negative for the higher percentile plots they were not statistically significant. Rural sites, however showed negative slopes for all percentiles with statistically significant decreases in maximum, 95th and 75th percentile 8h ozone. The urban results illustrate the effect of NO reductions in reducing ozone scavenging and resulting in a net apparent upward trend in lower percentile and average ozone concentrations. The rural sites show that on a regional scale ozone has responded to emission reductions and upper percentile 8h ozone concentrations show a statistically significant decrease.
- Ozone concentrations in eastern Canada appear to have dropped more quickly in the 2004-2007 period than in the past (and although not shown in this report, through the 2007-2009 period), likely a result of reductions in U.S. NO_x emissions.

- There was a large reduction in urban $PM_{2.5}$ and $PM_{10-2.5}$ between 1985 to 1998 and little change in $PM_{2.5}$ since then, but $PM_{10-2.5}$ continues to decline. The limited data on compositional change restricts conclusions on its trends.
- Between 2002 and 2006, SO_2 and NO_x emission reductions in Eastern Canada and the Eastern U.S. were highly effective at reducing the ambient concentrations of SO_2 , HNO_3 , $p-SO_4^{2-}$, $p-NH_4^+$ and $p-NO_3^-$ at rural/remote sites in eastern Canada.
- Urban SO_2 reductions have occurred but some locations still experience very high ambient SO_2 levels due to large point sources (also applies to $PM_{2.5}$). Urban sites also show a decrease in SO_4 but it has only represented a small fraction of the overall change in $PM_{2.5}$ mass.
- Results from observations and models have been used to assess the sensitivity of ambient PM levels to changes in NH_3 emissions for six agriculturally-intensive regions of Canada. The results indicated that PM levels exhibit relatively low sensitivity to NH_3 in five of the six regions.

3.8 Recommendations for Changes to the Monitoring Networks and for Additional Monitoring and Special Studies

- The TEOM monitors deployed in the NAPS network significantly underestimate $PM_{2.5}$ mass in the cold season. NAPS monitoring agencies have agreed to accept the U.S. Class III Federal Equivalency Method (FEM) instruments (reference) as meeting the NAPS data quality objectives (DQOs) for $PM_{2.5}$ CWS reporting. Monitoring agencies across the country have begun to transition their $PM_{2.5}$ networks over to FEM instruments. This transition is expected to be completed over the 2010 – 2011 timeframe. In the meantime, interpreting $PM_{2.5}$ levels and trends across Canada will be challenging. It is expected that the reported concentrations from $PM_{2.5}$ FEM instruments deployed in the network will be higher relative to the TEOM measurements. Guidelines should be developed for future handling of PM data for the purpose of trend reporting.
- As ozone and PM precursor emissions continue to decline in North America, an understanding of the influence of baseline levels and how they change over time becomes increasingly important and it is recommended additional measurements be resumed or initiated at remote, high elevation, and arctic sites. Such measurements would enable a much better assessment of the changing influence of baseline and the effect on air quality.

- The lack of long-term PM_{2.5} measurement data at regionally-representative sites made it impossible to assess the long-term temporal trends of baseline PM_{2.5} (as was done for background ozone in Section 3.3.1.4). Such analyses are recommended when sufficient data sets are available.
- Most NO_x measurement sites in NAPS are located in urban environments which are impacted by local emissions and thus reduce the positive interference due to other nitrogen species. The over-prediction of NO₂ however, should increase as the distance from emission sources increases. Quantifying the positive interference in Canadian urban environments should be investigated.
- There is some evidence to suggest that declining SO₂ emissions in the late 1990s may have led to increases in nitrate particle mass in eastern Canada during that time. Further exploration of this potential disbenefit should be carried out.
- The apparent dominance of roadway emissions on measured levels of PM and ozone precursors suggests that more near-roadway measurement sites should be established to better track trends in motor vehicle emissions and to provide a platform to carry out special studies.
- There are some serious discrepancies between emission inventory estimates and ambient observations of coarse PM and biogenic and anthropogenic VOC. Additional analysis of observations using tools such as PMF is recommended in order to resolve discrepancies. Carefully designed long and short term studies involving measurement of better ‘marker’ compounds may be required to provide more observation power.
- In light of decreasing SO_x and NO_x emissions in various areas of North America, NH₃ concentration may become more important to total PM_{2.5}, raising a series of questions: Will emission reductions for NH₃ be effective in reducing PM_{2.5} concentration? If so, starting from which areas and which season will give the most effective result? Knowing different sensitivity regimes across the continent is an important first step to understanding PM_{2.5} response, but the temporal changes of these regimes will play an important role in the effectiveness of NH₃ reduction as a result of best agricultural practices. More NH₃ and PM measurements are required in areas downwind of the agriculturally-intense areas to investigate the sensitivity of PM to changing NH₃ emissions.

References

- ACCENT, 2006. First ACCENT Symposium, Urbino, Italy, Sept. 2005, Ed. F. Raes and J.Hjorth. <http://www.accent-etwork.org/index.cfm?objectid=6023C479-BCDC-BAD1-A0D3EB5D0C950580>.
- Ainslie, B and D.G. Steyn, 2007: Spatiotemporal Trends in Episodic Ozone Pollution in the Lower Fraser Valley, B.C. in Relation to Meso-scale Atmospheric Circulation Patterns and Emissions. *Journal of Applied Meteorology*, 46, 10, 1631-1644.
- Allen, G., Sioutas, C., Koutrakis, P., Reiss, R. Lurmann, F.W., Roberts, P.T., 1997. Evaluation of the TEOM method for measurement of ambient particulate mass in urban areas, *Journal of the Air and Waster Management Association*, 47, 682-689.
- Altshuller, A.P., 1978. Association of oxidant episodes with warm stagnating anticyclones. *Journal of the Air Pollution Control Association*, 28, 152-155.
- Amann, M., Cofala, J., Klimont, Z., 2006. Projections of global emissions of air pollutants. Presented at the TF HTAP Workshop on Emission Inventories and Projections, Beijing, October 18-20, 2006.
- Ansari, A.S., Pandis, S.N., 1998. Response of inorganic PM to precursor concentrations. *Environmental Science and Technology*, 32, 2706-2714.
- Bottenheim, J.W., Shepherd, M.F. 1995. C2-C6 Hydrocarbon Measurements at Four Rural Locations Across Canada, *Atmospheric Environment*, 29, 647-664.
- Bovis, P. E. 2003. Stratospheric troposphere exchange and its influence on surface ozone concentrations in the Lower Fraser Valley. Thesis, Atmospheric Science Program, University of British Columbia , 119 pp.
- Brook, J., Dann, T., 1998. Contribution of Nitrate and Carbonaceous Species to PM₁₀ and PM_{2.5} Observed in Canadian Cities. *Journal of the Air and Waste Management Association*, 49, 193-199.
- Brook J.R., Burnett R.T., Dann T.F., Cakmak S., Goldberg M.S., Fan X., Wheeler A.J., 2007. Further interpretation of the acute effect of nitrogen dioxide observed in Canadian time series studies. *Journal of Exposure Science and Epidemiology*, 17, S36-S44.
- Brook, J.R., Dann, T., Burnett, R.T., 1997. The Relationship Among TSP, PM₁₀, PM_{2.5} and Inorganic Constituents of Atmospheric Particulate Matter at Multiple Canadian Locations. *Journal of the Air and Waste Management Association*, 47, 2-19

- Brankov, E., Henry, R.F., Civerolo, K.L., Hao, W., Rao, S.T., Misra, P.K., Bloxam, R., Reid, N., 2003. Assessing the effects of transboundary pollution between Ontario, Canada and New York, USA. *Environmental Pollution*, 123, 403–411.
- Buhr, M.P., Parish, D.D., Norton, R.B., Fehsenfeld, F.C., Sievers, R.E., Roberts, J.M., 1990. Contribution of organic nitrates to the total reactive nitrogen budget at a rural eastern U.S. site. *Journal of Geophysical Research*, 95, 9809-9816.
- Burnett, R.T., Stieb, D., Brook, J.R., Cakmak, S., Dales, R., Raizenne, M., Vincent, R., Dann, T., 2004. Associations between short-term changes in nitrogen dioxide and mortality in Canadian cities. *Archives of Environmental Health*, 59, 228–236
- Camalier, L., Cox, W., Dolwick, P, 2007. The effects of meteorology on ozone in urban areas and their use in assessing ozone trends. *Atmospheric Environment*, 41, 7127–7137
- Canada-USA, 2008. Canada-United States Air Quality Agreement 2008 Progress Report, Environment Canada and US Environmental Protection Agency available at http://www.ec.gc.ca/cleanair-airpur/caol/canus/report/2008CanUs/eng/tdm-toc_eng.cfm.
- Carmichael, G.R., Calori, G., Hayami, H., Uno, I., Cho, S.Y., Engardt, M., Kim, S.-B., Ichikawa, Y., Ikeda, Y., Woo, J.-H., Ueda, H., Amann, M., 2002. The MICS-Asia study: Model intercomparison of long-range transport and sulphur deposition in East Asia. *Atmospheric Environment*, 36, 175-199.
- Carter, W.P.L., 1994. Development of Ozone Reactivity Scales for Volatile Organic Compounds. *Journal of the Air and Waste Management Association*, 44, 881-899
- CCME (Canadian Council of Ministers of the Environment). 2006. Canada Wide Standards for Particulate Matter and Ozone: Five Year Report: 2000-2005.
- Canadian Councils of Ministers of the Environment. PN1374. http://www.ec.gc.ca/cleanair-airpur/caol/pollution_issues/cws/toc_e.cfm
- CCME (Canadian Council of Ministers of the Environment), 2007. Guidance Document on Achievement Determination, Canada-wide Standards for Particulate Matter and Ozone, CCME Report PN 1391 downloadable from http://www.ccme.ca/assets/pdf/1391_gdad_e.pdf.
- Chameides, W.L., Fehsenfeld, F., Rodgers, M.O., Cardelino, C., Martinez, J., Parrish, D., Lonneman, W., Lawson, D.R., Rasmussen, R.A., Zimmerman, P., Greenberg, J., Middleton, P., Wang, T., 1992. O₃ Precursor Relationships in the Ambient Atmosphere. *Journal of Geophysical Research*, 97, 6037-6055.

Chameides, W.L., Xingsheng, L., Xiaoyan, T., Xiuji, Z., Chao, L., Kiang, C.S., St. John, J., Saylor, R.D., Liu, S.C., Lam, K.S., Wang, T., Giorgi, F., 1999. Is ozone pollution affecting crop yields in China? *Geophysical Research Letters*, 26, 867–870.

Chan, C.Y., Chan, L.Y., Harris, J.M., 2003. Urban and background ozone trend in 1984-1999 at subtropical Hong Kong, South China. *Ozone-Science and Engineering*, 25, 513-522.

Chan, E., 2009, Regional ground-level ozone trends in the context of meteorological influences across Canada and the eastern United States from 1997 to 2006. *Journal of Geophysical Research*, 114, D05301.

Chan, E. and Vet, R. J., 2010. Baseline levels and trends of ground level ozone in Canada and the United States, *Atmospheric Chemistry and Physics*, 10, 8629-8647.

Cleveland, W.S., 1979. Robust locally weighted regression and smoothing scatterplots. *Journal of the American Statistical Association*, 74, 829-836.

Chevalier A., Gheusi, F., Delmas, R., Ordonez, C., Sarrat, C., Zbinden, R., 2007.

Air Quality Health Index Report and Guidance Document, Environment Canada and Health Canada.

Cooper, O.R., D. D. Parrish, A. Stohl, M. Trainer, P. Nédélec, V. Thouret, J. P. Cammas, S. J. Oltmans, B. J. Johnson, D. Tarasick, T. Leblanc, I. S. McDermid, D. Jaffé, R. Gao, J. Stith, T. Ryerson, K. Aikin, T. Campos, A. Weinheimer & M. A. Avery, 2010. Increasing springtime ozone mixing ratios in the free troposphere over western North America. *Nature*, 463, 344-348 (21 January 2010) | doi:10.1038/nature08708;

Dann, T. and Wang, D., 1992a. Measurement of volatile organic compounds in Canada 1987-1990. Environment Canada, C&P, PMD Report 92-3

Dann, T. and Wang, D., 1992b. Volatile organic compounds measurements in Canadian urban and rural areas: 1989-1990. In: AWMA Annual Conf.

Dann, T., White, L., Biron, A., 2006. Performance of Continuous PM_{2.5} Monitors at a Monitoring Site in Ottawa, Canada. EPA National Air Monitoring Conference, November 2006.

Dennis R.L., Binkowski F.S., Clark T.L., McHenry J.N., Reynolds S., Seilkop S.K., 1990. Selected Applications of RADM (Part II), App. 5F, NAPAP SOS/T Report 5, In: National Acid Precipitation Assessment Program: State of Science and Technology, National Acid Precipitation Assessment Program, Washington, D.C.

- Dibb, J. E., Talbot, R.W., Scheuer, E., Seid, G., DeBell, L., Lefer, B., Ridley, B., 2003. Stratospheric influence on the northern North American free troposphere during TOPSE: 7Be as a stratospheric tracer. *Journal of Geophysical Research*, 108, 11.1-11.8, doi:10.1029/2001JD001347
- Diem, J., 2004. Explanations for the spring peak in ground-level ozone in the southwestern United States. *Physical Geography*, 25, 105-129
- Dorling S. R., Davies, T.D., Pierce, C.E., 1992. Cluster analysis: A technique for estimating the synoptic meteorological controls on air and precipitation chemistry—Method and applications. *Atmospheric Environment*, 26, 2575–2581
- Eder, B. K., Davis, J.M., Bloomfield, P., 1993. A Characterization of the Spatiotemporal Variation of Non-Urban Ozone in the Eastern United States. *Atmospheric Environment*, 27, 2645-2668
- EMEP, 2005. The development of European surface ozone. Implications for a revised abatement policy. EMEP/CCC-Report 1/2005, NILU, Oslo, Norway.
- Environment Canada, 1997. “Ground Level Ozone and Its Precursors in Canada. (1980-1993).” Canadian 1996 NO_x/VOC Science Assessment: Report of the Data Analysis Working Group. (Edited by T. Dann and P. Summers).
- Environment Canada, 2001. Precursor contributions to ambient fine particulate matter in Canada. Environment Canada, Gatineau, 237 pp.
- Environment Canada, 2004a. Canada-United States Transboundary Particulate Matter Science Assessment. Environment Canada, Toronto, ON.
- Environment Canada, 2004b. Performance of Continuous PM_{2.5} Monitors at Canadian Monitoring Locations. NAPS Managers Technical Working Group on PM Measurement Technology, November 2004.
- Environment Canada, 2005a. Speciation Network Preliminary Data Features Report 2003-2005. Analysis and Air Quality Division Internal Report, November 2005.
- Environment Canada, 2005b. Recent Trends in Ozone in Southern Ontario and Southern Quebec. Analysis and Air Quality Division Internal Report, November 2005.
- Environment Canada, 2007. Criteria Air Contaminants Branch, Pollution Data Division, Environment Canada, Place Vincent Massey, Gatineau, QC

Environment Canada, 2009. The 2008 Canadian Atmospheric Assessment of Agricultural Ammonia. Environment Canada, Gatineau.

Fay, J.A., Kumar, S., Golomb, D., 1986. Annual and semi-annual anthropogenic sulphur budget for eastern North America. *Atmospheric Environment*, 20, 1497-1500.

Fehsenfeld, F., Calvert, J., Fall, R., Goldan, P., Guenther, A.B., Hewitt, C.N., Lamb, B., Liu, S., Trainer, M., Wetberg, H., Zimmerman, P., 1992. Emissions of Volatile Organic Compounds from Vegetation and the Implications for Atmospheric Chemistry. *Global Biogeochemical Cycles*, 6, 389-430.

Fiore, A., Jacob, D.J., Liu, H., Yantosca, R.M., Fairlie, T.D., Li, Q., 2003. Variability in surface ozone background over the United States: Implications for air quality policy. *Journal of Geophysical Research*, 108, 19.1-19.16, doi:10.1029/2003JD003855.

Fiore, A.M., Jacob, D. J., Bey, I., Yantosca, R. M., Field, B. D., Wilkinson, J. G., 2002. Background ozone over the United States in summer: origin and contribution to pollution episodes. *Journal of Geophysical Research*, 107, 11.1-11.27, doi:10.1029/2001JD000982.

Fuentes, J.D., Dann, T., 1994. Ground-Level Ozone in Eastern Canada: Seasonal Variations, Trends and Occurrences of High Concentrations. *Journal of the Air and Waste Management Association*, 44, 1019-1026.

Fuentes, J.D., Dann, T.F., 1993. Ground-Level Ozone in Canada during 1980 to 1990. Report: ARD-93-010. Atmospheric Environment Service, Downsview, Ontario.

Fuentes, J.D., den Hartog, G., Neumann, H.H., Dann, T.F., and Puckett, K.J., 1996. Ambient biogenic hydrocarbon concentrations and isoprene emissions from deciduous forests. *J. Atmos. Chem.*, 29, 1-29.

Fuentes, J.D., Wang, D., Gu, L., 1999. Seasonal Variations in Isoprene emissions from a Boreal Aspen forest. *Journal of Applied Meteorology*, 38, 855-869.

Fuentes, J.D., Wang, D., Bowling, D., Potosnak, M., Monson, R.K., Goliff, W., Stockwell, W.R., 2007. Biogenic Hydrocarbon Chemistry Within and Above a Mixed Deciduous Forest. *Journal of Atmospheric Chemistry*, 56, 165-185.

Fusco, A. C., Logan, J. A., 2003. Analysis of 1970-1995 trends in tropospheric ozone at Northern Hemisphere mid-latitudes with the GEOS-CHEM model. *Journal of Geophysical Research*, 108, ACH 4-1-ACH 4-25, doi:10.1029/2002JD002742.

Gégo, E., Porter, P.S., Gilliland A., Rao, S.T., 2007. Observation-based assessment of the impact of nitrogen oxides emissions reductions on ozone air quality over the eastern United States. *Journal of Applied Meteorology and Climatology*, 46, 994-1008.

Goldstein, A. H., Millet, D. B., McKay, M., Jaeglé, L., Horowitz, L., Cooper, O., Hudman, R., Jacob, D. J., Oltmans, S., and Clarke, A., 2004. Impact of Asian emissions on observations at Trinidad Head, California, during ITCT 2K2. *Journal of Geophysical Research*, 109, D23S17, doi:10.1029/2003JD004406.

Government of Canada, 2007. Five-year Progress Report: Canada-wide Standards for Particulate Matter and Ozone. January 2007.

Health Canada and Environment Canada, 1999a. National ambient air quality objectives for ground-level ozone science assessment document: a report by the Federal-Provincial Working Group on Air Quality Objectives and Guidelines. Environment Canada, Gatineau, QC.

Health Canada and Environment Canada, 1999b. National ambient air quality objectives for particulate matter science assessment document: a report by the Federal-Provincial Working Group on Air Quality Objectives and Guidelines. Environment Canada, Gatineau, QC.

Helmig, D., Oltmans, S. J., Carlson, D., Lamarque, J-F., Jones, A., Labuschagne, C., Anlauf, K., Hayden, K., 2007. A review of surface ozone in the polar regions. *Atmospheric Environment*, 41, 5138-5161.

Hessel, C., 2003. A climatological evaluation of elevated ozone levels at a background Site in the Foothills of Alberta, Canada. Presented at the 96th A&WMA Annual Conference, San Diego CA, Air and Waste Management Association.

HTAP (Task Force on Hemispheric Transport of Air Pollution), 2010. Hemispheric Transport of Air Pollution 2010 Report. Prepared by the Task Force on Hemispheric Transport of Air Pollution acting within the framework of the Convention on Long-range Transboundary Air Pollution. Report available online at <http://www.htap.org>.

Hudman, R.C., Jacob, D.J., Cooper, O.R., Evans, M.J., Heald, C.L., Park, R.J., Fehsenfeld, F., Flocke, F., Holloway, J., Huber, G., Kita, K., Koike, M., Kondo, Y., Neuman, S., Nowak, J., Oltmans, S., Parrish, D., Roberts, J.M., Ryerson, T., 2004. Ozone production in transpacific Asian pollution plumes and implications for ozone air quality in California. *Journal of Geophysical Research*, 109, D23S10, doi:10.1029/2004JD004974.

Jacob, D.J., Logan, J.A., Murti, P.P., 1999. Effect of rising Asian emissions on surface ozone in the United States. *Geophysical Research Letters*, 26, 2175-2178.

Jaffe, D.A., Parrish, D., Goldstein, A., Price, H., Harris, J., 2003. Increasing background ozone during spring on the west coast of North America. *Journal of Geophysical Research*, 30, doi:10.1029/2003GL017024.

Jaffe, D., Bertschi, I., Jaegle, L., Novelli, P., Reid, J.S., Tanimoto, H., Vingarzan, R., Westphal, D.L., 2004. Long-range transport of Siberian biomass burning emissions and impact on surface ozone in western North America. *Geophysical Research Letters*, 31, L16106, doi:10.1029/2003JDO04436.

Jaffe D., Tamura, S., Harris, J., 2005. Seasonal cycle, composition and sources of background fine particles along the west coast of the U.S. *Atmospheric Environment*, 39, 297-306

Jenkin, M. E., 2008: Trends in ozone concentration distributions in the UK since 1990: Local, regional and global influences. *Atmospheric Environment*, 42, 5434- 5445.

Jobson, B.T., Wu, Z., Niki, H., Barrie, L.A., 1994. Seasonal Trends of Isoprene, C2-C5 Alkanes, and Acetylene at a Remote Boreal Site in Canada. *Journal of Geophysical Research*, 99, 1589-1599.

Lefohn, A.S. Oltmans, S.J., Dann, T. Singh, H.B., 2001. Present day variability of background ozone in the lower troposphere. *Journal of Geophysical Research*, 9, 9945-9958.

Lehman, J., Swinton, K., Bortnick, S., Hamilton, C., Baldrige, E., Eder, B., Cox, B., 2004. Spatio-temporal characterization of tropospheric ozone across the Eastern United States. *Atmospheric Environment*, 38, 4357-4369.

Lelieveld, J., van Aardenne, J., Fischer, H., de Reus, M., Williams, J., Winkler, P., 2004. Increasing ozone over the Atlantic Ocean. *Science*, 304, 1483.

Li, Q., Jacob, D., Bey, I. Palmer, P., Duncan, B.N., Field, B.D., Martin, R.V., Fiore, A.M., Yantosca, R.M., Parrish, D.D., Simmonds, P.G., Oltmans, S., 2002. Transatlantic transport of pollution and its effects on surface ozone in Europe and North America. *Journal of Geophysical Research*, 107, doi:10.1029/2001JD001422.

Lindskog, A., Kindbom, K. 2001, Ozone in Remote Areas: Seasonal Cycles, EUROTRAC-2 Symposium2000 Proceedings. Ed. Midgley, P. M., Reuther, M., Williams, M. Springer-Verlag, Berlin

Lyons, W. A., Cole, H.S., 1976. Photochemical oxidant transport: mesoscale lake breeze and synoptic-scale aspects. *Journal of Applied Meteorology*, 15, 733–743.

McKendry, I.G., 1993. Ground-Level Ozone in Montréal, Canada. *Atmospheric Environment*, 27, 93-113.

- McKendry, I. G., 2006. Background concentrations of PM_{2.5} and Ozone in British Columbia, Canada. University of British Columbia report prepared for the British Columbia Ministry of the Environment, Vancouver, B.C.
- Meng, Z., Seinfeld, J.H., 1996. Time scales to achieve atmospheric gas-aerosol equilibrium for volatile species. *Atmospheric Environment*, 16, 2889-2900.
- Merrill, J.T., 1989. Atmospheric long-range transport to the Pacific Ocean. *Chemical Oceanography*, 10, 15-50.
- Monks, P.S., 2000. A review of the observations and origins of the spring ozone maximum. *Atmospheric Environment*, 34, 3545-3561.
- Nowak, J.B., Parrish, D.D., Neuman, J.A., Holloway, J.S., Cooper, O.R., Ryerson, T.B., Nicks, D.K. Jr., Flocke, F., Roberts, J.M., Atlas, E., de Gouw, J.A., Donnelly, S., Dunlea, E., Hubler, G., Huey, L.G., Schauffler, S., Tanner, D.J., Warneke, C., Fesenfeld, F.C., 2004. Gas-phase characteristics of Asian emission plumes observed during ITCT 2K2 over the eastern North Pacific Ocean. *Journal of Geophysical Research*, 109, doi:10.1029/2003JD004488.
- Olson M.P., Oikawa K.K., 1989. Interannual variability of transboundary sulphur flux. *Atmospheric Environment*, 23, 333-340.
- Olson, M.P., Voldner, E.C., Oikawa, K.K., 1983. Transfer matrices from the AES-LRT model. *Atmosphere Ocean*, 31, 344-361.
- Olszyna, K.J., Bailey, E.M., Simonaitis, R., Meagher, J.F., 1994. Ozone and NO_y Relationships at a Rural Site. *Journal of Geophysical Research*, 99, 14557-14563.
- Oltmans, S. J., Lefohn, A.S. Harris, J.M., Galbally, I., Scheel, H.E., Bodeker, G., Brunke, E., Claude, H., Tarasick, D., Johnson, B.J., Simmonds, P., Shadwick, D., Anlauf, K., Hayden, K., Schmidlin, F., Fujimoto, T., Akagi, K., Meyer, C., Nichol, S., Davies, J., Redondas, A., Cuevas, E., 2006. Long-term changes in tropospheric ozone. *Atmospheric Environment*, 40, 3156-3173.
- Paraskevopoulos, G., Singleton, D.L., McLaren, R., 1995. Hydrocarbon Reactivity Scales: A Critical Review. National Research Council Report No. ER-1344-955, March 1995.
- Pryor, S.C., McKendry, I.G., Steyn, D.G., 1995. Synoptic-Scale Meteorological Variability and Surface Ozone Mixing Ratios in Vancouver, British Columbia.” *Journal of Applied Meteorology*, 34, 1824-1833.

Raven, H., 2004. ⁷Be as a Tracer of Stratospheric Contribution to Ground Level Ozone at Harlech, Alberta. 39th CMOS Annual Congress, Vancouver BC, Canadian Meteorological and Oceanographic Society.

Rizzo, M.J., Scheff, P.A., 2004. Assessing ozone networks using positive matrix factorization. *Environmental Progress*, 23, 110-119.

Roberts, J.M., Flocke, F., Chen, G., de Gouw, J., Holloway, J.S., Hubler, G., Neuman, J.A., Nicks, D.K., Jr., Nowak, J.B., Parish, D.D., Ryerson, T.B., Sueper, D.T., Warneke, C., Fesefeld, F.C., 2004. Measurement of peroxy-carboxylic nitric anhydrides (PANs) during the ITCT 2K2 aircraft intensive experiment. *Journal of Geophysical Research*, 109, doi:10.1029/2004JD004960.

Savoie, D.L., Prospero, J.M., Salzman, E.S., 1989. Nitrate, non-seasalt sulfate and methanesulfonate over the Pacific Ocean. *Chemical Oceanography*, 10, 220-251

Schichtel, B.A., Husar, R.B., 2001. Eastern North American transport climatology during high- and low-ozone days. *Atmospheric Environment*, 35, 1029-1038.

Simmonds, P., Derwent, R., Manning, A., Spain, G., 2004. Significant growth in surface ozone at Mace Head, Ireland. 1987-2003. *Atmospheric Environment*, 38, 4769-4778.

Singh, H.B., Ludwig, F.L., Johnson, W.B., 1978. Tropospheric ozone: concentrations and variabilities in clean remote atmospheres. *Atmospheric Environment*, 12, 2185-2196.

Sirois A., 1998. A Brief and Biased Overview of Time-Series Analysis or How to Find that Evasive Trend. In *Proceedings of the Workshop on Advanced Statistical Methods and their Application to Air Quality Data Sets*, (Helsinki, 14-18 September 1998). Report WMO TD No. 956, World Meteorological Organization, Geneva, Switzerland.

Streets, D.G., Tsai, N.Y., Akimoto, H., Oka, K., 2001. Trends in emissions of acidifying species in Asia, 1985–1997. Part 2. *Water, Air, Soil Pollution*, 130, 187–192.

Tanimoto H., 2007. Interannual variations and recent trends of surface ozone in East Asia: Integrated observations and chemical transport model analysis. National Institute for Environmental Studies, Japan. Presented at the Joint Task Force on Hemispheric Transport of Air Pollution and World Meteorological Organization Workshop 24-26, Geneva, Switzerland, January, 2007.

Tarasick, D.W., Fioletov, V.E., Wardle, D.I., Kerr, J.B., Davies, J., 2005. Changes in the vertical distribution of ozone over Canada from ozone sondes: 1980–2001. *Journal of Geophysical Research*, 110, D02304.

Thompson, M.L., Reynolds, J., Cox, L.H., Guttorp P, Sampson, P.D., 2001. A review of statistical methods for the meteorological adjustment of tropospheric ozone. *Atmospheric Environment*, 35, 617–630.

U.S. EPA, 1998. Reference Method for Determination of Fine Particulate matter as PM_{2.5} in the Atmosphere, U.S. Environmental Protection Agency.

U.S. EPA, 1999. Compendium of Methods for the Determination of Toxic Organic Compounds in Ambient Air - Second Edition, U.S. Environmental Protection Agency, EPA/625/R-96/010b, January 1999.

U.S. EPA, 2003. National Air Quality and Emissions Trends Report, 2003 Special Studies Edition, EPA 454/R-03-005. US Environmental Protection Agency, Washington, D.C.

U.S. EPA, 2006a. NO_x Budget Trading Program: 2005 Program Compliance and Environmental Results. Office of Air Quality Planning and Standards and Office of Atmospheric programs, EPA430-R-06-013, September 2006.

U.S. EPA, 2006b. VOC Fugitive Losses: New Monitors, Emission Losses, and Potential Policy Gaps. Proceedings of Workshop, Research Triangle Park

U.S. EPA, 2007. United States Environmental Protection Agency National Emissions Inventory (NEI), Emissions Inventory & Analysis Group; Air Quality Assessment Division, Office of Air Quality Planning and Standards U.S. EPA, Research Triangle Park, NC.

U.S. EPA, 2008. NO_x Budget Trading Program Report: 2007 Compliance and Environmental Results. Office of Air and Radiation, Office of Atmospheric Programs, Clean Air Markets Division, Washington, D.C., EPA-430-R-08-008, December 2008.

Vet, R., Brook, J., Ro, C., Shaw, M., Narayan, J., Zhang, L., Moran, M., Lulis, M., 2005. Chapter 3: Atmospheric response to past emission control programs In: 2004 Canadian Acid Deposition Science Assessment, Environment Canada, Gatineau.

Vet R., Ro C.-U., 2008. Contribution of Canada-United States transboundary transport to wet deposition of sulphur and nitrogen oxides – a mass balance approach. *Atmospheric Environment*, 42, 2518-2529.

Vingarzan, R. Fleming, S. Meyn, S., Schwarzhoff, P., Belzer, W., 2007. Air Quality and Transboundary Transport at Christopher Point, British Columbia. Meteorological Services of Canada, Environment Canada.

Vingarzan, R., 2004. A review of surface ozone background levels and trends. *Atmospheric Environment*, 38, 3431–3442.

- Vingarzan, R., Taylor, B., 2003. Trend analysis of ground level ozone in the greater Vancouver/Fraser Valley area of British Columbia. *Atmospheric Environment*, 37, 2159-2171.
- Vukovich F. M., Fishman J., 1986. The climatology of summertime O₃ and SO₂ (1977–1981). *Atmospheric Environment*, 20, 2423–2433.
- Walker, J. T., Robarge, W.P. Shendrikarc, A., Kimball, H., 2004. Ambient ammonia and ammonium aerosol across a region of variable ammonia emission density. *Atmospheric Environment*, 38, 1235–1246.
- Wang, D.K., Austin, C.C., 2006. Determination of Complex Mixtures of VOC in Ambient Air: An Overview. *Analytical & Bioanalytical Chemistry*, 386, 1089-1098.
- Wang, D.K., Austin, C.C., 2006a. Determination of Complex Mixtures of VOC in Ambient Air: Canister Technology. *Analytical & Bioanalytical Chemistry*, 386, 1099-1120.
- Winkler, P., 1988. Surface ozone over the Atlantic. *Journal of Atmospheric Chemistry*, 7, 73-91.
- Wolff G. T., Lioy, P.J., Wight, G.D., Meyers, R.E., Cederwall, R.T., 1977. An investigation of long-range transport of ozone across the Midwestern and Eastern United States. *Atmospheric Environment*, 11, 797–802.
- Wolff G., Lioy, P.J., 1980. Development of an ozone river associated with synoptic scale episodes in the Eastern United States. *Environmental Science. and Technology*, 14, 1257–1260.
- Yienger, J.J., Galanter, M, Holloway, T.A., Phadinx, M.J., Guttikunda, S.K., Carmichael, G.R., Moxim, W.J, Levy II, H., 2000. The episodic nature of air pollution transport from Asia to North America. *Journal of Geophysical Research*, 105, 931-945.
- Yu, X-Y, Lee, T., Ayres, B., Kreidenweis, S., Malm, W., and Collett, J.L.-Jr., 2006. Loss of fine particle ammonium from denuded nylon filters. *Atmospheric Environment*, 40, 4797-4809.
- Zbinden, R., Cammas, J.-P., Thouret, V., Nedelec, P., Karcher, F., Simon, P., 2006. Mid-latitude Tropospheric Ozone Columns from the MOZAIC program: climatology and interannual variability. *Atmospheric Chemistry and Physics*, 6, 1053–1073.
- Zhang, L., Vet, R., Wiebe, A., Mihele, C., Sukloff, B., Chan, E., Moran, M.D., and Iqbal, S., 2008. Characterization of the size-segregated water-soluble inorganic ions at eight Canadian rural sites. *Atmospheric Chemistry and Physics*, 8, 7133-7151.

CHAPTER 4: Emissions and Sources of Smog Precursors

David Niemi, Patrick George

KEY MESSAGES AND IMPLICATIONS

- Emissions of most smog precursors have decreased over the 1985 to 2006 period except for ammonia. Emissions of primary fine particulate matter have remained relatively stable over this time period.
- Current smog precursor emissions projections are indicating continued reductions into the future, with the exception of ammonia and volatile organic compounds (VOC).
- Past and ongoing efforts to reduce emissions from major industrial and commercial sources are being offset by recent large increases in the petroleum sectors.
- While the emissions inventories adequately capture point source emissions, additional efforts are required to improve the emissions estimates for diffuse (or area) sources.
- To better support air quality modelling, improvements are necessary to better characterize emissions (such as particulate matter and VOC speciation, as well as temporal and spatial emissions distribution).
- The current emissions projections need to be updated to reflect the more recent economic conditions and the latest economic projections using the departmental economic modelling platform to the year 2020 and/or 2030.

4.1 Introduction

Canada compiles comprehensive emissions inventories (EIs) for the following substances, including precursors and contributors to smog formation:

- Criteria Air Contaminants (CAC): total particulate matter (TPM), particulate matter with diameter $< 10 \mu\text{m}$ (PM_{10}), particulate matter with diameter $< 2.5 \mu\text{m}$ ($\text{PM}_{2.5}$) sulphur oxides (SO_x), nitrogen oxides (NO_x), volatile organic compounds (VOC), carbon monoxide (CO) and ammonia (NH_3)
- Heavy Metals (HM): mercury, cadmium and lead, and
- Persistent Organic Pollutants (POPs – 4 polycyclic aromatic hydrocarbons (PAH), dioxins and furans (PCDD/F), and hexachlorobenzene (HCB).

The criteria air contaminants of sulphur oxides (SO_x), nitrogen oxides (NO_x), volatile organic compounds (VOC), ammonia (NH₃), and to some extent primary particulate matter (TPM, PM₁₀, PM_{2.5}) are precursors and contributors to the formation of and ambient levels of ground level ozone (O₃) and particulate matter (PM). The CAC emissions inventories have been compiled annually since 2002 and on a periodic basis since 1970, namely every 2 years from 1970 to 1980, and every 5 years from 1980 to 2000. The emissions inventories from 1985 and onwards have been updated with the latest estimation methodologies and annual inventories have been developed to allow for comparison and trends analysis over time.

The National Pollutant Release Inventory (NPRI) and the Greenhouse Gas (GHG) emissions inventory are the other two main release or emissions inventories compiled by Environment Canada (EC). The GHG emissions inventory compiles emissions of the substances contributing to global climate change and stratospheric ozone depletion, and while comprehensive, will not be discussed in detail within this chapter. The NPRI is an inventory of the reported releases and transfers of over 300 substances by industrial and commercial facilities meeting the reporting requirements. The NPRI is not comprehensive, as its target is mainly releases from individual facilities. The emissions of the CAC substances from facilities have been reported under the NPRI since 2002. The point source emissions form part of the comprehensive CAC emissions inventory, which also includes area or non-point source data. Caution should be exercised when performing any emissions level comparisons between the NPRI and CAC inventories as they vary in purpose, method of calculation, organization and comprehensiveness.

The comprehensive CAC emissions inventories for substances contributing to ground level ozone and ambient fine PM (PM_{2.5}) are compiled using comparable methodologies to the United States and other countries around the world. Canada continually exchanges emissions inventory information and methodologies with the United States Environmental Protection Agency (U.S. EPA). Emissions information is also reported annually to the United Nations Economic Commission for Europe (UNECE) and other bodies under the various protocols and agreements Canada has signed and ratified. Through this exchange of information, Canada and other countries can conduct air quality modelling, quantify transboundary influences, and more adequately characterize and predict ambient ground level O₃ and PM.

Canada has been continuously working on improving the emissions inventories, methodologies and estimation models, working with industries and the U.S. EPA to further the improvements. The methods used to calculate the area sources are updated with the latest information available from the various partner agencies. Some of the sectors recently updated are On-Road Vehicles, Non-Road Engines, and the Oil Sands (see a more complete list in Section 4.5). For the industrial and commercial emissions, Environment Canada works with industries and associations to update their estimation methodologies and perform testing. Most recently, the Upstream Oil and Gas and the Pulp and Paper sectors have been updated through these efforts.

Further information and details on the emissions inventories, historical trends and projections can be found on Environment Canada's website at: www.ec.gc.ca/inrp-npri/.

4.1.1 Chapter Organization

This chapter will focus on emissions of smog precursors, mainly in Canada, but with some information on U.S. trends. The chapter provides an overview of the development of the Canadian emissions inventories, projections of smog precursors and analysis of the changes in the emissions levels. It is not intended to be an extensive treatise on the development of the emissions inventories.

A summary of conclusions from previous assessments is provided first (section 4.2), as many of the emissions updates draw on recommendations from these prior reports. Information is provided on how the emissions inventories (EIs) are updated in the Canadian context with respect to point and area (or non-point) sources, with focus on the CAC pollutants (which are described in section 4.3) and some specific sectors of interest (section 4.4). A discussion follows on improvements that have been made in the most recent EIs (section 4.5). Emissions of smog precursors, their sources and spatial distribution in Canada from the 2005 inventories are discussed in section 4.6. Section 4.7 focuses on the trends and emissions forecasts to 2015 in both Canada and the U.S. The chapter ends with a summary and recommendations for future work in section 4.8

4.2 Conclusions from Previous Assessments

A number of past science assessments have investigated the emissions and sources of smog and smog precursor compounds: 1996 NO_x/VOC Science Assessment (CCME, 1997); 1999 Federal/Provincial Working Group on Air Quality Objectives and Guidelines O₃ and PM Science Assessments (WGAQOG, 1999a, b); 2003 Canada-Wide Standards Science Review of PM and O₃ (CCME 2003a, b); 2001 Precursor Contributions to Ambient Fine Particulate Matter in Canada Report (Environment Canada, 2001); 2004 Canada-United States Transboundary PM Science Assessment (Environment Canada, 2004); and Particulate Matter Science for Policy Makers (NARSTO, 2004). In 2005, NARSTO also conducted an assessment on improving EIs for effective air quality management (NARSTO, 2005). The emissions information presented within this chapter builds upon the knowledge from these past assessments on Canadian emissions of PM and the precursor pollutants which form secondary PM and O₃. Key conclusions from these previous assessments are discussed in the following sections.

4.2.1 Ozone Precursor Emissions

The following list is a summary of findings from previous assessment reports on ozone and ozone precursor emissions:

- Emissions of O₃ precursor compounds vary geographically and seasonally across Canada.
- Anthropogenic emissions of O₃ precursor gases, NO_x and VOC have decreased from 1980 to 1995, although emission changes occurred in different proportions across Canada.
- Observed decreases in urban nitric oxide (NO) concentrations correspond mainly to reductions in motor vehicle emissions.
- Total biogenic emissions of VOC are approximately five times greater than the contribution from anthropogenic VOC sources. However in most urban areas in Canada, anthropogenic VOC exceed biogenic emissions.
- In the 1990 Canadian national emissions inventory, an uncertainty level of approximately 20% was associated with the NO_x emissions estimates; the uncertainty level for VOC emissions was greater than 20%.

4.2.2 PM and PM Precursor Emissions

The following list is a summary of findings from previous assessment reports on PM and PM precursor emissions:

- Emissions of primary PM and PM precursor compounds vary geographically and seasonally across Canada.
- Emissions of primary PM_{2.5} originate mostly from open (non-point) sources such as forest fires, dust and agricultural processes, and to a lesser extent from sources such as industrial facilities, non-industrial fuel combustion, transportation and power generation. (See section 4.4.2.3 for more information on the Open Sources sector.)
- Emissions of the coarse fraction of particulate matter (from PM_{2.5} to PM₁₀) are mainly the result of natural sources such as dust storms, sea salt and forest fires, and anthropogenic sources such as fossil fuel combustion, construction and road salt.
- SO_x is the largest contributor to summer secondary PM_{2.5} formation in eastern Canada. The major sources of SO_x are industrial activities, electrical power generation, transportation and other fuel combustion.
- Transportation is the largest source of NO_x emissions, a major contributor to secondary PM formation; industrial sources, power generation and other fuel combustion activities also contribute to NO_x emissions.

- NH₃ emissions are primarily emitted from agricultural activities, and to a much lesser extent, industrial sources.
- In North America, emissions of SO_x and NO_x are mostly concentrated in the industrial Midwest, north-eastern United States, southern Ontario and southern Quebec. Emissions of NH₃ are typically mostly concentrated in southern Ontario, southern Quebec and the U.S. central Midwest.

4.2.3 NARSTO Emissions Inventory Assessment

NARSTO published an assessment in 2005 (NARSTO, 2005) which provided a more in-depth look into the history and reasons behind the past and current performance of emissions inventories. The following bullets from the NARSTO report summarize the significant weaknesses of the emissions inventories for ambient air quality management in North America:

- Quality assurance and quality control procedures are not strictly applied in the development of most emissions models and inventories, and the documentation of uncertainties and data sources in emissions inventories is not adequate.
- There are significant uncertainties in mobile source inventories particularly regarding the speciation of VOC, the magnitude of CO emissions, and the temporal trend of NO_x emissions.
- Emissions for many important categories such as fine particulates and their precursors, biogenic emissions, toxic air pollutants, NH₃, fugitive emissions, open biomass burning and many other area sources are uncertain and inadequately characterized.
- Emission estimates are frequently based on a small number of emission measurements that may not be representative of real-world activity, either because the samples do not appropriately cover the range of real-world activity patterns or because the measurement methods are not intended to capture such patterns. Thus, the precision and accuracy of estimates developed from such measurements are limited.
- The process for developing information on emissions with the spatial and temporal resolution needed for location-specific air quality modelling is problematic and a source of uncertainty in model results that is not quantified.
- Methods used to estimate emissions of individual chemical species in many emission models are out-of-date and produce estimates that are not reliable.
- Current emission inventories are not developed and updated in a timely manner.

- Differences in current emission inventories in North America create difficulties for jointly managing air quality. (The "differences" are in the emissions estimated for some area sources such as Road Dust and Residential Wood Combustion where statistical and emission factor differences have resulted in discontinuities in emission levels along the borders between countries)

Nonetheless, the NARSTO report on the status of the North American emissions inventories also listed the following strengths in addition to the aforementioned weaknesses:

- The major sources of emissions that affect air quality are well characterized.
- North American emission inventories and models can provide quantitative estimates of emissions at national, state or provincial and county levels.
- Confidence is high in data on emissions of SO₂, NO_x, and carbon dioxide (CO₂) from electric generating units as the result of the development and deployment of Continuous Emissions Monitoring Systems (CEMS) at these facilities.
- Emission trends over time can be used to evaluate the effectiveness of control strategies and projects.

4.3 Smog Precursor Pollutants

4.3.1 Sulphur Oxides (SO_x)

Sulphur oxides are the sum of the gases sulphur dioxide (SO₂) and sulphur trioxide (SO₃). Sulphur oxides are emitted both naturally (e.g. volcanoes & biological processes) and from anthropogenic sources, with the base metals smelting sector accounting for approximately 35% of the Canadian national SO₂ emissions in 2006.

4.3.2 Nitrogen Oxides (NO_x)

Nitrogen oxides (NO_x) are the sum of the gases nitric oxide (NO) and nitrogen dioxide (NO₂). NO_x is a by-product of high temperature combustion and biological reactions in soils. In Canada, the transportation sector is the major contributor to NO_x emissions accounting for 54% of the 2006 national emissions. Other major sources are power plants, combustion sources and metal smelting operations.

4.3.3 Ammonia (NH₃)

Ammonia (NH₃) is the most abundant gas-phase alkaline chemical species in the troposphere. NH₃ emissions are expected to increase while those of other precursor gases (e.g. SO₂, NO_x) are expected to decline because of emission control strategies already in place. This may have implications for NH₃ becoming increasingly important in the formation of smog. Agricultural activity is the major source of NH₃ and is responsible for approximately 90% of national emissions.

4.3.4 Direct PM emissions (PM₁₀ & PM_{2.5})

Particulate matter consists of small discrete masses of solid or liquid material that are individually dispersed in the atmosphere. Direct PM refers to the particulate that is emitted into the atmosphere and not the secondarily formed particulate through atmospheric chemical processes. Only the finer fractions (PM₁₀, PM_{2.5}) of particulate matter will be discussed as they have more of an influence on air quality and are components of the total PM mass. Open sources (as described in section 4.4.2.3) are the major contributors to both primary PM₁₀ and PM_{2.5}. The open source contribution for PM₁₀ is about 90%, while for PM_{2.5} open sources it makes up about 61% of the emissions in 2006.

4.3.5 Volatile Organic Compounds (VOC)

Volatile organic compounds (VOC) are carbon compounds which participate in atmospheric photo-chemical reactions and/or partition to atmospheric aerosols. VOC can be sub-divided into gaseous volatile organic compounds which are in the gas-phase in ambient conditions, semi-volatile organic compounds which partition between gas and aerosol phase at ambient conditions and non-volatile organic compounds which exist only in the aerosol phase at ambient conditions. The transportation sector accounts for over 30% of the 2006 VOC emissions in the Canadian portion of the Pollution Emission Management Area (PEMA) of central and southern Ontario, southern Quebec, the District of Columbia and 18 U.S. states (IJC, 2008). Nationally, the industrial sectors contribute approximately 35% of the 2006 emissions, mainly from oil and gas production.

4.4 NPRI Reporting & CAC Emissions Inventory Process

Emissions inventories are a compilation of estimates for point, area and mobile sources that are combined to form the overall comprehensive inventory. Facilities reporting under the NPRI mandatory reporting program make up the point sources. The reported information includes

releases from various points such as smokestacks less than 50m in height, other lower level sources, fugitive, storage, and other emissions sources. VOC speciation is also reported under the NPRI.

Beginning in 2002, facilities meeting the emissions thresholds and other conditions for reporting were required to report their CAC emissions to the NPRI. The authority under Canadian Environmental Protection Act, 1999 (CEPA 1999) was used to add these emissions into the NPRI, allowing for facilities to estimate their own emissions and facilitate broader use of the detailed, facility level inventories.

Emissions reporting is required when emissions are at or above the thresholds which vary from 300 kg for PM_{2.5} through 20 tonnes for SO_x, NO_x, and TPM. Beginning in 2003, the requirements were changed to require reporting of 60 VOC species (isomers, compounds and compound groupings), and the exemption for the Upstream Oil and Gas sector was removed. This led to about 10,000 facilities reporting to the NPRI in 2005, up from about 2600 in 2001. Details on reporting, databases of reported information and additional information is available from Environment Canada's website (www.ec.gc.ca/pdb/npri/).

The area and mobile sources are estimated using various methodologies, statistics, emission factors and models. Canada estimates its emissions in a manner compatible to those of the United States and most UNECE countries. Some variations in methodologies are employed to account for available information, differences in technology, emissions control regimes and meteorological conditions.

CAC emissions inventories are prepared by Environment Canada in collaboration with the provincial, territorial and regional emissions inventory experts to ensure that the inventory is the best possible representation of the emissions for the year in question. The CAC emissions inventory process is a very detailed, time-intensive process which involves examining all the NPRI-reported emissions, obtaining statistics, estimating the area sources, searching and developing new methodology improvements, and reconciling point and area source emissions. The inclusion of area source emissions estimates results in improved comprehensiveness of the emissions inventories.

4.4.1 Point Sources

Point source emissions are those that are identified and specifically reported for an individual facility. In Canada, this information is obtained from facilities reporting to the NPRI mandatory reporting program and incorporated into the CAC emissions inventories. In conjunction with the NPRI program, the information is analyzed to ensure that the estimates for each facility are free from reporting errors (such as incorrect units) and that any large annual variations are in fact true and not due to a miscalculation.

Emission estimates for point sources are further analysed to ensure completeness. For example, if the reporting threshold was met for one of the smog precursor substances, the unreported emissions need to be adequately accounted for in the area sources emissions estimates, ensuring that double counting of emissions is avoided. While attempting to estimate and attribute the unreported emissions to facilities would improve the data for air quality modelling purposes, not enough information is available to accurately evaluate the emissions levels. In many cases, it is assumed that the emissions levels would not have a great impact on model results, and the resources are not available to perform these detailed calculations on over 8500 facilities annually.

The area source emissions estimates are also used to capture emissions not reported to the NPRI by facilities. For example, in the commercial fuel combustion sector, many facilities meet the requirements for NO_x reporting, but due to low sulphur concentration in fuels, are not required to report SO_x emissions. These SO_x emissions are then accounted for in the area source estimates for fuels burnt in this sector.

For the 2005 CAC emissions inventory of the smog precursors, the NPRI-reported facility emissions accounted for a high of about 90% of the SO_x emissions to a low of 15% of the VOC emissions. Facilities accounted for 38% of the NO_x emissions, 36% of the NH₃ emissions, and 23% to 28% of the emissions of the three PM fractions. These relative contributions of the NPRI-reported facility emissions were expected, as sources such as transportation, residential fuel use and others are not required to report to the NPRI. Further, in some sectors such as the Upstream Oil and Gas sector, there are numerous sources which do not individually meet the requirements for reporting, but due to their number (over 3700 Upstream Oil and Gas installations report to the NPRI), are relatively large contributors to the emissions inventory

4.4.2 Non-Point Sources

Non-point sources are those that are generally large in number and occur over large areas. The non-point sources include area, transportation and natural sources, which are often compiled or estimated based on calculations or model results. It should also be noted that area source calculations are done for most sectors, even where information is reported under the NPRI. This is performed to ensure complete coverage of the emissions from the sectors when point and non-point emissions are reconciled.

For discussion purposes, the non-point sources are broken down into Area Sources, Transportation Sources, Open Sources and Natural Sources.

4.4.2.1 Area Sources

The Canadian emissions inventories of the smog precursors comprise over 60 non-point or area sources such as Fuel Combustion in the various Industrial, Commercial and Residential sectors, Residential Wood Combustion, and many Solvent Use categories. Many of these sectors also include sub-classes in order to further refine the emissions estimates. For example, the Agriculture sector includes sub-classes for livestock type, source of emission, livestock housing type, manure spreading, and manure fermentation and spreading.

Environment Canada's comprehensive emissions inventories of the precursors (www.ec.gc.ca/inrp-npri/default.asp?lang=en&n=F2B66EB1-1) are highly dependent on the quantitative information produced by Statistics Canada (SC) for the calculation of the area source emissions estimates. Some examples of the types of statistical information used are fuel consumption, population, construction amount information, mining data, cement production, etc.

Environment Canada and Statistics Canada (SC) are working together to ensure the continued flow of information to meet Canada's emissions reporting needs and to determine if there is additional information collected by SC that may be of use to EC. Emissions inventories require and utilize physical quantity information and not economic or dollar value information. Attempting to use dollar value of expenditures or gross domestic product for the sector/activity to derive emissions quantities adds another layer of complexity and potential error to the calculations due to factors such as inflation, commodity price variation in response to supply and demand, and the need to account for imports and exports. Construction is a good example of this complexity. Dollar value is available for the expenditures on road construction but this then needs to be translated into the actual lengths of road constructed and material removed and hauled.

The Industrial and Commercial sectors area source estimates follow mainly the methodologies published by the U.S. EPA (2008) in their Compilation of Air Pollutant Emission Factors (AP 42) manual. Some variations occur due to differences in the statistical information available and the results of specific studies to investigate the emissions from the sectors. Section 4.5 lists many of the sectors that EC has worked on since the NO_x/VOC Science Assessment (CCME, 1997) to improve the emissions inventories. The work on these sectors has resulted in improved methodologies, updated emission factors, and/or improved allocation of the emissions geographically across Canada.

Most statistical sources of information are not available until one to one and a half years after the year in question. For the 2005 emissions compilation, most statistics didn't start becoming available until late spring/early summer of 2007. This is after the emissions inventories are published, so the initial version of the inventories utilizes many of the statistics for the area

sources from the previous year, in this case, 2004. Where the statistics for major sources such as fuel combustion and production are available prior to publication, every effort is made to incorporate these.

Previous year statistical data is used rather than trying to predict annual sector growth for the area sources, as uncertainties can be large when using predictive techniques. The use of expected annual sector growth from the year 2000 for emissions projections was analysed for feasibility of use. It was found that often the expected changes on the annual level did not match the actual changes. Furthermore, meteorological conditions and economic and other factors had a large impact on the actual annual variations, which are impossible to predict on a yearly basis. For example, in the Agriculture and Solvents sectors, which are predominantly accounted for by area sources, the use of projected statistics was shown to cause higher variations compared to the updated statistics than was observed when comparing previous year data to the updated statistics. Also, for area source estimates for Industrial and Commercial sectors where the area source contribution is small, analysis showed that there was minimal impact in using previous year over the current year statistics.

4.4.2.2 Transportation

The Transportation category is made up of emissions of many types of on and off road vehicles and equipment. There are 28 different classes of on-road vehicles, over 100 types of off-road engines (outboards, mining trucks, lawn mowers, etc.), as well as aviation estimates for many engine types, rail locomotives, and even estimates of the particulates generated from brake and tire wear. This encompasses everything from aviation, commercial marine, cars and trucks, mining and other industrial or commercial equipment, outboard motors, yard equipment to rail transportation, and for the purposes of this discussion, dust from on-road vehicles (dust from paved and unpaved roads are normally included in the Open Sources sector - see section 4.4.2.3).

To estimate the emissions from such a diverse collection of engine types, ages, usage pattern and other factors, Environment Canada utilizes models which account for all of these factors and more to produce emissions estimates:

- On-Road Transportation is estimated using a Canadian version of U.S. EPA's MOBILE 6.2 model. The model has been modified to account for years when emission standards were not harmonized between Canada and the U.S.; additional improvements to PM and other pollutants that were being implemented in the U.S. EPA emissions modelling system Motor Vehicle Emission Simulator (MOVES); and to incorporate additional Canadian vehicle testing information and developments in Canadian policy.

- Commercial Marine is estimated using details of domestic and international ship movements and ferry vessels in conjunction with information on engine types, speeds, and fuel usage characteristics. Work is underway with the U.S. EPA to incorporate GPS movement data and more detailed ship characteristics along with typical operation procedures in response to legal requirements to develop more precise spatially and temporally allocated emissions.
- The emissions from industrial, commercial, private and recreational equipment are based on the U.S. EPA's NONROAD model which incorporates Canadian details on the numbers and types of engines, usage patterns ages, and emissions characteristics to produce emissions estimates. Work has been performed to ensure that the mining fleet from the Oil Sands is adequately characterized as well as to improve the estimates of the various types of equipment and engines in use across the country.
- Aviation emissions are estimated with information from Transport Canada, utilizing detailed movement information, aircraft engine and fuel use information in conjunction with emission rates for the various engine types and classes.
- Rail emissions are developed with data provided by the Rail Association of Canada, utilizing details on the numbers and operational characteristics of the various types of engines in use across the country.
- Road Dust emissions are estimated using a model, developed by Environment Canada, which is based on the EPA's road dust methodology (U.S. EPA, 2006b). The model utilizes weather observations across the country and road silt content information to estimate emissions. Work is underway to continually improve this model to incorporate more traffic volume information from municipalities across the country and their dust mitigation efforts.

4.4.2.3 Open Sources

The Open Sources sector is a collection of sources that are not entirely the direct result of human activity, but do not readily fit into any other category. This category incorporates agricultural emissions, construction operations, mine tailings, and prescribed burning. Road dust is discussed in the Transportation section (4.3.2.3) and forest fires in the Biogenics section (4.3.2.5) of this chapter, although these two categories are normally included in the Open Sources sector in the inventories.

Sources under this category are generally large emitters of PM and NH₃. Emissions from Prescribed Burning (the controlled burning of forested areas for forest fire prevention, vector control, and public safety) are estimated using U.S. EPA methodologies (U.S. EPA, 1996), with variations to account for local burning conditions and vegetation. The incidence of prescribed burning varies annually from province to province.

Agricultural emissions under the Open Sources sector include emissions from livestock and dust from agricultural tillage. Canada utilizes emission rates derived from mainly Canadian and United States sources in conjunction with agricultural statistics (e.g.: crops, tillage, livestock counts, fertilizer sales) to estimate the emissions of NH_3 and some VOCs. Agricultural tillage is estimated using U.S. EPA methodologies along with surface area obtained from crop statistics.

Particulate emissions from mine tailings are estimated using U.S. EPA methodologies along with information on mine tailing surface areas. The latter are derived from consultant reports and statistical information.

4.4.2.4 Natural Sources (Biogenics & Forest Fires)

Biogenics are the VOC emissions from vegetation and nitric oxide (NO) emissions from soils. These are estimated by Environment Canada utilizing the US EPA's BEIS v3.09 biogenics model in combination with the national weather observations data and forest/crop acreage. The model is updated with emission rates of NO_x for Canadian soils and VOC from tree species.

Forest Fires are estimated using a model developed to address the various types of vegetation and fires that occur while incorporating impacts of meteorological conditions. For example, the emissions from a fire burning rapidly across the crowns of trees are different from the emissions from a slower burning fire at the forest floor, which slowly consumes the vegetation as it advances. Therefore there is a need to characterize forest fire type.

For Forest Fires and Prescribed Burning, newer methodologies exist that utilize satellite observations, but due to resource constraints these methodologies have not been implemented.

4.4.3 Quality Control and Uncertainties

4.4.3.1 Quality Control

To ensure the quality of the national emissions inventories, annual quality control verifications are performed on the statistics, the emissions reported by facilities, and the emission estimates for the point, area, transportation and natural sources. Quality control verifications include comparison with previous year statistics and emission estimates; identification of the causes for the variations in the emissions and the statistics; and validation of the emission estimates with ambient air quality measurements and air quality modelling results.

The information submitted under the NPRI mandatory reporting program is analyzed to ensure that the estimates for each facility are free from reporting errors (such as incorrect units) and that any large annual variations are in fact true and not due to a miscalculation.

Another portion of the emission inventory quality control involves feedback from air quality modellers. During modelling for ground-level ozone and ambient PM, the modellers occasionally observe model concentration results which are in disagreement with ambient measurements. Back trajectory and other model analyses are performed to identify potential causes for the discrepancy, and these are forwarded to the emissions inventory personnel for review. At issue may be the magnitude of the emissions, or the temporal distribution or VOC speciation. Depending on the source type (point, area, or transportation), these are addressed through the NPRI mandatory reporting QC process or through examination of the area and transportation source data and spatial allocation.

The quality control process requires many iterative steps and the information is reviewed several times for the individual sources and sectors, and at different aggregate levels for each pollutant.

4.4.3.2 Uncertainties

It is important to recognise that the uncertainty of the emission estimates for selected sectors and pollutants can vary considerably. For example, many of the diffuse sources such as road dust, construction activities and residential biomass combustion have a relatively high uncertainty compared to the information reported by industrial facilities to the NPRI program.

Table 4.1 Proportions of NPRI reported emissions by estimate method (Environment Canada, 2010a)

	PM _{2.5}	SO _x	NO _x	VOC	NH ₃
Mass Balance	1.01%	24.30%	0.78%	15.29%	7.93%
Emission Factors	Not Used				
Site Specific Emission Factors	19.76%	3.60%	8.01%	8.97%	5.47%
Published Emission Factors	40.26%	5.08%	50.96%	46.17%	28.91%
Monitoring or Direct Measurement	Not Used				
Continuous Emission Monitoring	0.02%	42.22%	23.70%	0.02%	0.64%
Predictive Emission Monitoring	0.75%	0.99%	0.47%	0.13%	8.01%
Source Testing	19.64%	4.71%	8.95%	12.96%	31.55%
Engineering Estimates	18.57%	19.09%	7.12%	15.53%	17.49%
Not Applicable				0.93%	0.00%
No Information Available	Not Used				

The information reported to the NPRI is based on a variety of estimation methods. Table 4.1 summarizes the percentage of the individual smog precursor emissions estimated by the various methods.

Highlighted in the table are the highest proportions of emissions by estimation method. For $PM_{2.5}$, SO_x , and NO_x , over 50% of the emissions are reportedly based on some form of emission factor, while for SO_x , continuous emissions monitors based estimates account for the highest proportion of emissions. Ammonia has the highest proportion of emissions based on source testing reported.

The NPRI mandatory reporting program requires reporting of SO_2 emissions, while the emission inventories are of SO_x . For most sources the proportion of the SO_3 is low – about 1% – but where electrostatic precipitators are installed, the proportion of SO_3 can be almost 30%, based on SO_x speciation profiles (Possiel *et al.*, 2001).

Efforts have been made to reduce the uncertainties in the inventories. Emissions testing has been implemented for a number of sectors. There is continued work on surveys and other collaborative work with industry to improve the detail and amount of information on which estimates are based. Additional Canadian vehicle testing information has been incorporated, as well as improved vehicle mileages based on Inspection and Maintenance (I&M) program data.

The Area, Transportation, Open and Natural sources have a wide variety of uncertainties that at the moment can only be qualified, not quantified. The joint Canada, United States and Mexico NARSTO PM Assessment provides a listing of the estimated confidence level of emissions estimates (see Table 4.8 of NARSTO, 2004). These estimates are provided for some of the major categorization of emissions sources, giving each a low–high confidence ranking.

Sources such as road dust and construction dust have a high degree of uncertainty given the variable nature of the silt fraction, moisture content, traffic volumes and the mitigation methods applied. Municipalities across the country have in place street cleaning regimes to reduce/minimize road dust emissions; however, implementing this in the estimation methodologies on a provincial or national basis has not been realized to date. Similarly with construction, it is difficult to implement dust mitigation efforts or requirements in the estimation methodology.

Other sources such as fuel combustion have variable certainty depending on the pollutant. SO_x estimates have a higher degree of certainty nationally and provincially as the sulphur contents are quite well known. NO_x emissions, however, are highly dependant on combustion devices.

The spatial allocation of emissions is another area of uncertainties. Emissions allocations are constantly being evaluated in conjunction with air quality modellers and efforts are ongoing to improve them.

4.5 Inventory Updates and Improvements

4.5.1 Inventory & Data Quality Updates and Improvements

Environment Canada continuously improves the emissions inventories for many sectors through specific studies, collaborative efforts by EC and industries, emissions testing, and through the incorporation of methodological improvements instituted by other agencies such as the U.S. EPA.

Since the NO_x / VOC Science Assessment (CCME, 1997), Environment Canada has made many improvements to the emissions inventories of precursors. Chief among these are:

- Industrial and Commercial emissions reporting under the NPRI
- Emission by stacks and low level sources
- Speciation of VOC
- Temporal information
- Residential wood combustion: New surveys and updated emission factors representing how wood burning devices are actually used.
- On-road and non-road vehicles and engines using MOBILE 6.2C & NONROAD models: Upgrade of the previous MOBILE 5C model and fuel calculations.
- Road dust and Construction: Incorporation of new emission rates, more detailed statistical information, and meteorological impacts.
- Solvents: Updated studies of the individual substances.
- Oil sands: Updated equipment use and emission rate information; improved facility estimates.
- Upstream oil and gas: Collaborative federal, provincial and industry survey of emissions sources, equipment and usage correlating to the actual production of oil and gas at individual installations.
- Agricultural sources: In-depth review of the major livestock categories, ammonia emissions sources and characterization, survey of farming practices, feed manufacturers and fertilizer use.

The above updates to the emissions inventories have led to some fairly large changes (see sections 4.4.2 for some examples) in the emissions inventories of the precursors. Work is still underway to continuously improve the current, historical and projected emissions from all sources. These updates and other newly available information are reflected in Environment Canada's revised historical emissions inventories for the years 1985 to 2000.

Some future enhancements to the inventory include: a version of the U.S. EPA's new on-road transportation model MOVES adapted to Canadian conditions (not finalized at the time of scoping for this assessment); incorporation of transportation demand modelling for major urban centres; updated upstream oil and gas inventory; and incorporation of collaborative work on oil sands mine face emissions.

Through the NPRI, Environment Canada has undergone stakeholder negotiations from 2005 to 2007 to improve the data reported to the NPRI. As a follow-up to this effort, Environment Canada has begun working with specific industrial sectors to improve the data submitted to the NPRI. In 2007, work began with the Aluminum, Iron and Steel, and Coal Fired Electricity Generation sectors. The work includes updating historical emissions where possible, ascertaining what is included in the currently reported emissions, and working towards emissions measurements and reporting guidelines for the sectors.

4.5.2 Emissions Inventory Reorganization

The emissions inventories of the smog precursors and other pollutants were reorganized in 2007–2008 to account for their evolution since the 1985 emissions inventory. The inventories initially focused on larger emitting facilities of 100 tonnes or more of any CAC. About 2000 to 4000 facilities reported for 1985 through 1995. Up to and including the year 2000, inventories of facility emissions were developed by the provincial experts, forming the basis of the CAC emissions inventories. Facility-level emissions were not available to the public due to confidentiality concerns.

Beginning with the inception of the CAC emissions reporting under the NPRI in 2002, the facilities emissions data for the year 2002 and beyond became publicly available. They now form the basis for the provincial/territorial and national inventories. The year 2005 emissions inventory now contains over 8000 facilities (Environment Canada, 2009a). This large increase in the number of included facilities as well as sectors of interest to various programs has led to a reorganization of the inventory.

Each facility included in the inventory was briefly researched to determine the most appropriate sector allocation. The following is a brief summary of the changes made:

- Clean Air Industrial Regulatory Agenda (CAIRA) sectors singled out;
- Sectors broken down to provide finer resolution of emitting sources;
- Facilities moved to more appropriate sectors (e.g.; Secondary Iron and Steel, Waste Water Treatment, etc.);
- “Other Industries” broken up into sub-sectors;

- Some sector organization made to accommodate emissions projections;
- New sectors created to accommodate areas of increasing interest, e.g. Waste: Landfills, Sewage Treatment, and Energy from Waste.

Generally, the emissions levels for the major categories (e.g. Industrial, Miscellaneous, etc.) have remained the same, with only minor adjustments.

4.6 Canadian Smog Precursor Emissions

The latest comprehensive CAC emissions inventory available at the time of this assessment is for the 2006 data year. Table 4.2 is a summary of the national emissions information for this data year, divided by the major sector categories. The EI incorporates the improvements in the inventories as listed in Section 4.5 (except for ammonia which will be incorporated at a later date).

Table 4.2 2006 smog Precursor Emissions by Category (Environment Canada, 2010b)

	PM ₁₀	PM _{2.5}	SO _x	NO _x	VOC	NH ₃
Industrial Sources	199.7	113.8	1337.4	719.7	828.6	21.6
Non Industrial Fuel Combustion	127.6	119.5	518.9	305.9	161.4	2.2
Transportation	67.7	61.3	62.1	1201.3	573.5	21
Incineration	0.5	0.4	1.9	1.9	1.3	0.1
Miscellaneous	8.8	8.7	0.1	0.8	367.3	1.7
Open Sources	5422	814.4	0.6	3.4	308.4	504.3
Biogenics and Forest Forest	256.5	211.2	0.2	79.2	340.8	5.3
Total With Open Sources	6,083	1,329	1,921	2,312	2,581	556
Total Without Open Sources, Biog, & Forest Fires	404	304	1920	2230	1932	46.6

4.6.1 Sources

4.6.1.1 National

Table 4.3 Major Sectors Contributing to the 2006 National Emissions Inventory (Environment Canada, 2010b)

	PM _{2.5}	SO _x	NO _x	VOC	NH ₃
Industrial Sources					
Aluminum	0.40%	4%	0.10%	0%	0%
Cement and Concrete	0.80%	2%	1.70%	0%	0.20%
Non-Ferrous Smelting	0.40%	35%	0.20%	0%	0.10%
Wood & Pulp and Paper	4.20%	3.10%	2.30%	4.00%	0.70%
Chemical Industry	0.10%	1.20%	1.20%	0.60%	1.90%
Upstream Petroleum	1.10%	17%	21%	24%	0.90%
Downstream Petroleum	0.30%	5.10%	3.40%	5.10%	0%
Other Industrial	2.80%	3.00%	2.60%	2.90%	0.10%
Non-Industrial Fuel Combustion					
Electricity Generation	0.50%	24%	10%	0.10%	0.10%
Residential Wood	10%	0.10%	0.50%	7.00%	0.20%
Transportation					
Marine Transport	0.50%	1.70%	5.20%	0.40%	0.10%
Heavy Duty Diesel Vehicles	0.60%	0.20%	12%	0.40%	0.10%
Non-Road	4.30%	1.30%	26%	14%	0.10%
Other Onroad Transport	0.20%	0.10%	11%	11%	3.60%
Miscellaneous					
Solvents and Printing	0.00%	0%	0%	16%	0%
Opent Sources					
Agriculture (Fertilizer)	0.10%	0%	0%	0%	29%
Agriculture (Animals)	2.70%	0%	0%	13%	61%
Agriculture (Tilling)	2.20%	0%	0%	0%	0%
Construction	19%	0%	0%	0%	0%
Road Dust	48%	0%	0%	0%	0%
Sum of Sources	98%	97%	97%	99%	99%
Total without Biogenics [kt]	1,118	1,921	2,233	2,240	551

There are many sectors that contribute a large proportion of the emissions inventory for individual contaminants. Table 4.3 shows the major sectors contributing to the emissions inventory on a national basis.

The numbers in bold in Table 4.3 indicate the sectors that are the major contributors to the emission totals for the individual contaminants. Many of these sectors are major contributors for one or two of the smog precursors, while a few sectors have a larger spectrum of pollutant emissions (e.g. the Petroleum sectors.) Table 4.3 shows the magnitudes of the large emitting sectors such as Smelting, Petroleum, and Electricity Generation and other Canadian industrial activities. Other non-industrial sectors also contribute substantially to the national emissions picture, including Transportation, Residential Wood and Agriculture.

4.6.1.2 Regional

Canada is a large country with a range of economic or industrial bases that vary by region or province. These differing bases lead to each province contributing in varying proportions to the total national emissions of each of the smog precursors.

Figures 4.1 to 4.5 show the relative contribution by province to the total national 2006 emissions of $PM_{2.5}$, SO_x , NO_x , VOC and NH_3 , including Open Sources but excluding Biogenics and Forest Fires to emphasize the anthropogenic portion of the emissions. The major sectors contributing to the national smog precursor emissions vary depending on the pollutant (see Table 4.2).

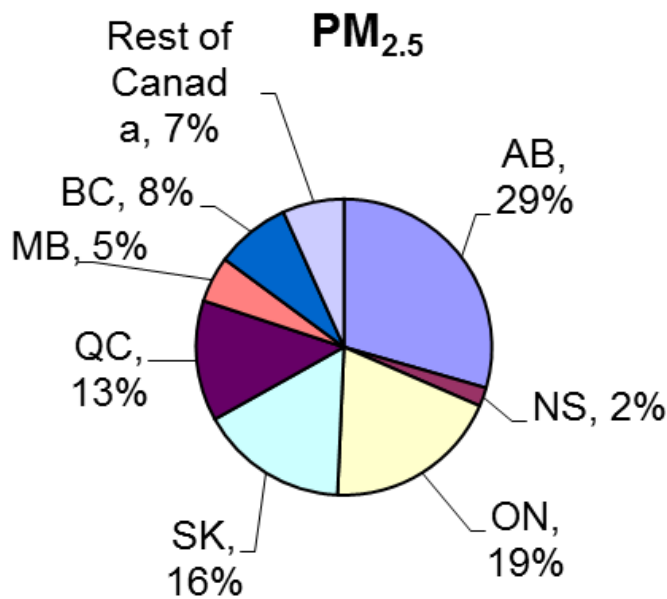


Figure 4.1 Relative Provincial Contributions to the 2006 National Emissions of $PM_{2.5}$ (Environment Canada, 2010b)

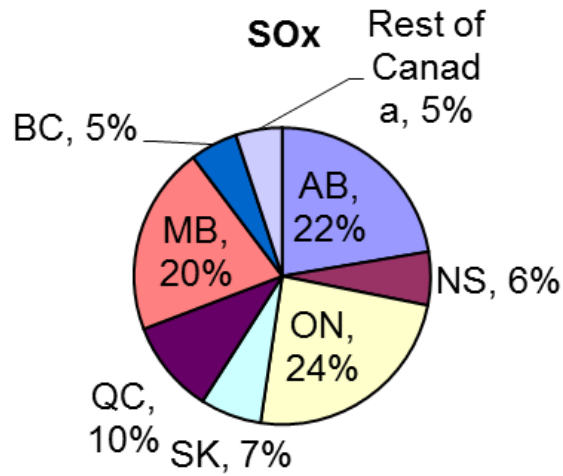


Figure 4.2 Relative Provincial Contributions to the 2006 National Emissions of SO_x (Environment Canada, 2010b).

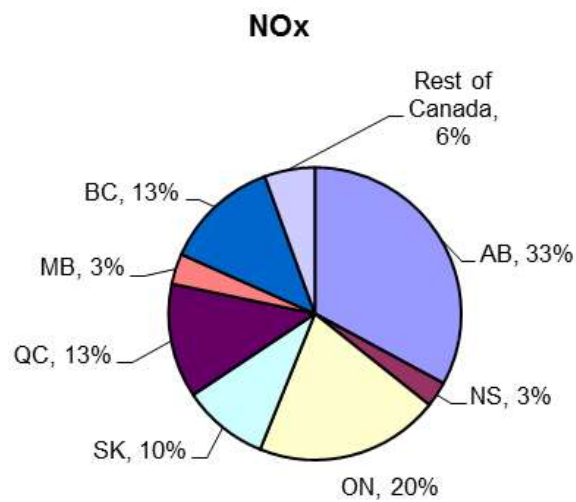


Figure 4.3 Relative Provincial Contributions to the 2006 National Emissions of NO_x (Environment Canada, 2010b).

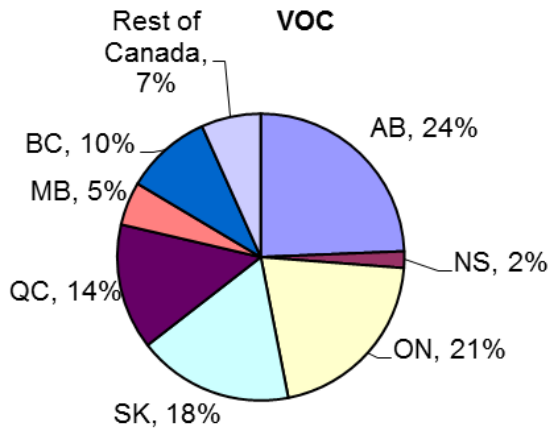


Figure 4.4 Relative Provincial Contributions to the 2006 National Emissions of VOCs (Environment Canada, 2010b).

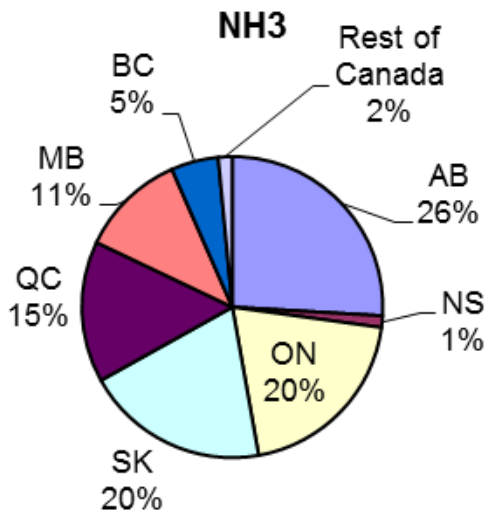


Figure 4.5 Relative Provincial Contributions to the 2006 National Emissions of NH₃ (Environment Canada, 2010b).

The 2006 relative provincial contributions are influenced by the dominant contributing sectors in each province. Alberta, with its large Agriculture sector and Upstream and Downstream Petroleum industry, is the largest contributor of smog precursors except for SO_x. Ontario, with 39% of Canada's population in 2006, large Non-Ferrous Smelting and Refining, fossil-fuel fired Electricity Generation, Agriculture, and other contributing sectors, is the second largest smog precursor emitting province and the leader in SO_x emissions. Quebec, Manitoba and Saskatchewan rank third or lower depending on the pollutant. Their dominant contributing sectors are Non-Ferrous Smelting and Refining and Agriculture.

For the most part, the territories and Atlantic Canada are generally minor contributors to Canada's overall emissions. In Atlantic Canada, however, the Fossil Fuel Electricity Generation and Non-Ferrous Smelting and Refining sectors in Nova Scotia and New Brunswick are the major contributors of SO_x and NO_x . While generally the levels are not significant at the national level, they are important in the regional context.

4.6.1.3 Geographical Distribution of Emissions in North America

Air quality is influenced by local emissions as well as by emissions upwind of the monitoring location. Figures 4.6 to 4.10 provide graphical representations of the location and magnitude of emissions across the northern United States and southern Canada on a 42 km modelling grid domain. The emissions density maps show relative intensity. They are based on the national annual 2006 emissions (US EPA, 2002a; Environment Canada, 2009b), spatially distributed across the two countries for atmospheric modelling.

Figures 4.6 to 4.10 show the locations of the major $\text{PM}_{2.5}$ emissions sources from industrial activity, Agriculture and Road Dust. The SO_x and NO_x images clearly show the locations of the Smelting and Refining and Fossil Fuel Fired Electricity Generation facilities. Major urban centres with high traffic density are visible (see the green & yellow in the figures). The VOC image depicts the influence of the Agriculture sector (mainly animal operations) and Biogenic emissions. Industrialized regions are clearly visible as sources of many pollutants in Alberta and the Northeastern United States/Windsor–Quebec corridor (again mainly seen in the green & yellow in the figures.)

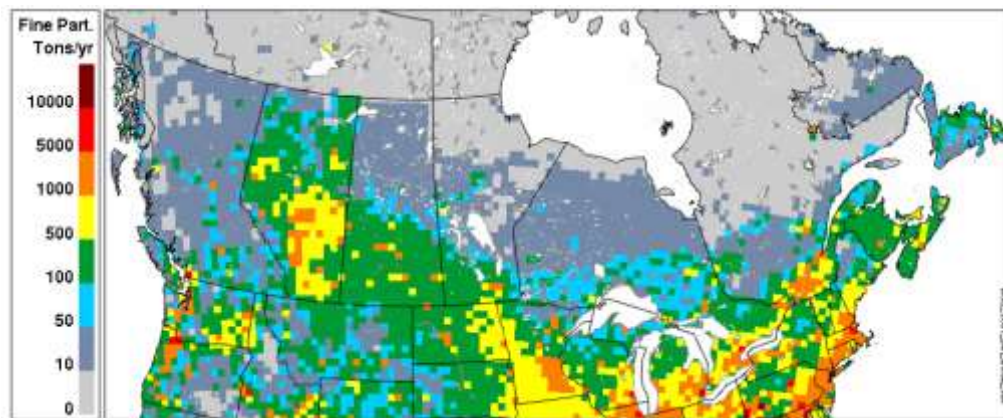


Figure 4.6 Emissions Density Map of the 2006 North American $\text{PM}_{2.5}$ Emissions (Environment Canada, 2009b)

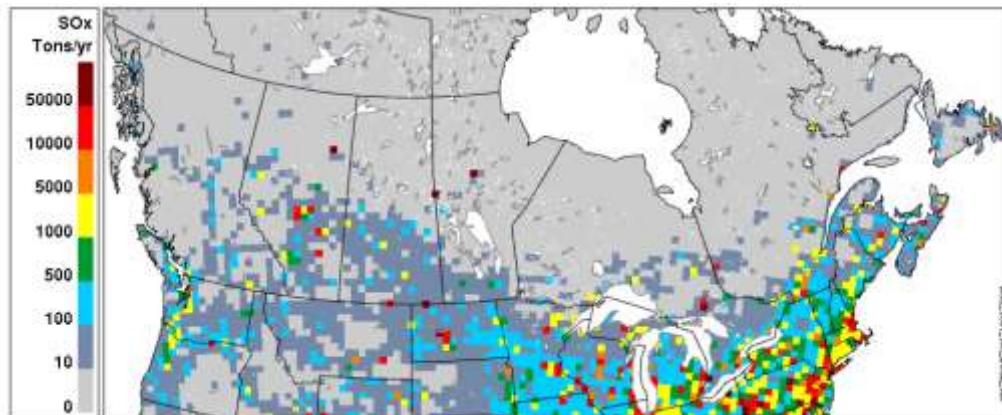


Figure 4.7 Emissions Density Map of the 2006 North American SO_x Emissions (Environment Canada, 2009b)

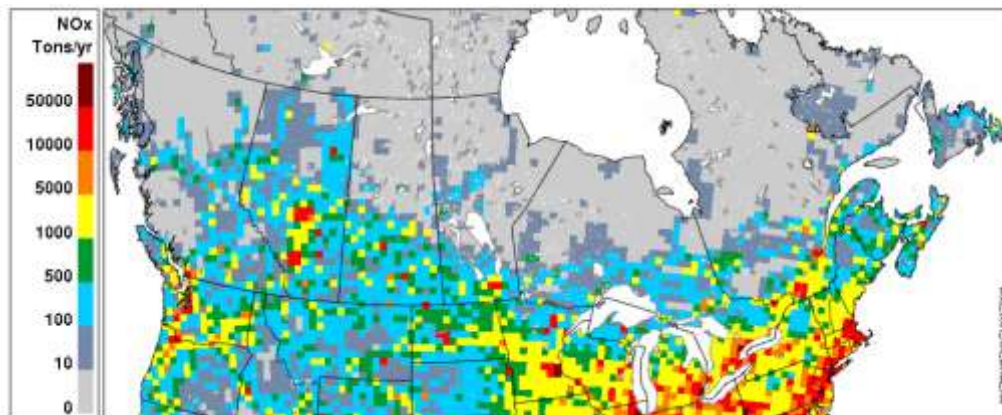


Figure 4.8 Emissions Density Map of the 2006 North American NO_x Emissions (Environment Canada, 2009b)

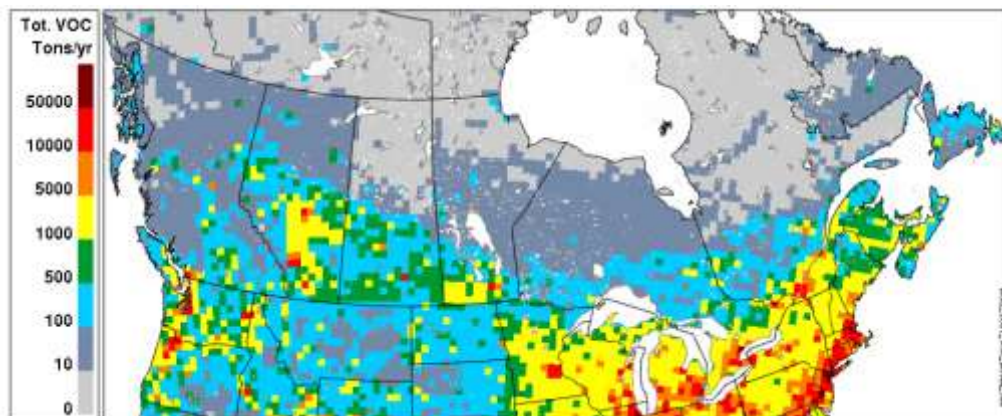


Figure 4.9 Emissions Density Map of the 2006 North American VOC Emissions (Environment Canada, 2009b)

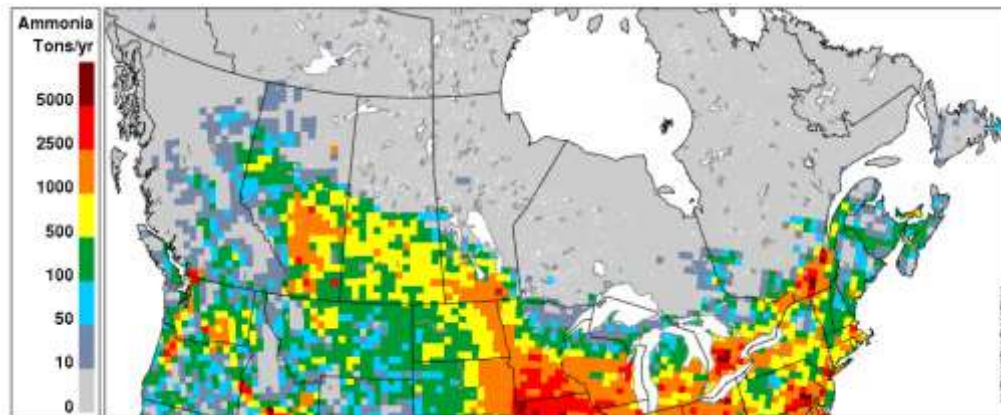


Figure 4.10 Emissions Density Map of the 2006 North American NH₃ Emissions (Environment Canada, 2009b)

4.6.2 Emissions Inventories for Modelling

Emissions inventories need to be processed into a format suitable for use in air quality models. Processing emissions inventories for ambient air quality models requires detailed process-specific information to develop temporally and chemically speciated emissions. To meet this requirement, the information provided under the NPRI has been pre-processed to provide sufficient information to enable the further processing of the emissions inventories for use in VOC, PM, and temporal speciation models.

4.6.2.1 VOC Speciation

Environment Canada consulted with industry representatives of the NPRI Multi-stakeholder Work Group on Substances to identify a list of 60 VOC species to be reported to the NPRI concurrently with existing VOC reporting. A minimum threshold of one tonne was established for each of these species, and reporting began in 2003. Six of these VOC species are common to the traditionally reported NPRI substances. In total, about 250 VOC species are reported (Environment Canada, 2008a).

For facilities that met the VOC and VOC speciation reporting triggers for 2003 through 2005, the amount of the speciated VOC reported varied from 0% to about 300% of the total VOC mass reported (values greater than 100% are due to variations in testing methods for total VOC and individual species, and in some cases, total VOC is reported as carbon). Including the traditional substances and accounting for common substances (substances reported as both a traditional NPRI substance and as a VOC species), an average of about 55% of the total VOC mass is reported to the NPRI as species. The remaining non-speciated amount can be due to any of a combination of any of the following factors: only 60 of potentially 1000+ species are required to be reported; facilities not meeting the reporting triggers for all the 60 species;

facilities not emitting some of the species; and lack of information available on the species emitted (the NPRI does not require testing). Also, the Pulp and Paper sector generally reported VOC as Carbon instead of sum of VOC species, although when the carbon content of the VOC species is calculated there is generally an agreement between the reported VOC total and the reported Carbon emissions.

For modelling, the VOC species reported to NPRI were used as the basis to develop VOC speciation profiles for facilities. As ambient air quality modelling requires as complete a speciation profile as possible, historical emissions inventory details were used with the U.S. EPA's SPECIATE Model 3.2 and 4.2 (US EPA, 2002b) (US EPA, 2006a) to generate facility level and sector average speciation profiles. These sector profiles were then reconciled with the facility profiles to remove the duplicate species. The remaining speciation was then applied to the unspiciated portion of the reported total VOC.

In total, there are about 600 VOC species in the developed point source speciation, accounting for 92% of the 2005 point source VOC. To assist in the emissions processing for models, cross reference tables were prepared for input of the species data into the different aggregate model species for model chemistry calculations (e.g. RADM, ADOM II, SAPRC, CB4, CB05). These were based on tables available in Carter (2008), which describe reactions and interactions between chemicals in the atmosphere.

4.6.2.2 Particulate Matter Speciation

For ambient air quality modelling, speciation of particulate matter is required. The most common components include elemental carbon, organic carbon, sulphate, nitrate, ammonium, crustal material and sea salt.

Table 4.4 Speciated Particulate from the 2002 Emissions Inventory (Environment Canada, 2005)

	Organic Carbon	Elemental Carbon	Sulphate	Nitrate	Ammonium	Other
PM ₁₀	1.80%	1.60%	1.10%	0.03%	0.10%	95.40%
PM _{2.5}	2.00%	1.10%	1.50%	0.02%	0.10%	95.30%

As there is currently no requirement for facilities to report PM species, Environment Canada has utilized the detailed process level historical emissions inventories along with speciation profiles (CMAQ, SPECIATE) to develop facility-level PM speciation profiles suitable for ambient air quality modelling purposes. Although the use of historical information will introduce some inconsistencies, these will be minimized taking into consideration that the PM speciation profiles are in many cases sectoral generalizations for aggregated processes,

combustion sources and equipment. Environment Canada's PM speciation profiles were based on the U.S. EPA's SPECIATE model (versions 3.2 and 4), with input from the PM species profiles found in the Community Multiscale Air Quality (CMAQ) modelling system, as these models have a more detailed information base. Table 4.4 provides a summary of the speciated particulate matter emissions from the point source portion of the 2002 emissions inventory, with the bulk of the mass coming from crustal material (included in the "Other" category in the table).

4.6.2.3 Temporal Profiles

Reporting of temporal information is also required under the NPRI. Reporting facilities are required to provide their emissions by month for each of the contaminants, along with typical days of operation, hours per day and any periods of operational shutdown. This information has been used to develop updated facility and contaminant temporal profiles.

As part of the National Agri-Environmental Standards Initiative (NAESI) with Agriculture and Agri-Foods Canada (AAFC), ammonia emissions are estimated on a monthly basis with a fine grid resolution utilizing monthly meteorological information. At the moment it is not possible to provide a further temporal breakdown. However, a model is under development which will utilize the meteorological data to estimate the ammonia emissions at a finer temporal resolution.

The remainder of the temporal profiles for area sources are generated based on information from the 1980s or by using the U.S. EPA temporal profiles distributed with the Sparse Matrix Operator Kernel Emissions (SMOKE) emissions processor. SMOKE is an emissions processing system that creates gridded, speciated, hourly inputs for air quality models (UNC, 2009). Work needs to be performed to update the temporal distribution of emissions from these sources.

4.6.2.4 Spatial Allocation of Non-point Emissions

As noted in Section 4.4.1, the point source emissions account for a varying percentage of the national emissions totals for each of the pollutants. The emissions from the non-point sources (Section 4.4.2) need to be allocated spatially across Canada. To spatially allocate the emissions, a variety of geospatial layers with percents of an activity (e.g.: fuel combustion, construction, etc) are used.

These layers consist of the usual population and dwelling information as well as:

- About 26 different labour force statistics, over 50 animal types and counts and acreages of crops for the agriculture sectors from Statistics Canada;
- Road and rail networks from Natural Resources Canada;

- Forest fire polygons from Canadian Forestry Service;
- Aviation corridors developed from Transport Canada information;
- Over 200 000 locations for the upstream oil and gas emissions, developed by the Canadian Association of Petroleum Producers.

Many of the above layers have been created by the originators to suit specific purposes. Emissions inventories have a large number of highly varied sources. Many of the geospatial layers have been modified slightly to remove allocations to areas where the emissions wouldn't be expected (e.g. agricultural animal emissions inside urban areas, or allocation of large diesel mining truck emissions to the downtown core of urban centres.)

4.6.2.5 Projected Emissions Inventories

For ambient air quality modelling in Canada and joint transborder modelling with the United States, model(s)-ready emissions inventories must be prepared for future years to develop and analyse the impacts of new emissions reductions programs and scenarios in both countries and globally.

The SMOKE emissions processor that is widely used in Canada and the United States has built into it a means to prepare projected emissions inventories based on user supplied sector growth and control factors. With the Canadian emissions being reported at the facility level, it is not possible for Canadian emissions inventory projections to be detailed to the processes level to allow for the utilization of the projection capacity in SMOKE.

To overcome this inventory limitation, a major development has been undertaken over the past few years to produce projected emissions inventories using the latest inventories and output from the E3MC model, accounting for any provincial/territorial adjustments and projecting the base emissions inventory year based on expected sectoral changes (see section 4.7.4.1 for details on the E3MC model). These improvements produce a projected emissions inventory on the same basis as the base year inventory. The need for projected emissions inventories is another reason why the emissions inventory was reorganized. Any possible information on future facility level emissions, facility openings or closures, and other information are also incorporated into the production of future emissions inventories for modelling. Speciation and temporal information currently remain constant into the future due to a lack of additional information to enhance these characterizations. Emissions projections are discussed further in section 4.7.4.

4.7 Trends and Projections

Historical trends are maintained by Environment Canada as well as provincial and territorial authorities to meet domestic and international requirements, inform the public, and support policy and modelling development. For the year 2000 and earlier, the provinces, regions and territories performed their own inventories in cooperation with facilities. These inventories were created with the understanding that the details would not be made public, as some of the information could affect the competitiveness of some industries. This provincially-owned information was provided to Environment Canada with a similar understanding, in order to meet the national reporting needs. Due to this restricted use of the information, the facility reporting of smog precursor and other emissions was moved into the NPRI to provide public access to and use of the information.

As previously mentioned, the emissions inventories are under a constant state of improvement resulting in individual inventory years not being directly comparable for individual sectors. A major effort was undertaken to re-estimate all of the area sources using the latest methodologies and to ensure that, as much as possible, the same facilities exist in all data years where appropriate, from 1985 through 2005. These updated inventories were published by Environment Canada in 2008. The inventories are available on the NPRI website.

Environment Canada also generates emission projections of the smog precursors to meet similar demands and commitments.

4.7.1 National Trends

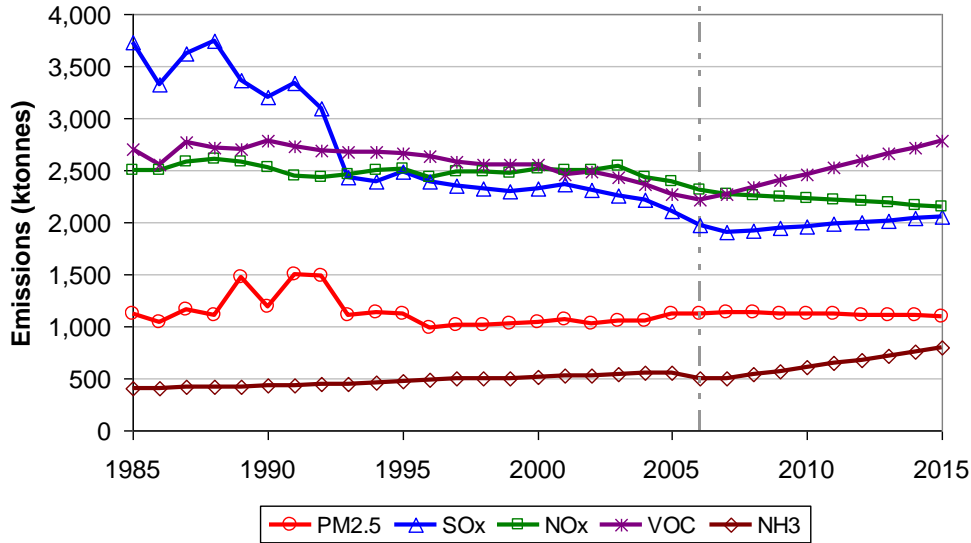


Figure 4.11 Canadian National Emissions Trends and Projections (Environment Canada, 2006; 2010b).

Figure 4.11 shows the smog precursor emissions from 1985 through 2020 with the vertical line at 2006, the latest data year. Shown on the graph are the emissions for all sources except forest fires and biogenics. The latter are too variable, and the biogenic signal would dwarf all other contributions to the VOC emissions. The projection to 2020 is a previous version based on the year 2000 emissions inventory and was published on in 2006. New projections including new control measures are in progress and should be available in 2012.

From 1985 to 2006, the emissions of SO_x and VOC have decreased by 47% and 18% respectively. PM₁₀ emissions have continued to climb due to the influence of road and construction dust. PM_{2.5} emissions remained stable. NO_x emissions decreased by 8%. Ammonia emissions are estimated to have increased by 22% due to increases in the agriculture sector. This sector dominates the ammonia emissions inventory, with an average 87% contribution to the national total. Except for NO_x, most emissions were projected to continue, increasing in varying amounts into the future.

Through various national and provincial regulatory and other emissions reduction initiatives, emissions reductions in smog precursors have been observed in many sectors.

Sulphur oxides emissions have been reduced through provincial level caps in Eastern Canada (Manitoba east) and provincial regulation of sulphur emissions on sources, lowering of the sulphur contents of fuels (gasoline, diesel and other fuels), and phasing out of coal-fired electricity generation units. Some of these reductions have been achieved through process changes at metal smelting facilities and fuel use changes for coal fired electricity generation,

Nitrogen oxides reductions have been achieved through provincial caps on coal-fired electricity generation units, implementation of vehicle emissions standards and provincial requirements for NO_x emissions rates for combustion devices.

VOC emissions have been reduced through implementation of guidelines on solvent use, provincial requirements on solvent use, regulated fuel vapour pressures for gasoline and diesel and implementation of vehicle emissions standards.

The steadily increasing price of oil, expansion of the Alberta Oil Sands projects and increased development of oil and gas primarily in Alberta have lead to increased smog precursor emissions mainly in Alberta. The Upstream Oil and Gas sector is the extraction, preliminary treatment and transportation of the gas and crude oil before it reaches the refineries. The increased emissions from these sectors have somewhat offset the reductions realized as described above primarily in eastern Canada.

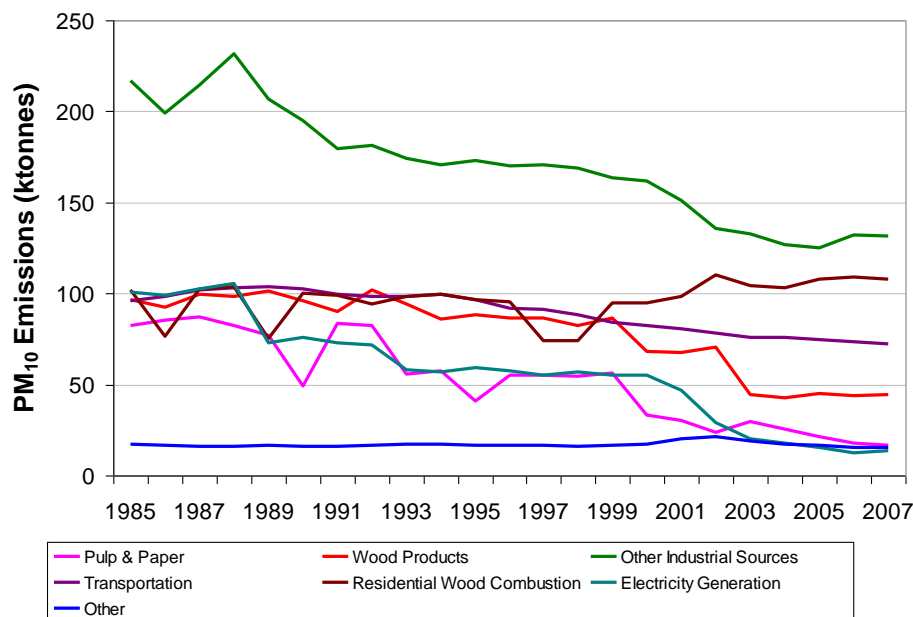


Figure 4.12 Sectors contributing to PM₁₀ Emissions without Open Sources (Environment Canada, 2010b)

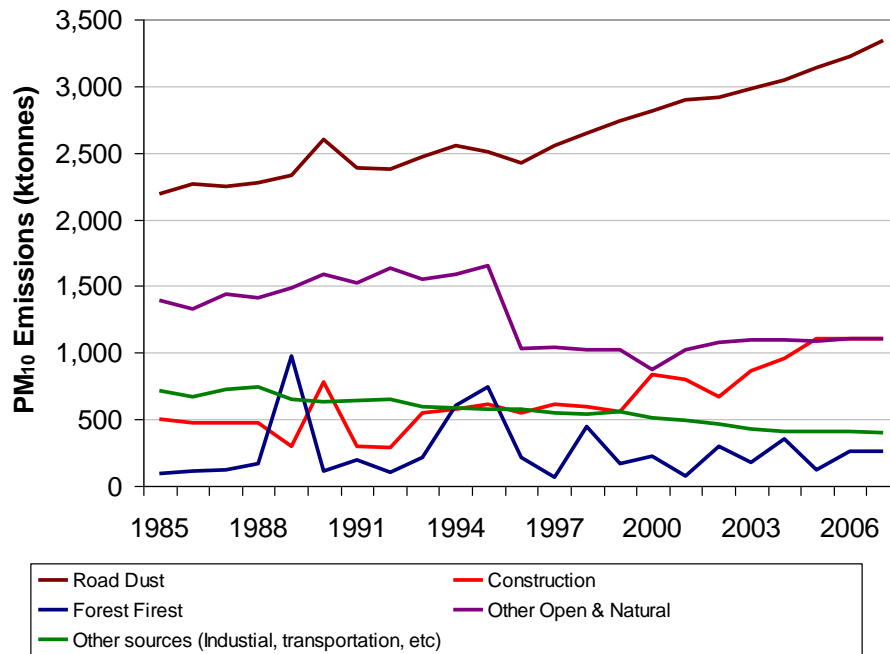


Figure 4.13 Sectors contributing to PM₁₀ Emissions with Open Sources (Environment Canada, 2010b)

When the Open Sources are included, PM₁₀ is increasing throughout the period. When the open sources are excluded, there is a decreasing emissions trend throughout the 1985–2006 period, achieved through reductions in many of the key sectors shown in Figure 4.12. Ambient monitoring data shows a decreasing trend in urban sites from 1985–2005 with little or no change in rural areas. This is seemingly contradictory to the national PM₁₀ trend with open sources included (Figure 4.13). Information on ambient monitoring data is available from the National Air Pollution Surveillance Network: www.etc-cte.ec.gc.ca/NAPS/index_e.html. This discrepancy may be due to provincial or territorial-level dust mitigation efforts not reflected here (e.g. for construction and road dust); a high uncertainty in the estimates; a large proportion of the PM₁₀ emissions are removed through impaction or deposit close to the source; or that PM₁₀ monitors are elevated two metres above the ground and are not capturing the dust.

Construction operations and road dust cause most of the increase in PM₁₀ emissions in response to increased construction activity and increased vehicle kilometres travelled. It should be noted that these sources have a high degree of uncertainty and emissions are predominantly of the size fraction greater than PM_{2.5}.

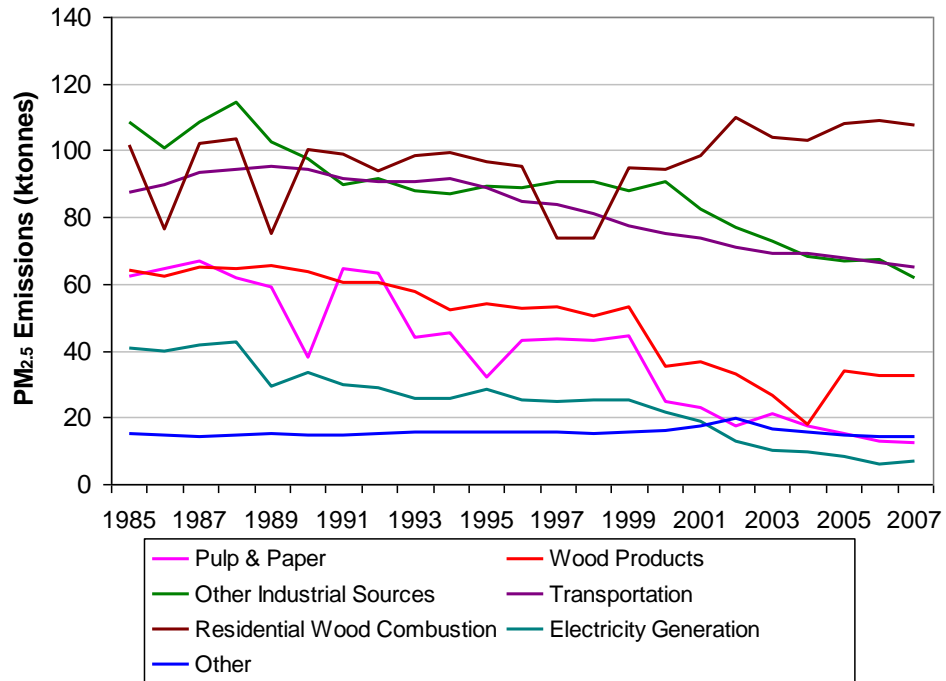


Figure 4.14 Sectors contributing to PM_{2.5} Emissions without Open Sources (Environment Canada, 2010b)

PM_{2.5} emissions have remained fairly stable throughout the period of 1985–2006 (Figure 4.11), and when Open Sources are excluded (Figure 4.14), a 35% decrease in emissions is evident. These reductions have occurred in various Industrial sectors such as Wood and Pulp and Paper, as well as Fossil Fuel Electricity Generation. These reductions have been achieved through process changes, changes in practices, and with add-on emissions control technologies.

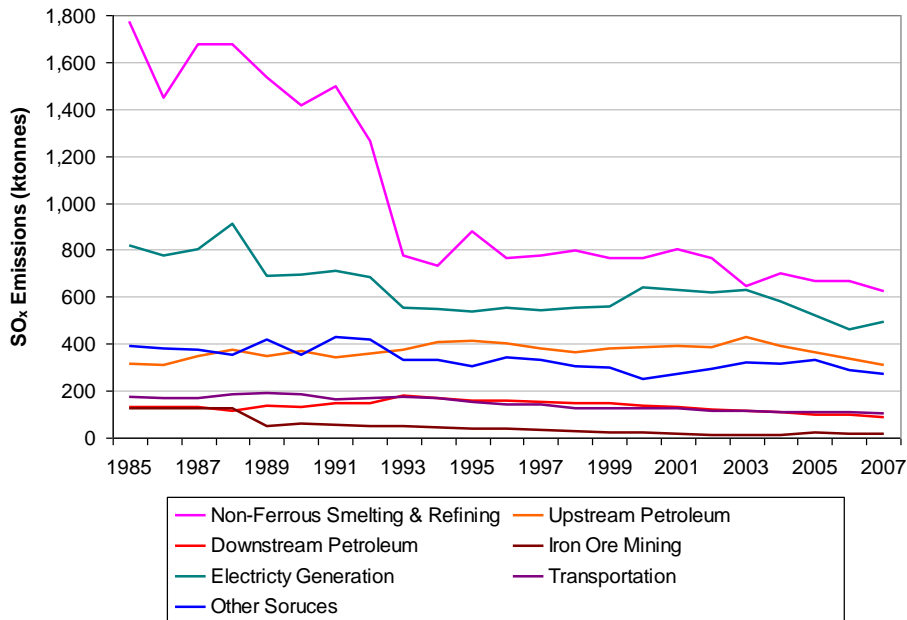


Figure 4.15 Sectors contributing to SO_x Emissions without Open Sources (Environment Canada, 2010b)

The SO_x emissions decreased by over 30% prior to 1995 (with most of the reductions occurring in eastern Canada resulting from the Eastern Canada Acid Rain Program), and since then have remained relatively constant nationally. Major reductions have occurred in the Non-Ferrous Smelting and Refining sector and in Fossil Fuel Electricity Generation (Figure 4.15). Smaller decreases have occurred in many other Industrial sectors. Since 1995, many of these sectors and the Transportation sector have continued to reduce SO_x emissions but these reductions have been offset by increases in the Upstream and Downstream Petroleum sectors.

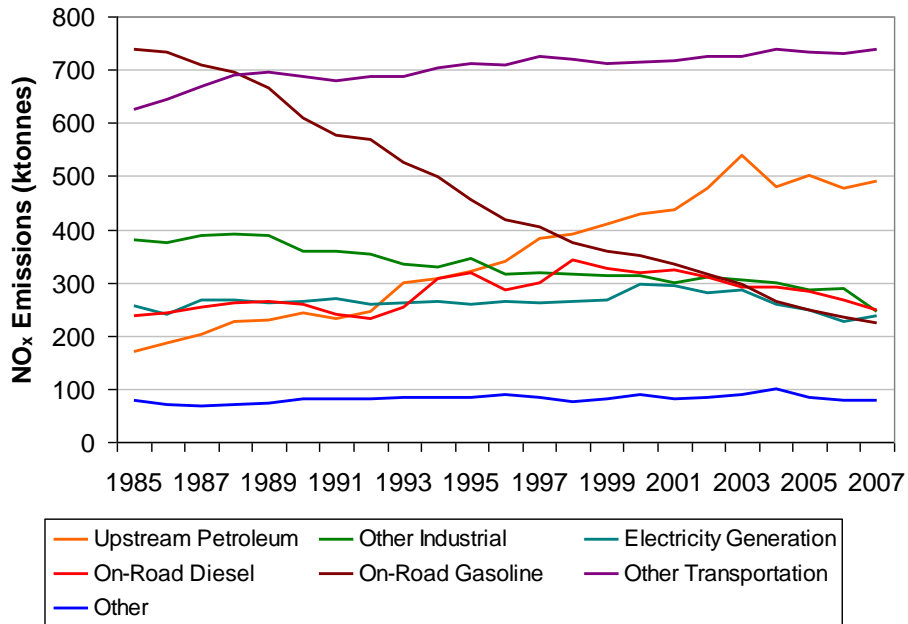


Figure 4.16 Sectors contributing to NO_x Emissions without Open Sources (Environment Canada, 2010b)

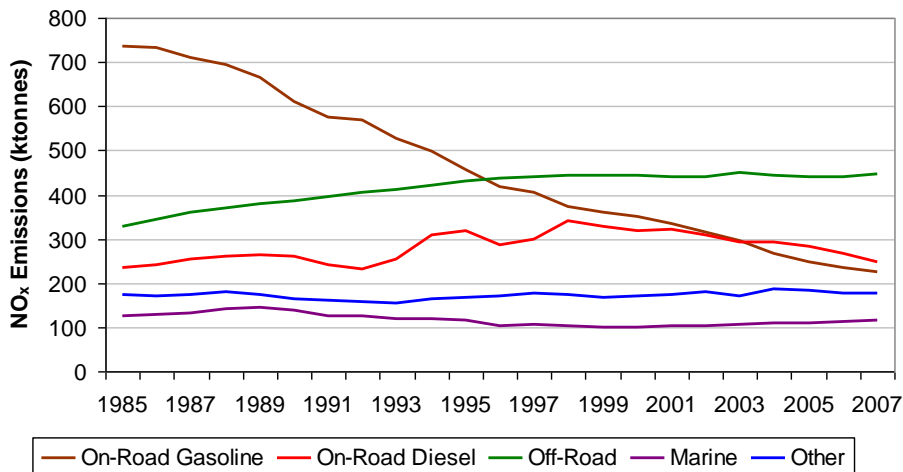


Figure 4.17 Breakdown of the Transportation Sectors NO_x Emissions Sources (Environment Canada, 2010b)

NO_x emissions have remained relatively constant throughout the entire 1985-2006 period. As seen in Figure 4.16, there has been approximately a 25% reduction in emissions from the Transportation sector (from gasoline vehicles emissions reductions), and decreases in some Industrial sectors. These NO_x reductions were offset by increases in the Upstream and Downstream Petroleum sectors. The Fossil Fuel Electricity Generation sector has remained relatively constant throughout the period.

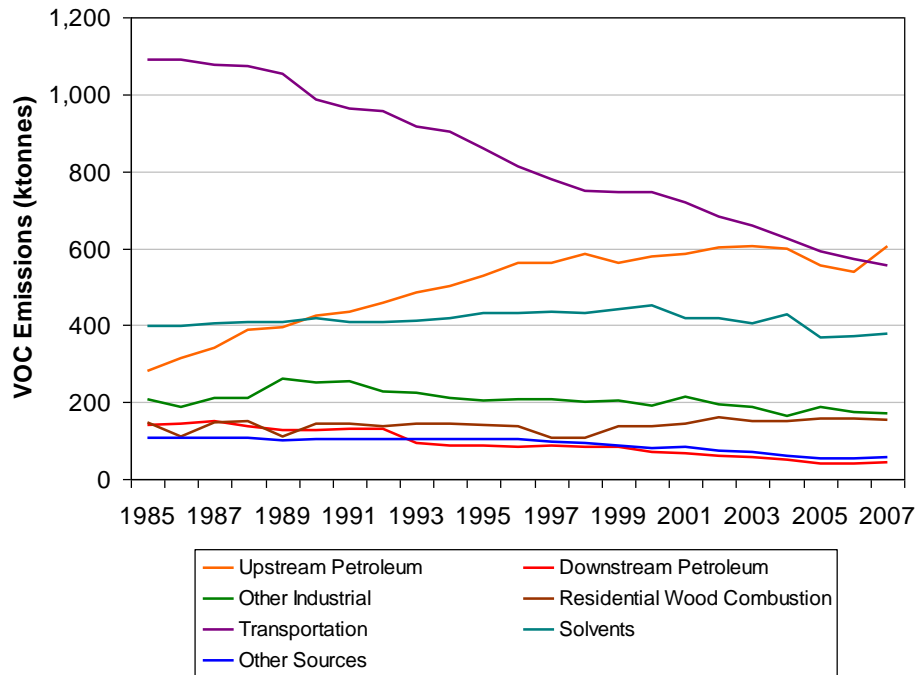


Figure 4.18 Sectors Contributing to VOC Emissions without Open Sources (Environment Canada, 2010b)

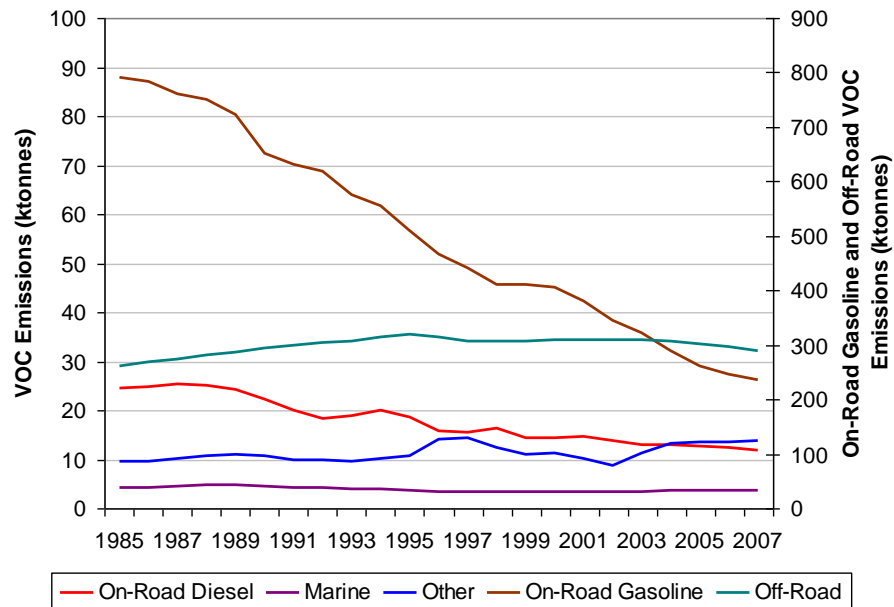


Figure 4.19 Breakdown of the Transportation Sectors VOC Emissions Sources (Environment Canada, 2010b)

VOC emissions have decreased by about 20% from 1995-2005 due to reductions primarily from the Transportation and Solvents sectors, with some contribution from the Industrial sector. The VOC emissions trend from major Canadian sources is shown in Figure 4.18, while Figure 4.19 shows the emissions trends from the Transportation sectors. The large reduction from the on-road gasoline vehicles can be seen in Figure 4.19 but these reductions in Transportation emissions have been offset by increases in the Upstream Petroleum sectors (which include Oil Sands and Upstream Oil and Gas), as shown in Figure 18.

The Agriculture sector dominates Canada's ammonia emissions, accounting for approximately 90% of the total emissions. Excluding the Agriculture sector, NH₃ emissions have remained fairly constant from 1985–2006. The decreases in the Industrial sectors have been offset by increases by the On-Road Gasoline emissions (ammonia is produced as a by-product from catalytic converters.)

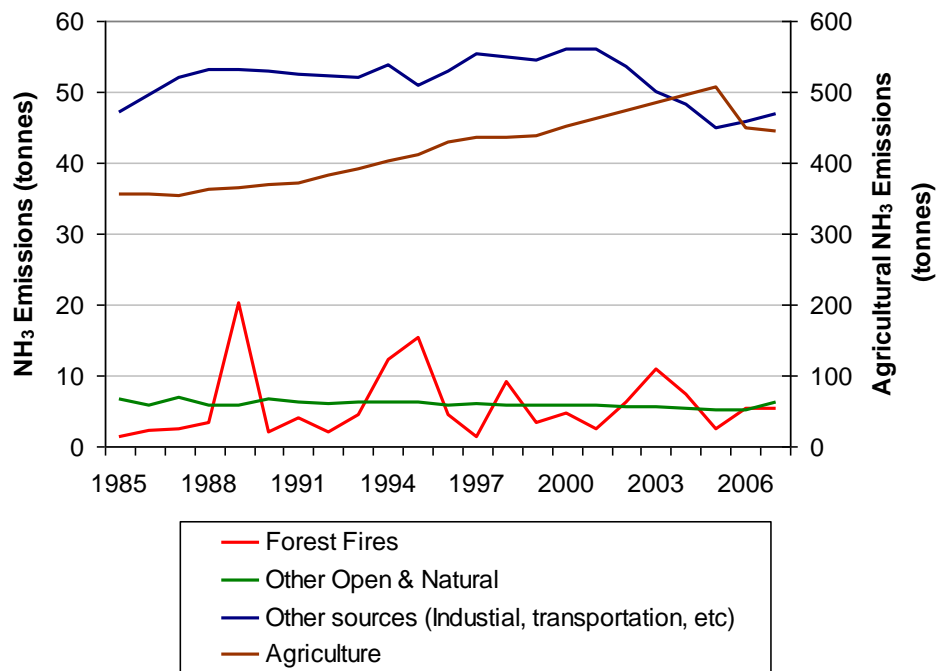


Figure 4.20 Sectors Contributing to NH₃ Emissions with Open Sources (Environment Canada, 2010b)

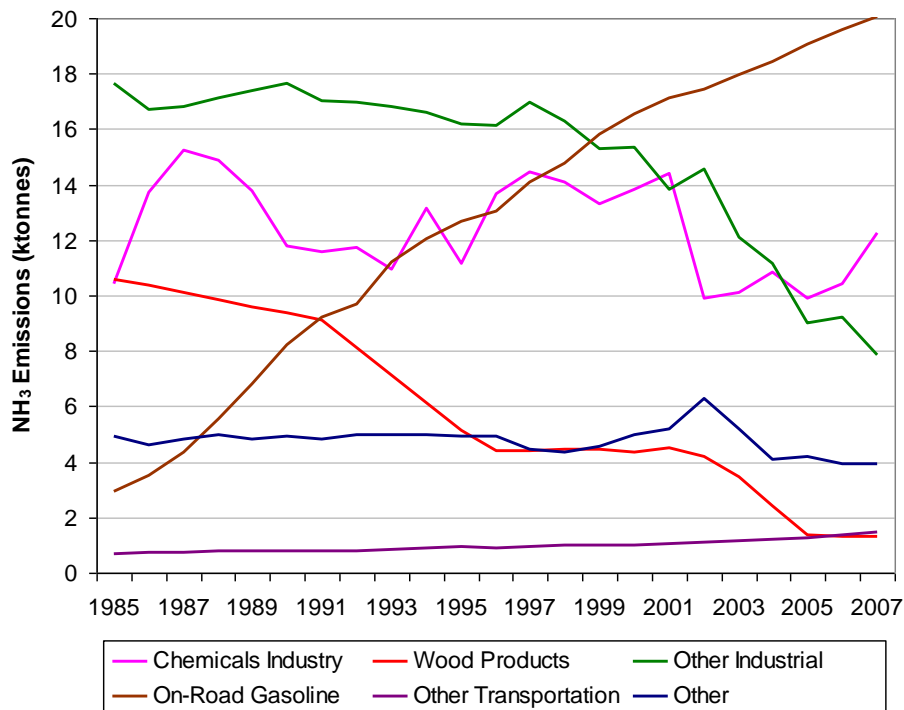


Figure 4.21 Sectors Contributing to NH₃ Emissions without Open Sources (Environment Canada, 2010b)

4.7.2 Regional Trends

The Maritimes: Emissions have generally decreased in the Maritime Provinces. There have been SO_x reductions in the Transportation, Fossil Fuel Electricity Generation and Petroleum sectors. These reductions have been partially offset by increases from the Upstream Oil and Gas sector.

Quebec: Transportation emissions of all substances have decreased in general in Quebec. Particulate emissions have remained relatively constant throughout the reporting period. SO_x emissions have decreased through reductions in the Non-Ferrous Smelting and Refining sector and other small industrial reductions. Non-Transportation NO_x emissions have remained relatively constant, as have VOC emissions. Ammonia emissions have increased by an estimated 16% from 1995–2006, through increases in most sectors.

Ontario: In Ontario, PM emissions decreased throughout the period, mainly through reductions in emissions from the Transportation sector. SO_x emissions have decreased by about 45%, primarily in the Non-Ferrous Smelting and Refining and Fossil Fuel Electricity

Generation sectors, and from some other smaller reductions in the Industry and Transportation sectors. NO_x emissions have decreased about 25%, from reductions in Transportation, Fossil Fuel Electricity Generation, and many smaller reductions from Industrial sources.

Manitoba and Saskatchewan: Manitoba and Saskatchewan are highly influenced by the Open Sources sector, especially in the increases in PM emissions, due to the large agricultural base and road networks. Excluding Open Sources, decreases of 20–30% have occurred in emissions from the Transportation and Fossil Fuel Electricity Generation sectors. Saskatchewan's SO_x emissions have increased from Fossil Fuel Electricity Generation, while Manitoba's SO_x emissions have decreased by 24% due to decreases from Non-Ferrous Smelting and Refining. Manitoba has realized a 15% decrease in NO_x emissions due to decreases from Transportation and Fossil Fuel Electricity Generation sources, while Saskatchewan's NO_x emissions have increased by 27%, largely due to the Fossil Fuel Electricity Generation sector. The ammonia emissions from these provinces have remained relatively constant, with some annual variability.

Alberta: When Open Sources are excluded, Alberta's PM emissions have decreased by more than 20% through reductions in the Transportation, Fossil Fuel Electricity Generation and Residential Wood Combustion sectors. However, particulate emissions from the main Open Sources – road dust, construction and agriculture – have been increasing. SO_x emissions have been variable throughout the period, with Oil Sands emissions generally increasing, and the Upstream Oil and Gas decreasing in recent years. SO_x emissions from Fossil Fuel Electricity Generation have also increased. NO_x emissions have increased by about 50% due to development in the Petroleum and Fossil Fuel Electricity Generation sectors. VOC emissions have decreased by about 30% due to reductions in the Solvent, Transportation and lately, the Upstream Oil and Gas sectors. These decreases have been offset by increases in emissions from the Oil Sands. Ammonia emissions have decreased somewhat, with decreases in Agricultural emissions which have been somewhat offset by increases in emissions from the Industrial and Transportation sectors.

British Columbia: British Columbia's particulate emissions have generally been decreasing throughout the reporting period. Excluding Open Sources, the Wood and Pulp and Paper sectors have realized decreases in particulate emissions, while most other sectors have experienced either little change or slight increases. SO_x emissions are showing an increase of about 8%, due mainly to increases in the Upstream Oil and Gas sector as well as some increase in most Industrial, Commercial Fuel Combustion, and Fossil Fuel Electricity Generation sectors. These increases have been counteracted by reductions from Transportation sectors. NO_x emissions have decreased about 13% due mainly to decreases in the Transportation sector, offset by increases in the Upstream Oil and Gas and some other Industrial sectors. VOC emissions decreased by about 40% due to reductions from the Transportation and Solvent sectors, although offset by increases in the Petroleum industries. Ammonia has decreased by about 12% due mainly to changes in the agricultural sector.

4.7.3 United States Emissions

4.7.3.1 National Trends

Smog levels in Canada are often influenced by emissions in the United States and vice-versa. The United States has made available up-to-date historical emissions inventories from 1990 and beyond.

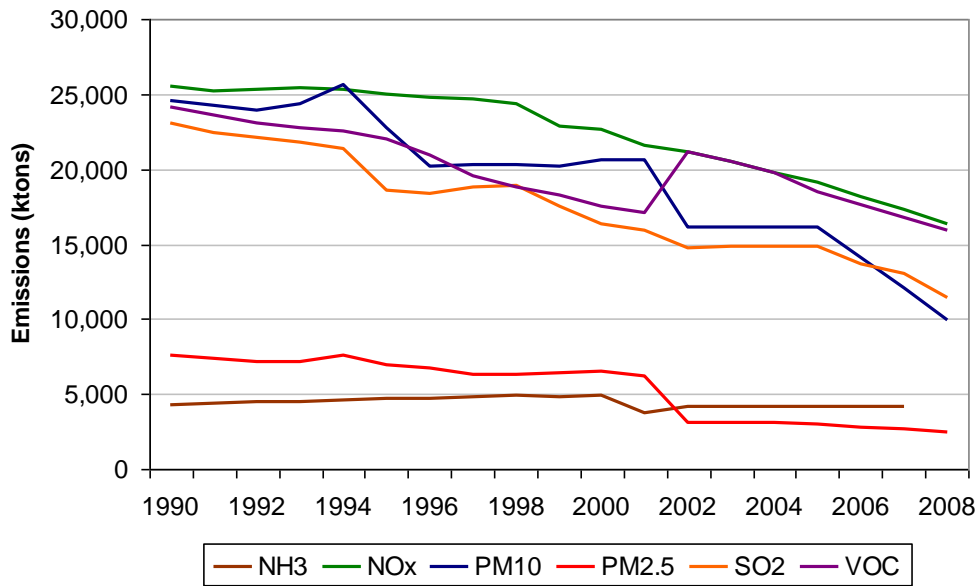


Figure 4.22 National U.S. Emissions Trend (US EPA, 2010f)

The emissions in the United States have generally decreased between 1990 and 2008. Figure 4.22 depicts the emissions trend for smog precursor emissions in the United States (US EPA, 2010f). For PM₁₀, PM_{2.5}, VOC and NH₃ there appears to be a methodological or coverage change to the emissions reported in the years 1999 to 2001, as the trend line for these pollutants displaces either down or up at this point. The change is most notable in the Miscellaneous category which includes agriculture and forest fires. In the Canada – United States Air Quality Agreement 2008 Progress Report it has been stated that these are due to improved characterization of the sources within the categories (IJC, 2008).

Major reductions in SO₂, NO_x, and VOC emissions reductions have been realized (50%, 36% and 34% respectively) through the implementation of regulations on large industrial and fossil fuel fired electricity generators for SO₂ and NO_x, as well as additional regulations on solvents for VOC emissions. The On-Road Transportation (Highway Vehicles) category has also been regulated to reduce NO_x and VOC emissions and fuel sulphur levels have been lowered to reduce SO₂ emissions.

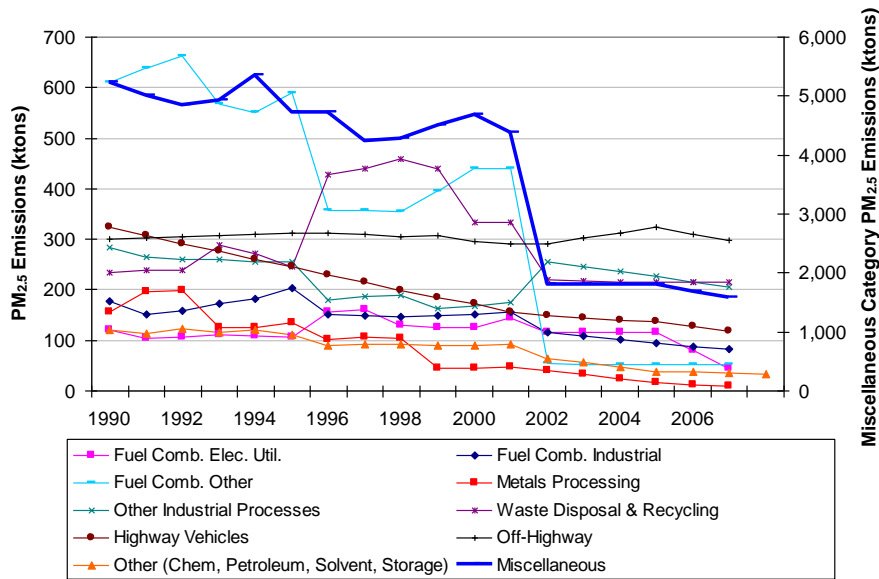


Figure 4.23 U.S. PM_{2.5} Emissions by Category (US EPA, 2010f)

PM_{2.5} emissions have reduced by about 65% since 1990. Reductions have been achieved in most of the major categories as depicted in Figure 4.23. For comparative purposes, only PM_{2.5} filterable has been used. The Off-Highway and Waste Disposal categories show the least reduction throughout the period. Due to the variation in magnitude of the Miscellaneous Sources category from the others, a secondary Y-axis has been used to show its emissions in the heavy blue line. The methodological or other changes to the inventories are visible for the Miscellaneous, Other Fuel Combustion and Other Industrial Processes categories, where there are very sharp changes in the trend in 2001.

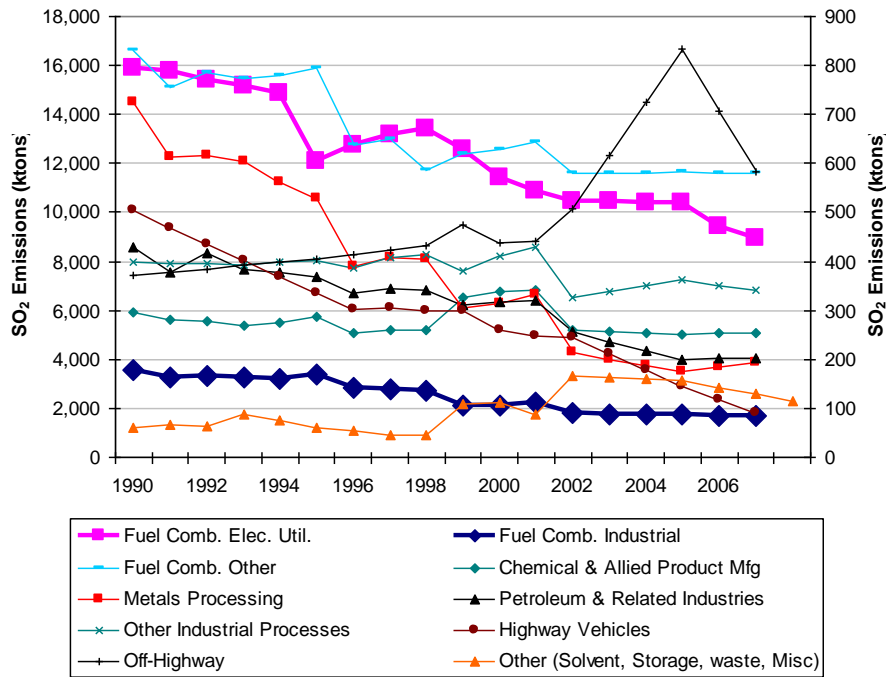


Figure 4.24 U.S. SO_x Emissions by Category (US EPA, 2010f)

Sulphur dioxide emissions have decreased by about 44% from 1990 to 2008. Figure 4.24 shows reductions primarily from the Electric Utility and Industrial Fuel Combustion categories (shown as heavy lines on the primary y-axis) which account for 80% of the emissions in 2008. Most of the other categories (shown as thin lines on the secondary axis) have reduced as well, except the Off-Highway and Miscellaneous categories. The Miscellaneous sector, included in the Other category, is made up of sources which are quite variable (e.g. agriculture and forest fires) and continually subject to improvement which may account for some of the increase.

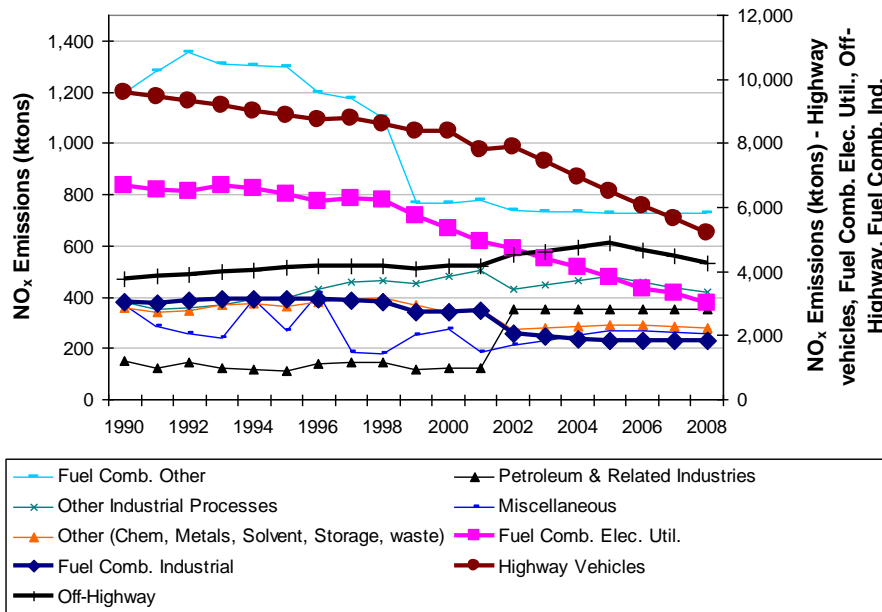


Figure 4.25 U.S. NO_x Emissions by Category (US EPA, 2010f)

Nitrogen Oxides (NO_x) emissions have decreased by 36% overall from 1990 to 2008, primarily from reductions in the On-Road Transportation (Highway), Electrical Utility Fuel and Industrial Fuel Combustion categories. Figure 4.25 depicts the aforementioned major categories in heavy lines on the secondary y-axis, along with emissions from the Off-Highway category which have increased by about 18%. A decrease in emissions has been observed for some of the minor contributing sectors, while emissions from the Petroleum and Related Industries appear to have increased. The increase in the Petroleum and Related Industries may be due to a method change due to the abrupt almost tripling of emissions between 2001 and 2002.

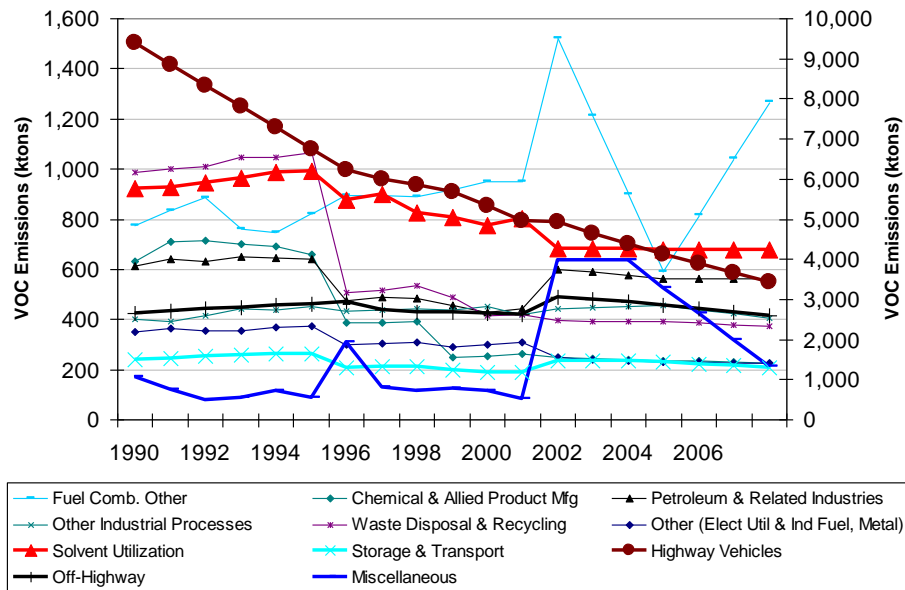


Figure 4.26 U.S. VOC Emissions by Category (US EPA, 2010f)

National VOC emissions have decreased by 30% from 1990 to 2008, primarily from reductions of 60% in the On-Road Transportation (Highway) and Solvent Utilization sectors. These reductions and some additional small reductions in other categories were offset by increases in the Miscellaneous and Other Industrial Fuel Combustion categories. Figure 4.26 shows the NO_x emissions changes for the various categories. The five larger emissions categories (e.g. Transportation, Solvent, etc) are shown with heavier lines on the secondary y-axis.

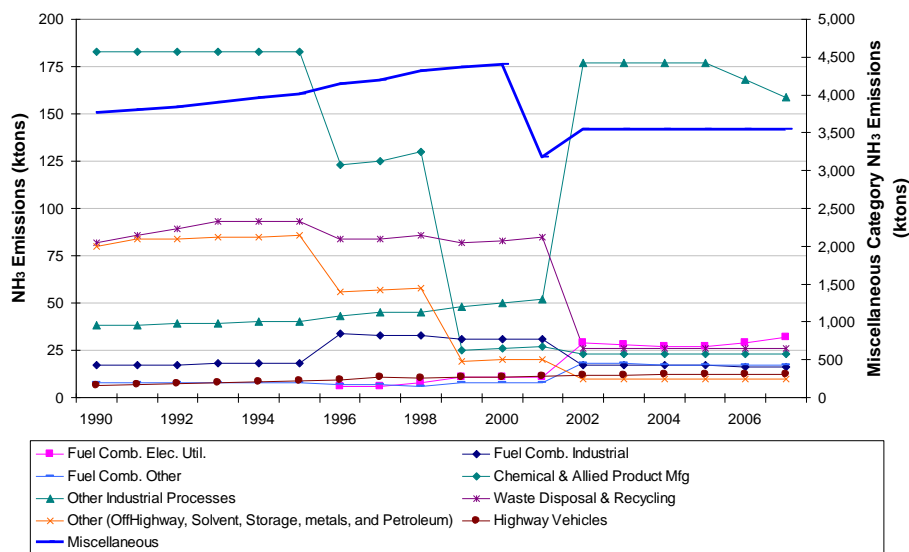


Figure 4.27 U.S. NH_3 Emissions by Category (US EPA, 2010f)

Like Canada, the United States ammonia emissions inventory is dominated by the Agriculture sector with an average 87% proportion of the U.S. emissions. The U.S. national ammonia emissions have decreased slightly (4%) over the period from 1990 to 2007, driven largely by a 4% decrease in agricultural NH_3 emissions (included in the Miscellaneous category) as shown in Figure 4.27. Decreased NH_3 emissions have also been realized in most sectors but these have been offset somewhat by increased emissions from Highway Vehicles (73%) and Industrial Processes (300%). Note that there is an obvious discrepancy in the emission magnitudes in the timeframe 2000 to 2002 for almost sectors. This has somewhat contributed to their overall increases or decreases in emissions.

4.7.3.2 Regional Trends



Figure 4.28 U.S. PEMA (IJC, 2008)

As described in the Canada – United States Air Quality Agreement Progress Reports, from 2004 to 2008, areas of both Canada and the United States are influenced by the transboundary flows of pollutants. The regional analysis will focus specifically on the United States portion of the Pollutant Emissions Management Area (PEMA), which covers the following 19 north-eastern states: Connecticut, Delaware, Illinois, Indiana, Kentucky, Maine, Maryland, Massachusetts, Michigan, New Hampshire, New York, New Jersey, Ohio, Pennsylvania, Rhode Island, Vermont, West Virginia, and Wisconsin, and the District of Columbia. These are depicted in Figure 4.28 from the 2008 report (IJC, 2008).

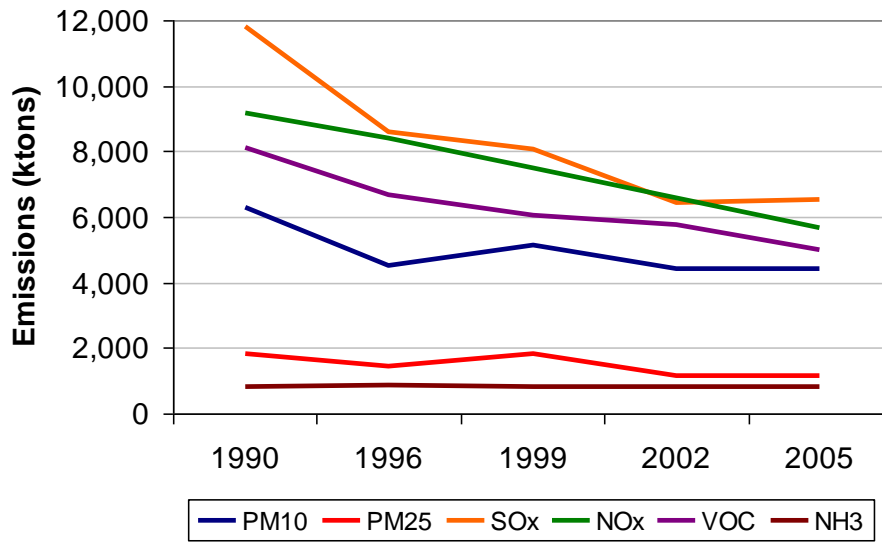


Figure 4.29 U.S. PEMA Emissions Trend (US EPA, 2010a,b,c,d,e)

When compared to the national emissions totals for 2005, these states accounted for: 20% of the national PM_{2.5} emissions, 48% of SO_x, 33% of NO_x, 30% of the VOC, and 22% of NH₃. Figure 4.29 depicts the trend from 1990 to 2005 utilizing the detailed inventories available from the EPA for 1990, 1996, 1999, 2002, and 2005 (US EPA, 2010a,b,c,d,e).

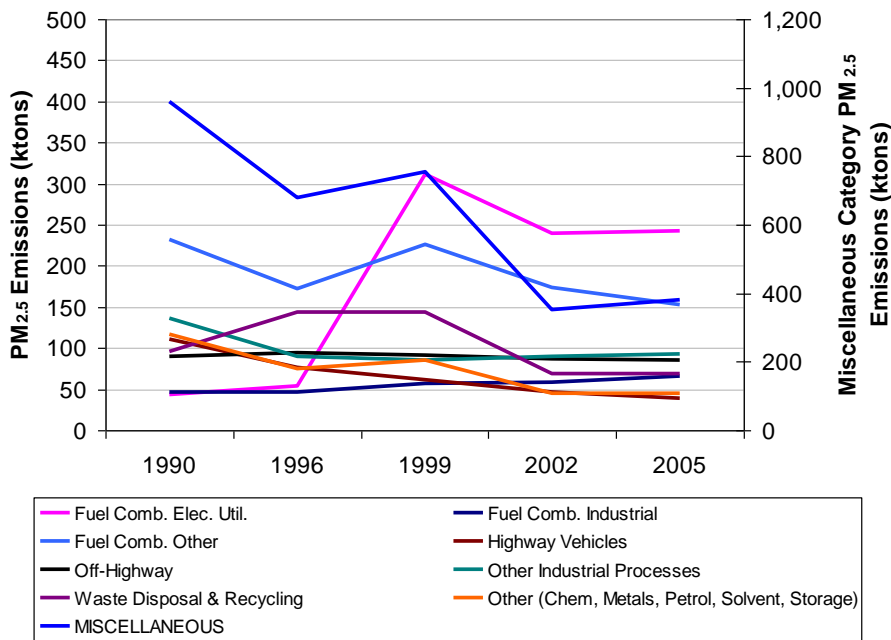


Figure 4.30 U.S. PEMA PM_{2.5} Emissions Trend (US EPA, 2010a,b,c,d,e)

PM_{2.5} emissions in the northeastern states have decreased by 36% overall. As in Canada this pollutant is dominated by dust emissions from road dust and agriculture dust included in the Miscellaneous category (Figure 4.30). The Miscellaneous category emissions have been estimated to have decreased by 60% (US EPA, 2010a,b,c,d,e). As has been noted in the Canada – United States Air Quality Agreement 2008 Progress Report (IJC, 2008), many categories have improved characterization which may be leading to some of the apparently large and abrupt increases or decreases.

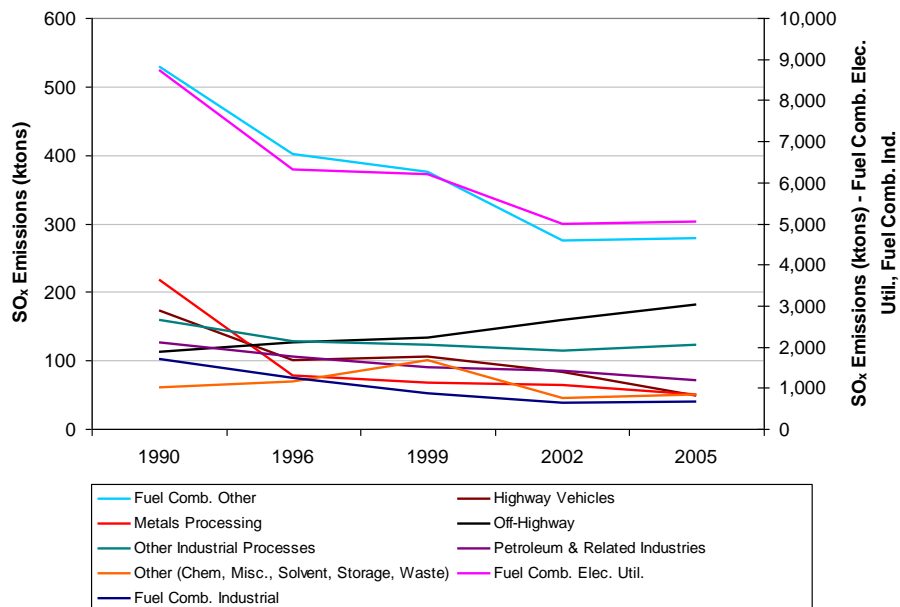


Figure 4.31 U.S. PEMA SO_x Emissions Trend (US EPA, 2010a,b,c,d,e)

The emissions of SO₂ have reduced 45%, largely from reductions in the dominant source, the Electric Utilities category of 42%. Figure 4.31 below shows how most other categories in the northeastern states have reduced the SO₂ emissions as well, except in the off-highway category, which has increased by about 60% (US EPA, 2010a,b,c,d,e).

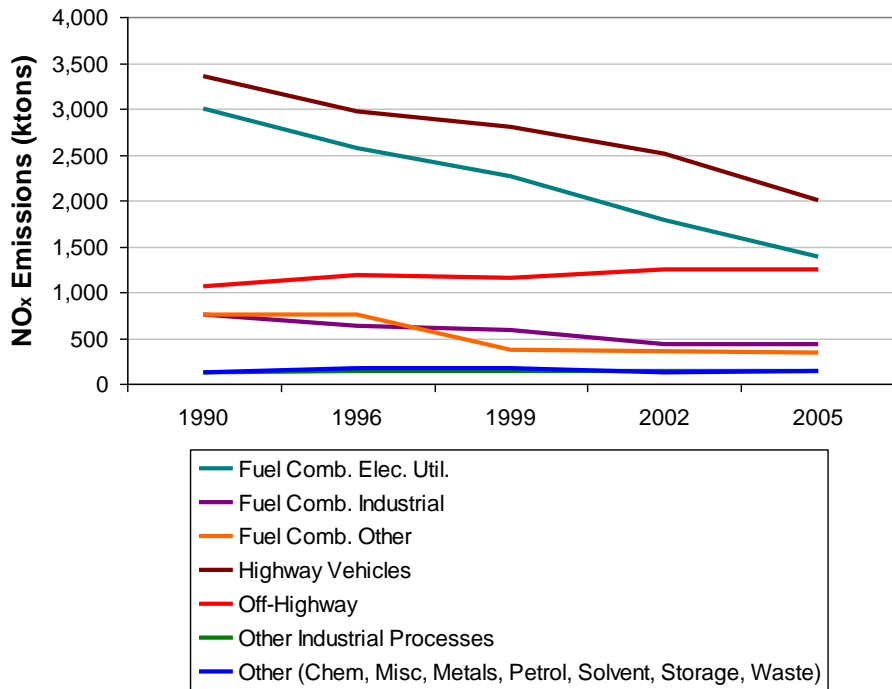


Figure 4.32 U.S. PEMA NO_x Emissions Trend (US EPA, 2010a,b,c,d,e)

Most sources of NO_x have decreased their emissions since 1990, except for Off-Highway Vehicles, which increased 16% (Figure 4.32). From 1990 to 2005, NO_x emissions have declined by 38% overall, primarily due to reductions from Highway Vehicles (40%) and Fuel Combustion from the Electric Utilities category (54%) (US EPA, 2010a,b,c,d,e).

NO_x emissions have decreased significantly since 1990 as a result of the implementation of the NO_x Budget Trading Program in the United States. As of 2007, 20 states and the District of Columbia are affected by this trading program. During the ozone season (May to September), NO_x emissions have decreased by almost 74% over the period from 1990 to 2006 (IJC, 2008). However, annual emissions have been relatively constant in the last 5 – 10 years of the reporting period. The sectors contributing to the reductions in this region are similar to those of the U.S. as a whole.

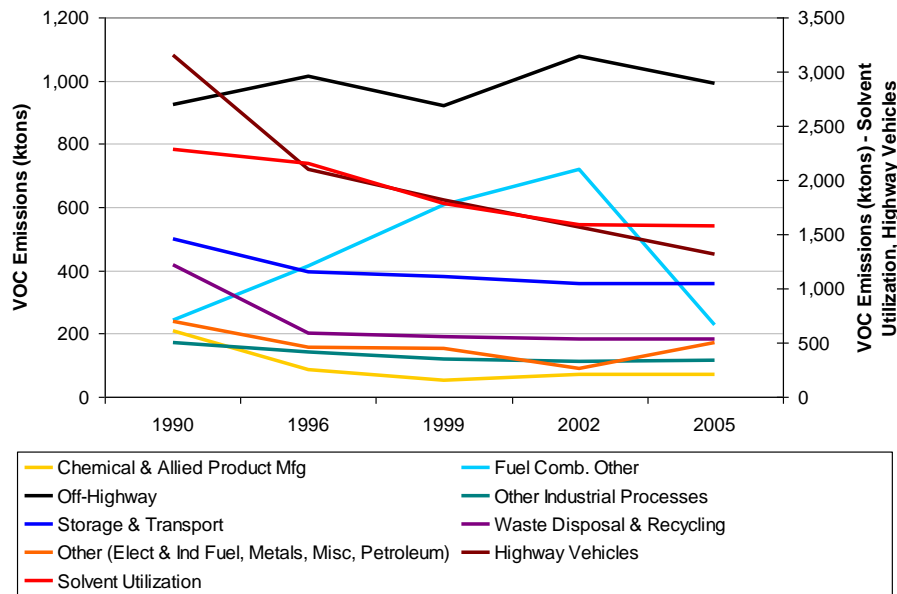


Figure 4.33 U.S. PEMA VOC Emissions Trend (US EPA, 2010a,b,c,d,e)

VOC emissions have reduced by 38% overall with the greatest reductions from the Highway Vehicles (56%) and Solvent Utilization sectors (31%). Figure 4.33 depicts the VOC emissions trends (US EPA, 2010a,b,c,d,e).

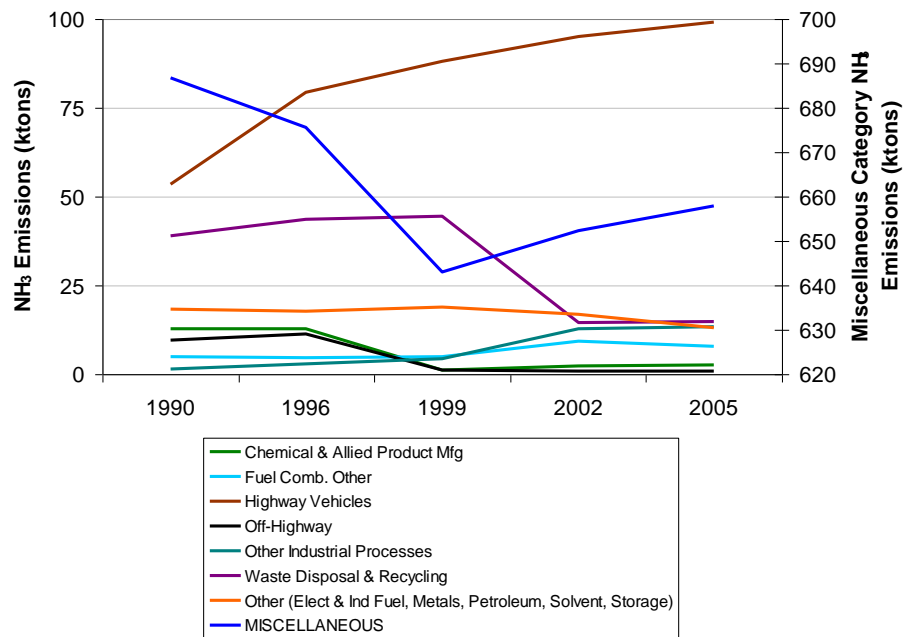


Figure 4.34 U.S. PEMA NH₃ Emissions Trend (US EPA, 2010a,b,c,d,e)

Ammonia emissions shown in Figure 4.34, have decreased slightly (2%) over the 1990 to 2005 period, influenced by the dominant Agriculture sector within the Miscellaneous category. Similar to Canada, emissions of ammonia from the Highway Vehicle sector in the U.S. have increased (85%) in the PEMA (US EPA2010a,b,c,d,e). Otherwise, emissions have decreased for the Chemical and Petroleum categories and increased for the Other Industrial Processes category. However it is not known if these are methodological or actual changes due to the reported improved characterization (IJC, 2008).

4.7.4 Emissions Projections

Environment Canada is responsible for Canada's projections of CAC emissions into the future. The projections currently available are based on the year 2000 emissions inventory. They were projected using accepted methodologies based on Natural Resources Canada's "Canadian Emissions Outlook 1999, an Update" with additional economic information from Infometrica Limited (2007). These projections, performed in 2004, utilized the latest available information as well as input from sector experts, provinces and territories, and industrial associations. The projections incorporate the impacts of all of the policies and agreements for emissions reductions in effect at the time.

Environment Canada is in the final stages of developing new projections utilizing a new methodology described in the next section. For more information on the old emissions projections methodology, please refer to the Emissions Inventory section in Chapter 2 of the 2004 Canadian Acid Deposition Science Assessment (Niemi, 2005).

4.7.4.1 New Emissions Projections Methodology

The Energy 2020 economic model is an integrated multi-region, multi-sector North American model simulating supply, price and demand for fuels. It can be tailored to suit specific client needs and was modified to suit CAC Emissions projections. This modified version is now called Energy, Emissions, and Economic Model for Canada (E3MC) (Environment Canada, 2008b).

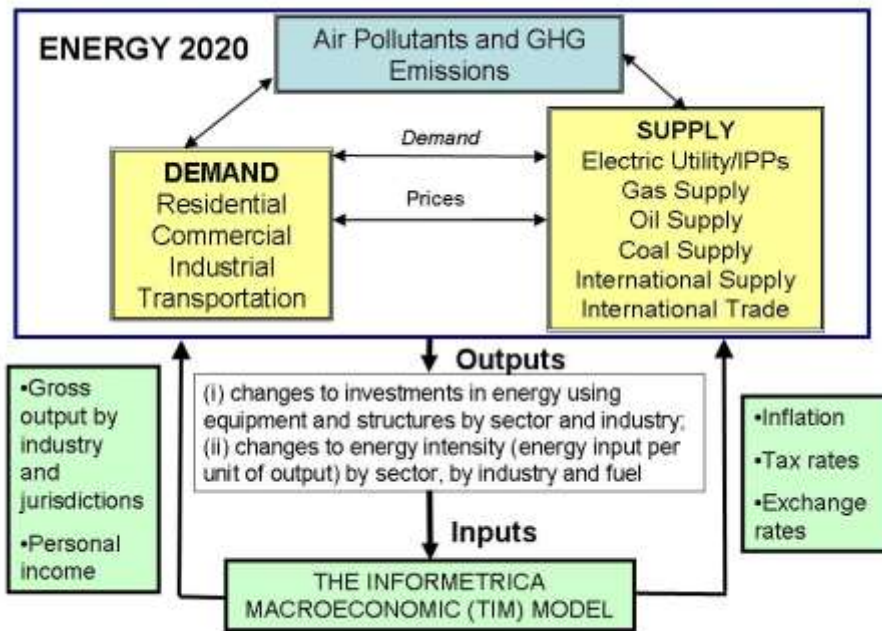


Figure 4.35 Schematic of the E3MC Interactions (Macaluso, 2009)

The E3MC model (Figure 4.35) is a multi-sector model that simulates supply and demand of energy (electricity, fossil fuels, etc.) and works with the Infometrica Limited macroeconomic model (Infometrica, 2007) to simulate the financial impacts in a feedback mechanism to E3MC. E3MC has been modified with the appropriate energy, economics and cost curves to suit CAC emissions projections for all 8 contaminants appropriate to the Canadian economy and industrial base. These curves have been developed using studies of major Canadian industrial sectors and other specific consultant studies. The latest available energy outlook from the National Energy Board (NEB, 2007) was also incorporated into the model. Coefficients of CAC emissions are then derived using the actual emissions and the appropriate driver (e.g. energy, economic activity, or other exogenous drivers) based on the latest available emissions inventories.

The E3MC model utilizes the past 20 years of CAC emissions data, energy supply and demand and economic information to “spin-up” (i.e. to prepare the model grids with background data) when performing the projections. It then utilizes the energy outlook (conventional and renewable), economic projections and other market expectations to project the various demands and outputs. During the simulation it works with the Infometrica Limited macroeconomic model and cost curves to simulate changes in financials and their feedback on the projections. Changes in policy and investment in emissions control technology are incorporated to determine their impact on the economy and resultant realignment of demands and outputs. E3MC has also factored into the output projections all of the impacts of current in-place and on-the-books regulations and emissions reductions programs.

The derived coefficients for CAC emissions are then applied to the resultant drivers, while incorporating the effects of the changes in policy and emissions controls, to arrive at a preliminary projection of emissions. These projections are then verified with Environment Canada’s sector experts and provincial/territorial authorities to ensure all national, provincial/territorial policies, initiatives and agreements have been adequately accounted for in the model results.

The E3MC model’s strength is in simulating all the various aspects at a national and aggregate sector level. However, when the results are broken down to the provincial or finer scale levels, the uncertainty increases due to assumptions made regarding the state of provincial/territorial economies and of the individual sectors.

4.7.4.2 North American Emissions Projections

	Canada	U.S.	North American Total
PM ₁₀	5,826	12,711	18,537
PM _{2.5}	1,118	4,212	5,330
SO _x	1,921	4,942	6,863
NO _x	2,233	10,272	12,505
VOC	2,240	11,844	14,084
NH ₃	551	3,629	4,180

The Canadian and United States national emissions projections of smog precursors in 2015 are summarized in Table 4.5. Spatially these data will be distributed similarly to the 2006 patterns in Figures 4.6 to 4.10, although with lower emissions expected in some regions.

Table 4.5: Canada and United States Projected 2015 Emissions Levels (Environment Canada, 2006; US EPA, 2005)

It must be noted that these are the previous Canadian projections based on the emissions inventory for the year 2000. Since their development in 2004, additional reduction initiatives have been implemented across Canada. Please see Section 4.7.4.3 for a more specific discussion on the Canadian emissions projections.

Canadian emissions of $PM_{2.5}$ have been projected to remain relatively stable to 2015 due to the high proportion of Canadian road and construction dust, and residential wood combustion. Emissions of $PM_{2.5}$ in the United States are projected to decrease by about 20% through the implementation of CAIR, the proposed legislation at the time these emissions projections were made.

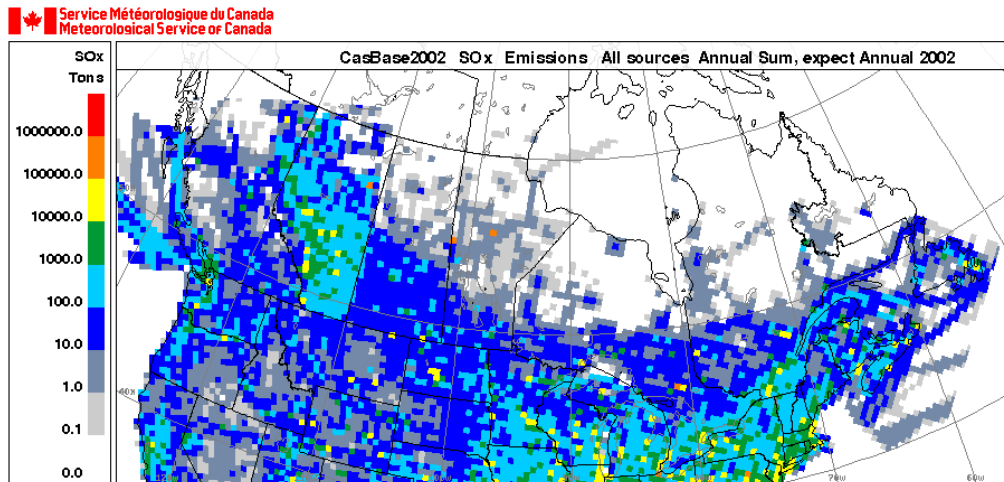


Figure 4.36 North American 2002 SO_x Emissions Density Map. (Environment Canada, 2009b)

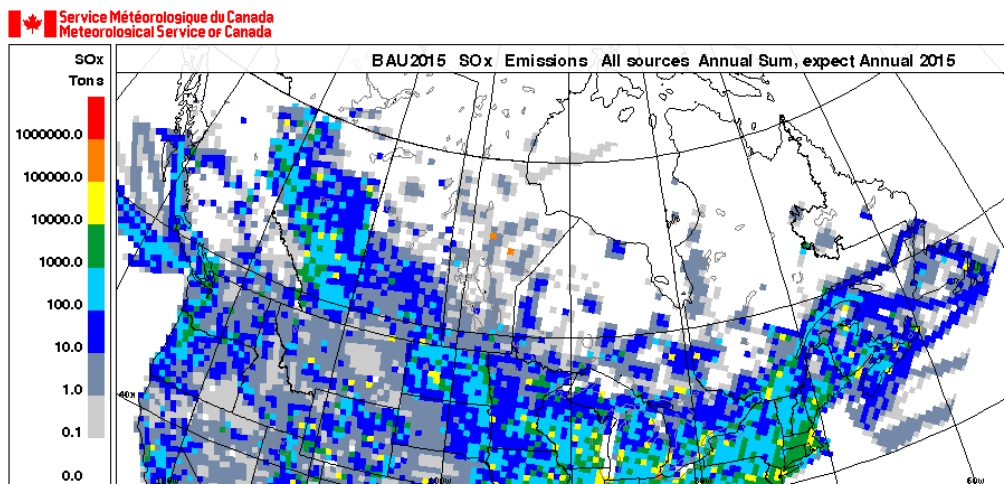


Figure 4.37 North American 2015 SO_x Emissions Density Map. (Environment Canada, 2009b)

With the projected changes in both Canadian and U.S. SO_x emissions there is a marked change in the magnitudes of emission across the region. The projected 2015 SO_x emissions show a distinct decrease in the emissions intensity in most regions in Canada and the United States. Emissions in western Alberta and the Windsor-Quebec City corridor remain elevated, but some reductions are visible. In the U.S., many areas from North Dakota through to Maine show a

decrease in emissions intensity while in many other regions, emissions intensities have remained constant or even increased. To illustrate the impacts of North American emissions changes, emissions density maps of SO_x emissions for the years 2002 and 2015 are shown in Figures 4.36 and 4.37. NO_x emissions projected for 2015 generally show a similar reduction pattern to that of SO_x in these figures.

4.7.4.3 Canadian Future Emissions

Table 4.5 provides estimates of the future emissions that have previously been published by Environment Canada. These emissions projections to 2015 are based on the 2000 emissions inventory performed in 2004. Figure 4.11 also provides this information in a graphical trend for the years 1985 to 2020.

For particulate matter, there is generally a continued increase projected in emissions from all sectors except for Transportation. The projected decrease in the Transportation sector emissions is due to changes in the emissions characteristics of the engines that are expected to be in use by 2015.

For SO_x, reductions are expected from the major contributing sectors (Smelting and Refining, Petroleum Production and Fuel Use, Pulp and Paper, Transportation, and Electricity Generation). These reductions are projected to be offset by increases in the Oil Sands and Upstream Oil and Gas sectors.

NO_x emissions are projected to slightly decrease overall. However, similar to SO_x emissions, reductions in the Transportation sector are projected to be offset by increases in the Oil Sands and Upstream Oil and Gas sectors emissions.

Ammonia emissions are generally projected to increase from most sectors due to continued economic growth and a lack of on-the-books initiatives to reduce ammonia emissions at the time the modelling of projections was performed.

4.8 Summary and Conclusions

While Canadian emissions (except for ammonia) have declined somewhat over the period of 1990 to 2006, emissions levels have been relatively stable or even increased during the last 5 to 10 years. The United States is for the most part showing continual decreases in emissions over the time period except for VOC and NH₃ which, though decreasing, are erratic or generally stable (see Figure 4.22).

Overall Canadian emissions of PM₁₀ have increased due to the influence of dust from roads, construction and agriculture. Excluding these sources, the PM₁₀ emissions have decreased for many other sources. For PM_{2.5}, emissions have remained relatively constant overall. When the PM_{2.5} dust from roads, construction and agriculture are excluded from the trend analysis, decreases from many sectors become apparent.

Substantial reductions in SO_x emissions have been realized, with additional reductions anticipated in the future. Reductions achieved in eastern Canada under the Canadian acid rain program have recently begun to be offset by emissions increases due to increased Petroleum industry development in the west. NO_x and VOC emissions have shown some modest decreases, but again these reductions are being offset by emissions from increased Petroleum industry development in the west.

Ammonia emissions in Canada are dominated by the agriculture sector for which current estimates show the emissions to be continually increasing. Most other sources (except on-road vehicles) have reduced ammonia emissions.

Emissions inventories have long been criticized for not adequately representing the best snapshots of emissions at any given time. This is primarily due to the high degree of uncertainty and variability of some sources and in the methodologies for estimation of the emissions of smog precursors. While industrial source emissions estimates have improved greatly, the estimation methodologies for non-point sources still need to be improved especially for fugitive sources such as dust emissions or Canada's Upstream Oil and Gas and Oil Sands sectors. It is also very important that work continue on improving the emissions estimates for historical emissions inventories as these time series generally form the basis for policy development and decision-making.

Improving the non-point estimates as well as the spatial and temporal distribution of emissions will allow for improved ambient air quality modelling. This will provide improved air quality forecasting and a better information base for policy makers on which to focus their continued efforts to improve air quality through targeted emissions reductions.

References

Canadian Council of Ministers of the Environment (CCME) 1997. Canadian 1996 NO_x/VOC Science Assessment. April 1997.

Canadian Council of Ministers of the Environment (CCME), 2003a. Atmospheric Science of Ground-Level Ozone: Update in Support of the Canada-Wide Standards for Particulate Matter and Ozone. Report available at: http://www.ccme.ca/ourwork/air.html?category_id=107

Canadian Council for Ministers of the Environment (CCME), 2003b. Atmospheric Science of Particulate Matter: Update in Support of the Canada-Wide Standards for Particulate Matter and Ozone. Report available at: http://www.ccme.ca/ourwork/air.html?category_id=107

Carter W.P.L, 2008 SAPRC Atmospheric Chemical Mechanisms and VOC Reactivity Scales, Air Pollution Research Center and College of Engineering Center for Environmental Research and Technology. University of California, Riverside, January 2008, Data available at: <http://www.cert.ucr.edu/~carter/SAPRC/>

Environment Canada, 2001. Precursor Contributions to Ambient Fine Particulate Matter in Canada: A Report by the Meteorological Service of Canada, May 2001. ISBN 0-662-30650-3. Report available at: http://www.msc-smc.ec.gc.ca/saib/smog/smog_e.html

Environment Canada, 2004. Canada – United States Transboundary PM Science Assessment: A Report by the Canada-U.S. Air Quality Committee. ISBN 0-662-38678-7 Report available at: http://www.msc-smc.ec.gc.ca/saib/smog/smog_e.html

Environment Canada 2005. Particulate Speciation of the 2002 Emissions Inventory, Unpublished. David Niemi. Gatineau QC, May 2005.

Environment Canada, 2006. Provincial Emissions Trends and Projections. Published on Internet November 2006. Gatineau, QC. August 2006

Environment Canada, 2008a. National Pollutant Release Inventory – Toolbox – Part 5: Speciated VOC – Complementary Information (Synonyms and Compound) Internet: http://www.ec.gc.ca/pdb/websol/ToolBox/other/part_5_speciated_voc_2006_e.cfm, last updated: 2008-11-12, accessed: 2009-04-21

Environment Canada, 2008b. Turning the Corner: Detailed Emissions and Economic Modelling Annex 1: Environment Canada's Modelling Framework. Internet: http://www.ec.gc.ca/doc/virage-corner/2008-03/571/Annex1_eng.htm, last updated: 2008-03-07, accessed: 2009-04-30

Environment Canada, 2009a. National Pollutant Release Inventory (NPRI) Databases. Internet: <http://www.ec.gc.ca/inrp-npri/default.asp?lang=en&n=0EC58C98->, last updated: 2009-04-02, accessed: 2009-06-03

Environment Canada, 2009b. National Prediction Operations (NPO). North American Emissions Maps (Unpublished), Dr. Veronique Bouchet, Montreal QC, Aug 2009.

Environment Canada, 2010a. National Pollutant Release Inventory (NPRI) Downloadable Databases. Internet: <http://www.ec.gc.ca/inrp-npri/default.asp?lang=en&n=0EC58C98-> , last updated: 2010-04-20, accessed: 2010-04-25

Environment Canada, 2010b. National Air Pollutant Emission Trends in MS Excel Format (as of July 2009). Internet: <http://www.ec.gc.ca/inrp-npri/default.asp?lang=en&n=0EC58C98-> , last updated: 2010-04-20, accessed: 2010-04-25

Infometrica Limited. Infometrica Forecast Services. 2007. Internet: <http://www.infometrica.com/>

International Joint Commission (IJC) 2008. Canada – United States Air Quality Agreement: 2008 Progress Report. ISBN: 978-1-100-10516-1. Report available at: http://www.ec.gc.ca/cleanair-airpur/caol/canus/report/2008CanUs/eng/tdm-toc_eng.cfm

Macaluso, Nick. E3MC slide on model interactions. September 2009.

NARSTO (2004). Particulate Matter Assessment for Policy Makers: A NARSTO Assessment. P. McMurry, M. Shepherd, and J. Vickery, eds. Cambridge University Press, Cambridge, England. ISBN 0 52 184287 5

NARSTO (2005). Improving Emission Inventories for Effective Air Quality Management Across North America: A NARSTO Assessment. M. Deslauriers, H. Fledman, C. Frey, D. Mobley, L. Rojas-Bracho, S. Wierman, chairs. . . Report available at: <http://www.narsto.org/section.src?SID=8>

National Energy Board (NEB). 2007 Summer Energy Outlook. May 30, 2007. Ottawa, Ontario.

Niemi, D., 2005. Chapter 2: Emissions of Pollutants Related to Acid Deposition in North American *In* Environment Canada, 2005. 2004 Canadian Acid Deposition Science Assessment. Meteorological Service of Canada, Environment Canada, Ottawa, ON. ISBN 0-662-38754-6. Report available at: http://www.msc-smc.ec.gc.ca/saib/acid/acid_e.html

Possiel, N., G. Stella, R. Ryan, T. Pace, W. Benjey, A. Beidler, E. Kinnee, M. Houyoux, and Z. Adelman, 2001. Development of an anthropogenic emissions inventory for annual nationwide Models-3/CMAQ simulations of ozone and aerosols. Proc. 10th International Emissions Inventory Conference, May 1-3, Denver, CO, 9 pp. Available from <http://www.epa.gov/ttn/chief/conference/ei10/modelling/possiel.pdf>

United States Environmental Protection Agency (US EPA), 1996. AP 42, Fifth Edition, Volume I Chapter 13: Miscellaneous Sources. Section 13.1 Wildfires and Prescribed Burning October 1996. Internet: <http://www.epa.gov/ttn/chief/ap42/ch13/index.html>, last updated: September 5th, 2008, accessed: April 2009

United States Environmental Protection Agency (US EPA), 2002a. National Emissions Inventories for the U.S. 2002 NEI. Internet : <http://www.epa.gov/ttn/chief/net/2002inventory.html>, last updated: 2009-04-29, accessed: 2009-06-03

United States Environmental Protection Agency (US EPA), 2002b. SPECIATE Version 3.2. November 2002. Internet: <http://www.epa.gov/ttn/chief/software/speciate/speciate32.html>. last updated: 2007-06-21, accessed: 2009-06-03

United States Environmental Protection Agency (US EPA), 2005 Projected 2015 CAIR emissions. Inventory files for SMOKE processing. Internet <http://www.epa.gov/CAIR/> downloaded spring 2005.

United States Environmental Protection Agency (US EPA), 2006a. SPECIATE Version 4.0. December 2006. Internet: <http://www.epa.gov/ttn/chief/software/speciate/index.html>. last updated: 2010-04-06, accessed: 2010-04-06

United States Environmental Protection Agency (US EPA), 2006b. AP 42, Fifth Edition, Volume I Chapter 13: Miscellaneous Sources. Section 13.2.1 Paved Roads and 13.2.2 Unpaved Roads November 2006. Internet: <http://www.epa.gov/ttn/chief/ap42/ch13/index.html>, last updated: September 5th, 2008, accessed: April 2009

United States Environmental Protection Agency (US EPA), 2008. Emissions Factors & AP 42. Internet: <http://www.epa.gov/ttn/chief/ap42/index.html>, last updated: 2009-02-10, accessed: February 2008

United States Environmental Protection Agency (US EPA), 2010a. 1990 Tier3 Summary database – September 8, 2005. Internet: ftp://ftp.epa.gov/EmisInventory/nei_criteria_summaries/1990criteriasummaryfiles/, September 8, 2005, accessed: April 2010.

United States Environmental Protection Agency (US EPA), 2010b. 1996 Tier3 Summary database – September 8, 2005. Internet: ftp://ftp.epa.gov/EmisInventory/nei_criteria_summaries/1996criteriasummaryfiles/, September 8, 2005, accessed: April 2010.

United States Environmental Protection Agency (US EPA), 2010c. 1999 Tier3 Summary database – September 8, 2005. Internet:
ftp://ftp.epa.gov/EmisInventory/nei_criteria_summaries/1999criteriasummaryfiles/, September 8, 2005, accessed: April 2010.

United States Environmental Protection Agency (US EPA), 2010d. 2002 All Sector Tier Summary Database – October 15, 2007. Internet:
ftp://ftp.epa.gov/EmisInventory/2002finalnei/all_sector_tier_summary_data/tier/, October 15, 2007, accessed: April 2010.

United States Environmental Protection Agency (US EPA), 2010e. 2005 Tier2 State & National Database – September 8, 2005. Internet:
<http://www.epa.gov/ttn/chief/net/2005inventory.html#inventorydata>, Last Updated April 06 2010, accessed: April 2010.

United States Environmental Protection Agency (US EPA), 2010f. 1970 - 2008 Average annual emissions, all criteria pollutants in MS Excel - June 2009. Internet:
<http://www.epa.gov/ttn/chief/trends/index.html> , Last Updated June 09, 2009. Accessed: April 2010.

University of North Carolina (UNC), 2009. SMOKE – Sparse Matrix Operator Kernel Emissions. Internet: <http://www.smoke-model.org/index.cfm>, accessed: April 2009

WGAQOG, 1999a. National Ambient Air Quality Objectives for Ground Level Ozone: Science Assessment Document. A report by the CEPA/FPAC Working Group on Air Quality Objectives and Guidelines. Minister, Public Works and Government Services

WGAQOG, 1999b. National Ambient Air Quality Objectives for Particulate Matter: Science Assessment Document. A report by the CEPA/FPAC Working Group on Air Quality Objectives and Guidelines. Minister, Public Works and Government Services

CHAPTER 5: Chemical Transport Models: Model Description and Evaluation

Wanmin Gong, Colleen Farrell, Paul A. Makar, Richard Ménard, Michael D. Moran, Gilles Morneau, and Craig Stroud

Contributor Authors: Véronique Bouchet & AQMAS, Colin di Cenzo, David Fox, Weimin Jiang, Steve Smyth, Junhua Zhang, Qiong Zheng

KEY MESSAGES AND IMPLICATIONS

- Chemical Transport Models (CTMs) are amongst the current state-of-science models capable of simulating atmospheric oxidants and particulate matter (PM). AURAMS, CHRONOS, and CMAQ models have been used and evaluated for a number of model simulations ranging from longer term (annual) continental scales to shorter term, episodic regional and local scales.
- AURAMS, CHRONOS and CMAQ are evaluated by comparing model predictions to observations. Collectively these individual evaluations provide an overall range of model performance variability. A summary of model performance specific to ozone and particulate matter is as follows:
- In general, model performance tends to be better for longer-term averages than on shorter time scales.
- On an annual time scale, the AURAMS predicted ozone (O_3) and fine particulate matter ($PM_{2.5}$) correlate well with observations geographically for 2002.
- Annually $PM_{2.5}$ is under-predicted, mainly due to the under-prediction of fine total organic matter ($TOM_{2.5}$).
- O_3 is over-predicted in summers (3rd quarter) mostly over eastern North America.
- Over shorter time scales, the models tend to better predict maximum O_3 (daily 1-hr or 8-hr) than daily means, mostly due to the over-prediction of night-time minimum O_3 concentrations.
- It is shown that model predicted annual PM-sulphate has the highest correlation with observations; correlations are also good for PM-nitrate and ammonium. The model simulation of elemental carbon and organic matter components are poor; crustal material is over-predicted mainly due to poor representation of the emissions.

- Models generally have better skills in predicting primary pollutants (given reliable emissions) than in predicting secondary pollutants due to the complexity of various atmospheric processes. In particular, boundary layer dynamics and mixing, cloud processing, and secondary organic aerosol (SOA) formation are some of the processes having significant impact on model performance.
- Dynamic evaluation is a relatively new concept, aimed at evaluating model response to changes in either meteorology or emission, and is particularly relevant to applying CTMs to support emission control strategy development. Dynamic evaluations of model simulations of the U.S. SIP Call NO_x control case indicate that the models are able to reproduce the observed trend in O₃, although the magnitude of the changes may be under predicted by the model particularly farther downwind from the source region. However, bearing in mind the difficulties in defining such an evaluation both in terms of resolving different changes in emission and meteorology and discerning clear response to the changes from observations, such an evaluation is subject to a significant level of uncertainty itself.
- Uncertainties in CTM predictions can arise from many sources, including uncertainties in model inputs, meteorology, initial and boundary conditions, incomplete model science and process parameterization, and model numerics. Confidence levels in CTMs simulations have not changed significantly from the previous assessment in Seigneur and Moran (2004), although there is considerable improvement in our confidence levels in the simulations for longer time scales and over larger spatial scales.
- There may also be a disconnect between confidence level in model prediction of the targeted pollutants and in model prediction of responses to changes in emissions. Amongst different CTMs there is indication that large performance differences may exist in predicting targeted pollutants, although the differences in predicting relative response to emission changes are smaller. It is argued that, for regulatory applications, emphasis should be shifted from operational evaluation to diagnostic and dynamic evaluations.

5.1 Introduction

Chemical transport models (CTMs) play an important role in the scientific investigation of the transport and transformation of pollutants in the atmosphere. They have also become an essential tool for providing science-based input into developing policies to manage air quality. CTMs are commonly referred to as source-oriented models consisting of mathematical representations of the relevant physical and chemical atmospheric processes, linking emissions of primary gaseous and particulate matter (PM) precursors quantitatively to ambient concentrations of air pollutants under a given set of meteorological conditions (e.g., Peters *et al.*, 1995; Seinfeld and Pandis, 1998; Jacobson, 1999; Russell and Dennis, 2000; Seigneur and Moran, 2004). CTMs are usually part of a larger air quality modelling system, which is also comprised of an emission processing component and a meteorological model.

CTMs have been frequently used to assess the sensitivity of ambient concentrations to changes in primary precursors and to predict the impact from anticipated changes in emissions on future air quality, e.g., the 1996 NO_x/VOC Science Assessment (Multi-stakeholder NO_x/VOC Science Program, 1997), the 2004 Canada-U.S. Transboundary PM Science Assessment (Canada-U.S. Subcommittee on Scientific Co-operation, 2004), and the 2004 Acid Deposition Science Assessment (Environment Canada, 2005). Some of the current CTMs applicable to smog issues on regional and urban scales in North America include AURAMS (Moran *et al.*, 1998; Gong *et al.*, 2006), CHRONOS (Pudykiewicz *et al.*, 1997; Sirois *et al.*, 1999), CMAQ (Byun and Ching, 1999; Byun and Schere, 2006), STEM (Tang *et al.*, 2003; Carmichael *et al.*, 2003), WRF-CHEM (Grell *et al.*, 2005; Tie *et al.*, 2007), GATOR (Jacobson, 1997, 2007), and CAMx/PMCAMx (Morris *et al.*, 2003, 2004; Gaydos *et al.*, 2007). On a global scale, CTMs have also been used to assess the impact of intercontinental transport on global and regional air quality (see Chapter 9 for a detailed discussion).

In this assessment three CTMs (namely, AURAMS, CHRONOS, and CMAQ) are run in a series of scenario applications to assess the changes in future ambient concentrations as a result of the anticipated changes in emissions (see Chapter 6). Several intercomparisons of regional CTM performance have suggested that these three models are broadly comparable in performance with respect to each other and to other state-of-the-science regional CTMs (McKeen *et al.*, 2005, 2007, 2009; Smyth *et al.*, 2007a,b, 2009).

This chapter provides an assessment of the current status of these models and levels of confidence in the model performance in the context of providing science support for policy development. An overview of the recent major achievements in CTM development and capabilities is given in section 5.2. This is followed by a brief description in section 5.3 of the CTMs used in this assessment. Section 5.4 summarises some of the important results from recent model evaluations, including operational and diagnostic evaluations, as well as model intercomparison and dynamic evaluation. Section 5.5 addresses the uncertainty issues, followed by a summary and conclusion in section 5.6. Finally recommendations regarding model development and evaluation are made in section 5.7.

5.2 Recent Major Advances in CTM Development and Capabilities

Over the past decade or so, the main advances in regional CTM development have been in the representation of atmospheric aerosols and relevant processes. The majority of CTMs capable of predicting PM_{2.5} nowadays include algorithms for aerosol dynamics, microphysics, and chemistry. Models do, however, differ significantly in their characterization of PM chemical composition and size distribution. They may also differ in the detailed algorithms for specific aerosol-related processes, e.g., gas-phase mechanism, aqueous chemistry, inorganic aerosol thermodynamics, secondary organic aerosol (SOA) formation, and cloud processing (including

wet deposition). Some of the main differences amongst a number of current CTMs relating to aerosol processes are reviewed in McKeen *et al.* (2007). Other comprehensive reviews of PM models are found in Seigneur (2001) and Seigneur and Moran (2004). Previously CTMs have been developed for other atmospheric issues such as photochemical oxidants and acid deposition. Since all of the atmospheric processes relevant to oxidants and acid deposition are also relevant to PM, the development of PM capabilities in CTMs has moved these models closer towards being unified, one-atmosphere air quality models capable of assessing multi-pollutant issues.

Another recent development is the integration of CTM in-line with a meteorological or numerical weather prediction (NWP) model. Traditionally, most of the regional CTMs, such as the ones covered in this chapter, have been developed independent of meteorological models. They are often driven “off-line” by the output fields from a meteorological model. The main advantage of an off-line model is the computational attractiveness for retrospective chemical transport simulations since in this case only a single meteorological dataset is required to support the multiple CTM runs. On the other hand, aside from heavy overhead on input/output (I/O), the off-line approach can create mass inconsistency in wind fields through the inevitable spatial and/or temporal interpolations (e.g., Byun, 1999a, b; Odman and Russell, 1999). In addition, the feedback responses between the chemistry and atmospheric dynamics cannot be modelled with an off-line approach. In recent years several in-line (or on-line) CTMs have been developed, e.g., GATOR-GCMM (Jacobson, 2001a, b), WRF-CHEM (Grell *et al.*, 2005), GEM-AQ (Kaminski *et al.*, 2008), and UAQIFS (Baklanov *et al.*, 2007). The in-line approach eliminates the need for interpolation and ensures no-loss of information between dynamics, physics and chemistry. Most importantly, the feedback between chemistry, dynamics and physics becomes possible, which may lead to improvement in weather prediction and may also enable the integrated assessment of air quality and climate interactions.

The use of CTMs to produce air quality forecasts has become a new application area in recent years. For example, Environment Canada (EC) was amongst some of the first national weather centres to issue air quality forecast based on CTM output (O_3 forecasts since summer 2001 and $PM_{2.5}$ forecasts since 2003). The U.S. National Weather Service has also started to provide CTM based next-day ground-level O_3 forecast for the eastern U.S. and is currently experimenting with the same forecast for conterminous U.S., with the expansion of the operational capacity to include fine PM anticipated in the very near future (Davidson *et al.*, 2007). Regional CTMs have also been used to provide real-time forecasts for guiding flight planning during several recent field campaigns (e.g., ICARTT 2004, PrAIRie2005, TEXAQs 2006, and BAQS-Met 2007). The ICARTT 2004 campaign included a first-ever real-time air quality forecast ensemble involving several regional CTMs (McKeen *et al.*, 2005, 2007). With the increase in computer power and improved computational techniques, longer term (e.g., season-long and year-long) simulations with regional CTMs are now much more common

(e.g., Eder *et al.*, 2006; Gilliland *et al.*, 2008; van Loon *et al.*, 2007; Vautard *et al.*, 2007; Moran *et al.*, 2007, 2008). Recently, a 12-year regional CTM simulation has been attempted for a health impact analysis (Hogrefe *et al.*, 2007a).

Data assimilation is a technique that brings observations into a prognostic model. The technique was originally developed to create initial conditions for numerical weather forecast. Over the years, the technique has been evolving and playing an increasingly important role in improving the quality of weather forecast in the numerical weather prediction community (Daley, 1991; Kalnay, 2003; Lewis *et al.*, 2006). Significant advancements have been made in recent years in transferring and extending the data assimilation techniques to the chemical transport modelling community through bringing the ever-increasing chemical observations into atmospheric CTMs. For example, chemical data assimilation has been used to produce analyses of atmospheric chemical constituents on regional and global scales (e.g., Blond *et al.*, 2003; Menard and Robichaud, 2006; Clerbaux *et al.*, 2001; Yudin *et al.*, 2004; Rasch *et al.*, 2001) and to improve CTM performance (e.g., van Loon *et al.*, 2000; Elbern and Schmidt, 2001; Chai *et al.*, 2007). There have been numerous applications of data assimilation techniques to improve emission estimates of several pollutants based on satellite observations (e.g., Arellano *et al.*, 2004; Muller and Stavrou, 2005; Pison, 2005). In particular, the use of adjoint modelling, a procedure employed by variational methods for either inverse modelling or data assimilation, is a powerful tool for emission sensitivity analysis which is relevant to air quality management (e.g. Menut *et al.*, 2000, Hakami *et al.*, 2006).

5.3 Description of the CTMs Used in This Assessment

5.3.1 Regional CTMs developed at Environment Canada

Table 5.1 Comparison of key characteristics of AURAMS, CHRONOS, and CMAQ circa 2008.

CHARACTERISTIC/ MODEL	AURAMS	CHRONOS	CMAQ
Meteorological Driver	GEM (off-line)	GEM (off-line)	MM5, [MC2, GEM, WRF] (off-line)
Emissions Processing System	SMOKE	SMOKE	SMOKE
Anthropogenic Emissions	PM _{2.5} and PM _c emissions speciated to 7 species and size disaggregated to 12 bins by primary source type (major and minor point, area, mobile); 17 gas-phase species emitted. Dynamic emission module for sea-salt (soil dust and DMS	PM _{2.5} and PM _c emission are assumed to be bulk emissions (no speciation, no further size disaggregation); 17 gas-phase species emitted	PM _{2.5} emissions are assumed to be mainly accumulation mode with constant composition; PM _c emissions are assumed to be in coarse mode; 16 gas-phase species emitted (CB-IV)

CHARACTERISTIC/ MODEL	AURAMS	CHRONOS	CMAQ
	planned)		
Biogenic Emissions	BEIS 3.09/BELD 3	BEIS2/BELD3	BEIS 3.09 or 3.13; BELD3
PM Size Distribution Representation	Sectional method (12 bins) based on Canadian Aerosol Module (Gong <i>et al.</i> , 1997a,b, 2003)	Sectional method (2 bins: PM _{2.5} and PM _c)	Modal method with 3 modes: Aitken; accumulation; coarse (Binkowski & Roselle, 2003)
PM Composition Representation	9 species: SO ₄ , NO ₃ , NH ₄ , EC, pOC, sOC, CM, SS, H ₂ O	6 species: SO ₄ , NO ₃ , NH ₄ , sOC, H ₂ O, primary	9 species: SO ₄ , NO ₃ , NH ₄ , EC, pOC, biogenic and anthropogenic sOC, other, SS
Advection	Positive-definite, nonoscillatory, semi-Lagrangian method (Smolarkiewicz and Pudykiewicz, 1992)	Positive-definite, nonoscillatory, semi-Lagrangian method (Smolarkiewicz and Pudykiewicz, 1992)	Piece-wise Parabolic Method (Colella and Woodward, 1984); Yamo global mass-conserving advection scheme?
Vertical Diffusion	Laasonen or Crank-Nicholson implicit differencing with diffusivity from the met driver model with TKE closure; urban heat island parameterization (Makar <i>et al.</i> , 2006)	Laasonen implicit differencing with diffusivity from the met driver model with TKE closure.	TKE closure solved using Crank-Nicholson implicit differencing, or non-local mixing
Subgrid Convective Mixing	Not included	Not included	User-selected option
Gas-Phase Chemistry Mechanism	ADOM-2 mechanism (Stockwell and Lurmann, 1989); 47 species (CO now as a dynamic species)	ADOM-2 mechanism (Stockwell and Lurmann, 1989; 47 species	1. Carbon Bond mechanism, version 4 (CB-IV; Gery <i>et al.</i> , 1989; 36 species); 2. CB05 (Sarwar <i>et al.</i> , 2008; 52 species); or SAPRC-99 (Carter, 2000a,b, 72 species)
Chemical Solver	Vectorized version of Young and Boris (1977); Makar (1995)	Vectorized version of Young and Boris (1977); Makar (1995)	Euler Backward Iterative
Photolysis	Table lookup	Table lookup	Table lookup
Aqueous-Phase Chemistry Mechanism	Based on ADOM mechanism (Young and Lurmann, 1984); nucleation scavenging reactions replaced by explicit particle activation, 20 reactions, 7 gas and 13 aqueous species (Gong, 2002)	None	Based on RADM mechanism (Chang <i>et al.</i> , 1987; Walcek and Taylor, 1986); 22 reactions; some updates made in v 4.7.
Chemical Solver	Vectorized Young & Boris (based on Makar, 1995)		
Aerosol Physics	Nucleation, Condensation/evaporation, Coagulation, Sedimentation, Hygroscopic growth, Aerosol/CCN activation	Sedimentation	Nucleation Condensation/evaporation Coagulation Sedimentation (Binkowski & Roselle, 2003)
Heterogeneous Chemistry	HETV (vectorized inorganic heterogeneous chemistry based on the ISORROPIA solver (Makar <i>et al.</i> , 2003)	HETV as in AURAMS	ISORROPIA (Nenes <i>et al.</i> , 1998) excluding Halogen (Sea Salt) chemistry;
Secondary Organic (sOC) Yields	Based on Odum <i>et al.</i> (1996), or Jiang (2003, 2004)	Based on Pandis <i>et al.</i> (1992)	Based on SORGAM (Schell <i>et al.</i> 2001; Byun and Schere, 2006)

CHARACTERISTIC MODEL	AURAMS	CHRONOS	CMAQ
Cloud (Physical) Processes	Cloud attenuation and enhancement of photolysis rates (based on ADOM algorithm). Aerosol activation (based on Jones <i>et al.</i> , 1994) Droplet scavenging of interstitial aerosol	Cloud attenuation and enhancement photolysis rates (based on ADOM algorithm).	Cloud attenuation and enhancement of photolysis rates. Aerosol activation (only accumulation mode)
Dry Deposition	New resistance-based methods for gases (Zhang <i>et al.</i> , 2002) and size-segregated model for particles (Zhang <i>et al.</i> , 2001); 15 land-use categories	Resistance-based method, Wesley and Hicks (1977), Zhang <i>et al.</i> (2002), and Robichaud (1991), Robichaud <i>et al.</i> (2003)	Particle deposition is treated as in Regional Particulate Matter model Gaseous deposition model is based on RADM (Wesely, 1989) with Pleim-Xiu land-surface model (Xiu and Pleim, 2000).
Wet Deposition	Cloud-to-rain tracer transfer based on precip. Production from the met model; Precipitation scavenging and removal of particles (size-dependent) and soluble gases parameterized by precipitation fluxes and terminal velocity with consideration of evaporation (Gong <i>et al.</i> , 2006)	Distribution of LWC is used to calculate the wet scavenging term by applying Sundqvist formulae for the rate of release of precipitation	Based on Regional Particulate Matter model (RPM) (Binkowski and Shankar, 1995).
Horizontal Discretization	Structured grid defined on polar stereographic projection	Structured grid defined on polar stereographic projection	Structured grid defined on polar stereographic, Mercator or Lambert projections
Vertical Discretization	Gal-Chen terrain-following coordinates (model top at 30 km)	Gal-Chen terrain-following coordinates (model top at 8 km)	Generalized vertical coordinates (model top at 14 km)
Initialization	Model is integrated from either user-specified 1D profiles or objectively-analyzed 3D fields (if mmts available); no data assimilation	Model is integrated using spin up from arbitrarily -specified initial conditions; no data assimilation	Model is integrated starting from user-specified 1D profiles; no data assimilation
Lateral Boundary Conditions and Nesting	Zero-gradient inflow and open outflow boundary conditions; no nesting,	Zero-gradient inflow and open outflow boundary conditions; no nesting,	Default profiles on 4 boundaries; nesting is frequently used with typical horizontal resolutions of 36, 12 and 4 km
Model Application	Policy guidance / real-time forecasts	Policy guidance / real-time forecasts	Policy guidance / real-time forecasts
Model Status	Version 1.3.1 ²³ (released Nov. 2005)	Current operational version (until 18 Nov. 2009)	Latest release versions: 4.6 (Oct. 2006), 4.7 (Dec. 2008).

²³ Version 1.3.2 prototype (final version released officially as version 1.4.0 on 3 Feb. 2009) was used for some of the more recent simulations included in this assessment (as indicated).

Two regional CTMs developed by EC have been used in this Assessment. CHRONOS (Canadian Hemispheric and Regional Ozone and NO_x System) is currently the Canadian national air quality forecast model (AQFM) for O₃ and PM_{2.5}. It is based on the off-line photochemical CTM developed at EC (Pudykiewicz et al., 1997; Sirois et al., 1999), and it has been used operationally since 2001. AURAMS (A Unified Regional Air-quality Modelling System) was designed by EC to be a regional PM modelling system with a size- and composition-resolved representation of PM (Moran et al., 1998; Gong et al., 2006). The off-line AURAMS CTM started from the 1998 version of the CHRONOS CTM code, so despite their largely independent development after that time, they share a number of model components. The main difference in the science between the two CTMs lies in the sophistication of the parameterizations used to represent atmospheric aerosol processes (see Table 5.1). These two modelling systems are therefore described together here, with their differences specified wherever necessary.

Table 5.1 summarizes the various process representations employed by CHRONOS and AURAMS. Both models use the same three-dimensional advection schemes and vertical diffusion schemes, although AURAMS also includes a mass-conservation adjustment step and another, higher-order, vertical diffusion scheme (Crank-Nicholson). Both models use the ADOM-II gas-phase chemistry scheme and the same 46 gas-phase model species plus H₂SO₄ in AURAMS. To represent PM size distribution, both models use a sectional approach but CHRONOS considers only two size bins (0-2.5 and 2.5-10 µm diameter) whereas AURAMS considers 12 size bins from 0 to 41 µm. To represent PM chemical composition, CHRONOS considers six chemical components (primary PM plus particulate sulphate (p-SO₄), particulate nitrate (p-NO₃), particulate ammonium (p-NH₄), secondary organic aerosol (SOA), and particle-bound water (WA)) versus nine components in AURAMS (p-SO₄, p-NO₃, p-NH₄, elemental carbon (EC), primary organic aerosol (POA), SOA, crustal material (CM), sea salt (SS), and WA).

CHRONOS and AURAMS use different parameterizations of SOA formation, i.e., Pandis *et al.* (1992) is used in CHRONOS whereas Odum *et al.* (1996) or Jiang (2003) is used in AURAMS, but use the same treatment of inorganic gas-particle partitioning. CHRONOS does not consider aqueous-phase chemistry but AURAMS does. Unlike CHRONOS, AURAMS includes explicit parameterizations for such aerosol microphysical processes as nucleation, coagulation, activation in cloud, and droplet scavenging of interstitial aerosol. CHRONOS and AURAMS employ different parameterizations for dry deposition and for wet deposition of gases and particles (Table 5.1). Finally, both models use the same zero-gradient treatment of chemical lateral boundary conditions as default. In newer versions of AURAMS an option for time-independent chemical lateral boundary conditions (e.g., Samaali et al., 2009) has been implemented.

Both CHRONOS and AURAMS obtain the meteorological input fields that they require from the EC Global Environmental Multiscale (GEM) meteorological model, which is an integrated weather forecasting and data assimilation system designed to meet Canada's operational needs for both short- and medium-range weather forecasts (Côté *et al.*, 1998a,b; Mailhot *et al.*, 2006). AURAMS requires more meteorological fields from GEM than CHRONOS does, particularly cloud-related fields needed for its parameterization of aqueous-phase chemistry. Also, a pre-processing step is needed to interpolate GEM output fields to the CHRONOS and AURAMS grids, since GEM uses a rotated latitude-longitude horizontal grid coordinate and a hybrid vertical coordinate whereas CHRONOS and AURAMS both use a uniform horizontal grid on a polar stereographic projection and a modified Gal-Chen terrain-following vertical coordinate, with 28 unevenly spaced levels from surface to about 22 km in the case of AURAMS, and 24 levels up to about 6 km in the case of CHRONOS.

The gridded, speciated, hourly anthropogenic emission files needed by CHRONOS and AURAMS are prepared using the SMOKE (Sparse Matrix Operator Kernel Emissions) emissions processing system (e.g., Houyoux *et al.*, 2000; CEMPD, 2007). Emissions of 18 model gas-phase species and two bulk PM species are included in these files. Biogenic emissions of four model gas-phase species are calculated internally by CHRONOS and AURAMS during a simulation using algorithms from Biogenic Emissions Inventory System (BEIS) developed by the U.S. EPA (e.g., Pierce *et al.*, 1998a,b). CHRONOS uses an older version of BEIS (version 2), and version 3 of the Biogenic Emissions Landcover Database (BELD3) whereas AURAMS uses version 3.09 of BEIS and BELD3 (e.g., Kinnee *et al.*, 1997; Pierce *et al.*, 1998a,b; Morneau, 2007; U.S. EPA, 2007a).

5.3.2 US EPA CMAQ

The Community-Multiscale Air Quality (CMAQ) modelling system was developed at the U.S. EPA (e.g., Byun and Ching, 1999; Byun and Schere, 2006). CMAQ, like the AURAMS CTM, is an off-line regional PM CTM that employs a size- and composition-resolved representation of PM. CMAQ uses a modal representation of the PM size distribution that consists of three log normal sub-distributions or modes: Aitken or nucleation mode; accumulation mode; and coarse mode. Eleven chemical components are tracked: p-SO₄; p-NO₃; p-NH₄; EC; POA; anthropogenic SOA; biogenic SOA; CM; SS; WA; and "other". Unlike AURAMS, the CM and SS components are assumed to be restricted to the coarse mode whereas p-NO₃, p-NH₄, and the carbonaceous species are assumed to be restricted to the two smaller modes.

As described in Table 5.1, CMAQ includes a suite of process parameterizations similar to AURAMS, but the individual parameterizations are different from those in AURAMS (and CHRONOS) in every instance. AURAMS and CMAQ thus constitute independent descriptions of the processing governing atmospheric ozone and PM.

The usual meteorological driver for CMAQ is MM5, the fifth-generation version of the Penn State meteorological model (Dudhia *et al.*, 2004)²⁴. MM5 uses a uniform grid on a Lambert conformal conic map projection. A utility program called Meteorology Chemistry Interface Program (MCIP) is used to interpolate and/or diagnose MM5 output fields to CMAQ meteorological input fields. CMAQ (when driven by MM5) uses a pressure-sigma coordinate system in the vertical similar to MM5 but with typically 15 unevenly spaced vertical levels extending from surface to 100 hPa, or about 16 km (Byun and Ching, 1999). The National Research Council of Canada has developed a modified version of MCIP, called GEM-MCIP, to interpolate GEM output fields to CMAQ meteorological input fields (Smyth *et al.*, 2006b). Anthropogenic and biogenic emission files for CMAQ are generated using SMOKE and meteorological fields from MM5 or GEM. Version 3.09 of BEIS was used by SMOKE until mid 2007, when version 2.4 of SMOKE, which uses BEIS v3.13, was released.

5.4 Model Evaluation

Model performance evaluation plays an important role in both model development and application processes. It is essential to establish the credibility of a model before it can be used for guiding policy development. There are several levels of model performance evaluation. An operational evaluation usually involves comparing model predictions against routine monitoring data of the major pollutants of interest. This evaluation is conducted mainly to address whether the model is capable of predicting the end-point pollutants correctly. A diagnostic evaluation involves more detailed probing of a model, *i.e.*, evaluating both precursor and intermediate species, sensitivity tests on various model component/processes. A diagnostic evaluation addresses whether the predicted ambient concentrations are a result of correct or incorrect processes (or “right results for the right reasons”). A so-called probabilistic evaluation is an attempt to assess model uncertainty (or confidence level) given uncertainties in model inputs and formulations (Gilliland *et al.*, 2007; Seigneur, 2007). This can be done through model ensemble (*e.g.*, using multi-model or single-model, with perturbed inputs or model parameters). Model inter-comparison, particularly involving multiple models, is also an effective way of establishing uncertainties or confidence level (*e.g.*, McKeen *et al.*, 2005 and 2007; Vautard *et al.*, 2006; van Loon *et al.*, 2007). There is an increased realization that a

²⁴ Recently CMAQ is also being driven by WRF (the Weather Research and Forecasting model, Skamarock *et al.*, 2007) particularly with the latest release of CMAQ version 4.7.

dynamic evaluation, i.e., evaluating model response to changes in either meteorology or emissions, is particularly relevant when applying CTMs to support emission control strategy development.

Model evaluation relies heavily on available observational data from a variety of sources, e.g., monitoring networks, special intensive studies, and field campaigns. As mentioned briefly in section 5.2 (and discussed further in Chapter 8), satellite based measurements are also starting to play an important role in air quality model evaluation. Various existing monitoring networks in Canada and the U.S. provide routine measurements of O₃, PM_{2.5} (mass and composition) and several other targeted pollutants (see Chapter 3). These monitoring data are particularly useful for operational evaluation as they tend to cover a wide geographical area over a long time period. However, the data are limited to ground-level observations and, with current measurement techniques, mostly at infrequent sampling rates (e.g., weekly or one in several days). Many of the networks are also focused on urban, suburban, and industrial areas. As will be discussed in sections 5.4.1 and 5.4.2 below, the data coverage is poor for U.S. Midwest and the less populated Canadian North. On the other hand, diagnostic evaluation requires more chemically, spatially (including in the vertical), and temporally resolved measurements in order to reveal the relevant atmospheric processes. These data are usually acquired through intensive field studies targeting specific region or area over a limited time period (see section 5.4.3.2). One of the important issues with comparing model results with observations is the incommensurability between the measurement at one point in space and volume-averaged model results at a given spatial resolution (Seigneur and Moran, 2004). Other issues to be considered when comparing model results with observations include measurement standards and protocols (Moran *et al.*, 2010), matching between measured and modelled parameters, e.g., VOC representation in model versus measurement (section 5.4.3.1) and PM size representation in model versus size-cut from measurements (Jiang *et al.*, 2006; Moran *et al.*, 2010).

Table 5.2 Model simulations included in this evaluation.

	Model	Simulation period	Model domain and resolution	Emissions	Lateral boundary conditions
Annual	AURAMS (v1.3.1)	Dec. 1, 2001 to Dec. 31, 2002	NA continental domain @ 42-km resolution	Can. 2000/U.S. 2001/ Mexico 1999; BEIS v3.09	Ozone climatology; zero-gradient BC for other species/components
ICARTT (retrospective)	AURAMS (v1.3.2*)	July 7 – August 19, 2004	Eastern NA @ 42-km	Can. 2000 / U.S. 2001; BEISv3.09	Time-invariant LBC:
PrAIRie 2005 (retrospective)	AURAMS (v1.3.2*)	Aug.22 – Sept.9, 2005	western Canada & U.S. @ 21-km; nested Edmonton hi-res @ 3-km	21-km: Can. 2000/ U.S. 2001; 3-km: Can. 2000 with updates using CEMS data for three coal-fired power-plants; BEIS v3.09	Time-invariant LBC for the 21-km domain
Que /Atlantic	AURAMS (v1.3.1)	July 28 – Aug. 5, 2001; Feb. 5 – 8, 2005	Quebec-Atlantic domain @ 21-km resolution	Can. 2000 / US 2001; BEISv3.09	Zero gradient
Operational CMC	CHRONOS	Operational since summer 2001	NA continental domain @ 21-km resolution	Can. 2000 / US 2001 with EGU updates; BEISv3.09	Zero gradient
Alberta (PNR)	CMAQ-MM5 (CMAQ version 4.5)	June, July, and August 2002	Alberta @ 12-km, nested in a larger 36-km resolution domain	Can. 2000 with updates for oil sand emission / U.S. 2001; BEISv3.09/BELD3	CMAQ default (time-invariant) for the 36-km domain
BC-LFV (PYR/RWDI)	CMAQ-MC2 (RADM2 for 12-km; SAPRC-99 for 4-km), CMAQ version 4.3	Aug. 9 - 31, 2001	LFV @ 4-km, nested in a larger 12-km resolution domain	Can. 2000 + GVRD 2000 / U.S. 1999; BEIS2	CMAQ default (time-invariant) for the 12-km domain
BC-LFV (NRC)	CMAQ-MM5 (CMAQ version 4.3)	Aug.9 - 21, 2001	LFV @ 4-km, nested in a larger 12-km resolution domain	Can. 1995 + GVRD 2000 / U.S. 1999 projected to 2001; BEISv3.09/BELD3	CMAQ default (for 12-km domain) adjusted to observations during the study period for O ₃ , CO, SO ₂ , NO, and NO ₂
Model comparative study (NRC)	AURAMS (v1.3.1b)	July 1 – 30, 2002	NA continental domain @ 42-km resolution	Can. 2000 / U.S. 2001; BEISv3.09 (processed on-the-fly)	Zero-gradient lateral boundary condition
	CMAQ-GEM (CMAQ version 4.6)	July 1 -30, 2002	NA continental domain @ 42-km resolution (Lambert projection)	Can. 2000 / U.S. 2001; BEISv3.09 (processed by SMOKE)	Time-invariant CMAQ default

This section summarises the existing evaluations of the CTMs used in this assessment. To the largest possible extent, this section describes the current status of the models' ability to predict ambient O₃ and fine PM concentrations at different spatial and temporal scales, simulate the precursor-concentration relationship, and simulate the change in response to the changes in precursor emissions. The evaluations in this section draw from a number of model simulations which differ from each other in a variety of ways: the CTM itself (e.g., AURAMS, CHRONOS or CMAQ), model domain, resolution, time period, and other model configurations. A full list of the model simulations used in this model performance assessment is given in Table 5.2.

Evaluation data include routine monitoring data from various networks operated in Canada and U.S. and observations from a number of recent measurement field campaigns.

Different sets of evaluation metrics were used by the different groups for their model evaluation, but most of them, particularly those for operational evaluation against monitoring network data, involved the commonly used standard statistical measures, such as mean bias (MB), normalized mean bias (NMB), mean error (ME), normalised mean error (NME), root-mean-square error (RMSE), and correlation coefficient (r). The definitions of these standard statistical measures are given in the Appendix in Section 5.9. The model evaluations included in this section also cover a range of spatial and temporal scales, from continental to regional to local and from annual to seasonal to episodic. A variety of temporal (in particular) and spatial averaging were used in applying the evaluation metrics in these evaluations depending on individual objectives (see the Appendix in Section 5.9 for details).

5.4.1 Model Prediction of Ozone and Total PM_{2.5} at Ground Level

In this sub-section, we assess the current model performance in predicting ambient O₃ and fine PM (diameter less than 2.5 μm), the two most monitored components of smog.

5.4.1.1 Continental, Annual, and Seasonal Scales

An annual simulation with AURAMS was carried out for the year 2002 on a 42-km resolution grid, covering most of the North American continent (Moran *et al.*, 2007). Extensive model performance evaluation has been carried out against a large monitoring data set consisting of filter-based and continuous surface air chemistry measurements and precipitation chemistry measurements from several Canadian and U.S. networks. A full description of this evaluation is found in Moran *et al.* (2008, 2010).

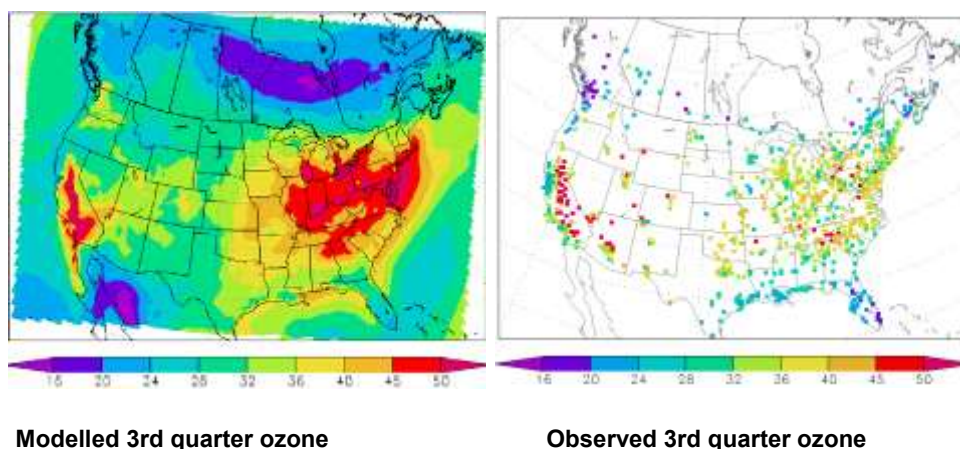


Figure 5.1 AURAMS predicted (left panel) 3rd quarter (July, August, and September, 2002) average ozone concentration (ppbv) compared to the observations (right panel).

Table 5.3 Ozone evaluation statistics, i.e., mean bias (MB), normalised mean bias (NMB), and linear correlation coefficient (r), from the AURAMS annual simulation of 2002

	Quarter 1	Quarter 2	Quarter 3	Quarter 4	Annual
# of pairs	447	811	859	461	458
Obs. mean	25.1	35.7	33.9	21.3	28.4
Model mean	22.2	36.0	39.8	21.7	28.6
MB (ppb)	-2.9	0.4	6.0	0.3	0.1
NMB (%)	-11.7	1.1	17.6	1.5	0.4
RMSE (ppb)	6.8	6.7	10.3	5.8	6.2
r	0.54	0.44	0.52	0.62	0.52

Modelled ground-level O₃ concentrations were compared to observations from four networks, two in Canada (CAPMoN and NAPS) and two in the U.S. (AQS and CASTNet). Figure 5.1 shows the modelled 3rd quarter (July, August, and September) average O₃ concentration compared to the observations. It is seen that the model captured the observed high O₃ concentrations over California in the west but over-predicted mid-western to eastern U.S and south eastern Canada (Windsor-Quebec corridor, in particular) for the 3rd quarter (a main part of O₃ season). Selected evaluation statistical measures, namely mean bias (MB), normalized mean bias (NMB), root-mean-square error (RMSE), and correlation coefficient (r), are presented in Table 5.3 for both quarterly and annual averages. Averaged over all sites, the model has a small positive bias in terms of annual mean O₃, though seasonally biased low in winter (1st quarter) and biased high in summer (e.g., 3rd quarter). As seen in Figure 5.1, the positive bias was mostly attributed to the model over-predicting O₃ in the eastern part of the domain. There is also a significant over-prediction in the Lower Fraser Valley of BC.

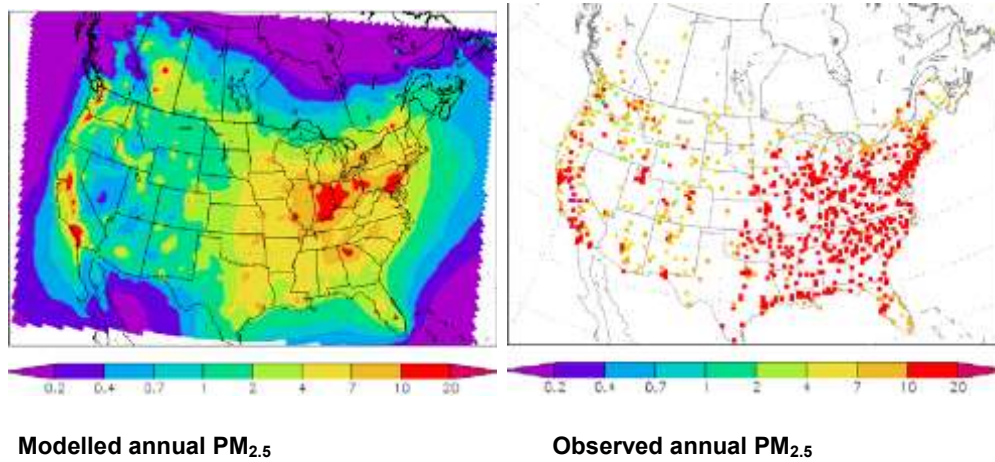


Figure 5.2 Comparison between AURAMS predicted (left panel) and observed (right panel) annual (2002) ground-level PM_{2.5} mass concentration ($\mu\text{g m}^{-3}$).

Table 5.4 PM_{2.5} evaluation statistics from the AURAMS annual simulation of 2002

	Quarter 1	Quarter 2	Quarter 3	Quarter 4	Annual
# of pairs	811	832	836	837	845
Obs. mean	9.7	10.0	12.6	9.9	11.3
Model mean	5.5	7.2	8.9	6.2	7.0
MB ($\mu\text{g m}^{-3}$)	-4.2	-2.8	-3.7	-3.7	-4.4
NMB (%)	-43.7	-28.1	-29.5	-37.7	-38.4
RMSE ($\mu\text{g m}^{-3}$)	5.9	4.7	5.6	5.7	5.6
r	0.48	0.63	0.67	0.52	0.59

A comparison between modelled and observed annual ground-level PM_{2.5} is shown in Figure 5.2. The PM_{2.5} measurements are from eight networks, three in Canada (CAPMoN, NAPS-continuous, NAPS-filter) and five in the U.S. (AQS-continuous, AQS-filter, AQS-STN, CASTNet, and IMPROVE). The modelled annual mean PM_{2.5} concentrations compared well with the observations in terms of geographical distribution but the modelled values were biased low particularly over the eastern U.S. This is reflected in the biases shown in Table 5.4. The under-prediction is more significant in the cold seasons (1st and 4th quarters). The model PM_{2.5} correlates better with the observation in warm seasons (2nd and 3rd quarter), while the opposite is true for O₃ (Table 5.3).

5.4.1.2 Regional, Episodic Scales

At shorter time scales, several evaluation exercises were conducted with different models focusing on different regions. These include a simulation of the International Consortium for Atmospheric Research on Transport and Transformation (ICARTT) study period (summer 2004) over eastern North America using AURAMS (Gong *et al.*, 2007), a simulation focussed over Alberta for three summer months (June, July, and August) in 2002 using CMAQ (Fox and Kellerhals, 2007), and two separate high-resolution CMAQ simulations (RWDI, 2003; Smyth *et al.*, 2006b) for the Pacific 2001 field study period (Li, 2004) focusing on southern BC (Lower Fraser Valley or LFV). Table 5.2 describes the specifics of these simulations.

Eastern NA (AURAMS ICARTT run):

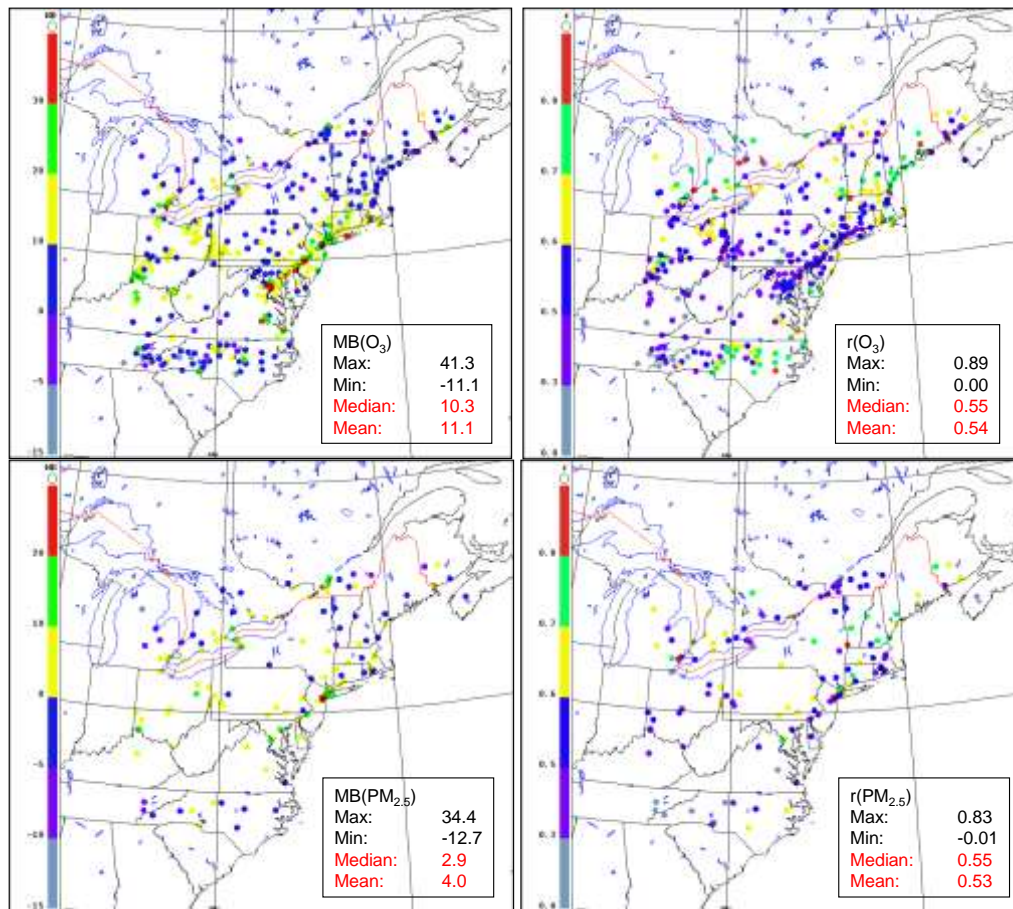


Figure 5.3 Spatial distribution of the correlation coefficient (r) and the mean bias (MB) for daily 1-hour maximum ozone (top panels) and daily average PM_{2.5} (bottom panels) for the AURAMS simulation of the ICARTT 2004 field study period.

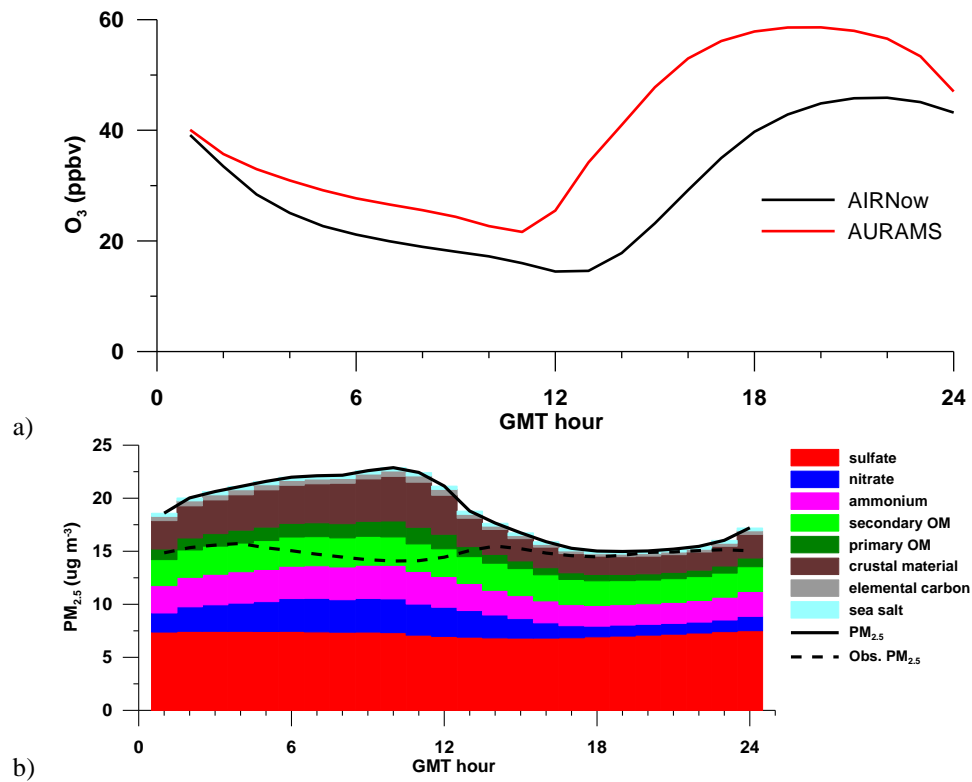


Figure 5.4 Model-observation comparisons of averaged diurnal (a) ozone and (b) PM_{2.5} over the AIRNOW sites for the ICARTT 2004 field study period. Modelled averaged diurnal speciated PM_{2.5} components are also shown in (b).

Table 5.5 Ambient ozone and PM_{2.5} evaluation statistics from the AURAMS ICARTT simulation against AIRNow observations.

	O ₃ daily 1-hr max.	O ₃ daily mean	PM _{2.5} daily 1-hr max	PM _{2.5} daily mean
Obs. mean	53.0	29.1	25.8	15.0
Model mean	63.8	40.3	32.0	18.9
MB (ppb, µg m ⁻³)	10.8	11.2	6.2	3.9
NMB (%)	21.9	41.8	24.7	29.0
RMSE (ppb, µg m ⁻³)	18.8	15.4	20.8	11.5
r	0.54	0.45	0.46	0.53

The AURAMS ICARTT retrospective simulation was conducted over eastern North America on a 42-km resolution grid for the period of July 7 to August 19, 2004 (Gong *et al.*, 2007). The first week of the simulation is treated as model spin-up (i.e., to allow the model to adjust to a

state of chemical equilibrium from its initial conditions). The model-predicted ground-level O_3 and $PM_{2.5}$ are compared with observations from the AIRNow surface network (<http://airnow.gov/index.cfm>). Figure 5.3 shows the spatial distribution of the correlation coefficient (r) and the mean bias (MB) for daily 1-hour maximum O_3 and daily average $PM_{2.5}$. A set of evaluation statistics is summarized in Table 5.5. It can be seen that the model over-predicts the daily 1-hr maximum O_3 , more significantly around the southern Great Lakes and the U.S. Mid-Atlantic States. Compared to the annual simulation described above (section 5.4.1.1) and with reference to the 3rd quarter in Table 5.3, the O_3 bias is significantly higher in this regional case. Several factors need to be considered when comparing the 2002 annual AURAMS run to the 2004 AURAMS ICARTT run. Most importantly, there is a significant difference in meteorological conditions between the summers of 2002 and 2004 over eastern North America. White *et al.* (2007) contrasted the July-August 2004 with the same period in 2002 and found that these two years represent the two extremes, both in meteorological conditions and in observed O_3 levels. Relative to the 1996-2005 decade, the summer of 2002 was much warmer and drier than normal and recorded the maximum O_3 exceedances in this region, while the summer of 2004 was considerably cooler and wetter and saw the minimum O_3 exceedances during this decade. Comparing the annual AURAMS run to the ICARTT AURAMS run indicates that AURAMS performs better in predicting O_3 under higher O_3 conditions compared to low O_3 conditions. This is a phenomenon also experienced by the CMAQ model (Arnold and Dennis, 2001). Figure 5.4a presents the model to observation comparison of averaged diurnal O_3 over the simulation period at the AIRNow sites. It shows that the model bias is associated with the under-prediction of night-time depletion and the over-prediction of the net production of O_3 during the day. The model predicted timing for the early-morning minimum and the afternoon maximum also appears to be about two hours earlier than observation.

The modelled daily average $PM_{2.5}$ is also biased high (mostly over source areas) from the ICARTT simulation, which contrasts with the negative bias from the annual simulation ($-3.7 \mu\text{g m}^{-3}$ for the 3rd quarter in Table 5.4). This is at least in part due to the revised SOA formation parameterization used in the ICARTT simulation (see discussion in section 5.4.3.3) which resulted in a significant increase in modelled SOA. The model to observation comparison for averaged diurnal $PM_{2.5}$ over all the AIRNow sites in the domain is presented in Figure 5.4b. The modelled average $PM_{2.5}$ diurnal time series is decomposed into the individual components (speciated PM measurements are not available at AIRNow sites). Figure 5.4b seems to suggest that the over-prediction may be attributable to over-prediction of night-time concentrations. Of all the components, the modelled nitrate is seen to have a night-time high, which may be due to higher partitioning to particle phase at night due to lower temperature, higher humidity and enhanced N_2O_5 hydrolysis. Surprisingly, all the primary components from the model, i.e., primary organic matter, elemental carbon, and crustal material, also exhibit night-time highs, which could imply insufficient vertical mixing leading to the accumulation of emitted primary particles.

LFV (CMAQ/MC2 and CMAQ/MM5):

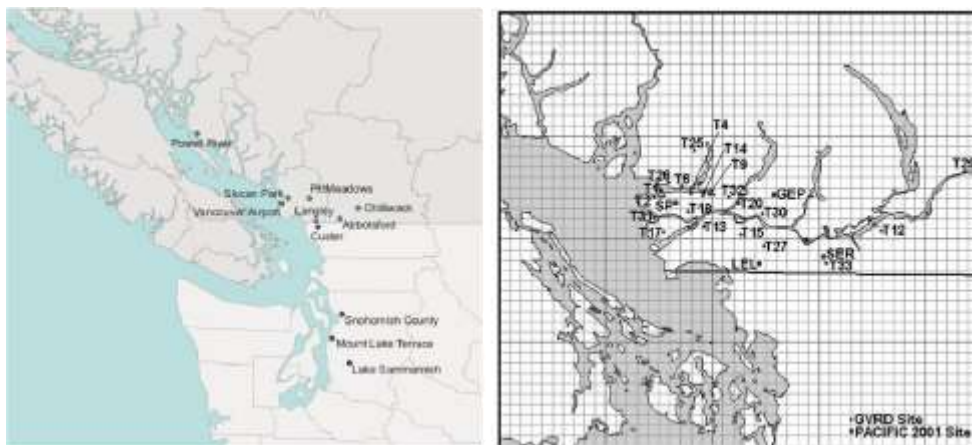


Figure 5.5 (a) Selected sites from the GVRD (Greater Vancouver Regional District) monitoring network and from Washington state used for evaluating RWDI CMAQ/MC2 Pacific 2001 simulation; (b) the nested 4-km NRC CMAQ/MM5 domain and locations of GVRD and Pacific 2001 measurement sites.

During August 2001, a major field campaign (Pacific 2001) led by Environment Canada scientists was conducted in the Lower Fraser Valley (LFV) of British Columbia, focused on ambient PM (Li, 2004). Two high-resolution (4-km) CMAQ simulations of the Pacific 2001 period (Aug 9 – 21, 2001) were conducted separately by RWDI (RWDI, 2003 and 2005) and by the National Research Council Institute for Chemical Process and Environmental Technology (NRC-ICPET) (Smyth et al, 2006a). Both runs were nested within a coarser resolution CMAQ run (12-km) with a larger domain, but the RWDI run was driven by MC2, a Canadian mesoscale community model (CMAQ/MC2) and the NRC run was driven by MM5 (CMAQ/MM5). There were also differences in emission data used for the two runs (see Table 5.2). Furthermore, in the NRC CMAQ/MM5 simulation the CMAQ default lateral boundary profiles were adjusted to match the observations obtained during the field campaign for a number of species, including O₃, CO, SO₂, NO, and NO₂. The CMAQ/MC2 simulation was evaluated against observations at 7 sites from the Greater Vancouver Regional District (GVRD) monitoring network (Atmospheric Science Data Center, 2004) and 4 U.S. sites in Washington State as shown in Figure 5.5a, while the CMAQ/MM5 simulation was evaluated against the observations from 20 GVRD monitoring stations and 4 Pacific 2001 sites as shown in Figure 5.5b.

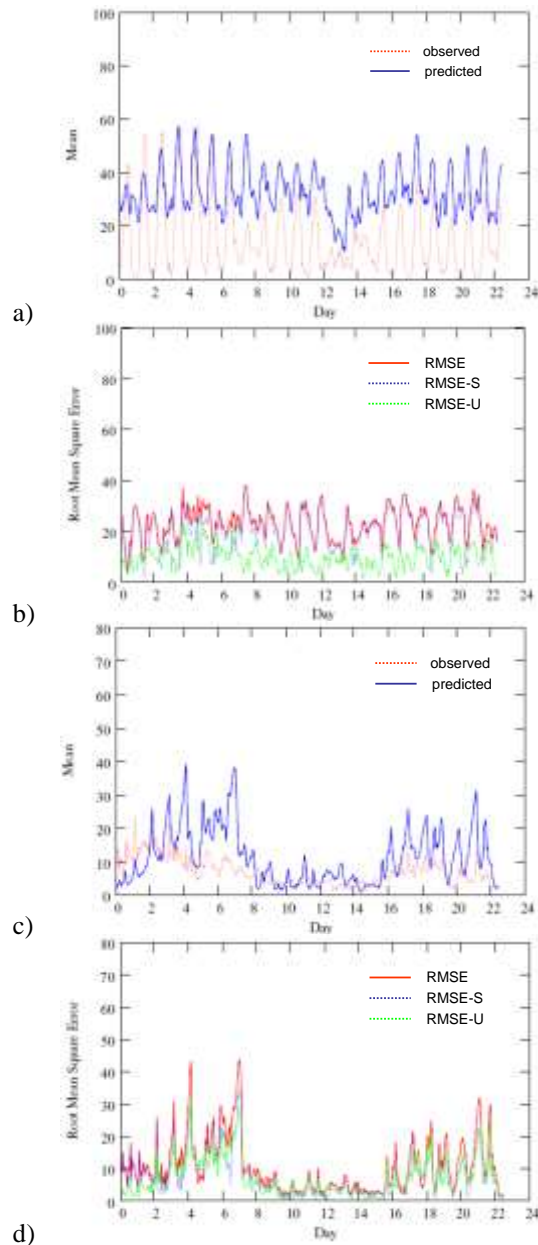


Figure 5.6 Time series comparison between the CMAQ/MC2 simulation and observed (a) O₃ and (c) PM_{2.5} averaged over the sites for the period between August 9 and 31, 2001. Time series of root-mean-square-errors (RMSE), including the systematic RMSE (RMSE-S) and unsystematic RMSE (RMSE-U), are shown in (b) for O₃ and (d) for PM_{2.5}.

Figure 5.6 shows the time series comparison between the CMAQ/MC2 simulation and observed O₃ and PM_{2.5} averaged over the sites for the period between August 9 and 31, 2001. For O₃, the model did a better job at predicting the daily peaks, particularly during the relatively high O₃ period towards the beginning of the simulation. The model had some

difficulty predicting the night-time lows and tends to over-predict the peaks when O₃ levels are low. The mean RMSE over the period is about 20 ppbv. For PM_{2.5}, the large over-predictions are mostly influenced by the model over-prediction at urban sites.

Table 5.6 Ambient ozone and PM_{2.5} evaluation statistics from the NRC CMAQ/MM5 simulation for the Pacific 2001 period.

	All O ₃	Daily peak O ₃	All PM _{2.5}
Mod. mean (ppb, µg m ⁻³)	21.8	41.9	15.8
Obs. Mean (ppb, µg m ⁻³)	19.2	42.8	12.0
MB (ppb, µg m ⁻³)	2.6	-0.92	3.7
NMB (%)	13.3	-2.2	30.9
ME (ppb, µg m ⁻³)	9.8	10.4	8.0
NME (%)	51.2	24.3	66.2

Some of the standard model evaluation statistics for the NRC CMAQ/MM5 simulation are included in Table 5.6. A better performance in predicting O₃ may be partly due to a better defined lateral boundary condition in this case. However, the modelled PM_{2.5} suffered similar over-prediction particularly over urban sites as in the case of RWDI CMAQ/MC2 simulation.

Alberta (CMAQ/MM5):

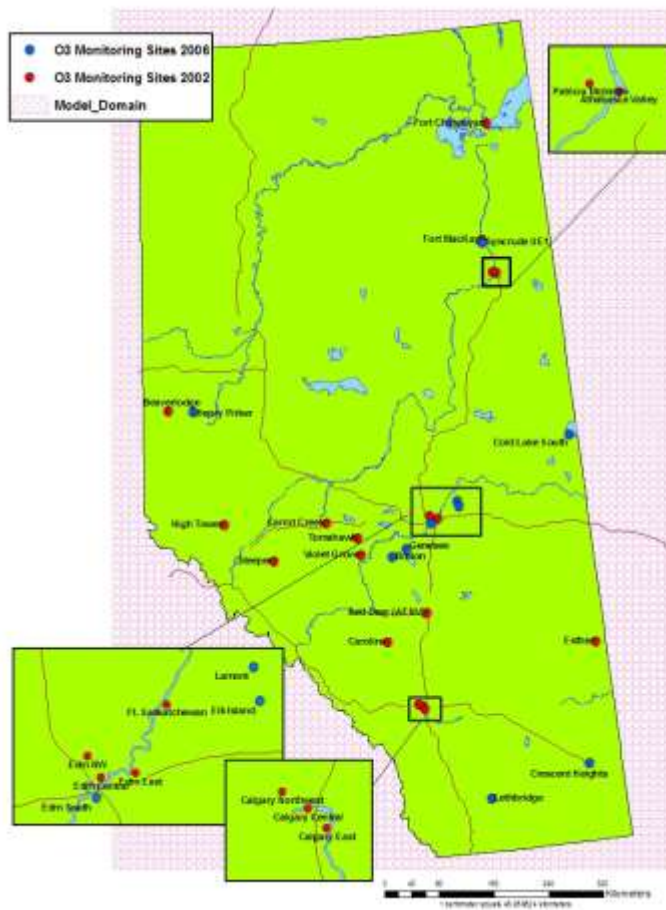


Figure 5.7 The model domain for PNR CMAQ simulation of 2002 summer season and Alberta ozone monitoring sites. Stations in red were operating in 2002. Additional stations shown in blue were also measuring ozone in 2006.

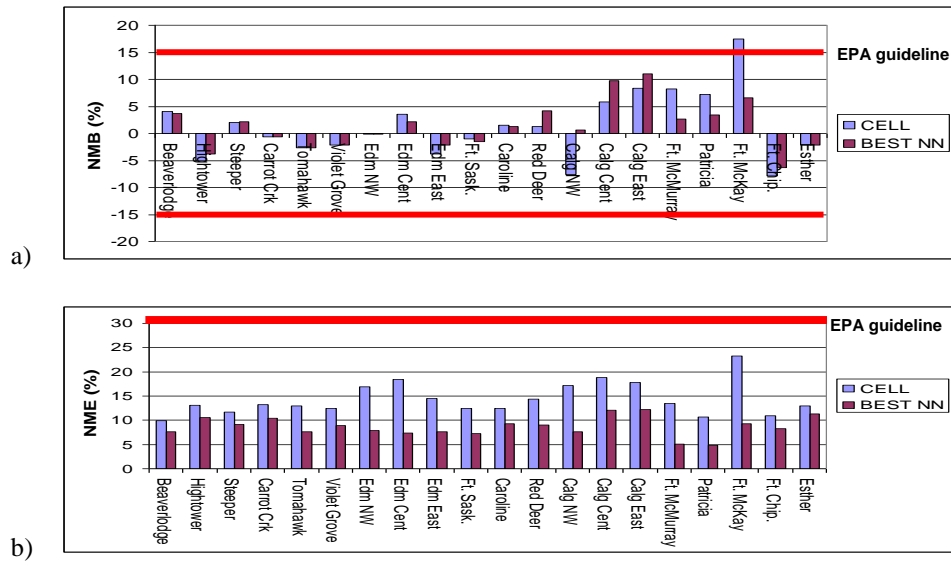


Figure 5.8 Normalized mean bias (a) and normalized mean error (b) of CMAQ-predicted ozone compared to observations at Alberta ozone monitoring sites for summer 2002.

The 12-km resolution CMAQ simulation that focussed on Alberta was evaluated primarily for O₃ only (Fox and Kellerhals, 2007). O₃ observations from twenty monitoring stations (Figure 5.7) were used for the evaluation. Two evaluation statistical measures, normalized mean bias and normalized mean error, are shown in Figure 5.8 for all twenty sites for hourly O₃ greater than 40 ppbv. Two sets of statistics are calculated, one based on the model prediction for the grids containing observation sites and the other based on a “best nearest-neighbour” approach, i.e., the modelled values are taken from any of the 9 grids surrounding the site which gives the best comparison with the observation. It is seen that the model was able to predict O₃ (for most of the sites) well within the U.S. EPA guidelines (Tesche *et al.*, 1990; U.S. EPA, 1991, 2005) for regulatory models in terms of NMB ($\pm 15\%$) and normalized mean error (NME) ($\pm 30\%$). The best nearest-neighbour approach significantly improved the performance statistics in term of normalized errors. The model showed more significant over-prediction at two Calgary sites and at the sites around Fort McMurray, due possibly to a combination of the local NO_x emission not being represented correctly and the incommensurability (between “point” observations and modelled finite grid volumes) issue.

5.4.2 Model Prediction of Speciated $PM_{2.5}$ at Ground Level

The model performance in predicting major chemical components of the ambient fine PM is evaluated in this sub-section.

5.4.2.1 Continental, Annual, and Seasonal Scales

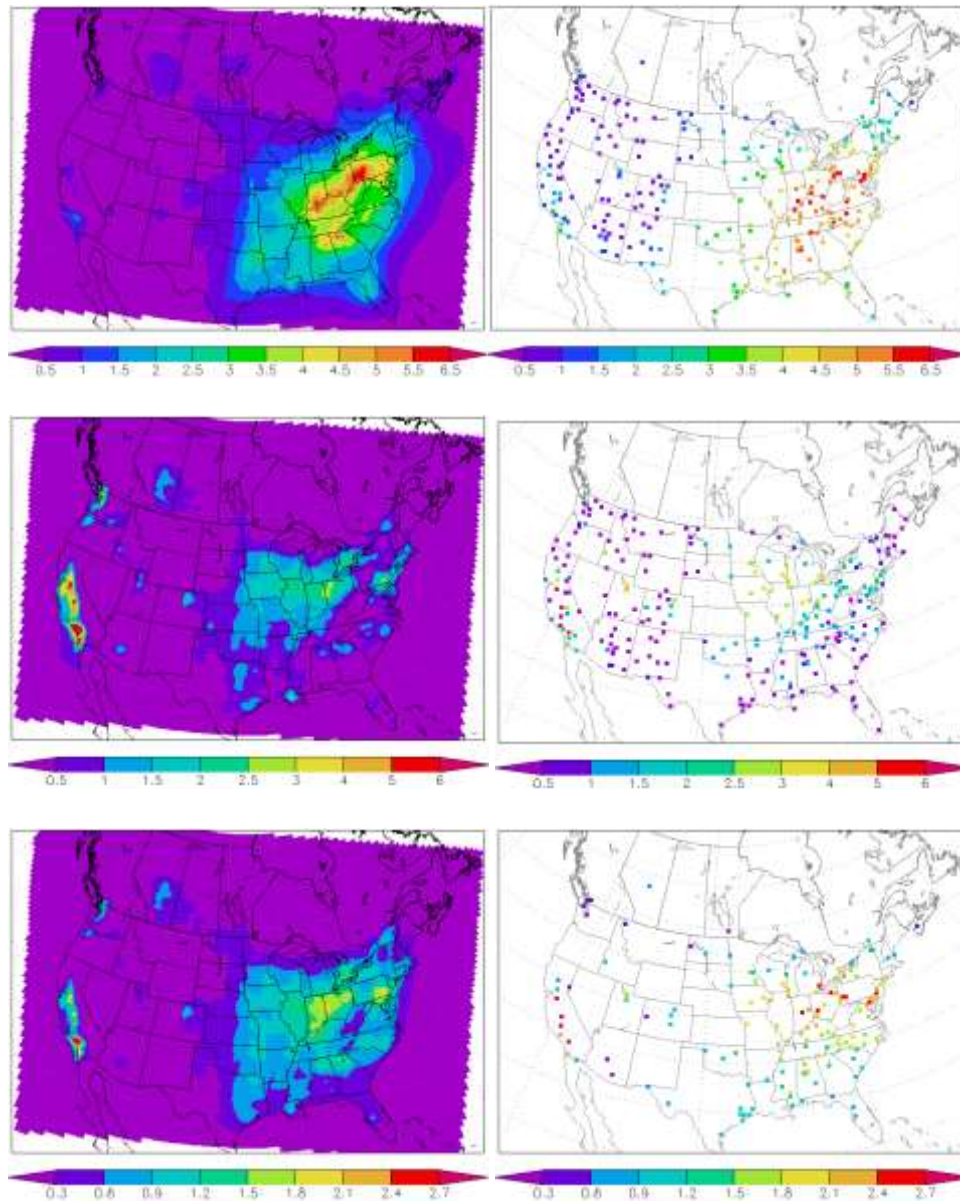


Figure 5.9 Comparison between AURAMS predicted (left panel) and observed (right panel) annual (2002) ground-level speciated $PM_{2.5}$ mass concentration ($\mu\text{g m}^{-3}$): sulphate – top panels, nitrate – middle panels, and ammonium – bottom panels.

Table 5.7 Sulphate_{2.5} evaluation statistics from the AURAMS annual simulation of 2002

	Quarter 1	Quarter 2	Quarter 3	Quarter 4	Annual
# of pairs	230	273	301	292	265
Obs. mean	1.8	3.0	4.2	2.0	2.8
Model mean	0.6	2.2	3.5	0.9	1.7
MB ($\mu\text{g m}^{-3}$)	-1.2	-0.8	-0.8	-1.1	-1.1
NMB (%)	-66.7	-26.1	-18.4	-55.7	-38.2
RMSE ($\mu\text{g m}^{-3}$)	1.4	1.3	1.6	1.3	1.3
r	0.91	0.86	0.91	0.90	0.92

Table 5.8 Nitrate_{2.5} evaluation statistics from the AURAMS annual simulation of 2002

	Quarter 1	Quarter 2	Quarter 3	Quarter 4	Annual
# of pairs	220	260	288	285	254
Obs. mean	1.8	1.0	0.7	1.9	1.3
Model mean	1.0	1.0	0.9	1.1	1.0
MB ($\mu\text{g m}^{-3}$)	-0.8	-0.0	0.3	-0.8	-0.3
NMB (%)	-45.0	-4.9	38.0	-41.3	-24.9
RMSE ($\mu\text{g m}^{-3}$)	1.5	1.3	1.2	1.4	1.0
r	0.86	0.62	0.63	0.87	0.76

Table 5.9 Ammonium_{2.5} evaluation statistics from the AURAMS annual simulation of 2002

	Quarter 1	Quarter 2	Quarter 3	Quarter 4	Annual
# of pairs	110	155	175	169	141
Obs. mean	1.5	1.5	1.7	1.5	1.5
Model mean	0.8	1.1	1.3	0.8	0.9
MB ($\mu\text{g m}^{-3}$)	-0.7	-0.4	-0.5	-0.7	-0.6
NMB (%)	-49.2	-25.8	-27.2	-46.0	-38.7
RMSE ($\mu\text{g m}^{-3}$)	0.9	0.6	0.8	0.9	0.7
r	0.79	0.77	0.77	0.81	0.79

The predicted PM_{2.5} components from the 2002 AURAMS annual simulation are compared with the speciated data from three networks, NAPS in Canada, AQS-STN and IMPROVE in the U.S.. Figure 5.9 shows the modelled and observed annual concentrations of sulphate_{2.5}, nitrate_{2.5}, and ammonium_{2.5}. Again the model seems to simulate the spatial distribution well for all three inorganic components. The annual and quarterly performance statistics for these three components of PM_{2.5} mass are shown in Tables 5.7-5.9. In general the correlation coefficients for all three components, sulphate in particular, are significantly higher than that for PM_{2.5}. As in the case of PM_{2.5}, the model predictions for all three inorganic components were biased low. There is also a marked seasonal (quarterly) variation particularly in biases. For example, sulphate was more significantly under-predicted in colder seasons (1st and 4th quarters) than warmer seasons (2nd and 3rd quarters). This coincided with model over-prediction of precipitation for the 1st and 4th quarters and under-prediction of precipitation for the 2nd and 3rd quarter; the model predicted wet deposition of sulphate was also more negatively biased for the 2nd and 3rd quarters (see Moran *et al.*, 2010). Ammonium followed a similar pattern to sulphate. Nitrate was considerably over-predicted in the 3rd quarter while it was significantly under-predicted in the 1st and 4th quarters. While the seasonal bias for PM-nitrate may point to the model's potential difficulty in simulating the gas-particle partition (as well as the model bias in wet removal similar to sulphate above), PM-nitrate measurements are also subject to a considerable level of uncertainty due to its semi-volatile nature.

As for other components, such as total organic matter (TOM), elemental carbon (EC), and crustal matter (CM), the model predictions correlated poorly with the observations (Moran *et al.*, 2007, 2010). The model under-predicted TOM and EC but over-predicted CM significantly. While emission may be the main factor for EC and CM, the under-prediction of TOM is at least partly due to the SOA formation not being represented adequately in the

version of AURAMS used for the simulation (see discussion later in this sub-section). The model also seriously over-predicted sea salt concentration, which can be attributed to the sea-salt generation scheme in AURAMS, as will be discussed later in section 5.4.3.3.

5.4.2.2 Regional, episodic scales

Eastern NA (AURAMS ICARTT run):

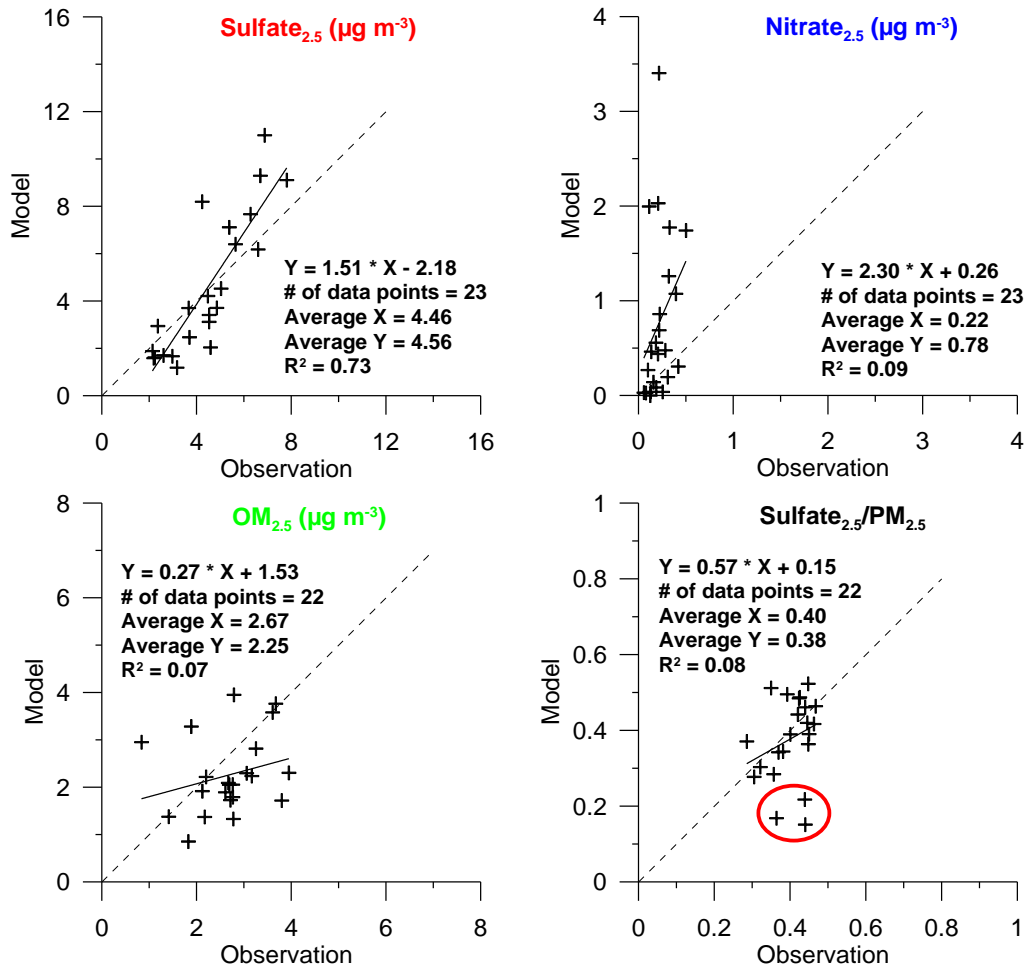


Figure 5.10 Model vs. observation scatter-plots of (a) sulphate_{2.5}, (b) nitrate_{2.5}, (c) organic matter, OM_{2.5}, and (d) sulphate fraction. Both model (AURAMS) results and observations are averaged over the ICARTT simulation period.

The model predictions of PM_{2.5} components from the AURAMS ICARTT simulation (Gong *et al.*, 2007) were compared with the measurements at 23 sites from the IMPROVE network (<http://vista.cira.colostate.edu/views/Web/Data/DataWizard.aspx>). The measurements at these sites are 24-hour averages (midnight-to-midnight, local daylight saving time) every three days. The hourly model outputs are therefore averaged over the same 24-hour periods and sampled every three days so as to match the observations. Figure 5.10 shows the model-observation

scatter plots for speciated $PM_{2.5}$: sulphate_{2.5}, nitrate_{2.5}, total organic matter TOM_{2.5}, and sulphate_{2.5}-to- $PM_{2.5}$ ratio averaged over the 5-week simulation period. As seen in Figure 5.10, averaged over the simulation period, the model performed well for sulphate_{2.5}, with very little bias and good correlation coefficient. The model however, over-predicted high concentrations and under-predicted low concentration resulting in a slope > 1. On the other hand, nitrate_{2.5} was significantly over-predicted by the model. Here with a more up-to-date SOA formation parameterization (see discussion later in 5.4.3.3), the modelled organic particulate matter (OM_{2.5}) values were comparable to the observations in magnitude, although correlation coefficient was still low. For example, the mean bias for organic particulate matter was $-5.5 \mu\text{g m}^{-3}$ (not shown, or -93 % in terms of normalized mean bias) from the annual run with the older SOA scheme in AURAMS. Sulphate fraction (sulphate-to-total ratio) was predicted reasonably well, except for several coastal sites (as indicated by the red circle on Figure 5.10d) where the model significantly under-predicted the sulphate fraction due to a combination of under-predicting sulphate and over-predicting sea salt at these sites.

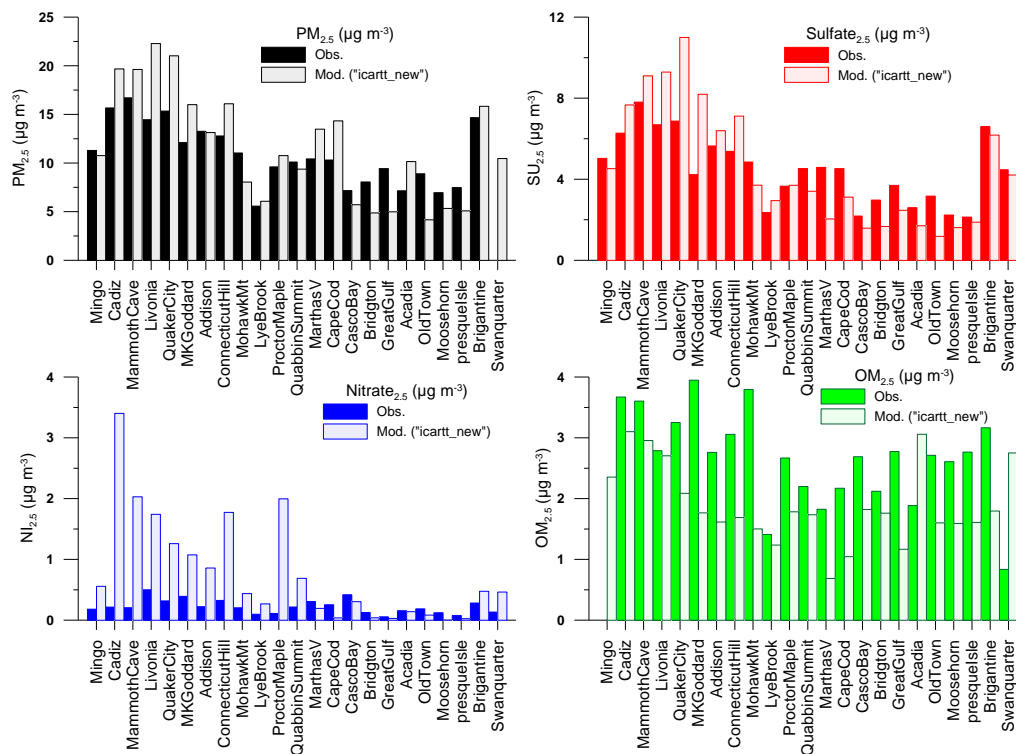


Figure 5.11 Comparison of AURAMS predicted $PM_{2.5}$ (a) and its components, (b) sulphate, (c) nitrate, and (d) organic matter, with observations at IMPROVE sites over the ICARTT simulation period. The sites on the x-axis are arranged to move from the U.S. Midwest and Ohio Valley source regions to northeast coastal areas.

Site-specific model to observation comparisons for sulphate, nitrate, and organic components are presented in Figure 5.11. The sites on the x-axis are arranged to move from the U.S. Midwest and Ohio Valley source regions to northeast coastal area. Geographically, the model

over-predicted sulphate over source regions but under-predicted sulphate farther downwind. As for nitrate, the model significantly over-predicted areas in the midwest, which is the region with high ammonia emissions.

LFV (CMAQ/MC2, CMAQ/MM5):

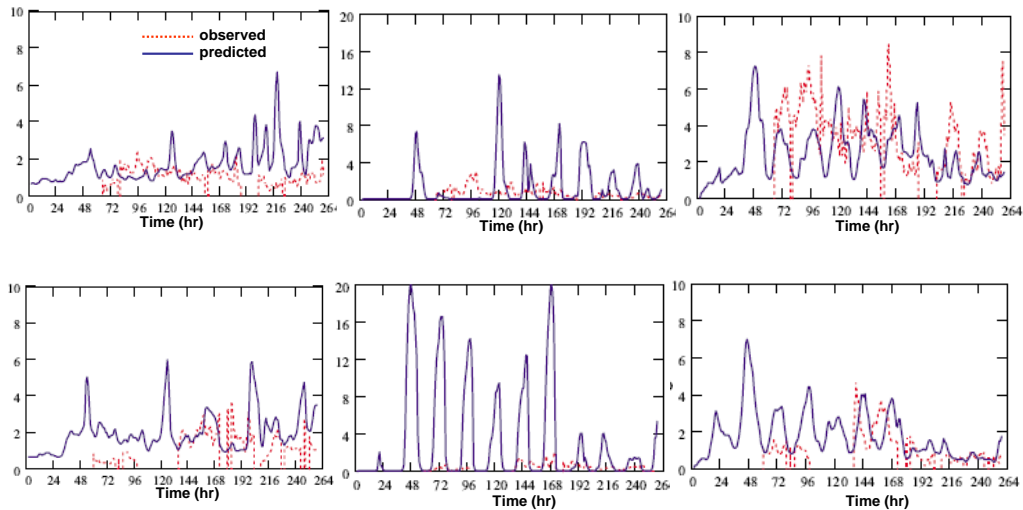


Figure 5.12 Time series comparison at two sites, Slokan Park (urban; upper panels) and Langley (rural; lower panels), from the CMAQ/MC2 simulation for sulphate (left), nitrate (centre), and organic component (right), all in $\mu\text{g m}^{-3}$.

Table 5.10 Ambient speciated $\text{PM}_{2.5}$ evaluation statistics from the NRC CMAQ/MM5 simulation for the Pacific 2001 period.

	Sulphate _{2.5}	Nitrate _{2.5}	Ammonium _{2.5}	OM _{2.5}
Mod. mean ($\mu\text{g m}^{-3}$)	2.25	4.25	1.86	2.69
Obs. Mean ($\mu\text{g m}^{-3}$)	1.01	0.29	0.55	2.86
MB ($\mu\text{g m}^{-3}$)	1.23	3.96	1.31	-0.17
NMB (%)	122	1340	238	-5.98
ME ($\mu\text{g m}^{-3}$)	1.34	3.96	1.35	1.44
NME (%)	133	1340	246	50.5

Both RWDI CMAQ/MC2 and NRC CMAQ/MM5 simulations of the Pacific 2001 period were evaluated with very limited $\text{PM}_{2.5}$ composition data. Figure 5.12 shows time series comparison at two sites, Slokan Park (urban) and Langley (rural), from the CMAQ/MC2 simulation. Sulphate and organic components were predicted well in terms of magnitude, while nitrate was

significantly over-predicted. The performance statistics for the NRC CMAQ/MM5 prediction of the major PM_{2.5} components for the same two sites are shown in Table 5.10. In this case, the organic component was predicted relatively well in comparison to the other components in terms of normalized mean bias (NMB) and normalized mean error (NME). There was a significant over-prediction of sulphate component, and nitrate was greatly over-predicted. The over-prediction of nitrate in summer time was shared by all model simulations (i.e., AURAMS 2002 annual and ICARTT simulations and CMAQ Pacific 2001 simulations).

To summarize the findings from the rather broad-brush assessment of model performance in predicting ground-level O₃ and PM_{2.5} over different spatial and time scales presented so far (5.4.1 and 5.4.2), we can see that annually, at a North American continental scale, the model captures the observed spatial distribution of O₃ and PM_{2.5} well. Seasonally, O₃ is under-predicted in winter and over-predicted in summer; PM_{2.5} is more significantly under-predicted in winter. Regionally, the model tends to over-predict O₃ over eastern Canada and U.S., particularly around the southern Great Lakes and the U.S. Mid-Atlantic States; PM_{2.5} is more significantly under-predicted annually over eastern U.S. At shorter time scales, over eastern North America, O₃ is over-predicted (both daily 1-hour maximum and daily mean), particularly around the southern Great Lakes and the Mid-Atlantic States; daily average PM_{2.5} is over-predicted mostly over the source regions. Over western Canada, the high-resolution model simulations over Vancouver-LFV capture the daily O₃ peaks well, but the model does not consistently capture the night-time lows, particularly at the sites in the LFV; PM_{2.5} is over-predicted in the region particularly at urban sites. In Alberta the model simulation at 12-km resolution is able to predict O₃ well within U.S. EPA guidelines for regulatory models in terms of NMB and NME.

For speciated PM_{2.5} components at ground level, averaged annually, modelled inorganic components correlate well with observations. Comparatively, the model performs the best in predicting annual sulphate_{2.5}. Seasonally, there is a significant under-prediction of sulphate in the cold season (i.e., 1st and 4th quarter) and nitrate is significantly over-predicted in summer (3rd quarter). Regionally on a shorter time scale (e.g., six weeks during summer), sulphate_{2.5} is overall well predicted by the model over eastern North America in terms of regional average and correlation but geographically over-predicted in the source regions and under-predicted farther downwind; nitrate is over-predicted over the Midwest where the model has significant ammonia emissions; the organic component is comparable to the observations in magnitude, but the correlation coefficient is low. Over western Canada, sulphate and organic components are predicted well in terms of magnitude only over LFV for the Pacific 2001 period (based on very limited observations available); nitrate is significantly over-predicted.

It needs to be stressed again that an attempt is made here to provide an overall assessment of the models' operational performance at various spatial and temporal scales. It is nevertheless based on limited individual model evaluations with different CTMs and model configurations. For example, the assessment at annual, seasonal, and continental scale is based on a single year

(2002) run which can not account for any inter-annual variability. On the regional and shorter time scale, the assessment is based on evaluations of different model runs for different regions and specific time periods. One needs to be careful in generalizing these results.

5.4.3 Diagnostic and process evaluation

The operational evaluation described in the first two sub-sections (5.4.1 and 5.4.2) above is usually a first step to be pursued in any model evaluation exercise (e.g., Seigneur and Moran, 2004). It is done to establish how well a CTM does in predicting the ambient targeted pollutants. However, for policy applications of the CTMs, it is more critical to evaluate the model's ability in simulating the atmospheric processes in order to establish confidence in a model's ability to correctly represent the precursor-concentration relationship. This is often termed as diagnostic evaluation (e.g., Seigneur and Moran, 2004; Gilliland *et al.*, 2007), which will be the focus of this sub-section. The diagnostic evaluation here will include the evaluation of model-predicted precursor species to O₃ and PM_{2.5} with available routine monitoring data, the comparison of model prediction with data obtained from intensive field campaigns, and sensitivity tests with regard to model inputs and parameterizations of various modelled processes.

5.4.3.1 Evaluation of Model Prediction of Precursor Species Against Network Data

VOC

As described in Chapter 2, VOCs are key precursors to O₃ and SOA formation. VOC mixing ratios predicted by AURAMS were evaluated over eastern Canada between July 8 and August 19, 2004 and western Canada between August 26 and September 9, 2005. These are based on the simulations carried out for the ICARTT 2004 and PrAIRie 2005 field studies (see section 5.4.3.2 and Table 2). Predicted VOCs were compared to observations from the NAPS network (24-hr samples for urban sites and 4-hr samples for rural sites, every 3 or 6 days). Measured VOCs were mapped to the model's ADOM-II chemical speciation. For comparison, modelled and measured VOCs were expressed as their OH-reactivity ($k_{OH}[\text{VOC}]$). The OH-reactivity metric better represents a VOC's contribution to O₃ formation than a VOC mixing ratio.

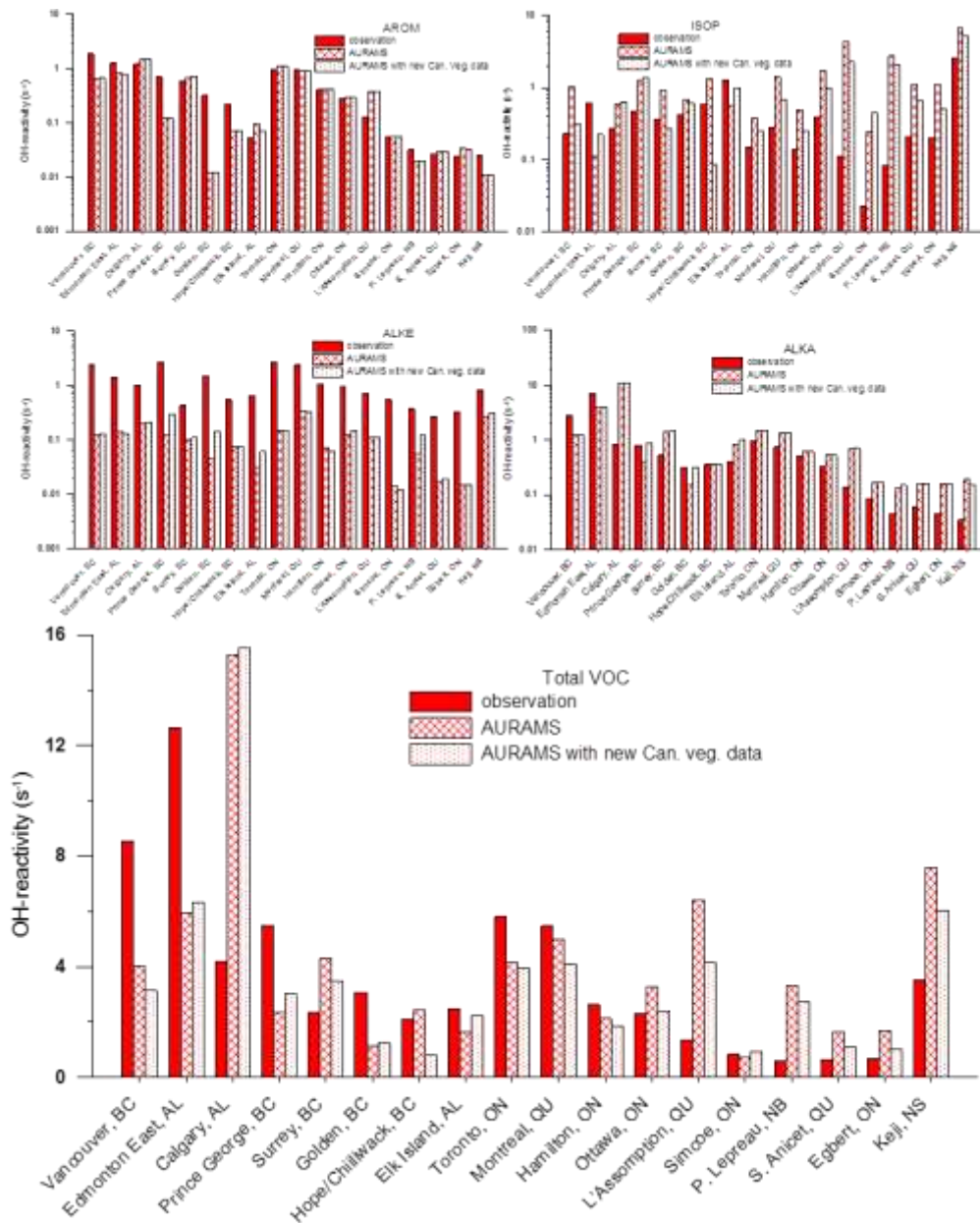


Figure 5.13 Comparison of model-predicted and measurement-based average OH-reactivity for lumped VOC species: AROM, ISOP, ALKE, and ALKA, as well as total VOC, at sites across Canada. Two model runs are included: base case and a sensitivity run with new vegetation data.

Figure 5.13 presents the results for each site as average VOC modelled and measured OH-reactivity (s^{-1}) with panels for AROM (multi-substituted aromatics; anthropogenic origin), ISOP (isoprene; biogenic origin), ALKE (higher alkenes; mixed anthropogenic and biogenic), ALKA (higher alkanes; mixed anthropogenic and biogenic), and TOTAL (sum for all species). Also included are results from a sensitivity run with updated Canadian vegetation data (see section 5.4.3.3). Comparisons for TOLU (mono-substituted aromatics; anthropogenic origin),

C3H8 (propane, acetylene and benzene; anthropogenic origin) and ETHE (ethene, some reactive isoprene product species; mixed anthropogenic and biogenic) are not shown here since they play a lesser role in contributing to TOTAL. The complete comparison can be found in Stroud *et al.* (2008). The first 8 sites presented on Figure 5.13 are in the western domain and ordered, from left to right, in decreasing observed AROM. The remaining 10 sites are in the eastern domain also ordered by decreasing observed AROM. For the lumped AROM species, contributed by species of mostly anthropogenic origin, the model predicted well for urban sites in general except for Vancouver where the model under-predicted significantly. As for the rural sites, AROM was under-predicted at several sites over the western domain, particularly seriously at Golden BC, Prince George BC, and Hope/Chilliwack BC. On the other hand, AROM was considerably over-predicted at L'Assomption QU in the east. Similar model-measurement agreement was also observed for the TOLU and the C3H8 lumped species.

ISOP was over-predicted for the majority of sites, particularly severely over the eastern domain. In general, the updated vegetation data improved the ISOP model-measurement comparison, most significantly in the west, e.g., Vancouver, Surrey, and Elk Island. In the ADOM-II chemical mechanism, the first-generation products of ISOP oxidation, methyl-vinyl-ketone and methacrolein, are lumped into the ETHE species. As a result, the ETHE model-measurement comparison (not shown here) followed a similar pattern to ISOP.

ALKE and ALKA are both emitted from anthropogenic and biogenic sources. Overall, the biogenic source of ALKE dominates the anthropogenic source for rural sites. Interestingly, ALKE showed an across-the-country under-prediction for urban and rural sites alike, suggesting significant under-predictions in both biogenic and anthropogenic ALKE emissions. The biogenic ALKE emissions are likely monoterpenes. The updated Canadian vegetation data resulted in some improvement in the ALKE comparison for several sites. The ALKA lumped species includes contributions from non-terpene biogenic species and anthropogenic species. In the west, ALKA was underpredicted in Vancouver, Edmonton East, and over-predicted in Surrey, Calgary, and Elk Island. In the east, there is a general over-prediction particularly for rural sites.

As for the total VOC OH-reactivity, it was significantly under-predicted at two of the western urban locations, Vancouver and Edmonton East, but significantly over-predicted at Calgary. For rural western sites, the total VOC OH-reactivity was under-predicted except for Surrey where it was over-predicted. Interestingly, the ISOP over-predictions tended to be offset by ALKE under-predictions to some degree. In the urban eastern locations, the total OH-reactivity was somewhat under-predicted, while at the rural eastern sites, the total OH-reactivity was over-predicted due to ISOP over-predictions.

At high NO_x , O_3 production increases with total OH-reactivity (e.g. urban centres with low biogenic VOC emissions). At low NO_x , O_3 production increases less sharply with total OH-reactivity and can even reach the regime at low NO_x and high VOC where O_3 becomes

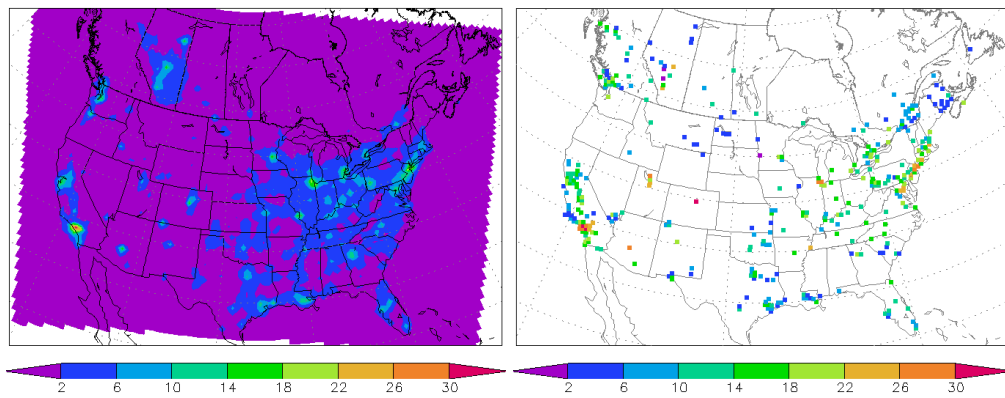
insensitive to VOC changes. For most major cities across Canada, with the exception of Calgary, the total OH-reactivity was under-predicted which will lead to less modelled urban O₃ production. Conversely, AURAMS over-predicted total OH-reactivity for rural locations in the east which may lead to more modelled rural O₃ production. Kejimikujik had particularly large total OH-reactivity and coupled with the low NO_x levels may result in O₃ at Kejimikujik being insensitive to VOC changes.

The findings from the VOC comparison suggest a need for further improvements in the biogenic emissions algorithms and databases (both isoprene and monoterpenes) and their explicit representation in terms of model chemical speciation. Sub-grid scale variability in vegetation cover and biogenic emissions adds further uncertainty for regional scale model grid sizes. The isoprene over-prediction has a particular implication for model prediction of O₃. Dégardin (2007) showed that AURAMS prediction of O₃ was very sensitive to biogenic emissions. The urban emissions for ALKA and ALKE are a further area for model improvement. It should be noted that the comparison performed was for a limited period of time during the summer months and future comparisons should be extended to other seasons. Chapter 3 includes a discussion on maximum incremental reactivities (MIRs) derived from longer term NAPS VOC measurements (section 3.4.3).

NO_x, SO₂, and HNO₃

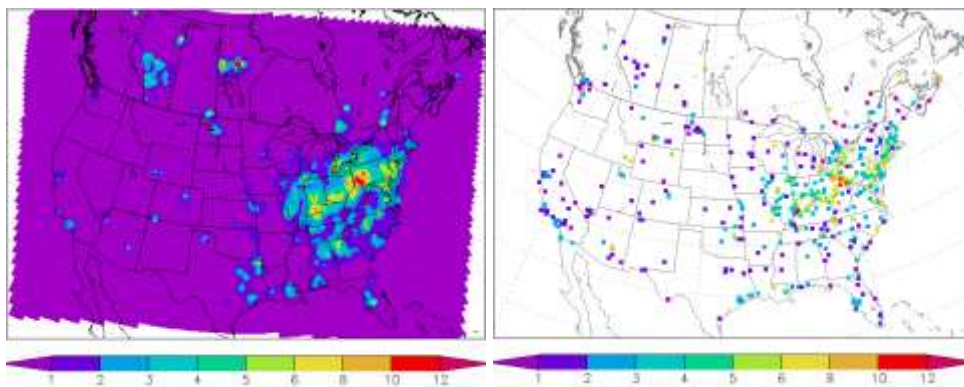
Other important precursor species to the formation of smog include NO_x (NO + NO₂) and SO₂, (see Chapter 2). Nitric acid (HNO₃) is a secondary product from NO₂ oxidation. It is a termination species (or, sink) for NO_x due to its fast removal from the atmosphere (through dry and wet deposition) and rather slow photolysis. On the other hand, owing to its semi-volatile nature HNO₃ is also an important precursor to particle nitrate.

AURAMS predictions of NO₂, SO₂, and HNO₃ from the 2002 annual simulation were evaluated against observations from a number of monitoring networks in terms of annual and seasonal averages (Moran *et al.*, 2010). Both the NAPS network in Canada and the AQS network in U.S. include continuous measurement of NO₂ and SO₂, but are both focused on populated areas. SO₂ measurements (filter-based, daily or weekly samples) are also available from the Canadian CAPMoN and U.S. CASTNet networks whose sites are primarily located in rural areas. The CAPMoN and CASTNet networks also provide filter-based monitoring data for HNO₃.



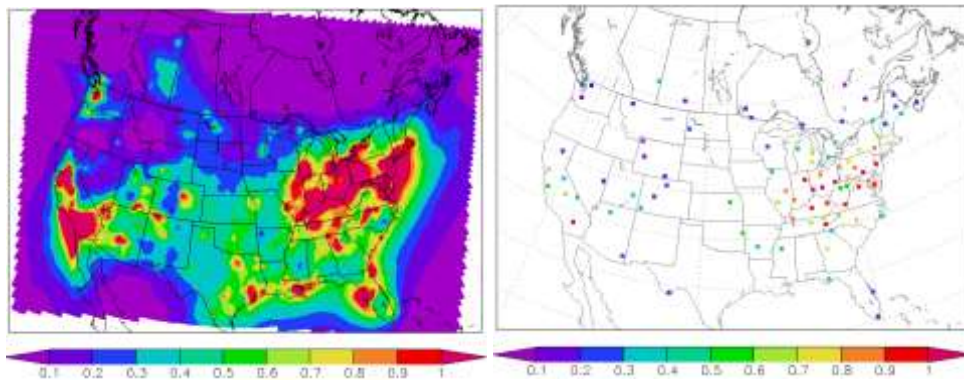
Modelled annual NO₂

Observed annual NO₂



Modelled annual SO₂

Observed annual SO₂



Modelled annual HNO₃

Observed annual HNO₃

Figure 5.14 Comparison between AURAMS predicted (left panel) and observed (right panel) annual (2002) ground-level NO₂ concentration (top panels), SO₂ (middle panels), and HNO₃ (bottom panels), all in ppbv.

Table 5.11 Evaluation statistics for NO₂, HNO₃, and SO₂ from the AURAMS annual simulation of 2002

		Quarter 1	Quarter 2	Quarter 3	Quarter 4	Annual
NO ₂ (ppb)	# of pairs	364	368	373	354	363
	MB (ppb)	-6.342	-4.222	-4.126	-5.478	-5.11
	NMB (%)	-45.87	-42.88	-39.35	-41.09	-42.64
	RMSE (ppb)	8.663	6.76	7.515	7.954	7.52
	r	0.658	0.626	0.579	0.672	0.65
SO ₂ (ppb)	# of pairs	447	452	456	454	451
	MB (ppb)	-0.714	-0.733	-0.608	-0.333	-0.599
	NMB (%)	-18.30	-25.45	-20.76	-9.55	-18.06
	RMSE (ppb)	3.123	2.753	2.99	2.985	2.832
	r	0.49	0.392	0.386	0.488	0.456
HNO ₃ (ppb)	# of pairs	85	87	89	91	86
	MB (ppb)	-0.026	0.097	0.284	0.024	0.09
	NMB (%)	-5.61	16.61	43.93	5.98	17.14
	RMSE (ppb)	0.189	0.355	0.585	0.189	0.278
	r	0.791	0.773	0.751	0.741	0.778

Figure 5.14 compares the model-predicted and observed annual concentrations of NO₂, SO₂ and HNO₃. In general, the model captured the observed spatial distributions of the precursor species (NO₂ and SO₂) well, indicating a reasonable representation of sources. The model under-predicted NO₂ over some of the major urban centres which is at least partly due to the incommensurability issue, i.e., the network measurements are point measurements made at sites located in populated areas (urban and suburban in nature) whereas the model predictions were volume averages for 42 km by 42 km by 15 m grid boxes. Another contributing factor is likely to be the positive biases due to interferences from other nitrogen species such as HNO₃, PAN, alkyl nitrates, HONO, and NO₃ that are known to be a problem for the molybdenum-converter chemiluminescent instruments widely used to make routine NO₂ measurements (e.g., Lamsal *et al.*, 2010). SO₂ was over-predicted over central Alberta and around large smelters in Manitoba (Flin Flon and Thompson, Manitoba) but under-predicted over eastern Quebec and

Nova Scotia. There were considerably fewer observations available for HNO₃. There is, however, a clear indication that the model over-predicted HNO₃ particularly over the west (e.g., California, Washington and BC) but also over the east. Table 5.11 includes a selected set of evaluation statistics for the three species. It is seen that, despite the considerable negative bias, model-predicted NO₂ correlated relatively well with the observations. The correlation coefficients for quarterly and annual SO₂ were lower in comparison to those for NO₂, partly due to the fact that most of the SO₂ emissions are from large point sources (power generation facilities) which were less well resolved at the model resolution in comparison to urban sources for NO₂ (particularly for models such as AURAMS which do not have a representation for sub-grid scale plumes from point sources). For the precursor species (NO₂ and SO₂), there were relatively small differences in the quarterly and annual statistics. In comparison there were strong quarterly differences in HNO₃ biases and RMSE. HNO₃ was clearly more significantly over-predicted in warm seasons (particularly the 3rd quarter). This is consistent with the over-prediction of nitrate_{2,5} shown above (Table 5.8).

5.4.3.2 Evaluation against Recent Field Study Data

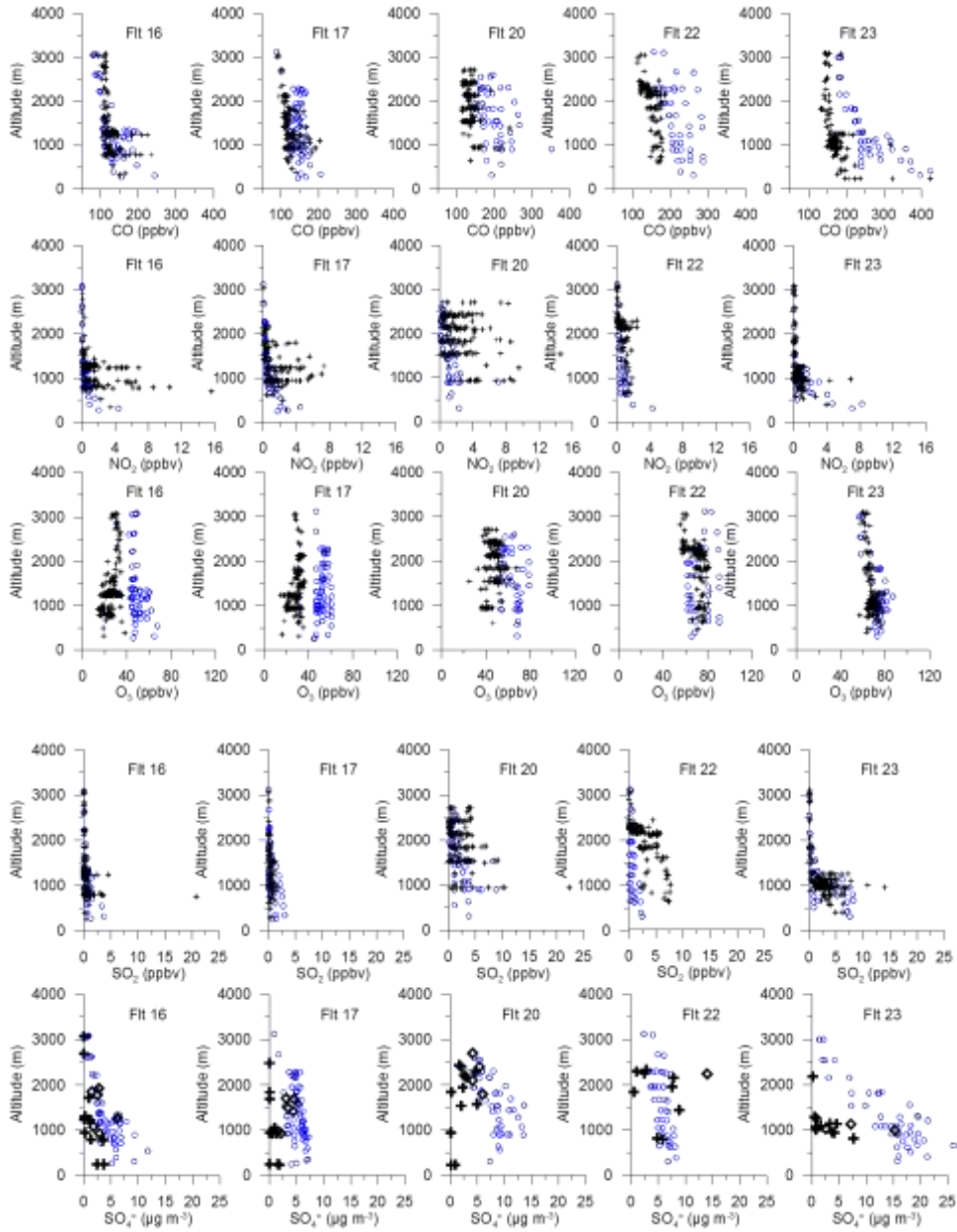
Intensive field measurement campaigns are particularly valuable sources of data for diagnostic evaluation. They provide observations that are not routinely available, for example details in atmospheric multi-phase chemistry, better spatial and temporal resolution (for targeted geographical area and time period), and observations aloft (usually from aircraft) which provide important information on atmospheric processes. Recent field campaigns also often incorporate model evaluation data needs into their study plans. Examples of how field data are used for model evaluation from two recent field campaigns are given in this section.

ICARTT

During the summer of 2004, several coordinated field campaigns were conducted over North America, the North Atlantic, and Western Europe as part of the International Consortium for Atmospheric Research on Transport and Transformation (ICARTT). These field programs were designed to study the emission of aerosol and O₃ precursors, their chemical transformations and removal during transport to and over the North Atlantic, and their impact downwind on the European continent (Fehsenfeld *et al.*, 2006). One of the campaigns, an aircraft study conducted by the Environment Canada scientists using the National Research Council of Canada (NRCC) Convair 580, focused on the chemical transformation of gases and aerosols by clouds.

Twenty-three research flights were flown with the NRCC Convair 580 based in Cleveland, Ohio. Measurements onboard the aircraft included trace gases, aerosol particle size distribution and chemistry, and cloud microphysics and chemistry (see Hayden *et al.*, 2008; Li *et al.*, 2008; and Zhang *et al.*, 2007 for details on the measurement and instrumentation). Complementary to

the surface-based observations, these airborne measurements provide information on both primary and secondary pollutants aloft which is valuable for improving our knowledge of the atmospheric processes and for evaluating model representations of these processes.



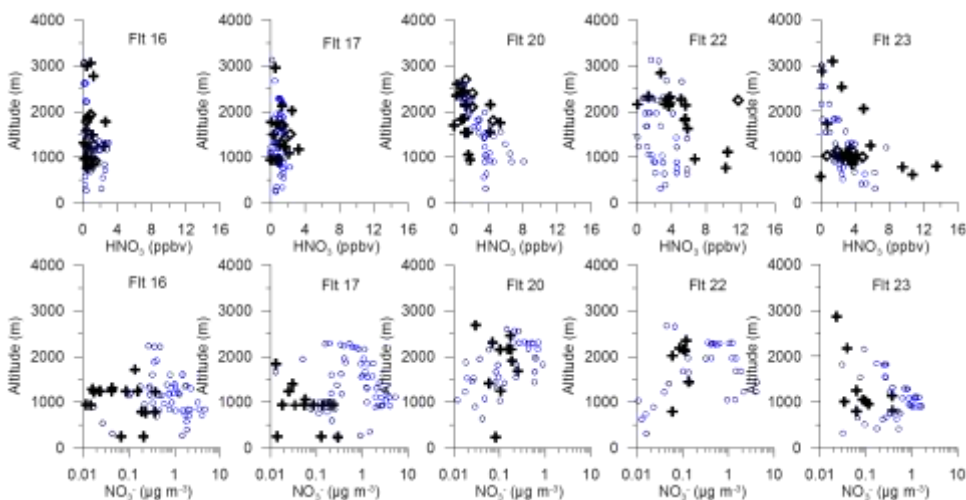


Figure 5.15 In-situ comparison of observed (in black) and AURAMS modelled (in blue) gaseous and particle species (from the top row down: CO, NO₂, O₃, SO₂, SO₄⁻², HNO₃, and NO₃) for selected Convair 580 flights during ICARTT 2004 field campaign. Measurements of the gaseous species (SO₂, NO₂, CO, and O₃) are at 1-s frequency; HNO₃ measurements are 5-minute averages; measurements of inorganic ions are from the 10-minute integrated PILS; also included is air equivalent cloud-water sulphate (black diamonds) from bulk cloud water samples (varying in sampling duration).

The AURAMS predictions from the retrospective ICARTT simulation, as mentioned earlier in this chapter, were compared to various measured gaseous and particulate species. One comparison was done by plotting the model results and the observations along the flight track against height in the form of “vertical profiles”. This was an attempt to get a sense of whether the model comes close to the aircraft observation over the flight area in terms of the range of magnitudes and vertical structure, since a true point-to-point in-situ comparison was not appropriate given the model resolution (i.e., an incommensurability issue). The sampling through the modelled fields was done based on the given grid locations along the flight path over the entire flight period. Figure 5.15 shows such comparison for CO, NO₂, SO₂, O₃, HNO₃, particulate sulphate (p-SO_{4,2,5}), and particulate nitrate (p-NO_{3,2,5}) from five flights, over the southern Great Lakes area.

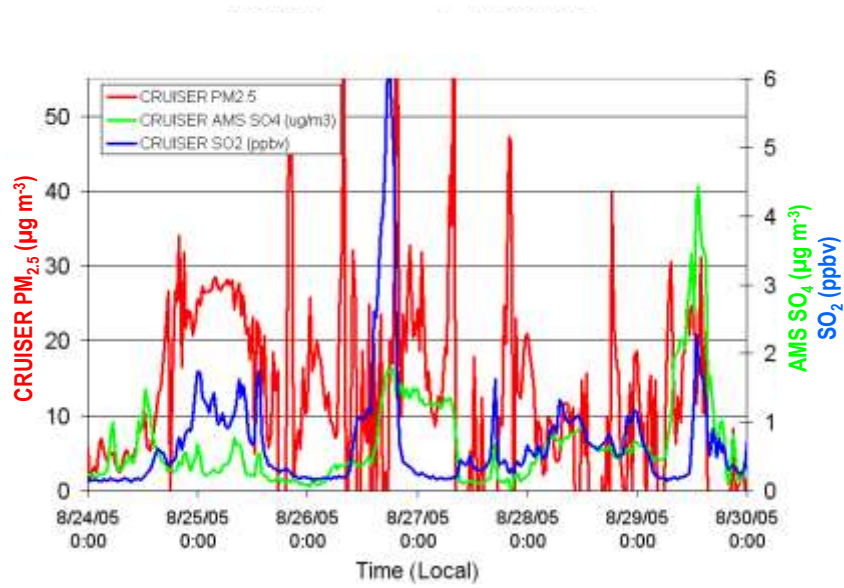
CO is often used as a tracer (or indicator) for regional anthropogenic pollutants. The monthly MOPPIT (Measurements Of Pollution In The Troposphere) CO data was used for the model’s lateral boundary condition. As shown in Figure 5.15, the model performed well in predicting CO particularly for the two flights (16 and 17) over southern Michigan. There was some over-prediction of CO for the flights over central Ohio (Flight 22) and south-western Ontario (Flight 23), but the vertical structure was reproduced by the model. The model also performed well in predicting other primary (precursor) species, SO₂ and NO₂, both in terms of magnitude and vertical variations. The model, however, performed less well in predicting secondary pollutants. O₃ was over-predicted in most of the cases, particularly over southern Michigan (Flights 16 and 17) where the observations showed much lower O₃ throughout the boundary layer. Nevertheless the observed vertical structures were correctly captured by the model.

Particulate sulphate was over-predicted at lower levels. Considering that the primary precursor, SO₂, was predicted very well, the over-prediction of sulphate implies that total sulphur (SO₂ + SO₄) was over-predicted in the model. This can be attributed to many factors, such as emission, removal, and atmospheric conversion of sulphur to sulphate. Particulate nitrate was generally over-predicted for most of the flights (by about an order of magnitude, or several µg m⁻³). Interestingly the model prediction of nitric acid (HNO₃) was quite good, and the over-prediction of nitrate does not seem to be associated with an over-prediction of HNO₃. For the two flights where nitrate was more significantly over-predicted (Flights 16 and 17), there is an indication that total nitrate may also be over-predicted.

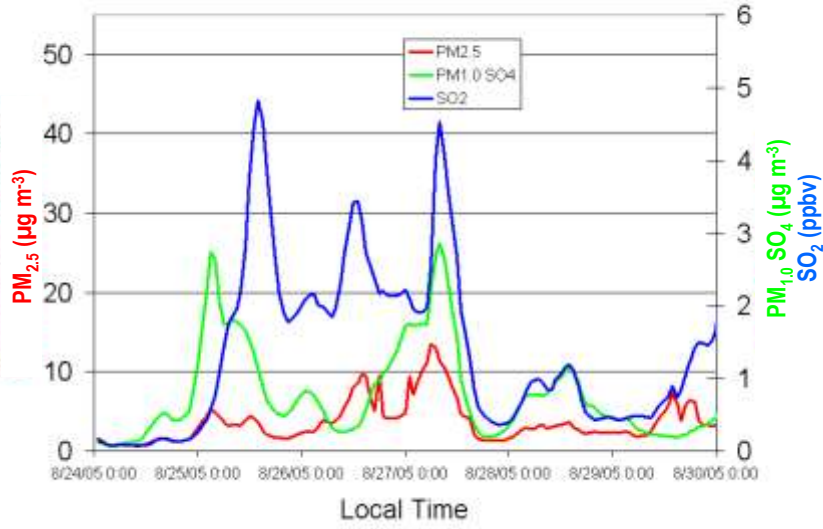
McKeen *et al.* (2007) compared the model predictions from six PM forecast models (including AURAMS and CHRONOS) with the measurements onboard NOAA-WP3, which also flew during ICARTT making aerosol composition and aerosol size measurements over and around the New England area (<http://www.al.noaa.gov/2004>). The analysis based on this comparison showed that the models with in-cloud oxidation over-predicted particle sulphate aloft more significantly than those models which did not include this process, raising the question of possible over-estimate of sulphate in-cloud production. This issue will be discussed further in the next subsection (section 5.4.3.3).

PrAIRie2005

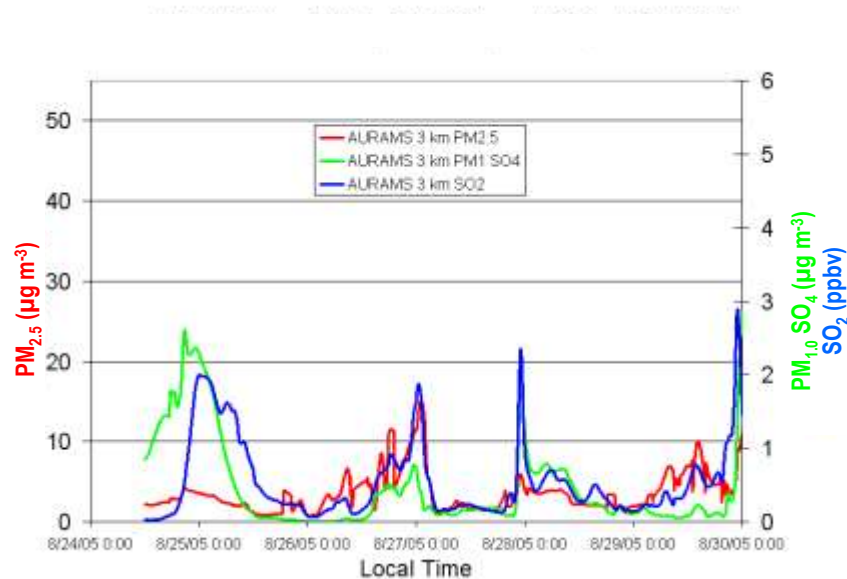
The PrAIRie2005 campaign was designed and led by EC air quality modellers with the scientific objective of determining the extent to which air pollution events in Edmonton result from local emissions versus long-range transport (Makar *et al.*, 2007). Several ground-based platforms and two instrumented aircrafts (Cessna 207 and 188) were deployed to characterize trace gases and aerosol physics and chemistry over and around the Edmonton area during late summer (August 17 to September 9) 2005.



a)



b)



c)

Figure 5.16 (a) ground-based measurements of PM_{2.5}, PM_{1.0} sulphate, and SO₂ 80 km east of Edmonton; (b) AURAMS prediction at the grid containing the site at 21 km resolution; (c) AURAMS predictions at 3-km resolution.

During the field study, AURAMS was used to produce 48-hour forecasts to direct the ground-based mobile laboratories and plan aircraft flight paths. Post field campaign, retrospective AURAMS simulations were carried out with a number of updates (model codes and emission data) at two different resolutions, a 21-km resolution domain covering western Canada and north-western U.S. and a nested 3-km resolution domain focused on the Edmonton area (see Table 5.1 for details). Figure 5.16 compares the observed time series of SO₂, PM_{2.5} and PM_{1.0} sulphate (or SO₄ measured by Aerodyne Mass Spectrometer, AMS) with model predictions at one of the ground sites about 80 km southeast of Edmonton. At 21-km resolution, the overall PM_{2.5} mass is under-predicted. The first three peaks in the modelled PM_{1.0} sulphate (Figure 5.16b) are similar in timing to the observation (Figure 5.16a), but the final peak on the 29th is missed in the simulation. The SO₂ concentrations are over-predicted, aside from the observed peak value at 18:00 on August 26. At higher resolution (Figure 5.16c), the model predictions for SO₂ and PM_{1.0} sulphate at this site are considerably improved relative to the observations (better timing and magnitude), although the total PM_{2.5} concentration is still low.

Table 5.12 Ozone and PM statistics for PrAIRie2005 flights.

	R	Slope	MB	NMB (%)	ME	NME (%)
Ozone (ppbv) (C207)	0.516	0.655	7.25	18.9	11.6	30.22
Ozone (ppbv) (C188)	0.525	0.678	3.50	8.79	9.77	24.5
PM1 SO ₄ (µg m ⁻³)	0.284	0.590	0.295	49.3	0.549	91.9
PM1 OC (µg m ⁻³)	0.523	0.143	-2.80	-64.6	2.86	66.0
PM1 NH ₄ (µg m ⁻³)	0.192	1.15	0.631	263.	0.678	283.
PM1 NO ₃ (µg m ⁻³)	0.214	1.37	0.688	255.	0.990	366.
NO (ppbv)	0.440	1.04	1.79	79.9	3.57	159.
NO _x (ppbv)	0.482	1.03	2.58	41.5	7.30	117.

Model predictions at 3-km resolution are compared with aircraft observations by sampling along flight tracks in space and time through the model. Table 5.12 summarizes the overall comparison statistics for all available flights for each aircraft; the two aircrafts did not always fly on the same flight-paths and days, hence the difference in the O₃ statistics between the aircraft. The best correlations are for O₃, NO and NO_x, and PM_{1.0}-OC. NO, and NO_x, have near unity (1:1) slopes yet positive normalized mean biases. The NO_x over-predictions led to PM_{1.0}-NO₃ and NH₄ high biases via excessive particle nitrate formation; ground-based measurements indicate HNO₃ over-prediction. Despite the high correlation for the PM_{1.0}-OC, the slope and normalized mean bias values are low, indicating a substantial under-prediction. It should be noted that the comparison statistics for an individual flight can be quite different from the overall statistics shown.

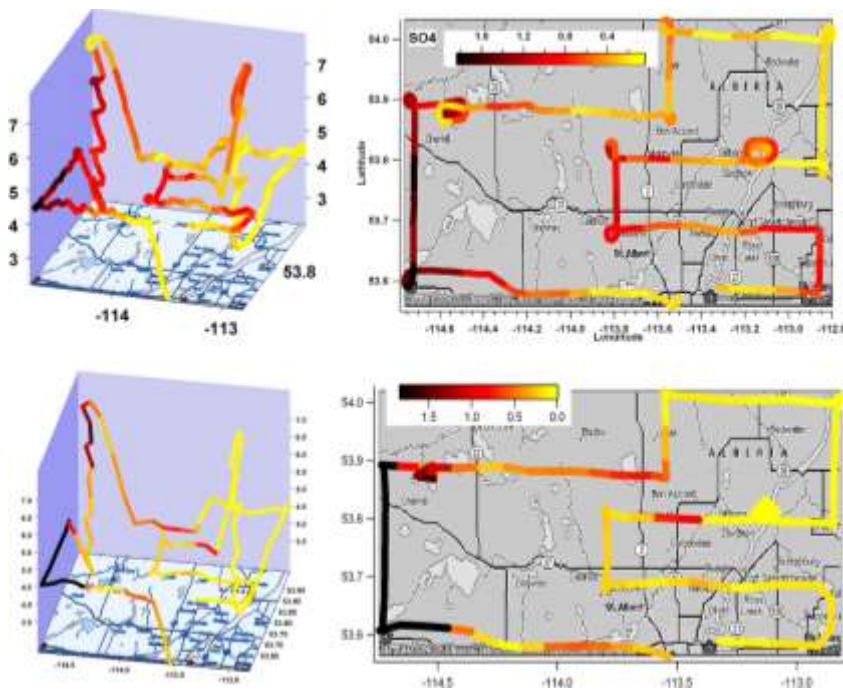


Figure 5.17 An example of model-observation comparison along a flight track for $PM_{1.0}$ -sulphate: 3-D plots of SO_4 along flight track shown on the left with corresponding plan view shown on the right, (top – observation; bottom – model).

Figure 5.17 shows an example of a 3-D model-observation comparison along a flight track for $PM_{1.0}$ -sulphate. It is seen that the model captured well some of the plumes particularly for the power plants west of Edmonton, but missed the plumes over the city. Further study indicates that the local flow can be quite complex, likely influenced by the anabatic/katabatic (or upslope/down-slope) winds in the nearby Rockies, and that predicting the boundary of the local circulation correctly is critical in getting the plume in the right place and time (Stroud *et al.*, 2007). The retrospective model evaluation also indicates that there is a significant discrepancy between the gas and particle mass emissions in the inventory used by the model and the actual emission based on continuous emissions monitoring system (CEMS) data. The correction to the emissions from three coal-fired power plants based on CEMS data resulted in considerable improvement in model evaluation statistics (Cho *et al.*, 2009).

5.4.3.3 Process Evaluation and Sensitivity Studies

In this subsection we summarize some of the recent sensitivity studies aimed at establishing uncertainties in model prediction resulting from uncertainties in model input (emission, meteorology) and parameterization of the physical and chemical processes.

Emission

Biogenic emission processing (isoprene emission factor and vegetation data)

Biogenic emissions play an important role in the formation of smog. As mentioned in section 5.3, both AURAMS and CMAQ use BEIS v3.09 or higher for biogenic emission processing. The evolution of BEIS has been an increase in details in the representation for both vegetation types and biogenic VOC speciation (Pierce *et al.*, 2002). Uncertainties in biogenic emission processing arise from the uncertainties in emission factors (for the various VOC species from the various vegetation types) and in the land-cover information available for the detailed vegetation categories over the area of interest. For example, BEIS 3.09 considers emissions of NO, isoprene, monoterpenes, and “other VOCs” from 230 vegetation land-cover categories (Pierce *et al.*, 1998a,b). Recently, based on BOREal Ecosystem Atmosphere Study (BOREAS) measurements (Pattey *et al.*, 1999; Westberg *et al.*, 2000; Isebrands *et al.*, 1999), the isoprene emission factor for spruce was reduced by half (Schwede *et al.*, 2005). As for the land-cover data, BELD3 provides a default database containing land-cover of the predominant vegetation categories over most of North America obtained from remote sensing. Over the continental United States, the land-cover base map has been refined with more detailed agriculture and forestry information, while over Canada the information needed for refining the vegetation land-cover data required by BEIS v3.09 has not been available until very recently (Morneau, 2007). Most of the simulations included in this assessment used the satellite-derived default land-cover base map over the Canadian domain.

Sensitivity runs with AURAMS were conducted with two different biogenic emissions. In the first (base) run, the biogenic emissions of VOCs and NO were computed using BEIS v3.09 with original emission factors and BELD3 with satellite-derived land-cover for Canada, while the second simulation (“sensitivity run”) was conducted using the updated isoprene emission factors and a recently upgraded BELD3 using the Canadian agriculture and forestry inventory data (see Morneau, 2007 for details). The model domain covers north-eastern North America at a resolution of 21 km, and the simulations were conducted over the period of 28 July to 5 August 2001.

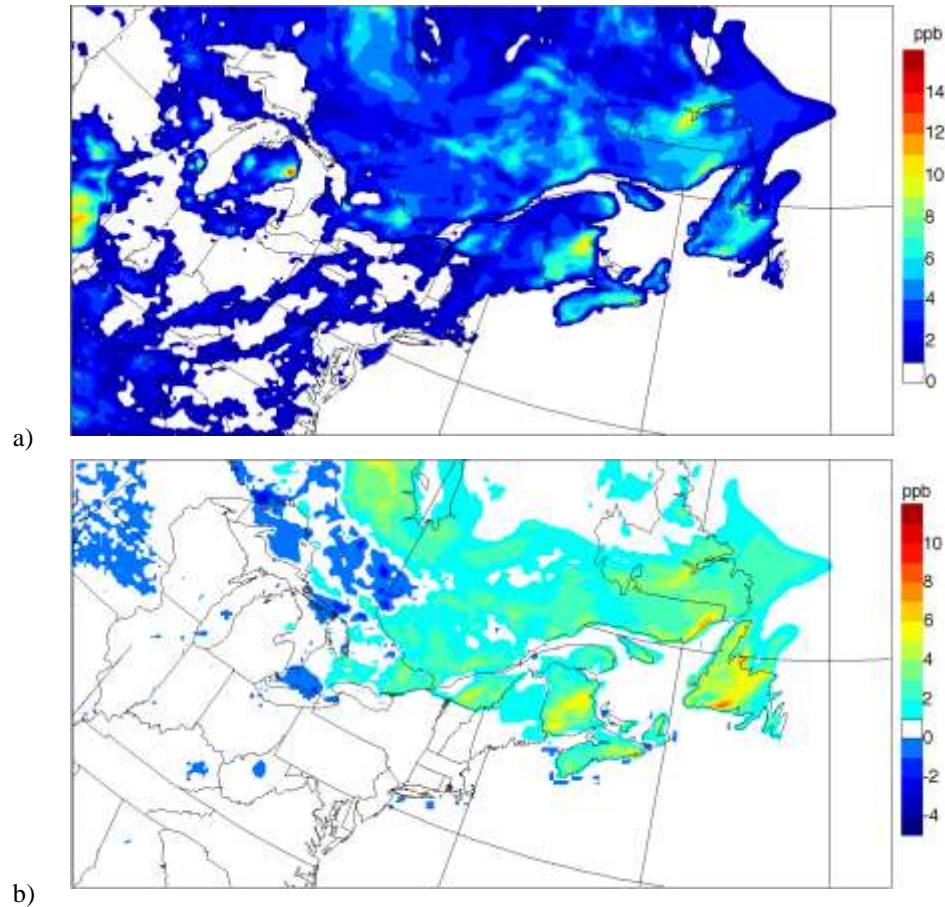


Figure 5.18 (a) Modelled isoprene concentration at the lowest model level from the base run for 1800 UTC, August 2, 2001, and (b) difference in isoprene concentration between the base-case run and the sensitivity run with new vegetation data and revised isoprene emission factors, positive values corresponding to decreases from the base run.

Figure 5.18 shows the modelled isoprene concentration at the lowest model level from the base run and the concentration difference between the two runs for 1800 UTC, August 2, 2001. Positive values correspond to decreases from the base run. It is seen that the modelled isoprene concentrations from the sensitivity run are reduced substantially over Atlantic Provinces and southern Quebec. This is mainly due to the fact that the default satellite-derived vegetation land-cover data used in the base run has very broad categories. For example, there is only a single deciduous forest category. The result of using only one deciduous forest category with an averaged emission factor is the overestimation of isoprene emissions over the area (such as eastern Canada) with the deciduous tree species which are not high isoprene emitters and the underestimation of emissions over the area (such as north-western Canada) with other deciduous tree species which are high emitters of isoprene.

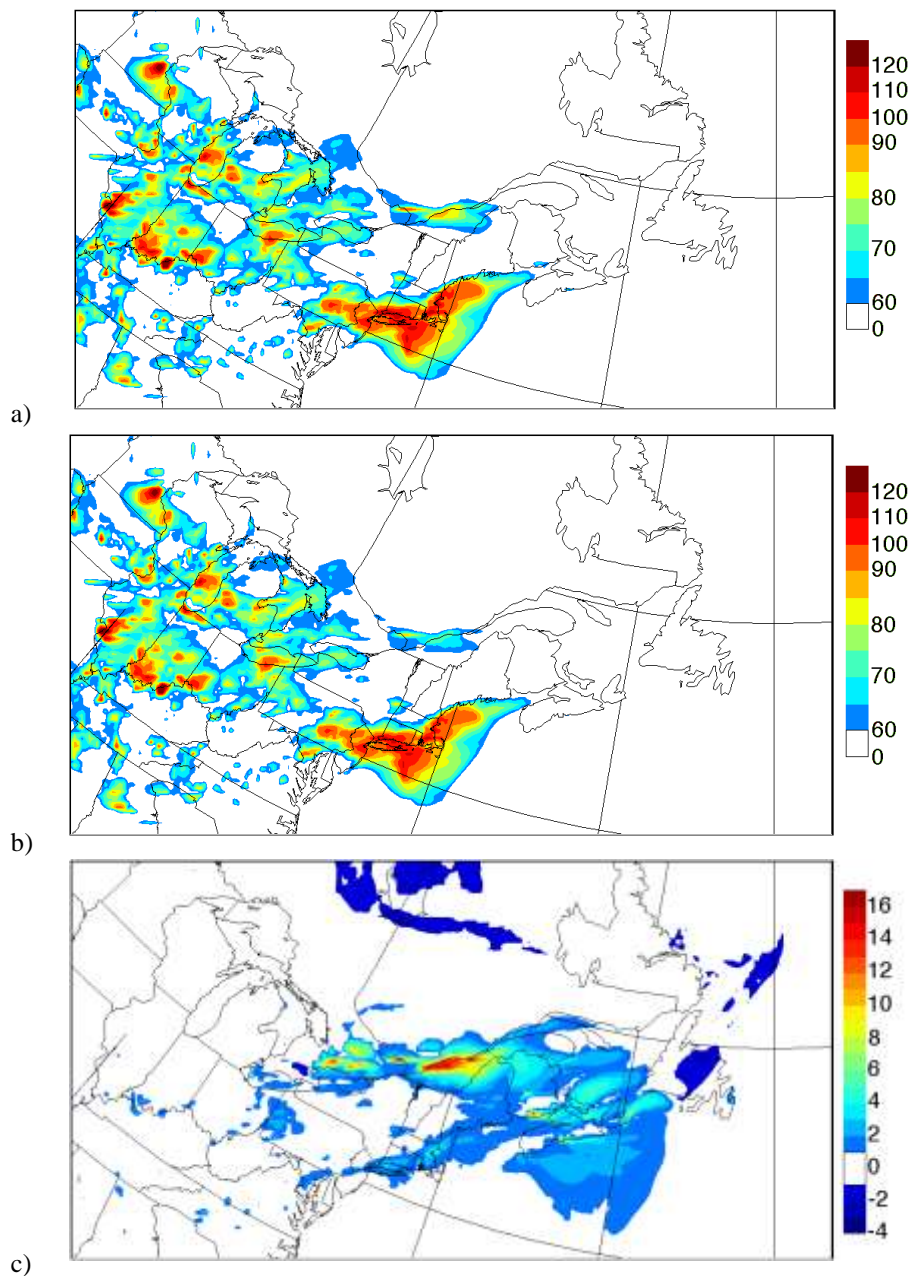


Figure 5.19 The model predicted maximum one-hour ozone concentrations for August 2, 2001: (a) base-case run and (b) sensitivity run with new vegetation data and revised isoprene emission factors, with the difference field (base run – sensitivity run) shown in (c), all in ppbv.

The model predicted maximum one-hour O_3 concentrations for August 2, 2001, from the two runs are shown in Figure 5.19(a) and (b), with the difference field (base run – sensitivity run) shown in Figure 5.19(c). Up to 15 ppbv of reductions in the daily maximum hourly O_3 are seen downwind of

major urban centres along the Windsor-Quebec Corridor with the use of upgraded land-cover data. The O₃ maxima simulated with the new vegetation database are closer to the observed values of 68 to 76 ppb along the St. Lawrence River Valley during that day.

Meteorology

Most of the CTMs are driven either off-line or in-line by meteorological models. Meteorological parameters, such as wind, temperature, humidity, boundary layer depth, turbulence, cloud and precipitation, radiation, all have important influence on the fate of atmospheric pollutants through their influence on the transport, transformation, and removal processes. Consequently, errors in simulated meteorology will have a major impact on the overall performance of CTMs. Some air quality models make use of the objectively analysed meteorology (e.g., LOTOS-EURO, see Schaap *et al.*, 2008) in order to minimize potential errors in simulated meteorology. Almost inevitably the analysis fields will have to be spatially and temporally interpolated for the use in air quality model simulations, which will introduce errors. Furthermore, not all the meteorological parameters required to drive CTMs are available from the objective analysis. The regeneration of the missing meteorological parameters within air quality models will introduce dynamic inconsistency. The use of available data assimilation capability in meteorological simulation (on-line or off-line) may be a way to reduce errors input meteorology. For example Otte (2008a, b) showed significant improvements in model predicted surface ozone from using nudging in meteorological model.

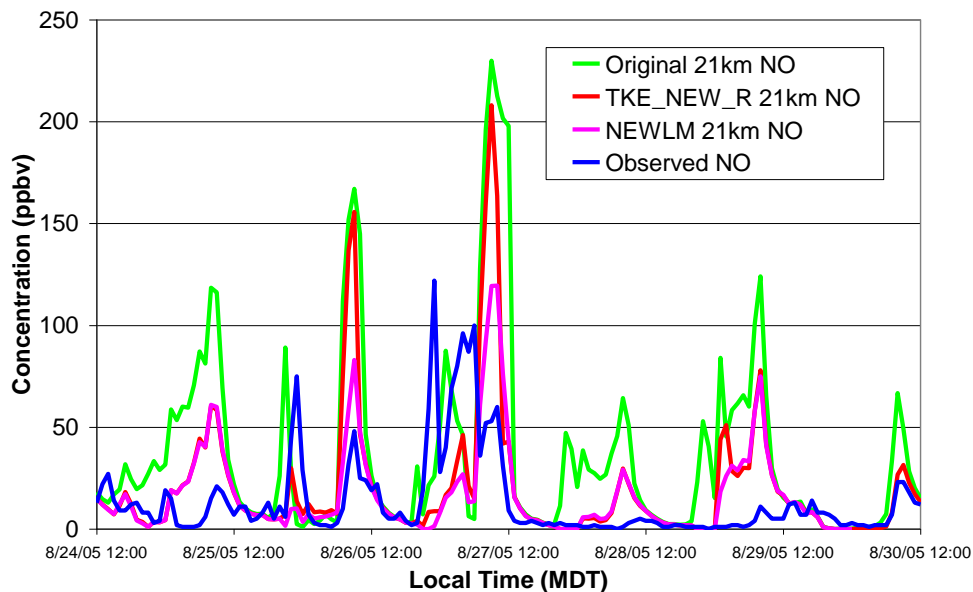


Figure 5.20 Comparison of modelled and measured NO at Edmonton Central from the PrAIRie2005 simulations (Original denotes the current operation GEM, while TKE_NEW_R includes new parameterizations for urban heat islands, boundary layer height, and turbulent kinetic energy and NEWLM includes an additional observation-based lower limit in TKE).

It is known that the errors in the simulated meteorology mainly come from initial and boundary conditions (IC and BC) and the representation of unresolved, parameterized physical processes (Seaman, 2007; Nance *et al.*, 2007). Atmospheric boundary layer dynamics and clouds are amongst the fields that are least evaluated and most difficult to predict. When it comes to air quality modelling, these are amongst the most important variables affecting CTM's performance. Traditionally the meteorological community has focused model evaluations mostly on the state variables (such as pressure, temperature, humidity). To illustrate the impact of different parameterizations of mixing in atmospheric boundary layer on CTM performance, Figure 5.20 shows model predicted NO time series from the PrAIRie2005 simulations (see 5.4.3.2) at 21 km resolution driven by meteorology from three different GEM runs compared with observations: (i) the current operational GEM (denoted as "Original"); (ii) as in (i) but with new parameterizations for urban heat islands (Makar *et al.*, 2006), boundary layer height, and turbulent kinetic energy (Han *et al.*, 2000) (denoted as "TKE_NEW_R"); and (iii) same as (ii) but with an additional lower limit in TKE based on the observations of Nastrom and Eaton (2005) (denoted as "NEWLM"). The model over-predicts NO in the urban core, but the parameterizations with the highest mixing (TKE_NEW_R and NEWLM) tend to be the closest to observations, suggesting that the vertical diffusion in the current operational GEM model is insufficiently strong in urban core areas (see section 9.4 for further discussion). The sensitivity in CTM's performance to the PBL mixing parameterizations has also been reported by others (e.g., McKeen *et al.*, 2007).

Evaluation of model predicted 3-D cloud properties remains to be a major challenge for the lack of suitable data and pertinent evaluation methodologies. Yet cloud properties such as 3-D fraction and liquid water content directly influence photolysis and in-cloud oxidation which are important transformation processes for the formation/production of O₃ and PM in the atmosphere. Zhang *et al.* (2007) pursued an evaluation of GEM predicted cloud water content at 15- and 2.5-km resolutions with aircraft observations during the ICARTT/CTC 2004 field campaign. Both stratocumulus and towering cumulus cases were included. The conventional "point-by-point" in-situ statistical evaluation proved to not work well given the temporal and spatial mismatch between model simulation and aircraft observation. The evaluation using a broader statistical approach showed that the model was able to capture the observed vertical distribution of liquid water content (LWC) and also reproduced the observed variation in the LWC statistics amongst different flights. However, the model at both resolutions generally overestimated the cloud water content, considering both in-cloud and cloud-scale values, for the cases investigated. This will subsequently impact the modelled in-cloud oxidation in AURAMS simulations.

Physical and Chemical Processes

SOA formation

As shown in Chapter 3, the organic component can account for a significant fraction of the $PM_{2.5}$ mass observed in both urban and rural ambient air, of which a large portion can be secondary organic aerosol (SOA) (e.g., Turpin and Huntzicker, 1995; Volkamer *et al.*, 2006; Yu *et al.*, 2007). Most of the CTMs for predicting atmospheric aerosols these days do include some representation for SOA formation. Several SOA formation algorithms are currently used in CTMs. For example, as listed in Table 5.1, AURAMS includes two SOA algorithms, an overall aerosol yield (OAY) algorithm based on Odum *et al.* (1997) and an instantaneous aerosol yield (IAY) algorithm which is derived from the Odum's OAY parameterization but aimed at representing the incremental increase in organic aerosol mass due to small changes in reacted precursor VOC (Jiang, 2003). CHRONOS, on the other hand, uses a constant yield scheme based on Pandis *et al.* (1992), while a more detailed algorithm based on Schell *et al.* (2001) is implemented in CMAQ.

Most of these SOA parameterization schemes share the basic concept of a two-step process involving (1) gas-phase production of condensable vapour products followed by (2) gas-to-particle partitioning (see Chapter 2). The first step is determined based on the stoichiometric (or production/yield) coefficients of the condensable vapour products. As for the second step, the Pandis' scheme assumes that the condensation of vapour-phase products only occurs when its saturation vapour pressure is exceeded, while Odum's and Schell's algorithms follow an absorption partitioning based on Pankow (1994) which allows the partitioning of the condensable products to particle phase below their saturation concentrations. The various SOA schemes and their implementations also differ in the representation of precursor and products classes. Additional uncertainties arise from the uncertainties in determining stoichiometric coefficients, saturation vapour pressures, and gas-to-particle partitioning coefficients for the various condensable classes represented.

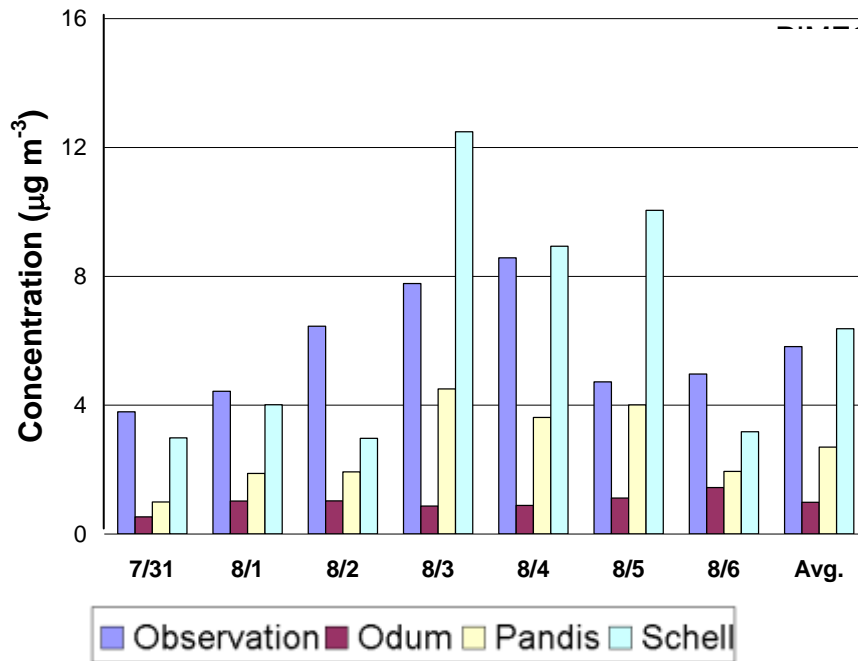


Figure 5.21 Comparison of 24-hour average modelled and measured organic aerosol concentrations at the Pitts Meadows site in the Lower Fraser Valley during the PACIFIC 2001 study.

Jiang *et al.* (2003) compared the Schell, Pandis and Odum parameterizations within CMAQ for characterization of the Lower Fraser Valley (southern BC) during the PACIFIC 2001 study. Figure 5.21 shows a comparison of the 24-hr averaged organic aerosol model results against observations for the Pitts Meadows (PIME3) location. Results from Schell’s algorithm compare favourably with the measurement data, in terms of magnitudes, while both Pandis’ and Odum’s algorithms consistently under-predict the 24-hour average organic aerosol concentrations.

Table 5.13 AURAMS statistics for SOA comparison with observations from the IMPROVE and NAPS networks (20 sites in the northeastern US and eastern Canada, number of points = 235, 24-hr samples every 3 days)

	Modelled average	Observed average	NMB	NME	R
Jiang (AURAMS v1.3.1)	0.34	2.6	-0.87	0.87	0.26
Odum (AURAMS v1.3.1)	0.041	2.6	-0.98	0.98	0.12
Jiang (AURAMS v1.3.2*)	1.8	2.6	-0.31	0.52	0.29
Odum (AURAMS v1.3.2*)	0.72	2.6	-0.72	0.73	0.27
Jiang (AURAMS v1.3.2*, with aqueous phase)	3.0	2.6	0.15	0.66	0.25

Table 5.14 AURAMS statistics for POA and EC comparison with observations from the IMPROVE and NAPS networks (20 sites in the northeastern US and eastern Canada, number of points = 235, 24-hr samples every 3 days)

	Modelled average	Observed average	NMB	NME	R
Primary Organic	0.54	1.3	-0.66	0.68	0.45
Elemental Carbon	0.13	0.38	-0.67	0.68	0.47

The implementations of Odum's and Jiang's schemes in AURAMS are compared for the characterization of the eastern North American domain during the ICARTT 2004 study. Table 5.13 presents the evaluation statistics comparing model predictions with organic aerosol observations from the IMPROVE and NAPS networks, using the OC/EC tracer method (Yu *et al.*, 2004) to estimate the observational split between secondary and primary organic aerosol. Several sets of results are included. The first pair is from an older implementation of Odum's and Jiang's schemes (AURAMS v1.3.1), where primary organic aerosol component is not included as absorbing organic aerosol component. This is the same implementation used in the 2002 AURAMS annual simulation presented earlier. The second pair is from an updated implementation where all organic components (primary and secondary) are considered to be absorbing. The revised implementation also includes updates on some of the stoichiometric and partitioning coefficients based on newer data (e.g., Chung and Seinfeld, 2002; Song *et al.*, 2005) and the inclusion of isoprene as SOA precursor (Kroll *et al.*, 2006). This is the implementation used in the more recent AURAMS simulations (e.g., ICARTT and PrAIRie2005). It can be seen that both schemes underestimate SOA formation but the Jiang's IAY scheme consistently predicts higher SOA compared to the Odum OAY scheme, and that the updated implementation also significantly improves model prediction in terms of magnitudes. However, both parameterizations yield poor linear correlation coefficients. Table 5.14 lists the model-measurement comparisons for primary organic aerosol (POA) component and elemental carbon (EC). AURAMS underpredicts POA and EC both by factors of 2.4 and 2.9, respectively. Both POA and EC have similar linear correlation coefficients which are considerably better than for SOA.

The last row in Table 5.13 presents the results from a sensitivity run where aerosol-bound water was included with the organic component as the absorbing medium. This is to assess the uncertainties related to the chemical nature of the absorbing medium for partitioning (Griffin *et al.*, 2003). As expected, the modelled SOA increased under this scenario with improved bias score (now positive) but no apparent improvement in mean error and correlation coefficient. Other approaches, based on more explicit gas-phase mechanisms including multi-generation products and their gas-particle partitioning, are being developed (Griffin *et al.* 2005). These more explicit approaches do provide estimates of aerosol-phase speciation; however they are computationally expensive which currently precludes their use in operational air quality

forecasting and long-term policy related simulations. Explicit mechanisms have also not necessarily resulted in improved skill in terms of modelling total SOA (Pun *et al.*, 2003; Chen *et al.*, 2006).

Recently, the volatility of primary organic aerosol (POA) emissions has been measured with dilution flow tube experiments and thermal denuders. Robinson *et al.* (2007) showed that POA emissions can evaporate in the gas-phase and subsequently oxidize to form SOA. This process will add mass to the organic aerosol in terms of functional groups (-OH, -C(O)-, -ONO₂) and will shift the burden of organic aerosol from urban to regional scales. Furthermore, it has been found that intermediate volatile organic compounds (IVOC) represent a pool of emitted gas-phase organic compounds which can oxidize in one reaction step and form significant amounts of SOA (Murphy and Pandis, 2009).

Other studies have looked at the sensitivity of SOA predictions to NO_x and VOC reductions (Chen *et al.*, 2006). Interestingly, under rural NO_x limited conditions, the explicit SOA schemes show an opposite SOA trend for NO_x reductions as compared to the empirical SOA parameterizations. The explicit schemes show an SOA increase with decreasing NO_x, due to the lower volatility of carboxylic acid products, which are favoured over organic nitrate products at lower NO_x/VOC ratios. This has implications on the effectiveness of NO_x emission reduction strategies as SOA can be a large fraction of PM_{2.5}. Both explicit and empirical parameterizations show a decrease in SOA with decreasing VOC. Other studies have looked at the temperature dependence of SOA predictions and found considerable variability among results (Pun *et al.*, 2003; Chen *et al.*, 2006). The temperature dependence of SOA is largely due to the values chosen for the enthalpy of vapourization of SOA products in the parameterization. Modelled temperature dependence predicted by both empirical and explicit algorithms is currently greater than measured experimentally in smog chambers. These temperature sensitivity studies have implications on the response of SOA to, for example, future climate change.

In-cloud oxidation

As discussed in 5.4.3.2, comparing with aircraft data obtained during ICARTT, AURAMS tends to over-predict sulphate in the lower atmosphere. It was also found from a multi-model intercomparison and evaluation study (McKeen *et al.*, 2007) that those models that include in-cloud sulphur oxidation (e.g., AURAMS and CMAQ) over-predicted sulphate between 400 and 700 m comparing with observations, hence raising the question that the in-cloud oxidation may be over-predicted in the models.

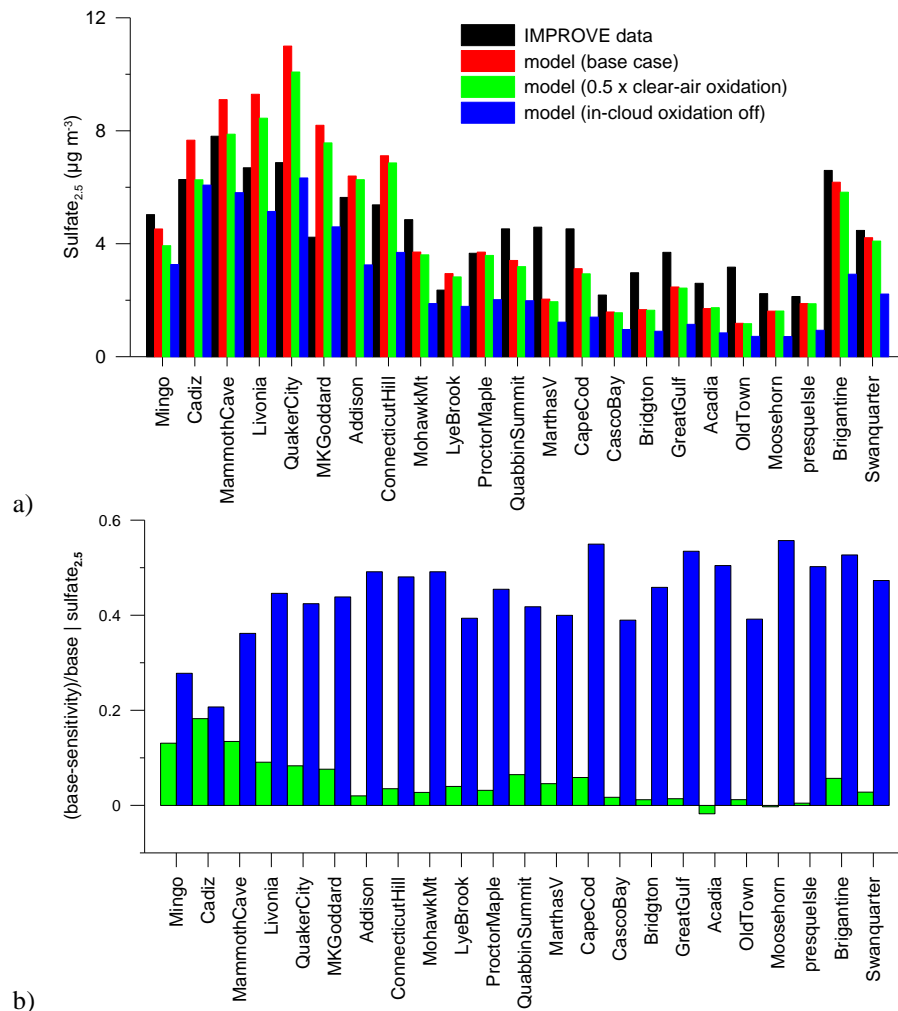


Figure 5.22 (a) Model-observation comparison of sulphate_{2.5} at the IMPROVE sites (arranged by locations from Midwest source region to eastern seaboard along the x-axis, left to right); (b) relative difference of the two sensitivity runs with respect to the base-case run.

To investigate the relative impact from in-cloud versus clear-air sulphur oxidation, two sensitivity runs were conducted using AURAMS for the ICARTT period, one with in-cloud oxidation turned off and the other with clear-air sulphur oxidation rate reduced by half. Figure 5.22 shows the model-observation comparison of sulphate_{2.5} at the IMPROVE sites. Recall from the discussion in 5.4.2.2, the model tended to over-predict over the source region (e.g., Ohio River Valley) and under-predict over more downwind regions (e.g., east coast). The clear-air oxidation has a relatively small impact on the modelled sulphate, in comparison to the in-cloud oxidation. Nevertheless, the impact is clearly greater close to the sources than farther downwind (Figure 5.22b). The in-cloud oxidation contributed to about 50% of the modelled ambient sulphate and about same fraction of the total column loading below 5 km during the ICARTT period over eastern NA (Gong *et al.*, 2007). While turning off in-cloud oxidation may bring model closer to observation at sites located in source area, it worsens the comparison at

sites over east coast and New England area. As discussed above, Zhang *et al.* (2007) found that the meteorological model (GEM) tended to over-predict cloud water content compared with aircraft observations over south-western Ontario and Ohio during the ICARTT period. It is therefore reasonable to expect that in-cloud oxidation may be overestimated. On the other hand, other processes and emission may have also contributed to the model over-prediction of sulphate_{2,5}.

Mathur *et al.* (2007) also explored the possible causes for the apparent over-prediction of sulphate_{2,5} from CMAQ comparing with aircraft observations during ICARTT 2004. It was postulated that the tendency for over-predicting H₂O₂ by the CB-4 mechanism could be responsible for the over-prediction of in-cloud sulphur oxidation. Interestingly when the CB-4 mechanism was replaced by SAPRC mechanism, H₂O₂ was indeed reduced and so was the in-cloud oxidation. However, the reduction was almost completely compensated by an increase in model prediction in OH and clear-air sulphur oxidation.

Sea salt production

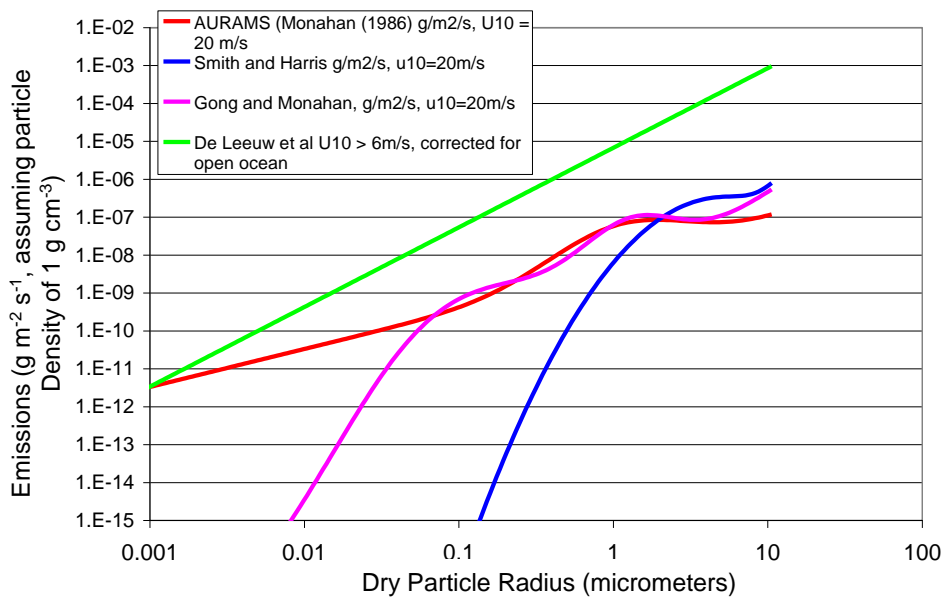


Figure 5.23 Comparison of Sea-salt fluxes at $u_{10} = 20 \text{ ms}^{-1}$ for four different parameterizations.

Sea salt can contribute a significant fraction of fine particle mass in marine and coastal environments particularly under high wind conditions (O’Dowd and Smith, 1993). The concentration of sea salt particles has been found to have a strong correlation with wind speed for all size ranges (O’Dowd and Smith, 1993). Both AURAMS and CMAQ (version 4.6) include sea salt as one of the aerosol components. AURAMS uses a sea salt generation

algorithm based on Monahan *et al.* (1986). Gong (2003) further extended the Monahan scheme to better represent sea salt generation at both sub- and super-micron size ranges. CMAQ on the other hand uses an algorithm based on Smith and Harrison (1998). Figure 5.23 shows a comparison between the three sea salt generation schemes (source functions) in terms of mass emission at 20 m s^{-1} wind speed (at 10 m). It is seen that the Monahan (1986) parameterization used in AURAMS has the highest mass in the 0.001 to $0.1 \text{ }\mu\text{m}$ radius range. The Gong (2003) parameterization drops rapidly for radii less than $0.1 \text{ }\mu\text{m}$, and the Smith and Harrison parameterization drops rapidly for radii less than $2 \text{ }\mu\text{m}$. Note that all three source functions are for open ocean. De Leeuw *et al.* (2000) also proposed a set of source functions, given different ranges of wind speed, for surf zone conditions.

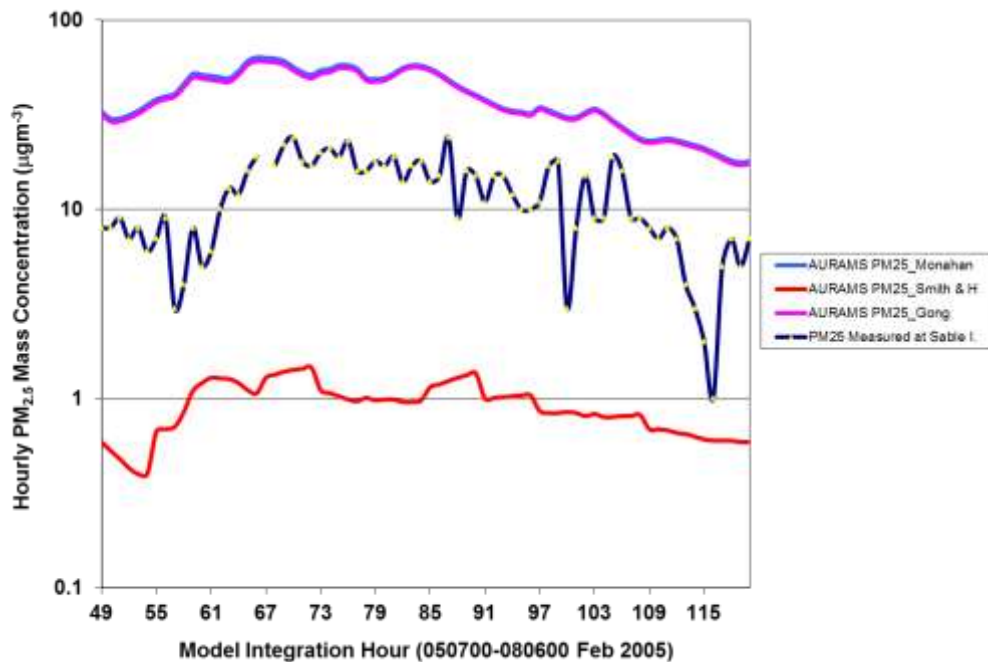


Figure 5.24 AURAMS predicted surface fine particulate mass concentration ($\text{PM}_{2.5}$) using various sea-salt generation parameterizations versus measured $\text{PM}_{2.5}$ at Sable Island 5-8 Feb 2005.

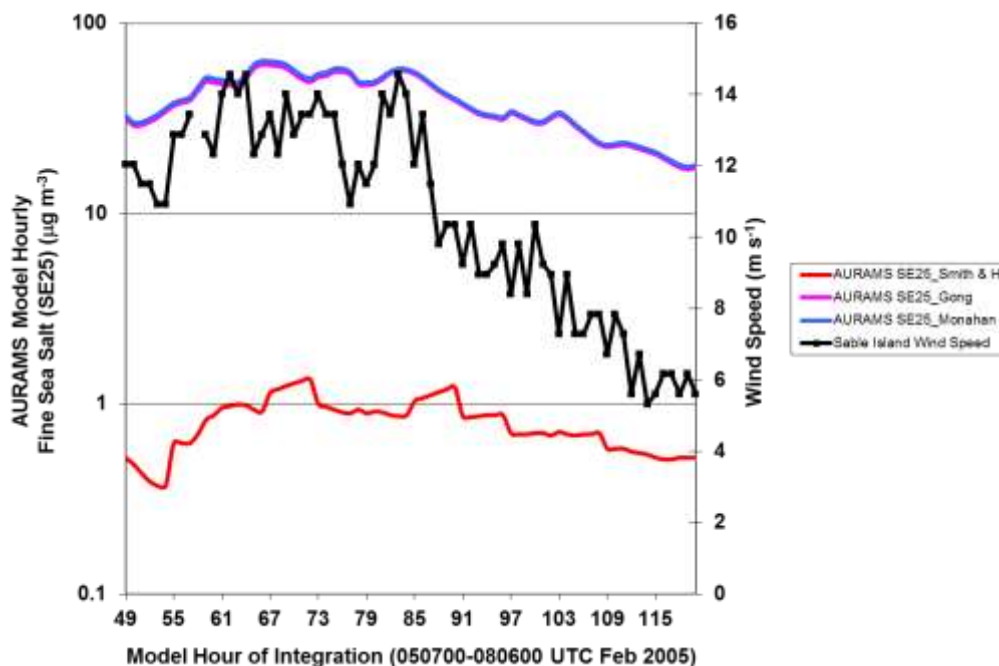


Figure 5.25 AURAMS predicted surface fine sea salt aerosol (SE25) versus hourly wind speed at Sable Island, NS, 5-8 February 2005.

To test the sensitivity of modelled sea salt aerosols to the various sea-salt generation parameterizations, three separate AURAMS runs were conducted, each with a different open-ocean source function. The simulations were conducted for the period of Feb. 5 to 8, 2005 at 21 km resolution (see Table 5.2 for details), focussed on Quebec and Atlantic region. The period coincided with an elevated PM episode in the region. In Figure 5.24, the model predicted $PM_{2.5}$ time series are compared with the observation at the Sable Island site. The model simulations with the Monahan and Gong-Monahan parameterizations over-predicted, while the simulation with the Smith-Harrison parameterization under-predicted fine PM mass compared with the observations. Both the over- and under-predictions were significant. Figure 5.25 compares the model predicted fine sea salt component with different sea-salt source functions with observed 10-m wind speed at Sable Island. It is seen that the modelled $PM_{2.5}$ is dominated by sea-salt component at this site for this period. The Monahan and Gong-Monahan schemes behaved similarly and correlated with the wind speed while the Smith-Harrison scheme generated much lower sea salt in comparison.

Model Resolution and IC/BC

CTM's performance may also be influenced by model resolution and chemical initial and boundary conditions. At urban scale and for areas with complex terrain (e.g., LFV), higher model resolution is required to properly resolve small scale variations in forcing functions (dynamic, thermal, and emission sources), although it also requires that the processes are resolved accurately at smaller scales. Comparison between the 12-km and 4-km CMAQ

simulation results for the Pacific 2001 period over LFV (RWDI, 2003; see 5.4.1.2 and Table 5.2) found that the model at finer resolution captured the night-time O₃ minimum somewhat better than at coarser resolution but found little difference in daytime maximum O₃ between the two runs. The improvement in model predicted PM_{2.5} at 4-km over the 12-km resolution was slightly more appreciable at some sites but without significant improvement in overall performance statistics. Zhang *et al.* (2006) evaluated CMAQ simulations for a 10-day period in July 1999 during the Southern Oxidant Study (SOS) at 32-km and 8-km resolutions. They found that, in terms of 1-hr and 8-hr O₃ statistics, the model at 32-km resolution produced better correlation coefficients than at 8-km resolution but higher bias at rural sites. At urban and suburban sites however, the correlation coefficients are similar from the two model runs but much smaller bias from the coarse than the finer resolution runs. As for the evaluation statistics for PM mass and components, the coarse resolution run performed somewhat better except for sulphate_{2.5}, though both model runs significantly under-predicted total PM mass and most of the components.

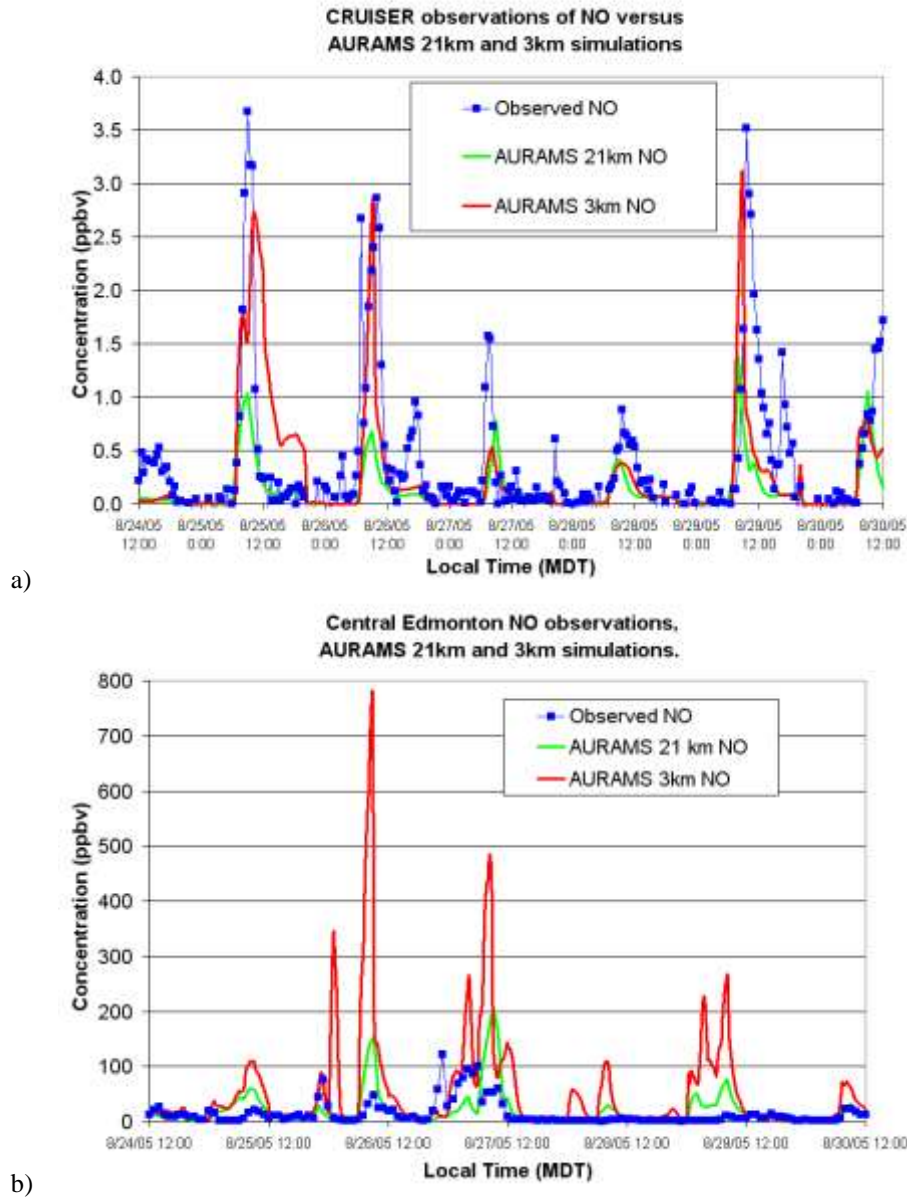


Figure 5.26 (a) Comparison of modelled and measured NO 80 km downwind of Edmonton and; (b) Comparison of modelled and measured NO at Edmonton Central.

Figure 5.26 shows the modelled NO time series at two sites, Edmonton central and the Cruiser site (80 km east of Edmonton), from the PrAIRie2005 AURAMS simulations at 21-km and 3-km resolutions compared with observations. It is seen that increasing the horizontal resolution from 21km to 3km substantially improved the model fit to observations for locations downwind of the urban core, but the insufficient vertical mixing at night over the city was exacerbated in the urban core itself (hence more over-prediction at the finer resolution at the Edmonton central site). AURAMS simulation for the ICARTT period was also carried out at 15-km resolution as opposed to the retrospective run at 42-km resolution included in this

assessment. It was found that the overall evaluation statistics (at AIRNow sites) was not improved by going to a finer resolution grid. What this means is that higher resolution model simulation does not always result in better model performance. It depends on a number of things, e.g., model input and process representation at higher resolution as well as the particular performance measure.

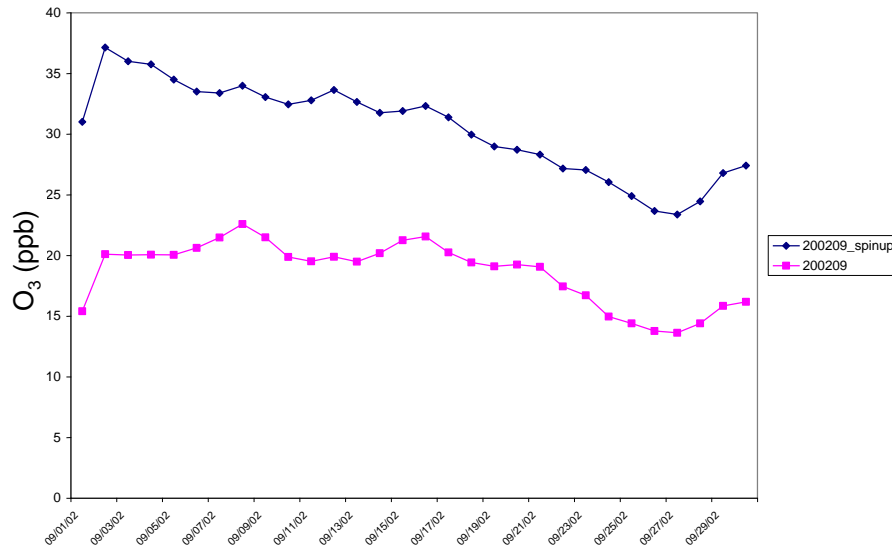


Figure 5.27 Domain-averaged ozone time series for the month of September 2002 from two AURAMS runs, one starting on May 1, 2002 (denoted as “200209”) and the other starting on September 1, 2002 (denoted as “200209_spinup”), both from the same initial conditions and with zero-gradient boundary conditions.

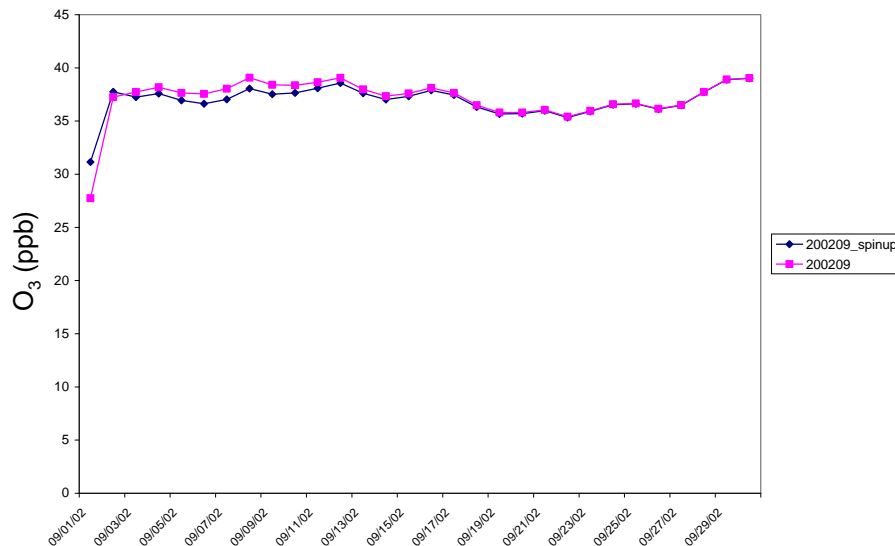


Figure 5.28 Same runs as in Figure 5.27 but with time-independent first-order boundary conditions.

The treatment of chemical lateral boundary conditions (CLBCs) can also impact CTM's performance (e.g., Brost, 1988; Hogrefe *et al.*, 2004; Tong and Mauzerall, 2006). CHRONOS and the earlier versions of AURAMS (v1.3.1 and earlier) use a closed-boundary zero-gradient CLBC for their semi-Lagrangian advection algorithm, while CMAQ uses a Dirichlet lateral boundary condition, i.e., concentrations on the boundary grids are specified by either time-invariant profiles or time-dependent fields provided by a larger-scale model (Appel *et al.*, 2007). The zero-gradient boundary condition was shown to be problematic when used for an extended simulation with inflow boundaries located over ocean and remote area (see Samaali *et al.*, 2009 and Tarasick *et al.*, 2007). Figure 5.27 shows domain-averaged O₃ time series for the month of September 2002 from two AURAMS runs, one starting on May 1, 2002 and the other starting on September 1, 2002, both from the same initial conditions. It is seen that with the zero-gradient lateral boundary condition the two runs never converged. Figure 5.28 shows the same pair of runs but with time-independent Dirichlet boundary conditions. Now the two runs converge after two days (in terms of domain-wide average).

Even for the Dirichlet CLBC, the CTM performance can still be affected by the actual concentrations prescribed at the boundaries. The zero-gradient lateral boundary conditions were replaced by time-invariant Dirichlet CLBC in more recent AURAMS simulations (e.g., ICARTT and PrAIRie2005 retrospective runs; see Table 5.2), where gridded monthly O₃ climatology (Logan, 1999), MOPITT CO (<http://neo.sci.gsfc.nasa.gov/Search.html?group=35>), and long-term particle measurements (e.g., Macdonald *et al.*, 2006) were used, along with other representative profiles, to set values at in-flow boundary grid cells. Appel *et al.* (2007) showed that the CMAQ performance statistics was improved by replacing the time-invariant CMAQ default profiles with the ones provided by a global CTM, GEOS-CHEM (Bey *et al.*, 2001) for their 2001 annual simulation. Tang *et al.* (2007) described a series of sensitivity runs where the lateral boundary conditions for the regional CTM were provided by three different global models. There was considerable variability amongst the boundary conditions provided from the different global models, which led to important differences in the regional CTM's performance. Furthermore, the study also showed that by reducing the time-varying, geographically dependent boundary conditions to spatially and temporally averaged boundary conditions, the performance of the regional CTM deteriorated with each averaging step.

Before turning to the next sub-section on model inter-comparison, it is worthwhile to highlight some of the issues and findings from the diagnostic and process evaluation, which is aimed at assessing model's ability in representing the precursor-concentration relationship.

Firstly, model performance in predicting the major precursors to smog (namely, NO_x, SO_x, and VOC) is assessed. Based on AURAMS simulation of 2002, the modelled annual NO_x and SO₂ concentrations correlated well with the observations over NA, though SO₂ is over-predicted over central Alberta and near two major sources in Manitoba, indicating possible discrepancies between the emission used by the model and actual emissions. Nitric acid, both a secondary pollutant and precursor to particle nitrate, is modelled less well in comparison, with significant

over-prediction for summer (3rd quarter), consistent with the over-prediction of particle nitrate for the same quarter. Modelled VOC is evaluated with observations in terms of OH-reactivity. It is seen that comparatively the model performs better in predicting anthropogenic than biogenic VOCs. Isoprene is significantly over-predicted in AURAMS despite the update in Canadian vegetation data. This will have an impact on modelled O₃ production and SOA formation.

Several recent field studies have provided valuable additional datasets for diagnostic model evaluation. Model evaluations against two of the field studies, ICARTT and PrAIRie2005, are discussed. Over the Great Lakes area, the comparison of AURAMS simulation with aircraft (Convair 580) data during ICARTT shows that the model performs better in predicting primary than secondary species. While the model captures the observed vertical distribution of O₃ well in the lower atmosphere, there is an indication that there is an over-prediction in regional background O₃. As well, while SO₂ is predicted well, sulphate is often over-predicted, indicating possible over-estimation of production and/or under-estimation of removal. Over Edmonton area, the evaluation of high-resolution AURAMS simulation with PrAIRie2005 aircraft observations indicates that the model's ability of predicting local circulations is critical in getting the plumes in the right place and time. The model sensitivity studies also indicate that there is a significant discrepancy between the gas and particle mass emissions in the inventory used by the model and the actual emission. The correction to the emissions from three coal-fired power plants based on the continuous emissions monitoring data resulted in considerable improvement in model evaluation statistics.

Finally, model sensitivities with regard to the representation of various processes are reviewed based on a number of existing studies. These processes include biogenic emission, meteorology, secondary organic aerosol formation, in-cloud oxidation, and sea-salt generation. It shows that the estimate of biogenic emission is sensitive to the input information on vegetation cover, which in turn impacts on modelled O₃ production and also the SOA formation. Boundary layer parameterization, including the effect of urban heat island and turbulence mixing, is shown to have important impact on CTM performance particularly over urban areas. Several different algorithms are available to model SOA formation, and existing sensitivity tests show that there can be significant differences in the modelled organic aerosol concentrations resulting from the different SOA formation algorithms. In-cloud oxidation is shown to be the more important contributor (compared to clear-air oxidation) to modelled ambient sulphate concentration during ICARTT period particularly farther downwind from the sources. It is shown that there is considerable uncertainty in the meteorological model's ability to predict cloud microphysics, which is expected to have a significant impact on model performance particularly for sulphate prediction. It is also shown that there are considerable uncertainties in modelled sea salt concentrations due to the uncertainty in the parameterization of sea salt generation, which can impact CTM performance in predicting total PM mass in coastal areas. Model sensitivities to resolution, initial and boundary conditions are also discussed. It is shown that the type of lateral boundary condition can have a significant impact

on model predictions as well as the actual concentrations prescribed on the lateral boundaries. The benefit of higher resolution modelling is shown to be dependant on model input and process representation pertinent at the higher resolution as well as on the particular performance measure.

5.4.4 Model Intercomparison

Model intercomparison is a valuable exercise for (1) establishing model uncertainties (or a collective confidence level) and (2) diagnosing model deficiencies (or areas for improvement) in representing various processes. Model intercomparison can be carried out in a range of ways. On one end of the spectrum, the intercomparison can be conducted with very little constraint with participating models running in their native states, each with its own meteorology and emission data. This is to aim at assessing the maximum variability (or uncertainties) amongst model predictions. To the other end, the intercomparison can be done with as much constraints in model inputs as feasible in order to assess the uncertainties related to model parameterizations only. Recently there have been a number of intercomparison exercises involving multiple models conducted in North America (e.g., McKeen *et al.*, 2005, 2007) and in Europe (e.g., van Loon *et al.*, 2004, 2007; Vautard *et al.*, 2007; Cuvelier *et al.*, 2007).

As part of the ICARTT field campaign, a real-time collective air-quality model intercomparison, evaluation, and ensemble project was undertaken (Fehsenfeld *et al.*, 2006; McKeen *et al.*, 2005, 2007). Both AURAMS and CHRONOS from Environment Canada and CMAQ/Eta from NOAA participated in this exercise amongst a group of six regional air-quality forecast models. All models were run in their native states with different anthropogenic emission inventories and biogenic emission processing. Statistical evaluations of the model predictions (from the individual models as well as model ensemble) were performed against near real-time O₃ and PM_{2.5} data from the AIRNow network. There was a range of performance amongst the participating models. All models had positive bias for O₃, ranging between 5 and 25 ppb in terms of daily 8-hour maximum concentrations. The over-prediction can at least be partly attributable to the use of older emission inventories by a number of models which did not reflect the important changes in NO_x and VOC emissions in recent years, particularly the significant changes in NO_x emission due to the U.S. NO_x State Implementation Plan which came into effect during 2003-2004 (Frost *et al.*, 2006; also 5.4.5 below). Models also tended to over-predict under low O₃ concentration conditions which dominated the summer of 2004 over eastern North America (White *et al.*, 2006). Nevertheless the ensemble always outperformed any individual members in terms of both O₃ and PM_{2.5} mass. The models showed similar (if not better) skills in predicting PM_{2.5} compared to predicting O₃. Most of the models tended to predict better for urban and suburban sites (or close to anthropogenic sources) than at rural sites (or farther downwind of anthropogenic sources) indicating processes affecting secondary aerosol as being a model weakness.

Despite the large heterogeneity in models' configurations and emissions, the inter-comparison study was able to allude to a number of areas which may have affected the model performance and warrant further investigations, such as PBL parameterization and vertical diffusion/mixing, SOA parameterization, the representation of in-cloud sulphur oxidation (McKeen *et al.*, 2007).

On the other hand, a more "controlled" model intercomparison has been conducted recently between AURAMS and CMAQ (see Smyth *et al.*, 2007a,b, 2009, for more detailed description of the study). In this comparative performance evaluation, both models were run in their native states but a number of model configurations were made as common as possible, e.g., model horizontal resolution and domain, meteorological driver model, anthropogenic emission inventories and processing system. The evaluation was carried out for the month of July 2002, using the same GEM meteorology as for the AURAMS 2002 annual run (see 5.4.1). Although best effort was made to eliminate as many uncertainties as possible in order to focus on the differences in model science and algorithms (see Table 5.1), there were still other important differences between the two models in, for example, vertical resolution, initial and lateral boundary condition, and speciation of primary PM emission, which will lead to the differences in model performance.

Table 5.15 Ambient ozone and PM_{2.5} evaluation statistics from the NRC AURAMS-CMAQ comparative evaluation for July 2002.

	O ₃		Daily peak O ₃		PM _{2.5}	
	AURAMS	CMAQ	AURAMS	CMAQ	AURAMS	CMAQ
Mod. mean (ppb, µg m⁻³)	42.03	51.46	66.66	70.16	12.21	5.11
Obs. Mean (ppb, µg m⁻³)	35.64	35.62	60.77	60.72	14.43	14.40
MB (ppb, µg m⁻³)	6.38	15.85	5.89	9.44	-2.23	-9.29
NMB (%)	17.91	44.50	9.68	15.56	-15.42	-64.52
ME (ppb, µg m⁻³)	16.25	18.82	16.38	14.29	9.69	10.16
NME (%)	45.59	52.83	26.96	23.54	67.12	70.59
r²	0.393	0.438	0.350	0.505	0.074	0.151

Table 5.15 shows the evaluation statistics for O₃, PM_{2.5} mass for both models, against hourly data from the NAPS and Air Quality Service (AQS) networks. As seen, both models are biased high for O₃ and biased low for PM_{2.5} mass, with AURAMS' biases considerably smaller than CMAQ's. The smaller biases in AURAMS prediction however, did not translate to smaller errors. The normalised mean errors (NME) were comparable between the two models, and CMAQ performed better in terms of correlation coefficients overall. The higher O₃ bias in CMAQ prediction was, to a significant extent, due to the over-prediction of night-time minimum concentration, but may also be contributed at least in part from the default CMAQ profiles used for lateral boundary condition (see Appel *et al.*, 2007). It should be noted that the version of the AURAMS code used in this study was with the zero-gradient lateral boundary condition, which may have also impacted the O₃ prediction in particular (see discussion in 5.4.3.3 above).

Table 5.16 Speciated PM_{2.5} (sulphate, nitrate, ammonium, and organic components) evaluation statistics from the NRC AURAMS-CMAQ comparative evaluation for July 2002.

	SO ₄		NO ₃		NH ₄		TOA	
	AURAMS	CMAQ	AURAMS	CMAQ	AURAMS	CMAQ	AURAMS	CMAQ
Modelled mean (ppb, µg m⁻³)	5.31	2.44	2.00	0.263	1.64	0.821	3.92	0.928
Observed Mean (ppb, µg m⁻³)	5.03	5.03	0.902	0.902	1.63	1.63	10.56	10.56
MB (ppb, µg m⁻³)	0.29	-2.59	1.09	-0.64	0.009	-0.811	-6.64	-9.64
NMB (%)	5.72	-51.51	121.2	-70.87	0.58	-49.68	-62.85	-91.22
ME (ppb, µg m⁻³)	3.03	2.83	1.58	0.71	0.885	0.929	6.93	9.64
NME (%)	60.34	56.26	174.7	79.00	54.20	56.90	65.64	91.25
r²	0.367	0.524	0.397	0.437	0.428	0.458	0.0005	0.0066

The evaluation statistics for speciated PM_{2.5} are presented in Table 5.16. The 24-hour average data from NAPS and STN networks were used for the evaluation. Again, AURAMS performed well for sulphate_{2.5} and ammonium_{2.5} in terms of bias, but significantly over-predicted nitrate_{2.5}. CMAQ, on the other hand, predicted much lower inorganic ions. Both models under-predicted TOA_{2.5}, with AURAMS somewhat closer to the observations which mainly resulted

from the use of the updated SOA parameterization in AURAMS as discussed earlier in 5.4.3.3. In addition, AURAMS and CMAQ predicted very different sea salt component (not shown) in that AURAMS predicted much higher sea salt concentrations which had significant impact on PM_{2.5} even over land (mostly coastal areas). This confirms the finding from the sensitivity test discussed above in 5.4.3.3. The comparative evaluation study reinforced the need for further investigations in several science components, e.g., SOA formation, inorganic heterogeneous chemistry, and sea salt generation.

5.4.5 Dynamic Evaluation

The so-called dynamic evaluation is a more recent concept in model evaluation. It is focused on the evaluation of a model's ability to simulate the responses in ambient concentration to the changes in either meteorological conditions or emissions (Gilliland *et al.*, 2007; Seigneur 2007). It may be most relevant to establishing model's confidence for policy relevant applications. It is also more, if not the most, challenging evaluation to pursue in reality because it requires that the changes in meteorology or emission be clearly qualified (and, most desirably, isolated) and the responses due to these changes be clearly discerned from the observations.

A feasible test of dynamic evaluation may be to look at the comparison between modelled and observed "day-of-the week" (or weekdays versus weekends) variability in ambient concentrations (Seigneur, 2007). One such example can be found in Yarwood *et al.* (2003), where modelled sensitivity to the weekday versus weekend change in motor vehicle emission over the Los Angeles area was compared to the observed weekday versus weekend change in daily O₃ maximum. The model (CAMx: Environ Intl. Co., 2002) was found to simulate the observed weekday versus weekend changes in O₃ quite well.

Another unique candidate for model dynamic evaluation is the case of the implementation of the U.S. EPA NO_x Budget Trading Program (NBP) in recent years. Since 2003 (and particularly between 2003 and 2004), significant reductions in NO_x emission (during O₃ season), mostly from large power generation facilities, have occurred over eastern U.S. in response to the U.S. NO_x SIP (State Implementation Plan, <http://www.epa.gov/>) Call requirement. The reduction is evident based on satellite-retrieved summertime NO₂ columns (Kim *et al.*, 2006). The progress of NBP has been closely monitored in terms of emission reductions and environmental response. Gégó *et al.* (2007) showed that the meteorologically adjusted O₃ concentration in eastern U.S. is about 13% lower than prior to the NO_x SIP Call. Several dynamic evaluation studies have been conducted based on this case (e.g., Gilliland *et al.*, 2008, Hogrefe *et al.*, 2008). Gilliland *et al.* (2008) conducted CMAQ simulations of three summers (June, July, and August) for 2002 (pre-NO_x SIP Call), 2004, and 2005 (both post-NO_x SIP Call) with the appropriate emission change, and showed that the model underestimated the changes in maximum daily 8-hour O₃ compared to the observations (by about one-third to a

half). The underestimation was particularly significant farther downwind from the Ohio Valley, or the model-predicted changes in O₃ due to the emission change did not extend as far downwind from the source region as indicated from the observations. Hogrefe *et al.* (2008) also looked into model predicted changes in O₃ design value in response to the NO_x SIP Call reductions with the observed changes, and found that, while they agreed well in terms of spatially-averaged magnitude, the model-predicted and observed changes in O₃ design values can differ substantially at individual sites.

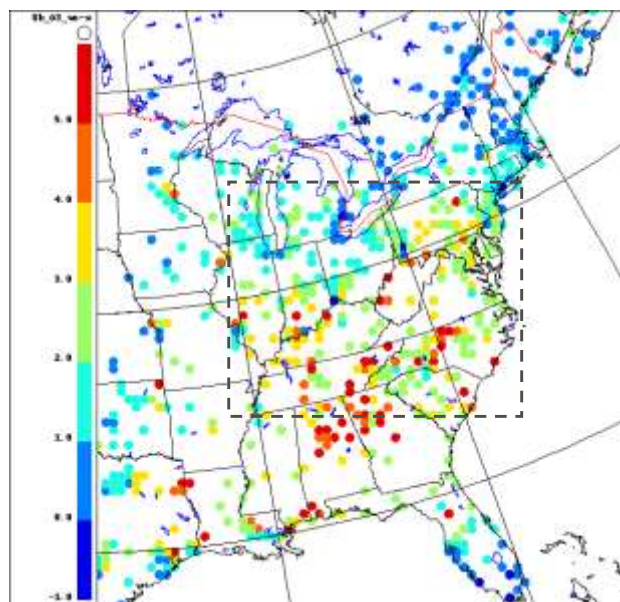


Figure 5.29 The difference (ppbv) in modelled daily maximum 8-hour ozone concentrations averaged over the ICARTT period between the base case (i.e., without the NO_x emission adjustment) and the sensitivity run (i.e., with the emission adjustment). Positive values correspond to a decrease in ozone concentration due to the adjustment to NO_x emission. A statistical comparison with observation was done over the boxed area.

For a simple test, AURAMS sensitivity runs with and without the U.S. SIP Call NO_x control were conducted for the ICARTT period. The base emission inventories were Canadian 2000 and U.S. 2001. To account for the NO_x SIP Call reduction in NO_x emissions, simple state-specific adjustment ratios, based on the U.S. EPA published season NO_x emissions for 2000 and 2005 state trading budgets (U.S. EPA, 2007b), were applied to the base NO_x emissions from major point sources. In addition to the adjustment to the NBP states major point source emissions, adjustments to account for the change in NO_x emissions from EGU for the non-NBP states between 2004 and 2001 (Pouliot, 2005) were also included in the sensitivity run. Figure 5.29 shows the difference in modelled daily maximum 8-hour O₃ concentrations averaged over the ICARTT period between the two cases. Greater than 5 ppbv of decrease in averaged daily 8-hour maximum O₃ concentrations is found along the Ohio River Valley and over areas in Alabama, Tennessee, and North Carolina, where most of the large power plants

affected by the NBP are located. This can be qualitatively compared to observed change in seasonal 8-hour O₃ between 2002 and 2005 reported by U.S. EPA (Figure 14 in U.S. EPA, 2006) after meteorological adjustment. In comparison, the modelled changes in percentage are in general smaller than the observations. However there is a resemblance between the model and the observation in terms of spatial distribution of the reductions in O₃ due to the implementation of the U.S. US SIP Call reductions in NO_x emissions. The fact that the 2004 summer meteorology was used in the model simulations may have an impact on the model-predicted response. As mentioned earlier in 5.4.1.2, the 2004 summer was unusually cool and wet. In contrast the 2002 and 2005 summers were comparable and were relatively warm and dry compared to the climatology for the decade of 1996 – 2005. A comparison was made between the three-year average of May-to-September daily 8-hour maximum O₃ for 2000 – 2002 and 2003 – 2005, prior and post the implementation of the U.S. SIP Call NO_x emission reductions in 2003 that there was on average of 6% reduction in the O₃ season 8-hour maximum O₃ over the area affected by the NO_x Trading Budget Program, after the adjustment for meteorology. In comparison, an average of about 5% reduction over a similar area (indicated in Figure 5.29) was predicted by the model due to the NO_x emission reduction under US EPA NBP.

5.5 Uncertainties

Uncertainties in CTM predictions can arise from many sources, including model emission (inventory data and emission processing for both anthropogenic and biogenic), model meteorology (particularly boundary layer and cloud microphysics parameters), initial and boundary conditions, model science and process parameterization, and model numerics. The diagnostic evaluation above (section 5.4.3) explored many of these sources of uncertainties. To systematically address the model uncertainty issue is a considerable undertaking. The methodology and strategy depend on the objectives and are still being developed. Error propagation and formal sensitivity analysis may be more readily performed with existing techniques, such as “Decoupled Direct Method” (e.g., Napelenok *et al.*, 2006) with regard to input parameters, but the uncertainties arising from process representations are not as easily assessed in a systematic manner. The intention here is to synthesize the information on model uncertainties based on the collection of existing model diagnostic/process evaluation and sensitivity studies and to provide an overall assessment of model uncertainty or confidence levels, an update from the previous assessment.

Seigneur and Moran (2004) made a qualitative assessment of model confidence levels in various aspects of PM CTM simulations at the time. They used four broad degrees, “very low”, “low”, “medium”, and “high”, to scale the confidence levels. The levels of confidence in many aspects have not changed significantly since. For example, our confidence in simulating/predicting ambient O₃ does not seem to have improved. There is an overall positive bias from all models particularly over summertime O₃ season. Models tend to predict daily

maximum (1-hr or 8-hr) better than daily mean. Hogrefe *et al.* (2007b) examined over ten separate CTM simulations of summer O₃ season between 1993-2005 conducted over the past decade and found that, although there was improvement in model confidence from the earlier simulations (measured in terms of RMSE), the recent simulations seemed to have reached a plateau of about 15 ppbv in RMSE (based on both temporal and spatial analysis of simulated and observed daily maximum 8-hour O₃). The evaluations included in this assessment also indicate a similar magnitude of RMSE from the various model simulations. As for PM_{2.5}, the model confidence level was assessed to be medium by Seigneur and Moran (2004) which is the same confidence level as for O₃. This also remains to be the case based on this assessment: the evaluation statistics are similar between model predicted O₃ and PM_{2.5} (in terms of mean error, correlation coefficient, and RMSE, for example; see 5.4.1). This being said, we know that our understanding of precursor sources and processes affecting atmospheric PM is generally poorer than those affecting O₃. The fact that evaluation statistics indicate similar skill level in predicting O₃ and PM_{2.5} may mean more compensating errors in the modelling of PM. Concerning the composition of PM_{2.5}, sulphate remains the best predicted component amongst others. The confidence level however, particularly at shorter time scales, is affected by the uncertainties from secondary processes, e.g., in-cloud production and wet removal, which are highly dictated by the meteorological model's ability to predict cloud and precipitation reliably. Based on recent evaluations our confidence in predicting particle nitrate is not high: models tend to over-predict in summer and under-predict in winter, partly due to the uncertainties in HNO₃ prediction but mostly due to the uncertainties in gas-particle partition. Ammonium is mostly driven by sulphate and to a lesser degree by nitrate but, due to the recent improvement in NH₃ emission one can expect better level of confidence in modelled PM_{2.5}-NH₄. Organic component continues to be one of the components with low level of model confidence. Uncertainties in primary organic particle emission are still high, and there are still large uncertainties in SOA formation mechanism. Sea salt can be an important component of PM_{2.5} over coastal area but our level of confidence in modelling sea salt is largely limited by the significant uncertainty in parameterization of the source functions. It should also be mentioned that there are significant uncertainties in model versus measurement comparisons (i.e., what is modelled and what is measured) for some of the particulate matter components, such as nitrate and organics (due to their semi-volatile nature and measurement techniques; see Chapter 3 for more discussion on measurement), which can have important implication for model evaluation.

The most significant change from previous assessment in level of confidence in CTM simulations may be in terms of the simulations for longer time scales and at larger spatial scales. Previously our levels of confidence in CTM simulations at continental and annual or seasonal scales were limited at least partly by computational considerations. With increased computing power and improved computational efficiency, CTM simulations at both continental and longer time (annual, seasonal) scales are considerably more feasible now. Issues such as being able to handle all seasons correctly are still valid, however. Existing evaluations of long-term CTM simulations (e.g., Eder and Yu, 2006; Moran *et al.*, 2010)

demonstrated better performance statistics for longer time averages (annual, seasonal, monthly) than for shorter time scales (e.g., daily, hourly). Hogrefe *et al.* (2007b) showed that temporally regional CTMs seem to perform best in capturing signals on time scale of about a week, while spatially CTMs are better able to capture the larger-scale concentrations patterns than localized features.

Model confidence (or uncertainty) level in terms of predicting the targeted pollutants may not translate to the level of confidence (or uncertainty) in predicting the changes in response to changes in emission (e.g., Jones *et al.*, 2005; Hogrefe *et al.*, 2008). An encouraging finding from these studies, where model predictions were compared from multiple models (and configurations) of response to emission change, is that despite the large difference in performance amongst models for base case, only relatively minor differences were found in the relative response of O₃ concentrations to emission reductions. On the other hand, this also argues that for regulatory applications emphasis be shifted from operational evaluation to diagnostic and dynamic evaluations, so as to ensure that precursor-ambient concentration relationships are being correctly represented by the CTMs.

5.6 Summary and Conclusions

The main advancements in regional CTM development over the past decade have been in the representation of atmospheric aerosols and the relevant processes. The three CTMs used in this assessment, AURAMS, CHRONOS, and CMAQ, are amongst current state-of-science models capable of simulating atmospheric oxidants and PM. AURAMS and CMAQ, in particular, share a similar level of complexity in the science components involving atmospheric aerosols. Nevertheless, the two models do differ in the characterization of PM chemical composition and particularly size distribution (e.g., sectional vs. modal) and in the individual parameterizations and algorithms, such as chemistry mechanics or SOA formation algorithm. They also differ in model configurations.

Extensive evaluations of the three models have been conducted in recent years based on different model simulations, ranging from longer term (annual) over continental scale to shorter term, episodic regional and local scales. Of the simulations included in this chapter, the AURAMS annual simulation of 2002 is the base-case for a number of scenario applications to be discussed in the following chapter; as well the three CMAQ simulations over LFV and Alberta are the base-cases for some of the regional scenario simulations. The retrospective AURAMS simulations for the two recent field campaigns (ICARTT 2004 and PrAIRie2005) are primarily focused on diagnostic evaluation and sensitivity studies. Since the simulations are for different periods over several years (2001, 2002, 2004, and 2005) over different regions (and with different models), the individual evaluations are not directly comparable between each other. For example over eastern North America, summers of 2002 and 2004 represent two extremes, both in meteorological conditions and in observed O₃ levels, for the 1996-2005

decade, and model performance can be quite different under these different conditions. However, collectively these individual evaluations provide an overall range of model performance variability.

On an annual time scale, the AURAMS predicted O_3 and $PM_{2.5}$ correlate well with observations geographically for 2002. Annually $PM_{2.5}$ is under-predicted, mainly contributed by the under-prediction of $TOM_{2.5}$. O_3 is over-predicted during summer (3rd quarter) mostly over the eastern NA. At shorter time scales, the models tends to have better skill in predicting maximum O_3 (daily 1-hr or 8-hr) than for daily means, mostly due to the overprediction of night-time minimum O_3 concentrations. Concerning model prediction of speciated $PM_{2.5}$, annually sulphate has the highest correlation with observations; correlations are also good for nitrate and ammonium. Sulphate is significantly under-predicted during cold months; nitrate is over-predicted over summer months (3rd quarter) but under-predicted for other quarters. Regionally, sulphate tends to be over-predicted over the source region in the east (e.g., Ohio River Valley) but under-predicted farther downwind of the sources. The model simulation of elemental carbon and organic matter components are poor; crustal material is overpredicted mainly due to poor representation of the emissions.

The model (AURAMS) is shown to be able to predict inorganic precursors well, such as NO_2 and SO_2 , comparing to monitoring data and aircraft measurement at regional scale. The model's performance in predicting these precursors is largely tied to the quality and the processing of emission inventory data. HNO_3 as precursor to $PM_{2.5}$ nitrate is predicted well annually (for 2002) in terms of mean and correlation. There is however an over-prediction during summer (3rd quarter) which coincides with the $PM_{2.5}$ -nitrate over-prediction over the same time period, linking the particle nitrates over-prediction to the over-prediction of HNO_3 . However this does not seem to be the case for the ICARTT simulation where $PM_{2.5}$ -nitrate is over-predicted but HNO_3 is not, indicating possible partitioning problem.

Comparison of modelled VOC with observations shows that the total OH-reactivity is under-predicted by AURAMS over most of the urban sites and over-predicted over rural sites particularly over the eastern part of the country. Individually, ALKE is under-predicted over all sites, while isoprene is over-predicted over most of the sites particularly in the east. There is some compensation between the ALKE under-prediction and the isoprene over-prediction. However the impact of the discrepancies between model and observation in the total and individual VOC reactivity on modelled O_3 and $PM_{2.5}$ (via secondary organic aerosols) needs to be further investigated.

Diagnosis of model processes and sensitivities shows several important sources contributing to the overall model uncertainty, including biogenic emission processing, parameterizations of the boundary layer and vertical diffusion, modelled cloud and subsequent in-cloud oxidation,

algorithms for SOA formation, parameterization for sea salt generation, model resolution and IC/BC. All these need further investigation and improvement in order to improve on the model overall performance.

While a less constrained model intercomparison can provide a good assessment of model uncertainty, a more controlled model intercomparison is more useful for diagnosing uncertainties related to model processes only. One such comparative evaluation of AURAMS and CMAQ shows that while AURAMS performed better in bias scores, CMAQ performed better in correlation coefficients. The predictions for inorganic ions from the two models are quite different, with CMAQ under-predicting all inorganic ions while AURAMS over-predicting nitrate. Both models significantly under-predicted SOA. The differences in model performance can be linked to the differences between the two models in the parameterization of several processes, e.g., heterogeneous chemistry, SOA formation, sea salt generation.

To conduct a dynamic evaluation is to evaluate model response to changes in either meteorology or emissions, and is particularly relevant to applying CTMs to support emission control strategy development. The recent U.S. EPA NO_x budget Trading Program provided a unique case for such an evaluation. Based on a dynamic evaluation of this case using CMAQ (Gilliland *et al.*, 2008) and a simple sensitivity analysis using AURAMS (this assessment), it is indicated that while the models are able to reproduce the observed trend, the magnitude of the changes may be under-predicted by the model particularly farther downwind from the source region. Bearing in mind that difficulties arise in defining such an evaluation, both from resolving changes in emissions and meteorology, and discerning clear response to the changes from observations, dynamic evaluation itself is subject to a significant level of uncertainty.

Our overall confidence level in modelling smog has not changed significantly since the last assessment (Seigneur and Moran, 2004), particularly with regard to O₃ measured by model performance. There is a significant (positive) bias in predicted O₃ at regional scale particularly over eastern North America from most current CTMs, which is at least in part due to uncertainties in lateral and upper boundary conditions. Our understanding and model representation of PM_{2.5} related processes have progressed but our confidence level in modelling PM_{2.5} is still medium. In general, we are better in modelling longer time averages (e.g., annual) than modelling the variations on shorter time scales (e.g., daily, hourly), and we are more confident in modelling summer time than winter time. With regard to PM_{2.5} components, comparatively, current models tend to do better in predicting inorganic ions (particularly sulphate) than organic matter due to the complexity and the lack of understanding of the sources, characteristics, and processes of the various organic compounds involved. Particulate nitrate, a minor contributor to total PM in summer but a significant component in winter, is poorly predicted by current CTMs. Our confidence level in modelling black carbon and crustal materials (dust) at regional scale is also low, mainly due to poor representation of the sources in current CTMs. It is also important to assess our confidence in predicting the changes in smog components in response to changes in emissions, particularly for regulatory

policy applications. Based on limited studies, there is an indication that, for certain pollutants (O_3 , for example) and under certain circumstances, our confidence in predicting concentration change in response to emission change may be higher than predicting concentration itself. However, this needs to be systematically assessed by carefully designed diagnostic and dynamic evaluations.

5.7 Recommendations for Future Research

The current uncertainties can be improved through better representations of a number of processes:

Planetary boundary layer and vertical mixing are particularly important in urban and source regions. Deficiencies in representing nighttime vertical mixing in the PBL may be one of the main contributors to the model's inability to represent night-time O_3 values accurately.

The processing and representation of anthropogenic emissions remains a major source of uncertainties for air quality model predictions. There is a large uncertainty in generating spatially, temporally, and chemically segregated emission input for air quality models from inventory data, and continued improvement on emissions processing and modelling is needed. Within the air quality models, there is also a need to improve the representation of sub-grid scale plumes from point sources, which has a significant impact on model performance in source regions.

- Biogenic VOC emissions play an important role in atmospheric oxidant and SOA formation and need to be better resolved.
- Inorganic heterogeneous chemistry needs to be further examined in order to improve model predictions of PM nitrate which is poorly predicted currently.
- SOA can contribute to a significant portion of the total $PM_{2.5}$ mass, but its formation mechanisms are not currently well understood and its parameterization in CTMs needs to be improved. Improvement in POA and BC emissions inventories are needed, as well as a wintertime speciated PM evaluation study.
- In-cloud process and scavenging have a significant degree of uncertainty related in part to the uncertainties in modelled cloud and precipitation. Additional processes for cold season (e.g., mixed-phase and ice clouds) need to be better represented in models. There is experimental evidence that cloud may play a role in SOA formation.
- The uncertainty in model prediction of sea salt is substantial due to the uncertainty in source functions used in current regional models.

- Feedback between air quality and meteorology is emerging from recent studies as being a factor affecting the performance of both meteorological and air quality models.
- Integrated modelling and coupling to exposure model;

Diagnostic and dynamic evaluations are critical to modelling: the former ensures that the model simulates the atmospheric processes correctly so that the model predicted changes in response to the changes in future meteorology and/or emission are credible, while the latter is a direct check on model's ability in reproducing the observed responses. Model evaluations using spatial and temporal analysis are useful in shedding light on the strengths and weaknesses of modelled processes. However, further development in diagnostic and dynamic evaluation methodologies is needed.

As discussed, model evaluation depends critically on the availability of appropriate observational data. Although the existing monitoring networks (such as those described in Chapter 3) provide reasonably good spatial and temporal resolution for O₃ and bulk PM_{2.5} observations particularly in populated areas of North America, the routinely available PM speciation data are relatively few in number of sites and are mostly from filter-based measurements with relatively poor temporal resolution. The availability of continuous and semi-continuous PM composition measurements from some of the existing monitoring networks would be valuable for model evaluation and development as well as advances in our understanding of the processes. As also demonstrated in Chapter 7 additional insights can be gained from more time-resolved PM composition information. There is also a lack of observational data for evaluating modelled wet and dry removal (particularly for diagnostic evaluation). Specially designed network observations may be required for specific diagnostic and dynamic evaluations. There is a continuing need for both the monitoring and the field study activities to occur in closer coordination to insure that our understanding and capabilities advance as efficiently as possible.

Methodologies to systematically assess air quality model uncertainties still need further development. Probabilistic modelling approaches may better address model uncertainties for both forecasting and policy applications and should be further explored.

Data assimilation and inverse modelling is an area of active research recently in air quality modelling community. While data assimilation is seen as an effective tool for improvement in model forecast, inverse modelling is being increasingly used to improve emission estimates (in particular "top-down" estimate from satellite observations, see Chapter 8 for more discussion) and in air quality management related applications.

References

- Appel, K.W., Gilliland, A.B., Sarwar, G., Gilliam, R.C., 2007. Evaluation of the Community Multiscale Air Quality (CMAQ) model version 4.5: Sensitivities impacting model performance: Part I—Ozone. *Atmospheric Environment*, 41, 9603-9615
- Arellano, A. F., Kasibhatla, P.S., Giglio, L., van der Werf, G.R., Randerson, J.T., 2004, Top-down estimates of global CO sources using MOPITT measurements, *Geophysical Research Letters*, 31, L01104, doi:10.1029/2003GL018609.
- Arnold, J.R., Dennis, R.L., 2001. First results from operational testing of the U.S. EPA Models-3/Community Multiscale Model for Air Quality (CMAQ). In: Gryning, S.-E., Schiermeier, F.A. (Eds.), *Air Pollution Modelling and its Application XIV*. Kluwer Academic/Plenum Publishers, New York, NY, pp. 651–658.
- Atmospheric Science Data Center, 2004.
- http://eosweb.larc.nasa.gov/GUIDE/dataset_documents/narsto_pac2001_gvrd_capmon_air_qual_data.html
- Baklanov, A., Hänninen, O., Slørdal, L. H., Kukkonen, J., Bjergene, N., Fay, B., Finardi, S., Hoe, S. C., Jantunen, M., Karppinen, A., Rasmussen, A., Skouloudis, A., Sokhi, R. S., Sørensen, J. H., Ødegaard, V., 2007. Integrated systems for forecasting urban meteorology, air pollution and population exposure. *Atmospheric Chemistry and Physics*, 7, 855-874
- Bey, I., Jacob, D.J., Yantosca, R.M., Logan, J.A., Field, B.D., Fiore, A.M., Li, Q., Liu, H.Y., Mickley, L.J., Schultz, M.G., 2001. Global modelling of tropospheric chemistry with assimilated meteorology: model description and evaluation. *Journal of Geophysical Research* 106, 23073–23096.
- Binkowski, F.S., Shankar, U., 1995, The Regional Particulate Matter Model: Part 1. Model description and preliminary results. *Journal of Geophysical Research*, 100, 26191-26209
- Binkowski, F.S., Roselle, S.J., 2003. Models-3 community multiscale air quality (CMAQ) model aerosol component: 1. Model description. *Journal of Geophysical Research*, 108, 4183, doi:10.1029/2001JD001409.
- Blond, N., Bel, L., Vautard, R., 2003. Three-dimensional ozone data analysis with an air quality model over the Paris area. *Journal of Geophysical Research*, 108, 4744, doi:10.1029/2003JD003679.

Brost, R.A., 1988. The sensitivity to input parameters of atmospheric concentrations simulated by a regional chemical model. *Journal of Geophysical Research*, 93, 2371-2387

Byun, D.W., 1999a. Dynamically consistent formulations in meteorological and air quality models for multiscale atmospheric studies. Part I: Governing equations in a generalized coordinate system. *Journal of Atmospheric Science*, 56, 3789-3807.

Byun, D.W., 1999b. Dynamically consistent formulations in meteorological and air quality models for multiscale atmospheric issues. Part II: Mass conservation issues. *Journal of Atmospheric Science*, 56, 3808-3820.

Byun, D.W., Ching, J.K.S., 1999. Science algorithms of the EPA Models-3 Community Multiscale Air Quality (CMAQ) modelling system. U.S. EPA Report EPA/600/R-99/030

Byun, D., Schere, K.L., 2006. Review of the governing equations, computational algorithms, and other components of the Models-3 Community Multiscale Air Quality (CMAQ) modelling system. *Applied Mechanics Reviews*, 59 (1-6), 51-76.

Canada-U.S. Subcommittee on Scientific Cooperation, 2004. Transboundary PM Science Assessment, available at <http://www.msc-smc.ec.gc.ca/saib>.

Carmichael, G.R., Tang, Y., Kurata, G., Uno, I., Streets, D., Woo, J.-H., Huang, H., Yienger, J., Lefer, B., Shetter, R., Blake, D., Atlas, E., Fried, A., Apel, E., Eisele, F.,

Cantrell, C., Avery, M., Barrick, J., Sachse, G., Brune, W., Sandholm, S., Kondo, Y., Singh, S., Talbot, R., Bandy, A., Thornton, D., Clarke, A., Heikes, B., 2003. Regional-scale chemical transport modelling in support of the analysis of observations obtained during the TRACE-P experiment, *Journal of Geophysical Research - Atmospheres*, 108, 8823, doi:10.1029/2002JD003117.

Carter, W. P.L., 2000a, Documentation of the SAPRC-99 chemical mechanism for VOC reactivity assessment, Volume 1 of 2, Final Report to California Air Resources Board Contract 92-329 and Contract 95-308, 00-AP-RT17-001-FR.

Carter, W. P.L., 2000b, Implementation of the SAPRC-99 chemical mechanism into the Models-3 framework, Report to the United States Environmental Protection Agency pp. 101

CEMPD, 2007. Center for Environmental Modelling for Policy Development SMOKE website, University of North Carolina at Chapel Hill, <http://www.smoke-model.org/index.cfm>.

Chai, T., Carmichael, G.R., Tang, Y., Sandu, A., Hardesty, M., Pilewskie, P., Whitlow, S.,

- Browell, E.V., Avery, M.A., Nedelec, P., Merrill, J.T., Thompson, A.M., Williams, E., 2007. Four-dimensional data assimilation experiments with international consortium for atmospheric research on transport and transformation ozone measurements. *Journal of Geophysical Research*, 112, D12S15
- Chang, J.S., Brost, R.A., Isaksen, I.S.A., Madronich, S., Middleton, P., Stockwell, W.R., Walcek, C.J., 1987. A three-dimensional Eulerian acid deposition model: Physical concepts and formation. *Journal of Geophysical Research*, 92, 14681-14700.
- Chen, J., Mao, H., Talbot, R.W., Griffin, R.J., 2006, Application of the CACM and MPMPO modules using the CMAQ model for the eastern United States, *Journal of Geophysical Research*, 111, D23S25, doi:10.1029/2006JD007603.
- Cho, S., Makar, P.A., Lee, W.S., Herage, T., Liggio, J., Li, S.-M., Wiens, B., Graham, L. 2009. Evaluation of A Unified Regional Air-quality Modelling System (AURAMS) using PrAIRie2005 field study data: The effects of emissions data accuracy on particle sulphate predictions. *Atmospheric Environment*, 43, 1864-1877.
- Chung, S. H., Seinfeld, J.H., 2002. Global distribution and climate forcing of carbonaceous aerosols. *Journal of Geophysical Research D: Atmospheres*, 107, 14-1-14-33.
- Clerbaux, C., Hadji-Lazaro, J., Hauglustaine, D., Megie, G., 2001. Assimilation of carbon monoxide measured from satellite in a three-dimensional chemistry-transport model. *Journal of Geophysical Research*, 106, 15385-15394.
- Colella, P., Woodward, P.R., 1984. The piecewise parabolic method (PPM) for gas-dynamical simulations. *Journal of Computational Physics*, 54, 174-201.
- Côté, J., Desmarais, J.-G., Gravel, S., Méthot, A., Patoine, A., Roch, M., Staniforth, A., 1998a. The operational CMC/MRB Global Environmental Multiscale (GEM) model. Part 1: Design considerations and formulation. *Monthly Weather Review*, 126, 1373-1395.
- Côté, J., Desmarais, J.-G., Gravel, S., Méthot, A., Patoine, A., Roch, M., Staniforth, A., 1998b. The operational CMC-MRB Global Environment Multiscale (GEM) model. Part II: Results. *Monthly Weather Review*, 126, 1397-1418.
- Cuvelier, C., Thunis, P., Vautard, R., Amann, M., Bessagnet, B., Bedogni, M., Berkowicz, R., Brandt, J., Brocheton, F., Builtjes, P., Carnavale, C., Coppalle, A., Denby, B., Douros, J., Graf, A., Hellmuth, O., Hodzic, A., Honore, C., Jonson, J., Kerschbaumer, A., de Leeuw, F., Minguzzi, E., Moussiopoulos, N., Pertot, C., Peuch, V.H., Pirovano, G., Rouil, L., Sauter, F., Schaap, M., Stern, R., Tarrason, L., Vignati, E., Volta, M., White, L., Wind, P., Zuber, A., 2007.

CityDelta: A model intercomparison study to explore the impact of emission reductions in European cities in 2010. *Atmospheric Environment*, 41, 189-207.

Daley, R., 1991. *Atmospheric Data Analysis*. Cambridge University Press, New York, 1991, 457 pp.

Davidson, P., Schere, K., Draxler, R., Kondragunta, S., Wayland, R.A., Meagher, J.F., Mathur, R., 2007. Toward a U.S. national air quality forecast capability: current and planned capabilities, in 'Air pollution modelling and its application XIX', edit. C. Borrego and A.I. Miranda, Kluwer Academic/Plenium Publishers.

Dégardin, 2007, Intercomparaison de trois modèles Canadiens de qualité de l'air à l'échelle régionale, Master's Thesis, Université du Québec à Montréal

De Leeuw, G., Neele, F.P., Hill, M., Smith, M.H., Vignatti, E., 2000. Production of sea spray aerosol in the surf zone. *Journal of Geophysical Research*, 105, 29397-29409.

Dudhia, J., Gill, D., Manning, K., Wang, W., Bruyere, C., 2004. PSU/NCAR Mesoscale Modelling System Tutorial Class Notes and User's Guide: MM5 Modelling System Version 3, Mesoscale and Microscale Meteorology Division, National Center for Atmospheric Research, U.S., January 2004. <http://www.mmm.ucar.edu/mm5/mm5-home.html>, Accessed: November 24, 2004.

Eder, B., Yu, S., 2006. A performance evaluation of the 2004 release of Models-3 CMAQ. *Atmospheric Environment*, 40, 4811-4824

Eder, B., Kang, D., Mathur, R., Yu, S., Schere, K., 2006. An operational evaluation of the Eta-CMAQ air quality forecast model. *Atmospheric Environment*, 40, 4894-4905

Elbern, H., Schmidt, H., 2001. Ozone episode analysis by four-dimensional variational chemistry data assimilation. *Journal of Geophysical Research*, 106, 3569-3590

Environ International Corp. 2002. User's Guide, Comprehensive Air Quality Model with Extensions (CAMx) Version 3.10; Available at: <http://www.camx.com> (accessed June 2003).

Environment Canada, 2005. 2004 Canadian acid deposition science assessment, Environment Canada, pp. 440

Fehsenfeld, F.C., Ancellet, G., Bates, T., Goldstein, A., Hardesty, M., Honrath, R., Law, K., Lewis, A., Leitch, R., McKeen, S., Meagher, J., Parrish, D.D., Pszenny, A., Russell, P., Schlager, H., Seinfeld, J., Trainer, M., Talbot R., 2006. International Consortium for Atmospheric Research on Transport and Transformation (ICARTT): North America to Europe:

Overview of the 2004 summer field study. *Journal of Geophysical Research*, 111, D23S01, doi:10.1029/2006JD007829.

Fox, D., Kellerhals, M., 2007, Modelling of ozone levels in Alberta: base case, sectoral contributions and a future scenario, Environment Canada Internal Report, 83pp. Available from Air Quality Science Unit, Prairie and Northern Region, Environment Canada.

Frost, G.J., McKeen, S.A., Trainer, M., Ryerson, T.B., Neuman, J.A.,

Roberts, J.M., Swanson, A. Holloway, J.S., Sueper, D.T., Fortin, T., Parrish, D.D., Fehsenfeld, F.C., Flocke, F., Peckham, S.E., Grell, G.A., Kowal, D., Cartwright, J., Auerbach, A., Habermann, T., 2006. Effects of changing power plant NO_x emissions on ozone in the eastern United States : Proof of concept. *Journal of Geophysical Research*, 111, D12306, doi:10.1029/2005JD006354.

Gaydos, T.M., Pinder, R., Koo, B., Fahey, K.M., Yarwood, G., Pandis, S.N., 2007. Development and application of a three-dimensional aerosol chemical transport model, PMCAMx. *Atmospheric Environment*, 41, 2594-2611.

Gégo, E., Porter, P.S., Gilliland, A., Rao, S.T., 2007. Observation-based assessment of the impact of nitrogen oxides emissions reductions on ozone air quality over the eastern United States. *Journal of Applied Meteorology and Climatology*, 46, 994–1008

Gery, M.W., Whitten, G.Z., Killus, J.P., Dodge, M.C., 1989. A photochemical kinetics mechanism for urban and regional scale computer modelling. *Journal of Geophysical Research*, 94, 12925–12956.

Gilliland, A.B., Godowitch, J.M., Hogrefe, C., Rao, S.T., 2007, Evaluating regional-scale air quality models, in 'Air pollution modelling and its application XIX', Eds. C. Borrego and A.I. Miranda, Kluwer Academic/Plenium Publishers.

Gilliland, A.B., Hogrefe, C., Pinder, R.W., Godowitch, J.M., Foley, K.L., Rao, S.T., 2008. Dynamic evaluation of regional air quality models: Assessing changes in O₃ stemming from changes in emissions and meteorology. *Atmospheric Environment*, 42, 5110-5123

Gong, S. L., Barrie, L.A., Blanchet, J.-P., 1997a. Modelling sea-salt aerosols in the atmosphere 1. Model development. *Journal of Geophysical Research*, 102, 3805–3818

Gong, S. L., Barrie, L.A., Prospero, J.M., Savoie, D.L., Ayers, G.P., Blanchet, J.-P., Spacek, L., 1997b. Modelling sea-salt aerosols in the atmosphere 2. Atmospheric concentrations and fluxes. *Journal of Geophysical Research*, 102, 3819–3830.

Gong, S.L., Barrie, L.A., Blanchet, J.-P., Salzen, K.v., Lohmann, U., Lesins, G., Spacek, L., Zhang, L.M., Girard, E., Lin, H., Leaitch, R., Leighton, H., Chylek, P., Huang, P., 2003. CAM: A Size Segregated Simulation of Atmospheric Aerosol Processes for Climate and Air Quality Models 1. Module Development. *Journal of Geophysical Research*, 108, 4007, doi: 10.1029/2001JD002002.

Gong, S.L., 2003. A parameterization of sea-salt aerosol source function for sub- and super-micron particles. *Global Biogeochemical Cycles*, 17, 1097, doi:10.1029/2003GB002079.

Gong, W., 2002. "Modelling cloud chemistry in a regional aerosol model: bulk vs. size resolved representation", in 'Air pollution modelling and its application XV', edit. C. Borrego and G. Schayes, pp285-293, Kluwer Academic/Plenium Publishers.

Gong W, Dastoor A.P., Bouchet V.S., Gong S., Makar P.A., Moran, M.D., Pabla B., Ménard S., Crevier L.-P., Cousineau S., Venkatesh S., 2006. Cloud processing of gases and aerosols in a regional air quality model (AURAMS). *Atmospheric Research*, 82, 248-275

Gong, W., Zhang, J., Moran, M.D., Makar, P.A., Gong, S.L., Stroud, C., Bouchet, V.S., Cousineau, S., Ménard, S., Samaali, M., Sassi, M., Pabla, B., Leaitch, R., Macdonald, A.M., Anlauf, K., Hayden, K. Toom-Sauntry, D., Leithead, A., Strapp, J.W., 2007. Modelling regional aerosols: impact of cloud processing on gases and particles over eastern North America and in its outflow during ICARTT 2004, in 'Air Pollution Modelling and Its Application XIX', Eds. Corrego and A.I. Miranda, Springer, Dordrecht, 539-547.

Grell, G.A., Peckham, S.E., Schmitz, R., McKeen, S.A., Frost, G., Skamarock, W.C., Eder, B., 2005. Fully coupled "online" chemistry within the WRF model. *Atmospheric Environment*, 39, 6957-6975.

Griffin, R. J., Nguyen, K. Dabdub, D., Seinfeld, J.H., 2003. A coupled hydrophobic-hydrophilic model for predicting secondary organic aerosol formation. *Journal of Atmospheric Chemistry* 44, 171-190.

Griffin, R. J., Dabdub, D., Seinfeld, J.H., 2005. Development and initial evaluation of a dynamic species-resolved model for gas phase chemistry and size-resolved gas/particle partitioning associated with secondary organic aerosol formation. *Journal of Geophysical Research D: Atmospheres*, 110, 1-16.

Hakami, A., Seinfeld, J.H., Chai, T., Tang, Y., Carmichael, G.R., Sandu, A., 2006. Adjoint sensitivity analysis of ozone nonattainment over the continental United States. *Environmental Science and Technology*, 40, 3855-3864

- Han, J., Arya, S.P., Shen, S., Lin, Y.-L., 2000. An Estimation of Turbulent Kinetic Energy and Energy Dissipation Rate Based on Atmospheric Boundary Layer Similarity Theory, National Aeronautics and Space Administration Report NASA/CR-2000-210298, NASA Center for Aerospace Information, 7121 Standard Drive, Hanover, MD, 21076-1320, 35 pp.
- Hayden, K.L., Macdonald, A.M., Gong, W., Toom-Sauntry, D., Anlauf, K.G., Leithead, A., Li, S.-L., Leaitch, W.R., Noone, K., 2008. Cloud processing of nitrate. *Journal of Geophysical Research*, (ICARTT special issue), 113, D18201, doi:10.1029/2007JD009732.
- Hogrefe, C., Biswas, J., Lynn, B., Civerolo, K., Ku, J.Y., Rosenthal, J., Rosenzweig, C., Goldberg, R., Kinney, P.L., 2004. Simulating regional-scale ozone climatology over the eastern United States: model evaluation results. *Atmospheric Environment* 38, 2627–2638
- Hogrefe, C., Lynn, B., Knowlton, K., Goldberg, C. Rosenzweig, P.L. Kinney, 2007a. Long-term regional air quality modelling in support of health impact analysis, To appear in ‘Air Pollution Modelling and Its Application XIX’, Eds. C. Borrego and A.I. Miranda, Springer, New York.
- Hogrefe, C., Ku, J.-Y., Sistla, G., Gilliland, A., Irwin, J.S., Porter, P.S., Gégó, E., Kasibhatla, P., Rao, S.T., 2007b, Has the performance of regional-scale photochemical modelling systems changed over the past decade? in ‘Air Pollution Modelling and Its Application XIX’, edit. C. Borrego and A.I. Miranda, Springer, New York.
- Hogrefe, C., Civerolo, K.L., Hao, W., Ku, J.-Y., Zalewsky, E.E., Sistla, G., 2008. Rethinking the assessment of photochemical modelling systems in air quality planning applications. *Journal of the Air and Waste Management Association*, 58, 1086-1099.
- Houyoux, M.R., Vukovich, J.M., Coats, Jr. C.J., Wheeler, N.J.M., 2000. Emission inventory development and processing for the Seasonal Model for Regional Air Quality (SMRAQ) project. *Journal of Geophysical Research*, 105, 9079-9090.
- Isebrands, J.G., Guenther, A.B., Harley, P., Helmig, D., Klinger, L., Vierling, L., Zimmerman, P., Geron, C., 1999. Volatile organic compound emission rates from mixed deciduous and coniferous forests in Northern Wisconsin. *Atmospheric Environment*, 33, 2527-2536.
- Jacobson, M.Z., 1997. Development and application of a new air pollution modelling system--II. Aerosol module structure and design. *Atmospheric Environment*, 31, 131-144.
- Jacobson, M.Z., 1999. *Fundamentals of atmospheric modelling*, Cambridge University Press, 656 pp.

- Jacobson, M. Z., 2001a. GATOR-GCMM: A global- through urban-scale air pollution and weather forecast model 1. Model design and treatment of subgrid soil, vegetation, roads, rooftops, water, sea ice, and snow. *Journal of Geophysical Research*, 106, 5385–5401.
- Jacobson, M. Z., 2001b. GATOR-GCMM 2. A study of daytime and nighttime ozone layers aloft, ozone in national parks, and weather during the SARMAP field campaign. *Journal of Geophysical Research*, 106, 5403–5420
- Jacobson, M.Z., 2007. Effects of ethanol (E85) versus gasoline vehicles on cancer and mortality in the United States. *Environmental Science and Technology*, 41, 4150-4157.
- Jiang, W., 2003. Instantaneous secondary organic aerosol yields and their comparison with overall aerosol yields for aromatic and biogenic hydrocarbons. *Atmospheric Environment*, 37, 5439-5444
- Jiang, W., Giroux, É., Yin, D., Roth, H., 2003. Comparison of three secondary organic aerosol algorithms implemented in CMAQ, presented at the 2003 CMAS Models-3 Users' Workshop, Oct 27-19, 2003, RTP, NC, extended abstract, 4 pp.
- Jiang, W., 2004. Reply to the “Comment on ‘Instantaneous secondary organic aerosol yields and their comparison with overall aerosol yields for aromatic and biogenic hydrocarbons’, by Knipping *et al.* (2004)”. *Atmospheric Environment*, 38, 2763-2767
- Jiang, W., Smyth, S., Giroux, E., Roth, H., Yin, D., 2006. Differences between CMAQ fine mode particle and PM_{2.5} concentrations and their impact on model performance evaluation in the lower Fraser valley. *Atmospheric Environment*, 40, 4973–4985.
- Jones, A., Roberts, D.L., Slingo, J., 1994. A climate model study of indirect radiative forcing by anthropogenic sulphate aerosols. *Nature*, 370, 450-453.
- Jones, J.M., Hogrefe, C., Henry, R.F., Ku, J.-Y., Sistla, G., 2005. An Assessment of the Sensitivity and Reliability of the Relative Reduction Factor (RRF) Approach in the Development of 8-hr Ozone Attainment Plans. *Journal of the Air Waste Management Association*, 55, 13–19.
- Kalnay, E., 2003. *Atmospheric Modelling, Data Assimilation and Predictability*, Cambridge University Press, New York, 339 pp.
- Kaminski, J. W., Neary, L., Struzewska, J., McConnell, J. C., Lupu, A., Jarosz, J., Toyota, K., Gong, S. L., Côté, J., Liu, X., Chance, K., Richter, A., 2008. GEM-AQ, an on-line global multiscale chemical weather modelling system: model description and evaluation of gas phase chemistry processes. *Atmospheric Chemistry Physics*, 8, 3255-3281

Kim, S.-W., Heckel, A., McKeen, S.A., Frost, G.J., Hsie, E.-Y., Trainer, M.K., Richter, A., Burrows, J.P., Peckham, S.E., Grell, G.A., 2006. Satellite-observed U.S. power plant NO_x emission reductions and their impact on air quality. *Geophysical Research Letters*, 33, L22812, doi:10.1029/2006GL027749.

Kinnee, E., Geron, C., Pierce, T., 1997. United States land use inventory for estimating biogenic ozone precursor emissions. *Ecological Applications*, 7, 46-58.

Kroll, J. H., Ng, N.L., Murphy, S.M., Flagan, R.C., Seinfeld, J.H., 2006. Secondary organic aerosol formation from isoprene photooxidation. *Environmental Science and Technology* 40, 1869-1877.

Lamsal, L.N., Martin, R.V., Van Donkelaar, A., Celarier, E.A., Bucsela, E.J., Boersma, K.F., Dirksen, R., Luo, C., Wang, Y., 2010. Indirect validation of tropospheric nitrogen dioxide retrieved from the OMI satellite instrument: Insight into the seasonal variation of nitrogen oxides at northern midlatitudes. *Journal of Geophysical Research D: Atmospheres*, 115, art. no. D05302, doi:10.1029/2009JD013351.

Lewis, J.M., Lakshmiarahan, S., Dhall, S.K., 2006. *Dynamic Data Assimilation: A Least Squares Approach*. Cambridge University Press, New York, 654 pp.

Li, S.-M., 2004. A concerted effort to understand the ambient particulate matter in the Lower Fraser Valley: the Pacific 2001 Air Quality Study. *Atmospheric Environment*, 38, 5719-5731

Li, S.-M., Macdonald, A.M., Leithead, A., Leitch, W.R., Gong, W., Anlauf, K.G., Toom-Saunry, D., Hayden, K., Bottenheim, J., Wang, D., 2008. Investigation of carbonyls in cloud-water during ICARTT. *Journal of Geophysical Research*, 113, D17206, doi:10.1029/2007JD009364.

Logan, J.A. 1999. An analysis of ozonesonde data for the troposphere: Recommendations for testing 3-D models and development of a gridded climatology for tropospheric ozone. *Journal of Geophysical Research*, 104, 16115-16149

Macdonald, A.M., Anlauf, K.G., Leitch, W.R., Liu, P., 2006. Multi-year chemistry of particles and selected trace gases at the Whistler high elevation site. *Eos. Trans. AGU*, 87(52), Fall Meet. Suppl., Abstract A53B-0179.

Mailhot, J., Belair, S., Lefàivre, L., Bilodeau, B., Desgagné, M., Girard, C., Glazer, A., Leduc, A.-M., Methot, A., Patoine, A., Plante, A., Rahill, A., Robinson, T., Talbot, D., Tremblay, A., Vaillancourt, P., Zadra, A., Qaddouri, A., 2006. The 15-km version of the Canadian regional forecast system. *Atmosphere Ocean*, 44, 133-149.

- Makar, P.A., 1995. Fast use chemical numerics methods: the use of “vectorization by gridpoint”. In: 3rd International Conference on Air Pollution, Computational Mechanics Publications, Volume 1, 327-334.
- Makar, P.A., Bouchet, V.S., Nenes, A., 2003. Inorganic chemistry calculations using HETV □ a vectorized solver for the $\text{SO}_4^{2-}\text{NO}_3^-\text{NH}_4^+$ system based on the ISORROPIA algorithms. *Atmospheric Environment*, 37, 2279-2294.
- Makar, P.A., Gravel, S., Chirkov, V., Strawbridge, K.B., Froude, F., Arnold, J., Brook, J., 2006. Heat flux, urban properties, and regional weather. *Atmospheric Environment*, 40, 2750-2766
- Makar, P.A., Stroud, C., Wiens, B., Cho, S., Zhang, J., Sassi, M., Liggio, J., Moran, M., Gong, W., Gong, S., Li, S.-M., Brook, J., Strawbridge, K., Anlauf, K., Mihele, C., Toom-Saunty, D., 2007. High Resolution Nested Runs of the AURAMS Model with Comparisons to PrAIRie2005 Field Study Data, in *Air Pollution Modelling and Its Application XIX*, Borrego, C., Miranda, A.I., (eds), Springer, New York.
- Mathur, R., Roselle, S., Pouliot, G., 2007. Diagnostic analysis of the three-dimensional sulphur distributions over the eastern United States using the CMAQ model and measurements from the 2004 ICARTT field experiment, in ‘*Air Pollution Modelling and Its Application XIX*’, Eds. C. Borrego and A.I. Miranda, Springer, New York.
- McKeen, S., Wilczak, J., Grell, G., Djalalova, I., Peckham, S., Hsie, E.-Y., Gong, W., Bouchet, V., Ménard, S., Moffet, R., McHenry, J., McQueen, J., Tang, Y., Carmichael, C., Pagowski, M., Chan, A., Dye, T., 2005. Assessment of an ensemble of seven real-time ozone forecasts over Eastern North America during the summer of 2004. *Journal of Geophysical Research*, 110, D21307, doi:10.1029/2005JD005858
- McKeen, S., Chung, S.H., Wilczak, J., Grell, G., Djalalova, I., Peckham, S., Gong, W., Bouchet, V., Moffet, R., Tang, Y., Carmichael, G.R., Mathur, R., Yu, S. 2007. Evaluation of several real-time $\text{PM}_{2.5}$ forecast models using data collected during the ICARTT/NEAQS 2004 field study. *Journal of Geophysical Research*, 112, D10S20, doi:10.1029/2006JD007608
- McKeen, S., Grell, G., Peckham, S., Wilczak, J., Djalalova, I., Hsie, E.Y., Frost, G., Peischl, J., Schwarz, J., Spackman, R., Middlebrook, A., Holloway, J., de Gouw, J., Warneke, C., Gong, W., Bouchet, V., Gaudreault, S., Racine, J., McHenry, J., McQueen, J., Lee, P., Tang, Y., Carmichael, G.R., Mathur, R., 2009. An evaluation of real-time air quality forecasts and their urban emissions over Eastern Texas during the summer of 2006 TexAQS field study. *Journal of Geophysical Research*, 114, D00F11, doi:10.1029/2008JD011697.

- Ménard, R., Robichaud, A., 2006. The chemistry-forecast system at the Canadian Meteorological Service of Canada. ECMWF Seminar Proceedings on Global Earth-System Monitoring, Reading UK, 297-308.
- Menut, L., Vautard, R., Beekmann, M., Honnoré, C., 2000. Sensitivity of photochemical pollution using the adjoint of a simplified chemistry-transport model. *Journal of Geophysical Research*, 105, 15379-15402
- Monahan, E.C., Spiel, D.E., Davidson, K.L., 1986. A model of marine aerosol generation via whitecaps and wave disruption, in *Oceanic Whitecaps*, edited by E. Monahan and G.M. Niocaill, 167-174, D. Redel Publishing, Dordrecht, Holland.
- Moran, M.D., Dastoor, A.P., Gong, S.-L., Gong, W., Makar, P.A., 1998. Conceptual design for the AES unified regional air quality modelling system (AURAMS), Internal Report, 100 pp., Air Quality Research Division, Environment Canada, Toronto, Ontario.
- Moran, M.D., Zheng, Q., Samaali, M., Narayan, J., Pavlovic, R., Cousineau, S., Bouchet, V.S., Sassi, S., Makar, P.A., Gong, W., Gong, S., Stroud, C., Duhamel, D., 2007. Comprehensive surface-based performance evaluation of a size- and composition-resolved regional particulate-matter model for a one-year simulation. *Proc. 29th NATO/CCMS ITM on Air Pollution Modelling and Its Application*, Aveiro, Portugal, Sept. 24-28, 9 pp. [Published in *Air Pollution Modelling and its Application XIX*, 2008, C. Borrego and A.I. Miranda, Editors, Springer, Dordrecht, pp. 434-442].
- Moran, M.D., Zheng, Q., Pavlovic, R., Cousineau, S., Bouchet, V.S., Sassi, M., Makar, P.A., Gong, W., Stroud, C., 2008. Predicted acid deposition critical-load exceedances across Canada from a one-year simulation with a regional particulate-matter model. *Proc. 15th Joint AMS/A&WMA Conf. on Applications of Air Pollution Meteorology*, Jan. 21-24, New Orleans, American Meteorological Society, Boston, 20 pp. [Available from weblink <http://ams.confex.com/ams/pdfpapers/132916.pdf>].
- Moran, M.D., Zheng, Q., Samaali, M., 2010. Long-term multi-species performance evaluation of AURAMS for first 2002 annual run. Environment Canada internal report, Toronto, Ontario (in preparation).
- Morneau, G., 2007. Biogenic emissions in AURAMS. EC internal report, Quebec region, Montreal, Quebec, 7 pp. (Available from author: gilles.morneau@ec.gc.ca)
- Morris, R.E., Yarwood, G., Emery, C.A., Koo, B., Wilson, G.M., 2003. Development of the CAMx One-Atmosphere Air Quality Model to Treat Ozone, Particulate Matter, Visibility and Air Toxics and Application for State Implementation Plans (SIPs), A&WMA Specialty

Conference, Guideline on Air Quality Models: The Path Forward, Mystic, CT (October 2003), paper # 9, 15 pp.

Morris, R.E., Yarwood, G., Emery, C.A., Koo, B., 2004. Development and Application of the CAMx Regional One- Atmospheric Model to Treat Ozone, Particulate Matter, Visibility, Air Toxics and Mercury, 97th Annual Conference and Exhibition of the A&WMA, Indianapolis, IN (June 2004), paper # 549, 15 pp.

Müller, J.-F, Stavrakou, T., 2005. Inversion of CO and NO_x emissions using the adjoint of the IMAGES model. *Atmospheric Chemistry and Physics*, 5, 1157-1186.

Multi-stakeholder NO_x/VOC Science Program, 1997. Modelling of ground-level ozone in the Windsor-Quebec City corridor and in the southern Atlantic region. Report of the WQC Corridor and Souther Atlantic Region Modelling Working Group. Venkatesh, S. and Beattie, S. Eds., pp. 265

Murphy, B. N., Pandis, S. N., 2009. Simulating the formation of semivolatile primary and secondary organic aerosol in a regional chemical transport model. *Environmental Science and Technology*, 43, 4722-4728.

Nance, L., Bernardet, L.R., Weatherhead, B., Noonan, G., Fowler, T., Smirnoa, T.G., Benjamin, S.G., Brown, J., Loughe, A., 2007. Weather research and forecasting core tests. AMS 22nd Conf. on Wea. Anal. & Fcstng/18th Conf. on NWP, Park City, UT. 25-29 June, 1pp.

Napelenok, S.L., D.S. Cohan, Y. Hu, A.G. Russell, 2006. Decoupled direct 3D sensitivity analysis for particulate matter (DDM-3D/PM). *Atmospheric Environment*, 40, 6112–6121.

Nastrom, G., Eaton, F.D., 2005. Seasonal variability of turbulence parameters at 2 to 21 km from MST radar measurements at Vandenberg Air Force Base, California. *Journal of Geophysical Research*, 110, D19110, doi:10.1029/2005JD005782.

Nenes, A., Pilinis, C., Pandis, S.N., 1998. ISORROPIA: a new thermodynamic equilibrium model for multiphase multicomponent marine aerosols. *Aquatic Geochemistry* 4, 123–152.

Odman, M.T. , Russell, A.G., 1999. Mass conservative coupling of non-hydrostatic meteorological models with air quality models, in “Air Pollution Modelling and Its Applications XII”, Eds. S.-E. Gryning and E. Batchvarova, 651-660.

O’Dowd, C. D., Smith, M. H., 1993. Physicochemical Properties of Aerosols Over the Northeast Atlantic: Evidence for Wind-Speed-Related Submicron Sea-Salt Aerosol Production. *Journal of Geophysical Research*, 98, 1137-1149

- Odum, J.R., Hoffmann, T., Bowman, F., Collins, D., Flagan, R.C., Seinfeld, J.H., 1996. Gas/particle partitioning and secondary organic aerosol yields. *Environmental Science and Technology*, 30, 2580-2585.
- Odum, J. R., Jungkamp, T. P. W., Griffin, R.J., Forstner, H.J.L., Flagan, R.C., Seinfeld, J.H., 1997. Aromatics, reformulated gasoline, and atmospheric organic aerosol formation. *Environmental Science and Technology*, 31, 1890-1897.
- Otte, T.L. 2008a. The impact of nudging in the meteorological model for retrospective air quality simulations. Part I: Evaluation against national observation networks. *Journal of Applied Meteorology and Climatology*, 47, 1853-1867.
- Otte, T.L. 2008b. The impact of nudging in the meteorological model for retrospective air quality simulations. Part II: Evaluating collocated meteorological and air quality observations. *Journal of Applied Meteorology and Climatology*, 47, 1868-1887.
- Pandis, S.N., Harley, R.A., Cass, G.R., Seinfeld, J.H., 1992. Secondary organic aerosol formation and transport. *Atmospheric Environment*, 26A, 2269-2282.
- Pankow, J.F., 1994. An absorption model of the gas/aerosol partitioning involved in the formation of secondary organic aerosol. *Atmospheric Environment*, 28, 189-193
- Pattey, E., Desjardins, R.L., Westberg, H., Lamb, B., Zhu, T., 1999. Measurement of isoprene emissions over a black spruce stand using a tower-based relaxed eddy-accumulation system. *Journal of Applied Meteorology*, 28, 870-877.
- Peters, L.K., Berkowitz, C.M., Carmichael, G.R., Easter, R.C., Fairweather, G., Ghan, S.J., Hales, J.M., Leung, L.R., Pennell, W.R., Potra, F.A., Saylor, R.D., Tsang, T.T., 1995. The current state and future direction of Eulerian models in simulating the tropospheric chemistry and transport of trace species: a review. *Atmospheric Environment*, 29, 189-222.
- Pierce, T., Geron, C., Bender, L., Dennis, R., Tonnesen, G., Guenther, A., 1998a. Influence of increased isoprene emissions on regional ozone modelling. *Journal of Geophysical Research*, 103, 25611-25629.
- Pierce, T., Kinnee, E., Geron, C., 1998b. Development of a 1-km resolved vegetation cover database for regional air quality modelling. Proc. 23rd AMS Conference on Agricultural and Forest Meteorology, Albuquerque, NM, Nov., American Meteorological Society, Boston.
- Pierce, T., Geron, C., Pouliot, G., Kinnee, E., 2002. Integration of the biogenic emissions inventory system (BEIS3) into the Community Multiscale Air Quality modelling system.

Proceedings of the 12th Joint AMS/A&WMA Conf. on the Applications of Air Pollution Meteorology, Norfolk, Virginia, May, American Meteorological Society, Boston.

Pison, I., 2005. Modélisation inverse pour l'optimisation des sources primaires de pollution atmosphérique à l'échelle régionale. PhD Thesis, Université de Paris XII, 174 pp.

Pouliot, G.A., 2005. The emissions processing system for the Eta/CMAQ air quality forecast system. Proc. Seventh AMS Conf. on Atmospheric Chemistry, Jan. 9-13, San Diego, 6 pp.

Pudykiewicz, J.A., Kallaur, A., Smolarkiewicz, P.K., 1997. Semi-Lagrangian modelling of tropospheric ozone. *Tellus*, 49B, 231-248.

Pun, B. K., Wu, S.-Y., Seigneur, C., Seinfeld, J.H., Griffin, R.J., Pandis, S.N., 2003. Uncertainties in modelling secondary organic aerosols: Three-dimensional modelling studies in Nashville/Western tennessee. *Environmental Science and Technology* 37, 3647-3661.

Rasch, P.J., W.D. Collins, B.E. Eaton, 2001. Understanding the Indian Ocean Experiments INDOEX aerosol distributions with an aerosol assimilation. *Journal of Geophysical Research*, 106, 7337-7355.

Robichaud, A., 1991. Évaluation des vitesses de dépôts secs aux sites du réseau REMPFAAQ. Internal Report M-91-06. Ministère de l'Environnement du Québec. Direction des réseaux atmosphériques, June 1991.

Robichaud, A., Kallaur, A., Pudykiewicz, J., Ménard, R., Moffet, R., 2003. Effects of an Improved Gas Dry Deposition Formulation in Reducing CHRONOS Model Error, 37th CMOS Congress, June 2-5, 2003, Ottawa, ON.

Robinson A. L., Donahue, N.M., Shrivastava, M.K., Weitkamp, E.A., Sage, A.M., Grieshop, A.P., Lane, T.E., Pierce, J.R., Pandis, S.N., 2007. Rethinking organic aerosols : Semivolatile emissions and photochemical aging. *Science*, 315, 1259.

Russell, A., Dennis, R., 2000. NARSTO critical review of photochemical models and modelling. *Atmospheric Environment*, 34, 2283-2324.

RWDI, 2003. Phase 1 report – Pacific Northwest IAQMP. Project # W03-121

RWDI, 2005. The Pacific Northwest air quality scenarios modelling report: PNW CMAQ scenarios, Project # W04-227

Samaali, M., Moran, M.D., Bouchet, V.S., Pavlovic, R., Cousineau, S., Sassi, M., 2009. On the influence of chemical initial and boundary conditions on annual regional air quality model simulations for North America. *Atmospheric Environment*, 43, 4873-4885.

- Sarwar, G., Luecken, D., Yarwood, G., Whitten, G.Z., Carter, W.P.L., 2008. Impact of an updated Carbon Bond mechanism on predictions from the CMAQ modelling system: Preliminary assessment. *Journal of Applied Meteorology and Climatology*, 47, 3-14.
- Schaap, M., Renske M.A. Timmermans, Michiel Roemer, G.A.C. Boersen, Peter J.H. Bultjes, Ferd J. Sauter, Guus J.M. Velders, Jeanette P. Beck, 2008. The LOTOS–EUROS model: description, validation and latest developments. *International Journal of Environment and Pollution*, 32, 2, 270-290.
- Schell, B., Ackermann, I.J., Hass, H., Binkowski, F.S., Ebel, A., 2001. Modelling the formation of secondary organic aerosol within a comprehensive air quality model system. *Journal of Geophysical Research D: Atmospheres*, 106, 28275-28293.
- Schwede, D., Pouliot, G., Pierce, T., 2005. Changes to the Biogenic Emissions Inventory System version 3 (BEIS3). Proc. Fourth Annual CMAS Models-3 Users' Conference, UNC, Chapel Hill, NC, Sept 26-28, 2005.
- Seaman, N.L., 2007. Evaluating the performance of meteorological processes within air quality modelling systems. Extended abstract, AMS/EPA Workshop on the Evaluation of Regional-Scale Air Quality Modelling Systems, Aug. 7-8, Research Triangle Park, North Carolina, American Meteorological Society, Boston, 9 pp.
- Seigneur, C., 2001. Current status of air quality modelling for particulate matter. *Journal of the Air and Waste Management Association* 51, 1508-1521.
- Seigneur, C. Moran, M.D. 2004. Using models to estimate particle concentration. Chapter 8 in *Particulate Matter Science for Policy Makers: A NARSTO Assessment*, P. McMurry, M. Shepherd, and J. Vickery, Editors, February, 42 pp., Cambridge University Press, Cambridge.
- Seigneur, C., 2007. Evaluating the performance of chemical and aerosol processes within air quality models. Extended abstract, AMS/EPA Workshop on the Evaluation of Regional-Scale Air Quality Modelling Systems, Aug. 7-8, Research Triangle Park, North Carolina, American Meteorological Society, Boston, 4 pp.
- Seinfeld, J.H. Pandis, S.N., 1998. *Atmospheric Chemistry and Physics: From Air Pollution to Climate Change*. John Wiley & Sons, Inc., New York, 1326 pp.
- Sirois, A., Pudykiewicz, J.A., Kallaur, A., 1999. A comparison between simulated and observed ozone mixing ratios in eastern North America. *Journal of Geophysical Research*, 104, 21397-21423

- Skamarock, W.C., J.B. Klemp, J. Dudhia, D.O. Gill, D.M. Barker, W. Wang and J.G. Powers, 2007. A description of the advanced research WRF version 2. NCAR Technical Note, NCAR/TN-468+STR, Boulder, Colorado.
- Smith, M.H., Harrison, N.M., 1998. The sea spray generation function. *Journal of Aerosol Science*, 29, 5189-5190.
- Smolarkiewicz, P.K., Pudykiewicz, J.A., 1992. A class of semi-Lagrangian approximations for fluids. *Journal of Atmospheric Science*, 49, 2082-2096.
- Smyth, S.C., Jiang, W., Yin, D., Roth, H., Giroux, E., 2006a. Evaluation of CMAQ O₃ and PM_{2.5} performance using Pacific 2001 measurement data. *Atmospheric Environment*, 40, 2735-2749.
- Smyth, S., Yin, D., Roth, H., Jiang, W., Moran, M.D., Crevier, L.-P., 2006b, The impact of GEM and MM5 meteorology on CMAQ air quality modelling results in eastern Canada and the northeastern United States. *Journal of Applied Meteorology*, 45, 1525–1541,
- Smyth, S.C., Jiang, W., Roth, H., Yang, F., Bouchet, V.S., Moran, M.D., Landry, H., Makar, P.A., 2007a. A comparative performance evaluation of the AURAMS and CMAQ air quality modelling systems, presented at the 6th annual CMAS conference, Oct. 1-3, 2007, Chapel Hill, NC, extended abstract, 6 pp.
- Smyth, S.C., Jiang, W., Roth, H., Yang, F., 2007b. A comparative performance evaluation of the AURAMS and CMAQ air quality modelling system – revised., ICPET Report # PET-1577-07S, National Research Council of Canada.
- Smyth, S.C., Jiang, W., Roth, H., Moran, M.D., Makar, P.A., Yang, F., Bouchet, V.S., Landry, H., 2009. A comparative performance evaluation of the AURAMS and CMAQ air quality modelling systems. *Atmospheric Environment*, 43, 1059-1070.
- Song, C., Na, K., Cocker III, D.R., 2005. Impact of the hydrocarbon to NO_x ratio on secondary organic aerosol formation. *Environmental Science and Technology* 39, 3143-3149
- Stockwell, W.R., Lurmann, F.W., 1989. Intercomparison of the ADOM and RADM Gas-Phase Chemical Mechanisms, Electrical Power Research Institute Topical Report, EPRI, 3412 Hillview Avenue, Palo Alto, Ca., 254 pp.
- Stroud, C. A., Makar, P., Moran, M., Gong, W., Gong, S., Li, S.-M., Liggio, J., Hayden, K., Anlauf, K., Wiens, B., Zhang, Q., Jimenez, J., 2007. Primary and Secondary Contributions to Organic Aerosol in the Greater Edmonton Air Shed: Results with Environment Canada's

Unified Regional Air Quality Model, The 2007 CMOS Annual Congress, May 28 – June 1, 2007, St John's, NF.

Stroud, C.A., Morneau, G., Makar, P.A., Moran, M.D., Gong, W., Pabla, B., Zhang, J., Bouchet, V.S., Fox, D., Venkatesh, S., 2008. OH-Reactivity of volatile organic compounds at urban and rural sites across Canada: evaluation of air quality model predictions using speciated VOC measurements. *Atmospheric Environment*, 42, 7746-7756.

Tang, Y., Carmichael, G.R., Uno, I., Woo, J.-H., Kurata, G., Lefer, B., Shetter, R.E., Huang, H., Anderson, B.E., Avery, M.A., Clarke, A.D., Blake, D.R., 2003. Impacts of aerosols and clouds on photolysis frequencies and photochemistry during TRACE-P: 2. Three-dimensional study using a regional chemical transport model. *Journal of Geophysical Research*, 108, 8822, doi:10.1029/2002JD003100.

Tang, Y., Carmichael, G.R., Thongboonchoo, N., Chai, T., Horowitz, L.W., Pierce, R.B., Al-Saadi, J.A., Pfister, G., Vukovich, J.M., Avery, M.A., Sachse, G.W., Ryerson, T.B.,

Holloway, J.S., Atlas, E.L., Flocke, F.M., Weber, R.J., Huey, L.G., Dibb, J.E., Streets, D.G., Brune, W.H., 2007. Influence of lateral and top boundary conditions on regional air quality prediction: A multiscale study coupling regional and global chemical transport models. *Journal of Geophysical Research*, 112, D10S18, doi:10.1029/2006JD007515.

Tarasick, D.W., Moran, M.D., Thompson, A.M., Carey-Smith, T., Rochon, Y., Bouchet, V.S., Gong, W., Makar, P.A., Stroud, C., Ménard, S., Crevier, L.-P., Cousineau, S., Pudykiewicz, J.A., Kallaur, A., Moffet, R., Ménard, R., Robichaud, A., Cooper, O.R., Oltmans, O.S., Witte, J.C., Forbes, G., Johnson, B.J., Merrill, J., Moody, J.L., Morris, G., Newchurch, M.J., Schmidlin, F.J., Joseph, E., 2007. Comparison of Canadian air quality forecast models with tropospheric ozone profile measurements above mid-latitude North America during the IONS/ICARTT campaign: Evidence for stratospheric input. *Journal of Geophysical Research*, 112, D12S22, doi:10.1029/2006JD007782.

Tesche, T.W., Georgopoulos, P., Lurmann, F., Roth, P., 1990. Improvement of Procedures for Evaluating Photochemical Models, Prepared by Radian Corporation for the California Air Resources Board, August 1990.

Tie, X., Madronich, S., Li, G., Ying, Z., Zhang, R., Garcia, A.R., Lee-Taylor, J., Liu, Y., 2007. Characterizations of chemical oxidants in Mexico City: A regional chemical dynamical model (WRF-Chem) study. *Atmospheric Environment*, 41, 1989-2008.

Tong, D.Q., Mauzerall, D.L., 2006. Spatial variability of summertime tropospheric ozone over the continental United States: Implications of an evaluation of the CMAQ model. *Atmospheric Environment*, 40, 3041-3056.

Turpin, B. J., Huntzicker, J.J., 1995. Identification of secondary organic aerosol episodes and quantitation of primary and secondary organic aerosol concentrations during SCAQS. *Atmospheric Environment*, 29, 3527-3544.

U.S. EPA, 1991. Guideline for Regulatory Application of the Urban Airshed Model. US Environmental Protection Agency, Office of Air Quality Planning and Standards, Research Triangle Park, NC.

U.S. EPA, 2005. Guidance on the Use of Models and Other Analyses in Attainment Demonstrations for the 8-hour Ozone NAAQS, October 2005.

U.S. EPA, 2006, NO_x Budget Trading Program: 2005 Program Compliance and Environmental Results, EPA430-R-06-013, U.S. Environmental Protection Agency, Washington, D.C., September 2006, 38 pp. (Available from <http://www.epa.gov/airmarkets/progress/progress-reports.html>: accessed 5 May 2008)

U.S. EPA, 2007a. Biogenic Emissions Inventory System (BEIS) Modelling <http://www.epa.gov/asmdnerl/biogen.html>

U.S. EPA, 2007b, NO_x Budget Trading Program: 2006 Program Compliance and Environmental Results, Clean Air Markets Program, Office of Air and Radiation, U.S. Environmental Protection Agency, Washington, D.C., September, 53 pp. + App. (Available from <http://www.epa.gov/airmarkets/progress/progress-reports.html>: viewed 5 May 2008)

Van Loon, M., Builtjes, P.J.H., Segers, A.J., 2000. Data assimilation of ozone in the atmospheric transport chemistry model LOTOS. *Environmental Modelling and Software*, 15, 603-609.

Van Loon, M., Roemer, M.G.M., Builtjes, P.J.H., 2004. Model inter-comparison in the framework of the review of the unified EMEP model. TNO-Report R2004/282, Apeldoorn, The Netherlands.

van Loon, M., Vautard, R., Schaap, M., Bergstrom, R., Bessagnet, B., Brandt, J., Builtjes, P.J.H., Christensen, J.H., Cuvelier, C., Graff, A., Jonson, J.E., Krol, M., Langner, J., Roberts, P., Rouil, L., Stern, R., Tarrason, L., Thunis, P., Vignati, E., White, L., Wind, P., 2007. Evaluation of long-term ozone simulations from seven regional air quality models and their ensemble. *Atmospheric Environment*, 41, 2083-2097.

Vautard, R., Van Loon, M., Schaap, M., Bergstrom, R., Bessagnet, B., Brandt, J.,

Builtjes, P.J.H., Christensen, J.H., Cuvelier, C., Graff, A., Jonson, J.E., Krol, M., Langner, J., Roberts, P., Rouil, L., Stern, R., Tarrason, L., Thunis, P., Vignati, E.,

- White, L., Wind, P., 2006. Is regional air quality model diversity representative of uncertainty for ozone simulation? *Geophysical Research Letters*, 33, L24818, doi:10.1029/2006GL027610.
- Vautard, R., Builtjes, P.J.H., Thunis, P., Cuvelier, C., Bedogni, M., Bessagnet, B., Honore, C., Moussiopoulos, N., Pirovano, G., Schaap, M., Stern, R., Tarrason, L., Wind, P., 2007. Evaluation and intercomparison of Ozone and PM₁₀ simulations by several chemistry transport models over four European cities within the CityDelta project. *Atmospheric Environment*, 41, 173-188.
- Volkamer, R., Jimenez, J.L., San Martini, F., Dzepina, K., Zhang, Q., Dalcedo, D., Molina, L.T., Worsnop, D.R., Molina, M.J., 2006. Secondary organic aerosol formation from anthropogenic air pollution: Rapid and higher than expected. *Geophysical Research Letters*, 33, L17811, doi:10.1029/2006GL026899
- Walcek, C.J., Taylor, G.R., 1986. A theoretical method for computing vertical distributions of acidity and sulphate production within cumulus clouds. *Journal of Atmospheric Science*, 43, 339-355.
- Wesely, M.L., Hicks, B.B., 1977. Some factors that affect the deposition rates of sulphur dioxide and similar gases on vegetation. *Journal of the Air Pollution Control Association* 27, 1110-1117.
- Wesely, M. L., 1989. Parameterization of surface resistances to gaseous dry deposition in regional-scale numerical models. *Atmospheric Environment*, 23, 1293– 1304
- Westberg, H, Lamb, B., Kempf, K., Allwine, G., 2000. Isoprene emission inventory for the BOREAS southern study area. *Tree Physiology*, 20, 735-743.
- White, A. B., Darby, L.S., Senff, C.J., King, C.W., Banta, R.M., Koermer, J., Wilczak, J.M., Neiman, P.J., Angevine, W.M., Talbot, R., 2007. Comparing the impact of meteorological variability on surface ozone during the NEAQS (2002) and ICARTT (2004) field campaigns. *Journal of Geophysical Research*, 112, D10S14, doi:10.1029/2006JD007590
- Xiu, A., Pleim, J.E., 2001. Development of a Land Surface Model. Part I: Application in a Mesoscale Meteorological Model. *Journal of Applied Meteorology*, 40, 192–209.
- Yarwood, G., Stoeckenius, T.E., Heiken, J.G., Dunker, A.M., 2003. Modelling Weekday/Weekend Ozone Differences in the Los Angeles Region for 1997. *Journal of the Air and Waste Management Association*, 58, 864-875.

Young, T.R., Boris, J.P., 1977. A numerical technique for solving stiff ordinary differential equations associated with the chemical kinetics of reactive-flow problems. *Journal of Physical Chemistry*, 81, 2424–2427.

Young, J.R., Lurmann, F.W., 1984. ADOM/TADAP Model Development Program, Volume 7: Aqueous Phase Chemistry. ERT Document No. P-B980-535, Environmental Research and Technology, Inc., Newbury Park, CA, 133 pp.

Yu, S., Dennis, R., Bhawe, P.V., Eder, B.K. 2004. Primary and secondary organic aerosols over the United States: estimates on the basis of observed organic carbon (OC) and elemental carbon (EC), and air quality modelled primary OC/EC ratios. *Atmospheric Environment*, 38:5257-5268.

Yu, S., Bhawe, P.V., Dennis, R.L., Mathur, R., 2007. Seasonal and regional variations of primary and secondary organic aerosols over the continental united states: Semi-empirical estimates and model evaluation. *Environmental Science and Technology*, 41, 4690-4697

Yudin, V.A., Petron, G., Lamarque, J.-F., Khattatov, B.V., Hess, P.G., Lyjak, L.V., Gille, J.C., Edwards, D.P., Deeter, M.N., Emmons, L.K., 2004. Assimilation of the 2000-2001 CO MOPITT retrievals with optimized surface emissions. *Geophysical Research Letters*, 31, L20105, doi:10.1029/2004GL021037.

Zhang, L., Moran, M.D., Brook, J.R., 2001. A comparison of models to estimate in-canopy photosynthetically active radiation and their influence on canopy stomatal resistance. *Atmospheric Environment*, 35, 4463-4470.

Zhang, L., Moran, M.D., Makar, P.A., Brook, J.R., Gong, S., 2002. Modelling gaseous dry deposition in AURAMS -- A Unified Regional Air-quality Modelling System. *Atmospheric Environment*, 36, 537-560.

Zhang, Y., Liu, P., Queen, A., Misenis, C., Pun, B., Seigneur, C., Wu, S.-Yu., 2006. A comprehensive performance evaluation of MM5-CMAQ for the Summer 1999 Southern Oxidants Study episode--Part II: Gas and aerosol predictions. *Atmospheric Environment*, 40, 4839-4855.

Zhang, J., Gong, W., Leitch, W.R., Strapp, J.W., 2007. Evaluation of modelled cloud properties against aircraft observations for air quality applications. *Journal of Geophysical Research*, 112, D10S16, doi:10.1029/2006JD0

Appendix

Statistical evaluation metrics used in this Chapter

The various existing model evaluation studies included in this chapter largely used some or all of the following standard statistical measures as their evaluation metrics:

Mean bias (MB):

$$MB = \frac{1}{N} \sum (C_{\text{mod}} - C_{\text{obs}})$$

Normalised mean bias (NMB):

$$NMB = \frac{\sum (C_{\text{mod}} - C_{\text{obs}})}{\sum C_{\text{obs}}} \times 100\%$$

Mean error (ME):

$$ME = \frac{1}{N} \sum |C_{\text{mod}} - C_{\text{obs}}|$$

Normalised mean error (NME):

$$NME = \frac{\sum |C_{\text{mod}} - C_{\text{obs}}|}{\sum C_{\text{obs}}} \times 100\%$$

Root-mean-square error (RMSE):

$$RMSE = \left[\frac{1}{N} \sum (C_{\text{mod}} - C_{\text{obs}})^2 \right]^{1/2}$$

Correlation coefficient (r):

$$r = \frac{\sum (C_{\text{mod}} - \bar{C}_{\text{mod}})(C_{\text{obs}} - \bar{C}_{\text{obs}})}{\left(\sum (C_{\text{mod}} - \bar{C}_{\text{mod}})^2 \sum (C_{\text{obs}} - \bar{C}_{\text{obs}})^2 \right)^{1/2}}$$

Where $\bar{C}_{\text{mod}} = \frac{1}{N} \sum C_{\text{mod}}$ and $\bar{C}_{\text{obs}} = \frac{1}{N} \sum C_{\text{obs}}$

For each pair of C_{mod} (model prediction) and C_{obs} (observation), different spatial and temporal averaging may be used by different groups.

1. AURAMS 2002 annual run evaluation (Moran *et al.*, 2007): Annual and quarterly averages are computed and the statistics are done on the basis of annual and quarterly means over all sites (Table 5.3, 5.4, 5.7, 5.8, 5.9, and 5.11).
2. AURAMS ICARTT 2004 evaluation (this assessment): The evaluation statistics are computed for daily 1-hour mean and daily 1-hour maximum at each monitoring site separately to provide geographical distribution of the statistics (shown in Figure 3), and the averaged statistics (over all sites) are shown in Table 5.5.
3. CMAQ-MM5 Pacific 2001 evaluation (Smyth *et al.*, 2006): The statistics are computed based on hourly data over all hours and all sites (Table 5.6, 5.10).
4. CMAQ-MC2 Pacific 2001 evaluation (RWDI, 2003 and 2005): Hourly statistics over all monitoring sites are computed to provide a temporal evolution of the statistics (e.g., RMSE shown in Figure 5.6) over the study period.
5. CMAQ-MM5 Alberta summer 2002 (Fox and Kellerhals, 2007): The statistics are computed for each monitoring sites over the 3-month (June, July, August 2002) period based on hourly data (but for data pairs when observed O_3 exceeds 40 ppbv only; Figure 5.8).

CMAQ-AURAMS inter-comparison (Smyth *et al.*, 2007a,b): The statistics are computed based on all pairs of both hourly O_3 and $PM_{2.5}$ and the daily peaks (Table 5.15, 5.16).

CHAPTER 6: Model Scenarios and Applications

Lead Authors: Véronique Bouchet and Kathleen Buset

Contributing Authors: Robert Bloxam, Silvina Carou, Sophie Cousineau, Colin di Cenzo, Didier Davignon, Colleen Farrell, Weimin Jiang, Markus Kellerhals, Paul Makar, Gilles Morneau, Simon Pelletier Steve Smyth, and Roxanne Vingarzan

KEY MESSAGES AND IMPLICATIONS

- A number of modelling studies on a continental and regional scale were conducted to assess the sensitivity of ambient levels of $PM_{2.5}$ and O_3 to a number of sector-specific changes in precursor emissions. Results indicate that ambient $PM_{2.5}$ is highly sensitive to reductions in precursor emissions from the Agricultural, Marine Transportation, Upstream Oil and Gas, Electricity Generation and Residential Wood Combustion sectors. Ambient O_3 is impacted by emissions from the Upstream Oil and Gas and the Electricity sectors, and to a lesser extent by those from the Marine Transportation and Refinery and Chemical sectors.
- Model projections for 2015 of the impact of combined reductions in precursor emissions upon the implementation of current Canadian and U.S. legislation, suggest a general improvement in O_3 levels on a national and regional scale translating into a reduction of CWS exceedance days. Although improvements in ambient $PM_{2.5}$ are also projected in some areas, increases are projected in large urban areas, where wintertime chemistry may play an important role, and in parts of western Canada, where emissions are increasing.
- Model projections of ambient $PM_{2.5}$ and O_3 levels for 2015, resulting from the implementation of additional nationwide and provincial emission reductions for various industrial sectors indicate a fairly widespread improvement in summertime $PM_{2.5}$ and O_3 in the Prairies (linked to emission changes from the Upstream Oil and Gas, Electricity Generation and Smelting sectors) but marginal improvements in other regions.
- These additional nationwide emission reductions beyond current legislation also have the potential to lower the number of CWS exceedance days in densely populated areas, as well as the potential to reduce the magnitude and geographic extent of sulphur and nitrogen acidity critical load exceedances across Canada.

- Sensitivity studies show that ambient PM_{2.5} and O₃ levels in eastern Canada are still strongly influenced by emissions transported from the U.S. while in western Canada, the transboundary influence from the U.S. is relatively equal to that from Canada. Canadian emissions influence ambient levels in the U.S. almost continuously across the border with the strongest influence south of Ontario and Quebec. Even with the inception of U.S. legislation, eastern Canada will remain strongly influenced by U.S. emissions; however, decreases in ambient levels and the number of exceedance days should be measurable given the magnitude of expected reductions in U.S. precursor emissions.
- Inter-provincial transport is most significant in eastern and Atlantic Canada, as the region lies downwind of major emissions areas, in southern Ontario, in Québec, and in the north-eastern United States.

6.1 Introduction

6.1.1 Topic Introduction

The atmosphere is a challenging system to characterize due to its complexity (Chapter 2). Regional air quality models (such as those described in Chapter 5) are valuable tools to predict how changes in pollutant emissions will impact ambient air quality and to examine the potential consequences of emissions changes prior to enforcing them. The use of air quality model scenarios makes it possible to improve the understanding of the relationship between emissions and ambient concentrations, to estimate current and future air quality, and to evaluate the impacts of emissions management or regulatory options aimed at improving air quality and reducing the associated impact on human and ecosystem health.

This chapter provides a review of air quality scenario modelling studies focused on Canada that have been performed between 2000 and 2007. The study results address several policy-relevant science questions that were initially identified and which guided the modelling studies of this assessment, including: what is the sensitivity of particulate matter (PM) and ozone (O₃) to changes in smog precursors? [in section 6.3]; what are the anticipated impacts of future emissions reduction? [in sections 0 and 6.5]; and, how will the observed and predicted changes in PM and O₃ impact ecosystem health? [throughout the chapter]. The analyses also provide insights into a few other policy-relevant science questions such as: what is the spatial and temporal distribution of the smog problem in Canada? [in sections 0 and 6.6]; and, what are the factors that contribute to elevated levels of smog in Canada? [in section 6.6].

The air quality model scenarios discussed in this chapter span a variety of models, geographic domains, spatial resolutions, time periods, meteorological conditions and emissions data. Whenever possible, the authors have tried to examine the results of a number of studies on a

single topic together, in order to assess the convergence of the results and, if possible, identify an overall consensus. Within the constraints of this chapter, a weight-of-evidence approach is used to draw an overall modelling perspective on a topic through analyses of the outputs of the various model scenarios from the different modelling platforms. This provides additional certainty in the modelling conclusions when all models converge towards a similar answer and insight into the state of knowledge when differing answers are obtained. Modelling conclusions are then examined in light of other types of analyses within the context of this assessment to derive overall conclusions on the various policy-relevant science questions.

The air quality modelling results presented in this chapter are by and large, summaries of analyses published in internal government reports, along with a few studies published in the peer-reviewed literature. As extensive use of air quality models in support of air quality policy analyses is fairly recent, and the capacity to model air quality has only improved dramatically in recent years, there is limited depth to the peer-reviewed scientific literature relevant to the results presented in this chapter.

6.1.2 Organization of Chapter

This chapter presents the results of model scenario analyses covering a number of air quality issues:

- Section 6.2 discusses the use and limitations of modelling analyses to assess atmospheric outcomes from various emissions scenarios;
- Section 6.3 presents a review of model scenario analyses that investigate the sensitivity of $PM_{2.5}$ and O_3 to changes in precursor pollutant emissions from individual sectors of activity under current conditions (2002 reference case);
- Sections 6.4 and 6.5 investigate the impact of future emissions projection scenarios, set at or around the year 2015. Section 6.4 focuses on estimating the projected changes in air quality that will result from emissions reduction legislation that had been promulgated as of January 2008. The emissions projections used in the analyses presented in Section 6.4 include the impact of the United States' Clean Air Interstate Rule (U.S. CAIR), which was disputed in U.S. courts in 2008 and which will now be implemented with some modifications as the Cross-State Air Pollution Rule (CSAPR). Section 6.5 investigates the impact of proposed legislative activities, including the impact of emissions reductions as proposed under Canada's Regulatory Framework for Air Emissions;
- Section 6.6 assesses the influence of transboundary flow of pollutants and their impact on $PM_{2.5}$, O_3 and precursor pollutant concentrations;
- Section 6.7 reviews current uncertainties associated with the modelling scenario results presented within this chapter;

- Section 6.8 presents a summary of the overall conclusions presented within this chapter;
- Section 6.9 discusses potential areas for further research.

Whenever possible, the topics addressed in this chapter include a review of the issue at the national level and, in addition, provide regionally-focused discussions that incorporate highly spatially-resolved model scenario results. Although the overall focus is on ambient concentrations, where possible, the impacts on acid deposition and critical load exceedances are also presented. In addition, short case studies that relate model scenario results to impacts on vegetation and visibility are discussed in Chapters 10 and 11, respectively.

6.1.3 Definitions and Terminology

6.1.3.1 Scenario Definitions

Model scenarios analyses are the most common means by which air quality models are used to estimate the impact of emission changes on atmospheric pollutant concentrations. Model scenarios analyses most often consist of a comparison of a reference case with a second predicted simulation that is referred to as a scenario. The same meteorology is generally used for both the reference and scenario cases. In some cases, such as those presented in Sections 6.3 and 6.4, the reference case represents recent conditions. The model input fields are the best available emission estimates for the given time period. The resulting simulation output may then be compared to measurements made during the same time period, and statistics generated to evaluate the model's performance (as presented in Chapter 5).

The scenario usually involves a perturbation to the input emissions fields used in the reference case, in order to understand the model's or atmosphere's sensitivity to a given pollutant or to predict the air quality impacts that would result from a proposed or projected change in emissions. The results of a scenario analysis are most often presented as the difference in the model-predicted atmospheric conditions between the simulation with the modified emission fields (i.e., the scenario) and the reference case.

When evaluating the impact of any proposed air quality management or regulatory action on future conditions, on the other hand, the emissions for the reference case are produced using a projection of the future emissions that will occur in the absence of the proposed action. This is often referred to as a "business-as-usual" (BAU) case. The emissions for the scenario are then generated using future emission levels representative of the proposed regulatory action. Such analyses are presented in Section 6.5, where the impact on air quality of Canada's proposed Regulatory Framework for Air Emissions is compared against a 2015 BAU case.

6.1.3.2 Canada-wide Standards Metrics

Many of the results presented within this chapter are framed in the context of how changes in emissions in the model scenario impact attainment of the current Canada-wide Standards (CWS) for PM_{2.5} and O₃. The metric used to calculate the CWS for PM_{2.5} is 30 µg m⁻³ for the 24-hour average, with attainment based on the annual 98th percentile of the 24-hour average values, averaged over 3 consecutive years. The metric used to calculate the CWS for O₃ is 65 ppbv for the maximum daily 8-hour average, with attainment based on the 4th highest daily 8-hour average measured annually, averaged over 3 consecutive years (see CCME, 2000 for details on CWS attainment).

In the results presented in this chapter, only the frequency of exceedances of the CWS numerical values are assessed for the time period simulated in the scenarios. None of the studies reviewed here span simulation periods long enough to calculate 3-year average values, although the number of days in which the CWS numerical thresholds are exceeded still provides valuable insight to describe how a particular emissions scenario affects the number of high pollution events. At this time, the limitation on using the full CWS metrics in modelling studies is associated with the computing time required to produce results for multi-year periods.

The CWS-based metrics adopted within this chapter are hence for PM_{2.5}, the number of days on which the 24-hour average concentration value exceeds 30 µg m⁻³, and for O₃, the number of days on which the 8-hour rolling average exceeds 65 ppb at least once during that 24-hour period. The calculations of exceedances are performed on a grid cell basis.

6.1.3.3 Acid Deposition – Critical Loads

Although the results presented in this chapter focus on impacts on ambient pollutant concentrations, where possible the impacts on acid deposition and critical load exceedances are also discussed. Acid deposition refers (a) to the removal of acidic compounds from the atmosphere through precipitation and (b) to the dry deposition of gases and particles onto the Earth's surface. High levels of acid deposition can harm both aquatic and terrestrial ecosystems.

The potential impact of acid deposition on an ecosystem can be quantified using the “critical load” concept. The critical load of an ecosystem refers to its ability to withstand the effects of acidifying deposition. The underlying concept is that an ecosystem will have the ability to absorb a certain amount of acidifying sulphur and nitrogen compounds without damage to the ecosystem itself. If the rate of deposition of these compounds exceeds the rate at which the ecosystem can naturally absorb the compounds, ecosystem damage occurs. The maximum amount of acidifying mass that an ecosystem can absorb per unit area in a given time is known as its critical load, and any additional deposited mass that exceeds that amount is known as a

critical load exceedance (e.g., Jeffries *et al.*, 1999; McNulty *et al.*, 2007). In Canada, acid deposition critical loads and their exceedances have been estimated and mapped for forest soils and lakes over large areas of the country (Jeffries *et al.*, 1999; Jeffries and Ouimet, 2005; Ouimet *et al.*, 2006; Aherne 2008a, 2008b, Wong and Dennis, 2008). Many sensitive areas receive acid deposition (sulphur plus nitrogen) at levels that exceed the ecosystem critical loads and in turn are at risk of further and/or future damage. Such damage includes a depletion of essential soil nutrients, acidification of lakes and groundwater, and related impacts to terrestrial and aquatic biota.

Critical load exceedances can be calculated using two different assumptions: the first examining critical load exceedances for sulphur species only, the second for sulphur + nitrogen, where both oxidized and reduced nitrogen species are included. In Canada, the former is a measure of the extent to which changes in deposition may have an immediate impact on ecosystem damage, and the latter is a measure of the extent to which ecosystem damage may occur in the future. Despite no widespread evidence of N-based acidification in Canadian watersheds, the capacity of ecosystems to retain N is finite and it is possible that N-based acidification may occur in the future should ecosystems become N-saturated (Environment Canada, 2005a). Thus, considering critical load exceedances due to total S+N total deposition corresponds to a situation where all deposited S and N species are acidifying.

6.2 Use and Limitations of Modelling Scenarios

As with the application of any analytical tool, there are limitations associated with the use and application of air quality model scenarios. One of these limitations is that the conclusions derived from the modelling work apply only to the specific time period and meteorological conditions being evaluated. Despite continuous improvements to the regional air quality models discussed in this chapter, a level of error and uncertainty remains inherent. In an effort to minimize the impact of the modelling error, the general consensus of the modelling community (e.g., U.S. EPA, 2005; Sistla *et al.*, 2004) is that instead of discussing the absolute values of the model outputs, the difference (deltas) between a model scenario output and a reference case should be the primary result to be analysed. By discussing deltas, the focus is on the direction and magnitude of the resulting air quality impacts rather than on the absolute values.

When comparing the results from among a number of scenario runs that are similar, but which may vary slightly in terms of emissions, time period, or spatial coverage, a weight-of-evidence approach is used to analyze and synthesize the results. Through this approach, similarities in the direction and magnitude of the deltas are compared and used to draw conclusions.

As discussed thoroughly in Chapter 5, the evaluation of an air quality model's skill is based on the comparison of the model scenario results with past and present ambient air quality monitoring site data. It is assumed that the same acceptable level of modelling skill will pertain when a model is used to predict future scenarios. If future conditions are significantly different from the current or past conditions used to evaluate the model, the model's skill level may change but this cannot be easily verified.

The quality of the air quality modelling scenario results presented within this chapter relies not only on the performance of the models themselves, but also on the quality of the model inputs, including emissions and meteorology (see Chapter 5, Section 5.4 for a more thorough discussion). There are ongoing improvements being made to the estimation of emissions and the prediction of meteorological conditions, with the objective of narrowing the range of uncertainties. As a result, modelling scenarios need to be updated on a regular basis to reflect these improvements as well as improvements to the models themselves.

Despite limitations and uncertainties, the models discussed within this chapter are among the current state-of-the-art in terms of their capacity to model PM, O₃, and their precursors. The information generated through their application to simulate scenarios is invaluable in improving our understanding of the atmosphere's response and ability to predict the impact of potential changes in emissions on current or future ambient air quality.

6.3 Sensitivity of PM_{2.5} and O₃ To Changes In Smog Precursors – Sector-Based Analysis

6.3.1 Sensitivity of PM_{2.5} and O₃ to Emissions from the Agricultural Sector (Ammonia)

The sensitivity of ambient levels of PM_{2.5} and O₃ to changes in emissions from the agricultural sector has been investigated in three different studies, a national study and two regional studies focused on British Columbia.

6.3.1.1 Continental-Wide Analysis

Modelling work carried out under the National Agri-Environmental Standards Initiative (NAESI) focused on assessing the impact of agricultural emissions of ammonia (NH₃) on particulate matter concentrations across Canada and the United States using a newly updated ammonia emissions inventory for Canada. This study, performed with AURAMS on a North American domain, evaluated the effect of a 30% reduction, from a 2002 reference level, of Canadian and U.S. ammonia emissions from the agricultural sector. Emissions for all species aside from gaseous NH₃, were based on the 2002 Canadian and U.S. national emissions

inventories; NH_3 emissions in the U.S. were based on the U.S. EPA 2002 national inventory as well, whereas the newly compiled NAESI Canadian ammonia inventory (base year 2002) was used for Canada. Details of the modelling setup for this annual scenario analysis, labelled S1, are presented in the Appendix.

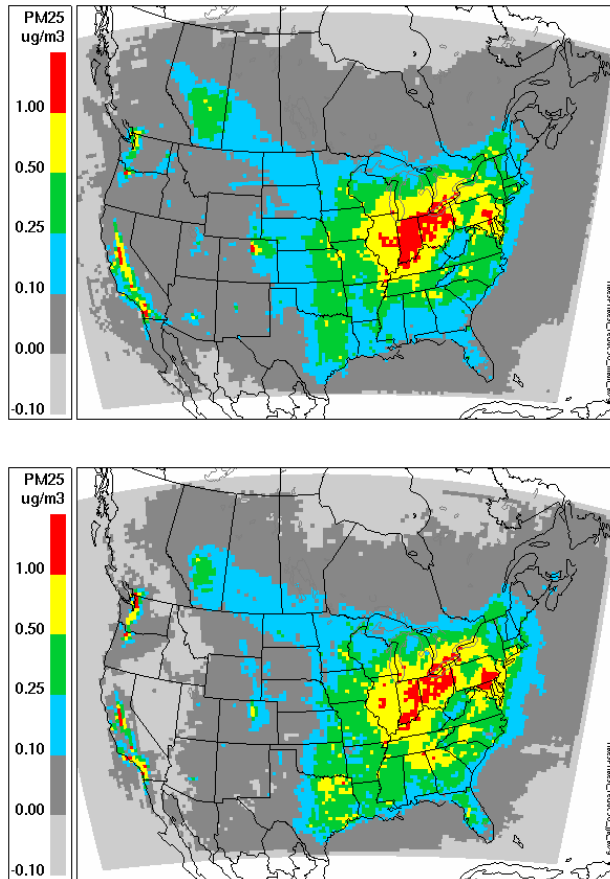


Figure 6.1 Average seasonal changes in $\text{PM}_{2.5}$ mass associated with a 30% Canada and U.S. ammonia emission reduction for March, April May (top) and June, July and August (bottom). Positive values indicate decreases in $\text{PM}_{2.5}$ mass associated with a 30% reduction in ammonia emissions. [S1]²⁵

²⁵ The captions for all figures and tables within this chapter include a scenario reference number (e.g. [S1]). Details of all the modelling scenarios presented in this chapter are tabulated in the Appendix and sorted according to the scenario reference number.

The S1 scenario showed that ambient PM_{2.5} concentrations are sensitive to NH₃ emission levels. Seasonally averaged reductions of ambient PM_{2.5} concentrations of up to 3.9 µg m⁻³ were observed, with typical reduction values ranging from 0.5 to 1.9 µg m⁻³. The largest percentage reductions in median hourly PM_{2.5} concentrations were found in Southern Ontario (3.5 to 7.4%), Saskatchewan (1.8 to 6.4 %), Alberta (1.0 to 4.6%), the Lower Fraser Valley (2.3 to 3.8%) and Quebec (1.7 to 3.4%). Very little impact of ammonia emissions reductions was seen in the Maritime Provinces (maximum median change of 2%). In addition, the reduction in particulate mass had a strong seasonal variability; the highest reductions (by mass) occurred in the spring defined as a March, April, May average and the summer, defined as a June, July, August average (Figure 6.1), while the lowest change in mass occurred in the winter when emissions are lower and the absolute change in emissions represented by a 30% reduction is also lower (not shown). However, if expressed as a percentage of the total PM_{2.5} mass, NH₃ reductions across the domain during the winter period had a greater proportional impact on PM_{2.5} mass, as particle nitrate formation is dependent on temperature and lower temperatures lead to greater proportions of NH₃ being converted to particle ammonium nitrate, ammonium and nitrate ions (Makar *et al.*, 2009).

The reasons behind the reduction in PM_{2.5} mass are fairly straightforward: the decrease in NH₃ emissions results in a decrease in atmospheric NH₃ concentration, hence decreasing the NH₃ available for particle formation. This in turn leads to less NH₃-related compounds in the particles, i.e. ammonium and particulate nitrate, which are both dependant on the presence of NH₃ for their formation. Interestingly, of the remaining NH₃ available for particle formation, more of it tends to partition to the particle phase but the overall impact is a decrease of PM_{2.5} mass.

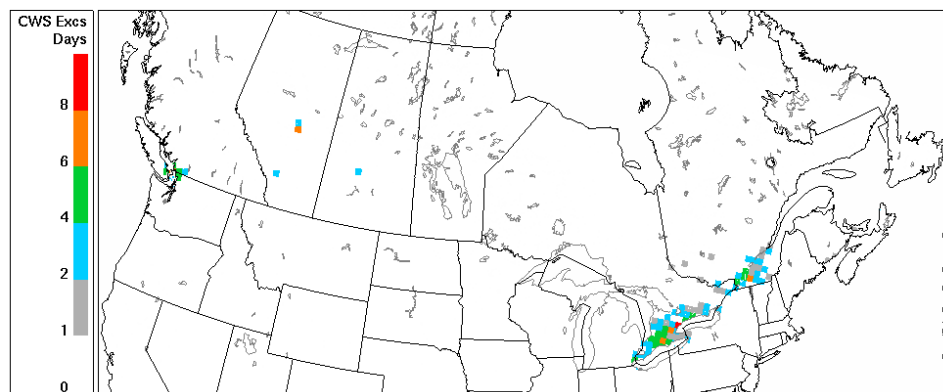


Figure 6.2 Changes in the annual number of exceedance days in which the 24-hour average PM_{2.5} mass exceeds 30 µg m⁻³ associated with a 30% reduction in ammonia emissions [S1]. Positive values indicate areas where the PM CWS exceedance days have decreased in response to decreasing ammonia emissions.

The number of days in exceedance of the PM CWS numerical value behaved like $PM_{2.5}$ mass. Annual summations (Figure 6.2) showed that the decrease in the annual number of exceedance days associated with a 30% reduction in agricultural NH_3 emissions in both Canada and the U.S. varied from 0 to 8 days, with the greatest reductions in the Vancouver area (5 to 7 fewer exceedance days), the “Golden Horseshoe” area of southern Ontario (5 to 7 fewer exceedance days) and the Montreal area (3 to 5 fewer exceedance days). This analysis suggests that NH_3 emissions reductions would result in a significant decrease in CWS exceedances in specific regions of the country. However, additional scenarios are needed in order to determine the relative impact of Canadian or U.S. emission reductions alone (transboundary transport is discussed in further detail in section 6.6).

In contrast to what is seen for ambient $PM_{2.5}$, the 30% reduction in NH_3 emissions had virtually no effect on the O_3 levels, e.g., a maximum domain-average O_3 difference in the summer period of less than 0.1 ppbv. This behaviour is consistent with the fact that chemical reactions involving ammonia are only very weakly linked to the chemical reactions responsible for O_3 formation.

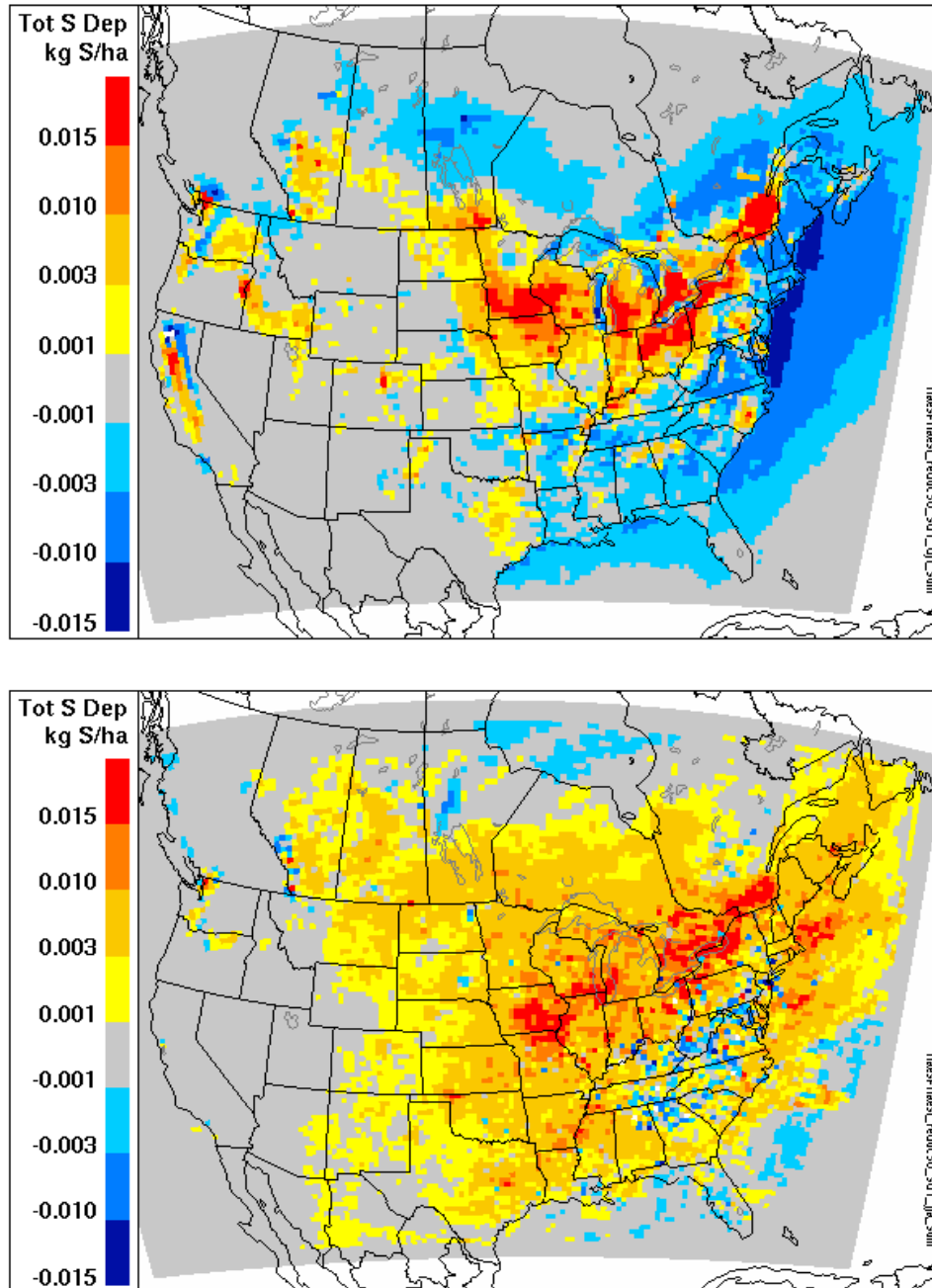


Figure 6.3 Changes in total sulphur deposition (kg S /ha per season) associated with a 30% reduction in NH₃ emissions for December, January, February(top) and June, July, August (bottom). Positive values indicate decreases in sulphur deposition resulting from decreasing NH₃ emissions; negative values indicate increases. [S1].

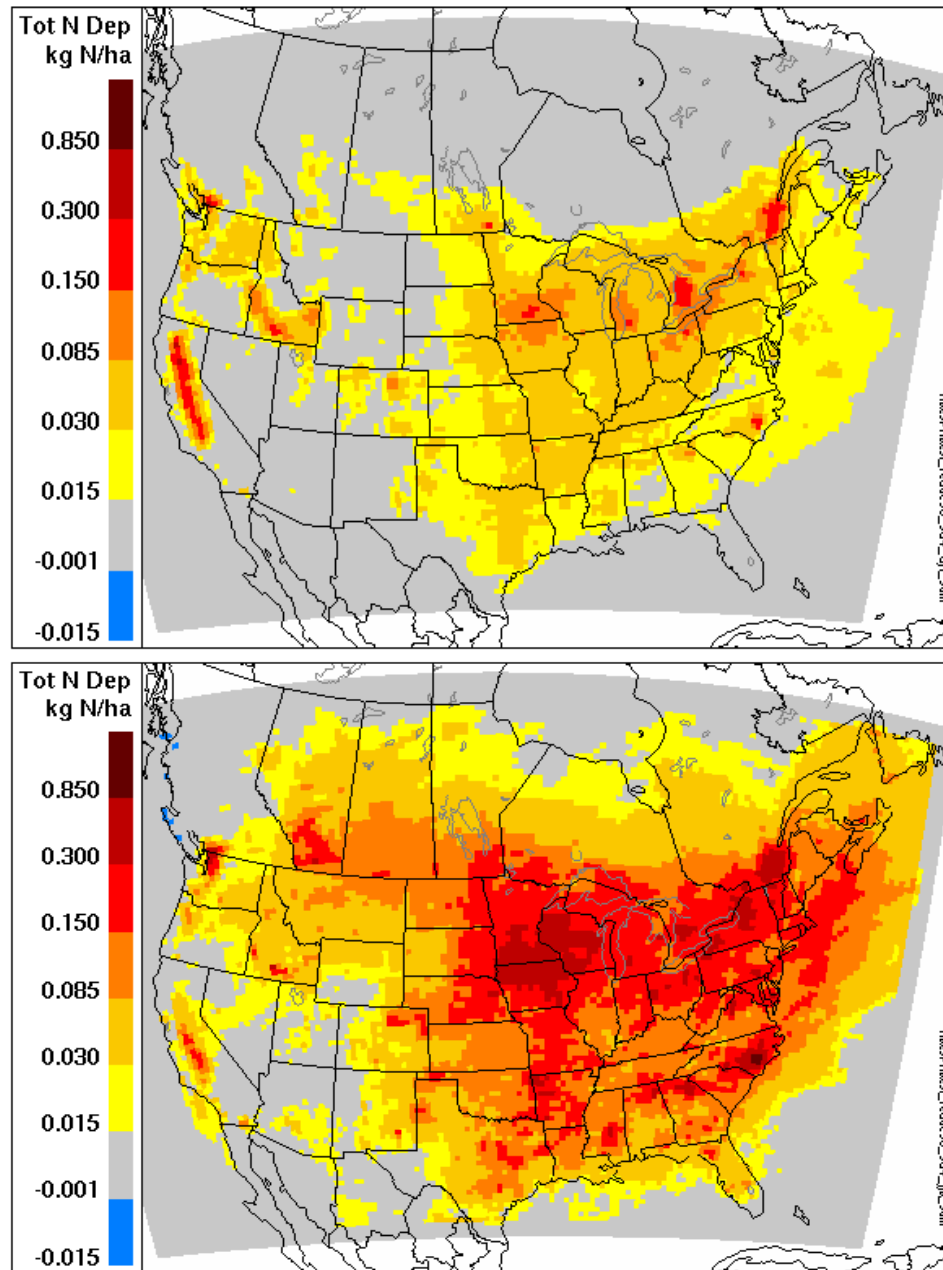


Figure 6.4 Changes in total nitrogen deposition (kg N/ha per season) associated with a 30% reduction in NH₃ emissions for December, January, February (top) and June, July, August (bottom). Positive values indicate decreases in N deposition resulting from decreasing NH₃ emissions; negative values indicate increases. [S1]

The reduction in NH₃ emissions, however, resulted in seasonal and geographic changes in deposition of various atmospheric compounds including sulphur. Total deposition of sulphur compounds generally decreased slightly in the spring (not shown) and summer (Figure 6.3), while in winter, the location of maximum total sulphur deposition shifted, indicating that the mechanisms of deposition have likely changed. A detailed chemical analysis showed that the

decreases in NH_3 emissions led to increases in particle and cloud water acidity, reducing conversion of sulphur dioxide (SO_2) to sulphuric acid in clouds. The atmospheric residence time of SO_2 was thus increased. Since SO_2 has a smaller scavenging ratio in comparison to particle sulphate, this led to a net shift of sulphur total deposition to locations farther from the sources. Ammonia (NH_3) and ammonium (NH_4^+) total deposition decreased, as expected, in the NH_3 source regions, such as south-west Minnesota. Similarly, total nitrogen total deposition (i.e., all oxidized and reduced nitrogen species in both wet and dry deposition) also decreased as it is dominated by the (NH_3 , NH_4^+) mass (Figure 6.4).

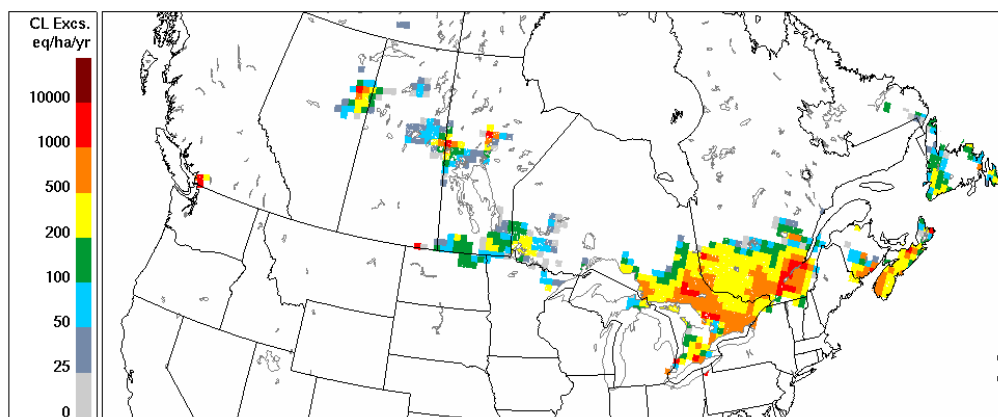


Figure 6.5 Canadian (S + N) critical load exceedances (eq/ha/y) for 2002 for the reference case simulation.

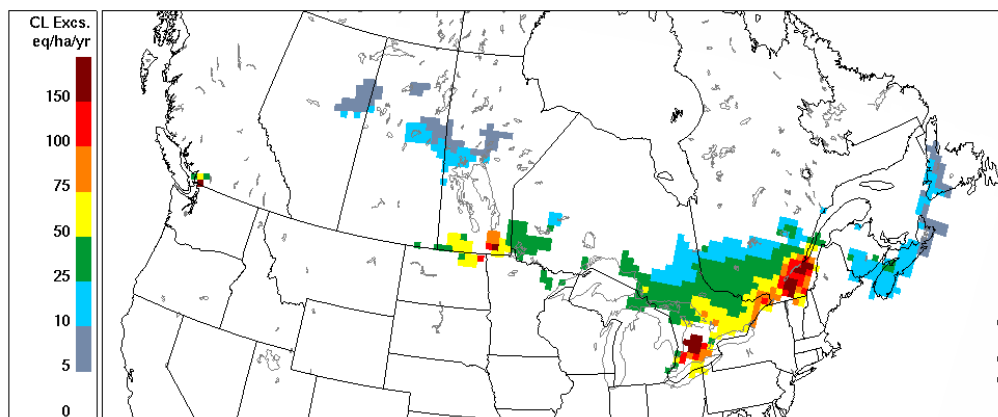


Figure 6.6 Changes in the magnitude of (S + N) critical load exceedances for 2002 associated with a 30% reduction in NH_3 emissions. Positive values indicate areas where critical load exceedances have decreased in response to decreasing ammonia emissions. [S1].

Comparisons of sulphur and nitrogen critical load exceedances (see Moran *et al.*, 2008 for methodology) for the 2002 reference case and the 30% reduction scenario showed that NH_3 reductions had a minimal impact on sulphur critical load exceedances (not shown), implying that reductions in NH_3 emissions would have a minimal impact on acidification of sensitive

ecosystems. On the other hand, sulphur + nitrogen critical load exceedances are notably different for the two cases (Figures 6.5 and 6.6), which suggests that NH₃ emission reductions have the potential to reduce future ecosystem acidification, if current sulphur deposition rates result in a permanent reduction in ecosystem buffering capacity.

Overall, this scenario illustrated that reductions in North American emissions of NH₃ are predicted to lead to reductions in predicted ambient PM_{2.5} levels. Although the impact of these reductions on median concentrations was low to moderate (a fraction to a few $\mu\text{g m}^{-3}$), additional analysis of the impact during short-term episodes revealed much more significant improvements (e.g., a factor of 10 higher than the median values). This led to a reduction in the number of days in which the 24-hour average of PM_{2.5} was above 30 $\mu\text{g m}^{-3}$. NH₃ emissions reductions would therefore result in a decrease in CWS numerical exceedances, and reductions of PM_{2.5} concentrations and deposition levels downwind of the NH₃ emissions sources. This has implications with respect to the transboundary transport of PM_{2.5} that may result from NH₃ emission changes as well as ecosystems health as a result of reduction in nitrogen and sulphur deposition.

6.3.1.2 High-Resolution Regional Analyses: British Columbia

Simulations at very high resolution have also been performed to investigate the sensitivity of ambient PM_{2.5} to changes in NH₃ emissions in the Lower Fraser Valley region of British Columbia, an area of intensive agriculture within the confines of high topography. Two different modelling studies were carried out for episodes in August 2001 coinciding with the Pacific 2001 intensive measurement campaign (Li, 2004; Vingarzan and Li, 2006).

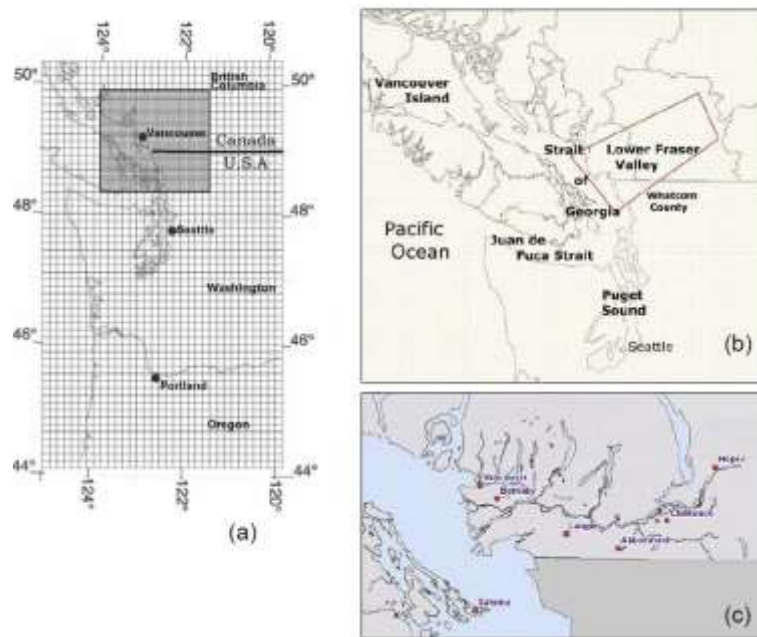


Figure 6.7 The CMAQ model domains for the Lower Fraser Valley scenarios: (a) S2 and (b) S3; (c) Major geographic references within the Lower Fraser Valley model domains.

Sensitivity tests to NH_3 emissions were conducted with the CMAQ model by the National Research Council of Canada (NRC) (Smyth *et al.*, 2006b). NH_3 emissions across all emission source sectors were reduced by 50, 70, and 80% over the entire modelling domain, which consisted of an outer 12-km grid and an inner nested 4-km grid encompassing an area of south-western BC and north-western Washington centered over the Lower Fraser Valley and the city of Vancouver (Figure 6.7a). Emissions were based on the 1995 Canadian emission inventory for British Columbia, except for the Greater Vancouver and Fraser Valley regional districts where year 2001 data were used (GVRD/FVRD, 2002, 2003). In addition, 2001-specific mobile emissions were generated for the purpose of the study. For the U.S. part of the domain, the 2001 projection of the U.S. EPA 1999 National Emission Inventory (NEI) version 3 and 2001 year-specific mobile emissions were used. The study spans 13 days in August 2001 and initially focussed on identifying an over-prediction of $\text{PM}_{2.5}$ nitrate and ammonium. Details of the model setup for this scenario, labelled S2, are presented in the Appendix.

Table 6.1 Comparison of daily maximums of 24-hour rolling average PM_{2.5} concentrations averaged over entire modelling domain for base case and NH₃ sensitivity simulations over the entire simulation period. [S2]

	Base Case	NH ₃ reductions		
		50 %	70 %	80 %
Avg. of daily maximums of 24-hr rolling avg. ($\mu\text{g m}^{-3}$)	10.8	10.3	10.0	9.8
Absolute difference ($\mu\text{g m}^{-3}$)	-	-0.5	-0.8	-1.0
Relative difference (%)	-	-4.6 %	-7.4 %	-9.2 %

Table 6.1 provides the results from the comparison between the reference case and the three scenario runs for the daily maximum 24-hour average PM_{2.5} concentrations, averaged over the entire domain and the entire simulation period. In the reference case, the domain-and time-averaged daily maximum was $10.8 \mu\text{g m}^{-3}$. This value was $0.5 \mu\text{g m}^{-3}$ (4.6%) lower in the 50% NH₃ emissions reduction case, $0.8 \mu\text{g m}^{-3}$ (7.4%) lower in the 70% NH₃ emissions reduction case, and $1.0 \mu\text{g m}^{-3}$ (9.2%) lower in the 80% NH₃ emissions reduction case. The maximum of the daily domain-averaged maxima also exhibited similar reductions from $45.8 \mu\text{g m}^{-3}$ in the reference case to 40.9, 39.5, and $38.8 \mu\text{g m}^{-3}$ for the respective reduction scenarios

Table 6.2 Summary of exceedances over Canada-Wide Standard of $30 \mu\text{g m}^{-3}$ for PM_{2.5} for reference case and three NH₃ sensitivity cases. [S2]

	Base Case	NH ₃ reductions		
		50 %	70 %	80 %
Number of days with one exceedance (days)	10	6	6	6
Absolute difference (days)	-	-4	-4	-4
Relative difference (%)	-	-40 %	-40 %	-40 %
Percentage of days with one exceedance (%)	76.9 %	46.2 %	46.2 %	46.2 %
Absolute difference (%)	-	-30.7 %	-30.7 %	-30.7 %
Relative difference (%)	-	-39.9 %	-39.9 %	-39.9 %
Total grid cells with one exceedance (# grids)	144	78	42	29
Percentage of grid cells with one exceedance (%)	7.6 %	4.1 %	2.2 %	1.5 %
Total number of rolling periods in exceedance	3800	1377	672	422
Percentage of rolling periods in exceedance (%)	0.7 %	0.3 %	0.1 %	0.1 %

The corresponding number of exceedance days of the PM_{2.5} CWS numerical value is provided in Table 6.2. In the reference case, 10 out of the 13 days are in exceedance. The number of daily exceedances decreases to 6 days for each of the sensitivity cases. Furthermore, the total number of 24-hour rolling periods in exceedance over the entire simulation period and all grid

cells decreases for each successive NH₃ reduction, as does the total number of grid cells with exceedances. These sensitivity simulations show that reducing NH₃ emissions in the Lower Fraser Valley result in improvements in both PM_{2.5} concentrations and CWS numerical exceedances.

As found with the S1 scenario, the impact of the NH₃ reduction scenarios on O₃ concentrations is negligible, with differences in the average daily maxima of the 8-hour average O₃ concentrations not exceeding -0.3% for the 80% NH₃ reduction scenario.

These results are consistent with the national-scale S1 scenario. However the magnitude of the PM_{2.5} changes in the S2 study should only be considered qualitatively as limitations in the spatial distribution information at the time these older NH₃ inventories were compiled, may have led to the unrealistic allocation of a significant fraction of NH₃ emissions to downtown Vancouver.

A second high-resolution sensitivity study, also carried out with CMAQ, investigated the effect of a 60% reduction in agricultural ammonia emissions in the Lower Fraser Valley. The objective of this study was to simulate the reduction in emissions that occurred from the summer 2004 chicken cull due to an Avian Flu outbreak in the region. A 12-km coarse-grid modelling domain stretching from central Oregon to central British Columbia and from western Idaho to the Pacific Ocean was used to drive a nested 4-km fine-grid resolution sub-domain centred over the Georgia Basin and Puget Sound (Figure 6.7b). In comparison, the geographical area covered is over nine times larger than the one in the S2 study. The emissions data used for the reference case and scenario were for the year 2000 for Canada, and the year 2002 for the U.S portion of the domain (or for 1999 if 2002 data were unavailable). The study covered two periods: a summer period (August 09-31, 2001) and a winter period (December 01-13, 2002). Details of the model setup for this scenario, labelled S3, are presented in the Appendix.

Consistent with the S1 and S2 studies, the 60% reduction in emissions of ammonia from agricultural sources had only a very minor impact on ground-level ozone concentrations, with changes not exceeding 1 ppbv throughout the summer episode when ozone is a potential issue. The summer PM_{2.5} domain-averaged 24-hour daily maximum decreased by an average of 1% (from 7.5 to 7.4 µg m⁻³), a reduction that is significantly smaller than the domain-averaged reductions obtained in the S2 study. However differences in the allocation of NH₃ emissions between the S2 and S3 studies could explain this variability. At certain times during the modelling period, reductions in NH₃ emissions did lead to widespread PM_{2.5} reductions, as sea-land breezes and mountain-valley flows transported the effects of the emission changes throughout the study area. The maximum one-hour PM_{2.5} reduction was approximately 23 µg m⁻³ or about 35%. Similarly, during the winter period, the maximum one-hour reduction in

PM_{2.5} concentrations was 40 µg m⁻³ or about 35%, again due to the greater proportional impact of NH₃ concentrations in particle nitrate formation as a result of cooler temperatures, with the most widespread reductions occurring on Vancouver Island.

Table 6.3 Summary of exceedances over Canada-Wide Standard of µg m⁻³ for PM_{2.5} for the reference case and the summer-time 60% NH₃ reduction scenario. [S3]

	Base Case	NH ₃ reductions 60%
Number of days with one exceedance	9	9
Percentage of days in exceedance (%)	69.2%	69.2%
Total grid cells in exceedance during episode	1621	1399
Percentage of grid cells in exceedance (%)	9.1%	7.9%
Total number of rolling periods in exceedance	46,563	36,549
Percentage of rolling periods in exceedance (%)	0.9%	0.7%

Table 6 3 summarizes statistics on the number of exceedance days of the PM_{2.5} CWS numerical value for the S3 scenario for the summer period. The decrease in NH₃ emissions did not produce any changes in the number of exceedance days during this period (based on the domain-averaged 24-hour daily maximum). However, the number of grid cells in exceedance decreased as well as the total number of 24-hour rolling periods in exceedance.

A detailed analysis of the distribution of the hourly change in PM_{2.5} at Abbotsford Airport was performed for both the summer and winter periods. It was observed that the median differences in PM_{2.5} concentrations are more than 15 times smaller than the differences in the 98th percentile, suggesting that the effects of the NH₃ emission reductions are very episodic and location-specific, as the model grid also includes areas not impacted by NH₃ emissions, which are included in the spatially-averaged median. Similar results were obtained for the S1 scenarios, again an indication that the impact of emissions reductions is the greatest in short-term episodes close to emissions regions (Makar *et al.*, 2009)²⁶.

²⁶ A more detailed discussion of the S1 and S3 studies and the impacts of ammonia emissions reductions on particulate matter may be found in Chapter 8 of the 2008 Canadian Atmospheric Assessment of Agricultural Ammonia (Environment Canada, 2010).

The three studies discussed here provided consistent information about the impact of NH_3 emissions on $\text{PM}_{2.5}$ and O_3 . Reductions in NH_3 emissions have very little to no effect on O_3 levels, whereas they affect ambient $\text{PM}_{2.5}$ levels by anywhere from a few percent up to 35% depending on the temporal and spatial averages that are applied to the results. There are also indications that locally, average and median changes to $\text{PM}_{2.5}$ may be small, but short-term episodic $\text{PM}_{2.5}$ reductions can be substantial. In all three cases, the modelling results indicate that reductions in NH_3 emissions will result in a reduction in $\text{PM}_{2.5}$ ambient levels.

6.3.2 Sensitivity of $\text{PM}_{2.5}$ and O_3 to Emissions from the Marine Transportation Sector

The sensitivity of ambient levels of $\text{PM}_{2.5}$ and O_3 to emissions from marine transportation was investigated in the Pacific Northwest region, where there are significant marine activities associated with major ports such as Vancouver and Seattle. Using the same CMAQ model and setup as scenario S3, high-resolution simulations were carried out to illustrate air quality conditions under three cases: one with no marine emissions included; one with marine emissions at their current level (reference case); and a last case where marine emissions are doubled. Simulations were performed for a summer and a winter period. Details of the model setup for this scenario, labelled S4, are presented in the Appendix. The study domain is presented in Figure 6.7b.

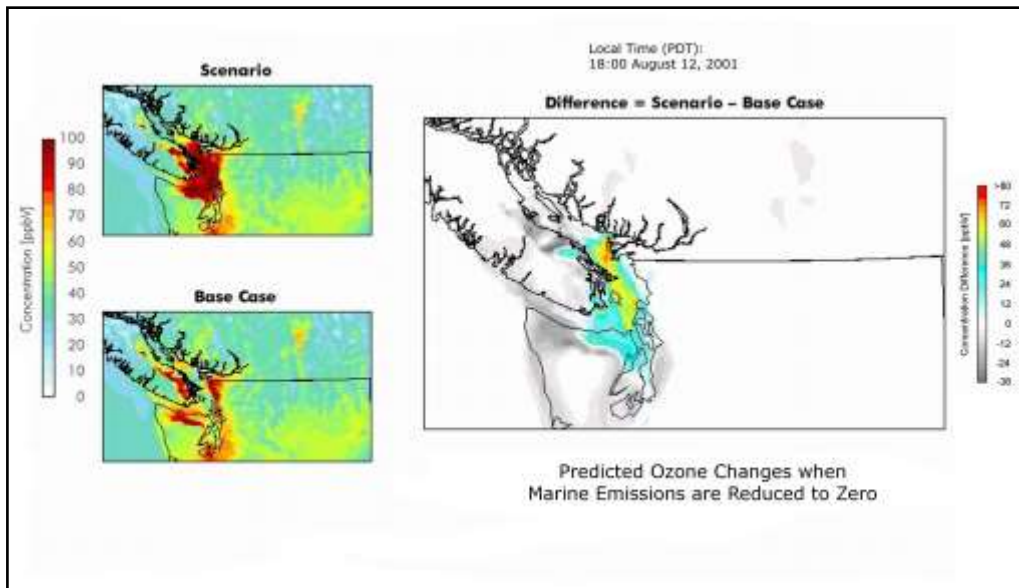


Figure 6.8 Predicted changes in ground-level ozone concentration at 18:00 PDT on August 12, 2001 associated with the no-marine emission case. [S4]

The comparison between the no-marine emission case and the reference case highlighted the complexity of O₃ behaviour. Near the marine seaways in the Strait of Georgia, Juan de Fuca Strait and Puget Sound, the removal of marine emissions resulted in an increase in O₃ concentrations while farther downwind O₃ levels generally decreased. This behaviour is consistent with the Marine sector being a major but locally-constrained source of NO_x in an area that is occasionally subject to elevated O₃ levels at the regional scale. The removal of NO_x emissions from the Marine sector resulted in less NO being available to titrate²⁷ existing O₃ close to the marine sources (near the marine seaways), but also to less production of NO₂ and therefore less O₃ being generated photochemically downwind (for more information on NO_x / O₃ chemistry, see Chapter 2 Atmospheric Processes, section 2.2.1 Chemistry of Ozone: General Concepts). An example of the changes in surface O₃ levels at the height of the summer episode studied is provided in Figure 6.8.

When marine emissions were doubled, the opposite behaviour was observed with ozone decreasing near the marine seaways where titration is enhanced and increasing farther downwind due to increased photochemical production (not shown). The model results suggest that marine emissions contribute significantly to O₃ levels over coastal areas but that farther inland the impact decreases rapidly in magnitude.

The response in ambient PM_{2.5} levels was found to be more linear. Removing PM_{2.5}, NO_x and SO₂ emissions from marine vessels in the summertime (“zeroing out”) significantly reduced primary and secondary PM_{2.5} levels along the seaways as well as downwind, although to a lesser extent (not shown). The same behaviour was observed for the winter episode with the change in season mostly affecting the magnitude of the response but not its spatial distribution.

This scenario suggests that marine emissions are a potentially significant contributor to air pollution in coastal areas, with variations that can exceed 40 ppbv for O₃ and 20 µg m⁻³ for PM_{2.5} on an hourly basis. Further analyses are needed, however, to refine a quantitative estimate of their impact and to assess how much they influence inland concentrations and deposition.

²⁷ The titration reaction during daytime is only the first step to a more complex radical chemistry mechanism in a NO_x limited environment. The full set of reactions is provided in Chapter 2.

6.3.3 Sensitivity of O₃ to emissions from the Oil and Gas Sector (related to upstream and oil sands activities)

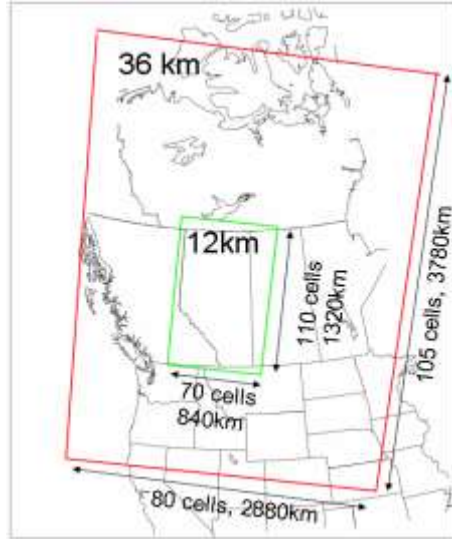


Figure 6.9 CMAQ model domain showing the coarse (36km by 36km) and fine (12 km by 12km) grid domains used in the S5, S6, S7 and S8 scenarios.

A sensitivity study of O₃ levels to emissions from the oil and gas sector was conducted over Alberta using the CMAQ model (Fox and Kellerhals, 2007). Although the study was regional in nature, it conservatively captured between 65 and 75%, of all Canadian upstream oil and gas related emissions within its domain, depending on the pollutant (Figure 6.9). Results from this study can therefore provide a good insight into the impact of this sector at the national scale.

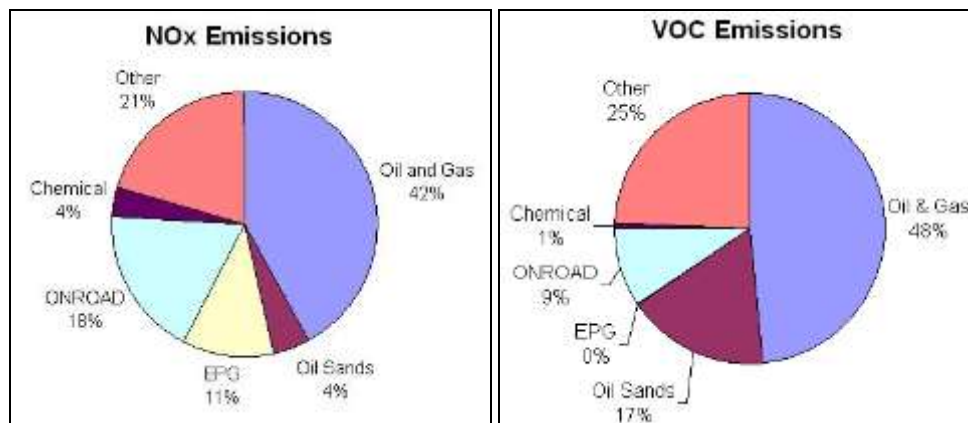


Figure 6.10 Sectoral contributions to Alberta total emission inventory of NO_x and VOC used in the reference case for S5, S6, S7 and S8. "EPG" stands for "electric power generation".

The simulations were performed for a summer period spanning June 1st to August 31st 2002. Anthropogenic emissions were based on the 2000 Canadian emission inventory and the 2001 U.S. National Emission Inventory, with specific updates for the oil sands, for the Upstream Oil and Gas sector, and for the Fort Air Partnership area²⁸. The make up, by sector, of the emissions for the reference case is shown in Figure 6.10. The simulations consisted of a reference case and two scenarios where emissions from conventional oil and gas sources and from the oil sands were alternatively zeroed out. Details of the modelling setup for these simulations, labelled S5 and S6, are provided in the Appendix.

²⁸ The Fort Air Partnership is an airshed association in the industrial area located north-east of Edmonton

6.3.3.1 Conventional Upstream Oil and Gas Industry

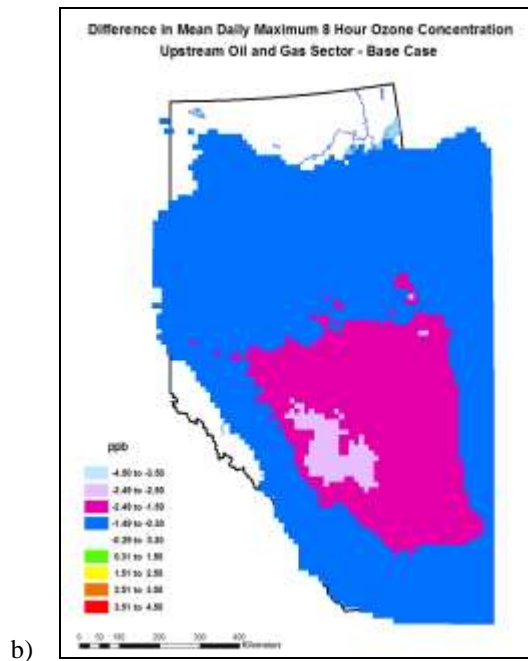
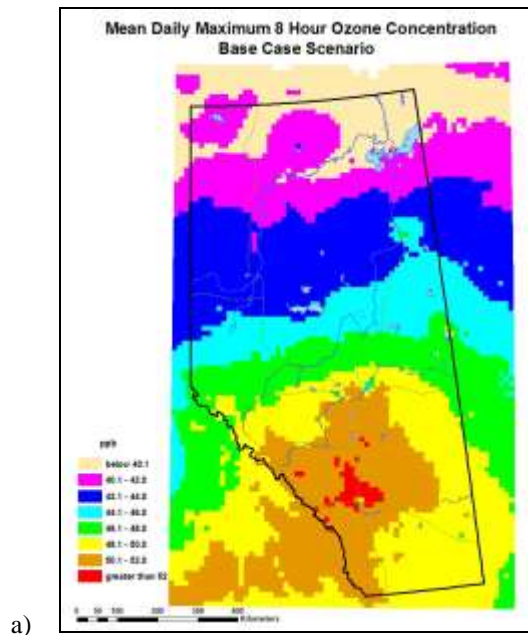


Figure 6.11 (a) Predicted mean daily 8-hour O₃ maximum with in the reference case for the 12-km grid; (b) difference in the mean daily 8-hour O₃ maximum (no-upstream oil and gas-emissions scenario minus reference case). [S5]

Removing upstream oil and gas emissions from the modelling domain had an impact on O₃ levels in the entire province, resulting in seasonally-averaged differences in the daily 8-hour O₃ maxima of 1.5 to 3.5 ppbv (3% to 8%) in southern Alberta, especially southwest of Edmonton, and between 0.3 and 1.5 ppbv (0.5% to 4%) in most of the rest of the province as well as downwind into Saskatchewan (Figure 6.11). This behaviour is consistent with the fact that the sector contributes 42% and 48% of provincial NO_x and VOC emissions respectively (Figure 6.10). The Upstream Oil and Gas sector has a large number of facilities (flares, compressors, storage tanks, dehydrators, gas plants, etc.) widely dispersed across the province. Individually most of these are small sources, but collectively they add up to a significant emissions total, which explains the sensitivity that is observed in the S5 scenario. The heaviest concentration of oil and gas activity is in a band along and to the east of the Rocky Mountain foothills, and corresponding roughly to the area of largest decrease, both in terms of magnitude and spatial extent, in the daily 8-hour O₃ mean. The other area of strong decreases, straddling the Alberta–Saskatchewan border, corresponds to emissions from heavy oil operations around Cold Lake.

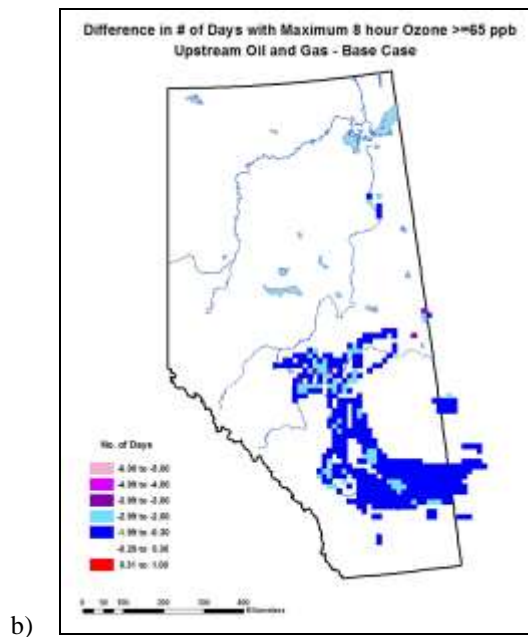
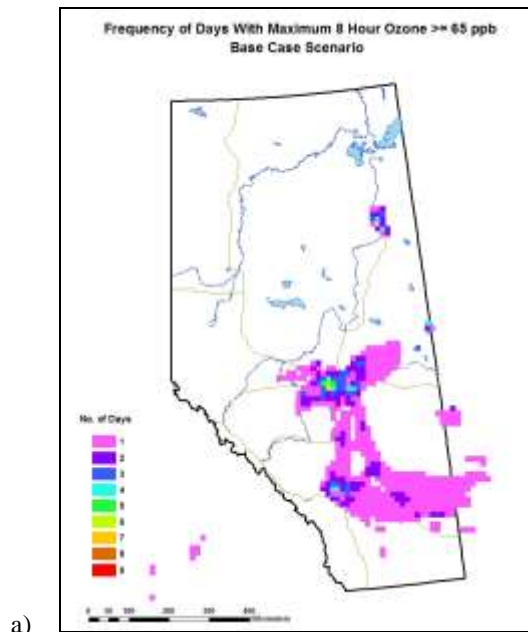


Figure 6.12 (a) Predicted number of days with 8-hour average ozone > 65 ppbv in the reference case for the 12-km grid; (b) difference in the number of days with 8-hour average ozone > 65 ppbv (no upstream oil and gas emissions scenario minus reference case) (b). [S5]

The Upstream Oil and Gas sector also has a strong influence on the pattern of exceedance days in central Alberta. The large area of central Alberta experiencing 1 to 4 days of O₃ exceedances in the reference case diminished into smaller exceedance areas around Edmonton and Calgary

once emissions from the Upstream Oil and Gas sector were removed (Figure 6.12). An analysis by Fox and Kellerhals (2007) found that oil and gas emissions were important contributors to ozone in a 108-km by 108-km square centred on Red Deer and a similarly sized area centred on Calgary. In both areas the oil and gas sector was approximately equivalent to on-road transportation as the most important contributor to ozone on days with ozone above 65 ppb. In a similar area centred on Edmonton the oil and gas industry was, along with on-road transportation, the second most important contributor to high ozone days after the electricity sector.

6.3.3.2 Oil Sands

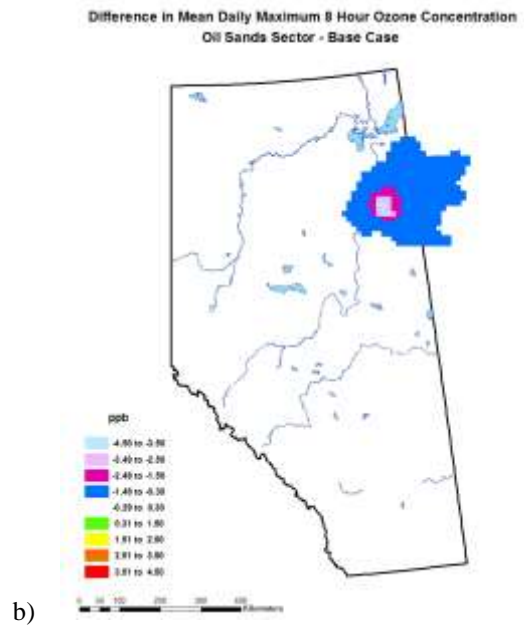
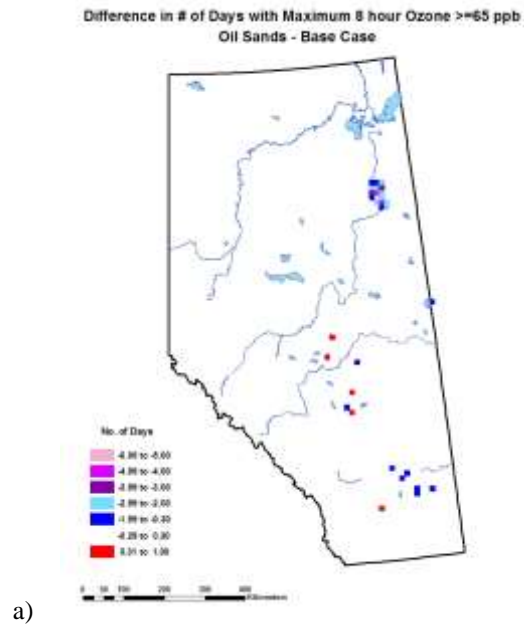


Figure 6.13 (a) Difference in the number of days with 8-hour average ozone $>$ 65 ppb (no-oil sands emission scenario minus reference case); (b) difference in the mean daily 8-hour O_3 maximum (no-oil sands-emissions scenario minus reference case). [S6]

Results from the oil sands scenario, investigated in S6, suggest that the impact of oil sands emissions on O₃ concentrations is restricted to the area immediately surrounding Fort McMurray and the existing oil sands facilities. With emissions from the oil sands removed, the area of exceedances in northern Alberta disappeared, while the area of exceedances in south-central Alberta was largely unchanged (Figure 6.13(a)). The same applies to the mean daily 8-hour O₃ maximum (Figure 6.13(b)): with oil sands emissions removed, there was a significant reduction of O₃ (exceeding 3.5 ppbv at its peak) centred on the oil sands operations and extending east into Saskatchewan, and very little change to mean daily 8-hour O₃ maximum in the southern half of the province.

Uncertainties associated with the S6 modelling results are likely larger than for other scenarios focused on other parts of Alberta. VOC emissions from oil sands tailing ponds and from exposed bitumen in oil sands mines as well as NO_x emissions from the large diesel engines in the oil sands mining fleet are some of the emissions from or associated with the oil sands known to be poorly quantified. In addition, modelling work in the oil sands region (Fox, 2002) demonstrated that simulated O₃ formation was strongly sensitive to the model's representation of biogenic VOC emissions due to the fact that the boreal forest around the oil sands is composed of a large fraction of poplar trees, which are major emitters of isoprene, a very reactive VOC. Direct comparisons with O₃ measurements at three oil sands sites (Fort McMurray, Patricia McInnes, and Fort McKay), suggested that the O₃ levels in the S6 reference case were consistently over-predicted. Also, at least two of the measurement sites, Fort McKay and Fort McMurray, are located near the bottom of the Athabasca Valley, and adjacent to significant NO_x sources not associated with the oil sands that which would alter their representativeness at the regional scale.

Despite uncertainties in the magnitude of the impact of the oil sands emissions, the S6 scenario outlined the spatial extent of the impact from the source area and especially showed that it is mostly constrained to northern Alberta and Saskatchewan. These results are consistent with national simulations discussed in section 6.6.

6.3.4 Sensitivity of O₃ to Emissions from the Refinery and Chemical sector

Using the same approach as for scenarios S5 and S6, the impact of the Refinery and Chemical sector on O₃ levels in Alberta was also investigated. Alberta's emissions for this sector represents approximately 25% and 20% of the Canadian national total emissions of NO_x and VOC, respectively, from the refinery and chemical sectors, hence results obtained here can not be generalized to the national level. Details of the model setup for this scenario, labelled S7, are presented in the Appendix.

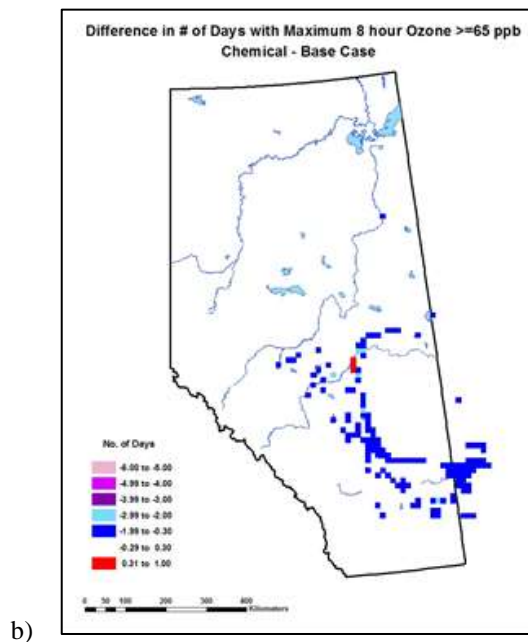
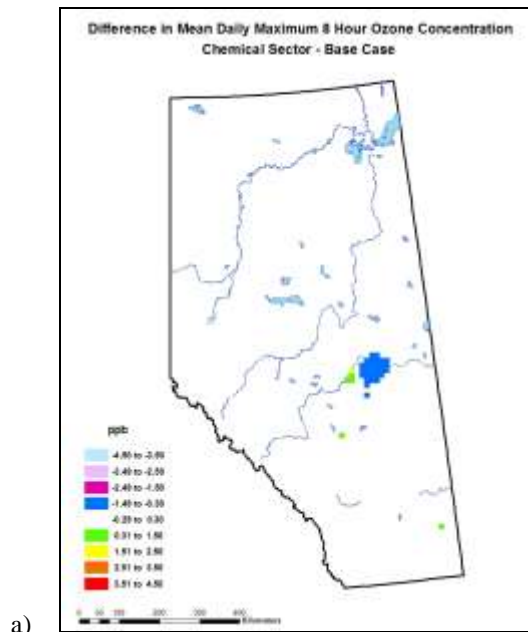


Figure 6.14 Difference in (a) the mean daily 8-hour O₃ maximum (no-refinery-and-chemical-sector emission scenario minus reference case); (b) the number of days with 8-hour average O₃ > 65 ppbv (no-refinery-and-chemical-sector emissions scenario minus reference case). [S7]

Removing the emissions from the sector resulted in a fairly constrained reduction in the mean daily 8-hour O₃ maximum northeast of Edmonton where much of the chemical and refinery industry is concentrated, a behaviour that is consistent with the fact that the sector only

contributes 4% and 1% of Alberta NO_x and VOC emissions, respectively (Figure 6.14a). An increase in the mean daily 8-hour O_3 maximum was also observed in a small area east of Edmonton and upwind from the area where O_3 decreased. This increase is due to a reduced titration of O_3 by NO emissions in this small source region with otherwise high NO emissions. The same NO emissions that were removed, by not transforming into NO_2 , lead to the reduced O_3 levels farther downwind. A few other isolated increases can also be noted in the vicinities of Calgary and Medicine Hat.

In terms of exceedance days, the frequency is generally reduced by one day in a band running east of the Calgary-Edmonton corridor and extending east into Saskatchewan (Figure 6.14b), which suggests that this sector, despite its relatively small contribution to the total Alberta emissions, plays a non-negligible role in O_3 pollution in central Alberta.

6.3.5 Sensitivity of O_3 to Emissions from the Electricity sector

The sensitivity of O_3 to emissions from the Electricity sector (EPG) was assessed for Alberta where it represents a substantial contributor of NO_x emissions (11%) and a negligible contributor of VOC emissions (see Figure 6.10). The same modelling approach as for scenarios S5, S6 and S7 was used. Many other provinces in Canada have significant emissions related to the electricity sector, hence the results discussed here are only illustrative in the Alberta context. Details of the model setup for this scenario, labelled S8, are presented in the Appendix.

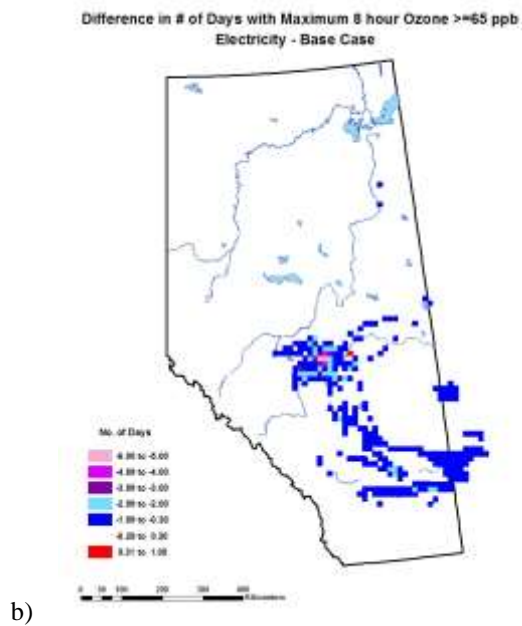
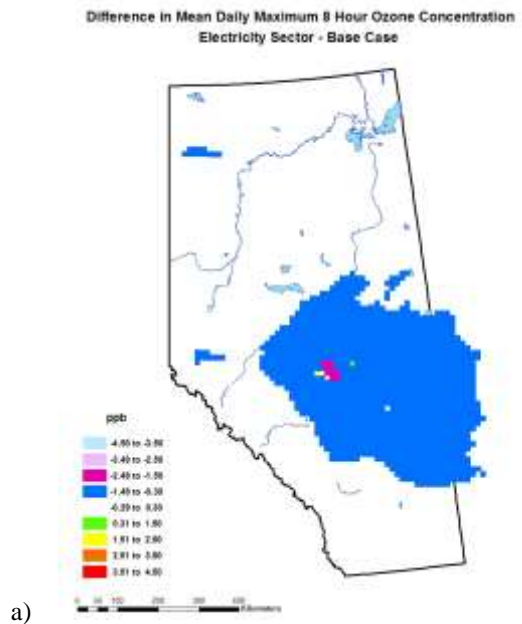


Figure 6.15 Difference in (a) the mean daily 8-hour O₃ maximum (no-electricity-sector emission scenario minus reference case); (b) the number of days with 8-hour average O₃ > 65 ppbv (no electricity sector emissions scenario minus reference case). [S8]

Removing the emissions from the Electricity sector led to a substantial reduction of up to 2.5 ppbv in the mean daily 8-hour O₃ maximum centred west of Edmonton and extending east into Saskatchewan (Figure 6.15a). Correspondingly, the exceedance day frequency decreased, primarily in Edmonton and to the west of Edmonton where four coal fired power plants are

located (Figure 6.15b). Further analysis of S8 results by Fox and Kellerhals (2007) showed that Electricity sector emissions were the leading contributor to O₃ on days with O₃ above 65 ppbv within a 156-km by 132-km square centred on Edmonton. In the rest of the province, on-road transportation and oil and gas emissions are also large contributors.

An additional investigation focusing on the influence of the Electricity sector on ground-level ozone concentrations and transboundary transport at the national level is found in Section 6.6 (Transboundary influences on PM_{2.5}, O₃ and smog precursors)

6.3.6 Sensitivity of PM_{2.5} to Emissions from Residential Wood Combustion

Emissions of primary PM_{2.5} from residential wood combustion are amongst the largest emissions of primary PM_{2.5} in Canada. Residential wood combustion also emits significant amounts of PM_{2.5} and O₃ precursors (VOCs especially), and it is characterized by strong seasonal variations whereby emissions are concentrated in the winter months.

An analysis of the influence of residential wood combustion on winter-time air quality in Quebec was performed with AURAMS for the period of November 20 to 26, 2006 over a domain covering eastern Canada and the eastern U.S. The grid spacing was 21-km by 21-km. This particular period was chosen because meteorological conditions were conducive to the accumulation of high levels of PM_{2.5}. Anthropogenic emissions were based on the 2000 Canadian national inventory and the 2001 U.S. national inventory. The on-road vehicle emissions over an area of 15,000 km² centered on Montreal was generated by the GRID software (Centre for Research on Transportation, 2005). For wood combustion emissions, the number, spatial distribution, and wood consumption of stoves and fireplaces of different technologies were estimated for the province of Quebec using the results of two recent surveys: (a) Environment Canada's surveys conducted in 2006 in residential areas of Montreal and Quebec City (TNS Canadian Facts, 2006); and (b) the Montreal Public Health department survey of 2000 (Labrèche *et al.*, 2000). In addition, data from the Montreal municipal database, which document the presence or absence of a stove or fireplace in each dwelling, were used where available.

The scenarios considered were designed to evaluate the effectiveness of a potential wood-stove upgrade or change-out strategy as a mechanism to reduce emissions contributing to wintertime smog episodes in urban areas in Quebec. Two scenarios were analyzed: (a) the replacement of 25% of the conventional stoves and fireplaces with EPA-certified products (or CSA B415.1-00 standard) across Quebec; and (b) the replacement of 50% of the stoves and fireplaces by certified products. EPA-certified stoves and fireplaces result in less primary PM_{2.5} emissions compared to conventional appliances. For both scenarios, it was assumed that replacement occurred homogeneously across the province, and emissions from residential wood

combustion were adjusted accordingly. As a result, emissions from residential wood combustion are 12% and 25% lower, respectively, in the scenarios. Details of the model setup for this scenario analysis of the influence of residential wood combustion, labelled S9, are presented in the Appendix.

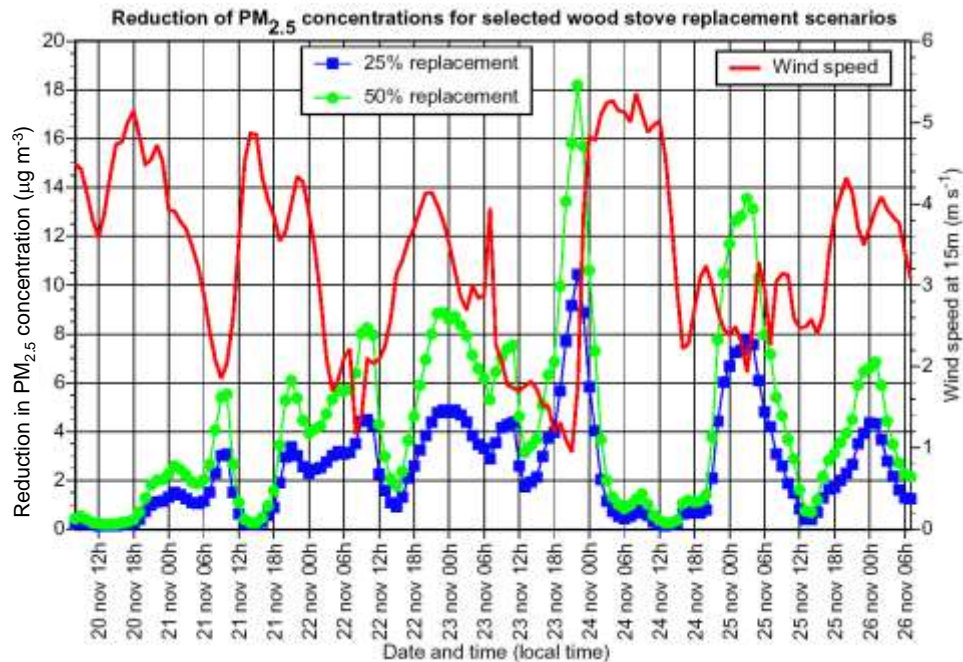


Figure 6.16 Reduction in hourly ambient $PM_{2.5}$ concentrations resulting from the conversion of non-certified wood-burning appliances to EPA-certified products for the Nov. 20-26, 2006 period. The results are averaged over Montreal Island. The modelled wind speed is also plotted to show the relationship between reduction in $PM_{2.5}$ concentration and local meteorological conditions. [S9]

Figure 6.16 presents time series of the average decrease in $PM_{2.5}$ concentrations associated with the two conversion scenarios with respect to the reference case. The results were averaged over the grid cells covering Montreal Island. During this particular episode, a conversion of 25% of the wood stoves was predicted to provide an average reduction of ambient $PM_{2.5}$ concentrations of 2 to 4 $\mu\text{g m}^{-3}$ in the evening and night time, with extremes up to 10 $\mu\text{g m}^{-3}$ on some nights with weak winds. The conversion of 50% of the wood-burning devices would provide a greater reduction, averaging from 4 to 8 $\mu\text{g m}^{-3}$, with peaks up to 18 $\mu\text{g m}^{-3}$ on some nights. It is worthwhile to note that during conditions with high wind speeds, the reduction of $PM_{2.5}$ emissions had little effect on the ambient concentrations, which are low in all cases.

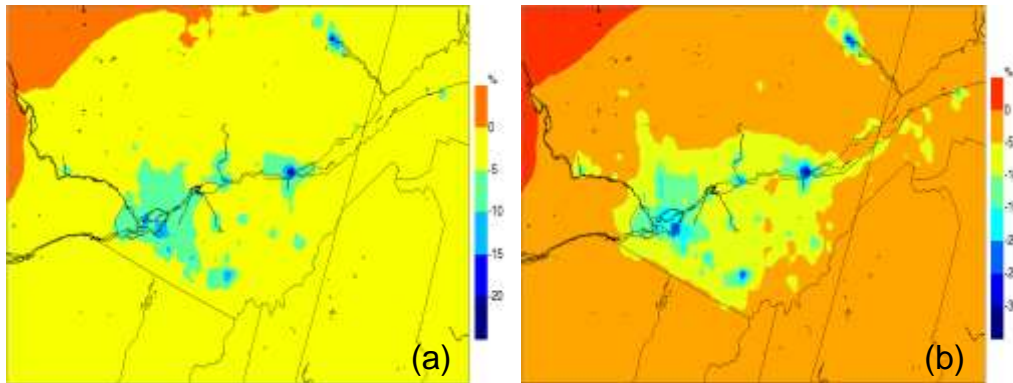


Figure 6.17 Relative difference in time averaged $PM_{2.5}$ concentrations as a percentage between the base case and (a) the 25% conversion scenario and (b) the 50% conversion for the Nov. 20-26, 2006 period. Please note that the colour scale is different in (a) and (b). [S9]

The $PM_{2.5}$ concentrations were also averaged over the entire modelling period, and the difference between the base case and each of the two scenarios computed as a percentage of the base case value (Figure 6.17). The results showed that decreases in the average $PM_{2.5}$ concentrations due to the conversion scenarios would be most pronounced in urban areas, where 10-30% reductions in average $PM_{2.5}$ concentrations were predicted. Even if per capita wood consumption in urban areas is less than in rural areas, air quality benefits resulting from the conversion of wood-burning appliances would be most significant in urban areas due to the higher density of dwellings and wood-burning appliances. Noticeable improvements in ambient $PM_{2.5}$ concentrations were predicted for Montreal, Sherbrooke, Quebec City and Saguenay, whereas in the more rural areas, reductions in average $PM_{2.5}$ concentration of less than 10% occurred.

The accuracy of the number and geographical distribution of wood-burning appliances, along with the annual wood consumption, is limited by the number of respondents in the surveys. Most of the data used for this study is based on the TNS Canadian Facts (2006) survey of 2000 respondents in Quebec, of which 31% reported the use of wood burning equipment. The error in the wood consumption estimates, and therefore also in the emissions of pollutants, is about 25% at the 95% confidence level.

6.3.7 Influence of Background O₃ Concentrations

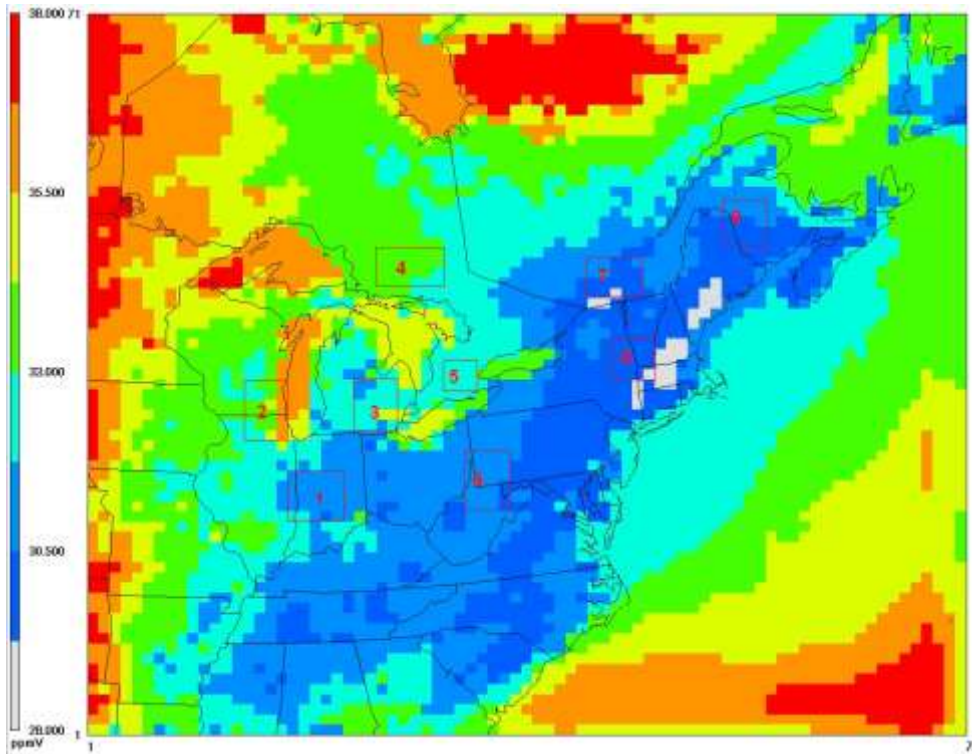


Figure 6.18 Averaged daily 8-hour maximum background O₃ concentration (ppbv) for May-September 2005. [S10]

Background O₃ is defined in the context of regional modelling as O₃ formed from biogenic precursor emissions as well as O₃ transported into the modelling domain from areas beyond its boundaries. An estimate of background O₃ levels in eastern Canada and the eastern U.S. states was derived from a simulation where all anthropogenic emissions within the domain were set to zero. The simulation was performed with CMAQ for a 5-month period from May 1 to September 30, 2005. Since the domain is centered over the Great Lakes and with the western boundary stretching from western Ontario to Arkansas (Figure 6.18), background O₃ from outside the modelling domain includes tropospheric O₃ from hemispheric sources such as Europe and Asia as well as O₃ generated in western and central Canada and U.S.. In the modelling approach chosen for this study, the transported fraction of background O₃ is represented through the application of fixed (time-independent) chemical lateral boundary conditions. The boundary conditions for all chemical species were based on the default settings of CMAQ. For ozone specifically, the southern and western boundaries were set to 35 ppbv near the surface, increasing to 40, 45, 50, 60 and 70 ppbv in 5 layers to the model top (100 hPa). The eastern and northern boundaries were set to 30 ppbv in the lowest layer. The boundary values were based on average observed O₃ profiles. Details of the model setup for this scenario analysis, labelled S10, are presented in the Appendix.

Figure 6.18 shows the average daily 8-hour maximum background O₃ concentrations across the model domain for the five months of simulation. The background 8-hour maxima generally fell in a 30 to 34 ppbv range in the inner portion of the model domain, with higher background concentrations over large bodies of water due to slower O₃ dry deposition rates over water. In addition, ground-level O₃ concentrations around the boundaries of the domain tended to be higher. This was in response to the regular meteorological conditions transporting outside O₃ charged air (represented here as air with a constant 35ppbv O₃ loading at the surface), especially on the western and southern boundaries in areas with smaller precursor emission sources (hence less chemically reactive). This study provides an estimate of biogenic generated and transported O₃ levels for eastern Canada for very specific conditions reflective of a clean environment. Further investigations with dynamic inflow conditions representative of the alternately clean and polluted events experienced by the region will be needed to refine that estimate.

6.4 Projected Levels of PM_{2.5} and O₃ in Canada Based on Implementation of Current Legislation

6.4.1 Outlook on Canadian Air Quality and the Canada-Wide Standards for PM_{2.5} and O₃

A study of the projected levels of PM_{2.5} and O₃ in Canada under a business-as-usual (BAU) emission scenario was performed with AURAMS at the national level for the emission year 2015. Details of the model setup for this scenario are presented in the Appendix under label S11. The emission levels underlying the BAU scenario were based on projections to 2015 of the 2000/2001 Canadian and U.S. inventories assuming that emission levels would evolve in response to changes in economic activity and population growth within the bounds of existing and/or already proclaimed emission legislations. More specifically, the 2015 U.S. projected emission levels included the reduction imposed by the NO_x SIP call and the Clean Air Interstate Rule (CAIR) as proposed prior to the courts dispute in 2008, while the 2015 Canadian emission levels did not include the emission reductions proposed under Canada's Turning the Corner Plan. For the purpose of the analysis discussed here, the 2015 simulation is compared to a present-day simulation corresponding to the 2002 emission year. The meteorological year was identical between the two studies and was set to 2002. Note that due to a reporting error in the 2015 projected inventory, northern Alberta trends in the Fort McMurray vicinity are slightly displaced, appearing north of the Peace River area instead. This slight displacement can be seen in all modelling results for S11 and Figures 6.20 to 6.24.



Figure 6.19 Map of U.S. states covered by the CAIR rule (U.S. EPA, 2009)

Table 6.4 Emissions (Tonnes/Year) and overall changes in NO_x, SO₂, VOC and PM_{2.5} emissions between the 2002 and 2015 Canada + United States combined inventory. [S11]

Emissions	Tonnes/Year	NO _x	SO ₂	VOC	PM _{2.5}
Canada	NEI 2002 ²⁹	2,821,665	2,393,193	2,676,655	532,428
Relative to Can. inv	NEI 2015	2,130,755	1,867,949	2,300,905	636,475
Relative to Can+U.S	% change	-24.5%	-22.0%	-14.0%	+19.6%
	% change	-3.2%	-3.3%	-1.7%	+1.3%
US	NEI 2002	14,195,089	11,768,017	12,289,133	4,420,302
CAIR States	NEI 2015	8,502,814	7,861,358	8,370,946	2,727,129
Relative to Can+US	% change	-26.0%	-24.8%	-18.0%	-21.1%
US	NEI 2002	4,907,950	1,619,485	6,831,138	3,064,239
Non-CAIR States	NEI2015	3,528,368	1,551,691	2,925,836	1,162,251
Relative to Can+US	% change	-6.3%	-0.4%	-17.9%	-23.7%
US (total)	NEI 2002	19,103,039	13,387,502	19,120,271	7,484,541
Relative to Can+US	NEI 2015	12,031,182	9,413,048	11,296,782	3,889,380
	% change	-32.3%	-25.2%	-35.9%	-44.8%

²⁹ 2002 Canadian emission inventory version 2.3 and 2015 Canadian Business As Usual projection (BAU_NOI_2015_smoke_report.xls), excludes emissions from forest fires and assumes 0.75 discount factor for open sources..

Table 6.4 provides a summary of national and regional emission totals for the scenario and the reference case for NO_x, SO₂, VOC and primary PM_{2.5}. These emissions levels describe the conditions that were used as the basis for the simulations and their analysis. The reader is referred to chapter 4 for the background information on how the projections were established. Subtotals for the U.S. states covered by CAIR, as shown in Figure 6.19, and for the remainder of the states are also presented. From a national perspective, Canadian NO_x, SO₂ and VOCs emissions were projected to decrease by 24.5%, 22% and 14%³⁰ respectively from their 2002 reference levels. Although these reductions are relatively small in the North American context (3.2%, 3.3% and 1.7% of the combined Canadian and U.S. inventories), these changes represent substantial decreases in Canada. Primary PM_{2.5} emissions however were projected to increase in Canada by more than 19%. In the U.S., all precursor and primary emissions were projected to decrease significantly due to the implementation of a couple of programs. The projected reductions were particularly marked for the eastern U.S. states covered by CAIR where emission reductions would decrease the total North American NO_x emission by 26%, SO₂ by 24.8%, VOC by 18% and primary PM_{2.5} by 21.1%. In the west, the largest decreases would be associated with primary PM_{2.5} reductions (23.7% of the North American inventory total) and VOC reductions (17.9%). With the exception of primary PM_{2.5} emissions in Canada, the projected emission levels were much lower than the 2002 reference ones.

³⁰ Note that the 2015 BAU scenario was based on an earlier version of the 2015 Canadian inventory and does not reflect recent updates in emissions projections presented in Chapter four of this Assessment. As a result, the projected changes in Canadian PM_{2.5}, NO_x and SO₂ emissions based upon the latest information are smaller than the projections in this scenario, and the direction of the projected VOC emissions is actually reversed (+12% versus -14%). Nonetheless, the modelling results of this scenario are indicative of the expected directional response of PM_{2.5} and O₃ relative to such emissions changes.

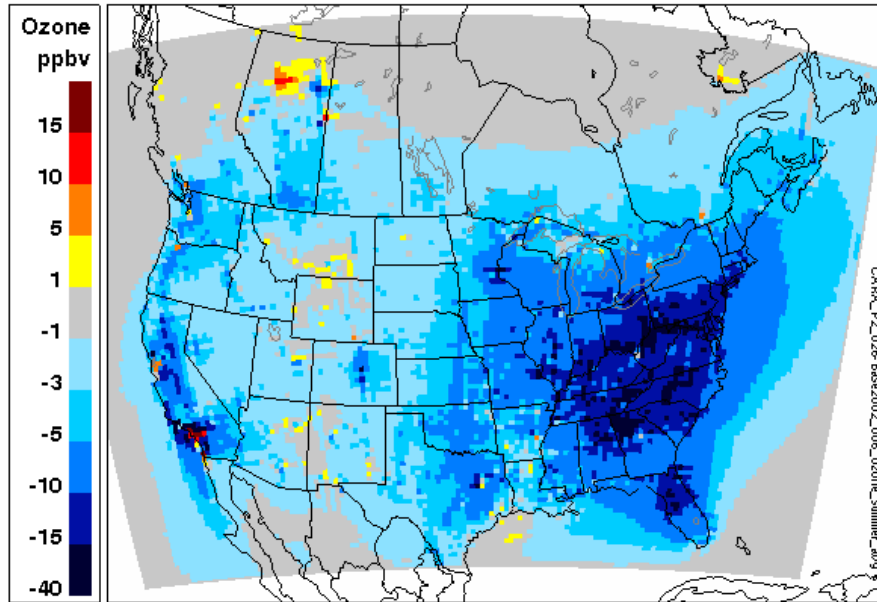


Figure 6.20 Absolute difference in the average O₃ summertime (June-July-August) 8-hour daily maximum between the 2015 BAU simulation and the 2002 reference case. [S11]

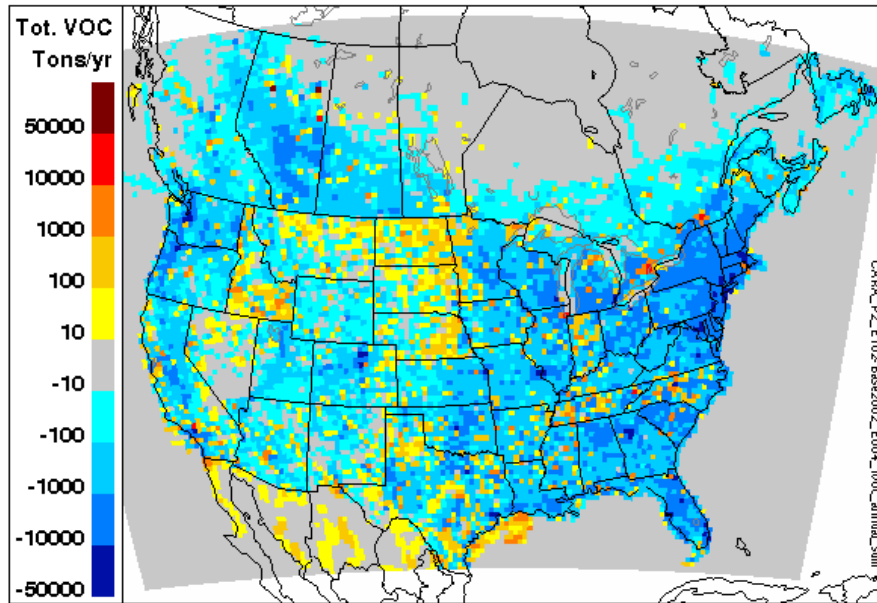


Figure 6.21 Differences in monthly averaged VOC emission levels between the 2015 and 2002 inventories. [S11]

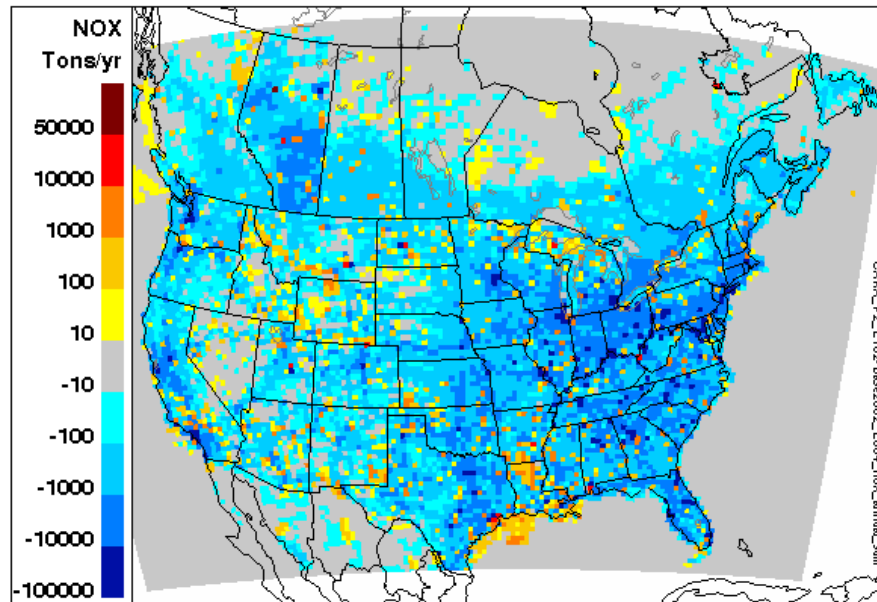


Figure 6.22 Differences in monthly averaged NO_x emission levels between the 2015 and 2002 inventories. [S11]

Figure 6.20 presents a comparison between the 2002 reference case O₃ levels and the 2015 BAU levels. A marked improvement in the average summertime 8-hour daily maximum, consistent with the changes in emissions outlined above, was predicted for the eastern half of North America, including eastern Canada, south of the 50th parallel. The average summertime 8-hour daily maximum was generally predicted to decrease by 3 to 10 ppb (10 to 30%) in most of the populated area in southern Ontario, southern Quebec and the Atlantic provinces. This behaviour is explained in part by the fact that a large fraction of the Canadian VOC and NO_x emission reductions were projected to occur in the Windsor-Quebec City corridor, as outlined in Figure 6.21 and Figure 6.22; and in part by the fact that these Canadian provinces are downwind of northeastern American states where pollution levels were predicted to be much lower. O₃ improvements hence reflected the cumulative effect of the Canadian emission reductions in the east and the decrease in the long-range transport of precursors and pollutants from the U.S. There are a few exceptions to the general improvement in Eastern Canada, namely the close vicinities of Toronto and Montréal. Although NO_x and VOC emissions did decrease in average, Figure 6.21 and Figure 6.22 show that there were some local increases which generally coincide with urban centres. These local increases of both precursors were especially strong in Montréal and Toronto, and likely explain, given that the transboundary transport of pollution from the U.S. is also lower, the local deterioration of the O₃ concentration seen in the projections. As both the component from long-range transport of O₃ and precursors and the component due to local emissions of precursors were fluctuating simultaneously in the scenario, it would require additional analyses to confirm the exact reason that gave rise to the local urban increases. Higher resolution simulations could also provide additional insights on these local behaviours.

Western Canada was projected to experience O₃ improvements of comparable magnitude to eastern Canada in the areas of southern Alberta, in the Edmonton vicinity as well as in the south-west of British Columbia, near the U.S. border. Improvements throughout Saskatchewan and Manitoba were more moderate but reached 1 to 3 ppb (5 to 10%) in the southern half of the provinces. In the Prairies, areas of improvement generally corresponded to regions of marked reductions in both VOC and NO_x Canadian emissions (Alberta especially) and areas downwind of these; in British Columbia, on the other hand, O₃ improvements were likely due to a combination of local and U.S. reductions in the Northern part of Washington State (Figure 6.21 and Figure 6.22). Contrasting with the general trend, northern Alberta was predicted to experience significant increases in O₃ levels in the future (Figure 6.20). Due to a reporting error in the 2015 projected inventory³¹, the largest increase was incorrectly simulated north of Peace River rather than in the Fort McMurray vicinity. Despite the slight displacement, elevated O₃ levels in Northern Alberta are consistent with the growth in local NO_x and VOC emissions that are simulated between the two cases. New emissions associated with the projected increase in Canadian oil sands exploitation are releasing O₃ precursors in a fairly isolated area, creating favourable conditions for O₃ formation. Although only a single meteorological year was studied, the impact of the oil sand sources on air quality seem constrained to Northern Alberta and Saskatchewan as observed in section 6.3.3.2 (Oil Sands).

³¹ A fraction of the emissions from a company operating in the Fort McMurray area were reported with incorrect latitude. The error was later corrected in NPRI and the 2002 inventory but only identified in the projected inventory from the simulations discussed here. Because there are very few sources of anthropogenic emissions in Northern Alberta, some general conclusions can be derived despite the displacement.

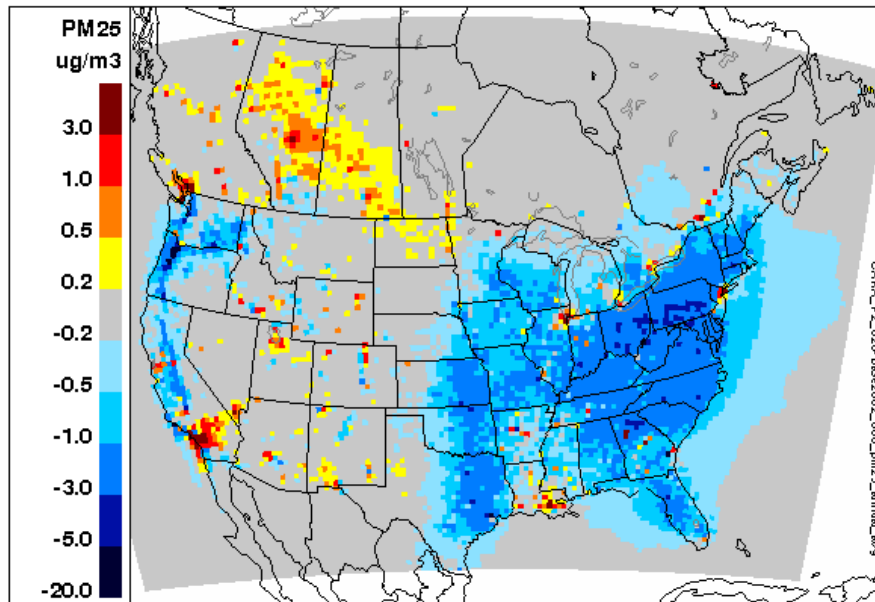


Figure 6.23 Absolute difference in the annual PM_{2.5} 24hr average between the 2015 BAU simulation and the 2002 reference case. [S11]

PM_{2.5} annual ambient levels were predicted to improve in most of the U.S. with the exception of southern California, a few major centers in the intermountain states and the vicinities of Chicago and New York. In Canada, however, the trends were projected to be quite different as outlined in Figure 6.23. Although levels were predicted to decrease by 0.2 to 3 $\mu\text{g m}^{-3}$ (10 to 30%) in southern Ontario, the remaining parts of the Windsor-Quebec City corridor and most of the Atlantic provinces were only projected to experience marginal improvements or actual increases of PM_{2.5} levels by 0.2 to 3 $\mu\text{g m}^{-3}$ (15 to 30%). Similarly, urban centres in Manitoba, Saskatchewan and British Columbia were predicted to experience a worsening of air quality due to PM_{2.5} increases of 1 to 3 $\mu\text{g m}^{-3}$ (20 to 50%), while the surrounding areas stayed unchanged. A maximum increase exceeding 3 $\mu\text{g m}^{-3}$ was projected in Alberta in the vicinity of Edmonton, and also in southern Saskatchewan. This would represent an increase of 20 to 40% of the PM_{2.5} ambient levels in Alberta and Saskatchewan but was not predicted to bring average annual levels above 10 $\mu\text{g m}^{-3}$ throughout the Prairies except in the main urban centres (not shown).

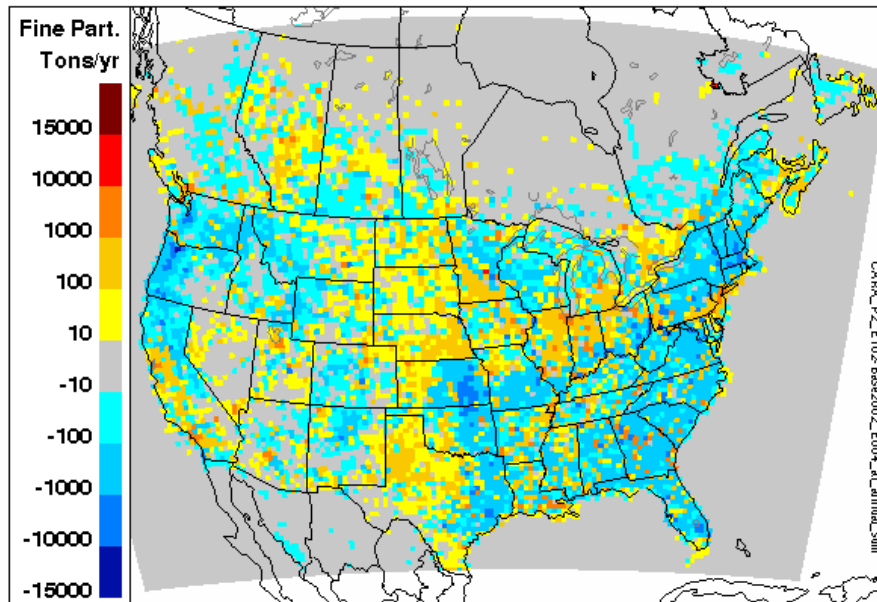


Figure 6.24 Differences in monthly averaged primary PM_{2.5} emission levels between the 2015 and 2002 inventories. [S11]

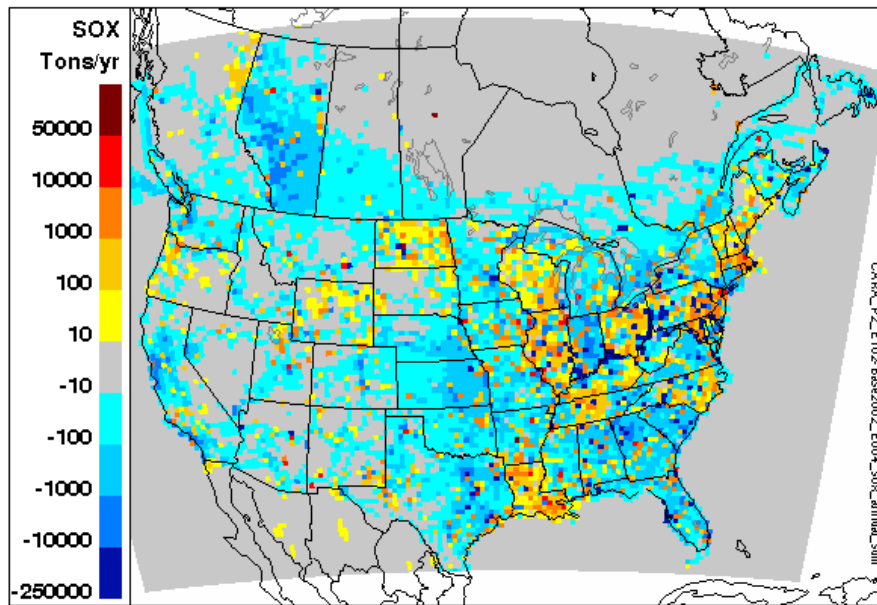


Figure 6.25 Differences in monthly averaged SO_x emission levels between the 2015 and 2002 inventories. [S11]

Relating the ambient PM_{2.5} changes to changes in emissions was more complex for PM species as primary PM_{2.5} emissions as well as emissions from precursors of secondary PM (NO_x, SO_x and VOC) come into play. Figure 6.24 shows that primary PM_{2.5} emissions were projected to increase in the Windsor-Quebec City corridor, in upwind regions such as the Ohio valley as well as in Alberta and to some extent in Saskatchewan. However this did not provide a

complete explanation for the projected ambient $PM_{2.5}$ changes. For example, emissions of NO_x , SO_x (Figures 6.22 and 6.25) and VOC (Figure 6.21) were all projected to decrease substantially overall in Alberta where ambient $PM_{2.5}$ are projected to increase. Only NH_3 emissions were projected to increase moderately in 2015 in the Prairies and the Windsor-Quebec City Corridor (not shown).

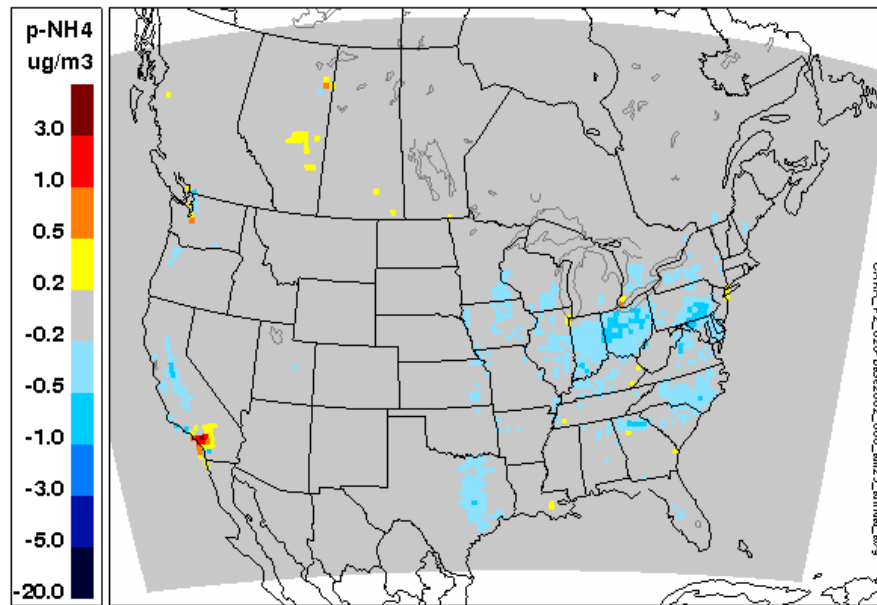


Figure 6.26 Differences in annual 24-hour average $PM_{2.5}$ -ammonium levels between the 2015 BAU simulation and the 2002 reference case. [S11]

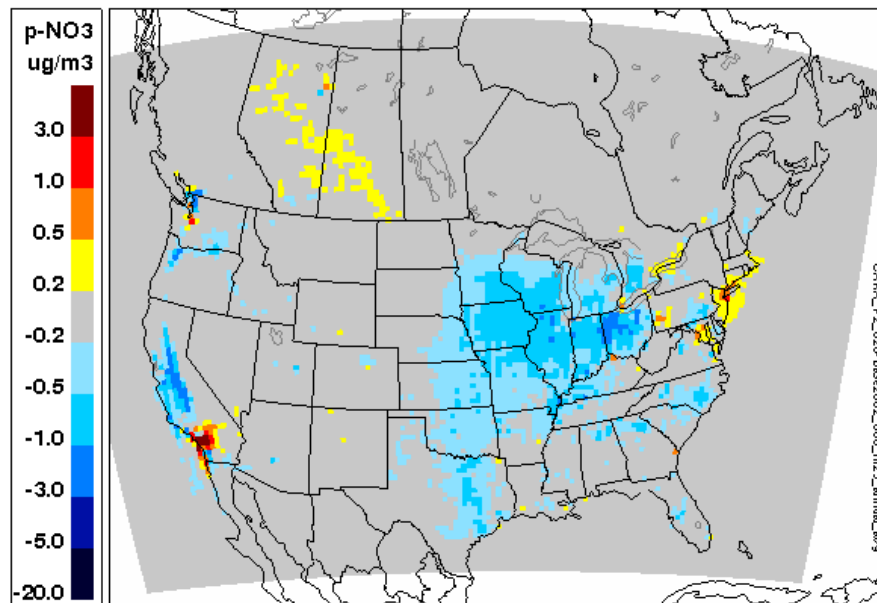


Figure 6.27 Differences in annual 24-hour average $PM_{2.5}$ -nitrate levels between the 2015 BAU simulation and the 2002 reference case. [S11]

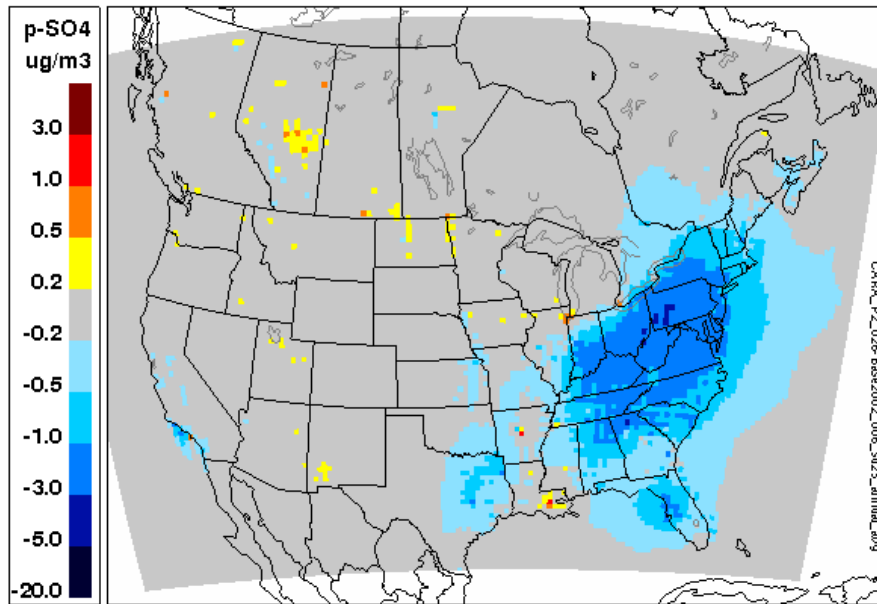


Figure 6.28 Differences in annual 24-hour average PM_{2.5}-sulphate levels between the 2015 BAU simulation and the 2002 reference case. [S11]

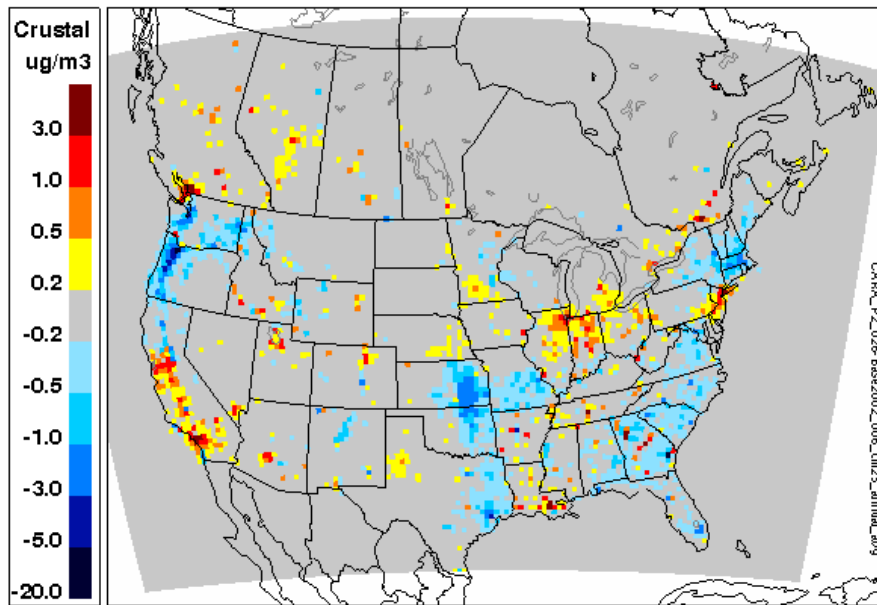


Figure 6.29 Differences in annual 24-hour average PM_{2.5}-crystal material levels between the 2015 BAU simulation and the 2002 reference case. [S11]

From an analysis of the detailed PM chemical composition (Figure 6.26 to Figure 6.29) corresponding to the total ambient PM_{2.5} changes presented in Figure 6.23, it can be deduced that the changes in PM_{2.5} mass in Canada were primarily driven by changes in PM_{2.5}-sulphate, PM_{2.5}-nitrate and PM_{2.5}-crystal material, and to a lesser extent PM_{2.5}-ammonium. The remaining chemical components modelled by AURAMS (elemental carbon, primary and

secondary organic carbon and sea salt) are not shown here as they only presented marginal differences. In general, looking at the changes of each chemical component individually, it is possible to relate most of the increase or decrease in ambient level to increases or decreases in the corresponding precursor emissions. In the Prairies however, these four PM chemical components increased despite the general decrease in precursors in the same area, suggesting that chemical reactions likely play an important role in the behaviour of the system.

The increases in PM_{2.5}-crustal material (Figure 6.29), a fairly non-reactive species which dominated the PM_{2.5} changes in Canadian urban centres, can be directly correlated to the increase in PM_{2.5} primary emissions, its only source, in the scenario (Figure 6.24). In most of the Windsor-Quebec City corridor, the PM_{2.5} crustal material component increased enough to result in local deteriorations of PM_{2.5} ambient levels, despite the general trend of decreasing PM_{2.5}-sulphate, PM_{2.5}-nitrate and PM_{2.5}-ammonium components in that area (Figure 6.26 to Figure 6.28). As it was the case for O₃, PM_{2.5}-sulphate, PM_{2.5}-nitrate and PM_{2.5}-ammonium levels decreased in eastern Canada as a result of the lower SO_x and NO_x emissions in Canada and even lower emissions in the CAIR U.S. states, but isolated increases in local emissions in western Canada only provided a partial explanation for PM_{2.5}-nitrate dominated increases in Alberta and Saskatchewan.

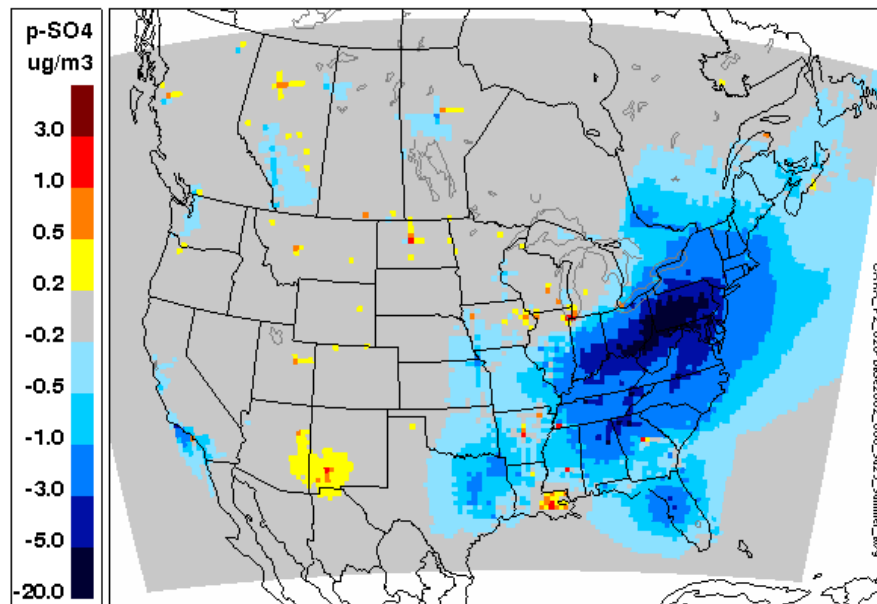


Figure 6.30 Differences in summer (June-July-August) 24-hour average PM_{2.5}-sulphate levels between the 2015 BAU simulation and the 2002 reference case. [S11]

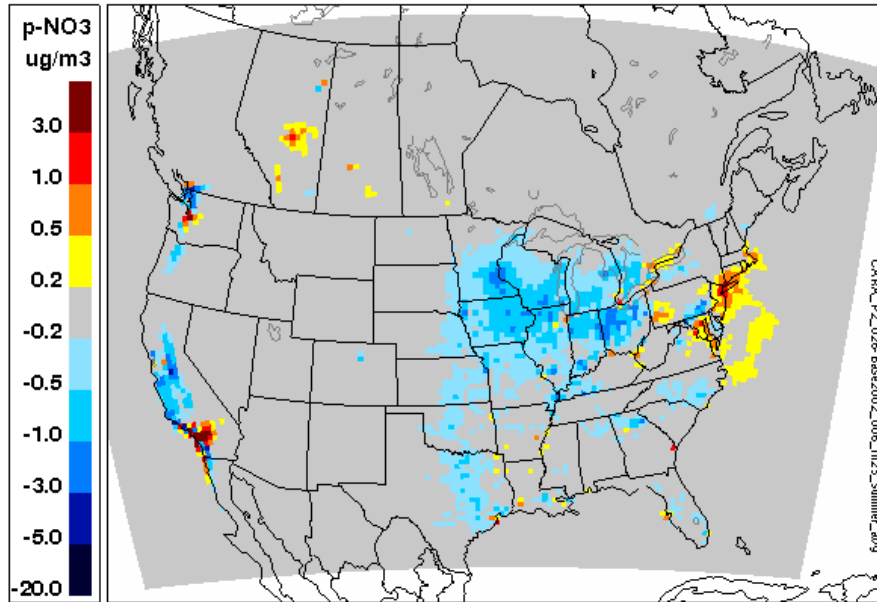


Figure 6.31 Differences in summer (June-July-August) 24-hour average PM_{2.5}-nitrate levels between the 2015 BAU simulation and the 2002 reference case. [S11]

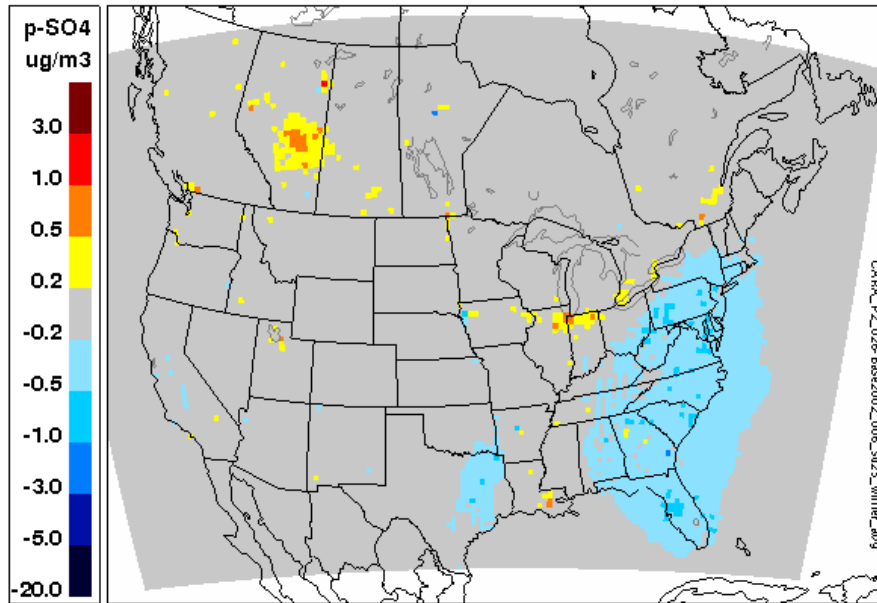


Figure 6.32 Differences in winter (January-February-March) 24-hour average PM_{2.5}-sulphate levels between the 2015 BAU simulation and the 2002 reference case. [S11]

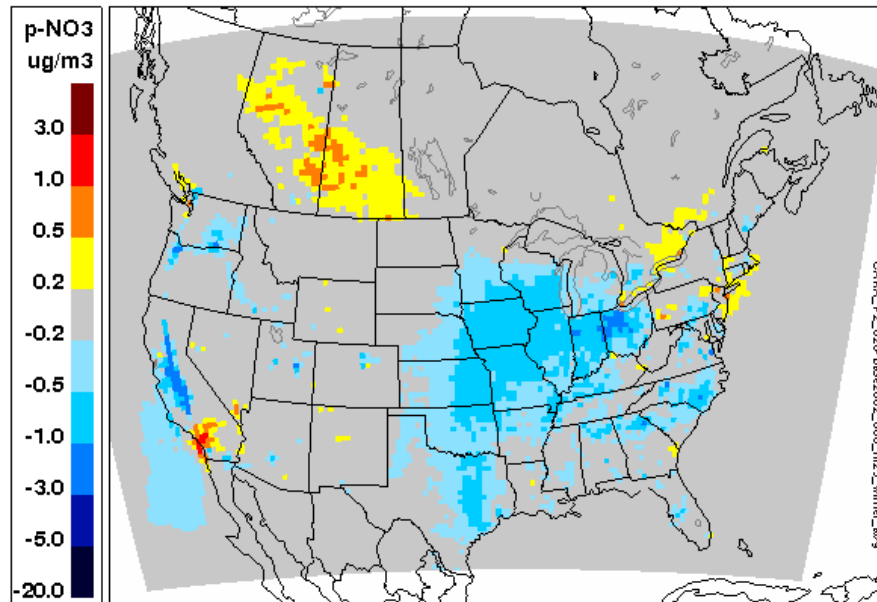


Figure 6.33 Differences in winter (January-February-March) 24-hour average PM_{2.5}-nitrate levels between the 2015 BAU simulation and the 2002 reference case. [S11]

A finer temporal analysis was necessary to obtain more insight on the predicted ambient PM_{2.5} trends. Figure 6.30 to Figure 6.33 present the summertime and wintertime changes in the average levels of PM_{2.5}-sulphate and PM_{2.5}-nitrate between the BAU simulation and the 2002 reference case. PM_{2.5}-sulphate levels were generally predicted to decrease across Canada, including in most of Alberta in the summer, while PM_{2.5}-nitrate levels were predicted to experience only a few local changes, decreasing in Southern Ontario and increasing in the vicinities of Vancouver, Edmonton and around Lake Ontario). In contrast to the summer situation, the winter averages (Figure 6.32 and Figure 6.33) showed very little change in the PM_{2.5}-sulphate levels in Canada except for an area in Central Alberta which coincides with local SO_x emissions increase in the vicinity of Edmonton, wide areas of increase of PM_{2.5}-nitrate levels in Alberta and Saskatchewan, and smaller increases in the Windsor-Quebec City corridor.

Under cold conditions, the formation of nitrate-based particles (ammonium nitrate) is favoured. Due to the non-linearity in the chemistry of the sulphate-nitrate-ammonium system, for each sulphate-based particle that disappears, up to two nitrate-based particles can form, resulting in most cases in an increase in total PM_{2.5} mass (Meng *et al.*, 1997). At this point however, we can only speculate that the local increases of NO_x emissions at a few point sources in Alberta and Saskatchewan (Figure 6.22) provide the necessary precursor species to support the winter chemistry.

Correlating the seasonal analysis with the predicted annual changes of ambient $PM_{2.5}$ (Figure 6.23), one can see that the increases in Alberta and the limited decreases in the Windsor-Quebec City corridor in the annual plot were the results of increases under winter conditions that were not necessarily offset by the summertime changes. Since this study was carried out, it was identified that the version of AURAMS used for S11 overestimated the amount of $PM_{2.5}$ -nitrate under certain conditions. Additional simulations are necessary to evaluate how much, if any, it affected the magnitude of the levels simulated in S11, especially in the winter. These results nonetheless suggest that wintertime regimes could play an important role in the response of ambient $PM_{2.5}$ to emission changes, and may need to be given more attention.

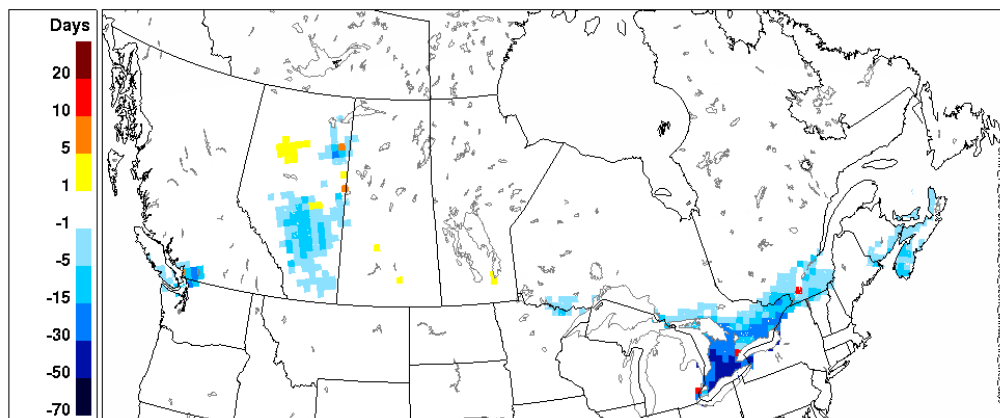


Figure 6.34 Differences in the number of CWS exceedance days for O_3 between the 2015 BAU simulation and the 2002 reference case. [S11]

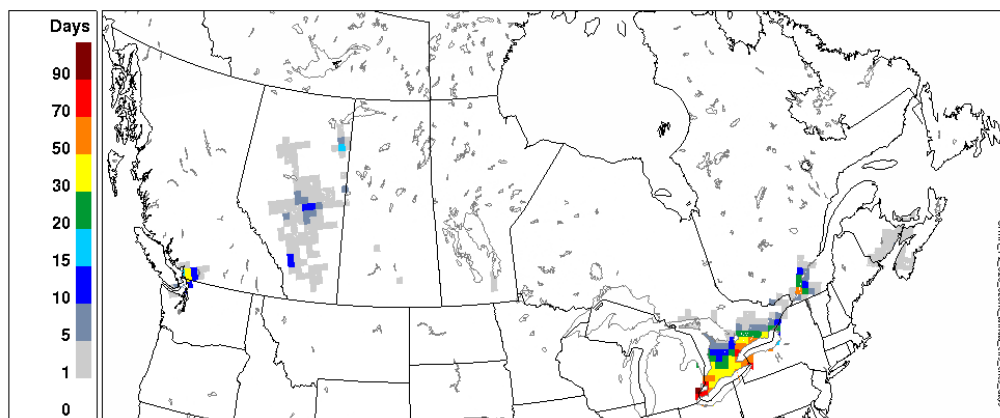


Figure 6.35 Number of O_3 CWS exceedance days for the 2015 BAU simulation. [S11]

Changes in the number of exceedance days of the CWS numerical value of 65 ppb for O_3 , as presented in Figure 6.34, largely correspond to the changes in the ambient levels. Large decreases in O_3 daily maxima were reflected by similar decreases in the number of exceedance days by more than 50% in southern Alberta (5 to 15 days less) and south-eastern Canada (15 to 30 days less, with decrease along lake Erie in excess of 30 days), while predicted increases of

O₃ daily maxima resulted in predicted increases in the number of CWS exceedance days. As for the 8-hour averaged daily maximum, the appearance of O₃ exceedances in northern Alberta in 2015 was the result of the misplacement of some emission sources and should be expected to occur further east. Despite the overall decrease in the number of exceedances, it was predicted that the vicinity of Vancouver, most of Alberta, southern Ontario and Quebec and part of Atlantic Canada would still experience exceedances of the O₃ CWS numerical values under the 2015 BAU scenario (Figure 6.35).

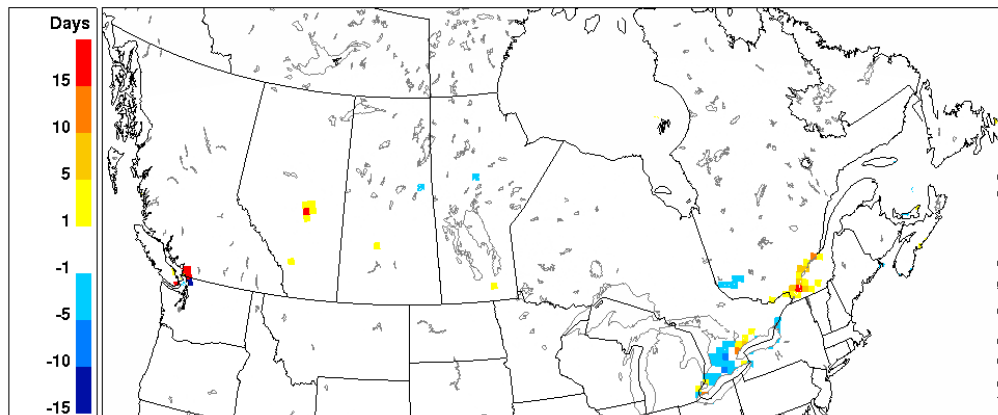


Figure 6.36 Differences in the number of CWS exceedance days for PM_{2.5} between the 2015 BAU simulation and the 2002 reference case. [S11]

In the case of PM_{2.5}, it was predicted that exceedances of the CWS numerical value of 30 µg m⁻³ for PM_{2.5} would increase in the large urbanized areas across Canada with the exception of south west Ontario (Figure 6.36). As outlined for the average ambient PM_{2.5} levels, there was a seasonal dependency to this behaviour, with the increases of the number of exceedances occurring mostly during the winter (not shown) and the decrease in southwestern Ontario reflecting summertime reductions of the PM_{2.5} levels (not shown). It should be noted that the 2015 BAU simulation did not predict the appearance of exceedances in new locations compared to the 2002 reference case but rather showed an increase in the frequency of exceedances in places already in exceedance of the PM_{2.5} CWS numerical value.

In summary, the comparison between the 2015 BAU simulation and the 2002 reference case suggested that O₃ and PM_{2.5} levels in Canada would evolve in different directions. While O₃ levels were generally predicted to improve as a result of combined reductions in precursor emissions in Canada and the U.S., PM_{2.5} levels were projected to improve in some areas but to deteriorate in others, in particular in large urbanized areas, despite the large projected reductions in U.S. emissions of primary PM_{2.5} and PM precursors. The analysis also implied that the projected increase in PM_{2.5} primary emissions in Canada could play a significant role in defining future levels of ambient PM_{2.5} and possibly modulating the improvements that might result from U.S. emission reductions. The analysis outlined the importance of

considering the influence of seasonality on the ambient $PM_{2.5}$ response to emission changes as the winter behaviour of the ambient $PM_{2.5}$ could be responsible for the deterioration that was predicted overall.

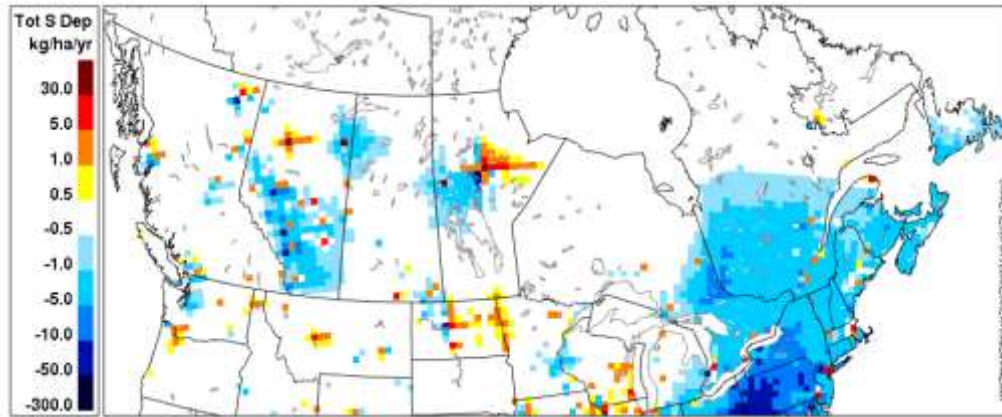


Figure 6.37 Difference in annual total sulphur deposition between the 2015 BAU simulation and the 2002 reference case. [S11]

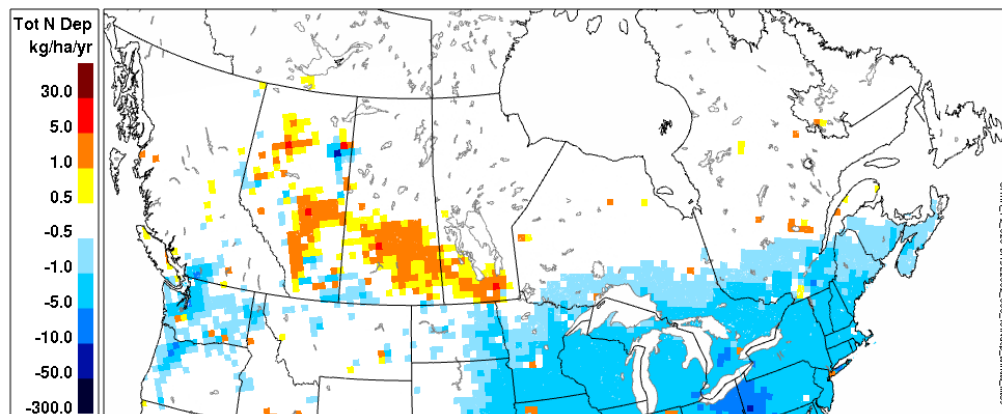


Figure 6.38 Difference in annual total nitrogen deposition between the 2015 BAU simulation and the 2002 reference case. [S11]

The predicted evolution of acid deposition between 2002 and 2015 closely followed the evolution of ambient $PM_{2.5}$ levels. The maps of the difference in total sulphur deposition and total nitrogen deposition between the 2015 BAU and the 2002 reference case (Figure 6.37 and Figure 6.38) presented the same east/west divide. Eastern Canada was predicted to experience a general reduction, with very few exceptions, of 1 to 5 kg/ha/yr (or 10 to 50%) in sulphur deposition levels and 1 to 5 kg/ha/yr (or 25 to 50 %) in nitrogen deposition. In western Canada, areas of reduction of sulphur deposition of 1 to 5 kg/ha/yr (or 25 to 50 %) with pockets of increases around major point sources were projected for Alberta and Manitoba, especially in the north of the provinces. Nitrogen deposition across most of Alberta and

Saskatchewan, on the other hand, was predicted to increase by 1 to 5 kg/ha/yr (or 10 to 50 %); this behaviour was associated with the predicted winter increase in ambient particulate nitrate across the same area.

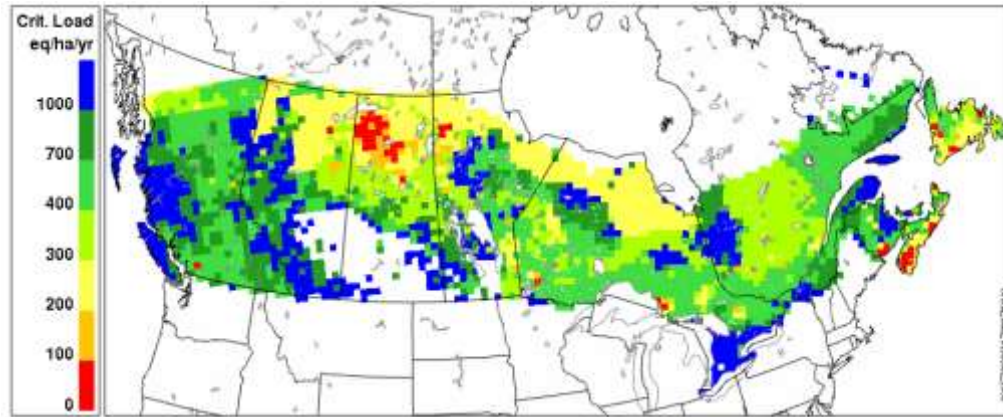


Figure 6.39 Combined aquatic and terrestrial critical load map for Canada. White regions on the map represent areas where no data is available. (Wong *et al.*, 2008). [S11]

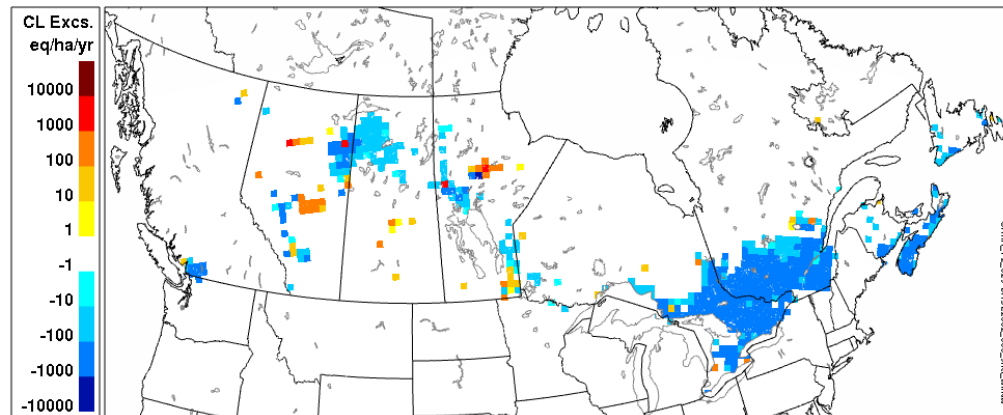


Figure 6.40 Difference in annual critical load exceedances for sulphur+nitrogen between the 2015 BAU simulation and the 2002 reference case based on critical load map from Wong and Dennis (2008). [S11]

Critical load exceedance maps for acid deposition (see Moran *et al.*, 2008 for methodology), were derived by combining the AURAMS deposition output with the latest aquatic and terrestrial ecosystem critical load map by Wong and Dennis (2008) (Figure 6.39). As a result of the lower deposition levels in the east, critical load exceedances were projected to decrease in major parts of Ontario, Québec and the Atlantic provinces for both sulphur (not shown) and sulphur + nitrogen (Figure 6.40). Additional exceedances were predicted in northern Manitoba around major point sources associated with the increased sulphur deposition in these areas. In northern Alberta, as with previous results, the projections of increases or decreases in critical load exceedances were affected by the misplacement of the few point sources west of the oil sands. In southern Alberta, Saskatchewan and Manitoba,

where most of the nitrogen deposition increase was predicted a lack of critical load data prevented the calculation of critical load exceedances. However from the calculations performed on the edges of the no-data area in the vicinity of Edmonton and in the few isolated locations with aquatic critical load data in Saskatchewan and Manitoba, the analysis suggest that increases in nitrogen deposition would lead to increase in the sulphur + nitrogen critical load exceedances for ecosystems in the southern part of the Prairies. Finally, sulphur + nitrogen critical load exceedances were also predicted to decrease in the vicinity of Vancouver due largely to the projected decreases in nitrogen deposition. Overall, critical load exceedances were projected to improve in most of eastern Canada, while the analysis pointed towards deterioration in a large part of western Canada.

6.4.2 Outlook on British Columbia Air Quality and PM_{2.5} and O₃ Levels

6.4.2.1 High-Resolution Business-As-Usual Projection For 2015

The projected levels of PM_{2.5} and O₃ under a 2015 Business-as-usual scenario similar to S11 were investigated in a high resolution study. The episodic simulations were performed with CMAQ at a 12-km spatial resolution over a domain encompassing the Pacific Northwest and at a finer 4-km spatial resolution on a sub-domain centred over the Georgia Basin and Puget Sound (Figure 6.7(b)). The 2015 emission fields for Canada were based on the same projection of the 2000 Canadian inventory as in S11; for the U.S. emission fields, a 2015 projection of the 2001 U.S. inventory were used. In both cases, the emissions were processed at a much finer resolution than in the case of S11 and would diverge from the S11 emission fields at the local scale. The simulations were performed for periods of August 9 to 31st 2001 and December 1 to 13th, 2002. The reference case used the 2000 Canadian inventory and 2001 U.S. inventory. Details of the model setup for this scenario analysis, labelled S12, are presented in the Appendix.

The high resolution results were in general agreement with the S11 results, but provided a more refined delineation of the areas where levels were projected to increase or decrease. Compared to the reference case, the 2015 summertime O₃ levels in the vicinity of Metro Vancouver, Whatcom County, and parts of Vancouver Island were predicted to increase due to weaker O₃ titration effects associated with a reduction of NO_x emissions in the local metro Vancouver area and Whatcom County. O₃ levels were on the contrary projected to decrease in the eastern Lower Fraser Valley, along the Strait of Georgia, and Juan de Fuca Strait, and Puget Sound as NO_x emissions in the Puget Sound and Seattle areas were projected to increase by 2015, leading to enhanced titration in that case.

In the case of $PM_{2.5}$, levels were predicted to increase significantly throughout the year and throughout the study domain, with the exception of Metro Vancouver, where $PM_{2.5}$ levels mostly decreased due to a projected reduction in the local NO_x and primary PM emissions. Projected increases in primary $PM_{2.5}$, NO_x and SO_2 emissions in the rest of the domain caused the overall increase in $PM_{2.5}$ levels.

6.4.2.2 Analysis of Legislated Standards for Motor Vehicles

The impact on ambient $PM_{2.5}$ levels of three sets of motor vehicle emission standards, which were set to come into force in 2004 and 2007, was investigated in a study centered over British Columbia for the projected year 2020 (Jiang *et al.*, 2004). Although the projection year was different in this scenario compared to S11 and S12, the analysis provided insights on the impact of the legislated vehicles standards which have a general relevance for all projected years beyond 2007.

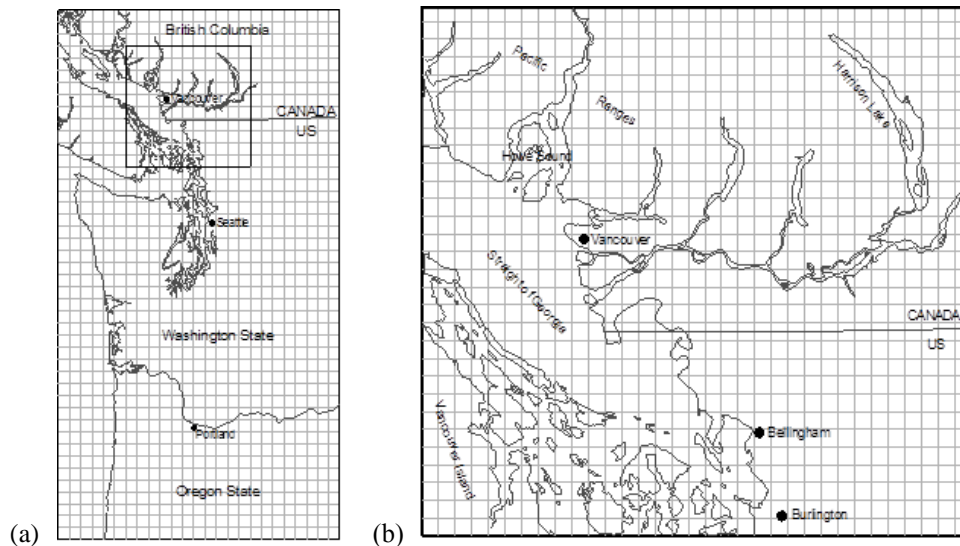


Figure 6.41 Modelling domains of the S13 scenario: (a) 15 km domain; (b) nested 5 km domain.[S13]

Four simulations, which included a 1993 reference case, a 2020 business-as-usual scenario, a 2020 no-mobile scenario, and a 2020 policy scenario combining the three on-road emission standards, were performed with CMAQ version 4.1. The modelling covered the period of July 31st to August 8, 1993. The domain consisted of an outer 15-km grid and a nested inner 5-km grid, as shown in Figure 6.41(a). The inner grid, encompassing an area of south-western British Columbia and north-western Washington, was centered on the Lower Fraser Valley region and the city of Vancouver (Figure 6.41(b)), and was the focus of the analysis.

Emissions for the 1993 reference case were generated by merging 1993 specific data (Levelton Engineering Ltd, 1995) with backcasted 1995 emission inventories for Canada and the U.S. Emissions for the 2020 business-as-usual scenario (FBA) were generated by projecting the 1993 reference case fields to 2020. They did not include any of the three vehicle emission standards being assessed, but reflected all current (as of 2004) and committed federal, provincial, and regional activities and measures, including existing on-road vehicle regulations. Emissions for the 2020 future no-mobile emissions scenario (FNM) were the same as for the FBA scenario except that all on-road mobile emission sources were removed. Finally, the 2020 future vehicle emission standard scenario (ES) built on the FBA scenario, where on-road mobile sources were modified to reflect the implementation of the following three vehicle emission standards (SENES/AIR, 2002): the light-duty Tier 2 vehicles standards; the heavy-duty vehicle (HDV) non-methane hydrocarbons and NO_x emission standards; and the HDV NO_x and PM emission and low sulphur on-road diesel standards. Details of the model setup for this scenario analysis, labelled S13, are presented in the Appendix.

Table 6.5 Total emissions and emission changes for the 1993 reference case (BA), 2020 business as usual scenario (FBA), implementation of mobile emission standard 2020 scenario (ES) and 2020 no-mobile scenarios (FNM). [S13]

Pollutant	Short Tons				% Change			
	BA	FBA	ES	FNM	FBA vs BA	ES vs FBA	ES vs BA	FNM vs FBA
NO _x	3709	1870	1056	876	-49.6	-43.5	-71.5	-53.1
VOC	9672	8942	8916	8756	-7.6	-0.3	-7.8	-2.1
SO _x	1034	1034	940	932	-0.1	-9.1	-9.1	-9.8
NH ₃	471	768	768	728	63.0	0.0	63.0	-5.2
PM _{2.5}	417	373	350	340	-10.4	-6.3	-16.0	-9.0
PM ₁₀	781	901	842	810	15.4	-6.6	7.8	-10.1
CO	14 157	6437	5684	2605	-54.5	-11.7	-59.8	-59.5

Table 6.5 summarizes the total emissions as well as the emission changes between the various simulations. From 1993 to 2020, NO_x emissions in the modelling domain were projected to drop by 49.6%, primary PM_{2.5} and VOC emissions by 10.4% and 7.6% respectively, while SO_x emission levels stayed mostly unchanged. With the implementation of the vehicle emission standards, 2020 NO_x emissions were projected to be further reduced by 43.5%, SO_x by 9.1%, and primary PM_{2.5} by 6.3%.

Table 6.6 Comparison of daily maximums of 24-hour rolling average PM_{2.5} concentrations averaged over entire modelling domain and simulation period for base case (BA), future base case (FBA), future no-mobile case (FNM), and future emission scenario (ES). [S13]

	BA	FBA	ES	FNM
Avg. of daily maximums of 24-hour rolling avg. ($\mu\text{g m}^{-3}$)	8.5	8.9	8.7	8.6
Absolute difference ($\mu\text{g m}^{-3}$)*	-	0.4	-0.2	-0.3
Relative difference (%)*	-	4.7 %	-2.2 %	-3.4 %

Table 6.7 Summary of exceedances over Canada-Wide Standard of 30 $\mu\text{g m}^{-3}$ for PM_{2.5} for reference case (BA), future base case (FBA), future no-mobile case (FNM), and future emission scenario (ES). [S13]

	BA	FBA	ES	FNM
Number of days with one exceedance (days)	6	3	2	2
Absolute difference (days)*	-	-3	-1	-1
Relative difference (%)*	-	-50.0 %	-33.3 %	-33.3 %
Percentage of days with one exceedance (%)	66.7	33.3	22.2	22.2
Absolute difference (%)*	-	-33.4 %	-11.1 %	-11.1 %
Relative difference (%)*	-	-50.0 %	-33.3 %	-33.3 %
Total grid cells with one exceedance (# grids)	27	54	28	21
Percentage of grid cells with one exceedance (%)	2.7	5.5	2.8	2.1
Total number of rolling periods in exceedance	376	526	338	280
Percentage of rolling periods in exceedance (%)	0.2	0.3	0.2	0.1

Table 6.6 shows the 24-hour average daily PM_{2.5} maxima for the four modelling scenarios averaged over the modelling domain and simulation period. The average daily maximum PM_{2.5} concentration increased by approximately 4.7% between 1993 and 2020. The implementation of the three emissions standards was predicted to reduce the average daily maximum PM_{2.5} levels by 2.2%, from the 2020 business-as-usual case, and by 3.4% if all on-road mobile emissions were removed. Table 6.7 summarizes how the changes in PM_{2.5} ambient levels translate into changes in exceedances of the Canada-wide standard numerical value for PM_{2.5}. In comparison to the 1993 reference case, there was a 50% reduction in the number of daily exceedances for the 2020 future business-as-usual case as well as a reduction in the average number of hours in exceedance per day. However, there is an increase in both the number of grid cells with one exceedance as well as the total hours in exceedance for the FBA scenario. This shows that although the daily exceedances have decreased for the simulation, the exceedances are more widespread spatially.

When the on-road emissions standards were implemented or on-road mobile emissions removed, there was a reduction of 33% in daily exceedances versus the future business-as-usual case. There were reductions in both the number of grid cells with exceedances and the total number of hours in exceedance of the CWS numerical value. However, the results showed that the average number of hours in exceedance per day was expected to increase for the ES scenario versus the FBA scenario.

In terms of O₃, the results showed a slight increase of 2% in O₃ levels in the 2020 business-as-usual case over the 1993 reference case. For both the ES and FNM simulations, increases in O₃ of approximately 6% were predicted in comparison to the 2020 business-as-usual case due, in all likelihood, to reductions in NO_x emissions resulting in less NO available for the titration of O₃. Correspondingly, both the number of grid cells with one exceedance of the O₃ CWS numerical value and the total number of hours in exceedance were predicted to increase with each successive modelling scenario, although all four modelling scenarios were predicted to have 3 days with at least one exceedance (not shown).

Overall, the three vehicle emission standards were predicted to decrease the number of daily exceedances of average PM_{2.5} concentration and the number of areas in exceedance in comparison to the 2020 business-as-usual case, but were expected to slightly increase O₃ concentrations in the year 2020 due to the reductions in NO_x emissions.

6.4.3 Outlook on Alberta Air Quality and PM_{2.5} and O₃ Levels

A projection of O₃ levels in Alberta was performed using CMAQ with emissions forecasted for the 2012-2015 timeframe, assuming a full implementation of current environmental legislations for 5 sectors of activities. The model domain for this scenario is depicted in Figure 6.9, and details of the model setup, labelled S14, are presented in the Appendix.

Emission projections for the electric power generation, chemical, refineries and cement sectors were based on work completed by Cheminfo (2007). Oil sands emission projections were prepared by RWDI (2003a) and updated with information provided in the Imperial Kearn Lake Project application (2005)³². Emissions for approved and proposed bitumen upgraders in Fort

³² The “Cumulative Effects Assessment” case from this environmental impact assessment, which includes approved and announced projects, was used to update the future case emissions.

Saskatchewan were taken from AMEC (2007)³³. Emission projections derived from Environmental Impact Assessments (EIAs) tend to be conservative, and in this particular case oil sands VOC emission projections were a factor of 4 lower than the national ones in S11 (projections for other pollutant emissions were similar). Emissions for the remaining sectors were kept constant at their reference case level. The choice to keep emissions constant was motivated by difficulties in spatially allocating the future emissions for the Upstream Oil and Gas sector. Cheminfo (2007) projected a small increase in NO_x emissions from that sector in the 2010-2015 timeframe and a sizeable decrease in VOC emissions. The impact of keeping this sector at the reference level was not fully assessed. Mobile emissions from on-road vehicles were also kept constant. It was expected that these emissions would continue to decline due to the phase-in of regulated improvements in emissions control, but that the decline would be partially offset by increasing population and vehicle-kilometres travelled.

Overall the future scenario amounted to projected provincial emissions increases of 25%, 19% and 18% for NO_x, SO₂ and VOCs, respectively. On a sectoral basis, emissions from the oil sands sector were expected to increase by over 450% for NO_x and 100% for VOCs by 2015, reflecting the expected increase in production. NO_x emissions from the electricity sector were projected to increase by approximately 20% in the future case, assuming some older plants would be shutting down and new plants coming online in other areas. Finally, emissions from the chemical sector were projected to increase by approximately 50% for NO_x and 10% for VOCs. This growth was primarily driven by the projected construction of new bitumen upgraders (refineries and upgraders outside of the Fort McMurray area are considered as part of the chemicals sector in the sector simulations) in the Redwater/Fort Saskatchewan area north-east of Edmonton.

A comparison of the assumptions in the projected emissions between S11 and S14 showed that two very different situations were examined. At the national level, the S11 scenario investigated the impact of NO_x, SO₂ and VOCs emissions reductions of 24%, 22% and 14% respectively and an increase of primary PM_{2.5} emission of 19%. For Alberta specifically, the S11 scenario amounted to increases of 6% in NO_x and 80% in primary PM_{2.5} emissions, and to decreases of 23% and 6% in SO_x and VOC emissions. Although the projected emission

³³ Emissions from the following approved and proposed upgraders in the Fort Air Partnership area (NE of Edmonton) were included in the future case simulation: BA Energy Heartland Upgrader, Petro-Canada Sturgeon Upgrader, North West Upgrader, Synenco Northern Lights Upgrader and the Shell Scotford Expansion

changes for the 5 sectors modified in S14 were of the same order of magnitude between the S11 and S14 studies (with the exception of a 4 time larger forecast for VOCs emissions from oil sands activities in S11), the S11 scenario included significant changes to emissions from the upstream oil and gas sector (-46% in SO_x and -22% in VOCs) and from the transportation sector (-58% for NO_x and -55% for VOCs). As a result, little comparison can be done of the projected ambient levels between the two studies, but both are informative of how Alberta levels would respond to the various scenarios.

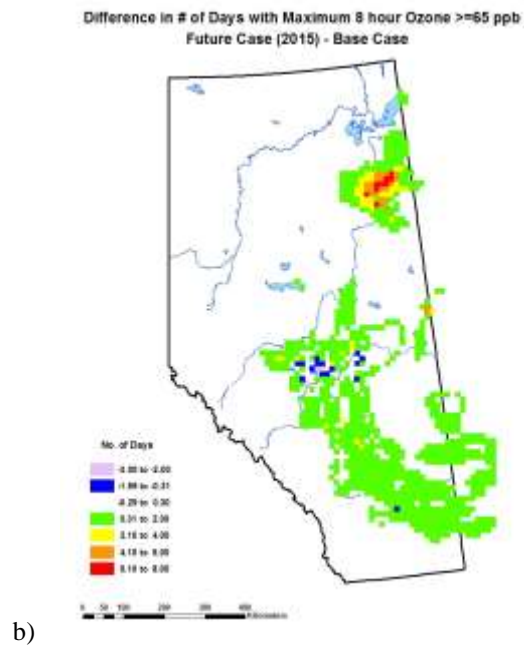
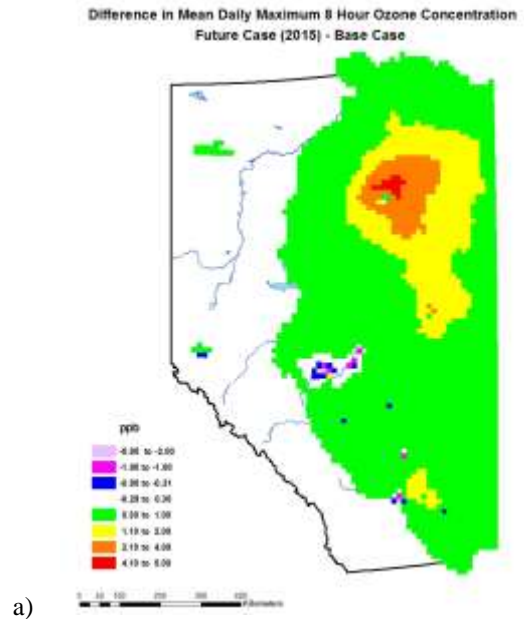


Figure 6.42 Difference over Alberta in (a) mean daily 8-hour O_3 maximum between the 2015 future case and the 2002 reference case; and (b) the number of days with 8-hour average $O_3 > 65$ ppb between the 2015 future case and the 2002 reference case. [S14]

Figure 6.42a presents the difference in the mean 8-hour averaged O_3 daily maximum between the projected S14 scenario and the 2002 reference case. The projected emissions generated a significant increase of 1 to 8 ppb in O_3 levels around the oil sands and a more modest increase

(0-2 ppb) over central and eastern Alberta. A small decrease in O₃ levels is predicted around Edmonton, presumably due to titration from increased NO_x emissions. Correspondingly, the difference in the number of days in exceedance of the CWS numerical value between the projected scenario and the 2002 reference case (Figure 6.42b) showed at least one extra exceedance day over a large area of central Alberta and a greatly increased area around the oil sands experiencing one or more additional exceedance days. The most robust feature of the scenario simulation was the projected increase in O₃ levels around Fort McMurray. Although the oil sands emissions used for the scenario in this study may have been conservative, nearly all projections for this area project a substantial increase in NO_x and VOC emissions from oil sands extraction and processing.

6.5 Projected Levels of PM_{2.5} and O₃ in Canada from Emission Reductions Above and Beyond Current Legislation

6.5.1 Outlook upon Implementation of Additional Nationwide Emissions Reductions

The effect of Canada-wide emission reductions above and beyond the ones imposed by current legislations (as discussed in section 0) were investigated with AURAMS for the emission year 2015. The study considered additional emission reductions in Canada only; emissions in the U.S. were kept at the 2015 reference level. Scenario results were analyzed in comparison to the 2015 Business-as-Usual case discussed in section 0. Details of the model setup for this scenario, which is identical to S11 except for the Canadian emission fields, are presented in the Appendix under label S15.

Table 6.8 Percentage reductions in the 2015 S15 emission levels in each of the 16 sectors compared to their 2015 BAU case levels (PM_{2.5} refers to primary PM_{2.5} emissions).[S15]

Sector	NO _x	SO _x	VOC	PM _{2.5}
Upstream Oil & Gas (excl. oil sands)	45%	14%	59%	0%
Oil Sands	41%	35%	50%	0%
Petroleum Refining	36%	68%	44%	71%
Pipelines	43%	43%	43%	43%
EGU by combustion	61%	58%	0%	73%
Alumina	0%	2%	24%	59%
Aluminum	2%	0%	1%	32%
Iron and Steel (incl. titanium)	65%	80%	70%	70%
Cement	49%	52%	1%	85%
Lime	8%	20%	1%	86%
Pulp and Paper	19%	40%	10%	19%
Wood Products	0%	1%	24%	60%
Chemicals (incl. fertilizers)	25%	0%	11%	1%
Iron Ore Pelletizing	30%	75%	0%	65%
Base Metal Smelters	0%	64%	19%	78%

Canadian NO_x, SO_x, VOCs and primary PM (including PM_{2.5}) emissions from 15 industrial sectors were reduced from their 2015 business-as-usual reference level. A full list of the sectors considered in this scenario along with the details of the emission reductions within each sector is provided in Table 6.8. Overall, this scenario represented a 41% reduction in the 2015 Canadian SO_x emissions, and a 23%, 16% and 6% reduction in the NO_x, VOCs and primary PM_{2.5} Canadian emissions, respectively.

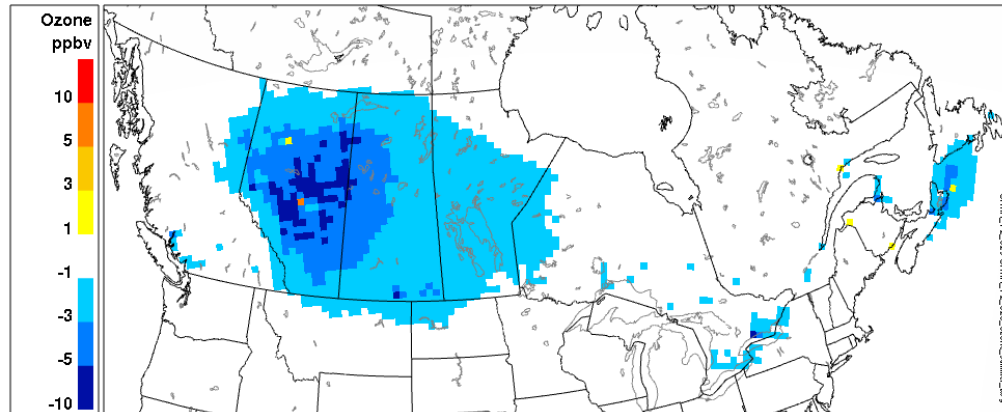


Figure 6.44 Change in average summertime daily 8-hour O₃ maximum (in ppb) between the S15 scenario and the BAU case (S15 scenario minus 2015 BAU). [S15]

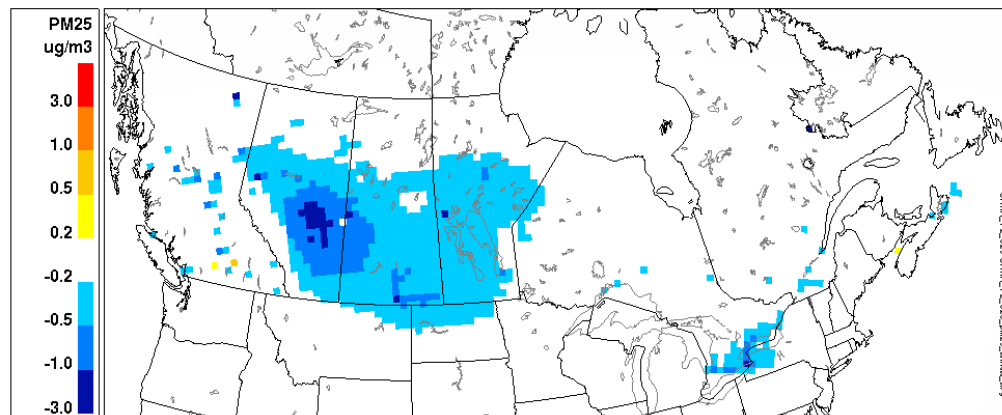


Figure 6.45 Change in annual PM_{2.5} levels (in $\mu\text{g m}^{-3}$) between the S15 scenario and the BAU case (S15 scenario minus 2015 BAU). [S15]

Figure 6.44 and Figure 6.45 present the changes in the summertime O₃ and annual PM_{2.5} ambient levels that were predicted to occur as a result of the emission reductions. AURAMS predicted a fairly widespread improvement in the summertime daily 8-hour O₃ maxima levels in the Prairies, ranging from 1 to 3 ppb (i.e. 5 to 10%) with higher levels of improvements exceeding 5 ppb in a large portion of Alberta. In the densely populated areas which generally experience higher O₃ levels, in the vicinity of Vancouver, in the Windsor-Quebec City corridor and in the Maritimes, the predicted improvements were marginal and only exceeded 3 ppb or 5% in a single location east of Toronto.

PM_{2.5} levels presented similar features with the largest improvements predicted in the Prairies (exceeding 1 $\mu\text{g m}^{-3}$ or 10% in central Alberta). The magnitude of the improvements in the Windsor-Quebec City corridor was larger than in the case of O₃ (ranging from 0.2 to 1 $\mu\text{g m}^{-3}$ or 2 to 30%) but the Maritimes and Vancouver area were only projected to experience marginal improvements on an annual basis (Figure 6.45).

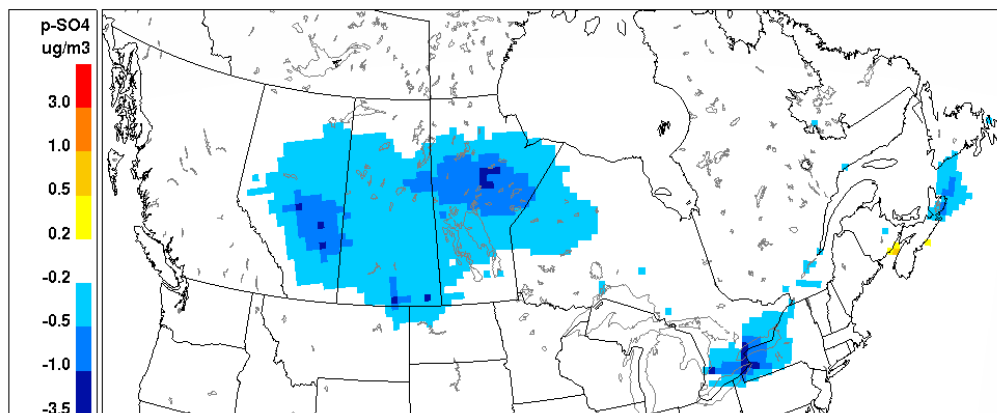


Figure 6.46 Change in average summer fine particle sulphate level (in $\mu\text{g m}^{-3}$) between the scenario and the BAU (S15 scenario minus 2015 BAU). [S15]

Changes in $\text{PM}_{2.5}$ ambient levels corresponded largely to decreases in secondary particulate matter and its components. On an annual basis, decreases in sulphate levels drove the improvements in $\text{PM}_{2.5}$ ambient levels in all areas across the country (not shown). This was in turn associated with the large and sulphate dominated improvements predicted for the summer period (Figure 6.46). More moderate improvements were predicted in the winter and, in that case, were exclusively driven by decreases in nitrate (not shown). In areas such as Alberta and Northern Manitoba, where the amount of chemically formed particles dropped by 5 to 30 percentage points (not shown), a shift in the chemical composition of the particles was projected. This shift meant that the primary fraction, which is directly correlated to primary emissions, became an equal fraction of the $\text{PM}_{2.5}$ mass. In the Windsor-Québec City corridor, the ratio of primary versus secondary formed particles remained largely unchanged, with secondary particles dominating the composition. A shift in the primary versus secondary nature of the particles could necessitate a different approach, with more emphasis on primary PM emissions, to further reduce air pollution in these areas.

Additional analyses were performed to better understand the role played by emission reductions in each sector in the atmospheric response. Three additional simulations were studied, with the following perturbations applied to the emission field: 1) emission reductions for the Oil and Gas sectors (including Upstream Oil and Gas, Petroleum Refining and Oil Sands) omitted, other sectors as per Table 8; 2) emission reductions for the Smelting and Electricity Generation sectors omitted, other sectors as per Table 8; 3) emission reductions for all but the Oil and Gas, Smelting and Electricity Generation sectors omitted (as per Table 8). When emission reductions were omitted in a simulation, emissions from that sector were set at their 2015 reference levels.

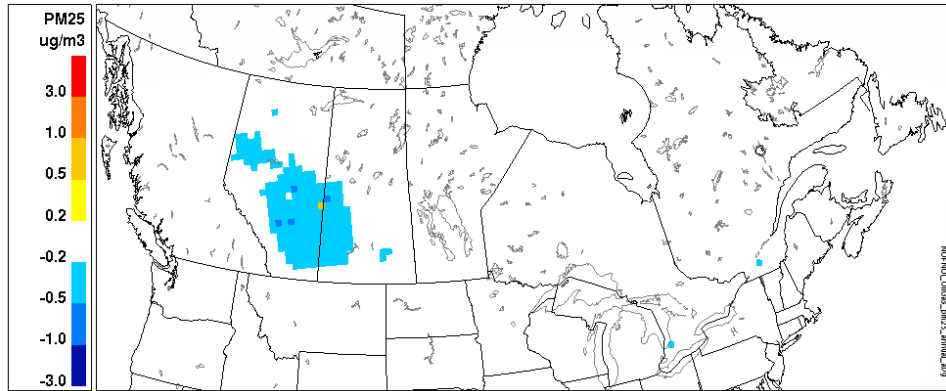


Figure 6.47 Change in annual $PM_{2.5}$ levels (in $\mu g m^{-3}$) between S15 scenario and the no-oil-and-gas emission reduction scenario (S15 scenario minus S15 scenario with no oil and gas reduction). [S15]

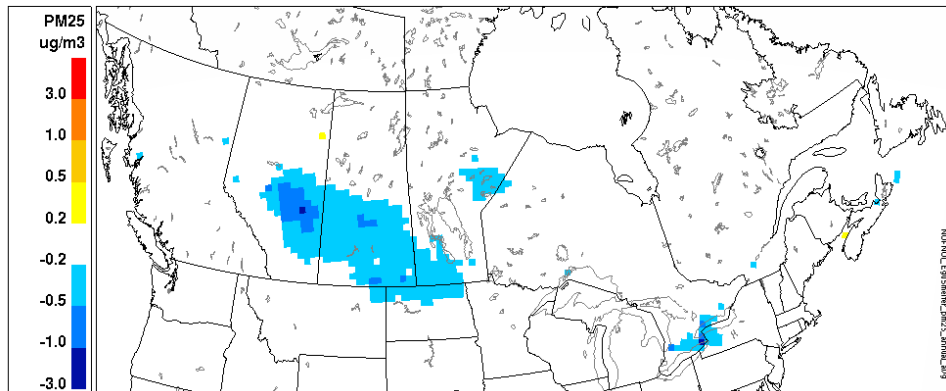


Figure 6.48 Change in annual $PM_{2.5}$ levels (in $\mu g m^{-3}$) between the S15 scenario and the no-smelting-and-electricity generation industries emission reduction scenario (S15 scenario minus S15 scenario with no smelting-and-electricity generation reduction). [S15]

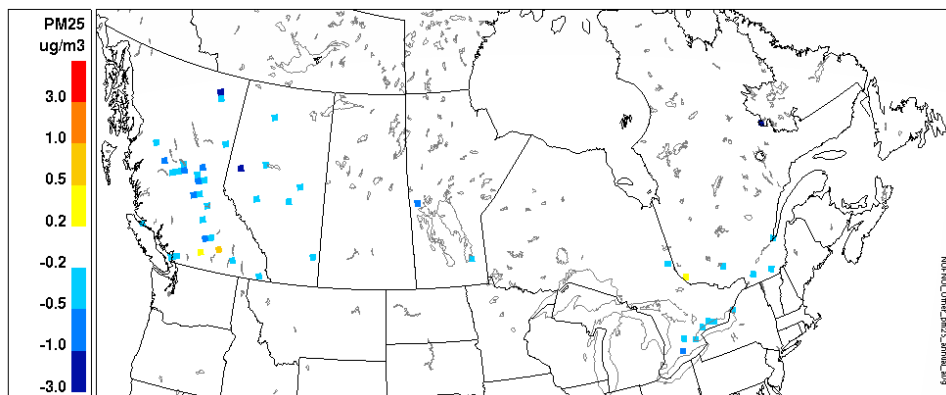


Figure 6.49 Change in annual $PM_{2.5}$ levels (in $\mu g m^{-3}$) between the S15 scenario and the no 'other sectors' emission reduction scenario (S15 scenario minus S15 scenario with no 'other sectors' reduction). [S15]

Figure 6.47 to Figure 6.49 present the results of these additional analyses. Each figure isolates the contribution that can be linked to the emission reductions in the sector or sectors being examined. Figure 6.47 suggests that emission reductions in the Upstream Oil and Gas sector were responsible for a large fraction of the decrease in ambient $PM_{2.5}$ shown in Figure 6.45, but solely in Alberta. In other parts of the country, emission reductions in the Upstream Oil and Gas sector did not generate changes in ambient levels in excess of $0.2 \mu g m^{-3}$, with the exception of two isolated locations along the Windsor-Quebec City Corridor. The impact of emission reductions in the electricity generation and smelting sectors on ambient $PM_{2.5}$ levels were far more wide-ranging (Figure 6.48). It was associated with changes in large parts of Alberta, Saskatchewan, Manitoba and Ontario. In areas where the impact of emission reductions from the Oil and Gas sector were also important, the magnitude of the impact of emission reductions in the Electricity Generation and Smelting sectors was larger (in the particular emission reductions scenario studied here). The impact of emission reductions in the remaining sectors (Figure 6.49) was much lower and spatially dispersed over the domain. It should however be noted that, especially in the east, it was associated with changes in ambient $PM_{2.5}$ levels in the major cities and hence had the potential to impact densely populated areas.

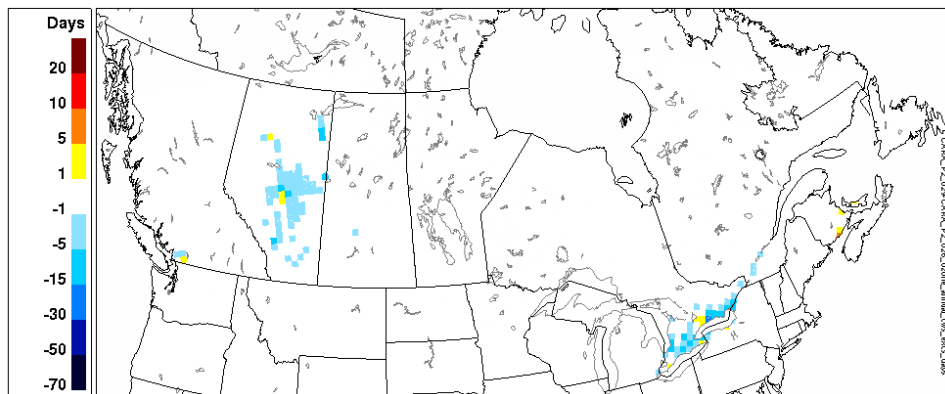


Figure 6.50 Difference in the number of CWS exceedance days for O_3 (S15 scenario minus 2015 BAU). [S15]

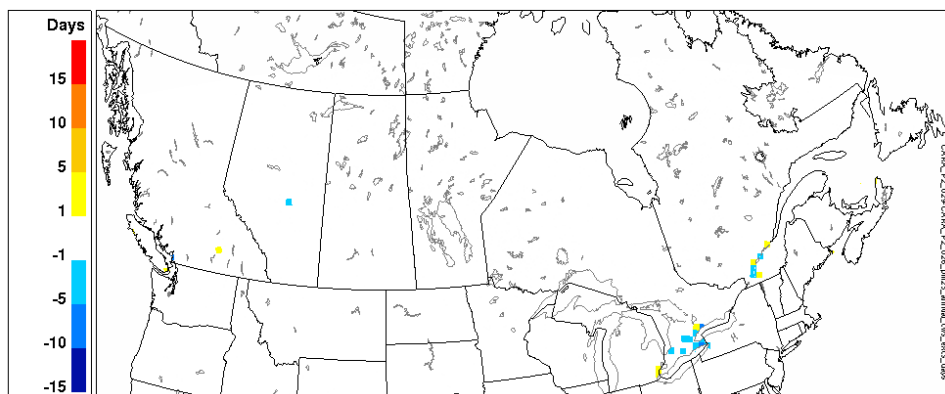


Figure 6.51 Difference in the number of CWS exceedance days for $PM_{2.5}$ (S15 scenario minus 2015 BAU). [S15]

From a CWS perspective, the emission reductions in the S15 scenario resulted in a general decrease by 1 to 10 days of the O₃ exceedance days (Figure 6.50). The largest decreases were projected to happen in the Windsor-Quebec City corridor, then Alberta and the vicinity of Vancouver. A few scattered places were projected to experience 1 to 3 additional exceedances; with the exception of Edmonton and Peace River, these increases have no equivalent in the mean daily 8-hour O₃ maximum (Figure 6.44) and hence would be related to a slight displacement of the location of some exceedances rather than the occurrence of new exceedances. Emission reductions also decreased the number of exceedances of PM_{2.5} in the Edmonton and Montréal vicinities and the Hamilton-Toronto area (Figure 6.51). As for O₃, a few isolated increases in the number of exceedances, located in the same vicinities as decreases, suggested a slight change in the locations experiencing the exceedances. For both PM_{2.5} and O₃, the emission reductions presented here had the potential to lower the number of CWS exceedance days.

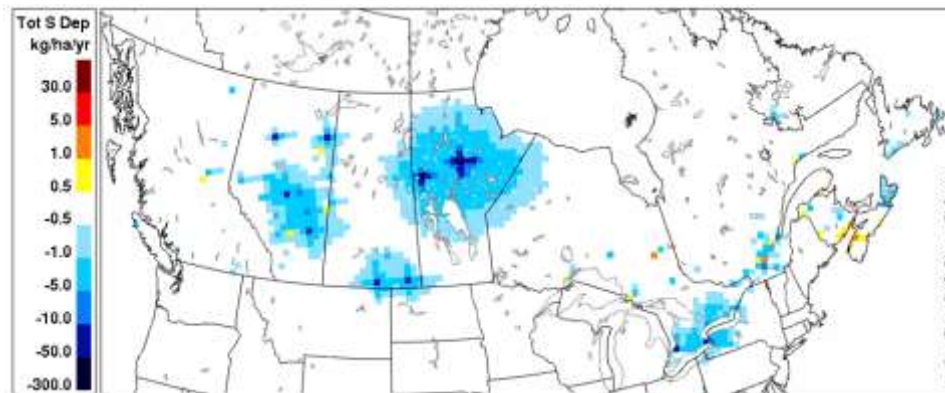


Figure 6.52 Changes in total sulphur deposition in eq/ha/yr (S15 scenario minus 2015 BAU). [S15]

The S15 emission reductions also resulted in significant decreases in sulphur deposition of the order of 0.5 to 5 kg/ha/yr in large regions of Alberta, southern Saskatchewan and the Windsor-Quebec City Corridor (Figure 6.52). In Manitoba, the projected reductions exceeded 50 kg/ha/yr at their peak (more than 50%) and the area affected by reductions up to 5 kg/ha/yr covered the entire northern half of the province. The decreases amounted to a 10 to 50% reduction in total sulphur deposition levels across most of western Canada, and to a 10 to 30% reduction in the Windsor-Quebec City corridor. In eastern New Brunswick and Nova Scotia however, the model predicted an increase in total sulphur deposition which seemed to be associated with an isolated emission source increase. Projected changes in total nitrogen deposition presented a similar pattern with decreases in western Canada and the Windsor-Quebec City corridor (amounting to 5 to 30% across much of western Canada, but less than 5% in eastern Canada) and increasing slightly in Nova Scotia (nitrogen deposition map not shown).

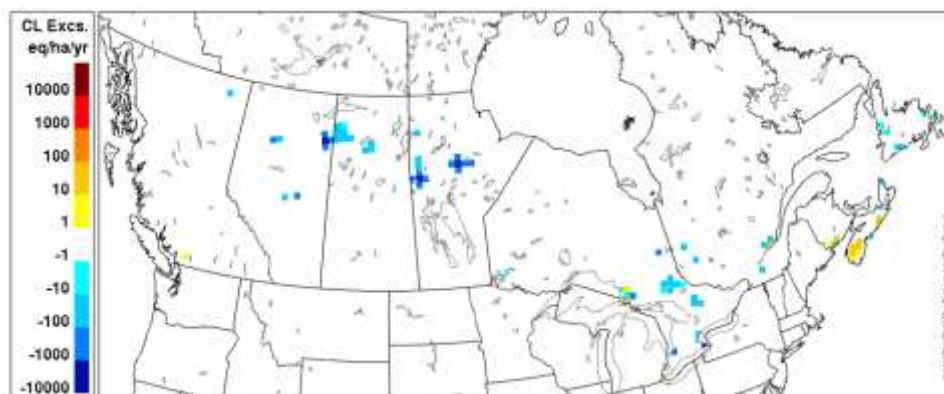


Figure 6.53 Changes in total sulphur critical load exceedances between (S15 scenario minus 2015 BAU), based on critical load map from Wong and Dennis (2008). [S15]

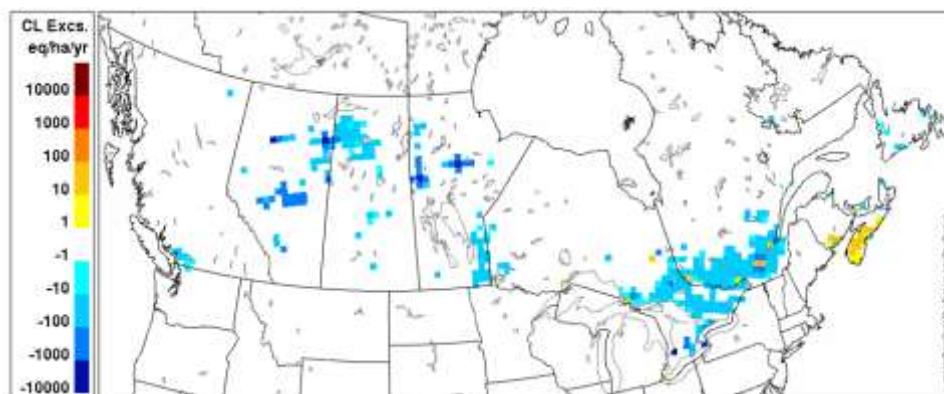


Figure 6.54 Changes in total sulphur + nitrogen critical load exceedances (S15 scenario minus 2015 BAU), based on critical load map from Wong and Dennis (2008). [S15]

The resulting projected changes in the number of critical load exceedances are presented in Figure 6.53 and Figure 6.54. Due to a lack of critical load data in southern Alberta, Saskatchewan and Manitoba, changes in critical load exceedances in these areas could not be calculated (see Figure 6.39 for coverage of critical load data). The emission reductions underlying the S15 scenario were projected to lower the number of critical load exceedances for both sulphur and sulphur + nitrogen metrics except in Nova Scotia and a few scattered locations in the vicinities of Quebec City, Algoma and Vancouver. In the case of both metrics, the emission reductions were not sufficient to completely eliminate exceedances of critical loads in Canada (not shown), but would decrease the magnitude of the exceedances and the extent of the geographical areas that are affected.

6.5.2 Outlook upon Implementation of Additional Provincial Level Emissions Reductions

Two emission reduction scenarios above and beyond reductions imposed by current legislation were investigated in British Columbia. The first scenario (S16) studied the impact of reductions from two point sources in the metro Vancouver area in 2015. The second scenario, also set in 2015, investigated a broader regional air quality management plan (S17) which includes the point source reductions in the first scenario as well as emission reductions in the marine and non-road sectors. A 12-km resolution modelling domain stretching from central Oregon to central British Columbia and from western Idaho to the Pacific Ocean was used to drive a nested 4-km fine resolution sub-domain centred over the Georgia Basin and Puget Sound (Figure 6.7 (b)). The meteorological periods chosen for the studies were a typical summer period (August 09-31, 2001) and a typical winter period (December 01-13, 2002). The emissions for the reference case as well as for all other sources not affected by the reductions were 2015 projections. Details of the model setup for these two scenarios, labelled S16 and S17, are presented in the Appendix.

The S16 scenario was designed to investigate the impact of emission reductions from modest point sources in the Metro Vancouver area. Specifically, NO_x was reduced at two plants by 2100 tonnes, and SO_x and $\text{PM}_{2.5}$ from refineries by 850 tonnes and 50 tonnes, respectively. These reductions amounted to decreases of approximately 2%, 1% and 0.1% respectively of all emissions within the modelling domain. The emission reductions had minor impacts on O_3 levels. Generally speaking, when O_3 levels were in the higher ranges (> 40 ppb), the O_3 reductions amounted to 0 to 2 ppb, and where O_3 levels were low or at baseline levels in the vicinity of Metro Vancouver, modest O_3 increases of up to 9 ppb were predicted. The impact on ambient $\text{PM}_{2.5}$ levels was also very limited with maximum reductions of hourly $\text{PM}_{2.5}$ levels not exceeding $5 \mu\text{g m}^{-3}$ in summer and $11 \mu\text{g m}^{-3}$ in winter. The small emission reductions that were modelled here were likely at the limit of the model capacity and results should be considered with caution.

The S17 scenario was designed to study the impacts of a potential air quality management plan in the major Vancouver metropolitan region. Three areas of reductions were considered: reductions from the point sources investigated in S16; reductions in the marine sector from the use of low sulphur fuel for ocean-going vessels, increased use of shore power for hotelling operations, retrofitting of BC Ferries with emission controls, and re-powering and retrofitting of working harbour vessels; and reductions in the non-road sector arising from the use of diesel oxidation catalysts in non-road engines and re-powering. These three sets of reductions were applied to the Canadian portion of the lower Fraser Valley, namely Metro Vancouver and the Fraser Valley Regional District. The reductions amounted to decreases, relative to the total emissions within the modelling domain, of 8% in NO_x emissions, 6% in VOC emissions, 11% in SO_2 emissions and 2% in $\text{PM}_{2.5}$ emissions.

The S17 scenario resulted in a moderate increase in hourly O₃ levels extending from the marine seaways to the Metro Vancouver areas as lower NO_x emissions in these areas weakened the titration of already formed O₃ (that is either transported to or pooled in these locations). Correspondingly, small areas of decreased O₃ levels occurred just downwind of the areas experiencing the increases. In those cases, less NO_x is available to form the O₃ that is otherwise generated from emissions of precursors from these sources. Net hourly differences between the scenario and the 2015 reference case ranged from -6 ppb to +16 ppb and vary greatly depending on location, day and hour. The inland extent of the impact was limited, illustrating the relative importance of marine emission reductions to the other modelled reductions. Ambient levels of PM_{2.5} were also reduced with both the primary and secondary components (mainly nitrate and sulphate) decreasing across the domain in both the summer and winter modelling periods. Decreased emissions affected not only local PM_{2.5} levels near the emission source region but also ambient levels in downwind areas. Summertime net hourly differences ranged anywhere between 0 µg m⁻³ to -18 µg m⁻³ in and around the coastal and downtown areas of Vancouver. Wintertime hourly PM_{2.5} levels decreased by as much as 18 µg m⁻³ (December 02, 2002). Further modelling and analysis would be needed to evaluate the impact of the S17 emission reduction scenario on the seasonal O₃ maxima, annual PM_{2.5} levels and CWS exceedances.

6.6 Transboundary Influences on PM_{2.5}, O₃ and Smog Precursors

6.6.1 Modelling Methodology for Transboundary Impact Studies

Recent Canadian studies of the transboundary influences on PM_{2.5} and O₃ levels have largely been performed with zero-out simulations. In these studies, all anthropogenic emissions from a given source of interest (sector of activity or geographical area) are set to zero. Results from the simulation with the zeroed emissions are then compared to the results from an unperturbed simulation. The difference between the two simulations provides an estimate of the effects of the emissions from the source region of interest. Although not a quantitative method, this approach provides a first order approximation of the quantity of emissions and/or secondary pollution from a given source region and the distance these travel. In the studies discussed in this section, zero-out simulations have been used to estimate the transboundary influence of Canada on the United States and vice-versa. Similar approaches have also been used to derive estimates of inter-provincial transport and transboundary transport at the local scale.

6.6.2 Influences of Canadian Emissions on PM_{2.5} in the U.S.

The impact of Canadian emissions on PM_{2.5} ambient levels in the U.S. has been the focus of 3 different studies. The first two studies, S18 and S19, were performed with CHRONOS for 2003 and 2004 summers using the 1995 Canadian and 1999 U.S. emission inventories, while the third study (S20) used AURAMS to assess transboundary flows under future conditions (represented by 2015 projected emission inventories for Canada and the U.S.). In the S20 study, the reference meteorological year was 2002. Details of the modelling set-up for these three studies are provided in the Appendix.

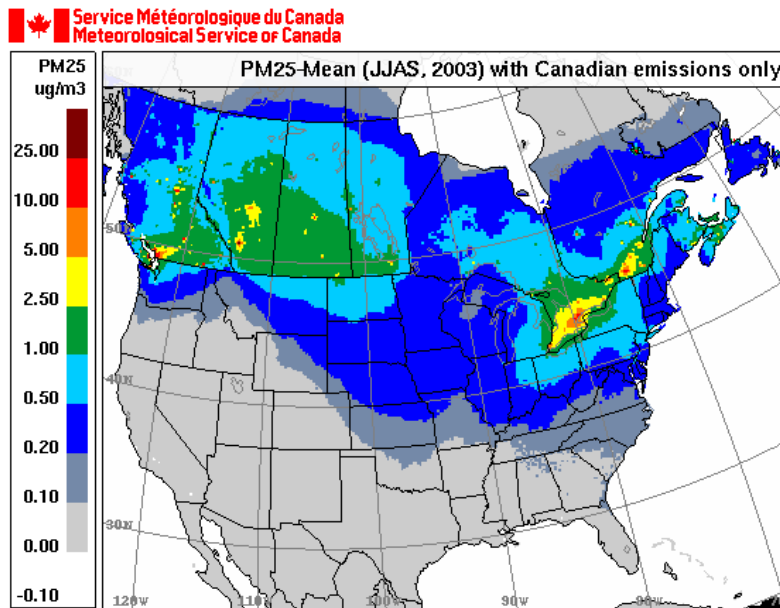


Figure 6.55 Composite map of the influence of Canadian emissions on PM_{2.5} levels in the U.S. for summer 2003 (expressed as relative sensitivity of PM_{2.5} levels in $\mu\text{g m}^{-3}$). [S18]

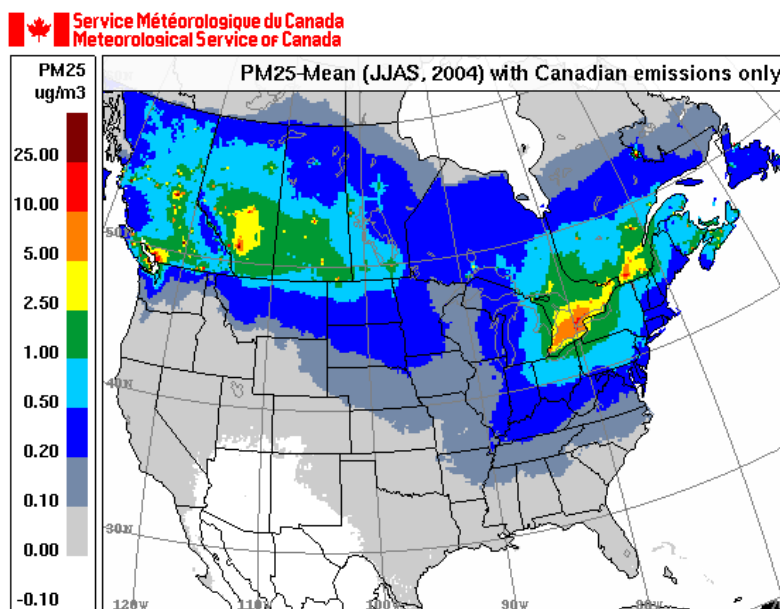


Figure 6.56 Composite map of the influence of Canadian emissions on PM_{2.5} levels in the U.S. for summer 2004 (expressed as relative sensitivity of PM_{2.5} levels in $\mu\text{g m}^{-3}$). [S19]

Figure 6.55 and Figure 6.56 present maps of the influence of Canadian emissions on U.S. PM_{2.5} ambient levels for the 2003 (S18) and 2004 (S19) summers, respectively. The maps were compiled from a series of CHRONOS provincial zero-out simulations, each providing the influence of a given province on its neighbours. The results of the individual simulations were then assembled to obtain composite image of an overall Canadian area of influence. The composite map was created by taking the maximum influence calculated from any of the individual simulations in any given location. The maps allowed the identification of U.S. areas that are sensitive to changes in Canadian emissions and provided a first estimate of their level of sensitivity. Assuming that reductions of ambient PM_{2.5} mean levels in excess of $0.2 \mu\text{g m}^{-3}$ were significant³⁴. Figure 6.55 and Figure 6.56 showed that the significance of transboundary transport of Canadian pollution to the U.S. varied across the country. Directly south of British Columbia, transboundary transport appeared limited spatially, while Canadian emissions appeared to significantly influence ambient PM_{2.5} levels as far south as Nebraska in the south central plains and Kentucky and Virginia in the east.

³⁴ The threshold of $0.2 \mu\text{g m}^{-3}$ is identical to the criteria used by the U.S. EPA for the establishment of the Clean Air Interstate Rule (CAIR).

There were notable fluctuations in the spatial extent of the influence of Canadian emissions between the S18 and S19 scenarios. These differences were directly attributed to variations in meteorology between 2003 and 2004 since both modelling studies were performed with the same model CHRONOS and the same emission input (see Appendix). In particular, while transboundary flows from the Canadian Prairies were consistently transported to the south east of the prairies, the spatial extent of the flows in the U.S. varied by up to 500 km between the two summers. In the east however, transboundary flows from Ontario and Quebec seemed more consistent from one year to the next.

Generally speaking, it was inferred from S18 and S19 that Canadian emissions influence ambient $PM_{2.5}$ levels in most of the northern half of the U.S., but that the magnitude is relatively limited, reaching 10 times the threshold of $0.2 \mu\text{g m}^{-3}$ at its maximum directly across from Lakes Erie and Ontario and in the Puget Sound area in British Columbia.

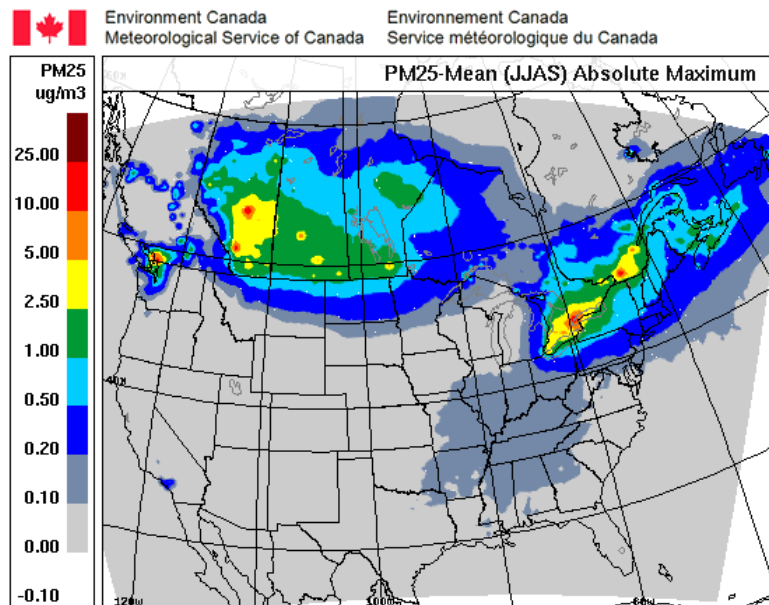


Figure 6.57 Composite map of the projected influence of Canadian emissions on $PM_{2.5}$ levels in the U.S. in 2015 during summertime (expressed as relative sensitivity of $PM_{2.5}$ levels in $\mu\text{g m}^{-3}$). [S20]

The S20 AURAMS study investigating Canadian emissions' influence on ambient U.S. $PM_{2.5}$ levels in the future (2015) confirmed that northern American states would continue to experience transboundary flows in the future, and at levels projected to be similar to today's levels (Figure 6.57). This particular study did not consider any of the proposed regulations that are being assessed as part of the Turning the Corner Plan.

While Figure 6.55, Figure 6.56 and Figure 6.57 present contrasting information as to the spatial extent of the influence of Canadian emissions in the U.S., and especially south of the Prairies, it should not hastily be concluded that the differences are solely the results of a

decrease in Canadian emissions between the 1995 inventory used in the CHRONOS studies S18 and S19 and the 2015 projected inventory used in the AURAMS study S20. In fact, on a national basis, primary $PM_{2.5}$ and VOC emission levels are similar between 1995 and 2015, and only SO_x and NO_x emissions decreased by approximately 20% between the two inventories (PDB: <http://www.ec.gc.ca/inrp-npri>). Other differences between the studies included different representations of PM processes and different meteorological years (2002 versus 2003 and 2004), which had a direct impact on the spatial extent as discussed previously in the context of the S18 and S19 CHRONOS analyses. As a result, it is difficult to ascertain without additional simulations which one of these factors is predominantly responsible for the differences.

Nonetheless, all three studies agreed on the fact that Canadian emissions had an influence in the U.S. almost continuously across the border, with the strongest influence, in absolute terms, south of Ontario and Quebec. In addition, the magnitude of the changes above the significance criteria of $0.2 \mu g m^{-3}$ induced by zeroing out Canadian emissions, was estimated to range from 0.2 to $2.5 \mu g m^{-3}$, translating into variations of U.S. $PM_{2.5}$ ambient levels of 5 to 30% on a seasonal basis.

6.6.3 Influence of U.S. Emissions on $PM_{2.5}$ in Canada

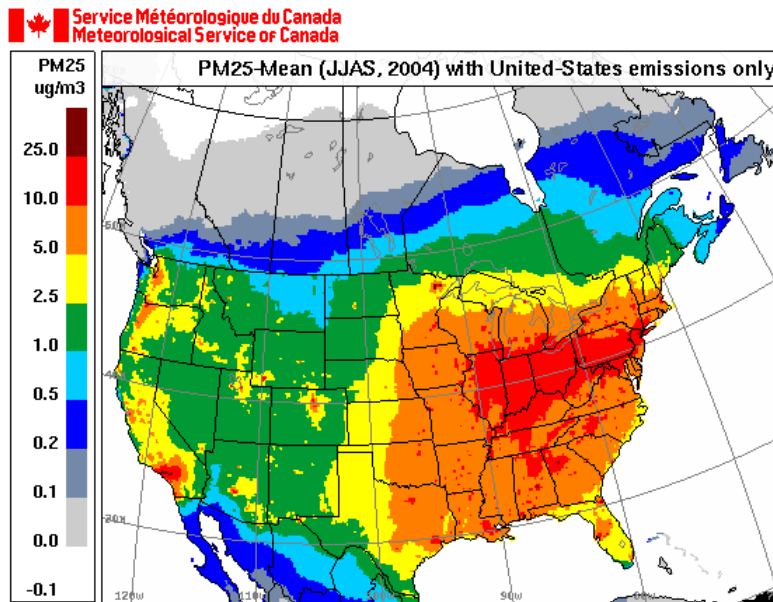


Figure 6.58 Map of influence of U.S. emissions on Canadian $PM_{2.5}$ levels in Canada for summer 2004 (expressed as relative sensitivity of $PM_{2.5}$ levels in $\mu g m^{-3}$). [S19]

The influence of U.S. emissions on Canadian $PM_{2.5}$ ambient levels were analysed in the same three studies S18, S19 and S20 described above. Due to the similarities between the results of S18 and S19, only the S19 and S20 are discussed in this section. The map of influence of U.S. emissions in Canada resulting from the S19 CHRONOS zero-out simulations for the summer 2004 is depicted in Figure 6.58. There were two distinct patterns identified across Canada. In the four western provinces, transboundary flows from the U.S. were estimated to be of the same magnitude as the ones from Canada. Their impact was generally characterized by variations in $PM_{2.5}$ ambient levels between 0.2 and $1.0 \mu\text{g m}^{-3}$, with a peak above $1.0 \mu\text{g m}^{-3}$ at the border between Puget Sound and the Georgia basin in British Columbia, and a spatial extent generally within 500 km of the border. In contrast to the situation western Canada, eastern provinces were estimated to have a much higher level of sensitivity to U.S. emissions. In Ontario and Quebec, the magnitude of the influence was estimated to range from 5 to 50 times the significance threshold in most areas south of the 50^{th} parallel, and exceeding 50 times the threshold (between 10 and $25.0 \mu\text{g m}^{-3}$) at the southern tip of Lake Erie. In all eastern provinces, including in the Maritimes, the spatial extent of the area of influence appeared to commonly reach 1000 to 1500 km.

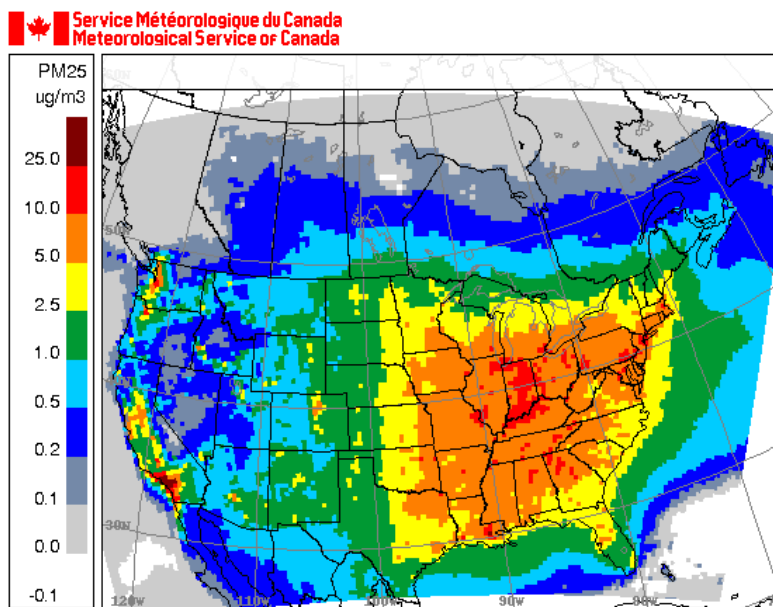


Figure 6.59 Map of influence of 2015 projected U.S. emissions on Canadian $PM_{2.5}$ levels during summer (expressed as relative sensitivity of $PM_{2.5}$ levels in $\mu\text{g m}^{-3}$). [S20]

The map of influence of U.S. emissions derived from the S20 AURAMS zero-out simulations for the 2015 projected emission levels (Figure 6.59) presents a similar footprint in Canada to the one resulting from the S19 CHRONOS study for 2004. The magnitude of the changes was estimated to range from 0.2 to $1.0 \mu\text{g m}^{-3}$ in the western provinces (10 to 30% of the $PM_{2.5}$ ambient concentrations), and from 0.2 to above $5.0 \mu\text{g m}^{-3}$ in eastern provinces (30 to 80% of the $PM_{2.5}$ ambient levels, with variations above 50% in the southern half of Ontario, map not

shown). Although there was a slight displacement to the south of the contour lines in Ontario and Quebec indicating a small reduction in the influence of U.S. emissions on Canadian $PM_{2.5}$ levels, the strong similarities between Figure 6.58 and Figure 6.59 suggest that despite emission reduction efforts in the U.S. such as CAIR, ambient $PM_{2.5}$ levels in eastern Canada will remain strongly influenced by U.S. emissions.

6.6.4 Influence of the U.S. NO_x SIP Call and the Clean Air Interstate Rule (CAIR)

Changes in the transboundary influence of U.S. emissions on O_3 levels have been investigated in two recent studies: a study performed with CMAQ (S21) specifically focused on the effect of the NO_x SIP call, and the S11 study where the projected levels of pollution in 2015 were analysed with AURAMS and compared to present day levels (2002). Details of the model setup are provided in the Appendix.

The NO_x SIP Call was intended to reduce the regional transport of O_3 and O_3 precursors, and required that 22 eastern States and the District of Columbia put NO_x control measures in place by May 1, 2003. The State Implementation Plans (SIPs) most often targeted reductions in NO_x emissions from Electric Generation Units (EGUs) and some large Non-EGU boilers. During the O_3 season (May – September), NO_x emissions in these states decreased by more than half between 2002 and 2005. The resulting effect on summertime O_3 concentrations was studied over the period of May 1 to September 30, 2005 by comparing a simulation with 2002 emission levels for EGUs and on-road sources to one with 2005 emission levels for EGUs and on-road sources. Emissions from all other sources were kept unchanged at their 2002 level in both simulations.

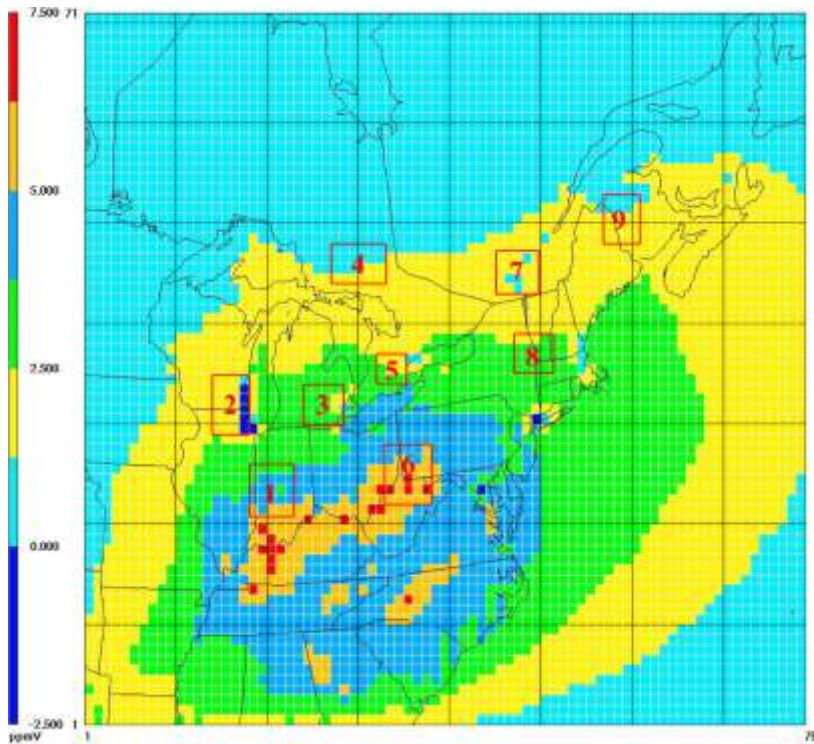


Figure 6.60 Averaged change in the daily 8-hour O₃ maximum levels (ppb) between the 2002 reference case and the 2005 emission scenario for the May to September 2005 period (2002 reference case minus 2005 scenario). Sub-domains are depicted by the red boxes. [S21]

Table 6.9 Change in the daily 8-hour O₃ maximum levels (ppb) between a 2002 reference case and a 2005 emission case for May-September 2005 across model sub-domains as referenced in Figure 6.60 (2002 reference case minus 2005 scenario). [S21]

Sub-domain	Average Change (ppb)	Maximum (ppb)	Minimum (ppb)	Standard deviation	Average on "dirty" days (ppb)
1	4.2	11.1	-0.9	2.4	8.4
2	1.4	5.9	-0.7	1.3	3.0
3	2.8	9.0	-0.7	2.0	6.4
4	1.2	6.4	0.0	1.4	3.4
5	2.6	8.8	-0.5	2.1	5.4
6	5.5	14.9	-3.2	3.1	10.0
7	1.5	6.8	-1.1	1.5	4.5
8	2.7	10.2	0.0	1.8	5.7
9	1.3	4.3	0.0	1.1	3.9

Figure 6.60 shows the average change in the daily 8-hour O₃ maximum levels for eastern North America over the length of the study. Southern Ontario and Quebec as well as most of the Maritime Provinces were predicted to experience reductions in the daily 8-hour O₃ maximum ranging, on average, from 1 to 3.5 ppb. In addition, in southwestern Ontario, about 90% of the days modelled exhibited a reduction in the daily 8-hour O₃ maximum. A detailed analysis of the nine sub-domains outlined in Figure 6.60 showed that the average reductions ranged from about 1% in northern Ontario to 5.5% in southern Ohio/western Pennsylvania. A summary table is presented in Table 9.

Table 6.9 also gives the variability in the response of the daily 8-hour O₃ maximum to changes in EGU and mobile emissions. On ‘dirty’ days when the modelled O₃ concentrations exceeded 70 ppb, the O₃ reductions were generally 2 to 3 times higher than the average improvements. Although the predicted concentrations on ‘dirty’ days were still above the CWS benchmark of 65 ppb, the improvements were substantial. There were also some days when O₃ levels increased in the 2005 emission simulation. Usually these were cleaner days with limited regional O₃ production (not shown). The decreases were likely due to less titration of O₃ resulting from lower NO_x emissions from on-road vehicles in the 2005 emission simulation.

Similar conclusions were reached in the S11 study comparing the forecasted O₃ levels for 2015, when both the NO_x SIP call and the CAIR regulations would be in place, to the current 2002 levels. As discussed in section 6.4.1, most of the reductions in O₃ levels in eastern Canada were driven by emission reductions in the eastern U.S. Changes in Southern Ontario and Quebec and most of the Atlantic provinces are shown in Figure 6.20 to range from 3 to 10 ppb (i.e., 10 to 30%). As would be expected, the absolute changes were larger in the S11 study than in S21 which only investigated the effect of the NO_x SIP call and focused on a projected year (2005) that was much closer to 2002. In S11, the resulting concentrations led to decreases of more than 50% of the number of days exceeding the CWS numerical threshold for O₃ in the Windsor-Quebec city corridor, New Brunswick and Nova Scotia (not shown), except in large cities where the reductions were closer to 5 to 10% (Figure 6.34).

Both of these studies suggested that transboundary flows from the U.S. that impact O₃ levels in eastern Canada should have decreasing levels of pollutants as time goes by (starting with full implementation of the NO_x SIP call). These studies also suggest that this trend is expected to continue in the future and that the effect on O₃ should be measurable given the magnitude of the expected changes.

6.6.5 Investigation of Transboundary Influences in British Columbia

Information on transboundary influences in British Columbia was derived from three studies: a zero-out study (S22) performed with CMAQ at high resolution for the Georgia Basin/Puget Sound area (Figure 6.7b) for month-long simulations in the summer 2001 and winter 2002 (RWDI, 2003b); and specific analyses of provincial zero-out simulations from the S19 CHRONOS and S20 AURAMS studies. Details of the model setup are provided in the Appendix.

Results of the S22 study indicated that most of the O₃ and PM_{2.5} in the Georgia Basin was of Canadian origin in summer as well as in winter. There was however evidence of episodic transboundary transport under the right meteorological conditions. During one episode, characterized by southwest wind conditions, transported O₃ and precursors from the Puget Sound airshed were seen to contribute approximately 10 ppb to ambient levels of O₃ and to increase PM_{2.5} concentrations over southern Vancouver Island by 50-60%. Conversely, during another episode characterized by northerly flows, Canadian PM_{2.5} was observed to contribute to the overall concentrations in the Puget Sound by as much as 15-20 µg m⁻³. The results of these studies suggest that transboundary transport of both O₃ and PM_{2.5} occurs between the two airsheds throughout the year, depending on existing weather patterns. Significant transport of air pollutants appeared to occur primarily across the Canadian and U.S. portions of the Lower Fraser Valley, in a 100 km wide band along the border, with transport occasionally reaching westward to Vancouver Island (Environment Canada, 2004).

Results from the S19 and S20 national scale studies agreed well with the conclusions of the S22 study. As discussed in previous sections and in the S19 and S20 studies, there was evidence of transboundary flows between British Columbia and Washington State influencing PM_{2.5} levels, and that these flows were confined to the most western part of the Canada-U.S. border. In addition, each area's influence on the other appeared to be of the same order of magnitude in all three scenarios, and that it is a year-round phenomenon (Figure 6.56 to Figure 6.59).

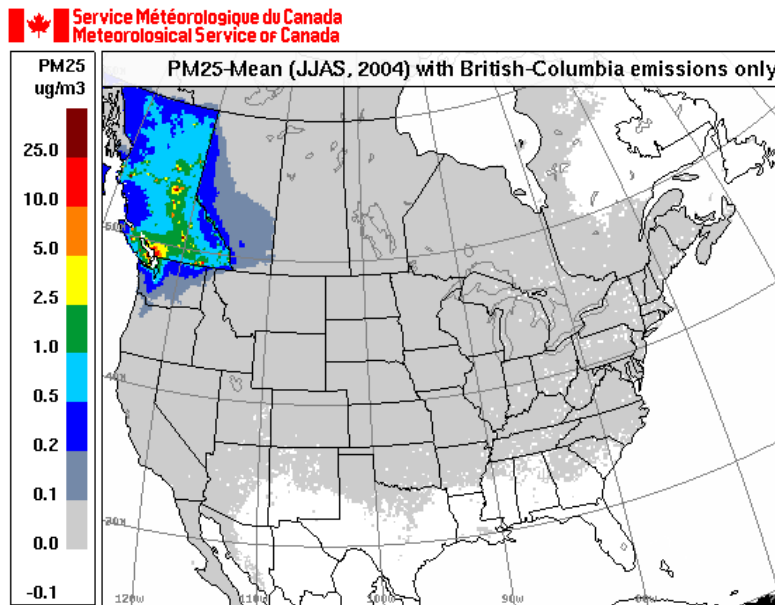


Figure 6.61 Map of influence of British Columbia emissions on ambient PM_{2.5} levels in rest of Canada and the U.S. for summer 2004 (expressed as relative sensitivity of PM_{2.5} levels in $\mu\text{g m}^{-3}$).[S19]

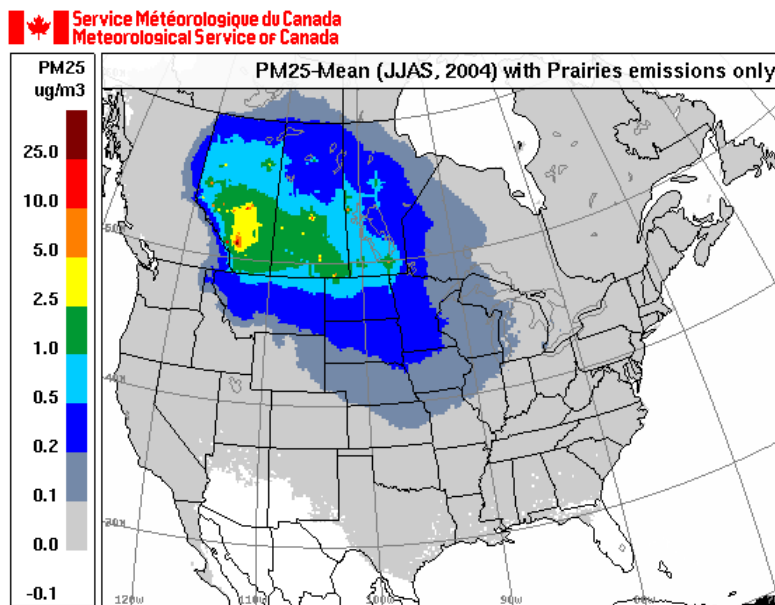


Figure 6.62 Map of influence of emissions from the Prairies on ambient PM_{2.5} levels in the rest of Canada and the U.S. for summer 2004 (expressed as relative sensitivity of PM_{2.5} levels in $\mu\text{g m}^{-3}$).[S19]

In addition, for the province of British Columbia, there was little evidence of inter-provincial transport contributing to PM_{2.5} ambient levels. Figure 6.61 and Figure 6.62 show the influence of emissions from British Columbia and from the Prairies (Alberta-Saskatchewan-Manitoba)

on the rest of Canada as derived from individual zero-out simulations from the S19 CHRONOS study. As a result of the prevailing meteorology, which tends to transport pollution eastward, and the natural geographical barrier made by the Rockies, pollution in the lower atmospheric levels did not appear to travel much in either direction across the British Columbia-Alberta border.

6.6.6. Investigation of Transboundary Influences in Alberta, Saskatchewan and Manitoba

Information on inter-provincial contributions to $PM_{2.5}$ concentrations in the Prairies was derived from specific analyses of provincial zero-out scenarios from the S19 CHRONOS study.

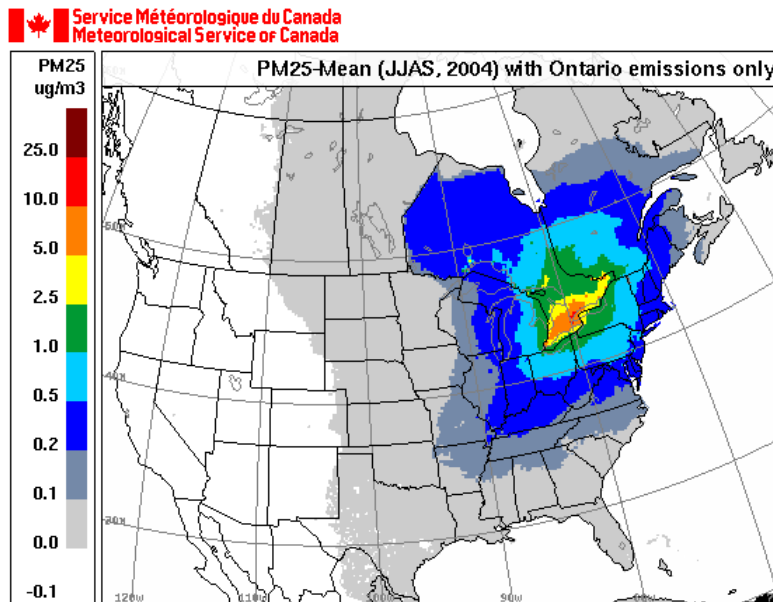


Figure 6.63 Map of influence of Ontario emissions on ambient $PM_{2.5}$ levels in the rest of Canada and the U.S. for summer 2004 (expressed as relative sensitivity of $PM_{2.5}$ levels in $\mu g m^{-3}$). [S19]

As discussed in the previous section, results from S19 individual simulations showed that there was little inter-provincial transport at the border between British Columbia and Alberta (Figure 6.61 and Figure 6.62). The analysis also indicated that inter-provincial transport from Ontario to the Prairies, as expected from the prevailing meteorology, was small to insignificant (Figure 6.63) and that $PM_{2.5}$ ambient levels in Alberta, Saskatchewan and Manitoba were mostly influenced by emissions originating from these three provinces and from the U.S. to a certain extent. On the other hand there was some evidence that emissions from the three Prairie provinces were influencing $PM_{2.5}$ levels in Ontario, although the effect seemed contained to Northern Ontario (Figure 6.62 and Figure 6.63).

6.6.7 Investigation of Transboundary Flows in Ontario, Québec and Atlantic Provinces

Transboundary influences in eastern Canada have been analysed in a couple of studies: specific analyses of provincial zero-out scenarios from the S19 CHRONOS study; zero-out analyses with AURAMS (S23) of an August 2001 episode in Quebec; and zero-out studies with CHRONOS of a June 2001, an August 2001 and a February 2005 (S24) episode in Atlantic Canada. Details of the models' setup are provided in the Appendix.

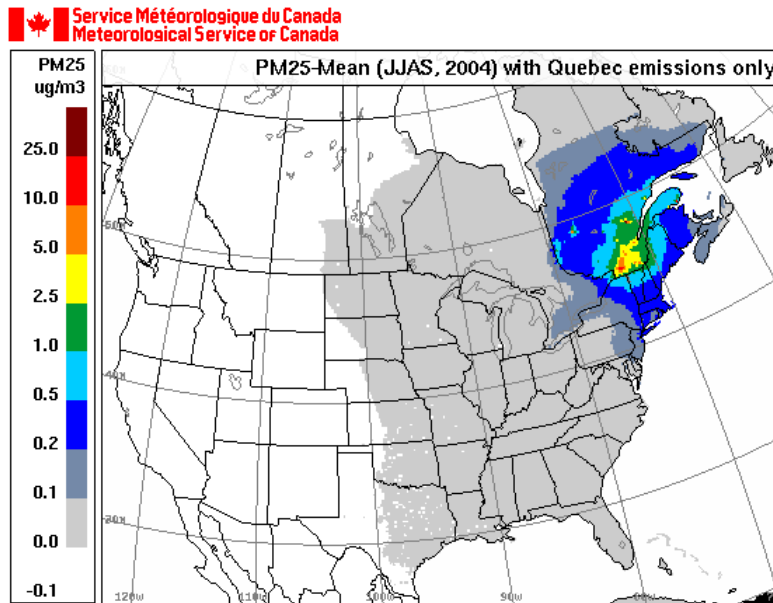


Figure 6.64 Map of influence of Québec emissions on ambient PM_{2.5} levels in the rest of Canada and the U.S. for summer 2004 (expressed as relative sensitivity of PM_{2.5} levels in µg m⁻³). [S19]

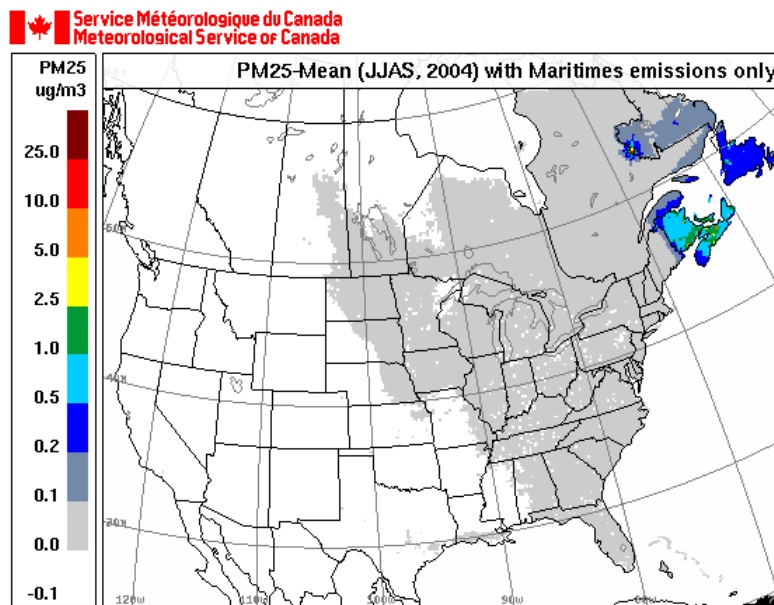


Figure 6.65 Map of influence of emissions from Maritime provinces on ambient PM_{2.5} levels in the rest of Canada and the U.S. for summer 2004 (expressed as relative sensitivity of PM_{2.5} levels in µg m⁻³). [S19]

The influence of emissions from Ontario, Québec and the Atlantic Provinces on PM_{2.5} ambient levels in other provinces, as derived from the S19 zero-out simulations, is shown in Figure 6.63 to Figure 6.65. Results showed that, due to the prevailing meteorology, transboundary flows tended to occur predominantly to the east of a given province. In the case of Ontario, that meant that Ontario's influence on other provinces was larger than the impact of surrounding provinces on Ontario. Despite evidence that emissions from the three Prairie provinces influenced PM_{2.5} levels in Ontario, the effect seemed contained to Northern Ontario (Figure 6.62 and Figure 6.63). On the other hand, the analysis suggested that emissions from Ontario significantly influenced PM_{2.5} levels in most of southern Québec and as far as the border with New Brunswick (Figure 6.63). Similarly, emissions from Québec were estimated to have a significant influence on PM_{2.5} levels in the Atlantic Provinces (Figure 6.64), while emissions from Atlantic Canada appeared to have little impact on the rest of the country (Figure 6.65).

From the various zero-out analyses of the S19 study, it was possible to compare the relative strength of transboundary contributions in Québec. PM_{2.5} levels in the segment between Montreal and Québec City varied by 2.5 to 10.0 µg m⁻³ when anthropogenic emissions from within the province were zeroed (Figure 6.64), by 0.5 to 1.0 µg m⁻³ when emissions from Ontario were zeroed (Figure 6.63) and by 1.0 to 5.0 µg m⁻³ when U.S. emissions were zeroed (Figure 6.58). These results highlighted that both local (provincial) emissions and transboundary flows are of competing importance in defining the air quality in the province of Québec. It also suggested that, at least for the summer of 2004, transboundary flows from the

U.S. were likely more important than the ones from Ontario in contributing to Québec ambient $PM_{2.5}$ levels.

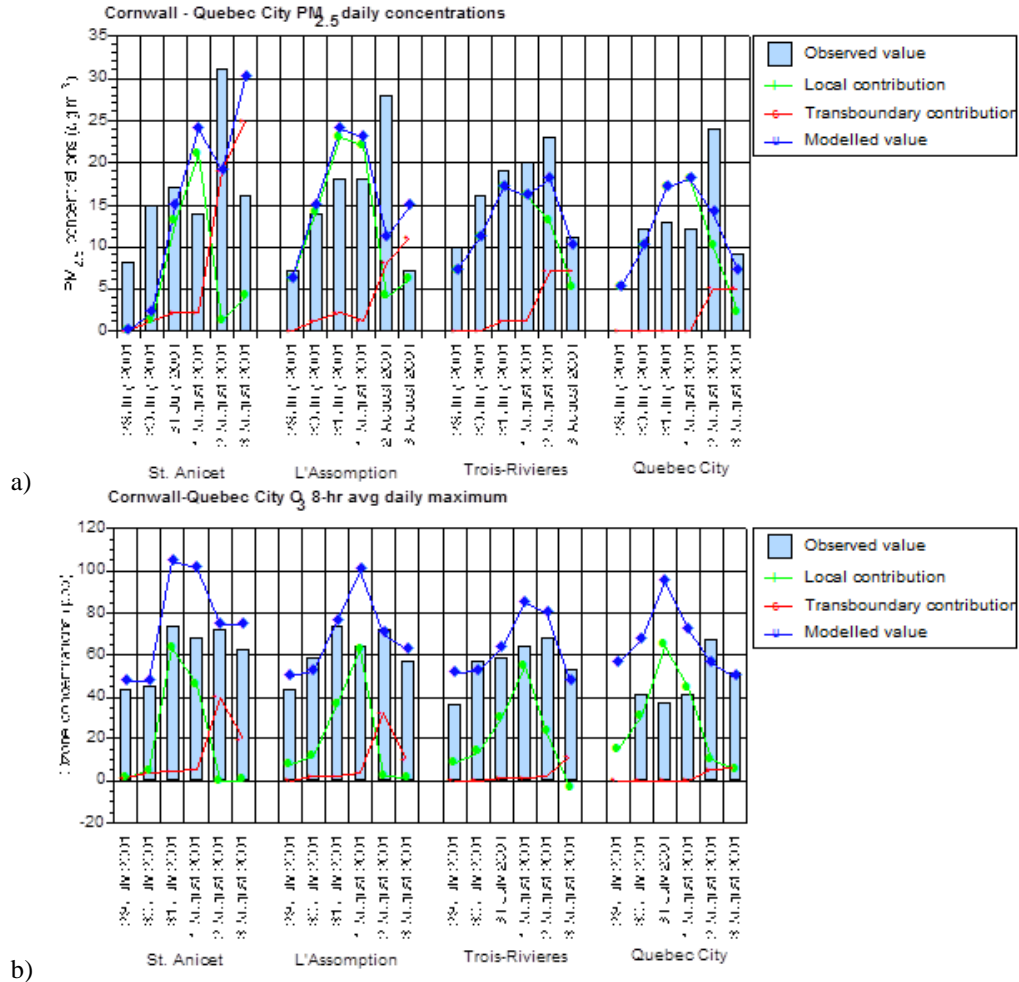


Figure 6.66 Daily (a) $PM_{2.5}$ (b) 8-hour O_3 maximum measured and modelled for four locations along the St. Lawrence valley from west to east. Also shown are computed estimates of the local and transboundary contributions. [S23]

The S23 study of the August 2001 episode in Québec presented a specific example of the role of long-range transport in the province of Québec. A high pressure system on the East of the continent on July 31st allowed pollutants to accumulate and cause local smog episodes in the Montreal area. Then, once the system reached the Atlantic Ocean, the south-westerly flow behind the ridge transported accumulated smog precursors from the Midwest and southern Ontario into the area of interest, causing regional smog episodes on August 2nd, 2001. Three simulations of the episode were performed: one with all emissions, a second with anthropogenic emissions within the province of Quebec set to zero, and a third with anthropogenic emissions outside the province set to zero. Figure 6.66 presents the apportionment results derived from the simulations interpolated at four locations in the Cornwall-Quebec City corridor for $PM_{2.5}$ (a) and O_3 (b). For both pollutants, the transboundary

contribution was negligible on July 31st, the first day of the episode, and increased sharply on August 2nd due to the strong south-westerly flow prevailing that day, to the point that it explained at least half of the modelled concentrations of either pollutant in the two western locations. The transboundary contribution diminished gradually from west to east suggesting that the more eastern locations were farther from the transboundary sources in this particular episode. The zero-out analyses provided different results for PM_{2.5} and for O₃. For PM_{2.5}, the reference values modelled with all the emissions could be almost exactly reconstructed from the local and transboundary contributions derived from the zero-out simulations, while it was not the case for O₃ as biogenic sources also contribute to the atmospheric levels.

The importance of transboundary influences in Atlantic Canada was investigated with similar case studies of a June 2001 episode, the continuation of the August 2001 episode simulated in S23, and a February 2005 episode (S24). Tables 10 and 11 provide the relative contributions of U.S. and Canadian anthropogenic emissions to modelled PM_{2.5} and ozone levels at individual monitoring sites estimated from the CHRONOS zero-out simulations. Transboundary transport of PM, O₃ and their precursors from the U.S. was found to have a predominant influence of the order of 40% for O₃ and greater than 80% for PM_{2.5} during the two summertime episodes of poor air quality in the Atlantic Region. During the wintertime episode, on the other hand, contributions from Québec and Ontario were found to dominate (exceeding 60% for PM_{2.5}), but anthropogenic emissions of precursors and primary fine particulate originating in the Atlantic Region were also found to contribute a relatively high percentage (close to 30%) to local concentrations of PM_{2.5}. The transboundary contribution from the U.S. was found to be low in the wintertime case. As for the Québec case study (S23), only zeroing-out anthropogenic sources explained only part of the atmospheric levels of O₃ in the summer. The estimated contribution from biogenic sources in New Brunswick and Nova Scotia for the two summer episodes was approximately 50%.

A similar ranking analysis can be performed from the S19 CHRONOS zero-out simulations for the summer 2004. On a seasonal basis, PM_{2.5} levels in New Brunswick and Nova-Scotia varied by 0.1 to 0.2 µg m⁻³ when anthropogenic emissions from Ontario were zeroed (Figure 6.63); by 0.1 to 1.0 µg m⁻³ when anthropogenic emissions from Québec were zeroed (Figure 6.64); by 0.2 to 2.5 µg m⁻³ with a few isolated sensitivity peaks above 5.0 µg m⁻³ when anthropogenic emissions from within the province were zeroed, and by 0.2 to 2.5 µg m⁻³ when U.S. emissions were zeroed (Figure 6.58). The S19 study outlined the role of flows from Québec and the U.S. in setting the PM_{2.5} ambient levels in Atlantic Canada, but seemed to suggest a larger contribution from local anthropogenic emissions than the case studies (S23). The discrepancy is likely related to the fact that only high pollution episodes were examined for the case studies while the S19 considered an entire summer season.

All the studies discussed here added more evidence that long-range transport from both transboundary and inter-provincial origin is a defining component of PM_{2.5} and O₃ levels for all the eastern Canadian provinces. As a consequence, smog issues in one province cannot be addressed in isolation to other provinces or to the U.S.

Table 6.10 Average percent contribution to CHRONOS modelled O₃ at New Brunswick and Nova Scotia monitoring sites on days when the Canada-Wide Standard was exceeded [S24]

% Contribution to CHRONOS Model Ozone	Atlantic	Quebec & Ontario	Trans-boundary (US)	Biogenic /Background
June 2001		7	37	56
August 2001	4	8	46	42

Table 6.11 Average percent contribution to CHRONOS modelled PM_{2.5} at New Brunswick and Nova Scotia monitoring sites on days when the Canada-Wide Standard was exceeded [S24]

% Contribution to Model PM _{2.5}	Atlantic	Quebec & Ontario	Trans-boundary (US)	Biogenic / Background
August 2001	5	4	86	5
February 2005	29	67	2	2

6.7 Assessments of Uncertainties

As in previous sections, recent studies and/or information which provide additional insights on known areas of modelling uncertainties are discussed in the following subsections. The focus here relates to the sensitivity of modelling results to changing meteorology and to external (to the modelling domain) or episodic sources of pollution. Prefacing these analyses, a short summary of uncertainties associated with model abilities is also presented and is based on the detailed discussions of Chapter 5.

A detailed discussion of uncertainties pertaining to emission inventories would be beyond the scope of the present chapter. Models' sensitivities to differing levels of emissions have been discussed in Section 6.3 and the conclusions can be directly used in the context of an uncertainty analysis. Where O₃ and PM_{2.5} ambient levels were found to be sensitive to a given emitted precursor and/or pollutant, any uncertainty in the emitted field will be carried forward to the modelling results; conversely where O₃ and PM_{2.5} ambient levels were found not to be sensitive, uncertainties in the emitted field of a given precursor and/or pollutant will be compounded by the lack of sensitivity. Emission inventories and confidence levels in emission levels from different sources are discussed in Chapter 4.

6.7.1 Influence of Uncertainties in Process Representations on Model Results

The air quality models used in the studies reviewed in this chapter are amongst the current state-of-science models available. There are however multiple areas of active research in the development and evaluation of algorithms representing the processes responsible for the release, formation, transportation and removal of both atmospheric oxidant and particulate matter. A detailed discussion of strengths and weaknesses of these models is the objective of Chapter 5.

Chapter 5 highlights that all three models used here still exhibit significant biases in their ability to predicted both O₃ and PM_{2.5} at the regional scale, and have different levels of success in simulating particulate matter composition. Models generally have better skills in predicting primary pollutants (given reliable emissions) than in predicting secondary pollutants due to the complexity of various atmospheric processes. In particular, boundary layer dynamics and mixing, cloud processing, and secondary organic aerosol (SOA) formation are some of the processes having significant impact on model performance.

Chapter 5 provides also two conclusions of particular relevance to the studies conducted here:

- although confidence levels in air quality model simulations have not changed significantly from the previous assessment (Seigneur and Moran, 2004), there is considerable improvement in the confidence levels for the simulations over longer time periods and larger spatial scales;
- while there are indications that large differences in performance may exist in predicting targeted pollutants, the differences in predicting relative response to emission changes are smaller between different models.

Knowing the strengths and weaknesses of the models used for scenario simulations is a fundamental part of interpreting the results of the studies. Specialized analysis methods, such as examining the differences between a scenario and a reference case, are generally recommended as a means to minimize the influence of biases in model prediction. Moreover, weight of evidence approaches, where scenarios are performed with multiple modelling platforms and the results corroborated with evidence from other type of analysis, are strongly suggested as the scientific understanding of oxidant and especially particulate matter is still evolving.

Given the large increase in model applications and the increasing reliance on these approaches to advise policy decisions, modelling teams throughout the community are participating in large intercomparison studies. Multiple ensemble air quality predictions projects have also been initiated in various contexts. These initiatives should provide very valuable information over the next few years.

6.7.2 Influence of Uncertainty in Meteorological Input on Model Results



Figure 6.67 S25 modelling domain with locations of selected major cities. [S25]

Uncertainties in the meteorological input and their influence on air quality model results were investigated using CMAQ over a nine-day period by the National Research Council of Canada (Smyth *et al.*, 2005, 2006a). The study consisted of comparing two simulations of the same episode where meteorological fields were generated in one case by the U.S. MM5 model (Dudhia *et al.*, 2004), and in the second by Environment Canada’s GEM model (Côté *et al.*, 1998a, b). Emission fields that are meteorologically dependent (on-road mobile and biogenic emissions) were processed with the corresponding meteorological set using SMOKE (MCNC, 2000). Except for meteorology and those modelled emissions dependent on meteorology, all other inputs were identical for the two CMAQ simulations. The study was focused on eastern Canada and northeastern U.S. states (Figure 6.67) and span the July 11 to 19, 1999 period. Details of the model setup for this scenario analysis, labelled S25, are presented in the Appendix.

Comparison of the two modelled meteorological datasets against surface measurements revealed that GEM and MM5 gave comparable results. When comparing the two meteorological sets against each other, the modelled pressures matched each other very well with normalized mean differences (NMDs) of less than 1%. For temperatures, the NMD was 6%. The average MM5 temperature was higher than the average GEM temperature by approximately 1.3°C when averaged over all surface-level grid cells, with a significant portion occupied by the Atlantic Ocean. When only land-grid cells were used in the calculations, the average MM5 temperature was 2.2°C greater than GEM. GEM wind speeds were on average 0.6 m s⁻¹ greater than MM5, with a NMD of 15%, while GEM average relative humidity (RH) was 11% higher than MM5, with a NMD of 16.6%.

On-road emissions of VOC and NO_x based on the MM5 meteorology were greater than GEM-based results by 3.3% and 0.3%, respectively. The average land temperature difference of 2.2°C between the models had a small effect on the on-road mobile source emissions. GEM CO emissions were 0.1% greater than MM5, and emissions of NH₃, PM, and SO_x were not impacted at all as their emission factors are not dependent upon temperature in the version of the on-road emission model MOBILE used in this study (details on the MOBILE model can be found in Environment Canada, 2005b). The surface temperature difference had a much larger influence on biogenic emissions, resulting in a relative difference of 11.8% between GEM- and MM5-based biogenic NO emissions, and of 16.6% for biogenic VOCs (with the MM5-based fields higher than the GEM-based ones). In the case of biogenic VOCs, although the variation is mainly attributable to the difference in temperature fields, differences in solar radiation fields also had some impact.

The average O₃ concentrations obtained by using the GEM and MM5 meteorology were very similar and gave similar statistical performance scores when compared with network observations for that time period. The mean GEM-based O₃ concentration was less than 1 ppb lower than the mean MM5-based concentration, corresponding to a NMD of only -1.7%. The combined effects of increased temperature in the MM5 model resulting in increased isoprene and NO_x emissions are likely the main reasons for the higher average MM5 O₃ concentrations.

The average GEM- and MM5-based PM_{2.5} levels exhibited more differences than the O₃ fields, although both simulations under-predicted average dry PM_{2.5} concentrations significantly compared to measured data (by 16.6 µg.m⁻³ and 14.3 µg.m⁻³ respectively). The differences between GEM and MM5 results were partially controlled by differences in relative humidity (RH), as analysed and discussed in detail by Jiang *et al.* (2006) and Smyth *et al.* (2006a). The increased RH in the GEM results caused CMAQ to predict increased total PM_{2.5} mass due to an increased concentration of particle-bound water, which facilitated the formation of sulphate, nitrate, and ammonium ions in aerosols. The higher RH also enlarged particle diameters which, in the GEM results had the effect of causing the levels of most PM_{2.5} chemical components to be lower than the MM5-based results. For ‘wet’ PM_{2.5} containing all aerosol components, GEM-based model results were 6.1% greater than MM5 results, while for ‘dry’ PM_{2.5} containing aerosol dry components only, MM5-based model results were 18.8% greater than the GEM-based results. Overall, however, the performance statistics for PM_{2.5} mass were not drastically different between the two simulations, suggesting that minor differences in the meteorological input only translate into minor changes in the O₃ and PM_{2.5} ambient levels in the types of conditions studied here

6.7.3 Influence of Meteorology on Model Results

In all the scenarios presented in the chapter, the same meteorological conditions were used in both the reference case and the scenario, hence isolating the impact of emission changes. This is a common simplification in the modelling community given current computational constraints. Studies such as the ones presented in S25 are investigating the various ways in which meteorological conditions influence the system's response in terms of atmospheric pollution. An area of active research presently deals with the relationship between changing climate conditions and regional air quality, as discussed in Chapter 8. This is of particular concern for scenarios set in the future since it is currently projected, for example, that regional increases in O₃ concentrations due to climate change could be as large as predicted increases associated with increasing emissions.

The current consensus (see Chapter 8 for a detailed review) is that in the absence of emission growth, global O₃ background levels would decrease, but regional O₃ levels would tend to increase in most industrialized regions such as Canada, the U.S. and Europe. In addition, the inclusion of projected increases in emissions, at the global scale, is projected to offset the global O₃ background level decrease associated with climate change and to result overall in a global background O₃ increase. In terms of PM_{2.5}, although aerosols in general are extensively studied in the context of climate change for their direct and indirect effects on the atmosphere, there is limited information on how surface PM_{2.5} levels would be affected. Initial studies hint at a mixed response with increases expected in some regions and decreases in others, hence the need to pursue more focused investigations.

There are significant efforts underway in Canada and throughout the global scientific community to incorporate air quality and climate interactions into regional and global air quality modelling systems, with the objective of informing the design of air quality policies. All indications are that policies based on emission reductions, without the consideration of climate change effects, may fall short of the desired outcomes by underestimating the emission reductions actually required.

6.7.4 Influence of External and Episodic Emission Sources

The choice of limited area models to assess atmospheric impacts at the regional scale implies that boundary conditions are provided at the edges of the domain to represent levels of pollutants transported from outside the considered domain. As mentioned in the previous section, global emissions of smog precursors are predicted to increase (IPCC scenario A2P, Brasseur *et al.*, 2006 – see Chapter 8 for additional discussions). This in turn will impact background concentrations of O₃ which is expected to reduce the effectiveness of domestic emission reduction strategies. A similar trend could be expected for PM_{2.5} although scientific literature is still limited at this time. Air quality model simulations presented in this chapter did

not account for any future change in background concentrations. Efforts are underway to address this limitation by adapting model boundary conditions to incorporate the influence of increasing global emissions.

Another source of uncertainty in the modelling results presented in this chapter is linked to the absence of some natural emissions such as biomass burning. Due to a lack of specific information on the spatial and temporal extent of wild and prescribed forest fires for a given model year, forest fires emissions are not usually included in scenario simulations such as the ones discussed in this Chapter. This is especially true when studying projected years. Forest fire emissions do amount to a substantial fraction of annual primary $PM_{2.5}$ emissions in any given year; the 2002 Quebec fires, for example, were estimated to have released close to 50% of the annual Canadian anthropogenic $PM_{2.5}$ emissions in about 12 days (Lavoué et al, 2007). Forest fire emissions would be a consideration when evaluating air quality conditions against ambient targets. However, limitations inherent to the nature of this emission source prevent it from being included in projection scenarios. The current consensus in the scientific community is to exclude such episodic sources from both reference and scenario cases so as to have information that is comparable. Any synergistic effect that could happen in the atmosphere due to this additional loading of primary PM on an episodic basis is de facto neglected.

6.8 Summary and Conclusions

6.8.1 General Summary

Insights on several policy-relevant science questions were gathered through a review of recent modelling scenarios focused on Canadian air quality. Conclusions and state of knowledge that can be derived as a result of this review, from a modelling perspective, are discussed in the following sections. They will contribute, with the analyses of the other chapters, to addressing the policy relevant science questions defining this assessment.

The majority of studies were performed with multi-pollutants models, providing a comprehensive outlook of the effects of a given set of emission changes on O_3 , $PM_{2.5}$ and acid deposition levels. This approach highlighted that whereas ambient O_3 and $PM_{2.5}$ share a number of precursors (NO_x and VOCs), and although conditions that are conducive to high levels of O_3 also generally result in high levels of $PM_{2.5}$, emission changes do not necessarily induce similar changes in O_3 and $PM_{2.5}$ (sections 0 and 0). Differences in the chemical pathways leading to their respective formation are largely responsible for the differences in behaviour.

A behaviour specific to O_3 , and observed in most of the scenarios reviewed, is its two-phase response to changes in precursor emission. NO_x reductions typically result in a lowering of O_3 levels in areas downwind of emission sources; they can also be associated with a very local and contained increase in O_3 at the location of the source itself, especially when the NO_x reductions are not wide-ranging (sections 0, 0, 0, 0). In such situations, the regional improvements in O_3 levels usually outweigh the local disbenefit.

Changes in ambient $PM_{2.5}$ in response to emission changes are more complex due to the many variables involved, from the type of pollutant reduced to the season in which it happens. The scenarios provided examples of cases in which emission reductions lead to decreases in ambient $PM_{2.5}$ (section 0) and examples where reductions lead to increases (section 0). Some analyses also suggested that winter PM chemistry may need further attention due to its potential to form secondary, nitrogen-based, $PM_{2.5}$.

O_3 and $PM_{2.5}$ do behave similarly under certain circumstances: they both increase when new sources are added to otherwise pristine environments and decrease when deep emission reductions are applied. In the latter case, the proportions of the decreases are not usually linearly correlated to the corresponding precursor emission reductions. In addition, long-range transport from the U.S. has a large influence on both O_3 and $PM_{2.5}$ levels in eastern Canada (section 0) while the transboundary flux tends to be more balanced across the western boundaries.

O_3 levels are currently projected to decrease across Canada in the next 5 to 10 years due to the combined reductions in the projected Canadian and U.S. NO_x and VOCs emissions (assuming a CAIR equivalent rule in the U.S). On the other hand, under the future business-as-usual projections studies analyzed in this chapter, $PM_{2.5}$ levels are projected to experience more limited improvements, and even deteriorate in places such as in major urbanized areas, despite the large projected reductions in U.S. emissions of primary $PM_{2.5}$ and PM precursors (section 0). Additional reductions would be needed to curb this trend (section 0), especially if the effects of climate change on air quality are taken into account (section 0).

6.8.2 Specific Conclusions

Specific summaries pertaining to the science-policy questions listed in section 0 are provided below.

What is the sensitivity of PM and O_3 to changes in smog precursors?

Of the six major sectors of activity investigated (agriculture, marine, oil and gas -including oil sands-, refinery and chemical, electricity generation, and residential wood combustion), NH_3 emissions from agriculture and primary $PM_{2.5}$ emissions from residential wood combustion

had a definite influence on ambient $PM_{2.5}$ levels. O_3 showed no sensitivity to NH_3 emissions nor to emissions from residential wood combustion since the issue is confined to winter periods and did not, in the residential wood combustion scenario reviewed, involve any changes in NO_x or VOC emissions.

The marine sector, which emits all criteria air contaminants, seemed to have the potential to influence O_3 and $PM_{2.5}$ ambient levels significantly, especially in coastal areas and along seaways, but limitations with the reviewed study did not permit any quantification (it should be noted that additional studies investigating the role of marine emissions in North America have now been released in support of the Canada-U.S. Sulphur Emission Control Area joint applications to the International Marine Organization³⁵).

O_3 sensitivity to NO_x and VOC emissions was the subject of many of the reviewed scenarios. The findings confirm the importance of the oil and gas sector as a major sector influencing O_3 levels in Alberta; so was the electricity generation sector in Alberta and southern Ontario. The sensitivity of O_3 to NO_x and VOCs was detected by the models even for relatively low emission levels such as the ones represented by the refinery and chemical sector in Alberta. From the limited information available for $PM_{2.5}$, the oil and gas sector also appeared to have a large role in setting ambient $PM_{2.5}$ levels in Alberta, and the electricity generation sector in Alberta and southern Ontario.

³⁵ ECA proposal (<http://www.epa.gov/otaq/regs/nonroad/marine/ci/mepc-59-eca-proposal.pdf>) available from EPA's website for Oceangoing vessel regulation (<http://www.epa.gov/otaq/oceanvessels.htm>)

Table 6.12 Schematic summary of O₃ and PM_{2.5} changes, with qualitative estimates of confidence level, as a result of a change in a given precursors or set of precursors based on the studies reviewed in this chapter.

Sector	Precursor emission change	No. of studies	Effect on PM _{2.5}	Confidence level for PM _{2.5} results	Effect on O ₃	Confidence level for O ₃ results	Comment
Agriculture	↓ NH ₃	3 O ₃ + PM _{2.5} (6.3.1)	↓	High	Nil	High	The average magnitude of the resulting PM _{2.5} reduction is moderate but indications are that sensitivity during episodes can be high.
Marine Transportation	↓ NO _x + ↓ SO _x + ↓ VOC+ ↓ PM _{2.5}	1 O ₃ + PM _{2.5} (6.3.2)	↓	Low	↓downwind ↑ locally	Low	Indications are that the magnitude of the impact on O ₃ and PM _{2.5} is large but more studies are needed to confirm.
Conventional Oil and gas (upstream) S5	↓NO _x + ↓VOC	1 PM _{2.5} (6.5.1) 2 O ₃ (6.3.3, 6.5.1)	↓	Medium	↓	Medium	Largest impacts are concentrated in Alberta where this sector's activities are most prevalent.
Oil sands S6	↑NO _x + ↑VOC	2 PM _{2.5} (6.4.1, 6.5.1) 3 O ₃ (6.3.3,6.4.3, 6.5)	↑	Medium	↑	High	Increase in O ₃ restricted to area surrounding sector activity. For PM _{2.5} , impact is extrapolated from ensemble of simulations where precursors emissions are both increased and decreased.
Refinery and chemical S7	↓NO _x + ↓VOC	1 O ₃ (6.3.4)	No information	NA	↓	Low	Impacts seems constrained to the near vicinity of the emission sources.
EGU	↓NO _x + ↓VOC	1 PM _{2.5} (6.5.1) 2 O ₃ (6.3.5,6.5.1)	↓	Medium	↓	Medium	Appears as a dominant contributor to O ₃ and PM _{2.5} levels in most Canadian provinces.
Residential wood combustion	↓ PM _{2.5}	1 PM _{2.5} (6.3.6)	↓	Medium	No information	NA	Magnitude of atmospheric response needs to be further investigated (confidence level is high for direction of response but low for the magnitude).

Table 6.12 summarizes these findings in a schematic way and attempts to provide a confidence level for each assessment based on the strength of the studies and the weight-of-evidence of the multiple analyses where available. Confidence levels were assigned by examining the following questions for each sector studied: 1) do the reviewed results agree with the expected theoretical outcomes?; 2) were the studies comprehensive enough to generalize the results (in terms of length of time, spatial coverage, and analysis)?; 3) Were there limitations identified by the authors of the studies that have some bearing on their significance?; and 4) were there more than one study for the sector of interest and, if so, were the results in agreement? Areas where information is insufficient and additional studies needed are also highlighted.

What are the anticipated impacts of future emission reductions?

Emission reductions in the U.S., represented by the Clean Air Interstate Rule (CAIR) in most of the reviewed scenarios, are anticipated to have large and beneficial impacts on Canadian O₃ and PM_{2.5} levels, especially in eastern Canada. Projected increases in primary PM_{2.5} emissions in Canada would however have the potential to offset some of the improvements associated with lower levels of transboundary transport, and deterioration of PM_{2.5} levels are projected in large urbanized areas. Deteriorations are also anticipated for O₃ levels around Fort McMurray if the expected substantial increase in NO_x and VOC emissions from oil sands extraction and processing does occur.

Future reductions of precursor emissions are projected to result in decreases in O₃ levels, although the analyses suggested that improvements would be smaller in urban cores than in other parts of Canada. Given the magnitude of the predicted changes in PM_{2.5} and especially O₃ levels, it is expected that measurements should reflect these trends over the next 5 to 10 years if emissions evolve as currently projected.

Additional reductions in Canada above and beyond current legislation are predicted to be beneficial for both O₃ and PM_{2.5} levels, although none of the reductions investigated here were sufficient to bring all of Canada below the numerical Canada-Wide Standards threshold for either pollutant. In addition, the review suggests, however, that as SO_x and NO_x precursor emissions are reduced, a shift in the primary versus secondary nature of the particles could occur and necessitate a different approach, with more emphasis on primary PM emissions, to further reduce air pollution. A certain seasonality was also observed in the chemical formation of particles with winter chemistry showing a potential to dampen or even offset summer improvements due to emission reductions. Both aspects will need further investigations.

How will the observed and predicted changes in PM and ozone impact ecosystem health?

In all scenarios reviewed, the predicted evolution of acid deposition follows closely the behaviour of ambient PM_{2.5} levels. Total sulphur deposition reflects the decrease in particulate sulphate associated with SO_x emission reductions. Changes in total nitrogen deposition are more complex as they are controlled by changes in both particulate nitrate and particulate ammonium resulting from a chemical response of the sulphate-nitrate-ammonium system to

reductions in NO_x and NH₃ emissions. As a result, the scenarios provide examples of cases, especially during the winter period, where emission reductions overall result in local increases in both PM_{2.5} mass and nitrogen deposition.

From total deposition, the impact on ecosystem health can be evaluated through the assessment of critical load exceedances across most of Canada (data is lacking at this time to perform the evaluation in southern Alberta, Saskatchewan and Manitoba). The sensitivity of the critical load exceedances varied with the various scenarios but in all cases investigated, the emission reductions were not sufficient to eliminate exceedances of critical loads in Canada. The emission reductions in the majority of cases result in decreases in the magnitude of the exceedances and the extent of the geographical areas that are affected.

What are the factors that contribute to elevated levels of smog in Canada? What is the spatial and temporal distribution of the smog problem in Canada?

The reviewed analyses provide elements of information that help characterize smog levels in Canada. A study on the influence of background O₃ concentrations adds further evidence that biogenic emissions contribute to O₃ levels in the order of 30 to 35 ppb in eastern Canada.

Scenarios focused on the transboundary flows in and out of Canada highlight that inter-provincial transport from British Columbia to Alberta and the rest of Canada is minimal, that inter-provincial transport from Ontario to the Prairies, as expected from the prevailing meteorology, is small to insignificant and that PM_{2.5} ambient levels in Alberta, Saskatchewan and Manitoba were mostly influenced by emissions originating from within these three provinces and from the U.S. to a certain extent. On the other hand the scenario showed that emissions from the three Prairie Provinces are influencing PM_{2.5} levels in Ontario, although the effect seemed contained to Northern Ontario.

All the studies discussed in this review add more evidence that long-range transport from both transboundary and interprovincial origin is a defining component of PM_{2.5} and O₃ levels for all the eastern Canadian provinces. As a consequence, smog issues in one province cannot be addressed in isolation to other provinces or the U.S. and at this time, all indications are that despite emission reduction efforts in the U.S. such as through the implementation of CAIR (now in the form of CSAPR following some modifications), ambient O₃ and PM_{2.5} levels in eastern Canada will remain strongly influenced by U.S. emissions.

6.9 Recommendations for Future Research

The new knowledge that has been gathered in this chapter results from the review of a much larger array of Canadian modelling studies than has been available in the past. Improvements in technology and accessibility of models are largely responsible for this new capacity, and as a result, many scientific questions which could only be identified as gaps in the past are slowly being addressed.

As reliance upon scenario analyses increases, continued efforts in the development and evaluation of air quality models will be critical to improve the accuracy and confidence in the guidance provided by scenario studies. Many aspects of the modelling framework, from the scientific understanding of PM chemistry to the ability to represent appropriately subgrid-scale processes, are still evolving and, accordingly, so is the accuracy of the model projections. Model projections need to be revisited on a regular basis to reflect the most up-to-date understanding and, where large uncertainties are known to exist and impact on the projections, sustained model development is required.

Similarly, evaluations targeting the way models are used in the context of scenario analysis should also be undertaken in addition to the conventional performance evaluation against a given set of observations. Areas of particular interest range from investigating the use of the differences between a scenario and a reference case to systematic sensitivity studies where changes in emissions from individual pollutants are analysed, to determining the magnitude of emission changes to which a model is sensitive or can respond without too much distortion due to non-linearities in the chemical processes.

Another area of focus over the next couple of years should be on adding a temporal dimension to the studies that are undertaken. Policy scenarios are typically framed within a fixed meteorological year; yet all indications are that climate change may influence the conclusions of such analyses and potentially the efficiency of proposed emission regulations, an aspect that needs further investigation. An integral part of characterizing the impact of climate change will be to initially understand the inherent variability induced by year to year changes in meteorology. In addition, reductions in emissions are generally achieved through incremental reductions over a number of years rather than overnight as currently simulated, requiring the ability to assess transient changes and any associated synergistic or compounding effects. Modelling studies should therefore evolve into multi-year simulations, which would have to be supported by faster models and computer technology.

More information is also needed within multiple spatial scales. The focus on the regional scale has so far been a compromise between computing resources and the need to characterize the smog issue within a North American context. As we improve our understanding of the potential influence of global background O₃ and PM_{2.5} on the conclusions reached by modelling existing and future scenarios, studies where models can interactively exchange

information between the global to regional to local scales are required. In addition, given the weight of epidemiological information which is surfacing, the need to better characterize the local to human exposure scales will become critical.

Intermittent sources, such as wildfires or wind-dust or even lightning, which are highly variable from year to year and for which the onset is challenging to model, were excluded from the studies reviewed as is the case in most similar analyses in the rest of the modelling community. Approaches to consider these sources should be entertained as their significance likely increases in future years where emissions are reduced and climate change influences more pronounced.

In many ways, this review highlighted many first studies of specific activity sectors. In many cases, the initial estimates of impact and contributions need to be verified and refined and more comprehensive studies performed to investigate the role of individual sectors at the national level. The review also pointed out initial results in terms of the possible role of seasonality on ambient $PM_{2.5}$ levels for certain ranges of emission reduction. Again these unique results need to be confirmed and investigated further. In addition, efforts should be made to publish such studies in the peer-reviewed literature.

The method of choice for the scenario studies reviewed here was through turning emissions on and off or reducing them by significant fractions. Although providing important insights, this approach is not always optimal especially when the chemistry of the target pollutants is highly nonlinear, as can be the case for secondary pollutants. New methods are emerging allowing the investigation of smaller perturbations in the emission input and their applications to scenario analyses should be encouraged. Such methods also have the potential to help in the assessment of uncertainties in scenario predictions, information that would greatly improve the usefulness of model projections.

Finally, this faster and more accessible modelling capacity has heightened the need for more thorough and coordinated studies. Of particular attention in the design of new studies should be the characterization of the emission input, possibly against a set emission benchmark, the establishment of standard analysis metrics and the rationalization and documentation of emission projections. The reach of modelling reviews would be greatly improved by integrating a more uniform framework to individual studies.

References

- Aherne, J., 2008a. Critical Load and Exceedance Estimates for Upland forest Soils in Manitoba and Saskatchewan: Comparing Exceedance Outputs of Different Models. Final Report, Environmental and Resource Studies, Trent University, Peterborough, Ontario.
- Aherne, J., 2008b. Calculating Critical Loads of Acid Deposition for Forest Soils in Alberta: Critical load, exceedance and limitations. Final Report, Environmental and Resource Studies, Trent University, Peterborough, Ontario.
- AMEC, 2003. *Analysis of 2001-2002 Airborne Ozone and Ozone Precursor Measurements in the Oil Sands*. Prepared for CEMA, by AMEC Earth & Environmental Limited, September 2003
- AMEC, 2007, Fort Air Partnership Air Quality Database.
- Brasseur, G.P., M. Schultz, C. Granier, M. Saunio, T. Diehl, M. Botzet, E. Roeckner, and S. Walters, 2006. Impact of climate change on the future chemical composition of the global troposphere. *Journal of Climate*, 19, 393203951.
- Byun, D.W., J.K.S. Ching, 1999: Science Algorithms of the EPA Models-3 Community Multiscale Air Quality (CMAQ) Modelling System. EPA/600/R-99/030, US Environmental Protection Agency, Washington, DC, United States, March 1999.
- Canadian Council of Ministers of the Environment (CCME), 2000. Canada-wide standards for particulate matter (PM) and ozone. Report available at: http://www.ccme.ca/ourwork/air.html?category_id=99
- Centre for Research on Transportation, 2005. Calculation of mobile emissions on a fine grid. Final project report, Université de Montréal, Canada, October 2005, 145 pp.
- Cheminfo Services Inc., 2007. *Forecast of Common Air Contaminants in Alberta (2002 to 2020)*. Prepared for Environment Canada by Cheminfo Services, May 2007
- Clearstone Engineering Ltd, 2007. *2002 Inventory of CAC Emissions from the Oil Sands Region of Alberta*. Prepared for NSMWG of CEMA, May 2007
- Clearstone Engineering Ltd., 2005. *A National Inventory of Greenhouse Gas (GHG), Criteria Air Contaminant (CAC) and Hydrogen Sulphide (H2S) Emissions by the Upstream Oil and Gas Industry: Volume 2 - Overview of the CAC and H2S Inventory*. Prepared for CAPP, January 2005

Côté, J., S. Gravel, A. Méthot, A. Patoine, M. Roch, and A. Staniforth, 1998a: The operational CMC-MRB Global Environmental Multiscale (GEM) model: Part I - Design considerations and formulation. *Monthly Weather Review*, 126, 1373-1395.

Côté, J.-G. Desmarais, S. Gravel, A. Méthot, A. Patoine, M. Roch, and A. Staniforth, 1998b: The operational CMC-MRB Global Environmental Multiscale (GEM) model: Part II – Results. *Monthly Weather Review*, 126, 1397-1418.

Dudhia, J., D. Gill, K. Manning, W. Wang, and C. Bruyere, 2004: PSU/NCAR Mesoscale Modelling System Tutorial Class Notes and User's Guide: MM5 Modelling System Version 3, Mesoscale and Microscale Meteorology Division, National Center for Atmospheric Research, US, January 2004. Available online at <http://www.mmm.ucar.edu/mm5/mm5-home.html> (accessed 24 November 2004).

Environment Canada, 2005a. 2004 Canadian Acid Deposition Science Assessment: Summary of Key Results. Toronto: Environment Canada.

Environment Canada, 2005b. The Development of the MOBILE6.2C Model. Environment Canada Tech. Rep. M6C-06-E, 37 pp.

Environment Canada. 2004. Characterization of the Georgia Basin/Puget Sound Airshed. Environment Canada. United States Environment Protection Agency. http://www.pyr.ec.gc.ca/Air/gb_ps_airshed/report_e.pdf

Environment Canada, 2010. The 2008 Canadian Atmospheric Assessment of Agricultural Ammonia. Environment Canada, Gatineau, QC, Canada. ISBN: 978-1-100-12420-9

Farrell, T. C., 2005a. Canada-Wide Standards Achievement in the Atlantic Region: Modelling Results for New Brunswick, Meteorological Service of Canada, Atlantic Region Science Report Series 2005-06, May 2005.

Farrell, T. C., 2005b. Canada-Wide Standards Achievement in the Atlantic Region: Modelling Results for Nova Scotia, Meteorological Service of Canada, Atlantic Region Science Report Series 2005-07, May 2005.

Farrell, T. C., 2006a. Canada-Wide Standards Achievement in the Atlantic Region: Model Results for Nova Scotia, Part II, Meteorological Service of Canada, Atlantic Region Science Report Series 2006-02, August 2006.

Farrell, T. C., 2006b. Canada-Wide Standards Achievement in the Atlantic Region: Model Results for New Brunswick, Part II, Meteorological Service of Canada, Atlantic Region Science Report Series 2006-03, August 2006.

Farrell, T. C., 2007. Canada-Wide Standards Achievement in the Atlantic Region: Supplementary Model Results for Prince Edward Island and Newfoundland and Labrador Meteorological Service of Canada, Atlantic Region Science Report Series 2007-04, December 2007.

Fox D, Influence of biogenic emission uncertainties on ozone predictions in the Oil Sands Region, Air Quality and Health: State of the Science 2002 Science Symposium, Clean Air Strategic Alliance (CASA), 2002.

Fox, D. and Kellerhals, M., 2007. Modelling of ozone levels in Alberta: Base case, sectoral contributions and a future scenario. Environment Canada, Edmonton AB.

GVRD/FVRD, 2002: 2000 emission inventory for the Lower Fraser Valley airshed. Greater Vancouver Regional District, Policy and Planning Department, Burnaby, British Columbia, Canada, October 2002.

GVRD/FVRD, 2003: Forecast and backcast of the 2000 emission inventory for the Lower Fraser Valley airshed 1985–2025. Greater Vancouver Regional District, Policy and Planning Department, Burnaby, British Columbia, Canada, July 2003.

Jeffries, D.S., R. Ouimet, 2005. Chapter 8: Critical loads: Are they being exceeded? In: 2004 Canadian Acid Deposition Science Assessment. Environment Canada, Ottawa.

Jeffries, D.S., Lam, D.C.L., Moran, M.D., Wong, I. 1999. The effects of SO₂ emission controls on critical load exceedances for lakes in southeastern Canada. *Wat. Sci. Technol.* 39, 165-

Jiang, W., É. Giroux, D. Yin, and H. Roth, 2004. A modelling study on the impact of three sets of future vehicle emission standards on particulate matter loading in the Lower Fraser Valley: Interim report. ICPET Tech. Rep. PET-1557-04S, 86 pp. [Available from National Research Council of Canada, Institute for Chemical Process and Environmental Technology, 1200 Montreal Road, Ottawa, ON, Canada K1A 0R6]

Jiang, W., S. Smyth, É. Giroux, H. Roth, and D. Yin, 2006. Differences between CMAQ fine mode particles and PM_{2.5} concentrations and their impact on model performance evaluation in the Lower Fraser Valley. *Atmospheric Environment*, 40, 4973-4985.

Labrèche, France, Yvette Bonvalot and Marie-Claude Boivin, 2000. Enquête téléphonique sur la possession et l'acquisition d'un système de chauffage au bois dans la région de Montréal. Report, Direction de la santé publique de Montréal-Centre, 54 pp.

Lavoué D, S. Gong and B. J. Stocks, 2007. Modelling emissions from Canadian wildfires: a case study of the 2002 Quebec fires. *International Journal of Wildland Fire*, 16, 649-663

Levelton Engineering Ltd., 1995: Pacific 93 air emissions inventory draft report. Technical Report 495-195, Levelton Engineering Ltd., 150 – 12791 Clarke Place, Richmond, British Columbia, Canada, V6V 2H9, July 1995.

Li, S.-M., 2004. A concerted effort to understand the ambient particulate matter in the Lower Fraser Valley: the Pacific 2001 Air Quality Study. *Atmospheric Environment*, 40, 5719-5731.

Makar, P., Moran, M., Zheng, Q., Cousineau, S., Sassi, M., Duhamel, A., Besner, M., Crevier, L.-P., di Cenzo, C., Vingarzan, R., Nissen, R., Bouchet, V., 2009 Chapter 8: Modelling the Effects of Ammonia on Regional Air Quality. *In* Environment Canada, 2010. The 2008 Canadian Atmospheric Assessment of Agricultural Ammonia, Environment Canada, Gatineau, QC, Canada.

MCNC, 2000: Sparse Matrix Operator Kernel Emissions (SMOKE) Modelling System. Available at <http://www.emc.mcnc.org/products/smoke/>.

Meng Z., D. Dabdub, and J.H. Seinfeld, Chemical coupling between atmospheric ozone and particulate matter. *Science*, 277 (5322), 116-119, doi:10.1126/science.277.5322.116, 1997.

Moran, M.D., Q. Zheng, R. Pavlovic, S. Cousineau, V.S. Bouchet, M. Sassi, P.A. Makar, W. Gong, and C. Stroud, 2008. Predicted acid deposition critical-load exceedances across Canada from a one-year simulation with a regional particulate-matter model. *Proc. 15th Joint AMS/A&WMA Conference on Applications of Air Pollution Meteorology*, Jan. 21-24, New Orleans, 20 pp. [Available from weblink <http://ams.confex.com/ams/pdfpapers/132916.pdf>]

McNulty, S.G., E.C. Cohen, J.A. Moore Myers, T.J. Sullivan, H. Li. 2007. Estimates of critical acid loads and exceedances for forest soils across the conterminous United States. *Environmental Pollution*, 149: 281-292.

Ouimet, R., P.A. Arp, S.A. Watmough, J. Aherne, I. Demerchant, 2006. Determination and mapping critical loads of acidity and exceedances for upland forest soils in eastern Canada. *Water, Air, and Soil Pollution*, 172: 57-66.

Pollution Data Division http://www.ec.gc.ca/pdb/cac/Emissions1990-2015/emissions_e.cfm.

RWDI, 2003a. *Oil and Gas Industrial Emissions Project*. RWDI West Project No. W03-280, prepared for Environment Canada, May 2003

RWDI, 2003b. *Pacific Northwest International Air Quality Modelling Project, Phase 2 Report*. Environment Canada, Pacific and Yukon Region, Vancouver, BC.

Seigneur, C. Moran, M.D. 2004. Using models to estimate particle concentration. Chapter 8 in *Particulate Matter Science for Policy Makers: A NARSTO Assessment*, P. McMurry, M. Shepherd, and J. Vickery, Editors, February, 42 pp., Cambridge University Press, Cambridge.

SENES/AIR, 2002: Updated estimate of Canadian on-road vehicle emissions for the years 1995–2020. SENES Consultants Limited, Air Improvement Resources Inc., Revised October 2002.

Sistla, G., C. Hogrefe, W. Hao, J.-Y. Ku, E. Zalewsky, R.F. Henry, and K. Civerolo, 2004.

An operational assessment of the application of the relative reduction factors in the demonstration of attainment of the 8-hr ozone National Ambient Air Quality Standard. *J. Air & Waste Manage. Assoc.*, 54, 950-959.

Smyth, S., D. Yin, H. Roth, and W. Jiang, 2005: A study of the impact of GEM and MM5 meteorology on CMAQ modelling results in Eastern Canada and the Northeastern United States. ICPET Tech. Rep. PET-1561-04S, 77 pp. [Available from National Research Council of Canada, ICPET, 1200 Montreal Road, Ottawa, ON]

Smyth, S.C., D. Yin, H. Roth, W. Jiang, 2006a. The Impact of GEM and MM5 Modelled Meteorological Conditions on CMAQ Air Quality Modelling Results in Eastern Canada and the Northeastern United States. *Journal of Applied Meteorology and Climatology*, 45, 1525-1541.

Smyth, S.C., W. Jiang*, D. Yin, H. Roth, and É. Giroux, 2006b. Evaluation of CMAQ O₃ and PM_{2.5} performance using Pacific 2001 measurement data. *Atmospheric Environment*, 40, 2735-2749.

TNS Canadian Facts, 2006. Residential fuelwood Combustion in Canada, volume 1. Report presented to Environment Canada, April 2006, 72 pp.

US EPA, 2003: User's Guide to MOBILE6.1 and MOBILE6.2: Mobile Source Emission Factor Model. U.S. EPA Rep. EPA420-R-03-010, 261 pp.

U.S. Environmental Protection Agency. 2005. Guidance on the use of models and other analyses in attainment demonstrations for the 8-hour ozone NAAQS. Publication No. EPA-454/R-05-002, October, U.S. Environmental Protection Agency, Research Triangle Park, North Carolina, 128 pp. [Available at www.epa.gov/scram001/guidance/guide/8-hour-O3-guidancefinal-version.pdf]

US EPA, 2009. Clean Air Interstate Rule. <http://www.epa.gov/interstateairquality/> [Wednesday, May 13th, 2009]

Vingarzan, R., Li, S.-M., 2006. The Pacific 2001 Air Quality Study – synthesis of findings and policy implications. *Atmospheric Environment*, 40, 2637-2649.

Wong I. and Dennis I. 2008. Interim Ecosystem critical load map, Air Quality Program, Environment Canada, September 2008

Yin, D., W. Jiang, H. Roth, É. Giroux, 2004: Improvement of biogenic emissions estimation in the Canadian Lower Fraser Valley and its impact on particulate matter modelling results, *Atmospheric Environment*, 38, 507–522.

Appendix – Table of Model Versions Used in the Modelling Scenarios Presented in Chapter 6

The following table is a summary of the 25 modelling scenarios discussed throughout chapter 6. The table should be referred to while reading chapter 6 to obtain the specific parameters of the modelling scenarios. The first column entitled Scenario identifies the scenario with a number and gives a brief description of the scenario. The Model version column specifies the air quality model used for the particular scenario. The following columns give the spatial resolution, the emissions inventory and meteorology used for the particular scenarios, respectively. The ‘model time period’ gives the duration of the scenario simulation. Additional comments on the model scenario to complete the information are added in the last column.

Scenario	Model Version	Spatial Resolution and domain coverage	Modelled Time Period(s)	Emissions	Meteorology	Notes
Section 6.3						
S1	AURAMS 1.3.1	Resolution: 42 x 42 km; 30 vertical levels up to 25km (first thermodynamic level at 14m) Domain: continental	Period: 2002 Length: Annual	Canadian 2002 CAC inventory except for agricultural NH ₃ sources; Canadian NH ₃ emission from NAESI inventory (base year 2002); US 2002 National inventory; Mexican 1999 emission; Processing: SMOKE v. 2.0; On-line biogenic emission calculations (BEIS v.3.9)	Base year: 2002 Generated using GEMDM v. 3.2.0 with a 24 km grid configuration	Uses a modified version of AURAMS 1.3.1 with explicit O ₃ and PM species boundary conditions; Publication: Makar <i>et al.</i> , 2009
S2	CMAQ 4.3	Resolution: Nested 4 x 4 km within a 12 x 12 km; 15 vertical levels up to 100mb (first level above surface at $\sigma=0.995$) Domain: SW British Columbia and NW Washington state	Period: August 09-21, 2001 Length: Episodic	Canadian 1995 CAC inventory except for the Greater Vancouver (GVRD) and Fraser Valley (FVRD) regional districts and mobile emissions; 2001 local inventory for GVRD and FVRD (GVRD,FVRD,2002,2003); 2001 specific mobile emissions generated with MOBILE; US 1999 national inventory; Processed with SMOKE including biogenic emissions.	Base year 2001 Generated using MM5 v. 3.6.2	Chemistry mechanisms included modified RADM2 and AERO ₃ modules; Publication: Smyth <i>et al.</i> , 2006.
S3	CMAQ 4.3	Resolution: Nested 4 x 4 km within a 12 x 12 km; 16 vertical levels up to 16km above ground (first level at 38m above surface) Domain: Central British Columbia to central Oregon	Periods: August 09-31, 2001; December 01-13, 2002. Length: Episodic	Canadian 2000 CAC inventory; US 2002 national inventory (with 1999 inventory data when 2002 data were unavailable); Processed with SMOKE including biogenic emissions.	Base year 2001 and 2002 respectively; Generated using MC2 with a 3.3km grid resolution, (dynamicsv.4.9.1; physics v. 3.7)	Used the SAPRC-99 photochemical mechanism;
S4	CMAQ 4.3	Resolution: Nested 4 x 4 km within a 12 x 12 km; 16 vertical levels up to 16km above ground (first	Periods: August 09-31, 2001; December 01-13, 2002	Same as S3	Base year 2001 and 2002 respectively; Generated using MC2 with a 3.3km	Used the SAPRC-99 photochemical mechanism;

Scenario		Model Version	Spatial Resolution and domain coverage	Modelled Time Period(s)	Emissions	Meteorology	Notes
			level at 38m above surface) Domain: Central British Columbia to central Oregon	Length: Episodic		grid resolution, (dynamics v.4.9.1; physics v. 3.7)	
S5	On-off of oil and gas sector, over a domain covering Alberta	CMAQ 4.5	Resolution: Nested 12 x 12 km within a 36 x 36 km; 14 vertical levels up to 100mb (first level above surface at $\sigma=0.995/36$ m) Domain: Alberta	Period: June 01-August 31, 2002 Length: Seasonal	Canadian 2000 CAC inventory (AQMAS September 2006 version) except for oil sands, oil and gas sector and for the Fort Air Partnership ³⁶ ; Oil sands emissions from environmental assessments including the 2002 Canadian Natural Resources Ltd Horizon application and the 2003 Shell Canada Jackpine application (RWDI, 2003a), adjusted to Clearstone (2007) totals - base year 2000; For the Upstream Oil and Gas sector, emission totals and spatial allocation are based on <i>Clearstone, (2005)</i> ; Emission inventories from Fort Air Partnership based on the FAP Air Quality Database (<i>AMEC, 2007</i>); US 2001 national inventory ; Processed with SMOKE including biogenic emissions.	Base year: 2002; Generated using MM5 v. 3.6.	Publication: Fox and Kellerhals, 2007.
S6	On-off of oil sands sector, over a domain covering Alberta	CMAQ 4.5	Resolution: Nested 12 x 12 km within a 36 x 36 km; 14 vertical levels up to 100mb (first level above surface at $\sigma=0.995/36$ m) Domain: Alberta	Period: June 01-August 31, 2002 Length: Seasonal	Same as S5	Base year: 2002; Generated using MM5 v. 3.6.	Publication: Fox and Kellerhals, 2007.
S7	On-off of chemical and refineries sectors, over a domain covering Alberta	CMAQ 4.5	Resolution: Nested 12 x 12 km within a 36 x 36 km; 14 vertical levels up to 100mb (first level above surface at $\sigma=0.995/36$ m) Domain: Alberta	Period: June 01-August 31, 2002 Length: Seasonal	Same as S5	Base year: 2002; Generated using MM5 v. 3.6.	Publication: Fox and Kellerhals, 2007.

³⁶ The Fort Air Partnership is an airshed association in the industrial area located north-east of Edmonton

Scenario		Model Version	Spatial Resolution and domain coverage	Modelled Time Period(s)	Emissions	Meteorology	Notes
S8	On-off of electricity sector, over a domain covering Alberta	CMAQ 4.5	Resolution: Nested 12 x 12 km within a 36 x 36 km ¹⁴ vertical levels up to 100mb (first level above surface at $\sigma=0.995/36$ m) Domain: Alberta	Period: June 01-August 31, 2002 Length: Seasonal	Same as S5	Base year: 2002; Generated using MM5 v. 3.6.	Publication: Fox and Kellerhals, 2007.
S9	Woodstove replacement scenario, over a domain covering eastern Canada and the U.S.	AURAMS 1.3.1	Resolution: 21 x 21 km; 30 vertical levels up to 25km (first thermodynamic level at 14m) Domain: North-eastern North America	Period: November 20-26, 2006 Length: Episodic	Canadian 2000 CAC inventory except for on-road for the Montréal area and wood combustion emissions; On-road vehicle emissions for Montréal area: generated using the GRILLE software (Centre for Research on Transportation, 2005); Wood combustion emissions for the province of Québec: estimated from results from recent surveys - TNS Canadian Facts (2006), Environment Canada's 2006 survey conducted in a residential area of Montreal and Quebec City, and the Montreal public Health department survey of 2000 (Labrèche et al, 2000). US 2001 national inventory; Processed using SMOKE; On-line biogenic emission calculations (BEIS v.3.9).	Base year: 2006; Generated using GEM.	
S10	Influence of background ozone in eastern Canada/US	CMAQ 4.6	Resolution: 36 x 36 km; 14 vertical levels up to 100mb (first level above surface at $\sigma=0.995$) Domain: North-eastern North America	Period: May 1 to September 30, 2005 Length: Seasonal	All anthropogenic emissions were set to zero; Biogenic emissions processed using SMOKE v. 2.1.	Base year: 2005; Generated using WRF v. 2.2	
Section 6.4							
S11	Business-as-usual projection to 2015 over a North American domain	AURAMS v.1.3.1	Resolution: 42 x 42 km; 30 vertical levels up to 25km (first thermodynamic level at 14m) Domain: North America	Period: 2015 Length: Annual	Canadian 2015 CAC business-as-usual projection (November 2007 version) of 2000 Canadian inventory; U.S. 2015 CAIR (Clean Air Interstate Rule) projection of 2001 national inventory; Mexican 1999 emission inventory (not projected due to lack of data); Processed with SMOKE; On-line biogenic emission calculations (BEIS v.3.9).	Base year: 2002; Generated using GEMDM v. 3.2.0 with a 24 km grid configuration.	AURAMS v.1.3.1 includes explicit boundary conditions for O ₃ only; Reference case: 2002 simulation using the Canadian 2002 CAC emission inventory (version Can2002V2.3), the U.S. 2002 national inventory and the Mexican 1999 inventory.

Scenario		Model Version	Spatial Resolution and domain coverage	Modelled Time Period(s)	Emissions	Meteorology	Notes
S12	Business-as-usual projection to 2015 for British Columbia over a domain centred on the Georgia Basin and Puget sound area	CMAQ 4.3	Resolution: Nested 4 x 4 km within a 12 x 12 km; 16 vertical levels up to 16km above ground (first level at 38m above surface) Domain: Central British Columbia to central Oregon	Periods: 2015 summer and winter episodes Length: Episodic	Canadian 2015 CAC business-as-usual projection (April 2007 version) of 2000 Canadian inventory; U.S. 2015 CAIR (Clean Air Interstate Rule) projection of 2001 national inventory; Processed with SMOKE including biogenic emissions.	Base year 2001 (summer) and 2002 (winter); Generated using MC2 with a 4.0km grid resolution, (dynamics.v.4.9.1; physics v. 3.7)	Used the SAPRC-99 photochemical mechanism; Reference cases: August 09-31, 2001 and December 1-13, 2002 using the same emissions as S3.
S13	Analysis of vehicle emissions standards in a 2020 projection over a domain centred on the Lower Fraser Valley of BC	CMAQ 4.1 (Byun and Ching, 1999)	Resolution: Nested 5 x 5 km within a 15 x 15 km; 15 vertical levels. Domain: SW British Columbia and NW Washington state	Period: July 31 – August 08, 1993 Length: Episodic	Canadian 2020 projection of 1993 specific inventory (see notes column) including the three vehicle emission standard under study (SENES/AIR, 2002); U.S. 2020 projection of 1993 inventory (see notes column); Biogenic emissions generated with NRC/BEIS (Yin <i>et al.</i> , 2004) Processed with SMOKE v.1.4 including biogenic emissions.	Base year 1993; Generated using MM5 v.3.	Used modified RADM2 and AERO2 modules; Present reference case: July 31 - August 8, 1993 using Pacific'93 daily emission inventory (Levelton Engineering Ltd, 1995) for inner Canadian domain with 1995 Canadian and 1995 U.S. (Models-3 version 3.0) emissions inventories backcasted to 1993 for the remainder of the domain; Specific 1993 mobile data were generated with MOBILE6.2 and 6.2C for both Canada and the U.S.; Future reference case: same July 31 to August 8 1993 period simulated with 2020-representative emissions generated by projecting the 1993 inventories for Canada and U.S. Projection factors for area, point, and non-mobile sources were calculated by using data from the Greater Vancouver Regional District (GVRD/FVRD, 2003) while projection factors for on-road mobile sources were generated using data from a report by SENES/AIR (2002). Publication: Jiang <i>et al.</i> , 2004.

Scenario		Model Version	Spatial Resolution and domain coverage	Modelled Time Period(s)	Emissions	Meteorology	Notes
S14	Alberta specific business-as-usual projection for 2012-2015 for domain covering Alberta	CMAQ 4.5	Resolution: Nested 12 x 12 km within a 36 x 36 km; 14 vertical levels up to 100mb (first level above surface at $\sigma=0.995/36$ m) Domain: Alberta	Period: June 01 - August 31, 2002 Length: Seasonal	Modified Canadian 2000 inventory (see S5) with 2012-2015 projections for electricity power generation, chemical, refineries and cement emissions (Cheminfo, 2007; Yin <i>et al.</i> , 2004; SENES/AIR, 2002; Levelton Engineering Ltd., 1995; GVRD/FVRD, 2003) and oil sands emissions (RWDI, 2003a; Imperial Kearn Lake Project application, 2005; AMEC, 2007); US 2001 national inventory; Processed using SMOKE v. 2.1 including biogenic emissions.	Base year: 2002; Generated using MM5 v. 3.6.	Reference case: 2002 using the same emission inventory as S5; Publication: Fox and Kellerhals, 2007.
Section 6.5							
S15	2015 projection with additional emission reductions for a number of Canadian industrial sectors over a north American domain	AURAMS v.1.3.1	Resolution: 42 x 42 km ; 30 vertical levels up to 25km (first thermodynamic level at 14m) Domain: North America	Period: 2015 Length: Annual	Canadian 2015 CAC business-as-usual projection (November 2007 version) from 2000 Canadian inventory for anthropogenic emissions except for sectors cited below; Specified sectoral emission reductions for the following Canadian sectors: Upstream Oil and Gas, oil sands, petroleum refining, pipelines, electricity power generation, aluminum, alumina, iron and steel, cement, lime, pulp and paper, wood product, chemical, iron ore pelletizing, base metal smelter (see <i>Table 8</i> for details) U.S. 2015 CAIR (Clean Air Interstate Rule) national inventory; Mexican 1999 emission inventory (not projected due to lack of data); Processed with SMOKE; On-line biogenic emission calculations (BEIS v.3.9).	Base year: 2002; Generated using GEMDM v. 3.2.0 with a 24 km grid configuration.	AURAMS v.1.3.1 includes explicit boundary conditions for O ₃ only; Reference case: 2015 business-as-usual simulation described in S11.

Scenario		Model Version	Spatial Resolution and domain coverage	Modelled Time Period(s)	Emissions	Meteorology	Notes
S16	2015 projection with additional emission reductions for identified point sources in the vicinity of Vancouver over a domain centred on the Georgia Basin and Puget sound area	CMAQ 4.3	Resolution: Nested 4 x 4 km within a 12 x 12 km; 16 vertical levels up to 16km above ground (first level at 38m above surface) Domain: Central British Columbia to central Oregon	Periods: 2015 summer and winter episodes Length: Episodic	Canadian 2015 CAC business-as-usual projection (April 2007 version) of 2000 Canadian inventory except for an ensemble of point sources in the vicinity of Vancouver; Reduction of NO _x emissions at two plants and SO ₂ and primary PM _{2.5} emissions at refineries in the vicinity of Vancouver; U.S. 2015 CAIR (Clean Air Interstate Rule) projection of 2001 national inventory; Processed with SMOKE including biogenic emissions.	Base year 2001 (summer) and 2002 (winter); Generated using MC2 with a 3.3km grid resolution, (dynamics.v.4.9.1; physics v. 3.7)	Used the SAPRC-99 photochemical mechanism; Reference cases: 2015 projection of August 09-31, 2001 and December 1-13, 2002 described in S11.
S17	2015 projection with additional emission reductions as prescribed by a GVRD air quality management plan over a domain centred on the Georgia Basin and Puget sound area	CMAQ 4.3	Resolution: Nested 4 x 4 km within a 12 x 12 km; 16 vertical levels up to 16km above ground (first level at 38m above surface) Domain: Central British Columbia to central Oregon	Periods: 2015 summer and winter episodes Length: Episodic	Canadian 2015 CAC business-as-usual projection (April 2007 version) of 2000 Canadian inventory except for an ensemble of point sources in the vicinity of Vancouver, marine emissions and non-road emissions; Reduction of NO _x emissions at two plants and SO ₂ and primary PM _{2.5} emissions at refineries in the vicinity of Vancouver as for S16; Specified reductions in marine sector resulting from estimates of use of low sulphur fuel for ocean-going vessels, increased use of shore power for hotelling operations, retrofitting of BC Ferries with emission controls, and re-powering and retrofitting working harbour vessels; Specified reductions in non-road emissions from estimates of use of diesel oxidation catalysts in non-road engines and re-powering; U.S. 2015 CAIR (Clean Air Interstate Rule) projection of 2001 national inventory; Processed with SMOKE including biogenic emissions.	Base year 2001 (summer) and 2002 (winter); Generated using MC2 with a 3.3km grid resolution, (dynamics.v.4.9.1; physics v. 3.7)	Used the SAPRC-99 photochemical mechanism; Reference cases: 2015 projection of August 09-31, 2001 and December 1-13, 2002 described in S11.
Section 6.6							
S18	On-off of Canadian and U.S. emissions during summer 2003 over a North American domain	CHRONOS	Resolution: 21 x 21 km; 24 vertical levels up to 6km (first thermodynamic level at 10m) Domain: North America	Period: Summer 2003 Length: Seasonal	Canadian 1995 inventory grown from 1990 Canadian CAC inventory; U.S. 1999 national inventory; On-line biogenic emission calculations.	Base year: 2003; Generated using GEMDM with a 24 km grid configuration.	

Scenario		Model Version	Spatial Resolution and domain coverage	Modelled Time Period(s)	Emissions	Meteorology	Notes
S19	On-off of Canadian and U.S. emissions during summer 2004 over a North American domain	CHRONOS	Resolution: 21 x 21 km; 24 vertical levels up to 6km (first thermodynamic level at 10m) Domain: North America	Period: Summer 2004 Length: Seasonal	Canadian 1995 inventory grown from 1990 Canadian CAC inventory; U.S. 1999 national inventory; On-line biogenic emission calculations.	Base year: 2004; Generated using GEMDM with a 24 km grid configuration.	
S20	On-off of Canadian and U.S. emissions in 2015 over a North American domain	AURAMS v.1.3.1	Resolution: 42 x 42 km; 30 vertical levels up to 25km (first thermodynamic level at 14m) Domain: North America	Period: 2015 Length: Annual	Canadian 2015 CAC business-as-usual projection (November 2007 version) from 2000 Canadian inventory; U.S. 2015 CAIR (Clean Air Interstate Rule) national inventory; Mexican 1999 emission inventory (not projected due to lack of data); Processed with SMOKE; On-line biogenic emission calculations (BEIS v.3.9).	Base year: 2002; Generated using GEMDM v. 3.2.0 with a 24 km grid configuration.	AURAMS v.1.3.1 includes explicit boundary conditions for O ₃ only.
S21	NO _x SIP Call study in 2005 over an eastern North American domain	CMAQ 4.6	Resolution: 36 x 36 km 14 vertical levels up to 100mb (first level above surface at $\sigma=0.995$) Domain: north-eastern North America	Period: May 01 – September 30, 2005 Length: Seasonal	Canadian 2002 CAC emission inventory except for on-road and point source emissions; U.S. 2002 national inventory except for on-road and electricity power generation point sources emissions; 2005-specific on-road emissions generated with MOBILE; 2005-specific electricity power generation emissions; Processed with SMOKE v.2.1 including biogenic emissions.	Base year: 2005; Generated using WRF v. 2.2.	Reference case: 2002 simulation using the Canadian 2002 CAC emission inventory and the U.S. 2002 national inventory.
S22	On-off of Canadian and U.S. emissions during typical BC episodes over a domain centred on the Georgia Basin and Puget sound area	CMAQ 4.3	Resolution: Nested 4 x 4 km within a 12 x 12 km; 16 vertical levels up to 16km above ground (first level at 38m above surface) Domain: Central British Columbia to central Oregon	Periods: August 09-31, 2001; December 01-13, 2002 Length: Episodic	Same as S3.	Base year 2001 and 2002 respectively; Generated using MC2 with a 3.3km grid resolution, (dynamics v.4.9.1; physics v. 3.7)	Used the SAPRC-99 photochemical mechanism;

Scenario		Model Version	Spatial Resolution and domain coverage	Modelled Time Period(s)	Emissions	Meteorology	Notes
S23	On-off of Canadian and U.S. emissions during a typical Quebec episode over a domain covering eastern Canada and the U.S.	AURAMS	Resolution: 21 x 21 km; 30 vertical levels up to 25km (first thermodynamic level at 14m) Domain: Eastern Canada and U.S.	Period: July 27 to August 3, 2001 Length: Episodic	Canadian 1995 inventory grown from 1990 Canadian CAC inventory; U.S. 1996 national inventory; On-line biogenic emission calculations.	Base year: 2001; Generated using GEM.	
S24	On-off of Canadian and U.S. emissions during typical summer and winter episodes in the Atlantic provinces over domain covering eastern Canada and the U.S.	CHRONOS (v. 2005-2006)	Resolution: 21 x 21 km; 24 vertical levels up to 6km (first thermodynamic level at 10m) Domain: Eastern Canada and U.S.	Periods: 14-22 June 2001; August 2 -12 2001; 5-10 February, 2005 Length: Episodic	June 2001 case: Canadian 1995 inventory grown from 1990 Canadian CAC inventory US 1996 national inventory; August 2001 and February 2005 cases: Canadian 2000 CAC inventory; U.S. 2001 national inventory; All cases: Emissions processed using SMOKE. On-line biogenic emission calculations.	Base years: 2001 and 2005; Generated using GEM v. 1.3.1 with a 24km grid configuration.	Publications: Farrell, 2005a, 2005b, 2006a, 2006b, 2007
Section 6.7							
S25	Comparison of GEM versus MM5 meteorology on air quality predictions over a domain covering eastern North America	CMAQ 4.3	Resolution: 36 x 36 km; 14 vertical levels up to 100mb (first level above surface at $\sigma=0.995$) Domain: North-eastern US and Canada	Period: July 11 to 19, 1999 Length: Episodic	Canadian 1995 inventory grown from 1990 CAC emission inventory for point, area and non-road mobile sources; U.S. 1999 national inventory for point, area and non-road mobile sources; Specific 1999 on-road mobile emissions generated with MOBILE 6.2c and 6.2 for Canada and U.S.; Processed with SMOKE v.2.0; Biogenic emissions for both Canada and the U.S. generated using the Biogenics Emissions Inventory System (BEIS) version 3.09.	Base year: 1999; Generated with : GEM v.3.1.1 with physics v.4.0 for one case (post processing of the meteorological results was performed using GEM-MCIP v. 2.2) and with MM5 v.3.3 for the other case	Used modified RADM2 and AERO2 modules; Publications: (Smyth <i>et al.</i> , 2005, 2006a)

CHAPTER 7: Air Quality at the Regional and Local Scale: The What, Where, Why and How of Concentration Variations

Jeffrey R. Brook, Julie Dion, Private Consultant, Colleen Farrell, Kristina Friesen, Lisa Phinney Langley, Markus Kellerhals, Gilles Morneau, Neville Reid, Roxanne Vingarzan, David Waugh, Brian Wiens, Mario Benjamin, Claude Gagnon, Jacques Rousseau.

KEY MESSAGES AND IMPLICATIONS

- Transboundary movement of pollutants occurs all across Canada. Long-range transport of pollutants has a greater impact on air quality over southern Ontario, Québec and Atlantic Canada compared to the Prairies and British Columbia. The regional differences in the nature of transboundary transport imply that smaller Canada-U.S. border sub-regions could be defined and assessed more comprehensively to address air quality issues more effectively.
- Despite the important influence of long-range transport in the eastern half of Canada, local emissions and local formation of secondary air pollutants (O_3 and $PM_{2.5}$) have a large enough impact to degrade air quality and in some areas to the extent that Canada-wide Standard levels are surpassed or nearly surpassed.
- Wintertime air quality, while always an issue, has become a more apparent problem because of the greater recognition of the importance of $PM_{2.5}$ and NO_2 . Winter pollution events are different from those in the summer in that local emission sources and primary pollutants (e.g., NO_x) play a greater role.
- There is considerable variability in concentrations over Atlantic Canada. This is due to long-range transport over the ocean and complex meteorology associated with the coastal environment. These features result in the redistribution of both transported and locally emitted pollutants leading to pollutant layers above the surface that impact higher elevation inland areas more frequently. This complex meteorology also leads to locations with relatively higher concentrations (hotspots) near sources and over surrounding inland and coastal locations.
- Ontario and Québec face problems associated with local industrial regions, but the large urban areas and accompanying high traffic density have widespread impacts on population exposures. In Southern Ontario, the Great Lakes and the close proximity to U.S. sources represent important influences on air quality. In Southern Québec, pollutant transport from the U.S. is not as significant and thus the frequency of poor air quality events tends to be equal between seasons if not slightly more important in winter.

- O₃ across Ontario remains a key issue with only small improvements in peak concentrations (frequency of high hourly concentrations) during the past 15+ years. While NO_x concentrations have declined, baseline O₃ levels in the main population centres of Ontario, as well as Québec and many other urban areas in Canada, have risen, highlighting some of the challenges facing future air quality management.
- Emissions of NO_x, VOCs and PM_{2.5} in Alberta in 2006 are the largest of any Canadian province but are often dispersed quickly so that ambient concentrations remain low. However, during cold and calm periods in winter, urban and industrial areas experience some of the highest concentrations of primary pollutants in Canada. Summertime photochemical air pollution is detectable in Alberta, but tends to be limited in duration and typically leads to the highest levels in less populated areas. Further expansion of the oil industry may threaten future air quality in parts of Alberta, including Edmonton.
- Air quality remains an issue in the Lower Fraser Valley (LFV), especially owing to the impact on visibility from locally formed particles arising from human, biogenic and agricultural emissions. Although trends in most pollutant concentrations are currently stable or decreasing in most of the LFV, ozone levels have remained stable or have been rising at individual sites since the early 1990s. Maintaining and improving air quality in the LFV will be a challenge in future decades due to population growth and expansion of marine shipping and agricultural industries.
- During the cold season in interior BC and northern communities across the country residential wood combustion is a major contributor to high PM_{2.5}. This is also a problem in some areas of Québec, especially along the St-Lawrence River Valley, and the Atlantic provinces and in all areas where topographic features (i.e., valleys) enhance the impact of wood burning and other local sources.
- Forest fires are important contributors to regional pollution and to periodic extreme air quality events in the Prairies, British Columbia and the north, including northern Ontario and Québec.
- Conceptual models describing and relating emissions, atmospheric processes and observations, as well as their implications for regional and local air quality management, are now documented for six specific regions in Canada. These are described in the first sections of Chapter 7 (this chapter).

7.1 Introduction

Our understanding of the basic processes influencing the concentrations and fate of ozone, PM_{2.5} and their precursors once released in the atmosphere continues to improve (Chapter 2). Similarly, Canadian data on the quantity of air pollutants emitted, as well as their distribution in time and space, is being tracked in an increasingly consistent and reliable manner (Chapter 4). Given these emission patterns, variations in meteorology, terrain, coastal

boundaries, population, industry and energy generation and consumption lead to a diverse range of observed pollutant behaviour across Canada. Although concentrations are generally higher where the emission density, either locally or upwind, is greater, a complete understanding of why they are high in certain locations and/or at certain times requires an in-depth focus involving examination of the conditions region-by-region.

The goal of this chapter is to provide information on some of the unique features, as well as similarities, in the factors controlling air pollutant concentrations within six main regions of the country:

1. The **Atlantic Region** with busy coastal cities and long complex coast lines leading to the northeast U.S.;
2. **Southern Québec and Eastern Ontario** with the relatively complex terrain of the St. Lawrence and Ottawa River Valleys and Eastern Townships, a region which includes several large population centers;
3. The densely populated and industrialized **Southern Great Lakes Region**;
4. **Alberta and the Prairies**, a relatively flat, open region extending from Manitoba into Alberta;
5. The densely populated **Lower Fraser Valley (LFV)** of British Columbia;
6. The **Interior Valleys of British Columbia** and Yukon;

Chapter 3 of this assessment focuses on how the concentrations of ozone, $PM_{2.5}$ and its chemical constituents, and the precursors of both, vary temporally on the national scale. This chapter examines the behaviour of air pollutants and the factors that control them in more detail to provide insight on why concentrations vary. Such an understanding is necessary in order to predict when and where levels will be high (i.e., for issuing air quality forecasts) and to develop strategies to reduce pollutant concentrations and ultimately reduce the impact on human health and the environment. A closer examination of the available measurement data on a region-by-region basis is necessary because, although the underlying science behind smog formation is the same everywhere, it is local emissions, physical features and meteorology that modulate local air quality. Consideration of these local factors is essential to effective air quality management.

7.2 Overview of Air Pollutant Behaviour and Issues across Canada - Regional Conceptual Models

To better understand air quality within the six regions identified above specialized studies, generating and/or examining a variety of measurement datasets, have been carried out during the past ten years. These have ranged from more in-depth analyses of monitoring data and short term special studies to intensive, multi-partner field campaigns that often involve the application of air quality models. Such detailed efforts help in emission inventory and model

development, identification of potential problems and solutions and contribute to the formulation of conceptual models (e.g., Pun and Seigneur, 1999; NARSTO, 2004) for different parts of the country.

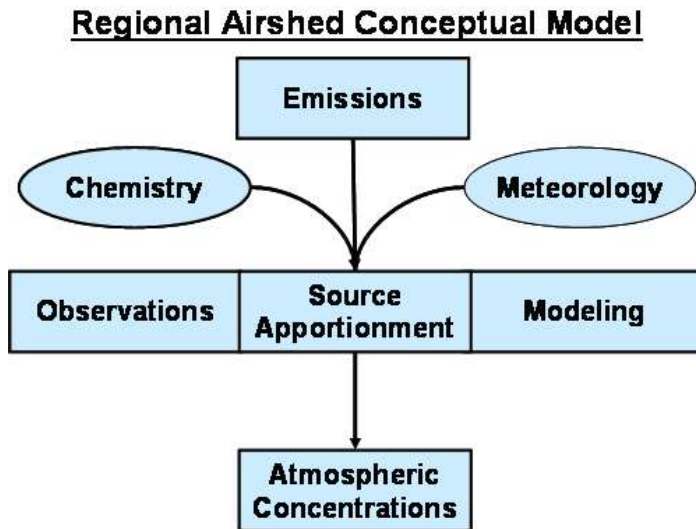


Figure 7.1 A conceptual model represents initial hypotheses of how emissions, chemistry and meteorology interact to produce the observed pollutant concentrations. Observations, source apportionment analyses with this observations and applications of models are the tools used to develop and test the conceptual model.

An air quality conceptual model is a qualitative mental model for a specific geographic region that is based on a synthesis and simplification of available information obtained from analysis of emissions, measurements and model results (Figure 7.1). The goal is to distill the primary factors contributing to increases in air pollutant concentrations, including key emission sources, terrain characteristics, and local weather and climate, into an integrated picture. Air quality model results from emissions scenarios and/or from sensitivity studies, as well as source apportionment studies, can contribute significantly to the development or refinement of a conceptual model (Craig *et al.*, 2008). Conceptual models, which are rarely considered complete, guide future scientific studies and potentially help in the development of local air quality management strategies.

In order to provide concise air quality information, region-specific conceptual models describing how the observed concentrations relate to upwind and local emissions and meteorology and chemical processes are presented in the first six sections of this chapter. Although the core of these conceptual models stems from basic scientific knowledge, there are important factors that are unique from region to region. The main body of this chapter then presents more detailed data and analyses that serve as the basis for the conceptual models and also provide an overview of our current state of knowledge. This is accomplished by comparing, among or within regions, contributions from the main source sectors, the regional

and local meteorological factors influencing air quality, temporal and spatial patterns in O_3 , $PM_{2.5}$ and NO_2 concentrations, including contributions from local/urban emissions, and the features of medium scale to long-range transport.

The information presented in this chapter is not intended to be uniform for each region. This is because over the past ten years there have been regional differences regarding which air quality issues have received the greatest attention, differences in the rate of expansion of monitoring and conducting of field intensives or special studies and differences in approach (i.e., emphasis on modelling analyses vs. measurement analyses). In particular, the last main section of this chapter provides insights into a variety of issues as shared through case studies of local, regional and/or national importance. This includes a discussion on issues such as urban scale pollutant variations and concentration gradients near highways, a major wintertime $PM_{2.5}$ episode in Ontario and Québec, recent detailed studies on $PM_{2.5}$, including source apportionment, and brief overviews of two summertime intensive field campaigns: Prairie 2005 and Pacific 2001. This chapter concludes with a discussion of key knowledge gaps that will require attention in the future in order to improve each of the regional conceptual models.

7.2.1 Atlantic Region

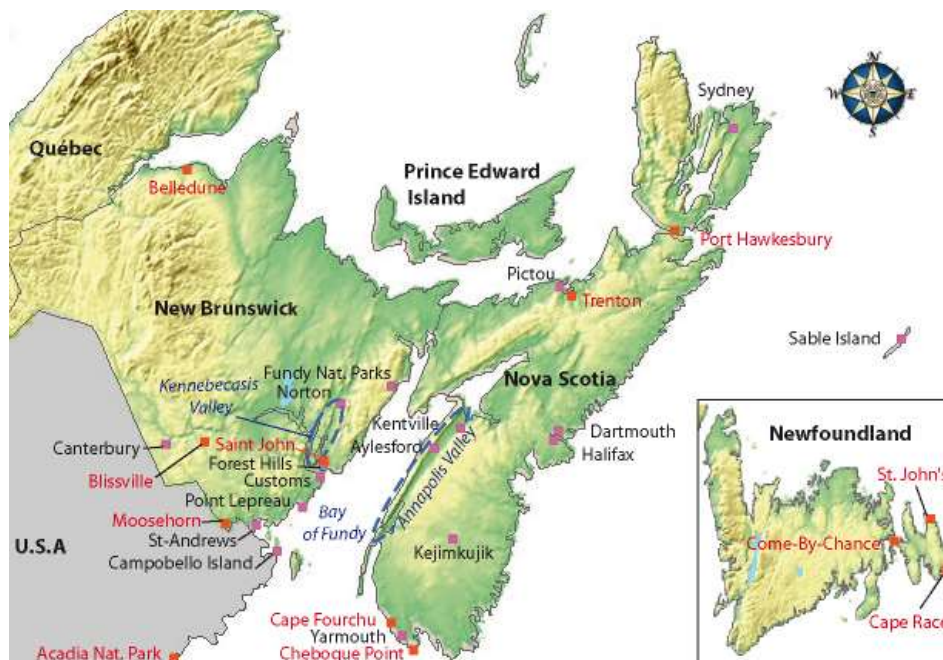


Figure 7.2 Map of Southern Atlantic Region with locations of main sites, cities and geographic regions discussed in this chapter.

Atlantic Canada is defined geographically as the provinces of Newfoundland and Labrador, Prince Edward Island, Nova Scotia, New Brunswick and adjacent offshore areas. The population of 2.3 million people consists of a 54/46% split between those living in urban and rural areas. The region spans a distance of 2000 km from north to south, varies topographically with mountain ranges in the north and low lands in the south, has extensive river valley systems, and thousands of kilometers of coastline, much of which is frequented by marine inversions and becomes ice-bound in winter. The climate varies from continental Arctic in the far north to maritime in the south. This diversity of topography and weather patterns adds complexity to the understanding of air quality issues, dynamics and processes in the region. A map of the Atlantic Region is provided in Figure 7.2.

Because of its location on the eastern end of the continent and a prevailing westerly flow through the lower portion of the troposphere, the Atlantic Region lies downwind from the major emission areas of southern Canada, the Ohio Valley and the northeastern U.S. Proximity to these source areas in combination with local emissions continues to result in high concentrations of both PM and ozone in some areas of Atlantic Canada. The impact of upwind emissions on acid deposition in the region was highlighted in the 1980s (Beattie and Whelpdale, 1989), with the first estimates of transboundary contributions during an ozone episode given in the 1997 NO_x/VOC Science Assessment (Environment Canada, 1997). Anthropogenic activities on a continental and global scale are affecting local air quality (Shepherd, 2004) and field research programs that have included the southern portion of the region have continued to delve into factors associated with degraded air quality in this continental outflow area. Upwind emissions of NO_x and SO₂ result in a regional south to north gradient in acid deposition concentrations (Environment Canada, 2004b).

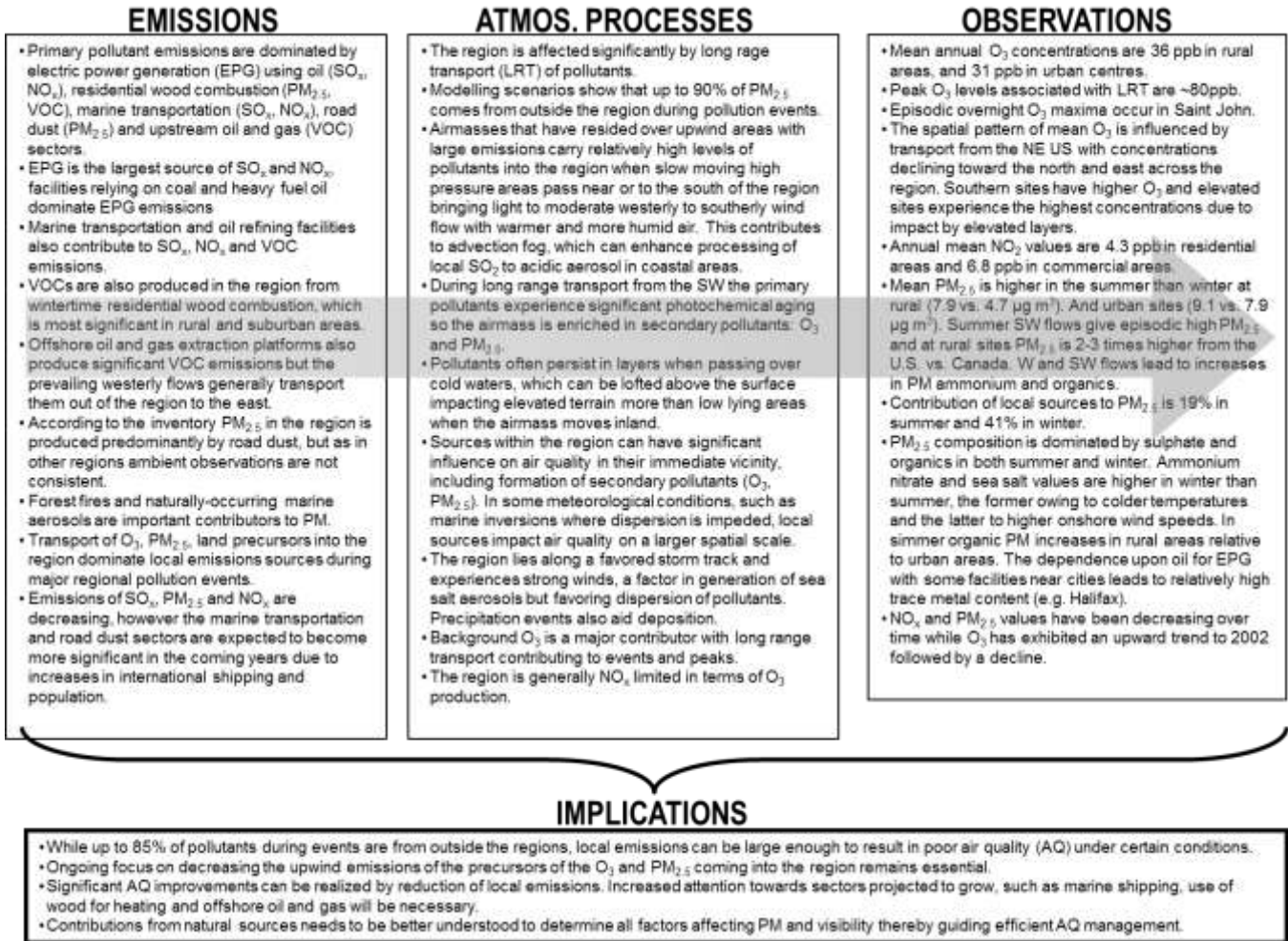


Figure 7.3 Southern Atlantic Canada Conceptual Model.

A summary of conditions or conceptual model for the Atlantic Region is provided in Figure 7.3. As highlighted above, smog in Atlantic Canada is dominated by long-range transport, so much so that pollutant concentrations can peak in the overnight hours. Under this regime the concentrations of primary pollutants NO_x and SO_2 tend to be low relative to secondary pollutants (O_3 and $\text{PM}_{2.5}$) over most of the rural areas. Pollutant plumes drift back and forth over the region bringing ‘aged’ air masses to the area resulting in smog episodes that generally last from one to two days. These episodes occur most often in summer (but can also occur in winter) when stagnant high pressure systems move slowly over emission areas of the northeastern U.S., southern Canada and the upper Ohio Valley, picking up smog and its chemical ingredients. Subsequently, these air masses push eastward carrying the smog into Atlantic Canada especially as southerly flows develop when the ridge passes. Transport over the cooler Atlantic water results in the pollutants being isolated from the surface so that as they move over land, they remain aloft impacting elevated terrain more frequently and with

sufficient downward mixing, more widespread parts of the province. Under long-range transport conditions local emissions can also build up and thus the region does produce its own smog-forming compounds.

Emissions in the Atlantic Region are based on significant use of fossil fuels for energy production and, while generally declining, can still contribute to exceedances of established national ambient air quality standards. Due to low ammonia emissions, wintertime particle nitrate episodes are not frequent, but when they occur they are usually due to regional scale transport.

Although the region is dominated by a greater portion of long-range transport than other regions in Canada, there are a few areas where emissions are significant and air quality is compromised as a result. Halifax and Saint John, two of the larger cities, have considerable local emissions with large amounts of SO₂ released from various sources. This leads to some of the highest urban SO₂ levels in the country, and to formation of acidic particles, especially when mixed with fog. Local formation of O₃ in these regions also plays a role, albeit small. Marine transportation emissions are having an increasingly recognized impact on the local air quality in the seaports.

Several field studies have been conducted in the airshed and measurements in the pollutant plumes coming over the region indicate that sulphate dominates the composition of the particles. Modelling studies conclude that up to 90 percent of the fine particles come from outside the region during smog episodes. Plumes from naturally occurring forest fires can also affect the region. Transport on a continental and even the hemispheric scale has been implicated in smog being carried over this region.

The expansive coastline combined with the adjacent cool ocean waters lead to marine temperature inversions which restrict dispersion, resulting in the complex behaviour of sea and land breezes, and contributing to deteriorated air quality in coastal cities. On the other hand, the marine inversions can also force incoming pollutant plumes aloft thereby isolating the incoming smog plumes from reaching the surface. One positive aspect of the location of the region is its proximity to the favoured track of low pressure systems. This results in frequent precipitation and/or wind events, both of which help to improve the dispersion and removal of pollutants from the air.

Since the previous assessments on ozone and PM air quality in Canada (Health Canada and Environment Canada, 1999a,b; Environment Canada, 1997, 2001, 2004a), the spatial and temporal variation, the magnitude, and chemical composition of smog in this region have been better quantified, yet there remains a lack of knowledge of biogenic and marine aerosol formation and their influences on regional air quality. The long-range transport of pollution will continue to be controlled in large part by the weather factors, but local contributions to smog will be a significant factor as continued growth occurs in the region.

7.2.2 Southern Québec and Eastern Ontario



Figure 7.4 Map of the Southern Québec and Eastern Ontario region with locations of main sites, cities and geographic regions discussed in this chapter.

Approximately 80% of the population of Québec lives in the St. Lawrence River Valley, a wide, flat area that channels air between the Great Lakes and the Gulf of St. Lawrence. In addition, as shown in Figure 7.4, this region includes eastern Ontario and industrial cities such as Cornwall, as well as the Ottawa River Valley and the National Capital Region. These two large river valleys are where most industries are located, where most of the farming activity takes place and where most vehicular traffic is concentrated. The topography and land use, combined with the wide range of weather conditions that characterizes the temperate climate of the mid-latitudes, allow for multiple air quality regimes within the region. However, air quality issues most often arise in the area from Ottawa to Cornwall to Montréal and occasionally extend eastward to Québec City. Cases of poor air quality are a result of relatively high pollutant emissions in the populated area, combined with the fact that the region is frequently located downwind of southern Ontario and the Midwest U.S. North and east of the Ottawa and St. Lawrence River valleys regional air pollutant levels decrease rapidly as distance from the large source areas to the south increases. However, under stable or stagnant

conditions, which occur at night in summer and often in winter, local industries and wood burning can affect the air quality of the towns located in the smaller valleys found throughout the region.

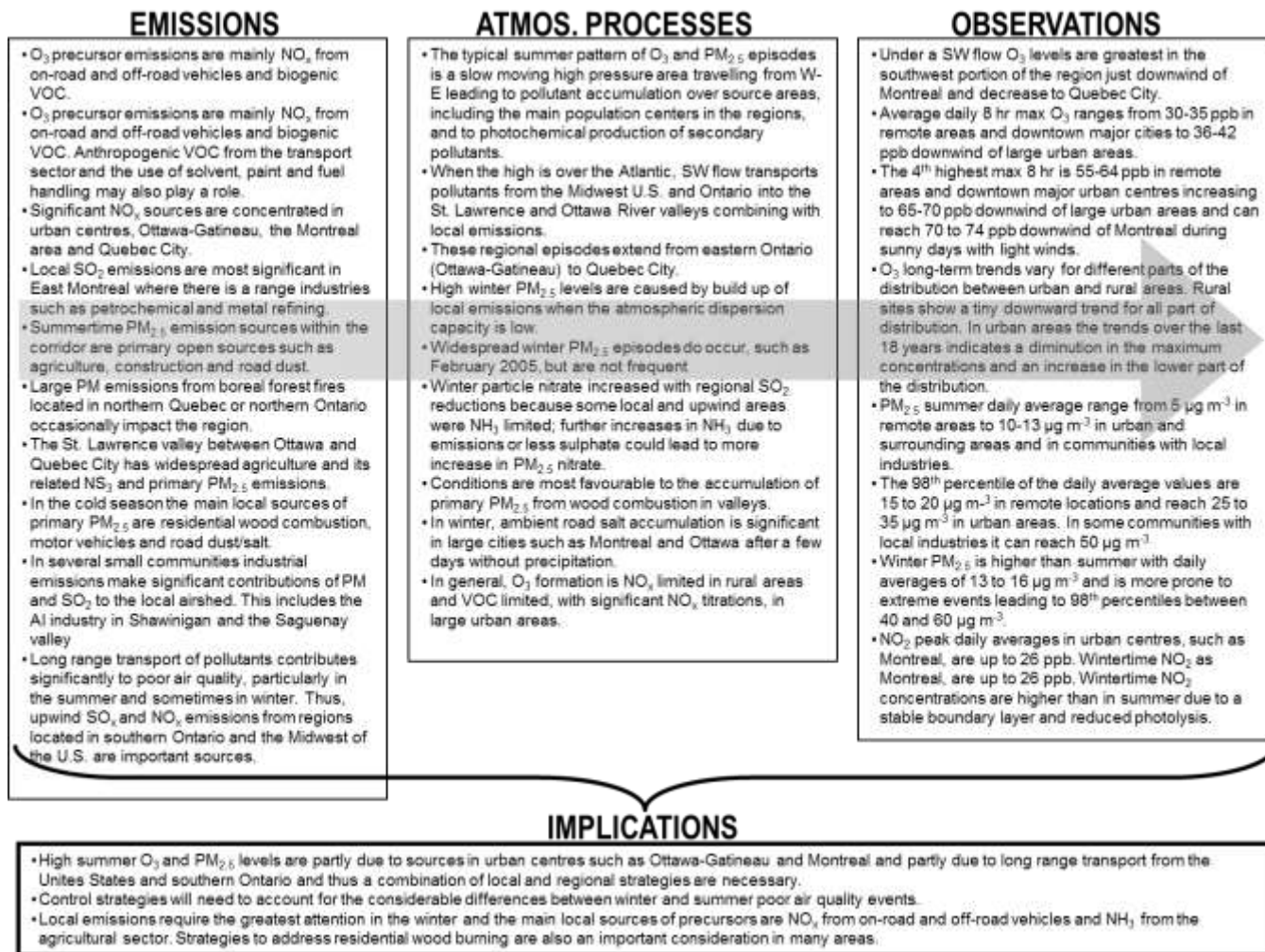


Figure 7.5 Southern Québec and Eastern Ontario Conceptual Model.

A summary of air quality conditions in the region is provided in Figure 7.5. In the densely populated parts of the eastern end of the Windsor-Québec City Corridor (EWQC), ozone and PM_{2.5} have many local and regional sources. Specific meteorological conditions lead to high smog levels many times per year in all seasons. In some communities away from major urban centres, local industries and residential wood combustion may lead to high levels of particles and some other primary pollutants. At higher elevations in mountain areas of western Québec, summer ozone may be as high as in the populated regions of the St. Lawrence River valley.

The St. Lawrence River Valley channels the wind, often containing both primary and secondary pollutants, along its southwest-northeast axis. Under this pattern, southern Ontario and the U. S. have a significant impact on O₃ and PM_{2.5} levels over eastern Ontario and southern Québec. Superimposed on top of this somewhat more local pattern are relatively large secondary sulphate and organic levels from regional scale transport, leading to more spatial homogeneity during episodes. These periods are characterized by increased PM_{2.5} and O₃ levels. However, high summertime events in the EWQC are less frequent than in southern Ontario because the region is more distant from the high emission areas. In the winter the St. Lawrence River valley contributes to the pooling of cold air leading to lower mixing heights and the build up of more local pollutants. A high pressure ridge entrenched over this area for a week in February 2005 led to the highest PM_{2.5} event in Canada over the past ten years. Peak concentrations were in Montréal, but in addition to high levels in the cities (e.g., Ottawa, Cornwall), this event caused rural areas to experience high concentrations due to local activities, but also likely due to the spreading of the urban air mass into outlying areas in the valley. Residential wood combustion compounds (such as metals, polycyclic aromatic hydrocarbon, etc), secondary ammonium nitrate and motor vehicle emissions are key contributors to wintertime PM.

Given that topography and land use, combined with the wide range of meteorological conditions, influence the behaviour of air pollutants and lead to multiple air quality regimes over the EWQC, air quality management programs need to be multi-faceted. This will require both local measures and cooperation with other jurisdictions to the west and south. Strategies to reduce local SO₂, NO_x and major local primary PM_{2.5} sources can be expected to be fruitful in reducing ambient fine particles, especially in winter. However, air quality benefits of local controls on summertime ozone levels and regional sulphate haze events are not likely to be as readily observable due to a greater contribution from regional scale transport.

7.2.3 Southern Great Lakes Region

Ontario is Canada's most populous province, home to approximately 40% of the total population of Canada. The vast majority of these 12.5 million people live in the southern and southwestern part of the province (Statistics Canada, 2006). The population of Toronto is 2.5 million, while approximately 5.5 million people live in the Greater Toronto Area (GTA), which stretches along Lake Ontario from Burlington in the west to Clarington in the east and as far north as Lake Simcoe. The GTA does not include Hamilton, which has a population in excess of 600,000. With some notable exceptions, such as Sudbury, the majority of the province's large point emission sources are located in the same region, particularly in the Toronto-Hamilton and Windsor-Sarnia areas. The largest point sources are associated with ferrous and non-ferrous metal processing, electrical power generation, and the petrochemical industry. Toronto itself does not have any of the province's major point sources, but is the location of a large number of smaller sources, and generates a large quantity of motor vehicle emissions.

Aside from effects due to its own emissions, Ontario experiences significant impact from sources located in the U.S. Midwest which is in relatively close proximity. The region is thus impacted by significant emissions of SO_2 , NO_x , PM and VOC, both from within and outside its borders.



Figure 7.6 Map of the Southern Great Lakes Region with locations of the main sites, cities and geographic regions discussed in this chapter.

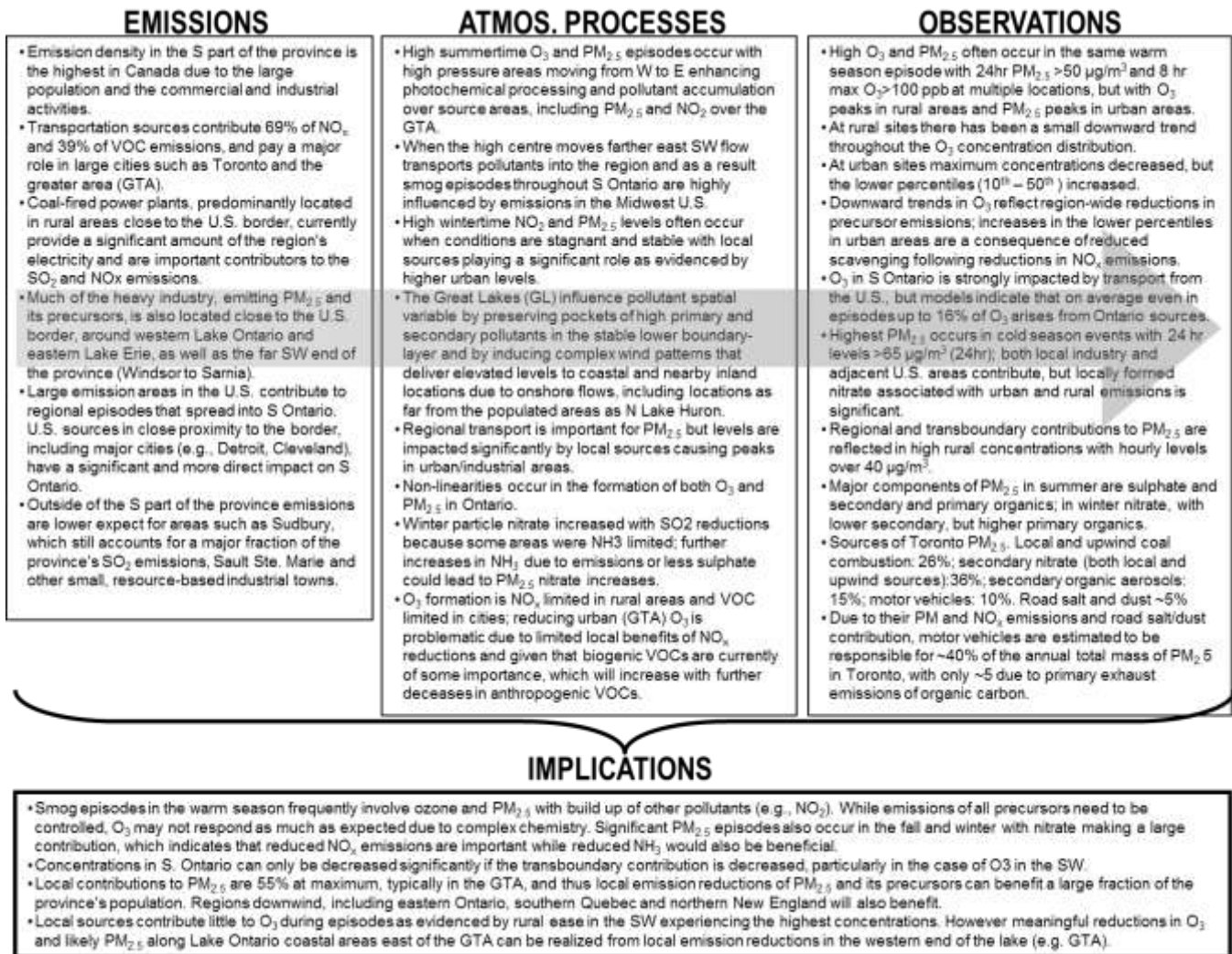


Figure 7.7 Southern Great Lakes Region Conceptual Model.

The Southern Great Lakes region is depicted in Figure 7.6. Southern Ontario is quite flat, with some elevation provided by the Niagara escarpment, which runs from Niagara up to the Bruce Peninsula on Lake Huron. The conceptual model or summary of conditions is provided in Figure 7.7. The pollutants of major concern are ozone and fine particulate matter, which tend to share common precursor emission sources or source regions. Episodes of high concentrations of both pollutants typically occur in the summer in association with winds from the southwest, which bring emissions from U.S. sources, and which also pick up emissions from the within Ontario sources. If the winds are light, local build-up over emission areas in Ontario can precede the transport of smog and its precursors from the U.S. Consequently, on the order of 30% of the $\text{PM}_{2.5}$ in the Toronto area during episodes is from local urban emissions. During these periods the pollutants emitted locally and upwind have ample time to react, forming a wide range of photochemical pollutants, including secondary organic and

inorganic particles. Superimposed on this pattern is the influence of the Great Lakes, which redistribute pollutants within the region, possibly enhancing local photochemistry and leading to greater spatial heterogeneity. As well, high pollutant concentrations, particularly surface O_3 , tend to persist over the Great Lakes, and subsequently can impact shoreline areas during onshore flow such as under the influence of the lake breeze.

In winter, southwesterly flow also has a role to play in delivering pollutants to locations in Ontario, but stagnant or near-stagnant conditions are a key factor in the production of high concentrations since they allow the accumulation of locally emitted pollutants. In the winter O_3 is not of concern, but high concentrations of PM and NO_2 are a relatively common occurrence. In contrast with the summertime situation, fine particulate matter composition in winter is dominated by nitrate rather than sulphate. Ammonium nitrate particles form readily and, due to colder temperatures, persist under shallow inversions or in low-lying areas. Increases in cold season nitrate in the late 1990s and early 2000s, which were in response to decreases in sulphate, demonstrate that particle nitrate concentrations are ammonia limited. Thus, under some conditions there is some non-linearity in the $PM_{2.5}$ mass response associated with SO_2 emission reductions.

Air pollutant concentrations and formation processes in the region have been the subject of extensive routine monitoring, special studies and field campaigns. Examples are several special studies carried out to elucidate the composition and formation of fine particle formation (e.g., Border Air Quality and Meteorology Study). These studies have involved the use of particle mass spectrometry to provide information not previously available by other means.

An extensive measurement campaign was carried out in the Windsor-Sarnia border area to improve understanding of the impacts of pollutant sources in the transboundary region. The measurement work in the province has been supported and extended by a considerable amount of mathematical modelling.

7.2.4 Alberta and the Prairies

The Prairie Provinces of Manitoba, Saskatchewan, and Alberta are home to 5.5 million people (Statistics Canada, 2006), roughly 17% of Canada's population and nearly 20% of Canada's land area. They are bounded on the southwest by the Rocky Mountains, on the northeast by the coast of Hudson Bay, on the south by the U.S. border and on the north by the border of Nunavut and Northwest Territories ($60^\circ N$). Outside of the Rocky Mountains the terrain in the Prairies is mostly flat and sloping gently down from southwest to northeast.

The major geographic features of the region include the Interior Plains, covering most of Alberta, the southern two thirds of Saskatchewan, and the southwest quarter of Manitoba; and the Canadian Shield, covering the northern portion of Saskatchewan and most of Manitoba. Although included in Section 7.2.6 as part of Interior British Columbia, the northeast corner of British Columbia fits more logically in this region given its relatively flat terrain and the importance of the energy industry. This highlights the challenge of dividing Canada into a relatively small number of regions and the likelihood that the boundaries can shift depending upon the criteria involved in creating them.

Few people live in the Canadian Shield portions of the Prairie Provinces. The southern portion of the Prairie Provinces is mostly natural grassland and agricultural areas, while the northern portion is primarily boreal forest of pine, spruce and poplar mixed with many lakes. The majority of the population of the Prairie region lives in the southern portion of the Interior Plains within 600 km of the U.S. border. The Edmonton-Calgary corridor, with a combined population approaching 2.5 million people, has the largest amount of industrial activity and also the busiest transportation corridors in the region.



Figure 7.8 Map of the Alberta and the Prairie Region showing locations of the main sites, cities and geographic features discussed in this chapter.

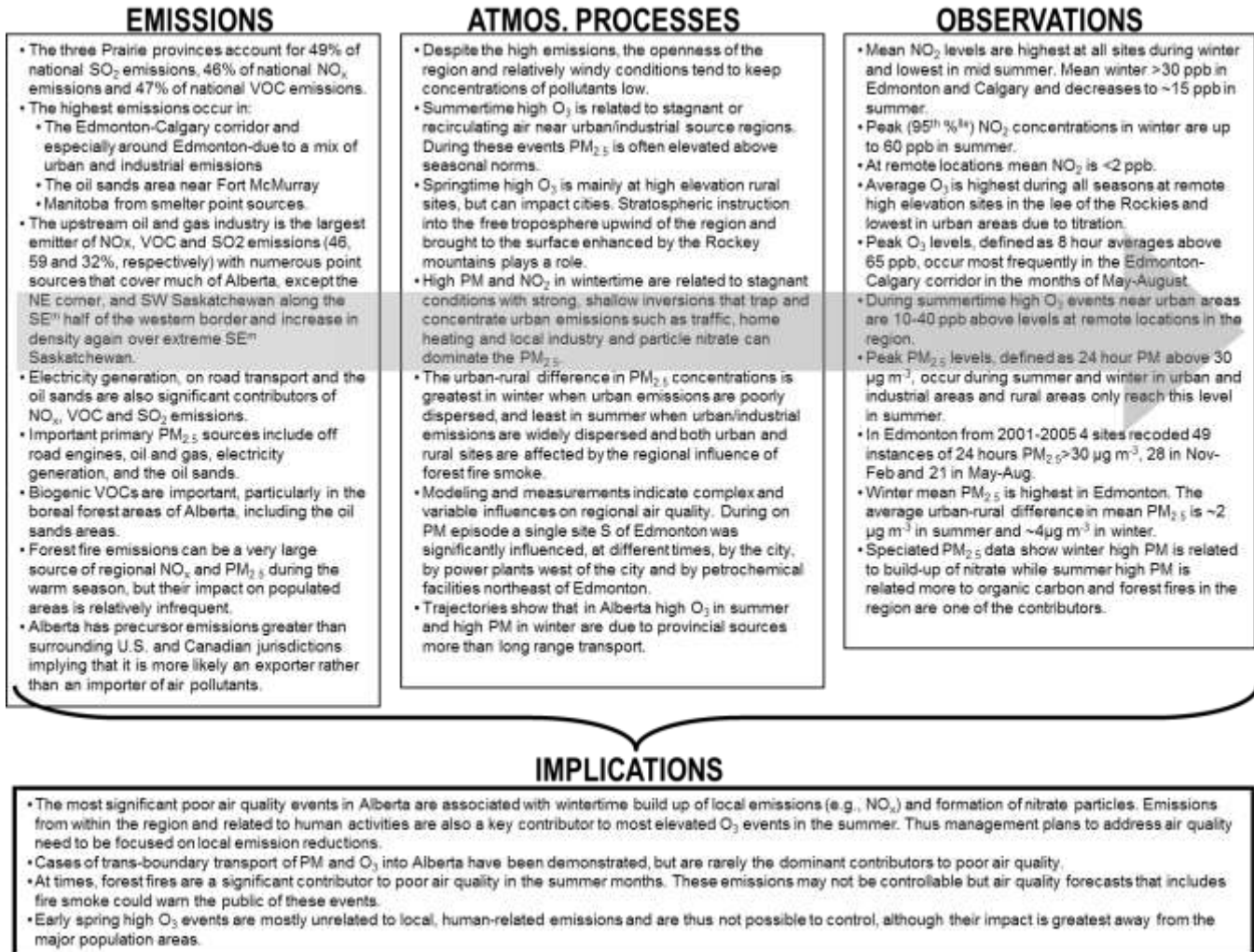


Figure 7.9 Alberta and the Prairie Region Conceptual Model.

Figure 7.8 shows the geographic area covered by the Alberta and Prairie Region and a summary of the air quality conditions is provided in Figure 7.9. Despite the presence of the highest emissions of smog precursors in Canada, air quality in the region is relatively good compared to the Windsor-Québec City corridor. This is largely by virtue of major pollution emitters being spaced far apart, and prevailing meteorological conditions, such as higher wind speeds, that are only occasionally conducive to pollutant build-up and summertime smog formation.

The occurrence of elevated O₃ in summer is typically related to stagnant conditions so contribution from other areas (i.e., regional scale transport) is likely of limited importance. Field and modelling studies indicate that considerable O₃ also forms along discrete plumes downwind of Alberta’s major cities and industrial areas (e.g., Fort McMurray, Fort

Saskatchewan). Thus, despite low annual average O₃ levels, occasional summertime episodes have brought the Edmonton area close to the Canada-wide Standard (CWS) level when local emissions linger or re-circulate in the area.

Western Alberta has several high elevation monitoring sites that experience pronounced springtime ozone maxima and high annual values due to a relatively high background level. Several other Alberta sites also have higher background ozone. A contributor to these observations is downward flux of ozone from the upper troposphere which is a result of stratospheric intrusions, which can occur far upwind (to the west) of the province (see text box below).

Elevated PM and NO_x levels occur in the winter under stagnant conditions with poor vertical mixing, and therefore trans-boundary sources are not important. These high wintertime levels, which also involve high CO and other primary pollutants, occur in Edmonton, Calgary and other industrialized regions when strong inversion conditions trap the local emissions. Concentrations of NO_x and CO often match or exceed those reported in most other Canadian cities. PM_{2.5} levels are also elevated under these inversions, but the available data suggest that they do not surpass levels observed in eastern cities. However, these observations are largely based upon TEOM measurements, which are biased low in the winter (see Section 3.2.6 in Chapter 3). Coarse PM levels are often higher in the Prairies compared to other regions in Canada due to the open spaces, the agricultural practices and higher wind speeds.

As indicated above, the air quality issues in Alberta are primarily domestic in origin, and thus management plans to address smog needs to focus on local emission reductions. The situation over Saskatchewan and Manitoba is less clear. Modelling work suggests an Alberta influence on O₃ formation in Saskatchewan. Trajectory analyses also show that southern Manitoba and southern Saskatchewan are the regions most influenced by emissions from the U.S. Midwest. In those locations transport from the U.S. Midwest is consistently associated with higher PM_{2.5} and O₃. However, even in Saskatchewan and Manitoba, the influence of local sources on NO₂ and PM_{2.5} in the cities is still dominant. Northern Manitoba also has two large base metal industrial facilities that release large quantities of SO₂ and PM yielding high levels for local populations. There are also indications of substantial dry and wet sulphate deposition over downwind areas.

Forest fires are a significant contributor to poor air quality episodes in the summer months throughout the region. While forest fire emissions may not be controllable, an effective smoke forecasting system could warn residents of potential smoke impacts.

Given the large oil and gas and petrochemical sectors in Alberta, investigations into smog should not overlook air toxics. Immediately adjacent to Edmonton is a major industrial centre, including several large refineries, chemical manufacturers and oil sands upgraders. This

collocation of a growing urban centre with a large and growing industrial centre is one of the key emerging issues in the region. The other key emerging issue is the dramatic growth in the oil sands, and its potential influence on local and regional air quality.

7.2.5 The Lower Fraser Valley

The Lower Fraser Valley (LFV) of southwestern British Columbia and northwestern Washington State is bounded by the Coast Mountains to the north, rising to approximately 2000 meters, by the North Cascades to the south and the Strait of Georgia to the west. The Canada-U.S. border bisects the valley with approximately one third of the area lying in Whatcom County, Washington State. A map of the region showing some of the main air quality measurement sites is given in Figure 7.10.

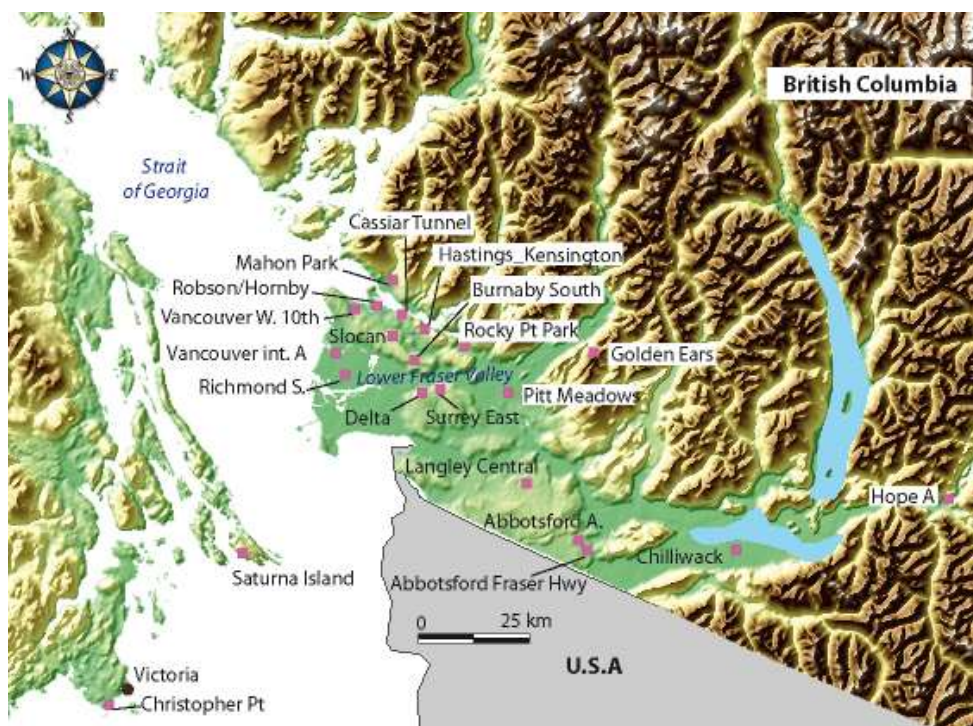


Figure 7.10 Map of the Lower Fraser Valley region with locations of the main sites, cities and geographic features discussed in this chapter.

The LFV is home to roughly 2.5 million people and comprises three jurisdictions: Metro Vancouver (formerly known as the Greater Vancouver Regional District), the Fraser Valley Regional District and Whatcom County. Metro Vancouver has delegated authority for air management and its jurisdictional area covers the largest part of the population. The valley becomes increasingly rural towards its central and eastern extent, where large portions of land are used for agriculture. An industrial area extends along the western portion of Whatcom County, ending at the city of Bellingham.

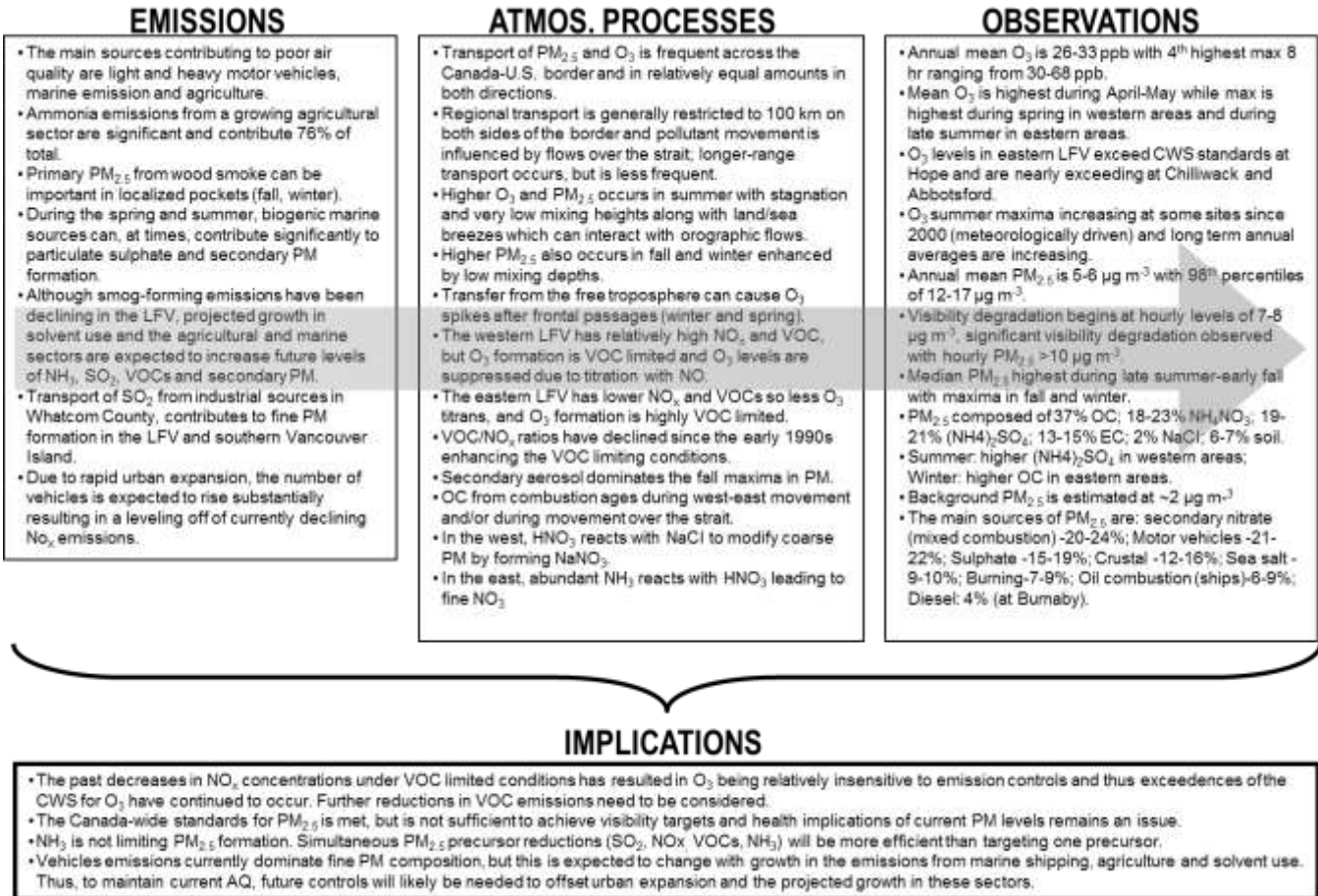


Figure 7.11 Lower Fraser Valley Conceptual Model.

Figure 7.11 summarizes our current conceptual model for the LFB. The mountainous terrain, river valleys and the surrounding Strait of Georgia leads to complex local scale meteorological patterns, which can make it difficult to trace observed pollutant levels back to their sources and also leads to significant vertical layering or stratification of pollutants above the ground. In addition, the funnel shape of the valley that narrows considerably towards the east confines pollutants to a smaller volume, enhancing concentrations. These features are key factors in the occurrence of air quality episodes. In the summer, stagnant conditions are generally most important in giving rise to ozone and $PM_{2.5}$ episodes, which increase in severity from west to east. Such episodes involve substantial photochemical processing, significant secondary particle formation and moderate to severe visibility impairment. Local scale wind patterns such as upslope flow and sea/land breezes ultimately move pollutants around within the valley drawing polluted air masses up into tributary valleys and towards Hope. The eastern LFB is considered to be an ozone hot-spot in British Columbia, as levels have been near or exceeding the CWS since 2003.

Regional trends in maximum summer ozone are also increasing, due to increasing temperatures in the post 2000 period and the effect of local NO_x reductions on O_3 . Increasing trends in the 10th percentile and mean annual ozone may in part be due to increasing background levels. $\text{PM}_{2.5}$, although not particularly elevated compared to other areas, is also of concern in the LFV due to significant impacts on visibility and on human health. The highest average levels tend to be in the late summer and early fall. Fine PM composition is dominated by organic carbon, especially in the winter in eastern areas of the LFV. Ammonium sulphate and ammonium nitrate dominate fine mode inorganic particulates, and their relative proportions are closely influenced by the spatial availability of ammonia and seasonal variations of sulphuric acid and sea salt, respectively. Ammonia emissions and concentrations are high in eastern portions of the LFV (e.g., Abbotsford) enhancing ammonium nitrate formation, which is limited by the availability of oxidized nitrogen species, not ammonia.

Closer to the coast, coarse nitrate formation, due to interaction of nitric acid with sea salt, represents an important sink for nitrogen species. Ammonium sulphate levels tend to be higher closer to Vancouver due to more available SO_2 . Sea salt interactions with oxidized nitrogen species can also influence ozone levels, but less is known about this process in the LFV. Winter $\text{PM}_{2.5}$ episodes are less frequent and are a result of inversions caused by cold arctic air masses moving westward from the interior of the province. During such inversions, $\text{PM}_{2.5}$ levels are typically higher than during summer photochemical episodes. Periods with strong easterly winds occur in the colder months and can push emissions from the LFV well out into the Strait of Georgia.

Dominant sources contributing to $\text{PM}_{2.5}$ are motor vehicles, nitrate (from general combustion, but dominated by transportation and agriculture) and sulphate (marine vessels, industrial and marine biogenic). Wood burning and vehicle sources are more important in the winter, while oil combustion and biogenic influences are more important in the summer. Regional transport of $\text{PM}_{2.5}$ and O_3 occurs back and forth across the Canada-U.S. border of the LFV in relatively equal proportions. Transport of SO_2 from industrial sources in Whatcom County, contributes to PM formation in the LFV and southern Vancouver Island. The extent of regional transport is generally restricted to <100 km on both sides of the border, but less frequent, longer-range regional transport also occurs.

Although smog-forming emissions have been declining in the LFV, projected growth in solvent evaporation and the agricultural and marine transport sectors are expected to increase future levels of NH_3 , SO_2 , VOCs and $\text{PM}_{2.5}$. In addition, due to rapid urban expansion, the number of vehicles is expected to rise substantially, resulting in a levelling off of currently declining NO_x emissions. In light of future emission projections and current O_3 , visibility and health issues, there is a clear need to continue to address airborne emissions in the LFV. The complex nature of emissions patterns and sources indicates that air quality management strategies need to be carefully crafted to maintain current emission reduction trends and address emerging sectors threatening future air quality in the area.

7.2.6 Interior Valleys of British Columbia

The interior of British Columbia is home to a number of communities, many nestled in valleys created by rugged mountainous terrain. The Yukon Territory and the mountainous parts of southwestern Alberta are similar in many respects. Although this latter area is included in Section 7.2.4 as part of Alberta and the Prairies for practical reasons related to preparation of this report, its air quality is likely to exhibit features that are more in common with Interior British Columbia. Throughout this mountainous region (BC, YK and southwestern AB) differences in sources, meteorology and local geography give rise to a variety of regionally-specific air quality issues and although they can be of concern throughout the region, detailed information is currently only available for the more-populated communities. Most emissions are locally generated, and there is little mixing of air pollutants between the valleys.



Figure 7.12 Map of the Interior BC region with locations of the main sites, cities and geographic features discussed in this chapter.

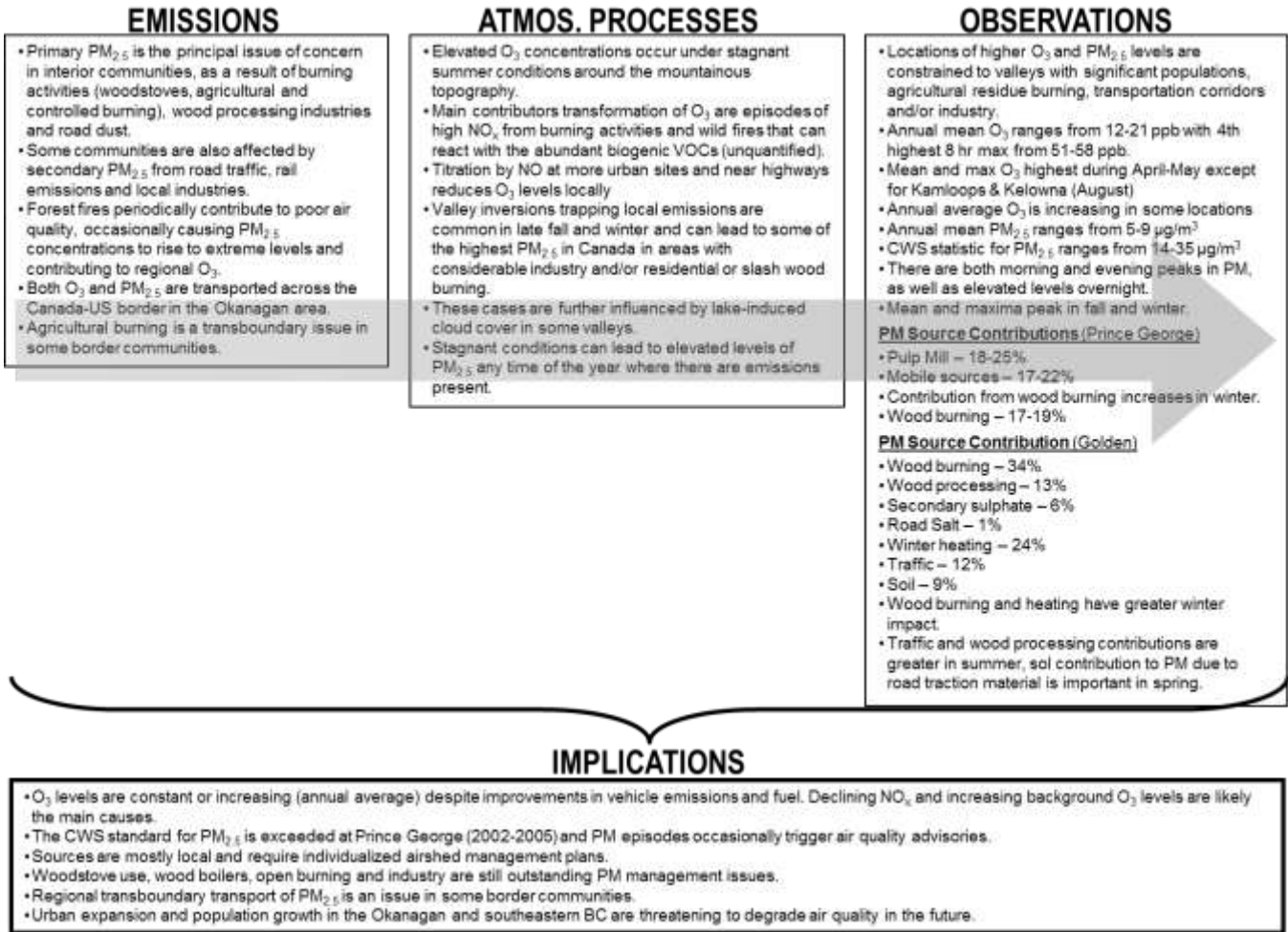


Figure 7.13 Interior British Columbia Conceptual Model

A map of this complex region is given in Figure 7.12 and an overview of the conceptual model is shown in Figure 7.13. Valley communities are subject to frequent inversions, especially during the winter, which effectively trap pollutants. Primary PM is the principal issue of concern in interior communities, as a result of burning activities (woodstoves, boilers, agricultural and controlled burning), wood processing industries, and road dust. Some communities are also affected by secondary $PM_{2.5}$ from road traffic, rail emissions and industry. Exceedances of the $PM_{2.5}$ CWS have occurred in both Prince George and Golden over the past five years. In some of the more rural interior communities, $PM_{2.5}$ episodes are associated with agricultural and open burning activities. Forest fires also periodically contribute to poor air quality, occasionally causing $PM_{2.5}$ concentrations to rise to extreme levels. At both Golden and Prince George, $PM_{2.5}$ composition is dominated by organic carbon, especially in the winter. During this season, wood burning, wood processing (drying) and winter heating dominate $PM_{2.5}$ sources in Golden, while at Prince George, wood burning, pulp mills and traffic sources contribute relatively equally. Throughout the interior towns, road dust

levels rise considerably in the spring leading to elevated coarse PM levels; pollutant levels tend to be lower in the summer due to higher mixing heights and less prevalence of inversions. The CWS ozone metric is near 60 ppb in a number of BC interior communities, including the Okanagan. Ozone is becoming an emerging issue in the Okanagan area due to increasing population, leading to rapid urbanization and economic growth. PM from summer wildfires can be transported over hundreds of kilometers, and, by fall, agricultural burning increases. Transboundary transport of PM between Canada and the U.S. occurs along the Okanagan and Creston valleys, and its effects are regionally limited.

The BC Ministry of Environment has been very active in addressing air quality issues in interior communities, and comprehensive air quality management plans have been implemented in a number of areas. As a consequence of specific mitigation measures, some BC interior communities have seen improvements in ambient PM levels in recent years. In spite of these efforts, fine PM levels are still episodically elevated in many communities and much work remains to be done in improving local air quality.

7.3 Regional Air Pollutant Emissions and Areas of Concern

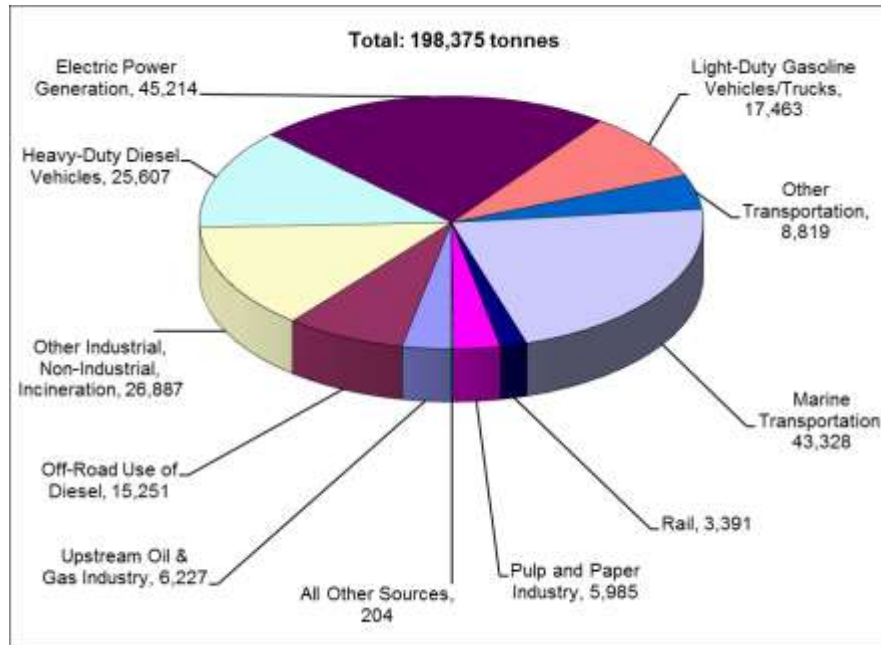
In this section, the main controllable emission sources of the criteria air contaminants (CAC) are described. The information in this section is generally presented according to the regions described above. However, due to the jurisdictional approach to reporting emissions, some of the material is organized by province, particularly for Ontario and Québec.

Emissions within each region can play a significant role in air quality problems. Thus to understand the issue information on which activities are responsible, where they are located and what is expected in the future is essential. Emissions information was presented in Chapter 4, including national totals, percent contributions by province, broad spatial patterns and trends and projections. The focus here is on discussing the main activities or sectors in each region producing the emissions, the geographic areas where they occur and specific locations where emissions are believed to be high enough to generate concern. On a local scale, emissions from a particular industrial area or busy transportation hub may lead to what is referred to as a “hotspot”. While some of these potential locations will be highlighted, it is beyond the scope of this chapter to list and describe all possible hotspots in each region. Given that such areas could present a local human health concern they are an issue that will require continued attention in the future.

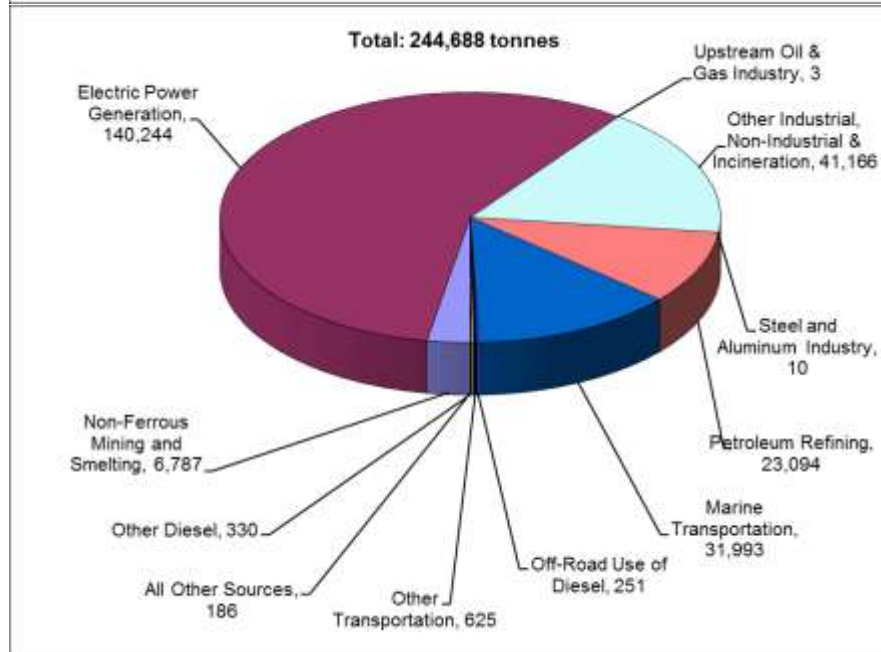
There are significant natural emissions of trace gases and particles that contribute to smog, such as VOCs from vegetation, wind blown dust, sea salt, marine sulphur and biomass burning. Stratospheric ozone, which often enters the troposphere and periodically impacts the surface, especially in high elevation areas, is also important to consider. Such natural sources

cannot be ignored in understanding air quality issues especially on the continental and hemispheric scale. However, they are not controllable and so can only be taken into consideration with respect to air quality modelling and in developing effective strategies to reduce emissions from human activities.

7.3.1 Atlantic Region



a)



b)

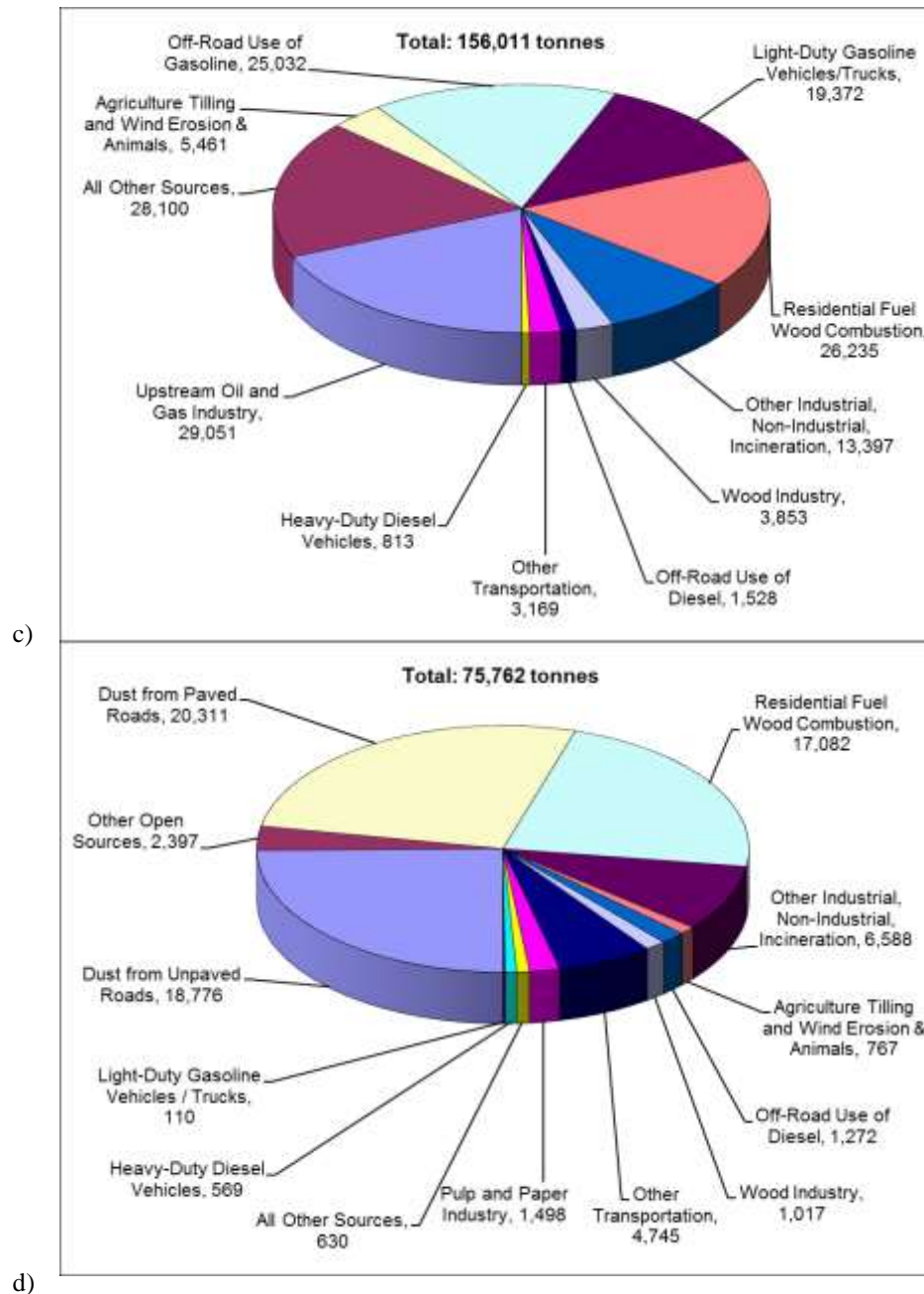


Figure 7.14 2005 Atlantic Provinces Criteria Air Contaminants (CAC) inventory by sector contribution for a) NO_x, b) SO_x, c) VOCs, and d) PM_{2.5}. Electrical Power Generation dominates NO_x and SO_x emissions while Residential Fuel Wood Combustion dominates VOC emissions and Dust from Paved and Unpaved Roads are the major contributors PM_{2.5} emissions. Environment Canada, 2007a.

Anthropogenic emissions upwind of the region have a significant impact on air quality in Atlantic Canada (see Section 7.6.1), but considerable impact also comes from emissions within the region. A summary of the regional anthropogenic contributions to NO_x, SO_x, VOC and

PM_{2.5} emissions by sector is shown in Figure 7.14a-d. The most significant anthropogenic contributors to PM and ozone and their precursor emissions are Electrical Power Generation (EPG), Marine Transportation, Road Dust, and Residential Fuel Wood Combustion.

In the Atlantic region, specifically New Brunswick and Nova Scotia, coal and oil-fired power plants remain the dominant energy source as alternatives such as hydro electric power are in limited use. Thus, Electrical Power Generation (EPG) is the most significant source of SO_x and NO_x in the region, producing 57% of the total SO_x emissions and 23% of the NO_x emissions.

Marine transportation is the second most important source of NO_x (22%) and is a major contributor to SO_x (13%). Emissions from the marine sector are concentrated within the major ports of Halifax and Saint John, where they can have a measurable impact on local air quality (Hingston 2005; Phinney *et al.*, 2006).

Dust from Paved and Unpaved Roads contribute 27% and 25% to PM_{2.5} emissions, respectively, and Residential Fuel Wood combustion (principally from uncertified wood stoves in rural areas) is the third most significant source of PM_{2.5} emissions (23%).

Although the Upstream Petroleum sector (which includes offshore oil and gas platforms in NL and NS) contributes 19% to VOC emissions in the Atlantic region, its impact on the region is minimal due to prevailing winds which carry pollutants eastward or northeastward away from the region. In contrast, the Downstream Petroleum (Oil Refining) sector is a significant source of SO_x in the region (contributing 9%), largely attributable to the three major centres of Come-by-Chance, NL, Dartmouth, NS, and Saint John, NB, which have had minimal emissions changes since 1995. Residential Fuel Wood combustion contributes 17% of VOC emissions, while off-road use of gasoline contributes 16%.

The agricultural sector in Atlantic Canada, as in all regions, is the number one contributor to NH₃ (40%), but these emissions comprise only 3% of total Canadian NH₃ emissions and thus are not considered to be a regional problem. However, because these emissions are concentrated in small areas that are often downwind of SO₂ source areas (i.e. Saint John, NE U.S.), they may be of importance for formation of ammonium sulphate. Ammonia emissions in the region have increased by 12% while emissions of PM_{2.5}, SO_x and NO_x have declined 15%, 18%, and 12%, respectively since, in the ten years since 1995 (not shown) (Environment Canada, 2007a).

Natural aerosols, which include sea salt and a portion of organic and sulphate aerosols, can play a significant role in the Atlantic region due to both its coastal location (the ocean is a source of natural sulphate and sea salt aerosols), and its abundance of forested areas (a source of biogenic organics, accounting for the dominating 87% contribution to VOC emissions)

(Levasseur *et al.*, 1997; Quinn *et al.*, 1998; Biesenthal *et al.*, 1998; Leaitch *et al.*, 1999). The role of natural aerosols in the Atlantic region is not well-quantified, however, and requires further study.

7.3.1.1 Local Areas of Concern

The major centers of Saint John, NB, Halifax, NS, and Sydney, NS, each with power plants, industry and shipping emitting a complex mix of pollutants represent the chief local concerns in the region. However, smaller centers in Nova Scotia, such as Pictou and Trenton, are home to medium to large emission sources including a power plant, the pulp and paper industry and tire manufacturing. Other localities include Port Hawkesbury, NS, with a pulp and paper and power plants; Belledune, NB, with a power plant and smelter; and the small town of Come-by-Chance, NL, which is home to a refinery and associated marine traffic. In addition to these industrial air pollutant releases, the terrain around these localities, including surrounding hills and proximity to the coast with marine inversions, are likely a factor contributing to instances of poor air quality. However, many of these smaller population centres have limited or no continuous air quality monitoring and thus the extent of any potential problems are not well documented.

7.3.1.2 Potential Future Concerns

As documented in Chapter 4, total CAC emissions have decreased over the past 20 years (with the exception of NH_3). Contributing to this have been decreases in many parts of the eastern part of Canada. Also important to the region are the decreases that have also occurred in the eastern U.S and further decreases in U.S. emissions of SO_2 , NO_x and VOCs are expected from 2005 to 2015 (Hidy, Niemi and Pace, 2004). However, economic development in Atlantic Canada and other local factors are projected to lead to increases in some emissions.

Rising electricity and fuel prices combined with the reality of natural disasters such as Hurricane Juan, which knocked out electricity to homes and felled thousands of trees which were then cut for firewood, have made woodstove use more attractive to homeowners in Atlantic Canada. Emissions from this sector are unlikely to decrease in the coming decade. Anecdotal evidence and a recent pilot survey by the Nova Scotia Department of Environment and Labour suggest that residential wood combustion is becoming increasingly important in urban and suburban areas in the region, and is most problematic in those areas located in valleys (M. Hingston, EC, and F. DiCesare, NSEL, *pers. comm.*, 2006).

Sulphur dioxide emissions from the mining, smelting, and commercial fuel combustion sectors are projected to increase 19% in the Atlantic Region by 2015 due in part to new oil refining facilities proposed for the region. Increases in NO_x emissions from the Upstream Oil and Gas sector will result from a new liquefied natural gas (LNG) facility currently under construction in Saint John, NB. While there are some new facilities proposed for the region, there are also

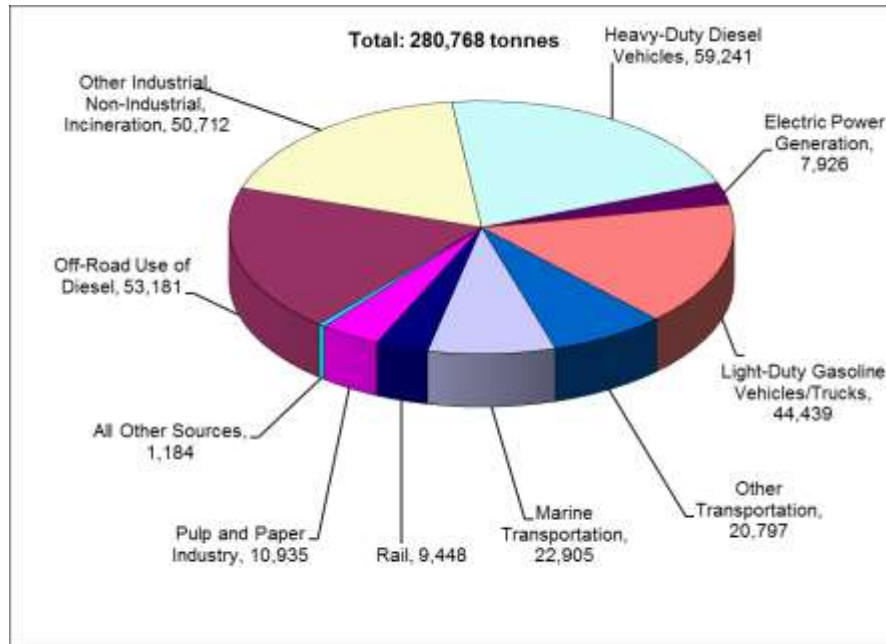
significant emission reduction commitments for SO₂ and NO_x from existing sources by 2010. These are likely to offset most, if not all, of the expected increases. For example Nova Scotia's regulated SO₂ cap alone, will be a greater reduction than the expected combined emissions from the two proposed refineries, two new offshore installations and the proposed LNG facilities.

The Port of Halifax has capacity to more than double container volumes now and can quadruple with terminal expansions (Oulton *et al.*, 2007), which would result in increased emissions of NO_x, CO, SO₂ and PM_{2.5}. However, changes in port activity are not imminent and will be tempered by the realities of the world markets. Overall shipping growth worldwide is expected, but the impacts vary regionally; the Port of Halifax has seen recent declines with little sign of turning around while Saint John can expect significant increases from LNG carriers and tankers if the proposed refinery is built. International Maritime Organization initiatives are expected to result in reduced emissions from ships, which may offset any emissions changes from shipping growth.

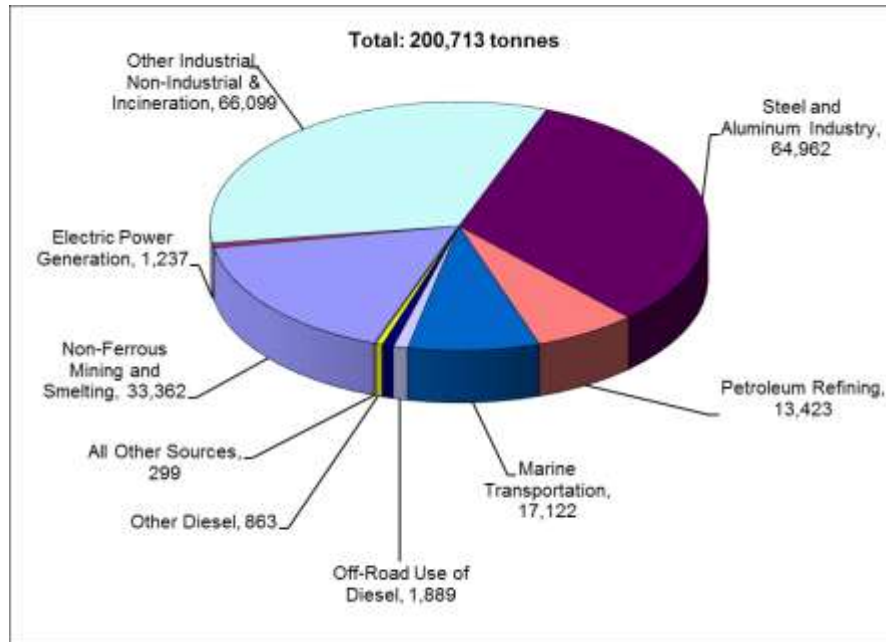
7.3.2 Québec

Emissions of smog precursors are not evenly spread over the province. Cities such as Montréal account for a large portion of emissions because of the size of its population and the number of industries in the area. Due to an abundance of hydro powered electricity in the province, emissions from fossil fuel-generated electricity are low compared to other jurisdictions.

Rural and forested areas account for most biogenic VOC emissions because of the surrounding vegetation (see text box), while agricultural areas emit ammonia and nitrogen oxides. Smaller cities such as Québec and Trois-Rivières will also add to the industrial and transportation emissions to a lesser degree, but may be affected by residential wood burning or local industries. Remote areas may also be affected by these two activities, but these will mainly cause air quality problems in and around their host locality.



a)



b)

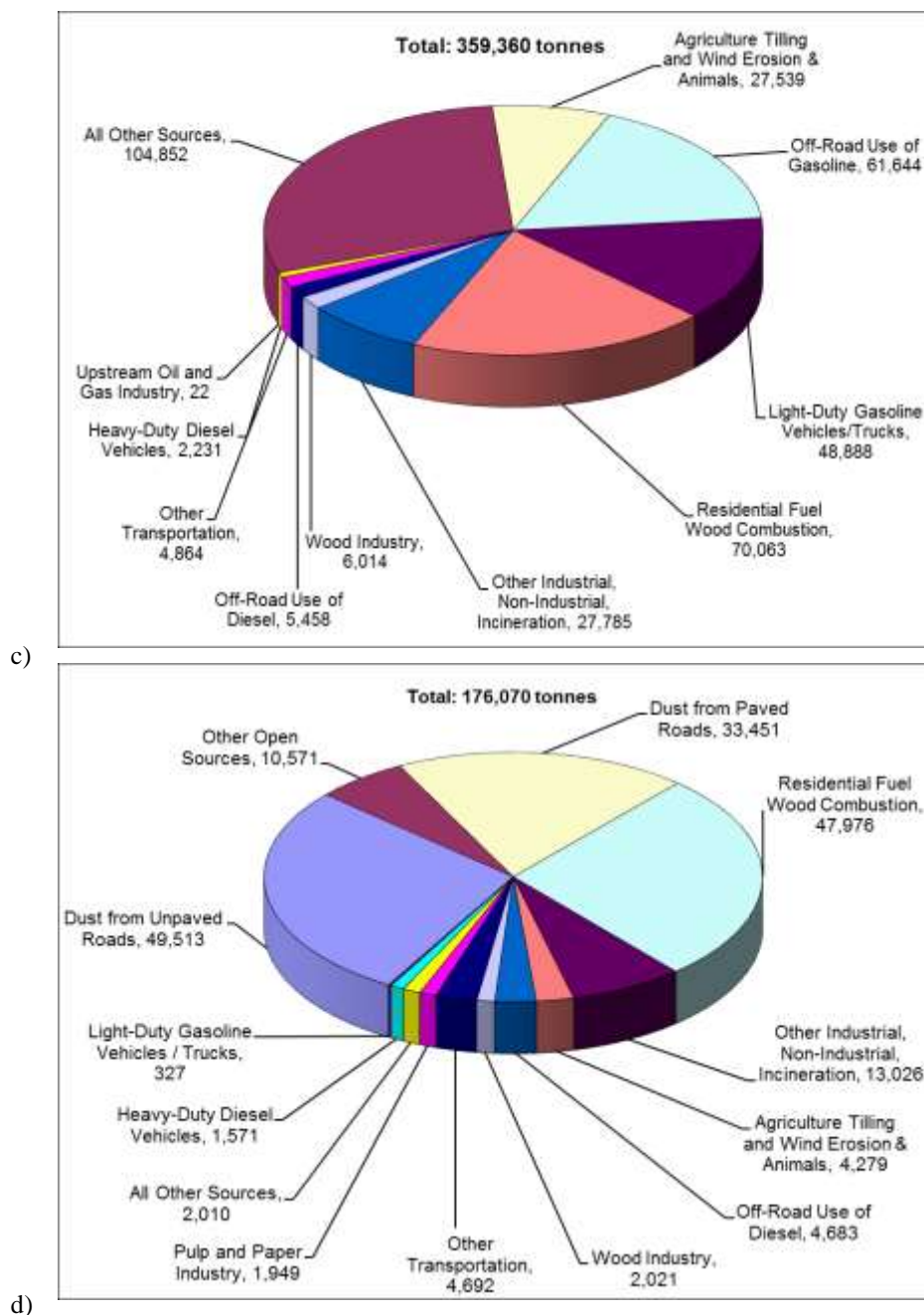


Figure 7.15 Quebec's anthropogenic criteria air contaminants emissions by sector contribution for a) NO_x, b) SO_x, c) VOCs, and d) PM_{2.5}. The transportation sector (which can be broken into on-road emissions (37%) and off-road emissions (19%)) dominates NO_x emissions while industrial activity is the major source of SO_x emissions. Transportation and residential fuel wood combustion dominate VOC emissions while road dust contributes to almost one half of regional PM_{2.5} emissions.

The transportation sector is responsible for close to 70% of NO_x emissions due to the dominance of the province's electricity generation by hydroelectric power (Figure 7.15a). Half of the transport emissions are produced by on-road vehicles and as a result, approximately

30% of the province's emissions are concentrated over the greater Montréal region, an area enclosed within a radius of about 40 km from the centre of the Montreal Island. The remaining half comes from off-road vehicles and engines, marine, rail and air transport.

More than 85% of the Québec's SO₂ emissions come from industrial sources, 32% of which are due to the aluminium industry (Figure 7.15b). Four aluminium plants are located in the vicinity of the city of Saguenay, the remaining six plants are dispersed along the St. Lawrence River from the extreme southwest of the province down to the Lower North shore. In the Montréal area 84% of industrial SO₂ comes from the petroleum and petrochemical industry—mostly located in the east end of the island (Gagnon *et al.*, 2006). These sources of SO₂ have an impact on air quality in the vicinity of the facilities and although not quantified, will contribute to local and downwind levels of fine particle sulphate.

As described in the “Biogenic VOCs” text box below, the majority of volatile organic compounds in Québec are emitted by vegetation in the warm season. During this time of year biogenic emissions are an order of magnitude higher than anthropogenic emissions. However, the natural emissions are spread over the whole forested areas so contribute to smog formation to a lesser extent in urban areas where anthropogenic emissions are more likely to play the greater role. Figure 7.15c shows that the main sources are the transportation sector and from the use of solvents and paints (combined in the “all other sources” category). Locally, the petrochemical industry can be important (e.g. East Montréal).

The main anthropogenic sources of PM_{2.5} (Figure 7.15d) are industries (14%), residential wood burning (27%), and road dust (47%). However, because a significant portion of road dust remains close to the ground and is believed to settle near roads its relative impact on airborne primary PM_{2.5}, which is shown later in Table 7.5 is much smaller than its emissions percent would suggest. Fully reconciling this discrepancy, particularly so that road dust emissions are properly included in air quality models, remains an ongoing issue requiring further research. Emission factor models and knowledge of near roadway meteorological processes and surface interactions are in need of improvement. As a result, wintertime residential wood combustion is likely responsible for a large percentage of the primary emissions of PM_{2.5} than the available inventory suggests. Even though surveys indicate that wood combustion is prevalent in rural areas, higher emission rates occur in urban areas due to a higher density of dwellings. It is worthwhile to note that Montréal and Québec have the highest emissions, followed by medium-size cities such as Gatineau, Sherbrooke, Trois-Rivières and Saguenay.

Overall NO_x emissions have been decreasing since 1990 and are expected to decrease in the transport sector by a further 10% by 2010 and another 18% by 2015. Anthropogenic VOC emissions have stabilized since 1995 but show a small decrease overall, mainly due to reductions in the transportation sector which is expected to release 50% less VOC in 2015 in comparison to 1990. This decrease, along with a decrease in NO_x emissions, is predicted to lead to lower regional ozone levels

The agricultural sector is concentrated along both shores of the St. Lawrence River's southwestern portion and in the Eastern Townships, contributing to emissions of ammonia.

Biogenic VOCs

Owing to an abundance of vegetation, biogenic VOC emissions are present throughout Canada. The dominant biogenic hydrocarbons are isoprene, emitted mostly by deciduous vegetation, and monoterpenes (alpha-pinene, beta-pinene, camphene and d-limonene) emitted mostly by coniferous trees (Wang *et al.*, 2005). Biogenic emissions of VOC are an important contributor to total VOC emissions, especially in the summer due to higher ambient temperatures and the presence of leaves in deciduous trees. In Canada, isoprene is mostly emitted by poplar trees (*populus tremuloides*) and black spruce trees. Poplar are abundant over northwestern Canada while black spruce are present throughout the country. Balsam fir, abundant in eastern Canada and British Columbia, and spruce trees are responsible for most of the monoterpenes emissions in the country. Subalpine fir in BC mountain ranges also contribute to the monoterpenes emissions in western Canada. Overall, Canadian biogenic VOC emissions are five to ten times higher than the anthropogenic VOC emissions. However, these emissions are spread and diluted over the whole country, unlike anthropogenic VOC emissions which are concentrated in industrial and populated areas. Biogenic VOC will contribute to the formation of smog only in the presence of NO_x sources such as an urban center.

Air quality modelling studies in the oil sands region of Alberta (Fox, 2002) demonstrated that ozone formation was strongly sensitive to the method of parameterizing biogenic VOC emissions and to the mix of tree species chosen to represent the boreal forest. Sensitivity tests in eastern Canada also show that ozone production is sensitive to the biogenic VOC emission intensity downwind of urban centers in eastern Ontario, southern Quebec, New Brunswick and Nova Scotia. As an example, by varying the spatial distribution of tree species in the mixed and boreal forests, the maximum ozone predicted by the AURAMS air quality model changed by as much as 15 ppb downwind of Montréal.

7.3.2.1 Local Areas of Concern

Near surface emissions of fine particles can easily accumulate on cold winter days characterized by a stable boundary layer and light air flow. Thus, as in Atlantic Canada, when local populations burn wood as an alternative to other sources of heat, high levels of PM_{2.5} result. This is a common problem in some residential areas of Montréal, Québec City, and the Saguenay and Abitibi regions. These areas all have significant wood burning emissions from households or industries and experience wintertime inversions trapping the pollutants within low lying areas such as the river valleys (St. Lawrence River, Saguenay fjord, La Mauricie River, etc.).

Some older technology aluminium smelters in the Shawinigan, Beauharnois, Baie-Comeau and Saguenay regions have a significant impact on their surroundings with an average contribution of 11-14 $\mu\text{g m}^{-3}$ of primary $\text{PM}_{2.5}$ added to the hourly ambient concentrations (RWDI, 2004). The Saguenay plant closed in 2004, Beauharnois is expected to close in June 2009, Baie-Comeau is undergoing modernization and the Shawinigan plant is expected to close in the near future and thus reduced $\text{PM}_{2.5}$ concentrations are expected in those areas. Nonetheless, there remain uncertainties in the estimation of primary $\text{PM}_{2.5}$ emissions from the aluminium industry because there is no sampling methodology available to measure $\text{PM}_{2.5}$ emissions from roof vents which are the main sources of emissions. Other pollutants, such as SO_2 , and to a lesser degree, NO_x and VOC contribute to the formation of secondary particulate matter and ozone. However, their contribution to the local problems is not quantifiable without models capable of simulating atmospheric chemistry.

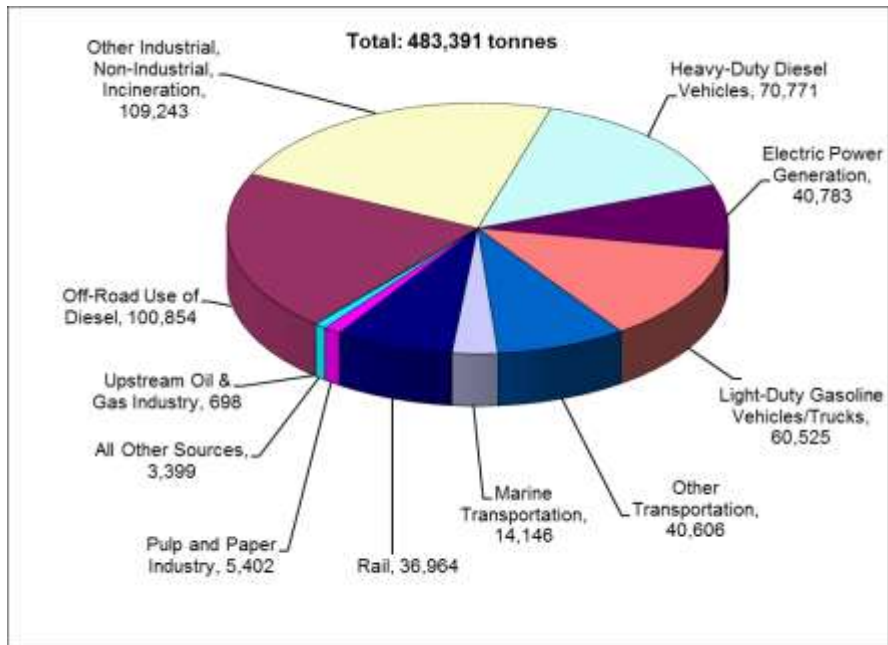
7.3.2.2 Future Areas of Concern

Residential wood combustion, a major source of $\text{PM}_{2.5}$, has increased by 25% in the last 15 years and recent socio-economic projections indicate there will be another 3% increase from 2005 to 2010 and again to 2015. Industrial releases of fine particles are expected to rise by 8% by 2010, then rise slightly more but remain below 1990 levels. As a result, the occurrence of poor air quality due to local sources of primary particles is expected to remain stable or increase slightly.

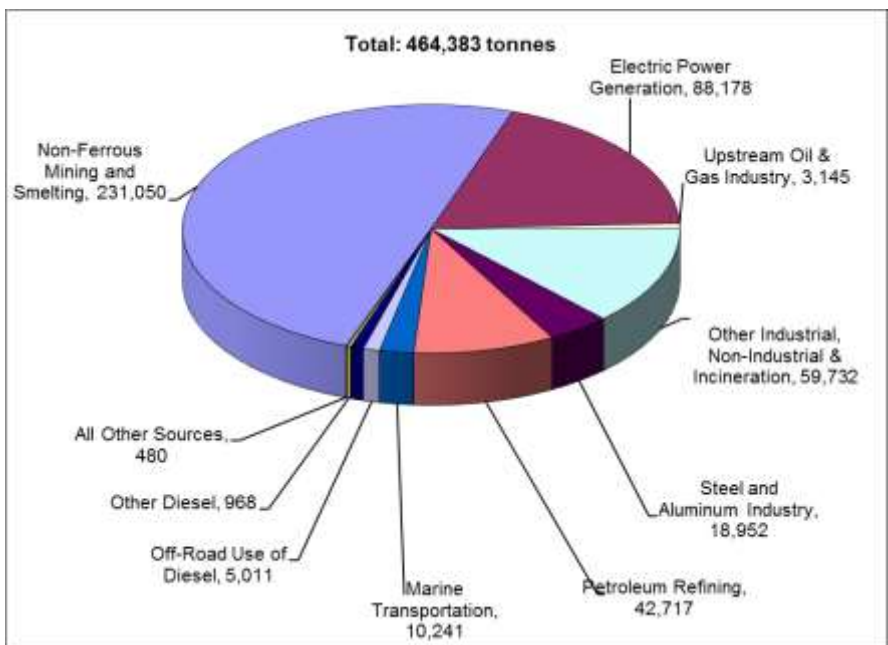
It is likely that SO_2 emissions from the aluminium industry will rise by around 40% by 2015 because of a projected increase in the sulphur content of the coke and also planned expansions in the Saguenay region in Alma and Arvida. In addition to higher SO_2 concentrations, this increase in emissions will lead to secondary $\text{PM}_{2.5}$ formation in the vicinity and downwind of these industrial regions.

7.3.3 Ontario

Not only does Ontario house a significant fraction of Canada's population, it is also home to a large part of the country's industry. Consequently, Ontario emissions are substantial, amounting to 464 kT of SO_2 , 480 kT of NO_x , 434 kT of VOC and 12 kT of ammonia in 2006. Excluding open sources, the Ontario emissions of $\text{PM}_{2.5}$ were 72 kT in 2006. (Although open source emissions of $\text{PM}_{2.5}$ are large, their effect is reduced as discussed in Section 7.3.2 because they occur at ground level). However, comparing these values to those in Figure 4.29, it is apparent that Ontario emissions are much lower than the total of the U.S. States within the airshed (U.S. EPA, 2007). The key message is that the combined emissions of the Midwest U.S. and Ontario are large and spread and accumulate over the area and downwind. These emissions have a significant impact on regional air quality.



a)



b)

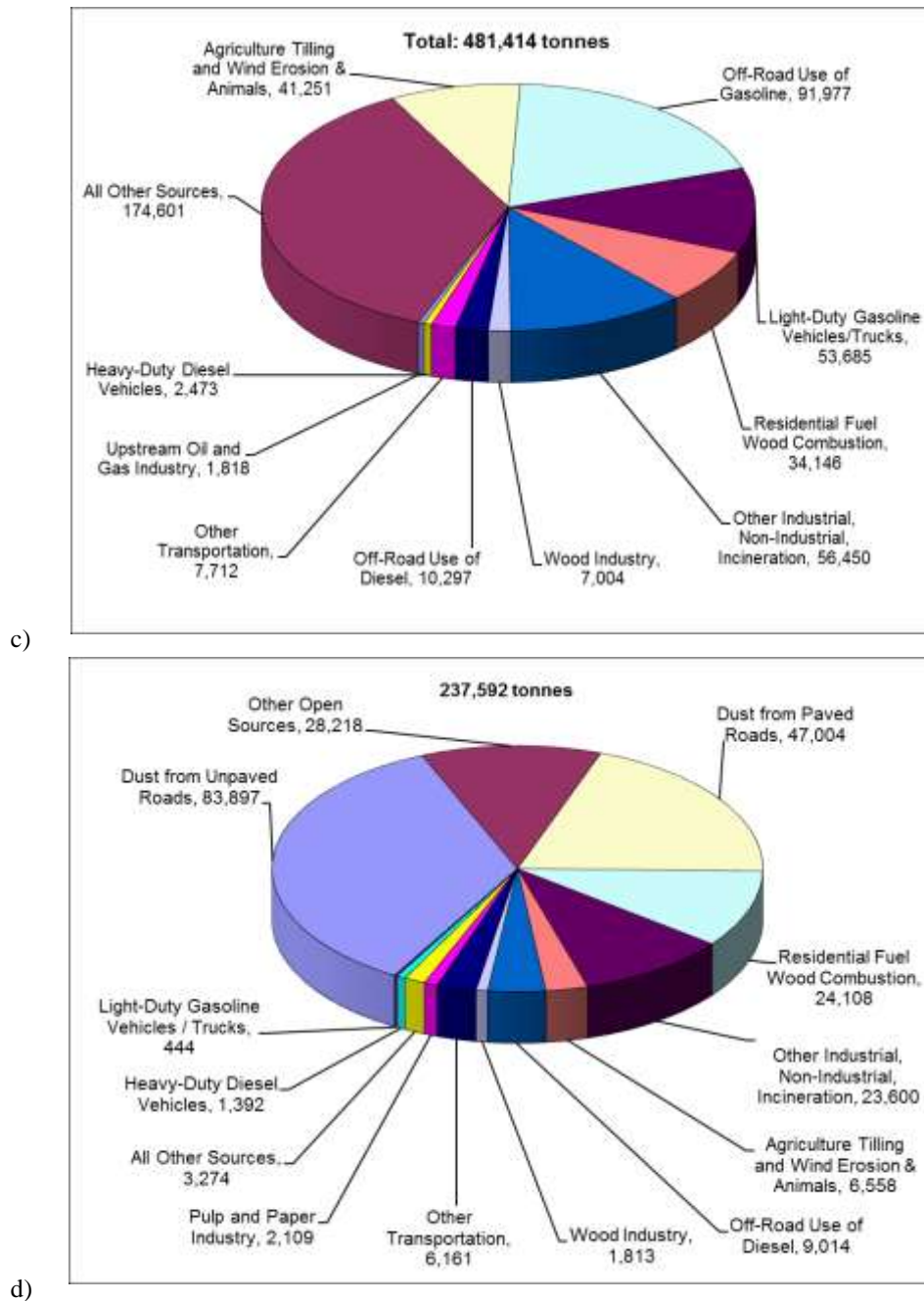


Figure 7.16 Ontario's anthropogenic criteria air contaminants emissions by sector. a) NO_x , b) SO_x , c) VOCs, and d) $\text{PM}_{2.5}$. (Pollution Data Branch, 2007). Environment Canada, 2007a.

Ontario's emissions of smog precursors are summarized in a breakdown by source sector in Figure 7.16a-d. Transportation sources dominate provincial NO_x emissions (67%), and also contribute 35% of anthropogenic VOC emissions. Industrial sources are the major contributors to Ontario emissions of SO_2 and primary $\text{PM}_{2.5}$ (Environment Canada, 2009a).

7.3.3.1 Local Areas of Concern

Table 7.1 Comparison of emissions from Windsor, Sarnia, Hamilton, Toronto and Ottawa, 2006 values in kilotonnes (NPRI, 2007b).

City	PM _{2.5}	SO ₂	NO _x	VOC
Windsor	1,814	925	4,582	10,639
Sarnia	1,405	34,194	6,801	8,904
Hamilton	6,671	12,523	20,340	20,506
Toronto	19,678	7,128	46,212	83,448
Ottawa	4,976	2,794	13,306	22,969

In general, the provincial emissions are concentrated in the most populated areas including Windsor, Sarnia, Hamilton, Toronto and Ottawa (Table 7.1). While Ottawa is also a significant population center, it is not highly industrialized. This city therefore contributes NO_x and VOC, mainly from motor vehicle emissions, but less SO₂ and primary PM_{2.5}. Hamilton is a major industrial and population center, which is reflected in the emissions. Consequently, air quality in Hamilton has presented a concern for many years (HAQI, 1997a), although a downward trend in concentrations has been noted (HAQI, 1997b). The city contains several large industrial facilities, and also has a significant motor vehicle population. The key industries contributing to poor air quality in this area include ferrous smelting, lime and gypsum manufacturing and the production of inorganic chemicals including black carbon. The emissions from these industries amount to approximately 15 kT SO₂, 10 kT NO_x and 1.5 kT PM_{2.5} per year.

The transboundary area encompassing Detroit and Port Huron on the U.S. side and Windsor and Sarnia on the Ontario side is densely populated. Ontario is responsible for a significant amount of emissions as located within this region is Sarnia's large petrochemical industry and accompanying SO₂ emissions as well as four of the province's ten largest SO₂ point sources. However, the dominating effect for Windsor is often emissions from the greater Detroit area associated with a variety of industries some of which are also present in Windsor (e.g., automotive and related activities) that are important to the economies in both countries. Due to the large amount of international trade flowing through this area significant local air quality concerns are associated with emissions from heavy duty diesel trucks lined up in Windsor to cross the border.

Table 7.2 10 largest point source emitters of NO_x and SO_x in Ontario.

Facility Name	City	On-Site Releases (tonne)
SO ₂		
Inco - Copper Cliff Smelter Complex	Copper Cliff	177631
Nanticoke Generating Station	Nanticoke	61958
Falconbridge Limited - Smelter Complex	Falconbridge	40445
Imperial Oil - Sarnia Refinery Plant	Sarnia	23770
Lambton Generating Station	Courtright	17227
Shell Canada - Sarnia Manufacturing Centre	Corunna	10763
Cabot Canada Ltd	Sarnia	7319
Falconbridge Limited - Kidd Metallurgical Site	Timmins	6646
Algoma Steel Inc	Sault Ste. Marie	6249
Essroc Canada	Picton	5892
Provincial total SO₂ emissions		512,000
NO _x		
Nanticoke Generating Station	Nanticoke	20048
Lambton Generating Station	Courtright	6179
St. Mary's Cement	Bowmanville	4415
Carmeuse North America	Dundas	3069
Dofasco	Hamilton	3057
Essroc Canada	Picton	2962
Algoma Steel Inc	Sault Ste. Marie	2757
Thunder Bay Generating Station	Thunder Bay	2701
Nova Chemicals	Corunna	2556
Lafarge Canada Inc. - Bath Cement Plant	Bath	2552
Provincial total NO_x emissions		515,000

There are major point sources throughout the southern part of the province, i.e., south of an east-west line drawn approximately through Barrie. The ten largest sources of SO₂ and NO_x are listed in Table 7.2. However, the largest sources of SO₂ are well outside the most populated areas of southwestern Ontario, being associated with the nickel smelting operations in the Sudbury area. In fact, SO₂ emissions from the Copper Cliff smelter complex, at 177 kT per year account for just over one third of the provincial total, and the three largest point sources emit more than half of the total. These can give rise to local impacts from time to time, but

significant improvements in the area should be recognized. Under a variety of control orders and programs, including the Countdown Acid Rain Program (Scott, 1989) smelter emissions of SO₂ have been reduced by over 90% since the early 1970s, and now stand at 177 kT annually. Vale Inco has stated their intention of reducing SO₂ emissions further, to 66 kT annually, by 2015.

Other major SO₂ sources outside large urban areas include metallurgical operations in Timmins and Sault Ste. Marie. Emissions of 7 kT per year are associated with the Kidd metallurgical site in Timmins, while Algoma Steel Inc., ninth of the top ten sources of SO₂ in Ontario, is located in Sault Ste. Marie. Air quality problems have been reported in Sault Ste. Marie in the past (Potvin Air Management Consulting, 2006). There has been a steady improvement over the past decade but excursions, though infrequent, still occur.

Cement plants figure in the list of the ten largest NO_x emitters that are outside southwestern Ontario, specifically those located in Bowmanville, Picton, Mississauga and Bath.

The thermal generating station in Thunder Bay, and Algoma Steel in Sault Ste. Marie must also be considered in assessing impacts of pollutants in Ontario. However, the largest point sources of NO_x are located in southern Ontario, being the thermal generating stations at Nanticoke and Lambton which contributed respectively 22 and 9 kT to the provincial total of 480 kT in 2007. These two generating stations also contributed respectively 67 and 31 kT of SO₂ to the 2007 provincial total of 464 kT. It should be noted that Ontario has plans in place to close these two generating stations by 2014, and has already closed the Lakeview generating station, which was located in Toronto. In addition to the Nanticoke generating station, annual emissions totaling approximately 4 kT of NO_x and 10 kT of SO₂ are reported by other sources in this area. These include an Imperial Oil refinery and Lake Erie Steel.

Unlike Québec and the Atlantic Provinces, residential wood burning is not believed to be a significant problem in the urbanized part of Ontario. Wood burning for residential heating is more common in communities in the northern part of the province, where local impacts may be experienced, especially under conditions of reduced mixing experienced in the winter time.

7.3.3.2 Future Areas of Concern

On a local and provincial level significant new sources or source regions are not anticipated, and existing major sources are all subject to abatement measures and are showing emission reductions. The continued growth of motor vehicle use is therefore seen as the most important area of concern for future air quality.

Transboundary influences on air quality in Ontario have been of concern for many years, starting with the identification of the acid rain problem. Analysis and interpretation of monitoring data, including use of mathematical models (MOE, 2005) confirm the importance

of transboundary transport, and it is clear that this will remain a factor into the future in contributing to elevated pollutant levels in Ontario. In particular, as long as U.S. air quality standards are set at numerical values higher than those in Canada, it will be possible for air parcels which are in compliance in the U.S. to cross the border and cause exceedances even before Canadian emissions are added.

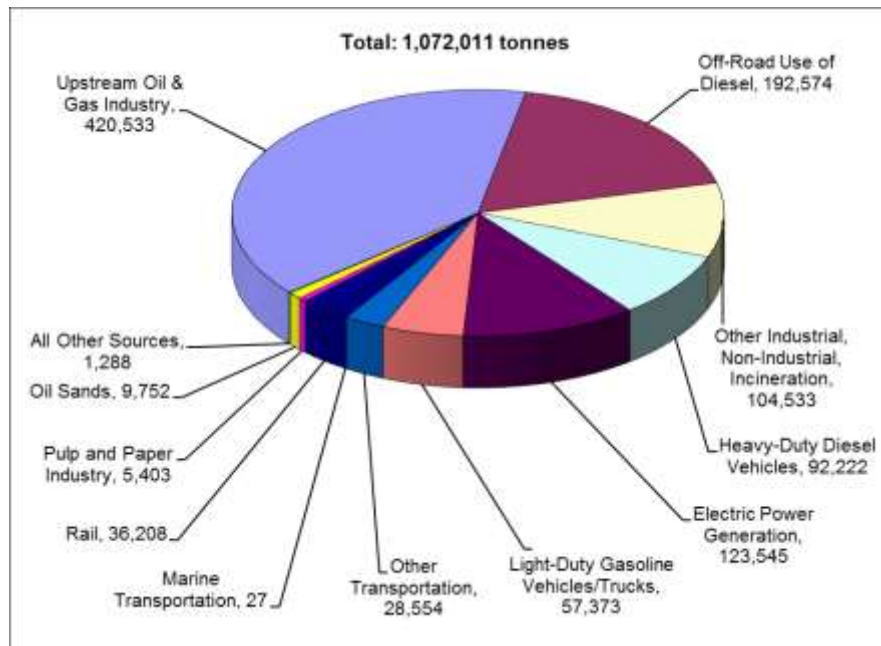
7.3.4 Alberta and the Prairies (and the North)

The three Prairie provinces account for 49% of national SO₂ emissions, 47% of national NO_x emissions and 47% of national VOC emissions in 2006 (see Chapter 4). These provinces have high per capita emissions, due to the reliance of Alberta and Saskatchewan on coal and natural gas for electricity generation, large emissions from the oil and gas industry – particularly in Alberta, and large emissions of SO₂ from smelters in Manitoba. The significant contribution of the three provinces to national emissions is shown in Figures 4.1 to 4.5.

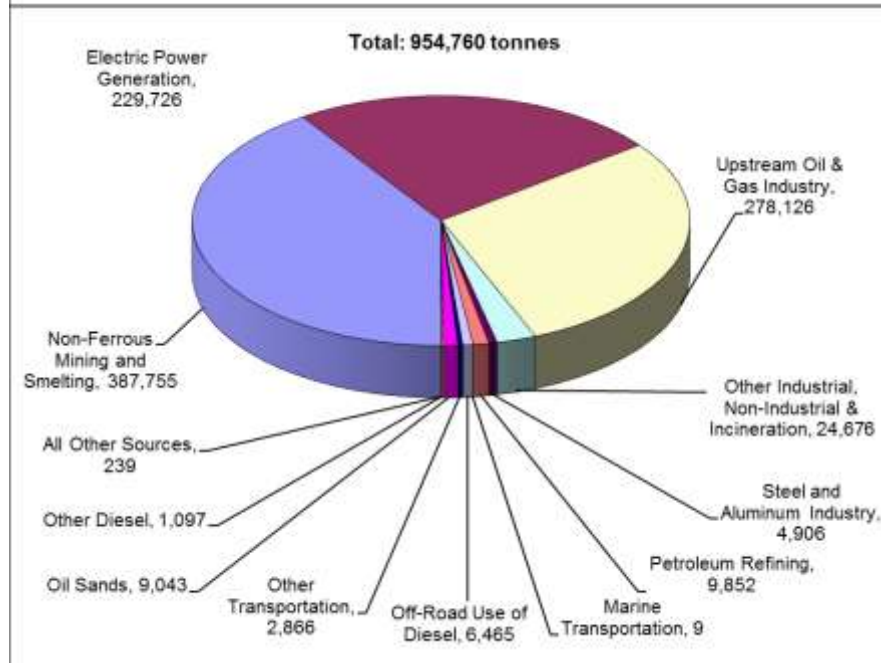
Alberta accounted for roughly 33% of total Canadian NO_x emissions, 24% of Canadian VOC emissions and 22% of Canadian SO₂ emissions in 2006. Furthermore, when compared to both adjacent provinces and U.S. states in the northwest, Alberta is the most significant emitter for these pollutants throughout this large region, suggesting that on average it is likely a net exporter of air pollutants to surrounding jurisdictions.

Major contributors to emissions in Alberta include the upstream³⁷ oil and gas industry, extraction of bitumen from the Athabasca oil sands, oil refineries and petrochemical production, and coal-fired electricity generation. The conventional oil and gas industry is spread across most of the province except for the extreme north-eastern corner; however areas with major concentrations of activity include the Rocky Mountain Foothills and the area around Cold Lake, where heavy oil is extracted. The oil sands industry is concentrated in the area surrounding Fort McMurray in northeast Alberta though oil sands deposits are also found in the Peace River area and the Cold Lake area, and these deposits are beginning to be developed. Refineries and petrochemical facilities are concentrated in the area northeast of Edmonton, while coal-fired electricity generation is concentrated just west of Edmonton.

³⁷ The “upstream” oil and gas industry refers primarily to the exploration for and extraction of oil and gas along with sufficient processing for the products to be shipped by pipeline. Refining of crude oil into gasoline and other fuels is part of the “downstream” industry.



a)



b)

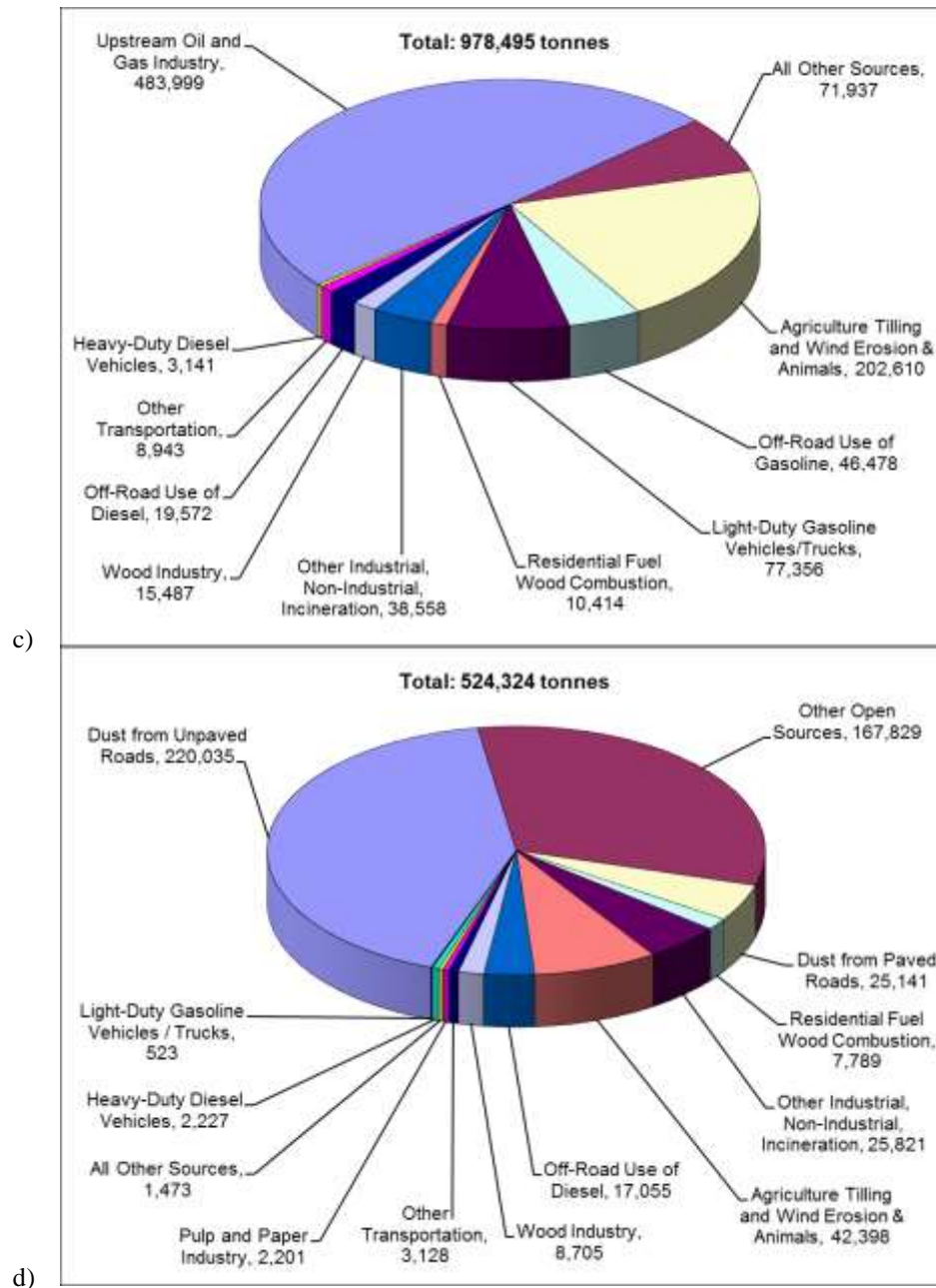


Figure 7.17 Alberta, Saskatchewan and Manitoba anthropogenic criteria air contaminants emissions by sector. a) NO_x, b) SO_x, c) VOCs, and d) PM_{2.5}. Environment Canada, 2007a.

The sectoral contribution to emissions from the Prairie Provinces of NO_x, SO_x, VOCs and primary PM_{2.5} is presented in Figure 7.17a-d. The upstream oil and gas sector is the dominant contributor to NO_x emissions, accounting for 39% of provincial emissions. Other important sectors include on road transport, electricity sector, off-road engines, and the oil sands. For SO₂ emissions, the mining and smelting industry, the upstream oil and gas sector and the

electricity sector each account for almost a third of emissions. For VOC emissions the oil and gas industry is again dominant, accounting for 59% of anthropogenic VOC emissions. The oil sands contribute 12% of VOC emissions, while on road transport contributes 10%.

The spatial distributions of emissions across the country were shown in Figures 4.7-4.11. As in other provinces, the spatial pattern within Alberta shows that there are discrete areas with a high proportion of the emissions. The census divisions containing the cities of Edmonton, Calgary, and Fort McMurray are the highest emitting areas. The Edmonton area has one of the highest total urban area emissions in Canada, accounting for on the order of 8% of national NO_x emissions and 6% of national SO₂ emissions. This is partly due to its large population and because the area has several large coal-fired power plants west of Edmonton as well as oil refineries and chemical plants to the east and northeast of the city.

7.3.4.1 Local Areas of Concern

7.3.4.1.1 The Athabasca Oil Sands Region

The Athabasca region, located approximately 500 km northeast of Edmonton, is one of three in Alberta containing oil sands deposits, and is the most extensively developed. This area is surrounded by largely intact boreal forest. Prevailing winds are from the west and north and there is minimal topography to impact ambient pollutant concentrations, other than the relatively small river valley where much of the population is located. The oil sands industry is the primary economic basis for the city of Fort McMurray, employing over 30% of the region's 65,000 inhabitants (Regional Municipality of Wood Buffalo, 2006).

In 2005 the oil sands sector contributed 9% of Alberta's NO_x emissions, 12% of VOC emissions and 32% of SO₂ emissions (these emission totals do not include the mine fleet so the actual proportions, particularly for NO_x, will be greater). Within the oil sands sector emission sources include SO₂, NO_x, and VOC from the upgraders, NO_x and PM_{2.5} from the mine fleet, NO_x from natural gas fired boilers, heaters and turbines, and VOC from upgraders, from tailings ponds and from exposed bitumen in the mines.

The majority of these emissions are concentrated within about a 100 km radius of the city of Fort McMurray. Air quality is a significant concern for people living in the area (Jardine and Ouellette, 2006). Among these concerns is the potential for ground-level ozone production as a result of these emissions (AMEC, 2003). Current concerns are exacerbated by dramatic projected increases in emissions between 2007 and 2015.

7.3.4.1.2 Alberta's Industrial Heartland

Alberta's Industrial Heartland is a 470 square kilometer area designated for long-term heavy and medium industrial growth. The Heartland includes four smaller municipalities and begins about 10 km northeast of the city of Edmonton (part of the Edmonton Census Metropolitan

Area). The area is Canada's largest processing center for petroleum, petrochemical and chemical industries³⁸ and is highly industrialized with more than 30 major industrial facilities and numerous smaller ones. Industries include oil refineries and bitumen upgraders, inorganic and pharmaceutical chemical manufacturing plants, a major nitrogen fertilizer plant, a major phosphorus plant and steel production. Growth in the Industrial Heartland is largely tied to growth in the oil and gas sector in Alberta and is being actively promoted. It is likely that industrial growth in this area will continue; there are currently eight new upgraders proposed and a total of \$46 billion in industrial construction planned or underway in the area.

The proximity of a major industrial area to a large urban population, the city of Edmonton, makes this an area of concern. Existing emissions of NO_x and SO₂ have already been identified as a concern and the provincial government has proposed regional caps of 25,000 tonnes per year of NO_x and 28,000 tonnes per year of SO₂. No caps have been proposed for VOCs or particulate matter, and much still remains unknown about the interaction of pollution from the cities of Edmonton and Fort Saskatchewan with industrial emissions raising the possibility of CWS exceedances.

7.3.4.1.3 Agricultural Emissions

The three Prairie Provinces account for 57% of national ammonia emissions. The bulk of these emissions are from agriculture – both livestock husbandry and fertilizer application (Environment Canada, 2009b). Ammonia emissions in Alberta are greatest in the southwest near Lethbridge, an area with numerous large cattle feedlots, and in the Edmonton-Calgary corridor. In Saskatchewan, ammonia emissions are broadly distributed over cropland in the southern third of the province. Ambient levels of ammonia in the Prairies, and the extent to which ammonia from agriculture contributes to PM_{2.5} concentrations in the Prairies is discussed extensively in the 2008 Canadian Atmospheric Assessment of Agricultural Ammonia (Environment Canada, 2009b).

An occasional contributor to smog in the Prairies is smoke from burning of agricultural residue (stubble burning). It is difficult to make quantitative statements about the impact of agricultural burning as the impacts tend to be localized and of brief duration, and the time and locations of burning are not typically available. Agricultural burning occurs in late summer and autumn.

³⁸ Alberta's Industrial Heartland <http://www.fortsask.ca/pdfweb/Heartland.pdf>

7.3.4.2 Future Areas of Concern

Due to its significant population and industrial growth, Alberta's emissions have been increasing over the past several years. The population of Alberta has been growing at twice the national rate and is projected to continue growing rapidly well into the future. Current trends would see Alberta add nearly one million new residents between 2006 and 2020. In contrast, the populations in Manitoba and Saskatchewan are projected to grow slowly if at all.

Within Alberta, the cities of Calgary and Fort McMurray have been growing faster than the provincial average. In particular, the city of Fort McMurray is projected to nearly double in size over the next 10 years. These population increases can be expected to increase the vehicle miles travelled on Alberta roadways, which may lead to increased emissions from the transportation sector, despite improved control technologies and fuels.

Industrial trends that will affect emission trends include the projected growth in production of bitumen and synthetic crude from the oil sands of Alberta. Production from the oil sands is projected to increase from 1 million barrels per day (Mbbbl day⁻¹) currently to between 2.0 and 3.5 Mbbbl day⁻¹ in 2015 (NEB, 2006; CAPP, 2007), with further increases beyond that. The majority of the bitumen will be produced in the Fort McMurray region in northeast Alberta, though some will also be produced in the Peace River region of northwest Alberta and near Cold Lake in eastern Alberta. A large expansion in the capacity to upgrade bitumen from the oil sands to synthetic crude oil is planned (and in some cases already approved) for Strathcona and Sturgeon Counties immediately northeast of Edmonton. The Athabasca oil sands deposits extend into northwest Saskatchewan, so it is possible that Saskatchewan may see production of bitumen from the oil sands as well.

Uncertainties in Emissions Inventories

Obtaining accurate numbers for emissions of the CACs, as well as their chemical speciation (e.g., composition of PM_{2.5} or VOC speciation) is a critical part of air quality risk management (Craig *et al.*, 2008). This is a challenging process requiring the use of emission factors and activity data, including a range of surrogates and industry cooperation, and uncertainties are difficult to quantify and vary significantly among pollutants, industries and over time. Actual measurements to produce more accurate emissions and to evaluate the reported or estimated values are limited and require additional effort to improve Canadian information, including continuous emissions monitoring (NARSTO, 2008). The recent improvements in Canadian ammonia emissions under the NAESI program (Environment Canada, 2009b) are a notable activity and should serve as a model for future efforts. Other recent activities in Canada include some measurements of fugitive VOC emissions in Edmonton (Chambers and Strosher, 2006), updates to the Canadian biogenic VOC inventory (see text box above) and

measurements in the vicinity of a cargo ship plume in Vancouver (Xu *et al.*, 2008). As an example of what is being learned more information on the work in Alberta is provided in this text box.

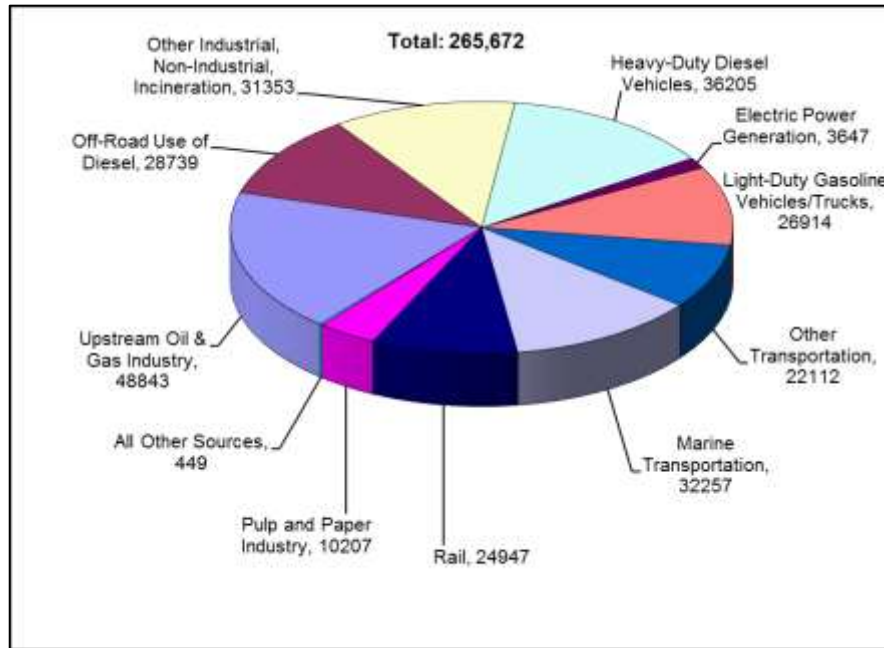
A defining characteristic of the oil and gas industry in Alberta and Saskatchewan is the very large number of facilities such as flares, compressors, storage tanks, dehydrators and gas plants, which are widely dispersed across both provinces. Individually many of these are small emitters, but collectively they add up to significant sources of smog precursors. Emissions from these sources are generally not as well quantified as emissions from larger point sources, and thus add considerable uncertainty to the emission inventories for this sector. A study in 2004 (Chambers, 2004) used a laser based technology, the Differential Absorption Laser technique (DIAL) to investigate fugitive methane and VOC emissions from a selection of gas plants. In most cases, DIAL measured fugitive VOC emissions were higher than emissions calculated using standard estimation techniques.

In 2005 the DIAL was used to study fugitive VOC emissions from a refinery near Edmonton. When fugitive emissions from this short term study were extrapolated over a year to compare to reported VOC emissions, measured VOC emissions were approximately 15 times greater than reported emissions. While extrapolating a few hours of measurement to represent an entire year involves many assumptions, the conclusion that actual emissions are greater than reported is likely robust. Measurements and modelling in Houston, Texas, an area with a similar but larger concentration of petrochemical plants found that reported VOC emissions could be understating true emissions by a factor of 10 or more (Ryerson, *et al.*, 2003; Jiang and Fast, 2004)

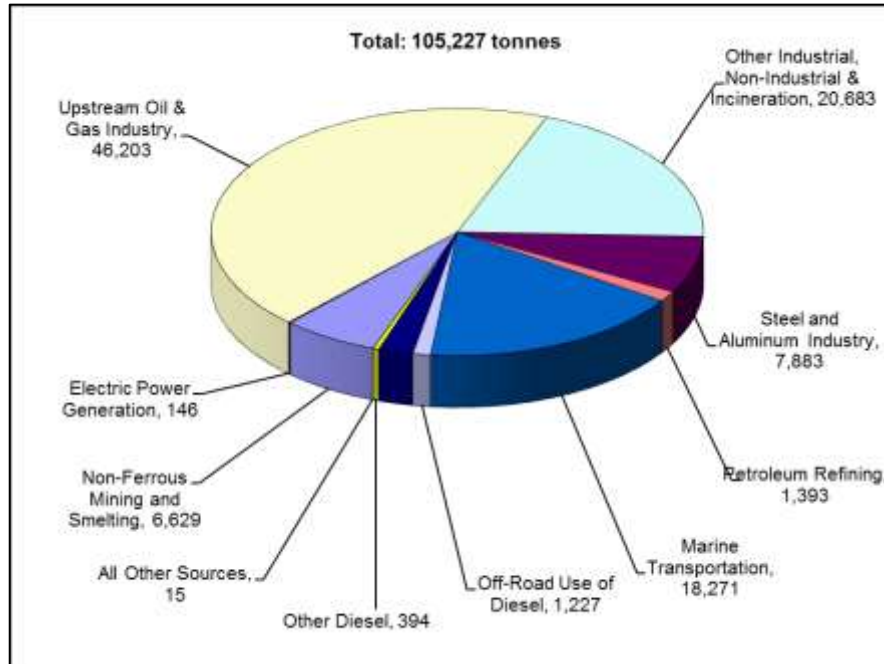
Conventional oil and gas production in Alberta and Saskatchewan has peaked and will decline in the future (NEB, 2007). Despite this, conventional oil and gas will support significant levels of activity well into the future, particularly if commodity prices are high. Production of lower quality heavy oil and production of oil and natural gas from smaller or more difficult reservoirs can be more energy and emissions intensive even with lower overall production.

Expansion of coal-fired electricity generation west of Edmonton is planned for the near future, with one 450 MW plant currently under construction and another permitted. However the oldest (and highest emitting) existing plant is slated to be shut down by 2010. Additional coal-fired generation has been proposed, including a 1000 MW facility in southern Alberta. Manitoba on the other hand is projected to extend its reliance on low emission hydro-electricity well into the future. In addition to expanding energy production, current mineral exploration activity, primarily in Manitoba and Saskatchewan, suggest that additional mines will be operating in the future, contributing some emissions in the lightly populated Canadian Shield areas. Emissions of SO₂ and PM_{2.5} from the two large base metal smelters in Manitoba are predicted to decline either due to reduced operations or equipment upgrades.

7.3.5 British Columbia



a)



b)

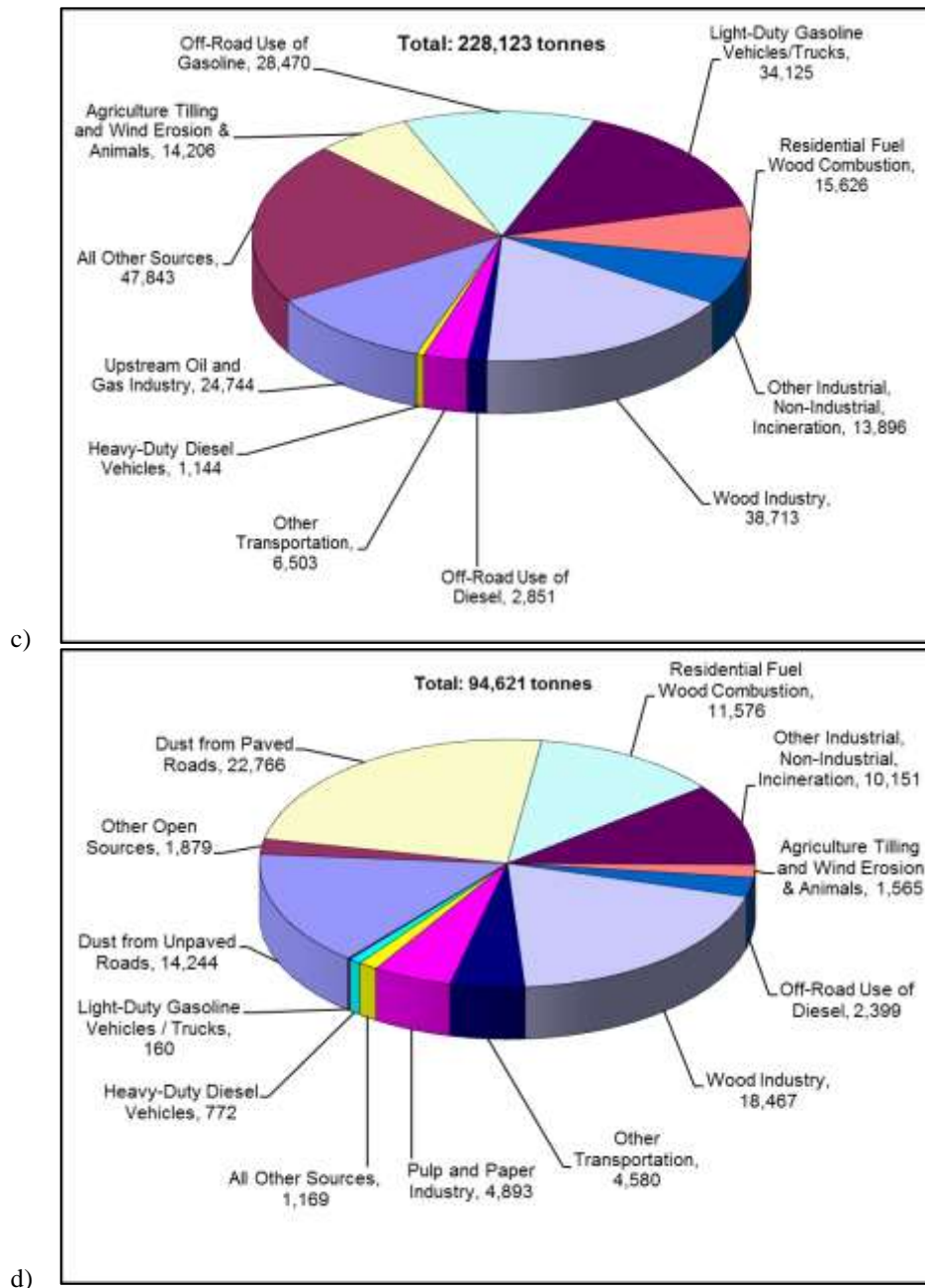


Figure 7.18 British Columbia's anthropogenic criteria air contaminants emissions by sector. a) NO_x, b) SO_x, c) VOCs, and d) PM_{2.5}. Environment Canada, 2007a.

Provincial emissions data by sector are summarized in Figures 7.18a-d. NO_x emissions in BC are shared by a number of sources among which the most notable are: upstream oil and gas (18%), heavy-duty diesel (14%), a mix of industrial, non industrial and incineration, marine transportation (12% each), light duty gasoline vehicles (10%) and off road diesel (11%). SO₂ emissions are dominated by the upstream oil and gas industry (44%), followed by a mix of other industrial, non industrial and incineration (20%) and marine transportation (17%). Major

industry (non ferrous mining and smelting, steel and aluminum and petroleum refining) collectively contribute to 15% of total SO₂ emissions in the province. VOC emissions in BC are relatively equally divided into four principal sources: the wood industry (17%), light duty gasoline vehicles (15%), off road gasoline use (12%) and upstream oil and gas (11%). Lastly, dust from paved and unpaved roads dominates PM_{2.5} (39%), followed by the wood industry (20%) and residential fuel wood combustion (12%).

7.3.6 The Lower Fraser Valley

Due to the urban and marine character of the area and its abundant vegetation, emissions of smog-forming pollutants in the LFV have unique characteristics compared to the remainder of the province. In the more urbanized western portion of the LFV, NO_x and SO₂ emissions are dominated by automobiles and marine vessels, while in the less urbanized eastern LFV, emissions are dominated by agriculture and automobiles. Light and heavy duty automobiles are the largest contributors to NO_x emissions (35%), while marine vessels, mostly ocean going, are the largest contributors to SO₂ emissions (47%) (Metro Vancouver, 2007). Ammonia emissions from agricultural practices are significant (76%) and originate from cattle, pig and poultry housing, nitrogen-based fertilizer and manure land-spreading. Industrial emissions account for less than 10% of smog forming pollutants in the LFV. Some of the more notable contributions are from the petroleum products sector (11% of SO₂) and the wood products industry (7.5% of PM₁₀).

7.3.6.1 Future Areas of Concern

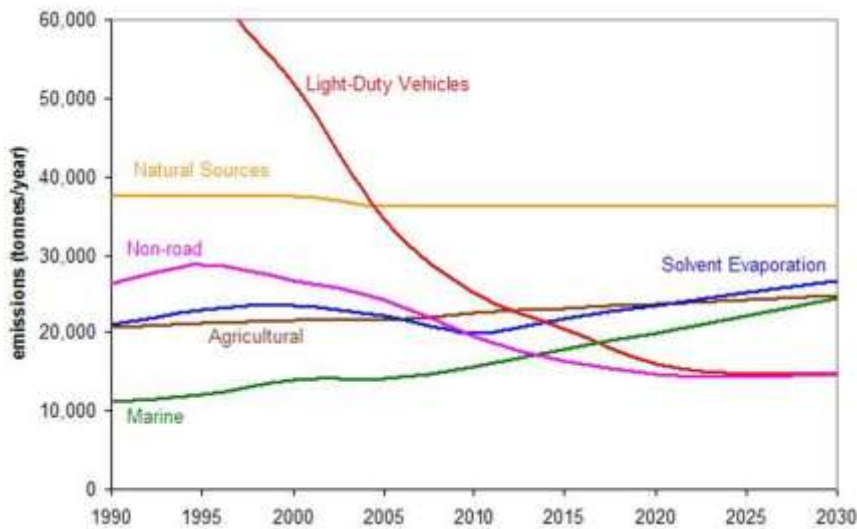


Figure 7.19 Forecast of smog forming pollutant sources for the LFV based on the 2005 emission inventory (Metro Vancouver, 2007).

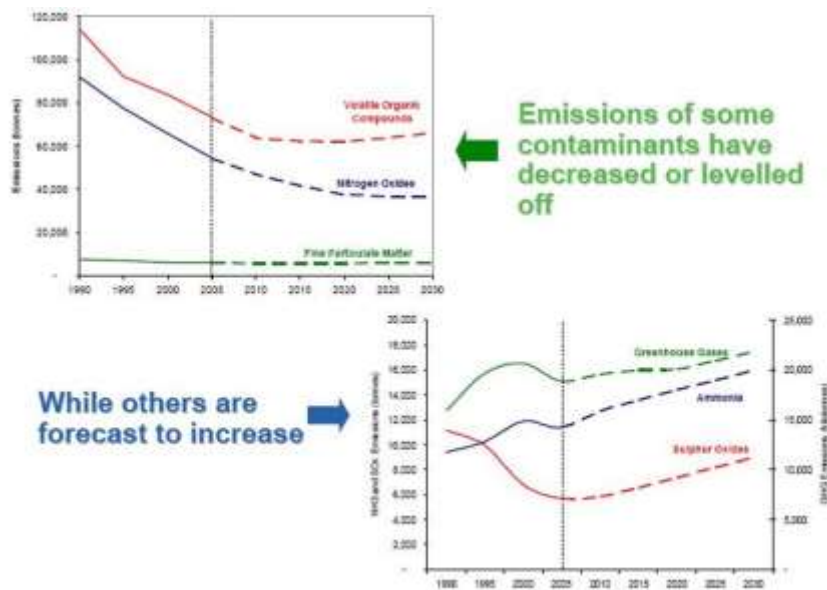


Figure 7.20 Emission forecasts of smog forming pollutants for the LFV based on the 2005 emission inventory (Metro Vancouver, 2007).

Emission projections were generated for dominant source sectors in the LFV for the period extending to 2030 (Figure 7.19) (Metro Vancouver, 2007; Metro Vancouver 2010). While vehicle emissions have been declining steadily in the LFV in response to federal vehicle regulations and the Air Care program, emissions from the marine, agricultural and solvent sectors are expected to rise over the next two decades. Projected trends of individual smog forming emissions are illustrated in Figure 7.20 (Metro Vancouver, 2007). Current declines in VOC emissions are expected to continue until about 2010 and then start rising again after 2020 (mostly due to population and economic growth). On the other hand, NO_x emissions are projected to continue to decline until about 2020 before leveling off. In contrast, ammonia is expected to increase significantly from growth in the agricultural sector. While SO_2 , has seen significant declines since 1990, emissions are expected to increase due to growth in the marine sector. Whereas primary $\text{PM}_{2.5}$ emissions are projected to remain constant, secondary $\text{PM}_{2.5}$ (not shown) is expected rise in response to increasing levels of ammonia and SO_2 .

7.3.7 Interior Valleys of British Columbia

Primary PM emissions are of particular concern in interior BC communities where meteorology acting on mountainous topography traps pollutants and causes the majority of pollution episodes. For primary $\text{PM}_{2.5}$, prescribed burning accounts for most (29%) of emissions followed by the wood industry (18%) and residential fuel wood combustion (15%)

(BCEnv, 2007). As such, considerable effort has been made on emission reduction measures such as open burning regulations (BCEnv, 2004a), wood-stove exchange programs, (BCEnv, 2007) and the “Burn it Smart Program” (BCEnv, 2008).

Industrial wood processing emissions are of particular concern in communities such as Williams Lake, Quesnel and Prince George. Although a number of communities have successfully eliminated emissions from beehive burners, others, such as Bulkley Valley, are still being impacted by this source (BVLD, 2006). Communities with rail yards, such as Golden, Quesnel and Prince George, are more heavily influenced by emissions of SO₂, NO_x (from diesel) and rail dust (from transported freight). Elevated SO₂ emissions from industry are of concern in both Trail and Prince George. Outdoor wood boiler emissions are an additional concern in some BC communities. Road dust affects air quality in many interior communities during the spring (BCEnv, 2004b; 2006a; 2006b).

In the Peace River area in the north-east sector of BC, emissions are mainly dominated by the upstream oil and gas industry which emits significant amounts of SO₂. This area may also occasionally be affected by emissions from the Alberta oil sands (Pankratz, 2004). In the Yukon Territory, emission sources include wood stoves, vehicles, diesel electric generators, garbage combustion and industrial activities. Emission regulations have been drafted under the Yukon Environment Act however, they do not address wood smoke or vehicle idling, two important factors contributing to deterioration of air quality in the region (Yukon Government, 2007). Forest fires affect air quality in both BC and Yukon communities causing PM_{2.5} ambient concentrations to sometimes rise to extreme levels. The severity of summer forest fires dominates the variability in the mean annual PM_{2.5} concentrations at Whitehorse.

7.3.7.1 Future Areas of Concern

Although there are no emission forecasts available for the rest of BC or the Yukon, there are, nevertheless, a few areas of concern. The Okanagan is an area of current concern due to its rapid population growth and associated increase in motor vehicle emissions which may increase ozone levels and degrade visibility. In addition, the development of the international port of Fairview at Prince Rupert is expected to impact both local air quality, due to an increase in marine emissions, and on the route between Prince Rupert and Prince George, as heavy duty truck traffic increases. Furthermore, rail emissions are expected to become more important in BC interior communities in terms of contributions to overall NO_x and SO₂ emissions, as light and heavy duty transport sectors continue to reduce tailpipe emissions. Additional concerns exist due to open and prescribed burning, which is common throughout the BC interior. Lastly, areas in the northern Yukon could be affected by an expected increase in ship emissions in the North-West Passage, as this area becomes more accessible to ship traffic due to climate change.

7.4 Meteorological Influences on Air Quality

Once air pollutants have been introduced into the atmosphere their transport, transformation and deposition is largely controlled by meteorology. This section provides background information on the meteorological factors influencing the observed pollutant concentrations. In subsequent sections, examples that highlight the influence of these factors and enhance our current understanding are presented.

Although hemispheric and continental scales of motion are important considerations and are discussed in Chapter 9, day to day and hourly variations in pollutant concentrations are largely dependent upon smaller scale features ranging from the synoptic or regional scale (i.e., low and high pressure areas) to the local or meso-scale phenomena, such as sea and lake breezes, upslope flows, terrain-induced drainage and nocturnal inversions. Microscale features, such as individual urban street canyons, are also important, particularly with respect to actual human exposure patterns, but are not discussed in this section or this chapter (see Chapter 8 for an in-depth discussion).

The relative importance of the different scales (hemispheric to micro) depends strongly upon a pollutant's atmospheric lifetime (see Chapter 2) and its origin. Those that are highly reactive (e.g., NO, some VOCs, ultrafine particles) will not travel far and thus it is only necessary to consider micro to local scale phenomena. Less reactive pollutants (e.g., CO, black carbon, SO₂, benzene) can travel further before being converted to other species, depositing and/or dispersing to low levels and hence somewhat larger scales of motion also play a role. Ozone and some chemical constituents of PM_{2.5} (e.g., ammonium sulphate, elemental and organic carbon) have relatively long lifetimes (5-10 days) and also continue to be formed outside of the main source areas (i.e., cities or industrial regions) due to the presence of precursors, natural or anthropogenic. Thus, in addition to the local scale, regional to continental scales are relevant. Consequently, long-range transport pathways are important to study to understand their day to day variations.

Regardless of location in Canada, areas with high emissions (e.g., cities) undergoing air mass stagnation and suppressed vertical motion, which are largely a function of the synoptic weather pattern, will typically experience elevated concentrations of pollutants. Local circulation patterns can be super-imposed upon such conditions leading to re-circulation of local emissions. These patterns serve to retain emissions within their source region for a longer period allowing for greater local formation of secondary pollutants, which is enhanced further under clear skies with warm temperatures and through aqueous processes due to fog, cloud and/or enhanced by higher absolute humidity.

The long-range or regional transport of air pollutants, which is dictated by synoptic scale patterns and is discussed in Section 7.6 below, is mainly an issue of importance from central Ontario to the east coast. This is due to the prevailing wind directions and the increasing

density of emissions east of the Mississippi River, including southern Ontario. In general, during air pollution episodes the relative importance of long-range transport increases towards the east, although, with the right meteorology local emissions can contribute significantly regardless of location. West of central Ontario, long-range transport plays a smaller role in the occurrence of elevated air pollution levels. Forest fire plumes are one of the main exceptions and on occasion detectable increases in concentrations occur due to trans-Pacific transport (see Chapter 9).

The Prairies and the north are vast with few terrain features to trap pollution, and the large emission regions are relatively distinct and isolated. Given the wide separation between major source regions, the relatively flat terrain and the frequency of strong winds, the pollutants from source areas, such as cities or industrial areas, move in relatively defined paths (i.e., narrow or wide plumes) as they disperse and mix with the background air mass. This is in contrast to the close proximity of emissions source regions in east central Canada and the U.S. Measurements and modelling studies (see Sections 7.5.5 and 7.7.13) support this view of discrete plumes, though they also illustrate that multiple plumes can affect a given location on the same day. In addition, emissions from the oil and gas industry occur over such a wide spatial area that in Alberta their influence is likely to be more general rather than confined to specific plumes. The situation is different again in the mountainous and coastal areas of British Columbia and Yukon Territory. The Pacific Ocean is upwind so long-range transport into the region of air masses containing high pollutant concentrations is rarely an issue. Poor air quality results when local emissions are not dispersed quickly, often accentuated by terrain (e.g., valleys) and/or are re-circulated, which also enhances the amount of secondary pollutants.

7.4.1 Southern Great Lakes to the Atlantic Coast: Common Synoptic Patterns

Certain weather patterns, which occur periodically and differ in frequency among seasons, are known to lead to the conditions that bring higher pollutant levels into eastern Canada and/or favour the build up of local emissions. Consequently, elevated concentrations of O₃ and PM_{2.5} are episodic in nature. The prime synoptic weather pattern for episodic summer smog events over the eastern part of Canada includes:

1. A high pressure system moving over the emission areas of southern Canada, the Ohio Valley and the eastern U.S. seaboard, or westward extension of the 'Bermuda' high pressure centre,
2. Stagnation and/or the presence of a subsidence inversion in the low to mid levels of the troposphere,
3. Warm temperatures to promote chemical reactions and biogenic emissions,
4. Two or more days of light winds (<4 m s⁻¹) and mainly sunny skies over the emission areas, allowing the build-up of pollutants, followed by:

5. An approaching cold frontal trough and/or low pressure area over areas immediately to the west or northwest (e.g., for Atlantic Canada this implies such a feature over Québec) with a southwesterly flow bringing pollution to the region.

Meteorological processes that influence the concentration of pollutants when they arrive over eastern Canada include the amount and location of vertical mixing over emission areas and along the wind transport path, the amount of sunshine and duration of stagnation upwind and the nature of upwind precipitation events. Extended periods of steady precipitation upwind, which are accompanied by cloudy conditions, reduce levels of O₃ and PM_{2.5} in the atmosphere. In addition, for Atlantic Canada, the three dimensional origin of the air parcels and their trajectories, the thickness and characteristic scales of horizontal plume layers and the horizontal transport speed and horizontal scale of the pollutant plume have been found to be important aspects of the meteorological pattern (Angevine *et al.*, 1996a). A detailed analysis of the meteorological factors of a multi-day pollution transport event over the western north Atlantic in the summer of 1993, which includes the Atlantic Canada, was discussed by Moody *et al.* (1996).



Figure 7.21 Example of a synoptic weather pattern typically associated with regional air pollution events affecting eastern Canada from southern Ontario to the southern Atlantic region. Common features are the high pressure system (H) to the south and lower pressures (L) toward the northwest and north. This pattern places eastern Canada in the warm sector of the low pressure system with southerly to southwesterly wind flow. On days prior to this pattern the 'Bermuda' high and ridge often lay over the eastern U.S. and southern Canada promoting stagnation, light winds and sunny weather over the emission areas. With the low pressure system moving into northern Ontario and then into Québec the wind flow transports pollutants northeastward in the warm sector or 'back of the high'. Depending upon the track of the low and the high this can lead to build up and transport into Ontario, Québec and Atlantic Canada. The black lines are isobars. The heavy red and blue lines indicate warm and cold fronts, respectively.

As described above, for southern Ontario and Québec (i.e., Windsor to Québec City corridor), episodes of elevated O₃ and PM_{2.5} are mainly associated with high pressure weather systems. While these may be related to the Bermuda High, it is often high pressure centers that move slowly out of central Canada into the U.S. Midwest or the Great Lakes area and then eastward to the Atlantic coast that lead to the highest levels of smog. The “back of the high” portion of such a slow moving high pressure area or the approaching warm sector of a low pressure system, which is shown schematically in Figure 7.21, generally has winds with a southerly component that have travelled over major precursor emission areas located in the Midwest and eastern U.S. As the high pressure system moves from west to east, precursors are emitted into the front (east side) of the high pressure system and circulate to the rear (west side) of the system over a period of 2 to 6 days depending on the wind speed. This results in the accumulation of pollutants (both primary and secondary) in the air mass. As a result, when the high pressure system moves east, the south to southwesterly flow transports this pollution into Ontario, Québec and at times, Atlantic Canada.

The relationship between the occurrence and position of high pressure areas and pollutant concentrations is more complex than the idealized case described above. Thus, under these situations the concentrations observed from Windsor into southern Québec, Nova Scotia and New Brunswick can vary considerably due to subtle variations in the larger scale synoptic and local weather patterns. For example, not all “back of the high” situations lead to high ozone concentrations. It is likely that high wind speeds limit the travel time between the source and receptor areas and therefore the atmospheric reaction time to the point that significant concentrations of ozone and secondary PM_{2.5} do not form (Reid *et al.*, 1996). Local and upwind precipitation, which can remove pollutants from the air mass, also likely plays a role. However, the analyses conducted to date show that precipitation occurs occasionally during both periods of high and low pollutant concentrations indicating that the situation is more complex. Maximum daily temperatures are also important to consider. In Québec when concentrations were lower the temperature was on average 4°C less than on days with high PM_{2.5} levels (Johnson, 2004)

Overall, the synoptic weather patterns leading to higher concentrations that were described above are associated with westerly to southerly wind flow. The longer this direction persists the farther north the emissions and their products (i.e., secondary pollutants) that accumulated over the high emission areas will penetrate. Given the prevailing westerlies of the mid-latitudes, these weather systems tend to move from west to east so that conditions conducive to air pollution episodes move from Ontario to Québec and into the Atlantic provinces. Consequently, episodes are more frequent over southern Ontario, somewhat less over southwestern Québec and even less so in New Brunswick and Nova Scotia. Some examples of the relationship between pollutant concentrations and long-range transport direction derived from back-trajectory analyses were shown in Chapter 3 in Figures 3.4, 3.5 and 3.45. In Section 7.6 below additional trajectory-based analyses for all regions in Canada will be presented.

The actual upwind area that contributes to regional air quality can differ across the regions as shown by Brook *et al.* (1997) who tracked a large episode as it evolved and moved from Ontario into Atlantic Canada. In Ontario, emissions from as far west as St. Louis and as far south as Texas most often play a role, while in the St. Lawrence River Valley, the Eastern Townships of Québec and Atlantic Canada the more important upwind areas are southern Ontario and the eastern Ohio River Valley. Additionally, the U.S. eastern seaboard (Boston to Washington corridor) is an important upwind area in Atlantic Canada, but rarely impacts Ontario and Québec.

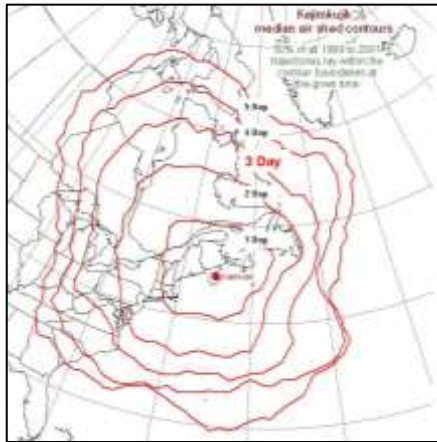


Figure 7.22 Median airshed contours for Kejimikujik, Nova Scotia based on 925 hPa back-trajectories for the period 1999-2001 (Ketch *et al.*, 2005). The 3-day median airshed encompasses the eastern half of Ontario, all of Québec, Atlantic Canada and the northeastern U.S. including the states of Ohio, West Virginia and Virginia where significant precursor emissions occur.

The region of influence to the air quality in a given geographic area can be defined as the median distance upwind indicated by a 3-day, 925 hPa back-trajectory. As an example, the region of influence for southern Nova Scotia and New Brunswick (i.e., Kejimikujik, NS and St. Andrews, NB monitoring sites) is shown in Figure 7.22. For this area, the region encompasses the eastern half of Ontario, all of Québec, Atlantic Canada and the northeastern U.S. including the states of Ohio, West Virginia and Virginia as well as a significant portion of the continental shelf east of these land masses (Waugh *et al.*, 2003). The relationship between transport direction, as defined by back-trajectories, and O_3 , $PM_{2.5}$ and NO_2 concentrations is discussed in the section below on long-range transport.



Figure 7.23 Typical pressure pattern leading to high winter PM_{2.5} levels (1000 hPa pressure surface in decameters above sea-level) shows a high pressure centre lying to the southwest of the Lower Great Lakes with a ridge extending across Ontario and Québec. This pattern can push air from high emissions areas into southern Ontario, the St. Lawrence River Valley and potentially Atlantic Canada.

The typical synoptic patterns leading to smog events in the winter have not been studied as extensively as those in the summer. Invariably, high pressure systems play a role, although from the cases studied it appears that their location, movement and shape differs from the summer. The typical configuration is depicted in Figure 7.23, which shows a high pressure centre lying to the southwest of the Lower Great Lakes with a ridge extending across Ontario and Québec. This pattern can push air from high emissions areas into southern Ontario, the St. Lawrence River Valley and potentially Atlantic Canada, but another important feature of these events is stagnation and very low vertical mixing heights under the ridge, enhancing the accumulation of local emissions and formation of fine particle nitrate. In Section 7.7.1 a case study describing an extreme PM_{2.5} event in Ontario and Québec in February 2005 is discussed in detail, including the meteorological conditions leading to the high concentrations that were observed.

7.4.1.1 Local Meteorological Features in the Atlantic Region

The terrain across Atlantic Canada, along with its complex coastal features and land-ocean temperature contrasts lead to many local factors that influence pollutants transported into the region and those emitted locally. Furthermore, its mid-latitude coastal location at the northeast part of the continent leads to very active weather. Consequently, the region has among the highest average wind speeds in Canada (Environment Canada, 2005). Newfoundland and Labrador are the windiest areas, a factor favouring the dispersion of locally emitted pollution, thereby reducing concentrations near the ground and/or transporting the pollutants out of the region.

The cooling waters of the Atlantic Ocean, Bay of Fundy and the Gulf of St. Lawrence lead to frequent marine inversions. In particular, they readily develop in spring and summer when warm south or southwesterly winds blow across the region. These inversions have several effects, including decoupling the surface from over-riding pollutant plumes, or in the case of sea breezes where these inversions are carried onshore, restricting dispersion of locally produced pollution, which can occur around Saint John, NB. Land breezes may push pollutants from coastal cities out over the water only to be re-circulated back to the land by the sea breeze in their original form and as secondary pollutants the next day (Lyons, Tremblack, Pielke, 1995) making it difficult to trace these pollutants back to their origin.

Temperature profiles in the lowest 2 km over the Gulf of Maine, when the flow is offshore, are similar, regardless of transport time over water or time of day (Angevine *et al.*, 2006). A surface-based stable layer forms within 10 km of the coastline during the daytime and persists over the cool water, suppressing the transfer of momentum, sensible and latent heat (Fairall *et al.*, 2006). This shallow stable boundary layer, averaging 50 m in depth, is ubiquitous over the Gulf of Maine waters and acts to decouple the layer aloft from the surface. This reduces dispersion in the layer aloft allowing it to travel forward as an intact plume. Locations in southwestern Nova Scotia and southeastern New Brunswick adjacent to the waters of the Gulf of Maine and the Bay of Fundy are most significantly impacted by this feature especially in southerly to southwesterly flow regimes.

Several field investigations have studied the layering of pollutants that is pervasive over the Atlantic region. Kleinman *et al.* (1996) found plumes with high concentrations of O₃ in both the near-surface marine inversion layer or in layers at higher altitudes during flights over the Gulf of Maine and southern Bay of Fundy. Observations at Sable Island revealed vertical stratification of the air from both aircraft and radiosonde data (Wang *et al.*, 1996). The vertical temperature stratification is a significant controlling factor in the chemical composition of the air reaching either Chebogue Point or Sable Island (Merrill and Moody, 1996). The presence of low-level nocturnal jets, which may also advect pollutant plumes at a faster rate, as was detected over southwestern Nova Scotia by Angevine *et al.* (1996b). Tethersonde flights were conducted on the southwestern tip of Nova Scotia (Chebogue Point) during the NARSTO field experiment in 1995. The pollutant layering and impact of the marine inversion layer were evident during a 5-day period in July where transported ozone was restricted to the 300 m deep marine boundary layer, with highest concentrations of ozone (>110 ppb) at an altitude of 200 m, and mean surface concentrations reaching 50 ppb (Gong *et al.*, 2000; Waugh, 2003).

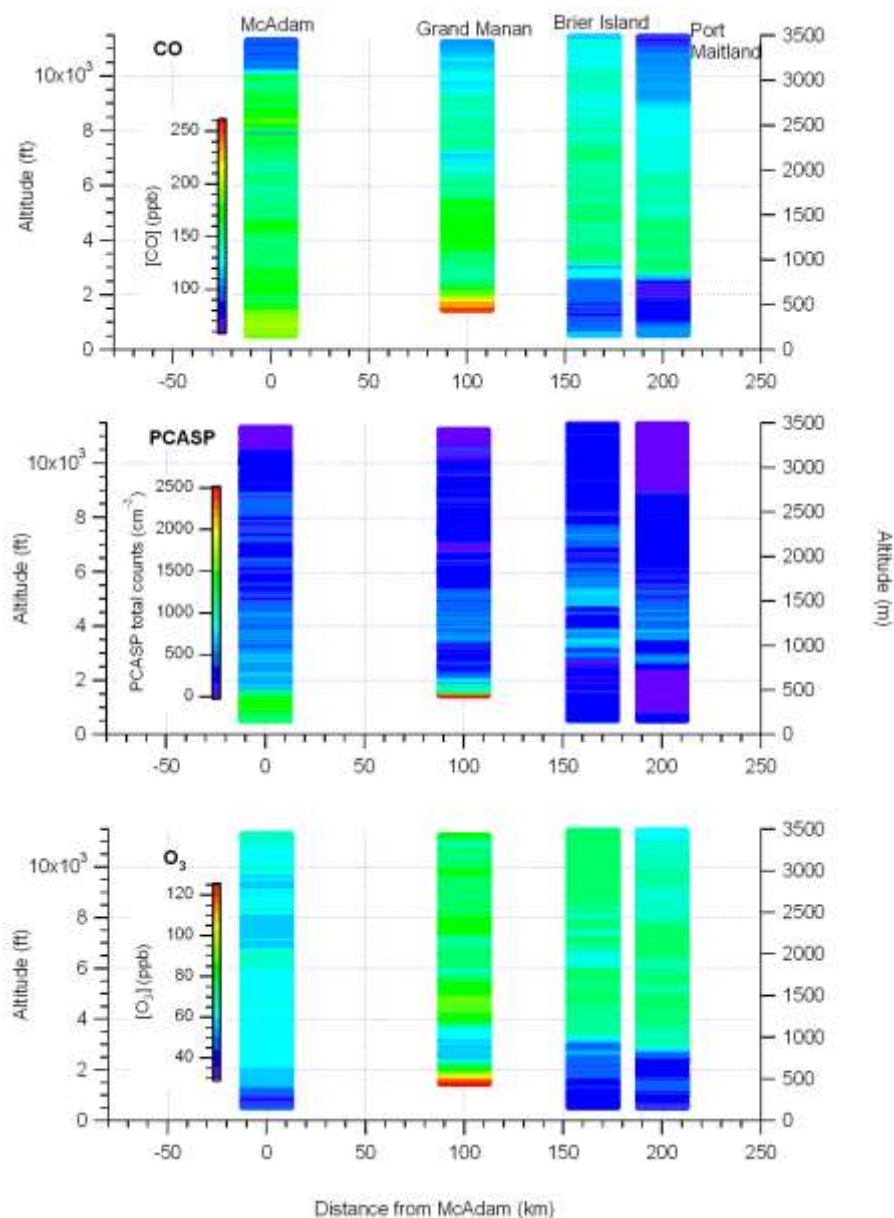


Figure 7.24 Vertical profiles of concentrations of a) CO, b) total number concentration (PCASP), and c) O₃, showing layering of pollutants during ICARTT – TIMs Flight 3, 16:18 – 18:12 UTC, July 22, 2004 (Waugh *et al.*, 2007). Colours indicate concentrations (red = high, blue = low), and the x-axis represents the location of the aircraft profiles (McAdam, NB, Grand Manan, NB, Brier Island, NS, and Port Maitland, NS) in relation to McAdam. Each plot can be considered as an interrupted view of a vertical cross section along the transect from McAdam to Port Maitland, across the Bay of Fundy. CO, particles, and O₃ all tend to be highest at an elevation of 500 m above Grand Manan Island, but in general the CO and O₃ plumes appear to ride over top of the marine boundary layer over Brier Island and Port Maitland.

As part of the ICARTT study in 2004 (Waugh *et al.*, 2007), several flight passes over the Bay of Fundy were initiated under the Transport Into the Maritimes Study (TIMS). Vertical pollutant structuring was observed in the resulting data as shown in Figure 7.24, with elevated

CO, particle number concentration, and ozone most evident in the lowest portions of the profiles over Grand Manan Island, near the mouth of the Bay of Fundy and above the surface boundary layer. A sharp increase in ozone concentrations was also noted in the ozonesonde data from Yarmouth detected on the day prior to the TIMS flights indicating that a plume of high ozone concentrations was present on two consecutive days, corroborating the flight results.

Another unique aspect of the meteorology in Atlantic Canada are fog banks, which develop over the cool waters to the south of the region, interacting with air masses moving in from the south and southwest. Under these situations, heterogeneous chemistry can lead to chemical conversion of primary pollutants forming compounds that will enhance fine particle levels or alter their chemical and physical characteristics. For example, Brook *et al.* (1997) found that fine particle acidity ('acid aerosols') is often very high in the Saint John area compared to other areas studied in Canada when advection fog increased the conversion of locally emitted SO₂ into sulphuric acid particles. Research by Beauchamp and Tordon (1993) at two coastal sites Cape Forchu, NS near Yarmouth, and Cape Race, NL highlighted the importance of fog water in the transport and deposition of atmospheric pollutants. Thus, fog can enhance ambient concentrations of certain pollutants and lead to areas of higher deposition, but it can also reduce ambient concentrations by reducing sunshine and thus photochemical processes.

The prevailing track of synoptic low pressure systems lies over the region during much of the year (Climate Prediction Centre, 2007) resulting in high wind speeds over adjacent waters and contributing to an increase in natural aerosols (i.e. O'Dowd and Smith, 1993). In addition to anthropogenic pollutants from local and regional emission sources, these conditions can lead to a significant contribution to PM mass by sea salt aerosol for communities near the coastlines (Farrell, 2006a; Phinney, 2007). The proximity to the storm track also leads to more frequent cloud cover and precipitation events resulting in removal of some smog precursors and particulate matter from the atmosphere.

7.4.1.2 Local Meteorological Features in Southern Québec and Eastern Ontario

Most of the emissions in the region are concentrated along the St. Lawrence and Ottawa River Valley. This feature and its interaction with the synoptic weather patterns play a dominant role in the fate and build up of local pollutants. Other smaller valleys in Québec, the Richelieu, the St-Maurice or the Saguenay fjord, also have a significant influence on local air quality by trapping pollutants or channelling winds along the valley. Light winds under stable high pressure systems provide a longer residence time and weak mixing, allowing the accumulation and transformation of primary pollutants to produce smog near source areas and in river valleys or valleys of the Laurentian Mountains.

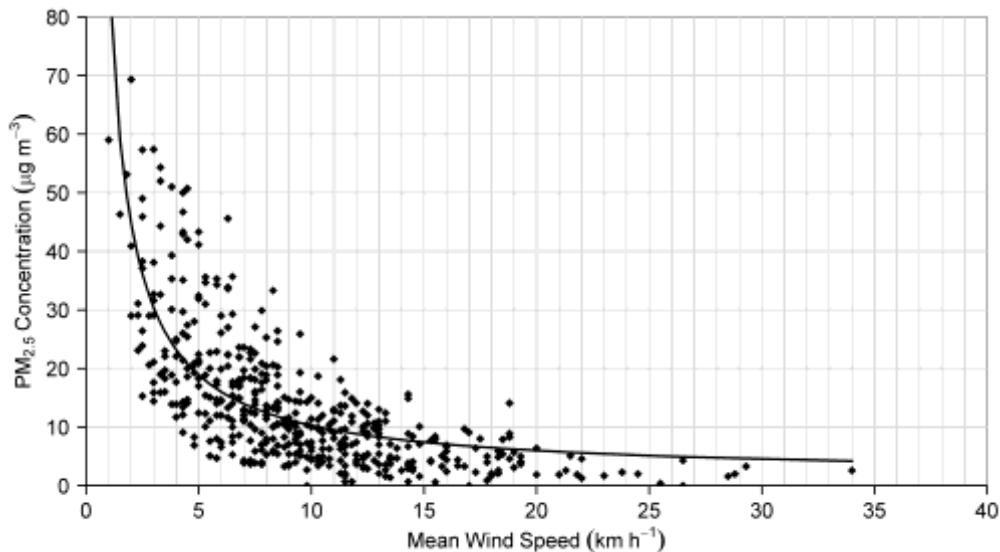


Figure 7.25 Typical relationship between evening wind speed and PM_{2.5} levels in East Montréal (Rivière-des-Prairies) in winter where local primary PM_{2.5} sources prevail (adapted from Carter *et al.*, 2004).

Although valley trapping can influence local pollutant levels any time of the year and can be important all across Canada, its greatest role in Québec is during the winter. This is partly due to reduced relative importance of long-range transport, stronger more persistent inversions and in some areas, greater use of residential woodstoves. Thus, in winter, high concentrations are mostly the result of the accumulation of locally emitted pollutants accentuated by valleys. In general, the meteorological conditions leading to local accumulation of PM_{2.5} and high concentrations in winter are a weak pressure gradient, such as under a high pressure system, light surface winds (see Figure 7.25) and large scale atmospheric subsidence.

7.4.1.3 Local Meteorological Features in the Southern Great Lakes Region

Compared to Québec and the Atlantic region, southern Ontario is closer to the high emission areas in the U.S. In addition, as documented above, the size of the population and thus vehicle usage, the amount of industrial and agricultural activity and the partial reliance on coal for electricity, leads to large local emissions in the region from the greater Toronto area and west (southwestern Ontario). Ozone and PM_{2.5} events often occur together and while O₃ at a given point is a result of both local and more distant upwind emissions and chemistry, PM_{2.5} levels are a result of a combination of both these upwind processes as well as primary emissions in the immediate vicinity of the measurement location.

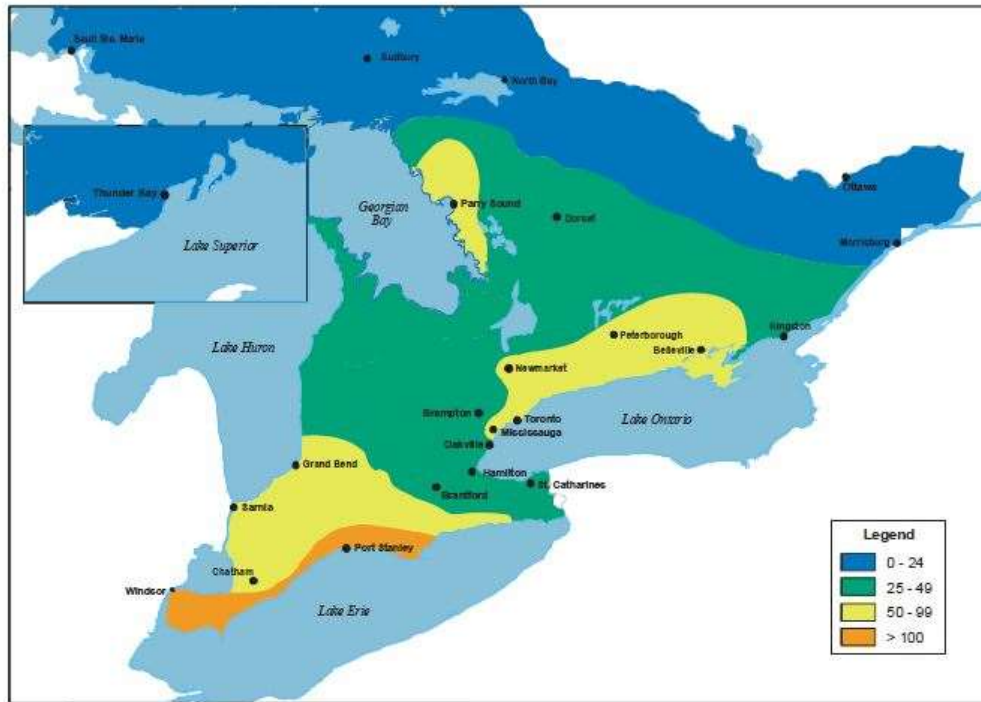


Figure 7.26 Geographical distribution of number of 1-hour O₃ exceedences across Ontario in 2005 (MOE, 2006).

The most important physical feature that influences air quality in Ontario is the Great Lakes. The preferential transport of ozone and other pollutants over large water bodies, as opposed to the land surface, has been understood for some time (e.g., Lyons and Cole, 1973, 1976; Sillman *et al.*, 1993; Lu and Turco, 1994). The phenomenon is a consequence of decoupling of the water surface from the mixed layer by the formation of a very shallow inversion above the cool water, as discussed above in relation to the influence of the Atlantic Ocean. The relative scarcity of emission sources over water as compared with on land also means that scavenging of pollutants such as O₃ by NO_x is generally negligible except along shipping routes. The result is an enhancement of pollutant concentrations, especially of O₃ with the potential for subsequent delivery to sensitive receptors on-shore by mechanisms including the lake breeze (Reid *et al.*, 1996). Figure 7.26 provides a clear picture of where, over and near the lakes, O₃ concentrations are most enhanced. It is believed that the concentration and composition of PM_{2.5} over southern Ontario are also influenced by the lakes, but less information is currently available.

A more detailed investigation of how lake breezes influence air quality was reported by Hastie *et al.* (1999), who documented several instances of sudden rises of ozone concentration at locations near the shore of Lake Ontario. A particularly well documented case occurred during the Southern Ontario Oxidant Study (SONTOS; Reid *et al.*, 1996), in August of 1993. Ozone concentrations at Hastings, Ontario (150 km northeast of Toronto, and 36 km from the shore of

Lake Ontario) increased from 42 to 80 ppb in approximately 20 minutes. At the same time, the temperature dropped from 33 to 31 °C, as the dew point temperature increased from 21 to 23 °C, signaling the arrival of cooler moister air from over the lake. The wind speed increased from 2 to 4 m s⁻¹ and the direction changed from westerly to southwesterly. A number of other pollutant species were measured at Hastings, and concurrent increases were seen in SO₂, PAN and NO_y. Hydrocarbon concentrations were also observed to increase with the arrival of the lake breeze (with the exception of isoprene which is ubiquitous at this rural location). Concentration profiles over Hastings, from an instrumented aircraft, showed little variation with altitude, confirming that the sudden increase in ozone concentration did not result from downward mixing from a polluted layer aloft. It is important to note that the extent of processing of the air parcel, as measured by a number of indicator species and the NO_x/NO_y ratio strongly suggested that the air parcel in question had received precursor emissions from land-based sources within the previous 24 hours, and had been transported out over the lake possibly by the night time land breeze. This suggests that more local emissions, such as in the Greater Toronto area, may have played an important role. Such emissions would have stayed over the lake in a low wind speed regime, undergoing photochemical processing, until being delivered to Hastings (and other locations on land) the following day.

7.4.2 Meteorological Factors Impacting Air Quality Alberta and the Prairies

Smog in the prairies is defined largely by two different types of events: winter events with high PM and NO_x concentrations resulting in reduced visibility, and summer events which are typically related to the formation of secondary pollutants and periodically influenced by forest fire emissions. In general, elevated PM concentrations occur with a wider range of synoptic conditions than elevated O₃ suggesting that local emissions and poor dispersion play an important role for PM.

East of the Rocky Mountains, the Prairies have few terrain features such as large valleys or continuous ranges of hills that act to trap pollution in certain areas, and thus, the primary meteorological factors are influenced by synoptic scale motions. Similar to most other areas in Canada, the local meteorological conditions at urban and near urban sites in the Prairies during elevated O₃ concentrations include warm temperatures and light to moderate wind speeds. In contrast, at rural sites in the Prairies, high O₃ episodes occur under a wider range of meteorological conditions (Johnson, 2004; Chaikowsky, 2001).

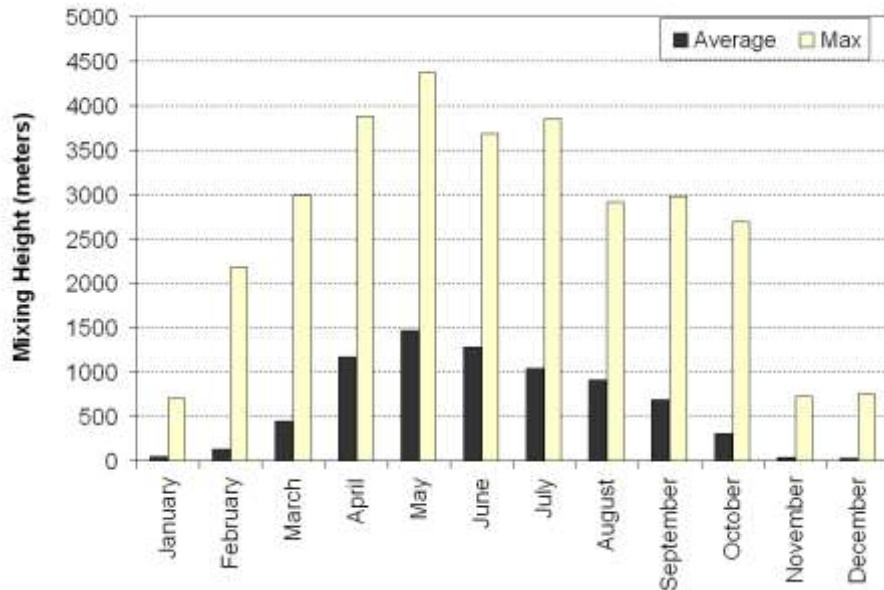


Figure 7.27 Mean and maximum mixing heights by month derived from measurements at Stony Plain, Alberta.

The Prairies experience considerable seasonal variation in mixing heights. The boundary-layer heights are high in the summer due to abundant insolation and long daylight hours promoting strong convection. Conversely, there are periods of very limited vertical mixing in the winter. Mixing heights derived from radiosonde launches at Stony Plain are shown in Figure 7.27. Average and maximum mixing heights peak in May and are at a minimum in November-January. Since May has both the highest wind speeds and the highest mixing heights it is on average the least favourable month for the build up of local pollution. On the other hand, free tropospheric air with high ozone concentrations and low levels of primary pollutants is most likely to be mixed to the surface during the spring months of April through June. Conversely the winter months have a high frequency of temperature inversions that can act to trap primary pollutants causing high concentrations, especially close to the emission sources. The consequence of this is evident in Figure 3.30, which shows that Edmonton and Calgary experience some of the highest NO and NO₂ concentrations in the country, particularly in the winter (Figure 3.31).

The meteorological conditions associated with high O₃ levels in summertime include temperatures above seasonal norms, moderate to light winds, and re-circulating surface trajectories (Chaikowsky, 2001). A study of summer time high O₃ events in Alberta in 2002 found that nearly all of them were associated with back trajectories that spent 24 or more hours over populated areas of Alberta. This is consistent with the trajectory analyses presented below in Section 7.6, which found elevated summertime O₃ in Alberta associated with the “stagnant flow” trajectory and with Johnson (2004) who found higher O₃ associated with slower moving trajectories.

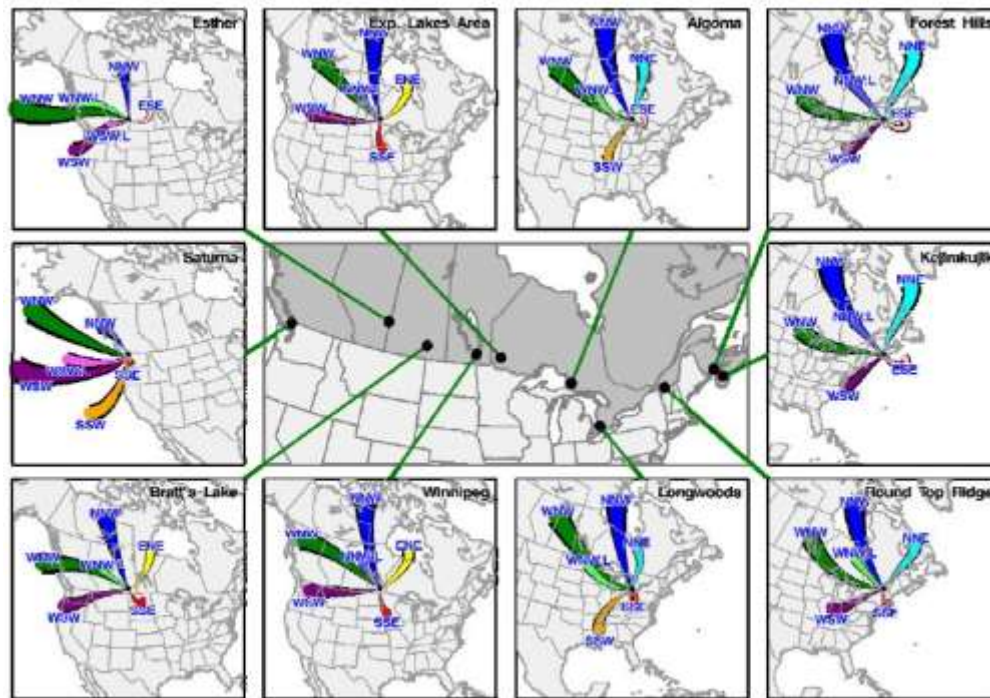


Figure 7.28 Trajectory cluster mean vectors at 10 O₃ sites. Six trajectory clusters were sorted by the k-means clustering technique similar to Dorling *et al.* (1992a,b) using Euclidean distance as the dissimilarity measure on CMC 3-day air parcel backward trajectories from 1994 through 2005 for all sites. This method primarily used here is to define synoptic flow patterns associated with these sites. The endpoint for the vectors shown represents the mean upwind distance three days back in time. Shorter vectors thus indicate slow travel speed and possible stagnation along the path while longer vectors are related to strong wind speeds. See Section 7.6.1 for more discussion on this figure.

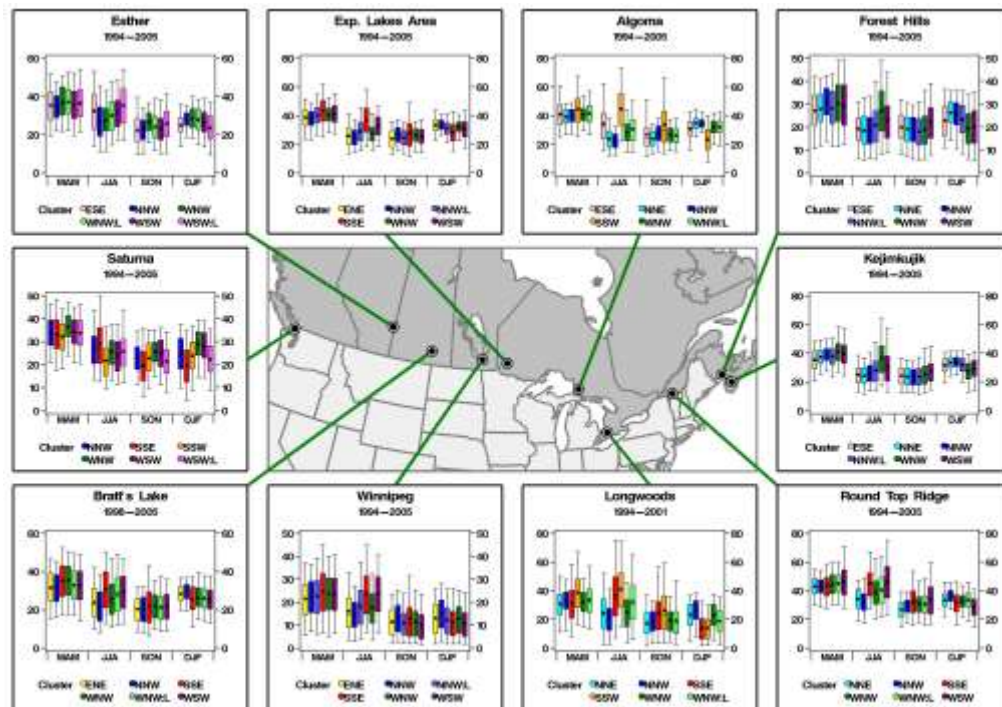


Figure 7.29 Seasonal box-and-whisker O_3 plots by trajectory clusters at 10 O_3 sites. The time period of the O_3 data record at any given site used in the analysis is shown below the site name in each panel. Seasonal breakdowns are as follows: March – April – May (MAM), June – July – August (JJA), September – October – November (SON) and December – January – February (DJF). Note that different vertical scales, which are in ppb, are used across sites to highlight location-specific differences in O_3 by transport direction. See Section 7.6.1 for more discussion on this figure.

Johnson (2004) investigated the synoptic weather patterns associated with high levels of PM and O_3 over the Prairies and found that elevated PM is not consistently correlated with ozone levels or with the synoptic patterns that are associated with higher ozone. This differs from eastern Canada where elevated summertime O_3 and $PM_{2.5}$ have a tendency to occur under similar situations. Over most of the Prairies the highest ozone levels occur with synoptic patterns that are most common in spring and summer. The highest summertime ozone levels in Alberta seem to occur mainly in light to moderate westerly flows with the passage of a weak trough or low across the Prairies. Synoptic flows are extremely light at the onset of this pattern, and then strengthen. These strengthening winds may account for the fact that most summertime ozone episodes in Alberta are relatively short-lived. Further east in the Prairies southerly flows tend to lead to the highest O_3 concentrations throughout the year (Figure 7.28 and 7.29). The synoptic patterns associated with northerly flow generally bring lower than average ozone in the summer months (Figure 7.28 and 7.29).

In spring and autumn, ozone tends to be elevated when an area of high pressure develops over the southern Northwest Territories yielding a north-easterly, easterly or south-easterly flow across the prairies (Johnston, 2004). In contrast to the rest of the region, ozone at Hightower

Ridge, a ridge-top site in the Rocky Mountain Foothills, is highest for synoptic patterns occurring in winter and spring suggesting that at this site ozone levels depend more on hemispheric background conditions and less on local weather patterns. This is further supported by the fact that ozone levels at Hightower Ridge are not well correlated with ozone levels at other Alberta sites.

Generally, strong synoptic scale flows, which result in strong or steady winds tend to be associated with lower ozone and PM levels, with the exception of some winter patterns where strong temperature inversions isolate the surface layers and permit PM to accumulate from local sources. Patterns that lead to widespread precipitation also have low PM and ozone levels. While in the Prairies elevated PM or ozone occurred more frequently under certain synoptic patterns, there are also many periods when such patterns do not lead to elevated pollution events. Thus, synoptic patterns are only one part of a complex puzzle controlling ambient air quality conditions.

Local weather features that induce high pollutant levels are important within and near (i.e., foothills) the Rocky Mountains. As discussed for British Columbia and Québec, mountain valleys and related inversions trap pollutants leading to higher concentrations predominantly in the winter. Another important local influence of the Rockies is their immense size (height and north-south extent), which leads to enhancements in downward mixing of free tropospheric air over the Alberta foothills. This air may be enriched in stratospheric O₃ affecting ground-based trace gas concentrations, particularly at high elevation locations. Another phenomenon in this region is the Chinook. However, the impact of the Chinooks on air quality is unclear. It has been suggested that the apparent correlation between Chinooks and poor air quality may be related to Chinook induced low mixing heights rather than dust re-suspension (Nkemdirim, 1988).

7.4.3 Meteorological Factors Impacting Air Quality in the Lower Fraser Valley

Air quality in the LFV is negatively influenced by periods of stagnation which often occur during the summer and winter seasons. During the summer, the LFV is frequently dominated by areas of high pressure over the eastern Pacific. During these periods, temperature inversions near the surface, cause the air to stagnate, often for several days. Episodes of elevated ozone and PM_{2.5} concentrations can occur under these conditions, and visibility is often degraded.

The topography of the LFV modulates the diurnal pollutant transport pattern driven by the sea breeze - land breeze cycle. Light flows associated with sea breeze conditions effectively funnel and concentrate primary and secondary pollutants originating from more populated urban source areas in the west towards the narrowing eastern extent of the valley and communities such as Chilliwack and Hope. Exceedances of the National Air Quality Ozone Objective of 82

ppb at the coastal Vancouver International Airport have been associated with sea-breeze conditions with coastal winds from the northwest and from the southwest (Ainslie and Steyn, 2007).

During sea-breeze conditions pollutants are advected inland during the day and this process can be enhanced by upslope flows along the mountains lining the north end of the valley from west to the east and north. Consequently by evening, pollutant plumes can move up mountain slopes and into elevated tributary valleys where they accumulate. This flow pattern also results in layers of concentrated pollutants aloft, especially towards valley apexes (Strawbridge and Snyder, 2004). During the night, drainage and land breeze flows and the formation of a shallow nocturnal boundary layer lead to a concentration of aerosols and primary pollutants near the surface and in elevated layers above the boundary layer. In many monitoring locations ozone drops to very low concentrations. During the late night and early morning, the land-breeze transports aerosols from the eastern part of the LFV and tributary valleys westward towards the Strait of Georgia, resulting in an increase in aerosols and primary pollutants (e.g., NO_x) over the water. In the morning, the nocturnal boundary layer breaks up, and elevated layers still containing ozone, primary and secondary PM and some precursors species (e.g., NO_x) are mixed down to the surface (McKendry *et al.*, 1997; Pisano *et al.*, 1997).

Pollutant transport has also been shown to be influenced by a process known as the Wake-Induced Stagnation Effect (WISE; Brook *et al.*, 2004c). This occurs as a result of light winds from the Strait of Georgia and Strait of Juan de Fuca converging together, coupled with a “wake” effect induced by the geographical features of the Vancouver, Gulf, and San Juan Islands. During the Pacific 2001 Air Quality Study, WISE was associated with the advection and buildup of concentrated aerosol layers over the Gulf/San Juan islands (Strawbridge and Snyder, 2004). Within these aerosol layers, pollutants underwent photochemical processing and were then re-circulated via the sea/land-breeze cycle. The advection of aged aerosols and gases (ozone, oxidized nitrogen compounds) from the WISE zone was observed to impact the LFV and adjacent Whatcom County area of northwestern Washington State, a phenomenon repeated over several days and resulting in a build-up of concentrated and increasingly aged pollutants.

In the winter, cold arctic air masses move westward from the interior of the province, creating stagnant conditions over the LFV with strong temperature inversions in tributary valleys. This can exacerbate air quality problems causing episodes of elevated particulate matter. If stagnant conditions are coupled with the presence of a ridge of high pressure inland and a Pacific weather system approaching from the west, strong easterly outflow winds can develop, stirring up dust from the Fraser Canyon and raising PM_{10} levels in the LFV, occasionally sometimes as far west as the Strait of Georgia.

7.4.4 Meteorological Factors Impacting Air Quality in the Interior Valleys of British Columbia

Communities in the interior of British Columbia are subject to air pollutant sources and meteorology that are quite different compared to the conditions affecting the LFV. Many communities are located in valleys, some mountainous, and are thus subject to valley flows and frequent winter-time inversions. These situations occur when cold air sinks to the valley floor or base of the mountains and then becomes trapped by the warm air above. These stagnant conditions prevent upward mixing of the air, allowing wood smoke and other pollutants to increase near the surface. This is most prevalent during the nighttime but can also occur during the day, especially during the winter season when daylight hours are reduced. In some locations, such as at Nelson, in south-eastern BC, the thermal effect of lakes can cause cloud cover lasting for several days which acts to inhibit the break-up of the inversions (BCEnv, 2006c). In the Yukon, wood smoke episodes occur throughout the territory, largely as a result of a combination of weather acting on topography. This is particularly evident in Whitehorse's Riverdale subdivision located on a valley floor where temperature inversions trap wood smoke during cold weather (SOE, 2002).

When Topography and Intensive Industrial Activity Combine

In Prince George, BC, the unique combination of emissions and topography has a profound effect on local air quality. Several emission sources contribute to high levels of particulate matter in the city, including pulp mills, saw mills, rail activity, a large freeway and wood smoke from indoor stoves. Road dust emissions can be significant during dry periods, especially after spring melt. The topography of the city is varied, featuring a large bowl intercepted by a north-south river valley surrounded by elevated terrain. This bowl-like topography severely restricts the dispersion of pollutants during temperature inversions which are frequent in the winter and fall. Buildup of particulate matter occurs within hours of the formation of capping inversions, indicating that the valley floor is the primary source of these emissions. Due to the combination of topography and industrial sources, Prince George exceeded the Canada Wide Standard for PM_{2.5} for the reporting period 2002 to 2005 (Government of Canada, 2007).

7.5 Regional Characteristics of Air Quality

The analyses in Chapter 3 provided an overall picture of where and when concentrations are higher, what the background levels are in different geographic regions and the trends in concentrations for up to 20 years. Variations in concentrations were also linked to large scale wind flow patterns showing, over different areas in the country, the pattern (i.e., transport directions) associated with the highest and lowest concentrations of O₃ and PM_{2.5}. In addition, Chapter 3 linked some of the annual and multi-year trends in concentrations to known

emission changes, such as eastern North American SO₂ and NO_x emission trends from 1990 to 2006. With this overarching background of information, this section examines regionally-specific issues or features of the observations to provide more detail. The purpose is to illustrate how concentrations vary, both spatially and temporally, on a local scale, including urban-rural differences and characteristics of periods of elevated concentrations. The information presented is not intended to provide an exhaustive analysis of all the conditions within each region. Instead it is hoped that this, along with the subsequent sections on long-range transport and selected case studies, will demonstrate the extent that local emissions, terrain, including the urban landscape, and meteorology influence air quality. This is to provide some insight into similarities and differences among regions, the complexity of the issue and the level of detail required to develop a useful conceptual model of the situation in each region.

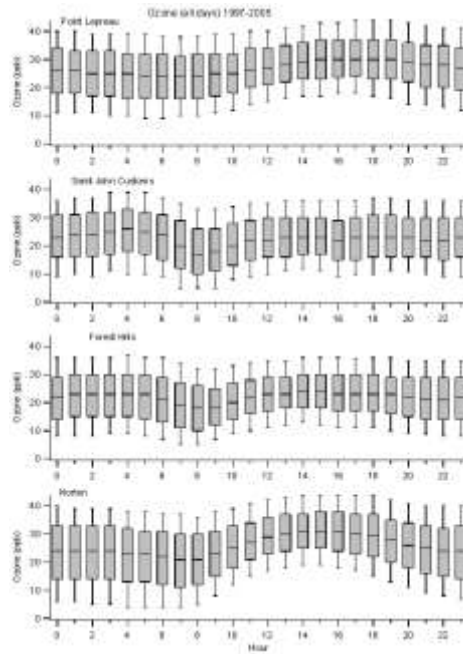
7.5.1 Atlantic Region

7.5.1.1 Spatial and Temporal Variability of O₃

As has been highlighted in Chapter 3, Atlantic Canada O₃ levels are considerably lower than southern Ontario and extreme southern Québec. Nonetheless, there is noticeable spatial variability in the concentrations (Figure 3.6), particularly in the southern part and some areas just surpass the CWS threshold (Figure 3.7). Mean O₃ is highest at Kejimikujik and Fundy National Parks and Aylesford Mountain (elevation 230 m), followed by Point Lepreau and Norton. All of these stations are generally around the Bay of Fundy, but at varying distances inland and at varying elevations. Other sites in this general area, such as Saint John and Moncton also have relatively high O₃ compared to other parts of Atlantic Canada. It is interesting to note that Kentville, which is close to Aylesford, but in the floor of the Annapolis Valley, has considerably lower levels. Spatial variability in O₃ in this region is discussed in more detail in Section 7.7.6 below. Ozone levels in most other parts of Atlantic Canada are also relatively low.

The overarching cause of the observed spatial pattern in O₃ is geographic location relative to the U.S. east coast population centers (e.g., Boston, New York City). However, differences between locations such as Campobello Island or St. Andrews and Yarmouth or Kejimikujik indicate that regional scale transport directions play a role with the U.S. east coast emissions tending to stay east and south of northeastern Maine as they move across the Atlantic forming O₃. Consistent with this pattern is the fact that Yarmouth had the highest O₃ peaks, followed closely by Kejimikujik and Aylesford Mountain, the latter of which has the greatest average and 75th percentile O₃ values. The O₃ behaviour at this location compared to Kentville suggests that elevation plays a role, with the high elevation Aylesford site tending to experience more of the O₃ transported from the east coast, assuming a greater amount resides above the marine layer. Vertical O₃ measurements discussed elsewhere in the chapter support this assumption. In

addition to elevation, the difference between these two sites is also the result of greater O₃ destruction in Kentville due to local NO emissions. These emissions, and more importantly those from the Saint John area, also contribute to some locally formed O₃. For example, the slightly higher concentrations at Fundy National Park, Norton and Pt. Lepreau may be due to Saint John area and its greater concentration of traffic, power plants and industry, including oil refining. Another key factor influencing the O₃ pattern in this region is the sea/land breeze circulation, which can redistribute O₃ and precursors horizontally and vertically and stabilize the lower boundary-layer near the coast.



a)

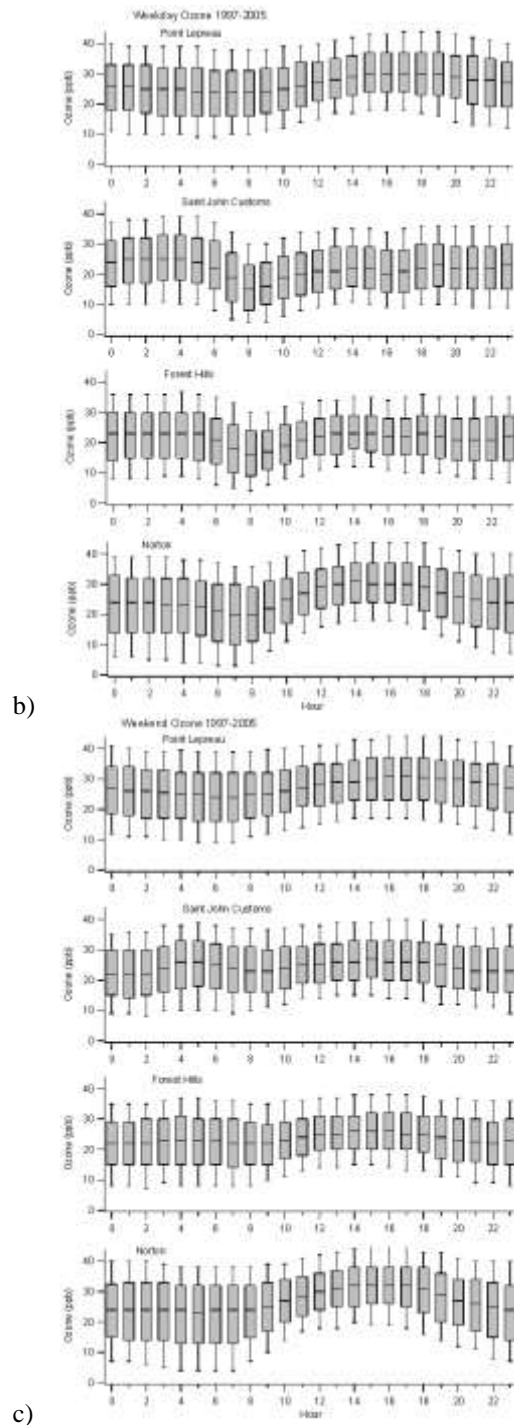


Figure 7.30 Mean Ozone diurnal cycles for a) All Days (Mon-Sun), b) Weekdays (Mon-Fri) and c) Weekends (Sat-Sun), for the years 1997-2005 at Point Lepreau, Saint John Customs, Forest Hills, and Norton, New Brunswick. Median values for each hour are shown as a short horizontal line, the shaded boxes indicate values that lie between the 25th and 75th percentile of all values, and the whiskers indicate the 10th and 90th percentiles. The rural site of Norton has the greatest daily range of ozone concentrations (10.4 ppb) while the urban site at Forest Hills and the coastal site (Point Lepreau) have the least daily variability (~6 ppb). The absolute levels are lower at the urban site due to

O₃ titration by NO. The rural sites of Norton and Point Lepreau ozone values exhibit a characteristic rural diurnal pattern, rising throughout the morning and early afternoon due to photochemistry, peaking at approximately 5pm, and decreasing through the dark evening and early morning hours to a minimum at about 7am. In contrast, Saint John Customs and Forest Hills indicate a strong O₃ titration by NO in the morning (8 am minimum due to urban traffic patterns), and a suppressed afternoon peak owing to continued titration which is enhanced by the shallow mixed-layer due to cool marine air.

To further highlight some of the local O₃ features of interest around Saint John, diurnal variations in O₃ at two rural sites (Point Lepreau and Norton) and two urban sites (the commercial site of Saint John Customs and the residential site of Forest Hills) in New Brunswick are compared in Figure 7.30a-c. Hourly mean values are compared amongst sites for all days, weekdays and weekends separately. The rural site of Norton has the greatest daily range of ozone concentrations (10.4 ppb) while the urban site at Forest Hills and the coastal site (Point Lepreau) have the least daily variability (~6 ppb). The absolute levels are lower at the urban site due to O₃ titration by NO.

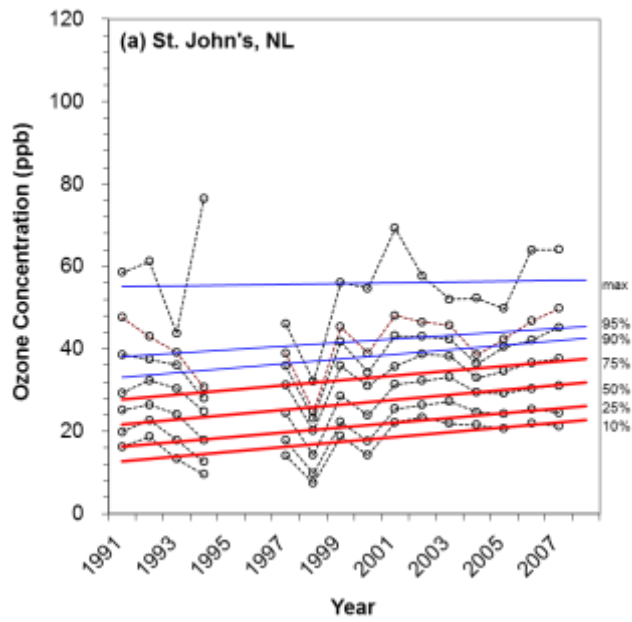
Ozone values at the rural sites of Norton and Point Lepreau exhibit a characteristic rural diurnal pattern, rising throughout the morning and early afternoon due to photochemistry, peaking at approximately 5pm, and decreasing through the dark evening and early morning hours to a minimum at about 7am. In contrast, Saint John Customs and Forest Hills indicate a strong O₃ titration by NO in the morning (8 am minimum due to urban traffic patterns), and a suppressed afternoon peak owing to continued titration which is enhanced by the shallow mixed-layer due to cool marine air. Halifax and St. John's (Fig. 3.12) exhibit a similar behaviour likely due to the same two factors. These patterns differ considerably from that of larger centers to the west, such as Toronto, Windsor and Vancouver (Figure 3.12), which experience the more classical afternoon peaks related to peak photochemical production, especially in the summer. While Saint John and these other Atlantic cities are less of a source area than the larger centers, leading to less local and regional O₃ production, it is likely that the most significant factor contributing to lower O₃ concentrations is the shallow mixing layer at these coastal cities, which enhances the destruction of O₃.

The overnight maximum in O₃ at Saint John Customs is unique to the region and is hypothesized to be due largely to its maritime setting. As described above, marine inversions and locally produced NO do not permit the build-up of O₃ concentrations at this downtown site during the photochemically active part of the daytime (as exhibited at Norton and Pt. Lepreau). This may result in the O₃ maximum at Saint John Customs occurring in the overnight period – pre-sunrise – due to overnight accumulation once NO_x emissions and concentrations decline. The effect may also be facilitated by the land breezes that often occur overnight that carry higher O₃ concentrations from inland areas outside the urban centre (e.g., Norton area) into the city. Reasons why Forest Hills does not show this pattern as strongly are not clear. It may be that higher O₃ draining from inland tends to follow the Kennebecasis Valley or the main river Valley, preferentially affecting downtown. These hypotheses for the overnight maximum in O₃

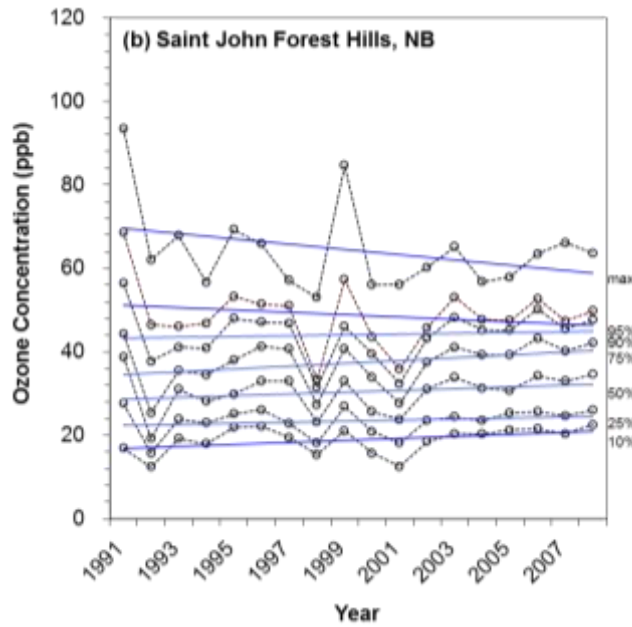
concentrations in downtown Saint John require verification through expanded monitoring and meso-scale analysis. In Section 7.7.7 the Saint John area sites are examined more closely to show evidence of formation of O₃ from the local precursor emissions.

As expected, local NO_x emissions on weekends are less than on weekdays. This results in a weaker minimum in the morning in Saint John and an overnight maximum that is not as pronounced as that of the weekday, and a daily maximum that occurs in mid-afternoon. In addition, the morning commuter effect is noticeably less at the Norton site on the weekend, while Point Lepreau, being well removed from traffic, shows little difference between the weekday and weekend.

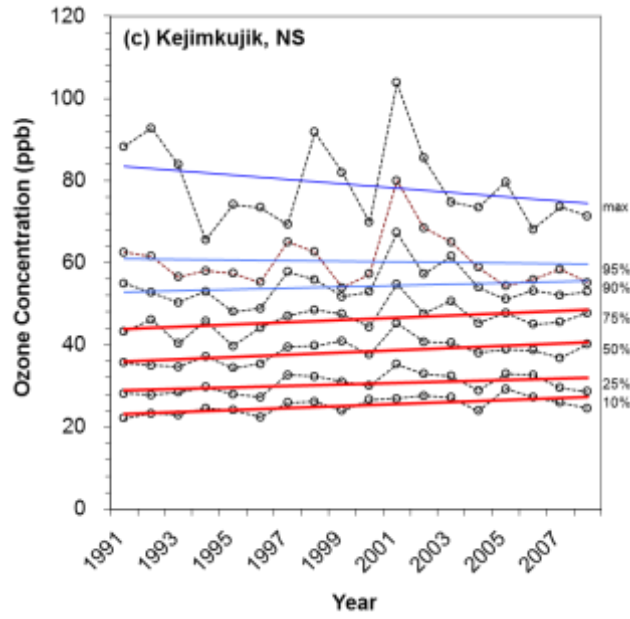
In Chapter 3 long term O₃ trends were examined using several different approaches. Comparison of daily warm season 8-hour maximum O₃ concentrations between 1997 – 2000 and 2003 – 2006 after adjustment for meteorological factors revealed that there have been statistically significant increases (Figure 3.21). This was for all five of the southern New Brunswick and southern Nova Scotia sites considered. Daily mean O₃ at the single rural site of Kejimkujik was determined to be rising significantly by 0.91 ppb/yr (Table 3.4). To provide additional insight Figures 7.31a-e show individual long term trends for five Atlantic Region sites. These plots are similar to those in Chapter 3 shown in Figures 3.24 and 3.25 in that they separate the trends for different parts of the O₃ distribution as was done by the Royal Society (2008) and Jenkin (2008).



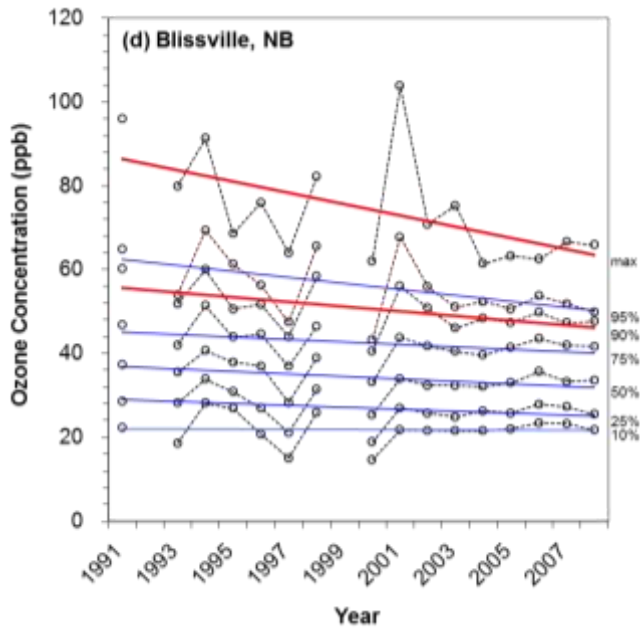
a)



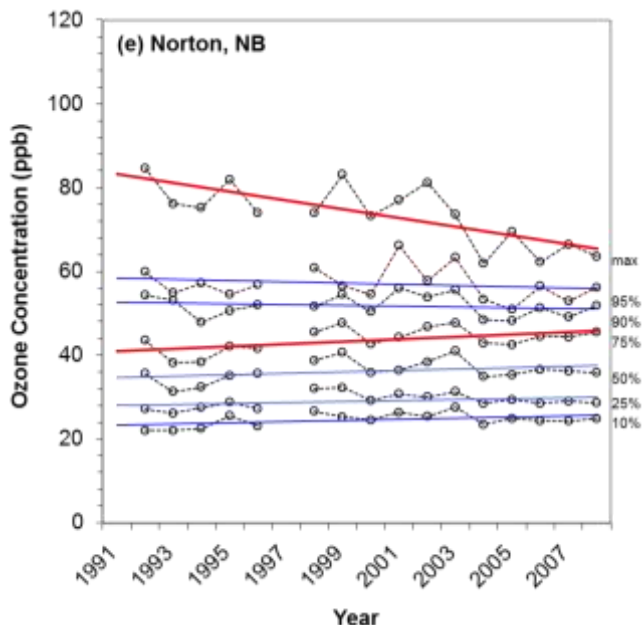
b)



c)



d)



e)

Figure 7.31 Trend plots of the 10, 25, 50, 75, 90, 95th and maximum percentiles for five Atlantic region sites: (a) St. John’s, NL, (b) Saint John Forest Hills, NB, (c) Kejimikujik, NS, (d) Blissville and (e) Norton, NB. The blue line indicates a non-statistically significant trend and the red line a statistically significant trend at the 95% confidence limit based upon the T-test.

Figures 7.31a-e tend to show that the variability in the April-September averages across much of the distribution in daily maximum 8-hour O_3 seems to have become smaller across the Atlantic region since 2001. This apparent damping in O_3 variability, which has persisted for several years, is difficult to explain. It implies that there has been an overall reduction in the number of large episodes, but also that the baseline concentrations have stabilized. Consistent with this behaviour, the maximum O_3 (upper percentiles in the graphs) has decreased since 1991 with either a significant trend or a non-statistically significant trend at all sites except St. John’s, NL.

The urban site of Forest Hills in Saint John, NB, (Figure 7.31b) does not show any statistically significant O_3 trends, but at the urban site of St. John’s, NL, ozone has increased since 1991, significantly in the lower 4 percentiles. The 10th, 25th and 50th percentiles are considered to represent the baseline levels. The rural site of Kejimikujik also shows a significant increasing trend in the lower four percentiles, while at Norton and Saint John there were slight, but largely non-significant, increases. These overall rises, which require further investigation to explain, may be what the analysis summarized in Figure 3.21 detected. The outlier in this behaviour is the rural site of Blissville where 8-hour O_3 appears to have been decreasing at all points in the distribution. These trends at Blissville are significant for the maximum 8-hour value and for the 90th percentile.

Decreasing trends in the upper percentiles of O₃ levels, which are also evident in the trends for Norton and Saint John, although not significant, indicate decreases in episodes of elevated O₃. Declines in NO_x emissions from the Oil Refining and Electrical Power Generation sectors in Saint John may explain these decreases in the upper parts of the O₃ distribution. In particular, these decreases may contribute to decreasing episodic behaviour at Norton, which lies directly downwind of Saint John in the typical warm season south to southwesterly flow, and may also be a factor at Blissville which can lie downwind of the local sources at times.

7.5.1.2 Spatial and Temporal Variability of PM_{2.5}

Table 7.3 Seasonal mean and peak concentrations of O₃, PM_{2.5} and NO₂ at urban and rural NAPS sites in the Atlantic region for years 2002-2006. Seasonal mean values refer to the mean of all hourly values in each season over these 5 years. Seasonal peak values are calculated as the average over these 5 years of the seasonal mean of the 98th percentile hourly values each day. Seasons that do not fulfill the completeness criteria are not included. Uncertainty is expressed as one standard deviation of the yearly seasonal mean values; where no uncertainty is given there is only one seasonal mean within the 5-year period that meets the completeness criteria. PM_{2.5} measurements are from the BAM instrument at each site, which is why the values differ from the seasonal PM_{2.5} values shown in Figures 3.62-3.65.

O ₃ (ppb)	SUMMER		WINTER	
	mean	peak	mean	peak
RURAL UNDEVELOPED	36.7±3.6	59.3±5.3	35.5±3.0	48.4±4.6
URBAN COMMERCIAL	31.3±4.0	51.3±6.2	31.3±3.1	43.7±4.0
<i>All Atlantic Region</i>	<i>34.6±4.2</i>	<i>56.3±6.3</i>	<i>33.3±3.5</i>	<i>46.7±4.6</i>
PM _{2.5} (µg m ⁻³)	SUMMER		WINTER	
	mean	peak	mean	peak
RURAL UNDEVELOPED	7.9±1.8	24.4±2.9	4.7	14.3
URBAN RESIDENTIAL	9.1±2.2	27.8±8.0	7.9±2.7	20.3±4.8
<i>All Atlantic Region</i>	<i>8.8±2.1</i>	<i>27.1±7.2</i>	<i>7.4±2.8</i>	<i>19.3±5.0</i>
NO ₂ (ppb)	SUMMER		WINTER	
	mean	peak	mean	peak
URBAN RESIDENTIAL	3.7±1.6	21.7±8.6	4.8±3.7	31.1±13.1
URBAN COMMERCIAL	6.5±5.1	29.2±14.6	7.1±3.1	40.2±16.1
<i>All Atlantic Region</i>	<i>5.2±4.1</i>	<i>25.7±12.6</i>	<i>5.8±3.1</i>	<i>36.4±15.4</i>

Rural undeveloped O₃ measurements are from Happy Valley-Goose Bay, Ferrole Point, Kejimikujik, Aylesford, Yarmouth, Fundy National Park, Point Lepreau, Central Blissville, Norton, Dow Settlement, St. Andrews, Campobello Island, St. Leonard, and Lower Newcastle

Urban Commercial O₃ sites include St. John's, Corner Brook, Grand Falls, Halifax, Sydney, Fredericton, and Saint John.

The Rural Undeveloped PM_{2.5} site is Canterbury, NB.

The Urban Residential PM_{2.5} sites are Pictou, Sable Island, Saint John Forest Hills, Saint John Champlain Heights and Saint John West Side.

The Urban Residential NO₂ sites include Mount Pearl, Sable Island, Saint John Forest Hills, Saint John Champlain Heights and Moncton.

The Urban Commercial NO₂ sites comprise St. John's, Corner Brook, Halifax, Fredericton and Saint John

Seasonal mean concentrations in PM_{2.5} at sites in the Atlantic region were not directly compared in Chapter 3. Therefore, although some patterns can be discerned from the figures in that chapter, mean PM_{2.5} concentrations (based on years that fulfill the completeness criteria between 2002 and 2006) measured by a continuous beta attenuation monitor (BAM) instrument are highlighted in Table 7.3. Unlike the TEOM, the BAM is not influenced by cold season mass losses. Three of the “urban” sites are in Saint John, which is relatively close to the “rural” site of Canterbury, which is located ~150 km inland to the northwest. Although mean PM_{2.5} concentrations are greater in the summer compared to the winter in both the urban and rural groupings, the difference is greater at the rural site ($7.9 \pm 1.8 \mu\text{g m}^{-3}$ vs. $4.7 \mu\text{g m}^{-3}$), compared to the urban sites ($9.1 \pm 2.2 \mu\text{g m}^{-3}$ vs. $7.9 \pm 2.7 \mu\text{g m}^{-3}$). Seasonal peak PM_{2.5} mass concentrations, based on the 98th percentile, are higher in the summer months than the winter months at both the rural and urban sites. The summer 98th percentiles are $24.4 \pm 2.9 \mu\text{g m}^{-3}$ at the rural site and $27.8 \pm 8.0 \mu\text{g m}^{-3}$ at the urban sites, while the winter 98th percentiles are $14.3 \mu\text{g m}^{-3}$ and $20.3 \pm 4.8 \mu\text{g m}^{-3}$, respectively.

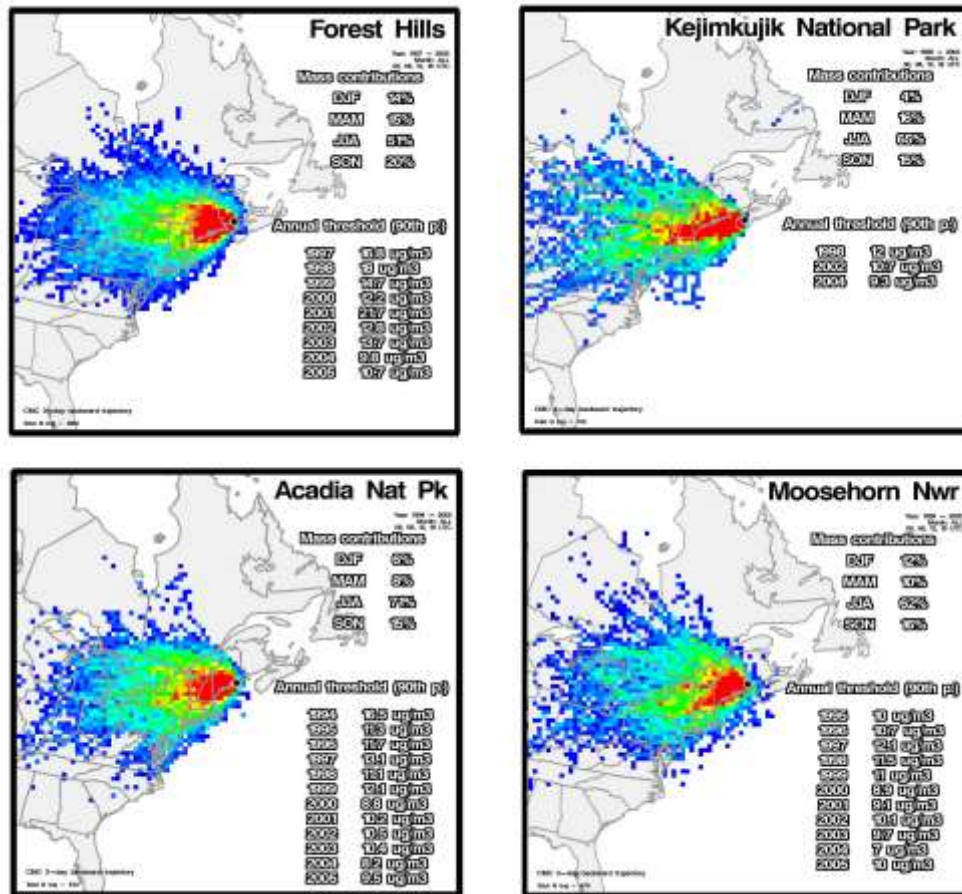


Figure 7.32 Probability density for the trajectories that result in 90th percentile values of $PM_{2.5}$ for two sites in the Atlantic region (Kejimikujik, NS; Forest Hills, NB) and two sites in the northeastern US near the Canadian border (Acadia National Park, ME; Moosehorn National Wildlife Refuge, ME). Mass contributions to annual 90th percentile are shown; at all stations the summer months (JJA) show the greatest contribution to 90th percentile values (51%, 65%, 71% and 62% for Forest Hills, Kejimikujik, Acadia and Moosehorn, respectively). Probability densities show the most influential trajectory at all stations to be that from the west-southwest.

The seasonality in $PM_{2.5}$ in the southern Atlantic region is examined more closely in Figure 7.32. These maps show the upwind probability densities derived from trajectories associated with all the 90th percentile values of $PM_{2.5}$. As the upper right of each panel in the figure shows, these 90th percentile events were more frequent in the summer months. The values are 51%, 65%, 71% and 62% for Forest Hills, Kejimikujik, Acadia, and Moosehorn, respectively. These percent frequencies are more than double of any of the other 3 seasons indicating that in addition to the mean concentrations being higher in summer compared to winter, this seasonal difference is more dramatic with respect to the occurrence of episodes. Summer episodes are due to more active photochemistry leading to greater sulphate concentrations (see Figure 3.64) and a greater frequency of favourable synoptic patterns with lighter winds and prevailing south-

westerly flows. The importance of this flow direction to $PM_{2.5}$ events is indicated by the higher probabilities towards the west southwest shown in Figure 7.32. Long-range transport will be discussed in detail in Section 7.6.

The higher urban $PM_{2.5}$ values in Table 7.3 and overall greater 90th percentile values at the Forest Hills site relative to the three rural sites in Figure 7.32 (see the bottom right of each panel) are a result of local sources. If the rural values in Table 7.3 are taken to represent the regional level of $PM_{2.5}$, then the difference between the mean urban values and mean rural values indicates the typical local urban contribution to $PM_{2.5}$ (Blanchard, 2004). In the summer, local sources contribute 19% of total $PM_{2.5}$ in urban areas, while in the winter the contribution increases to 41%. The lower local contribution in the summer season reflects the dominance of long-range transport throughout the region. U.S. sources likely play an important role given the prevailing southerly and south-westerly flows, which increase total $PM_{2.5}$ while decreasing the local contribution relative to the total. In winter, westerly and north-westerly flows passing over areas with a lower concentration of sources, coupled with less particle-generating photochemistry in the darker months, decreases the overall $PM_{2.5}$ concentrations while increasing the relative local contribution.

Although the majority of the urban and rural $PM_{2.5}$ sites in Table 7.3 are in relatively close proximity and can provide reasonable insight into urban-rural differences in southern New Brunswick, actual data completeness differed by station and year. Thus, a more direct station-to-station, year-to-year and case-by-case comparison, which removes the influence regional meteorology may have on the differences, can only be made between Saint John Forest Hills (urban) and Canterbury (rural) using 2005 data. In this case, local sources from Saint John result in a 36% increase in mean $PM_{2.5}$ over and above that measured at Canterbury in the summer, but only a 2% increase in the winter. In addition to the different time periods, the reasons for the different seasonal pattern between these two specific stations compared with urban and rural comparison from Table 7.3, are suspected to be two-fold. First, there are considerable emissions of SO_2 and VOCs from refineries and power plants in Saint John, which can react photochemically in the high solar intensity of the summer, resulting in higher local levels of sulphate and secondary organic aerosols. Second, the low local contribution in the winter is most likely due to residential fuelwood combustion in the Canterbury area which increases the rural PM concentrations relative to Saint John. As more years of $PM_{2.5}$ data in this region become available more robust estimates of local contributions will be possible.

Observations of $PM_{2.5}$ composition across the country were compared in Figures 3.63-3.66. Two of those sites are in the Atlantic region: Halifax, NS, and Canterbury, NB, which represent an urban and rural setting, respectively. Although the separation between these sites is too far to permit a rigorous urban-rural analysis as was done for total $PM_{2.5}$ above where the sites compared were both in New Brunswick, there are some interesting differences between the sites. Most noticeable are the higher percentages and magnitudes of elemental carbon (EC) and ammonium sulphate for all sampling days in Halifax. Greater EC in the city is typical, but the

increase in sulphate, given that it is usually more regionally homogeneous due to the contribution from long-range transport, is somewhat unusual. However, Canterbury, being considerably southwest of Halifax and hence closer to regional sources (i.e., Midwest and Eastern U.S., S. Ontario) should have higher concentrations. Thus, the fact that concentrations of sulphate are higher at Halifax suggests that the amount of locally produced secondary sulphate in the Halifax area is likely to be larger than just the difference between the two sites (i.e., $>1 \mu\text{g m}^{-3}$ in winter and $>0.5 \mu\text{g m}^{-3}$ in summer for sulphate). This evidence of local, urban sulphate formation also supports the above explanation for the relatively large summer $\text{PM}_{2.5}$ increase in Saint John over Canterbury.

Another interesting difference between Halifax and Canterbury is that, unlike sulphate, concentrations of organic mass are slightly higher in summer at the rural site. This difference suggests that particles from biogenic sources, primary and/or secondary, which are more abundant during the summer months, influence the rural and more continental areas to a greater extent than the coastal areas further to the east. Biogenic organic aerosol precursors are considered to be more likely responsible since there are clearly greater emissions of anthropogenic precursors in Halifax. However, more years of data and more detailed analyses are required to determine the true differences in organic mass and their causes.

The greater relative importance of regional scale $\text{PM}_{2.5}$ at Canterbury compared to Halifax is apparent when looking at the 10 highest $\text{PM}_{2.5}$ days in both the warm season and the cold season (Figures 3.64 and 3.65). During these days, which are not necessarily the same at each site, the total mass is *higher* at Canterbury due to greater concentrations of both sulphate and organic matter. As suggested above, the higher $\text{PM}_{2.5}$ days at Canterbury are more likely, compared to Halifax, to have been influenced by long-range transport.

7.5.1.3 NO_2 variability

The mean NO_2 concentration in both summer and in winter for all sites in Atlantic Canada between 2002 and 2006 with available data, excluding the more recent special study at Kejimikujik reported in Figure 3.27, is 5.2 ± 4.1 ppb in summer and 5.8 ± 3.1 in winter. A stronger seasonal pattern emerges when these sites are sorted into those that are in highly urbanized settings (“urban-commercial”) versus those that are on the edge of the commercial core (“urban-residential”). Table 7.3 shows that mean NO_2 is higher in the winter than the summer at both urban-commercial (7.1 ± 3.1 ppb vs. 6.5 ± 5.1 ppb) and urban-residential (4.8 ± 3.7 ppb vs. 3.7 ± 1.6 ppb) sites. Mean winter values are 4.8 ± 3.7 and 7.1 ± 3.1 ppb, respectively. As expected, peak NO_2 values are also highest at both sites in the winter, with urban-residential sites reaching 31.1 ± 13.1 ppb and urban-commercial sites reaching 40.2 ± 16.1 ppb. There is greater heterogeneity in NO_2 concentrations in summer with urban-commercial sites experiencing NO_2 values 75% higher than those of the urban-residential sites. This difference is only about 50% in winter. Higher summer values in urban-commercial areas are likely due to faster conversion of emitted NO to measured NO_2 due to more O_3 . Lower

summer NO₂ values in residential areas are likely due to greater overall vertical mixing of the urban-commercial NO₂ and faster photochemical conversion of NO₂ to other oxidized nitrogen species between the commercial and residential areas.

7.5.2 Spatial Patterns in O₃, PM_{2.5} and Precursors across Southern Québec and Eastern Ontario

Figure 3.7 shows that the large area of O₃ concentrations in Ontario exceeding the Canada-wide Standard (CWS) metric extends just into southwestern Québec. Based upon the existing monitoring site locations, the boundary separating areas or locations above and below this threshold is quite jagged with pockets of areas or sites below the threshold surrounded by others above it. CWS values by site for PM_{2.5} are mapped in Figure 3.48. Although the contouring in the map suggests that a large area of southern Québec is approaching the CWS, closer examination reveals that this is an artefact of the placement of a small number of sites with high PM_{2.5}. These are mainly in and around Montréal and Shawinigan. For example, the monitoring site in Shawinigan is highly influenced by the local aluminium industry and is not representative of the region. Thus, high PM_{2.5} levels are generally localized and are not widespread as implied in Figure 3.48.

Table 7.4 Frequency of exceedances of the CWS daily metric for ozone and PM_{2.5} in Quebec. Exceedance frequency is the frequency when at least one site in the region is in exceedance and WS33 is the frequency when at least 33% of the sites in the region are in exceedance. Ozone statistics are based on data from 15 monitoring sites during 1990 to 2002 while PM_{2.5} statistics use data from 6 sites from 1998 to 2002 (source: Johnson, 2004).

	Exceedance Frequency	Exceed %	WS33 Frequency	WS33 %
Ozone	355	7.5	127	2.7
PM _{2.5}	45	0.9	19	0.4

To provide a better indication of the occurrence of high concentration events across the region, the frequency of days above the CWS at multiple sites was examined over a multi-year period. These widespread exceedances were defined as a day in which 33% of the sites in the region (WS33) were above the CWS. Table 7.4 summarizes the results for O₃ and PM_{2.5} and shows that during the period widespread exceedances were more common for O₃. About 3% of the days had high concentrations simultaneously at 33% of the sites.

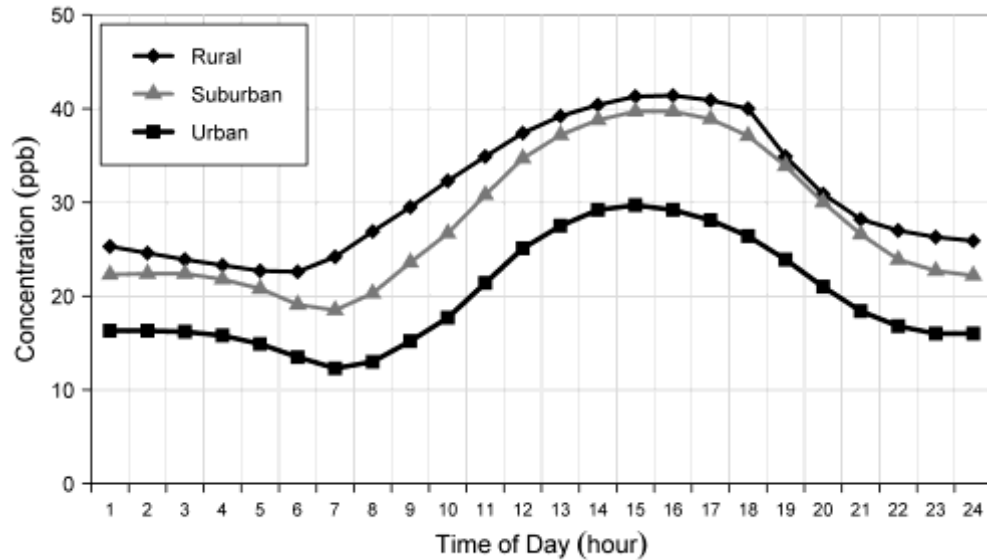


Figure 7.33 Summer (May to September) diurnal variation of ozone for a rural site (Saint-Anicet), an urban site (Ontario Street, downtown Montréal) and a suburban site (Rivière-des-Prairies) from 2003-2006.

In the St. Lawrence River valley, O_3 concentrations in summer vary according to the land use and the location of the sources of its precursors. Figure 7.33 shows the summer diurnal variation of O_3 at three sites representative of a rural (Saint-Anicet, located at the extreme southwest of the province near Cornwall), an urban (Ontario Street in Montréal) and a suburban (Rivière-des-Prairies, located near the eastern tip of the Montreal island) environment. Summer average O_3 levels at Saint-Anicet, Rivière-des-Prairies and Ontario Street are 31 ppb, 28 ppb and 20 ppb respectively.

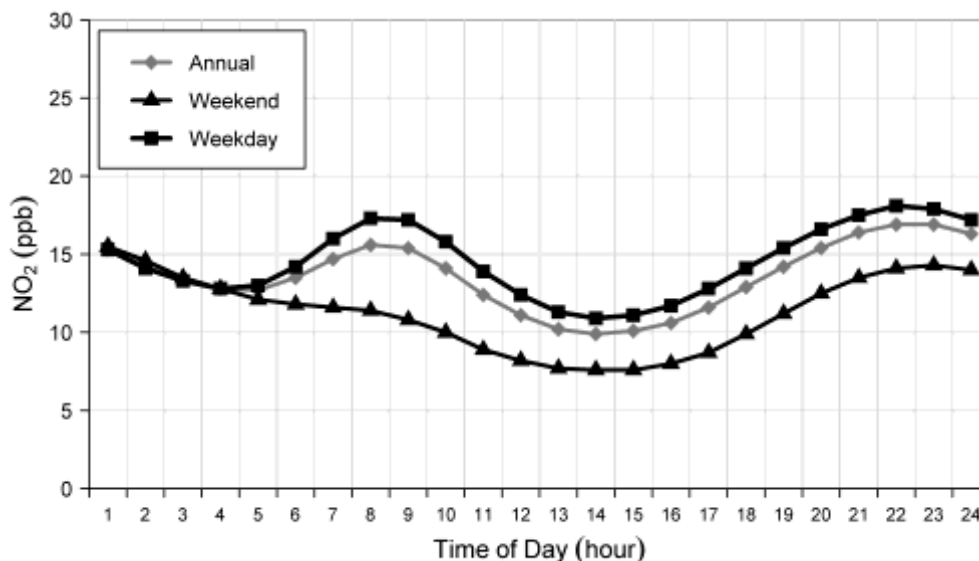
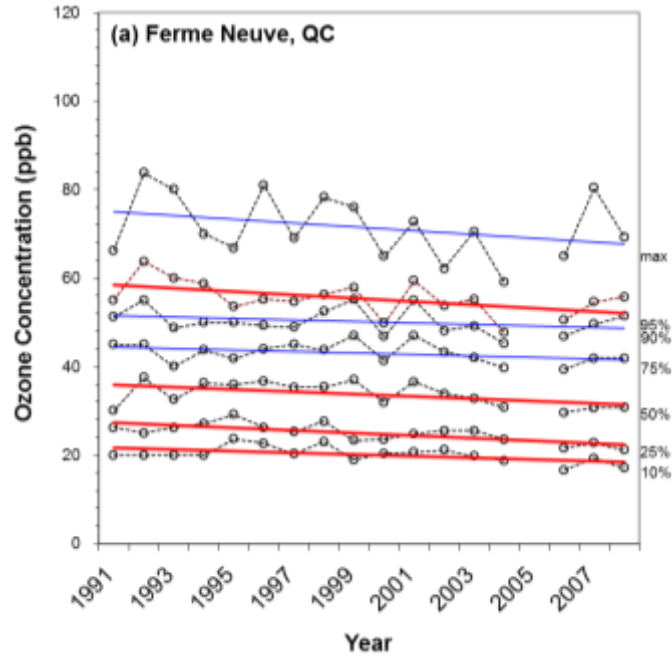
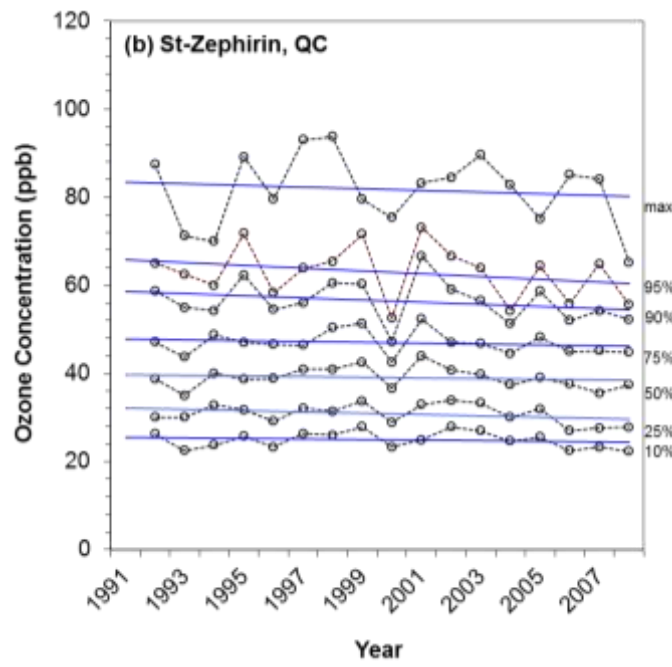


Figure 7.34 NO₂ mean diurnal cycle for all days (annual) and for weekends vs. weekdays averaged across six stations located in Montréal (Saint-Anne-de-Bellevue, Aéroport de Montréal, Parc Pilon, Jardin Botanique, St-Jean-Batiste and Verdun) for 2005 to 2006.

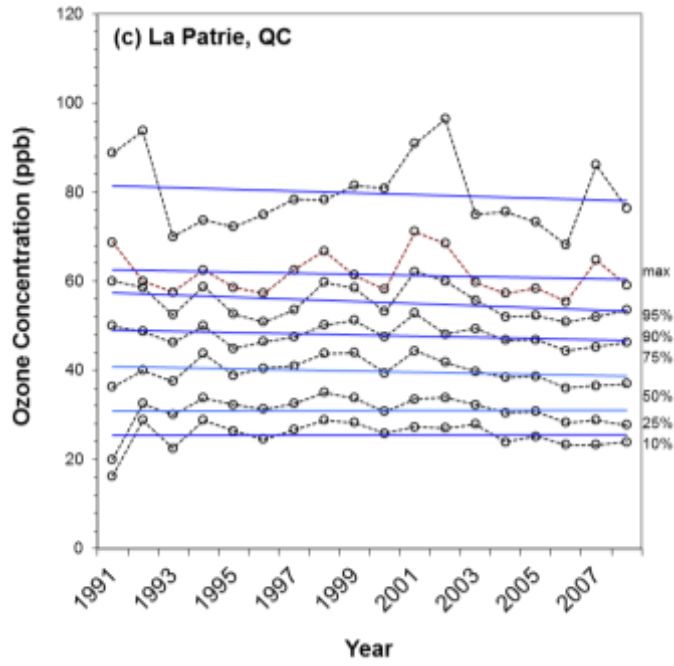
The rural environment of eastern Ontario and southwest Québec is an area of low local anthropogenic emissions, with the main locally-emitted precursors being biogenic VOCs. These VOCs are characterized by stronger release rates between noon and mid-afternoon as temperature and solar radiation reach a maximum. When combined with NO_x and VOCs and O₃ transported into the area from upwind regions, including urban centres, an O₃ maximum is produced in the late afternoon (16:00). At the opposite end of the spectrum is the urban downtown environment, a densely populated area characterized by elevated NO_x and VOC emissions from a variety of sources such as industry and on-road vehicles. The NO availability is high enough that O₃ equilibrium concentrations remain lower than its rural and suburban counterparts. As has been described in several earlier sections, high NO emissions scavenge O₃ by transforming it into NO₂. In many cases this is then carried outside the city to transform oxygen into O₃ again over the suburbs and the countryside. Low concentrations in the urban environment are even more obvious during morning and late afternoon rush hours. Figure 7.34 shows the diurnal variation of NO₂ in Montréal on weekends and on weekdays. It is obvious from both figures that O₃ and NO₂ peak at different times. Moreover, Figure 7.34 clearly shows that the urban input of NO₂ into the atmosphere is modulated by commuter traffic, with higher concentrations on weekdays and at rush hour times.



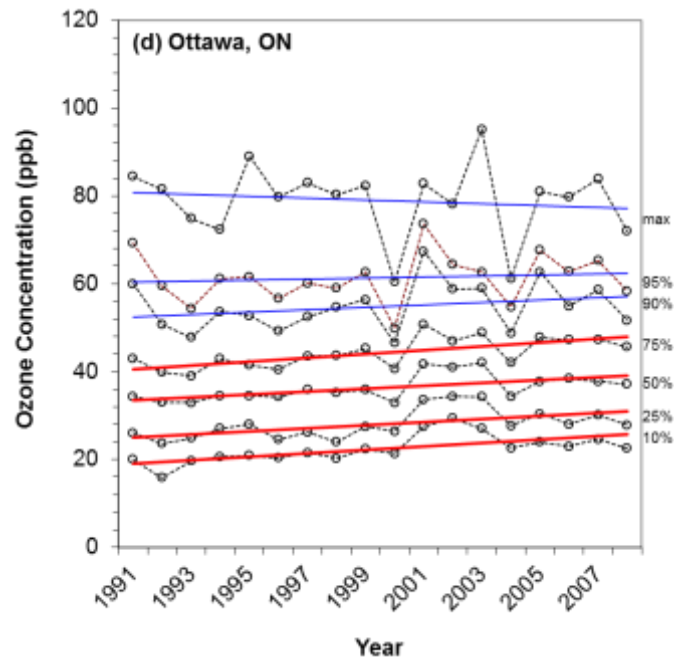
a)



b)

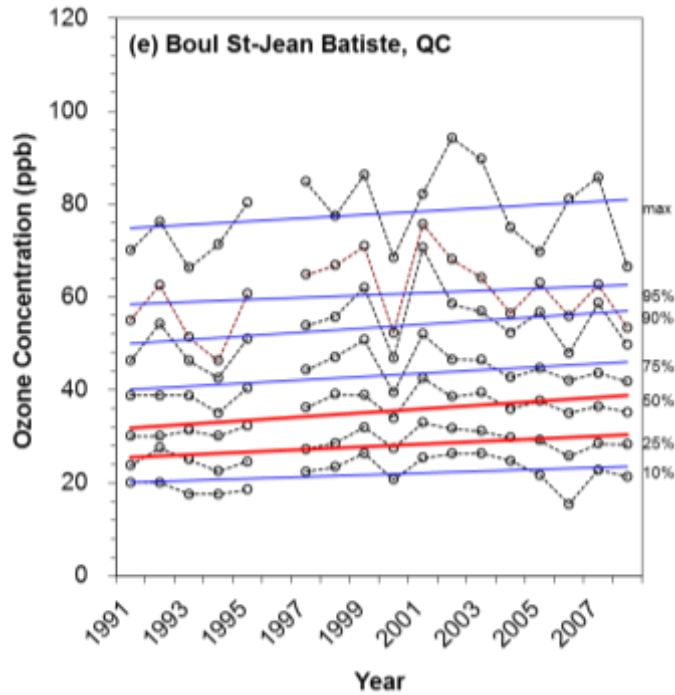


c)

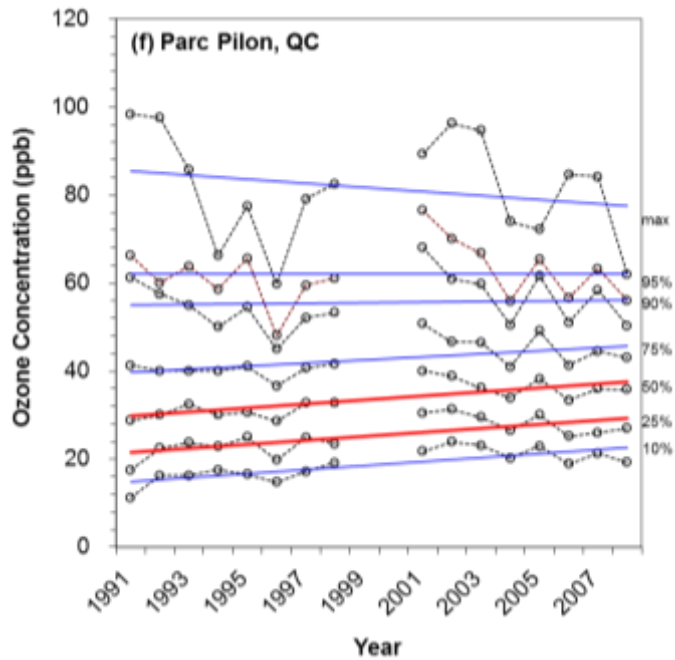


d)

e)



f)



g)

Figure 7.35 Trends in warm season daily 8 hour maximum ozone for five sites in southern Québec and one in eastern Ontario from 1991 to 2008. Background site: Ferme-Neuve (located 180 km northwest of Montréal). Urban sites: Saint Jean Baptiste, Parc Pilon (both on Montréal Island) and Ottawa. Rural sites: Saint Zéphirin, La Patrie. Trend lines shown in red are significant at the 95% confidence level based upon the T-test.

Meteorologically-adjusted trend analyses in Chapter 3 demonstrated that daily maximum 1 hr and 8-hr O₃ levels and daytime average O₃ levels decreased by an average of 0.5 %/yr from 1997-2006. These trends, which were based upon data from multiple sites in southwest Québec and northern New England (U.S.) were found to be highly significant (Table 3.7). Plots of 1991-2008 warm season trends for six sites in southwest Québec are shown in Figure 7.35a-f. As done for the Atlantic sites, separate trends are shown for several points in the O₃ distribution. Consistent with Table 3.7, the warm season maximum 8-hour O₃ concentrations in the baseline air over the region decreased significantly during the period. For example, at Ferme-Neuve (~120 km north of Ottawa) the median values decreased by about 5 ppb or 14% from 1991-2008. At this site and at the other rural locations (Saint-Zéphirin located in the Saint Lawrence River Valley mid way between Québec City and Montréal and La Patrie located in Eastern Townships close to the New Hampshire border), the 10th, 25th, 50th and 75th percentiles all decreased significantly and all other parts of the distribution were trending downward over the 18 years.

The urban locations in Figure 7.35d-f exhibited contrasting behaviour compared to the rural locations. At all the urban sites selected (Saint-Jean Batiste, Parc Pilon and Ottawa), the slope of the 25th through the 75th percentile trend lines are significant and upward. For the median O₃ concentration this amounted to about 24% or 7 ppb over the past 18 years. This is the same pattern, but larger than the increase shown in Figure 3.24 for the combination of urban 51 sites across the country. This urban increase is also seen at many of the other urban sites discussed in this chapter. Local decreases in NO concentrations in urban areas lead to less local destruction of the regional O₃ transported over the cities. The lower parts of the O₃ distribution are revealing an apparent disbenefit from NO_x emission reductions. However, it is important to note that despite the chemical reactions involved in the rise in O₃ there is a net decrease in NO₂, which is of significant benefit to overall air quality.

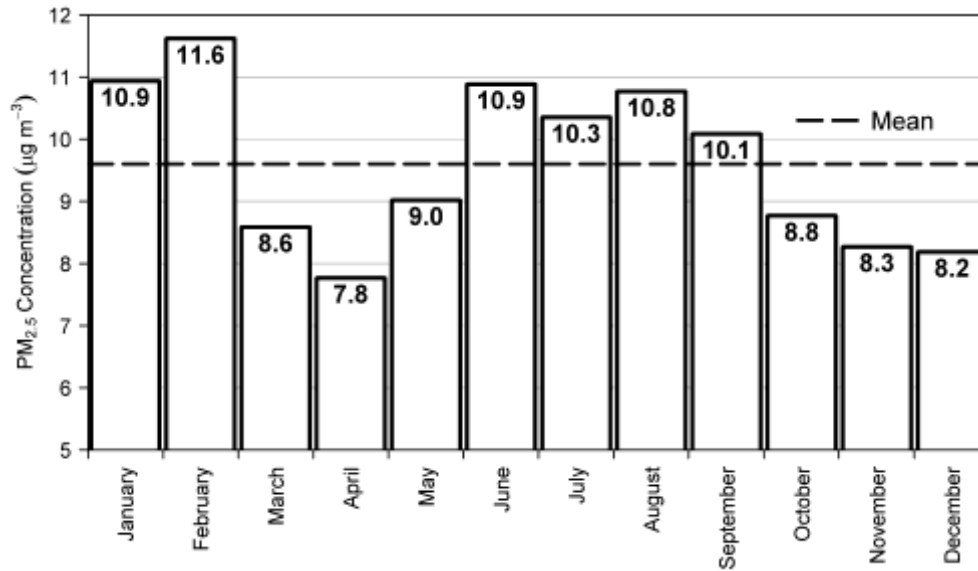


Figure 7.36 Mean monthly PM_{2.5} concentrations based upon TEOM measurements for Montréal (Drummond site), Québec, Trois-Rivières, Saint-Anicet, L'Assomption and L'Acadie from 1999 to 2002.

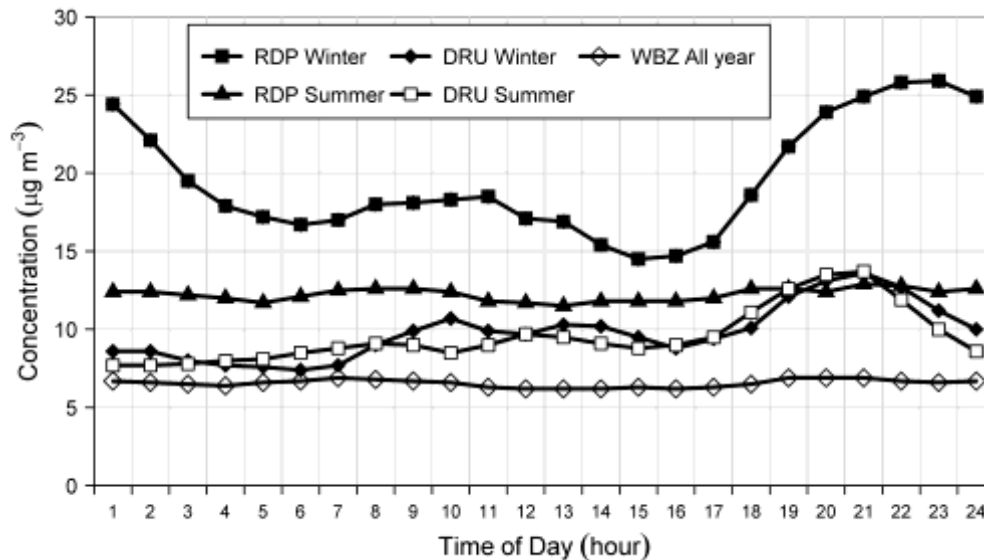


Figure 7.37 PM_{2.5} diurnal cycles based on TEOM measurements at a suburban (Rivière-des-Prairies, referred to as RDP) and urban (Maisonneuve, downtown Montréal, referred to as DRU) site over three summers and winters (2004-2006) compared to the annual average diurnal cycle at the rural site of Saint-Anicet (WBZ) site.

Across southern Québec, urban PM_{2.5} concentrations follow a strong seasonal pattern with one maximum in winter and another one in summer. Figure 7.36 illustrates the combined annual cycle of average PM_{2.5} concentrations at six sites. This pattern differs from the Atlantic Region where the winter maximum is less pronounced. Figure 7.37 shows the diurnal cycle of PM_{2.5}

and, as with the O₃ analysis discussed above, a rural, suburban and downtown site are shown. No significant diurnal cycle in PM_{2.5} concentration is evident in less populated areas of eastern Ontario and southwest Québec due to small local impacts from industrial and fossil fuel combustion emissions. At Saint-Anicet for example, labelled WBZ on Figure 7.37, and where the annual mean for both summer and winter time periods is approximately 6.6 µg m⁻³, there is little change in the concentration as a function of time of day.

In contrast to the rural locations the urban and suburban sites shown in Figure 7.37 exhibit some daily variation in PM_{2.5}. These locations are subject to local industrial and on-road vehicle sources of primary and secondary PM_{2.5}, including primary PM from road dust. However, the morning rush hour peak in PM_{2.5}, which was shown in Figure 3.54, is seen to be much more of a wintertime feature at the downtown Montréal location (DRU). Interestingly, the afternoon and evening rush hour peak occurs in both seasons and is more pronounced than the national average pattern in Figure 3.54. Overall the summer and winter curves in Figure 7.37 are similar implying that the sources are similar in both seasons.

A prominent feature in Figure 7.37 is the impact of winter wood burning at Rivière-des-Prairies (RDP), which appears as a late evening maximum in PM_{2.5}. This is related to ignition of wood stoves and fireplaces when local residents return from work (18:00-19:00), which combined with low mixing heights overnight leads to a broad peak in PM_{2.5}. Comparing this with the summer flat curve at Rivière-des-Prairies provides further evidence that wood burning is a major winter issue in this suburb. This is discussed further in Section 7.7.8.

Table 7.5 Average mass concentration and percent fractional chemical composition for Saint-Anicet and Montréal (Ontario Street) based on 24-hour mean PM_{2.5} reconstructed mass. All days with concurrent measurements at both sites from 2003 to 2007 (N=386) are included in the All Year columns. The last four columns are based upon the concurrent measurements but when PM_{2.5} ≥ 30. There were 13 days in Montréal (6 winter) and 8 days at Saint-Anicet (3 winter). Total mass corresponds to the reconstructed mass summed from the chemical fractions. Organic matter is estimated as 1.8xOC for Saint-Anicet and 1.6xOC for Montréal. Estimated water is determined from 0.32x(sulphate+ammonium).

	Saint-Anicet All Year $\mu\text{g}/\text{m}^3$ (%)		Ontario St. All Year $\mu\text{g}/\text{m}^3$ (%)		Saint-Anicet mass $\geq 30 \mu\text{g}/\text{m}^3$ $\mu\text{g}/\text{m}^3$ (%)		Ontario St. mass $\geq 30 \mu\text{g}/\text{m}^3$ $\mu\text{g}/\text{m}^3$ (%)	
	Mass	%	Mass	%	Mass	%	Mass	%
Total Mass	8.7	-	11.5	-	38.9	-	49.7	-
Ammonium Sulphate	2.8	33	3.0	26	11.5	30	12.6	25
Ammonium Nitrate	0.9	11	1.1	10	11.4	29	11.7	24
Organic Matter	2.7	32	4.4	38	8.8	23	15.4	31
Elemental Carbon	0.6	7	1.0	9	1.6	4	2.8	6
Soil	0.5	5	0.8	7	0.6	2	1.6	3
Salt	0.1	1	0.2	1	0.1	1	0.6	0
Estimated water	1.0	11	1.1	9	4.6	12	5.0	10

Routine chemical composition of measurements of PM_{2.5} have been made in downtown Montréal at the Ontario Street site and at the rural St. Anicet location since 2003. Figures 3.62 to 3.65 showed that ammonium sulphate, ammonium nitrate and organic matter are, on average, the three main constituents. Table 7.5 expands upon those figures summarizing the mass concentrations and percent contributions from each of the main chemical constituents based upon days when there were measurements for both sites. In addition, the percent contribution when reconstructed PM_{2.5} exceeded 30 $\mu\text{g}/\text{m}^3$ is also shown. Obviously, for these cases the mass concentration increases for all the constituents, although increases in the soil and salt fractions at Saint-Anicet were minimal. Of note is that in both the urban and rural areas there was a dramatic increase in the relative importance of ammonium nitrate during these episodes. In contrast, organic matter and elemental carbon decreased markedly in importance, particularly at the rural location. The rise in the ammonium nitrate contribution hints at the potential importance of wintertime episodes. One particular case of interest because it resulted in the highest PM_{2.5} in eastern Canada over the past 15 years is examined in detail below in Section 7.7.1.

The differences in the ammonium sulphate and nitrate concentration between the urban and rural locations are relatively small increasing by 7% and 18%, respectively. This indicates that throughout eastern Ontario and southwest Québec these components of $PM_{2.5}$, especially ammonium sulphate, are more likely regional pollutants and are influenced by long-range transport. The carbonaceous species OM and elemental carbon (EC) increase by 60% and 80%, respectively, from Saint-Anicet to Montréal. These large increases in the city provide an estimate of the amount of local input (e.g., $1.7 \mu\text{g m}^{-3}$ of additional OM). Soil-related components and road salt increase by 50-60% in the city. Collectively, the urban-rural differences indicate that, on average, local Montréal emissions contribute about $2.8 \mu\text{g m}^{-3}$ to the $PM_{2.5}$ concentrations in the city. This increase in mass is about $2 \mu\text{g m}^{-3}$ in the warm season (Figure 3.62) and $3.5 \mu\text{g m}^{-3}$ in the cold season (Figure 3.63). The majority of this additional cold season $PM_{2.5}$ is made up of OM with a much smaller contribution from ammonium nitrate. Possible sources of this additional OM are greater combustion activities related to heating (wood and/or fossil fuels) as well as lower mixing heights to concentrate these enhanced emissions more effectively over the city. Reduced temperatures may also lead to a greater fraction of the semi-volatile organics shifting to the particle phase. Urban enhancements in road salt components (Na^+ and Cl^- ions) and soil-related components are also greater in the cold season because they are used in greater quantities in the city where there are more roads in need of de-icing and traction materials.

At both the St. Anicet and Ontario Street (Montréal) sites, the compositional plots in Chapter 3 (3.62 and 3.63) indicate that the mean $PM_{2.5}$ is greater in the cold season. This contrasts with Figure 7.37 which shows similar levels in each season in downtown Montréal and with what was stated above for St. Anicet: $PM_{2.5}$ is the same in both seasons, at $6.6 \mu\text{g m}^{-3}$. The cause of the discrepancy can largely be explained by the different measurement methods. The value of $6.6 \mu\text{g m}^{-3}$ and those shown in Figure 7.37 were obtained from TEOM measurements. As explained in Chapter 3, the TEOMs deployed at these sites, as well as many others across Canada, lose semi-volatile $PM_{2.5}$ constituents. These are mainly ammonium nitrate and some organic carbon constituents. For example, ignoring all of the ammonium nitrate and a small amount of the organic matter at St. Anicet in Figures 3.62 and 3.63 reduces the total $PM_{2.5}$ concentration to about $6.6 \mu\text{g m}^{-3}$, which is then consistent with the TEOM. These losses are important to consider in the interpretation of TEOM measurements, as was shown in Figure 3.50. In order to gain a true understanding of $PM_{2.5}$, it is clearly important to obtain detailed information on chemical speciation and to avoid the loss of semi-volatile species in both mass determination and chemical analysis.

7.5.3 Spatial Patterns in O₃, PM_{2.5} and Precursors across the Southern Great Lakes Region

Ozone levels over the southern Great Lakes are higher than all other regions in Canada. Figure 3.7 shows that the 4th highest daily 8-hour maximum averaged during 2004-06 was above the Canada wide Standard of 65 ppb over virtually all of the Southern Great Lakes Region. Nineteen of the twenty locations that the Province of Ontario intends to use for reporting under the CWS are within this area. Only Thunder Bay, which is well removed from the high emission regions of southern Ontario, and the adjacent U.S. states, had concentrations below 65 ppb. The highest values of the CWS metric, in the range of 80 to 90 ppb, occurred over far southwestern part of the province. The cities of Chatham and Windsor, which are near the border with the U.S., experienced the highest levels.

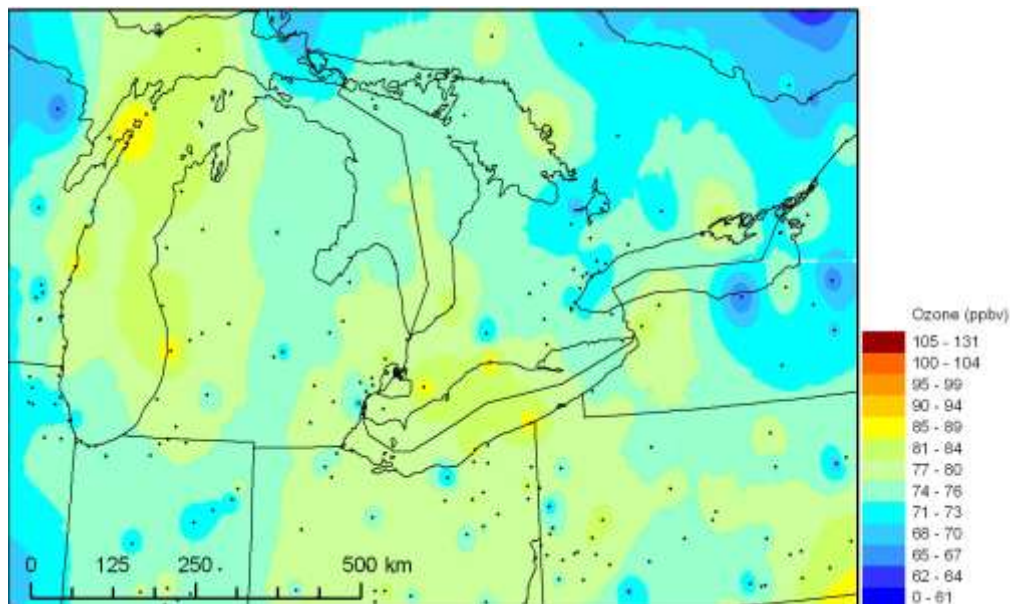


Figure 7.38 Spatial distribution of ozone in Ontario expressed as the CWS metric. Warm seasons of 2004–2006, fourth highest daily maximum 8-hour average ozone. The black dots show the locations of all the available monitoring sites used for the interpolation based upon an inverse distance weighting scheme.

Over much of the high O₃ region there is also a high density of local emissions and furthermore, where O₃ levels are the highest, the Great Lakes add complexity to the situation. To better understand the O₃ behaviour over this part of the country a close-up contour map of CWS metric values is provided in Figure 7.38, along with interpolated concentrations over the lakes. Not surprisingly, the patterns shown in this map and in Figure 7.26 – the 2005 O₃ exceedance map, based upon the 1 hour guideline of 82 ppb (MOE, 2006) - are similar. O₃ most often exceeded the 1 hr guideline and was farthest above the CWS over the southwest part of the province and along parts of the Lake Erie, Lake Huron, Georgian Bay and Lake

Ontario shorelines. The guideline value was exceeded more than 50 times in all of these areas and an even larger number of exceedances occurred in a narrow strip along the north shore of Lake Erie, under the influence of regional scale transport from the south and southwest.

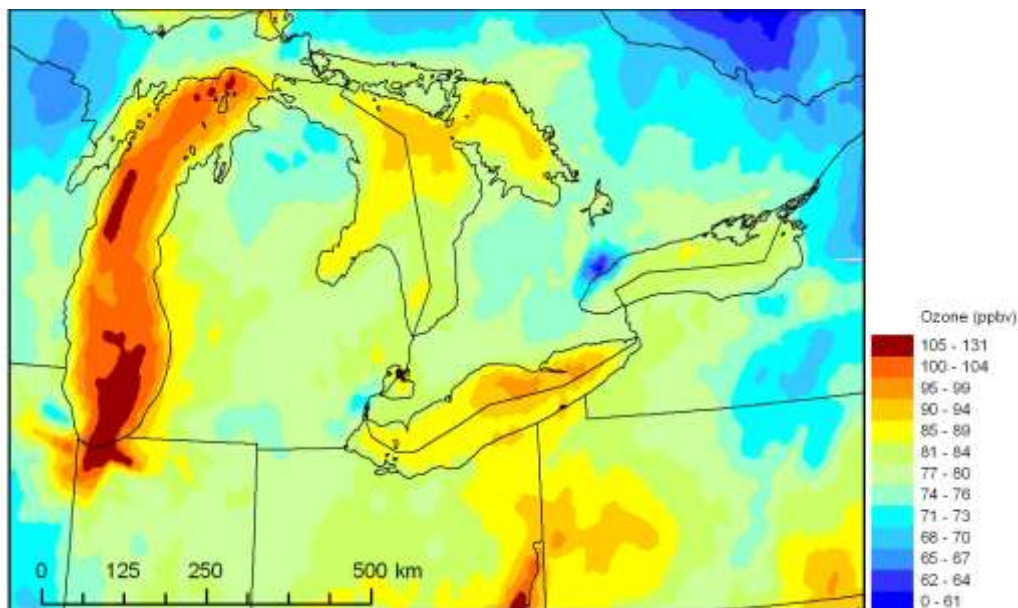


Figure 7.39 Spatial distribution of ozone in Ontario expressed as the CWS metric. Warm seasons of 2004–2006, fourth highest daily maximum 8-hour average ozone derived from an optimal interpolation of the monitoring site data typically available as of 2003 and output from the O₃ forecast model, CHRONOS.

Referring to the observation site locations shown on Figures 7.26 and 7.38 it can be seen that due to gaps in monitoring there is considerable latitude with respect to where the contour lines are drawn. For example, some areas with values above 80 ppb, which are based upon a small number of stations with higher concentrations, are portrayed as being isolated and discrete. Similarly, some of the areas below 74 ppb are portrayed this way. While these patterns may or may not reflect reality the key point is that a true picture of the spatial pattern of O₃ is difficult to obtain due to the limited number of monitoring sites, even in a relatively data-rich area like southern Ontario. Sites are still relatively far apart in rural areas and they are non-existent or even farther apart in more remote regions to the north or where the terrain can be more complex and also over large bodies of water. This includes the Great Lakes, which represents a significant gap in the O₃ picture for Ontario, given the evidence discussed above in Section 7.4.1.3 regarding how the lakes influence the pattern and magnitude of the concentrations. To address these shortcomings measurements and model output can be combined to fill in the gaps. A first attempt at this approach was undertaken for the warm seasons (May-Sept.) of 2004-06 and the map of the 4th highest daily 8-hr max is shown in Figure 7.39.

The difference between Figure 7.38 and Figure 7.39, which are based upon the same three years, is that the former map was derived from an interpolation based only upon the observations, while in the latter combined model runs predicting O₃ concentrations across a 21 km grid with the observations. This initial attempt at O₃ ‘data fusion’ is based upon work by Ménard and Robichaud (2005). This was carried out using hourly O₃ predictions from the Canadian air quality forecasting model, CHRONOS with the meteorology reinitialized every 24 hours, and hourly O₃ observations across Canada and the U.S. The observation sites selected for this work were those available in the USEPA AirNow reporting system as of 2003. An optimal interpolation approach based upon a least square combination of the CHRONOS and AirNow data that minimized the error variance was used hour by hour for the months of May through September of each of the three years. Using an air quality model to provide information between the observation sites enables inclusion of additional information, such as emissions, wind flow patterns and pollutant formation and loss processes. Thus the model serves as a “physics and chemistry based” interpolation tool helping improve spatial and temporal resolution in a realistic manner. This represents a valuable new application of air quality models potentially leading to greater scientific understanding of the behaviour and impacts of O₃ and other air pollutants.

Comparing Figures 7.38 and 7.39 brings out the enhancement, discussed in Section 7.4.1.3, of O₃ values over the Great Lakes. In particular, Figure 7.39 suggests there are high levels towards the eastern end of Lake Erie and over Lake Michigan, where CWS metric values exceed 95 ppb and 100 ppb, respectively. High values are also seen over northeastern Lake Huron and Georgian Bay, where concentrations are above 90 ppb. Lower, but still elevated levels are shown over Lake Ontario. Also of interest is the localized minimum in O₃ over the Greater Toronto Area, which is a result of scavenging by the substantial emissions of NO_x.

The high levels over the lakes and extending inland slightly are consistent with the observations near the shore. However, unlike the results from the interpolated map (Figure 7.38), use of the model predictions with the observations suggests that O₃ levels are even higher over the lake. While the actual magnitude of elevated surface O₃ over the lakes is the subject of ongoing research, there is a reasonably high potential for this phenomenon to be true. This is due to there being enhanced atmospheric stability over the lakes, which serves to keep O₃ and its precursors in a shallow concentrated layer near the surface, as well as there being more clear skies in the day due to the suppression of cumulus cloud formation, slower dry deposition and less O₃ destruction from NO titration over the water.

The “model-aided” concentration patterns provide insight into the origin of the high levels over the lakes. For example, the high O₃ reported in Parry Sound, which has been difficult to explain, appears to be “connected” to a pool of elevated O₃ that extends southwestward into the Saginaw Bay area of Michigan where there is industrial activity. Another “stream” of O₃ also merges with this area from the vicinity of Sarnia and Detroit, both regions of considerable emissions of O₃ precursors. Similarly, Figure 7.39 implies a potential link between the high O₃

over Lake Erie and some of the cities on its shore (e.g., Cleveland, Erie). It is also apparent that the high O₃ over Lake Michigan is likely influenced by emissions in the Chicago and Gary, IN, areas and potentially other coastal cities.

Toronto is seen to have some influence in terms of elevated O₃ east of the city over Lake Ontario where the local maximum surpasses 85 ppb. There are also areas of higher O₃ north of Toronto approaching Lake Simcoe. However, based upon Figure 7.39 the Toronto area's impact is surprisingly small. It is important to note that while this map appears more physically consistent and continuous and is also in agreement with rural Ontario observations near the lakes, there are areas near the sites shown in Figure 7.38 where there is considerable disagreement. In particular, the values over the Toronto area are lower than the observations while values near Pittsburg and the southern end of Lake Michigan are biased high. These discrepancies are partly due to the lack of observational data over these areas in the 2003 AirNow dataset and because there is no separate bias correction in the current approach. These limitations are being resolved for the future data fusion routines being applied across Canada and the U.S. Nonetheless, the insight provided by Figure 7.39 demonstrates the promise of this approach for studying air quality.

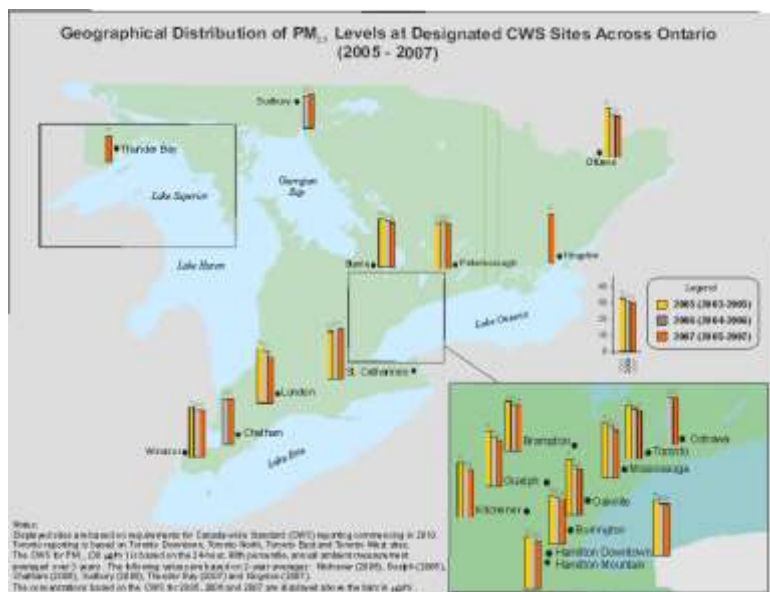


Figure 7.40 Geographical distribution across Ontario of PM_{2.5} concentrations expressed in terms of the Canada-wide standard metric (ending years of 2005, 2006 and 2007).

The spatial pattern of 24-hour average PM_{2.5} concentrations expressed in terms of the CWS metric for separate three year periods ending in 2005, 06 and 07 is shown in Figure 7.40. Although twenty sites are shown, at the present time only eighteen sites have been designated for assessment against the CWS for fine particulate matter PM_{2.5} in Ontario. Five of these (Hamilton Downtown, Mississauga, London, Toronto and Hamilton Mountain) exceeded the CWS metric for the period 2004 to 2006, with values of 31 or 32 µg m⁻³. Thus, while a number

locations were observed to exceed the CWS in southwestern Ontario, reflecting at least to some extent, long-range and/or transboundary transport, there was a substantial number in and around the Greater Toronto Area, which suggests that local emissions played a role.

While Sarnia is not shown in Figure 7.40, it is important to note that in 2005 it had the largest number of days above $30 \mu\text{g m}^{-3}$ with a maximum 24-hour $\text{PM}_{2.5}$ concentration of $54 \mu\text{g m}^{-3}$ during that year (MOE, 2005). In 2006, the maximum at Sarnia dropped to $39 \mu\text{g m}^{-3}$ and provincially, the peak $\text{PM}_{2.5}$ was observed in Burlington with a value of $49 \mu\text{g m}^{-3}$. Both the Sarnia and Burlington monitoring locations are in a populated, industrial region, with intensive petrochemical activities in Sarnia and the Hamilton steel mills and the Oakville refinery not far to the southwest of Burlington. While annual peak 24-hr values are variable in terms of their location of occurrence, over multiple years Sarnia had the highest median $\text{PM}_{2.5}$ in Ontario, followed closely by London (Figure 3.50). These two sites also had the highest median in the country, based upon 24-hr TEOM measurements.

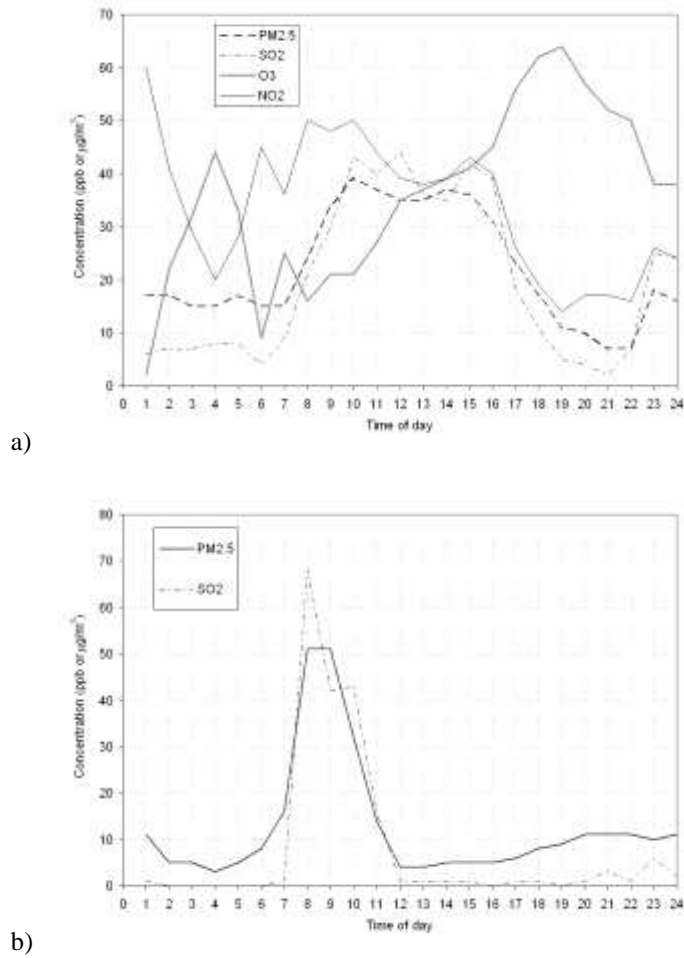


Figure 7.41 a) May 10, 2006 – a high SO₂ and PM_{2.5} concentration episode in Hamilton, Ontario. The gases have units of ppb while PM_{2.5} is in $\mu\text{g m}^{-3}$. b) June 15, 2006 – a high SO₂ (ppb) and PM_{2.5} ($\mu\text{g m}^{-3}$) concentration episode in Sault Ste. Marie, Ontario.

The role that local industry can play in PM_{2.5} peaks is exemplified in Figures 7.41a and 7.41b for Hamilton and Sault Ste. Marie, respectively. Sulphur dioxide, which is a good marker of local industrial emissions since its levels decrease considerably during long-range transport, can be seen to increase and decrease sharply at the same times as PM_{2.5}. Given its high PM_{2.5} levels, it is not surprising that Sarnia also experiences high SO₂ levels. It had the highest annual average (7.8 ppb) and 24-hour (73 ppb) SO₂ concentrations in the province in 2006, indicating that local sources likely contribute significantly to PM_{2.5}.

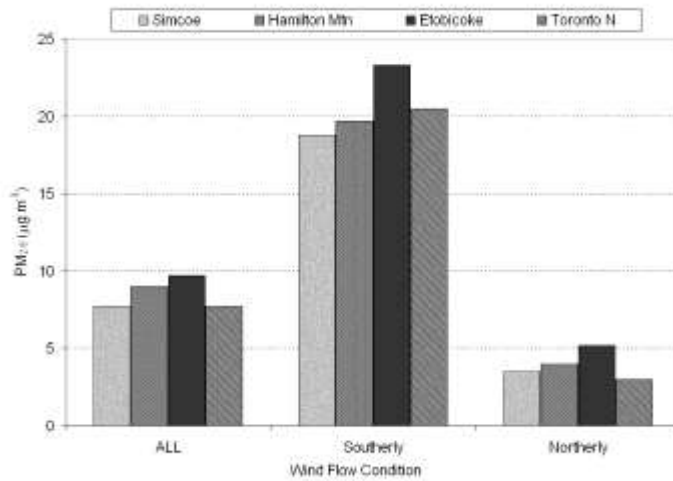


Figure 7.42 Median 6 hr PM_{2.5} concentrations for the warm seasons (May-September) of 1998-2001 (non-precipitating days). “All” represents all measurements in the period when each of the four sites were reporting simultaneously. The sites shown represent a southwest to northeast transect from a rural location (Simcoe) to the outskirts of Hamilton (Hamilton Mtn.) and two sites in Toronto. Etobicoke is in the southwestern part of Toronto and is impacted by traffic.

Although knowledge is limited, it is believed that PM_{2.5} is not preferentially transported, formed and stored over the Great Lakes in the same way as O₃. In addition, there is not a similar process of chemical destruction (i.e., NO titration) for PM_{2.5} in high NO emission areas. Thus, concentration patterns are determined by a combination of influences from local and upwind sources, as well as secondary formation processes. To provide insight on long-range and local contributions to PM_{2.5} in the region shown by the inset in Figure 7.40 concentrations at four sites, one rural (Simcoe), one suburban (Hamilton Mountain), one urban traffic-impacted (Toronto-Etobicoke) and one urban background (Toronto North) are compared in Figure 7.42 (Brook *et al.*, 2007a). The values shown are based upon the same observation periods at each site (i.e., equal sample size from the same 6-hr periods) and are based upon observations when there was no precipitation in the region. This approach provides a clearer picture of the differences between locations. Median PM_{2.5} was around 4-6 times higher under southerly transport conditions compared to northerly flow, depending upon location. While some differences in meteorological conditions (e.g., wind speed) may have contributed to this directional dependence of PM_{2.5}, the major cause was the difference in emissions to north of the region compared to south of the region.

Not surprisingly, PM_{2.5} was highest at Etobicoke and during high-concentration southerly flow periods its median PM_{2.5} was 12% higher than Toronto North. In contrast, it was 66% higher under northerly flow conditions, which is due to the smaller amount of PM_{2.5} in the regional background entering the city. Thus, when the background levels are low, the within-city variation in PM_{2.5} is more pronounced. To estimate the local contribution to urban PM_{2.5} the location of the rural site(s) with respect to the urban centre of interest is important (e.g., the

rural site should not be downwind of the city). As was the case for the Canterbury-Halifax comparison presented earlier, Simcoe is too far to the southwest to directly compare with Toronto concentrations since regional $PM_{2.5}$ levels gradually decrease from south to north. To address this difficulty Brook *et al.* (2002) used $PM_{2.5}$ from Simcoe and another rural site northwest of Toronto (Egbert) to estimate the likely range of the regional concentrations relevant for Toronto. The urban concentrations were then compared to this range to determine how much of the $PM_{2.5}$ in Toronto was due to local emissions. They found that for high concentration, southerly-transport-periods 30-38 % of the $PM_{2.5}$ in Toronto was due to local sources. During westerly flow conditions the local contribution was 30-45%, while the city was responsible for up to 52% when the flow was northerly due to the low background levels.

The chemical composition of $PM_{2.5}$ is monitored at three sites in Ontario – Windsor West, Simcoe and downtown Toronto. Chapter 3 showed the average warm and cold season composition at each of these locations. As discussed earlier, the total mass obtained by the filter-based samplers, from which some of the chemical constituents are determined, is higher than the value determined from the TEOM. This difference is reinforced by comparing the mass at Simcoe in Figures 7.42 and 3.47 to that shown in Figures 3.46, 3.62 and 3.63. As a result of the TEOM losses, it is best to focus on filter-based measurements for detailed comparison of urban-rural differences.

The compositional data show that in the southern part of Ontario, the average make up of $PM_{2.5}$ is generally quite similar. Ammonium sulphate dominates in the warm season, increases in importance when $PM_{2.5}$ is high and its concentration is similar in both the rural and urban locations, pointing towards the main sources being upwind of the region. In winter, ammonium nitrate increases in concentration at each location, surpassing ammonium sulphate in importance in the cities and equaling it at the rural location (Simcoe). This pattern suggests that there is a local, urban contribution to wintertime ammonium nitrate, but that there may be a significant regional contribution to wintertime ammonium nitrate. Several large scale nitrate episodes have been documented during the past 10 years. These have been characterized by widespread reductions in visibility with a tendency for a west to east propagation to the events and one of the common synoptic patterns is depicted in Figure 7.23. For example, a large event in February 1998, which has been examined closely, including by AURAMS runs (MOE, 2005), was observed building up in Minnesota and subsequently developing over the U.S. Midwest, southern Ontario and southern Québec. To some extent the southern Atlantic provinces were also impacted. Section 7.7.1 presents a case study examining the biggest anthropogenically-induced $PM_{2.5}$ event observed during the past 10 years, which occurred in early February 2005.

Other $PM_{2.5}$ species are also elevated in the wintertime $PM_{2.5}$ events, but nitrate dominates these cases and there is evidence that such events have been on the rise, as will be discussed below. Organic matter is an important $PM_{2.5}$ constituent across all three Ontario speciation sites. Its average concentration increases noticeably from winter to summer hinting at the

importance of secondary formation. Precursors of secondary organics include both biogenic and anthropogenic emissions of VOCs, but considerable uncertainty remains in their relative contributions. Organic matter increases from Simcoe to Windsor and Toronto (i.e., rural to urban), which are about equal in both seasons, providing an indication of the influence local emissions. Not surprisingly, a similar pattern is seen for elemental carbon concentration, but its seasonal change is difficult to interpret. At the rural site of Simcoe, EC concentrations in Figures 3.64 and 3.65 are very similar ($\sim 0.4 \mu\text{g m}^{-3}$), while at both of the urban sites there is a noticeable increase from cold to warm season. This behaviour is consistent with earlier results for Toronto presented by Brook *et al.* (2007a). If a seasonal difference in the long-range transport contribution to EC, which could be from upwind anthropogenic emissions (e.g., other cities) or upwind wildfires (a common summertime issue in North America), was the cause of the warm season increase, then the rural site should also be affected. Since it is not and an equal decrease in the influence of a different source at the rural location is also unlikely, the urban-rural comparison suggests that there is a more local scale cause of the increase in urban EC in the warm season. Given that mixing height differences from warm to cold season should lead to the opposite pattern to what is observed, the logical explanation is that warm season emissions of EC in the Toronto area and Windsor/Detroit area are greater. However, more research is needed to confirm this conclusion given that none of the other speciation sites in Figures 3.64 and 3.65 experienced greater EC in the warm season.

7.5.4 Temporal Patterns of O₃, PM_{2.5} and Precursors over Ontario

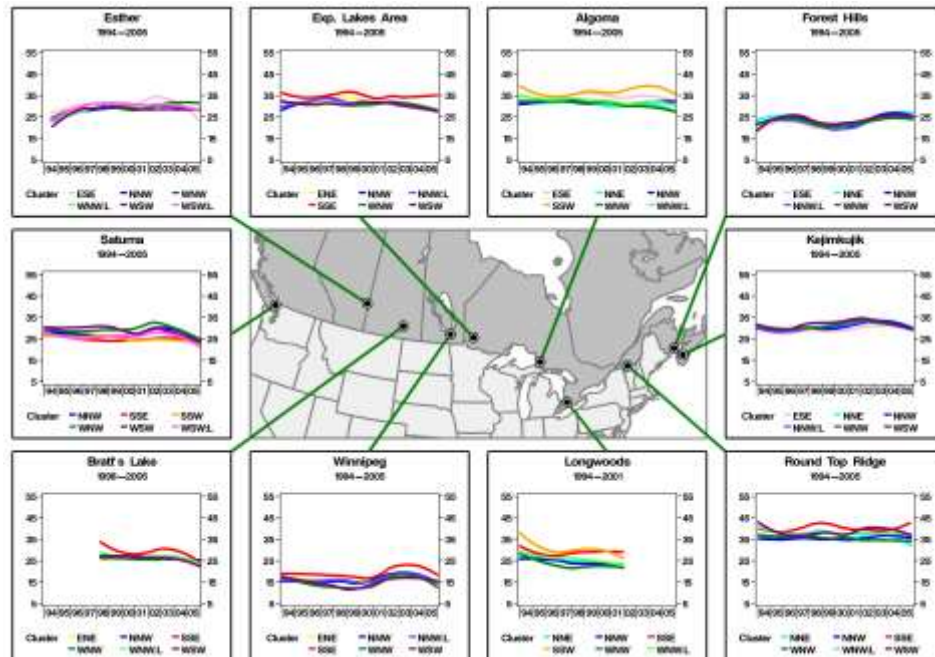
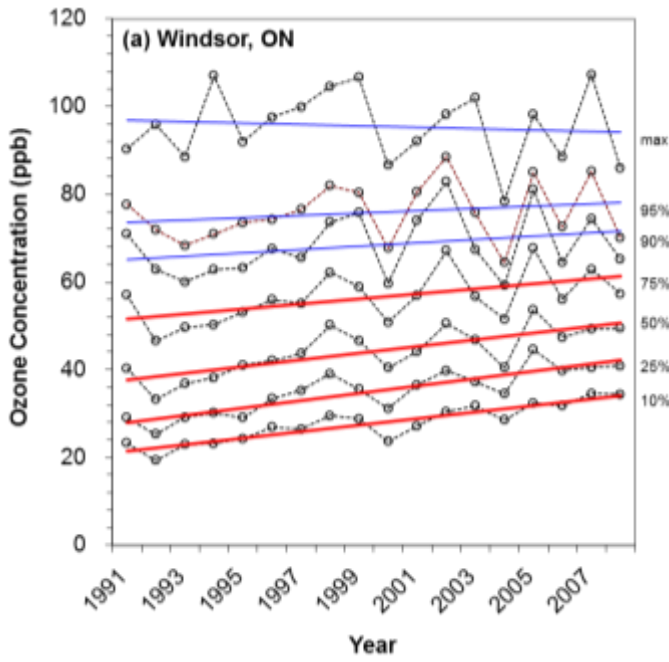
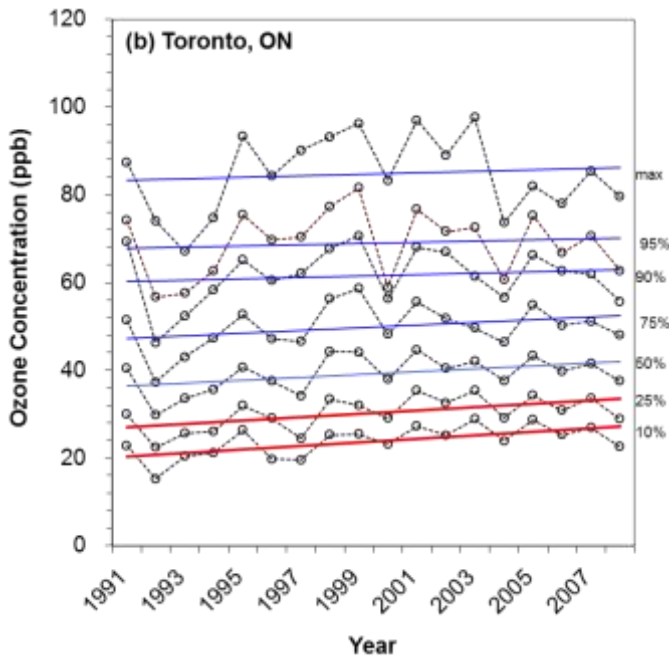


Figure 7.43 Inter-annual O₃ trend plots by trajectory cluster at 10 sites. The time period of the O₃ data record at any given site used in the analysis is shown below the site name in each panel. The curves associated with each cluster were generated using LOWESS (Cleveland *et al.*, 1988), a non-parametric smoothing technique. See Section 7.6.1 for more discussion on this figure.

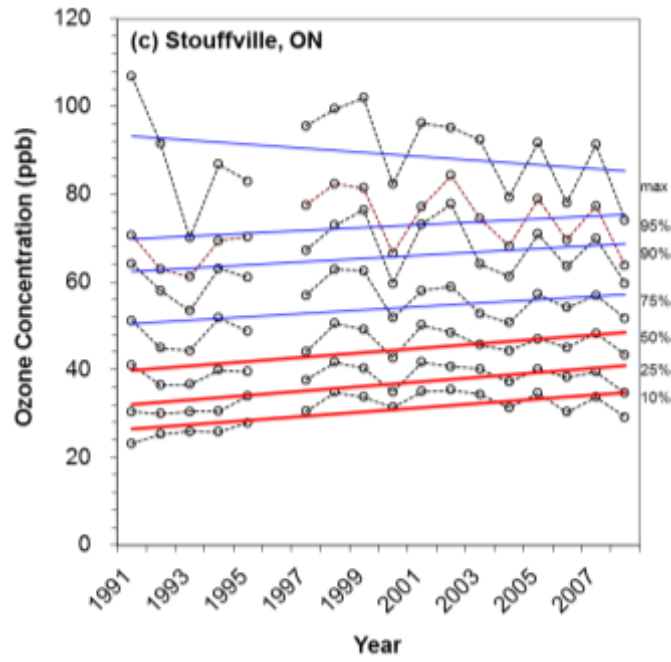
Long term trends in O₃ over Ontario were discussed in Chapter 3 and are also included for different transport pathways for two sites in Figure 7.43. In general, these analyses indicate that concentrations have not changed over the last 10 years or have decreased slightly in some cases. Even longer term trends, exceeding 25 years, were reported by the Ontario Ministry of the Environment (MOE, 2007). They combined provincial data across 19 urban and 4 rural sites to show that the yearly average of the 1-hour maximum O₃ concentration has decreased by 3% over the last ten years. This has amounted to a 3% decline over the period. For the period of 1997-2006, the meteorologically-adjusted trend analysis in Chapter 3 (Figure 3.21 and Table 3.7) also shows that the daily max O₃ levels are declining. For example, the daily 1 hr maximum was found to be decreasing by 1.4 %/yr, collectively across ten rural sites in southern Ontario and the upper Midwest U.S. In contrast, over the >25 year period the MOE reported that seasonal mean O₃, again pooled across a consistent set of urban and rural sites, increased by about 28% and 47% from 1980 to 2005 for the summer and winter, respectively.



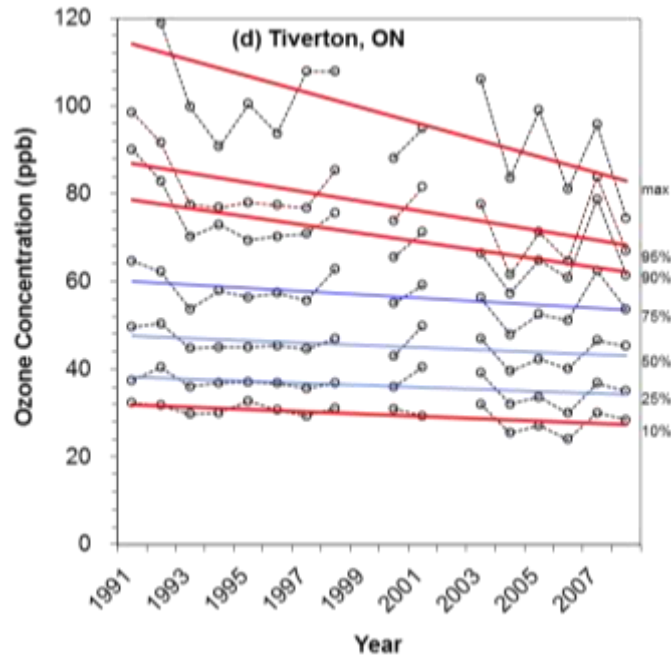
a)



b)



c)



d)

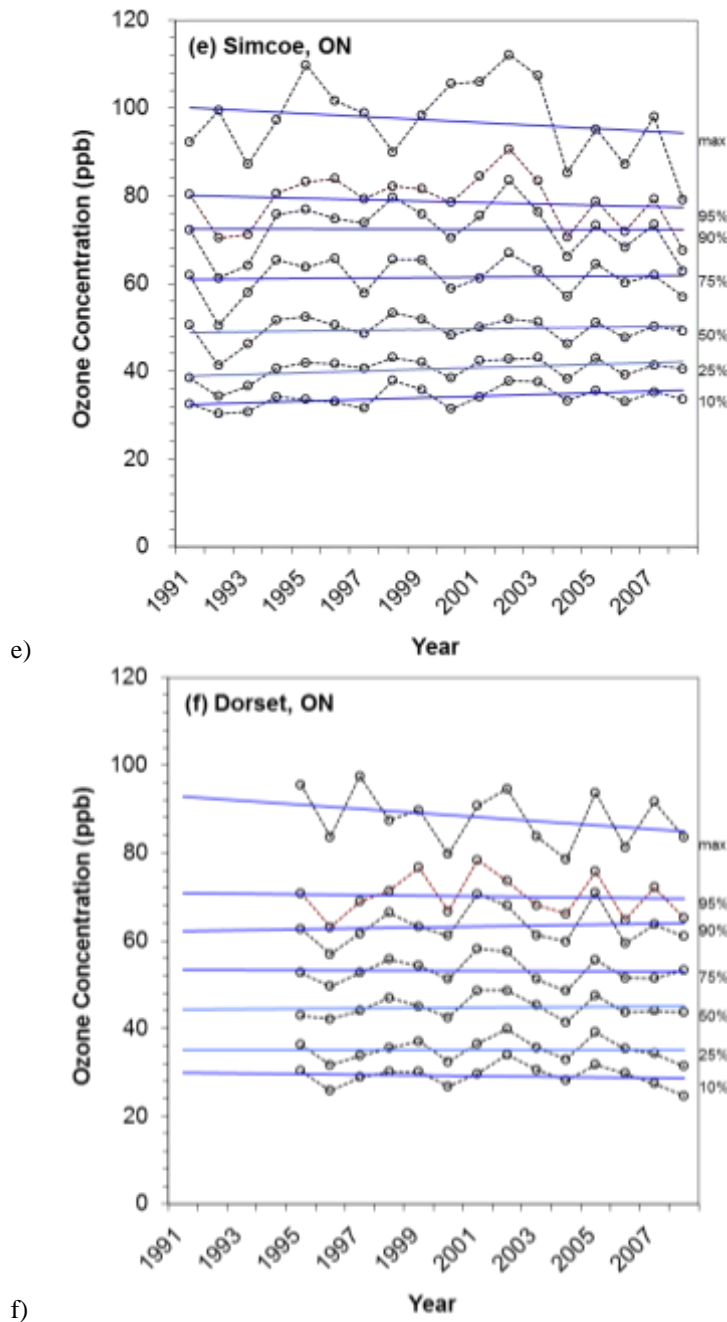


Figure 7.44 Southern Ontario trends in warm season (May-September) daily 8 hour maximum ozone concentrations for 1991-2008. Trend lines shown in red are statistically significant with 95% confidence based upon the T Test.

The difference in the trends based upon the hourly maximum and the seasonal average reported by MOE (2007) reflects how different parts of the O_3 distribution respond to changes in emissions and meteorology during the period. As was undertaken above for the Atlantic and Southern Québec and Eastern Ontario Regions, long term O_3 changes are examined in more detail in Figure 7.44a-f. These plots focus only on warm season trends and are from 1991 to

2008 for six sites in Ontario. Two of the sites are urban (Windsor and Toronto), one site is suburban (Stouffville – NE of Toronto) and the remaining three (Tiverton, Simcoe and Dorset) are rural. In Figure 7.44a-f trends are displayed separately for the 10th, 25th, 50th, 75th, 90th and 95th percentiles as well as for the maximum value for the 8-hour average ozone concentration. Slopes of trend lines shown in red are significantly different than zero with 95% confidence based upon the T-test.

The trends in Figure 7.44a-f indicate that the urban and rural sites exhibit contrasting behaviour, which was masked by the pooling of sites done in the MOE report. The three rural sites are spread across the southern part of the province and were selected to provide an indication of conditions throughout the area. The daily maximum 8 hr ozone concentrations appear to have been decreasing slightly at all points in the data distribution, but none of the slopes are significant. The exception is Tiverton, where the 10th, 90th, 95th and maximum trends are significant and downward. This tendency for decreases at the rural locations is consistent with the Chapter 3 results discussed above. However, in that more sophisticated analysis that pooled data across ten sites and looked at a shorter period, the decreases were found to be highly statistically significant for the maximum hourly, maximum 8-hour and daytime average O₃ and marginally significant (P=0.067) for the daily average O₃ (year round).

In Windsor and Stouffville the maximum concentration has a slight downward, but non-significant trend. The Toronto site (Scarborough) is an exception, in that the trend in the maximum 8-hour O₃ has been increasing, but not significantly. A key feature of the urban and suburban plots is that at each of these sites all other parts of the data distribution have had an upward trend. While these data are only from a few sites, they were selected to provide a general indication of major urban areas throughout the province. At the Windsor location, it appears that concentrations from the 75th percentile and lower were increasing significantly. At the Stouffville and Toronto sites, the lower half and lower quartile of their 8 hr O₃ distributions have been increasing significantly, respectively.

The rural-urban differences in the trends (i.e., downward trends for all percentile levels for rural sites but downward only for the maxima for urban sites) are consistent with what has been observed for averages across Canada, as shown in Figures 3.24 and 3.25, and also with some of the trends shown above for sites in the Atlantic and Southern Québec and Eastern Ontario regions. The analysis presented by Jenkin (2008) shows similar effects for sites in the United Kingdom, with decreases in the maxima and increasing trends in the lower parts of the distribution being especially marked for urban sites. Figure 7.42 trends are also consistent with Geddes *et al.* (2009), who have reported little change in ozone concentrations in and around Toronto, in spite of substantial changes in emissions both in Ontario, and in upwind regions. Trends in the ambient concentrations of the main ozone precursors and in their emissions are discussed in Chapters 3 and 4, respectively.

The decrease in maximum concentrations (i.e., the upper part of the distribution) is attributed (e.g., by Geddes *et al.*, 2009) to decreasing emissions of O₃ precursors in eastern North America, in particular in those upwind areas within Ontario and in the Midwest U.S., which impact frequently on southern Ontario. On the other hand, upward trends in the lower percentiles in urban locations have been attributed (Jenkin, 2008; Royal Society, 2008; Geddes *et al.*, 2009) to local decreases in NO_x emissions, leading to more O₃ due to less loss through reaction with NO (i.e., less titration). As in the other regions discussed in the chapter this effect is limited to urban areas because there is a far higher concentration of sources of NO_x emissions in the cities, most notably motor vehicles. This means, in turn, that the loading of NO to the atmosphere is higher in urban areas, so that changes in scavenging or titration of ozone are more readily observable. The lower emission densities in rural locations mean that scavenging is less important and thus less provincial NO_x emissions do not have the apparent disbenefit of rising O₃ concentrations seen in the cities. Conversely, as rural areas are downwind of the NO_x reductions, there is greater potential for benefits to be realized.

As reported by Reid (2007) it has been suggested by a number of researchers that increases at the lower end of the ozone concentration distribution may be influenced by increasing hemispheric background concentrations of O₃. The same conclusion was presented by Jenkin (2008) and, according to Vingarzan (2004) and Reid (2007), background O₃ concentrations have been reported to be increasing at between about 0.2 and 2% per year. Although all the reasons for and implications of a rising background are not known, it is likely to be partly related to increasing hemispheric precursor emissions. However, increasing background levels are not evident in the trend lines for the rural sites shown in Figure 7.44d-f. This also implies that, even if the confounding by the reduced amount of NO titration could be accounted for, no such pattern has occurred at the urban sites either.

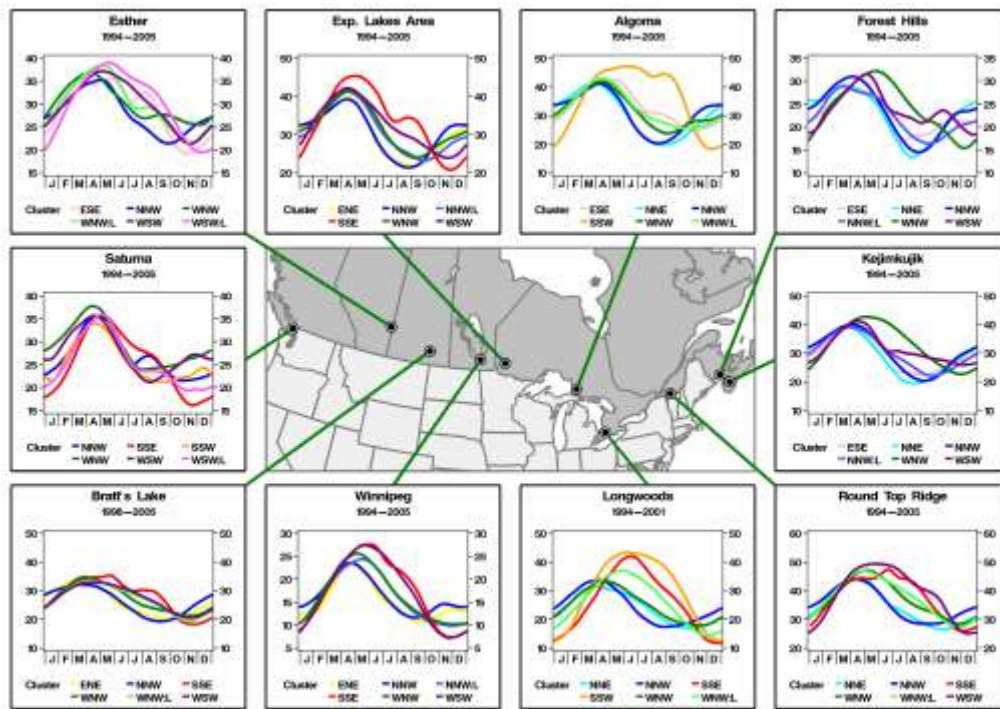


Figure 7.45 Seasonal O₃ trend plots by trajectory clusters at 10 O₃ sites. The time period of the O₃ data record at any given site used in the analysis is shown below the site name in each panel. The O₃ trends were generated using LOWESS (Cleveland *et al.*, 1988), a non-parametric smoothing technique, associated with these cluster. Note that different scales are used across sites. See Section 7.6.1 for more discussion on this figure.

Seasonal variations in maximum and mean O₃ at selected locations across the country are shown in Figure 3.9 and these patterns were examined according to transport pathways in Figure 7.28. One of the main characteristics is that mean O₃ and mean daily hourly maximum is highest in the spring at many locations. However, in areas where O₃ is higher in concentration (e.g., southern Ontario) and/or where precursor emissions are larger due to greater population density, the seasonal peak in the mean and/or the daily maximum has a greater tendency to occur in the summer. Thus, in Ontario, Figure 3.9 shows that somewhere between Experimental Lakes Area (ELA, near Kenora, Ontario, in the far west of the Province) and the Simcoe/Windsor area the O₃ seasonal pattern switches from a spring max to a summer max. There is evidence in the figure that the transition zone from a summer to spring peak is in the vicinity of Egbert since the data at that site show that the monthly averages are slightly higher in spring while the monthly average of the daily max is in the summer. Comparison of Longwoods and Algoma in Figure 7.45 also suggest there is a transition zone in this region. Three of the six transport pathway at Longwoods have a summer peak and at Algoma only one of them peaks in the summer. Slightly further north and nearer the western edge of the province at ELA there is still one transport pathway with some evidence of a summer maximum, but not nearly as pronounced as at Algoma.

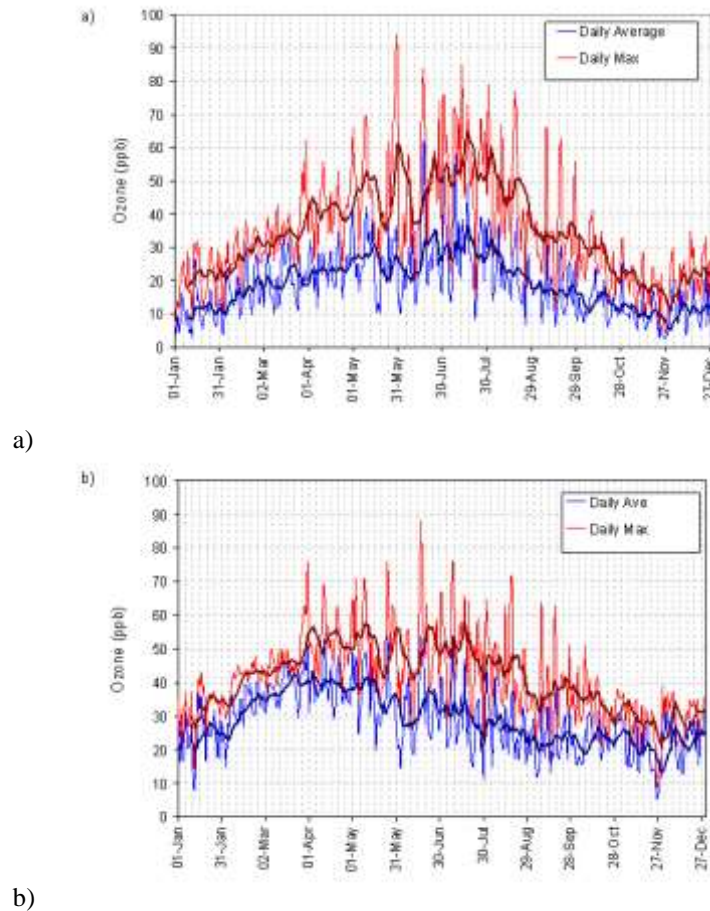


Figure 7.46 The daily average and maximum ozone concentrations at two Ontario sites: (a) Toronto West and; (b) Dorset. The solid line is the 10-point running mean. Note that data for other years, not shown here, exhibit essentially identical patterns.

To gain more insight into the transition zone from a dominant spring to a dominant summer peak in O_3 the 2006 daily average and maximum O_3 concentration for two sites in this region, Toronto West and Dorset, are shown in Figures 7.46a and 7.46b, respectively. There is considerable day to day variation in both measures, driven by day to day changes in meteorology. However, the overall patterns are clear, especially as seen in the 10-day moving averages plotted as black lines through the data points. For Toronto, there is a broad maximum for both the daily maximum and daily mean, peaking in the late July/early August period. Maximum concentrations exceeded 80 ppb several times during this period, even though this is an urban site, influenced by urban-scale vehicular emissions and therefore subject to scavenging of O_3 . Maximum values at Dorset, a rural site approximately 150 km north of Toronto, approached 80 ppb on a number of days, and exceeded this value once.

For Dorset the maximum in the annual distribution of the daily averages occurred in the spring (late March/early April). The daily maximum had a broader flat peak starting in spring extending into summer, which is similar to the Egbert plot shown in Figure 3.9. Thus, this site

still appears to be in the transition zone. The smoothed plot of O₃ concentrations shows common features between Toronto and Dorset, most notably the peak on May 31, with a dip in concentration either side of it. These features are clearly responding to regional scale changes in meteorology.

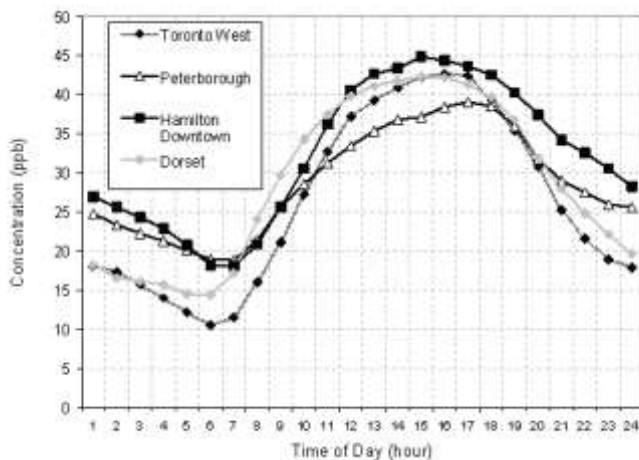
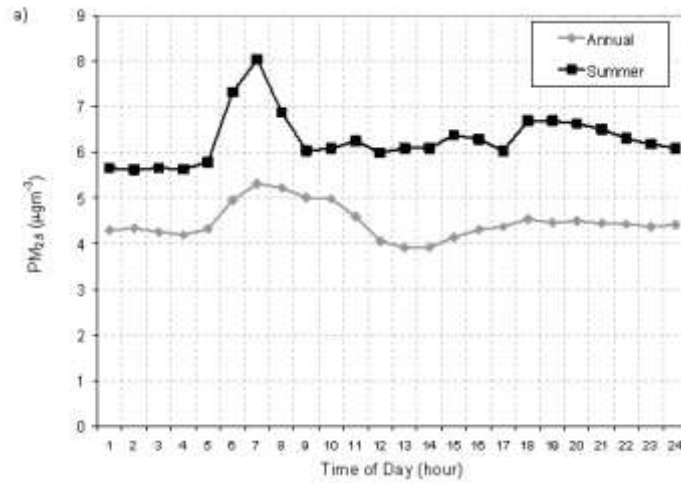


Figure 7.47 Diurnal pattern in ozone concentration for sites in Ontario for 2006.

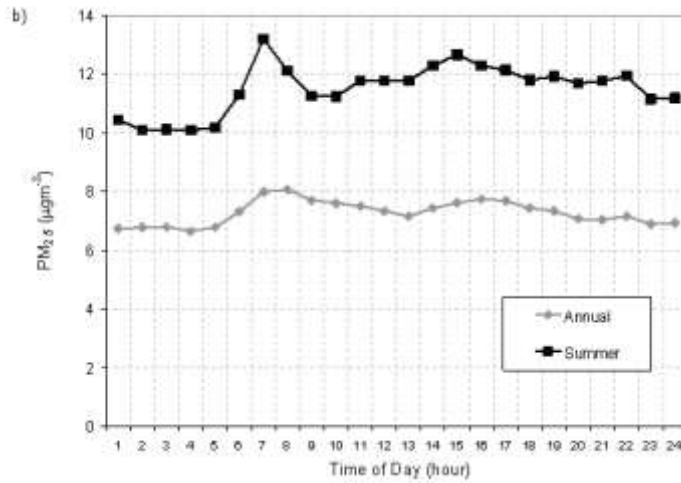
Closer examination of the diurnal pattern of O₃ concentration in the region around Toronto also reveals interesting features, as may be seen in Figure 7.47. This figure shows the average of the O₃ concentration for each hour of the day for the summer of 2006 (June, July, and August). The mean hourly O₃ concentrations typically have hourly standard deviations at all sites in the range of 11 to 17 ppb. These are largely due to meteorology-driven day-to-day and seasonal variations. Clearly, this variability exceeds the concentration differences between sites in Figure 7.47. However, there is strong consistency year-to-year in these differences and in the details of the diurnal patterns indicating that the interpretations discussed below are robust and are warranted. The curves for Toronto West and Hamilton show the classic behaviour of O₃ in urban locations, with a deep dip in the morning, and a fairly broad peak at about 3 p.m. Peterborough, a less urbanized location, shows a similar pattern, but the morning dip is somewhat less pronounced, while at Dorset the morning dip is smaller again, on the order of 4 ppb. Both these sites also have afternoon maxima.

The morning dip in concentration is a result of multiple processes. These include both depositional loss of O₃ from the shallow surface layer during the overnight period and the additional effect, particularly in urban areas, of the scavenging by fresh emissions of NO_x as traffic increases in the morning. The smaller dip at Dorset is likely due to the much smaller amount of traffic in this area. The increasing side of the dip later in the morning is initially due to the breakup of the nocturnal inversion leading to the mixing of higher O₃ concentrations from above the surface inversion layer(s). These higher O₃ levels are then enhanced by new photochemical formation of O₃. Of interest in the comparison in Figure 7.47 is the afternoon

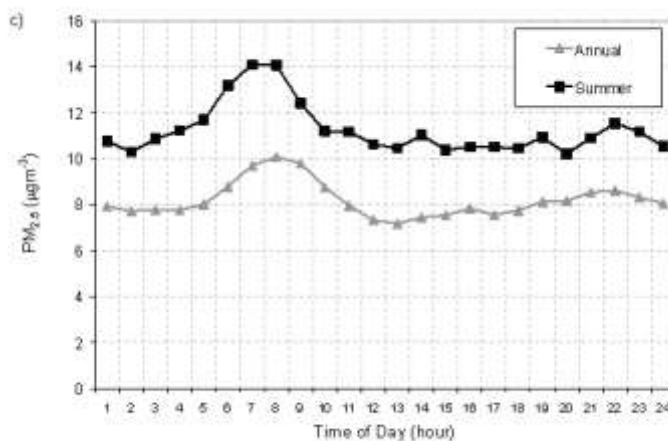
peak at Peterborough which occurs later in the afternoon compared to the other sites, and there is some suggestion of a double hump. The later portion of the O_3 peak may be associated with precursors emitted in the Greater Toronto Area earlier in the day and subsequently transported to Peterborough, either directly or by way of Lake Ontario and the lake breeze, as described by Reid *et al.* (1996).



a)



b)



c)

Figure 7.48 Diurnal patterns of PM_{2.5} (all year and summer only) for Dorset, Port Stanley, and Toronto West.

The period of record for PM_{2.5} measurements in Ontario is shorter than that for O₃, and similar long-term trends are therefore not available. However, a number of interesting temporal patterns may be seen in the available data. For example, Figure 7.48a-c shows hourly average PM_{2.5} concentrations for several locations for summer (June, July and August) and for the whole year. Data for a rural site (Dorset) a regional site influenced by pollution transport (Port Stanley) and an urban site (Toronto West) are shown in the figure. All three sites exhibit a morning peak in PM_{2.5} concentration for the summer plots. This is in contrast with previous results for the rural Egbert site (Brook *et al.*, 1999) and for St. Anicet as discussed above, in which no early morning peak was observed. Reasons for this difference are unclear and require further investigation. The magnitude of the peak is greater for Toronto West (about 4 µg m⁻³) than Port Stanley (3 µg m⁻³) and Dorset (2 µg m⁻³), which is due to local rush hour. There may be contributions to the rural morning peak from both downward mixing of polluted air with the break up of the nocturnal inversion and some addition of vehicular emissions of PM_{2.5} during the morning. However, in comparison to the rural sites, the contribution from rush hour would be expected to be larger than shown here for Toronto, again implying that these observations require further investigation. As in the case of O₃, despite the fact that the standard deviation of the hourly PM_{2.5} measurements, which ranges from 4 to 5 µg m⁻³, exceeds the concentration differences between sites, the diurnal patterns are robust and thus help reveal insight into some of the important processes affecting air quality.

7.5.4.1 Increasing Cold Season Concentrations of Fine Particle Nitrate

As indicated above, smog episodes are not only a summertime phenomenon due to the potential for high PM_{2.5} in all seasons. In fact, the highest filter-based 24 hour PM_{2.5} in Canada during the past 10 years occurred in the winter. This event is described in detail in Section 7.7.1. In the warmer months, ammonium sulphate tends to be the main contributor to episodes

(Figure 3.64) while in the winter increased ammonium nitrate is the main culprit (Figure 3.65 and Table 7.5). The colder temperatures favour the formation and build up of ammonium nitrate when coupled with light winds, sunshine and low mixing heights. These conditions are usually associated with high pressure ridges and twenty-four hour average $PM_{2.5}$ concentrations have been observed to exceed $50 \mu\text{g m}^{-3}$ with up to $15\text{--}20 \mu\text{g m}^{-3}$ of nitrate. In the warmer months nitrate may form overnight, but it typically evaporates in the day so that there is no sustained build-up.

There is reason to suspect that there may have been upward trends in particulate nitrate due to changes in sulphate concentration and Figures 3.79 and 3.81 suggest that such a pattern did occur in the latter half of the 1990s and the early part of this current decade. This was due to preference for NH_3 to react with acidic SO_4^{2-} before contributing to fine nitrate formation. Ansari and Pandis (1998) and West, Ansari and Pandis (1999) discussed the interplay between NH_3 and SO_4^{2-} in eastern North America, while conditions in southern Ontario and Québec were examined in the Canadian assessment on particulate matter (Shepherd *et al.*, 2001), as well as in this assessment in Chapter 3. This interplay can lead to situations when the total fine particle mass ($PM_{2.5}$) can respond non-linearly and even negatively to changes in SO_4^{2-} and/or NH_3 (i.e., $PM_{2.5}$ increases when SO_4^{2-} is decreased). The potential for this to happen can be estimated using the gas ratio (see Chapter 3) and for both the present conditions (Chapter 3) and those in the late 1980's and early 1990's (Shepherd *et al.*, 2001). The potential for $PM_{2.5}$ decreases to be less than the actual SO_4^{2-} decreases or even to increase, was estimated to be greatest in the winter over southern Ontario. Careful examination of the available nitrate data has shown that these predictions were correct. This was based upon the changes in ambient concentrations observed in the mid 1990's when SO_2 controls were implemented to help mitigate acidic deposition.

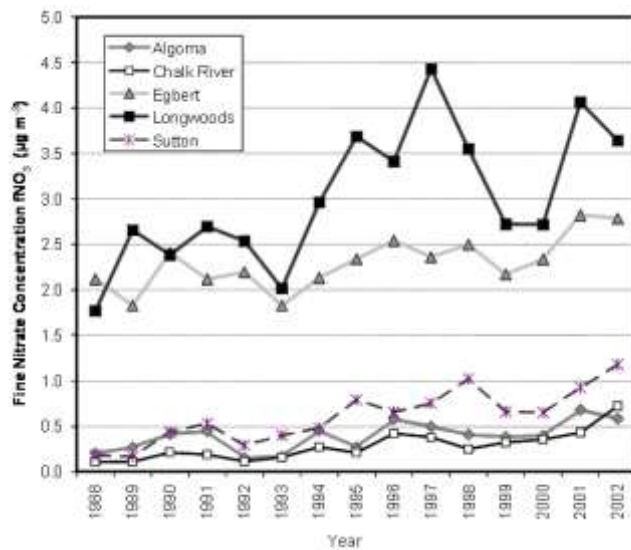


Figure 7.49 Annual average estimated fine nitrate from CAPMoN sites in southern Ontario and Québec.

Table 7.6 Percent Change in mean CAPMoN cold season concentrations of HNO₃, NH₄, NO₃, SO₂, SO₄, estimated fine nitrate (fNO₃), estimated coarse nitrate (cNO₃) and total nitrate (tNO₃) between the periods of 1988 – 1993 and 1996 – 2001.

CAPMoN	HNO ₃	NH ₄	NO ₃	SO ₂	SO ₄ ⁻²	fNO ₃	cNO ₃	tNO ₃
Longwoods	-22.7%	3.2%	12.5 %	-30.2%	-23.2%	48.7%	-42.0%	25.7%
Egbert	-19.1%	-10.2%	5.0%	-37.0%	-25.0%	17.9%	-20.4%	3.5%
Chalk River	-13.5%	-5.1%	55.7%	-38.7%	-26.1%	143.1%	17.8%	7.5%
Sutton	-21.6%	-8.3%	37.7%	-41.8%	-28.1%	133.5%	-18.4%	6.6%
Algoma	2.6%	0.3%	50.4%	-38.8%	-24.4%	78.7%	18.9%	20.6%
Chapais	-3.4%	-13.0%	148.1%	-49.8%	-33.6%	1791.3%	110.5%	11.0%
ELA	-0.7%	-3.0%	39.9%	-31.9%	-21.4%	61.3%	14.6%	24.0%
Kejimikujik	-21.7%	-21.4%	32.4%	-37.0%	-29.3%	238.7%	32.1%	-21.4%

Figure 3.75 showed that from 1994 to 1995 there was nearly a 3 million tonne reduction in eastern North American SO₂ emissions while NO_x emissions increased slightly and then started to decrease in about 1998. As mentioned above, Figures 3.79 and 3.81 showed that the CAPMoN observed an increase in nitrate. However, those results are for combined fine and coarse nitrate since CAPMoN uses an open-face filterpack. For Figure 7.49 an estimation procedure was used to determine the fine fraction of the CAPMoN nitrate (fNO₃). This approach, which assumes that all sulphate is in the form of ammonium sulphate (i.e., fully neutral) and that the remaining particle ammonium is in the form of ammonium nitrate, provides reasonably unbiased estimates of fNO₃ in the colder months. Consistent with the gas ratio predictions in Shepherd *et al.*, (2001), Figure 7.49 shows that average cold season fNO₃ at several eastern Canadian CAPMoN sites increased during the time SO₂ emissions decreased. Also as expected, the increase was most dramatic in southwestern Ontario. Percent changes in concentrations from the CAPMoN data comparing the five years before and after SO₂ emission reductions are shown in Table 7.6. Increases in fNO₃ ranged from 18% to almost 1800%, depending upon location. The larger percent increases are in areas where fNO₃ tends to be small, such as northern Québec (Chapais) and Nova Scotia (Kejimikujik). As expected, sulphur, in both gas (SO₂) and fine particle phases (SO₄⁻²), decreased relatively uniformly across the area. Total sulphur decreased by an average of 35%, which is consistent with the relative size of the eastern North American SO₂ emission reduction between the two periods (32%).

Additional CAPMoN measurements are included in Table 7.6 to demonstrate that the increase in fine NO_3 was not due entirely to more nitrogen in the atmosphere arising from the small increase NO_x emissions. This is best exemplified by total nitrate (tNO_3), which is the sum of the measured HNO_3 and measured NO_3 (combined fine and coarse). The last column in Table 7.6 shows that at all the sites except Kejimikujik tNO_3 increased between the two periods. However, these increases ranged from about 4% to 25% which are substantially less than the corresponding fNO_3 increases. There was a decrease in HNO_3 at all but one site and estimated coarse particle nitrate (cNO_3), which can form when HNO_3 reacts with the crustal elements found on larger particles, also decreased at several sites. The HNO_3 decreases and the smaller increases in tNO_3 relative to fNO_3 indicate that a shift in the N distribution was part of the reason for the fNO_3 increase. The 'free NH_3 ' provided by the reduction in SO_4^{2-} led to more of the gas phase nitrogen (i.e., nitric acid - HNO_3) shifting to the fine particle phase. Thus, measurement data indicate that wintertime fine particle NO_3 increased in eastern Canada through the late 1990s and early 2000's. The theory discussed above and in Chapter 3 suggests that this was largely in response to reductions in SO_2 emissions. This recent experience with fNO_3 demonstrates that future strategies to reduce $\text{PM}_{2.5}$ will need to carefully consider the complexities of atmospheric chemistry and the possibility that decreases in some components in smog could result in increases in others.

In other parts of Canada higher ammonium nitrate in the cooler months is also typical (see the next section), however, in the LFV, seasonality in nitrate is much less pronounced (Brook and Dann, 1999). Organic compounds can also be responsible for elevated cold season (Nov.-April) $\text{PM}_{2.5}$, but they are typically the driving force behind episodes in localities impacted by wood smoke such as the interior valleys of BC and in specific communities where wood is commonly used for heating (e.g., St. Lawrence River Valley).

A clearer picture of the behaviour of $\text{PM}_{2.5}$: Insights from high time resolution composition measurements

For over thirty years measurements of particulate matter have been dominated by integrated samples. Particles in the size range of interest were collected on a filter or impaction surface after multiple hours of sampling. The typical time length, which is still the norm for most monitoring programs, has been 24 hours. Increased interest in $\text{PM}_{2.5}$ due to health concerns led to large investments in R&D worldwide, but especially in the U.S. One result of these efforts has been significant advances in measurement technologies capable of automated sampling and sizing and/or chemical characterization of particles (Wexler and Johnson, 2008) with hourly or better time resolution. One of the most important new instruments evolving from this work has been the Aerodyne Aerosol Mass Spectrometer (AMS). Environment Canada was one of the first groups worldwide to deploy the AMS, which was during the Pacific 2001 field study. Since that initial beta test, a tremendous amount of new insight has been gained and the AMS is now a standard part of most field studies in Canada. The 5-15 minute time resolution of its typical operating mode has revealed complex and independent variations in the main chemical fractions of $\text{PM}_{1.0}$ ¹ and also in the different size fractions within $\text{PM}_{1.0}$. These

measurements are helping to unravel the processes controlling $PM_{1.0}$ variations, including source influences, secondary formation and meteorology. What were once observed by TEOMs as short term variations in total mass, with limited understanding of the factors causing such behaviour, can now be seen much more clearly to involve a variety of processes. This is exemplified in Figures 7.1 and 7.2, which are short time sequences of measurements in the Lower Fraser Valley and Toronto.

The first case (Figure 7.1) was discussed in detail in Brook *et al.* (2004c). $PM_{2.5}$ was observed to increase above $10 \mu\text{g m}^{-3}$ at four different times in the period shown. This included three separate peaks on August 26th, which would never have been resolved with 24 hour integrated samples. Furthermore, without the chemical constituents from the AMS, it would be very difficult if not impossible to uncover the fact that these peaks each were associated with different sources or processes. A standard midnight to midnight 24 hour sample for the 26th would have reported $1.0 \mu\text{g m}^{-3}$ of nitrate, $1.1 \mu\text{g m}^{-3}$ of sulphate, $3.7 \mu\text{g m}^{-3}$ of organic carbon and $7.8 \mu\text{g m}^{-3}$ of total $PM_{2.5}$, with no indication that the peak amounts occurred at entirely different points in the period.

From the AMS measurements in Figure 1 it can be seen that the first peak, the morning of the 26th, was related to a sharp increase in particle nitrate (pNO_3). This is the typical time for formation of pNO_3 in the warmer months. Cool temperatures and high humidity are required and the greatest potential for such conditions are overnight and into the early morning. Thus, the first peak is mostly associated with local formation of secondary ammonium nitrate particles. The second peak, early in the afternoon on that day, had elevated particle sulphate (pSO_4) and organics (pOC), while the third was largely associated with pOC . Combined with meteorological information, these two peaks were linked to the sea breeze. The first peak is the movement inland of an air mass residing over the Strait of Georgia. This air mass contained secondary sulphate and organics that had formed over the previous few days as particles and precursors accumulated and reacted offshore. The third peak was related to the outflow or land breeze bringing the particle-laden air mass back across the observing site. The most interesting feature is the reduced pSO_4 relative to the pOC in the outflow. The reason for this behaviour is related to the locations of pSO_4 sources and pOC sources. For the former there are few SO_2 emissions inland over the LFV so the air mass did not accumulate new pSO_4 during that period, but the pSO_4 it contained continued to disperse thereby having a lower concentration in the return outflow. However, there are ample sources of primary and secondary pOC inland over the LFV, which continued to accumulate in the air mass and then impacted the observation site during the return outflow.

The biggest $PM_{2.5}$ event during the period shown was on the 27th of August. At this time, concentrations rose to almost $20 \mu\text{g m}^{-3}$, sharply at first and then gradually, with a few ups and downs, and then sharply again in the early morning. The pSO_4 , pOC and pNO_3 each behaved differently. The start of the event was likely inflow from the Strait and was enhanced in pSO_4 . Then later as the event continued wind directions shifted and brought in more pOC . At this

time other pollutants (not shown) also rose, including elemental carbon and carbon monoxide, indicating that relatively fresh combustion sources of pOC, likely from the more populated parts of the LFV (e.g., Vancouver area) were contributing to the PM_{2.5} event. This lasted overnight and was enhanced by local formation of pNO₃ as temperatures decreased and humidity increased. The event ended abruptly, with mass and the three main constituents decreasing together as a cleaner air mass behind a weak cold front pushed through.

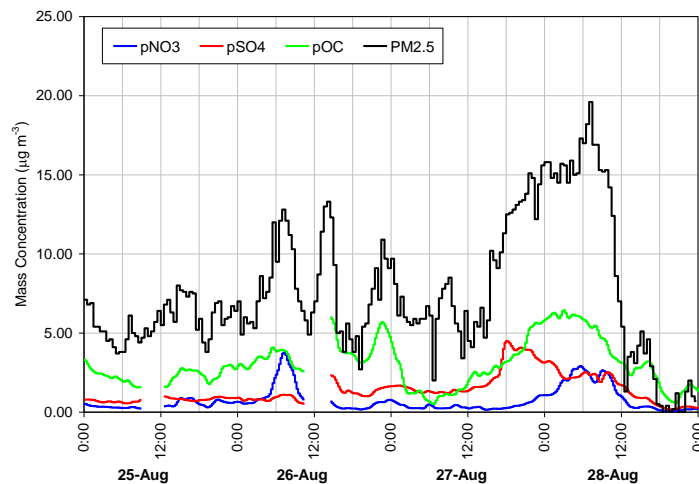


Figure 1 Aerosol Mass Spectrometer and TEOM measurements over four days in August 2001 at Langley, BC.

In Figures 2a and 2b, a short case study for Toronto is shown. TEOM PM_{2.5} data were not available at this location so only measurements from the AMS are shown. However, in addition to pSO₄, pNO₃, pOC, two useful marker ‘mass fragments’ are included. These are m/z 44 and m/z 57, which tend to be related to oxygenated, and hence more aged organics, and freshly emitted organics, respectively.

The first day of the episode, the middle of May 11th to middle of May 12th, was associated with PM_{1.0} consisting mostly of organics with two small separate nitrate peaks. The associated rises in m/z 57 suggest that these are fresh and more likely local emissions, which are building up over the city during this period due to stagnation. Traffic is suspected to be the major contributor. Closer examination shows that at the start of the time of build-up of NO₂ the pOC that increased was characterized by m/z 44 increases. This fragment indicates the presence of oxygenated organics, which can be from primary emissions, but also relates to secondary or more-aged organics. Overnight and into the morning of the 12th, m/z 57 rises sharply accompanied by increases in nitrate. This strong correlation suggests a common atmospheric process or source for the m/z 57 related organics and nitrate during this period. By the afternoon of the 12th a significant regional event started signified by a rapid increase in sulphate and shortly thereafter in aged organics (m/z 44). Then throughout the time of the highest PM_{1.0}, midday on the 12th to late on the 14th, the composition varied dramatically,

particularly the nitrate amount.

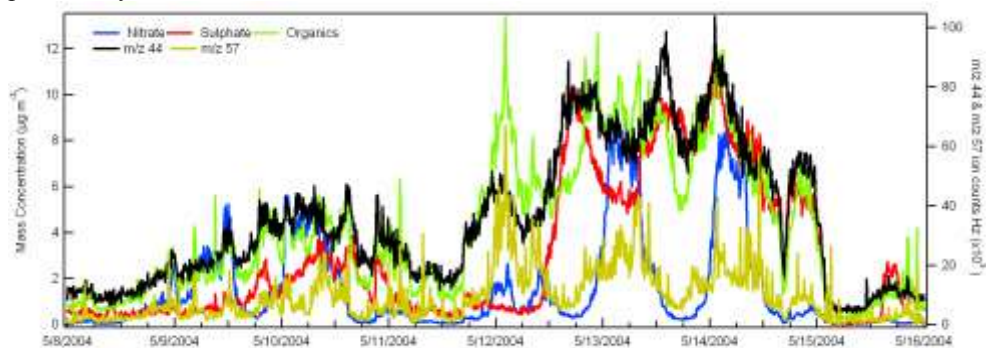


Figure 2a: Aerosol Mass Spectrometer time series for an eight day period in May 2004 In Toronto. PM_{1.0} is estimated by summing nitrate, sulphate and organics.

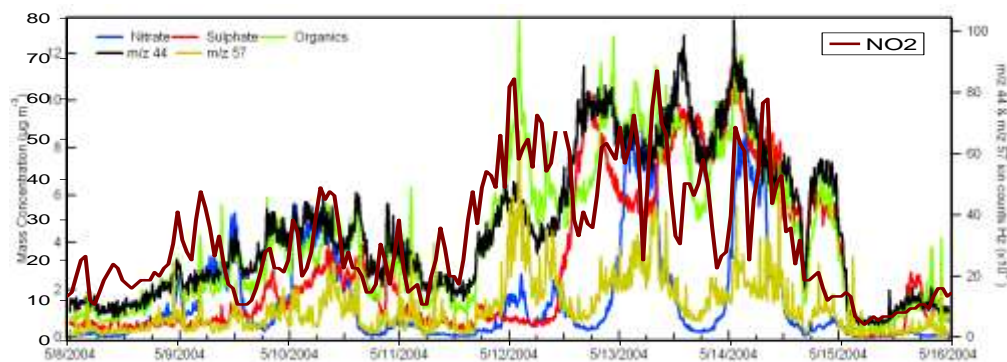


Figure 2b: Hourly NO₂ concentrations (ppb) averaged across Toronto are shown on top of the previous plot of AMS data. May 11 to 15 was a significant NO₂ episode. The AMS data show that the PM_{1.0} associated with that period varied significantly in terms of its chemical composition.

There were two major overnight to early afternoon nitrate formation events. These nights were associated with fog, which likely facilitated the formation of nitrate and also delayed the morning heating allowing nitrate to persist into the afternoon. During the first nitrate peak (PM_{1.0}~20 µg m⁻³ and NO₂~50 ppb) sulphate decreased and m/z 57 increased suggesting a decrease in mixing heights allowing the local emissions to build up and decoupling the surface from the more regional air mass that remained aloft above the inversion(s). Concentrations were low in the mid afternoon of the 14th (PM_{1.0}~13 µg m⁻³) due to a high mixing height and loss of nitrate caused by daytime heating. The highest particle mass concentrations occurred overnight on the 14th and into the morning of the 15th. PM_{1.0} was approximately 30 µg m⁻³. NO₂ levels were slightly lower compared to the previous night and this is also accompanied by slightly lower m/z 57 amounts. The greater amount of sulphate during this peak, as well as m/z 44, indicates that the particles and the air mass during this time were more homogeneous in composition in terms of contributions from local sources and the regional transport

component. By the end of the event early on the 15th NO₂ has decreased dramatically and particle levels are also somewhat lower. But the particle type was dominated by organics associated with m/z 44 and sulphate, with these two fractions appearing to co-vary closely. The overall message from Figures 2a and 2b is that this particle and NO₂ event was characterized by the build up of local emissions, followed by the arrival of transported particles. These two ‘air masses’, the local and regional, gradually interacted and mixed, becoming more homogeneous after the second day and becoming more aged later in the period. Analysis of other events in Toronto have shown a similar pattern of particle build-up (i.e., local then regional), suggesting that the case in Figures 2a and 2b may represent a relatively typical case urban build-up of particles in the Toronto area.

¹ The inlet to the AMS has a transmission efficiency which decreases above ~700 nm. Thus, it is considered to measure PM_{1.0}. Typically, a large percentage of the mass in PM_{2.5} is below 1.0 µm in the accumulation mode. Therefore, AMS measurements are highly indicative of PM_{2.5} and its behaviour.

7.5.5 Spatial and Temporal Patterns in PM_{2.5}, O₃ and Precursors over Alberta and the Prairies

There are significant challenges in understanding air quality problems in the Prairies. This is due to the influence of the Rocky Mountains on meteorology, the role of relatively unpolluted background air masses and natural phenomenon in regional air quality, the sporadic but important impact of forests, the poor coverage of monitoring in Saskatchewan and Manitoba and the near absence of full chemical speciation of PM_{2.5} across the Prairies. The available data indicate that air quality problems differ considerably from the cold season to the warm season. The former events are associated with greatly elevated PM_{2.5} and NO_x in urban and industrial areas resulting in reduced visibility. In contrast, warm season events, which are not as significant as those in the cold season, tend to exhibit more classic regional photochemical smog formation conditions, but forest fire emissions can play an important role.

In spite of the presence of the highest emissions of smog precursors in Canada, average O₃ and PM_{2.5} concentrations in the prairies are relatively low compared to the Windsor-Québec corridor. Despite their relatively low median concentrations, Edmonton and Calgary are both close to the Canada Wide Standard 2010 target for O₃. The lack of widespread monitoring in Saskatchewan and Manitoba limits the understanding of the regional transport of emissions from Alberta, the highest emitting province. The fate of these emissions is unclear and questions remain about the extent of secondary pollution formation and deposition downwind.

The relatively strong winds throughout the Prairies seem to ensure that PM_{2.5} and O₃ precursors are dispersed over a wide area, thus preventing widespread build up of air pollutant concentrations. Near high emission locations, high concentrations do occur when there is

reduced mixing in the lower boundary layer. As illustrated in Chapter 3 this becomes an issue of note in some Prairie cities, particularly with respect to nitric oxide (NO) concentrations in the winter and areas with high VOC emissions. This includes east Edmonton and Fort Saskatchewan, part of Alberta's Industrial Heartland. These high concentrations are related to lower mixing heights and periods of low wind speeds due to more frequent periods of cold and stable conditions. Mixing heights in winter are lower and less variable than in summer (Figure 7.27) leading to the observed seasonal patterns for PM_{2.5} and NO_x (Dawson, Adams and Pandis, 2007). Increased emissions for heating may also contribute to higher winter concentrations and for some periods and/or locations poorer performance of vehicles (e.g., cold starts, operating in cold conditions) may also play a role.

At all monitoring locations in Alberta, Saskatchewan and Manitoba, median and maximum NO concentrations tend to peak in December and January. Minimum average NO levels occur in spring and summer, typically between May and July. Since seasonal patterns are similar at all sites only Edmonton East is illustrated in Figure 7.51 as an example. NO₂ concentrations follow a similar pattern as NO, though with monthly maximum concentrations observed in January and February, and monthly minimum concentrations usually observed in July. Weekly cycles in both NO₂ and NO (see Chapter 3) are evident at urban sites such as Edmonton and Calgary, showing the important influence of road traffic on urban NO_x levels.

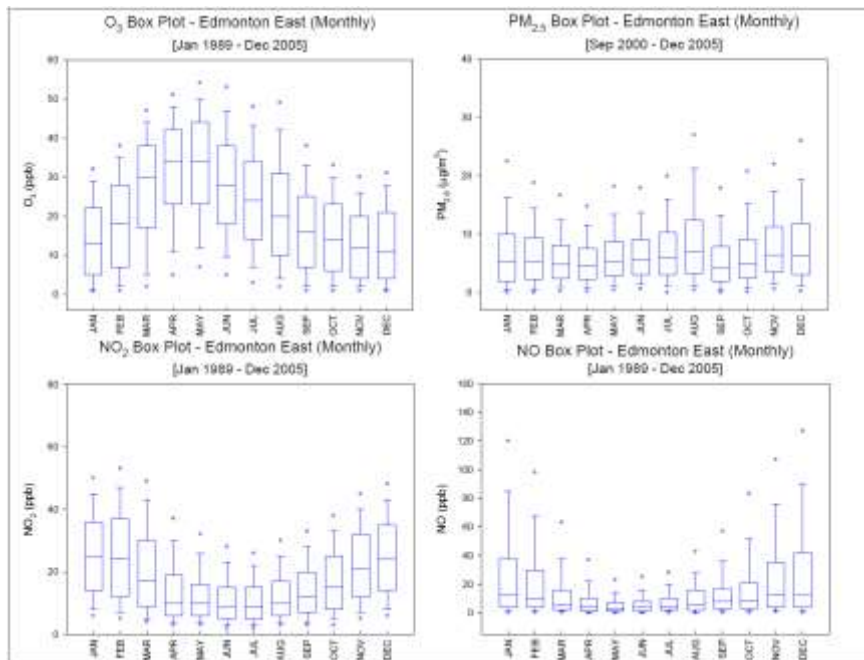


Figure 7.50 Seasonal cycle of O₃, PM_{2.5}, NO₂ and NO at Edmonton East monitoring site
 Box plots display: the 95th percentile (highest circle), 90th percentile (upper whisker), 75th percentile (upper boundary of box), median (horizontal line through box), 25th percentile (lower boundary of box), 10th percentile (lower whisker) and 5th percentile (lower circle) of all observations for each category.

Twenty four hour average $PM_{2.5}$ concentrations above the CWS metric value ($30 \mu\text{g m}^{-3}$) have been occasionally observed at most Alberta sites. At urban sites and sites influenced by urban and/or industrial emissions, $PM_{2.5}$ concentrations peak in winter and again in summer (e.g. Figure 7.50). At urban sites experiencing the greatest concentrations, the winter and summer peaks are approximately equal in magnitude. However, these data are from TEOM measurements which are known to lose mass in the winter (Chapter 3). Correction for this bias would likely result in winter $PM_{2.5}$ being greater than summer $PM_{2.5}$. Filter-based mass measurements are discussed below and they support this assumption and indicate that cold season $PM_{2.5}$ events have considerably higher concentrations than those in the warm season.

The summer peak in $PM_{2.5}$ is interpreted as due to the combined influence of forest fire smoke and greater prevalence of windblown dust during the snow free months. Moderately elevated $PM_{2.5}$ related to anthropogenic sources has been observed in the summer as discussed in Section 7.7.13. Few remote or regionally representative $PM_{2.5}$ measurements are available in the Prairies, however at these sites, observations $>30 \mu\text{g m}^{-3}$ occur almost exclusively in the May through September period. An analysis of episode causation (Johnson, 2005), attributed nearly all such episodes to forest fire influence.

Table 7.7 Edmonton mass reconstruction using speciation sampling results and formulae as described in Section 3.5.2 (Chapter 3). Concentration measurements to compute the contributions from Soil and TOE (total other elements) are not available for this period.

	Average $PM_{2.5}$ Mass	% Unaccounted	% ASO_4	% ANO_3	% OM	% EC	% SOIL	% TEO	% NACL
Average	8	12	14	26	31	13	-	-	3
Apr – Sep (warm)	6.3	23	21	11	33	12	-	-	1
Oct – Mar (cold)	8.9	7	12	33	31	13	-	-	4
10 highest warm	9.3	26	19	9	36	10	-	-	1
10 highest cold	17.3	9	15	47	20	8	-	-	1
Total mass $> 15 \mu\text{g m}^{-3}$	18.8	9	15	47	20	8	-	-	1

Limited $PM_{2.5}$ speciation data are available for the Prairies, with only one site in operation since May 2007 (see Table 3.16). Table 7.7 provides an overview of the percent contribution of the major constituents for the period from September 2006 to June of 2007. For this limited period of analysis it is interesting to note that all seven of the events with 24-hr filter-based $PM_{2.5}$ mass over $15 \mu\text{g m}^{-3}$ occurred in winter: one in November, three in December and three in February. On average, the major contributor to the mass was organic matter, reflecting the urban location of the site. As observed in eastern Canada, ammonium sulphate contributed

more to the total mass in the warm season than the cold and ammonium nitrate followed the opposite pattern. During the higher concentration events in the cold season, which were considerably greater in magnitude than the high warm season events, ammonium nitrate was the dominant constituent, responsible for nearly 50% of the total mass. The warm season events were characterized by an increase in the prevalence of organic matter on PM_{2.5}. Unlike eastern Canada, ammonium sulphate was less important during these periods. The importance of organic matter to these events suggests that regionally elevated PM_{2.5} associated with forest fires, as discussed above, has an impact on Edmonton. Figure 7.93 in Section 7.7.4.3 presents further evidence of this feature based upon receptor modelling results.

Median ozone concentrations at all sites in the region are highest during the spring months of March through June, which is in common with the majority of mid-latitude Northern Hemisphere sites (Monks, 2000). Northern Alberta sites such as Fort Chipewyan have highest median and 95th percentile O₃ in April. At southern Alberta and southern Saskatchewan sites, median O₃ peaks in May while 95th percentile O₃ has a broad maximum from April through August (Figure 7.50). Elevated O₃ in spring is suspected to be related to transport from the stratosphere or free troposphere (Refer to the “Stratospheric Ozone Influences in Alberta” text box), while O₃ in late summer is more-likely related to local photochemical production (Section 7.7.13).

Urban sites heavily impacted by NO_x emissions tend to have minimum O₃ in mid-winter, coincident with maximum NO concentrations. Minimum O₃ levels at high elevation sites and remote northern sites (Fort Chipewyan, Hightower Ridge and Steeper) are during August through September. This pattern has also been observed at Northern European sites (Monks, 2000) and Figure 7.45 illustrates that all of the Canadian sites included experience a springtime maxima for at least a few, if not all, transport pathways. Typically, sites that are only modestly influenced by urban or industrial NO_x emissions tend to have a broad minimum in median O₃ concentrations from August through January.

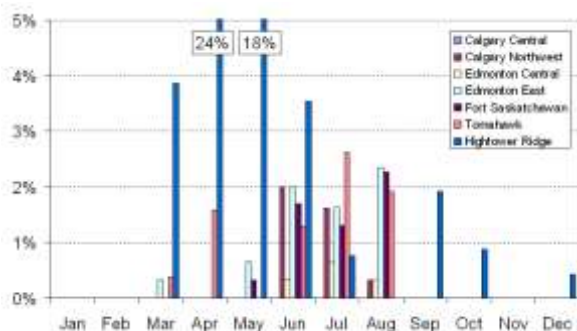


Figure 7.51 Percent exceedances of the CWS for O₃ in Alberta – comparison of urban and non-urban sites. (Percentage of days with 8 hour ozone >65 ppb at a selection of Alberta sites)

Eight hour average O₃ concentrations above the CWS metric value have been observed at many Alberta stations (Chaikowsky, 2001). They are most common at high elevation sites in western Alberta such as Hightower Ridge, where maximum daily 8-hour averages above 65 ppb have been observed in most months of the year, but are most common in April and May. Near the urban areas of Edmonton and Calgary, 8-hour ozone observations above 65 ppb are most common from June through August, though occasional 8-hour average observations above 65 ppb are observed in March through May and September. Central urban sites such as Edmonton Central and Calgary Central are strongly influenced by local NO_x emissions and so rarely exceed the CWS for O₃, while outlying sites such as Tomahawk, Edmonton East, Fort Saskatchewan and Calgary Northwest, experience more frequent observations above the CWS metric (see Figure 7.51). Calgary emissions may cause more frequent observations of O₃ above 65 ppb downwind of the city, as suggested by modelling work (Fox and Kellerhals, 2007), but there are no ambient O₃ observations in the vicinity to verify this. Eight hour O₃ levels above the CWS are rare at monitoring sites in southern Saskatchewan and southern Manitoba.

In Alberta, continuing to track the frequency, trend and spatial pattern of events with O₃ concentrations greater than 82 ppb for a one hour average is important to consider because most cases are associated with local smog production. In contrast, observations above the 65 ppb 8-hour CWS level occur regularly both during local smog episodes and perhaps even more often as a result of high springtime O₃ levels that can be heavily influenced by natural phenomena, including stratospheric O₃. Consequently, the provincial government continues to maintain an hourly objective. Observations above this threshold are less common than observations above the CWS benchmark and are most common in the area of Central Alberta centered on Edmonton and extending east and west. Occasional exceedances have also been observed at Red Deer, Calgary and Hightower Ridge. Exceedances are most common in August, July and June (Chaikowsky, 2001), further supporting this measure as being a more effective indicator of human-influenced smog events.

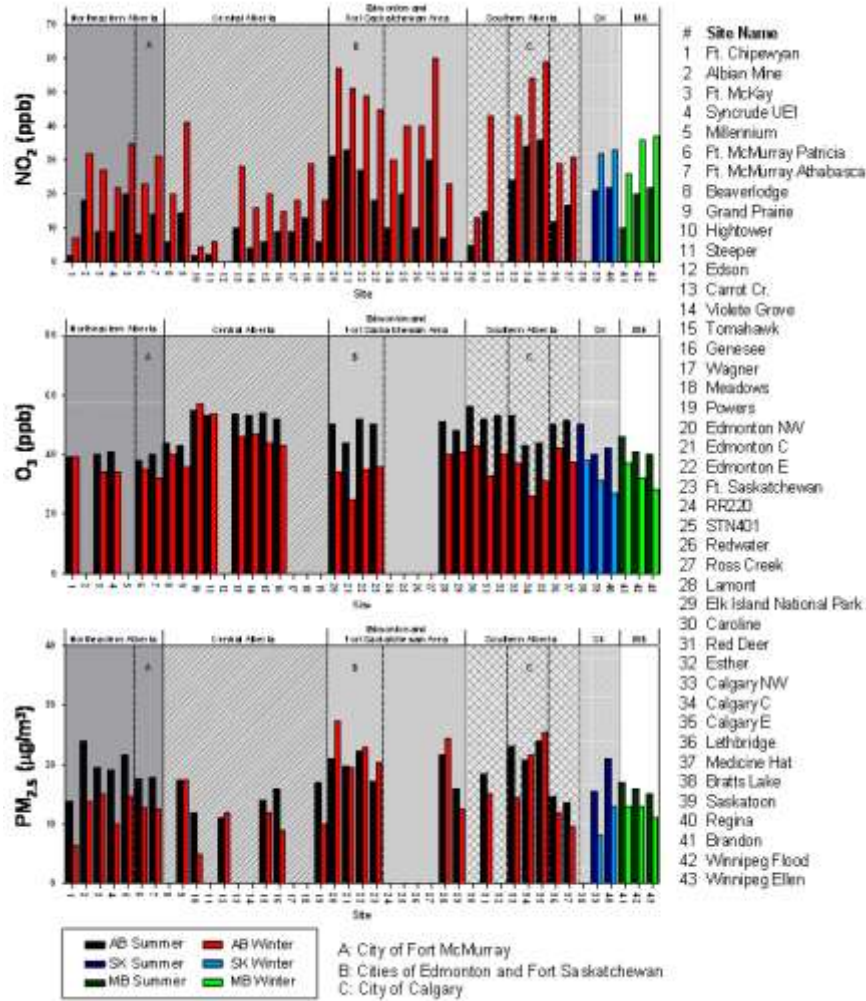


Figure 7.52 95th percentile NO₂ (top), O₃ (middle), and PM_{2.5} (bottom) concentrations in summer and winter (2000-2005) at sites across the Prairies.

Figure 7.52 shows the 95th percentile NO₂, O₃, and PM_{2.5} for all Prairie monitoring sites separated by summer and winter. Among the larger communities, 95th percentile NO₂ concentrations are highest in Edmonton and surrounding industrial areas followed by Calgary, Winnipeg, Regina and Saskatoon. Some smaller communities such as Red Deer and Grande Prairie also have relatively high NO₂ concentrations. NO₂ levels at sites in northern Alberta near oil sands industrial operations and in adjacent communities are comparable to those in medium size towns and cities. During the summer months, 95th percentile O₃ levels are fairly similar across the southern half of Alberta, except in city centre locations where it is lower due to NO titration. Summer time O₃ is lower in northern Alberta and in Saskatchewan and Manitoba. In the winter months, 95th percentile O₃ concentrations are consistently lower in those areas affected by NO emissions. During the summer period, 95th percentile PM_{2.5} concentrations are generally slightly higher in urban areas than rural areas, while in winter

urban areas have substantially higher $PM_{2.5}$ than rural areas. This is consistent with a regional forest fire influence in summer, and a proportionally greater impact of local emissions during winter.

Winter events with high $PM_{2.5}$, NO and NO_2 , are most frequent in the Edmonton and Calgary areas (Qiu and Pankratz, 2007) as reflected by greater average $PM_{2.5}$ concentrations in urban centers in winter. Of the nine independent wintertime $PM_{2.5}$ events recorded in the prairies between 1999 and 2003, seven of them were from the Edmonton area (Johnson, 2005). Investigation of specific winter smog events shows that correlations between NO_2 and $PM_{2.5}$ are lower than between NO and $PM_{2.5}$ (see 'winter smog' text box) The high NO to NO_2 ratios (see Figure 3.31) in winter are likely related to low O_3 concentrations and low temperatures resulting in slower conversion of NO to NO_2 (Jenkin and Clemitshaw, 2000).

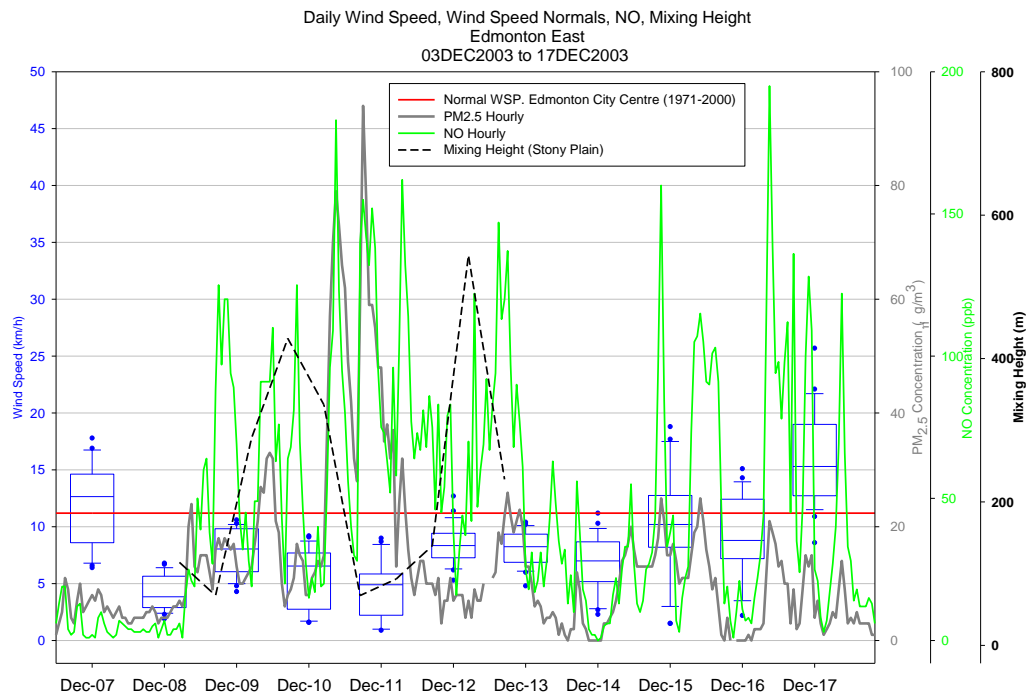


Figure 7.53 $PM_{2.5}$ concentration (heavy grey line) and NO (green line) mixing ratio along with wind speed and mixing heights during a winter episode in Edmonton. Pollutants and wind speed were measured at Edmonton East monitoring station, estimated mixing height was determined from Stony Plain radiosonde launches, 20km west of Edmonton. The blue box and whisker plots indicate the observed wind speeds on each day while the red line shows the long term average wind speed at the site. Note the observed wind speeds were much lower than average during the highest NO and $PM_{2.5}$ periods on Dec. 10 and 11.

An example of a winter smog event in Edmonton is shown in Figure 7.53. During this event 24 hour $PM_{2.5}$ levels on December 10th, 2003, as measured by TEOMs, rose to above the CWS level at three Edmonton sites and at Fort Saskatchewan. Peak hourly $PM_{2.5}$ concentrations reached $97 \mu\text{g m}^{-3}$. $PM_{2.5}$ concentrations elsewhere in Alberta were not highly elevated during

this time. In this event PM_{2.5} began to increase on December 8th with the onset of light southeast winds. Very light winds, low mixing heights and fluctuating wind direction possibly causing some recirculation of pollution accompanied the peak in PM_{2.5} levels on Dec 10th. The peak in PM was also accompanied by near saturated relative humidity (92%) and cold temperatures (-17.1°C). The smog event was terminated on December 17th by a return to a moderate westerly wind flow.

Summertime smog events in the Prairies, which consist of elevated O₃ with modestly elevated PM_{2.5} concentrations, occur relatively infrequently in Alberta. Nonetheless, they have been identified as a source of concern because O₃ levels in Calgary and Edmonton are close to the CWS and Alberta's ozone management framework (Alberta Environment, 2007) requires each area to develop a plan designed to prevent exceedances of the CWS.

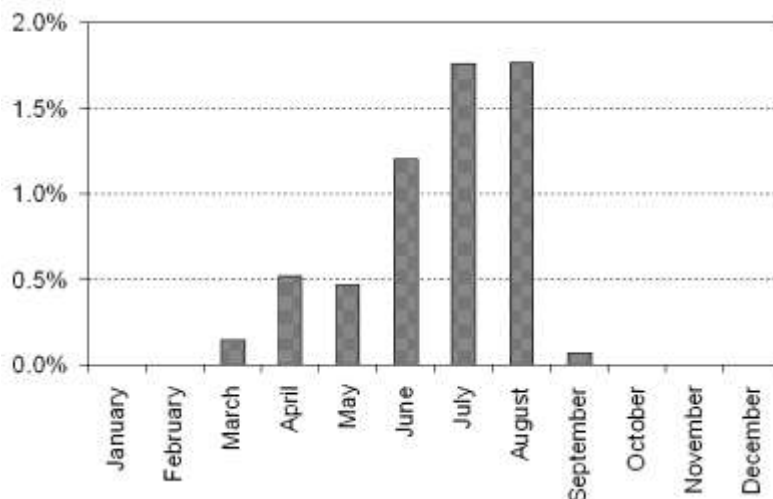


Figure 7.54 Mean frequency of days with 8-hour ozone above 65 ppb at five sites near Edmonton (1996-2005). The five Edmonton area sites are Edmonton Northwest, Edmonton Central, Edmonton East, Fort Saskatchewan and Tomahawk (80 km WSW of Edmonton) monthly frequency of ozone episodes in Edmonton 1989-2003. An ozone episode is defined as a day with one or more of the four Edmonton area sites (Northwest, Central, East and Fort Saskatchewan) reporting 8-hour O₃ above 65 ppb.

Ozone episodes above the CWS level of 65 ppb and above the Alberta one hour objective of 82 ppb are more frequent in Edmonton than Calgary. The Edmonton area has greater emissions of NO_x than Calgary, and mean summertime winds in Edmonton are weaker than in Calgary. To some extent, the lower frequency of high O₃ observations in Calgary may have to do with the placement of air quality monitoring sites. In Calgary two of the three monitoring sites are in locations that are strongly influenced by NO_x emissions most of the time, while in Edmonton area three of the four monitoring sites with long periods of record are outside the urban core. In Edmonton, O₃ episodes occur most frequently in the June-August period (Figure 7.54). Some of the early season (April-May) episodes happen under conditions not usually associated with photochemical smog, a description of the possible causes of these events is

included in the “Stratospheric Ozone Influence in Alberta” text box. Typical summertime high O₃ events in Alberta affect a limited number of stations, and often last only 1-2 days. Summertime O₃ events are often terminated by a return to strong synoptic flow or by the development of deep convection, both events that dilute precursor emissions. On occasion, O₃ episodes lasting 3-4 days with elevated levels over much of central Alberta, have been observed. Examples of this occurred in June and July 2002 (Fox and Kellerhals, 2007).

Stratospheric Ozone Influence in Alberta

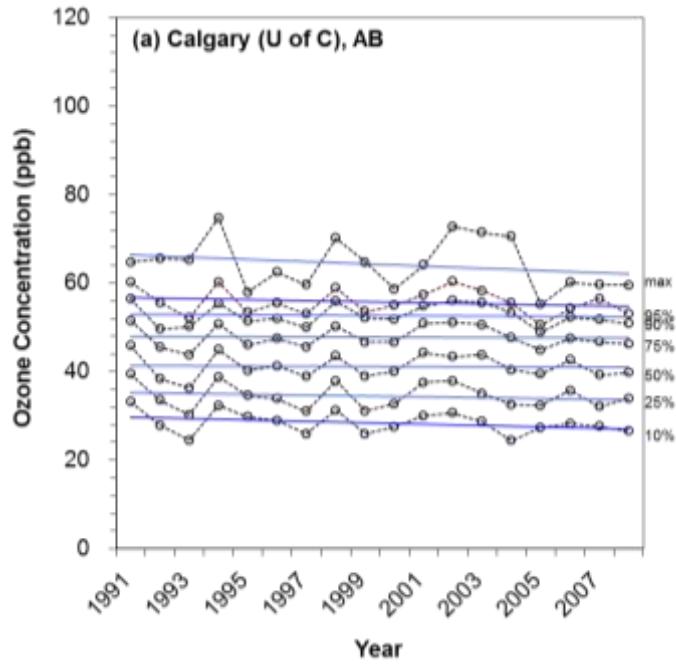
Investigations of surface O₃ concentrations at two high-elevation sites in the Rocky Mountain Foothills of Alberta have suggested that stratosphere/troposphere exchange (STE) is a source for the observed high O₃ levels in selected instances. There is consistent evidence of elevated ozone in the upper troposphere with occasional observations consistent with recent stratospheric injections of ozone. This upper tropospheric layer of elevated zone becomes a reservoir with a stratospheric origin and a source of downward ozone transport within the troposphere. The overall stratospheric contribution to surface O₃ concentrations at these two sites remains unknown and the importance of STE to surface O₃ at lower elevations has not been quantified. Measurements of O₃ and the stratospheric tracer ⁷Be, an isotope of beryllium, were made at Hightower Ridge in 1999 (1441 meters above sea level) and Harlech in 2004 (1569 meters above sea level).

Average concentrations of ⁷Be at Hightower Ridge were higher than those at lower elevation sites in Canada (Hessel, 2003), suggesting an overall greater proportion of stratospheric air at the high elevation site. Measurements of NO_x and wind direction ruled out significant local production of O₃ or transport of polluted air from nearby source regions (Hessel, 2003). On May 20th, 1999 a peak concentration of ⁷Be (9.81 mBq m⁻³), was observed, the highest seen during the study. The meteorology of this event was investigated in detail using the mesoscale meteorological model MM5 and a synoptic analysis. The MM5 simulation showed a stratospheric intrusion over west-central Alberta and meteorological evidence supports conditions favourable for STE. Measurements of ⁷Be at Stony Plain, a site 280 km east of Hightower Ridge, were also elevated on May 20th and 21st (Arthur, 2003). In this documented episode of STE, O₃ levels at Hightower and at lower elevation sites to the east were slightly elevated above seasonal norms.

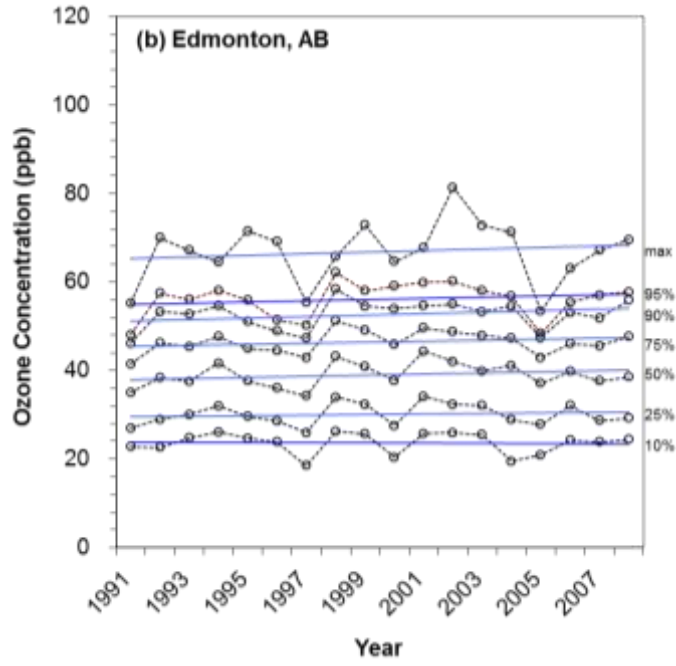
Surface O₃ and daily ⁷Be were measured at Harlech in 2004. O₃ concentrations observed at Harlech during the study period (March 3rd to June 30th, 2004) ranged from 16 ppb to 66 ppb with a mean of 43 ppb. These observations are consistent with other high elevation sites in Alberta (Hessel, 2003; Peake and Fong, 1990). Limited diurnal variation in the O₃ observations indicates little NO_x titration, suggesting the site is minimally influenced by local pollution. The peak ⁷Be and O₃ observations occurred on April 4th with ⁷Be concentration of 7.6 mBq m⁻³ and average O₃ for the filter period of 56 ppb (Raven, 2005). Meteorological conditions were favourable for STE and global Lagrangian dispersion modelling shows

instances of high level air descending into the mid-troposphere. These analyses indicate the event observed at Harlech is likely the result of an upper air source (possibly stratospheric) originating over Russia. The peak event was one of four instances observed where measured ^7Be was greater than 2 standard deviations above the average for the study period. No instances occurred when ^7Be concentrations were above the 8 mBq m^{-3} threshold sometimes employed to identify possible stratospheric intrusions (Cristofanelli *et al.*, 2006). Nevertheless, over the period of measurement O_3 and ^7Be levels were strongly correlated indicating likely input of O_3 from the stratosphere or upper troposphere.

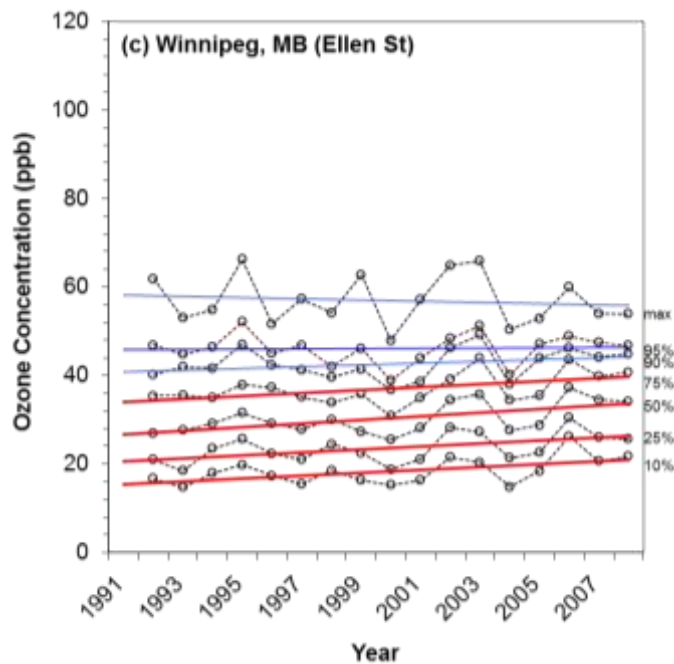
Hocking *et al.* (2007) observed frequent stratospheric intrusions over Ontario and Québec, most of which were dispersed in the mid-troposphere. Long-term ozonesonde measurements in Alberta demonstrate that high levels of O_3 are chronically present at mid-tropospheric elevations particularly in April through June. Both measurements and modelling, including back trajectory calculations, indicate that a significant portion of that O_3 is stratospheric in origin. Numerous studies have suggested that STE has a pronounced maximum in spring (e.g. Danielsen and Mohnen, 1977; Appenzeller *et al.*, 1996; Elbern *et al.*, 1997), but there is observational evidence from both North America and Europe (Merrill *et al.*, 1996; Beekmann *et al.*, 1997; also Holton *et al.*, 1995), as well as recent Canadian field studies using ozonesondes (He *et al.*, 2009) that the mechanisms of exchange are equally common in summer. However, the O_3 present in the free troposphere is most likely to be mixed to the surface, and hence be observed, in April and May when high O_3 concentrations coincide with higher mixing heights and more vigorous mixing in the lower troposphere. Early spring O_3 episodes that are associated with low levels of precursors, and that occur under weather conditions not typically associated with photochemical smog formation are likely due to down-mixing from this mid-tropospheric reservoir of O_3 .



a)



b)



c)

Figure 7.55 Trends in warm season (May-September) daily 8 hour maximum ozone concentrations for 1991-2008 in three Prairie cities. Trend lines shown in red are statistically significant with 95% confidence based upon the T Test.

Trend analyses in Chapter 3 showed that over the past 15-20 years the evidence that O₃ levels in Prairies have changed is inconclusive (see Figure 3.21 and Table 3.7). Figure 7.43 shows that there may have been a slight increase in rural background levels in the mid 1990's based upon observations at Esther, Alberta, and Bratt's Lake, Saskatchewan, but from the late 1990's to the late 2000's the mean O₃ levels have been relatively steady. Not surprisingly, Table 3.4 indicates that there were no significant trends at either of these sites. Trends for Calgary, Edmonton and Winnipeg based upon different parts of the O₃ distribution are shown in Figure 7.55a-c. Only the 10th to 75th percentile values in Winnipeg reveal a statistically significant upward trend. These increases in the lower part of the distribution are consistent with the Canadian urban site average pattern shown in Figure 3.24. This site is adjacent to the downtown core and since the city has seen only modest growth during the period of record it is likely that the decreasing NO_x emissions and subsequent decreases in urban NO_x concentrations have lead to the observed increases in O₃.

There is some weak evidence of change in Edmonton and Calgary, however they are opposite of each other with slight increases in Edmonton and slight decreases in Calgary. This latter site is located near the University of Calgary with residential development to the north and west. The location is primarily affected by transportation and space heating emissions. The lack of a significant change despite decreases in motor vehicle emissions may be because Calgary has been growing rapidly during the period so increases in traffic and population have counteracted the improvements in vehicle emission controls and fuels. The Edmonton location

shown is in the east part of the city, which is typically on the downwind side, but on the upwind or western edge of the industrial part of the region. Thus, this site most frequently represents emissions from an urban centre and is strongly influenced by NO_x emissions. The small rises through the period may reflect the decreases in NO_x , as in most urban locations.

It is worth noting that the Edmonton rises appear to be the largest for the upper parts of the O_3 distribution, which tends to reflect the levels experienced during photochemical events driven by relatively local formation. While anthropogenic emissions could be playing a role, the apparent larger rise in the maximum 8-hr O_3 is clearly influenced by the peak during the period of 81 ppb in 2002. This high value may have a link to forest fires in western Canada, which emit O_3 precursors. 2002-04 were periods of greater fire activity (Lavoué and Stocks, 2010) and the maximum 8-hour values in Figures 7.55a and 7.55b for both Calgary and Edmonton respectively, appear to reflect this. However, it is interesting to note that the largest maximum in Edmonton in 2002 was not seen in Calgary. The location of the fires may be the reason for this difference given that they were mostly located in northern parts of Alberta and Saskatchewan (Lavoué and Stocks, 2010), which would have influenced Edmonton more than Calgary. Clearly, O_3 behaviour in the Prairies should continue to be monitored to ensure that any upward trends are quickly identified and diagnosed. However, the lack of systematic rural measurements in regions that might be most influenced by the growing energy sector emissions in Alberta (see Section 7.7.13) will hinder determination of trends in the parts of the region where changes may be most rapid.

Wintertime Smog on the Prairies: Primary Pollutants and Stagnation

Events of elevated $\text{PM}_{2.5}$ and very high NO_x concentrations, which result in haze and notably degraded air quality, occur more frequently in the winter than in the summer (Qiu and Pankratz, 2007). Winter smog events occur more frequently in Edmonton than in Calgary (Figure 1). Of the nine independent winter high $\text{PM}_{2.5}$ events recorded in the prairies between 1999 and 2003, seven of them were in the Edmonton area (Johnson, 2005).

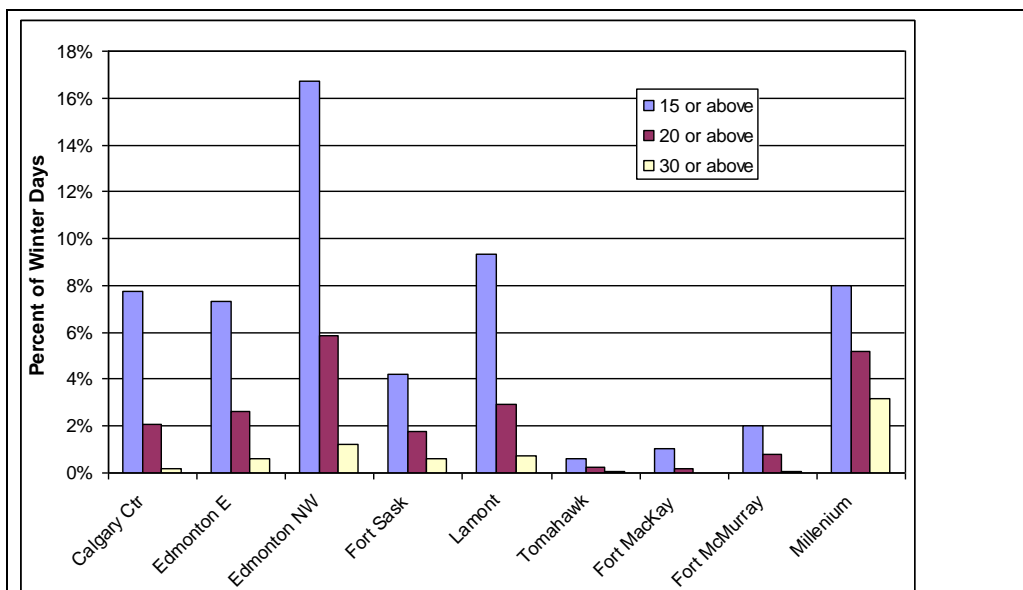


Figure 1 – Percentage of winter days (October to March) with 24-hour $PM_{2.5}$ above three thresholds ($30 \mu g m^{-3}$, $20 \mu g m^{-3}$, and $15 \mu g m^{-3}$) at selected Alberta sites. $PM_{2.5}$ from 1998 through 2006 (though many sites have shorter periods of record). All $PM_{2.5}$ measurements were made using non-FRM equivalent TEOM instruments and are likely under representing mass as a result of nitrate loss (see Chapter 3). All sites are urban except as follows: Millenium (industrial), Fort MacKay (small community), Tomahawk (rural/industrial), Lamont (industrial)

Unlike summer photochemical smog, winter events are largely the result of the build up of primary pollutants, particularly combustion products, and ozone levels are low. Investigation of specific winter smog events shows high NO_x concentrations and elevated $PM_{2.5}$, though high NO_x concentrations can also be observed without notable $PM_{2.5}$ concentrations (Table 1). Both NO_x and $PM_{2.5}$ are emitted from auto exhaust and other combustions sources and when NO_x is high it is reasonable to expect $PM_{2.5}$ to be present as well. The absence of elevated $PM_{2.5}$ is likely, at least in part, a result of the inability of the TEOMs used to capture and detect ammonium nitrate and semi-volatile organic compounds.

Analysis of high $PM_{2.5}$ events in the prairies between 1999 and 2003 showed that smog events were the result of local build up of pollutants under calm conditions (Johnson, 2005). However, calm conditions do not always result in high concentrations of $PM_{2.5}$ and NO_x . Detailed analysis of selected events suggests that the combination of low mixing height and calm winds is necessary to trigger the event. Temperature does not appear to be as important to the episodes as air movement. While no single synoptic pattern appears to be related to the winter smog events, common features are: a ridge of high pressure over or west of the area, northerly or westerly flow aloft, and light southerly or southeasterly surface flow (Johnson,

2005). Event termination seems to be associated with the breakdown of the ridge and a shift to westerly surface flow. Typically events break down quickly, lasting for only a few days.

Table 1: A summary of the highest 24-hr NO₂ and NO levels (ppb) observed in Alberta from 1998 to 2006. The two highest 24-hr average PM_{2.5} observations (µg m⁻³) are also included at the bottom of the list. Median PM_{2.5} mass for the cold season is: Calgary Central, 7.0 µg m⁻³, Edmonton Central, 5.7 µg m⁻³, Edmonton North West, 9.0 µg m⁻³. For PM_{2.5} 24 hour averages are calculated from hourly average TEOM data. Note: days with less than 75% available data were not included.

Date	Location	PM _{2.5}	NO ₂	NO
17-Jan-05	Calgary Central	14.7	61.1	224.6
20-Dec-02	Edmonton NW	31.5	68.7	335.7
20-Dec-02	Edmonton C.	22.1	57.2	236.5
19-Dec-02	Edmonton NW	20.2	52	281.8
10-Dec-02	Edmonton NW	16.1	48	235
29-Jan-02	Edmonton NW	17.8	60	203.3
08-Nov-01	Calgary Central	21.5	62.6	253.2
18-Jan-00	Edmonton NW	27.4	43.7	204.1
23-Jan-98	Calgary Central	22	60.1	215.2
17-Jan-98	Calgary Central	22.8	66.4	215.1
14-Jan-98	Calgary Central	21.5	66.5	227.4
25-Feb-04	Edmonton C.	51.5	47.8	100.5
10-Dec-03	Edmonton NW	54.3	49.9	152.7

Though only limited particulate composition data are currently available (Table 2), it is clear that the primary component of winter smog is ammonium nitrate (ANO₃). What is interesting to note is that the mass amount of elemental (EC) and organic carbon (OM) contributing to the total filter mass in Edmonton is similar to that in Toronto and Windsor even though the total PM_{2.5} is lower (Figure 3.47 and 3.51). However, on the ten highest PM_{2.5} concentration days the OM and EC mass only increase slightly above the seasonal average compared to the increase in ANO₃, which contributes a much greater proportion of the mass. As with the other western Canada sites, ammonium sulphate (ASO₄) is a relatively small contributor to winter PM mass (Figures 3.62 and 3.63). However, its concentration increases significantly during the peak winter episodes suggesting that there are local emissions sources (Figure 3.65).

Table 2: Edmonton cold season average filter-based mass and composition ($\mu\text{g m}^{-3}$) from October 2006 to March 2007. All available days are averaged in the first row and in the bottom row the ten days with the highest $\text{PM}_{2.5}$ are averaged separately. Unaccounted refers to the residual mass when all the measured chemical species are subtracted from the gravimetric mass measurement.

	Mass	Unaccounted	ANO3	ASO4	OM	EC
Overall average	8.95	0.67	2.91	1.04	2.80	1.14
Average from ten highest days	17.27	1.62	8.07	2.55	3.46	1.34

Future use of continuous $\text{PM}_{2.5}$ instruments that are less sensitive to semi-volatile loss (nitrate) can be expected to indicate that PM levels are higher during the cold season than currently reported (see Figure 3.50 for estimates of the magnitude of the current low bias). Additional analyses of the growing database of $\text{PM}_{2.5}$ chemical speciation will improve the understanding of its true levels and major sources.

7.5.5.1 Air Quality in the Oil Sands Region

Ozone, $\text{PM}_{2.5}$ and NO_x levels in the city of Fort McMurray are generally low compared to Edmonton or Calgary, are comparable to other cities of the same size, and exhibit the same seasonal and diurnal patterns. Under prevailing winds the city is likely upwind of the mines and upgrading facilities to the north. It is notable however that while NO_2 concentrations have been found to be declining in many areas of the province, NO_2 is increasing at the measurement site on the northern edge of Fort McMurray (Alberta Environment 2008), possibly as a result of the increasing population in the region, increasing industrial activity, or both. At several monitoring sites in the region, hydrogen sulphide (H_2S) concentrations have exceeded the provincial objectives for both the one hour average and the 24-hr average (Alberta Environment 2008). Since H_2S is ultimately oxidized to sulphate it could be a contributor to regional $\text{PM}_{2.5}$. Observed average benzene and styrene concentrations in Fort McMurray and Fort McKay are above the Canadian 75th percentile (Wade, Brown and Roberts, 2007).

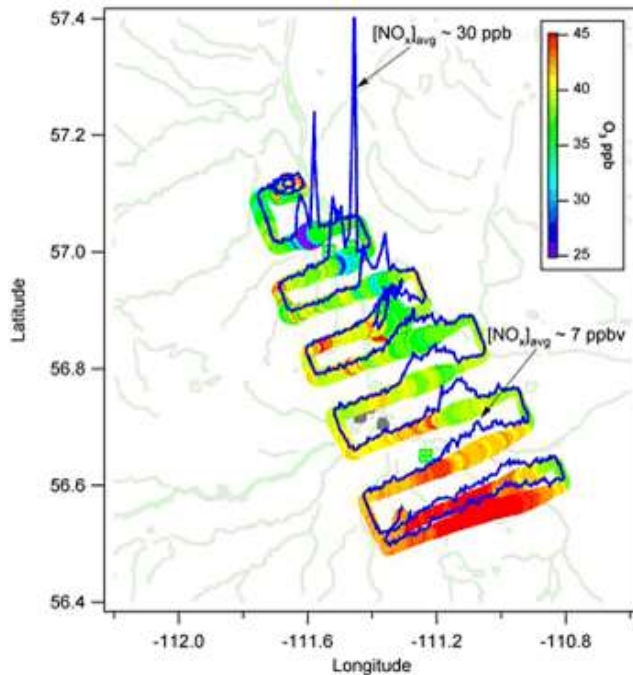


Figure 7.56 Ozone production and NO_x loss during a plume tracking sampling flight, August 10, 2001. The blue line represents NO_x concentrations observed during the flight, with concentrations increasing along the z-axis (not shown for simplicity). Ozone concentrations measured on the same flight are shown as a colored surface. Note the higher NO_x concentrations associated with lower ozone concentrations. Figure reproduced from AMEC, 2003. Ozone production and NO_x loss during a plume tracking sampling flight, August 10, 2001. Reproduced from AMEC (2003).

Understanding air quality in the oil sands region is complicated by the availability of measurements. For example, the current fixed monitoring sites in the oil sands area are likely not measuring peak secondary pollution formation. Most sites in the Wood Buffalo Environmental Association air monitoring network show O_3 levels influenced by NO_x titration and relatively high NO_x levels, often with high NO to NO_2 ratios, possibly indicating relatively fresh primary emissions. Prevailing wind direction most often moves air masses from the west to the east; while the existing monitoring network is located along a north-south axis along the Athabasca Valley. Measurements made by aircraft suggest that peak O_3 formation occurs at a distance of more than 70 km from the source, or at a plume age of at least three hours (Figure 7.56, AMEC 2003). Plumes from the oil sands facilities were found to favour HNO_3 formation and loss over O_3 formation until the plume became dilute enough to favour O_3 formation.

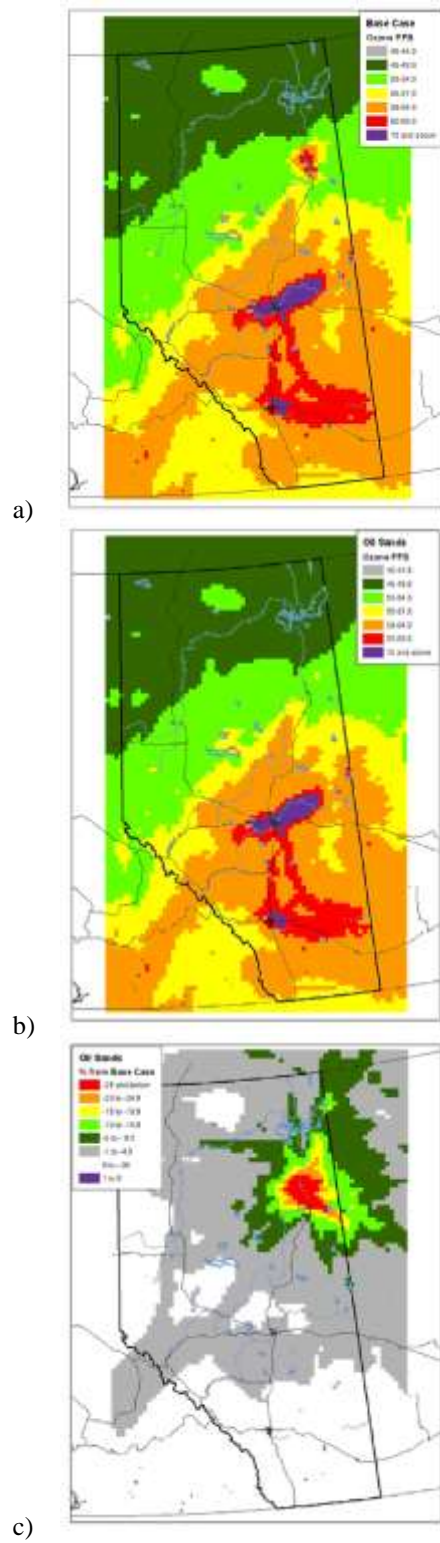


Figure 7.57 Oilsands sector scenario: (a) fourth highest daily maximum ozone (b) emissions from the oilsands sector excluded (c) maximum percent difference between (a) and (b).

Due to limited data, modelling studies (e.g., Fox and Kellerhals, 2007) have played an important role in understanding the impacts of emissions from the oil sands facilities on O_3 concentration in the region (Figure 7.57). Model to measurement comparisons show that O_3 is over predicted in Fort McMurray even though the model represents O_3 well in other areas in the province. The over-prediction could be the result of comparison to non-representative measurements, over estimation of emissions, or poor model representation of some aspect of atmospheric chemistry unique to the region (Fox and Kellerhals, 2007). Aircraft measurements downwind of the oil sands region suggest that in a mature plume, 2 molecules of O_3 were produced for every molecule of NO_x consumed (AMEC 2003). This O_3 production ratio matches that of the results of the modelling, suggesting that the “overestimation” of O_3 by the model might be related to non-representative measurements by the network (ibid.). As discussed in the “Uncertainties in Emissions Inventories” text box, some emission sources in the oil sands are poorly quantified, contributing additional uncertainty to the model simulation. This also includes emissions from tailings ponds, which may be an important contributor to photochemical ozone formation as seen when the highest level of ozone forming potential VOCs, expressed as propene equivalency, was measured downwind of a large oil sands tailings pond (AMEC, 2003). The in-use emissions of the oil sands mining fleet are also thought to be a significant area of uncertainty.

7.5.6 Spatial and Temporal Patterns of O_3 , $PM_{2.5}$ and NO_2 in the Lower Fraser Valley

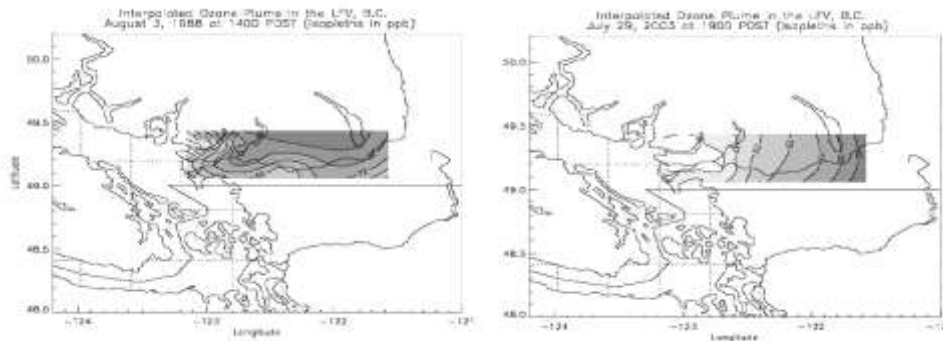


Figure 7.58 Interpolated ozone plumes for the LFV for August 3 1988 and July 29, 2003. From Steyn and Ainslie (2007).

In the LFV, O_3 episodes typically occur during July and August when the combined effect of ultraviolet radiation, temperature and regional stagnation are highest. During episodic conditions, hourly O_3 concentrations sometimes rise over 80 ppb and occasionally over 100 ppb. The highest O_3 concentrations occur in the eastern portion of the LFV, as a result of the sea-breeze flow concentrating precursor emissions towards its eastern extent. Consequently, between 2003 and 2007, O_3 concentrations at Hope met or exceeded the CWS (Government of Canada, 2007). In addition, in the eastern LFV several stations have come near the CWS

metric value over the past few years. A recent analysis by Ainslie and Steyn (2007), using 20 years of data, describes the spatial O₃ pattern during episodic conditions as having a centroid positioned over the eastern extent of the LFV in the area of Chilliwack and Hope. This centroid has shifted since the 1980s, at which time it was positioned over the central part of the LFV and closer to the north shore mountains (Figure 7.58). This shift may have occurred due to a combination of increasing precursor emissions in the central part of the LFV and changes in emissions resulting in VOC/NO_x ratios. In addition, the study found strong O₃ titration in and around the urban source region and higher values downwind. This suggests that precursor buildup prior to the exceedance day plays an important role in the spatial O₃ pattern on exceedance days.

Annual average PM_{2.5} concentrations in the LFV derived from TEOM measurements range between 5-6 µg m⁻³ (NAPS, 2006). Twenty-four hour average PM_{2.5} levels in the LFV tend to be well below the CWS (Government of Canada, 2007). Although lower than some eastern urban centers in Canada, PM_{2.5} is an issue of concern in the LFV. This is because its impact on visibility is readily apparent given the ease with which it can diminish the view of the mountains. Summer PM_{2.5} episodes occur during the late summer, as a consequence of optimal photo-chemical conditions for secondary aerosol formation coupled with stagnant meteorological conditions. Cold season PM_{2.5} episodes occur in the fall or winter months when emissions from wood burning and space heating add to the existing PM load. During episodic conditions, 24 hour maxima typically exceed 15 µg m⁻³ and occasionally exceed 20 µg m⁻³. Although rare, there have been occasional episodes where PM_{2.5} concentrations have reached extreme levels. The most recent such event occurred at the time of the Burns Bog fire in the summer of 2005. On September 19, a blanket of smoke covered the LFV causing hourly concentrations to exceed 274 µg m⁻³ at Burnaby South and 24 hour average PM_{2.5} concentrations to exceed 40 µg m⁻³ in some locations. PM_{2.5} levels occasionally exceed Metro Vancouver's 24 hour objective of 25 µg m⁻³ as a result of forest fires and localized fireworks activity (Metro Vancouver, 2006).

Urban-rural differences in the dynamics of smog-forming pollutants in the LFV are exemplified by comparing two sites: Robson, located in the heart of downtown Vancouver, and Hope, located at the eastern-most extent of the LFV. Robson is exposed to significant car, truck and bus emissions, much from idling vehicles. Hope is a largely rural location impacted by transported pollution from combined urban, agricultural and industrial sources from the Metro Vancouver and Whatcom County (U.S.) area.

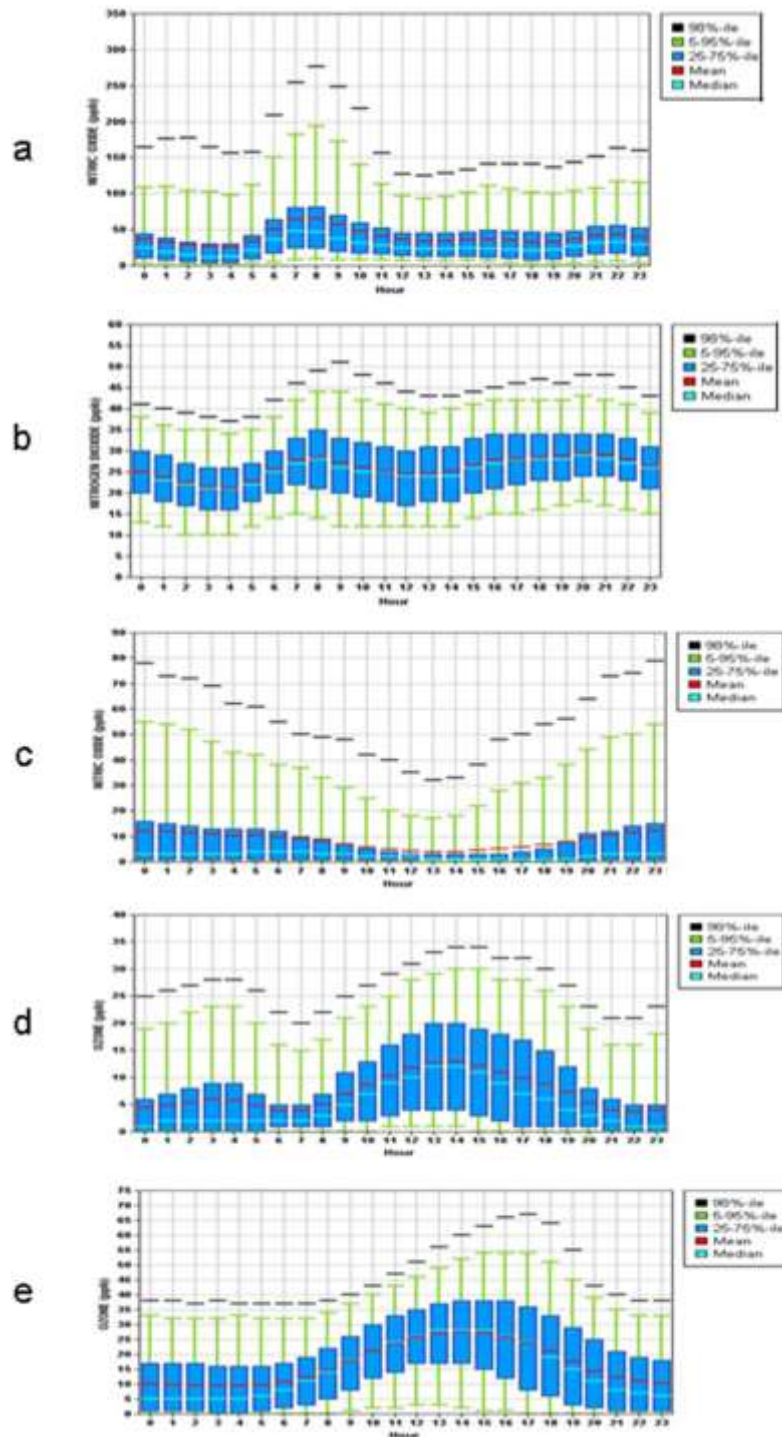


Figure 7.59 a) Diurnal pattern of NO concentrations at Robson, Vancouver (1995-2006). b) Diurnal pattern of NO₂ concentrations at Robson, Vancouver (1995-2006). c) Diurnal pattern of NO concentrations at Hope (1996-2006). d) Diurnal pattern of O₃ concentrations at Robson, Vancouver (1995-2006). e) Diurnal pattern of O₃ concentrations at Hope (1996-2006).

Robson has the highest annual NO_2 levels in the LFV (24 ppb), exceeding Metro Vancouver's annual air quality objective for NO_2 of 21 ppb (Metro Vancouver, 2006). Diurnal variations at Robson confirm the dominating influence of traffic on downtown air quality: NO_2 concentrations exhibit a pronounced morning peak (average concentration 70 ppb) coincident with the morning rush hour (Figure 7.59a). NO_2 levels (Figure 7.59b) also show a morning rush hour peak but also a second broader peak in the late afternoon-evening period. At the rural station of Hope, NO concentrations are significantly lower than at Robson, with annual mean values below 10 ppb (Figure 7.59c). NO concentrations at Hope are lowest during the mid-day and reach their highest concentrations during the night hours due to reduced boundary layer height. The diurnal cycle of NO_2 mirrors that of NO (not shown). The lack of a traffic related pattern at this site indicates that most of the NO_x is transported from urban areas located to the west.

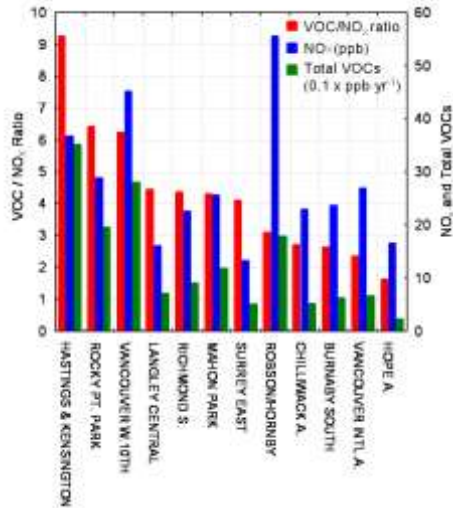


Figure 7.60 VOC: NO_x ratios, NO_x and total VOCs at NAPS stations in the LFV (May – September 1990-2006). Stations arranged in decreasing order of VOC/ NO_x ratios.

At Robson, low nighttime concentrations of O_3 (Figure 7.59d) indicate significant titration by NO (Figure 7.59c); this effect is considerably less at Hope (Figure 7.59e). Both Robson and Hope are VOC limited, with VOC/ NO_x ratios of 3.1 and 1.6, respectively (Figure 7.60). While NO_x concentrations are very high at Robson, levels at Hope are typical of rural-impacted locations in BC. Interestingly, total VOC levels are quite low at Hope, in spite of the fact that the town lies in the vicinity of steep tree covered mountain slopes. VOC limitation, indicated by VOC/ NO_x ratios below 8, is observed in various degrees at all sites in the LFV, with the exception of the Hastings and Kensington sites which are influenced by fugitive VOC emissions from adjacent petroleum storage tanks.

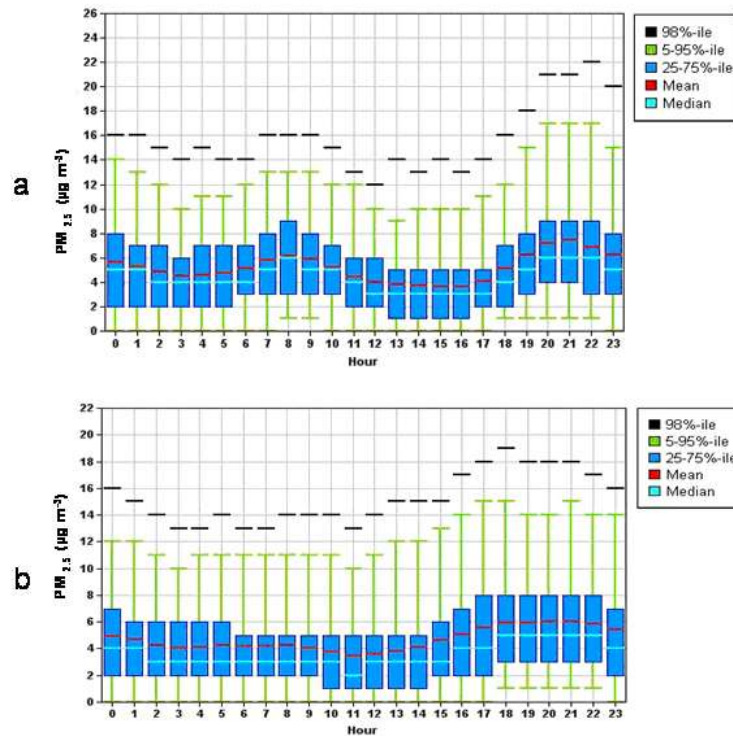


Figure 7.61 a) Diurnal pattern of PM_{2.5} concentrations at Vancouver, West 10th (2006). b) Diurnal pattern of PM_{2.5} concentrations at Hope (2005-2006).

PM_{2.5} concentrations are not measured at Robson, however at the nearby Kitsilano (West 10th) station, both a morning peak (rush hour) and a more pronounced evening peak are observed (Figure 7.61a). In addition, the diurnal NO_x and O₃ cycle at Kitsilano site also shows the same type of traffic dominated pattern as at Robson, however, at the latter site, enhanced ozone titration results in O₃ levels being generally lower. The morning PM_{2.5} peak is not observed at the more rural sites of Hope (Figure 7.61b) and Langley (not shown). The shallow nocturnal boundary layer keeps PM_{2.5} levels elevated overnight at all sites by concentrating the local emissions.

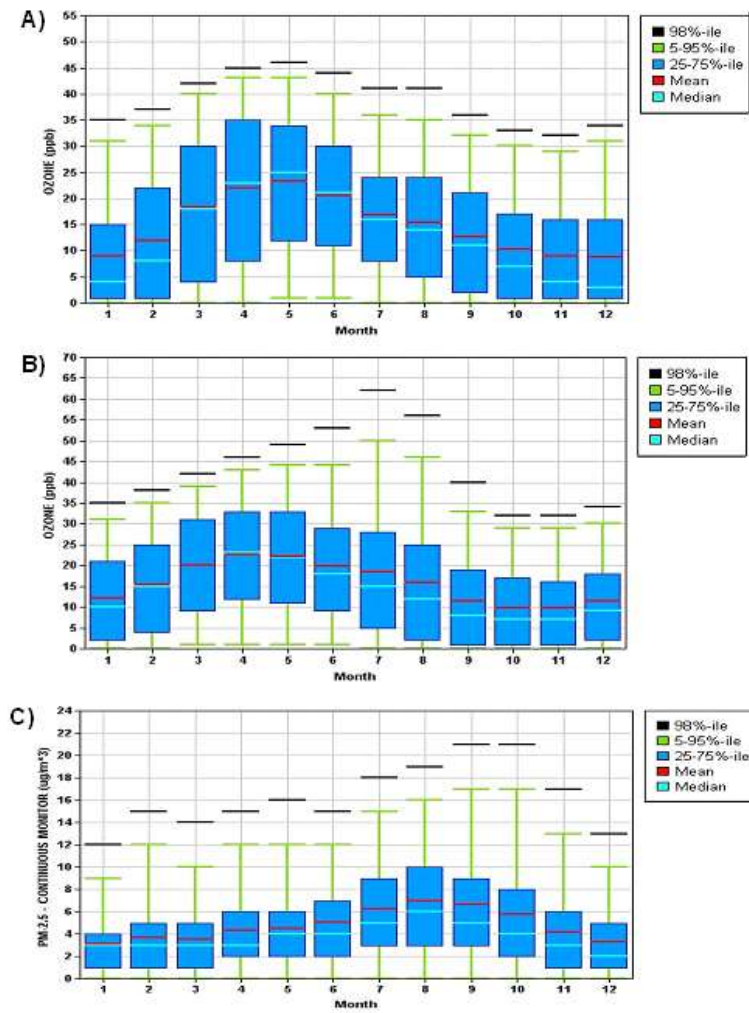


Figure 7.62 a) Seasonal pattern of O₃ concentrations at Vancouver Airport (1996-2006). b) Seasonal pattern of O₃ concentrations at Chilliwack (1995-2006). c) Seasonal pattern of PM_{2.5} concentrations at Chilliwack (1995-2006).

In the LFV, NO levels are generally lowest during the summer and tend to peak during the winter months. Average O₃ levels are highest during April-May, largely due to a combination of surface O₃ production in response to increasing ultraviolet radiation, inputs of background ozone from the free troposphere and stratospheric intrusion. Ozone maxima tend to occur during the spring in the western portion of the LFV (Figure 7.62a), due to the influence of background O₃ and during the summer in the eastern portion of the LFV (Figure 7.62b), reflecting more intense local photochemical production. Mean PM_{2.5} concentrations peak in the late summer at the majority of LFV sites (e.g. Figure 7.62c) and are associated with secondary aerosol production. Exceptions occur at Vancouver Airport and Pitt Meadows where mean PM_{2.5} peaks in the winter, due to the influence of wood smoke in nearby areas (Larson *et al.*, 2007).

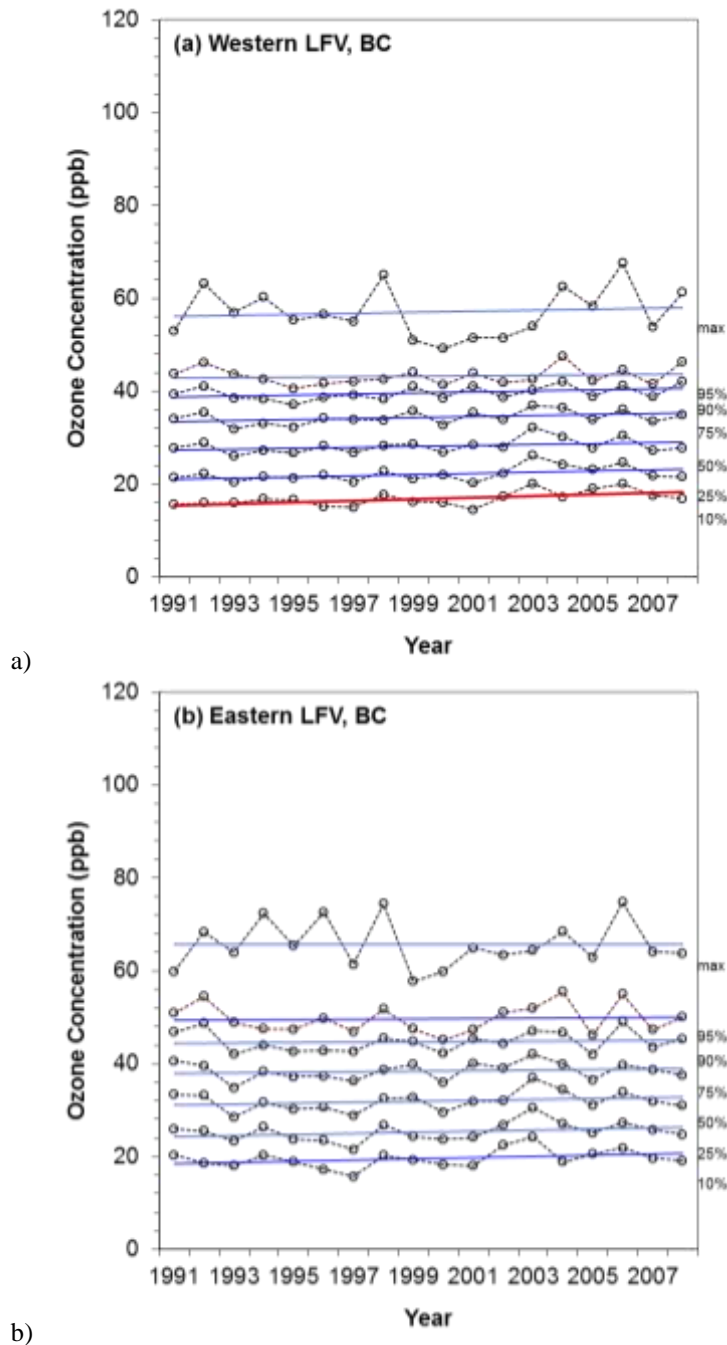
7.5.6.2 Trends in O₃ and PM in the LFV

Figure 7.63 Ozone trends for sites in the western (a) and eastern (b) LFV for different percentiles in the statistical distribution. Statistically significant trends at $p < 0.05$ shown in red. For the western LFV data were averaged for the following sites: Hastings and Kensington, Rocky Point, Vancouver West 10th, Delta, Burnaby Ring Road, Richmond South, Mahon Park. For the eastern LFV, data were averaged for the sites: Surrey East, Abbotsford S. Fraser Hwy., Chilliwack Airport.

Warm season O₃ trends were investigated for the western and eastern LFV, respectively, for the period 1991-2008, using simple linear regression performed on several parts of the statistical distribution as shown in Figure 7.63. The 1991-2008 period was chosen in order to capture the most current emission regime, including federal regulations on vehicles and fuels and the implementation of the Air Care program in the LFV. The western and eastern LFV were investigated separately to distinguish between source areas and downwind areas, respectively. Trends were positive for the western LFV, although not statistically significant, with the exception of the 10th percentile. Increasing trends at the lower percentiles have been discussed above for other regions in the country, in particular see the discussion for the Southern Great Lakes Region. The increase in the lowest percentile may be considered to reflect increases in background ozone (Royal Society, 2008), however this is confounded by the reduction in local NO concentrations. There were no statistically significant trends for the eastern LFV, although slopes were mostly positive, suggesting O₃ has been rising slightly.

Table 7.8 Meteorologically and seasonally adjusted ozone (ppb yr⁻¹) and PM_{2.5} (µg m⁻³ yr⁻¹) trends at PYR sites. All trends are statistically significant at p<0.05

Parameter	Time Period	Saturna CAPMoN	Pt. Moody Rocky Point	Langley Central	Chilliwack Airport	Hope Airport	Kelowna College
O ₃ 1-Hr Average	1995-2006	+0.14					
O ₃ 24-Hr Average	1995-2004				+0.32		+0.95
O ₃ 24-Hr Average	1997-2006	+0.26		+0.52		+0.46	
O ₃ Daytime Average	1997-2006	+0.26		+0.48		+0.55	
O ₃ Nighttime Average	1997-2006	+0.31		+0.62		+0.33	
O ₃ 1-Hr Daily Max	1995-2004				+0.41		
O ₃ 1-Hr Daily Max	1997-2006	+0.21		+0.25		+0.33	
O ₃ 8-Hr Daily Max	1997-2006	+0.23		+0.32		+0.46	
PM _{2.5} Dich. Daily Avg	1993-2004		-0.42				
O ₃ 1-Hr Average	1995-2006	+0.14					

Additional O₃ trend information for individual sites in the LFV is presented in Table 7.8. These trends were meteorologically and seasonally adjusted using multiple regression models described in Vingarzan and Taylor (2003). There is a consistent pattern of positive ozone

trends at all sites for all time averaging periods investigated. Ozone trends are larger at sites in the central and eastern areas compared to those at Saturna Island, located in the Strait of Georgia to the west. The trend results shown in Chapter 3 were based upon the combined annual data (meteorologically-adjusted) from four semi-rural sites in the LFV, including one site in Washington. Consistent with Table 7.8, a statistically significant upward trend of about 0.3 ppb/year was detected for the maximum hourly, maximum 8-hour and daytime average O₃.

Table 7.8 also presents PM_{2.5} trend results for Rocky Point, which is located in the north-central part of the western half of the LFV. The trend is negative based on 12 years of every sixth day 24-hr dichot filter samples. This trend is consistent with declines in NO_x, VOCs and CO ambient concentrations in the LFV since the mid 1990s. Recent analyses of particle backscatter (a surrogate for PM_{2.5} measurements) in the LFV also indicate statistically significant declining trends since 2002 (So and Vingarzan, 2010).

Information from Figure 7.63 and Table 7.8 suggests that, that as a whole, O₃ trends in the LFV have remained constant over the past two decades or have increased at selected sites. This occurred after a period of declining trends throughout the 1980s associated with declines in VOC and NO_x emissions. Although NO_x and VOC emissions and ambient levels continued to decline through the 1990s and 2000s, ozone levels did not follow the same trend. An analysis of O₃ reactivity for the LFV (Vingarzan and Schwarzhoff, 2010) concluded that declines in VOC/NO_x ratios over the past two decades have shifted the chemistry towards increased VOC limitation. The majority of this shift occurred during the early 1990s, coinciding with improvements in vehicles and fuels and the onset of the AirCare program in the LFV. In addition, the study found that VOC limitation is widespread throughout the entire airshed, with higher VOC limitation occurring in the eastern portion. Based on the current understanding of emission controls in VOC-limited airsheds (Finlayson-Pitts and Pitts, 1999) and current projections of VOC and NO_x emissions, is unlikely that the LFV will see significant ozone declines over the next decade.

7.5.6.3 Visibility in the Lower Fraser Valley

Poor visibility is a concern in the LFV due to loss of views of mountainous vistas, impacting both quality of life and the economy. Visibility is also the principal way that the public perceives the state of air quality in the LFV. Based on reconstructed extinction for the period 2003 to 2008 (So and Vingarzan, 2010), the visual range in the LFV is below 40 km 16% of the time, a publicly accepted visual threshold (Pryor, 1996). Although average annual PM_{2.5} levels in the LFV are comparatively low with respect to other parts of Canada, visibility effects become noticeable at hourly PM_{2.5} concentrations as low as 8-10 µg m⁻³, based on digital image data from the LFV visibility network. At concentrations between 10-20 µg m⁻³ visibility is significantly affected, while above 20 µg m⁻³ it is severely affected, often completely obscuring views of surrounding mountain ranges.

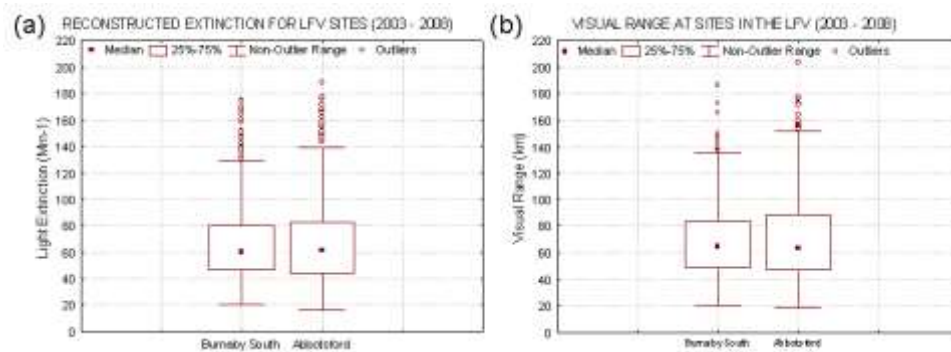


Figure 7.64 Statistical distributions for (a) reconstructed light extinction and (b) visual range at Burnaby South and Abbotsford Airport for the period 2003-2008.

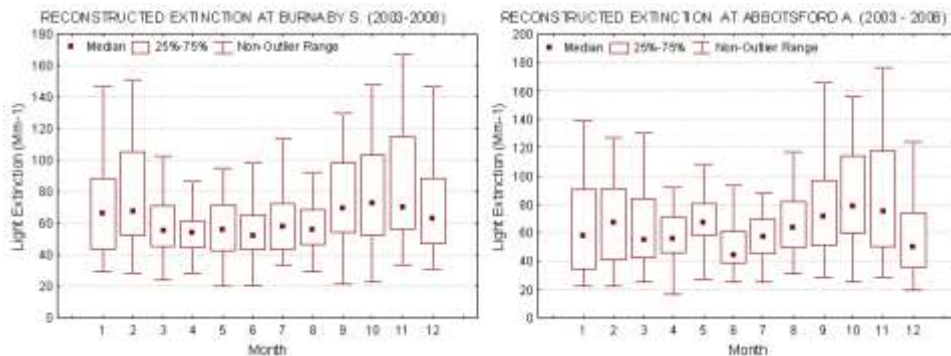


Figure 7.65 Seasonal pattern of reconstructed light extinction at Burnaby South and Abbotsford Airport for the period 2003-2008.

Measurements from Burnaby South and Abbotsford indicate that average reconstructed extinction is similar at the two sites, however at Abbotsford visibility is more impaired during poor visibility events as indicated by the whiskers in Figures 7.64 and 7.65 (So and Vingarzan, 2010). Average visual range, as derived from extinction) is 69 and 70 km, respectively at Burnaby South and Abbotsford (Figure 7.64b). For comparison, the range of natural visibility in western Canada is 185-210 km (Hoff *et al.*, 1997). This range is infrequently reached as indicated by the outliers in Figure 7.64b. Seasonally, average visibility is poorest during the fall months, as indicated in Figure 7.65. Reconstructed extinction was correlated with PM_{2.5} and ozone during the summer months and with PM_{2.5} during all other times of the year (So and Vingarzan, (2010).

7.5.7 PM_{2.5} and O₃ in British-Columbia Interior Valleys

Particulate matter is the primary air quality issue in most interior BC communities, due to the prevalence of open burning, wood combustion and emissions from wood processing industries. As such, annual average TEOM-derived PM_{2.5} concentrations in interior communities are higher than those in the LFV, ranging between 6-11 µg m⁻³ (NAPS, 2006). PM_{2.5} levels in

interior communities peak during the fall and winter seasons due to emissions being most intense at this time and the prevalence of capping inversions restricting the flow and vertical mixing of air. Communities with the highest episodic PM_{2.5} levels include Houston, Prince George, Quesnel, Williams Lake and Golden. However the location most impacted by PM is the city of Prince George (see text box “When Topography and Intensive Industrial Activity Combine” in Section 7.4.4).

Episodic PM_{2.5} concentrations are higher in Prince George than in most BC communities, resulting in an exceedance of the CWS for PM_{2.5} from 2002 to 2005. Since 1998, Prince George has also been exceeding the BC Ministry of Environment 24 hour interim objective of 25 µg m⁻³ an average of 4% of the time. In addition to anthropogenic sources of PM, interior communities are occasionally impacted by emissions from wildfires. In August 2003, large-scale wildfires affected air quality in several BC communities. Extremely high PM_{2.5} concentrations were recorded in Kelowna, where the 24 hour average reached 186 µg m⁻³ on August 21, 2003.

Although there have been no exceedances of the CWS for O₃ in the BC interior, recent analysis indicates that CWS metric is near 60 ppb in several communities, including Kelowna, Kamloops, Williams Lake, Grand Forks and Prince George. In Kelowna, O₃ is becoming an increasingly important issue due to significant population growth and expansion that is anticipated over the next decade. Given the rising ozone trend in Kelowna, (Table 7.8), achievement and maintenance of the CWS by the year 2010 and beyond may require continued and sustained efforts.

7.5.7.1 Diurnal and Seasonal Variation in Smog forming pollutants

In the interior valley communities of BC, NO exhibits two daily peaks, the first and usually larger one in the morning hours and a second in the evening. Diurnal peaks are most pronounced in the winter, due to the predominance of inversions and wood burning. At the rural site of Creston Piper Farms, NO persists into the mid-day hours in the winter due to slower conversion rates to NO₂ in the absence of sufficient O₃ and other oxidants. O₃ concentrations peak during the mid afternoon and various degrees of O₃ titration are seen at night depending on urban character of the site and proximity to highways. PM_{2.5} concentrations largely mirror those of NO, exhibiting either a bimodal peak in the early morning and evening periods, or a single morning peak. Morning peaks occur earlier in the summer than the winter, coinciding with the timing of the breakdown of the nocturnal boundary layer. In the winter, evening peaks are typically associated with wood stove emissions and are generally much more pronounced than those in the LFV.

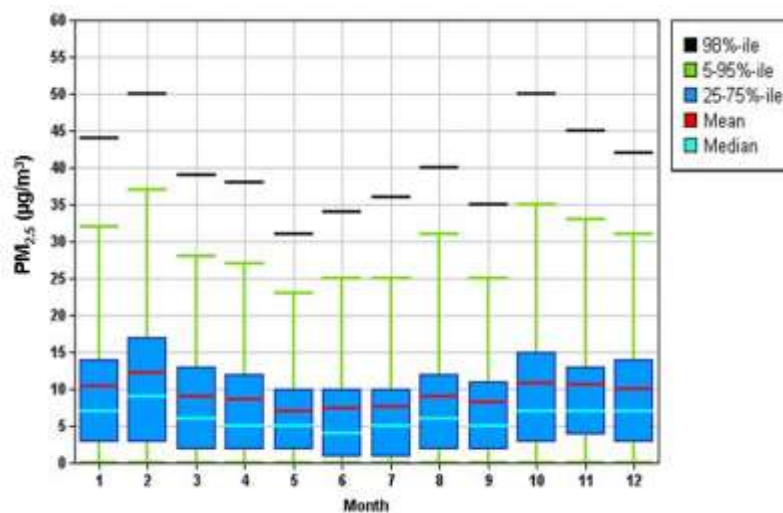


Figure 7.66 Seasonal pattern of PM_{2.5} concentrations at Prince George, Plaza 400 (1998-2006).

Seasonally, NO levels are highest during the fall and winter. Average and maximum O₃ concentrations peak in April-May at all stations with the exception of Kamloops and Kelowna, where maxima occur in August. PM_{2.5} concentrations mirror those of NO with maxima during the fall-winter period, as shown in the plot from Prince George (Figure 7.66). The seasonal patterns of NO and PM_{2.5} reflect increased open burning, woodstove use, lower mixing heights and frequent valley inversions.

7.5.8 Air Quality in the Yukon

Air quality in the Yukon is generally cleaner than in southern Canadian cities because there are fewer industrial activities and smaller, more dispersed populations. However episodes of high ambient air pollution occur occasionally in residential areas throughout the Yukon, because of residential wood smoke pollution and forest fires. Other causes of air pollution include vehicle exhaust and road dust. A single air quality station exists in the Yukon, located in downtown Whitehorse. Levels of carbon monoxide have declined substantially since the mid 1980s, with most of the decline having occurred in the early 1990s (SOE, 2002). Between 2002 and 2006, the range of the mean daily maximum O₃ concentration was 32-37 ppb and the 4th highest daily maximum ranged between 47-56 ppb, below the CWS standard of 65 ppb. Mean annual TEOM-derived PM_{2.5} concentrations were relatively low ranging between 2.4-4.7 µg m⁻³. PM_{2.5} concentrations at Whitehorse were highest during the summer months and at this site, annual variability appears to be influenced by the degree of forest fire activity. The summer of 2004 was the Yukon's busiest forest fire season recorded to date. More than 275 fires burned a record total of two million hectares, an area about the size of Wales (UpHere Publishing, 2007). From June to the end of August there were a total of 19 days with 24 hour average PM_{2.5} concentrations above 20 µg m⁻³. Very high hourly concentrations were recorded in

Whitehorse, with a one-hour maximum of $190 \mu\text{g m}^{-3}$ on June 27. Wood smoke episodes occur during the winter due to poor burning practices and inefficient wood stoves, which raise hourly concentrations to between $20\text{--}40 \mu\text{g m}^{-3}$. In spite of occasional extreme episodes, the Whitehorse station did not exceed the $\text{PM}_{2.5}$ CWS between 2003 and 2005 (Government of Canada, 2007).

7.5.9 Air Quality in Northern Communities

Canada's North is very sparsely populated, with the three territories jointly accounting for 39% of Canada's landmass and only 0.3% of Canada's population. The few communities are small and separated by large uninhabited areas. The small population is matched by small emissions of smog-forming pollutants; collectively the three territories contribute 0.4% of Canadian $\text{PM}_{2.5}$ emissions, 0.1% of SO_x emissions, 0.7% of NO_x emissions and 0.3% of VOC emissions. Taken together these small emissions are insufficient to contribute to any sort of regional smog problem.

Major contributors to current emissions in the region include electricity generation (usually with diesel generators), the mining industry, transportation, the oil and gas industry, and residential and commercial heating. It is expected that emissions from the region may increase in the future due to growing population and increasing activity in mining and oil and gas. It has also been proposed that emissions from shipping may increase if the Northwest Passage becomes seasonally ice-free.

Air quality measurements are available in several communities in the Northwest Territories. A NAPS station operates in Yellowknife, the capital and largest town, and the territorial government monitors air quality in three smaller communities in response to increasing resource development activity. Results of this monitoring indicate that air quality is generally good. Monthly average $\text{PM}_{2.5}$ concentrations typically range from 2 to $5 \mu\text{g m}^{-3}$. During the summer months there have been some days with 24-hour $\text{PM}_{2.5}$ concentrations greater than the CWS level. These events have been attributed to forest fire smoke. NO_2 levels are relatively low and consistent with measurements in small to medium sized Canadian communities. In common with other Canadian locations NO_2 concentrations peak during the winter months due to increased emissions and reduced dispersion. Ozone levels in the NWT are similar to background sites in northern Alberta, with highest levels in spring and lowest levels in early fall.

Levels of coarse PM can be high in northern communities due to a prevalence of unpaved roads and the extensive use of sand and gravel for traction on paved roads in winter. The impact of road dust can be particularly noticeable in Yellowknife during the spring months when the roads may be largely snow free, but the temperatures are considered too cold for street cleaning.

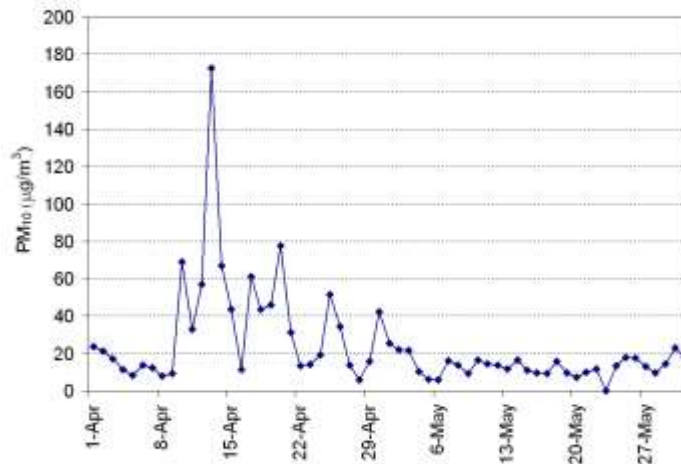


Figure 7.67 Daily average PM₁₀ in Yellowknife for April and May 2007.

An example of high PM₁₀ levels due to road dust is shown in Figure 7.67. In this case there were nine days in early April 2007 when 24 hour average PM₁₀ at the Yellowknife monitoring site was over 40 µg m⁻³. On the highest day of April 13th PM₁₀ was above 170 µg m⁻³. There were a number of other days with high PM₁₀ during the months of April 2007. In May daily mean PM₁₀ levels returned to normal values. The weather during those months was not unusual except that temperature in April was one standard deviation above the long term normal. The period from mid April to early May during which there were periodic days with high PM levels represents the period of time between snow melt and street cleaning, during which little precipitation fell.

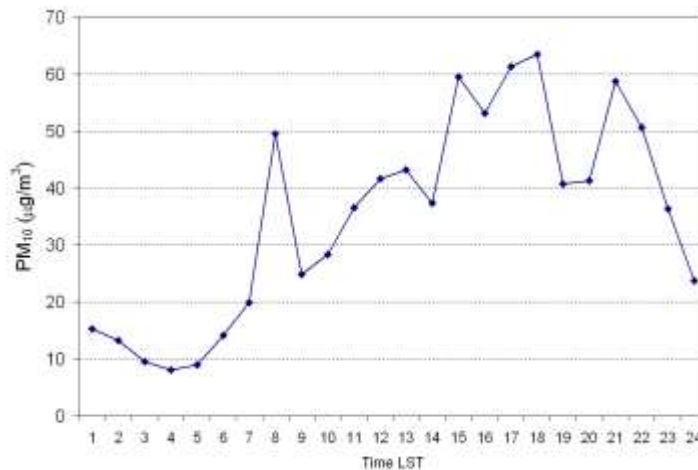


Figure 7.68 Hourly average PM₁₀ in Yellowknife during April and May 2007.

Although there was significant variability from day to day, the typical hourly pattern was a sharp spike in PM₁₀ around 8 AM local time and a second peak building through the rest of day then diminishing late in the evening and overnight (Figure 7.68). This pattern of PM is consistent with a source associated with road dust caused by vehicular traffic.

On 13th April, which was shown in Figure 7.67 to have experienced a high 24 hr average concentration, the hourly data showed that there was a very high peak in PM₁₀ in the evening when the concentration exceeded 500 µg m⁻³. On this day dust levels generally increased through the day to reach the highest values late in the evening. The highest PM₁₀ levels were observed during a period where wind speed was below the detection limit of the instrument or nearly still air. This is again consistent with a local dust source and concentrations building during poor dispersion conditions.

7.5.9.1 Arctic Haze

Arctic haze which can result in visibility as low as a few kilometres, was first noted by pilots in the 1950s and its anthropogenic origin was determined in the 1970s (AMAP, 2006). The arctic haze consists of very fine aerosol (mass median diameter $\approx 0.2 \mu\text{m}$) composed primarily of sulphates and organic matter and smaller amounts of nitrate, elemental carbon, crustal material and heavy metals (AMAP, 2006). Although the total PM concentrations resulting from the haze are a fraction of those at populated and industrial sites further south, the haze is still a concern as it provides a pathway for transport of contaminants emitted at lower latitudes to the arctic. In addition the haze may have important climatic impacts.

The haze primarily originates from emissions in northern Europe and Russia which are preferentially transported to the arctic during winter and spring (AMAP, 2006). Emissions from southern Canada, the U.S., or the heavily populated areas of Asia are less frequently transported to the arctic troposphere in winter. If emissions increased in northern Canada due to increased industrial activity, they could contribute to arctic haze. During winter the extremely cold and stable arctic air mass inhibits particle removal by dry or wet deposition and allows the trapping of haze for long periods. Haze concentrations peak in early spring. By May the breakdown of the inversion and increasing precipitation start to reduce haze concentrations.

Long term measurements of sulphate aerosol taken at Alert show a reduction in sulphate aerosol that has been linked to SO_x emission reductions, particularly from smelters and other sources in northern Russia (AMAP, 2006). Nitrate concentrations at Alert appear to be increasing in recent years, presumably because very little reduction in NO_x emissions has been realized in Arctic source regions.

7.6 Long-Range Transport of Air Pollutants

The focus in the previous section was on describing and explaining the observations of O₃, PM_{2.5} and NO₂ within each region. The purpose was to expand upon the information in Chapter 3 through a greater emphasis on regional to local scale spatial patterns and some of the features of the temporal trends, including further interpretation of the chemical composition of PM_{2.5}. Furthermore, the discussion attempted to highlight unique characteristics of smog in each region thereby highlighting the geographical differences. These differences are important to appreciate in order to develop strategies to improve air quality since in many cases optimal approaches will differ from one area to the next.

In addition to local, region-specific processes, movement of air pollutants over longer distances plays an important role in dictating the observed concentrations. In eastern Canada long-range transport from other jurisdictions can bring high enough concentrations into the area that local policies alone will not be sufficient to reduce levels below those known to have health impacts (e.g., achievement of the Canada-wide Standards). Therefore, the objective of this section is to demonstrate how different long-range or regional scale transport patterns (continental and smaller scales) influence air concentrations, including some discussion on transport across the Canada-U.S. border or across Provincial borders. Transport between adjacent cities or populated areas are not discussed specifically in this section, although it should be noted that this phenomenon can occur and is important to understand in assessing sources of pollutants experienced in any given populated area. Long-range transport, as it refers to hemispheric transport is not the focus in this chapter but is covered in Chapter 9.

On a continental scale it is now well-accepted that North America exports a considerable amount of O₃ and fine particles off the east coast and this impacts Europe (Li *et al.*, 2002; Singh *et al.*, 2006). Satellite remote sensing showed a maximum in ozone concentrations extending eastward over the North Atlantic (e.g., Fishman *et al.*, 1990) and Fehsenfeld *et al.* (1996) concluded that the summertime anthropogenic ozone originating from North America dominates the near-continent marine boundary layer ozone budget. More recently, the ICARTT study (Vaugh *et al.*, 2004) focused considerable attention on this issue in summer 2004. Quantitative studies during the North Atlantic Regional Experiment in the region over the Gulf of Maine, southern Bay of Fundy, southwestern Nova Scotia and adjacent waters to the east, calculated that the anthropogenic portion of ozone flowing eastward away from the continent, in a unit square vertical cross section, was 50% below 1 km, 35-50% from 1 to 3 km, 25-50% from 3 to 4 km and 10% from 4 to 5 km (Banic *et al.*, 1996). Plumes or layers of up to 1 km thick were have been observed several hundred kilometres downstream from the seaboard (Berkowitz *et al.*, 1996; Daum *et al.*, 1996), with ozone concentrations up to 150 ppbv. The outflow plumes, generally found below 1.5 km, (Buhr *et al.*, 1996) were characterized by defined layers of pollution, decoupled from the marine boundary layer (Neuman *et al.*, 2006). This vertical layering and the processes that create distinct layers and mix them to the surface is an important consideration for regional scale transport. While it has been studied in more

detail in Atlantic Canada, it is a feature of long-range transport everywhere and it remains a challenge to fully characterize due to the limited amount of measurements available above ground level.

Trans-Pacific transport impacting Canada, which is an emerging issue, is discussed specifically in Chapter 9. This is particularly important given the rapid growth in Asia. Within North America long-range transport continues to be an important international issue with emissions in the U.S. impacting Canada and Canadian emissions influencing levels in some areas of the U.S., although to a lesser extent.

7.6.1 The Relationship between Transport Patterns and O₃ and PM_{2.5}

Temporal variations in the synoptic weather patterns described above lead to specific regional scale or long-range air pollutant transport pathways that can significantly affect concentrations over downwind locations. The magnitude of this effect depends upon the presence or lack of emissions upwind and the rate of air mass movement, either over the source areas or between these areas and the observation site. A variety of techniques have been used to study how concentrations differ with transport path, but they all tend to utilize back-trajectories to characterize the transport. Overall, more meaningful conclusions can be drawn when concentrations are examined in relation to ensembles or large groupings of trajectories, as opposed to individual trajectories. The main goal of the trajectory analyses, which have been applied extensively in all regions in Canada, are to determine which upwind areas lead to higher and lower concentrations and how these flow paths relate to weather patterns.

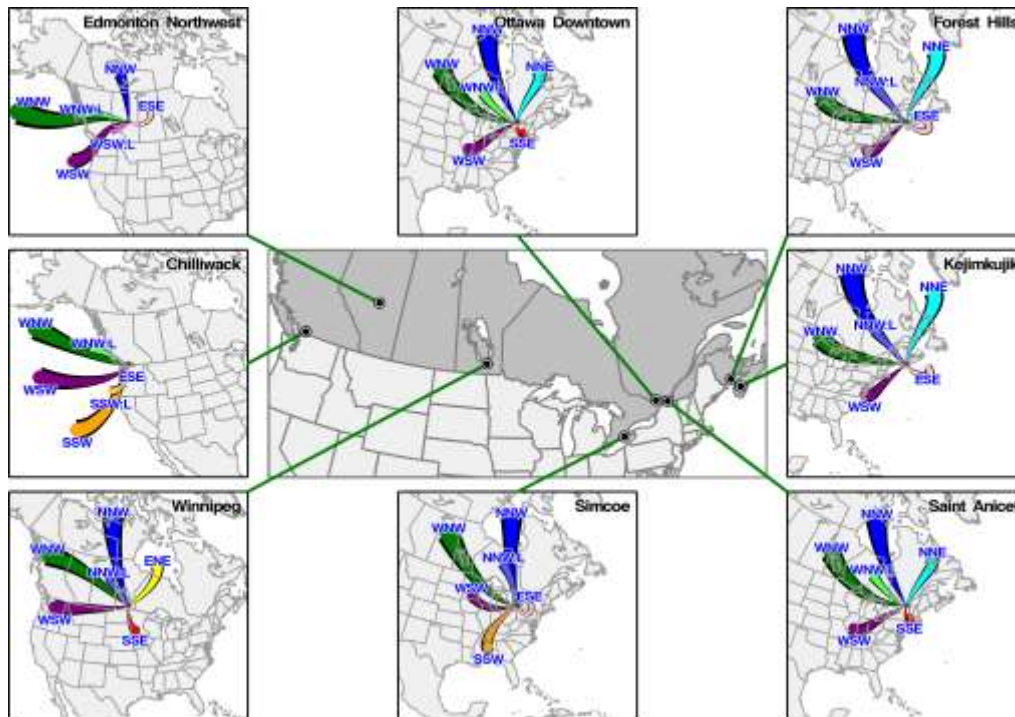


Figure 7.69 Trajectory cluster mean vectors derived from the time period (ranging from 1994 to 2005) of available $PM_{2.5}$ data at 8 selected sites. Note that although the time period used to derive these clusters and those in Figure 7.34 were considerably different very similar transport patterns were identified when the same sites (i.e., Kejimikujik and Forest Hills (Saint John)). Also note that the identified prevailing transport pathways at nearby sites (e.g., Kejimikujik and Forest Hills; Saint Anicet and Roundtop Ridge; Edmonton NW and Ester) are similar. This highlights the fact that, due to the input data used and the meteorological factors that are most influential, trajectories only resolve regional and larger scale phenomena as opposed to local scale features.

Cluster analysis has commonly been used to create ensembles of trajectories or “trajectory clusters” with common transport paths (Dorling and Davis, 1992a,b). The ensembles or clusters determined through this approach reflect the typical meteorological patterns in the area around the receptor site and upwind. A series of standard cluster analyses were undertaken for several locations spread across Canada to support of this assessment. These were done in relation to the available O_3 data in Figure 7.28 and the available $PM_{2.5}$ data in Figure 7.69. In both cases, six different clusters were deemed to be sufficient to differentiate to main transport patterns at each of the sites selected. Average seasonal and annual O_3 and $PM_{2.5}$ concentrations associated with each cluster for each site are compared in Figures 7.29, 7.43, 7.45 and 7.70. A large amount of insight can be gained from studying these figures, some of which will be discussed in the sections below.

7.6.1.1 Southern Great Lakes to the Atlantic Coast

Figure 7.29 shows the distribution of O₃ concentrations by season and transport cluster for each of the sites in Figure 7.28. At the two Atlantic Canada sites (Kejimkujik and Forest Hills), summertime O₃ is highest with the W to WNW flow (green). Both the mean and median are highest and the highest peaks in O₃ occur with this transport pattern across northern New England, southern Ontario and the upper Midwest (Michigan). Thus, the emissions of anthropogenic precursors in this area are important contributors to O₃ over the southern Atlantic region in the summer months when the potential for photochemical production is greatest. WSW flow along the U.S. eastern seaboard (Washington to Boston) also leads to relatively high summer O₃ and large peaks (i.e., episodes). High O₃ later in the season (August, September and even October) is associated with this transport pathway.

It is clear in Figure 7.29 that the spring maximum in average ozone documented in Chapter 3 prevails across all the Atlantic Canada trajectory clusters. However, it is interesting to note that springtime O₃ levels are higher with the WNW and WSW flow directions, suggesting that anthropogenic emissions have some role. This may be partly caused by higher peaks evident for these directions, which in general, are brought about by specific weather patterns leading to greater photochemical production of O₃ from anthropogenic emissions. This also implies that the spring (MAM) peaks shown in Figure 7.29 may be associated with conditions occurring later (i.e., May). The mean seasonal patterns highlighted in Figure 7.45 provide more insight on this feature, indicating that for the WNW flow the mean levels peak in May and into June. However, for the WSW flow the peak is clearly in April at Kejimkujik and late April or early May at Forest Hills. This may be a function of an earlier warm up and start to the growing season (i.e., release of biogenic VOCs) in the areas that are more directly to the south along the U.S. east coast. In the cold months the WSW and WNW flow directions do not stand out over the others and interestingly, mean O₃ is actually slightly higher with wind flow from the very low emission sectors (NNW, NNE and ESE). This likely reflects the reaction of regional background O₃ with NO_x emissions associated with areas within the SW quadrant from Kejimkujik.

The display in Figure 7.45 is useful for highlighting differences between the transport directions and the overall patterns. For example, other interesting features are the relative similarity in the seasonal pattern and the mean concentrations at Kejimkujik for each of the transport directions except WNW and WSW. In particular, in the winter and early spring months there is little difference in the mean O₃ for all the transport directions, which suggests a prominent influence of the regional background O₃. Mean O₃ is actually slightly higher with wind flow from the very low emission sectors (NNW, NNE and ESE), which likely reflects the reaction of regional background O₃ with NO_x emissions and higher regional NO_x associated with conditions over areas within the SW quadrant from Kejimkujik and Forest Hills. The interesting divergence, which was discussed to some extent above, is from the late spring to early fall. Comparing the patterns between Kejimkujik and Forest Hills reveals that, in general,

there appears to be greater differences in mean O₃ among the transport directions at Forest Hills (note that the scales are different for the two plots). Part of the reason for the greater spread is that Forest Hills is in an urban area and there is more local O₃ destruction due to NO titration, which appears to vary by transport direction. Another difference between these two Atlantic region sites is with the seasonal behaviour of the WSW and ESE transport directions. At Forest Hills, there are increases in the O₃ concentration for these directions in the fall, which are not apparent at Kejimikujik. However, it is important to note that actual mean and peak concentrations for these directions are the same or higher at Kejimikujik. Thus, it is just the shape of the seasonal change that differs between the sites, suggesting that there are subtle more-local scale influences at play in the region. Resolving such differences would require more detailed analysis of meteorology and the potential influences of local sources.

For interest, multi-year annual average O₃ concentrations (i.e., smoothed inter-annual variability) by transport path are shown in Figure 7.43. These trends will not be discussed in detail here as more formal trend analyses were presented in Chapter 3. Due to the influence of meteorology, detecting true O₃ trends is a challenge. In Chapter 3 a model for removing this influence was applied. Clearly, changes in the relative frequency of different transport directions from year to year is one factor that obscures the true trend and thus, by looking at the trend within each direction as in Figure 7.43 helps remove this effect. As an example, for Kejimikujik there was an increasing trend in ozone from 1994 to 2002 within most transport directions, and a declining trend since that time. Possible explanations for this pattern include increases in background concentrations, which in later years are offset by decreases in upwind precursor emissions. However, the pattern is quite different at Forest Hills indicating that more detailed study, including more rigorous meteorological adjustment (i.e., as done in Chapter 3), is necessary. Nonetheless, as was discussed in Chapter 3, a key feature of the Kejimikujik trend is that there has been a statistically significant increasing (~0.2%/year) in the springtime. This behaviour was observed at other sites in the region as well (e.g., Acadia NP) and agrees with the results from Monks (2000).

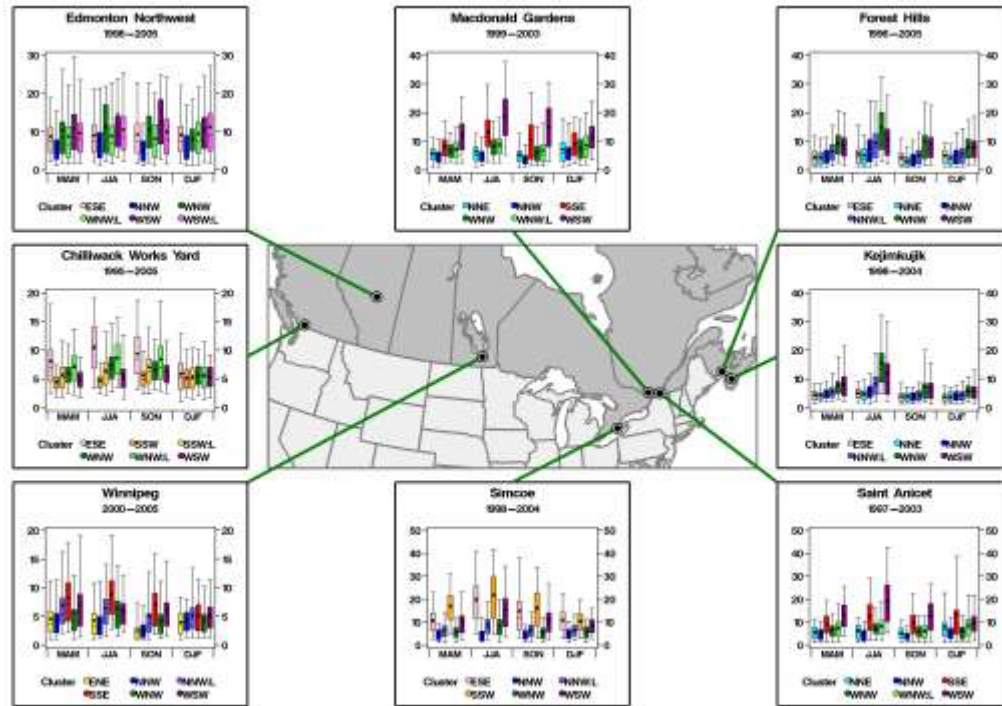


Figure 7.70 Seasonal box-and-whisker $PM_{2.5}$ plots by trajectory clusters at 8 $PM_{2.5}$ sites. The time period of the $PM_{2.5}$ data record at any given site used in the analysis is shown below the site name in each panel. Seasonal breakdowns are as follows: March – April – May (MAM), June – July – August (JJA), September – October – November (SON) and December – January – February (DJF). Note that different scales are used across sites.

Due to the smaller relative contribution from regional and hemispheric background concentrations, transport path has a large influence on $PM_{2.5}$ across all seasons over the southern Atlantic region (Kejimikujik and Forest Hills). One of the over-arching patterns shown in Figure 7.70 is that, with the exception of the WNW and WSW transport paths in the summer, $PM_{2.5}$ tends to be higher in Saint John (Forest Hills). This is not surprising given the contribution urban primary emissions make to $PM_{2.5}$. However, the similarity between these two locations when $PM_{2.5}$ is highest (i.e., summertime flows from the populated parts of the continent) clearly demonstrates that upwind sources and long-range transport patterns are more important causes of high average and peak $PM_{2.5}$ in this region. In all seasons, the WNW and WSW transport paths are associated with higher concentrations compared to each of the other directions, highlighting the influence of upwind anthropogenic emissions. In winter, however, the differences among the paths tend to be smallest, as do the $PM_{2.5}$ concentrations. Another feature apparent at the Forest Hills site, which is not as noticeable at the Kejimikujik site, is the increase in average and peak concentrations with flow from the ESE compared to the other “clean” directions. Along with the lower O_3 due to NO_x titration and the overall greater $PM_{2.5}$ at Forest Hills, this shows the extent to which, on average, local sources in the Bay of Fundy region can affect pollutant concentrations. Kejimikujik does not experience a rise in $PM_{2.5}$ for

this direction since the trajectories essentially originate over the ocean while for the Saint John area this oceanic flow passes southern Nova Scotia and the Bay of Fundy, as well as over the city itself.

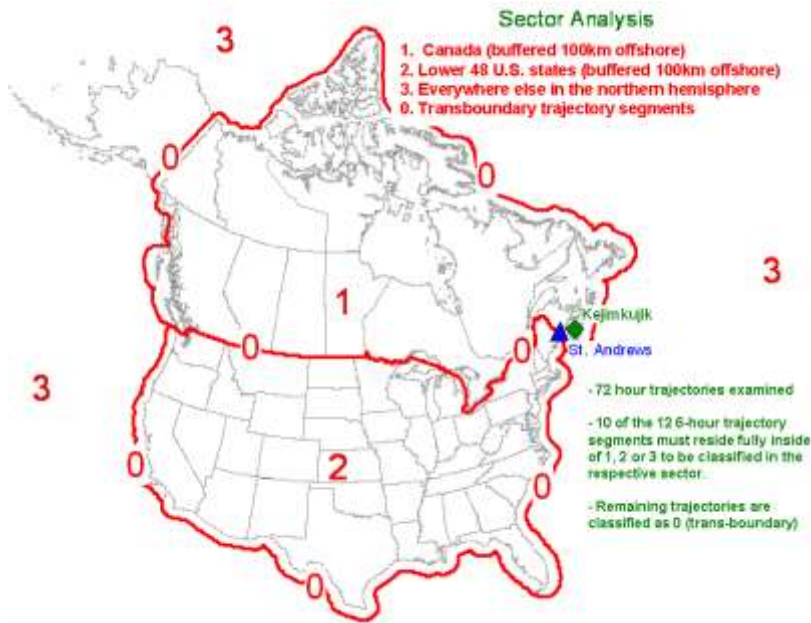


Figure 7.71 Source Sector geographic boundary definition (Ketch *et al.*, 2005) for St. Andrews, NB and Kejimikujik, NS. Trajectories (3-day, 925 hPa) arriving at each site were sorted according to three upwind regions or sectors: U.S., Canada and Ocean. A fourth grouping, “multi-sector”, was defined for any trajectory that did not have at least 10 of its 12 segments solely in one of these three regions. (Ketch *et al.*, 2005).

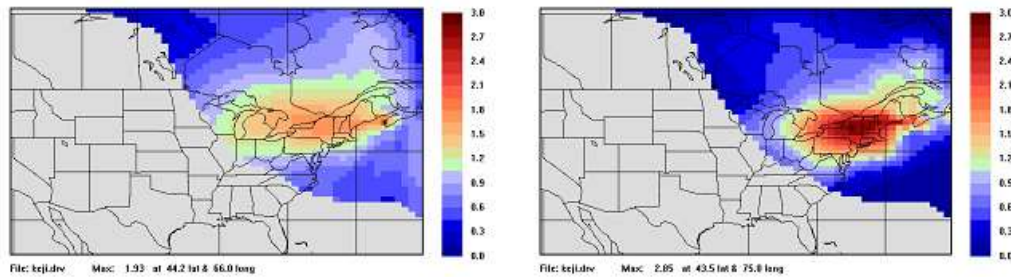


Figure 7.72 QTBA results showing the relative contribution to ozone concentrations during periods with widespread CWS metric exceedances of ozone (left panel) and $PM_{2.5}$ (right panel) for Kejimikujik (Johnson, 2004). Both panels illustrate that the trajectories contributing to the higher concentrations of these pollutants are generally from the west. Ozone data are based on the period 1990-2002 and $PM_{2.5}$ from 1998-2002. The transport path for elevated ozone is more westerly than the path for $PM_{2.5}$. The legend indicates the relative contribution of parcels passing over a grid square to the concentrations at Kejimikujik where the green colour represents a factor of 1 and the darkest red colour a factor of 3 above the average concentration.

Table 7.9 Percentage of trajectories from each sector for the data period 1999-2002 for St. Andrews, NB and Kejimikujik, NS, as well as the average ozone and PM_{2.5} concentrations attributed to each of these sectors.

Station	Pollutant	Sector Averages			
		Canada	US	Ocean	Multi-Sector
St. Andrews, NB	% of time trajectory was from sector	35	6	2	57
	Ozone (ppbv)	23.2	28.0	24.2	24.4
	PM _{2.5} (µg m ⁻³)	2.5	7.5	2.7	4.0
Kejimikujik, NS	% of time trajectory was from sector	33	5	5	57
	Ozone (ppbv)	30.5	36.6	39.8	32.2
	PM _{2.5} (µg m ⁻³)	3.4	9.5	2.6	4.9

Aside from cluster analysis, trajectories can also be manually sorted or sectorized according to the upwind areas they pass over, such as Canada vs. U.S. (Brook *et al.*, 2002). Trajectories (3-day 925 hPa) arriving at Kejimikujik, NS and St. Andrews, NB, were sorted according to three upwind regions or sectors: U.S., Canada and Ocean, as shown in Figure 7.71 (Ketch *et al.*, 2005). A fourth grouping, “multi-sector”, was defined for any trajectory that did not have at least 10 of its 12 segments solely in one of these three regions. With the exception of ozone at Kejimikujik, which was highest when transport was from the ocean sector, average pollutant concentrations shown in Table 7.9 were highest at both Kejimikujik and St. Andrews when transport was from the U.S. This was most notable for PM_{2.5} with the average concentration at St. Andrews a factor of 3 larger from the U.S. sector compared to the Canadian sector, and approximately 2.5 times larger at Kejimikujik. The differences between sectors for O₃ were not as pronounced because background O₃ is responsible for a large fraction of the long term average concentration and this is generally not dependant on transport direction. Quantitative Transport Bias Analysis (QTBA; Keeler and Samson, 1989; Brook *et al.*, 2004b) for Kejimikujik observations suggest that the relative contribution of Canadian sources areas (Ontario) compared to U.S. areas is slightly greater for O₃ than PM_{2.5}. Higher values indicated by orange and red in Figure 7.72 indicate where, during widespread CWS exceedances, the air more likely originated or passed over. Although the orientation of approach most likely to give the highest relative concentrations of O₃ and PM_{2.5} were similar, passing from Toronto, through New York State and then toward Kejimikujik, it appears in Figure 7.72 that transport paths were slightly longer and more westerly for O₃ compared to PM_{2.5} exceedances.

Switching to Québec, the locations considered for trajectory clustering were Roundtop Ridge (Mt. Sutton) for O_3 and St. Anicet for $PM_{2.5}$. The spring maximum in O_3 is clearly evident in Figures 7.29 and 7.45 for this rural, mountaintop site. Overall, O_3 at Roundtop can also be seen to be the highest among all the sites shown, which, as also indicated in Chapter 3, is due to its elevation. During the more photochemically active summer months Roundtop and all of SW Québec experiences the highest O_3 with transport from southerly directions. Very light flow from the SSE, which originates over the Boston-New York City area has slightly lower peaks and average levels than when the flow is across parts of southern Ontario and the lower Midwest U.S., but the minimum O_3 levels are higher from the SSE. This suggests that O_3 is more-consistently elevated from this direction. During the fall, for both of the southerly transport directions O_3 is also higher than for the other four directions. In contrast, in the spring there is less difference among the six transport paths, with only a slight enhancement in the mean and peak levels with the WSW flow.

Figure 7.45 shows that in March the mean O_3 is the same regardless of direction with the northerly directions having higher levels in the earlier months and the southerly, westerly and west-northwesterly directions bringing higher levels from March into the fall. Figure 7.45 shows that mean O_3 levels tend to fall into three groups with respect to transport paths. High concentrations from the SSE to WSW, medium from the WNW pathways and low from the NNW and NNE. Interestingly, in the winter O_3 is highest from these latter two directions and lowest from the two southerly directions. This reveals the importance of the regional and hemispheric wintertime background level, which is reduced when the flow is from the south towards Roundtop. This likely reflects the greater amount of NO_x in those areas, which will tend to suppress O_3 levels and also possibly the greater potential of precipitation during wintertime southerly flow patterns. Long-term trends in O_3 at Roundtop (Figure 7.43) were examined in detail in Chapter 3.

The relationship between transport path and $PM_{2.5}$ in southwest Québec resembles the O_3 relationship in the summer and fall. However, unlike O_3 , the $PM_{2.5}$ concentrations continue to be noticeably higher for the WSW and SE directions throughout the winter and spring as well. This behaviour is consistent with what was observed for the southern Atlantic region. $PM_{2.5}$ is not influenced by background levels to the extent that flow from clean or remote areas leads to concentrations that can match, much less surpass, the influence of anthropogenic-related source areas to the WSW and SE. One interesting feature of the tendency for higher $PM_{2.5}$ with these transport paths is that higher means and peaks are associated with the WSW flow across parts of southern Ontario and the U.S. Midwest for all seasons except winter. During these months, slow transport across rural New York from the New York City area brings noticeably greater $PM_{2.5}$ levels. Although transport from this direction is rare, the typical magnitude of the peaks and of the mean $PM_{2.5}$ is second only to summertime flows from the WSW. The conclusion from this analysis is that summertime transport from the WSW and wintertime transport from the SE most often lead to high $PM_{2.5}$ over southwest Québec. However, given these are opposite seasons and knowledge of the seasonal behaviour of $PM_{2.5}$ composition

from Chapter 3 would suggest that the chemical characteristics of these two types of high $PM_{2.5}$ situations are likely different. Given the available information, one can also not rule out the possibility that at St. Anicet light SE flow in the winter increases the influence of some local activities such as wood burning. A light SE flow at 925 hPa in winter at St. Anicet is indicative of a high pressure system lying to the northeast, cold temperatures and stagnant air flow conditions at the surface, favourable to the accumulation of local pollutants such as nitrate and primary $PM_{2.5}$ from combustion. In such conditions, St. Anicet is under a light NE flow at the surface that brings locally accumulated pollutants from Montreal and the suburbs.

To quantify the local and regional contributions to $PM_{2.5}$ in Québec a source-receptor analysis tool named START (Suivi du Transport Atmosphérique Régional et Transfrontalier), was developed (Dion, 2003) based upon back-trajectories and gridded hourly emission inventories. START estimates the pollutant load in an air mass when it arrives at a selected receptor point (i.e., air quality monitoring station). Although this method is based on the assumption of no chemistry or removal mechanisms along the transport path, the pollutant load that is estimated correlates quite well (up to 70%) with ambient measurements at the receptor stations. For the period from 1999 to 2001 START estimated that the average contributions to $PM_{2.5}$ affecting southern Québec were 40-50% from the U. S., 30-35% from Ontario and 20% from within the province.

In Ontario, the dependence of O_3 concentration on season and transport pathway is demonstrated for Longwoods and Algoma, which are rural sites near London and Sault Ste. Marie, respectively. Conditions were also examined at Experimental Lakes Area (ELA) in the far western part of the province. Consistent with the other regions and the commonality of the synoptic patterns associated with higher pollutant levels throughout eastern Canada, O_3 concentrations are highest in southwestern Ontario for transport from the SSE and SSW. Summertime concentrations are also elevated with light WNW transport which likely brings in O_3 and precursors from southern Michigan and the Chicago area.

As may be seen in Figure 7.28, the mean three-day SSE trajectories arriving at Longwoods are very short, implying light winds, if not stagnant conditions. Thus, the major influence on concentration is from emissions in the province or close to the border. The SSW trajectories are much longer, and are consistent with the transboundary transport of pollutants from the Ohio Valley and possibly as far away as the Gulf Coast. In the summer at the Algoma site, highest O_3 concentrations are also associated with trajectories from the SSW, while highest concentrations at Experimental Lakes Area (ELA) were found for trajectories from the SSE. Referring to Figure 7.28, it is clear that the transport pathways for maximum O_3 concentration at all three Ontario sites identify essentially the same source region.

Ozone concentrations at the Longwoods site are highest in the summer as is usually observed for areas influenced by anthropogenic emissions. However, for both Algoma and ELA, as well as for O_3 concentrations associated with transport to Longwoods from a predominantly

northerly direction, highest concentrations are observed in the spring (March, April, May). As in other areas, this is consistent with the observation that background O₃ concentrations typically show a spring maximum (Carslaw, 2005; McKendry, 2006). For both Algoma and ELA, concentrations for the SSW and SSE trajectories, which have an anthropogenic contribution, also show a summer hump or shoulder, corresponding to the summer maximum for O₃ of regional, anthropogenic origin.

It is noteworthy that for Longwoods and Algoma, and to a lesser extent for ELA, the sectors that exhibit the highest O₃ in the summer season, showing the maximum anthropogenic influence, have the lowest O₃ concentrations in the winter season. As in southern Québec and Atlantic regions, this is assumed to be a consequence of scavenging of O₃ by the higher winter season concentrations of NO_x seen for the anthropogenically influenced sectors to the south.

A trajectory analysis of concentrations of PM_{2.5} was carried out for two Ontario sites, Simcoe and Ottawa Downtown (Figures 7.69 and 7.70). Simcoe is a rural site, near the north shore of Lake Erie. Concentrations at this location are significantly higher in all seasons with transport from a southerly direction. Average and peak levels are highest in the summer and fall, however, it should be noted that due to losses associated with TEOM measurements (see Chapter 3) winter concentrations in Figure 7.70 are likely to be biased to a lower value. This effect is probably greatest in southern Ontario due to higher levels of fine particle nitrate, but probably plays a role at all the sites shown. In the spring, summer and fall, the longer SSW transport pathway has slightly higher peak and mean concentrations compared to the very light ESE pattern. As with O₃ at Longwoods (Figures 7.28 and 7.29), there is evidence that the Detroit-Windsor area, southern Michigan and the Chicago area contribute to higher PM_{2.5} levels over southwestern Ontario. These results clearly show the influence of transboundary flow, since there are essentially no emission sources in Ontario to the south of Simcoe. For the southerly trajectories, PM_{2.5} concentrations peak in the summer months, with concentrations as much as 15 µg m⁻³ higher than concentrations associated with air parcels from the clean NNW sector (22 vs. 5 µg m⁻³). This provides a measure of the transboundary contribution to concentrations at the site. As in areas further east, concentrations in southern Ontario were found to be higher when trajectories came from the south than when they originated in the north, reflecting the magnitude of the emissions in the south, particularly in the heavily populated and industrialized U.S. states (e.g., Brook *et al.*, 2002).

At the Ottawa site, an urban centre, PM_{2.5} concentrations are highest with transport from the WSW and SSE directions. Similar to the other Ontario site, average flow for the SSE trajectory cluster is very slow and thus concentrations will tend to reflect more build-up of local emissions. Trajectories from the WSW travel from and over the previously identified high emitting areas of the U.S. Midwest and also include the populated and industrialized parts of southern Ontario. Consequently, this transport path gives rise, for all months of the year, to concentrations approximately 5 µg m⁻³ higher compared to the light SSE pathway. Concentrations for both the WSW and SSE are, on average, highest in the summer and early

fall, as seen for other anthropogenically influenced measurements. In contrast, the concentrations for all of the other transport paths are essentially constant through the year. It is worth noting that the Ottawa monitoring site is in the north end of the city, which tends to maximize the impact of sources within Ottawa itself (e.g., motor vehicles) for the WSW and SSE trajectories. The concentrations for these two trajectories tend to decline more slowly into the winter months than is the case for the other sites shown in Figure 7.70. This is possibly a result of local emissions being trapped into a shallower mixed layer as the temperature decreases into the winter.

7.6.1.2 Alberta and the Prairies

Unlike the regions to the east, trans-boundary transport is not likely to be an important contributor to $PM_{2.5}$ and O_3 in the prairies. While air from the south typically brings higher PM into the Prairie Provinces, trans-boundary transport is not the dominant contributor to PM levels as air flow patterns tend to be heavily oriented to the east or west, as illustrated by the trajectory clusters at Esther, AB and Bratt's Lake, SK (Figure 7.28). Southern Manitoba has the most potential to be influenced by transport from the U.S. (Pankratz, 2004). Trajectory clusters with wind flow from the south were also identified by the cluster analysis of both Winnipeg and ELA trajectories, though in both cases these trajectories had the least average distance travelled, and could also be considered local in nature (Figure 7.28).

The O_3 concentrations shown in Figure 7.29 for the Esther trajectory clusters are typical of sites in the southern half of Alberta. The two transport patterns with the least average distance travelled over the three day period tended to have the highest median summertime O_3 concentrations, reflecting the relative importance of local (provincial) emissions and the influence of more stagnant flow conditions. These flow patterns were also the ones most likely to occur both overall and in summer (JJA) and, as observed in the east for flow from the southwest quadrant, they had lowest winter O_3 levels among the different transport pathways. This is potentially due to enhanced destruction of O_3 by regional NO emissions in winter. A transport pathway with rapid flow of air from the North Pacific (and presumably minimal local influence) had higher than average O_3 from October through May, while it had the second lowest median O_3 through the summer. Trajectories from the north had the lowest median O_3 in summer and high median O_3 in winter, presumably representative of the transport of natural background concentrations from northern Canada. Determination of the actual origin of O_3 along the transport path is complicated by the fact that observed concentrations result from both transport of O_3 or precursors along the path and local formation which is influenced by multiple weather conditions associated with a particular flow pattern.

The comparison of the Esther trajectory clusters (Figure 7.28) and Edmonton trajectory clusters (Figure 7.69) to those for the other prairie sites illustrates a slightly different pattern in south-central Alberta compared to the rest of the prairies. The Bratt's Lake, SK, Experimental Lakes Area, ON (ELA), and Winnipeg, MB sites each have a similar star like pattern of

trajectory clusters, with a SSE pathway associated with highest summer and lower winter O₃, suggesting the influence of photochemical formation and NO_x titration. Each of the ELA Bratt's Lake and Winnipeg SSE pathways also show a summer local maxima in seasonal O₃ patterns (Figure 7.45) though it is weakest at the Winnipeg site.

The influence of transport direction on PM_{2.5} is shown for the Edmonton Northwest monitoring site in Figures 7.69 and 7.70. Not surprisingly given the proximity, cluster analysis revealed essentially the same major transport pathways for Edmonton (Figure 7.69) as for Esther (Figure 7.28). The transport pattern associated with strong flow from the north was consistently associated with low PM_{2.5}, while transport from the southwest and the stagnant flow situation were associated with above average PM_{2.5}. This supports a conclusion of elevated PM_{2.5} at this urban site being primarily due to local pollutants, possibly with some long-range transport. Forest fires, a large but temporary source for PM, complicate back trajectory analysis for PM source regions.

At two IMPROVE sites, Lostwood and Medicine Lake, located near the U.S./Canada border in Montana and North Dakota, the highest PM_{2.5} concentrations were associated with transport from the southeast (U.S. Midwest). Both sites also had higher than average PM_{2.5} with transport from Alberta. The lowest PM_{2.5} concentrations were associated with rapid transport from the west or north. Since these sites are located away from local influences, PM concentrations should respond primarily to transport from source regions. Sirois and Vet (2002) conducted an analysis of speciated PM at Glacier National Park, stratified by trajectory origin, and concluded that SO₂ sources in Alberta contributed to visibility impairment by sulphate aerosol at that site, while sources on the west coast of Canada and the U.S. contributed to visibility impairment by EC and OC aerosol.

Source regions for high O₃ and PM_{2.5} levels were investigated (Johnson, 2004) using QTBA analysis with trajectories from seven Prairie sites for days when O₃ was above 55 ppb and from four Prairie sites for days when PM_{2.5} was above 20 µg m⁻³. All sites showed a pattern of higher ozone more frequently from the south. However there were some interesting inter-site differences. High ozone in Calgary had a favoured source region to the north over Edmonton and to the southwest over Puget Sound. Violet Grove had a high O₃ source to the northeast, possibly highlighting some influence from Edmonton. Both Brandon and Winnipeg had high O₃ source regions to the south east over the U.S. Midwest, while Brandon had a secondary source region over central Alberta. The QTBA for high PM_{2.5} showed less consistent results, possibly because of the influence of forest fires, an emission source with a different location from episode to episode. The QTBA for PM_{2.5} in Regina indicated a strong source region to the south-south-east including air that travels from the U.S. Midwest and over the Canadian coal-fired power plants near the U.S. border. Regina also had a secondary source region to the northeast near the Manitoba smelters.

Little work has been done to quantify the impact of trans-Pacific transport of pollutants on the Prairies. In spring 1998 a plume of dust from a dust storm in Asia crossed the Pacific and severely impacted $PM_{2.5}$ levels in the Lower Fraser Valley (McKendry *et al.*, 2001). The impact of this event was noted as far east as Minnesota and was detected at Esther, Alberta. Transport of forest fire smoke to Alberta from Yukon, Alaska and even Siberia has been noted on occasion. Episodes of trans-pacific transport of ozone have been documented (Jaffe, *et al.*, 2001), and global modelling results (Fiore *et al.*, 2002) suggest a 5-7 ppb contribution from anthropogenic emissions outside North America to peak ozone levels in the western U.S. Similar level of impacts on Alberta might be expected.

7.6.1.3 The Lower Fraser Valley and Southern Interior British Columbia

Air masses transported over British Columbia typically originate over the Pacific Ocean and are usually relatively clean, exhibiting the characteristics of northern hemispheric background concentrations. Since large-scale events of transported pollutants are episodic in nature and tend to be relatively infrequent, understanding pollutant transport over shorter distances is more relevant to air quality management opportunities in BC. Due to the varied topography of the west coast, high resolution (4 km) mesoscale back trajectories computed from mesoscale model output are best suited to study transport in this region. As will be shown below, they are better able to characterize features of fine scale flow compared to the coarser resolution trajectories, used for the other regions.



Figure 7.73 Clustered one day mesoscale back trajectories for O_3 at Saturna CAPMoN (December 2003-March 2005).



Figure 7.74 Clustered one day mesoscale back trajectories for O₃ at Chilliwack Airport (December 2003-March 2005).

Figure 7.73 presents mesoscale back trajectory clusters for Saturna Island. The transport direction associated with maximum summer O₃ concentrations (6-hr averages near 60 ppb) is a slow moving, clockwise rotating, stagnant flow (C3), typically associated with high pressure conditions. This is consistent with high pressure conditions associated with summertime regional stagnation and the WISE, which concentrates pollutants over the Strait of Georgia (refer to section 7.4.3). In contrast, elevated fall winter and early spring O₃ levels (C2) (6-hr average concentrations in the range of 40 ppb) were associated with a longer range, fast moving, northwesterly flow. This type of flow originates at higher elevations, and has been associated, in a previous study in the area, with frontal-associated downward transport of O₃ from aloft (Vingarzan *et al.*, 2007). Springtime O₃ concentrations at Saturna Island were associated with variable flow directions ranging from northwesterly flows in early spring giving way to southerly flows (C1) over the Puget Sound of Washington State and local stagnant flows as summer approaches. A similar flow pattern was found for Abbotsford (not shown). Further east in the LFV, at Chilliwack (Figure 7.74), two flow directions were associated with elevated summer ozone (6-hour average maxima between 60 and 70 ppb): a northeasterly outflow (C3) and a lighter, roughly southwesterly flow (C1) crossing the Whatcom County area of Washington State into British Columbia.



Figure 7.75 Clustered one day mesoscale back trajectories for O₃ at Kelowna College (December 2003-March 2005).

At Kelowna (Figure 7.75), 6-hour average summer maxima in the range of 70 ppb were associated with relatively localized, lower elevation flow from the north (C1). In contrast, maximum spring time O₃ (February to April) in the range of 45-50 ppb was associated with a higher altitude and longer range southwesterly flow (C3).

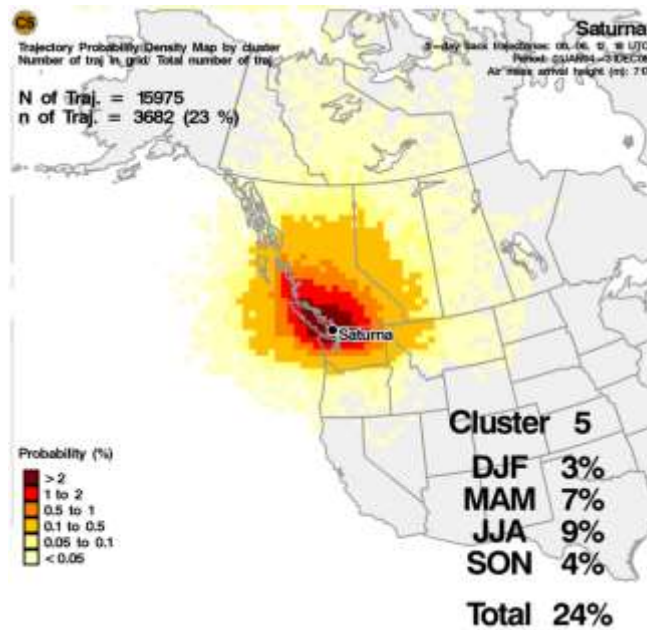


Figure 7.76 Trajectory probability density map of maximum summer O₃ at Saturna CAPMoN, based on three day CMC back trajectories.

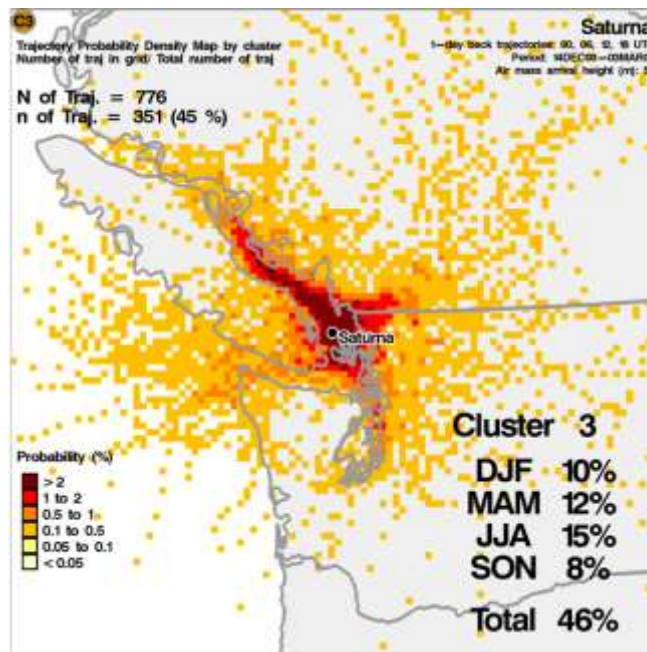


Figure 7.77 Trajectory probability density map of maximum summer O₃ at Saturna CAPMoN, based on one day mesoscale back trajectories.

The Saturna and Chilliwack mesoscale trajectory clusters can be compared with clusters derived from the lower resolution Canadian Meteorological Centre (CMC) trajectories by referring to Figures 7.28 and 7.69. This comparison is necessary because mesoscale

trajectories are currently only available for a short time period and thus, for analysis of O₃ and PM_{2.5} data over longer periods it remains necessary to rely on the CMC trajectories. For both sites, it can be seen that, although by default more clusters were derived using the CMC trajectories, they were all limited in their ability to characterize flow around geographical features. This is illustrated by comparing the probability density map for maximum summer O₃ at Saturna, created from CMC back trajectories (Figure 7.76), with that created from mesoscale back trajectories (Figure 7.77). The mesoscale trajectories are able to identify geographically defined areas of elevated O₃ concentrations and light flow over the Strait of Georgia. This level of resolution is absent with the CMC trajectories, demonstrating that with such trajectories there are significant limitations in the ability to confidently identify specific source areas. Nonetheless, both the CMC and mesoscale trajectories are able to identify, on a broad sense, the same general dominating flow patterns (*i.e.*, lighter flow or stagnant conditions vs. strong westerly flows) influencing maximum summer O₃ concentrations.

Chilliwack transport pathways related to PM_{2.5} observations and derived from the CMC trajectories are shown in Figure 7.69. In the spring, summer and fall higher PM_{2.5} concentrations (Figure 7.70) are associated with the two transport patterns associated with lighter, more stagnant flows. The mean ESE direction appears to resolve a pathway from the south and then west, possibly related with inflow from the southern Strait of Georgia across Whatcom County Washington. The other high concentration pathway can be seen to be a light flow coming from Vancouver area. This likely reflects the slow movement of primary PM_{2.5} and precursors up the valley where it gets concentrated by the narrowing of the terrain and by the formation of secondary particles. Lower PM_{2.5} levels result in all seasons under conditions of stronger westerly transport.

CMC cluster analyses were also performed for several sites from the U.S. IMPROVE network, located south of the BC border in Washington State (not shown). Results indicate that national park sites tended to have the highest PM_{2.5} during the summer period, while more urban-influenced sites, such as the Puget Sound, had maximum PM_{2.5} levels during the winter. The latter is consistent with wood burning during the cold season. In some cases, the flow direction associated with maximum PM_{2.5} concentrations coincided with westerly flow across the LFV (North Cascades NP) while in other cases it coincided with transport from the Puget Sound (Olympic NP). Note however that these sites were limited to 2-3 years of data and as such, the level of uncertainty is higher than for the Canadian sites.

7.6.1.3.1 Transport between Canada and the U.S.

In 2004, Canada and the United States launched a series of pilot projects under the Border Air Quality Strategy to study the transboundary transport of air pollutants in selected border regions. In British Columbia, three study sites were established: Christopher Point (Vingarzan *et al.*, 2007), on the southern tip of Vancouver Island, Osooyos (Meyn *et al.*, 2007a) in the

Okanagan Valley and Creston (Meyn *et al.*, 2007b) in the Kootenay area of BC. These sites were equipped with state of the art mobile trailers measuring air pollutants and meteorology continuously over a period of one to two years.

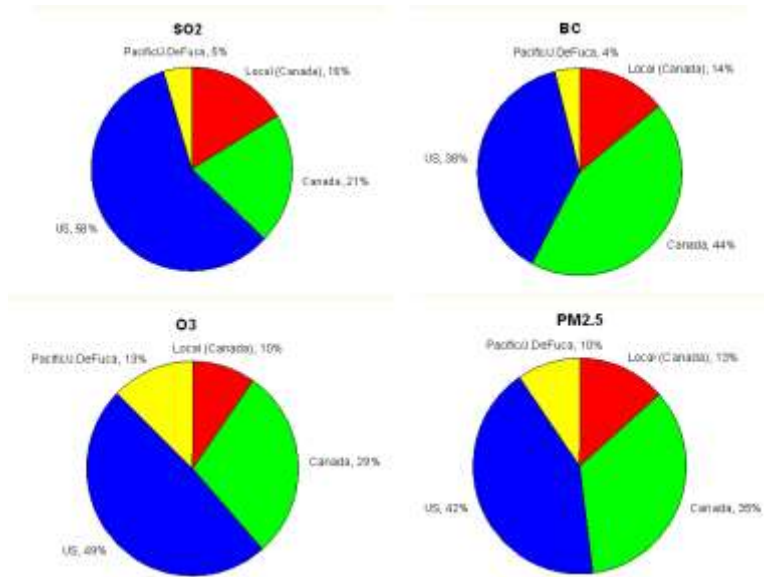


Figure 7.78 Wind sector analysis showing percentage contributions by each sector to pollutants measured at Christopher Point. Canadian contributions are shown as both local and transported.

At Christopher Point, elevated TEOM derived PM_{2.5} concentrations were associated with stagnant conditions throughout the year. In contrast, while O₃ was associated with stagnation in the summer, it was associated with westerly winds and post-frontal subsidence in the winter, indicating an influx of high altitude background O₃. Movement of air pollutants across the international border was observed and varied seasonally. U.S. source areas dominated during the spring and Canadian source areas dominating during the winter. On an annual basis, Canadian source sectors (sum of local and transported) dominated black carbon (BC) concentrations (58%) (Figure 7.78), while the U.S. source sector dominated SO₂ (58%) and O₃ (49%) concentrations (Vingarzan *et al.*, 2007). Contributions from Canadian and U.S. sectors were relatively similar for PM_{2.5}, and for NO, NO₂ (not shown). The site was found to be influenced by multiple sources from both sides of the border, including industry, vehicle and marine traffic.

At Osooyos, wood burning, road dust and forest fires were found to be important sources of air pollutants. TEOM derived PM_{2.5} concentrations were highest in winter, and its transport was influenced by seasonal winds from the south. Ozone transport also differed according to season. During the spring, the predominant transport direction was from Canada into the U.S., but the opposite was true in summer. Moreover, despite the presence of large population

centers to the north of Osoyoos (Kelowna, Penticton), during the summer, ozone concentrations associated with winds from U.S. were several ppb higher than those associated with winds from Canadian locations to the north.

At Creston, agricultural burning was identified as the greatest source of fine PM in the area. Meyn *et al.* (2007b) also found that the airshed shared by Creston, BC, and communities in northern Idaho is well-mixed, resulting in frequent transfer and sharing of air pollutants. Analysis of data and historic burn reports suggested that agricultural burning in northern Idaho is likely the dominant source of PM_{2.5}.

Collectively, the results of the border air quality studies indicate that air pollution moves across the international border at each of these sites, and that the movement of air pollution is closely linked to weather patterns and time of the year. Overall, the transboundary impact appears to be relatively equal at these sites, with Canada and the U.S. both contributing to pollutants crossing the international boundary.

7.7 Case Studies of Local, Regional and/or National Significance

The sections above have attempted to convey, in a relatively consistent fashion, information on the behaviour of O₃, NO_x, PM_{2.5} and its constituents in different regions of the country. Focus has been on insights from analysis of regional scale atmospheric transport and of local scale variations in concentrations. This information is needed to devise conceptual models of the factors influencing air quality with sufficient detail to impart some region-specific understanding. This ultimately helps in the development of air quality models, approaches to forecast air quality and strategies to reduce pollutant levels. To further advance understanding to achieve these goals ongoing research has been and is being undertaken within the regions on a variety of issues, from those of local interest to ones with national relevance. The purpose of this section is to summarize results from a range of specific studies or analyses to help complete the picture regarding our current understanding of air quality issues in Canada.

The first case study presented examines the largest PM_{2.5} event observed during the past ten years. This case is discussed because it affected a large populated area, it brings attention to the fact that high PM_{2.5} occurs in winter and because it provides an opportunity to demonstrate some of the links between meteorology and high PM_{2.5}, as well as some of the complexities.

The second topic discussed in this section is related to the air quality impacts of forest fires. These events are common, contribute to summer background PM_{2.5} and O₃ across Canada and on occasion can significantly impact cities anywhere in the country. Clearly, forest fires are of national significance and may increase in frequency and magnitude under future climate projections. Also of national significance are emissions from motor vehicles. Traffic is

ubiquitous in Canadian society with a sizeable proportion of the population living close enough (within 500 m) to a major road or a highway to be chronically exposed to elevated concentrations. Given that there has been considerable research in Canada on assessing the levels of some pollutants in relation to roadways and improving exposure estimates Section 7.7.3 provides a brief overview of some of this work.

The final topic in this section that is of national interest or scope and for which there are valuable results to present pertains to the sources of $PM_{2.5}$. Receptor modelling or source apportionment (e.g., Watson *et al.*, 2008) is a common approach to obtain quantitative information on $PM_{2.5}$ types and/or sources, although it has limitations, such as being able to discern the sources of secondary $PM_{2.5}$. Over the past several years the quantity and quality of $PM_{2.5}$ data for receptor modelling has improved for many locations. Consequently a range of results that provide insight into the sources of $PM_{2.5}$ are now available and are summarized in Section 7.7.4. The remaining case studies generally refer to specific studies conducted within the regions. They highlight some local issues of interest and/or importance and also contribute to a better overall understanding of the causes and or processes contributing to the levels of and variations in $PM_{2.5}$, O_3 and/or NO_2 observed in Canada.

7.7.1 Diagnosis of the Largest $PM_{2.5}$ Event in Canada – A Wintertime Occurrence

Monitoring capacity of both real-time and speciated $PM_{2.5}$ has improved over the past 10 years providing a clearer picture of and drawing attention to winter smog events. In recognition of the importance of such cases a widespread winter $PM_{2.5}$ event that occurred in February 1998 (MOE, 1998) was the focus of model case studies in support of an assessment of transboundary transport of $PM_{2.5}$ (Sub-Committee on Scientific Co-operation, 2004).

Although air quality advisories/alerts have been issued in winter for municipalities along the St. Lawrence River Valley for several years, it was a couple of events in February 2004 that raised awareness in Ontario. These cases laid the foundation for the first issuance of a formal winter air quality advisory by the Province of Ontario. This advisory, which was due to an event occurring from Feb. 1-8, 2005, was unique because of its spatial extent and the duration of high $PM_{2.5}$ levels, especially over eastern Ontario and southwest Québec. In fact, in Montréal the 24-hr filter-based $PM_{2.5}$ measurements, which represent the most robust and long-term monitoring approach in Canada, were the highest observed anywhere in the country during the past 15 years. While there have been other $PM_{2.5}$ events of similar or greater magnitude associated with forest fires (see below), this was the largest event entirely associated with anthropogenic emissions.

A ridge of high pressure, oriented SW-NE, remained entrenched over the lower St. Lawrence valley for the entire period and it extended outside of that area in various directions. However, as will be discussed below, these other regions of persistent high pressure and very light winds (i.e., Ontario and the upper Midwest U.S.) were not directly linked to the ridge over the St. Lawrence Valley. Thus, there were two synoptic features during the period:

1. A persistent St. Lawrence Valley ridge associated cold temperatures and strong inversions accentuated by the valleys.
2. A weak high and slack winds lingering for many days in late January over Minnesota and gradually moving east starting around Feb. 4th as an upper level ridge strengthened. Behind this high, a light and warm southerly flow of air over snow covered ground enhanced strong surface inversions.

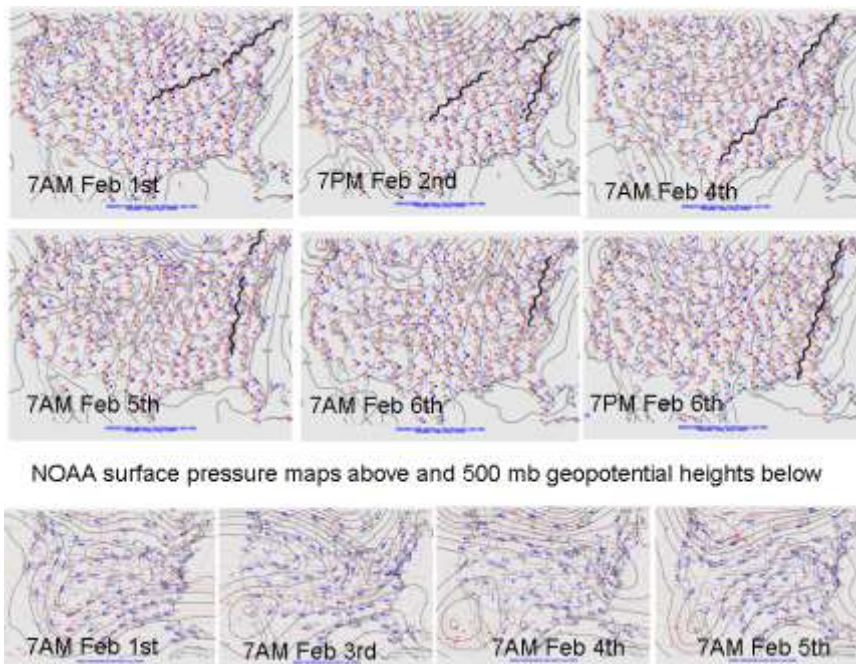
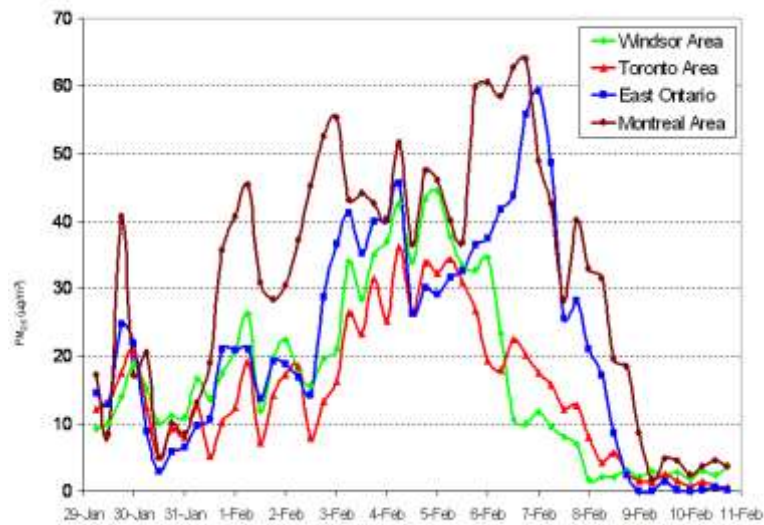
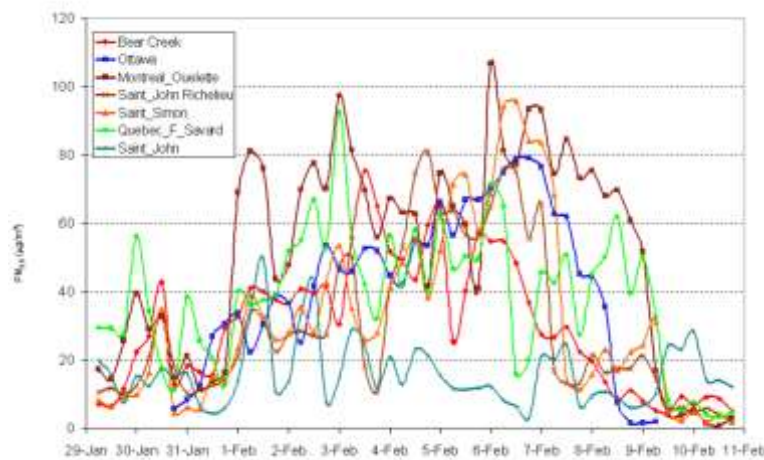


Figure 7.79 Weather maps associated with the February, 2005, $PM_{2.5}$ event in Ontario and Quebec. Map time stamps are EST with surface synoptic charts for February 1 – February 6 on the top two rows and 500 mb charts for February 1, 3, 4, 5 on the bottom row. The surface charts illustrate a ridge of high pressure (wavy line) lying nearly stationary over southern Ontario, the lower Great Lakes and southern Quebec during the period to February 6th.



a)



b)

Figure 7.80 a) Time series of unadjusted TEOM (SES) 6 hour average $PM_{2.5}$ concentrations for site group averages in the Windsor, Toronto, eastern Ontario and Montréal areas for the period 29 January to 10 February 2005. Although Montréal sites had the highest values and were elevated prior to the other areas the graph illustrates the rapid return to low concentrations as the cold front and attendant weather approached on February 8th. b) Beta Attenuation Monitor (BAM) 6 hour average $PM_{2.5}$ concentrations for selected sites in each region. This instrument is much less sensitive to loss of ammonium nitrate (especially in winter) and thus the concentrations shown tend to be larger than those in Figure 7.66a.

Weather maps covering this period are shown in several panels in Figure 7.79. On Feb. 1st there was a high pressure centre over eastern townships of Québec with a surface ridge towards southwestern Ontario and Nova Scotia. This was accompanied by a weak flow at 500 mb from New Jersey to the Dakotas. Figure 7.80a shows that 6-hour average $PM_{2.5}$ peaked at $20 \mu\text{g m}^{-3}$ or higher from southwest Ontario to Québec and Saint John, NB. Levels surpassed $40 \mu\text{g m}^{-3}$ around Montréal. These values were measured using TEOMs and although they

were equipped with a sample equilibration system (SES) to help remove water so that the instrument can be operated at a slightly lower temperature, they were still not able to correctly capture nitrate and semi-volatile organics.

The PM_{2.5} build-up started earlier, around January 28th, over Minnesota, Iowa and Wisconsin under this sprawling high pressure system and light flow aloft (i.e., the second feature listed above). This caused considerable stagnation along the Ohio River Valley with widespread morning fog or haze from Minneapolis to eastern Pennsylvania. However, the highest PM_{2.5} reported in the U.S. was in the upper Great Lakes, especially Michigan where Kenski and Sponseller (2005) reported peak 24-hour levels of over 60 µg m⁻³ at several stations in early February. At locations in Detroit and Port Huron, which were likely influenced significantly by nearby industry, 24-hour PM_{2.5} of over 90 µg m⁻³ and 100 µg m⁻³ were observed.

During the period, the two surface highs and the resulting PM_{2.5} concentrations were also affected by a 500 mb trough moving from the west and lower pressures off the coast of New England and over northwestern Ontario. With the 500 mb trough moving across Ontario (Figure 7.79) PM_{2.5} stayed at or below 20 µg m⁻³, while further east in Québec, where the high was dominant, levels climbed to over 50 µg m⁻³. On Feb. 4th the St. Lawrence Valley ridge weakened and, with falling pressures off the east coast, PM_{2.5} steadily dropped in Saint John due to increasing winds. The 500 mb trough moved over Québec later on the 3rd and into the 5th of Feb and Figure 7.80a shows that PM_{2.5} in Montreal and surrounding area decreased to below 40 µg m⁻³ for some 6-hour periods on those days. Over eastern Ontario the levels dipped below 30 µg m⁻³ for several hours with the passage of the trough.

Behind the trough a large 500 mb ridge developed over the Great Lakes, southern Ontario and Québec, allowing the surface high, which had retained some identity over Québec, to strengthen. The 'new' position of the high changed conditions significantly in eastern Québec and the Maritimes. Consequently, PM_{2.5} in Québec City (Parc Primevères) did not get as high as before the trough, although as seen in Figure 7.80b, it still reached 70 µg m⁻³ for six hours. Further east, in Saint John, concentrations steadily decreased and remained low through the rest of the episode. However, to the west, the high over the Great Lakes started to move east and the southerly flow in its wake brought warm air over snow cover as described above. Consequently, PM_{2.5} increased significantly, first surging above 30 µg m⁻³ in the Windsor and Toronto areas and eventually above 40 µg m⁻³ around Windsor. Of the Ontario sites, Sarnia had the highest concentration of around 55 µg m⁻³ on both Feb. 4th and 5th. This is consistent with the very high level reported for Port Huron (Kenski and Sponseller, 2005). A day or so later concentrations increased in southern Québec, but due to the orientation of the St. Lawrence Valley ridge, concentrations did not rise again in the Saint John area.

The highest PM_{2.5} in Canada with this episode was on Sunday Feb. 6th over the Montreal area and continuing until very early on the 7th over eastern Ontario. In contrast, on the 6th PM_{2.5} was decreasing quickly over southern Ontario due to increasing southerly winds caused by an

approaching low pressure area and cold front. This system ultimately led to the sharp decrease also seen on Figure 7.80a for eastern Ontario and the Montréal area on 7-8 Feb. Some of these regions also received some precipitation on Feb. 7th, thus decreasing $PM_{2.5}$ even further.

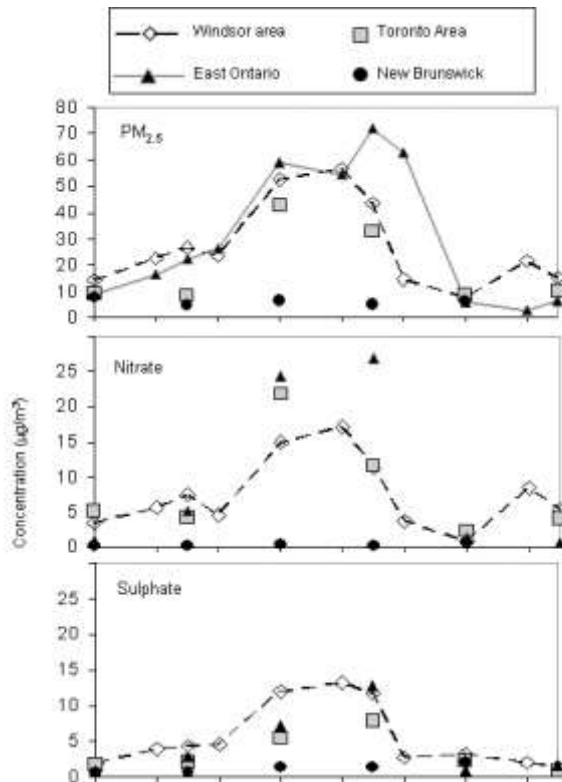


Figure 7.81 Filter-based $PM_{2.5}$ mass, nitrate and sulphate concentrations (24 hr averages) for the areas of Windsor, Toronto, East Ontario and New Brunswick during the February 2005 winter PM episode. Concentrations were averaged among the available sites in the four selected regions. The 24 hr mass measurements shown in the top panel are the best estimate of the true values.

Figure 7.81 presents measurements from filter-based samplers operating in the region during the period. Available observations from the different sites in the four regions were averaged for each day. There are considerably fewer sites operating manual samplers compared to the number of TEOM sites used for Figure 7.80a. The 24-hr mass measurements shown in the top panel of Figure 7.81 are the best estimate of the true values (i.e., the TEOM measurements in Figure 7.80a are known to be biased low; see Chapter 3). In the Windsor area, the filter measurements indicated that $PM_{2.5}$ was above $50-55 \mu g m^{-3}$ for the 3rd, 4th and 5th of Feb. and at $44 \mu g m^{-3}$ on the 6th. Around Toronto they surpassed $42 \mu g m^{-3}$ on Feb. 3rd and the mean filter-based mass on the 6th of Feb. was $33 \mu g m^{-3}$. Thus, it appears that the TEOM concentrations in 7.80a were about $15 \mu g m^{-3}$ lower than the true values. For the eastern Ontario average, which included a site in Montréal, the 24-hr average filter-based $PM_{2.5}$ peaked at $72 \mu g m^{-3}$ and there were four days above $54 \mu g m^{-3}$. Again, these are about $15 \mu g m^{-3}$ greater than the TEOM readings. The highest single site 24 hour filter-based $PM_{2.5}$ observed during the episode was 85

$\mu\text{g m}^{-3}$ in downtown Montréal on Feb. 6. This is the highest 24 hour $\text{PM}_{2.5}$, from the ‘gold standard’ filter-based method, observed in Canada during the past 10 years or more in any season. A three hour average of $105 \mu\text{g m}^{-3}$ was reported for Riviere des Prairies (east Montréal) based upon measurements from a FDMS-TEOM, which has been shown to match the filter-based measurements in side-by-side comparisons. Figure 7.80b shows the $\text{PM}_{2.5}$ measurements from sites operating Beta Attenuation Monitors (BAM). These are known to provide reliable measurements of $\text{PM}_{2.5}$ in the winter (i.e., limited nitrate loss). The Rivière des Prairies site also detected a 6-hr $\text{PM}_{2.5}$ of around $105 \mu\text{g m}^{-3}$.

Figure 7.81 also presents the available information on the composition of the $\text{PM}_{2.5}$. Consistent with expectations, nitrate was the main constituent with multi-site averages over $15 \mu\text{g m}^{-3}$ for ~ 3 days in the Windsor area. Closer examination in this region showed that 24-hr level peaked at $26 \mu\text{g m}^{-3}$ in Windsor, while at a nearby rural site (Essex) the peak was $19 \mu\text{g m}^{-3}$. This suggests that there was some urban enhancement in nitrate, which implies some local formation. The fact that peak 24-hr sulphate at these two locations was the same, at $14 \mu\text{g m}^{-3}$, further supports the conclusion that there was local particle nitrate formation enhancing levels in larger cities. On the same day as the Windsor peak (Feb. 3rd) Toronto observed $22 \mu\text{g m}^{-3}$ and St. Anicet, in extreme southwestern Québec experienced a level of $24 \mu\text{g m}^{-3}$. These concentrations are considerably higher than the available nitrate concentrations observed in the U.S. (Kenski and Sponseller, 2005).

At first glance, there appears to be widespread nitrate across southern Ontario and Québec in the $20\text{-}25 \mu\text{g m}^{-3}$ range. However sulphate mass concentrations at the Toronto and St. Anicet sites were only $5 \mu\text{g m}^{-3}$ and $7 \mu\text{g m}^{-3}$, respectively. Given that sulphate is typically more regionally homogeneous, but exhibited a decrease towards the east (i.e., from Windsor to Toronto and St. Anicet), while nitrate showed a much smaller relative decrease and an increase from Toronto to St. Anicet, leads to the conclusion that the observed nitrate was influenced by local formation. Furthermore, the large differences in the nitrate to sulphate ratio in Ontario vs. Québec suggests relatively little connection between these two air masses. Thus, in this large episode there appears to be both small scale (urban enhancement) and regional scale heterogeneity in nitrate.

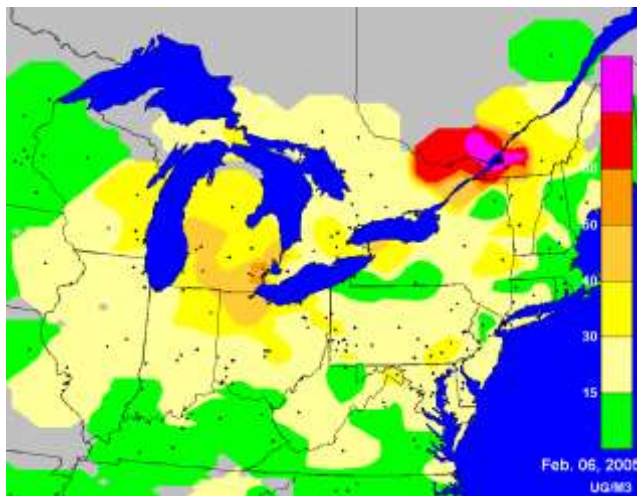


Figure 7.82 PM_{2.5} concentrations (24 hour average) on February 6, 2005, the day with the highest levels in southern Quebec, which were the highest PM_{2.5} (24 hour, filter-based samples) levels observed in Canada during the past 10 years.

One of the broad patterns in the PM_{2.5} observed during this episode was that concentrations were highest in Windsor-Sarnia and Michigan, lower in Toronto area and then higher again in eastern Ontario and southwestern Québec. Other available measurements indicate that there was a considerable low point in the levels over the area from Toronto to the eastern end of Lake Ontario. For example, at Pt Petre, which is south of Belleville on a point extending into Lake Ontario, the filter-based 24-hr concentration of PM_{2.5} was only 15 µg m⁻³ on Feb. 3rd. Similarly, the averaged TEOM readings for Belleville and Peterborough for Feb. 3-6 were 20 µg m⁻³ and peaked at 28 µg m⁻³ for the 24 hours centered on midnight of Feb. 4th. The concentration map for Feb. 6, in Figure 7.82 shows this pattern, consistent also with maps in Kenski and Sponseller (2005). Thus, this Feb. 2005 episode, with concurrent high concentrations in Ontario and Québec, consisted of two separate areas of PM_{2.5} build-up and local formation. There was no regional scale transport connecting these two regions, despite similar nitrate concentrations. In contrast, separate persistent high pressure areas with different driving forces helping to support shallow inversions, were at play. The particles in eastern Ontario and southwestern Québec were from relatively local emissions building up over a week or more. Relatively local influences were also most important in southern Ontario, but this was connected to a much larger area of high concentrations potentially with some amount of transport from the upper Midwest.

Overall, this case study shows that during major wintertime PM_{2.5} events the build-up of emissions from local sources is more important than regional scale transport. This is consistent with the analysis of some past events, particularly the February 1998 case.

7.7.2 Forest Fire Impacts on Air Quality in Canada

Nearly 50% of Canada is covered in forest with about a third of the world's boreal forest and one fifth of the world's temperate rainforest. Annually, an average of over 2 million hectares of Canada's forest burns³⁹, emitting large quantities of gaseous and particulate matter into the atmosphere. The bulk of fire emissions are carbonaceous particulate matter (both coarse and fine), CO, NO_x, VOCs and greenhouse gases (mainly CO₂ and CH₄). Other emissions include SO₂, NH₃, SVOCs, PAH, gaseous mercury and a variety of other air toxics (Clinton *et al.*, 2006, Andreae and Merlet, 2001). These emissions can be injected from the surface layers of the troposphere up to the lower stratosphere depending on the magnitude of the fires and the prevailing meteorology. Fires are highly variable in both space and time, which makes them difficult to include in inventories for atmospheric modelling.

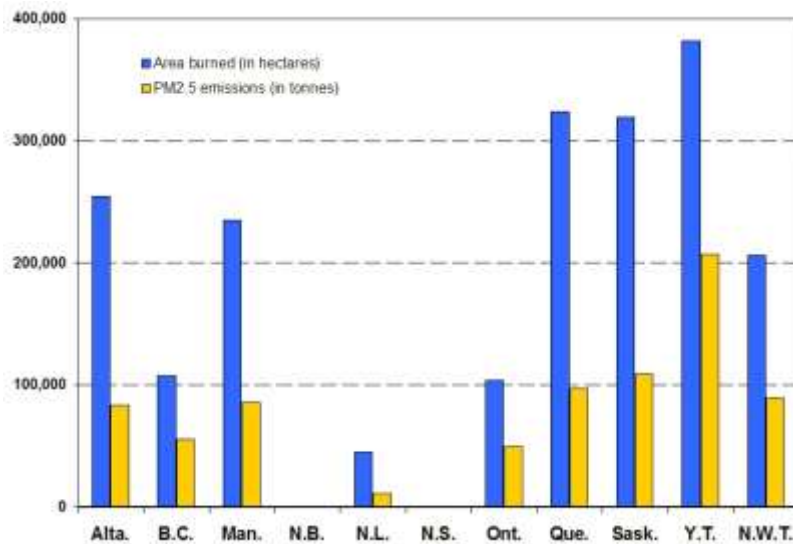


Figure 7.83 Average 2000-2004 forest fire PM_{2.5} emissions and area burned by Province (Lavoué *et al.*, 2007)

³⁹ Forest fires include both wildfires and prescribed burns (forest fires set intentionally, usually to achieve some forest management objective). In Canada far more area is burnt in wildfires than prescribed burns. For instance in 2006 wildfires burnt approximately 250 times the area of prescribed burns (Canadian Inter-Agency Forest Fire Centre, 2007).

Retrospective forest fire emissions have been calculated by year and province and the averages for the five year period from 2000 to 2004 are shown in Figure 7.83, along with hectares burned. These data provide some perspective on the total emissions related to human activities shown above and in Chapter 4 and are being used for air quality and climate modelling applications. The 2002 Québec fires, for example, were estimated to have released emissions equivalent to 50% of the total annual Canadian anthropogenic PM_{2.5} emissions in about 12 days (Lavoué *et al.*, 2007). The majority of forest fire emissions in Canada occur between April and October (peaking in June-August)⁴⁰ and the area of forest burnt varies from year to year by as much as a factor of ten. The locations of peak fire activity are highly variable from year to year. However, Figure 7.83 shows that the Yukon Territory, Québec and Saskatchewan experience the greatest amount of hectares burned on average, which leads to those areas having the largest annual PM_{2.5} emissions from fires.

Air quality impacts of forest fires have been observed on local, continental and global scale. On the global scale hemispheric enhancements of ozone and carbon monoxide have been reported, for instance Pfister *et al.*, (2006) reported an increase in tropospheric O₃ burden of 7-9% over Canada and 2-3% over Europe due to large fires in Alaska and northern Canada during 2004. Furthermore, intact ‘plumes’ of particles from the fires in Alaska were observed in Atlantic Canada during the ICARTT field study (Waugh *et al.*, 2007). The 2003 fires in Siberia are another example, they contributing to elevated levels of O₃, PM_{2.5}, and CO in north-western North America (Jaffe *et al.*, 2004; Bertschi and Jaffe, 2005).



Figure 7.84 View of downtown Calgary looking west at 7:30 PM August 13, 2003. Forest fire smoke from fires in southeastern B.C. Fine particulate matter levels = 125 µg m⁻³ (average of three Calgary monitoring stations).

⁴⁰ http://www.nofc.forestry.ca/fire/facts_e.php

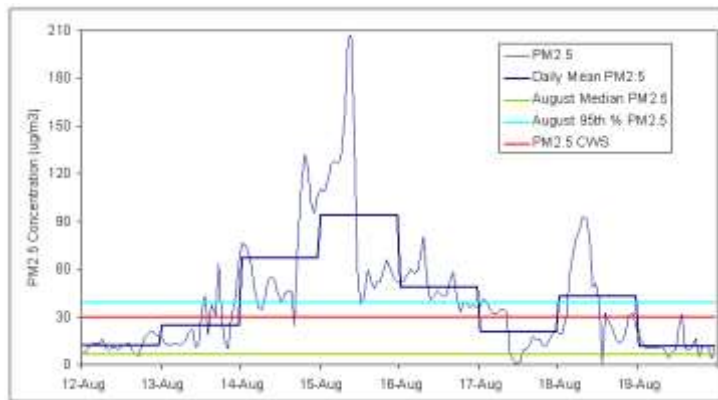


Figure 7.85 Hourly and daily PM_{2.5} at Calgary Northwest monitoring station during the August 2003 forest fire smoke episode. The green line shows August median hourly PM_{2.5} at this site, the light blue line shows the August 95th percentile hourly PM_{2.5} at this site and the red line shows the CWS fzzzor PM

Although air quality impacts from forest fires in populated areas are episodic, they can be severe when they do occur, elevating air pollutants far above the levels normally caused by anthropogenic pollutants. In the Prairie Provinces, nearly all the spring and summer exceedances of the PM_{2.5} CWS can be attributed to forest fire influence (Johnson, 2005). In August 2003 Calgary was heavily influenced by smoke (Figure 7.84) from a large number of forest fires in the Rocky Mountains and southern BC. The greatest impacts occurred between August 13th and the 18th (Figure 7.85), during which time the PM_{2.5} levels reached hourly averages of greater than 200 µg m⁻³, and daily averages up to 94 µg m⁻³. Among the fires in southern BC at that time were the fires that eventually threatened Kelowna, B.C. In Kelowna, hourly levels of PM_{2.5} above 100 µg m⁻³ were recorded and air traffic was forced to divert around the smoke plumes. A subsequent study of health impacts (Moore, *et al.*, 2006) found an increase of 46 to 78% (above the 10 year mean) in visits to doctors for respiratory conditions in Kelowna around the time of the fires.

In the summer of 2002 fires in northern Québec resulted in elevated PM_{2.5} concentrations over much of eastern Canada and northeastern U.S.. In southern Ontario twenty-four hour average PM_{2.5} concentrations over 70 µg m⁻³ were recorded at the Peterborough and Ottawa air monitoring locations (MOE, 2005). Daily PM_{2.5} concentrations between 55 and 75 µg m⁻³ were also recorded in southern Québec and as the smoke plume moved eastward, some sites in New Brunswick and Nova reported daily concentrations between 40 and 50 µg m⁻³. PM_{2.5} during this episode was at record levels at a number of sites across southern and eastern Ontario, including the Greater Toronto Area, Peterborough and Ottawa. High PM_{2.5} levels extended as far south as North Carolina in the U.S. This event is one of several where Canadian forest fire smoke crossed international boundaries and affected air quality in the U.S. (see Wotawa and Trainer, 2000; McKeen *et al.*, 2002; or Colarco *et al.*, 2004).

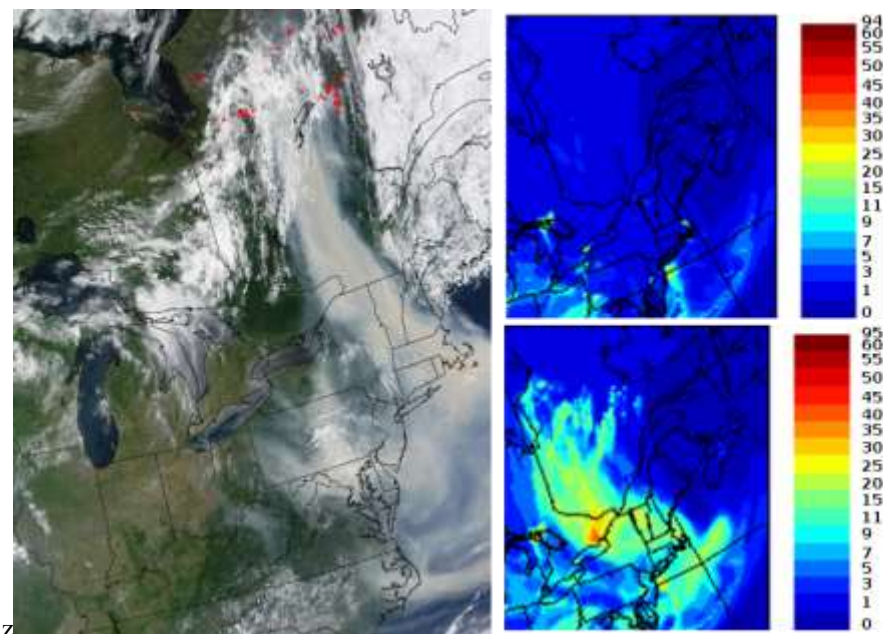


Figure 7.86 Results from the 2002 Québec case study for July 6, 2002. Left: Terra MODIS image at 15:50 UTC; Right: GEM/CHRONOS PM_{2.5} output at 16UTC with (bottom) and without (top) wildfire emissions. Without the inclusion of emissions from the forest fires the model is unable to forecast the elevated PM observed.

A retrospective study of the 2002 Québec fires that connected the wildfires emission estimates for the 2002 event (Lavoué *et al.*, 2007) to Environment Canada’s operational air quality forecasting system GEM/CHRONOS was performed (Rousseau and Lavoué, 2005). Figure 7.86 synthesizes the results of this case study which highlighted the limitations of the current air quality forecasting system in the absence of wildfire emissions. Nearly all areas of Canada have been affected, at one time or another, by smoke from forest fires (or other biomass burning). Some other documented cases include:

- Cheng *et al.* (1998) describe a 1995 event where a forest fire 300 km northwest of Edmonton contributed to high ozone in Edmonton. During this episode ozone and NO₂ concentrations were elevated 50-150% above seasonal medians.
- Chaikowsky (2001) describes an event in May 1998 where ozone at a rural site west of Edmonton rose rapidly to 185 ppb (the highest surface ozone measured in Alberta) along with a rapid rise in NO₂. The event was attributed to down-mixing of O₃ and NO₂ from an elevated forest fire plume identified in satellite photos.
- In May 2001, smoke from the Chisholm fire north of Edmonton affected Edmonton and Red Deer for a one day period causing PM_{2.5} concentrations as high as 261 µg m⁻³. Researchers at University of Alberta used the Air Quality Valuation Model to estimate the one-day health impacts from this fire (Rittmaster *et al.*, 2006), finding a health cost on the order of \$10,000,000. This figure was similar to the total cost of fighting the fire and greater than the cost of damage to infrastructure.

- In 2005 a portion of Burns Bog in the Lower Fraser Valley burnt, blanketing Vancouver in thick smoke and leading to record high PM_{2.5} concentrations at nearby air quality monitoring sites (274 µg m⁻³ at South Burnaby).
- In June 2005 in eastern Canada, wildfires ignited by thunderstorms in the Chibougamau region caused poor air quality in southern Québec and the Maritimes.

In 2004 Yellowknife and Whitehorse experienced extremely high PM_{2.5} concentrations due to large forest fires in Yukon and Alaska. PM_{2.5} levels in Whitehorse reached an hourly maximum of 190 µg m⁻³ on June 27. In Yellowknife PM_{2.5} reached an hourly maximum of 337 µg m⁻³ in early July (Northwest Territories Department of Environment and Natural Resources, 2004).

In the U.S., where wildfires are also a significant issue and often have a greater potential to impact populated areas, Park *et al.* (2007) estimated that biomass burning contributed approximately 30% of mean annual aerosol mass in the western U.S. and 20% in the east. Of the biomass burning component about 80% in the west and 50% in the east was accounted for by fires (wildfire, prescribed burning, and agricultural burning). Canadian wildfires were noted as significant contributors to aerosol in the northwest and northeast U.S. The methods of Park *et al.* (2007) were applied to one season (May-Sept 1998) of speciated PM_{2.5} data from Esther, Alberta. Forest fires were estimated to contribute, on average, 2.1 µg m⁻³ to PM concentration; approximately 1/3 of total PM_{2.5} mass. Esther is distant from the main forested areas, so forest fire contributions to PM concentrations at sites closer to forested areas may be greater.

In addition to forest fires, an occasional contributor to smog is smoke from the burning of agricultural residue (stubble burning). It is difficult to quantify the impact of agricultural burning as the impacts tend to be localized and brief, and the time and locations of burning are not typically recorded. Agricultural burning occurs mainly in late summer and autumn. At that time of year inversions can trap the smoke and inhibit dispersion. On occasion multiple fires will combine to create larger scale smoke events such as in Winnipeg on 5-6 September 2007 when numerous agricultural fires were lit following the lifting of a ban on burning. In this case widespread emissions combined with light flow to generate dense smoke over parts of the city.

Climate change projections suggest that climate change is likely to result in increased fire frequency in the boreal forest (Stocks *et al.*, 1998). In this case the issue of smoke impacts on air quality can be expected to increase in importance in the future.

7.7.3 Air Quality in the Vicinity of Traffic

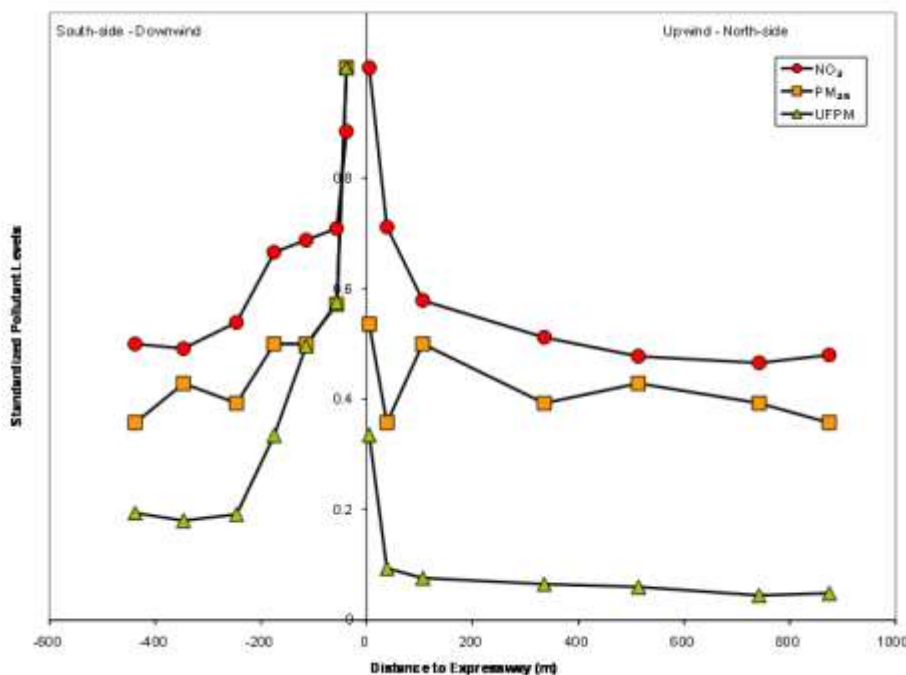


Figure 7.87 Concentration of NO₂ and particulate matter as a function of distance from a major highway (Beckerman *et al.*, 2007).

A large percentage of Canadians live in cities where one of the major sources of emissions is motor vehicles. Furthermore, many Canadians spend part of their day in close proximity to traffic, either travelling in vehicles (private or mass transit), or walking, biking, living or working in these source-impacted micro-environments. Therefore, it is important to better understand what impact traffic has on local air pollutant levels as well as the impact of these pollutants on human health. Gilbert *et al.* (2003) and Beckerman *et al.* (2008) examined the gradient in air pollutants away from major highways in Montréal and Toronto, respectively. Much of the focus of this work has been on NO₂ because it is easy to measure with passive samplers and it has a strong link to motor vehicle exhaust in cities. For example, two transects were sampled along Highway 401 in Toronto in August of 2004. Comparison of upwind and downwind concentrations of multiple pollutants, including NO₂, VOCs, PM_{2.5}, black carbon and ultrafine particles (total counts of particles less than 0.1 µm in diameter), generally showed that there is a clear impact of local highway traffic on air quality for 300 meters downwind. Figure 7.87 shows the concentrations of ultrafine PM (UFPM), PM and NO₂ as a function of distance (from Beckerman *et al.*, 2008). The peak near the highway and drop off with distance is relatively similar among the pollutants shown and NO₂ is seen to be a good indicator of the highway's influence. However, there are slight differences in the rate of decrease and the strength of the highway influence.

Ultrafine particle counts decrease the most rapidly with distance but appear to remain elevated above the upwind concentrations farthest downwind. $PM_{2.5}$ decreases somewhat less sharply and appears to have a smaller upwind-downwind increase as does NO_2 . For all the pollutants shown concentrations are much higher, perhaps double the levels elsewhere, within 50 meters of the highway. While the concentrations of all motor vehicle pollutants decrease due to dispersion and deposition, ultrafine particles are influenced by evaporation and possibly coagulation. Ultrafine particles are also more likely to deposit faster than accumulation mode particles (i.e., 0.1-1.0 μm) and compared to gases such as CO and NO_2 . NO decreases faster than NO_2 because, although it is one of the main gases emitted it reacts quickly to form NO_2 , thereby slowing the rate of decrease of NO_2 . The health impacts of traffic-related air pollutants is becoming widely recognized (see the Health volume of this Assessment) and thus there continues to be a need for more information on the levels and human exposures patterns related to traffic and on the chemical characteristics and local scale behaviour of motor vehicle emissions. Further, UFPM, which is seen above to be strongly related to traffic, is an increasingly being recognized as an important air quality-health issue requiring further study.

7.7.3.1 Characterization of Within-City Variations in NO_2 – A Surrogate for Traffic-Related Pollutants

Short term multi-site monitoring campaigns, referred to as saturation monitoring, have been carried out to obtain snapshots of NO_2 concentration patterns within cities. This information provides more insight on how traffic affects local air quality since, as shown above, urban NO_2 levels are a reasonable surrogate for traffic-related pollutants. Such measurements also help fill in gaps since standard monitoring network sites are costly to operate and so only a limited number of area representative locations can be maintained. Two week integrated sampling campaigns with 100 sites operating simultaneously were undertaken in Toronto in different seasons, including September 2002 and in May 2004. Passive samplers that capture NO_2 at a known rate were deployed to determine the average air concentrations.

Although 100 sites represents a large number, there remain many areas without measurements and thus isopleths (i.e., concentration contours) drawn from these data still cannot capture the details of the variation in concentrations given the high variability in the distribution of sources (i.e., traffic). Thus to produce spatial maps of NO_2 concentration a technique known as land-use regression (LUR) was used (Briggs *et al.*, 1997). Multivariate linear regression models were developed fitting the saturation monitoring NO_2 concentrations to predictors that can be mapped geographically. This includes traffic density where available, road type and size, commercial areas, industrial areas, green spaces and residential areas. Geographic information systems (GIS) was used to derive many of these predictors and subsequently to estimate NO_2 with very high spatial resolution using the LUR model. The resulting concentration maps appear more realistic than those produced by contouring the monitoring site data or even the saturation monitoring data. However, the limitation is that there is no temporal information in the map and the concentrations predicted are based upon the conditions during the saturation

campaigns used to develop the LUR model. Ideally, multiple campaigns should be carried out to generate a more representative input dataset since one or two week dataset could be overly influenced by the meteorological conditions during the measurement period.

LUR models based upon NO₂ have been developed for Toronto (Jerrett *et al.*, 2007), Montréal (Gilbert *et al.*, 2005), Hamilton (Sahsuaroglu *et al.*, 2006), Windsor (Wheeler *et al.*, 2007, 2008) and Vancouver (Henderson *et al.*, 2007). Research is underway to develop models for Winnipeg, London, Ottawa and Edmonton. The R² values for these models, which indicate how well the predictors can explain the variation in NO₂, range from 0.54 to 0.77 and some independent evaluation has shown that the models have reasonable skill. For Vancouver a NO model has also been developed (Henderson *et al.*, 2007), while for Windsor the largest number of pollutants have been considered, including NO₂, Benzene, Toluene and SO₂ (Wheeler *et al.*, 2008), as well as preliminary models for PM_{2.5} and BC (Wheeler *et al.*, 2007). In addition to land-use and roadway type predictors, the locations of major point sources were considered in Windsor and two-week saturation monitoring across 50+ sites was undertaken in each season. As expected, the spatial patterns determined in these four campaigns were quite strongly correlated (Wheeler *et al.*, 2007) due to the stability of the spatial distribution of the main local sources.

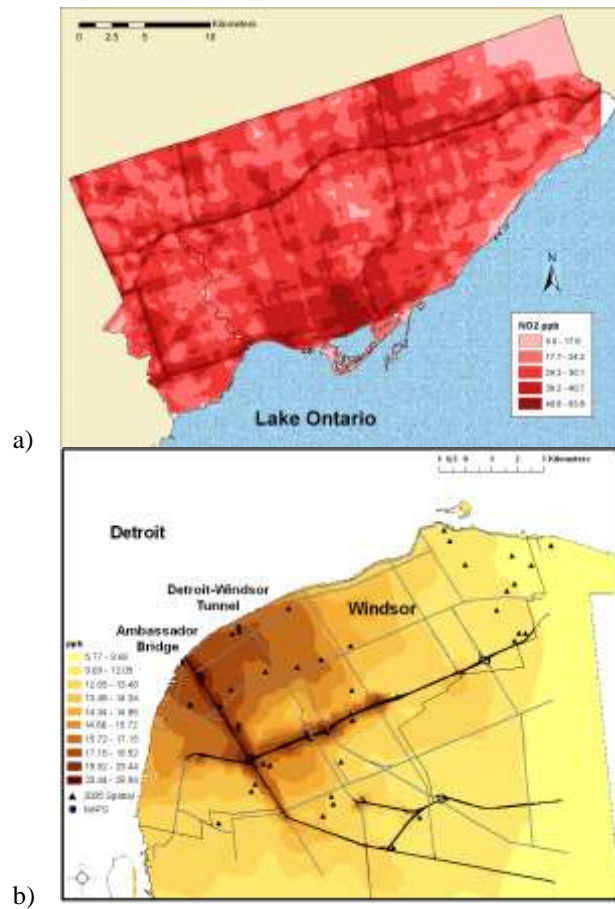


Figure 7.88 Map of NO₂ concentrations from a) Toronto (Jerrett *et al.*, 2007), and b) Windsor (Wheeler *et al.*, 2007), generated using a land-use regression (LUR) model.

Maps of NO₂ concentrations derived from LUR models are shown in Figure 7.88 for Toronto and Windsor. Jerrett *et al.* (2007) compared the Toronto map to a map produced by interpolating the saturation monitoring data using Kriging. This demonstrated clearly that LUR produces considerably more detail with patterns that appear realistic relative to the road network. In addition to providing a better picture of pollutant levels at many locations within cities, the LUR information is used to support health effect studies requiring estimates of the long-term or chronic exposure based upon an individual's home address. The validity of this assumption was tested for several Canadian cities by Xu *et al.* (2007).

7.7.4 Determining the Major Sources of PM_{2.5} using Receptor Models

Receptor-based source apportionment can be a valuable technique for gaining a better understanding of the likely sources contributing to the air pollutants in a given location. Many of the analyses described above, such as the trajectory analyses, have provided qualitative or

semi-quantitative insight regarding sources or source areas of importance. As such they generally fall within the classification of receptor-based methods (Brook *et al.*, 2004a). In combination with other types of information, such as source-oriented models like AURAMS (see Chapter 5) and emissions inventories (see Chapter 4), these methods can be used in the development of emissions control strategies. In addition, comparison of the results of applying these techniques helps advance overall understanding, leading to better conceptual models as well as improvements in the models and inventories. Receptor models are a type of a receptor-based method that is generally thought of as being more quantitative, typically using statistical approaches to apportion or attribute particulate mass ($PM_{2.5}$, PM_{10} or TSP) or VOCs to the sources or atmospheric processes responsible for the observed levels. There have been several applications of these models to observations in Canada since the 1980's. However, since more complete chemical speciation $PM_{2.5}$ measurements is a relatively recent activity, applications of receptor models have only been undertaken at a limited number of sites where sufficient $PM_{2.5}$ speciation data have been acquired. Given the potentially important role these analyses play in understanding air quality, the currently available results are summarized below.

7.7.4.1 Toronto

Lee *et al.* (2003) applied Positive Matrix Factorization (PMF) to a set of daily composition measurements of $PM_{2.5}$ carried out over the period of February 2000 to February 2001. Four main source categories were identified, namely coal combustion relating to regional transport (contributing 26% of the total particle mass), secondary nitrate related to both local and upwind sources of nitrate (contributing 36%), secondary organic aerosols from a variety of precursors (contributing 15%) and motor vehicles (contributing 10%). Four minor source categories were also identified: road salt which is important in the winter, and three groups of primary particulate matter, associated with smelters, fossil fuel combustion, industry and construction. In addition to the 10% noted above, motor vehicles are a significant source of secondary nitrate due to the NO_x emissions as well as road salt/dust. Thus, overall motor vehicles were estimated to be responsible for 40% of the total $PM_{2.5}$ mass in Toronto.

Brook *et al.* (2007a) extended the analysis using a different receptor modelling methodology known as UNMIX (Kim and Henry, 2000; Henry, 2002). While the results were similar, providing valuable confirmation of the analyses, they also separated the motor vehicle contribution with gasoline engine vehicles being a greater overall contributor compared to diesel vehicles at 13% and 8%, respectively. The UNMIX results also provided some insight into the sources of resuspended dust, estimating that road dust was responsible for 2% of the $PM_{2.5}$. Using more detailed organic analysis from the same site and source profiles for a specific class of organic tracers known as petroleum biomarkers Brook *et al.* (2007b) reported that 14% of the total organic carbon (OC) fraction of $PM_{2.5}$ was due to primary motor vehicle exhaust. Given that OC is responsible for 35% of the $PM_{2.5}$ suggests that only about 5% of the total $PM_{2.5}$ is from primary exhaust, which is considerably lower than the 20-25% derived from PMF and UNMIX. This discrepancy has not been fully resolved, but it is important to note that

the results from the biomarker approach were believed to be a lower limit on the contribution to OC. This is because the method could only focus on direct tailpipe emissions of OC and not on the contribution from organic gases emitted from vehicles that form secondary particles in the atmosphere and because there is some atmospheric degradation of the organic tracers. Furthermore, source apportionment based upon these organic tracers does not consider resuspension of road dust and tire and brake wear.

7.7.4.2 British Columbia

Several recent applications of PMF have been undertaken using speciated $PM_{2.5}$ data collected by speciation samplers from four NAPS stations in BC. This includes Burnaby South and Abbotsford (2003-2008) (So, *et al.* 2010), Prince George (2004-2006) (Rubin *et al.*, 2007) and Golden (2004-2006) (Evans and Jeong, 2007). Burnaby South, an urban-industrial site in the Greater Vancouver area, is impacted by traffic, mixed industry and marine (ship) emissions. Abbotsford a semi-rural site in central LFV, is impacted by significant ammonia emissions, vehicle traffic and growing urbanization. Prince George, a pollution hot spot in central BC, is impacted by large industrial sources, wood stove use and urbanization and is subject to significant episodes of poor air quality due to flow restrictions imposed by the topography of the area. Lastly, Golden, in south eastern BC, is a small town impacted by residential wood burning and an active forest products industry.

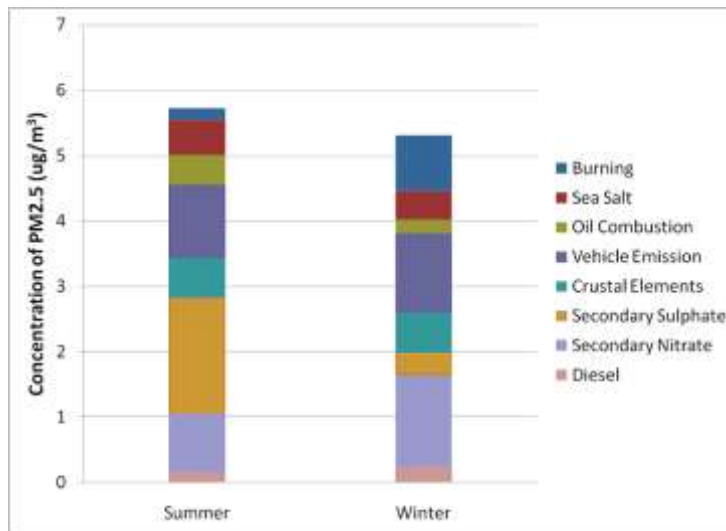


Figure 7.89 Seasonal variations in the contributions of the PMF modelled factors at Burnaby South (Dec 2003 – Dec 2008).

Figure 7.89 presents PMF source factor contributions to $PM_{2.5}$ mass for both summer and winter seasons for Burnaby South and Abbotsford (So, *et al.* 2010). At Burnaby South, the summer $PM_{2.5}$ composition is dominated by secondary sulphate (ammonium sulphate) and vehicle emissions. In the winter, the vehicle emission fraction remains the same but secondary nitrate (ammonium nitrate) and burning fractions increase. Note that the oil combustion

fraction (driven by the Ni/Va tracer) is larger in the summer, during the cruise ship season. In the Greater Vancouver area, SO₂ emissions from marine traffic, diesel vehicles and oil refining, the latter largely from Washington State, all contribute to particulate sulphate. Secondary sulphate is higher during the summer due to a combination of increased SO₂ oxidation and biogenic emissions. Marine biogenic emissions in the form of dimethyl sulphide are also significant during the spring and summer, contributing an estimated 26% of total sulphur emissions in the airshed during algal bloom periods (Sharma *et al.*, 2003). Most of the nitrate in the urban core comes from oxidation of NO_x from vehicle emissions, marine and industrial sources. Secondary nitrate contributions are less in the summer due to preferential formation of ammonium sulphate over ammonium nitrate and uptake of nitric acid on coarse mode sea-salt particles.

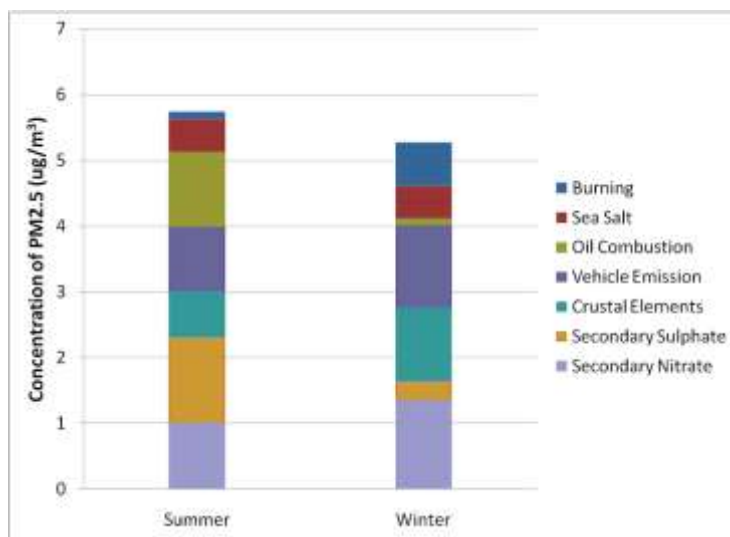


Figure 7.90 Seasonal variations in the contributions of the PMF modelled factors at Abbotsford (Dec 2003 – Dec 2008).

At Abbotsford (Figure 7.90) source contributions vary seasonally with secondary sulphate and oil combustion dominating in the summer, and secondary nitrate, crustal elements and vehicle emissions dominating in the winter. Contributions from wood burning were also more important in the winter. Secondary nitrate (a combined combustion-agricultural source factor) contributed significantly in both seasons.

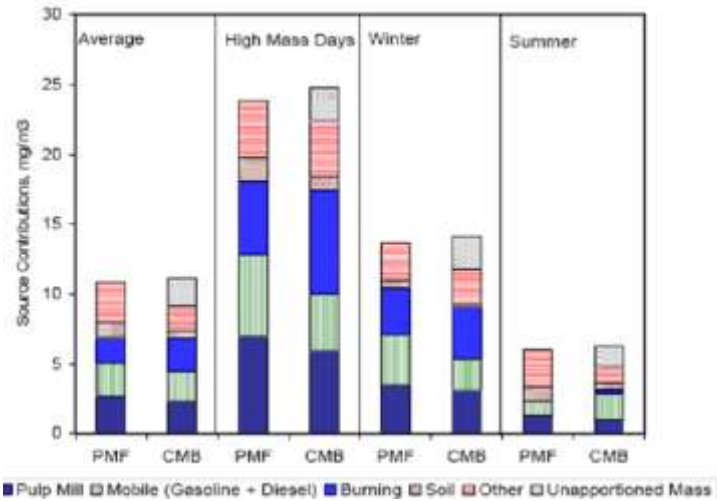


Figure 7.91 Seasonal PMF and CMB factor contributions to PM_{2.5} mass at Prince George, Plaza 400 (2004-2006). Courtesy of BC Environment.

Figure 7.91 presents PMF and CMB (chemical mass balance) source apportionment results for Prince George (Rubin *et al.*, 2007). Both analyses indicated that pulp mill emissions, mobile sources (gasoline and diesel) and wood burning were the largest contributors to PM_{2.5}, especially on high concentration days. On average, pulp mill emissions accounted for 18-25% of PM_{2.5} concentrations, mobile sources for 17-22% and wood burning accounted for 17-19%. Road salt, soil, and less important source types (*e.g.* K/Mn, Cu/Fe) were also identified. Predicted source contributions were similar between the two source receptor models, providing some additional confidence in the data and analyses.

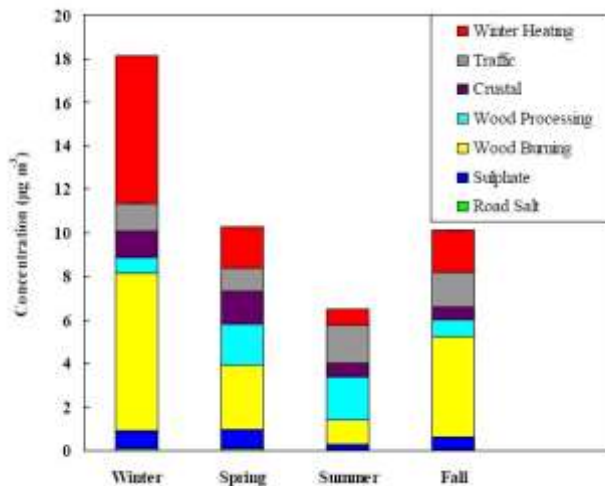


Figure 7.92 Seasonal factor contributions to PM_{2.5} mass at Golden (2004-2006). Courtesy of BC Environment.

At Golden (Evans and Jeong, 2007), PMF analysis identified wood burning and winter heating as the most important sources contributing to PM_{2.5} mass (Figure 7.92). On an annual basis, wood burning accounted for approximately 34% of the total PM_{2.5} mass, while winter heating (gas and wood furnaces) accounted for 24%. The latter was most affected by the frequent temperature inversions and stagnant air masses. Both sources were correlated with many VOCs, including benzene and 1,3-butadiene and were significantly higher in winter than in summer. The wood processing source, contributed 13% to the total PM_{2.5} mass and was highest during the spring and summer months. The traffic related source which contributed 12% to the total PM_{2.5} mass, contributed most during the summer. The crustal material source (assumed to be mostly road dust) accounted for 9% of the PM_{2.5} mass and peaked in the after spring melt. The secondary sulphate source contribution was quite low (6%), at this site. The contribution from road salt was also minor, representing approximately 1% of the PM_{2.5} mass.

7.7.4.3 Five City Report

Positive Matrix Factorization (PMF, Paatero 1997, Polissar *et al.* 2001, Jeong *et al.*, 2008), a type of bilinear multivariate receptor modelling, can be applied to identify PM sources and provide the contribution of each source in the absence of prior information on sources.

PMF (PMF2, Paatero 1998) has been applied to recent NAPS PM_{2.5} speciation data from Toronto and Montréal and available measurements from three additional cities in Canada (Windsor, Halifax, and Edmonton) (Jeong *et al.* 2008) For each site, the PM_{2.5} was apportioned into eight or nine “sources” related to both local and/or more distant emissions. Nine sources may be the limit of the model for the amount of data that were available.

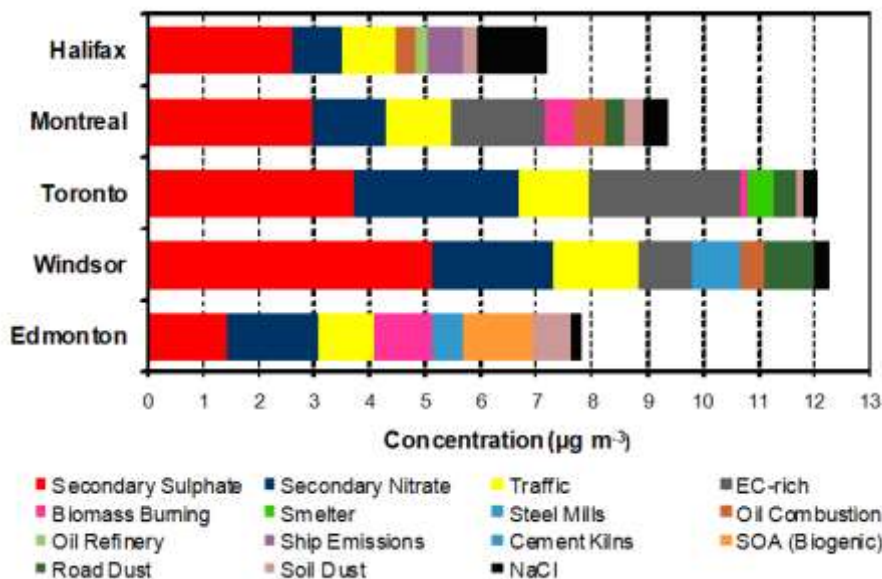


Figure 7.93 Source contributions to PM_{2.5} mass at five Canadian cities (2006-2007). SOA corresponds to secondary organic aerosols (Jeong *et al.*, 2009)

On average, the highest PM_{2.5} levels were observed in Windsor followed by Toronto and Montréal while lower concentrations were found in Halifax and Edmonton during the measurement period of 2006 to 2007 (Figure 7.93). Year-to-year and seasonal variations in PM_{2.5} concentrations and chemical species were observed at all sites. Consistent with the concentrations discussed above, the Edmonton site recorded significantly higher concentrations in the winter (Dec – Feb). Montréal also recorded higher levels in the winter; Toronto in the fall; Windsor summer; and Halifax in the spring. Strong seasonality was observed for most of the PMF sources with sulphate (except for Edmonton where the highest levels were measured in the winter) and elemental carbon (EC)-rich highest in the summer, nitrate and biomass burning highest in the winter, and salt and road dust highest in the winter-spring seasons. Stationary sources and traffic varied little from season to season.

Summarized below are some of the key findings from this study:

- Secondary sulphate and nitrate were the most significant contributors to PM_{2.5} mass at the urban sites, accounting for ~59% in Windsor, ~56% in Toronto, ~46% in Montreal, ~49% in Halifax, and ~40% in Edmonton.
- With the exception of Edmonton, the secondary factors were mostly contributed by regional sources with many located in Ohio, Pennsylvania, and New York, given the relatively large SO₂ and NO_x emissions in these areas.
- In the Edmonton area, supporting data analysis, such as high VOC correlations with the major PM_{2.5} sources, suggests that the secondary nitrate and sulphate mostly originated from local industrial sources under specific synoptic weather conditions.
- The combined contribution of motor vehicle-related sources (traffic and road dust factors) ranged from 13% to 20% at the urban sites.
- The elemental carbon (EC)-rich factor accounted for significant percentages of total PM_{2.5} mass in the summer (June-August) - 25% in Toronto, 23% in Montreal, 9% in Windsor).
- The EC-rich factor is normally identified as a diesel vehicle emission source, but in the present study it lacked correlation with local pollutants associated with traffic emissions. Supporting analysis indicates that this factor may be associated with coal combustion processes and is likely related to regional/transboundary sources. However, there is limited direct emissions of EC from coal combustion and regional background EC levels are generally very low.
- In Halifax, the contribution of the salt factor, the second largest contributor, was significantly higher (17%) as compared to other sites. Three oil-burning related factors were also identified for the Halifax site.
- In the Edmonton area, biomass burning in winter months was a major contributor (13%).

7.7.5 A Closer Look at the Vertical Layering of Particles over Nova Scotia

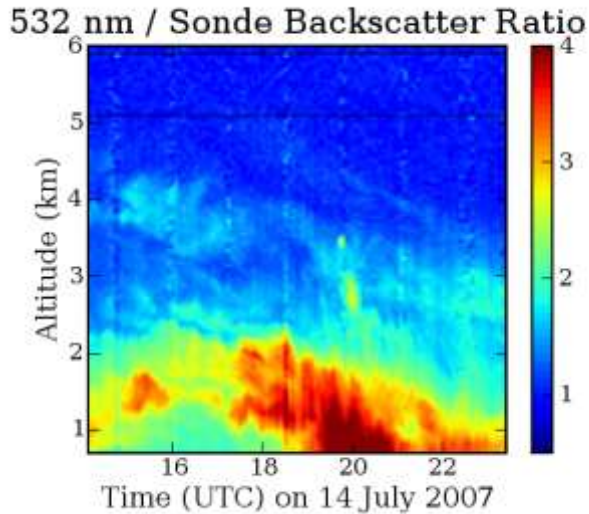


Figure 7.94 Backscatter ratio measurement obtained with the Dalhousie Raman Lidar on 14 July 2007. Aerosols are revealed by ratios greater than 1 (i.e. light blue to red on the colour scale). A separate low-altitude receiver is used for measurements between the ground and 1 km altitude. The particles were first detected between 1 and 2 km aloft and gradually descended toward the ground level. Elevated surface concentrations of O₃ and PM_{2.5} were measured when this layer reached the ground.

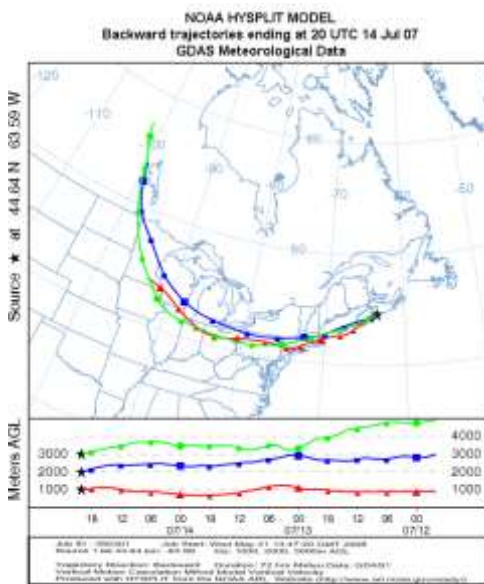


Figure 7.95 72-h back trajectory for air arriving at 1, 2 and 3 km altitude above Halifax at 2000 UTC on 14 July 2007 associated with the plume detected in Figure 7.85.

The Atmospheric-Optics Laboratory at Dalhousie University in 2004 operates a LIDAR during the summer months. This system (Duck *et al.*, 2007) profiles airborne particles and clouds at high spatial and temporal resolution from the ground to the lower stratosphere assisting in the study of long-range transport of particles for comparison with chemical transport models. The example profile given in Figure 7.94 shows an aerosol plume event on July 14, 2007. The particles were first detected between 1 and 2 km aloft and gradually descended toward the ground level. Elevated surface concentrations of O₃ and PM_{2.5} were measured when this layer reached the ground. Back trajectories associated with the event are given in Figure 7.95 and reveal that the aerosol plume originated over the Eastern Seaboard of the United States, and so likely represents a long-range pollution transport event. Thus, the LIDAR measurements are helping to support the hypothesis discussed above that pollutants from upwind regions often move into parts of Atlantic Canada above the ground, potentially due to the influence of the marine layer. For the event shown here, the elevated levels of pollution were anticipated by the CHRONOS Chemical Transport Model and were also simulated using AURAMS.

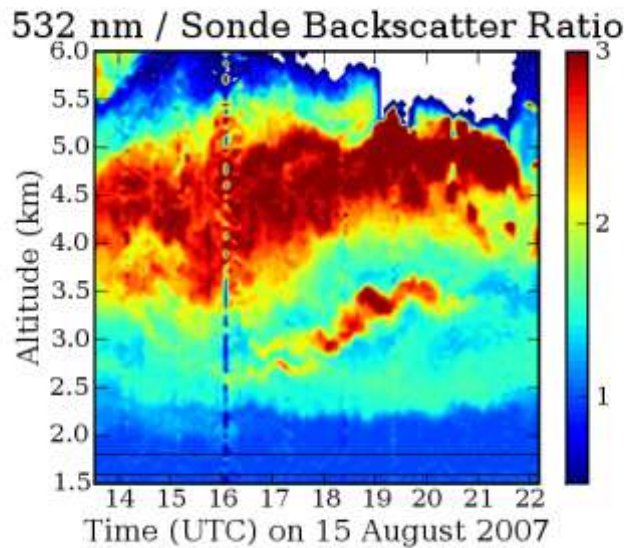


Figure 7.96 Dalhousie Raman Lidar measurement of a biomass burning plume originating from the state of Montana on 15 August 2007 where the plume shows a layer extending from 2.5 to 5.5 km in altitude.

The LIDAR has also revealed the presence of particles from biomass burning. In general, particles from nearby sources are observed at lower altitudes and others from pyro-convection events are seen up to 15.5 km in altitude. Consequently, the impact of forest fires as far south as Utah and as far north as Alaska/Yukon/Northwest Territories has been observed over Halifax. An example measurement is given in Figure 7.96, which shows a layer extending from 2.5 to 5.5 km in altitude on August 15, 2007. Trajectories suggest that these particles, which may never have been detected without the LIDAR, originated from intense forest fires

in the state of Montana. The ongoing measurement record reveals many long-range transport events of biomass burning particles. During the summer of 2007, particles from fires in Québec and as far away as Mongolia were detected above Halifax with the LIDAR.

7.7.6 Spatiotemporal Variability of Ozone in the Annapolis Valley

To investigate the spatial and temporal variations of O₃ in the Annapolis Valley, Nova Scotia, and the factors that contribute to the observed concentrations, seventeen locations were monitored simultaneously. The locations were arranged to study two transects perpendicular to the southwest to northeast orientation of the valley, through Middleton and Kentville. Sites on the valley floor, coastal locations and elevated sites on the North and South Mountains overlooking the Annapolis Valley were included. Integrated measurements using passive samplers took place over 18 sampling sessions ranging between 14, 21 and 28 days from August 29, 2006 to September 28, 2007.

Table 7.10 Seasonal mean O₃ concentrations at the 17 sites monitored during the Annapolis Valley, NS O₃ study.

Season	Mean [ppbv]	Standard Deviation [ppbv]
Sept to Nov 2006	22.6	4.8
Dec to Feb 2007	32.0	4.8
Mar to May 2007	43.2	6.3
Jun to Aug 2007	29.2	3.8
September 2007	34.7	4.3

Seasonal mean O₃ concentrations are provided in Table 7.10. The average concentration of the Valley floor sites (n=6) for the 13 month monitoring period was found to be 30.9 ± 8.7 ppbv, elevated sites (n=7) on the North and South Mountains was 36.3 ± 9.6 and the coastal sites (n=3) found to be 36.4 ± 10.7 ppbv (Gibson *et al.* 2009). An increase in O₃ concentration was observed in September 2007, which could be related to the record breaking temperatures experienced in the region and upstream sources during this period, allowing for enhanced O₃ formation. The minimum concentration observed was 8 ppbv for the sampling session spanning the September 19 to October 10 2006 period, at Middleton, NS. This low concentration was likely due to a combination of inversion conditions, surface scavenging by vegetation and NO titration due to local emissions. The maximum multi-day concentration observed was 72 ppbv at the Aylesford Mountain site from May 3 to 17 2007. This is a very

high concentration for such a prolonged period of time and requires further study. While the actual cause for this event is not fully understood it was most likely associated with the site's elevation and subsequent exposure to 'lofted' O₃. Possible sources of this O₃ include stratospheric intrusions, conversion of the winter time reservoir of PAN to NO₂ due to seasonal increases in temperature and solar radiation and possible upstream sources of O₃ and O₃ precursors.

7.7.7 Local Formation of Ozone from Emissions in Saint John

Urban centers produce the precursors of O₃, which are transported downwind of the city leading to increases in O₃ concentration. However, over short distances this process can be difficult to detect. Thus, to determine the extent to which cities in Atlantic Canada can produce O₃ by photochemical processes, data from the Saint John region were examined in detail. Simultaneous warm season daytime measurements for four sites were compared under conditions of southwest winds and < 50% cloud cover. Point Lepreau was considered to be an upwind rural site, Saint John Customs Building to be the urban site, Forest Hills a downwind suburban site, and Norton a downwind rural site. The southwest wind direction ensures that air parcels will travel in a path approximately aligned with the four stations, passing over Point Lepreau, the Saint John core, Forest Hills, and then finally Norton.

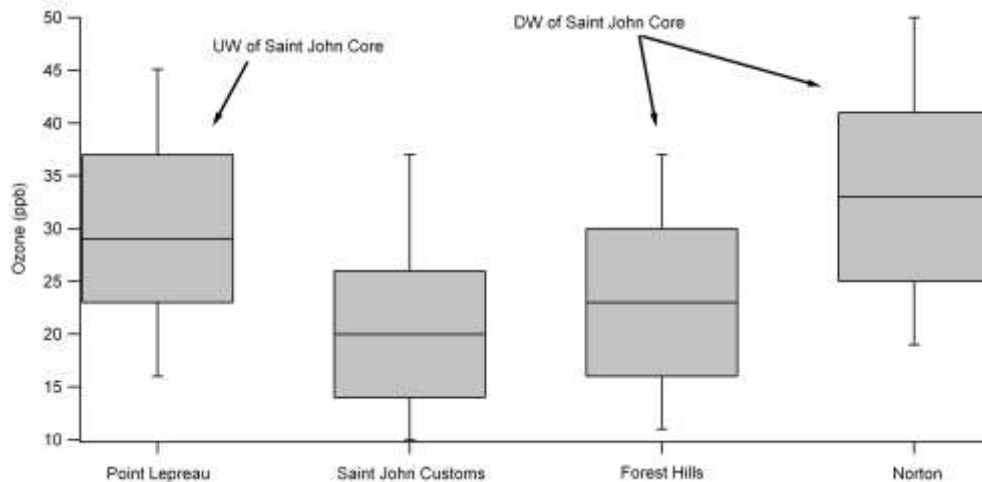


Figure 7.97 Median ozone concentration with SW winds and <50% cloud cover at each site near Saint John, NB, during daylight hours selected for optimal conditions for photochemistry, May-September, 1997-2005. Box represents values between the 25th and 75th percentiles; whiskers represent the 10th and 90th percentiles. "UW" refers to upwind, "DW" to downwind. Evidence of titration of O₃ by NO_x is indicated by the lower O₃ values at the Saint John customs site, which persist to the downwind suburban site of Forest Hills. The downwind rural site of Norton exhibits the highest O₃ concentrations during the selected hours, higher than the upwind rural site of Point Lepreau, indicating photochemical production from precursors released in the urban core.

Averaging the O₃ concentration for the 29 selected hours at each site reveals a decrease in O₃ at Saint John Customs as compared with Point Lepreau, followed by a recovery at Forest Hills and a further increase at Norton (Figure 7.97). This pattern indicates NO titration in the urban core, where NO sources are prevalent during the daylight hours, and suggests that the downwind suburban site of Forest Hills remains in the “shadow” of the urban core, with only slightly more elevated O₃ values. The downwind rural site of Norton has a median O₃ value that is 15% higher than at the upwind rural site of Point Lepreau, indicating that the Saint John area may also be a source for O₃ production downwind, as a result of emissions of NO_x and VOCs from traffic and industrial sources. This pattern of an O₃ “hole” over an urban centre followed by an increase in O₃ downwind has been documented in Lin *et al.* (1995) and Farrell (2006b), but in addition to the urban effect of traffic, the industrial core of Saint John may further increase the ozone production potential due to VOC emissions from the refinery, marine shipping, power plants, and pulp and paper plants. Very efficient O₃ production relative to the amount of NO_x reacted was found downwind of petrochemical/shipping areas in Houston, TX (Ryerson *et al.*, 2003), and the present analysis suggests a similar process in the Saint John area. Halifax, NS, is also home to a refinery, power plant, and marine shipping sources, and may also show evidence of this process; however monitoring stations are not currently positioned to test this hypothesis.

7.7.8 Wintertime Residential Wood Smoke in East Montréal

In Québec, wood smoke not only affects small communities, but also large cities such as Montréal, Laval, Québec City and Trois-Rivières. As shown earlier in this chapter (e.g., Figure 7.89-7.93) burning of wood for space heating is common in a number of regions in Canada. In 2008-09 more than 47 days of wintertime poor air quality in the Greater Montréal area were suspected as originating from wood burning for residential heat. Wood is an attractive alternative fuel for heating for people attempting to save on the costs of electrical or gas heat and thus, as indicated above in Section 7.3.2.2, there is potential for use of wood to continue to rise.

In East Montréal a number of special measurement studies were undertaken to learn more about the composition of wood smoke and exposure patterns (Bonvalot *et al.*, 2000; Carter *et al.* 2004). These studies, which ran from 1998 to 2002, showed that wood burning was the primary source of PM and other harmful substances, such as polycyclic aromatic hydrocarbons, dioxins and furans, in the Montréal area. In particular, in the suburb of Rivière-des-Prairies, where residential wood burning is a major source of heating in the winter compared to downtown heating sources, the levels were elevated significantly.

At the measurement site in Rivière-des-Prairies, polycyclic aromatic hydrocarbons (PAH) and PM_{2.5} concentrations were higher in the evening than during the day in the winter, but not in the summer, suggesting a heating source. Concentrations also tended to be higher on the week-

ends and holidays, likely reflecting longer daily time periods of woodstove or fireplace operation. The seasonal pattern in PAH and PM_{2.5} observed at Rivière-des-Prairies was not evident in downtown Montréal, where sources are mostly transportation-related), or at most other Montreal sites. In addition to PAHs, other chemical tracers on PM_{2.5} indicated that wood combustion was the likely cause of the increase in PM_{2.5} in Rivière-des-Prairies. For example, the PM_{2.5} was found to have a high potassium to iron ratio (a recognized tracer for wood combustion) and they were 200% higher in winter than in summer and 80% higher at Rivière-des-Prairies than downtown in the winter. Similar seasonal and spatial variation in dioxins and furans, substances emitted by the process of wood combustion, were observed.

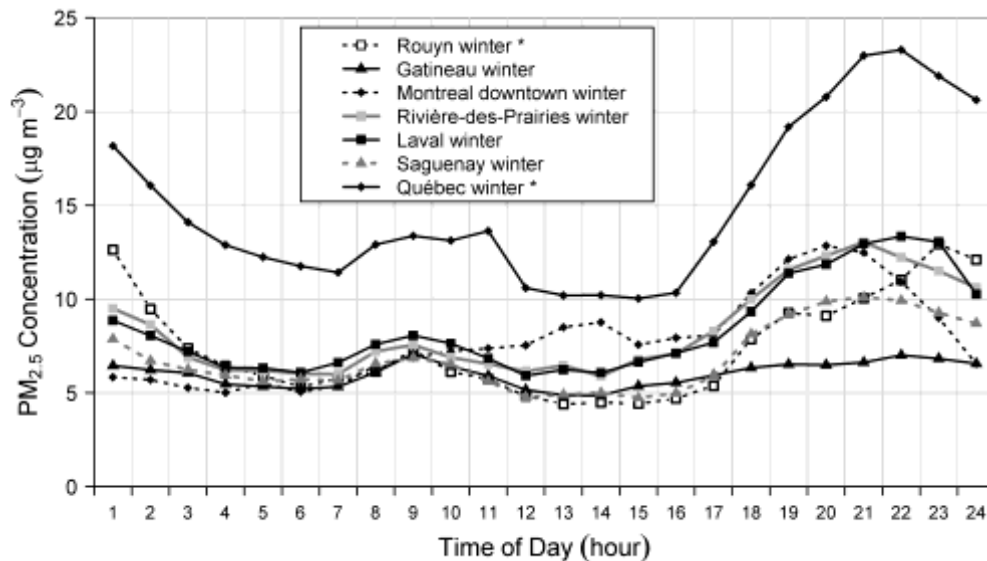


Figure 7.98 Average PM_{2.5} concentrations, hour by hour, in 2006 during winter months (November to March). The traffic site, Montreal downtown, is affected by the afternoon rush hour but concentration return to average values later in the evening. In contrast, communities affected by wood combustion are subject to an increase in PM_{2.5} concentrations later in the evening and return to average values well after midnight. The star (*) in the legend indicates that PM is measured by a BAMM instrument whose values are known to be higher than the TEOM with dry instrument (sites without the star).

Following these two studies, surveys conducted by the Montreal Health Department found that wood heating was an important issue throughout Montreal Island, not only in the suburb of Rivière-des-Prairies. Additionally, the spatial map of PM_{2.5} emissions used for model input (not shown) suggests that wood smoke may be a problem in many major and medium-size cities in southern Québec. Figure 7.98 shows the daily cycle of PM_{2.5} in the winter at 7 monitoring sites across Québec in the winter of 2006. The Gatineau monitor does not show a diurnal variation, as it is not affected by local sources. The traffic-influenced site in downtown Montreal shows an increase in PM_{2.5} concentrations beginning at 5 PM then a return to normal values by midnight. This increase is due to the lowering of the mixing height after sunset and the afternoon rush hour. The diurnal variation of the other sites show the pattern suspected to be reflective of the impact by local wood stove use. There was an increase beginning at 4 to 5

PM, similar to the traffic impact and reduced mixing height signature, but the levels reach their maximum later in the day, between 9 and 11 PM. Then there is a slow decrease to normal values, but not before 3 AM, which likely reflects the fact that people are asleep and so do not add more wood to the stove as the fuel is consumed.

7.7.9 The “En ville sans ma voiture” Annual Event

Every year since 2003, on September 22nd, the City of Montréal holds the “*En ville sans ma voiture*” event: a day where cars are not allowed in a specific area of the city centre in order to raise public awareness on the issue of air quality and other vehicular-related problems. In 2005, a mobile measuring station was used to compare nitric oxide (NO) and carbon monoxide (CO) levels within the area closed-off to traffic in concert with a nearby urban “control” station. As expected, NO levels within the car-free perimeter were much lower than levels measured at the control station where traffic remained as usual. That day between 9:30 a.m. and 3:30 p.m., NO was lower by 87%, while CO was down 95%, clearly demonstrating the impact of motor vehicles on local air quality.

7.7.10 Extreme Particulate Levels Produced by Fireworks

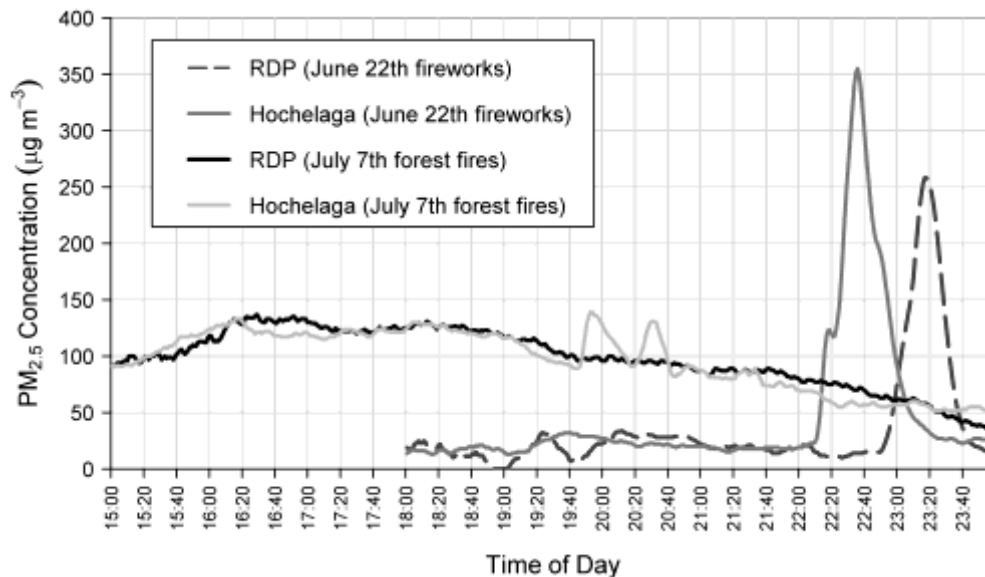


Figure 7.99 Comparison between PM_{2.5} from forest fires and fireworks in 2002 reported at Hochelaga (1.8 km north of the fireworks site) and Rivière-des-Prairies (RDP, 14 km north of the fireworks site) (Gagnon *et al.* 2003).

For the past few years, international fireworks competitions have been held on the Île Sainte-Hélène near Montréal on several days in the summer. The shows last for approximately 30 minutes and produce very large emissions of particulate matter from the rockets sending the fireworks aloft and the explosion of the fireworks themselves. This has been shown to have a brief but large impact on $PM_{2.5}$. For example, Gagnon *et al.*, (2003) reported that the hourly $PM_{2.5}$ levels at the nearby Hochelaga site have reached $162 \mu\text{g m}^{-3}$. The July 26th event in 2006 produced one of the highest $PM_{2.5}$ levels recorded in the history of the city's surveillance network at $570 \mu\text{g m}^{-3}$ over a period of a few minutes. Fortunately, this smoke disperses relatively quickly under most summer meteorological conditions, however as Figure 7.99 demonstrates, peak concentrations can remain relatively high for several kilometres downwind. In this figure, $PM_{2.5}$ related to the fireworks was observed sequentially at two stations separated by about 12 km. Over this distance the short term peak decreased by about $100 \mu\text{g m}^{-3}$, but was still over $350 \mu\text{g m}^{-3}$. In comparison, the $PM_{2.5}$ associated with the large forest fire event described above in the text box is also shown. In that case levels were sustained above $100 \mu\text{g m}^{-3}$ for several hours and there was little difference between sites, but interestingly, the short-term firework-related peak far surpassed these concentrations and due to the nature of the material burned, the composition of the particles likely differed considerably.

7.7.11 Detailed Characteristics of Submicron Particles

Approximately 70 km north of Toronto is Egbert, Ontario and the Centre for Atmospheric Research Experiments (CARE). This location serves as an important regional background research site for a wide variety of atmospheric studies and it is used heavily due to its accessibility to Toronto. Several routine air quality measurement networks operate at CARE, including CAPMoN, the Integrated Atmospheric Deposition Network (IADN) and the U.S. Clean Air Status and Trends Network (CASTNet). In addition, many research measurements are obtained at the site, to test instrumentation and develop advanced methods for data interpretation and to provide regional background readings to contrast with nearby urban measurements. One such instrument is the Aerodyne Aerosol Mass Spectrometer or AMS (see text box) and it, along with several other aerosol or particle measurement instruments, were operated in early to mid spring of 2003 (March 27 to May 8). This period represents an important transition time with respect to the start of "smog season" and the measurements were expected to shed some light on both winter and summer time formation of fine particles.

During the study, which is discussed in detail by Rupakheti *et al* (2005), it was found that particle composition and mass can vary widely in the course of a few hours, as exemplified in a text box above. As a general observation, the higher concentrations were associated with southerly winds and low wind speeds. The high particle concentrations tended to be dominated by nitrate. By contrast, winds from the northwest were associated mainly with organic aerosols, with short-lived contributions from sulphate. On average, the major contribution to

fine particle composition was organic matter. Sulphate and nitrate concentrations showed distinctly different diurnal profiles. Nitrate showed a maximum in the morning hours, with a minimum in the afternoon which is consistent with the enhanced stability of ammonium nitrate at lower temperatures. Sulphate concentrations were low in the mornings, and tended to rise in the afternoon hours, which was presumed to be a result of photochemical formation of sulphate. It is also possible that low morning concentrations of sulphate led to enhanced availability of ammonia, and thus to enhanced formation of ammonium nitrate concentrations.

Two contrasting episodes were considered in greater detail. The first occurred on April 10-11, 2003, and was characterized by relatively low temperatures (mean of 3.5 °C, range of -1.3 to 13 °C), and very low concentrations of O₃. The largest contribution to particle composition was nitrate, while sulphate was generally very low. Two modes were noted in the particle size distribution, nitrate and some of the organics in the smaller mode, and sulphate and other organics in a larger mode. The back trajectories for this episode originated in the north, passed over Toronto, then curled back to Egbert, leading to the conclusion that the larger particle size mode was present in the air mass before it reached Toronto, but that the precursors to the finer mode (NO_x and VOC) originated from Toronto sources. Thus, particle size can add a useful dimension in determining the source of PM_{2.5}.

The episode of April 15, had much warmer temperatures, ranging from 18.3 to 28.3 °C (mean of 25.6 °C), low humidity and high ozone concentrations. Consequently, nitrate concentrations were low and instead particle mass was dominated by organics, sulphate and ammonium. The AMS measurements showed a high fraction of oxygenated organics, indicating a processed or aged air parcel. This observation is consistent with the back trajectories, which were from the southwest, and had travelled over a number urban and industrial sources, possibly including the Nanticoke generating station in southwestern Ontario, and the coal-fired power plants in the Midwest U.S.

7.7.12 Regional-Scale Modelling to Estimate Trans-boundary Transport in Ontario

The Ontario Ministry of the Environment published (MOE 2005) the results of an application of the Community Multi-scale Air Quality model (CMAQ) to assess regional scale transport and the relative contributions of various jurisdictions to O₃ and PM_{2.5} in Ontario. CMAQ was run initially with all emissions turned on for a five-month period (May to October). The results of this base case run were evaluated against monitoring data to ensure that model performance was satisfactory. The model was then run again for the same five month period with all anthropogenic emissions in Ontario set to zero. Comparison of the two runs allowed assessment of the contribution to pollutant concentrations in Ontario of background biogenic emissions and material transported into the province.

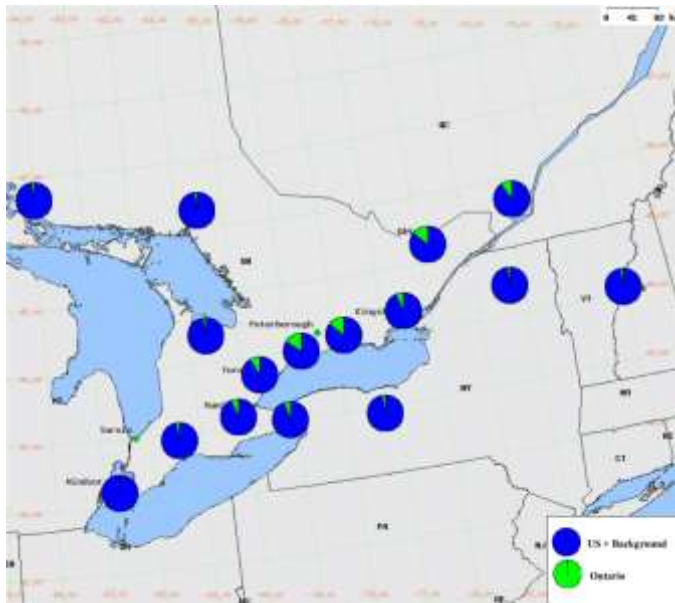


Figure 7.100 Transboundary and Ontario contributions to ozone on high concentration days for May – October (MOE, 2005).

From Figure 7.100 it can be seen that setting Ontario emissions to zero on high O_3 concentration days, i.e., days when 8-hour running average O_3 concentrations were above the CWS metric value of 65 ppb would have reduced ambient O_3 concentrations by 1% in Windsor, 9% in the GTA, 16% in Oshawa and 7% in Kingston. That is, on those days during the summer of 1988, when modelled O_3 levels in the province were above the CWS metric, Ontario emissions contributed to at most 16% of the O_3 concentration, and much less than that across much of the province. The largest contribution due to Ontario's emissions was downwind of the Greater Toronto/Hamilton areas.

Very large day-to-day variability was found in the reductions for each of the subdomains, due to changing meteorology. For Windsor through to the GTA, there were some days when modelled disbenefits were found; that is, by reducing the Ontario emissions to zero, O_3 concentrations actually increased. The disbenefits are believed to be a result of reduced O_3 scavenging when local NO_x emissions are reduced. The large contribution from U.S. emissions and background O_3 presents a significant challenge. Efforts to reduce O_3 on high concentration days by Ontario alone would have only small benefits for Windsor through to the GTA with larger benefits downwind of the GTA. Reductions in precursor emissions in the U.S. would be needed to affect O_3 significantly in southwestern Ontario on these days.

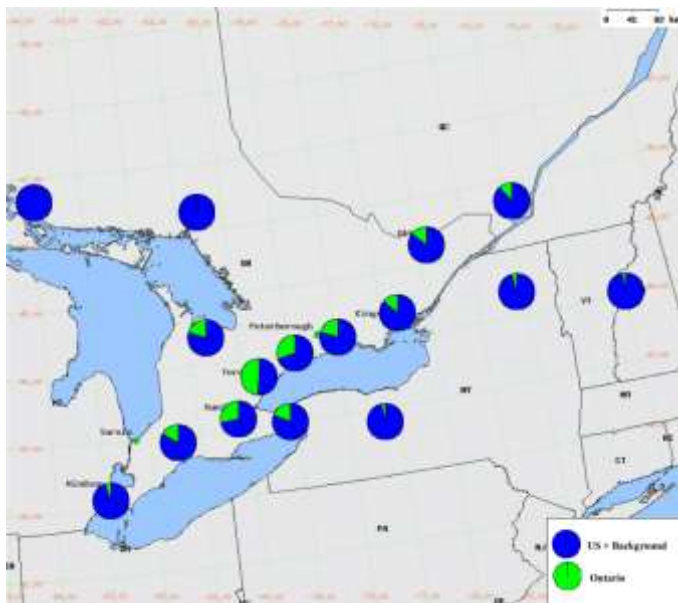


Figure 7.101 Transboundary and Ontario contributions to $PM_{2.5}$ on high concentration days for May – October (MOE, 2005).

The picture is similar for PM, with substantial contributions from U.S. sources. However, the relative contributions from local Ontario sources were much higher than for O_3 . Figure 7.101 shows $PM_{2.5}$ on days when daily average $PM_{2.5}$ levels exceeded the CWS metric value of $30 \mu g m^{-3}$. The Ontario contribution is highest in the GTA at approximately 49%, and declines in all directions from there. During a smog episode in the GTA, approximately half of $PM_{2.5}$ arises from emissions from human activity in Ontario (MOE, 2005). In Windsor the picture is similar to O_3 : where it appears that no amount of effort, by those living in the area will improve air quality in a significant way during smog episodes. In the area from Hamilton to east of Toronto, the impact of Ontario's emissions of $PM_{2.5}$ precursors and primary $PM_{2.5}$ is significant. However, further downwind in Kingston, the sum of transboundary and regional background concentrations again dominates the impacts.

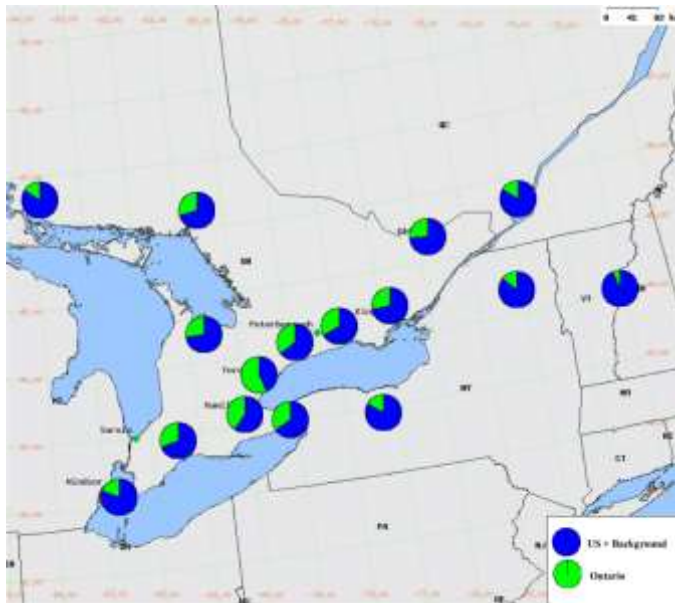


Figure 7.102 Transboundary and Ontario contributions to $PM_{2.5}$ on all days for May – October (MOE, 2005)

As illustrated in Figure 7.102 when the results of the air quality modelling of $PM_{2.5}$ are averaged over all days throughout the five-month period, Ontario emissions are seen to have a greater impact than on dirty days as was depicted in Figure 7.101. Even so, only in the GTA does the Ontario contribution exceed 50 per cent. Other communities from Windsor to Ottawa, had reductions in $PM_{2.5}$ concentrations by 20 to 40 % when Ontario's anthropogenic emissions were set to zero. These results are consistent with contributions determined by analysis of measurement data discussed above (e.g., as reported by Lee *et al.* (2003) and Brook *et al.* (2002, 2007a).

Regional scale transport also occurs out of Ontario, potentially carrying pollutants to neighbouring jurisdictions. Figures 7.100 to 7.102 include modelled predictions of the contribution of Ontario sources to concentrations of O_3 and $PM_{2.5}$ at locations in Québec, New York State and the border region between Maine and Vermont. These contributions are relatively small, approximately 16% in Québec, 20% in New York State, and 7% in New England when all $PM_{2.5}$ is considered, and about 12% in Québec, 5% in New York State, and 3% in New England on days of high O_3 .

7.7.13 The Prairie 2005 Field Study and other Model Applications

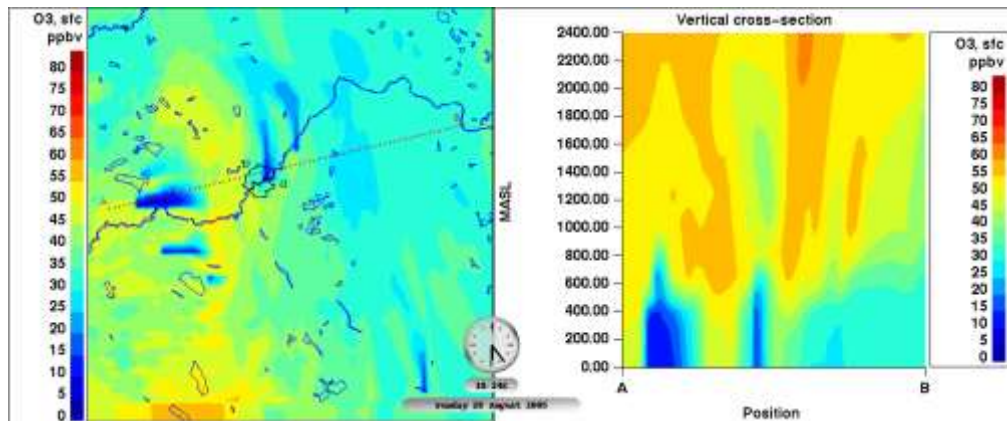


Figure 7.103 (a) AURAMS forecast for surface ozone for August 28th, 12:24 local daylight time during the PRAIRIE 2005 study; (b) vertical cross section of transect from A to B showing ozone depletion at the surface and two regions of high ozone aloft, from down mixing from the middle troposphere and local chemical enhancement at the 700 m level.

The PrAIRie2005 field study (Makar *et al.*, 2008) was conducted to explore the extent to which air pollution events in the city of Edmonton are the result of local emissions or long-range transport and to test various aspects of the air quality model AURAMS (see Chapter 5). Investigation of a $PM_{2.5}$ event between the 25th and 27th of August 2005 revealed multiple influences. The beginning of the event may have been influenced by long-range transport from the oil sands area, with subsequent peaks resulting from local sources such as the coal-fired power plants west of Edmonton, and the petrochemical facilities to the east. The O_3 observations and subsequent high resolution model runs revealed considerable complexity. Figure 7.103 shows that AURAMS predicted two areas of high O_3 in a vertical cross section roughly centered on the east side of Edmonton. Ground level titration of O_3 (blue) took place in the NO_x plumes from the power plants to the west of Edmonton (left side of the cross-section) and from sources east of Edmonton in the centre of the cross-section. Analysis of the time series of cross-sections from AURAMS suggested that local O_3 formation from Edmonton emissions may be taking place at ~700 m above ground level, in addition to downward mixing from the middle troposphere as a potential source of O_3 .

Consistent with expectations, low O_3 concentration areas correspond to regions with high NO levels at the surface. In Figure 7.103 it can be seen that the model also predicted, for this case, that there is an O_3 titration region at 1400m above the city core. As a consequence of this pattern there could be the intriguing possibility that the local circulation from Edmonton's heat island contributes to the downward mixing of middle tropospheric O_3 . That is, subsidence may be occurring on either side of the city in response to heat-island generated updrafts in the city core. Further data analysis and future studies will be needed to confirm if this feature of the model simulation is an important process influencing air quality around Edmonton. However,

previous measurements have revealed that the chemistry is relatively active in this area. For example, during an aircraft study focusing on the urban plume downwind of Edmonton, peak O₃ production on a moderately warm day under light wind conditions, was observed within 100 km of the Edmonton city center (Bates *et al.*, 2003). Ozone levels in the mature plume were estimated to represent a 20-30 ppb enhancement above observed background concentrations on that day.

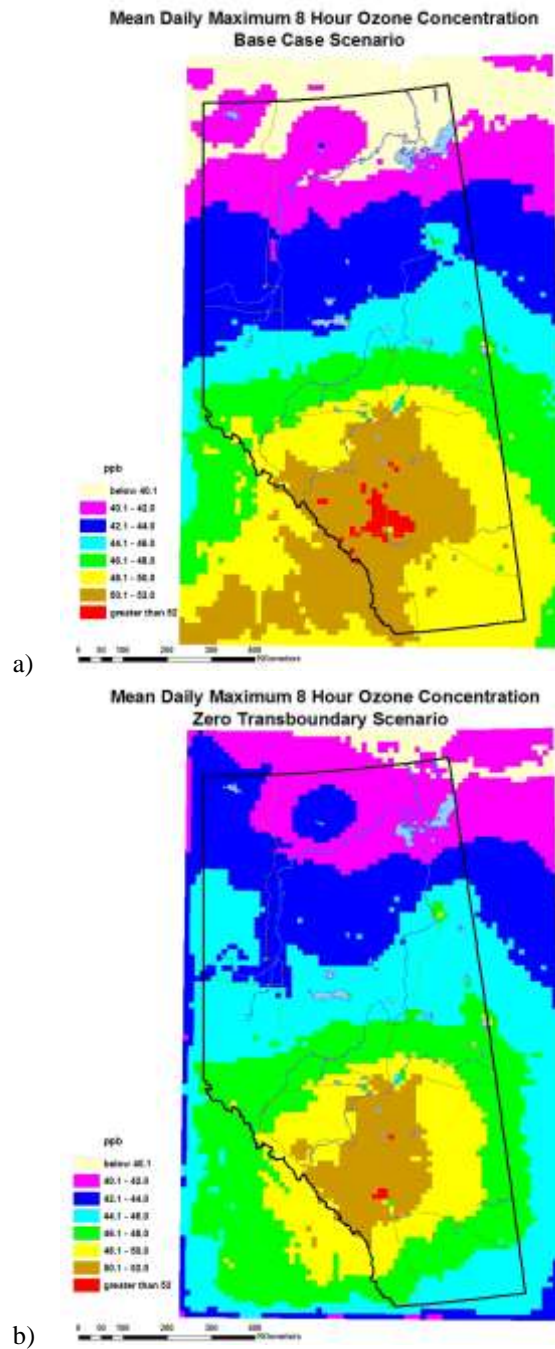


Figure 7.104 Model predicted daily mean of maximum 8 hour ozone for a three month simulation (JJA) for (a) the base case, (b) pollution sources outside Alberta set to zero (clean air boundary condition). Note that trans-boundary sources are more important to high ozone levels in Calgary than in Edmonton.(Model predicted daily mean of maximum 8 hour ozone for a three month simulation (JJA) for (a) the base case, (b) pollution sources outside Alberta set to zero (clean air boundary condition) (Fox and Kellerhals, 2007).

Other modelling studies have also suggested that O₃ can be expected to form downwind of key Alberta source areas. For example, Fox and Kellerhals (2007) simulated conditions in the summer 2002 and found that the highest modelled 4th highest daily maximum O₃ (Figure 7.104a) occurred around Edmonton, Calgary and Fort McMurray. These model runs were used to investigate the contribution of various industrial sectors to O₃ concentrations in Alberta. In Edmonton, the leading contributors to high O₃ were the electricity sector, the oil and gas sector and on-road transportation, while in Calgary the leading contributors to high O₃ were the oil and gas sector, on-road transportation, and emission sources from outside of the province (elsewhere in Canada and/or the U.S.). The influence of the oil and gas sector is not surprising given their relatively large emissions of NO_x and VOCs shown in Figures 7.17a and 7.17c. Overall, the model estimated that the combined emissions from refineries and the chemical sector contributed a modest increment to O₃ in Alberta, concentrated east of Edmonton and along the Edmonton-Calgary corridor. However, if VOC emissions from refineries are underestimated (Chambers and Strosher, 2006) the contribution of refinery emissions to O₃ may also be underestimated.

In addition to studying the impact of sources within Alberta Fox and Kellerhals (2007) also investigated the impact of trans-boundary sources on O₃ in Alberta. When all emissions outside Alberta were set to zero, the model showed a modest reduction to the area of elevated mean daily maximum 8-hour O₃ levels centered on the Edmonton/Calgary corridor (Figure 7.104b). Furthermore, trans-boundary sources were more important to high O₃ levels in Calgary than in Edmonton, though they were not the dominant cause of high summertime O₃ at either location. Despite the relatively small influence of sources outside Alberta, the model simulation demonstrated one case (not shown) where an O₃ plume originating in the Puget Sound area reached Alberta.

7.7.14 The Pacific 2001 Study

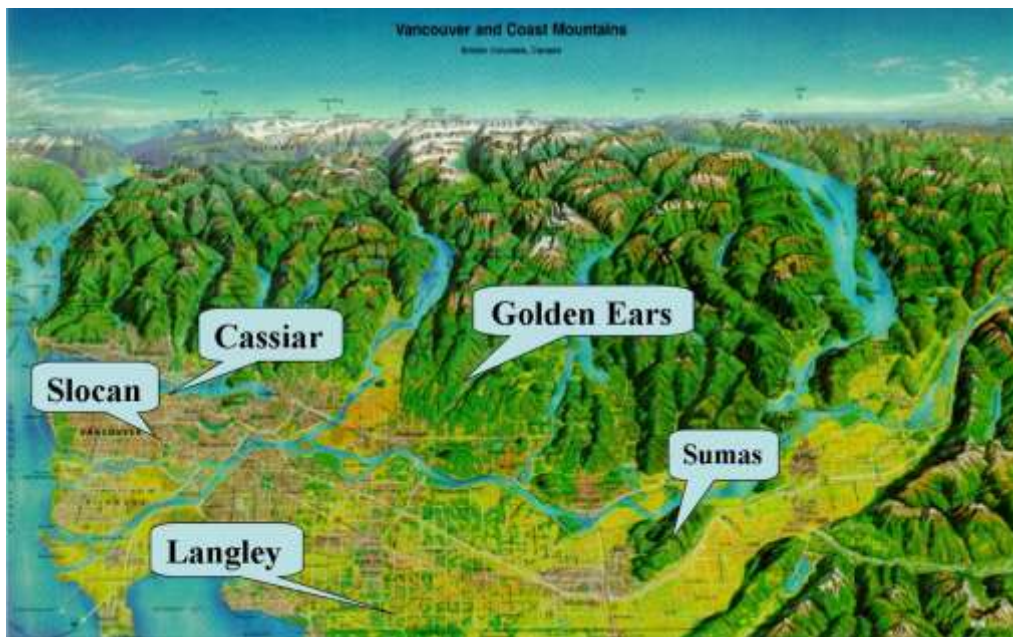


Figure 7.105 LFV station locations during the Pacific 2001 Study (Vingarzan and Li, 2006).

The Pacific 2001 Air Quality Study, was undertaken to characterize the physical and chemical properties of particulate matter in the Lower Fraser Valley (LFV) and to provide detailed data for air quality model development (Vingarzan and Li, 2006). Five main ground sites were used during the August 13–31 study period, as illustrated in Figure 7.105: Cassiar Tunnel in urban Vancouver, Slocan, an urban-suburban site in Vancouver; Langley, a rural site in the south-central LFV, Sumas, a semi-rural site in the eastern LFV, and Golden Ears, an elevated site on the north shore mountains. A large number of measurements were collected during the study and in addition to the ground monitoring, included LIDAR scans, vertical profiling, radiosonde and aircraft measurements.

Several chemical regimes were found to be influencing air quality in the LFV region. At Cassiar Tunnel, ambient aerosols were strongly dominated by gasoline and diesel emissions, as evidenced by elevated black carbon levels. At Slocan, the composition of ambient aerosols indicated an emission controlled regime dominated by organics, of both anthropogenic and biogenic origin. Anthropogenic emissions were strongly influenced by the vehicles and fugitive emissions of petroleum fuels. Plumes from ships operating around the area or at berth were observed to impact the city on a regular basis (Lu *et al.*, 2006). At the rural site of Langley, the $PM_{2.5}$ regime was controlled by secondary aerosol formation. Here the average particle composition was dominated by inorganics with contributions from sea salt, sulphate, nitrogen species and aged organics. Elevated ammonia and biomass burning markers reflected the influence of agricultural sources. At the semi-rural site of Sumas, the particle mass

composition indicated a mixed emission-formation regime dominated by urban, agricultural and biogenic sources. At the forested site of Golden Ears, the particle composition was dominated by biogenic organics. The chemistry at this site was impacted by anthropogenic sources due to upslope flow, while biogenically-derived secondary organic aerosols (SOA) were transported into the LFV by downslope flow.

Particle composition studies at many of the sites indicated that organic carbon comprised approximately half of the $PM_{1.0}$ mass, with the rest being comprised by inorganic species. Sulphate dominated the inorganic fraction of the fine particle mode at all sites. Sea salt chemistry was found to be important in the formation of coarse mode sodium nitrate aerosols. The fine particle fraction was dominated by ammonium sulphate aerosols, with occasional peaks in ammonium nitrate. Overall, elemental carbon comprised a minor part of the fine particle fraction. Isoprene and monoterpenes were the dominant biogenic hydrocarbons detected, and their presence at all sites indicated the broad influence of biogenic organics throughout the LFV.

Source analysis using isotopic methods suggested that the LFV was influenced by a well dispersed source of sulphate, consistent with gasoline, diesel and gas combustion. Biogenic contributions were found to be significant, with approximately 30% of the sulphate in $PM_{2.5}$ aerosols estimated to be derived from the oxidation of dimethyl sulphide (DMS). Organic aerosols were found to have significant contributions from terrestrial (plant material) sources during the summer months and from marine, biogenic and fossil fuel sources during the spring months. Biomass burning generally had a small, but measurable impact on the composition of ambient aerosols in the LFV.

Particle formation and growth were observed to occur via several mechanisms. Nucleation was observed on cleaner days, while on more polluted days, condensation and coagulation dominated particle growth. Ozone episodes were associated with an increase in both particle size and mass. Sulphate growth events were associated with photochemical production from advected SO_2 from industrial sources in northwestern Washington State. Within the city, sulphate peaks were associated with ship plume emissions, forming from the relatively large amounts of SO_2 emitted by individual ships. Fine particle nitrate events were associated with advection of HNO_3 into the eastern LFV reacting with local sources of ammonia. Organic particle growth events were associated with stagnant conditions and advection of air over urban Vancouver. The extent of processing of air masses was found to increase in a west to east direction, although photochemically aged pollutants from the WISE zone can reverse this gradient. Both biogenic and anthropogenic species were observed to be chemically reactive and contribute to secondary aerosol formation.

7.7.15 Ammonia and Particulate Matter in the Lower Fraser Valley

Ammonia has been identified as an important species in fine PM formation and degraded visual range in the Lower Fraser Valley (LFV) of British Columbia. The agricultural sector is the largest source of airborne atmospheric ammonia contributing approximately 76% of total ammonia in the LFV. The poultry industry is the largest contributing agricultural sector, accounting for 36% of total ammonia emissions in the LFV (Metro Vancouver, 2007). In the summer of 2004, a field study coinciding with the avian influenza poultry cull was undertaken in order to investigate the effects of large-scale ammonia emission reductions on ambient air quality. At the same time, modelling studies using CMAQ were conducted to investigate the effect of ammonia emission reductions. Results of field studies indicate that in spite of an approximate 67% decline in ammonia concentrations at Abbotsford in response to the cull, the effect on average TEOM-derived PM_{2.5} levels was relatively small (up to 6% decline). In addition, there was no statistical improvement in visibility during this period, based on extinction measurements at Abbotsford and Burnaby South (So and Vingarzan, 2010). CMAQ modelling studies using a hypothetical 60% agricultural emission reduction were in general agreement with field results, indicating average PM_{2.5} reductions of approximately 9%. These results suggest that due to the overabundance of ammonia in the LFV, control of ammonia emissions alone is likely to be only marginally effective at producing significant reductions in fine PM. Instead, a multi-pollutant reduction approach which would simultaneously target the principal precursors of fine PM (NO_x, SO₂ and VOCs), in addition to ammonia, would likely be more effective at reducing fine PM and improving visibility in the LFV.

7.8 Summary and Needs for Further Research

The information provided in this chapter has demonstrated that, despite the importance of long-range transport to air quality over the eastern half of Canada and the occurrence of transboundary exchange of pollutants all across the country, local emissions and local formation of secondary air pollutants contribute significantly to the observed air pollutant levels in each region.

In Atlantic Canada, understanding air quality processes necessitates that the impact of long-range transport over the ocean and of complex coastal meteorology be considered, while in Ontario and Québec the impact of large emissions from urban areas and industry and the influence of topographic features (Québec) and the Great Lakes (Ontario) on these emissions are of critical importance. Furthermore, southern Ontario is closest to high emission areas in the U.S. and these can have a large influence on air quality.

Emissions are large in Alberta, but generally only lead to high concentrations near the sources during cold and calm periods in winter and, although elevated photochemical air pollution levels do occur in summer, the highest levels are typically in less populated areas.

Air quality remains an issue in the Lower Fraser Valley, especially owing to the impact on visibility and although trends in most pollutant concentrations are stable or decreasing, ozone has remained as a whole stable since the early 1990s and is rising in certain locations of the valley.

Some of the highest particle levels occur in valley communities in the interior of British Columbia and Yukon during the colder times of the year. Residential wood burning contributes significantly to this problem, as it does in other provinces (e.g., Québec), and the wood industry also plays a significant role in BC. Rapid growth in some interior BC regions, such as the Okanagan Valley, is extending the potential for air quality problems to other times of the year due to increased precursor emissions of photochemical pollutants.

In the process of preparing this chapter a wide variety of air quality and meteorological data and special study results were assessed for each region of the country, tapping into a considerable base of local expertise. This has led to insight regarding air quality and enabled the development of the region-specific conceptual models presented at the beginning of the chapter. It is clear that there is considerable knowledge and that research in the past 5-10 years has added significantly to our understanding of a range of issues and atmospheric processes. In particular, the influence of both synoptic scale and meso to micro scale (i.e., local scale) meteorology on the movement of $PM_{2.5}$ and O_3 , as well as NO_2 and other precursors, is reasonably well understood.

Further advances in understanding are still needed. Clearly, there is a considerable amount of monitoring and special field study data available across Canada. However, it is also clear that there are areas where more measurements are needed. One of the pressing needs is for more $PM_{2.5}$ speciation measurements as there are relatively few sites across the country. This has limited our knowledge of issues such as the role of particles during winter smog events in Alberta and spatial patterns in the Southern Atlantic Region. Also related to $PM_{2.5}$ is the issue of continuous monitoring and the discrepancies among the instrumentation used and differences compared to the traditional filter-based approach. As raised in Chapter 3, this issue hinders assessment of temporal patterns (e.g., trends) and understanding of the role of semivolatile constituents in contributing to total mass and to $PM_{2.5}$ health and environmental effects.

The number of O_3 monitoring sites, while more than for the other pollutants, still imposes limitations in understanding, particularly where the spatial patterns are complex, including vertical layering, such as over and near the Great Lakes and over the Southern Atlantic Region. This also highlights the fact that information on O_3 and other pollutants above the surface, in

the boundary layer and free troposphere, is very limited. Such information is essential for obtaining a complete understanding of air quality issues, particularly for evaluating and improving models. There is also a lack of rural O₃ measurements in remote areas that are potentially impacted by human activities such as downwind of Edmonton and Calgary and eastern parts of the Lower Fraser Valley. Further headway on reducing O₃ is also hindered by too few locations with speciated VOC measurements in some regions of the country, including those with improved temporal resolution (i.e., hourly). While generally low in concentration outside of large cities, the number of NO₂ measurement sites in smaller communities and in rural areas is limited. Given its importance to the Air Quality Health Index more attention should be paid to NO₂ monitoring across Canada.

More detailed local studies of existing and new measurements in tandem with application and in-depth interpretation of model results will be needed to gain more insight into the interactions between complex meteorology and chemical processes forming O₃ and secondary particulate matter. The current conceptual models can serve as a base for designing these future studies. Improvements in emissions information, such as more spatial and temporal resolution and speciation of PM and VOCs, will need to go hand in hand with these activities. This continued research can be expected to provide better, more quantitative, information on local formation of secondary pollutants helping to explain some of the increases or less-than-expected decreases in O₃, and explain the causes of high O₃ and PM_{2.5} events. Furthermore, such coordinated efforts involving local scale model-measurement applications will challenge the models, leading to improvements, and enhance local expertise on the behaviour of air pollutants. Ultimately, the overall skill of the air quality forecasts will improve, further advances will be made in merged model-measurement products depicting O₃ and PM_{2.5} spatial and temporal patterns and there will be greater confidence in the results of model applications in support of policy.

In addition to the above relatively broad improvements in local emissions and measurement-model applications to study the combined effect of meteorology and chemistry, there are specific knowledge gaps relevant to each region, and nationally, these should be considered in future research efforts. Below is a list of the main gaps, starting first with those that are common (general) among all regions and then finishing with more region-specific issues. While in some cases the gaps identified below do link to specific issues presented in this chapter several of them are broader and reflect, in a general sense, the areas where knowledge is known to be lacking and hence where future research efforts would advance understanding and ability to inform future policy. As much as possible these gaps are presented in order of priority.

Knowledge Gaps

- Emissions, particularly for VOCs, particle chemical constituents and NH_3 , and improved spatial allocation of mobile emissions in major urban areas.
- The relative amounts of secondary and primary particulate organic carbon, their temporal and spatial variations (diurnal and seasonal; urban vs. rural). The potential for reversible and non-reversible exchanges of organic carbon between particles and gases and the impact on measurement uncertainty within current monitoring programs.
- The understanding of ozone formation and loss processes in airsheds with elevated ozone levels. There is a need to make better use of the existing VOC data from the NAPS network to understand airshed- specific VOC/ NO_x regimes and use this information to inform emission reduction strategies. Currently this has been done only for Toronto and Vancouver, where further analyses are still needed.
- Multi-pollutant concentrations, including air toxics, and their interactions and potential changes in toxicity that occur near significant source areas (within approx. 50-2500 meters) and how near source concentrations and processes (chemical and meteorological) impact population exposures.
- Contribution to $\text{PM}_{2.5}$ by biogenic emissions (organic gases and particles) from both local vegetation and upwind regions.
- The causes and implications of increasing background ozone on future trends and future air quality management strategies.
- Better characterization of urban scale atmospheric processes (horizontal and vertical) and how they can be represented in higher resolution air quality models capable of simulating the build-up and chemical and physical processes associated with local emissions and subsequent human exposure patterns.
- The effect of climate change and global emission trends on future ozone and $\text{PM}_{2.5}$ levels.
- The causes of the springtime ozone maxima, which dominates a considerable portion of the climatology of ozone in many regions.
- $\text{PM}_{2.5}$ chemical tracers for mobile emission sectors eg. aviation, rail, biodiesel.

Atlantic Region

- Concentrations of chemical components of PM need to be measured more frequently at several locations to improve knowledge of regional chemistry and the processes affecting regional air quality.
- Further understanding and modelling of the complex nature of the sea/land breeze and inversions as factors regulating concentrations and exposures related to both locally emitted and transported pollutants.

- Characterization of organic and inorganic aerosols of marine origin (both biogenic and anthropogenic), including sea salt, and their overall contribution to PM mass concentrations.
- The role of marine advection fog in particle transformation (heterogeneous chemistry) and subsequent deposition.
- The air quality impacts of the expanding offshore oil and gas industry and marine transportation.
- The extent of pooling of ozone and smog precursors over the Bay of Fundy and the potential for complex vertical structure in these pollutants and their impact inland.
- The characteristics of the decrease in O_3 and $PM_{2.5}$ from southern Nova Scotia and the Bay of Fundy towards southern New Brunswick and northern Maine and how this pattern relates to local and upwind emission regions.
- The role of sea salt in the formation of nitryl chloride and impacts on ozone and secondary particulate matter formation.

Southern Québec and Eastern Ontario

- A better understanding of how secondary air pollutant concentrations (O_3 and $PM_{2.5}$) change over the region in response to decreases in SO_x and NO_x emissions from upwind source regions and/or local emissions.
- The magnitude of the emissions in smaller communities and rural areas affected by local industries and/or residential wood combustion.
- Measurements of ambient concentrations of $PM_{2.5}$ in smaller communities and rural areas outside of the St. Lawrence river valley where local industries and topography play a role in pollutant accumulation.
- More detailed spatio-temporal information on NO_2 concentrations over southern Québec.
- Measurements of ambient concentrations of $PM_{2.5}$, O_3 and their precursors in far eastern Québec (east of Tadoussac).
- The sensitivity of $PM_{2.5}$ to increases in ammonia emissions from the local agricultural sector.
- The spatial variation of the relative contribution of natural and anthropogenic VOC emissions in ozone formation in summer over southern Québec.
- A better understanding of the fraction of road dust and road salt emissions that moves away from roadways and has a greater potential to impact PM levels throughout urban areas.

Southern Great Lakes

- The relationship between local sources, such as on and off road motor vehicle traffic and industry, and urban scale variations in primary and secondary PM_{2.5} and its precursors.
- The contributions that NO_x and VOC emissions from the densely populated parts of the province (i.e., greater Toronto area) make to downwind O₃ and PM_{2.5} levels, over land and water.
- The relative contribution of Sarnia/Lambton vs. upwind U.S. emissions on O₃ and PM_{2.5} in the southern Lake Huron area.
- The source(s) of elevated O₃ observed in Parry Sound and also predicted to extend through Georgian Bay towards Michigan and southern Lake Huron.

Alberta and the Prairies

- Speciation of emissions from Alberta sectors such as Upstream Oil and Gas, the oil sands and refineries.
- Baseline data and potential air quality and environmental impacts for potential growth areas throughout the far north.
- The impact on local and regional air quality and on population exposures as a consequence of projected growth in the oil sands and the related potential emission increases.
- Importance/role of air toxics to poor air quality and human exposures, especially given the collocation of a large urban centre (Edmonton) with an expanding petrochemical complex.
- Relative contribution from various sources at receptor points (detailed source apportionment studies)
- Emission and formation processes and their chemical and physical characteristics for wintertime primary and secondary particles, particularly over the major cities.
- The effect of Alberta emissions on Saskatchewan and Manitoba.
- Downwind wet and dry deposition amounts attributed to industry in the Prairies, in general and due to the unconventional oil industry, in particular.

Lower Fraser Valley

- Effective management strategies to address the lack of decline of warm season ozone in the Lower Fraser Valley. The current emission reduction strategy is ineffective at lowering ozone in the LFV, particularly in the far eastern end where exceedances of the CWS occur (e.g., Hope).

- Background concentrations of criteria air contaminants and toxics in the boundary layer of the west coast of BC to identify the portion that can be controlled by local and national reduction strategies.
- An understanding of VOC sources and chemical processes leading to ozone and fine PM formation in the LFV.
- The effect on ozone production in the LFV by the interaction of sea salt with N_2O_5 and the potential for this chemical pathway to regenerate NO_2 involved in ozone formation and to form nitryl chloride with subsequent impact on secondary particulate matter.
- The importance of air toxics to poor air quality and human exposures at the local scale (e.g., near industry, ship plumes), as well as throughout the valley.
- Effective management strategies to address visibility degradation in the LFV, particularly during the summer months.
- A better understanding of trans-Pacific transport events of smog-forming pollutants to the area to gain insight into the relative contributions of local and distant sources.
- A better understanding of mesoscale flows and pollution transport in the Georgia Basin-Puget Sound area in order to better understand source-receptor relations and the extent of air quality impacts.

Interior Valleys of British Columbia

- Improved understanding of the overall air quality impact of important and possibly increasing local emissions on local and regional air quality. e.g., SO_2 emissions from the energy sector in northeast BC; dust from open pit mining operations; Prince George bowl fumigation events; outdoor boiler smoke; rail industry. Emission information from emerging sectors is required for sound air quality management in these areas.
- Assessment of air quality impacts to the rail sector BC communities with large railyards.
- Development of a high-resolution emission inventory and photochemical modelling for the Okanagan Valley in order to inform air quality management strategies to minimize the impact of the significant population and agricultural growth in this area.
- Fine particle source apportionment during periods of visibility degradation in the Okanagan Valley and in National and Provincial parks.
- Measurements to establish baseline levels of air pollutants in Prince Rupert, prior to further expansion of the port terminal.
- A better understanding of the interaction between emissions, atmospheric chemistry and complex meteorology in valley/mountain environments.

- Additional characterization of background concentrations of O₃ and PM to improve understanding of the portion of the pollutants that can be controlled via local management actions.
- The impact of trans-Pacific transport on interior communities.

References

- Ainslie, B and D.G. Steyn, 2007: Spatiotemporal Trends in Episodic Ozone Pollution in the Lower Fraser Valley, B.C. in Relation to Meso-scale Atmospheric Circulation Patterns and Emissions. *Journal of Applied Meteorology*. 46 (10), 1631-1644.
- Alberta Environment, (2007). 2002-2004 Particulate matter and ozone assessment summary report. ISBN: 978-0-7785-5457-8
- Alberta Environment (2008) State of the Environment.
<http://www3.gov.ab.ca/env/soe/index.html>
- AMAP Assessment 2006: Acidifying Pollutants, Arctic Haze and Acidification in the Arctic. Arctic Monitoring and Assessment Programme (AMAP), Oslo, pp. 112
- AMEC, 2003. Analysis of 2001-2002 airborne ozone and ozone precursor measurements in the oil sands. Prepared for CEMA, by AMEC Earth & Environmental Limited, September 2003
- Andreae, M.O., Merlet, P., 2001. Emissions of trace gases and aerosols from biomass burning. *Global Biogeochemical Cycles*, 15, 955–966.
- Angevine, W.M., Trainer, M., McKeen, S. A., Berkowitz, C.M., 1996a. Mesoscale meteorology of the New England coast, Gulf of Maine, and Nova Scotia: Overview, *Journal Geophysical Research*, 101, 28893-29901.
- Angevine, W.M., Buhr, M.P., Holloway, J.S., Trainer, M., Parrish, D.D, MacPherson, J.I., Kok, G.L., Schillawski, R.D., Bowlby, D.H., 1996b. Local meteorological features affecting chemical measurements at a North Atlantic coastal site. *Journal of Geophysical Research*, 101, 28935-28946
- Angevine, W., Hare J. C. W., Fairall C., Wolfe, D., Hill, R., Brewer, W., White, A., 2006. Structure and formation of the highly stable marine boundary layer over the Gulf of Maine, *Journal of Geophysical Research*, 111, D23S22, doi:10.1029/2006JD007465.
- Ansari, A.S., Pandis, S.N., 1998. Response of inorganic PM to precursor concentrations. *Environmental Science and Technology*, 32, 2706-2714.

Appenzeller, C., J. R. Holton, and K. H. Rosenlof (1996), Seasonal variation of mass transport across the tropopause, *J. Geophys. Res.*, 101(D10), 15,071-15,078, doi:10.1029/96JD00821.

Arthur, J. A Tropopause Folding Study Using MM5 Simulation Results in West-Central Alberta, Canada. Poster presented at 96th A&WMA Annual Conference, San Diego CA, June 2003.

Banic, C.M., Leaitch, W.R., Isaac, G.A., Couture, M.D., 1996. Transport of ozone and sulphur to the North Atlantic atmosphere during the North Atlantic Regional Experiment. *Journal of Geophysical Research*, 101, 29091-29104.

Bates, D.L., Wiens, B.J., Hume, W.D., Shi, J., 2003. Rural-Urban Plume Evolution Experiment (RUPEE): A Summary of Atmospheric Chemistry Downwind of a Canadian Urban Centre. Presented at 96th A&WMA Annual Conference, San Diego CA, June 2003.

BCEnv. (British Columbia Ministry of the Environment, 2004a. Open Burning Smoke Control Regulation. PO Box 9341, Stn Prov Govt, Victoria, British Columbia, Canada. V8W 9M1. available at http://www.qp.gov.bc.ca/statreg/reg/E/EnvMgmt/145_93.htm

BCEnv (British Columbia Ministry of the Environment). 2004b. Quesnel Airshed Management Plan 2004-2014. BC Ministry of the Environment. available at <http://www.env.gov.bc.ca/air/>

BCEnv (British Columbia Ministry of the Environment), 2006a. Williams Lake Airshed Management Plan 2006-2016. BC Ministry of the Environment, available at <http://www.env.gov.bc.ca/air/>

BCEnv (British Columbia Ministry of the Environment). 2006b. An Emission Inventory for Golden, British Columbia. BC Ministry of the Environment, Kootenay and Okanagan Regions,. Environmental Quality Section, 205 Industrial Road G, Cranbrook, BC. V1C 6H3, available at http://wlapwww.gov.bc.ca/kor/epd/air_emissions_golden/air_emiss_golden.pdf

BCEnv. (British Columbia Ministry of the Environment). 2007. Reducing Wood Stove Smoke: A Burning Issue. PO Box 9341, Stn Prov Govt, Victoria, British Columbia, Canada. V8W 9M1. available at <http://www.env.gov.bc.ca/air/particulates/rwssabi.html>

BCEnv. (British Columbia Ministry of the Environment). 2008. PO Box 9341, Stn Prov Govt, Victoria, British Columbia, Canada. V8W 9M1. (British Columbia Ministry of the Environment). 2007. Reducing Wood Stove Smoke: A Burning Issue. PO Box 9341, Stn Prov Govt, Victoria, British Columbia, Canada. V8W 9M1. available at <http://www.env.gov.bc.ca/air/particulates/rwssabi.html>

Beattie, B.L., Whelpdale, D.M., 1989. Meteorological characteristic of large acidic deposition events at Kejimikujik, Nova Scotia, *Water Air and Soil Pollution*, 46, 45-59.

Beauchamp, S., Tordon, R., 1993. Marine Fog Chemistry and Acid Deposition at Two Coastal Sites in Atlantic Canada, in: Hall, J., Wadleigh, M., (Eds.), *Proceedings of Conference on Environmental Change in Newfoundland and Labrador and similar regions*, Canadian Global Change Program Secretariat, Ottawa, pp. 64-65

Beckerman, B., Jerrett, M., Brook, J.R., Verma, D. Arain, A., Finkelstein, M.M, 2008. Correlation of nitrogen dioxide to other traffic pollutants near a major expressway. *Atmospheric Environment*. 42, 275-290

Beekmann, M., G. Ancellet, S. Blonsky, D. Demuer, A. Ebel, H. Elbern, J. Hendricks, J. Kowol, C. Mancier, R. Sladkovic, H.G.J. Smit, P. Speth, T. Trickl and Ph. Van Haver (1997), Regional and global tropopause fold occurrence and related ozone flux across the tropopause, *J. Atmos. Chem.*, 28, 29–44.

Berkowitz, C.B., Daum, P.H., Spicer, W.S., Busness, K.M., 1996. Synoptic patterns associated with the flux of excess ozone to the western North Atlantic. *Journal of Geophysical Research*, 101, 28923-28933.

Bertschi, I.T., Jaffe, D.A., 2005. *Journal of Geophysical Research*, 110, 1-14

Biesenthal, T.A., Bottenheim, J.W., Shepson, P.B., Li, S.-M., Brickell, P.C., 1998. The chemistry of biogenic hydrocarbons at a rural site in eastern Canada. *Journal of Geophysical Research*, 103, 25487-25498.

Blanchard, C., 2004. Spatial and Temporal Characterization of Particulate Matter. In: McMurray, P., Shepherd, M., Vickery, J. (Eds), *Particulate Matter Science for Policy Makers, A NARTSO Assessment*. Cambridge University Press, Cambridge UK, ISBN 0 521 84287.

Bonvalot, Y., Gagnon, C., Benjamin, M., Germain, A., Dann, T., 2000. Sampling Program for Residential Wood Combustion: Winter of 1998-99 Study Report. Public Works and Government Services Canada, 80 pp.

Briggs, D.J., Collins, S., Elliott, P., Fischer, P., Kingham, S., Lebre, E., Pryl, K., Van Reeuwijk, H., Smallbone, K., Van der Veen, A. 1997, Mapping urban air pollution using GIS: a regression-based approach. *International Journal of Geographical Information Science*, 11, 699–718.

Brook, J.R., Wiebe, A.H., Woodhouse, S. A., Audette, C.V., Dann, T.F., Callaghan, S., Piechowski, M., Dabek-Zlotorzynska, E., Doughty, J.F., 1997. Temporal and spatial relationships in fine particle strong acidity, sulphate, PM₁₀, and PM_{2.5} across multiple Canadian locations. *Atmospheric Environment*, 31, 4223-4236.

Brook, J.R., Dann, T.F., 1999. Contribution of nitrate and carbonaceous species to PM₁₀ and PM_{2.5} observed in Canadian cities. *Journal of the Air and Waste Management Association*, 49, 174-185.

Brook, J. R., Lillyman, C. D., Shepherd, M. F., Mamedov, A., 2002. Regional Transport and Urban Contributions to Fine Particle Concentrations in Southeastern Canada, *Journal of the Air and Waste Management Association*, 52, 855-866.

Brook J.R., Vega E. and Watson J.G. 2004a, "Receptor Methods", Chapter 7 in *Particulate Matter Science for Policy Makers, A NARSTO Assessment*. Edited by P. McMurry, M. Shepherd and J. Vickery. Cambridge University Press, ISBN 0 521 84287 5 hardback. Pages 235-281.

Brook, J.R., Johnson, D, Mamedov, A., 2004b. Determination of the Source Areas Contributing to Regionally High Warm Season PM_{2.5} in Eastern North America. *Journal of Air and Waste Management Association*, 54, 1162-1169.

Brook, J.R., Strawbridge, K., Snyder, B.J., Boudries, H., Worsnop, D., Anlauf, K., Sharma, S., Lu, G., Hayden, K., 2004c. Towards an understanding of the fine particle variations in the LFV: integration of chemical, physical and meteorological observations. *Atmospheric Environment*, 38, 5775-5788.

Brook, J. R., Poirot, R. L., Dann, T. F., Lee, P. K. H., Lillyman, C. D., Ip, T., 2007a, Assessing Sources of PM_{2.5} in Cities Influenced by Regional Transport, *Journal of Toxicology and Environmental Health Part A*, 70, 191-199.

Brook, J.R., Graham, L., Charland, J.P., Cheng, Y., Fan, X., Lu, G., Li, S.M., Lillyman, C., MacDonald, P., Caravaggio, G., MacPhee, J.A., 2007b. Investigation of the motor vehicle exhaust contribution to primary fine particle organic carbon in urban air. *Atmospheric Environment*, 41, 119-135.

Buhr, M., Sueper, D., Trainder, M., Goldan, P., Kuster, B., Fehsenfeld, F., Kok, G., Shillawski, R., Schanot, A., 1996. Trace gas and aerosol measurement using aircraft data from the North Atlantic Regional Experiment, *Journal of Geophysical Research*, 101, 29013-29028.

- BVLD (Bulkley Valley Lakes District), 2006. Community Action Plan for Clean Air - A Five Year Strategy. Bulkley Valley- Lakes District Airshed Management Society, available at <http://www.env.gov.bc.ca/air/airquality/index.html>
- Canada – United States Transboundary Particulate Matter Science Assessment, 2004. Report by the Canada-United States Air Quality Committee, Subcommittee 2: Scientific Cooperation, December 2004, 150 pp.
- Canadian Interagency Forest Fire Centre, 2007, available <http://www.cifffc.ca/>
- Canadian Wind Energy Atlas, available at <http://www.windatlas.ca/en/index.php> (accessed Oct 2007)
- CAPP, 2007. Canadian Oil and Gas Industry Outlook, May 2, 2007. Accessed September 2007 available at <http://www.capp.ca/raw.asp?x=1&dt=PDF&dn=120884>
- Carter, A.-M., Germain, A., Rousseau, J., Bisson, M. Gagnon, C, 2004. Sampling Program for Residential Wood Heating Study Report: 1999 to 2002. Public Works and Government Services Canada, 88 pp.
- Carslaw, D. C., 2005. On the changing seasonal cycles and trends of ozone at Mace Head, Ireland, *Atmospheric Chemistry and Physics*, 5, 3441-3450
- CEPA/FPAC 1999. National Air Quality Objectives for Particulate Matter. Part 1: Science Assessment Document. CEPA/FPAC Working Group on Air Quality Objectives and Guidelines. Minister, Public Works and Government Services, 1999. ISBN 0-662-26715-X, available at <http://dsp-psd.pwgsc.gc.ca/Collection/H46-2-98-220-1-1E.pdf>
- Chaikowsky, C.L.A., 2001. Overview of ground-level ozone observations in Alberta, 1986-1998, Alberta Environment
- Chambers, A., 2004. Optical Measurement Technology for Fugitive Emissions from Upstream Oil and Gas Facilities. Alberta Research Council Project CEM – P004.03
- Chambers, A., Strosher, M., 2006. Refinery Demonstration of Optical Technologies for Measurement of Fugitive Emissions and for Leak Detection. Alberta Research Council Project CEM 9643-2006
- Chan, E., 2008, Trend Analysis using GLMM, in preparation
- Cheng, L. McDonald, K.M., Angle, R.P., Sandhu, H.S., 1998. Forest fire enhanced photochemical air pollution: A case study. *Atmospheric Environment*, 32, 673-681.

- Christofanelli, P., Bonasoni, P., Tositti, L., Bonafè, U., Calzolari, F., Evangelesti, F., Sandrini, S., Stohl, A., 2006. A 6- year analysis of stratospheric intrusions and their influence on ozone at Mt. Cimone (2165 masl). *Journal Geophysical Research*, 111, D03306.
- Cleveland, W.S., Devlin, S.J., 1988. Locally Weighted Regression: An Approach to Regression Analysis by Local Fitting. *Journal of the American Statistical Association*, 83, 596-610
- Climate Prediction Centre, 2007. Storm Tracks. Available at http://www.cpc.noaa.gov/products/precip/CWlink/stormtracks/strack_NH.shtml (accessed on 6 July 2007)
- Clinton, N. E., Gong, P., Scott, K., 2006. Quantification of pollutants emitted from very large wildland fires in Southern California, USA. *Atmospheric Environment*, 40, 3686-3695.
- Colarco P.R., M.R. Schoeberl, B.G. Doddridge, L.T. Marufu, O. Torres, E.J. Welton, 2004. Transport of smoke from Canadian forest fires to the surface near Washington, DC: injection height, entrainment and optical properties. *Journal Geophysical Research*, 109, D06203. doi:10.1029/2003JD004248.
- Craig L., Brook J.R., Chiotti Q., Croes B. *et al.*, 2008, Air pollution and public health: A guidance document for risk managers. *Journal of Toxicology and Environmental Health, Part A*, 71, 588–698.
- Danielsen, E.F., and V. Mohnen 1977, Project duststorm report: ozone transport, in situ measurements and meteorological analysis of tropopause folding. *J. Geophys. Res.*, 82, 5867-5877.
- Daum, P., Kleinman, L., Newman, L., Luke, W., Weinstein-Lloyd, J., Berkowitz, C., Busness, K., 1996, Chemical and physical properties of plumes of anthropogenic pollutants transported over the North Atlantic during the North Atlantic Regional Experiment. *Journal of Geophysical Research*, 101, 29029-29042.
- Dawson, J.P., Adams, P.J., Pandis, S.N., 2007. Sensitivity of PM_{2.5} to climate in the Eastern U.S.: a modelling case study, *Atmospheric Chemistry and Physics*, 7, 4295–4309.
- Dion, J., 2003. START – An Atmospheric Transport Analysis Tool. Proceedings of the 37th Congress of the Canadian Meteorological and Oceanographic Society, Ottawa, Canada, June 2003.
- Dorling, S.R., Davies, T.D., 1992a, Cluster analysis: A technique for estimating the synoptic meteorological controls on air and precipitation chemistry - method and applications. *Atmospheric Environment*, 26A, 2575-2581

Dorling, S.R., Davies, T.D., Pierce, C.E., 1992b, Cluster analysis: A technique for estimating the synoptic meteorological controls on air and precipitation chemistry - results from Eskdalemuir, South Scotland, *Atmospheric Environment*, 26A, 2583-2602

Duck, T., Firanski, B., Millet, D., Goldstein, A., Allan, J., Holzinger, R., Worsnop, D., White, A., Stohl, A., Dickinson, C., Donkelaar, A., 2007, Transport of forest fire emissions from Alaska and the Yukon Territory to Nova Scotia during summer 2004. *Journal of Geophysical Research* 112 (D10S44), doi: 10.1029/2006JD007716.

Elbern, H., J. Kowol, R. Sladkovic and A. Ebel 1997, Deep stratospheric intrusions: A statistical assessment with model guided analysis, *Atmospheric Environment*, 31, No. 19, 3207-3226.

Environment Canada, 1997, Canadian 1996 NO_x/VOC Science Assessment – Ground Level Ozone and its Precursors, 1980-1993, Report of the Data Analysis Working Group.

Environment Canada, 2001. Precursor contributions to ambient fine particulate matter in Canada. Environment Canada, Gatineau, 237 pp.

Environment Canada, 2004a. Canada-United States Transboundary Particulate Matter Science Assessment. Environment Canada, Toronto, ON.

Environment Canada, 2004b. 2004 Canadian Acid Deposition Science Assessment – Chapter 3. Vet, R., Brook, J., Ro, C., Shaw, M., Narayan, J., Zhang, L., Moran, M., Lulis, M. (Morrison, H., (Ed.)), pp. 15-90.

Environment Canada, 2005. Canadian Wind Energy Atlas. Updated 2006. available at <http://www.windatlas.ca/en/index.php>. (accessed 8 July 2007)

Environment Canada, 2007a, Criteria Air Contaminants national inventory in Canada for the year 2005. Based on March 2007 federal and provincial data. available at <http://www.ec.gc.ca/pdb/cac>. Also see: http://www.ec.gc.ca/pdb/cac/Emissions1990-2015/EmissionsSummaries/2006/2006_ON_e.cfm

Environment Canada, 2007b, The Border Air Quality Strategy, available at <http://www.ec.gc.ca/cleanair-airpur/default.asp?lang=En&xml=D6F2B21E-331A-455A-8F71-180B948E4589>

Environment Canada, 2008. Agricultural Ammonia Reduction Scenarios for the LFV using the CMAQ modelling system. Unpublished. Air Quality Science Unit, Meteorological Services of Canada, #201-401 Burrard Street, Vancouver, B.C.

Environment Canada, 2009a. National Pollutant Release Inventory (NPRI) Databases. Internet: <http://www.ec.gc.ca/inrp-npri>

Environment Canada, 2009b. The 2008 Canadian Atmospheric Assessment of Agricultural Ammonia. Environment Canada, Gatineau.

Evans, G.P., Jeong, C-H. 2007, Data Analysis and Source Apportionment of PM_{2.5} in Golden, British Columbia using Positive Matrix Factorization. Southern Ontario Centre for Atmospheric Research, University of Toronto, 200 College Street, Toronto, Ontario, M5S 3E5. Report prepared for Environment Canada, contract # K2313-06-0015. SOCAAR Report No. CR-WB-2007-02.

Fairall, C.W., Bariteau, L., Grachev, A.A., Hill, R.J., Wolfe, D.E., Brewer, W.A., Tucker, S.C., Hare, J.E., Angevine, W.M., 2006. Turbulent bulk transfer coefficients and ozone deposition velocity in the International Consortium for Atmospheric Research into Transport and Transformation. *Journal of Geophysical Research*, 111 (D23S20), doi: 10.1029/2006JD007597.

Farrell, C., 2006a. The Contribution of Naturally Occurring Sea Salt to Fine Particulate Concentrations in the Atlantic Region. Presented to the 40th Congress of the Canadian Meteorological and Oceanographic Society, Toronto, Ontario, June 1, 2006; Meteorological Service of Canada.

Farrell, T. C., 2006b, Canada-Wide Standards Achievement in the Atlantic Region: Model Results for New Brunswick, Part II, Meteorological Service of Canada, Atlantic Region Science Report Series 2006-03, August 2006.

Fehsenfeld, F. C., Trainer, M., Parrish, D.D., Volz-Thomas, A., Penkett, S., 1996. North Atlantic Regional Experiment 1993 summer intensive: Forward. *Journal of Geophysical Research*, 101, 28869-28875.

Finlayson-Pitts, B.J., Pitts, J.N. 1999. Chemistry of the Upper and Lower Atmosphere, Theory, Experiments and Application. Academic Press, San Diego, California.

Fiore, A.M., Jacob, D.J., Bey, I., Yantosca, R.M., Field, B.D., Fusco, A.C., Wilkinson, J.G., 2002. Background ozone over the United States in summer: Origin, trend, and contribution to pollution episodes. *Journal of Geophysical Research*, 107, 4275.

Fishman, J., Watson, C., Larsen, J., Logan, J., 1990, Distribution of tropospheric ozone determined from satellite data, *Journal of Geophysical Research*, 95, 3599-3617

Fox, D., 2002. Influence of biogenic emission uncertainties on ozone predictions in the Oil Sands Region, Air Quality and Health: State of the Science - 2002 Science Symposium, Clean Air Strategic Alliance (CASA)

Fox, D., Kellerhals, M., 2007. Modelling of ozone levels in Alberta: Base case, sectoral contributions and a future scenario. Environment Canada, Edmonton AB.

Gagnon, C., A. Boisvert, C. Vincent, P. Paquette, R. Mallet, 2003, Qualité de l'air à Montréal. Rapport annuel 2002. Ville de Montréal, Service de l'environnement, de la voirie et des réseaux, Direction de l'environnement, RSQA, 6 pp.

Gagnon, C., C. Bessette, Y. Garneau, R. Mallet, P. Paquette, 2006, Qualité de l'air à Montréal. Rapport Annuel 2006. Ville de Montréal, Service des infrastructures, transport et environnement, Direction de l'environnement et du développement durable, Planification et suivi environnemental, RSQA, 8 pp.

Geddes G.A., Murphy J.G., Wang D.K. (2009) Long term changes in nitrogen oxides and volatile organic compounds in Toronto and the challenges facing local ozone control. *Atmos. Envir.* 43, 3407-3415.

Gibson, M.D., Guernsey, J.R., Beauchamp, S., Waugh, D., Heal, M., Brook, J., Maher, R., Gagnon, G., McPherson, J., Bryden, B., Gould, R., Terashima, M., 2009. Quantifying the Spatial and Temporal Variation of Ground-Level Ozone in Rural Annapolis Valley, Nova Scotia, Canada Using Nitrite-Impregnated Passive Samplers, *Journal of the Air and Waste Management Association* 59, 310-320.

Gilbert N.L., Woodhouse S., Stieb D.M., Brook J.R., 2003. Ambient NO₂ monitoring near a major highway using passive diffusion samplers: a pilot study. *Science of the Total Environment*, 312, 43-46.

Gilbert N., Goldberg M.S., Beckerman B., Brook J.R., Jerrett M., 2005, Assessing spatial variability of ambient nitrogen dioxide in Montreal, Canada, with a land-use regression model. *Journal of the Air & Waste Managment Association*, 55, 1059-1063.

Gong, W., Mickle, R.E., Bottenheim, J., Froude, F., Beauchamp, S., Waugh, D., 2000. Marine and Coastal Boundary Layer and Vertical Structure of Ozone Observed at a Coastal Site in Nova Scotia During the 1996 NARSTO-CE Field Campaign. *Atmospheric Environment*, 34, 4139-4154.

Government of Canada, 2007. Government of Canada Five-year Progress Report. Canada-wide Standards for Particulate Matter and Ozone. Environment Canada, Gatineau, Québec, K1A0H3. ISBN 0-662-44480-9. available at www.ec.gc/publications

HAQI, 1997a, Summary Report: Hamilton Wentworth Air Quality Initiative

HAQI, 1997b, Environmental Work Group Final Report: Hamilton Wentworth Air Quality Initiative

Hastie, D. R., Narayan, J., Schiller, C., Niki, H., Shepson, P. B., Sills, D. M. L., Taylor, P. A., Moroz, W. J., Drummond, J. W., Reid, N., Taylor, R., Roussel, P. B., Melo, O. T., 1999, Observational Evidence for the Impact of the Lake Breeze Circulation on Ozone Concentrations in Southern Ontario, *Atmospheric Environment*, 33, 323-335

He, H., D.W. Tarasick, T. Carey-Smith, W.K. Hocking, Y. Rochon, M. Moran, S. Argall, K. Strawbridge, D. Jones and J.C. McConnell, Large-scale studies of stratosphere-troposphere exchange using trajectory modelling, satellite and ozonesonde measurements, MST-12 Workshop, London, ON, Canada, 18-23 May, 2009.

Health Canada and Environment Canada, 1999a. National ambient air quality objectives for ground-level ozone science assessment document: a report by the Federal-Provincial Working Group on Air Quality Objectives and Guidelines. Environment Canada, Gatineau, QC.

Health Canada and Environment Canada, 1999b. National ambient air quality objectives for particulate matter science assessment document: a report by the Federal-Provincial Working Group on Air Quality Objectives and Guidelines. Environment Canada, Gatineau, QC.

Henderson, S.B., Beckerman, B., Jerrett, M., Brauer M., 2007. Application of land use regression to estimate longterm concentrations of traffic-related nitrogen oxides and fine particulate matter. *Environmental Science and Technology*, 41, 2422-2428.

Henry, R. C., 2002. Multivariate receptor models—Current practice and future trends. *Chemometrics and Intelligent Laboratory Systems*, 60, 43–48.

Hessel, C., A Climatological Evaluation of Elevated Ozone Levels at a Background Site in the Foothills of Alberta, Canada. Poster presented at 96th Air and Waste Management Association Annual Conference, San Diego CA, June 2003

Hidy, G., Niemi, D., Pace, T., 2004. Perspective for Managing PM, in: McMurray *et al.* (Eds.), *Particulate Matter Science for Policy Makers, A NARSTO Assessment*, Cambridge University Press, Cambridge, pp 127-157.

Hingston, M., 2005, An Assessment of Marine Vessel Emissions and their Contribution to Air Quality in Halifax Harbour for the Year 2002. Report of the Environmental Protection Branch, Environment Canada – Atlantic Region. Available on request from the Environmental Protection Operations Directorate, Air Issues Unit, Michael.Hingston@ec.gc.ca.

Hingston, E.C., DiCesare, F., 2006. NSEL, personal communication

Hocking, W. K., Carey-Smith, T., Tarasick, D.W., Argall, P. S., Strong, K., Rochon, Y., Zawadzki, I., Taylor, P.A., 2007. Detection of stratospheric ozone intrusions by windprofiler radars. *Nature*, 450, 281-284.

Hoff, R.M., Guise-Bagley, L., Moran, M., McDonald, K., Nejedly, A., Campbell, I., Pryor, S., Golestani, Y., Malm, W., 1997, Recent visibility measurements in Canada. Proceedings (CD-ROM), 90th Annual Meeting of the Air and Waste Management Association, Toronto, Canada, June 8-13

Holton, J.R., P.H. Haynes, M.E. McIntyre, A.R. Douglass, R.B. Rood and L. Pfister (1995), Stratosphere troposphere exchange. *Rev. Geophys.*, 33, 403-439.

Isakson, J., Persson, T.A., Lindgren, E.S., 2001. Identification and assessment of ship emissions and their effects in the harbour of Göteborg, Sweden. *Atmospheric Environment*, 35, 3659-3666.

Jaffé, D., McKendry, I., Anderson, T., Price, H., 2001. Six 'new' episodes of trans-Pacific transport of air pollutants. *Atmospheric Environment*, 37, Issue 3, 391-404

Jaffé, D., Bertschi, I., Jaeglé, L., Novelli, P., Reid, J.S., Tanimoto, H., Vingarzan, R., Westphal, D.L., 2004. Long-range transport of Siberian biomass burning emissions and impact on surface ozone in western North America. *Geophysical Research Letters*, 31, L16106 1-4

Jardine, C., Ouellette, I. W., 2006. Risk communication plan for the issues surrounding the risk assessment of trace metal and air contaminants in the Athabasca oil sands region. Prepared for CEMA, August 2006.

Jenkin, M. E., Clemitshaw, K. C., 2000. Ozone and other secondary photochemical pollutants: chemical processes governing their formation in the planetary boundary layer. *Atmospheric Environment* 34, 2499 – 2527.

Jenkin, M. E., 2008: Trends in ozone concentration distributions in the UK since 1990: Local, regional and global influences. *Atmos. Environ.*, 42, 5434- 5445.

Jeong, C. -H., Evans, G. J., Dann T., Graham, M., Herod, D., Dabek-Zlotorzynska, E., Mathieu, D., Ding, L., Wang, D., 2008. Influence of Biomass Burning on Wintertime Fine Particulate Matter : Source Contribution at a Valley Site in Rural British Columbia. *Atmospheric Environment*, 42, 3684-3699.

- Jeong, C.-H., McGuire, M., Evans, G., Dann, T., Herod, D., PMF source apportionment for PM_{2.5} at the five national air pollution surveillance (NAPS) sites across Canada. Presented at the 27th Annual Conference of the American Association for Aerosol Research, Orlando, FL, October 2008
- Jerrett, M., Arain, M.A., Kanaroglou, P., Beckerman, B., Crouse, D., Gilbert, N.L., Brook, J.R., Finkelstein, N., 2007. Modelling the intra-urban variability of ambient traffic pollution in Toronto, Canada. *Journal of Toxicology and Environmental Health Part A*, 70, 200-212.
- Jiang, G., Fast, J.D., 2004. Modelling the effects of VOC and NO_x emission sources on ozone formation in Houston during the TexAQS 2000 field campaign. *Atmospheric Environment*, 38, 5071-5085.
- Johnson, D., 2004. Identification of Synoptic Conditions resulting in Widespread Ozone and PM_{2.5} exceedances. Draft report. Environment Canada – Environmental Stewardship Branch – Air Emissions Priorities, 43 pp
- Johnson, D., 2005. Analysis and determination of cause of PM_{2.5} CWS exceedance episodes in Canada's Prairie Provinces. Report prepared for Environment Canada.
- Kenski, D., Sponseller, B., 2005. The Great Midwestern PM_{2.5} Episode of February 2005, available at http://www.inawma.org/files/2005-10-11_The_Great_Midwestern_PM2.pdf
- Ketch, L., Waugh, D., Tordon, R., Beauchamp, S., 2005. Multi-pollutant Episodes Analysis for Kejimikujik, Nova Scotia and St. Andrews, New Brunswick – 1999 to 2002. Meteorological Service of Canada – Atlantic, Draft report.
- Kim, B. -M., Henry, R. C., 2000. Extension of self-modelling curve resolution to mixtures of more than three components. Part 3. *Chemometrics and Intelligent Laboratory Systems* 52,145–154.
- Kleinman, L.I., Daum, P.H., Springston, S.R., Leitch, W.R., Banic, C.M., Isaac, A.I., Jobson, B.T., Niki, H., 1996. Measurement of O₃ and related compounds over southern Nova Scotia, 2, Photochemical age and vertical transport. *Journal of Geophysical Research*, 101, 29061-29074.
- Keeler, G.J., Samson, P.J., 1989. Spatial representativeness of trace element ratios, *Environmental Science and Technology*, 23, 1358-1364.
- Lavoué D, S. Gong, B. J. Stocks, 2007. Modelling emissions from Canadian wildfires: a case study of the 2002 Québec fires, *International Journal of Wildland Fire*, 16, 649-663.
- Lavoué, D. and B.J. Stocks, 2010, Emissions of air pollutants by Canadian wildfires from 2000 to 2004, in review for publication in *International Journal of Wildland Fire*.

- Lee, P. K. H., Brook, J. R., Dabek-Zlotozynska, E., Mabury, S. A., 2003, Identification of the Major Sources Contributing to PM_{2.5} Observed in Toronto, *Environmental Science and Technology*, 37,4831-4840
- Leaitech, W.R., Bottenheim, J.W., Biesenthal, T.A., Li S.-M., Liu, P.S.K., Asalian, K., Dryfhout-Clark, H., Hopper, F., 1999. A case study of gas-to-particle conversion in an eastern Canadian Forest. *Journal of Geophysical Research*, 104, 8095-8111
- Levasseur, M., Sharma, S., Cantin, G., Michaud, S., Gosselin, M., Barrie, L., 1997. Biogenic sulphur emissions from the Gulf of St. Lawrence and assessment of its impact on the Canadian east coast. *Journal of Geophysical Research* 102, 28,025-28,039.
- Lin, X., Roussel, P.B., Meld, O.T., Selorio, M., 1995. The role of Toronto urban emissions in regional ozone episodes. *Atmospheric Environment*, 29, 565-577.
- Li, Q., Jacob, D., Bey, I. Palmer, P., Duncan, B.N., Field, B.D., Martin, R.V., Fiore, A.M., Yantosca, R.M., Parrish, D.D., Simmonds, P.G., Oltmans, S., 2002. Transatlantic transport of pollution and its effects on surface ozone in Europe and North America. *Journal of Geophysical Research*, 107, 4166, doi:10.1029/2001JD001422.
- Lu, R., Turco, R. P., 1994, Air pollutant transport in a coastal environment: Part I: two-dimensional simulations of sea breeze and mountain effects. *Journal of Atmospheric Science*, 15, 2285-2308
- Lu, G., Brook, J.R., Rami M., Alfarra, M.R., A., Anlauf, K., Leaitech, W.R., Sharma, S., Wang, D., Worsnop, D.R., Phinney, L., 2006, Identification and characterization of inland ship plumes over Vancouver, BC, *Atmospheric Environment*, 40, 2767-2782
- Lyons, W. A., Cole, H. S., 1973, Fumigation and plume trapping on the shores of Lake Michigan during stable onshore flow. *Journal of Applied Meteorology*, 12, 494-510
- Lyons, W. A., Cole, H. S., 1976, Photochemical oxidant transport: mesoscale lake breeze and synoptic-scale aspects. *Journal of Applied Meteorology*, 15, 733-743
- Lyons, W.A., Tremback, C.J., Pielke, R. A., 1995. Applications of the Regional Atmospheric Modelling System (RAMS) to Provide Input to Photochemical Grid Models for the Lake Michigan Ozone Study (LMOS). *Journal of Applied Meteorology*, 34, 1762-1786.

Makar, P.A., Stroud, C., Wiens, B., Cho, S.H., Zhang, J., Sassi, M., Liggio, J., Moran, M., Gong, W., Gong, S., Li, S.-M., Brook, J., Strawbridge, K., Anlauf, K., Mihele, C., Toom-Saunty D., 2008. High Resolution Nested Runs of the AURAMS Model with Comparisons to PrAIRie2005 Field Study Data Air Pollution Modelling and its Application, XIX Springer AK/NATO Publishing Unit, Dordrecht, The Netherlands (in press)

McKeen S.A., G. Wotawa, D.D. Parrish, J.S. Holloway, M.P. Buhr, G. Huebler, F.C. Fehsenfeld and J. F. Meagher, 2002. Ozone production from Canadian wildfires during June and July 1995. *Journal of Geophysical Research*, 107, 4192

McKendry, I.G., Hacker, J.P., Stull, R., 2001. Long-range transport of Asian dust to the Lower Fraser Valley, British Columbia, Canada. *Journal of Geophysical Research*, 106, 18361–18370.

McKendry, I.G., Steyn, D.G., Lundgren, J., Hoff, R.M., Strapp, W., Anlauf, K., Froude, F., Martin, J.B., Banta, R.M., Olivier, L.D. 1997. Elevated ozone layers and vertical down-mixing over the Lower Fraser Valley, BC. *Atmospheric Environment*, 31, 2135-2146

McKendry, I. G., 2006, Background concentrations of PM_{2.5} and ozone in British Columbia. Report to the BC Ministry of the Environment, available at

http://www.env.gov.bc.ca/air/airquality/pdfs/background_pm25_ozone.pdf

Ménard R., Robichaud A., 2005. The Chemistry-Forecast System at the Meteorological Service of Canada. Proceedings of ECMWF Seminar on Global earth-system monitoring 5-9 Sept. 2005. ECMWF 2005- Annual Seminar Proceedings.
<http://www.ecmwf.int/publications/library/do/references/show?id=86891>,
http://www.ecmwf.int/publications/library/ecpublications/_pdf/seminar/2005/sem2005_menard.pdf

Merrill, J.T., Moody, J.L., 1996, Synoptic Meteorology and transport during the North Atlantic Regional Experiment (NARE) intensive : Overview, *Journal of Geophysical Research*, 101, 28903-28921.

Merrill, J. T., J. L. Moody, S. J. Oltmans, and H. Levy II (1996), Meteorological analysis of tropospheric ozone profiles at Bermuda, *J. Geophys. Res.*, 101(D22), 29,201-29,211, doi:10.1029/95JD03432.

Metro Vancouver. 2006, Lower Fraser Valley Air Quality Report 2006. Metro Vancouver, 4330 Kingsway, Burnaby, BC, Canada, V5H 4G8. available at www.gvrd.ca.

Metro Vancouver, 2007. 2005 Lower Fraser Valley Air Emissions Inventory & Forecast and Backcast. Executive Summary. Metro Vancouver Policy Planning Department, 4330

Kingsway, Burnaby, BC, V5H 4G8. available at
http://www.gvrd.bc.ca/air/pdfs/ExecSummary_2005_LFV.pdf

Metro Vancouver. 2010. 2005 Lower Fraser Valley Air Emissions Inventory & Forecast and Backcast. Detailed Listing of Results and Methodology. Metro Vancouver Policy Planning Department, 4330 Kingsway, Burnaby, BC, V5H 4G8.
http://www.metrovancouver.org/about/publications/Publications/2005-LFV-Air_Emissions_Inventory-Forecast-Backcast.pdf

Meyn, S., Hay, J., Vingarzan, R., Farris, S. 2007a, Analysis of Air Quality at Osoyoos, British Columbia, Border Air Quality Station (November 2004-September 2006): An Analysis of Transboundary Air Pollution Transport. Environment Canada, Meteorological Services, Vancouver BC, V6S 3S5. available at
<http://www.pyr.ec.gc.ca/georgiabasin/documents/OsoyoosBorderAQ-FinalVersion.pdf>

Meyn, S., Farris, S. Vingarzan, R. 2007b. Analysis of Air Quality at the Creston, British Columbia Border Air Quality Station (Jun 2005 – Oct 2006): An Analysis of Trans-boundary Air Pollution Transport. Environment Canada, Meteorological Services, #201-401 Burrard, Vancouver, BC, V6S 3S5.

MOE, 1998, Air Quality in Ontario 2008 Report. Ontario Ministry of the Environment

MOE, 2005, Transboundary Air Pollution in Ontario. Ontario Ministry of the Environment.

MOE, 2006, Air Quality in Ontario 2005 Report. Ontario Ministry of the Environment

MOE, 2007, Air Quality in Ontario 2006 Report. Ontario Ministry of the Environment

Monks, P.S., 2000, A review of the observations and origins of the spring ozone maximum. Atmospheric Environment, 34, 3545-3561.

Moody, J.L., Davenport, J.C., Merrill, J.T., Oltmans, S.J., Parrish, D.D., Holloway, J.S., Levy II, H., Forbes, G.L., Trainer, M., Buhr, M., 1996. Meteorological mechanisms for transporting O₃ over the western North Atlantic Ocean: A case study for August 24-29, 1993.

Moore, D., Copes, R., Fisk, R., Joy, R., Chan, K., Brauer, M., 2006. Population Health Effects of Air Quality Changes Due to Forest Fires in British Columbia in 2003: Estimates from Physician-visit Billing Data. Canadian Journal of Public Health, Volume 97, #2, 105-108.

NAESI (National Agri-Environmental Standards Initiative), 2008, Environment Canada, document in preparation, <http://www4.agr.gc.ca/AAFC-AAC/display-afficher.do?id=1209128121608&lang=e>

NAPS (National Air Pollution Surveillance Network). 2006. NAPS Data Archive. Environment Canada, Environmental Protection Service, Ottawa, Ontario, K1A 0H3. <http://www.etc-cte.ec.gc.ca/Napsdata/Default.aspx>

NARSTO (North American Research Strategy for Tropospheric Ozone), 2008, "Narsto Multipollutant Assessment" Document in preparation, <http://www.narsto.org/>

NARSTO, 2004: Particulate Matter Science for Policy Makers, A NARSTO Assessment. Edited by P. McMurry, M. Shepherd and J. Vickery. "Receptor Methods", Chapter 7 by Brook J.R., Vega E. and Watson J.G. 2004. Cambridge University Press, ISBN 0 521 84287 5 hardback. Pages 235-281.

NEB (National Energy Board), 2006. Canada's Oil Sands: Opportunities and Challenges to 2015 an Update. An Energy Market Assessment, NE23-116/2006E, June 2006.

NEB (National Energy Board), 2007. Short Term Canadian Natural Gas Deliverability: 2007-2009. An Energy Market Assessment, NE2-1/2007E, October 2007.

Neuman, J.A., Parrish, D.D., Trainer, M., Ryerson, T.B., Holloway, J.S., Nowak, J.B., Swanson, A., Flocke, F., Roberts, J.M., Brown, S.S., Stark, H., Sommariva, R., Stohl, A., Peltier, R., Weber, R., Wollny, A.G., Sueper, D.T., Hubler, G., Fehsenfeld, F.C., 2006. Reactive nitrogen transport and photochemistry in urban plumes over the North Atlantic Ocean. *Journal of Geophysical Research*, 111, D23S54, doi:10.1029/2005JD007010.

Nkemdirim, L.C. ,1988. An assessment of the relationship between functional groups of weather elements and atmospheric pollution in Calgary, Canada. *Atmospheric Environment* 22, 2287-2296.

Northwest Territories Department of Environment and Natural Resources, 2004. Northwest Territories Air Quality Report 2004. Report by NWT Department of Environment and Natural Resources

NPRI, 2007b, National Pollutant Release Inventory: Major point source emissions http://www.ec.gc.ca/pdb/querysite/query_e.cfm

NPRI, 2009, National Pollutant Release Inventory: Major point source emissions http://www.ec.gc.ca/pdb/npri/npri_home_e.cfm

O'Dowd, C.D., Smith, M.H., 1993. Physicochemical properties of aerosols over the northeast Atlantic: evidence for wind-speed-related submicron sea-salt aerosol production. *Journal of Geophysical Research*, 98, 1137-1149.

Oulton, I., Blom, G., Oldfield, K., Brenton, L., MacIsaac, P., Cormier, M., Dempsey, K., Malec, G., Halifax Port Authority Stakeholder Report, June 2007. available at

<http://www.portofhalifax.ca/english/resources/documents/6087HPABiAnnualReport.pdf>,
(accessed September 2007)

Paatero, P., 1997. Least square formulation of robust, non-negative factor analyzer. *Chemometrics and Intelligent Laboratory Systems* 37, 23-35.

Paatero, P., 1998. User's guide for Positive Matrix Factorization Programs, PMF2 and PMF 3.

Pankratz, A., 2004. Climatology of wind trajectories for the prairie provinces. Environment Canada – Prairie and Northern Edmonton, AB.

Park, R. J., Jacob, D. J., Logan, J. A., 2007. Fire and biofuel contributions to annual mean aerosol mass concentrations in the United States, *Atmospheric Environment*, 41, 7389-7400.

Parliamentary Research Branch, 1998, Canadian Parliamentary Research Branch <http://dsp-psd.pwgsc.gc.ca/Collection-R/LoPBdP/CIR/7937-e.htm>

Peake, E., Fong, B.D., 1990. Ozone concentrations at a remote mountain site and at two regional locations in southwestern Alberta. *Atmospheric Environment* 24A, 475-480.

Pfister, G.G., Emmons, L.K., Hess, P.G., Honrath, R., Lamarque, J.-F., Val Martin, M.,

Owen, R.C., Avery, M.A., Browell, E.V., Holloway, J.S., Nedelec, P., Purvis, R., Ryerson, T.B., Sachse, G.W., Schlager, H., 2006. Ozone production from the 2004 North American boreal fires. *Journal of Geophysical Research D: Atmospheres*, 111, art. no. D24S07.

Phinney, L., Waugh, D., Beauchamp, S., Hingston, M., 2006a. Contribution of Marine Activities to Ambient Air Chemistry in Coastal Regions of Atlantic Canada, Phase I: Halifax Harbour. Meteorological Service of Canada, Atlantic Region, Science Report Series 2006-01.

Phinney, L., 2007. Sea Salt Aerosol Surface Concentrations and Vertical Profiles near the Atlantic Canadian Coast: A Literature Review. Meteorological Service of Canada, Atlantic Region, Science Report Series 2007-03.

Pisano, J.T., McKendry, I.M., Steyn, D.G., Hastie, D.R. 1997. Vertical nitrogen dioxide and ozone concentrations measured from a tethered balloon in the Lower Fraser Valley. *Atmospheric Environment*, 31, 2071-2078.

Polissar, A.V., Hopke, P.K., Poirot, R.L., 2001. Atmospheric aerosol over Vermont: Chemical composition and sources. *Environment Science and Technology* 35, 4604-4621.

Potvin Air Management Consulting, 2006. Informal Consultation on Local Air Issues in Sault Ste. Marie, Ontario-Michigan under the Canada-United States Air Quality Agreement: Technical Support Document on Air Quality 2001-2003, Summary Report Prepared for Environment Canada, U.S. Environmental Protection Agency, Ontario Ministry of the Environment, Michigan Department of Environmental Quality and Inter-Tribal Council of Michigan by Potvin Air Management Consulting, available at http://epa.gov/region5/air/transboundary_air_quality_study-final07-30-07.pdf

Pryor, S.C. 1996. Assessing public perception of visibility for standard setting exercises. *Atmospheric Environment*, 30, 2705-2716.

Pun, B.K., Seigneur, C. 1999. Understanding particulate matter formation in the California San Joaquin Valley: conceptual model and data needs. *Atmospheric Environment*, 33, 4865-4875.

Qiu, W., Pankratz, A., 2007. The AQHI in Alberta: 2001-2005. Internal analysis in support of AQHI evaluation.

Quinn, P.K., Coffman, J., Kapustin, V.N., Bates, T.S., Covert, D.S., 1998. Aerosol optical properties in the marine boundary layer during the first Aerosol Characterization Experiment (ACE 1) and the underlying chemical and physical aerosol properties. *Journal of Geophysical Research*, 103, 16,547-16,563.

Raven, H. (2005). 7Be as a Tracer of Stratospheric Contribution to Ground Level Ozone at Harlech, Alberta. Presented at 39th CMOS Annual Congress, Vancouver BC, May 2005

Regional Municipality of Wood Buffalo, 2006. The regional municipality of Wood Buffalo census 2006. Planning and Development Department, 2006.

Reid, N.W., Niki, H., Hastie, D.R., Shepson, P.B., Roussel, P.B., Melo, O.T., Mackay, G.I., Drummond, J., Schiff, H.I., Poissant, L., Moroz, W., 1996. The Southern Ontario Oxidant Study (SONTOS): Overview and Case Studies for 1992. *Atmospheric Environment*, 30, 2125-2132.

Reid, N. W., 2007, A Review of Background Ozone in the Troposphere. Available at <http://www.ene.gov.on.ca/en/publications/air/6424e.pdf>

Rittmaster R., Adamowicz, W.L., Amiro, B., Pelletier, R.T., 2006. Economic analysis of health effects from forest fires. *Canadian Journal of Forest Research*, 36, 868-877.

Rousseau, J., Lavoué, D., 2005. Integration of Real Time PM_{2.5} Emission Rates from Forest Fires with a Dynamic Model in order to Simulate Wildfires in CHRONOS to Improve the Air

Quality Forecasts . In the Proceedings of the 39th Canadian Meteorological and Oceanographic Society Congress, Vancouver/Richmond, Canada,

Royal Society. 2008. Ground-level Ozone in the 21st Century: Future Trends, Impacts and Policy Implications. ISBN: 978-0-85403-713-1. web royalsociety.org

Rubin, J., Brown, S.G., Hafner, H. R., Roberts, P.T., Graham, M., 2007, Source Apportionment and Positive Matrix Factorization at an Industrial City in Northern British Columbia. Presented at the 2007 Aerosol Conference, Reno, Nevada, September 24-28, 2007.

Rupakheti, M., Leitch, W. R., Lohmann, U., Hayden, K., Brickell, P., Lu, G., Li, S-M., Toom-Sauntry, D., Bottenheim, J. W., Brook, J. R., Vet, R., Jayne, J. T., Worsnop, D. R., 2005. An intensive study of the size and composition of submicron atmospheric aerosols at a rural site in Ontario, Canada. *Aerosol Science and Technology*, 39, 722-736

RWDI (Rowan Williams Davies & Irwin Inc.), 2004. Contribution des alumineries aux concentrations de matières particulaires. Report submitted to Association de l'aluminium du Canada, Montreal, Canada.

Ryerson, T.B., Trainer, M., Angevine, W.M., Brock, C.A., Dissly, R.W., Fehsenfeld, F.C., Frost, G.J., Goldan, P.D., Holloway, J.S., Hübler, G., Jakoubek, R.O., Kuster, W.C., Neuman, J.A., Nicks Jr., D.K., Parrish, D.D., Roberts, J.M., Sueper, D.T., Atlas, E.L., Donnelly, S.G., Flocke, F., Fried, A., Potter, W.T., Schauffler, S., Stroud, V., Weinheimer, A.J., Wert, B.P., Wiedinmyer, C., Alvarez, R.J., Banta, R.M., Darby, L.S., Senff, C.J., 2003. Effect of petrochemical industrial emissions of reactive alkenes and NO_x on tropospheric ozone formation in Houston, Texas. *Journal of Geophysical Research*, 108, ACH 8-1 – ACH 8-24.

Sahsuaroglu T., Arain, A., Beckerman, B., Kanaroglou, P., Brook, J.R., Finkelstein, N., Finkelstein, M., Gilbert, N., Newbold, B., Jerrett, M., 2006, A land-use regression model for predicting ambient concentrations of nitrogen dioxide in Hamilton, Canada. *Journall of Air & Waste Management Association*. 56, 1059-1069.

Scott, W., 1989, Acid Rain: What we know, what we did, what we will do, *Archives of Environmental Contamination and Toxicology*, 18, 75-82

Sharma, S., Vingarzan, R., Barrie, L.A., Norman A-L., Sirois, A., Henry, M., DiCenzo, C., 2003, Concentrations of dimethyl sulfide in the Strait of Georgia and its impact on the atmospheric sulphur budget of the Canadian West Coast, *Journal of Geophysical Research*, 108, 7.1–7.12

Shepherd, M.F., Brook, J.R., Makar, P.A., Moran, M.D., Vet, R.J., Dann, T.F., Dion, J., 2001
Precursor contributions to ambient fine particulate matter in Canada : a report by the
Meteorological Service of Canada, Environment Canada, pp. 237

Shepherd, M., 2004. Perspective for Managing PM, in: McMurray *et al.* (Eds.), Particulate
Matter Science for Policy Makers, A NARSTO Assessment, Cambridge University Press,
Cambridge, pp 53-68.

Sillman, S., Samson, P. J., Masters, J. M., 1993, Ozone production in urban plumes transported
over water: Photochemical model and case studies in the Northeastern and Midwestern United
States, *Journal of Geophysical Research*, 98, 12687-12699

Singh, G.B. Brune, W.H. Crawford, J.H. Jacob., D.J., Russel, P.B., 2006, Overview of the
summer 2004 Intercontinental Chemical Transport Experiment – North America (INTEX-A).
Journal of Geophysical Research, 111, D24S01, doi:10.1029/2006JD007905

Sirois, A., Vet, R., 2002. An Exploratory Evaluation of Potential Canadian Emission
Contributions to Reduced Visibility and Particulate Matter Concentrations at Glacier National
Park, Montana. Internal report.

SOE, 2002. Yukon State of the Environment Report. Yukon Department of Environment ISBN
1-55362-157-3. available at <http://www.environmentyukon.gov.yk.ca/pdf/2002soe.pdf>

So R. and Vingarzan R. 2010. Analysis of Visibility in the Lower Fraser Valley of British
Columbia. Environment Canada, Meteorological Services, #201-401 Burrard, Vancouver, BC,
V6S 3S5.

So, R., Vingarzan, R. and Meyn, S. 2010. Source Apportionment of PM_{2.5} at Burnaby South
and Abbotsford. Environment Canada. Environment Canada, Meteorological Services, #201-
401 Burrard, Vancouver, BC, V6S 3S5.

Statistics Canada, 2006. available at <http://www40.statcan.ca/101/cst01/demo02a.htm>

Strawbridge, K.B., Snyder, B.J. 2004. Daytime and nighttime aircraft measurements showing
evidence of particulate matter transport into the northeastern valleys of the Fraser Valley, B.C.
Atmospheric Environment, 38, 5873-5886.

Stocks, B.J., Fosberg, M.A., Lynham, T.J., Mearns, L., Wotton, B.M., Yang, Q. Jin, J.-Z.,
Lawrence, K. Hartley, G.R., Mason, J.A., McKenney, D.W., 1998. Climate change and forest
fire potential in Russian and Canadian boreal forests. *Climatic Change*, 38,1-13.

Sub-Committee on Scientific Co-operation (SC2). 2004. The Canada-U.S. Transboundary Particulate Matter Science Assessment. En56-203/2004E. 129pp. Available at: <http://www.msc-smc.ec.gc.ca/saib> or <http://www.epa.gov/airmarkt/usca/index.html>

UpHere Publishing, 2007. The Firing Squad. Nov/Dec 2004 Issue. Up Here Publishing Ltd. #800-4920 52nd Str. Yellowknife, NT X1A 3T1. available at <http://www.uphere.ca/node/61>

U.S. EPA, 2007. Emission summaries, available at <http://www.epa.gov/cair/technical.html#proposedrule>

Vingarzan, R., Taylor, B., 2003. Trend analysis of ground level ozone in the Greater Vancouver/Fraser Valley area of British Columbia. *Atmospheric Environment*, 37, 2159-2171.

Vingarzan R., 2004. A review of surface ozone background levels and trends, *Atmospheric Environment*, 38, 3431–3442

Vingarzan R., Li, S-M . 2006. The Pacific 2001 Air Quality Study – synthesis of findings and policy implications. *Atmospheric Environment*, 40, 2637-2649.

Vingarzan, R. Fleming, S. Meyn, S., Schwarzhoff, P., Belzer, W. 2007. Air Quality and Transboundary Transport at Christopher Point, British Columbia. Meteorological Services of Canada, Environment Canada, #201-401 Burrard Street, Vancouver, BC, V7R 2S5.

Vingarzan, R., Schwarzhoff, P. Ozone Trends and Reactivity in the Lower Fraser Valley. 2010. Meteorological Services of Canada, Environment Canada, #201-401 Burrard Street, Vancouver, BC, V7R 2S5.

Wade, K.S., Brown, S.G., Roberts, P.T., 2007. Characterization of ambient air quality in the oil sands area of Northern Alberta. Prepared for CEMA. Wang, T., Carroll, M.A., Albercook G.M., Owens K.R., Duderstadt, K.A., Markevitch, A.N., Parrish, D.D., Holloway, J.S., Fehsenfeld, F.C., Forbes, G., Ogren, J., 1996. Ground-based measurements of NO_x and total reactive oxidized nitrogen (NO_y) at Sable Island, Nova Scotia, during the NARE 1993 summer intensive, *Journal of Geophysical Research*, 101, 28972-29004.

Wang, D., J. D. Fuentes, D. Travers, T. Dann, T. Connolly, 2005. Non-methane hydrocarbons and carbonyls in the Lower Fraser Valley during PACIFIC 2001. *Atmospheric Environment*, 39, 5261-5272.

Watson J.G., Chen A L.-W., Chow, J.C., Draiwamy P, Lowenthal D.H. (2008) Source apportionment: Findings from the U.S. Supersites program. *J. Air & Waste Manage. Assoc.* 58, 265–288.

- Waugh, D., 2003. Low Altitude Ozone Concentrations over Southwestern Nova Scotia – Meteorological Factors and Model Sensitivity, MSc Thesis, Dalhousie University, 114 pp.
- Waugh, D., Tordon, R., Ketch, L., Beauchamp, S., 2003. Multi-pollutant Trajectory Analysis for Kejimikujik National Park, Nova Scotia and St. Andrews, New Brunswick – 1999 to 2001. Meteorological Service of Canada – Atlantic, CDROM.
- Waugh, D., Phinney, L., Beauchamp, S., Leaitch, R., Hayden K., 2007. Initial Results from the 2004 ICARTT / TIMs field study. Unpublished report.
- West, J.J., Ansari, A.S., Pandis, S.N., 1999. Marginal PM_{2.5}: Nonlinear aerosol mass response to sulphate reductions in the Eastern United States. *Journal of the Air and Waste Management Association*, 49, 1415-1424
- Wexler, A.S., Johnson, M.V., 2008. What have we learned from highly time-resolved measurements during EPA's supersites program and related studies?, *Journal of the Air and Waste Management Association*, 58, 303-319
- Wheeler A.J., Xu X., Smith-Doiron M., Gilbert N.L., Brook J.R., 2007, Intra-urban variability of air pollution – monitoring and modelling of PM_{2.5}, PM_{2.5-10} and NO₂. Poster presentation at: ISEE ISEA 2006, Paris, September
- Wheeler A.J., Smith-Doiron M., Xu X., Gilbert M.L., Brook J.R., 2008, Intra-Urban variability of air pollution in Windsor, Ontario – Measurement and modelling for human exposure assessment. *Environmental Research*, 106, 7-16
- Wotawa G., M. Trainer, 2000. The influence of Canadian forest fires on pollutant concentrations in the United States. *Science*, 288, 324-328.
- Xu X., Brook J.R., Guo Y., 2007, A statistical assessment of saturation and mobile sampling strategies to estimate long term average concentrations across urban areas, *Journal of the Air and Waste Management Association*, 57, 1396–1406.
- Xu X., Baoning Z., Brook J.R., Lu G. (2008) Dispersion modelling of ship plume in West Vancouver, British Columbia, Canada. *Air&Waste Mangement Association Annual Meeting*, Portland, OR. Paper 570.
- Yukon Government. 2007. Environment Yukon. available at <http://www.environmentyukon.gov.yk.ca/>

CHAPTER 8: New Directions in Smog Science

David Flagg, Janya Kelly, David Plummer, Paul Makar, Randall Martin

KEY MESSAGES AND IMPLICATIONS

- Recent advancements in climate change models have led to their use in air pollution projections based on future climate regimes.
- Modelled air quality projections from coupled air quality and climate models show that:
- If emissions were to remain constant at their current levels, changes to climate would cause the globally averaged background ozone (O₃) concentration to decrease by 1 to 3 parts per billion by volume (ppbv). However, projected increases in emissions will counteract this loss, with a net increase in O₃ for most continental regions at the surface.
- The modelled regional response of tropospheric O₃ to climate change varies locally, with a general trend of O₃ increases of 1 to 5 ppbv relative to the current climate, primarily in areas that are already known for O₃ pollution. Some areas show O₃ decreasing locally, depending on local climate, emissions and meteorology.
- The projected response of particulate matter to climate change is mixed, although increases can be expected in some areas.
- Sea and lake breeze fronts can have a significant impact on the boundary layer and on air quality, causing important changes in local surface pollutant concentrations. The presence of an urban area can significantly complicate the circulation, contributing to locally high pollutant concentrations on a diurnal timescale subject to the size of the city and the strength of the sea/lake breeze.
- Pollutant transport in urban environments is subject to the density, orientation and geometry of the buildings, in addition to the ambient wind speed, wind direction, and static stability. Very tall buildings lining narrow street canyons tend to inhibit daytime ventilation of surface source pollutants. Considerable work remains in modelling efforts of the dynamics and energy balance within the urban canopy and above.
- Satellite-based measurements have emerged in the last decade as a new means of studying air pollution, and their use is expected to grow. Satellite-based measurements may be used to provide information on surface air quality, provide constraints on emissions estimates, and track long-range transport on the regional and global scale.

8.1 Topic Introduction and Organization of Chapter

This chapter contains three separate reviews of recent scientific research, tied together under the theme “New Directions”. Although many of the chapters in this Assessment review the literature from the period 2003 to 2007, this chapter has been updated to include a review up to and including 2009 in order to adequately present new research directions. Each review describes either a part of smog science that did not exist in the previous decade, or a field in which new discoveries have greatly modified our understanding of air pollution formation and transport. They are not intended as an exhaustive list of all new or valuable research directions, rather, as highlights of research areas not covered in detail in other chapters of this assessment in which significant progress has been made. The reviews focus on:

The effects of climate change on air pollution (Section 8.2). Recent work with climate change models has led to their use for air pollution projections under future climate regimes. The work to date suggests that the impact of climate change on air pollution will be significant, rivalling that of expected increases in emissions.

The Atmospheric Boundary Layer (ABL) and its relationship with air pollution (Section 8.3). The movement of pollutant gases and particulate matter is especially sensitive to the local environment and meteorology. Assessment of the dispersion and large-scale transport from source areas requires careful study of the relevant physical processes, especially in complex environments like coastlines and cities.

Satellite observations of air quality constituents from space (Section 8.4). This is a new and exciting branch of air quality science with many possible future applications.

8.2 Climate Change and Air Quality

Janya Kelly, David Plummer, Paul Makar

8.2.1 Climate-Chemistry Interactions

8.2.1.1 Links between Climate Change and Air Quality

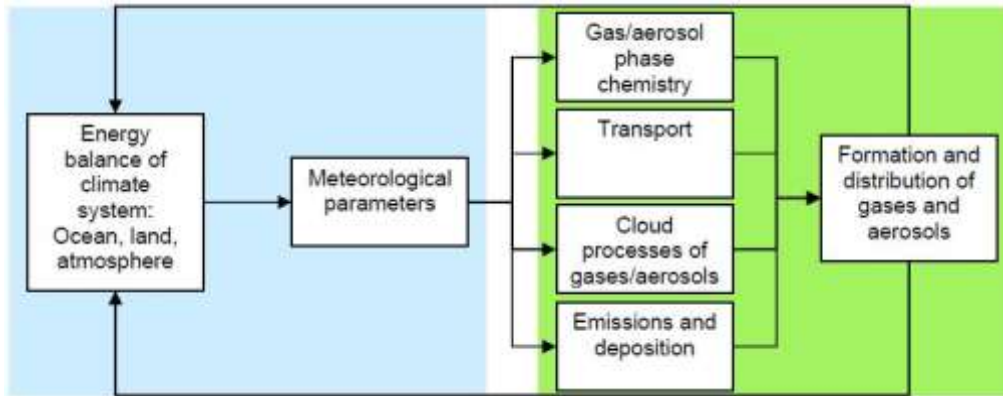


Figure 8.1 Representation of the links between climate change and air quality. Changes to the energy balance of the climate system can impact meteorological parameters, which can impact the formation and distribution of atmospheric species, changing air quality. Changes to the distribution and formation of atmospheric species can feedback and change the energy balance of the climate system.

A simplified outline of the links between climate change and air quality is provided in Figure 8.1. The complete climate system involves complex interactions between the atmosphere, oceans, cryosphere (snow and ice) and terrestrial biosphere (land and vegetation), with further complex interactions when considering climate change links to air quality. Climate change occurs through changes in the balance of incoming and outgoing radiation in the complete climate system. Meteorological parameters such as temperature, pressure, wind speed and direction, humidity, and precipitation can be either directly or indirectly impacted by radiation. These variables, in turn, impact gas phase and aerosol chemistry, transport, cloud processing of gases and aerosols, and emissions and deposition. Climate change may thus affect the formation and distribution of both ozone (O_3) and particulate matter (PM), two key indexes for air quality. Gases and aerosols may also affect climate, by interacting with the incoming (solar) and outgoing (terrestrial) radiation.

Climate change impacts on air quality include: (1) an increase in temperature causing an increase in water vapour concentrations with both water vapour and temperature changes affecting chemical reaction rates; (2) a change in the distribution of meteorological conditions, with local changes in weather patterns giving rise to changes in air quality – an example being climate change-induced changes in wind direction that prevent or allow pollutants to be

transported in a new direction; (3) modifications to global circulation dynamics (e.g. stratosphere-troposphere exchange, the distribution of convection and boundary layer ventilation, decrease in frequency of mid-latitude cyclones), resulting in changes to the distribution of pollutants; (4) changes to the emissions of natural precursor gases, which are meteorologically driven; and (5) decreased cloudiness, resulting in enhanced photochemical smog production (Jacob and Winner, 2009; Hogrefe *et al.*, 2004; Leung and Gustafson, 2005; Dawson *et al.*, 2007; Liao *et al.*, 2006; Stevenson *et al.*, 2006; Steiner *et al.*, 2006; Forkel and Knoche, 2006). Air quality projections from coupled air quality and climate models will include all of these effects; while temperature is often the focus of climate change, the role of all meteorological parameters is included in model projections.

Air quality can impact climate change via changes in the concentrations of atmospheric constituents that can modify the radiative balance of the atmosphere (e.g. O₃, methane and PM changes may result in changes to the radiative properties of the atmosphere) and the formation of clouds. PM can impact climate in two ways: directly, by the scattering and absorption of solar radiation and indirectly, by impacting cloud radiative properties. Depending on composition, PM will either scatter the solar radiation (sulphates) creating a cooling effect, or absorb the solar radiation (black carbon) creating a warming effect through interactions with the surrounding air. Possible outcomes include reduced low level cloud cover, increased numbers of cloud condensation nuclei, higher reflectivity, and increased or decreased radiation reaching the surface, depending on the balance of these effects.

Jacob and Winner (2009) provide a more in-depth discussion of the links between climate change and air quality, as well as the sensitivity of air pollution meteorology to climate change.

8.2.2 Studying Climate Change and Air Quality

The most comprehensive projections of future climate rely on global or regional scale numerical models of the climate system based on fundamental physical principles (CMOS, 2007). Although they are the best tools currently available, these models are only approximations with uncertainties resulting from the grid resolution, choice of processes to represent in the model, and the manner in which they are represented (especially those involving the formation and behaviour of clouds and precipitation) (Hogrefe *et al.*, 2004; Murphy *et al.*, 2004; Staniforth *et al.*, 2005). Different models handle processes occurring within the atmosphere in different ways, leading to a range of sensitivities to future climate change impacts (Hogrefe *et al.*, 2004). These uncertainties are derived from the representation of the climate system in models and by the internal climate variability in the system (IPCC, 2007). Multiple iterations of the models from a variety of initial conditions (consistent with observations) will reduce internal climate variability (IPCC, 2007). IPCC (2007) suggest the

use of multiple models (*ensemble modelling*) to reduce the effects of uncertainty in the representation of the climate system, however, some processes may still be missing and there may be shared systematic bias in the different parameterizations.

Projected changes in climate can be related to air quality indicators through statistical downscaling or dynamic downscaling of the climate modelling system. Further information about future air quality sensitivities and projections can be derived by using the ensemble modelling technique.

8.2.2.1 Statistical Downscaling

Statistical downscaling reduces large-scale climate variables to the regional/local scale, using derived statistical relationships between meteorological (predictors) and air quality (predictands) parameters from historical observational data for the given location (Cheng *et al.*, 2007a,b; Demuzere and van Lipzig, 2010a, b; Timbal *et al.*, 2009; Wise 2009). This method requires climate data from either a General Circulation Model (GCM) or a historical data record (e.g. local station observations). Demuzere and van Lipzig (2010a) provide an overview of the many different approaches to statistical downscaling approaches. Timbal *et al.* (2009) found the choice of large-scale climate predictor variables to be far more important than the choice of statistical downscaling technique.

The advantages of statistical downscaling include increased accessibility and flexibility, as well as the ability to provide local (station scale) data (Wise, 2009). Statistical downscaling also has the advantage of being less computationally expensive and intensive compared to dynamical downscaling as will be discussed in section 8.2.2.2 (Demuzere and van Lipzig, 2010). However, both dynamical and statistical downscaling are subject to the uncertainties of the GCM output they rely on (Wise, 2009). Similarly, statistical downscaling can require a historical data record that may be unavailable for regions of interest. A large disadvantage of this method is the assumption that the current climate statistical relationships between predictors and predictands will remain valid in a future climate (Demuzere and van Lipzig, 2010a, b; Timbal *et al.*, 2009; Wise, 2009). Changes in emissions (anthropogenic and biogenic) are not accounted for in statistical downscaling, as well as changes in transport and formation of chemical species (Demuzere and van Lipzig, 2010a, b; Wise, 2009). Wise (2009) noted that the inclusion of emissions and chemical transport changes are necessary to provide projections of air quality as without these values the results only show climate sensitivity. For example, Cheng *et al.* (2007a,b) included the impact of emissions by establishing a pollutant record for the period of 1981 – 2000. The study kept emissions at end of the century levels (the baseline period just mentioned) or scaled the baseline emissions by $\pm 20\%$, to account for future changes in emissions.

8.2.2.2 Dynamical Downscaling: GCM-CTM Studies

Beyond statistical downscaling, climate-chemistry studies often involve four different models: General Circulation Models (GCMs; resolution of a few hundreds of kilometers), global Chemical Transport Models (CTMs), Regional Climate Models (RCMs; resolution of a few tens of kilometres, simulating up to a single continent) and regional CTMs. Global CTMs are normally driven directly by meteorology from a given GCM, without any dynamical downscaling. In dynamical downscaling, global scale climate information at a coarse resolution is used to drive a higher resolution numerical model only run over a limited area. The limited area regional model receives boundary and initial conditions from the global model.

In many climate-chemistry studies, global-scale climate information from General Circulation Model (GCM) is used to drive a regional CTM, in either an on-line or off-line configuration. In an off-line configuration, the climate model is run first and the resulting meteorological fields are used to drive the regional CTM. There is no feedback between variables in the regional CTM and the climate fields. In the on-line configuration, a GCM and a global CTM are run simultaneously, exchanging information with each other, which may or may not include radiative feedback (Giorgi and Meleux, 2007). While on-line modelling systems have the advantage of feedback between the two models, they often include simplified chemistry and aerosol representations in order to make them computationally feasible. However, global atmospheric chemistry models constitute the best tools for making quantitative future projections of tropospheric composition, as they provide the best estimates of trace species (e.g. ozone and OH) distribution, oxidative capacity of the atmosphere and radiative forcings arising from changes in ozone and methane concentrations (Stevenson *et al.*, 2006). Global models can also capture important transport activities, such as intercontinental transport of emissions, which can have impacts on ground level ozone on the same order of emissions reductions (Fiore *et al.*, 2009). Global models allow the representation of the full climate-chemistry-aerosol system.

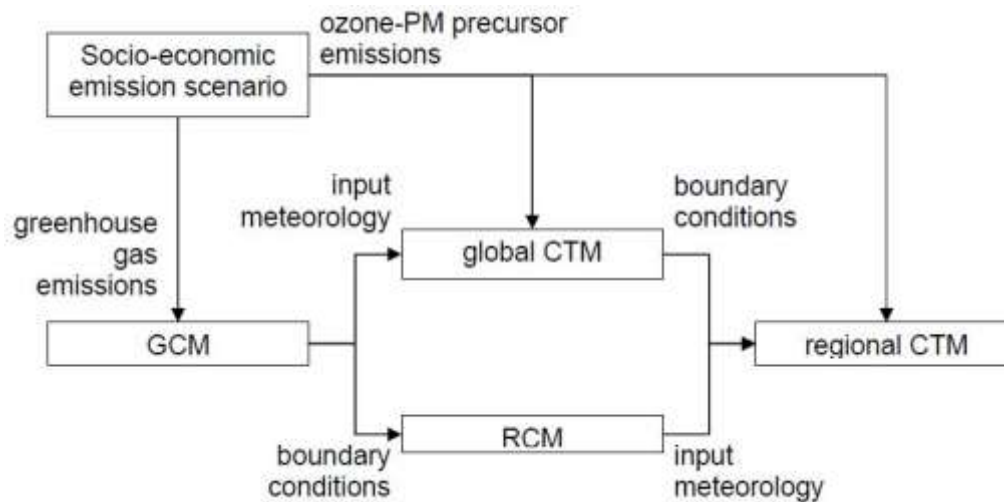


Figure 8.2 General off-line GCM-CTM set up for investigating the effect of climate change on air quality from Jacob and Winner (2009). GCM = general circulation model, RCM = regional climate model and CTM = chemical transport model.

Leung and Gustafson (2005) found that global climate and chemistry models do not have enough spatial resolution to resolve atmospheric, chemical, and surface processes used for assessing regional air quality. Resolving these processes necessitates dynamical downscaling from a GCM to a regional CTM. Off-line systems are chosen in the majority of studies as they retain the more complex representation of chemistry and aerosols required to address air quality issues (Giorgi and Meleux, 2007). Figure 8.2 shows a basic flowchart of how an off-line GCM-regional CTM modelling system is set up from Jacob and Winner (2009). The socio-economic emissions scenario dictates greenhouse gas emissions that are input into the GCM to project climate change over a desired time period. The socio-economic emissions scenario can also be used to estimate future anthropogenic and biogenic emissions at global and regional scales for input into the CTM. At global scales, the ozone and PM precursor emissions are input into a global CTM, along with input meteorology from the GCM run, to create boundary conditions for the regional CTM. At a regional scale, ozone and PM precursor emissions are input into the CTM directly. The GCM provides the boundary conditions for a regional climate model (RCM), providing finer resolution at a smaller scale of interest. The RCM corresponding output meteorology is input into the regional CTM to provide air quality projections. Studies often choose not to update emissions for future climate (beyond those fed into the GCM), isolating the impact of climate change alone. Other studies choose not to update the regional CTM boundary conditions for future climate, isolating impacts from climate change and regional emissions. Ideally, a GCM-regional CTM modelling system would include all the features shown in Figure 8.2. This retains information on a global scale through boundary conditions and input meteorology and allows for the finer resolution required to examine air quality on a regional scale. Leung and Gustafson (2005) found it is

important to include the complex interactions between emissions, atmospheric changes, and chemistry, in order to provide a comprehensive assessment of the influence of climate change on regional air quality.

Another important issue with climate chemistry studies is spatial and temporal scales. Studies often use a global scale GCM-CTM to look at air quality impacts on the regional scale. While this can provide some valuable information, Leung and Gustafson (2005) found that these models do not have enough spatial resolution to resolve atmospheric, chemical, and surface processes for assessing regional air quality. Racherla and Adams (2008) found that coarse resolution underestimates ozone in urban areas and overestimates it in background areas. Forkel and Knoche (2006) looked at near-surface ozone and found pronounced differences between coarse (60 km) and fine (20 km) resolutions for several regions due to smoothing of anthropogenic and biogenic emissions as well as flattened topography for the coarse resolution. The authors cautioned that regional interpretations of simulated changes in air quality due to changed regional climate must always be seen in the context of the grid resolution used for the simulations.

Accounting for interannual variability is essential to GCM-CTM studies. Racherla and Adams (2008) found it necessary to use five years or more of simulation data in order to separate the effects of future climate change and interannual variability on ozone episodes in the eastern United States. Leung and Gustafson (2005) used 10 year periods because interannual climate variations may obscure long term trends. Depending on the application of the study, it is not always necessary to simulate the full length of every year. Most studies look at the ozone season (June-July-August), or some portion within, over a number of simulation years, instead of simulating the full year.

Climate studies not only look at mean values of variables over long time scales, but at extreme values as well (when the values exceed a given threshold). For example, many studies will look at the mean value of summertime ozone concentrations and at the number of days these values exceed the national standard. In the case of GCM-CTM studies, it is a computational and technical challenge to include this much information in a study, especially when the ozone season is projected to lengthen with more pollution episodes in spring and fall (Chen *et al.*, 2009). Looking at only a portion of the ozone season or the ozone season over a small number of years may not provide the full impact of climate change on air quality.

Many modelling studies have demonstrated the impact of climate change on a global scale (Liao *et al.*, 2004; Mickley *et al.*, 2004a,b; Brasseur *et al.*, 2006; Stevenson *et al.*, 2006; Wu *et al.*, 2007), but it is also important to consider the impacts on a regional scale, as they are more complex, and spatially and temporally variant. The coarse resolution associated with global climate-chemistry simulations does not allow an accurate estimate of the effects of climate change on a regional scale (Forkel and Knoche, 2006). Many of the processes involved in the

formation of O₃ and PM depend on the regional distribution of their precursors, and O₃ and aerosols have relatively short atmospheric lifetimes (days to weeks) leading to spatially varying atmospheric distributions (Liao *et al.*, 2006).

For almost all studies, the socio-economic emission scenarios used for generating climate and emissions are those of the Intergovernmental Panel on Climate Change (IPCC), as outlined in the IPCC 4th Assessment Report (2007). As seen in Figure SPM.5 in IPCC AR4 (2007), there are much less significant differences over the first half of the century as the second half of the century. Depending on the time scale of interest (2050 vs. 2100), the socio-economic emission scenario chosen may not be as important. Avise *et al.* (2009) examined the impact of changes in future climate, anthropogenic U.S. emissions, background tropospheric composition and land use on summertime regional U.S. ozone and particulate matter. This study found changes in chemical boundary conditions have the largest impact on the average maximum daily 8-hour ozone concentration (md8hrO₃), followed by changes in anthropogenic emissions. Changes in land-use, combined with climate change, caused a decrease in average md8hrO₃ due to a reduction in biogenic ozone precursor emissions. Another source of uncertainty is the treatment of isoprene chemistry within the chosen chemical mechanism. There are fundamental uncertainties in the isoprene-O₃-NO_x chemistry (Racherla and Adams, 2008). Jacob and Winner (2009) provide an overview of isoprene and isoprene nitrate chemistry, along with their associated uncertainties. Particulate matter was most impacted by changes in anthropogenic emissions, with chemical boundary conditions having a negligible effect. Climate change alone decreased PM slightly. How boundary conditions, emissions (global and regional) and land-use are treated inside a modelling system varies between studies and is a source of uncertainty when comparing results.

8.2.2.3 Multi-model Ensemble Modelling

No single standard modelling methodology exists for representing many of the processes in the atmosphere, due to the large variety of mathematical and computational approaches available to simulate atmospheric transport and chemistry, leading to the use of different methodologies in different models. Multi-model ensemble modelling employs a group of models representing the same initial conditions, and examines the mean and range of outcomes produced. The Intergovernmental Panel on Climate Change (IPCC) uses multi-model ensemble modelling for regional climate projections in the 4th Assessment Report, involving approximately 20 GCMs (Christensen *et al.*, 2007). Since air quality modelling systems are developed independent of each other, the range of responses is hypothesized to be representative of the uncertainty in our knowledge about the physics and chemistry involved in air quality modelling, and the average between the model responses is the best prediction of the variable of interest (Cuvelier *et al.*, 2007). The net effect is a variation in projections resulting from similar initial conditions. Using many different models allows for identification of key areas of uncertainty and improves the robustness of results; the balance of evidence of many models is used to project future conditions (Stevenson *et al.*, 2006).

Déqué *et al.* (2007) performed an ensemble study for Europe involving ten regional climate models (RCM) to assess the factors that influence the extent of variation between future climate model projections. The uncertainty associated with the GCM (used to drive the local regional climate) was found to be larger than the uncertainty associated with the choice of the RCM itself, the scenario being represented, or the member of the ensemble chosen. In order to reduce the uncertainty involved with using several models, the authors suggested using a variety of GCMs, and at least as many GCMs as there are RCMs, in an ensemble study. To reduce the internal variability within a single model in an ensemble, the model may be started from slightly different boundary conditions and the spread in results assessed (Murphy *et al.*, 2004). Internal variability becomes more important at regional scales and when looking at extremes. Stevenson *et al.* (2006) found that the ensemble mean global tropospheric O₃ was not significantly impacted by individual model outliers and the use of an ensemble reduces the effects of specific parameterization choices on the resulting projections. Stevenson *et al.* (2006) also highlighted several areas of uncertainty in the models: deep tropical convection, including lightning NO_x production; isoprene emissions from vegetation and isoprene's degradation chemistry; stratosphere-troposphere exchange; biomass burning; and water vapour concentrations

8.2.3 Global and Regional Impacts

This section will summarize the global and regional impacts of ozone and particulate matter (PM) documented in the literature. These species are often quantified in similar terms to metrics used for air quality attainment. Ozone is often expressed as the mean daily maximum 8-hour ozone concentration (mdm8hO₃) and PM is expressed as the mean maximum 24-hour PM_{2.5} concentration (m24hPM). Exceedance days refer to the number of days with ozone or PM concentrations above the national standard. In Canada, the Canada Wide Standard (CWS) for ozone is an 8-hour average of 65 ppb (with achievement of the standard based on the 3 year average of the 4th highest annual value of this quantity). The Canada-wide standard for PM_{2.5} is a 24-hour average of 30 µg m⁻³ (with achievement of the standard based on the 3 year average of the annual 98th percentile of this quantity). In the U.S. the 2008 National Ambient Air Quality Standard (NAAQS) is 35 µg m⁻³ of PM_{2.5} in a 24 hour period and an 8-hour average of 75 ppb for ozone, with the same criteria for achievement of the standard as in Canada. The European air quality standard for maximum daily 8-hour average O₃ is 120 µg m⁻³ (~56 ppb) and 25 µg m⁻³ for annual average PM_{2.5}. For comparison, the annual NAAQS for PM_{2.5} is 15 µg m⁻³.

8.2.3.1 Ozone

The consensus among climate-change studies is that the globally averaged surface background O₃ concentration will decrease by approximately 10 % or ~3 ppb over the next century (2030 – 2100), in the absence of any increases in emissions (Brasseur *et al.*, 2006; Murazaki and Hess,

2006; Stevenson *et al.*, 2006). When expected increases in emissions are included, there is an overall increase in background ground-level O₃ of approximately 10 ppb by 2100 (Brasseur *et al.*, 2006). The global scale models thus suggest that the effects of expected changes in climate and emissions act against each other; the changes in climate reduce ground-level O₃, while the changes in emissions increase ground-level O₃.

Table 8.1 Future ozone projections for North America. Values given are for mean daily maximum 8-hour ozone and continental U.S. unless otherwise noted (table modified from Jacob and Winner, 2009).

Study	Method	Emission Scenario ^b	Model Scale	Region of Interest	Current Climate	Future Climate	Run Length	Study Period	Ozone Projections (change relative to current climate)
Cheng <i>et al.</i> , 2007b	SD ^a	A2, B2, IS92a	Regional	South-cent. Canada	1990	2050 2080	10 yrs	April - Sept	2.7 ppb 4.0 ppb
Wise, 2009	SD ^a	A2, B2	Regional	Southwestern U.S.	2001	2050 2100	50 yrs	Annual	2 to 7 ppb 8 to 15 ppb
Hogrefe <i>et al.</i> , 2004	DD	A2	Regional	Eastern U.S.	1990	2020 2050 2080	5 yrs	June - Aug	2.7 ppb 4.2 ppb 5.0 ppb
Liao <i>et al.</i> , 2006	DD	A2	Global	Global	2000	2100	5 yrs	July	Northeast: 4 to 8 ppb ^c
Murazaki and Hess, 2006	DD	A1	Global	U.S.	1990	2090	10 yrs	June - Aug	East: 2 to 5 ppb / West: insignificant Background: 0 to -2 ppb Continental: 0-6 ppb
Racherla and Adams, 2006, 2008	DD	A2	Global	Global	1990	2050	5yrs	June - Aug	East: 1 - 5 ppb ^c Continental: 5 ppb ^c
Kunkel <i>et al.</i> , 2007	DD	A1FI, B1	Regional	Northeastern U.S.	1990	2090	5 yrs	June - Aug	10 - 25% (A1FI) 0 - 10% (B1)
Tagaris <i>et al.</i> , 2007, 2008	DD	A1B	Regional	Continental U.S.	1990	2050	3 yrs	June - Aug	U.S.: -11to - 28% / Western Canada: -6% Eastern Canada: -8% / Northern Mexico: -4% Midwest US: -2.5 % Northeastern US: +2.8%
Lin <i>et al.</i> , 2008	DD	A1FI, B1	Global	U.S.	1990	2090	5 yrs	June - Aug	3 to 12 ppb (A1FI) 3 to 6 ppb (B1)
Nolte <i>et al.</i> , 2008	DD	A1B	Regional	U.S.	2000	2050	5 yrs	June - Aug	West: -1 to -8 ppb East: -8 to -15 ppb Texas, eastern U.S.: 1 to 8 ppb Midwest, northwestern U.S.: -1 to -3 ppb
Wu <i>et al.</i> , 2008a,b	DD	A1B	Global	U.S.	2000	2050	3 yrs	June - Aug	Midwest: 2 to 5 ppb / Northwest: 2 to 5 ppb Southeast: insignificant Background West: 2 to 5 ppb Background East: no change
Avise <i>et al.</i> , 2009	DD	A2	Regional	U.S.	2000	2050	10 yrs	July	Northeast: 4 ppb Southeastern U.S.: -6 ppb
Chen <i>et al.</i> ,	DD	A2	Regional	U.S.	1990	2050	10 yrs	Annual	9.6 ppb

Study	Method	Emission Scenario ^b	Model Scale	Region of Interest	Current Climate	Future Climate	Run Length	Study Period	Ozone Projections (change relative to current climate)
2009									
Liao <i>et al.</i> , 2009	DD	A1B	Regional	U.S.	2001	2050	1 yr	June - Aug	Continental U.S.: 1 ppb / West: negligible Northeast: negligible / Plains: 1.6 ppb Midwest: 1.2 ppb Southeast: 2.0 ppb

^a SD = statistical downscaling, DD = dynamical downscaling

^b Socio-economic scenarios from the IPCC Special Report on Emissions Scenarios (Nakicenovic *et al.*, 2000). IS92A is an older scenario with CO₂ increases comparable to the A1B scenario.

^c Mean surface ozone concentrations

Table 8.2 Future ozone projections for Europe and globally. Values given are for mean daily maximum 8-hour ozone unless otherwise noted.

Study	Method	Emission Scenario ^b	Model Scale	Region of Interest	Current Climate	Future Climate	Run Length	Study Period	Ozone Projection (change relative to current climate)
Demuzere and van Lipzig, 2010b	SD ^a	A1B, A2, B1	Regional	Netherlands (rural background)	2000	2050 2100 2050 2100	10 yrs	Annual June - Aug	1.4 to 3.3 ppbv* 3.1 to 5.6 ppbv* 2.8 to 6.4 ppbv* 6.8 to 14 ppbv*
Langner <i>et al.</i> , 2005	DD ^a	IS92A	Regional	Europe	2000	2060	10 yrs	April - Sept	South-central Europe 0 to 12% ^c Scandinavia 0 to -4% ^c
Brasseur <i>et al.</i> , 2006	DD	A2P	Global	Global	2000	2100	9 yrs	July January	12.6 ppb 10.5 ppb
Forkel and Knoche, 2006, 2007	DD	IS92A	Regional	Europe	1990	2030	10 yrs	June - Aug	Northern Italy: 10 ppb ^e Southern Germany: 5 to 7 ppb ^e Eastern France: 5 to 7 ppb ^e
Liao <i>et al.</i> , 2006	DD	A2	Global	Global	2000	2100	5 yrs	July	Central Europe: 2 to 6 ppb ^d
Stevenson <i>et al.</i> , 2006	DD	A2 ^e	Global ^f	Global	2000	2030	5 - 10 yrs	Annual	± 5 ppb ^g
Meleux <i>et al.</i> , 2007	DD	A2, B2	Regional	West-central Europe	1975	2085	30 yrs	June - Aug	10 to 18 ppb (A2) ^c 2 to 8 ppb (B2) ^c
Lin <i>et al.</i> , 2008	DD	A1FI, B1	Global	China	1990	2090	5 yrs	June - Aug	E. China: 3 to 12 ppb (A1FI) E. China: 1 to 5 ppb (B1)

^a SD = statistical downscaling, DD = dynamical downscaling

^b Socio-economic scenarios from the IPCC Special Report on Emissions Scenarios (Nakicenovic *et al.*, 2000). IS92A is an older scenario with CO₂ increases comparable to the A1B scenario.

^c Mean maximum daily ozone

^d Mean surface ozone concentration

^e see original reference for more information on other emission scenarios used.

^f Ensemble modelling study
^g Zonal mixing ratio
^{*} ppbv @ STP shown

Tables 8.1 and 8.2 respectively summarize the ozone projections from recent literature for a number of regions, time periods, emissions scenarios and conditions in North America as well as Europe and globally. Part of the variety in ozone projections can be attributed to whether or not changes in future anthropogenic emissions are accounted for, impacts of model resolution, boundary conditions and background ozone, chemical mechanism and interannual variability (Awise *et al.*, 2009; Racherla and Adams, 2008; Wu *et al.*, 2008b; Forkel and Knoche, 2007). The general consensus indicates that the eastern U.S. and parts of Europe will see an increase in the mdm8hO_3 . Areas with high pollution are expected to see increases in mdm8hO_3 , while rural areas are expected to see minimal impacts or decreases (Jacob and Winner, 2009).

Both increases and decreases in O_3 have been projected at the regional level, for different regions. This localized variability requires the use of increased resolution in regional models to allow for improved treatment of non-homogeneities in emission rates, land cover and dispersion (Cohan *et al.*, 2006). Regional projections are also affected by their boundary conditions (Awise *et al.*, 2009). Murazaki and Hess (2006) found that climate change results in a 0–2 ppbv decrease in background O_3 , but a 0 - 6 ppbv increase in O_3 produced within the United States. Wu *et al.* (2008) found that the uncertainty in the yield and fates of isoprene nitrates lead to a lack of consensus in modelling studies reporting on the south eastern U.S. The largest impacts of climate change are over the eastern United States in regions with the highest NO_x emissions.

Murazaki and Hess (2006) use well-known O_3 chemistry to explain the differing response between global background O_3 and regional urban O_3 to climate change. In the global case, one of the main meteorological effects of the increase in temperature is an increase in the amount of water vapour in the atmosphere. In clean environments (low nitrogen oxide concentrations), increases in water vapour due to climate change may result in decreases in the O_3 concentration ($\text{OH} + \text{O}_3$ and $\text{HO}_2 + \text{O}_3$ result in net ozone destruction). Conversely, in more polluted environments, ozone is produced by hydrocarbons and OH in the presence of NO_x ($\text{NO} + \text{NO}_2$). Further discussion of the impact of water vapour on ozone can be found in Jacob and Winner (2009).

On the global scale, a large portion of the atmosphere (close to the ground and above) is sufficiently far from urban locations so that the climate change-induced water vapour destruction of O_3 is the main effect of a future scenario. On the regional scale (noting that regional scale models usually focus on continental atmospheres with significant NO emissions sources), emissions increases associated with projections of future emissions and the NO chemistry described previously result in O_3 creation.

Regions experiencing high O₃ concentrations under the current climate can generally expect an increase of 1 to 6 ppbv in average daily maximum 8-hour O₃ concentration, with a large portion of this increase being attributed to changes in biogenic emissions (which tend to increase with increasing temperature until a threshold is reached; see Chapter 2) (Hogrefe *et al.*, 2004; Civerolo *et al.*, 2007; Forkel and Knoche, 2006; Murazaki and Hess, 2006; Steiner *et al.*, 2006; Bell *et al.*, 2007; Jacob and Winner, 2009). However, maximum O₃ level increases are not always spatially associated with maximum temperature and/or biogenic emission increases (Forkel and Knoche, 2006; Bell *et al.*, 2007), implying that the local conditions such as the emissions of other O₃ precursors also have a significant effect on local O₃ production. Bell *et al.* (2007) also found spatial variations in O₃ response. Cities currently experiencing elevated maximum 8-hour O₃ have the largest additional increases under future climate conditions. Projected increases in the extent of urbanization in the eastern United States may lead to increases in average daily maximum 8-hour O₃ concentration (Civerolo *et al.*, 2007). Small areas of O₃ level decreases were noticed just outside the urban center core, while O₃ increased in most counties outside of the metro area, largely due to the effects of projected increases in urbanization on local wind circulation and temperatures (Civerolo *et al.*, 2007).

Several studies present projections for ozone exceedance periods for future conditions (not included in Table 8.1). Cheng *et al.* (2007a,b) studied four weather stations in south-central Canada using statistical downscaling. Assuming emissions remain at the same level as at the end of the twentieth century, the number of exceedance days could increase by 50% in 2050 and 100% in 2080 from climate change alone. Demuzere and van Lipzig (2010a, b) applied statistical downscaling to a rural background area in the Netherlands. Their results found the number of exceedance days (maximum daily 8-hour ozone > 120 µg m⁻³ or 56 ppb) could increase by 4.3 – 12.3 days yr⁻¹ near 2050 and 7.1 – 21.1 days yr⁻¹ near 2090 during the summer season.

8.2.3.2 Particulate Matter

Table 8.3 Future air quality projections for particulate matter (PM). Values shown are mean 24-hour concentrations unless otherwise noted.

Study	Method	Emission Scenario ^b	Model Scale	Region of Interest	Current Climate	Future Climate	Averaging Period	Study Period	PM Projections
Wise, 2009	SD ^a	A2, B2	Regional	Southwestern U.S.	2001	2050 2100	50 yrs	Annual	-4 to -80 mg/m ³ -2 to -82 mg/m ³
Liao <i>et al.</i> , 2006	DD ^a	A2	Global	Global	2000	2100	5 yrs	Annual	Central Europe: 1 mg/m ³ (sulphate) 0.5 to 1 mg/m ³ (carbonaceous)
Racherla and Adams, 2006	DD	A2	Global	Global	2000	2100	5yrs	Annual	eastern U.S.: 1 mg/m ³ (sulphate)
Tagaris <i>et al.</i> , 2007, 2008	DD	A1B	Regional	U.S., Canada, Mexico	2000	2050	3 yrs	Annual	Continental U.S.: -9 to -32% Western Canada: -5% Eastern Canada: -11% Northern Mexico: -17%
Avisé <i>et al.</i> , 2009	DD	A2	Regional	U.S.	2000	2050	10 yrs	July	-1 mg/m ³

^a SD = statistical downscaling, DD = dynamical downscaling

^b Socio-economic scenarios from the IPCC Special Report on Emissions Scenarios (Nakicenovic *et al.*, 2000)

The direct and indirect effect of aerosols on radiative forcing is an active area of research, while the impact of future climate change on PM is an emerging area of study (recent literature highlighted in Table 8.3). Including the treatment of aerosols into a GCM-regional CTM system is computationally expensive and often left to global studies where resolution is coarse. Although PM_{2.5} is used as an air quality criteria index, most studies report increases in aerosol species components or aerosol burden. Generally an increase in sulphate and carbonaceous particulate matter is projected at mid-latitudes. Liao *et al.* (2006) found a significant increase in aerosol burden over the United States associated with the combined effects of future climate change and future emissions, while only a slight increase is associated with climate change alone. The authors recommended that future research focus on better treatment of emissions in models, especially the inclusion of changing land types and vegetation, and the creation of better aerosol feedback mechanisms to the driving GCM. Many studies link aerosol projections with future precipitation (Jacob and Winner, 2009). Racherla and Adams (2006) found that the particulate matter projections were highly dependent on the predicted regional precipitation changes, and values dependant on regional precipitation had a high degree of uncertainty associated with them. Much work remains to be done to gain a better understanding of the impact of future climate and emissions on particulate matter.

The circumstances favourable for particle formation coincide with those associated with an O₃ episode, and these circumstances are expected to increase with future climate change (Environment Canada, 2001). Synoptic patterns and winds impact the transport of precursor gases, with light winds allowing the precursor concentrations to build up. Temperature increase allows for more reactive chemistry and higher emissions of volatile organic hydrocarbons, while decreasing partitioning of semi-volatile gases into the aerosol phase. Climate-related modifications to precipitation and fog impact the wet deposition processes, and changes to vertical stability impacts mixing and dilution of emitted gases.

8.2.3.3 Policy and the Climate Penalty

Future climate may impact policy advice because of the increased demand for air conditioning with rising temperatures, increasing energy demands and associated emissions (Jacob and Winner, 2009); and changes in background ozone concentrations (Jacob and Winner, 2009). However, Liao *et al.* (2007) found that current climate emission control strategies should be applicable under future climate conditions, implying the dependence of ozone on emissions will likely not change under future climate conditions. Jacob and Winner (2009) highlight studies which find an increase in ozone sensitivity to NO_x emissions as temperature increases. In order to best advise policy, it is important to create regional projections for the area of interest, including the impacts of both climate change and changing emissions, boundary conditions (background ozone) and land-use.

Wu *et al.* (2008a) highlight another area of concern for policy makers called the “climate penalty”. The authors define the climate penalty as the additional emission controls necessary to meet a given ozone air quality target, beyond those required in the absence of climate change. Wu *et al.* (2008a) found that for the Midwest U.S. (area of greatest penalty), a 50% reduction in NO_x emissions is needed under future climate to achieve the same ozone air quality target as a 40% reduction under current climate. More stringent emissions controls are needed to maintain a given air quality target under future climate conditions, as climate change alone tends to increase surface ozone. It should be noted that some areas are found where the climate change penalty becomes a climate change benefit (western and south eastern U.S.) due to projected decreases of ozone with climate change in these areas. The decrease is linked to the large background ozone contribution in these regions (Wu *et al.*, 2008a).

8.2.4 Climate Change Air Quality in Canada: Emerging Science

Few studies currently exist that examine the future impact of climate change on air quality in Canada. Tagaris *et al.* (2008) and Cheng *et al.* (2007b) represent the only future projections and only cover southern Canada. While this is where the majority of Canadians live, the

impact of climate change on future air quality is an important issue for all Canadians. Therefore it is important to study the projected impacts of climate change and changing emissions on air quality across Canada and making this information available to all Canadians.

An ongoing Environment Canada project centres on coupling the Canadian Regional Climate model (Plummer *et al.*, 2006) with the AURAMS (A Unified Regional Air Quality Modelling System) regional air pollution model (see chapter 5 of this assessment and the references therein). The system will examine the impact of climate change and changing emissions on North America, with a special focus on Canada. This will provide multi-year, summertime simulations of air quality for both present day climate and future climate conditions, including assessment and analysis of the modelling results. The chosen CTM allows for the study of changes in ground level O₃ and size-resolved and chemically-resolved PM. The effect of climate change on air quality was found to be negative in this study: air pollution will deteriorate due to climate change. The changes were not uniform over the continent; in some localities conditions improved, while the average became worse. The impacts of climate change would be increases in human mortality, as well as the deposition of sulphur, nitrogen and ozone to ecosystems.

These effects were found to be considerably offset and often reversed with the use of the IPCC's Representative Concentration Pathway 6 (RCP 6) emission scenario under future climate conditions. An overall *improvement* to air quality compared to current conditions was found, with decreases in human mortality, and deposition of sulphur, and ozone to ecosystems. Nitrogen deposition, on the other hand, was projected to either increase or decrease depending on location, due to ammonia emissions increases included in RCP 6. The impact of changes to air pollution precursor emissions were found to be greater in magnitude than the effects of climate change alone.

The study thus suggests that:

6. Climate change will likely make air pollution and its effects worse in North America, compared to current conditions.
7. This effect may be counteracted and largely reversed through targeted emissions reductions such as those in RCP 6. The RCP 6 emissions would result in better air quality than is currently experienced over much of North America.

The study raises the possibility of co-benefits in emissions reduction strategies; that is, control programs that reduce emissions of both radiatively active gases and air pollution precursors would have benefits for both future air pollution and climate change. Decreases in precursor emissions would have the added benefit of an immediate reduction in the impacts of air pollution on human and ecosystem health.

8.2.5 Summary and Recommendations for Future Work

Recent modelling studies of the future climate impacts on air quality have shown that globally, in the absence of increases in emissions, the background concentration of O₃ is expected to decrease by 5 to 10%. The inclusion of projected increases in emissions results in an overall increase in global O₃ concentration. Regionally the responses are much more heterogeneous, but a general trend of O₃ increases by 1 to 5 ppbv from climate change alone is seen for the regions studied. Currently polluted areas are projected to deteriorate, especially for areas of projected urban growth. O₃ concentrations may increase as urban NO_x emissions are projected to increase in some areas. O₃ concentrations are also highly dependent on the role of biogenic emissions (especially isoprene), which are expected to increase with temperature, resulting in an increase in O₃.

A mixed response to climate change is expected for PM, although increases can be expected in some areas. While an increase in PM is hazardous to human and animal health and plant life, a decrease in PM, depending on the composition, can enhance the impacts of climate change directly (through scattering and absorption of solar radiation) and indirectly (through their role as cloud condensation nuclei) (Seinfeld and Pandis, 1998).

The future projection of air quality is still an emerging area of research within the atmospheric science community. The modelling systems are often complex and sensitive to many interacting initial conditions (emissions, boundary conditions, land-use, resolution and interannual variability for example). While much work has been done for some regions, such as the U.S., other regions lack projections. There is also a lack of consensus in the majority of projections available, primarily due to differences in the design of the modelling system and what factors are being accounted for scenario runs (future emissions, future boundary conditions, etc.).

In order to best advise policy, it is essential that systematic regional studies be performed at adequate resolution, accounting for both climate change and changing regional emissions. Ideally, an approach similar to that used by the IPCC for climate scenarios is recommended for climate/air quality studies: a multi-model ensemble using the same starting conditions being employed to produce data for a region of interest, for specified simulation periods. This would reduce the uncertainty associated with air quality projections and allow an estimation of its magnitude. Future work should be aimed at reducing uncertainty in the modelling systems (more ensembles and improved chemical mechanisms, for example) and providing additional information on size-resolved and chemically-speciated particulate matter.

8.3 Pollutant Transport in the Atmospheric Boundary Layer

David Flagg, Peter Taylor, Paul Makar, Craig Stroud

Pollutant transport in the lowest part of the atmosphere is governed largely by the local stability of the atmosphere, the characteristics of the land or sea surface and the large-scale (synoptic-scale) winds. This layer nearest to the surface, called the *atmospheric boundary layer* (ABL), is a highly dynamic part of the atmosphere, sensitive to forcing from local mesoscale circulations, diurnal fluctuations and surface properties. Its turbulent nature poses a challenge to our understanding of smog formation and dispersion. Field studies and modelling are necessary to better understand the relevant mechanisms and timescales for pollutant transport, and to validate empirical parameterizations and theories of fluid dynamics applied to the ABL.

Modelling the ABL is challenging. The ABL is sensitive to changes in the type of land cover, abrupt changes in the roughness of the surface and topography, and the smallest resolvable horizontal and vertical scales of the model. Some ABL features (its late-afternoon collapse, the vertical transfer of heat and momentum, and the development of the nocturnal boundary layer (NBL) remain difficult to simulate accurately. The choice of a simplified treatment (parameterization) of turbulence (e.g. Viana *et al.*, 2005; Mao *et al.*, 2006; Srinivas *et al.*, 2007; Fast, 2005; Pagowski *et al.*, 2006) can significantly affect predictions (e.g., ABL depth varying by up to 800 m (Mao *et al.* 2006)). The coastal and urban environments pose an especially difficult task for meteorological modellers. They are also frequently home to large human populations and pollutant emissions and hence have been the subject of considerable research in recent decades. Section 8.3 focuses on these two environments, including recent measurement campaigns, advances in modelling and how both can contribute to understanding pollutant transport in the ABL.

8.3.1 Coastal Environments

8.3.1.1 Summary

The atmospheric response to changes in roughness, temperature and elevation along the coastlines of major bodies of water partly depend on large-scale (synoptic-scale) surface wind-speed and direction. For *weak* large-scale winds, surface thermal property contrasts along coastlines can generate significant horizontal variability in the daytime vertical mixing of pollutants by turbulence. Sufficiently strong thermal contrasts will often give rise to a local thermal circulation. In the warmer months, during the daytime under relatively calm conditions, this circulation consists of buoyant, warm air rising over the land, replaced by

cooler air from over the water moving inland (a *sea-breeze* or *lake-breeze*). Convection over the land and subsidence over the water usually returns the air to the water. The depth of the sea-breeze/lake-breeze circulation may extend several hundred meters. At night the circulation often reverses, as the greater capacity of the water to store daytime heat compared to the land results in relatively warmer air rising over the water, and cooler air subsiding over land. This circulation is frequently referred to as a *land-breeze*. In other seasons, the development of such circulations will largely depend on the strength of the local thermal contrast at the coastline. In contrast, if the large-scale wind is sufficiently *strong*, an on-shore flow can create an internal boundary layer (IBL) caused by the local thermal and roughness contrasts between the water and adjacent land surface, called a thermal internal boundary layer (TIBL). Strong winds producing off-shore flow will limit the interaction of the marine air with that over land.

With the passage of a sea-breeze or lake-breeze across the coastline comes an accompanying locally sharp transition in air mass properties such as temperature and humidity (a *sea-breeze front* (SBF) or *lake-breeze front* (LBF)). The SBF/LBF can have a locally significant impact on the concentration, interaction and transport of airborne pollutants in the lower atmosphere. In cases of stronger, on-shore large-scale wind flow, precluding SBF/LBF development, the dispersion of pollutants near coastlines can be subject to the slope of the TIBL. Thus, the dispersion of pollutants along coastlines is subject to considerable change based on the ambient large-scale wind speed and direction and thermal and roughness contrasts. Moreover, modern coastlines are often highly populated (e.g. the southern Great Lakes region) and act as sources of various pollutants and precursors: large-scale winds change in speed and direction on a daily basis, blowing on-shore and off-shore in the vicinity of major urban populations and industrial emission sources. Thus, coastlines represent a uniquely challenging environment for understanding the transport of pollutants in the atmospheric boundary layer (ABL) in Canada.

8.3.1.2 Recent Observational Studies

The Nanticoke Shoreline Diffusion Experiment of 1978 (NSDE78) is an early example of extensive observational work of pollutant dispersion at coastal environments in Canada (Portelli, 1982; Kerman *et al.*, 1982; Hoff *et al.*, 1982; Anlauf *et al.*, 1982). NSDE78 observed the diffusion of plumes from 200m tall stacks at a major coal-fired plant on Lake Erie in late spring of 1978. NSDE78 evaluated the structure of the thermal internal boundary layer (TIBL) resulting from the warming of colder, on-shore flow from Lake Erie. Results demonstrated two common types of dispersion: rotating fumigation during lake-breeze flows and fixed fumigation during steady, on-shore flows. In both cases, the fumigation persisted throughout the afternoon beginning seven to 20 kilometres inland of the plant. NSDE78 provided a formidable fundamental resource for understanding plume dispersion in the presence of a lake-breeze and crucial ground work for later studies on the Pacific coast and in the Great Lakes region.

In contrast to terrestrial boundary layers, the marine boundary layer shows little sensitivity to the day-to-day change in solar energy since the water surface is more uniform and shows relatively little variation in heat emission (Garratt, 1992). It is also generally not well mixed (Garratt, 1992). During warmer months, the passage of the relatively colder air of the SBF/LBF or steady on-shore flow creates a local temperature inversion. In the case of strong off-shore flow, layers of high concentrations of pollutants may form over the water due to the greater static stability. These layers may become so distinct from each other that they may be transported in different directions, as was observed over the North Atlantic Ocean during the ICARTT study (Angevine *et al.*, 2006a).

The depth of the ABL has substantial influence on ambient pollutant concentrations. On days with a well-mixed layer (see section 2.5 in Chapter 2), the rising and falling thermal plumes and other turbulent motions disperse pollutants, reducing local concentrations. Processes causing a reduction in ABL depth therefore limit vertical mixing. Such a reduction in “mixing height” may take place along and several kilometres inland of the coastline, by the SBF/LBF or through the creation of a TIBL during strong on-shore flow (Yuan *et al.*, 2006). The effect of ABL depth reduction is particularly strong when the large-scale wind patterns associated are opposite in direction to the local SBF/LBF circulation (such as might occur along the western shore of Lake Ontario during the warmer months). In this case, the SBF/LBF may ‘stall,’ with the air stagnating over the coastal cities, resulting in high concentrations of pollutants. These effects have been observed over the Greater Houston Area (Banta *et al.*, 2005). The 2006 Texas Air Quality Study (TexAQS 2006) found higher variability of ozone deposition velocity over land (within eight kilometres of the coastline) as compared to over water (Grachev *et al.*, 2009). In another study, where halocarbons were used to track the SBF, elevated concentrations were found to correspond to stagnant conditions and a dominant land-breeze (Lee and Chiou, 2007).

The impact of sea-breezes on ABL heights over the land was observed in Canada during the Pacific 2001 study (Strawbridge and Snyder, 2004). The ABL height in the Lower Fraser Valley was found to be above two kilometres when sea-breeze was weak or absent, but only 300 to 900 m above ground level when sea-breezes were strong and the large scale flow was weak. Brook *et al.* (2004) found that the convergence of flows from the Strait of Georgia and Strait of Juan de Fuca coupled with the ‘wake’ effect induced by Vancouver, Gulf and San Juan Islands produce a recirculation pattern: a significant factor in the photochemical processing and distribution of pollutants during the PACIFIC 2001 study.

Similar effects occur in the Great Lakes. Hastie *et al.* (1999) noted that the arrival of a Lake Ontario lake-breeze coincided with an increase in O₃ mixing ratio of 30 ppbv. More recently, a joint study by Environment Canada, the Ontario Ministry of the Environment and several Canadian universities in the summer of 2007 (Border Air Quality and Meteorology Study – BAQS-Met) collected chemical measurements and meteorological observations to examine the effects of lake-breeze circulations and large-scale transport on local air quality in south

western Ontario (Makar *et al.*, 2008; Sills *et al.*, 2008). Analysis is on-going, but the intensive observation period included episodes of LBF flow fumigating local emissions and varying contributions from long-range sources. Arain *et al.* (2009) shows how on-shore flow reduces NO₂ concentrations in the Toronto-Hamilton region, with strong seasonal variation.

8.3.1.3 Recent Modelling Studies

Coastal ABL modelling often focuses on understanding the evolution and motion of the SBF/LBF and TIBL, due to their observed ability to create significant spatial discontinuities of ambient temperature, moisture, stability and wind flow, consequently affecting pollutant transport. The forecasting models of these processes can also be used to diagnose the relative importance of different meteorological processes towards SBF formation and interactions with pollution. Studies seeking to replicate the real coastal atmosphere will often couple or integrate models of air chemistry with a mesoscale numerical weather prediction (NWP) model. Such coupled models have been found to be reliable in reproducing the SBF/LBF (Harris and Kotamarthi, 2005; Angevine *et al.*, 2006b).

High coastal PM concentrations were shown to be related to the speed and direction of the SBF and a stable ABL along the Mediterranean Sea (Viana *et al.*, 2005). The passage of a second front in the afternoon can reduce PM concentrations. The night-time land-breeze, when associated with regions of high topography (Mediterranean coast, Australian coast), can result in significant accumulations of PM along the coastline (Viana *et al.*, 2005; Hess *et al.*, 2004; Cope *et al.*, 2005; Lo *et al.*, 2007). In line with observations, a model of an advancing SBF showed that the cooler air moving over land restricts the growth of the boundary layer to heights of less than 150 m and distances inland up to 5km, once the front has passed (Yuan *et al.*, 2006).

Studies in coastal Australia suggest that an accurate prediction of sea-breezes is essential in O₃ forecasting. Peak hourly O₃ underestimates and regional-scale O₃ overestimates were found to be related to errors in the forecasted wind fields and/or down-slope winds from coastal topography, boundary layer height, associated vertical mixing, and in the interaction between the SBF and larger scale wind field (Hess *et al.*, 2004; Cope *et al.*, 2005; Lo *et al.*, 2007). In contrast, the chemical transport model components unrelated to the flow field (such as the emissions) were found to have a much smaller effect on O₃ forecast accuracy.

Venkatram *et al.* (2008) examined a tracer release from a low-level and elevated release height (~ 64 m AGL) at the coastline. Their meteorological model did not adequately resolve the growth of the TIBL inland from the coastline, resulting in relatively poor performance for tracer dispersion from the elevated site. The meteorology estimated from a two-dimensional TIBL model and one-dimensional surface energy balance model provided superior tracer concentration estimates.

Kitada *et al.* (2008) employed a chemical transport model coupled with MM5 (Grell *et al.*, 1994) to model pollutant transport in the ABL over Jakarta, Indonesia. Simulations showed a nocturnal land-breeze transporting O₃ precursors to the Java Sea, consequent O₃ production in the morning hours, and subsequent on-shore transport in the early afternoon via the SBF. The model revealed that subsidence over water due to the circulation increased the background O₃ concentration by about 10 ppb, for a depth extending up to about 400-500 m above ground. Angevine *et al.* (2009), examined the Houston area using the WRF model (Skamarock *et al.*, 2007) at five kilometre resolution, and suggested that finer resolution would improve accuracy in modelling mountainous coastal areas or given cold water where thermal contrasts are particularly strong.

8.3.2 Urban Environments

8.3.2.1 Summary

As noted in section 2.5 of Chapter 2, the ABL may be subdivided into (from top to ground) an *Ekman or outer layer* (upper 90%, largely shielded from surface influences except for strong convection) and a *surface or inner layer* (lower 10%). The latter is in turn subdivided into *inertial sublayer* where the vertical transport of heat and momentum is considered constant, and (below) a *roughness sublayer* (RSL) that is particularly susceptible to change in surface conditions. In the urban boundary layer (UBL), the RSL further bifurcates into a shear layer overlying a canyon layer, divided by the mean canyon height (see Figure 2.10). The canyon layer (aka “street canyon”) describes the void of space above street level between buildings. Modelling of pollutant transport in the canyon layer is of particular societal relevance for its immediate impact on humans. Ventilation (vertical mixing and exchange) of pollutants from the street canyons to the shear layer and the overlying inertial sublayer, however, is also of great importance to understanding pollutant transport in the ABL. Advection of pollutants in the upper parts of the UBL is of interest at the regional scale.

The UBL poses a formidable challenge to both observation and modelling: structures create drag on the movement of air through the urban environment, generate turbulent wakes, affect the transfer of short and long-wave radiation, and can contribute an anthropogenic heat source, all of which may contribute to turbulent transport of heat and momentum. The urban heat island (see section 2.5 of Chapter 2) can reduce static stability over the UBL. Spatial variations in building height, width, density and orientation can cause vast discrepancies of pollutant concentration over relatively short horizontal or vertical distances by way of intermittent ‘sweeps’ and ‘ejections’ from the urban canopy. These effects suggest that a thorough assessment of pollutant concentration and dispersion in any urban environment requires a substantial and systematic field campaign, along with detailed modelling, as described below.

8.3.2.2 Modelling Strategies

Any model of the atmosphere above an urban area must contend with a complex surface boundary condition, hence is less amenable to broad-surface approaches of using a common “look-up table” of thermal and physical characteristics (albedo, thermal conductivity, surface emissivity, etc.). Researchers interested in ‘idealized’ modelling at smaller scales, such as a street canyon, intersection or uniform array of structures, can avoid this complexity. Coupled with traditional, idealized one and two-dimensional representations, a variety of three-dimensional modelling techniques are now available for the simulating the UBL. Below is a broad description of the more fundamental approaches with some references to recent and on-going work.

For large environments of complex fluid flows like the atmosphere within urban areas, researchers will often invoke numerical methods to discretize and solve these continuous flows. This approach is broadly labelled computational fluid dynamics (CFD). For more theoretical interests in the UBL, such as examining the behaviour of a single street canyon, researchers can use direct numerical simulation (DNS, Coceal *et al.*, 2006) to explicitly solve the equations describing three-dimensional momentum in the atmosphere and resolve all spatial and temporal scales of turbulence. This method is highly computationally expensive. However, DNS can be useful in providing a sub-grid scale turbulence model for evaluating less intensive strategies such as models of Reynolds-averaged Navier-Stokes (RANS) equations or large-eddy simulation (LES). RANS (Kim *et al.*, 2009; Yang and Li, 2009; Michioka and Sato, 2009; Liu *et al.*, 2009) methods employ a time-averaged version of the 3D momentum equations, splitting variables into constant and time-varying components. The LES approach (Li *et al.*, 2009; Ishida *et al.*, 2009; Michioka and Sato, 2009; Nakayama *et al.*, 2009) explicitly solves large-scale turbulent motions (eddies) in the atmosphere and parameterizes those at smaller scales. RANS describes the time evolution of turbulence, while the LES model estimates describe the turbulence at a given instant in time, the latter being more computationally intensive.

Many researchers opt to more fully replicate the real atmosphere on larger scales, using a numerical weather prediction (NWP) model. Most real urban surfaces are quite heterogeneous at scales smaller than those resolvable in NWP models, generally precluding methods such as described above and requiring parameterization. The incorporation of an urban environment into the NWP lower boundary condition can follow one of many techniques. One common method is through a coupled land-surface model (LSM) that treats the urban area analogously to vegetated surfaces with certain improvements and parameterizations. The LSM may represent the urban environment as a flat surface (‘tile’ or ‘slab’ approach; Khiem *et al.*, 2009; Angevine *et al.*, 2009), a canopy of one or more layers (Tewari *et al.*, 2009) or a combination of strategies (Chen *et al.*, 2009). Another approach is to couple a CFD model with an NWP model (Wyszogrodzki *et al.*, 2009; Hogue *et al.*, 2009), with the urban environment representation benefiting from the updated meteorology. The coupled NWP approach is

popular for retrospective and real-time simulation of real-data cases over real urban areas. Overall, the selection of any one particular approach (DNS, RANS, LES, NWP) for modelling the UBL typically involves a delicate compromise of the available computing resources, desired precision, and horizontal scale of interest.

8.3.2.3 Recent Observational Studies

Dynamics

The observations of the UBL and pollutant transport therein from the past decade derive from extensive field campaigns of meteorology and chemistry in the roughness sublayer (RSL) as well as weather stations, towers, soundings and remote sensing measurements. Most major campaigns in the last decade have focused on cities of varying sizes in Europe and North America. Some sites were selected to create urgently needed sets of verification data against which to test future model simulations and parameterizations. Others were selected for specific interest in susceptibility to pollutant or toxin dispersion, often in the interest of security, though these studies also often provide valuable test data. Roth (2000) and Arnfield (2003) both provide an extensive literature review of turbulence in the urban environment.

The recent, major European studies of the UBL include the *Basel Urban Boundary Layer Experiment* (BUBBLE; Rotach *et al.*, 2005), the *Expérience sur Sites pour Contraindre les Modèles de Pollution Atmosphérique et de Transport d'Emission* (ESCOMPTE; Mestayer *et al.* 2005), the *Canopy and Aerosol Particles Interactions in TOulouse Urban Layer* experiment (CAPITOU; Masson *et al.*, 2008) and the *Dispersion of Air Pollution and Penetration into the Local Environment* (DAPPLE) project (Robins *et al.*, 2008). BUBBLE and ESCOMPTE included extensive measurements within street canyons and over the urban environment using in-situ and remote sensing observations coupled with tracer releases. Whereas BUBBLE focused principally on the meteorology of the urban core of a small city (Basel, Switzerland), ESCOMPTE concentrated on the chemistry at the regional scale of a larger city (Marseille, France). Salmond *et al.* (2005) detected coherent structures of CO₂ and heat flux ventilated from street-level sources using the ESCOMPTE data. The authors emphasize the importance of turbulent transport within and above the canopy in models of pollutant dispersion in the UBL. CAPITOU examines the effect of the city (Toulouse, France) on UBL flow and the energy balance, throughout an annual cycle, in addition to study of urban aerosol mixing, aging, transport and radiative impact. Calvo *et al.* (2008) and Gomes *et al.* (2008) show substantial UBL heating and depth increases from increased black carbon concentration using the CAPITOU data. DAPPLE examines the dynamics within and ventilation from a street canyon intersection in central London (U.K.) through extensive in-situ meteorology and chemistry measurement and tracer releases. Early results indicate significant influence of street canyon vortices on pollutant accumulation on the windward and leeward sides of the canyon (Robins *et al.*, 2008).

Rotach *et al.* (2005) shows upward transport of turbulent eddies varying with height in the canyon and shear layers of the UBL, further confirmed by Fisher *et al.* (2006) and Christen (2005). This observation conflicts with an assumption of the commonly applied Monin-Obukhov similarity theory (MOST) used to describe ABL turbulence (Monin and Obukhov, 1954). The theory was devised for relatively uniform landscapes (e.g. flat terrain with relatively uniform “roughness elements” such as trees) and presumes constant flux with height in the surface (inner) layer. A second assumption of MOST is the logarithmic profile of wind with height. However, canyon layer observations show a distinctly different shape of the wind profiles, more closely aligned with an exponential shape (Macdonald, 2000), though some recent studies question this representation (Barlow and Coceal, 2009). Hanna *et al.* (2007) finds canyon scalar wind speed to be approximately 1/3 of that at the top of the building from the *Madison Square Garden* (MSG05) field experiment. Thus, although the turbulence spectra and statistics over cities share many similarities to that over vegetation canopies (Roth, 2000; Christen, 2005), MOST is best applied to the inertial layer and above. A universal theoretical framework of urban turbulence remains as an outstanding challenge in the research community (Barlow and Coceal, 2009).

Turbulent motion in the RSL and inertial sublayer of the UBL is three-dimensional. If the buildings are particularly variable in height, this may enhance the RSL depth (Cheng and Castro, 2002) and preclude the development of an inertial sublayer altogether (Barlow and Coceal, 2009). Winds in the vicinity of the canyon rooftop and the static stability appear to have greater impact on the canyon layer turbulence than do winds in the inertial sublayer and above (Allwine *et al.*, 2004; Klein and Clark, 2007). Wind direction with respect to the street orientation can affect the dynamics within the canyon (Allwine *et al.*, 2004; Calhoun *et al.*, 2007). Winds parallel or nearly parallel to the orientation of the street will ‘channel’ canyon air downstream. When the wind is more perpendicular, a local circulation (*canyon vortex*) will develop with sinking motion on the (windward) side of the canyon intersecting the wind and rising motion on the opposite (leeward) side. It is clear that both photochemistry and pollutant dispersion in an urban environment are subject to the local geometry and winds (Klein *et al.* 2007).

Among North American field campaigns, both the Joint Urban 2003 (JU2003) study (Allwine *et al.*, 2004) at Oklahoma City (U.S.A) and Urban 2000 (Allwine *et al.*, 2002) at Salt Lake City (U.S.A.) had as their primary interest the understanding of dispersion of toxic agents from an urban source, along with studying urban dynamics and the surface energy balance for verification of CFD and NWP models. This data was used to suggest that urban turbulent heat fluxes were reduced with increasing upwind stability (Ramamurthy *et al.*, 2007) – a similar effect would be expected to hold for concentrations of pollutants. In addition to remote sensing and in-situ meteorological instrumentation, both JU2003 and Urban 2000 used sulphur hexafluoride releases to observe the dispersion into, out of, and around buildings in the urban core and downwind several kilometres from the points of release, providing valuable model verification datasets (Hanna *et al.*, 2003).

In Canada, the *Environmental Prediction of Canadian Cities* (EPiCC) project involving the ongoing collaborative efforts of multiple universities and Environment Canada seeks to customize the coupled *Town Energy Balance* (TEB) model (Masson, 2000) and *Interactions Soil-Biosphere-Atmosphere* (ISBA) model (Noilhan and Planton, 1989) for Canadian climates, in order to improve forecasts of air quality and meteorology in Canadian cities (Voogt *et al.*, 2009). The study includes both modelling and measurements of radiation, energy balance, CO₂ concentrations and fluxes at sites in Montreal and Vancouver including measurements at outlying rural sites. Observation methods include meteorological mesonets, ceilometers, stationary towers and, at Montreal, a UHF wind profiler, RASS and Doppler radar. Elsewhere, assimilation of wind profiler data into NWP models has shown to produce noticeable improvement in wind direction simulation (Angevine *et al.*, 2009). EPiCC also employs additional remote sensing techniques, such as airborne lidar, to parameterize the vertical and horizontal structure of urban environments and improvements to the land use scheme for modelling. Using EPiCC data, Crawford *et al.* (2009) examined carbon dioxide fluxes above low-density residential neighbourhoods in Vancouver to understand the effects of source area characteristics, urban vegetation, soil, water use and traffic patterns. Other recent studies in Canada also combined in-situ and remote sensing measurements of O₃, PM_{2.5}, CO and O₃ precursors at Ottawa (Urquizo *et al.*, 2009).

Energy Balance

The energy balance at the urban surface is also a notable challenge pertinent to the development of the urban heat island and flow in the UBL. In addition to the sensible, latent and ground heat fluxes, the daytime heat uptake (storage) by buildings is typically ‘released’ at night, increasing the air temperature in the urban core and contributing to the urban heat island. In addition, vehicles, humans, ventilation and air conditioner units and other anthropogenic sources can contribute to heating of the UBL. Anthropogenic heat flux introduces a unique component to the surface energy budget of an urban area. There is no standard for measurement or quantification of anthropogenic heat, its magnitude or spatial distribution, which creates subjectivity with regard to its inclusion in the surface heat balance and models (Sailor, 2009). Understanding the urban energy balance is critical to canyon air temperature and turbulence structure.

Recent studies provide estimates of this flux for various cities across different seasons from a variety of approaches. The seasonal difference derives in part from variation in building illumination from the sun (Kanda *et al.*, 2005). Sailor and Lu (2004), using data widely available for U.S. cities, applied an inventory approach with diurnal distribution to estimate flux values up to 70-75 W m⁻² in winter and up to 30 W m⁻² in summer in major U.S. cities such as Chicago, Philadelphia and San Francisco (Fan and Sailor, 2005). Pigeon *et al.* (2007) and Offerle *et al.* (2005) provide comparable magnitude and seasonal variation for European cities. Measurements at various cities indicate upward heat flux throughout the night (Piringer and Joffre, 2005; Piringer *et al.*, 2007). This release of stored and anthropogenic heat along

with the shear generated near the canyon rooftops can enhance the depth of the UBL versus that seen over adjacent rural areas (Piringer *et al.*, 2007; Liu *et al.*, 2007a; Angevine *et al.*, 2003).

Of particular interest to Canadian cities is the role of snow in the surface energy balance. The EPiCC project includes substantial study on urban heat storage and anthropogenic heat in Montréal, including the *Montréal Urban Snow Experiment* (MUSE; Lemonsu *et al.*, 2008). Four weeks of radiation, temperature, humidity and turbulent flux observation in early 2005 demonstrate that the residual heat flux from the net radiation, sensible and latent heat flux account for more than 50 percent of the total, implying a significant contribution from heat storage and anthropogenic heat flux. MUSE found that snow played a significant role in the partitioning and daily pattern of the surface energy fluxes. The presence of snow melt contributed to the residual term and latent heat flux (Lemonsu *et al.*, 2008). Leroyer *et al.* (2009) further investigated the effect of the snow melting process. Results attributed some model deficiencies to the simulation of the latent heat flux during the freeze-thaw processes.

8.3.2.4 Recent Modelling Studies

Researchers have a vast array of tools available to model the urban boundary layer (UBL: see section 8.3.2.2). Today, substantial work remains on-going in both real and idealized studies of the UBL. Some studies seek to verify fundamental relationships, sensitivities, profiles and characteristics while others attempt to replicate the real environment, often comparing results against the field studies outlined in section 8.3.2.3. As discussed earlier, there are major outstanding research questions in UBL dynamics and the energy balance. Both will affect a model's capability to accurately model pollutant transport in the UBL.

Dynamics

Recent studies modelling motion and pollutant transport in urban environments extend in scales ranging from individual street canyons and single test sites to whole cities and metropolitan regions. Typically, these approaches do not include a thorough treatment of chemistry. For better chemistry representation, modellers may choose to couple a chemical transport model (CTM) with a CFD or other meteorological model. Modelling can also follow a more physical approach, building scale models of real or idealized urban surfaces and applying a controlled air flow to simulate dynamics and the advection and diffusion of scalar quantities. These “wind tunnel” experiments are often used to help validate or justify the results of a CFD or NWP model.

Among CFD studies, Michioka and Sato (2009) indicate that both a RANS and LES model of the urban environment represent the mean flow well, but the latter provides superior estimates of pollutant concentration due to RANS errors in turbulent scalar flux. Bezpalcová *et al.* (2009) found that dispersion through the idealized UBL is controlled by layout of buildings

near the source, which also governs the plume shape. Building density does not appear to significantly change the large-scale dispersion of pollutants, echoing a result of MacDonald *et al.* (1997). Locally, higher building density and variable building heights appear to enhance the turbulent transport and vertical ventilation, compensated by a suppression of horizontal ventilation (Nakayama *et al.* 2009). Li *et al.* (2009) indicated that decreasing stability facilitates canyon ventilation, caused by increased upward flux from the warmer canyon surface. Departing from the idealized nature of many CFD studies, the Canadian Urban Flow and Dispersion Model (CUDM; Hogue *et al.*, 2009) creates an operational system that can be applied to a real urban area in response to an emergency dispersion situation on micro to 2km scales.

Many studies of urban dynamics elect to focus on the role of a particular characteristic of the urban canyon, such as the aspect ratio (building height versus street width). Yang and Shao (2006) and Huq *et al.* (2007) found the aspect ratio to be inversely proportional to turbulent transfer and ventilation in the UBL; tall, narrowly spaced buildings inhibit vertical transport of pollutants and vice versa. Martilli (2002) found similar results in the daytime, due to reduced ground-level wind speed, but reduced concentrations and temperature inversion strength at night. Solazzo and Britter (2007) concluded that when the aspect ratio is sufficiently high, two counter-rotating vortices (one approximately atop the other) will tend to develop (also seen in Liu *et al.*, 2009). Liu *et al.* (2009) found differences in circulation strength, resulting in locally elevated pollutant concentrations.

Observations suggest that the top of the urban canopy is a site for the production of substantial turbulence. Dupont *et al.* (2004) found that a drag force representation of the urban surface fit observations better than a slab model, but noted that the predicted turbulence below the building height was still lower than observed. Harman and Finnigan (2007) found that extra turbulent mixing from the canopy top serves to greatly influence the mean profile in stable conditions. Traditional approaches account for the drag on the atmosphere through a roughness length enhancement in similarity theory equations. More recent studies include the explicit drag force terms in the equations of motion (Dupont *et al.*, 2004; Coceal and Belcher, 2005) or as a component of turbulent kinetic energy (TKE) dissipation (Maruyama, 1999).

Beyond dynamics within the urban canopy, modellers are interested in simulating pollutant dispersion at the regional scale. Urbanized mesoscale NWP models are a useful tool for this purpose. Lemonsu and Masson (2002) showed a neutral to slightly unstable stratification at night over the city (Paris, France), with a more stable stratification over adjacent rural areas. The model results confirmed observations of an enhanced well-mixed ABL depth over the city (Piringer *et al.*, 2007; Liu *et al.*, 2007a; Angevine *et al.*, 2003), together with elevated vertical velocities that produce a clear mesoscale (urban heat island) circulation extending 50 km outward from the center of the city under relatively calm large-scale ambient winds. The authors note the potentially significant implications of this circulation on pollutant dispersion, given that enhanced dispersion can drastically reduce local pollutant concentrations. There is

also considerable on-going work with urban applications of the WRF model (Skamarock *et al.*, 2007; Chen *et al.*, 2009). Tewari *et al.* (2009) applied WRF with a single layer canopy model and the National Urban Database and Access Portal Tools (NUDAPT) dataset (Ching *et al.*, 2009) to a study over the Houston region (Texas, U.S.A.).

Many recent efforts entail the coupling of a numerical weather prediction (NWP) model with a chemical transport model and/or computational fluid dynamics (CFD) model to track more complicated chemistry (Trini Castelli *et al.*, 2008; San Jose *et al.*, 2008; Peckham *et al.*, 2009; Chemel *et al.*, 2008). The latter study presented the added complication of modelling an urban area within varying topography (Grenoble, France), subject to frequent air stagnation in winter due to persistent temperature inversions and weak vertical mixing. This study can prove a useful proxy for urban pollution studies in the Canadian Rockies. Using data from the PrAIRie2005 field campaign, Makar *et al.* (2008) suggest a contribution of such mountain-induced flows to pollutant transport near Edmonton. The authors address the extent to which local versus long-range emissions contribute to air quality in Edmonton, analogous to the objectives of Kerschbaumer *et al.* (2008) for Berlin (Germany), using Environment Canada's *Unified Regional Air quality Modelling System* (AURAMS; Makar *et al.*, 2004) forced by the *Global Environmental Multiscale* model (GEM; Cote *et al.*, 1998). Results from four days in August of 2005 show a complex interaction, with long-range transport contributing heavily at the start and local sources toward the end. The boundary layer height estimates (verified against LIDAR measurements) appear particularly sensitive to the presence of an urban heat island in Edmonton.

There are also long-term applications for UBL modelling and pollutant transport. Civerolo *et al.* (2007) speculated on the meteorological consequences of increased 'urbanization' (conversion of "open space" to urban land cover) in the New York City (U.S.A.) area, as stipulated by one scenario of the Intergovernmental Panel on Climate Change (IPCC). The results predicted slightly warmer and drier conditions, with a small increase in ABL depth and increased average (+1-5 ppb) and maximum O₃ (> +6 ppb) episodic concentrations, subject to variability due to coastal interaction.

Energy Balance

Modelling the urban energy balance requires attention to particular challenges from the heat storage and anthropogenic heat flux terms, as well as changes to sensible, latent and ground heat flux. A major model inter-comparison project now underway involves the staged application of increasingly complex detail of the urban surface to many urban surface models to evaluate model approach and complexity performance (Grimmond *et al.*, 2009). The performance of individual parameterizations varies greatly. There is also broad model deficiency in latent heat flux, though simple models tend to perform best. The performance of individual parameterizations varies greatly. Most models show improved simulation with increasing detail of the environment and particular sensitivity to vegetation. The EPiCC goals

of improved simulation of latent heat flux in the UBL, in part through modelling the role of snow cover in the energy budget (Belair *et al.*, 2009) contribute towards the needs of the urban modelling community and Canadian cities.

An increasingly common trend in urban energy budget parameterization is the incorporation of an anthropogenic heating term (Ohashi *et al.*, 2007; Makar *et al.*, 2006; Dupont *et al.*, 2004; Taha, 1999; Sarkar *et al.*, 1998). There are several methods for representing anthropogenic heating in a model of the UBL (Sailor, 2009): gridded maps of energy consumption (a.k.a. inventory approach, Sailor and Lu, 2004; Fan and Sailor, 2005), as a residual of the net radiation, advection and storage (Pigeon *et al.*, 2007; Offerle *et al.*, 2005) or through a building energy model (Kikegawa *et al.*, 2003). Pigeon *et al.* (2007) compared the inventory and residual approaches and found comparable results. Pigeon *et al.* (2008) model the urban surface using TEB and ISBA modelling systems (TEB – Town Energy Budget; ISBA – Interactions Soil-Biosphere-Atmosphere) during the Fall and Winter similar to the approach of the EPiCC project (Voogt *et al.*, 2009). Comparisons against tower data at Toulouse (France) found strong coherence with the sensible heat flux, showing great promise for application of TEB-ISBA to NWP models. Using a building-energy model approach, Sailor *et al.* (2007) found that 50-80% of anthropogenic heat emissions in Houston (U.S.A.) are released as latent heat. Makar *et al.* (2006) demonstrated how the inclusion of anthropogenic heat flux reduces stability in the nocturnal boundary layer, increases ABL depth and enhances pollutant dispersion aloft over cities.

Recent studies also concentrate on improving the modelling of urban heat storage (Taha, 1999; Brown, 2000; Masson, 2000) and its nocturnal release (Rotach *et al.*, 2005). Roberts *et al.* (2006) implemented four approaches to modelling urban heat storage against verification from the ESCOMPTE (Mestayer *et al.* 2005) and other campaigns: the Energy balance residual method (RES), parameterization by the Objective Hysteresis Model (OHM; Grimmond *et al.*, 1991), numerical modelling with the Town Energy Balance (TEB; Masson, 2000) and modelling with the Thermal mass scheme (TMS; Peikorz, 1987). The lack of a common technique for measurement or error analysis of urban heat storage precludes direct comparison or ranking of these methods. However, Roberts *et al.* (2006) found generally common behaviour in the timing and magnitude of the diurnal oscillation with the storage heat flux reaching a maximum (heat up-take) around local noon and minimum (heat release) in the early evening. The geometry of canyon walls may affect mixing, with heating of windward walls being more likely to induce mixing and turbulent heat fluxes than leeward wall heating, which promotes vertical transfer out of the canyon without mixing (Offerle *et al.*, 2007). There are significant implications for proper accounting of heat storage. Taha and Bornstein (1999) and Taha (1999) show that improved heat storage modelling results in a ten percent increase in isoprene emissions and a one to two percent increase in NO_x and volatile organic compound (VOC) emissions for an Atlanta (U.S.A.) case study. These increased emissions produce a ten percent enhancement of average O₃ with a 5-10 ppbv increase during the mid-afternoon.

Coutts *et al.* (2007) modelled long-term effects of increased urbanization at Melbourne (Australia) and depicted increased urban heat storage, leading to elevated nocturnal temperatures.

8.3.3 Coastal-Urban Environment Interaction

8.3.3.1 Summary

Urban environments adjacent to coastlines are subject to the complex meteorology of both coastal and urban environments. In the presence of a coastline, steady on-shore flow can produce one or more IBLs, depending on whether the city is located immediately along the coastline. If large-scale winds are light, both a UHI circulation and SBF/LBF can develop. Both are three-dimensional mesoscale thermal circulations and can interact, subject to local geography and meteorology. The interaction can lead to abrupt changes in the depth of the local boundary layer, changes in air mass qualities and pollutant concentrations. Understanding this phenomenon is particularly challenging, being subject to the sensitivities of coastal environments, urban environments and all the outstanding uncertainties associated with modelling the ABL.

8.3.3.2 Recent Observational Studies

Comprehensive evaluation of the interaction of the UHI and SBF is difficult to capture since the circulations are three-dimensional and mesoscale in size but numerous studies are ongoing. The Border Air Quality Study (BAQS-Met) in 2007 (Makar *et al.*, 2008; Sills *et al.*, 2008) provides a new dataset for researchers interested in pollutant dispersion in south western Ontario, including urban areas such as Windsor and London. The field campaign included in-situ stationary and mobile chemical measurements, mesonet meteorological stations, wind profiler observations and remote sensing imagery. Keeler *et al.* (2009) and Harris and Kotamarthi (2005) also examined coastal urban environments in the Great Lakes region, at Chicago (U.S.A.). The presence of a coastal city causes a reduction in the speed of the SBF passage past the city due to the drag force of the buildings, functioning like a topographic barrier (Bornstein *et al.* 1993). The authors found reduced pollutant concentrations immediately after the SBF passage at New York City, with the ambient polluted air transported northwest of the city. Keeler *et al.* (2009), however, showed that less than 25% of the 49 spring and summer lake-breeze events examined showed this reduced speed of propagation. The authors also show that roughly two-thirds of the LBFs did not follow the shape of the adjacent coastline. Veron *et al.* (2009) presented a new dataset of SBFs over several months at Delaware Bay, showing impacts on surface winds at Philadelphia.

A city well removed from the coastline can induce the growth of multiple internal boundary layers under steady on-shore flow as roughness changes abruptly from the coastline inland. Kitada *et al.* (2008) found that near-surface O₃ concentrations increased monotonically after SBF passage, while a city 17 km inland had the greatest concentrations at 300 m above ground. At lower heights in the city, decreased stability due to the TIBL provided increased mixing and reduced the O₃ concentration. This study provides a useful comparison for air quality in Toronto, a comparably large ‘coastal’ city also with significant urban development well-removed from the coastline.

8.3.3.3 Recent Modelling Studies

Through modelling, researchers can achieve a more complete illustration of the intricate interactions of the UHI and SBF/LBF. Urbanized coastal cities can accelerate the development of the SBF/LBF, yet the drag of the buildings is typically shown to slow down the translation of the front through the city. The development of a UHI circulation may fumigate the urban core and carry the pollutants well outside the city, creating elevated nocturnal pollutant concentrations over ‘rural’ areas or over the water. During the day, however, the passage of the SBF/LBF can shift pollutants inland from the water and the lower level of the UHI circulation can return that ‘polluted’ rural air back to the urban core. However, the convergence of the UHI and SBF circulations can block this transport and loft pollutants at the point of intersection, which is highly sensitive to many conditions.

The interaction of the UHI and SBF/LBF is particularly sensitive to the orientation and location of the large-scale wind, the strength of the SBF/LBF and the placement of cities with respect to the coastline. For example, in the Pearl River Delta of China, Lo *et al.* (2007) showed that the UHI strengthens the coastal temperature gradient, thereby strengthening the SBF and its penetration distance, in contrast to other case studies that indicate SBF weakening (Yoshikado, 1992; Bornstein *et al.*, 1993; Martilli, 2003). Holt and Pullen (2009) also demonstrate sensitivity of the sea breeze circulation to sea-surface temperature perturbations, also showing sensitivity of tracer behaviour to anthropogenic heating, coastal upwelling and variation in building heights. Using an idealized, two-dimensional numerical model, Martilli (2003) found that a coastal city can accelerate SBF formation in the morning due, in part, to faster daytime heating and enhanced turbulence, but later inhibit the inland penetration of the SBF due to the convergence of the UHI circulation and the SBF (Martilli, 2003; Khiem *et al.*, 2009). Khiem *et al.* (2009) found that the return flow of the UHI circulation (blowing toward the urban core in the lower UBL) converged with the SBF as it passed inland through Tokyo. This convergence provoked lofting and effectively blocked high O₃ concentrations from advection further inland of the coastal city. Martilli (2003) also examined perturbations to rural soil moisture and showed a correlation to the inland SBF penetration and timing of the late afternoon ABL collapse. Thompson *et al.* (2007) simulated UHI-SBF interaction at New

York City using a mesoscale NWP model and confirm a reduced SBF propagation speed. Sensitivity tests reveal that the presence of the urban area elevated the leading edge of the SBF with substantial influence on direction and concentration of model tracer plumes.

One intriguing aspect of the UHI-SBF interaction is its detrimental effect on air quality well away from the urban sources. Although the UHI circulation may enhance dispersion over the urban core, pollutant concentrations may increase up to 100 km inland as the lofted, polluted air diverges then subsides, transporting its burden of pollutants accumulated over the city (Martilli, 2003; Yoshikado, 1992). The nocturnal land breeze can advect pollutants over the water, to be returned inland by the passage of the SBF the following day (Martilli, 2003). Martilli (2003) found the strongest concentration of tracers at night over the rural areas outside the city due to the shallower ABL depth. Over multiple days, inland concentrations can accumulate from a complex interaction of nocturnal advection strength, fumigation of pollutants from the urban area and the timing of the arrival of the sea-breeze front. Similar processes have been observed in the Fraser Delta of Vancouver, and this process has clear implications for the Great Lakes region. Thompson *et al.* (2007) show how large upward vertical motion at the leading edge of an SBF launches tracers aloft, dramatically reducing surface concentrations. In the wake of the SBF passage, however, the resulting profile generally confines newly released tracers to near the surface.

8.3.4 Summary and Recommendations for Future Work

8.3.4 1 Smog in the Atmospheric Boundary Layer

From the above studies, the following conclusions may be drawn from the state of the science for pollutant transport in the atmospheric boundary layer:

- 1) Measurement and modelling of the boundary layer depth is critical to understanding pollutant concentrations in the atmospheric boundary layer. In a well-mixed boundary layer, a larger depth increases fumigation and reduces surface concentration. Shallow, stable boundary layers will hinder the vertical mixing of a pollutant surface. Accuracy of wind speed profiles and wind direction is also critical to local pollutant dispersion, particularly over complex surfaces.
- 2) Coastal environments can be subject to sudden change in temperature, wind direction, boundary layer depth, stability and pollutant concentrations with the passage of a sea/lake breeze front. Mesoscale models capture this process well, though locally strong thermal and roughness contrasts may require increased resolution. Effects are dependent on the orientation of the coastline with respect to the large-scale wind direction.

- 3) Urban environments induce substantial influence on the momentum, stability and moisture content of the overlying atmospheric boundary layer. Heterogeneity of the density, height and orientation of buildings promotes shear turbulence production and produces complex horizontal and vertical flows within the urban environment. This complexity manifests in the exchange of turbulent momentum and mass fluxes from the street (canyon) level to the air above. The contribution of anthropogenic heat flux and heat storage complicates the surface energy balance. Turbulent exchanges near the canyon top contribute to the ventilation of pollutants from street canyon sources. The ventilation will depend, in part, on the background meteorology and the geometry of the canyon. Cities with clusters of tall structures surrounding narrow canyons appear subject to high daytime surface pollutant concentrations. Modelling of air quality at regional scales requires sufficient representation of the upper part of the urban boundary layer, as well, which likely requires additional study. Although a universal framework for turbulence theory in the urban boundary layer remains outstanding, copious field campaigns and modelling work in recent years provide a critical foundation.
- 4) The interaction of mesoscale circulations from the urban heat island and coastal flow as from a sea/lake breeze front or steady on-shore winds can produce drastic changes in local air mass characteristics over short periods. The nature of this interaction is highly sensitive to the speed and direction of the wind, the height of the buildings (drag) and the local geography. Studies suggest a diurnal process where the urban heat island circulation fumigates pollutants over the core of a city, transporting them laterally, aloft. The combination of the urban heat island circulation and the nocturnal land breeze can shift O₃ precursors and particular matter off-shore of a coastal city. The subsequent passage of a sea/lake breeze front and a new urban heat island circulation the following day can again return high O₃ and pollutant concentrations to the urban core.

8.3.4 2 Future Work

Extensive observations and modelling of tracer and pollutant transport in the atmospheric boundary layer in recent years has accelerated scientific understanding. There remain, however, a number of unknowns and outstanding questions. Understanding of the pollutant transport in the ABL requires improved understanding of the meteorology and land-atmosphere interaction, particular in the vicinity of cities. Future studies should focus on one or more of the following recommendations:

1. Understanding the Atmospheric Boundary Layer

Continued research into the observation and modelling of atmospheric boundary layer (ABL) depth over all types of surfaces is needed. This work should focus on (a) the accuracy of ABL depth forecast, (b) simulating the collapse of the ABL, (c) boundary-layer structure and wind

direction, (d) meteorology-air quality feedbacks, (e) the role of aerosol in the surface energy budget and in the moisture fields and (f) the effect of chemical data assimilation on weather forecasts (Oke, personal communication, 2009; Carmichael *et al.*, 2008).

2. Urban Influence on Dynamics

Despite recent valuable contributions to empirical parameterization, there remains a need for a universal theoretical framework to characterize urban flows (Barlow and Coceal, 2009). Past research has indicated further research is needed for (a) improved parameterizations of turbulent heat and momentum flux and exchange between the canyon layer and the overlying UBL under varying stability (Makar *et al.*, 2008; Chemel *et al.*, 2008; Rotach *et al.*, 2005; Dupont *et al.*, 2004), (b) better understanding of the effect of stability on canyon layer flow (Klein *et al.*, 2007), (c) improved definition of the urban RSL with respect to the urban morphology (Barlow and Coceal, 2009), (d) improved understanding of canopy drag's sensitivity to morphology and wind direction (Barlow and Coceal, 2009), (e) the evaluation of meteorology at the canopy morphology level of detail (Dupont *et al.*, 2004), and (f) the development of dimensionless morphological parameters to identify key combinations of relevant parameters (Barlow and Coceal, 2009). Some of these needs may be addressed by the implementation of urban observation networks (in-situ and remote sensing) to develop a climatology of the temperature and stability structure over Canadian cities (Oke, personal communication, 2009).

The above studies need to consider wind flows at scales from the urban canyon up to regional levels, and should examine how the urban influence varies in time, in space and with regard to local stability, urban morphology and geography. Future field campaigns should endeavour to evaluate cities of varying size, climate and morphology. For pollutant transport at larger (regional) scales, there is a considerable need to renew observation and modelling research of the Ekman (outer) layer of the ABL, well above the canyon (Oke, personal communication, 2009), which will be largely affected by advective processes (Rotach *et al.*, 2005). At these larger scales, studies should also continue to investigate the interaction of the urban heat island (UHI) circulation with synoptic-scale (large-scale) winds and other local mesoscale circulations (such as from sea/lake-breezes or elevation-induced flows) that can complicate the mixing and transport of pollutants downstream.

3. Urban Influence on Energy Balance

Additional work is necessary to understand and quantify the exchange of turbulent heat fluxes in the UBL, with the use of multi-dimensional energy balance parameterizations for urban dispersion models (Fisher *et al.*, 2006), multiple-layer canopy models (Skamarock *et al.*, 2007), improvements to latent heat flux estimation (Grimmond *et al.*, 2009; Voogt *et al.*, 2009), creation of standards for the measurement, quantification, magnitude or spatial

distribution of anthropogenic heat and its further observation (Sailor, 2009; Arnfield, 2003), and the impact of short and longwave radiative transfer in the UBL for potential photochemistry applications (Oke, personal communication, 2009).

8.4 Satellite Remote Sensing of Smog

Randall Martin

8.4.1 Remote Sensing of Trace Gases and Aerosols

Over the last decade a suite of remote sounding instrumentation has been successfully deployed in space, utilizing both naturally emitted and/or reflected light (“passive” sounding) and light reflected and scattered from a source on the spacecraft itself (“active” sounding). Noteworthy applications of remote sensing data include “top-down” constraints on emissions (constraining emissions using measurements of concentration, in contrast to “bottom-up” methodologies, in which emissions inventories are constructed based on reporting or estimates of emissions activities), improved estimates of radiative forcing, observation of long-range transport on regional to continental scales and air quality characterization.

Satellite remote sensing of the lower troposphere effectively began in 1995 with the launch of the GOME-1 instrument (Burrows *et al.*, 1999) aboard the ERS-2 satellite. Although GOME-1 was designed primarily to provide the research community with global observations of stratospheric ozone and related species, a secondary objective was to investigate the potential of nadir (i.e. measurements are made directly below the satellite) remote sounding of backscattered ultraviolet and visible radiation for the retrieval of tropospheric trace gases. The broad spectrum of observed wavelengths at a moderate resolution allows for the retrieval of several key species in tropospheric chemistry: O₃, NO₂, HCHO, BrO, SO₂, and H₂O. Tropospheric NO₂ and HCHO have strong signals in the lower troposphere and are of particular relevance for smog. The spatial resolution of a ground scene is variable but is typically 40 × 320 km². GOME-1 made global measurements from July 1995 to June 2003. Highlights of GOME include insight into emissions of nitrogen oxides (e.g. Martin *et al.*, 2003) and volatile organic compounds (e.g. Palmer *et al.*, 2003a).

The launch of NASA’s Terra satellite in December 1999 significantly expanded scientific perspective on the scale of tropospheric pollution. The MOPITT instrument (Drummond and Mand, 1996) onboard Terra is a nadir-viewing gas correlation radiometer that can be applied to retrieve CO. The MOPITT pixel is 22 x 22km at nadir with a 29 pixel wide swath. Near-complete global coverage is achieved in 3-4 days in the absence of clouds. Highlights of the

MOPITT observations include insight into the long-range transport of pollution (Heald *et al.*, 2003; Pfister *et al.*, 2005), the impact of frontal systems on CO transport (Liu *et al.*, 2006a), and improved estimates of CO emissions (Palmer *et al.*, 2003b; Pétron *et al.*, 2004).

The MISR and MODIS instruments provide unprecedented information about aerosol abundance and properties at high spatial resolution. A primary product is aerosol optical depth, a measure of light extinction over the atmospheric column. Other products include information on aerosol size and single scattering albedo. Information from MODIS and MISR is yielding insight into the global distribution of aerosols (King *et al.*, 1999; Kinne *et al.*, 2003), their long range transport (Li *et al.*, 2005), and increasingly about aerosol optical properties (Kahn *et al.*, 2001). The MISR instrument includes nine fixed cameras pointed at angles varying from +70°, through nadir, to -70°. Global coverage (in the absence of clouds) is obtained about once per week at mid-to-low latitudes, and every two days near the poles. A strength of MISR is the ability to retrieve aerosol optical thickness even over bright surfaces such as deserts (Martonchik *et al.*, 2004). The MODIS instrument uses a scanning mirror which allows full global coverage in 2 days in the absence of clouds or bright surfaces. A second MODIS instrument also is deployed onboard the Aqua satellite that was launched in 2002.

The SCIAMACHY instrument (Bovensmann *et al.*, 1999) was launched onboard Envisat in 2002. SCIAMACHY provides the capability for retrieval at ultraviolet through infrared wavelengths with a typical spatial resolution of 30 x 60 km. This enables retrieval of all the species observed by GOME-1, as well as glyoxal, CO, CH₄, and CO₂.

The launch of Aura in 2004 into the A-train began a period of unprecedented coverage of the lower troposphere from the OMI and TES instruments. OMI (Levelt *et al.*, 2006) is a nadir viewing imaging spectrometer that measures solar backscatter at ultraviolet and visible wavelengths with spatial resolution as high as 13 x 24 km and daily global coverage. This high resolution enables observation of more cloud-free scenes than previous backscatter measurements. OMI and MLS observations can be combined to infer the distribution of tropospheric ozone (Ziemke *et al.*, 2006). TES (Beer *et al.*, 2001) is a Fourier transform spectrometer observing thermal emission with both nadir and limb capability. The nadir version features a particularly high spatial resolution of 5 x 8 km, and is being applied to retrieve O₃ and CO with up to 2 degrees of freedom in the vertical such that the upper and lower troposphere can be resolved.

PARASOL (Deuzé *et al.*, 2001) offers the unique capability of measuring polarization, which yields additional insight into aerosol optical properties beyond aerosol optical thickness. Aerosol composition products are under development.

CALIOP (Winker *et al.*, 2003) is a nadir-pointing lidar that was launched in April, 2006 into the A-train. CALIOP offers unprecedented global vertical profiles of aerosol extinction at a vertical resolution of 120-360m, providing an exciting complement to the other satellite instruments.

Remote sensing instruments do not directly measure atmospheric composition, which is “retrieved” through a mathematical technique known as inversion from observed radiances leaving the top of the atmosphere. Such retrievals often require additional information on geophysical fields (e.g. temperature structure of the atmosphere, albedo at the surface, etc.), and may result in optical property data (e.g. aerosol optical depth, AOD) as opposed to chemical and physical properties (e.g. mass concentration). An integral aspect to the success of modern remote sensing has been the development of a variety of mathematical approaches and numerical techniques to extract physical parameters by accounting for atmospheric radiative transfer.

Table 8.4 Satellite remote sensing of surface air quality

Instrument	Platform	Global Meas Period	Typical Resolution (km)	Global coverage (days) ^b	Obs Time ^c	Spectral Range (µm)	NO ₂ ^a	HCHO ^a	SO ₂ ^a	CO ^a	O ₃ ^a	Other	Aero. Opt. Prop. ^a
GOME	ERS-2	1995-2003	320x40	3	10:30	0.23-0.79	X	X	X		0.5-1.5	BrO	
MOPIIT	Terra	2000-	22x22	3.5	10:30	4.7				0.5-2			
MISR	Terra	2000-	18x18 ^e	7	10:30	4 λ ^d 0.45-0.87							X
MODIS	Terra Aqua	2000-2002-	10x10 ^e	2	10:30 1:30	36 λ ^d 0.41-14.2							X
AIRS	Aqua	2002-	14x14	1	1:30	3.7-16			X	0.5-1.5			
SCIAMACHY	Envisat	2002-	60x30	6	10:00	0.23-2.3	X	X	X	X	0.5-1.5	Glyoxal, CH ₄ , CO ₂	
OMI	Aura	2004-	13x24	1	1:30	0.27-0.50	X	X	X		0.5-1.5		X
TES	Aura	2004-	5x8	n/a	1:30	3.3-15.4				0.5-1.5	1-2		
POLDER	PARASOL	2004-	16x18	1	1:30	9 λ ^d 0.44-1.0							X
CALIOP	CALIPSO	2006-	0.08x40	n/a	1:30	0.53, 1.06							>30
GOME-2	MetOp	2006-	80x40	1	9:30	0.24-0.79	X	X	X		0.5-1.5		
IASI	MetOp	2006-	12x12	0.5	9:30	3.6-15.5				0.5-1.5	1-2		
GOES	Various	Various	12x12	n/a	daytime	0.52-0.72							X

^aThe number of degrees of freedom (independent pieces of information) is given for each nadir measurement. A value of X indicates a tropospheric column.

^bValue given for clear-sky conditions. Clouds impede the retrieval.

^cValue given for the Equator.

^dNumber of discrete wavelengths.

^eRadiances for MISR and MODIS are acquired at between 205 m and 1.1 km, depending on channel. Resolutions reported here are for the standard operational aerosol products

References for Table 8.4: GOME-1: (Burrows *et al.*, 1999), MOPITT: (Drummond and Mand, 1996), MODIS: (Barnes *et al.*, 1998) MISR: (Diner *et al.*, 1998), AIRS: (Aumann *et al.*, 2003), SCIAMACHY: (Bovensmann *et al.*, 1999), OMI: (Levelt *et al.*, 2006), TES: (Beer *et al.*, 2001), POLDER: (Deuzé *et al.*, 2001), CALIOP : (Winker *et al.*, 2003), GOES: (Knapp *et al.*, 2005) .

Acronyms: **GOME:** Global Ozone Monitoring Experiment; **MOPITT:** Measurements Of Pollution In The Troposphere; **MISR:** Multi-angle Imaging Spectral Radiometer; **MODIS:** MODerate resolution Imaging Spectroradiometer; **SCIAMACHY:** SCanning Imaging Absorption spectroMeter for Atmospheric Cartography; **OMI:** Ozone Monitoring Instrument; **TES:** Tropospheric Emission Spectrometer; **PARASOL:** Polarization and Anisotropy of Reflectances for Atmospheric Sciences coupled with Observations from a Lidar; **CALIOP:** Cloud Aerosol Lidar and Infrared Pathfinder; **IASI:** Infrared Atmospheric Sounding Interferometer

Table 8.4 summarizes the capabilities of the major satellite instruments of relevance for remote sensing of smog. Thorough reviews of these instruments are in King *et al.* (1999), Fishman *et al.*, (2008), Martin (2008), and Hoff and Christopher (2009). Most of these satellites fly in low altitude “sun-synchronous” orbits of about 100 minutes which are timed with the Earth’s rotation and pass near the poles, arriving at the equator at a constant local time, with global coverage in one or more days. All of these instruments are nadir viewing, and thus return information on the entire “column” of the atmosphere below the instrument. The majority of instruments employ passive techniques, observing either scattered sunlight (solar backscatter) or emitted radiation (thermal emission). Solar backscatter measurements are the most common to date, in part due to their sensitivity to the lower troposphere, especially at visible and near infrared wavelengths where scattering by air molecules is weak. Measurements of thermal emission have the advantage of yielding both daytime and nighttime observations, and can provide useful information on the change of concentration with height within the troposphere. The sensitivity of thermal emission measurements is reduced in the boundary layer due to the lack of temperature difference between the atmosphere and the surface, with the result that these instruments are the least sensitive in the region with highest emissions of pollutants. In the ultraviolet the strong scattering by air molecules also reduces sensitivity to the boundary layer since some photons will be scattered back to space without passing through the boundary layer. Very recently, active LIDAR (light detection and ranging; analogous to radar) measurements have been deployed on satellites to yield relatively high resolution vertical profiles of aerosol parameters. In LIDAR instruments, a laser on board the satellite is used as a light source, with observation of the resulting backscattered light being used to determine aerosol location and light scattering properties. Clouds impede retrievals from all techniques.

Data from all of these instruments are publicly available from a variety of sites (NASA, ESA). Given the rapid developments in this field, scientific products are also available directly from research groups.

8.4.2 Applications of Satellite Data

8.4.2.1 Monitoring Surface Air Quality

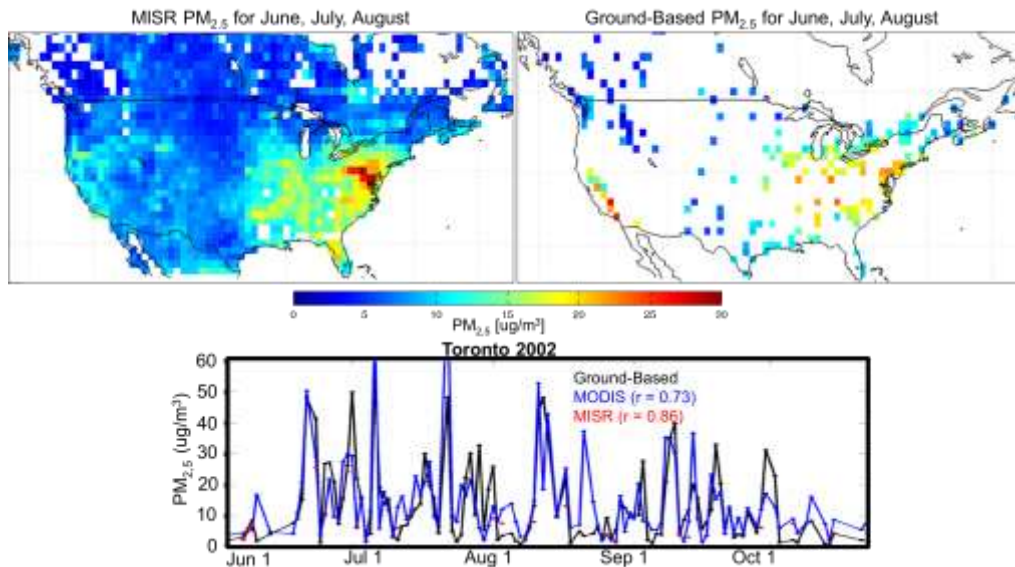


Figure 8.3 Surface $PM_{2.5}$ concentrations inferred from satellite observations of aerosol optical depth. The top panels show $PM_{2.5}$ for June – August from the MISR satellite instrument and from surface monitors. The bottom panel shows the temporal relationship of two satellite observations with a collocated ground-based monitor in Toronto. (Adapted from van Donkelaar *et al.*, 2006.)

Observation of surface air quality from space has focused on three primary areas: PM, NO_2 , and O_3 - NO_x -VOC sensitivity. PM has attracted the most attention. Recent findings for satellite retrievals of PM include: (a) AOD- PM_{10} and AOD- $PM_{2.5}$ relationships for, respectively, northern Italy (Chu *et al.*, 2003) and Alabama ($r > 0.9$, Wang and Christopher, 2003); (b) considerable variations in AOD- $PM_{2.5}$ correlation with region, with variations being higher in the eastern United States than the western United States (Al-Saadi *et al.*, 2005) or in Europe (Koelemeijer *et al.*, 2006); (c) AOD - surface $PM_{2.5}$ relationships for the southeast United States using both MODIS (Wang and Christopher, 2003) and MISR (Liu *et al.*, 2005); (d) the coupling of aerosol optical thickness from MISR with local scaling factors from a chemical transport model (GEOS-Chem) to estimate $PM_{2.5}$ (Wang *et al.*, 2007); (e) comparisons between MODIS and MISR-inferred $PM_{2.5}$ with surface $PM_{2.5}$ measurements in Canada and the United States (Figure 8.3), where the local vertical variation in aerosol light extinction was found to be the most important factor affecting the spatial relationship between AOD and surface $PM_{2.5}$ (van Donkelaar *et al.*, 2006); (f) the first near-real-time application of satellite data for air quality as part of the Infusing satellite Data into Environmental Applications (IDEA) partnership between NASA, EPA, and NOAA (Al-Saadi *et al.*, 2005). Aerosol data and

forecast products are available at <http://www.star.nesdis.noaa.gov/smcd/spb/aq/>. Recent global retrievals of aerosol extinction from CALIPSO should be of considerable value for improving satellite remote sensing of PM_{2.5}.

Tropospheric NO₂ columns feature strong signals from the lower mixed layer, in part due to the increase in the NO/NO₂ ratio with altitude in the troposphere. Several recent studies have made use of satellite-derived NO₂ measurements: GOME observations of tropospheric NO₂ columns were used to discern a weekly pattern with significant reductions on weekends (Beirle *et al.*, 2003); GOME NO₂ columns were used to infer a significant correlation with in-situ NO₂ concentration measurements (Ordonez *et al.*, 2006; Petritoli *et al.*, 2004); GEOS-Chem local scaling factors along with OMI tropospheric NO₂ columns were used to estimate surface NO₂ concentrations (Lamsal *et al.*, 2007). The overall agreement with in-situ USEPA Air Quality System (AQS) and Environment Canada National Air Pollution Surveillance (NAPS) networks for 2005 in the latter study was between 21 and 48%, with correlation coefficients up to 0.8. The satellite derived data base of ground-level NO₂ concentration should be valuable to epidemiological studies and the development of air quality control strategies.

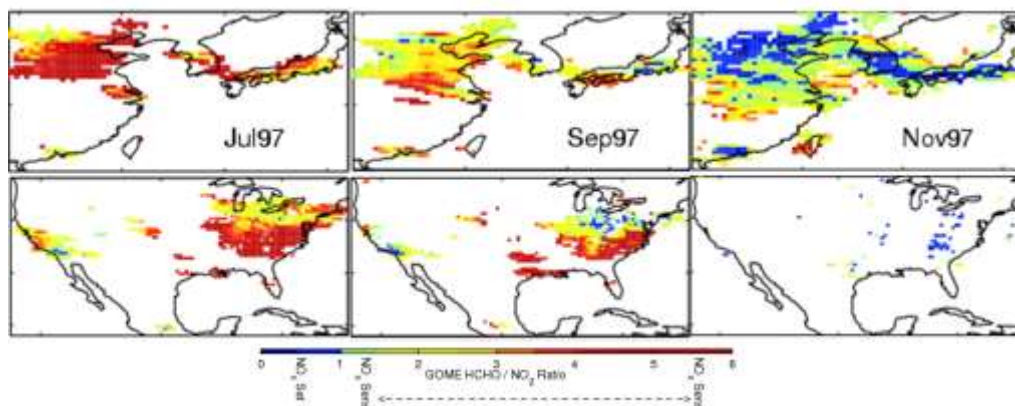


Figure 8.4 Monthly mean tropospheric HCHO/NO₂ column ratio retrieved from the GOME satellite instrument for East Asia and North America. Areas with ratios > 1 tend to be NO_x-limited while areas with ratios < 1 tend to be VOC-limited. White areas: less polluted regions (observed tropospheric NO₂ columns less than 2.5 x 10¹⁵ molecules cm⁻²) or below the HCHO column detection limit of 4x10¹⁵ molecules cm⁻². (After Martin *et al.*, 2004.)

The design of control strategies for surface O₃ has been impeded by sparse observations of O₃-NO_x-VOC sensitivity (Sillman, 1999). Martin *et al.* (2004) demonstrated the capability for satellite remote sensing of O₃-NO_x-VOC sensitivity in which the ratio of formaldehyde (HCHO) columns to tropospheric NO₂ columns was used as an indicator of the relative sensitivity of surface O₃ to emissions of NO_x and VOCs. Their diagnosis using observations from the GOME satellite instrument was broadly consistent with current understanding of surface O₃ chemistry based on in situ observations: the satellite-derived ratios indicate that surface O₃ is limited by NO_x emissions throughout most continental regions of the Northern

Hemisphere during summer (e.g. Figure 8.4). Exceptions include Los Angeles and industrial areas of Germany, which are VOC-limited. A seasonal transition occurs in the fall from NO_x-limited to VOC-limited conditions. Such observations should be of value for evaluating air quality models.

Numerous retrievals of tropospheric O₃ columns exist for the tropics (Fishman *et al.*, 1990; Hudson and Thompson, 1998; Ziemke *et al.*, 1998; Kim *et al.*, 2001; Newchurch *et al.*, 2002; Valks *et al.*, 2003). Retrievals of tropospheric O₃ columns have more recently become available for higher latitudes (Fishman and Brackett, 1997; Chandra *et al.*, 2003; Fishman *et al.*, 2003; Liu *et al.*, 2006b; Ziemke *et al.*, 2006). Vertical profile information is also becoming available (Newchurch *et al.*, 2001; van der A *et al.*, 2002; Müller *et al.*, 2003; Jourdain *et al.*, 2007; Worden *et al.*, 2007). However, retrievals of ground-level O₃ concentrations have been inhibited by several physical issues: (a) low thermal contrast reduces the instrument sensitivity of infrared measurements (Bowman *et al.*, 2006); (b) atmospheric scattering reduces the instrument sensitivity of ultraviolet measurements to near-surface concentrations (Klenk *et al.*, 1982); (c) O₃ in the boundary layer constitutes a small fraction (typically < 2%) of the total O₃ column; (d) the stratospheric O₃ column exhibits high variability at middle and high latitudes (Jing *et al.*, 2006). At the current state of the science, instrument sensitivity and stratospheric O₃ interference make accurate space-borne measurements of ground-level O₃ difficult to achieve. However, there are some encouraging recent developments in this area (Worden *et al.*, 2007).

Applications of satellite retrievals of SO₂ for air quality are emerging. Initial SO₂ observations found enhancements in major industrial regions used GOME (e.g. Eisinger and Burrows, 1998; Krotkov *et al.*, 1998). More recent developments have yielded more confidence in the retrieval by better accounting for aspects of spectral fitting and atmospheric scattering (Khokhar *et al.*, 2005; Krotkov *et al.*, 2008; Lee *et al.*, 2009).

8.4.2.2 Constraints on Emissions Estimates

Inverse modelling is a mathematical approach to infer pollutant source strength from observations of atmospheric concentrations. A modified chemical transport model may be used to calculate the emissions of various pollutants that would reproduce the observational data. This “top-down” information is being used to evaluate and improve “bottom-up” emission inventories (the latter resulting from the collection of emission data via reporting from sources, ground-based measurements, etc.). Satellites provide a major source of observations used for inverse modelling of emissions.

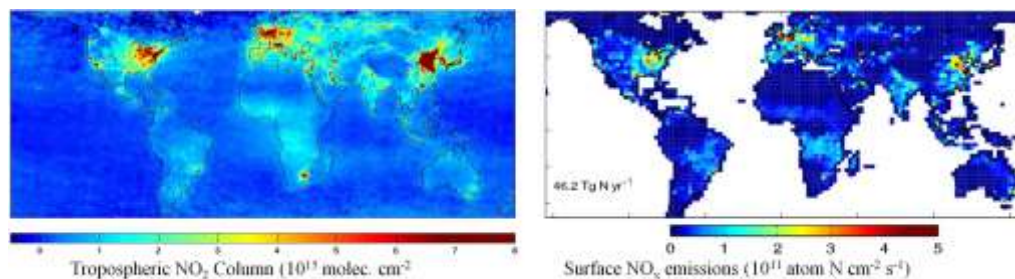


Figure 8.5 (Left) Tropospheric NO₂ columns for 2004-2005 determined from the SCIAMACHY satellite instrument. (Right) Surface NO_x emissions for 2004-2005 determined through inverse modelling of the SCIAMACHY observations using GEOS-Chem. The largest differences with bottom-up inventories occur over rapidly developing regions where the bottom-up inventory is out-of-date. Aircraft measurements were taken as part of the ICARTT aircraft campaign in support of the SCIAMACHY inventory program (Martin *et al.*, 2006).

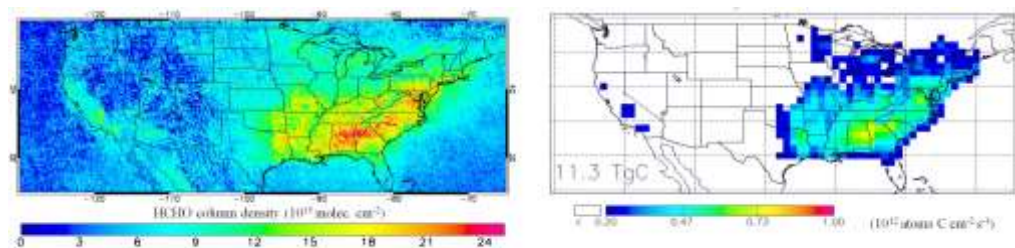


Figure 8.6 (Left) Formaldehyde (HCHO) columns over the United States determined from the OMI satellite instrument for summer 2006. (Right) Isoprene emissions determined through inverse modelling of the OMI observations using a chemical transport model (GEOS-Chem) (Millet *et al.*, 2008). Aircraft measurements show that isoprene is the dominant source of variability in column formaldehyde over North America (Millet *et al.*, 2006)

Figures 8.5 and 8.6 show examples of tropospheric NO₂ and HCHO columns retrieved from satellite, along with estimates of surface emissions of these species. Satellite data have been used to estimate NO_x emissions in several studies: (a) GOME retrievals of tropospheric NO₂ columns, a constant “typical” NO_x lifetime, and mass balance were used to derive a global NO_x emissions inventory (Leue *et al.*, 2001); (b) GEOS-Chem model-derived NO_x lifetimes, NO₂/NO ratios, top-down constraints and a bottom-up inventory were used to create an optimized inventory (Martin *et al.*, 2003), with resulting simulations that better matched in situ aircraft observations (Martin *et al.*, 2006); (c) the development of a method for global partitioning of satellite-derived NO_x sources into contributions from fossil fuel combustion, biomass burning, and soil emissions (Jaeglé *et al.*, 2005); (d) the development of an adjoint method for inference of emissions (Müller and Stavrou, 2005); (e) the application of regional models for inversion at higher resolution (Kim *et al.*, 2006; Kononov *et al.*, 2006); (f) better accounting of free tropospheric NO₂ in the inversion (Wang *et al.*, 2007).

Palmer *et al.* (2003a) developed a method for deriving emissions of VOCs using GOME retrievals of HCHO. This method was based on the relationship between the HCHO column and the sum of VOC emissions scaled by their HCHO yields from gas-phase oxidation. Long-lived species such as methane produce a spatially homogeneous HCHO column enhancement that is accounted for in the inversion using calculations from a chemical transport model. Abbot *et al.* (2003) found that the seasonal variation in GOME HCHO columns over North America is broadly consistent with the seasonal cycle of emissions of isoprene. Fu *et al.* (2007) applied GOME satellite measurements of HCHO columns over East and South Asia to improve regional emission estimates of reactive non-methane VOCs, and found the need for a 25% increase in anthropogenic VOC emissions and a 5-fold increase in biomass burning VOC emissions in order to be consistent with the satellite observations.

The availability of near-global and long-term CO observations from space, in conjunction with global chemical transport models, has allowed the use of inverse methods in constraining regional CO sources (Arellano *et al.*, 2004; Heald *et al.*, 2004; Pétron *et al.*, 2004; Müller and Stavrou, 2005; Pfister *et al.*, 2005). This has provided insight into the understanding of present-day fossil-fuel and biofuel use and on the patterns of biomass burning activity. For instance, inverse modelling studies using MOPITT CO retrievals consistently report that emissions from fossil-fuel and biofuel use in Asia are significantly larger than previously estimated. This finding contributed to recent efforts to revisit and update the bottom-up emission inventory in Asia (Streets *et al.*, 2006). In addition, these inverse modelling studies provide important constraints on the magnitude and spatio-temporal variability of biomass burning emissions.

Dubovik *et al.* (2007) applied inverse modelling techniques simultaneously to both pollutant and naturally occurring aerosols using MODIS aerosol optical thickness data with the GOCART model. The authors found and quantified the major aerosol sources during a 1-week period in August 2000. Sources were identified in the southeast United States, the Amazon basin, Europe, West Africa, southern Africa, the Indo-Gangetic Basin and East Asia.

Sources of PM in Canada are highly impacted by biomass burning which are difficult to inventory in models. Use of aerosol AOD to detect source emissions may be one of the only ways that remote emissions in boreal Canada can be quantified. Fire radiative power may serve as a useful emission estimation tool in this regard (Kaufman *et al.*, 1998, 2005; Weaver *et al.*, 2007).

8.4.2.3 Satellite Observations and Long-Range Transport

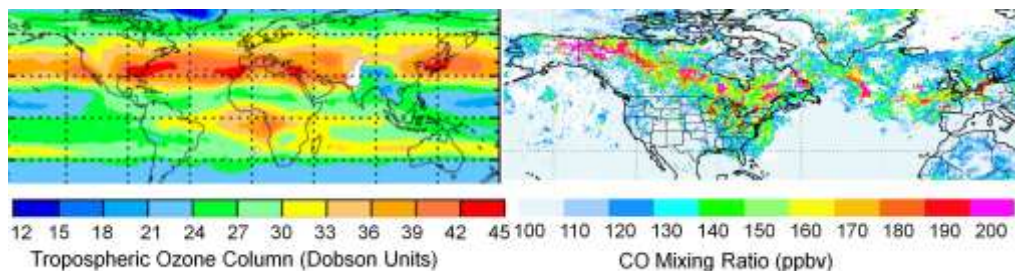


Figure 8.7 The left panel shows the seasonal average GOME tropospheric O_3 columns (Dobson units) for June – August 1997 (Liu *et al.*, 2006b). The right panel indicates the MOPITT 700 hPa CO mixing ratio (ppbv) for 15-23 July 2004 (Pfister *et al.*, 2006).

Recent advances in satellite capabilities allow a global view of tropospheric pollutant transport. Figure 8.7 presents example images that provide clear evidence of intercontinental transport of tropospheric O_3 and CO. The left panel of Figure 8.7 shows significant O_3 enhancements in the regions of greatest precursor emission, i.e. eastern United States, Europe, and East Asia, with a broad enhanced region in the mid-latitudes, associated with export of O_3 and its precursors from the adjacent continental regions. The right panel of Figure 8.7 shows that CO plumes from intense wildfires in Alaska and Canada that can be traced across North America and the Atlantic Ocean. Inverse modelling using the MOZART chemical transport model showed that these fires emitted about as much CO as did all human-related activities in the continental United States during the same time period, about 30 Tg of CO in the period of June-August, 2004 (Pfister *et al.*, 2006). Modelling and measurements also show that emissions from the 2004 North American wildfires caused ground-level concentrations of O_3 to increase by 25% or more in parts of northern continental United States and central North Atlantic Ocean and by 10% in areas as far away as Europe (Pfister *et al.*, 2006).

Several recent studies interpreted satellite observations to examine the long-range transport of aerosol and ozone from Asia to North America as part of the INTEX-B campaign (Singh *et al.*, ACP, 2008). Analysis of MODIS and in situ observations with a global model led to the conclusion that about a third of the sulphate in southern British Columbia in spring 2006 was from Asian sources (van Donkelaar *et al.*, 2008). Zhang *et al.* (2008) interpreted Tropospheric Emission Spectrometer (TES) and in situ O_3 with a global model and found that Asian pollution enhanced surface ozone concentrations by 5–7 ppbv over western North America in spring 2006 (Zhang *et al.*, 2008). Considerable opportunity remains for additional studies using satellite observations to examine transport of pollution from the United States to Canada.

8.4.3 Summary and Recommendations for Future Work

The current satellite database has yielded exciting developments in observations of surface air quality, constraining emissions, and long-range transport. Near-term prospects for additional advances are promising. Major near-term challenges include developing improved algorithms for the retrieval of near-surface concentrations from satellite observations, limited resources for the interpretation of satellite data sets, and few in situ observations for use in evaluating satellite retrievals of short-lived trace gases. As many of the examples provided are for applications outside of Canada, considerable opportunity exists to extend these analyses to more specific Canadian objectives.

A few emerging species from satellite observations would enhance existing capabilities. These include ammonia from TES (Beer *et al.*, 2008) and Infrared Atmospheric Sounding Interferometer (IASI; Clarisse *et al.*, 2009), HNO₃ from IASI (Wespes *et al.*, 2009), glyoxal (Wittrock *et al.*, 2006), and aerosol composition and size information (Liu *et al.*, 2007b; Mishchenko *et al.*, 2007; Chen *et al.*, 2008; Torres *et al.*, 2007). It would be valuable to continue developing instrumentation and retrievals with improved retrieval precision in the lower troposphere (IGOS-IGACO, 2004; Edwards, 2006; National Academy of Science, 2006). All of these satellite observations need to be better linked with ground-based measurements, and with modelling activities for their analysis.

A looming challenge is the small number of new instruments planned for observing atmospheric chemistry, coupled with the fact that many of the current missions are maturing and already past their design lifetimes. Given the rapid changes in atmospheric composition, high priority should be given to developing new missions in the near future. A few missions being considered with capability for remote sensing of Canadian smog include MCAP (CSA), Sentinel-5 precursor (ESA), GEOCAPE (NASA), and ACE (NASA). Canada has an opportunity to develop its smog remote sensing capability by supporting these missions and by preparing for them through the interpretation of existing satellite observations.

References

- Abbot, D.S., P.I. Palmer, R.V. Martin, K. Chance, D.J. Jacob, and A. Guenther, 2003. Seasonal and interannual variability of isoprene emissions as determined by formaldehyde column measurements from space. *Geophys. Res. Lett.* 30, 1886, doi:10.1029/2003GL017336.
- Allwine, K.J., M.J. Leach, L.W. Stockham, J.S. Shinn, R.P. Hosker, J.F. Bowers and J.C. Pace. 2004. Overview of Joint Urban 2003 – An Atmospheric Dispersion Study in Oklahoma City. Preprints: Symposium on Planning, Nowcasting, and Forecasting in the Urban Zone, Seattle, WA, Jan. 11-15, 2004, American Meteorological Society, CD-ROM, J7.1

- Allwine, K.J., J.H. Shinn, G.E. Strait, K.L. Clawson and M. Brown. 2002. Overview of URBAN 2000 – A Multiscale Field Study of Dispersion through an Urban Environment. *Bull. Amer. Meteor. Soc.*, 83, 521-536.
- Al-Saadi, J., J. Szykman, R. B. Pierce, C. Kittaka, D. Neil, D. A. Chu, L. Remer, L. Gumley, E. Prins, L. Weinstock, C. MacDonald, R. Wayland, F. Dimmick, and J. Fishman, 2005. Improving national air quality forecasts with satellite aerosol observations. *Bull. Amer. Meteor. Soc.*, 86, 1249-1261.
- Angevine, W. M., A. B. White, C. J. Senff, M. Trainer, R. M. Banta, and M. A. Ayoub. 2003. Urban-rural contrasts in mixing height and cloudiness over Nashville in 1999. *J. Geophys. Res. D: Atmospheres* 108, (3): AAC 3-1 - AAC 3-10.
- Angevine, W.M., M. Tjernstrom and M. Zagar. 2006a. Modelling of the Coastal Boundary Layer and Pollutant Transport in New England. *J. Appl. Met. Clim.*, 45, 137-154.
- Angevine, W. M., J. E. Hare, C. W. Fairall, D. E. Wolfe, R. J. Hill, W. A. Brewer, and A. B. White. 2006b. Structure and formation of the highly stable marine boundary layer over the gulf of maine. *J. Geophys. Res. D: Atmospheres* 111, D23S22, doi:10.1029/2006JD007465
- Angevine, W.M., M. Žagar, J. Brioude, R. Banta, C. Senff, H.C. Kim and D. Byun. 2009. How Well Can We Model the Houston Area for Air Pollution Studies? Proceedings of the 89th Annual Meeting of the American Meteorological Society, Phoenix, Arizona, U.S.A., 10-15 January 2009.
- Anlauf, K.G., P. Fellin, H.A. Wiebe, and O.T. Melo, 1982. The Nanticoke shoreline diffusion experiment, June 1978 – IV. A. Oxidation of sulphur dioxide in a power plant plume. B. Ambient concentrations and transport of sulphur dioxide, particulate sulphate and nitrate, and ozone. *Atmospheric Environment*, 16, 455-466.
- Arain, M.A., R. Blair, N. Finkelstein, J. Brook and M. Jerrett. 2009. Meteorological influences on the spatial and temporal variability of NO₂ in Toronto and Hamilton. *Canadian Geographer-Geographe Canadien*. 53, 165-190.
- Arellano, A.F., Jr., P.S. Kasibhatla, L. Giglio, G.R. van der Werf, and J.T. Randerson, 2004. Top-down estimates of global CO sources using MOPITT measurements. *Geophys. Res. Lett.*, 31, L01104, doi:10.1029/2003GL018609.
- Arnfield A. J., 2003: Two decades of urban climate research: a review of turbulence, exchanges of energy and water, and the urban heat island. *Int. J. of Climatol.*, 23, 1-26.

- Aumann, H.H., *et al.* 2003. AIRS/AMSU/HSB on the aqua mission: Design, science objectives, data products, and processing systems, *IEEE Transactions on Geoscience and Remote Sensing*, 41 (2), 253-264.
- Avise, J., J. Chen, B. Lamb, C. Wiedinmyer, A. Guenther, E. Salathé, C. Mass, 2009. Attribution of projected changes in summertime US ozone and PM_{2.5} concentrations to global changes. *Atmos. Chem. Phys.* 9, 1111 – 1124.
- Banta, R. M., C. J. Senff, J. Nielsen-Gammon, L. S. Darby, T. B. Ryerson, R. J. Alvarez, S. R. Sandberg, E. J. Williams, and M. Trainer. 2005. A bad air day in Houston. *Bull. Amer. Meteor. Soc.* 86, (5): 657-669.
- Barlow, J. and O. Coceal, 2009. A review of urban roughness sublayer turbulence. Met Office Meteorology Research and Development, Exeter, U.K.
- Barnes, W.L., T.S. Pagano, and V.V. Salomonson, 1998. Pre-launch characteristics of the Moderate Resolution Imaging Spectroradiometer (MODIS) on EOS AM-1, *IEEE Trans. Geosci. Remote Sens.*, 36 (4), 1088-1100.
- Bell, M.L., R. Goldberg, C. Hogrefe, P.L. Kinney, K. Knowlton, B. Lynn, J. Rosenthal, C. Rosenzweig, J.A. Patz, 2007. Climate change, ambient ozone, and health in 50 US cities. *Climatic Change* 82, 61-76.
- Beer, R., T.A. Glavich, and D.M. Rider, 2001. Tropospheric emission spectrometer for the Earth Observing System's Aura satellite. *Appl. Opt.* 40, 2356-2367.
- Beer, R., M.W. Shephard, S.S. Kulawik, S.A. Clough, A. Eldering, K.W. Bowman, S.P. Sander, B.M. Fisher, V.H. Payne, M. Luo, G.B. Osterman, J.R. Worden, 2008. First satellite observations of lower tropospheric ammonia and methanol, *Geophys. Res. Lett.*, 35, L09801, doi:10.1029/2008GL033642.
- Beirle, S., U. Platt, M. Wenig, and T. Wagner, 2003. Weekly cycle of NO₂ by GOME measurements: A signature of anthropogenic sources. *Am. Chem. Phys.* 3, 2225-2232.
- Bélair, S., M. Abrahamowicz, S. Leroyer, E. Christensen, Y.-C. Chung, A. Lemonsu, J. Mailhot and I. Strachan. 2009. Evolution of Snow Packs in the Town Energy Balanced (TEB) Model, Based on Results at EPiCC Rural, Suburban and Urban Sites. Proceedings of the 7th International Conference on Urban Climate, Yokohama, Japan, 29 June – 3 July 2009.
- Bezpalcová, K., M. Ohba and Z. Jaňour. 2009. Influence of Building Packing Density and Building Height Distribution on Vertical Mass Transport. Proceedings of the 7th International Conference on Urban Climate, Yokohama, Japan, 29 June – 3 July 2009.

Bornstein, R., P. Thunis and G. Schayes. 1993. Simulation of Urban Barrier Effects on Polluted Urban Boundary Layers using the Three-Dimensional URBMET/TVM Model with Urban Topography – new results from New York City. Invited Paper In: “Air Pollution ’93.” Eds: Zannetti, P., C.A. Brebbia and J.E.G. Gardea. Computational Mechanics Publications: Boston, First International Conference on Air Pollution, Feb. 23-25, 1993, Monterrey, Mexico, 15-34.

Bovensmann, H., J.P. Burrows, M. Buchwitz, J. Frerick, V.V. Rozanov, K.V. Chance, and A.P.H. Goede, 1999. SCIAMACHY: Mission objectives and measurement modes. *J. Atmos. Sci.* 56, 127-150.

Bowman, K.W.; Rodgers, C.D.; Kulawik, S.S.; Worden, J.; Sarkissian, E.; Osterman, G.; Steck, T.; Ming Lou; Eldering, A.; Shephard, M.; Worden, H.; Lampel, M.; Clough, S.; Brown, P.; Rinsland, C.; Gunson, M.; Beer, R., 2006. Tropospheric Emission Spectrometer: Retrieval method and error analysis. *IEEE Trans. Geosci. Remote Sens.* 44, 1297-130.

Brasseur, G.P., M. Schultz, C. Granier, M. Saunois, T. Diehl, M. Botzet, E. Roeckner, S. Walters, 2006. Impact of climate change on the future chemical composition of the global troposphere. *J. Climate* 19, 3932-3951.

Brook, J. R., K. B. Strawbridge, B. J. Snyder, H. Boudries, D. Worsnop, S. Sharma, K. Anlauf, G. Lu, and K. Hayden. 2004. Towards an understanding of the fine particle variations in the LFV: Integration of chemical, physical and meteorological observations. *Atmos. Env.* 38, (34): 5775-5788.

Brown, M.J. 2000. Urban Parameterizations for Mesoscale Meteorological Models. In: “Mesoscale Atmospheric Dispersion” (Ed: Boybeyi, Z.) Southampton: WIT Press 193-255.

Burrows, J.P., M. Weber, M. Buchwitz, V. Rozanov, A. Ladstätter-Weissenmayer, A. Richter, R. DeBeek, R. Hoogen, K. Bramstedt, K.-U. Eichmann, M. Eisinger, and D. Perner 1999. The Global Ozone Monitoring Experiment (GOME): Mission concept and first scientific results. *J. Atmos. Sci.* 56, 151-175.

Calhoun, R., R. Heap, M. Princevac, R. Newsom, H. Fernando and D. Ligon. 2007. Virtual Towers Using Coherent Doppler Lidar during the Joint Urban 2003 Dispersion Experiment. *J. Appl. Met. Clim.* 45, 1116-1126.

Calvo, A.I., V. Pont, C. Liousse, B. Dupré, A. Mariscal, C. Zouiten, E. Gardrat, P. Castera, C.G. Lacaux, A. Castro, R. Fraile. 2008. Chemical composition of urban aerosols in Toulouse, France during CAPITOUL experiment. *Meteorology and Atmospheric Physics.* 102, 307-323

Canadian Meteorological and Oceanographic Society, 2007. Statement on Climate Change. *Canadian Meteorological and Oceanographic Society Bulletin* 35, 99-106.

- Carmichael, G.R., A. Sandu, T. Chai, D. Daescu, E.M. Constantinescu and Y. Tang. 2008. Predicting Air Quality: Current Status and Future Directions (in) Air Pollution Modelling and Application XIX, 481-495, Borrego C and Miranda A.I. Eds., Springer: Dordrecht
- Chandra, S., J.R. Ziemke, and R.V. Martin, 2003. Tropospheric ozone at tropical and middle latitudes derived from TOMS/MLS residual: Comparison with a global model. *J. Geophys. Res.*, 108, 4291, doi:10.1029/2002JD002912.
- Chemel, C., J.-P. Chollet and E. Chaxel. 2008. On the Suppression of the Urban Heat Island over Mountainous Terrain in Winter (in) Air Pollution Modelling and Application XIX, 46-53, Borrego C and Miranda A.I. Eds., Springer: Dordrecht.
- Chen, F., M. Tewari, Y. Liu, J. Dudhia, S.G. Miao, A. Martilli, S. Grossman-Clarke, J.K. Ching and H. Kusaka. 2009. Application of an integrated WRF/urban modelling system to urban environmental problems. Proceedings of the 89th Annual Meeting of the American Meteorological Society, Phoenix, Arizona, U.S.A., 10-15 January 2009.
- Chen, J., Avise, J., Lamb, B., Salathé, E., Mass, C., Wiedinmyer, C., Lamarque, J.-F., O'Neill, S., McKenzie, D., Larkin, N., 2009. the effects of global changes upon regional ozone pollution in the United States. *Atmos. Chem. Phys.* 9, 1125 – 1141.
- Chen, W.-T., R. Kahn, W.-H. Li, and J. Seinfeld, 2008. Sensitivity of multi-angle imaging to optical and microphysical properties of biomass burning particles, *J. Geophys. Res.*, 113, D10203, doi:10.1029/2007JD009414.
- Cheng, C.S., Campbell, M., Li, Q., Li, G., Auld, H., Day, N., Pengelly, D., Gingrich, S., Yap, D., 2007a. A synoptic climatological approach to assess climatic impact on air quality in south-central Canada. Part I: Historical analysis. *Water, Air, and Soil Pollution* 182, 131-148.
- Cheng, C.S., Campbell, M., Li, Q., Li, G., Auld, H., Day, N., Pengelly, D., Gingrich, S., Yap, D., 2007b. A synoptic climatological approach to assess climatic impact on air quality in south-central Canada. Part II: Future estimates. *Water, Air, and Soil Pollution* 182, 117-130.
- Cheng, H. and I.P. Castro. 2002. Near Wall Flow Over Urban-like Roughness. *Boundary-Layer Meteorology*. 104, 229-259.
- Ching, J.K., F. Chen, H. Taha, M. Tewari and T.L. Otte. 2009. MM5, WRF, CMAQ using NUDAPT for advanced urban applications. Proceedings of the 89th Annual Meeting of the American Meteorological Society, Phoenix, Arizona, U.S.A., 10-15 January 2009.

Christen, A. 2005. Atmospheric Turbulence and Surface Energy Exchange in Urban Environments. Stratus, 11, Instit. Meteorol., Klimatol. Und Fernerkundung, Univ. Basel, Basel, 140 pp.

Christensen, J.H., B. Hewitson, A. Busuioc, A. Chen, X. Gao, I. Held, R. Jones, R.K. Kolli, W.-T. Kwon, R. Laprise, V. Magana Rueda, L. Mearns, C.G. Menendez, J. Raisanen, A. Rinke, A. Sarr, and P. Whetton, 2007: Regional Climate Projections. In: Climate Change 2007: The Physical Science Basis. Contribution of Working Group I to the Fourth Assessment Report of the Intergovernmental Panel on Climate Change, [S. Solomon, D. Qin, M. Manning, Z. Chen, M. Marquis, K.B. Averyt, M. Tignor, and H.L. Miller, (eds.)], Cambridge University Press, Cambridge, United Kingdom, and New York, NY USA, 847-845.

Chu, D.A., Y.J. Kaufman, G. Zibordi, J.D. Chern, J. Mao, C. Li, and B. Holben, 2003. Global monitoring of air pollution over land from the Earth Observing System-Terra Moderate Resolution Imaging Spectroradiometer (MODIS). *Journal of Geophysical Research*, 2003, 4661, doi:10.1029/2002JD003179.

Civerolo, K., Hogrefe, C., Lynn, B., Rosenthal, J., Ku, J.-., Solecki, W., Cox, J., Small, C., Rosenzweig, C., Goldberg, R., Knowlton, K., Kinney, P., 2007. Estimating the effects of increased urbanization on surface meteorology and ozone concentrations in the New York City metropolitan region. *Atmos. Env.* 41, 1803-1818.

Clarisse, L., C. Clerbaux, F. Dentener, D. Hurtmans, and P.-F. Coheur, 2009. Global ammonia distribution derived from infrared satellite observations, *Nature Geosci*, 2 (7), 479-483.

Coceal, O., and S. E. Belcher, 2005: Mean wind through an inhomogeneous urban canopy. *Bound.-Layer Meteor.*, **115**, 47–68.

Coceal, O., T.G. Thomas, I.P. Castro and S.E. Belcher. 2006. Mean flow and turbulence statistics over groups of urban-like cubical obstacles. *Boundary-*

Layer Meteorology. 125, 537-552.

Cohan, D.S., Hu, Y., Russell, A.G., 2006. Dependence of ozone sensitivity analysis on grid resolution. *Atmos. Env.* 40, 126-135.

Cope, M.E., G.D. Hess, S. Lee, K.J. Tory, M. Burgers, P. Dewundege and M. Johnson. 2005. The Australian Air Quality Forecasting System: Exploring First Steps Towards Determining the Limits of Predictability for Short-Term Ozone Forecasting. *Boundary-Layer Meteorology*. 116, 363-384.

- Cote, J., S. Gravel, A. Methot, A. Patoine, M. Roch and A. Staniforth. 1998. The operational CMC-MRB Global Environmental Multiscale (GEM) model. Part 1: Design considerations and formulation. *Monthly Weather Review*, 126, 1373-1395.
- Coutts, A.M., J. Beringer and N.J. Tapper. 2007. Impact of Increasing Urban Density on Local Climate: Spatial and Temporal Variations in the Surface Energy Balance in Melbourne, Australia. *J. Appl. Met. Clim.* 46, 477-493.
- Crawford, B., A. Christen, T. R. Oke, J.A. Voogt and S. Grimmon, 2009. Carbon dioxide fluxes in two suburban neighborhoods in Vancouver, Canada. Paper J13.1 Proc. Of the AMS Eight Conference on the Urban Environment, Phoenix, AZ, January 11-15, 2009.
- Cuvelier, C., Thunis, P., Vautard, R., Amann, M., Bessagnet, B., Bedogni, M., Berkowicz, R., Brandt, J., Brocheton, F., Builtjes, P., Carnavale, C., Coppalle, A., Denby, B., Douros, J., Graf, A., Hellmuth, O., Hodzic, A., Honoré, C., Jonson, J., Kerschbaumer, A., de Leeuw, F., Minguzzi, E., Moussiopoulos, N., Pertot, C., Peuch, V.H., Pirovano, G., Rouil, L., Sauter, F., Schaap, M., Stern, R., Tarrason, L., Vignati, E., Volta, M., White, L., Wind, P., Zuber, A., 2007. CityDelta: A model intercomparison study to explore the impact of emission reductions in European cities in 2010. *Atmos. Env.* 41, 189-207.
- Dawson, J.P., Adams, P.J., Pandis, S.N., 2007. Sensitivity of ozone to summertime climate in the eastern USA: A modelling case study. *Atmos. Env.* 41, 1494-1511.
- Déqué, M., Rowell, D.P., Lüthi, D., Giorgi, F., Christensen, J.H., Rockel, B., Jacob, D., Kjellström, E., De Castro, M., Van Den Hurk, B., 2007. An intercomparison of regional climate simulations for Europe: Assessing uncertainties in model projections. *Climatic Change* 81, 53-70.
- Demuzere, M. and N.P.M. van Lipzig, 2010a. A new method to estimate air quality levels using a synoptic-regression approach. Part I: Present-day O₃ and PM₁₀ analysis. *Atmospheric Environment*, 44, 1341-1355.
- Demuzere, M. and N.P.M. van Lipzig, 2010b. A new method to estimate air quality levels using a synoptic-regression approach. Part II: Future O₃ concentrations. *Atmospheric Environment*, 44, 1356-1366.
- Deuzé, J. L., F. M. Bréon, C. Devaux, P. Goloub, M. Herman, B. Lafrance,
- F. Maignan, A. Marchand, F. Nadal, G. Perry, and D. Tanré, 2001. Remote sensing of aerosols over land surfaces from POLDER/ADEOS-1 polarized measurements. *J. Geophys. Res.*, 106, 4913-4926.

Diner, D.J., J.C. Beckert, T.H. Reilly, C.J. Bruegge, J.E. Conel, R.A. Kahn, J.V. Martonchik, T.P. Ackerman, R. Davies, S.A.W. Gerstl, H.R. Gordon, J.-P. Muller, R.B. Myneni, P.J. Sellers, B. Pinty, M.M. Verstraete, 1998. Multi-angle Imaging SpectroRadiometer (MISR) instrument description and experiment overview, *IEEE Trans. Geosci. Remote Sens.*, 36 (4), 1072-1087.

Drummond, J.R., and G.S. Mand, 1996. The Measurements of Pollution in the Troposphere (MOPITT) Instrument: Overall Performance and Calibration Requirements. *J. Atmos. Ocean. Tech.* 13, 314-320.

Dubovik, O., T. Lapyonok, Y.J. Kaufman, M. Chin, P. Ginoux, and A. Sinyuk, 2007. Retrieving global sources of aerosols from MODIS observations by inverting the GOCART model. *Am. Chem. Phys. Discuss.* 7, 3629-3718.

Dupont, S., T.L. Otte and J.K.S. Ching. 2004. Simulation of Meteorological Fields within and above Urban and Rural Canopies with a Mesoscale Model (MM5). *Boundary-Layer Meteorology.* 113, 111-158.

Edwards, D.P., 2006. Air quality remote sensing from space. *EOS Trans. AGU* 87, 327.

Eisinger, M., and J.P. Burrows, 1998. Tropospheric sulfur dioxide observed by the ERS-2 GOME instrument. *Geophys. Res. Lett.*, 25, 4177-4180.

Environment Canada, 2001. Precursor Contributions to Ambient Fine Particulate Matter in Canada. Government of Canada. pp 26 – 27.

Fan, H. and D.J. Sailor. 2005. Modelling the Impacts of Anthropogenic Heating on the Urban Climate of Philadelphia: A Comparison of Implementations in two PBL schemes. *Atmos. Env.* 39, 73-84.

Fast, J. 2005. Evaluation of the Boundary Layer Characteristics and Pollutants in Mexico City Predicted by WRF. WRF/MM5 Users' Workshop, Boulder, Colorado, USA. June 27-30, 2005.

Fiore, A. M., F.J. Dentener, O. Wild, C. Cuvelier, M.G. Schultz, P. Hess, C. Textor, M. Schulz, R.M. Doherty, L.W. Horowitz, I.A. MacKenzie, M.G. Sanderson, D.T. Shindell, D.S. Stevenson, S. Szopa, R. Van Dingenen, G. Zeng, C. Atherton, D. Bergmann, I. Bey, G. Carmichael, W.J. Collins, B.N. Duncan, G. Faluvegi, G. Folberth, M. Gauss, S. Gong, D. Hauglustaine, T. Holloway, I.S.A. Isaksen, D.J. Jacob, J.E. Jonson, J.W. Kaminski, T.J. Keating, A. Lupu, E. Marmer, V. Montanaro, R.J. Park, G. Pitari, K.J. Pringle, J.A. Pyle, S. Schroeder, M.G. Vivanco, P. Wind, G. Wojcik, S. Wu, and A. Zuber, 2009: Multimodel estimates of intercontinental source-receptor relationships for ozone pollution. *J. Geophys. Res.*, **114**, D04301, doi:10.1029/2008JD010816.

Fisher, B., J. Kukkonen, M. Piringer, M.W. Rotach and M. Schatzmann. 2006. *Meteorology Applied to Urban Air Pollution Problems: Concepts from COST 715*. *Atmos. Chem. Phys.* 6, 555-564.

Fishman, J., K.W. Bowman, J.P. Burrows, A. Richter, K.V. Chance, D.P. Edwards, R.B. Martin, G.A. Morris, R.B. Peirce, J.R. Ziemke, J.A. Al-Saadi, J.K. Creilson, T.K. Schaack, A. M Thompson, 2008. Remote sensing of tropospheric pollution from space, *Bull. Am. Meteorol. Soc.*, 89 (6), 805-821.

Fishman, J., A.E. Wozniak, and J.K. Creilson, 2003. Global distribution of tropospheric ozone from satellite measurements using the empirically corrected tropospheric ozone residual technique: Identification of the regional aspects of air pollution. *Atmos. Chem. Phys.* 3, 893-907.

Fishman, J., and V.G. Brackett, 1997. The climatological distribution of tropospheric ozone derived from satellite measurements using version 7 Total Ozone Mapping Spectrometer and Stratospheric Aerosol and Gas Experiment data sets. *J. Geophys. Res.* 102, 19275-19278.

Fishman, J., C.E. Watson, J.C. Larsen, and J.A. Logan, 1990. Distribution of tropospheric ozone determined from satellite data. *J. Geophys. Res.* 95, 3599-3617.

Forkel, R., Knoche, R., 2006. Regional climate change and its impact on photooxidant concentrations in southern Germany: Simulations with a coupled regional climate-chemistry model. *J. Geophys. Res. D: Atmospheres* 111, D12302 1-13.

Forkel, R., Knoche, R., 2007. Nested regional climate-chemistry simulations for central Europe. *Compt. Rendus Geosci.* 339, 734-746.

Fu, T.-M., D.J. Jacob, P.I. Palmer, K. Chance, Y.X. Wang, B. Barletta, D.R. Blake, J.C. Stanton, and M.J. Pilling, 2007. Space-based formaldehyde measurements as constraints on volatile organic compound emissions in East and South Asia. *J. Geophys. Res.*, 112, D06312, doi: 10.1029/2006JD007853.

Garratt, J.R., 1992. *The Atmospheric Boundary Layer*, Cambridge University Press, Cambridge, U.K., 316 pp.

Giorgi, F. and F. Meleux, 2007. Modelling the regional effects of climate change on air quality. *Comptes Rendus Geosciences*, 339, 721-733.

Gomes, L. M. Mallet, J.C. Roger and P. Dubuisson. 2008. Effects of the physical and optical properties of urban aerosols measured during the CAPITOUL summer campaign on the local direct radiative forcing. *Meteorology and Atmospheric Physics.* 102, 289-306.

Grachev, A.A., L. Bariteau, C.W. Fairall, J. Hare, D. Helmig, J. Hueber and E.K. Lang. 2009. Turbulent Transfer and Mixing of Trace Gases in the Houston Urban Area and the Surrounding Coastal Zone of Gulf of Mexico during TexAQS 2006. Proceedings of the 89th Annual Meeting of the American Meteorological Society.

Grell, G., J. Dudhia, D. Stauffer. 1994. A Description of the Fifth Generation Penn State/NCAR Mesoscale Model (MM5). NCAR Tech. Note, TN-398 + STR, 117 pp.

Grimmond, C.S.B., H.A. Cleugh and T.R. Oke, 1991. An objective urban heat storage model and its comparison with other schemes. *Atmospheric Environment*, 25B, 311-326.

Grimmond, C.S.B., M. Blackett, M. Best, J.J. Baik, S. Belcher, S. Bohnenstengel, I. Calmet, F. Chen, A. Dandou, K. Fortuniak, M. Gouvea, R. Hamdi, M. Hendry, H. Kondo, S. Krayenhoff, S.-H. Lee, T. Loridan, A. Martilli, V. Masson, S. Miao, K. Oleson, G. Pigeon, A. Porson, F. Salamanca, G.-J. Steeneveld, M. Tombrou, J. Voogt and N. Zhang. 2009. The International Urban Energy Balance Comparison Project: Initial Results from Phase 2. Proceedings of the Seventh International Conference on Urban Climate, Yokohama, Japan, 29 June – 3 July, 2009.

Hanna, S., J. White and Y. Zhou. 2007. Observed winds, turbulence, and dispersion in built-up downtown areas of Oklahoma City and Manhattan. *Boundary-Layer Meteorology*. 125, 441-468.

Hanna, S.R., R. Britter and P. Franzese. 2003. A Baseline Urban Dispersion Model Evaluated with Salt Lake City and Los Angeles Tracer Data. *Atmos. Env.* 37, 5069-5082.

Harman, I. and J.J. Finnigan. 2007. A Simple Unified Theory for Flow in the Canopy and Roughness Sublayer. *Boundary-Layer Meteorology*. 123, 339-363.

Harris, L. and V.R. Kotamarthi. 2005. The Characteristics of the Chicago Lake Breeze and its Effects on Trace Particle Transport: Results from an Episodic Event Simulation. *J. Appl. Meteor.* 44, 1637-1654.

Hastie, D. R., J. Narayan, C. Schiller, H. Niki, P. B. Shepson, D. M. L. Sills, P. A. Taylor, Wm. J. Moroz, J. W. Drummond, N. Reid, R. Taylor, P. B. Roussel, O. T. Melo, 1999. Observational evidence for the impact of the lake breeze circulation on ozone concentrations in southern Ontario. *Atmos. Env.*, 33 (2), 323-335.

Heald, C.L., D.J. Jacob, D.B.A. Jones, P.I. Palmer, J.A. Logan, D.G. Streets, G.W. Sachse, J.C. Gille, R.N. Hoffman, and T. Nehrkorn, 2004, Comparative inverse analysis of satellite (MOPITT) and aircraft (TRACE-P) observations to estimate Asian sources of carbon monoxide, *J. Geophys. Res.*, 109, (D23), D23306, doi:10.1029/2004JD005185

- Heald, C.L., D.J. Jacob, P.I. Palmer, M.J. Evans, G.W. Sachse, H. Singh, and D.R. Blake, 2003. Biomass burning emission inventory with daily resolution: application to aircraft observations of Asian outflow. *J. Geophys. Res.*, 108, 8811, doi:10.1029/2002JD003082.
- Hess, G.D., K.J. Tory, M.E. Cope, S. Lee, K. Puri, P.C. Mannis and M. Young. 2004. The Australian Air Quality Forecasting System. Part II: Case Study of a Sydney 7-day Photochemical Smog Event. *J. Appl. Meteor.* 43, 663- 679.
- Hoff, R.M., N.B.A. Trivett, M.M. Millan, P. Fellin, K.G. Anlauf, H.A. Wiebe, and R. Bell, 1982. The Nanticoke shoreline diffusion experiment, June 1978 – III. Ground-based air quality measurements. *Atmospheric Environment*, 16, 439-454.
- Hoff, R.M., and S.A. Christopher, 2009. Remote sensing of particulate pollution from space: have we reached the promised land?, *J. Air. & Waste Manage. Assoc.*, 59 (6), 645-675.
- Hogrefe, C., Lynn, B., Civerolo, K., Ku, J.-., Rosenthal, J., Rosenzweig, C., Goldberg, R., Gaffin, S., Knowlton, K., Kinney, P.L., 2004. Simulating changes in regional air pollution over the eastern United States due to changes in global and regional climate and emissions. *J. Geophys. Res. D: Atmospheres* 109, D22301 1-13.
- Hogue, R., N. Benbouda, J. Mailhot, S. Belair, A. Lemonsu, Y. Yee, F. Lien, and J.D. Wilson. 2009. The Development of a Prototype of a Canadian Urban Flow and Dispersion Modelling System. Proceedings of the 89th Annual Meeting of the American Meteorological Society, Phoenix, Arizona, U.S.A., 10-15 January 2009.
- Holt, T.R. and J. Pullen. 2009. An Examination of Urban Heat Island and Sea Breeze Interactions Using High Resolution Coastal-Urban Mesoscale Ensembles. Proceedings of the Seventh International Conference on Urban Climate, Yokohama, Japan, 29 June – 3 July 2009.
- Hudson, R.D., and A.M. Thompson, 1998. Tropical tropospheric ozone from total ozone mapping spectrometer by a modified residual method. *J. Geophys. Res.* 103, 22129-22145.
- Huq, P., A. Carrillo, L.A. White, J. Redondo, S. Dharmavaram and S. Hanna. 2007. The Shear Layer above and in Urban Canopies. *J. Appl. Met. Clim.* 46, 368-376.
- IGOS-IGACO, 2004. An Integrated Global Atmospheric Chemistry Observation Theme for the IGOS Partnership, ESA SP-1282.

Nakicenovic, N. *et al* (2000). *Special Report on Emissions Scenarios: A Special Report of Working Group III of the Intergovernmental Panel on Climate Change*, Cambridge University Press, Cambridge, U.K., 599 pp. Available online at:

<http://www.grida.no/climate/ipcc/emission/index.htm>. See also IPCC (2000). *Emissions Scenarios*, N. Nakicenovic and R. Swart (Eds), Cambridge University Press, UK, pp 570.

IPCC, 2007: Summary for Policymakers. In: *Climate Change 2007: The Physical Science Basis. Contribution of Working Group I to the Fourth Assessment Report of the Intergovernmental Panel on Climate Change* [Solomon, S., D. Qin, M. Manning, Z. Chen, M. Marquis, K.B. Averyt, M. Tignor and H.L. Miller (eds.)]. Cambridge University Press, Cambridge, pp. 12–17.

Ishida, Y., Y. Endo, A. Mochida, T. Shirasawa, R. Yoshie, H. Tanaka. 2009. Large Eddy Simulation of Flow and Pressure Fields around Buildings in High Dense Cities – Effects of nonuniformity of building heights on drag force and momentum transport. *Proceedings of the Seventh International Conference on Urban Climate*, Yokohama, Japan, 29 June – 3 July 2009.

Jacob, D.J. and Winner, D.A., 2009. Effect of climate change on air quality. *Atmospheric Environment*, 43, 51-63.

Jaeglé, L., L. Steinberger, R.V. Martin, and K. Chance, 2005. Global partitioning of NO_x sources using satellite observations: Relative roles of fossil fuel combustion, biomass burning and soil emissions. *Faraday Discussions* 130, 407-423, doi:10.1039/b502128f.

Jing, P., D.M. Cunnold, Y. Choi, and Y. Wang, 2006. Summertime tropospheric ozone columns from Aura OMI/MLS measurements versus regional model results over the United States. *Geophys. Res. Lett.*, 33, L17817, doi:10.1029/2006GL026473.

Jourdain, L., H. M. Worden, J. R. Worden, K. Bowman, Q. Li, A. Eldering, S. S. Kulawik, G. Osterman, K. F. Boersma, B. Fisher, C. P. Rinsland, R. Beer, and M. Gunson., 2007. Tropospheric vertical distribution of tropical Atlantic ozone observed by TES during the Northern African biomass burning season. *Geophys. Res. Lett.*, 34, L04810, doi:10.1029/2006GL028284

Kahn, R., P. Banerjee, and D. McDonald, 2001. The sensitivity of multiangle imaging to natural mixtures of aerosols over ocean. *J. Geophys. Res.* 106, 18219-18238.

Kanda, M., R. Moriwaki and Y. Kimoto. 2005. Temperature Profiles within and above an Urban Canopy. *Boundary-Layer Meteorology*. 115, 499-506.

- Kaufman, Y.J., C.O. Justice, L.P. Flynn, J.D. Kendall, E.M. Prins, L. Giglio, D.E. Ward, W.P. Menzel, and A.W. Setzer, 1998. Potential global fire monitoring from EOS-MODIS, *J. Geophys. Res.*, 103, 32215-32238.
- Kaufman, Y.J., C. Ichoku, and E.M. Prins, 2005. A method to derive smoke emission rates from MODIS fire radiative energy measurements, *IEEE Trans. Geosci. Remote Sens.*, 43 (11), 2636-2649, doi: 10.1109/tgrs.2005.857328.
- Keeler, J.M. and D.A.R. Kristovich. 2009. An Observational Study of the Movement of Lake Breeze Fronts in the Vicinity of Chicago, IL. Proceedings of the 89th Annual Meeting of the American Meteorological Society, Phoenix, Arizona, U.S.A., 10-15 January 2009.
- Kerman, B.R., R.E. Mickle, R.V. Portelli, N.B. Trivett and P.K. Misra, 1982. The Nanticoke shoreline diffusion experiment, June 1978 – II. Internal boundary layer structure. *Atmospheric Environment*, 16, 423-437.
- Kerschbaumer, A., R. Stern and M. Lutz. 2008. Origin and Influence of PM₁₀ Concentrations in Urban and in Rural Environments (in) *Air Pollution Modelling and Application XIX*, 72-80, Borrego C and Miranda A.I. Eds., Springer: Dordrecht.
- Khiem, M. R. Ooka, H. Huang, H. Hayami and H. Yoshikado. 2009. Analysis of Relationship between changes of Meteorological Conditions and the Variation of O₃ Levels in Summer over the Central Kanto Area.
- Kikegawa, Y., Y. Genchi, H. Yoshikado and H. Kondo. 2003. Development of a Numerical Simulation System toward Comprehensive Assessments of Urban Warming Countermeasures Including their Impacts upon the Urban Buildings' Energy-Demands. *Applied Energy*, 76, 449-466.
- Kitada, T., A. Sofyan and G. Kurata. 2008. Numerical Simulation of Air Pollution Transport Under Sea/Land Breeze Situation in Jakarta, Indonesia in Dry Season (in) *Air Pollution Modelling and Application XIX*, 243-251, Borrego C and Miranda A.I. Eds., Springer: Dordrecht.
- Kim, J.H., M.J. Newchurch, and K. Han, 2001. Distribution of tropical tropospheric ozone determined by the scan-angle method applied to TOMS measurements. *J. Atmos. Sci.* 58, 2699-2708.
- Kim, M.-W., J.-J. Baik and S.H. Park. 2009. Modelling Aerosol Dispersion in a Street Canyon Using a Coupled CFD-Aerosol Model. Proceedings of the Seventh International Conference on Urban Climate, Yokohama, Japan, 29 June – 3 July 2009.

- Kim, S-W., A. Heckel, S. A. McKeen, G. J. Frost, E.-Y. Hsie, M. K. Trainer, A. Richter, J. P. Burrows, S. E. Peckham, and G. A. Grel, 2006. Satellite observed U.S. power plant NO_x emission reductions and their impact on air quality. *Geophys. Res. Lett.*, 33, L22812, doi:10.1029/2006GL027749.
- King, M.D., Y.J. Kaufman, D. Tanré, and T. Nakajima, 1999. Remote sensing of tropospheric aerosols from space: Past, present, and future. *Bull. Am. Meteorol. Soc.* 80, 2229-2259.
- Kinne, S., U. Lohmann, J. Feichter, M. Schulz, C. Timmreck, S. Ghan, R. Easter, M. Chin, P. Ginoux, T. Takemura, I. Tegen, D. Koch, M. Herzog, J. Penner, G. Pitari, B. Holben, T. Eck, A. Smirnov, O. Dubovik, I. Slutsker, D. Tanre, O. Torres, M. Mishchenko, I. Geogdzhayev, D. A. Chu, and Y. Kaufman, 2003. Monthly Averages of Aerosol Properties: A Global comparison among models, satellite data and AERONET ground data. *J. Geophys. Res.*, 108 (D20), 4634,
- Khokhar, M.F., C. Frankenberg, S. Beirle, S. Köhl, M. Van Roozendael, A. Richter, U. Platt, and T. Wagner, 2005. Satellite observations of atmospheric SO₂ from volcanic eruptions during the time period of 1996 to 2002. *Adv. Space Res.* 36, 879-887.
- Klein, P. and J.V. Clark. 2007. Flow Variability in a North American Downtown Street Canyon. *J. Appl. Met. Clim.*. 46, 851-877.
- Klein, P. and J.V. Clark, 2007. Flow variability in a North American downstreet Canyon. *J. Appl. Meteor. Climatol.*, 46, 851-877.
- Klein, P., B. Leidl, and M. Schatzmann, 2007. Driving physical mechanisms of flow and dispersion in urban canopies. *Int. J. Climatol.*, 27, 1887-1907.
- Klenk, K.F., P.K. Bhartia, A.J. Fleig, V.G. Kaveeshwar, R.D. McPeters, and P.M. Smith, 1982. Total ozone determination from the backscattered ultraviolet (BUV) experiment. *J. Appl. Meteorol.* 21, 1672-1684.
- Koelemeijer, R.B.A., C.D. Homan, and J. Matthijsen, 2006. Comparison of spatial and temporal variations of aerosol optical thickness and particulate matter over Europe. *Atmos. Environ.* 40, 5304-5315.
- Konovalov, I.B., M. Beekmann, A. Richter, and J.P. Burrows, 2006. Inverse modelling of the spatial distribution of NO_x emissions on a continental scale using satellite data. *Am. Chem. Phys.* 6, 1747-1770.

- Knapp, K. R., Frouin, R., Kondragunta, S., Prados, A., 2005. Toward aerosol optical depth retrievals over land from GOES visible radiances: determining surface reflectance. *Int. J. Rem. Sens.* 26, (18), 4097-4116, doi: 10.1080/01431160500099329.
- Krotkov, N.A., B. McClure, R.R. Dickerson, S.A. Carn, C. Li, P.K. Bhartia, K. Yang, A.J. Krueger, Z. Li, P.F. Levelt, H. Chen, P. Wang, D. Lu, 2008. Validation of SO₂ retrievals from Ozone Monitoring Instrument (OMI) over NE China, *J. Geophys. Res.*, 113, D16S40, doi:10.1029/2007JD008818.
- Krotkov, N.A., P.K. Bhartia, J.R. Herman, V. Fioletov, and J. Kerr, 1998. Satellite estimation of spectral surface UV irradiance in the presence of tropospheric aerosols - 1 - cloud-free case. *J. Geophys. Res.* 103, 8779-8793.
- Kunkel, K.E., Huang, H.-C., Liang, X.-Z., Lin, J.-T., Wuebbles, D., Tao, Z., Williams, A., Caughey, M., Zhu, J., Hayhoe, K., 2007. Sensitivity of future ozone concentrations in the northeast USA to regional climate change. *Mitig. Adapt. Strat. Glob. Change.* doi:10.1007/s11027-007-9137-y.
- Lamsal, L.N., R.V. Martin, M. Steinbacher, E.A. Celarier, E. Bucsela, E.J. Dunlea, and J. Pinto, 2007. Ground-level nitrogen dioxide concentrations inferred from the satellite-borne Ozone Monitoring Instrument. *J. Geophys. Res.*, 112, D2, doi:10.1029/2005JD006865.
- Langner, J., Bergstrom, R., Foltescu, V., 2005. Impact of climate change on surface ozone and deposition of sulphur and nitrogen in Europe. *Atmos. Environ.* 39, 1,129-1,141.
- Lee, B-S. and C-B. Chiou. 2007. The Use of CFC-12, CFC-11 and CH₃CCl₃ to Trace Terrestrial Airborne Pollutant Transport by Land-Sea Breezes. *Atmos. Env.* 41, 3360-3372.
- Lemonsu, A. and V. Masson, 2002. Simulation of a summer urban Breeze over Paris. *Boundary-Layer Meteorol.*, 104, 463-490.
- Lemonsu, A., S. Bélair, J. Mailhot, M. Benjamin, F. Chagnon, G. Morneau, B. Harvey, J. Voogt, M. Jean. 2008. Overview and First Results of the Montreal Urban Snow Experiment 2005. *J. Appl. Met. Clim.* 47, 59-75.
- Leroyer, S., J. Mailhot, S. Bélair, A. Lemonsu, I.B. Strachan. 2009. The Urban Surface Energy Budget During the Early Spring Period of the Montréal Urban Snow Experiment (2006). *Proceedings of the 89th Annual Meeting of the American Meteorological Society, Phoenix, Arizona, U.S.A., 10-15 January 2009.*
- Leue, C., M. Wenig, T. Wagner, O. Klimm, U. Platt, and B. Jahne, 2001. Quantitative analysis of NO_x emissions from GOME satellite image sequences. *J. Geophys. Res.* 106, 5493-5505.

- Leung, L.R., Gustafson Jr., W.I., 2005. Potential regional climate change and implications to U.S. air quality. *Geophys. Res. Lett.* 32, L16711 1-4.
- Levelt, P.F., G.H.J. van den Oord, M.R. Dobber, A. Mslkki, H. Visser, J. Vries, P. Stammes, J.O.V. Lundell, and H. Saari, 2006. The Ozone Monitoring Instrument. *IEEE Trans. Geosci. Remote Sens.*, doi:10.1109/TGRS.2006.872333.
- Li, Q.B., D.J. Jacob, R. Park, Y.X. Wang, C.L. Heald, R. Hudman, R.M. Yantosca, R.V. Martin, and M.J. Evans, 2005. Outflow pathways for North American pollution in summer: A global 3-D model analysis of MODIS and MOPITT observations. *J. Geophys. Res.* 110, D10301, 10.1029/2004JD005039.
- Li, X.-X., T.-Y. Koh, R. Britter, C.-H. Liu, L.K. Norford, D. Entekhabi and D.Y.C. Leung. 2009. Large-Eddy Simulation of Flow Field and Pollutant Dispersion in Urban Street Canyons Under Unstable Stratifications. *Proceedings of the Seventh International Conference on Urban Climate, Yokohama, Japan, 29 June – 3 July 2009.*
- Liao, H., J.H. Seinfeld, P.J. Adams, L.J. Mickley, 2004. Global radiative forcing of coupled tropospheric ozone and aerosols in a unified general circulation model. *J. Geophys. Res. D: Atmospheres* 109, D16207 1-33.
- Liao, H., Chen, W.-T., Seinfeld, J.H., 2006. Role of climate change in global predictions of future tropospheric ozone and aerosols. *J. Geophys. Res. D: Atmospheres* 111, D12304 1-18.
- Liao, H., Henze, D.K., Seinfeld, J.H., Wu, S., Mickley, L.J., 2007. Biogenic secondary organic aerosol over the United States: Comparison of climatological simulations with observations. *J. Geophys. Res. D: Atmospheres* 112, D06201 1-19.
- Liao, K.-J., E. Tagaris, K. Manomaiphiboon, C. Wang, J.-H. Woo, P. Amar, S. He and A.G. Russell, 2009. Quantification of the impact of climate uncertainty on regional air quality. *Atmos Chem. Phys.*, 9, 865-878.
- Lin, J.-T., K. O. Patten, X.-Z. Liang, and D. J. Wuebbles: Effects of future climate and biogenic emissions changes on surface ozone over the United States and China, *J. Appl. Meteor.* 47(7), 1888-1909, doi: 10.1175/2007JAMC1681.1, July 2008
- Liu, C.-H., W.C. Cheng and D.Y.C. Leung. 2009. Estimates of Air and Pollutant Exchange for Street Canyons in Combine Wind-Buoyancy Drive Flow using the RANS renormalization Group $k-\epsilon$ Turbulence model. *Proceedings of the 89th Annual Meeting of the American Meteorological Society.*

- Liu, Y., F. Chen, T. Warner, J. Basara. 2007a. Verification of a Mesoscale Data-Assimilation and Forecasting System for the Oklahoma City Area during the Joint Urban 2003 Field Project. *J. Appl. Met. Clim.*. 45, 912-929.
- Liu, Y., R. Kahn, and P. Koutrakis, 2007b. Estimating PM_{2.5} component concentrations and size distributions using satellite retrieved fractional aerosol optical depth: Part I - method development, *Journal of Air & Waste Management Association*, 57 (11), 1351-1359.
- Liu, J., J.R. Drummond, D.B.A. Jones, Z. Cao, H. Bremer, J. Kar, J. Zou, F. Nichituu, and J.C. Gille, 2006a. Large horizontal gradients in atmospheric CO at the synoptic scale as seen by spaceborne Measurements of Pollution in the Troposphere. *J. Geophys. Res.* 111, D02306, doi:10.1029/2005JD006076.
- Liu, X., K. Chance, C. E. Sioris, T. P. Kurosu, R. J. D. Spurr, R. V. Martin, T.-M. Fu, J. A. Logan, D. J. Jacob, P. I. Palmer, M. J. Newchurch, I. A. Megretskaia, and R. B. Chatfield, 2006b. First directly-retrieved global distribution of tropospheric column ozone: comparison with the GEOS-CHEM model. *J. Geophys. Res.* 111, D02308, doi:10.1029/2005JD006564.
- Liu, Y., J.A. Sarnat, V. Kilaru, D.J. Jacob, and P. Koutrakis, 2005. Estimating ground-level PM_{2.5} in the eastern United States using satellite remote sensing. *Environ. Sci. Technol.* 39, 3269-3278.
- Lo, J.C.F., A.K.H. Lau, F. Chen, J. Fung and K.K.M. Leung. 2007. Urban Modification in a Mesoscale Model and the Effects on the Local Circulation in the Pearl River Delta Region. *J. Appl. Met. Clim.*. 46, 457-476.
- MacDonald, R.W. 2000. Modelling the mean velocity profile in the urban canopy layer. *Boundary-Layer Meteorology*. 97, 25-45.
- MacDonald, R.W., R.F. Griffiths and S.C. Cheah. 1997. Field Experiments of Dispersion through Regular Arrays of Cubic Structures. *Atmos. Env.*. 31, 783-795.
- MacDonald, R.W., R.F. Griffiths and S.C. Cheah. 1997. Field experiments of dispersion through regular arrays of cubic structures. *Atmos. Env.*. 31, 783-795.
- Makar, P.A., V.S. Bouchet, W. Gong, M.D. Moran, S. Gong, A.P. Dastoor, K. Hayden, H. Boudries, J. Brook, K. Strawbridge, K. Anlauf, S.-M. Li. 2004. "AURAMS/Pacific 2001 Measurement Intensive comparison." Proceedings of the 27th NATO/CCMS ITM on Air Pollution Modelling and its Application, Banff, Canada, Oct. 25-29.
- Makar, P.A., C. Stroud, B. Wiens, S. Cho, J. Zhang, M. Sassi, J. Liggio, M. Moran, W. Gong, S. Gong, S.-M. Li, J. Brook, K. Strawbridge, K. Anlauf, C. Mihele and D. Toom-Sauntry. 2008.

High Resolution Nested Runs of the AURAMS Model with Comparisons to PrAIRie2005 Field Study Data (in) Air Pollution Modelling and Application XIX, 163-172, Borrego C and Miranda A.I. Eds., Springer: Dordrecht.

Makar, P.A., S. Gravel, V. Chrikov, K.B. Strawbridge, F. Froude, J. Arnold and J. Brook. 2006. Heat Flux, Urban Properties, and Regional Weather. *Atmos. Env.* 40, 2750-2766.

Mao, Q., L.L. Gautney, T.M. Cook, M.E. Jacobs, S.N. Smith and J.J. Kelsoe. 2006. Numerical Experiments on MM5-CMAQ sensitivity to various PBL schemes. *Atmos. Env.* 40, 3092-3110.

Martilli, A. 2002. Numerical Study of Urban Impact on Boundary Layer Structure: Sensitivity to Wind Speed, Urban Morphology, and Rural Soil Moisture. *J. Appl. Meteor.* 41, 1247-1266.

Martilli, A. 2003. A Two-Dimensional Numerical Study of the Impact of a City on Atmospheric Circulation and Pollutant Dispersion in a Coastal Environment. *Boundary-Layer Meteorology*. 108, 91-119.

Martin, R.V. 2008. Satellite remote sensing of surface air quality, *Atmos. Environ.*, 42, 7823-7843.

Martin, R.V., A.M. Fiore, and A. van Donkelaar, 2004. Space-based diagnosis of surface ozone sensitivity to anthropogenic emissions. *Geophys. Res. Lett.* 31, L06120, doi:10.1029/2004GL019416.

Martin, R.V., D.J. Jacob, K. Chance, T.P. Kurosu, P.I. Palmer, and M.J. Evans, 2003. Global inventory of nitrogen oxide emissions constrained by space-based observations of NO₂ columns. *J. Geophys. Res.* 108, 4537, doi:10.1029/2003JD003453.

Martin, R.V., C. E. Sioris, K. Chance, T. B. Ryerson, T. H. Bertram, P. J. Wooldridge, R. C. Cohen, J. A. Neuman, A. Swanson, and F. M. Flocke, 2006. Evaluation of space-based constraints on nitrogen oxide emissions with regional aircraft measurements over and downwind of eastern North America. *J. Geophys. Res.*, D15308, doi:10.1029/2005JD006680.

Martonchik, J.V., D.J. Diner, R.A. Kahn, B.J. Gaitley, and B.N. Holben, 2004. Comparison of MISR and AERONET aerosol optical depths over desert sites. *Geophys. Res. Lett.* 31, L16102, doi:10.1029/2004GL019807.

Maruyama, T., 1999: Surface and inlet boundary conditions for the simulation of turbulent boundary layer over complex rough surface. *J. Wind. Eng. Ind. Aerodyn.*, 81, 311-322.

- Masson, V., L. Gomes, G. Pigeon, C. Liousse, V. Pont, J.-P. Lagourade, J. Voogt, J. Salmond, T.R. Oke, J. Hidalgo, D. Legain, O. Garrouste, C. Lac, O. Connan, X. Briottet, S. Lachérade and P. Tulet. 2008. The Canopy and Aerosol Particles Interactions in TOulouse Urban Layer (CAPITOUL) experiment. *Meteorology and Atmospheric Physics*. 102, 135-157.
- Masson, V. 2000. A Physically-Based Scheme for the Urban Energy Budget in Atmospheric Models. *Boundary-Layer Meteorology*. 94, 357-397.
- Meleux, F., Solmon, F., Giorgi, F., 2007. Increase in European summer ozone amounts due to climate change. *Atmos. Environ.* 41, 7,577–7,587.
- Mestayer, P.G., P. Durand, P. Augustin, S. Bastin, J-M. Bonnefond, B. Bénech, B. Campistron, A. Coppalle, H. Delbarre, B. Dousset, P. Drobinski, A. Druilhet, E. Fréjafon, C.S.B. Grimmon, D. Groleau, M. Irvine, C. Kergomard, S. Kermadi, J-P. Lagouarde, A. Lemonsu, F. Lohou, N. Long, V. Masson, C. Moppert, J. Noilhan, B. Offerle, T.R. Oke, G. Pigeon, V. Puygrenier, S. Roberts, J-M. Rosant, F. Saïd, J. Salmond, M. Talbaut, and J. Voogt. 2005. The Urban Boundary-Layer Field Campaign in Marseille (UBL/CLU-ESCOMPTE): Set-Up and First Results. *Boundary-Layer Meteorology*. 114, 315-365.
- Michioka, T. and A. Sato. 2009. Numerical simulations of gas dispersion in a residential area. *Proceedings of the Seventh International Conference on Urban Climate, Yokohama, Japan, 29 June – 3 July 2009*.
- Mickley, L.J., Jacob, D.J., Field, B.D., Rind, D., 2004a. Climate response to the increase in tropospheric ozone since preindustrial times: A comparison between ozone and equivalent CO₂ forcings. *J. Geophys. Res. D: Atmospheres* 109, D05106 1-13.
- Mickley, L.J., Jacob, D.J., Field, B.D., Rind, D., 2004b. Effects of future climate change on regional air pollution episodes in the United States. *Geophys. Res. Lett.* 31, L24103 1-4.
- Millet, D.B., D.J. Jacob, T.-M. Fu, T.P. Kurosu, K. Chance, C.L. Heald, and A. Guenther, 2008. Spatial distribution of isoprene emissions from North America derived from formaldehyde column measurements by the OMI satellite sensor. *J. Geophys. Res.*, 113, D02307, doi: 10.1029/2007JD008950.
- Millet, D. B., D. J. Jacob, S. Turquety, R. C. Hudman, S. Wu, A. Fried, J. Walega, B. G. Heikes, D. R. Blake, H. B. Singh, B. E. Anderson, and A. D. Clarke., 2006. Formaldehyde distribution over North America: Implications for satellite retrievals of formaldehyde columns and isoprene emission. *J. Geophys. Res.* 111, D24S02, doi:10.1029/2005JD006853.

Mishchenko, M.I., B. Cairns, G. Kopp, C.F. Schueler, B.A. Fafaul, J.E. Hansen, R.J. Hooker, T. Itchkawich, H.B. Maring, L.D. Travis, 2007. Accurate monitoring of terrestrial aerosols and total solar irradiance: introducing the Glory Mission, *Bull. Am. Meteorol. Soc.*, 88, 677-691.

Monin, A. and A. Obukhov. 1954. Basic laws of turbulent mixing in the atmosphere near the ground. *Tr. Akad. Nauk SSSR Geofiz. Inst.* 24, 151, 163-87.

Müller, J.-F., and T. Stavrakou, 2005. Inversion of CO and NO_x emissions using the adjoint of the IMAGES model. *Am. Chem. Phys.* 5, 1157-1186.

Müller, M.D., A.K. Kaifel, M. Weber, S. Tellmann, J.P. Burrows, and D. Loyola, 2003. Ozone profile retrieval from Global Ozone Monitoring Experiment (GOME) data using a neural network approach (Neural Network Ozone Retrieval System (NNORSY)). *J. Geophys. Res.* 108, 4497, doi:10.1029/2002JD002784.

Murazaki, K., Hess, P., 2006. How does climate change contribute to surface ozone change over the United States?. *J. Geophys. Res. D: Atmospheres* 111, D05301 1-16.

Murphy, J.M., Sexton, D.M.H., Barnett, D.N., Jones, G.S., Webb, M.J., Collins, M., Stainforth, D.A., 2004. Quantification of modelling uncertainties in a large ensemble of climate change simulations. *Nature* 430, 768 - 772

Nakayama, H. T. Takemi and H. Nagai. 2009. LES Analysis of Plume Dispersion through Urban-Like Building Arrays. *Proceedings of the Seventh International Conference on Urban Climate, Yokohama, Japan, 29 June – 3 July 2009.*

National Academy of Science (2006), *Earth Science and Applications from Space: National Imperatives for the NExt Decade and Beyond*, National Academy Press, Washington, D. C.

Newchurch, M.J., D. Sun, J.H. Kim, and X. Liu, 2002. Tropical tropospheric ozone derived using Clear-Cloudy Pairs (CCP) of TOMS measurements. *Atmos. Chem. Phys.*, 3, 683-695.

Newchurch, M.J., X. Liu, and J.H. Kim, 2001. Lower-Tropospheric Ozone (LTO) derived from TOMS near mountainous regions. *J. Geophys. Res.* 106, 20403-20412.

Noilhan, J. M, and S. Planton. 1989. A simple parameterization of land surface processes for meteorological models. *Monthly Weather Review.* 117, 536-549.

Nolte, C.G., Gilliland, A.B., Hogrefe, C., Mickley, L.J., 2008. Linking global to regional models to assess future climate impacts on surface ozone levels in the United States. *J. Geophys. Res.* 113, D14307. Ordóñez, C., Mathis, H., Furger, M., Henne,

- Offerle, B., I. Eliasson, C.S.B. Grimmond and B. Holmer. 2007. Surface heating in Relation to Air Temperature, Wind and Turbulence in an Urban Street Canyon. *Boundary-Layer Meteorology*. 122, 273-292.
- Offerle, B., C.S.B. Grimmond and K. Fortuniak. 2005. Heat storage and anthropogenic heat flux in relation to the energy balance of a central European city centre. *International Journal of Climatology*, 25, 1405-1419.
- Ohashi, Y., Y. Genchi, H. Kondo, Y. Kikegawa, H. Yoshikado and Y. Hirano. 2007. Influence of Air-Conditioning Waste Heat on Air Temperature in Tokyo during Summer: Numerical Experiments using an Urban Canopy Model Coupled with a Building Energy Model. *J. Appl. Met. Clim.*. 46, 66-81.
- Ordonez, C., A. Richter, M. Steinbacher, C. Zellweger, H. Nuß, J.P. Burrows, and A.S.H. Prevot, 2006. Comparison of 7 years of satellite-borne and ground-based tropospheric NO₂ measurements around Milan, Italy. *J. Geophys. Res.* 111, D05310, doi:10.1029/2005JD006305.
- Pagowski, M., J. Hacker and D. Rostkier-Edelstein, 2006. Behavior of WRF BL Schemes and Land Surface Models in 1-D Simulations during BAMEX. 7th WRF Users' Workshop, Boulder, Colorado, USA, June 19-22, 2006.
- Palmer, P.I., D.J. Jacob, A.M. Fiore, R.V. Martin, K. Chance, and T.P. Kurosu, 2003a. Mapping isoprene emissions over North America using formaldehyde column observations from space. *J. Geophys. Res.* 108, 4180, doi:10.1029/2002JD002153.
- Palmer, P.I., D.J. Jacob, D.B. Jones, C.L. Heald, R.M. Yantosca, J.A. Logan, G.W. Sachse, and D. Streets, 2003b. Inverting for emissions of carbon monoxide from Asia using aircraft observations over the western Pacific. *J. Geophys. Res.* 108, 8828, doi:10.1029/2003JD003397.
- Peckham, S., G.A. Grell and S.A. McKeen. 2009. Description and application of a state-of-the-art online multi-scale air quality and weather prediction model (WRF/Chem). Proceedings of the American Meteorological Society 89th Annual Meeting, Phoenix, Arizona, U.S.A., 10-15 January 2009.
- Peikorz, G., 1987: Die Energiebilanz einer städtischen Struktur. Diplomarbeit, Department of Meteorology, Rheinische Friedrich-Wilhelms-Universität, Bonn, Germany.

- Petricoli, A., P. Bonasoni, G. Giovanelli, F. Ravegnani, I. Kostadinov, D. Bortoli, A. Weiss, D. Schaub, A. Richter, and F. Fortezza, 2004. First comparison between ground-based and satellite-borne measurements of tropospheric nitrogen dioxide in the Po basin. *J. Geophys. Res.* 109, D15307, doi:10.1029/2004JD004547.
- Pétron, G., C. Granier, B. Khattotov, V. Yudin, J.-F. Lamarque, L. Emmons, J. Gille, and D.P. Edwards, 2004. Monthly CO surface sources inventory based on the 2000–2001 MOPITT satellite data. *Geophys. Res. Lett.* 31, L21107, doi:10.1029/2004GL020560.
- Pfister, G. G., K. Emmons, P. G. Hess, R. Honrath, J.-F. Lamarque, M. V. Martin, R. C. Owen, M. A. Avery, E. V. Browell, J. S. Holloway, P. Nedelec, R. Purvis, T. B. Ryerson, G. W. Sachse, and H. Schlager, 2006. Ozone production from the 2004 North American boreal fires. *J. Geophys. Res.* 111, D24S07, doi:10.1029/2006JD007695.
- Pfister, G., P.G. Hess, L.K. Emmons, J.-F. Lamarque, C. Wiedinmyer, D.P. Edwards, G. Pétron, J.C. Gille, and G.W. Sachse, 2005. Quantifying CO emissions from the 2004 Alaskan wildfires using MOPITT CO data. *Geophys. Res. Lett.* 32, L11809, doi:10.1029/2005GL022995.
- Pigeon, G., D. Legain, P. Durand and V. Masson. 2007. Anthropogenic Heat Release in an old European Agglomeration (Toulouse, France). *International Journal of Climatology.* 27, 1969-1981.
- Pigeon, G., M.A. Moscicki, J.A. Voogt and V. Masson. 2008. Simulation of Fall and Winter Surface Energy Balance over a Dense Urban Area using the TEB Scheme. *Meteorology and Atmospheric Physics.* 102, 159-171.
- Piringer, M. and S. Joffre (eds). 2005. “The Urban Surface Energy Budget and Mixing Height in European Cities: Data, Models and Challenges for Urban Meteorology and Air Quality.” Final Report of Working Group 2 COST-715 Action. Sofia: Demetra Limited Publishers. 239p.
- Piringer, M., S. Joffre, A. Baklanov, A. Christen, M. Deserti, K. De Ridder, S. Emeis, P. Mestayer, M. Tombrou, D. Middleton, K.B. Stanzer, A. Dandou, A. Karppinen and J. Burzynski. 2007. The Surface Energy Balance and the Mixing Height in Urban Areas – Activities and Recommendations of COST-Action 715. *Boundary-Layer Meteorology.* 124, 3-24.
- Portelli, R.V., 1982. The Nanticoke shoreline diffusion experiment, June 1978 – I. Experimental design and program overview. *Atmospheric Environment,* 16, 413-421.
- Racherla, P.N., Adams, P.J., 2006. Sensitivity of global tropospheric ozone and fine particulate matter concentrations to climate change. *J. Geophys. Res.* 111, D24103.

- Racherla, P.N., Adams, P. J., 2008. The response of surface ozone to climate change over the Eastern United States. *Atmos. Chem. Phys.* 8, 871 – 885.
- Ramamurthy, P., E.R. Pardyjak and J.C. Klewicki. 2007. Observations of the Effects of Atmospheric Stability on Turbulence Statistics Deep within an Urban Street Canyon. *J. Appl. Met. Clim.*. 46, 2074-2085.
- Roberts, S.M., T.R. Oke, C.S.B. Grimmond, and J.A. Voogt, 2006. Comparison of four methods to estimate urban heat storage. *J Applied Meteorology and Climatology*, 45, 1766-1781.
- Robins, A., H. Smethurst and R. Mohan. 2008. DAPPLE (Dispersion of Air Pollution and its Penetration into the Local Environment) Experiments and Modelling. *HPA Chemical Hazards and Poisons Report*. 13, 24-28.
- Rotach, M.W., R. Vogt, C. Bernhofer, E. Batchvarova, A. Christen, A. Clappier, B. Feddersen, S-E. Gryning, H. Mayer, V. Mitev, T.R. Oke, E. Parlow, H. Richner, M. Roth, Y-A. Roulet, D. Ruffieux, J. Salmond, M. Schatzmann and J.A. Voogt. 2005. BUBBLE - An Urban Boundary Layer Project. *Theoretical Applied Climatology*. 81, 231-261.
- Roth, M. 2000. Review of atmospheric turbulence over cities. *Quarterly Journal of the Royal Meteorological Society*. 126, 941-990
- Sailor, D.J. 2009. Anthropogenic Heat and Moisture Emissions in the Urban Environment. *Proceedings of the 7th International Conference on Urban Climate, Yokohama, Japan, 29 June – 3 July 2009*.
- Sailor, D.J., A. Brooks, M. Hart and S. Heiple. 2007. A Bottom-Up Approach for Estimating Latent and Sensible Heat Emissions from Anthropogenic Sources. *Proceedings of the 7th Symposium on the Urban Environment, San Diego, California, U.S.A., 10-13 September 2007*.
- Sailor, D.J. and L. Lu. 2004. A Top-Down Methodology for Developing Diurnal and Seasonal Anthropogenic Heating Profiles for Urban Areas. *Atmos. Env.*. 38, 2737-2748.
- Salmond, J.A., T.R. Oke, C.S.B. Grimmond, S. Roberts and B. Offerle. 2005. Venting of Heat and Carbon Dioxide from Urban Canyons at Night. *J. Appl. Meteor.*. 44, 1180-1194
- San Jose, R., J.L. Pérez, J. L. Morant and R. M. González. 2008. Advances on Real-Time Air Quality Forecasting Systems for Industrial Plants and Urban Areas using the MM5-CMAQ-EMIMO (in) *Large-Scale Scientific Computing*, 450-457, Lirkov, I., Margenov, S. and Waśniewski J. Eds., Springer: Berlin.

Sarkar, A., R.S. Saraswat and A. Chandrasekar, 1998. Numerical Study of the Effects of Urban Heat Island on the Characteristic Features of the Sea Breeze Circulation. Proceedings of the Indian Academy of Sciences (Earth and Planetary Sciences). 107, 127-137.

Seinfeld, J.H., Pandis, S.P., 1998. Atmos. Chem. Phys.: From Air Pollution to Climate Change. Wiley-Interscience Publication, New York, pp. 1139-1184.

Sillman, S., 1999. The relation between ozone, NO_x, and hydrocarbons in urban and polluted rural environments. Atmos. Environ. 33, 1821-1845.

Sills, D., J. Brook and P. Taylor, 2008: Lake Breezes in Southwestern Ontario and Their Influence During BAQS-Met 2007. *Invited Presentation, AGU Fall Meeting, December 15-19, San Francisco, CA.*

Singh, H.B., W.H. Brune, J.H. Crawford, and D.J. Jacob, 2008. Chemistry and transport of pollution over the Gulf of Mexico and the Pacific: Spring 2006 INTEX-B campaign overview and first results, Atmos. Chem. Phys., 9, 2301-2318.

Skamarock, W.C., J.B. Klemp, J. Dudhia, D.O. Gill, D.M. Barker, W. Wang and J.G. Powers. 2007. A Description of the Advanced Research WRF Version 2, NCAR Technical Note NCAR/TN-468 + STR, NCAR, Boulder, CO, USA.

Solazzo, E. and R.E. Britter. 2007. Transfer Processes in a Simulated Urban Street Canyon. Boundary-Layer Meteorology. 124, 43-60.

Srinivas, C.V., R. Venkatesan and A. B. Singh. 2007. Sensitivity of Mesoscale Simulations of Land-Sea Breeze to Boundary Layer Turbulence Parameterization. Atmos. Env.. 41, 2534-2548.

Staniforth, D.A., Alna, T., Christenson, C., Collins, M., Faull, N., Frame, D.J., Kettleborough, J.A., Knight, S., Martin, A., Murphy, J.M., Piani, C., Sexton, D., Smith, L.A., Spicer, R.A., Thorpe, A.J., Allen, M.R., 2005. Uncertainty in predictions of the climate response to rising levels of greenhouse gases. Nature 433, 403 – 406.

Steiner, A.L., Tonse, S., Cohen, R.C., Goldstein, A.H., Harley, R.A., 2006., Influence of future climate and emissions on regional air quality in California. J. Geophys. Res. D: Atmospheres 111, D18303 1-22.

Stevenson, D.S., Dentener, F.J., Schultz, M.G., Ellingsen, K., van Noije, T.P.C., Wild, O., Zeng, G., Amann, M., Atherton, C.S., Bell, N., Bergmann, D.J., Bey, I., Butler, T., Cofala, J., Collins, W.J., Derwent, R.G., Doherty, R.M., Drevet, J., Eskes, H.J., Fiore, A.M., Gauss, M., Hauglustaine, D.A., Horowitz, L.W., Isaksen, I.S.A., Krol, M.C., Lamarque, J.-., Lawrence,

- M.G., Montanaro, V., Müller, J.-., Pitari, G., Prather, M.J., Pyle, J.A., Rast, S., Rodriguez, J.M., Sanderson, M.G., Savage, N.H., Shindell, D.T., Strahan, S.E., Sudo, K., Szopa, S., 2006. Multimodel ensemble simulations of present-day and near-future tropospheric ozone. *J. Geophys. Res. D: Atmospheres* 111, D08301 1-23.
- Streets, D.G., Q. Zhang, L. Wang, K. He, J. Hao, Y. Wu, Y. Tang, and G.R. Carmichael, 2006. Revisiting China's CO emissions after the Transport and Chemical Evolution over the Pacific (TRACE-P) mission: Synthesis of inventories, atmospheric modelling, and observations. *J. Geophys. Res.* 111, D14306, doi:10.1029/2006JD007118.
- Taha, H. 1999. Modifying a Mesoscale Meteorological Model to Better Incorporate Urban Heat Storage: A Bulk-Parameterization Approach. *J. Appl. Meteor.* 38, 466-473.
- Tagaris, E., Manomaiphiboon, K., Liao, K.-J., Leung, L.R., Woo, J.-H., He, S., Amar, P., Russell, A.G., 2007. Impacts of global climate change and emissions on regional ozone and fine particulate matter concentrations over the United States. *J. Geophys. Res.* 112, D14312.
- Tagaris, E., K.J. Liao, K. Manomaiphiboon, J.-H. Woo, S. He, P. Amar and A.G. Russell, The Role of Climate and Emission Changes in Future Air Quality over Northern Mexico and Southern Canada, 2008, *Atmospheric Chemistry and Physics*, 8, 3973-3983
- Taha, H. and R. Bornstein. 1999. Urbanization of Meteorological Models and Implications on Simulated Heat Islands and Air Quality. Invited Paper: Proceedings of the 15th International Congress of Biometeorology & International Conference on Urban Climatology. Eds: R. De Dear, J. Johnson and J. Potter, Nov. 8-12, 1999, Sydney, Australia. International
- Tewari, M., F. Chen, K.W. Manning, S. Grimmon, T. Lioridan, J.K. Ching and S.G. Miao. 2009. Numerical experiments using WRF/Urban Canopy Model over Houston region. Proceedings of the 89th Annual Meeting of the American Meteorological Society, Phoenix, Arizona, U.S.A., 10-15 January 2009.
- Thompson, W.T., T. Holt and J. Pullen. 2007. Investigation of a Sea Breeze Front in an Urban Environment. *Quarterly Journal of the Royal Meteorological Society.* 133, 579-594.
- Timbal, B., E. Fernandez, and Z. Li (2009), Generalization of a statistical downscaling model to provide local climate change projections for Australia. *Environmental Modelling & Software*, 24, 341-358.
- Torres, O., A. Tanskanen, B. Veihelmann, C. Ahn, R. Braak, P.K. Bhartia, J.P. Veefkind, and P.F. Levelt, 2007. Aerosols and surface UV products from Ozone Monitoring Instrument observations: An overview, *J. Geophys. Res.*, 112, D24S47, doi:10.1029/2007JD008809

- Trini Castelli, S., T.G. Reisin and G. Tinarelli. 2008. Development and Application of MicroRMS Modelling System to Simulate the Flow, Turbulence and Dispersion in the Presence of Buildings (in) Air Pollution Modelling and Application XIX, 81-89, Borrego C and Miranda A.I. Eds., Springer: Dordrecht.
- Urquizo, N., D. Spitzer, W. Pugsley and M. Robinson, 2009. Mapping small scale air pollution distribution using satellite observation in a large Canadian city. Environmental Sustainability. City of Ottawa.
- Valks, P.J.M., R.B.A. Koelemeijer, M. van Weele, P. van Velthoven, J.P.F. Fortuin, and H. Kelder, 2003. Variability in tropical tropospheric ozone: analysis with GOME observations and a global model. *J. Geophys. Res.* 108, 4328, doi:10.1029/2002JD002894.
- van der A, R.J., R.F. van Oss, A.J.M. Piters, J.P.F. Fortuin, Y.J. Meijer, and H.M. Kelder, 2002. Ozone profile retrieval from recalibrated Global Ozone Monitoring Experiment data. *J. Geophys. Res.* 107, 10.1029/2001JD000696.
- van Donkelaar, A., R.V. Martin, W.R. Leitch, A. M. MacDonald, T.W. Walker, D.G. Streets, Q. Zhang, E.J. Dunlea, J.L. Jimenez, J.E. Dibb, L.G. Huey, R. Weber, M.O. Andreae, 2008. Analysis of aircraft and satellite measurements from the Intercontinental Chemical Transport Experiment (INTEX-B) to quantify long-range transport of East Asian sulphur to Canada, *Atmos. Chem. Phys.*, 8, 2999-3014.
- van Donkelaar, A., R.V. Martin, and R.J. Park, 2006. Estimating ground-level PM_{2.5} with aerosol optical depth determined from satellite remote sensing. *J. Geophys. Res.* 111, D21201, doi:10.1029/2005JD006996.
- Venkatram, A., W. Qian, T. Zhan and M. Princevac. 2008. Comparison of Methods to Generate Meteorological Inputs for Modelling Dispersion in Coastal Areas (in) Air Pollution Modelling and Application XIX, 313-321, Borrego C and Miranda A.I. Eds., Springer: Dordrecht.
- Veron, D.E., N.P. Barton, A. Satinsky and E. Geiger. 2009. Observational Analysis and Simulation of the Delaware Sea/Bay Breeze. Proceedings of the 89th Annual Meeting of the American Meteorological Society, Phoenix, Arizona, U.S.A., 10-15 January 2009.
- Viana, M., C. Pérez, X. Querol, A. Alastuey, S. Nickovic and J. M. Baldasano. 2005. Spatial and Temporal Variability of PM levels and Composition in a Complex Summer Atmospheric Scenario in Barcelona (NE Spain). *Atmos. Env.* 39, 5343-5361.
- Voegt, J, T.R. Oke, O. Bergeron, N.R. Goodwin, S. Leroyer, B.R. Crawford, E. Christensen, B.E. Nanni, R. Tooke, D. van der Kamp, D. Aldred, S. Bélair, F. Chagnon, A. Christen, N. Coops, J. Mailhot, I. McKendry, I.B. Strachan, J. Wang, M. Benjamin, S. Grimmond, A.

- Lemonsu and V. Masson. 2009. The Environmental Prediction in Canadian Cities (EPiCC) network. Proceedings of the 89th Annual Meeting of the American Meteorological Society, Phoenix, Arizona, U.S.A., 10-15 January 2009.
- Wang, J., and S.A. Christopher, 2003. Intercomparison between satellite-derived aerosol optical thickness and PM_{2.5} mass: Implications for air quality studies. *Geophys. Res. Lett.* 30, 2095, doi:10.1029/2003GL018174.
- Wang, Y., M.B. McElroy, R.V. Martin, D.G. Streets, Q. Zhang, and T.-M. Fu, 2007. Seasonal variability of NO_x emissions over east China constrained by satellite observations: Implications for combustion and microbial sources. *J. Geophys. Res.* 112, D06301, doi:10.1029/2006JD007538.
- Weaver, C., A. da Silva, M. Chin, P. Ginoux, O. Dubovik, D. Flittner, A. Zia, L. Remer, B. Holben, W. Gregg, 2007. Direct insertion of MODIS radiances in a global aerosol transport model, *J. Atmos. Sci.*, 64, 808-826.
- Wespes, C., D. Hurtmans, C. Clerbaux, M.L. Santee, R.V. Martin, and P.F. Coheur, 2009. Global distributions of nitric acid from IASI/MetOP measurements, *Atmos. Chem. Phys.*, 9, 7949-7962.
- Winker, D.M., J. Pelon, and M.P. McCormick, 2003. The CALIPSO mission: Spaceborne lidar for observation of aerosols and clouds. *Proc. SPIE* 4893, 1-11.
- Wise, E.K., 2009. Climate-based sensitivity of air quality to climate change scenarios for the southwestern United States. *International Journal of Climatology*, 29, 87-97.
- Wittrock, F., A. Richter, H. Oetjen, J.P. Burrows, M. Kanakidou, S. Myriokefalitakis, R. Volkamer, S. Beirle, U. Platt, T. Wagner, 2006. Simultaneous global observations of glyoxal and formaldehyde from space, *Geophys. Res. Lett.*, 33, L16804, doi:10.1029/2006GL026310.
- Worden, J., X. Liu, K. Bowman, K. Chance, R. Beer, A. Eldering, M. Gunson, and H. Worden, 2007. Improved tropospheric ozone profile retrievals using OMI and TES radiances, *Geophys. Res. Lett.*, 34, L01809, doi:10.1029/2006GL027806.
- Wu, S., Mickley, L.J., Jacob, D.J., Logan, J.A., Yanyosca, R.M., Rind, D., 2007. Why are there large differences between models in global budgets tropospheric ozone?. *J. Geophys. Res. D: Atmospheres* 112, D05302 1-18.
- Wu, S., Mickley, L. J., Leibensperger, E. M., Jacob, Rind, D., Streets, D.G., 2008a. Effects of 2000 – 2050 global change on ozone air quality in the United States. *J. Geophys. Res. D: Atmospheres* 113, D06302 1 – 12.

Wu, S., Mickley, L. J., Jacob, D. J., Rind, D., Streets, D.G., 2008b. Effects of 2000 – 2050 changes in climate and emissions on global tropospheric ozone and the policy-relevant background surface ozone in the United States. *J. Geophys. Res. D: Atmospheres* 113, D18312 1 – 12.

Wyszogrodzki, A.A., F. Chen, S.G.Miao and J. Michalakes. 2009. Two-way coupling approach between WRF NWP and EULAG LES models for urban area transport and dispersion modelling. Proceedings of the 89th Annual Meeting of the American Meteorological Society, Phoenix, Arizona, U.S.A., 10-15 January 2009.

Yang, L. and Y Li. 2009. Ventilation Potential by Thermal Buoyancy in an Urban City: Numerical Simulation and Field Experiment Study. Proceedings of the Seventh International Conference on Urban Climate, Yokohama, Japan, 29 June – 3 July 2009.

Yang, Y. and Y. Shao. 2006. A Scheme for Scalar Exchange in the Urban Boundary Layer. *Boundary-Layer Meteorology*. 120, 111-132.

Yoshikado, H. 1992. Numerical Study of the Daytime Urban Effect and its Interaction with the Sea Breeze. *J. Appl. Meteor.* 31, 1146-1164.

Yuan, J., A. Venkatram and V. Isakov. 2006. Dispersion from Ground-Level Sources in a Shoreline Urban Area. *Atmos. Env.* 40, 1361-1372.

Zhang, L., D. J. Jacob, K.F., Boersma, D.A. Jaffe, J.R. Olson, K.W. Bowman, J.R. Worden, A. M. Thompson, M.A. Avery, R.C. Cohen, J.E. Dibb, F.M. Flocke, H.E. Fuelberg, L.G. Huey, W.W. McMillan, H.B. Singh, A.J. Weinheimer, 2008. Transpacific transport of ozone pollution and the effect of recent Asian emission increases on air quality in North America: an integrated analysis using satellite, aircraft, ozonesonde, and surface observations, *Atmos. Chem. Phys.*, 8 (20), 6117-6136.

Ziemke, J.R., S. Chandra, and P.K. Bhartia, 1998. Two new methods for deriving tropospheric column ozone from TOMS measurements; Assimilated UARS MLS/HALOE and convective-cloud differential techniques. *J. Geophys. Res.* 103, 22115-22127.

Ziemke, J.R., S. Chandra, B.N. Duncan, L. Froidevaux, P.K. Bhartia, P.F. Levelt, and J.W. Waters, 2006. Tropospheric ozone determined from Aura OMI and MLS: Evaluation of measurements and comparison with the Global Modelling Initiative's Chemical Transport Model. *J. Geophys. Res.* 111, D19303, doi:10.1029/2006JD007089

Chapter 9: Air Pollution from Intercontinental Transport (ICP) and Natural Sources

S.L. Gong

Contributing Authors: A.M. Macdonald and W.R. Leitch

KEY MESSAGES AND IMPLICATIONS

- Trans-Pacific transport affects Canadian air quality by increasing annual mean ozone (O_3) by 2-5 ppbv and mean sulphate by $0.1 \mu\text{g m}^{-3}$, while episodic influences can be even higher. The influence of trans-Pacific transport is highest in the spring, but distributed unevenly across the country, where the degree of impact in the west is about one order of magnitude higher than in eastern Canada.
- There are substantial increases in PM_{10} by dust from East Asia. The increase in anthropogenic $PM_{2.5}$ is primarily in sulphate. Any increase in organic $PM_{2.5}$ is below detectable limits.
- Natural sources affect air quality in Canada, where 20-30% of total annual PM is identified as being emitted from natural sources. Sources of natural emissions include dust aerosols (contributing $1-2 \mu\text{g m}^{-3}$ to the ambient spring PM in Canada), biomass burning (up to $1.0 \mu\text{g m}^{-3}$ in summer PM), and sea salt (contributing up to 20% of the ambient PM levels in coastal areas).
- Both trans-Pacific and natural contributions are episodic and have large seasonal and inter-annual variations.

9.1 Topic Introduction

Quantification of smog levels over the North American continent is complicated by the transport of particles and gases from other continents. The transport of particles and gases from Asia, Europe and Africa across the Pacific Ocean increases the background concentrations over North America (Fischer *et al.*, 2009; Gong *et al.*, 2006; Jacob *et al.*, 1999; Jaffe *et al.*, 1999). Conversely, North America contributes to global pollution levels with the aid of the prevailing atmospheric circulation that carries particles and gases away from the continent and over the Atlantic Ocean (Parrish *et al.*, 1993). Although some fraction of the pollution exported by North America across the Atlantic can circle the Northern Hemisphere and return to North America, this fraction is small in comparison to more direct sources, such as the trans-Pacific transport from Asia. The fast growing economy in Asia has both increased

the levels of pollution that reach North America and increased the difficulty with which their impact can be accurately quantified in a timely manner. In addition, pollutants such as sulphur and nitrogen compounds, persistent organic pollutants, lead and mercury from Eurasia can be transported to the North American Arctic through the trans-Arctic pathways in winter and early spring (Bottenheim *et al.*, 2004). This has increased the ambient levels of these compounds in the Arctic to levels comparable to polluted regions in North America. However, the impact of such trans-Arctic transport on the lower to the middle latitude North America is still rather small. Consequently, this chapter focuses on trans-Pacific transport of Asian pollutants.

The occurrence of trans-Pacific transport of trace gases and particles from the Eurasian continent to the northeast (NE) Pacific has been well established throughout the past two decades. The first evidence of such transport was reported by Andreae *et al.* (1988) who provided detailed airborne-based measurements of the long-range transport (LRT) of Eurasian emissions to the remote NE Pacific troposphere during May 1985. Many subsequent ground-based and airborne measurement campaigns have confirmed that under certain circumstances, pollutant gases including ozone (O₃), carbon monoxide (CO), radon, nitrogen oxides (NO_x), volatile organic compounds (VOCs), and particles of Eurasian origin (Cahill, 2003; Clarke *et al.*, 2004; Huebert *et al.*, 2003; Seinfeld *et al.*, 2004) may be transported to the NE Pacific within 5 to 6 days (Jaffe *et al.*, 2003; Jaffe *et al.*, 1999; Kotchenruther *et al.*, 2001; Kritz *et al.*, 1990; McKendry *et al.*, 2001; Parrish *et al.*, 1992; Price *et al.*, 2004; Price *et al.*, 2003). These pollutants may consequently influence the smog levels in North America (Jacob *et al.*, 1999; Jaffe *et al.*, 2004). Among the pollutants that are transported across the Pacific, the most distinguishable ones, either by surface monitoring or by satellite observations, are the soil dust and bio-mass burning from natural sources. They have contributed to noticeable increments in ambient particulate matter (PM) levels during episodic transport events reaching North America (Zhao *et al.*, 2007). Therefore, the contributions of natural sources to ambient PM are assessed also in the context of intercontinental transport.

9.2 Organization of the Chapter

This chapter will discuss the features of intercontinental transport (ICT) (Section 9.3), and the observational evidence of pollutant transport across the Pacific to North America in the form of monitoring data and intensive field campaign data up to the end of 2007 (Section 9.4). It will also evaluate results from modelling studies that assessed the enhancement of smog levels from both ICT and natural sources of pollutants (Section 9.5 and 9.6). The chapter concludes with a discussion of uncertainties (Section 9.7) and a summary of current understanding as well as recommendations for future research (Sections 9.8 and 9.9).

9.3 Features of ICT

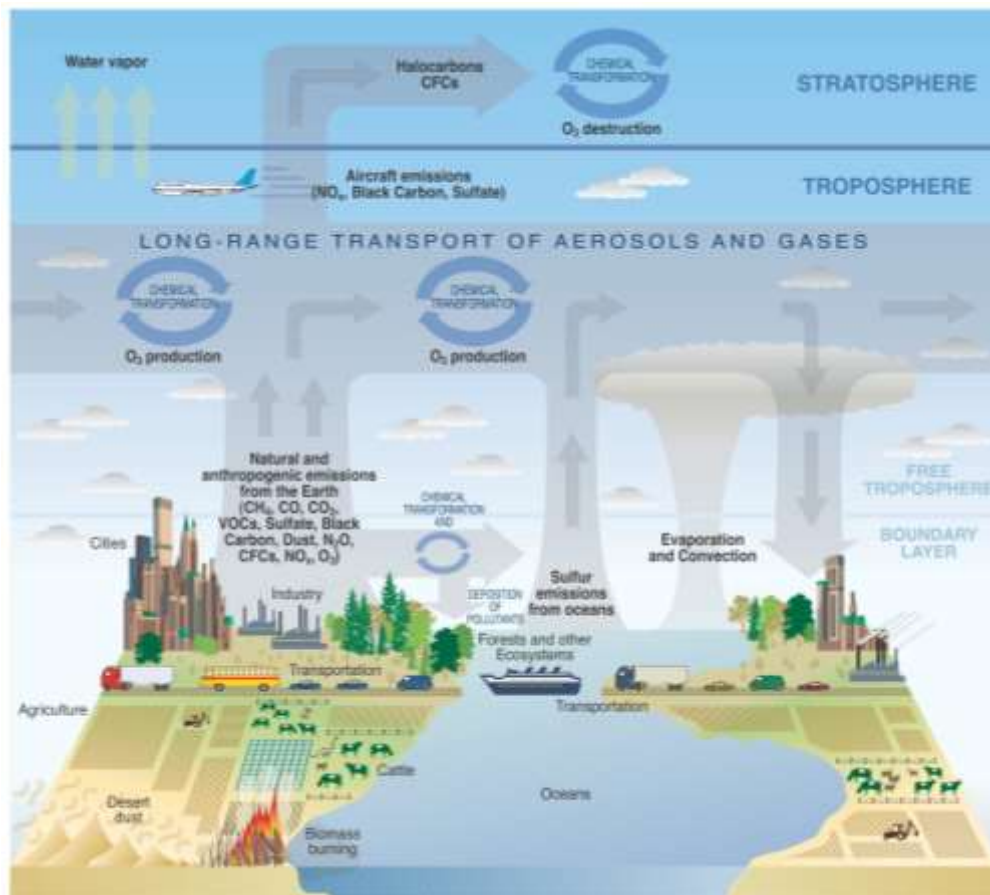


Figure 9.1 Chemical and transport processes related to atmospheric composition. These processes link the atmosphere with other components of the Earth system, including the oceans, land, and terrestrial and marine plants and animals. Credit: Climate Change Science Program Strategic Plan, 2005 (illustrated by P. Rekacewicz).

Figure 9.1 illustrates the main components and processes of trans-continental (e.g. trans-Pacific) transport of gases and PM. Many components of smog such as O₃ from NO_x, VOCs and sulphate from sulphur dioxide (SO₂) are formed from precursor gases that are en route from Asia to North America. Long-lived VOCs are also a source of organic carbon (OC) aerosols. An analysis of historical dust aerosol data combined with modelling results showed that the highest concentrations of particles and gases in the outflow from eastern Asia are found in the boundary layer (BL) (i.e. 0-2 km above the surface). Due to the wind direction and higher wind speeds, the strongest outflow fluxes are in the lower free troposphere (2-5 km above the surface) in spring time (Zhao *et al.*, 2006). Particles and gases reach a height above 2 km due to episodic lifting of pollution over central and eastern China ahead of eastward moving cold fronts. The combination of frontal lifting followed by westerly transport in the lower free troposphere is the principal process responsible for the export of anthropogenic

pollution, dust and biomass burning pollution from Asia (Bey *et al.*, 2001). Trans-Pacific transport of Asian pollution takes place mainly in the free troposphere with subsidence bringing the air down near North America (Jacob *et al.*, 1999; Yienger *et al.*, 2000). In contrast, export of North American pollutants over the Atlantic Ocean takes place in the lower troposphere year round. The shorter distance between North America and Europe and the prevailing westerly flow extending down to the surface favour trans-Atlantic transport in the BL. Trans-Atlantic transport in the middle and upper troposphere is important mostly during the summertime (Li *et al.*, 2002b).

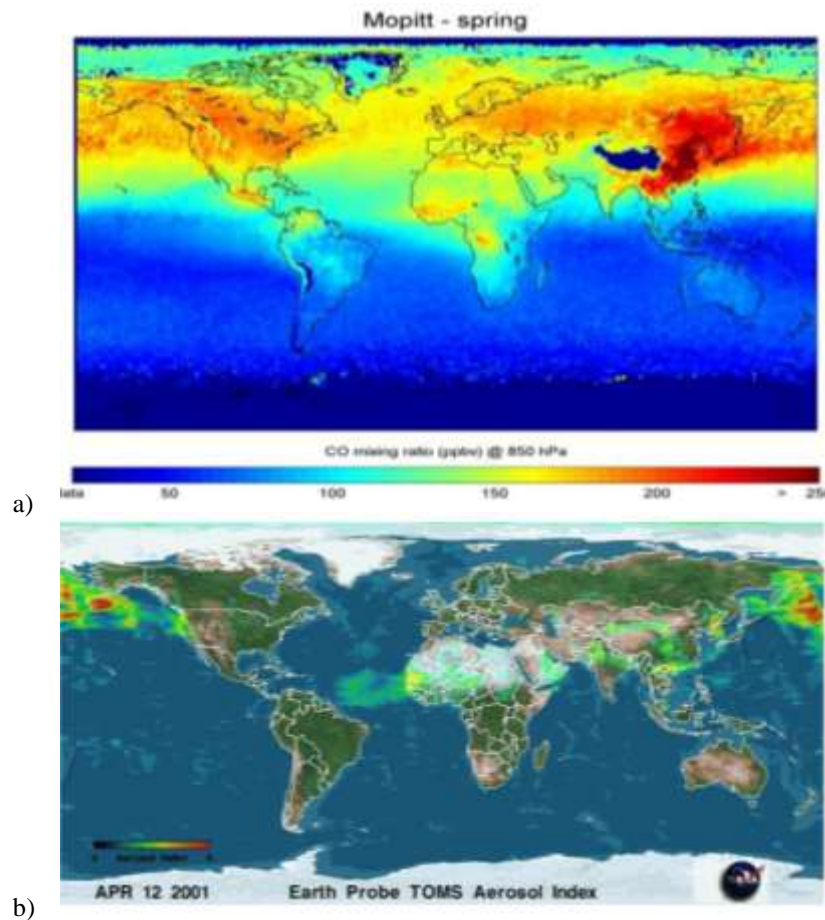


Figure 9.2 Satellite observation of (a) the Trans-Pacific Transport of Asian CO and (b) sand and dust storms.

Excellent pictures of the intercontinental transport of CO and dust aerosols have been captured from Measurements Of Pollution In The Troposphere (MOPITT) on the NASA EOS Terra satellite (Fig. 9.2a) and by the Total Ozone Monitoring Satellite Sensor (TOMS) on the Earth Probe Satellite (Fig. 9.2b), respectively. The TOMS AI (Aerosol Index) in Figure 9.2b represents the atmospheric column loading of absorbing aerosols such as dust and black carbon (BC) from biomass burning (Herman *et al.*, 1997). Figure 9.2b shows the well-

documented dust episode of April 2001 (Arimoto *et al.*, 2006), which was observed at North American surface monitoring stations (Cahill, 2003) and was simulated and compared with aircraft measurements (Gong *et al.*, 2003b).

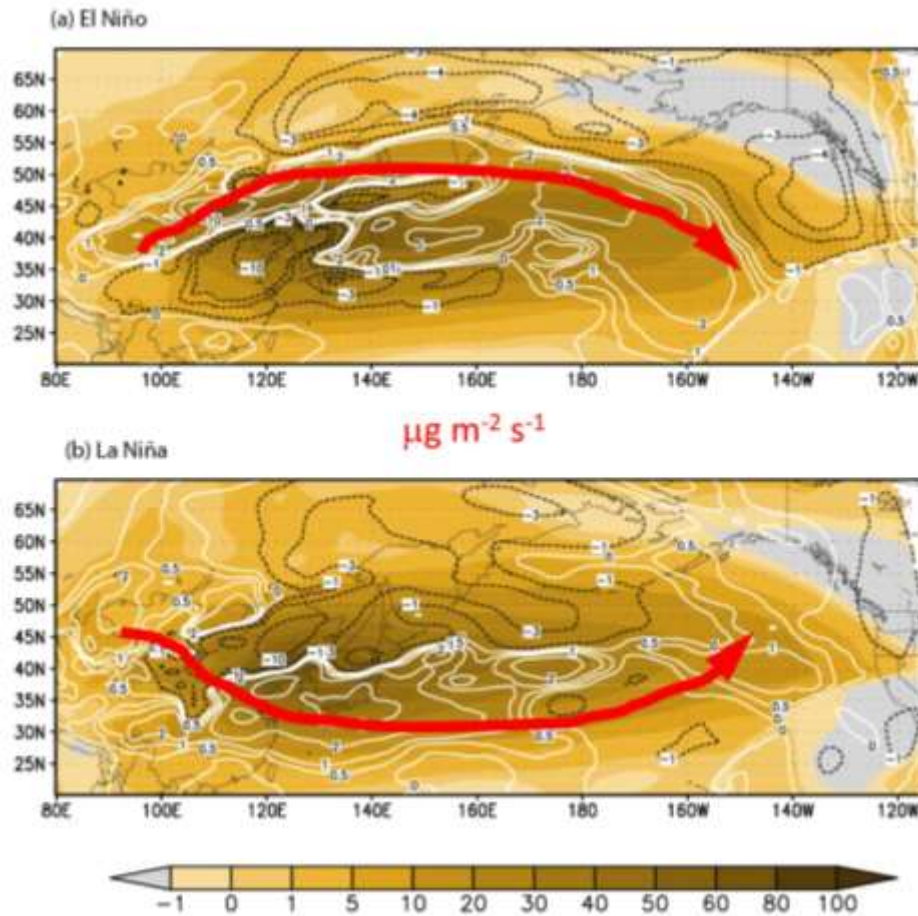


Figure 9.3 The zonal transport fluxes ($\text{mg m}^{-2} \text{s}^{-1}$) of Asian dust in spring of (a) 8 El Niño years (1966, 73, 83, 87, 87, 92, 98 and 2003) and (b) 8 La Niña years (1965, 71, 74, 76, 86, 89, 99 and 2000). The contour lines are for the anomalies relative to the 44-year mean of Asian dust aerosol in spring (Zhao *et al.*, 2006). The red dark arrow lines indicate the dominant pathways of intercontinental transport.

Intercontinental transport is also modulated by climate fluctuations (Liang *et al.*, 2005). Through a numerical modelling study of the transport of Asian dust to North America over the last 44 years, Gong *et al.* (2006) identified shifts in the intercontinental pathways for dust aerosols related to the El Niño Southern Oscillation. The developed phase of El Niño is characterized by a temperature elevation of a few degrees Celsius at the ocean surface extending from the coasts of Peru and Ecuador to the center of the equatorial Pacific Ocean. A consequence of such warming is the long-term perturbation of the weather systems over the surrounding lands, notably heavy rains in usually dry areas, and drought in normally wet regions. Conversely to El Niño, the cold phase, La Niña, occurs with some cooling of the

surface waters in the equatorial Pacific Ocean. Analysis of the variability of the 44-year zonal mass transport flux (i.e. concentrations multiplied by westerly/easterly wind speeds) was conducted for eight typical El Niño and eight La Niña years. Figures 9.3 (a) and (b) show the averaged dust transport flux (filled contours) integrated from 3 to 10 km above the surface for El Niño and La Niña years, respectively. On the same plot, the anomalies from the 44 year averaged values are also plotted as dashed contour lines.

As discussed above, most transport of Asian dust across the Pacific occurs in the middle troposphere (2-5 km above the surface) (Zhao *et al.*, 2006). However, a sharp difference between zonal transport during El Niño and La Niña years is evident in the centre of the transport path (Figure 9.3). During El Niño years, trans-Pacific transport is centred about 45° N while during La Niña years it is around 35° N. The zonal transport fluxes of Asian dust through 125° E in spring for the same El Niño and La Niña years indicate a shift of the main outflow point in Asia from 45° N to 40° N respectively. In the eastern Pacific (140° W) where the outflow reaches the coast of North America, the peak transport moves southward from 45° N to 40° N during El Niño years. The main transport heights also differ during El Niño (5000 m) and La Niña years (6500 m).

9.4 Observational Evidence

It has been documented that the Asian continent is a source of pollutants with the potential to influence North American background levels (Jaffe *et al.*, 1999). Asian dust plumes tracked by satellite have been observed to cause exceedances of air quality standards on the west coast of North America (Husar *et al.*, 2001). Large-scale field experiments such as the Aerosol Characterization Experiment (ACE-Asia) (Huebert *et al.*, 2003) and the NASA global TRANsport & Chemical Evolution over the Pacific (TRACE-P) campaigns have clearly shown the outflows of various gases and aerosols with elevated concentrations (Seinfeld *et al.*, 2004). Recently, the Intercontinental Chemical Transport Experiment (INTEX-B) over the Northeast Pacific examined the evolution and transport of the Asian plume to North America with the objective of assessing its implications on regional air quality.

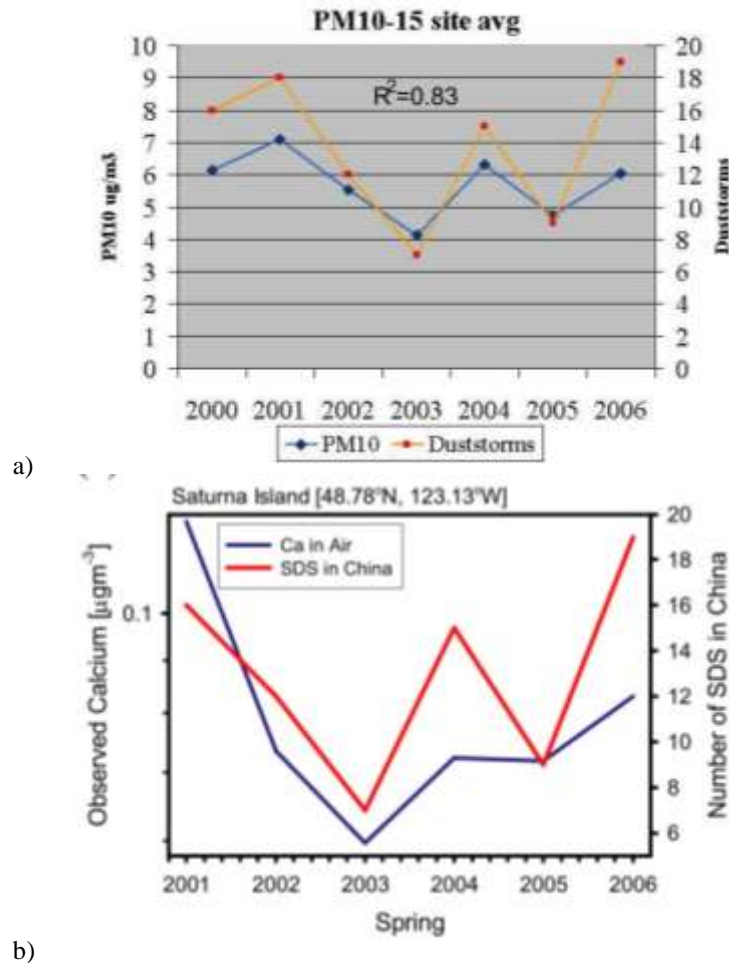


Figure 9.4 (a) Time series of spring mean PM_{10} concentrations at 15 sites in the western U.S and the total SDS process numbers in China from spring 2000 to 2006. The 15 sites are Bliss State Park, CA; Bridger Wilderness, WY; Columbia River, WA; Crater Lake, OR; Craters of the Moon, ID; Lassen, CA; Mt. Rainier, WA; Pinnacles, CA; Redwood NP, CA; Sawtooth NF, ID; Snoqualimie Pass, WA; Sula Peak, MT; Three Sisters, OR; Yellowstone, WY; and Yosemite, CA. (b) Same as in Figure 9.4(a) but for spring mean Ca concentrations contained in aerosols collected at Saturna Island, Canada, from 2001 to 2006.

Trans-Pacific transport of pollutants is episodic and occurs most frequently in the spring (Yienger *et al.*, 2000). Figure 9.4a shows the time series of the annual spring mean PM_{10} concentration at 15 American IMPROVE (Interagency Monitoring of Protected Visual Environments) sites, along with the total SDS (Sand and Dust Storm) process numbers in China each year (Zhao *et al.*, 2007). The SDS process number is a quantitative index systematically characterizing the occurrence of SDS in Asia through surface observations at various sites and the accompanying weather system (Yang *et al.*, 2007). The correlation between the American spring mean PM_{10} concentrations and the Chinese SDS process number yields an R^2 value of 0.83 (over 7 years). This relationship was also observed between the surface calcium measurements at the Canadian CAPMoN station on Saturna Island (Figure

9.4b) and the annual Chinese SDS process number, with a smaller R^2 value of 0.34 (6 years). The results imply that the number of sand and dust storms in China has a significant influence on the variability in springtime background PM over much of western North America. Furthermore, episodic PM events can cause even more significant increases in local concentrations in western Canada and the United States (U.S.). The largest such event documented occurred in April 1998, causing hourly $PM_{2.5}$ to rise to $44 \mu\text{g m}^{-3}$ and PM_{10} to rise to $120 \mu\text{g m}^{-3}$ at Chilliwack, B.C. (BCEnvironment, 2002).

VanCuren and Cahill (2002) provided evidence for continuous influence of the Asian plume throughout the year. Through analysis of 1989-1998 monitoring data from the IMPROVE network, they found a nearly continuous Asian dust transport across the Pacific above the marine BL, contributing between 0.2 to $1.0 \mu\text{g m}^{-3}$ to $PM_{2.5}$ levels in the eastern Pacific and in western North America. They also illustrated that the west coast high elevation sites are impacted by Asian dust to a greater extent than lower elevation sites. Analysis by Jaffe *et al.* (2005) using data from pristine Crater Lake, Oregon, identified the background $PM_{2.5}$ component, also referred to as Combined Marine/Asian aerosol (CMA) to be approximately $2.0 \mu\text{g m}^{-3}$. CMA exhibited a seasonal cycle with higher concentrations during the summer and lower concentrations during the winter. Although no long-term trend has been observed in CMA since 1988 (Jaffe *et al.*, 2005), studies using the Community Multiscale Air Quality Model (CMAQ) suggest that Asia contributes 0.6 - $1.6 \mu\text{g m}^{-3}$ to monthly average $PM_{2.5}$ in western North America (Keating *et al.*, 2005).

Year-round measurements of particles and trace gases at high elevation sites have been made at Mount Bachelor, Oregon (Weiss-Penzias *et al.*, 2006) and at Whistler, British Columbia (Harner *et al.*, 2006; Macdonald *et al.*, 2006; McKendry *et al.*, 2007). Import of total gaseous mercury (TGM) and CO has been observed at Mount Bachelor during Asian transport events. During spring 2004, specific transport events were identified based on the ratios of changes in TGM to changes in CO (Weiss-Penzias *et al.*, 2006). The ratio of TGM to CO enhancements during these events was similar to that found in plumes directly downwind of Asia.

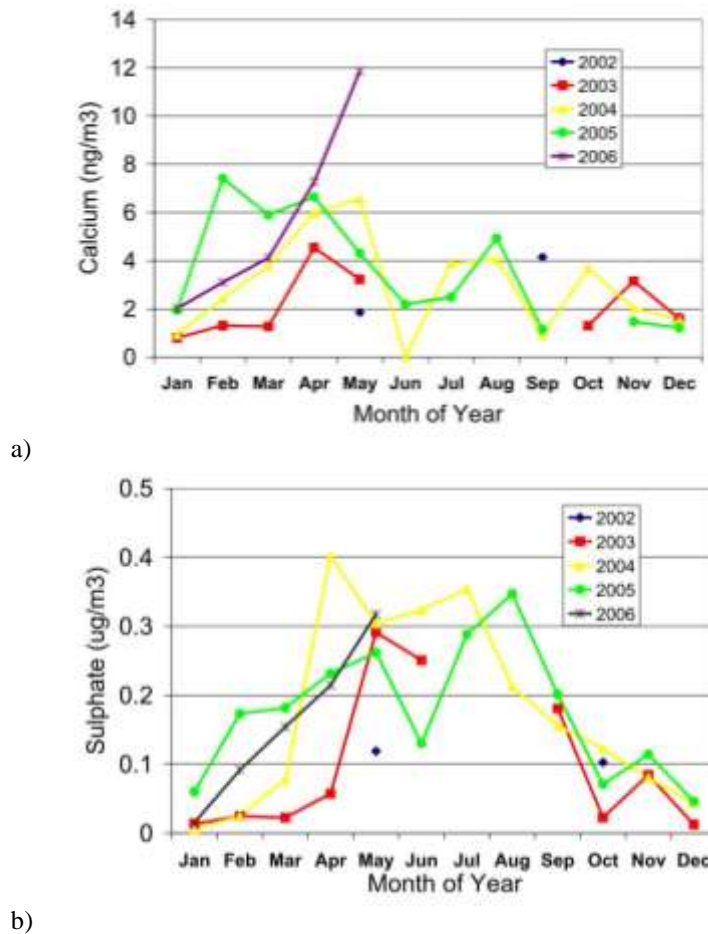


Figure 9.5 Monthly averages of (a) calcium and (b) sulphate less than 2.5 µm, collected at Whistler from 2002-2006.

Particle chemical and physical properties studied at the Whistler site yield information on the seasonal and inter-annual variability of fine aerosol composition. Dust events, identified by the presence of coarse mode aerosol and calcium, occur most often in springtime. It appears that even Saharan dust is observed at Whistler (McKendry *et al.*, 2007). Average springtime calcium concentrations in Whistler (Figure 9.5a) from 2003 to 2006 show an increase over the 4-year measurement period and are highly correlated with those (not shown) from Saturna Island ($R^2=0.99$). Calcium in the Whistler samples was an order of magnitude lower than at Saturna, a difference expected because the Whistler samples were collected with a 2.5 micron (μm) size cut and thus only a fraction of the coarse aerosol was collected, while at Saturna, open filter packs with no size cut device were used.

The range of sulphate concentrations in the fine particles at Whistler for 2002-2006 is similar to that of the 1989-1998 IMPROVE data measured at Crater Lake and Mt Lassen, discussed by VanCuren (2003). Sulphate in the fine particle fraction at Whistler peak (Figure 9.5 b) exhibits an annual variation with a summertime maximum. Geometric means weighted by sample

period show summer values of up to $0.4 \mu\text{g m}^{-3}$. Although the overall seasonal pattern is repeated from year to year, there are some notable differences. In particular, during 2005 and 2006, the sulphate during the winter months was elevated relative to earlier years resulting in a broader annual distribution and a less well-defined increase during the transport season.

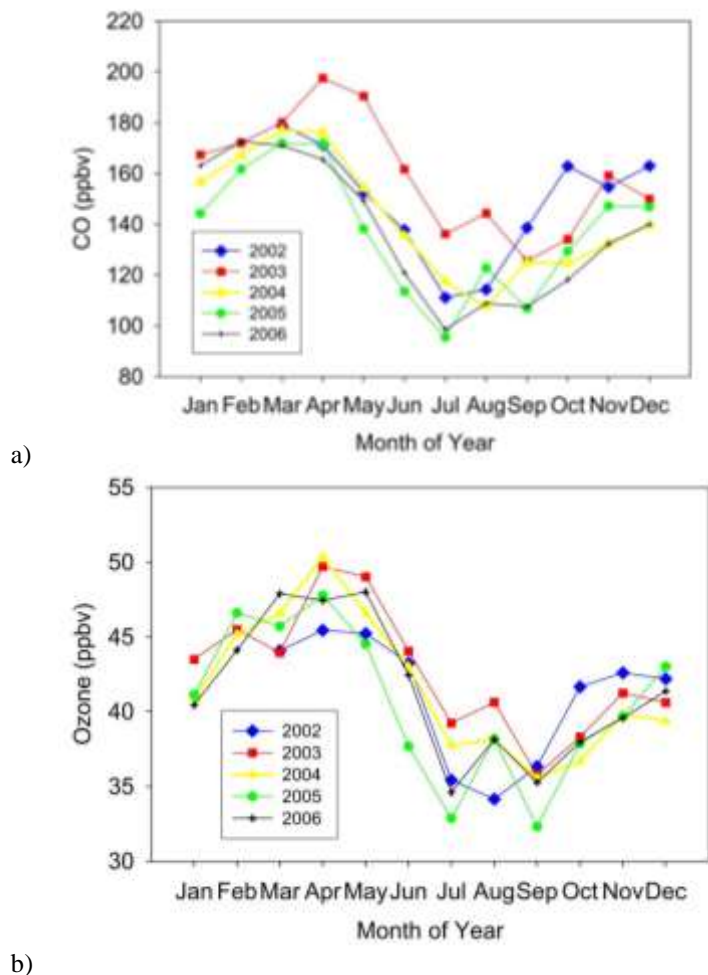
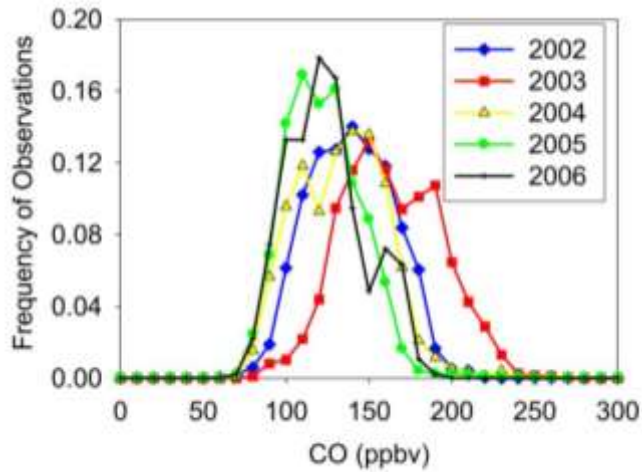


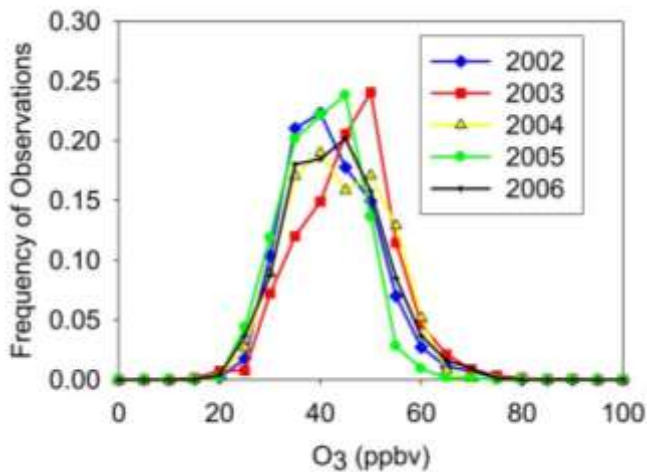
Figure 9.6 Monthly averages of (a) carbon monoxide and (b) ozone during nighttime at the Whistler high elevation site from March 2002 to November 2006.

This inter-annual variability is also observed in gas-phase species. Monthly mean values for CO and O₃ during 2002-2006 are shown in Figure 9.6. The springtime maxima in the annual cycle of both species has also been observed at other Northern Hemisphere sites and is thought to be the result of both transport and chemical processes. Higher CO concentrations in 2003 are attributed to biomass burning in Siberia and subsequent transport across the Pacific. Jaffe *et al.* (2004) related the total area burned to the changes in CO and O₃ concentrations observed on the west coast of North America; increases in CO at Alaskan sites ranged from 23-37 ppbv. One such event linked to large-scale forest fires in Siberia, occurred in June 2003 and caused 8-hour surface ozone levels in Enumclaw, Washington to reach 94 ppb, exceeding U.S. air

quality standards. The proportion of O_3 due to emissions from Siberian fires was estimated to be 15 ppb. This was superimposed on the background component (~ 35 ppb) and that locally produced (~ 50 ppb).



a)



b)

Figure 9.7 Frequency distributions of night-time (a) CO and (b) O_3 at Whistler, BC during summertime periods (May-August) during 2002-2005.

Frequency distributions of CO and O_3 at Whistler from May to August for 5 years (Figure 9.7) more closely illustrate this inter-annual variability. In 2003, the entire distribution is shifted to higher values for both CO and O_3 . Thus, not only are the direct transport events from Siberia affecting the monthly means, but the overall background CO and O_3 is elevated. The average CO for the summer of 2003 is 158 ppbv, approximately 26% higher than the mean of the four other summers. The average O_3 is higher during the summer of 2003 by approximately 4 ppbv

compared with the other years. During trans-Pacific transport events, the mean O_3 is 47 ppbv in contrast to the average of 37 ppbv for clean background air originating in the south-Pacific during summer 2003.

Measurements obtained at Whistler represent a mixture of the free troposphere and of the BL. Analyses of temperature profiles with increasing elevation and diurnal changes in water vapour at the peak site suggest that typically the site will be influenced by the BL during spring and summer from approximately 9 am to 8 pm local time. Monthly averages of O_3 and CO presented in Figure 9.7 are from night-time data only although the differences between these values and all data at Whistler are less than 3% as filter pack PM samples are collected over 24 or 48 hours, so the influence from the BL cannot be removed. Vertical profile data from the Intex-B experiment in spring 2006 indicate that during transport events, sulphate levels in the free troposphere are several times higher than in the BL. Thus the 24-hour samples may be a conservative estimate of sulphate in the transport layers.

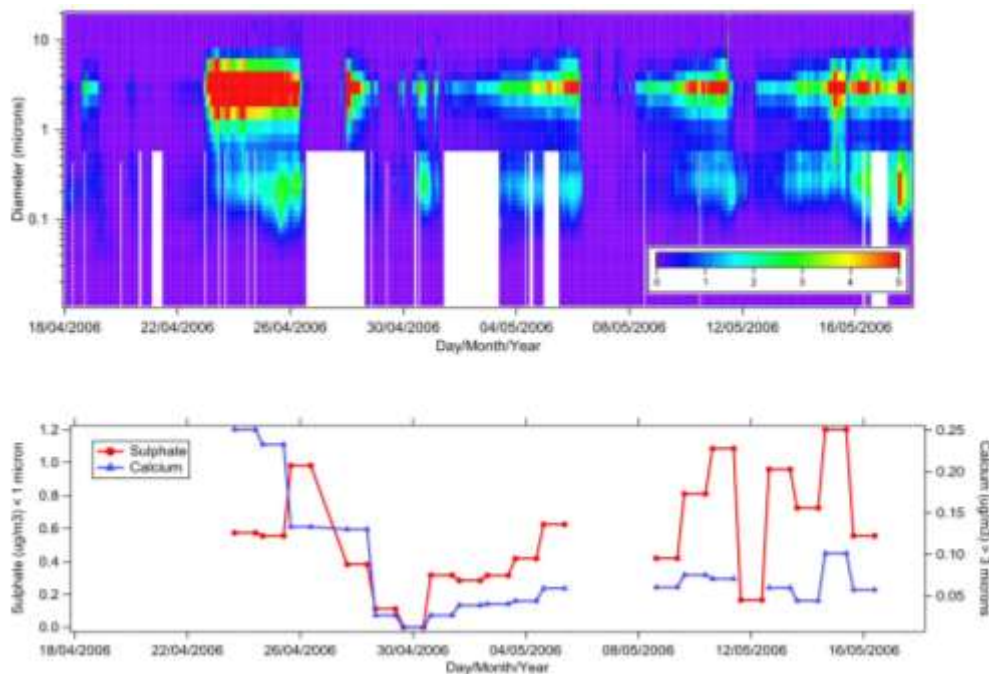


Figure 9.8 Time series of particle measurements at the Whistler, BC high elevation site during the Intex-B spring 2006 period, (a) Particle volume distributions ($dV/d\log D$), major transport events are identified by increase in coarse particle volume. (b) Fine fraction sulphate and coarse fraction calcium from impactor samples.

During the Intex-B experiment, transport of particles and gases to the west coast of Canada was characterized both at the Whistler high elevation site and with aircraft vertical profiles. Spring 2006 was a relatively active period for Asian dust storms (Zhou *et al.*, 2007) with these transport events being regularly observed throughout the period. Time series of the volume distribution of the fine and coarse mode aerosol and of sulphate and calcium mass

concentrations for the Intex-B period are shown in Figure 9.8a and 9.8b. Dust transport events are evident by increases in the coarse mode aerosol, in particular the periods around April 23-25, April 28, May 5, 10, and 15. These events are coincident with increases in calcium, an indication of an increased influence from soil dust. Variations in sulphate partially correspond to increases in coarse particle volume, but sulphate coincides more with the fine particle volume (e.g. April 25). Size-segregated samples collected during Intex-B show that more of the sulphate was in particle sizes $<1 \mu\text{m}$.

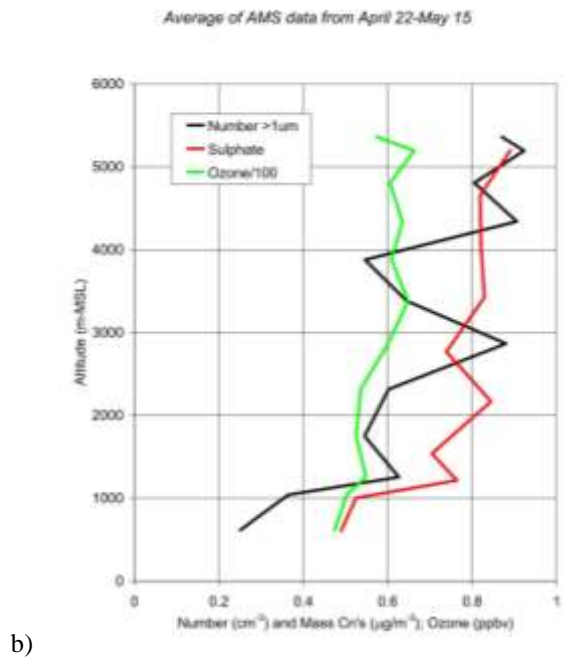
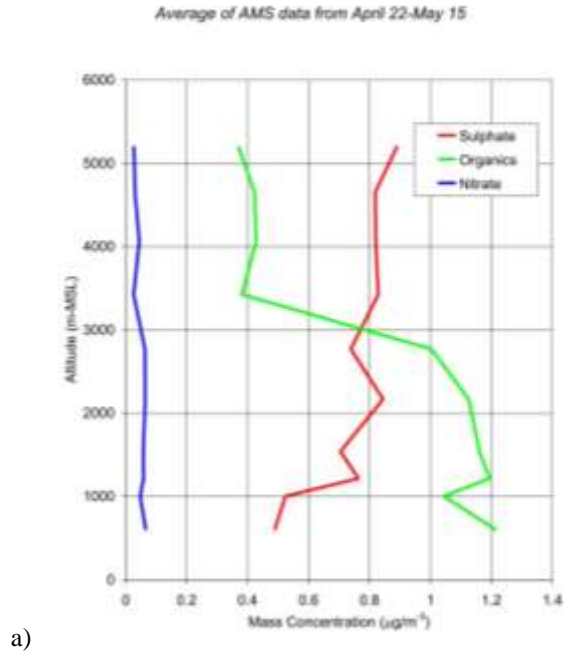


Figure 9.9 Average profiles of the mass concentrations (in $\mu\text{g m}^{-3}$) of nitrate, sulphate and total organics measured with the AMS. Also, the average profile of coarse particle number concentration profiles (in cm^{-2}) from 19 flights from April 22 to May 15, 2006 are used in the averages.

Average profiles of sulphate, nitrate and total organic material measured in the fine particles at Whistler from April 22, 2006 to May 15, 2006 inclusive (19 flights) are shown in Figure 9.9a. Figure 9.9b shows the average coarse particle number concentration and O₃ profiles (scaled by 0.01) for the same period. For O₃, two flights are removed from the average because of suspected direct influence from the stratosphere. At this location, the dominant source of organic material and particle nitrate is in the BL, whereas the sulphate, O₃ and coarse particle profiles indicate their dominant source was from aloft, as the concentrations increase with elevation. If we use the change in organic material from below to above 3 km as a scaling for the BL influence, then the contribution from transport to the upper level sulphate is estimated to be 0.5-0.6 µg m⁻³. Comparing the mean O₃ below and above 2.5 km indicates an increase from 52 to 62 ppbv in the upper level O₃ concentration.

9.5 Modelling the Contributions of Anthropogenic Pollutants to ICT

Isolating the contribution to Canadian smog levels from other continents by using observations is a difficult process. Model simulations provide an alternative to quantifying such contributions. The UNECE (United Nations Economic Commission for Europe) Task Force for the Hemispheric Transport of Air Pollutants (TF HTAP) has used an ensemble of models to assess the inter-continental transports and their impacts on local air quality (HTAP, 2007). The same approach has also been adapted in the most recent NAS report (NAS 2009).

In this section, results from two independent global 3-D chemical transport modelling systems (GEM-AQ/EC and GEOS-CHEM) are used to simulate and isolate the contribution of different sources from various regions. GEM-AQ/EC is an improved version of GEM/AQ that was jointly developed by a group of Canadian institutes (Kaminski *et al.*, 2007). GEM-AQ builds on the current operational weather forecasting system in Canada - GEM (Global Environmental Multiscale model) (Côté *et al.*, 1998) developed at MSC (Meteorological Service of Canada) through the addition of a gas phase chemistry module, the Acid Deposition and Oxidant Model (ADOM), (Venkatram *et al.*, 1988) and an aerosol module, the Canadian Aerosol Module (CAM) (Gong *et al.*, 2003a). The new features in GEM-AQ/EC include the estimates of biomass burning emissions and high resolution emissions inventories (42 km) of other species developed at Environment Canada. The GEM-AQ/EC was run with a spatial resolution of 2°×2° and vertical levels of up to 0.1 hPa, which may not be able to adequately simulate ozone peaks or ozone titration but is totally adequate to study long range transport of pollutants. As one of the models participating in HTAP, the GEM-AQ/EC has comparable results with other global transport models in providing reasonable ozone and PM concentrations.

9.5.1 Particulate Matter

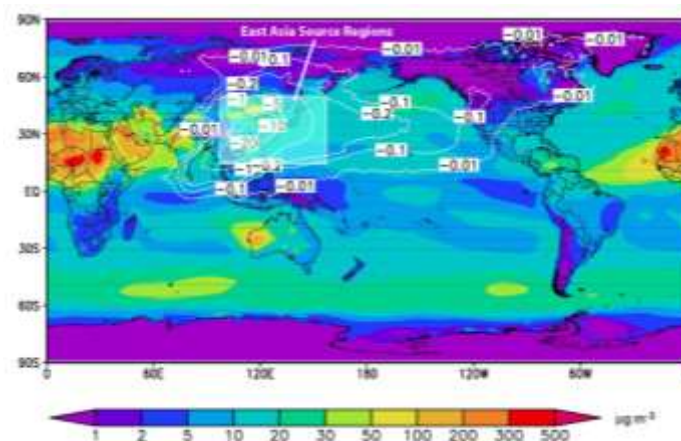


Figure 9.10 Annual averaged PM surface concentrations (colour filled contours) and the reduction (dashed contour lines) due to the elimination of the East Asian anthropogenic sources (sulphate, BC and OC). PM includes sulphate, BC, OC, dust and sea-salt in this figure.

Dust aerosol transported across the Pacific and reaching North America has been exclusively identified by surface observations, satellites and field campaigns (see Section 9.3). However, it is more difficult to identify other intercontinentally transported PM species as they can originate from both local and long range transport. Model simulations suggest that anthropogenic aerosols from Asia can also be transported to the United States (Park *et al.*, 2004). It was estimated that about $0.13 \mu\text{g m}^{-3}$ of sulphate could be attributed to the Asian anthropogenic emissions with negligible contributions of carbonaceous aerosols ($<0.01 \mu\text{g m}^{-3}$). The GEM-AQ/EC model estimates that $0.1 \mu\text{g m}^{-3}$ of the annual PM in the surface air at the west coast of Canada is due to anthropogenic sulphate, black carbon (BC) and organic carbon (OC) emissions from East Asia (Figure 9.10). The contribution from transport over the Pacific to PM concentrations on the east coast of Canada is estimated at approximately ten times less than on the west coast. The Asian contribution estimates in western Canada from GEM-AQ/EC results are comparable to the estimates of sulphates by Park *et al.* (2004) for the U.S. However, Park *et al.* (2004) predicted an almost equal influence of Asian emissions on both the western and eastern U.S. Chin *et al.* (2007) pointed out that even though Asian pollution may make significant contributions to the background sulphate level, its influence is about 6 times smaller in the western United States and 60 times smaller in the eastern United States than North American regional sources. In addition, only 2–6% of the annual average surface fine aerosol mass in the U.S. is estimated to be from the intercontinental transport of aerosol pollutants, including SO_4 , BC, and OC (Koch *et al.*, 2007).

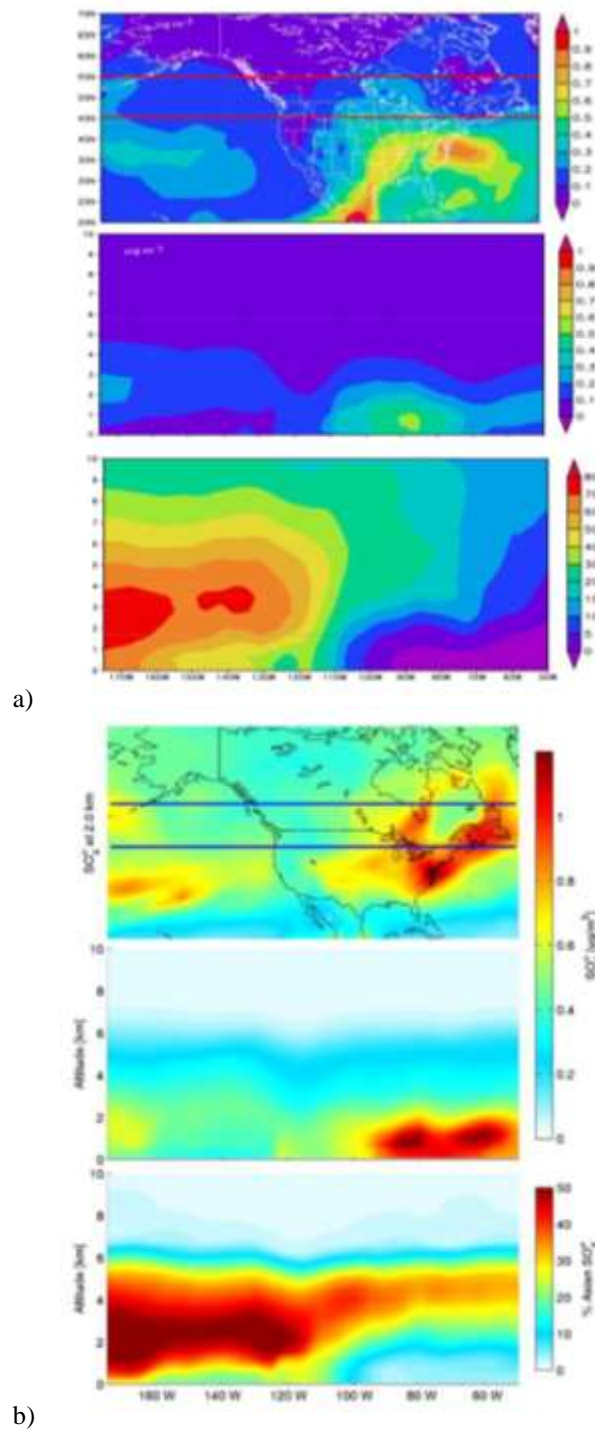


Figure 9.11 Simulated sulphate (top panels) over April and May 2006 from two models (a) GEM-AQ/EC and (b) GEOS-CHEM vertically averaged from 0 to 2 km (note the differences between colour scales). The middle panels show the average vertical profile between the red (blue) lines, and the bottom panels show the percent of sulphate that is of Asian origin from both models. This suggests that for much of Canada, East Asian sulphur emissions have little influence on the surface. A notable exception to this is the west coast, where Asian emissions account for 20-30% of the surface sulphate. At higher altitudes, Asian sulphate appears significant across the country.

In terms of the regional perspectives and vertical profiles in North America, Figure 9.11 shows the simulated average sulphate in April and May of 2006 by both GEM-AQ/EC and GEOS-CHEM (VanDonkelaar *et al.*, 2008). The top panel illustrates the sulphate concentrations at 2 km above the surface. The middle panel shows the average vertical profile between the red (blue) lines, and the bottom panel shows the percent of sulphate that is of Asian origin along the vertical profile. There are some differences between the two model results in terms of the absolute magnitude of the sulphate concentrations and the vertical profiles of Asian contributions above North America. However, some general conclusions can be drawn from them. It is found that for much of Canada, Asian sulphur emissions have little influence on the surface sulphate concentrations. A notable exception to this is the west coast, where Asian emissions account for 20-30% of the surface sulphate. At higher altitudes, Asian sulphate appears to be significant across the country. However, GEM-AQ/EC predicts a much lower fraction of Asian influence to eastern North America than GEOS-CHEM. A recent NASA study using the improved satellite sensor capabilities estimated that during 2002 to 2005 the amount of particulate pollution arriving in North America from Asia is equivalent to about 15% of local emissions from the U.S. and Canada (Yu *et al.*, 2008).

In an interim report by the UNECE TF HTAP based on the analysis of an ensemble of 21 models (HTAP, 2007), it was concluded that the impact of intercontinental transport on surface air quality is primarily episodic, especially associated with major emission events such as fires or dust storms. The intercontinental transport of fine particles has a larger impact on total atmospheric column loading (which in turn has significant implications for climate change) than on the surface concentrations.

9.5.2 Ozone

The contribution of O₃ to the ambient concentrations in North America from Asia has been subject to intensive studies (Jacob *et al.*, 1999; Wild and Akimoto, 2001). Through a modelling study, Li *et al.* (2002a) estimated the surface O₃ enhancement in North America due to Asian anthropogenic emissions to be in the range of 2-5 ppbv in June-August 1997. A more recent study (Zhang *et al.*, 2008) yielded a 5-7 ppbv ozone enhancement over western North America, reflecting the increased emissions in 2000-2006. Sensitivity investigations (Wild and Akimoto, 2001) of emission change scenarios for the O₃ precursors indicate that a 10% increase in Asian emissions would increase the surface O₃ in the U.S. region by 0.1 to 0.2 ppbv and by 0.2-0.4 ppbv at 650 hPa (3.6 km) and 200 hPa (11.8 km). Larger contributions were found to occur in spring and fall.

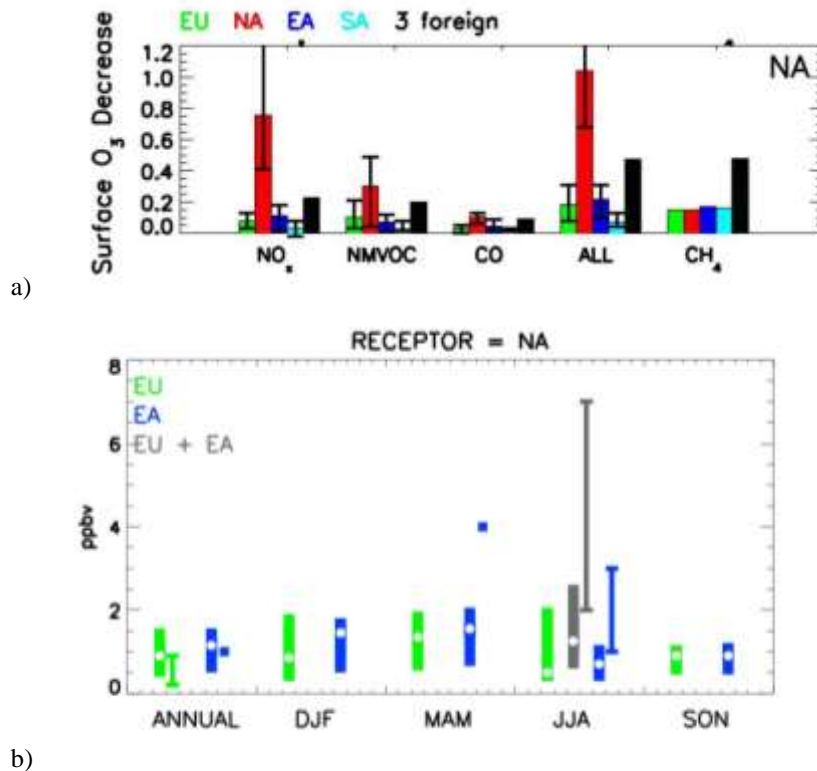


Figure 9.12 (a) Model ensemble surface O₃ response (ppb) over North America (NA, in red) to 20% reductions in anthropogenic O₃ precursor emissions individually (NO_x, NMVOC, and CO), combined (ALL), and to CH₄ originating from three foreign source regions (where EU is Europe, EA is East Asia and SA is South Asia). (b) Annual and seasonal mean contribution to total surface O₃ from foreign source regions to North America (Europe only, EU in green; East Asia only, EA in blue; combination of both Europe and East Asia, EU + EA in grey) as estimated from the individual model results of HTAP and from studies in the published literature (thin vertical bars for ranges across studies and regions; squares indicating where only one value is reported). The white circles represent the multimodel median value. (Fiore *et al.*, 2009)

From the TF HTAP Interim Assessment Report (HTAP, 2007), the contribution of surface O₃ enhancement in North America from hemispheric transport is summarized in Figure 9.12 (Fiore *et al.*, 2009). The modelled response of surface O₃ to a theoretical 20% reduction in emissions of individual O₃ precursors from the three regions of East Asia (EA), South Asia (SA) and Europe (EU) is shown in Figure 9.12a. The reduction in surface O₃ ranges from 0.05 to 0.2 ppb and is dependent on the individual precursor. The total reduction in surface O₃ from the combined emissions reductions of all precursor species from all three regions is approximately 0.4 ppb, with East Asia alone accounting for 0.2 ppb of that decrease.

By linearly scaling the simulated North American surface O₃ response to the combined 20% decrease in foreign sources of anthropogenic emissions of NO_x, CO, and non-methane volatile organic compounds (NMVOC) to a 100% emissions reduction, i.e., 5 times the values in Figure 9.12a, the annual and seasonal mean contribution to total surface O₃ in North America

was estimated in the range of 2 ppbv with a peak in the spring and low in the summer (Fig. 9.12b). Previous studies have reported higher summertime values of 2-8 ppbv as indicated by the grey bars in Figure 9.12b.

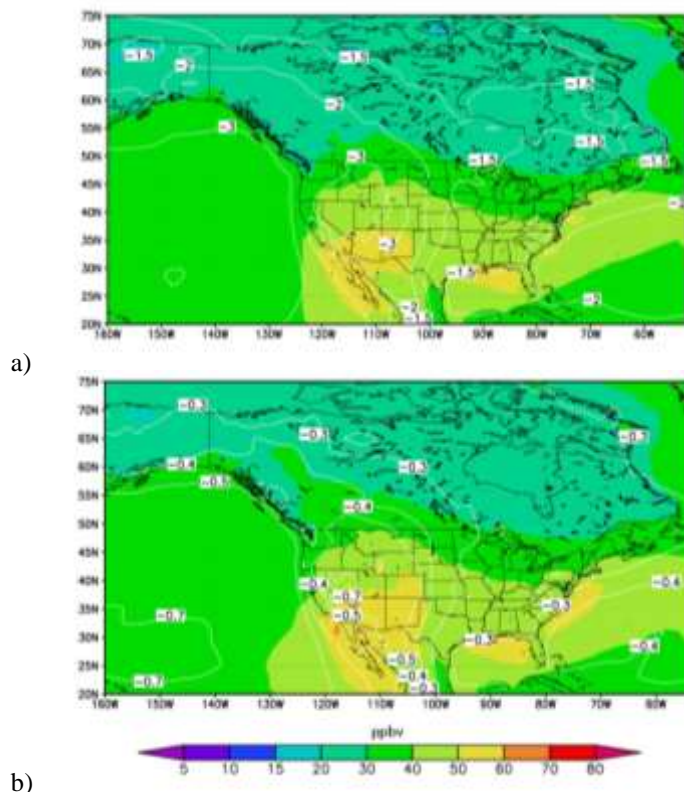


Figure 9.13 O₃ concentrations and reductions due to (a) 100% and (b) 20% reductions in NO_x and VOC in Asia (annual average), showing the non-linear response of ambient concentrations to emissions reductions. The coloured filled contours are the ozone surface concentrations and the dashed contour lines are the reductions (ppbv).

Figure 9.13 illustrates the GEM-AQ/EC results as part of the TF HTAP efforts to model the changes of surface O₃ in North America for 2001 due to reductions in East Asian emissions of NO_x and VOCs by (1) 100% (Figure 9.13a) and (2) 20% (Figure 9.13b), from two separate simulations. The reduction in annual surface O₃ due to the 100% cut is between 2-3 ppbv in western North America and 1.5 ppbv in eastern Canada and U.S. The peak reduction in North America is in the northwest U.S. where more than 3 ppbv of annual surface O₃ could be attributed to the East Asian emissions. Though the O₃ enhancement by the Asian emissions could range as high as 10 ppbv episodically, a 20% cut in its precursors can only result in a 0.3-0.5 ppbv O₃ reduction in western Canada and less than 0.3 ppbv in the east. The highest reduction of 0.5-0.7 ppbv occurs in the northwestern U.S.

9.6 Modelling the Contributions from Natural PM Components

In addition to the contributions from intercontinental transport to the total PM levels in Canada, natural sources also play an important role. It should be pointed out that some of the natural components are also from intercontinental transport. Since both of these contributions are primarily beyond our control in terms of emission reduction strategies in Canada, this section will focus on the quantitative information of PM constituents in Canada. The natural components included in the modelling study by GEM-AQ/EC are sea salt, soil dust, black and organic carbons from biomass burnings (not including volcanoes and biogenic secondary organics).

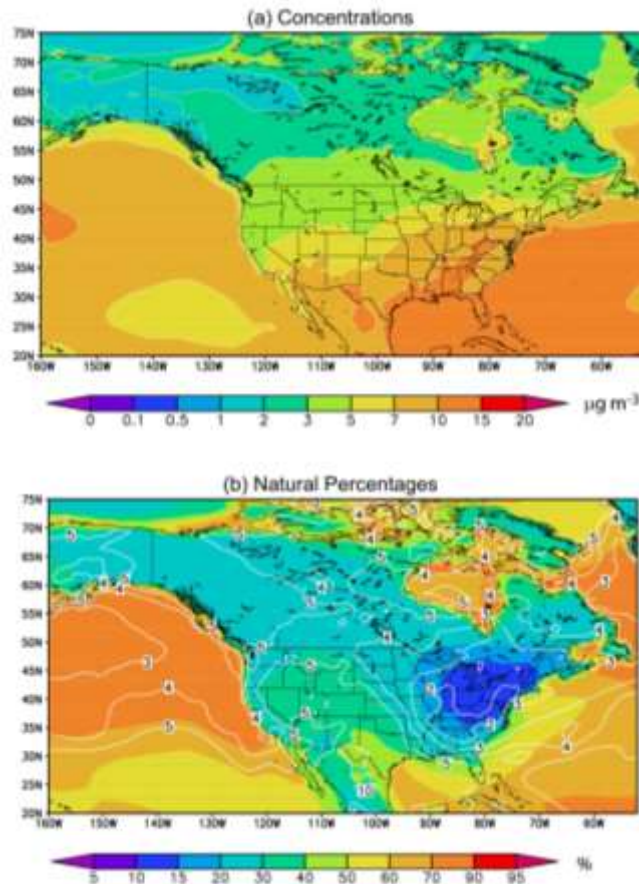


Figure 9.14 (a) The annual average concentration ($\mu\text{g m}^{-3}$) of PM from 1998-2004 simulations in North America. (b) Percentage of PM from natural contributions in North America. The coloured filled contours are the percentages and the contour lines are the standard deviations.

Figure 9.14a shows the model-simulated total PM concentrations in North America averaged from 1998-2004. The simulated spatial distribution and magnitudes are generally consistent with the observations of PM₁₀ by the IMPROVE network (Malm *et al.*, 2004).

For the 7 years of simulations (Figure 9.14b), the percentage of the natural contributions to ambient PM levels averages almost 20-30% over a large part of Canada. However, around the Great Lakes region and large part of northern and eastern U.S., where anthropogenic emissions are high, the natural contribution is about 10-15%. In contrast, the natural fraction increases to 30-40% in the western U.S. where dust and biomass burning aerosols dominate. In the figure, it is also shown that there are degrees of inter-annual variation of the natural contributions to the PM levels from the 7 years of results. The standard deviation of the percentage contributions is in the range of 3-5% for all natural aerosols but is higher for soil dust and BC/OC from boreal biomass burning.

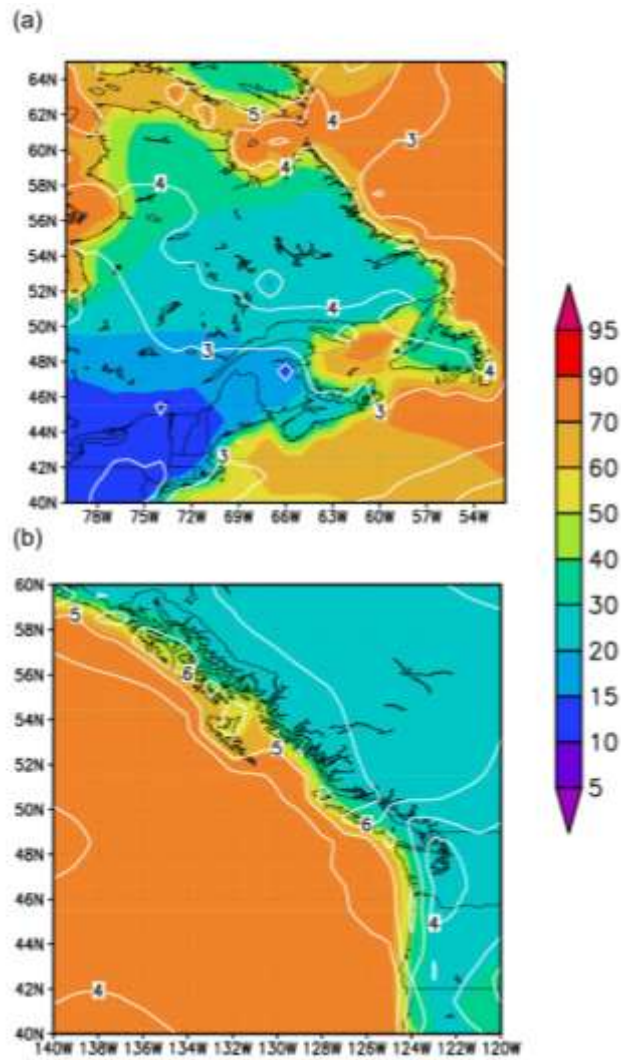


Figure 9.15 Percentage of PM from natural contributions in Canadian coastal areas (a) east and (b) west. The coloured filled contours are the percentages and the contour lines are for the standard deviations.

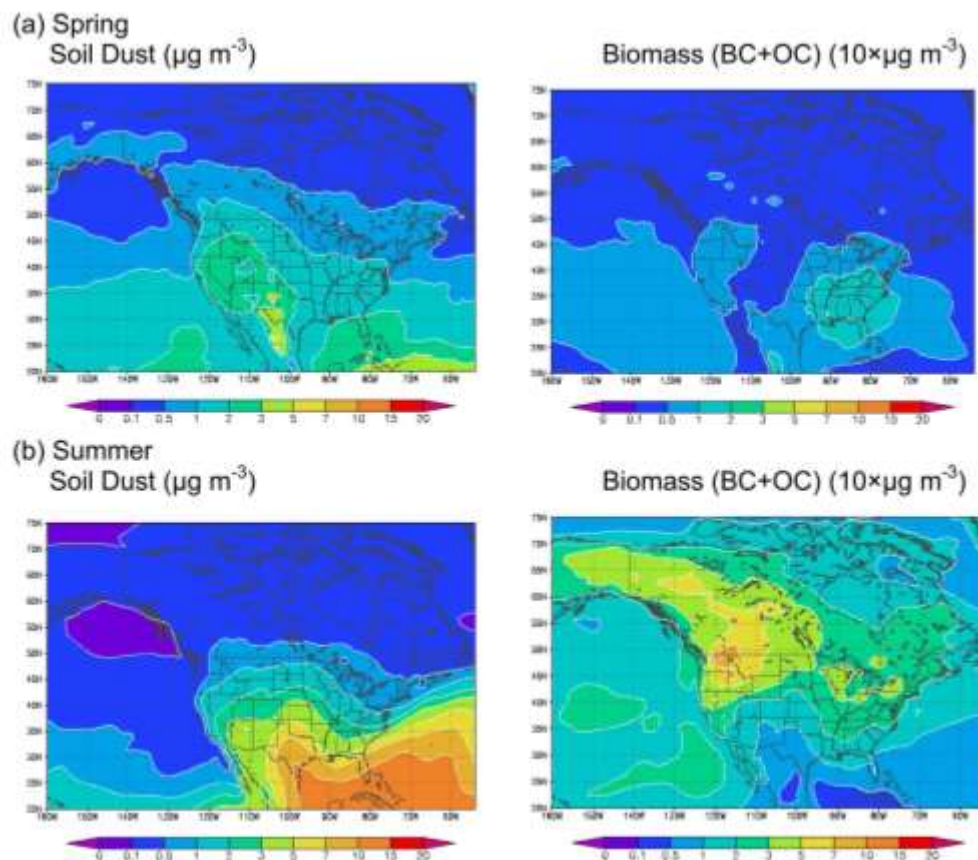


Figure 9.16 Ambient dust and carbonaceous aerosol concentrations from natural sources in (a) Spring and (b) Summer.

In Canada, the natural contributions in the east coast accounts for more than 20% of the total PM, mostly from sea salt, with a standard deviation of about 3% (Figure 9.15a). The percentage of natural components increases to about 40% on the west coast (Figure 9.15b) with significant contributions from sea salt all year round but also from dust in the spring and biomass burning in the summer. This is clearly shown in the seasonal variations of the natural contributions (Figure 9.16). In spring, Canada receives not only the dust aerosols from Asia but also from the U.S. (Park *et al.*, 2007) with an approximate $1\text{-}2 \mu\text{g m}^{-3}$ contribution to the ambient spring levels. In summer, Canada's natural ambient PM levels are largely influenced by biomass burning, especially in the west and northwest, and to a much lesser extent by aerosols from Africa. The summer carbonaceous aerosols can account for $0.7\text{-}1.0 \mu\text{g m}^{-3}$ of the PM concentrations in western Canada.

9.7 Uncertainties

There are three major areas of uncertainties in this assessment of intercontinental transport and natural contributions to air pollution: inter-annual variations of transport patterns, emissions changes and climate variability.

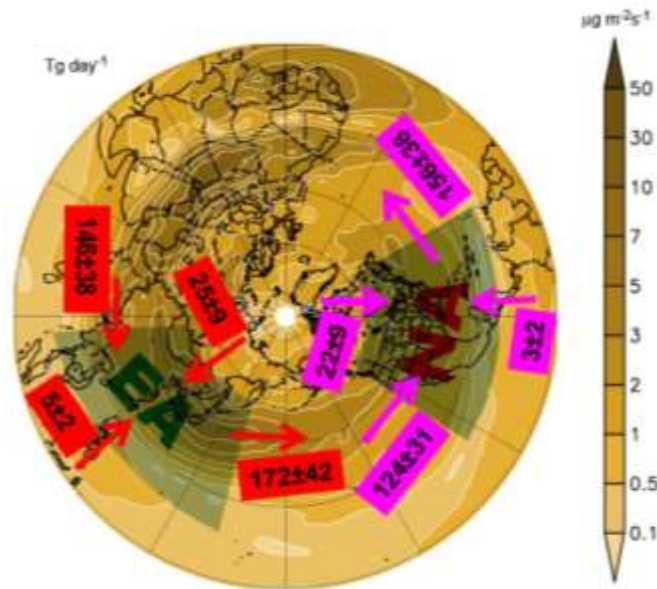


Figure 9.17 Averaged Import and export fluxes from East Asia and North America for total PM and standard deviations from 10 year simulations. The background contour illustrates the averaged spring transport fluxes ($\text{mg m}^{-2} \text{s}^{-1}$) vertically integrated from 3-10 km while the numbers with arrows show the 10 year averaged transported fluxes (Tg day^{-1}) and deviations crossing each boundary of the two HTAP defined regions (East Asia and North America) from surface to the model upper boundary.

As is demonstrated in this chapter, the routes of trans-Pacific transport change significantly from year to year, and the percentage of the air pollutants from Asia reaching North America will vary significantly even if the emissions remain unchanged. This effect is magnified between the El Niño and La Niña years. Most of the modelling results in this assessment and the HTAP interim assessment report were from a single year simulation. Through a 10-year simulation by GEM-AQ/EC with a fixed global anthropogenic emissions, the averaged import and export fluxes from North America and East Asia of total anthropogenic PM were calculated and are shown in Figure 9.17 with standard deviations. It is evident that the deviation of the import and export fluxes can reach as high as 25% from the averages due to the inter-annual variations in the circulation patterns. Such impact on ozone and its precursors still remains unclear. For a single year simulation, the results of source-receptor relationship could be subject to a 25% uncertainty.

The estimates of trans-Pacific contributions in this chapter are largely based on the results of large-scale models. In addition to the uncertainties in the transport paths, the uncertainty in the emissions of ozone precursors and PM in Asia remains high for two reasons: (1) the lack of information for accurate emissions data for Asia and (2) the rapid change in the economy that makes Asian emissions a moving target. As a result, future impacts will remain uncertain.

Model errors constitute other uncertainties to the quantification of intercontinental transport. These include the model transports, process parameterizations and modelled meteorology that influence the removal processes such as clouds and precipitation.

Finally, the uncertainty in climate change also plays a role in the uncertainty of the estimate as the changes in climate will impact atmospheric chemistry, transport and removal processes.

9.8 Summary and Conclusions

Evidence from both observations and model simulations link the enhancement of ambient levels of ozone and PM in Canada to intercontinental transport. The contribution of intercontinental transport to annual surface O₃ concentrations in Canada can range between 2-3 ppbv in the west and 1.5 ppbv in the east. However, the episodic contributions can reach as high as 7 ppbv in western North America. For fine PM, direct and consistent observations have identified the influence of Asian dust to North America in spring time, which could contribute as much as 4 µg m⁻³ to average spring time PM levels at west coast locations. The anthropogenic contributions to PM from Asian sulphate and carbonaceous aerosols are much smaller and are approximately 0.1 µg m⁻³ on an annual basis.

It is also found that natural contributions to the ambient PM levels in most of Canada ranges between 20-30%, with a lower contribution in the Great Lakes region (10-15%), around 20% in the east coast and about 30% in the west coast. Due to the fluctuations in meteorology which influences the natural emissions and transport of natural aerosols, large inter-annual variations were found.

9.9 Recommendations for Future Research

Although both observations and model simulations were able to explain some of the observed short-term trends and levels of trans-Pacific transport pollution to Canada, more research is needed to satisfactorily assess the significance of the transport and long-term trends. In particular, further efforts are needed to improve the observational ability to isolate the local and intercontinental transported chemical species with more spatial and temporal coverage and to enhance the modelling capacity to accurately simulate the chemical and physical processes. Model evaluations using surface and free troposphere O₃ observations along the west coast at

daily and monthly timescales and surface PM data across North America, by month to capture large seasonal changes, are needed. Research to better understand the relationship between ozone, sulphur, dust and organic matter during ICT should be carried out. It will greatly benefit our understanding to couple the global results into a regional modelling system to assess the intercontinental influence in more detail.

Improvements in the emissions inventories of the source region (e.g. Asia) are needed to provide more accurate outflows. Since there is inter-annual variability in trans-Pacific transport, multi-year simulations are required to characterize the spatial and temporal variation of the impacts.

References

- Andreae, M. O., Berresheim, H., Andreae, T. W., Kritz, M. A., Bates, T. S. and Merrill, J. T., 1998. Vertical distribution of dimethylsulfide, sulphur dioxide, aerosol ions, and radon over the Northeast Pacific Ocean *J. of Atmos. Chem.*, 6, 149-173.
- Arimoto, R., Kim, Y. J., Kim, Y. P., Quinn, P. K., Bates, T. S., Anderson, T. L., Gong, S. L., I. Uno, M. C., Huebert, B. J., Clarke, A. D., Shinozuka, Y., Weber, R. J., Anderson, J. R., Guazzotti, S. A., Sullivan, R. C., Sodeman, D. A., Prather, K. A. and Sokolik, I., 2006. Characterization of Asian Dust during ACE-Asia, *Global and Planetary Change*, 52, 23-56, doi:10.1016/j.gloplacha.2006.02.013.
- BCEnvironment, 2002. BC Environment Archive of Air Quality Data, PO Box 9341, Stn Prov Govt, Victoria, British Columbia, Canada. V8W 9M1.
- Bey, I., Jacob, D. J., Logan, J. A. and Yantosca, R. M., 2001. Asian chemical outflow to the Pacific: origins, pathways and budgets, *Journal of Geophysical Research*, 106, 23,097-23,114.
- Bottenheim, J. W., Dastoor, A., Gong, S. L., Higuchi, K. and Li, Y.-F., 2004. Long range Transport of Air Pollution to the Arctic. In: A. Stohl (Editor), *Intercontinental Transport of Air Pollution. The Handbook of Environmental Chemistry*. Springer Verlag, Berlin Heidelberg, pp. 13-39.
- Cahill, C. F., 2003. Asian aerosol transport to Alaska during ACE-Asia, *J. Geophys. Res.*, 108, 8664, doi:10.1029/2002JD003271.
- Chin, M., Diehl, T., Ginoux, P. and Malm, W., 2007. Intercontinental transport of pollution and dust aerosols: implications for regional air quality, *Atmos. Chem. Phys.*, 7, 5501-5517.

Clarke, A. D., Shinozuka, Y., Kapustin, V. N., Howell, S., Huebert, B., Doherty, S., Anderson, T., Covert, D., Anderson, J., Hua, X., II, M. K. G., McNaughton, C., Carmichael, G. and Weber, R., 2004. Size distributions and mixtures of dust and black carbon aerosol in Asian outflow: Physiochemistry and optical properties. , . *J. Geophys. Res.*, 109, D15S09, doi:10.1029/2003JD004378.

Climate Change Science Program Strategic Plan (CCSP Strategic Plan), 2006. Our Changing Planet - The U.S. Climate Change Science Program for Fiscal Year 2006, November 2005. Report available online at: <http://www.usgcrp.gov/usgcrp/Library/ocp2006/ocp2006.pdf>

Côté, J., Gravel, S., Méthot, A., Patoine, A., Roch, M. and Staniforth, A., 1998. The operational CMC-MRB Global Environmental Multiscale (GEM) model: Part I - Design considerations and formulation, *Mon. Wea. Rev.*, 126, 1373-1395.

Fiore, A. M., Dentener, F. J., Wild, O., Cuvelier, C., Schultz, M. G., Hess, P., Textor, C., Schulz, M., Doherty, R. M., Horowitz, L. W., MacKenzie, I. A., Sanderson, M. G., Shindell, D. T., Stevenson, D. S., Szopa, S., Dingenen, R. V., Zeng, G., Atherton, C., Bergmann, D., Bey, I., Carmichael, G., Collins, W. J., Duncan, B. N., Faluvegi, G., Folberth, G., Gauss, M., Gong, S., Hauglustaine, D., Holloway, T., Isaksen, I. S. A., Jacob, D. J., Jonson, J. E., Kaminski, J. W., Keating, T. J., Lupu, A., Marmer, E., Montanaro, V., Park, R. J., Pitari, G., Pringle, K. J., Pyle, J. A., Schroeder, S., Vivanco, M. G., Wind, P., Wojcik, G., Wu, S. and Zuber, A., 2009. Multi-model estimates of intercontinental source-receptor relationships for ozone pollution, *J. Geophys. Res.*, 114, D04301, doi:10.1029/2008JD010816.

Fischer, E. V., N. C. Hsu, D. A. Jaffe, M.-J. Jeong, and S. L. Gong, 2009. A decade of dust: Asian dust and springtime aerosol load in the U.S. Pacific northwest, *Geophysical Research Letters*, 36, L03821, doi:10.1029/2008GL036467.

Gong, S. L., Barrie, L. A., Blanchet, J.-P., Salzen, K. v., Lohmann, U., Lesins, G., Spacek, L., Zhang, L. M., Girard, E., Lin, H., Leaitch, R., Leighton, H., Chylek, P. and Huang, P., 2003a. Canadian Aerosol Module: A size-segregated simulation of atmospheric aerosol processes for climate and air quality models 1. Module development, *J. Geophys. Res.*, 108, 4007, doi:10.1029/2001JD002002.

Gong, S. L., Zhang, X. Y., Zhao, T. L., McKendry, I. G., Jaffe, D. A. and Lu, N. M., 2003b. Characterization Of Soil Dust Distributions In China And Its Transport During ACE-ASIA 2. Model Simulation and Validation, *Journal of Geophysical Research*, 108, 4262, doi:10.1029/2002JD002633.

Gong, S. L., Zhang, X. Y., Zhao, T. L., Zhang, X. B., Barrie, L. A., McKendry, I. G. and Zhao, C. S., 2006. A Simulated Climatology of Asian Dust Aerosol and its Trans-Pacific Transport 2. Interannual Variability and Climate Connections, *Journal of Climate*, 19, 104-122.

Harner, T., Farrar, N. J., Shoeib, M., Jones, K. C. and Gobas, F. A. P. C., 2006. Global pilot study for persistent organic pollutants (POPs) using PUF disk passive air samplers, *Environ. Pollut.*, 144, 445-452.

Herman, J., Bhartia, P., Torres, O., Hsu, C., Seftor, C. and Celarier, E., 1997. Global distribution of UV-absorbing aerosols from Nimbus 7/TOMS data, *Journal of Geophysical Research*, 102, 16911-16922.

HTAP, 2007. HEMISPHERIC TRANSPORT OF AIR POLLUTION 2007, UNITED NATIONS, New York and Geneva.

Huebert, B. J., Bates, T., Russell, P. B., Shi, G., Kim, Y. J., Kawamura, K., Carmichael, G. and Nakajima, T., 2003. An overview of ACE-Asia: Strategies for quantifying the relationships between Asian aerosols and their climatic impacts, *J. Geophys Res.*, 108, 8633, doi:10.29/2003JD003550.

Husar, R. B., Tratt, D. M., Schichtel, B. A., Falke, S. R., Li, F., Jaffe, D., Gassó, S., Gill, T., Laulainen, N. S., Lu, F., Reheis, M. C., Chun, Y., Westphal, D., Holben, B. N., Gueymard, C., McKendry, I., Kuring, N., Feldman, G. C., McClain, C., Frouin, R. J., Merrill, J., DuBois, D., Vignola, E., Murayama, T., Nickovic, S., Wilson, W. E., Sassen, K., Sugimoto, N. and Malm, W. C., 2001. Asian dust events of April 1998, *Journal of Geophysical Research*, 106, 18317-18330.

Jacob, D. J., Logan, J. A. and Murti, P. P., 1999. Effect of rising Asian emissions on surface ozone in the United States, *Geophysical Research Letters*, 26, 2175-2178.

Jaffe, D., Bertschi, I., Jaeglé, L., Novelli, P., Reid, J. S., Tanimoto, H., Vingarzan, R. and Westphal, D. L., 2004. Long-range transport of Siberian biomass burning emissions and impact on surface ozone in western North America, *Geophysical Research Letters*, 31, L16106, doi:10.129/2004GL020093.

Jaffe, D., McKendry, I., Anderson, T. and Price, H., 2003. Six 'new' episodes of trans-Pacific transport of air pollutants, *Atmospheric Environment*, 37 391-404.

Jaffe, D., Tamura, S. and Harris, J., 2005. Seasonal cycle, composition and sources of background fine particles along the west coast of the U.S., *Atmospheric Environment*, 39, 297-306.

Jaffe, D. A., Anderson, T., Covert, D., Kotchenruther, R., Trost, B., Danielson, J., Simpson, W., Berntsen, T., Karlsdottir, S., Blake, D., Harris, J., Carmichael, G. and Uno, I., 1999. Transport of Asian air pollution to North America, *Geophysical Research Letters*, 26, 711-714.

Kaminski, J. W., Neary, L., Struzewska, J., McConnell, J. C., Lupu, A., Jarosz, J., Toyota, K., Gong, S. L., Côté, J., Liu, X., Chance, K. and Richter, A., 2007. GEM-AQ, an on-line global multiscale chemical weather system: model description and evaluation of gas phase chemistry processes, *Atmospheric Chemistry and Physics Discussions*, 7, 14895-14937.

Keating, T., West, J. and Jaffe, D., 2005.: Air Quality Impacts of Intercontinental Transport, *EM (Environmental Management)*, October, 28-30.

Koch, D., Bond, T. C., Streets, D., Unger, N. and van der Werf, G. R., 2007. Global impacts of aerosols from particular source regions and sectors - art. no. D02205, *Journal of Geophysical Research-Atmospheres*, 112, 2205-2205.

Kotchenruther, R. A., Jaffe, D. A., Beine, H. J., Anderson, T., Bottenheim, J. W., Harris, J. M., D., B. and Schmitt, R., 2001. Observations of Ozone and Related Species in the Northeast Pacific During the PHOBEA Campaigns: 2. Airborne observations, *Journal of Geophysical Research*, 106, 7463- 7483.

Kritz, M. A., LeRouley, J. C. and Danielsen, E. F., 1990. The China Clipper - Fast advective transport of radon-rich air from the Asian boundary layer to the upper troposphere near California, *Tellus, B*, 42, 46-61.

Li, Q., Jacob, D. J., Bey, I., Palmer, P. I., Duncan, B. N., Field, B. D., Martin, R. V., Fiore, A. M., Yantosca, R. M., Parrish, D. D., Simmonds, P. G. and Oltmans, S. J., 2002a. Transatlantic transport of pollution and its effects on surface ozone in Europe and North America, *Journal of Geophysical Research*, 107, 4166, doi:10.1029/2001JD001422.

Li, Q. B., Jacob, D. J., Bey, I., Palmer, P. I., Duncan, B. N., Field, B. D., Martin, R. V., Fiore, A. M., Yantosca, R. M., Parrish, D. D., Simmonds, P. G. and Oltmans, S. J., 2002b. Transatlantic transport of pollution and its effects on surface ozone in Europe and North America, *J. Geophys. Res.*, 107(D13) doi:10.1029/2001JD001422.

Liang, Q., Jaeglé, L. and Wallace, J. M., 2005. Meteorological indices for Asian outflow and transpacific transport on daily to interannual timescales, *Journal of Geophysical Research*, 110, D18308, doi:10.1029/2005JD005788.

Macdonald, A. M., Anlauf, K.G., Leaitch, W.R., and Liu, P., 2007. Multi-year chemistry of particles and selected trace gases at the Whistler high elevation site, *EOS Trans. AGU*, 87(52), Fall Meet. Suppl., Abstract A53B-0179.

Malm, W. C., Schichtel, B. A., Pitchford, M. L., Ashbaugh, L. L. and Eldred, R. A., 2004. Spatial and monthly trends in speciated fine particle concentration in the United States, *Journal of Geophysical Research*, 109, D03306, doi:10.1029/2003JD003739.

- McKendry, I. G., Hacker, J. P., Stull, R., Sakiyama, S., Mignacca, D. and Reid, K., 2001. Long-range transport of Asian dust to the Lower Fraser Valley, British Columbia, Canada, *Journal of Geophysical Research*, 106, 18361-18370.
- McKendry, I. G., Strawbridge, K. B., O'Neill, N. T., Macdonald, A. M., Liu, P. S. K., Leaitch, W. R., Anlauf, K. G., Jaegle, L., Fairlie, T. D. and Westphal, D. L., 2007. Trans-Pacific transport of Saharan dust to western North America: A case study, *Journal of Geophysical Research*, 112, D01103, doi:10.1029/2006JD007129.
- National Academy of Sciences (NAS), 2009. Global Sources of Local Pollution: An Assessment of Long-Range Transport of Key Air Pollutants to and from the United States, National Academy of Science.
- Park, R. J., Jacob, D. J., Field, B. D., Yantosca, R. M. and Chin, M., 2004. Natural and transboundary pollution influences on sulfate-nitrate-ammonium aerosols in the United States: implications for policy, *Journal of Geophysical Research*, 109, D15204, 10.1029/2003JD004473.
- Park, S. H., Gong, S. L., Zhao, T. L., Vet, R. J., Bouchet, V. S., Gong, W., Makar, P. A., Moran, M. D., Stroud, C. and Zhang, J., 2007. Simulation of entrainment and transport of dust particles within North America in April 2001 ("Red Dust Episode"), *Journal of Geophysical Research*, 112, D20209, doi:10.1029/2007JD008443.
- Parrish, D. D., Hahn, C. J., Williams, E. J., Norton, R. B., Fehsenfeld, F. C., Singh, H. B., Shetter, J. D., Gandrud, B. W. and Ridley, B. A., 1992. Indications of Photochemical Histories of Pacific Air Masses From Measurements of Atmospheric Trace Species at Point Arena, California *Journal of Geophysical Research*, 97, 15,883–15,901.
- Parrish, D. D., Holloway, J. S., Trainer, M., Fehsenfeld, P. C. M. F. C. and Forbes, G. L., 1993. Export of North American Ozone Pollution to the North Atlantic Ocean *Science*, 259, 1436 - 1439.
- Price, H. U., Jaffe, D. A., Cooper, O. R. and Doskey, P. V., 2004. Photochemistry, ozone production, and dilution during long-range transport episodes from Eurasia to the northwest United States, *Journal of Geophysical Research*, 109, D23S13, doi:10.1029/2003JD004400.
- Price, H. U., Jaffe, D. A., Doskey, P. V., McKendry, I. and Anderson, T. L., 2003. Vertical profiles of O₃, aerosols, CO and NMHCs in the Northeast Pacific during the TRACE-P and ACE-ASIA experiments - art. no. 8799, *Journal of Geophysical Research Atmospheres*, 108, 8799.

Seinfeld, J. H., Carmichael, G. R., Arimoto, R., Conant, W. C., Brechtel, F. J., Bates, T. S., Cahill, T. A., Clarke, A. D., Doherty, S. J., Flatau, P. J., Huebert, B. J., Kim, J., Markowicz, K. M., Quinn, P. K., Russell, L. M., Russell, P. B., Shimizu, A., Shinozuka, Y., Song, C. H., Tang, Y., Uno, I., Vogelmann, A. M., Weber, R. J., Woo, J.-H. and Zhang, X. Y., 2004. ACE-ASIA: Regional Climatic and Atmospheric Chemical Effects of Asian Dust and Pollution, *Bulletin of the American Meteorological Society*, 85, 367-380.

VanCuren, R. A., 2003. Asian aerosols in North America: Extracting the chemical composition and mass concentration of the Asian continental aerosol plume from long-term aerosol records in the western United States, *Journal of Geophysical Research*, 108 4623, doi:10.1029/2003JD003459.

VanCuren, R. A. and Cahill, T. A., 2002. Asian aerosols in North America: Frequency and concentration of fine dust, *Journal of Geophysical Research*, 107, 4804, doi:10.1029/2002JD002204.

Van Donkelaar, A., Martin, R. V., Leaitch, W. R., Macdonald, A. M., Walker, T. W., Streets, D. G., Zhang, Q., Dunlea, E., Jimenez, J. L., Dibb, J. E., Huey, G., Weber, R., and Andreae, M. O.: Analysis of aircraft and satellite measurements from the Intercontinental Chemical Transport Experiment (INTEX-B) to quantify long-range transport of East Asian sulphur to Canada, *Atmos. Chem. Phys.*, 8, 2999–3014, 2008.

Venkatram, A., Karamchandani, P. K. and Misra, P. K., 1988. Testing a comprehensive acid deposition model, *Atmospheric Environment*, 22, 737-747.

Weiss-Penzias, P., Jaffe, D. A., Swartzendruber, P., Dennison, J. B., Chand, D., Hafner, W. and Prestbo, E., 2006. Observations of Asian air pollution in the free troposphere at Mount Bachelor Observatory during spring of 2004, *Journal of Geophysical Research*, 111, D10304, doi:10.1029/2005JD006522.

Wild, O. and Akimoto, H., 2001. Intercontinental transport of ozone and its precursors in a three-dimensional global CTM, *Journal of Geophysical Research Atmospheres*, 106, 27729-27744.

Yang, Y. Q., Hou, Q., Zhou, C. H., Liu, H. L., Wang, Y. Q. and Niu, T., 2007. A Study on Sand/dust Storms over Northeast Asia and Associated Large-Scale Circulations in Spring 2006, *Atmospheric Chemistry and Physics Discussions*, 7, 9259-9281.

Yienger, J. J., Galanter, M., Holloway, T. A., Phandnis, M. J., Guttikunda, S. K., Carmichael, G. R., Moxim, W. J. and Levy II, H., 2000. The episodic nature of air pollution transport from Asia to North America, *Journal of Geophysical Research*, 105, 26,93-26,946.

Yu, H., Remer, L.A., Chin, M., Bian, H., Kleidman, R.G. and Diehl, T., 2008. A satellite-based assessment of transpacific transport of pollution aerosol, *Journal of Geophysical Research*, 113, D14, doi: 10.1029/2007JD009349.

Zhang, L., Jacob, D. J., Boersma, K. F., Jaffe, D. A., Olson, J. R., Bowman, K. W., Worden, J. R., Thompson, A. M., Avery, M. A., Cohen, R. C., Dibb, J. E., Flock, F. M., Fuelberg, H. E., Huey, L. G., McMillan, W. W., Singh, H. B. and Weinheimer, A. J., 2008. Transpacific transport of ozone pollution and the effect of recent Asian emission increases on air quality in North America: an integrated analysis using satellite, aircraft, ozonesonde, and surface observations, *Atmospheric Chemistry and Physics*, 8, 6117-6136.

Zhao, T. L., Gong, S. L., Zhang, X. Y., Blanchet, J.-P., McKendry, I. G. and Zhou, Z. J., 2006. A Simulated Climatology of Asian Dust Aerosol and its Trans-Pacific Transport 1. Mean climate and validation, *Journal of Climate*, 19, 88-103.

Zhao, T. L., Gong, S. L., Zhang, X. Y. and Jaffe, D. A., 2007. Asian dust storm influence on North American ambient PM levels: observational evidence and controlling factors, *Atmospheric Chemistry and Physics Discussions*, 7, 9663-9686.

Zhou, C. H., Gong, S. L., Zhang, X. Y., Wang, Y. Q., Niu, T., Liu, H. L., Zhao, T. L., Yang, Y. Q. and Hou, Q., 2007. Development and Evaluation of an Operational SDS Forecasting System for East Asia: CUACE/Dust *Atmospheric Chemistry and Physics Discussions*, 7, 7987-8015.

CHAPTER 10: Impact of Smog on Vegetation and Materials

Beverley Hale and Barbara Dowsley

Contributing Authors: Tom Dann and Markus Kellerhals

KEY MESSAGES AND IMPLICATIONS

- Ozone can have negative effects on plant health which can lead to ecosystem changes (e.g. shifts in species composition). Plant response to ozone varies with species, and genotype within species, and is modified when combined with other ecosystem stressors. Recent studies show that multi-year exposures of perennial plants to O₃ lead to changes in biomass that would not otherwise be detected in studies of shorter duration.
- The 4th highest daily maximum 8-hour O₃ concentration (used to calculate the Canada-Wide Standard for O₃) and the cumulative O₃ exposure indices (i.e. AOT40, SUM60, W126, etc.) are well correlated. This indicates that actions aimed at reducing the 8-hour average O₃ concentration would also reduce vegetation exposure to O₃.
- The recent literature does not contain sufficient new information to support the identification of a secondary O₃ air quality standard to protect vegetation,
- In order to adequately evaluate the regional efficacy of the current CWS in protecting vegetation, future research needs to contribute to the development of exposure metrics in areas of known elevated O₃ occurrence across Canada, in the form of the current CWS as well as cumulative indices (i.e. AOT40, SUM60, W126, etc.), against which vegetation effect thresholds identified by current literature studies and future studies (ideally for Canada-relevant species and ecosystems) can be compared.
- The recent literature did not contribute new understanding to the impact of PM on vegetation but confirmed that vegetation response to PM is dependent upon PM speciation, and that is largely due to changes in soil chemistry rather than direct deposition. The impact to materials from PM is also dependent upon speciation of the PM. The recent literature does not contain any new information which would result in the modification of the air quality standard for PM to protect vegetation.
- The recent literature does not contain sufficient new information to support modifying the metric of an air quality standard for O₃ to protect materials, and it does not contain any new information which would result in the modification of the air quality standard for PM to protect materials.

10.1 Introduction

10.1.1 Impact of Ozone on Vegetation and Materials

Ozone is an oxidant that is taken up by plants almost exclusively via the stomates underneath plant leaves. The diffusion of ozone is driven by the concentration gradient between the ambient air and the substomatal cavity as well as by the size of the stomatal aperture. Significant uptake through the leaf surface is not likely as diffusion through the cuticle is not favoured. However, the exception to this generalization is surface absorption by the guard cells of the stomates, which are not cuticularized.

O₃ degrades into a number of reactive oxygen species (e.g. superoxide radical, hydroxyl radical, peroxide) which have the potential to react with biological molecules. Because of its reactivity, O₃ is not thought to travel far within a cell; however, the spongy mesophyll cells that form the lower layer of the leaf and the boundary of the substomatal cavity typically have chloroplasts adjacent to the cell wall that optimize carbon dioxide (CO₂) absorption. This means that some chloroplasts are close to the site of O₃ uptake by the spongy mesophyll cells, and therefore impacts to the chloroplasts can occur more readily. O₃ can diffuse through the leaf in the spongy mesophyll (so named because of the loose organization of these cells with plenty of air spaces to optimize diffusion of CO₂ from stomates) to palisade mesophyll cells, which are tightly packed, and which are most active in photosynthesis. Young leaves which are not fully expanded have undeveloped spongy mesophyll, that is, those cells are tightly packed – thus, the stomates of these leaves typically are not very active as the leaf cannot process CO₂ very efficiently. In addition, younger leaves have a less active pool of antioxidant to draw from in detoxifying ozone. Hence, young plants, or the young leaves of active plants, are not very sensitive to O₃. Older leaves deep in the canopy also do not have very active stomates as there is little light penetration for photosynthesis. These lower leaves may not be exposed to significant concentrations of O₃ because O₃ concentration decreases with distance from the top of the plant canopy, due to plant uptake or reaction with plant surfaces. Therefore, the upper canopy level leaves are generally exposed to higher concentrations of ozone than lower level leaves. Most of the reported values for exposure and subsequent response are actually measured at the top of the plant canopy rather than ambient (i.e. within canopy), which will be lower concentrations.

Once taken up by the plant, O₃ or its reactive oxygen species (ROS) are believed to do the most direct damage to membranes, specifically the fatty acids that compose the bi-layer, typically leading to visible necrosis (cell death). The plant can also be damaged indirectly by requirements for energy to detoxify O₃ or its ROS. Detoxification pathways are part of the plant's metabolism to generally deal with the ROS arising from photosynthesis, for example. These detoxification mechanisms include the oxidation of glutathione, which must be converted back (energy-requiring) to the reduced form in order to be available to again

“receive” a ROS. The ultimate plant effects of this indirect damage is loss of productivity and premature senescence, the latter being a process that is in itself related to production of ROS that are not detoxified. The effects of O₃ on photosynthesis can be both direct and indirect. Direct absorption of O₃ or ROS by guard cells can disrupt their function, altering CO₂ uptake. Absorption of O₃ or ROS by chloroplasts is thought to disrupt the organelle’s membranes reducing fixation of CO₂ (direct effect) thus causing stomatal closure (in response to the subsequent increasing partial pressure in the substomatal cavity) and indirectly reducing photosynthesis. At the whole-plant level, certain stages of development can be critical to the success of various processes. For example, yield of bean species can be very sensitive to photosynthesis at the pod-filling stage; thus, the ontogenic timing of or the physiological development stage of the plant at O₃ exposure can be critical to its effects.

Plant response to O₃ is a function both of duration and concentration of exposure. The response to acute exposure (short duration of high concentration) can include stomatal closure, which prevents the uptake of O₃, as well as extensive necrosis. O₃ also impairs stomatal control on water losses which can influence plant water balance. Response to chronic exposure (long duration at lower concentrations) is more typically yield or growth reduction, resulting from the disruption of primary production and/or additional energy requirements. Mathematical relationships linking O₃ fumigation with plant response are variably referred to as “Dose Response Functions” and “Exposure Response Functions”, the meaning of which continues to evolve. There is no agreement in the scientific community as to the difference (or, whether there is a difference at all) between the two terms, and thus they are used interchangeably in the literature. “Dose” should refer to the actual (or inferred actual) amount of O₃ taken up by the plants, whereas “Exposure” would refer to the amount of O₃ in the air fumigating the plants.

Much of the scientific literature is focussed on the mathematical expression of O₃ exposure or dose, sometimes referred to as exposure or dose metrics. For air quality standards setting, exposure metrics are discussed as they relate to secondary standards for the protection of vegetation. Investigators have explored various exposure metrics in an effort to relate vegetation’s exposure to plant response. Those frequently used in the literature include:

- SUM 00: sum of all hourly concentrations in a year without a threshold;
- SUM60: sum of the hourly concentrations above a threshold of 60 ppb in a year or a given portion of the year;
- W126: sum of the hourly concentrations from 8 a.m. to 8 p.m. from May to September (or the maximum consecutive 3-month summation period) within a year, where each concentration is weighted by a sigmoidal function that assigns greater weight to higher concentrations;

- AOT40: sum of hourly concentration over 40 ppb over daylight hours, or conventionally between 8 a.m. and 8 p.m., in a year or a given portion of the year;
- AF_{st}Y: accumulated stomatal flux above a threshold Y.

Ozone's greatest impact to materials has been shown to be the degradation of rubber and other elastopolymers. Exposure to O₃ can also cause fading or degradation in pigments and dyes as well as the degradation of surface coatings (i.e. paint, varnish, etc.). Minor increased corrosion of metal may be realized in the presence of sulphur dioxide. Stone or other building materials are affected by O₃ only when it is in combination with other environmental factors and pollutants.

10.1.2 Impacts of Particulate Matter on Vegetation and Materials

The mechanisms of action through which PM impacts vegetation include smothering of the leaf, physical blocking of the stomata, biochemical interactions and indirect effects via changes to the physical and chemical properties of soil. It should be noted that changes in soil characteristics from PM deposition were addressed in the 2004 Canadian Acid Deposition Science Assessment (Environment Canada, 2005); thus, are not revisited in this assessment.

The main impact of PM to materials is the impact to aesthetic appearance due to soiling and discolouration. Depending upon the speciation of the PM, it can also increase the rate of physical and chemical degradation of a material. Corrosion and erosion of materials can be accelerated via exposure to PM.

10.1.3 Organization of the Chapter

The intent of this chapter is to provide scientific guidance for the review of ambient air quality standards for Canada as it relates to the impact of ground-level ozone (O₃) and particulate matter (PM) - the principle components of smog - on vegetation and materials. The chapter includes a review of scientific material examining the effects of O₃ and PM on vegetation and materials subsequent to those captured in previous assessments. This corresponds to scientific literature published from 2003 to December 2007 inclusive. A focus was placed on reviewing the scientific literature within the context of closing the scientific gaps or limitations that were noted in the 2003 Update in Support of the Canada-wide Standards (CWS) for O₃ and PM (CCME, 2003a, b), the USEPA Air Quality Criteria Document (USEPA, 2006), the USEPA Office of Air Quality Planning and Standards (OAQPS) Staff Paper (USEPA, 2007) and the USEPA Air Quality Criteria for Particulate Matter (USEPA, 2004). The main findings of these previous assessments are included in Section 10.3.

Section 10.2 provides a quantifiable estimate of the current levels of vegetation exposure to O₃ in Canada using measured and modelled data. Section 10.3 includes a summary of previous assessment and their main findings. Section 10.4 provides a summary of the recent literature addressing the impacts of O₃ on vegetation and materials. Section 10.4.1 considers the literature according to studies examining individual plant effects, ecosystem responses, the effect of O₃ in combination with other stressors and in mixtures and O₃ dose expression. Section 10.4.2 considers recent literature on the impacts of O₃ on materials. Section 10.5 is a summary of the recent literature addressing the impacts of PM on vegetation and materials. Uncertainties that were identified as a result of reviewing the recent scientific literature in detail are provided in Section 10.6. Section 10.7 provides a summary of the main findings of the review of recent literature and provides conclusions as they apply to the objectives of this assessment. Section 10.8 briefly discusses the emerging issue of direct PM and O₃ effects on wildlife. Although only limited research is currently available, these effects may be important to assessing broader ecosystem risks. Recommendations for future research and references are included in Sections 10.9 and 10.10, respectively.

10.2 Characterization of Vegetation Exposure to Ozone

10.2.1 Measurement of Vegetation Exposure to Ozone

Ambient measurements of O₃ concentrations have been used to estimate vegetation exposure to O₃ using a number of metrics. Below are the definitions of the three O₃ index forms considered in this section:

- **12-hr SUM06:** 3-month sum of all hourly O₃ concentrations greater than or equal to 60 ppb observed during the daily 12-hr period between 8 am and 8 pm. The 3 months are those with a consecutive maximum summation value in the period of May to September. The sum is adjusted to account for missing observations and divided by 1000 to produce a result in ppm-hours. SUM06 is analogous to SUM60, but the results are presented in ppm-hours (1 ppm-hour = 1,000 ppb-hours) rather than ppb-hours.
- **12-hr W126:** Sigmoidally weighted 3-month sum of all hourly O₃ concentrations observed during the daily 12-hr period between 8 am to 8 pm. The 3 months are those with a consecutive maximum summation value in the period of May to September. The hourly values are divided by 1000 to produce a result in ppm-hours.

W126 is defined in Lefohn *et al.*, 1988 as:

$$W126 = \sum_{i=8AM}^{i=8PM} w_{C_i} C_i,$$

where C_i = hourly O_3 concentration in ppbat hour i , and

$$w_{C_i} = \frac{1}{1 + 4403e^{-126C_i}}$$

- **AOT40:** 3-month sum of all hourly O_3 concentrations greater than or equal to 40 ppb adjusted by subtracting 40 ppb, for the daily 12-hr period between 8 am and 8 pm. The 3 months are those with a consecutive maximum summation value in the period of May to September. The sum is adjusted to account for missing observations and divided by 1000 to produce a result in ppm-hours.

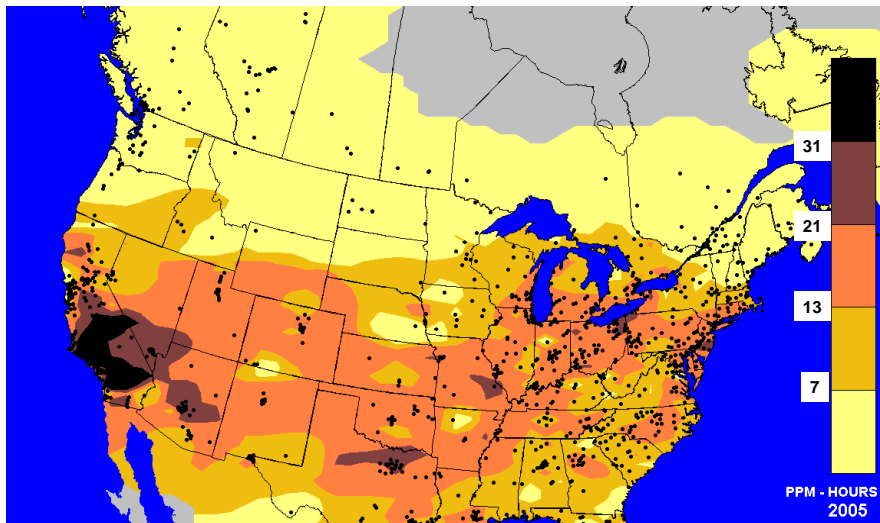


Figure 10.1 Spatial pattern of vegetation exposure to O_3 concentrations (2005) in North America based on the W126 Exposure Index (ppm-hours). The dots represent the locations of monitoring sites used in the analysis

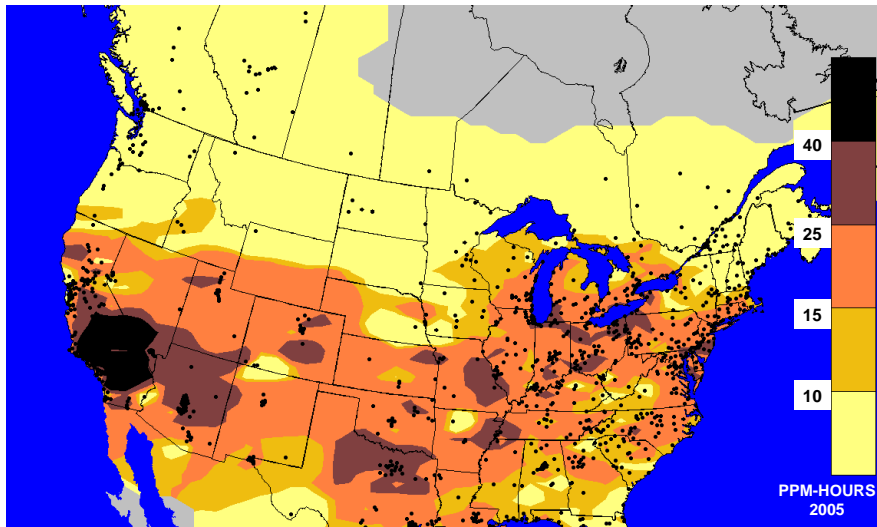


Figure 10.2 Spatial pattern of vegetation exposure to O₃ concentrations (2005) in North America based on the SUM06 Exposure Index (ppm-hours). The dots represent the locations of monitoring sites used in the analysis.

Table 10.1 Vegetation exposure indices calculated for rural Canadian sites in 2005. Right column presents the 4th highest daily maximum O₃ concentration (ppb) as measured at each site. Sites were selected to provide a cross-section of results across Canada

NAPS ID	Measurement Site	SUM06 (ppm-hrs)	W126 (ppm-hrs)	AOT40 (ppm-hrs)	4 th High Daily Max O ₃ Concentration (ppb)
30501	KEJIMKUJIK, NS	1.66	2.3	2.24	64
30701	AYLESFORD, NS	1.86	2.0	1.90	65
40501	POINT LEPREAU, NB	1.14	1.8	1.72	58
41001	CAMPOBELLO ISLAND, NB	0.55	1.5	1.69	58
52201	SAINT-SIMON, QC	2.90	2.8	3.01	61
52301	SAINT-FAUSTIN-LAC-CARRÉ, QC	4.52	3.8	3.64	77
52401	LA PÊCHE, QC	6.04	4.8	4.48	80
53801	TINGWICK, QC	3.20	3.4	3.52	63
54102	SUTTON, QC	3.75	4.3	4.36	72
55301	SAINT-JEAN-SUR-RICHELIEU, QC	4.84	4.5	4.69	68
55501	FRELIGHSBURG, QC	7.53	6.4	6.57	71
62501	TIVERTON, ON	9.12	6.6	6.00	82
62601	SIMCOE, ON	25.46	18.4	14.99	84
63301	DORSET, ON	14.40	11.6	9.86	80
64001	EXPERIMENTAL LAKES AREA, ON	1.92	2.9	3.52	64
64101	ALGOMA, ON	4.83	4.1	4.49	70
64401	EGBERT, ON	15.01	12.1	10.31	79
66001	FRASERDALE, ON	0.25	1.1	1.18	54
80901	BRATT'S LAKE, SK	0.06	1.5	1.82	53
91101	ELK ISLAND, AB	1.11	2.6	3.58	59
91901	CAROLINE, AB	2.87	4.1	5.13	61
101401	HOPE, BC	2.53	2.4	2.34	62
102001	SATURNA, BC	0.53	1.1	0.89	60

Ambient O₃ concentrations data collected at National Air Pollution Surveillance (NAPS) Network sites in combination with data obtained from U.S. monitoring sites available through the EPA Air Quality System (AQS) data repository, were used to develop spatial plots for W126 and SUM06 for the year 2005 and are shown in Figures 10.1 and 10.2. The maps were created using an inverse distance weighted interpolation scheme. Table 10.1 presents a cross-section of the vegetation exposure index values for a selection of rural sites across Canada and the 4th highest daily maximum 8-hour O₃ concentrations measured at those sites. Within

Canada, the highest O₃ exposures occur in southern Ontario, as calculated using both index methods (W126 of up to 18.4 ppm-hrs; SUM06 of up to 25.46 ppm-hrs). Outside of southern Ontario, W126 values of less than 7 ppm-hrs and SUM06 values of less than 10 ppm-hrs are observed across Canada. The patterns are similar to those of AOT40 (not shown).

Although each of the exposure metrics calculates vegetation exposure to O₃ slightly differently, the various techniques produce results which are well correlated.

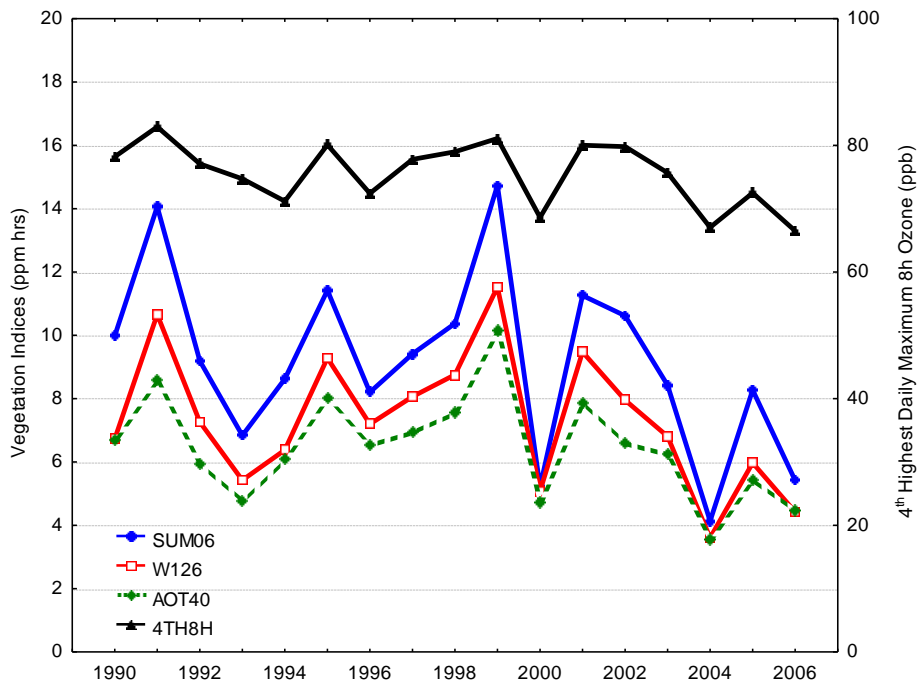


Figure 10.3 Interannual relationship between SUM06 (top left), W126 (top right), and AOT40 (bottom) and annual values of the 4th highest daily maximum 8-hour O₃ concentration calculated for all National Air Pollution Surveillance (NAPS) network sites for 1990-2006.

The form of the CWS for O₃ is the 4-year average of the 4th highest daily maximum 8-hour O₃ concentration. The relationship between the annual values of the 4th highest daily maximum 8-hour O₃ concentration and vegetation O₃ exposure metrics (SUM06, W126 and AOT40) are presented in Figure 10.3. Data from all sites (rural and non-rural) from 1990-2006 were used in this analysis. A Lowess smoothing was used to fit a line to the data, and the correlation coefficients (r) for the metrics were calculated to be 0.880, 0.882 and 0.887 for SUM06, AOT40 and W126, respectively. These results indicate that the 4th highest daily maximum 8-hour O₃ concentration is well correlated with vegetation exposure to O₃ as calculated using the three exposure metrics. This relationship indicates that actions aimed at reducing the 8-hour average O₃ concentration would also reduce vegetation exposure to O₃ measured using the

seasonal exposure indices. However, these relationships as seen in Figure 10.3, are not linear and as the indices are based on different effects thresholds, a reduction in the 4th highest daily maximum 8-hour O₃ concentration would have different benefits under each individual index.

10.2.2 Application of Regional Air Quality Modelling to Estimate Vegetation Exposure to Ozone in Alberta

A regional air quality modelling analysis was used to investigate the potential effects of O₃ exposure to vegetation in the province of Alberta. Ozone concentrations were modelled over a three month summer time period using the state-of-the-art Community Multiscale Air Quality Modelling System (CMAQ) for a base-case (2002) and a future case (2012-2015) emissions scenario. Details of the emissions inputs and model set-up for these scenarios are described in Chapter 6 (Section 6.3.3). Predicted O₃ concentrations for the base case scenario agreed reasonably well with available observations. The results of the future case simulation represent only one possible future scenario and are dependent on forecast emissions with conservative assumptions included. Vegetation exposure to O₃ was calculated using both the SUM60 and AOT40 metrics.

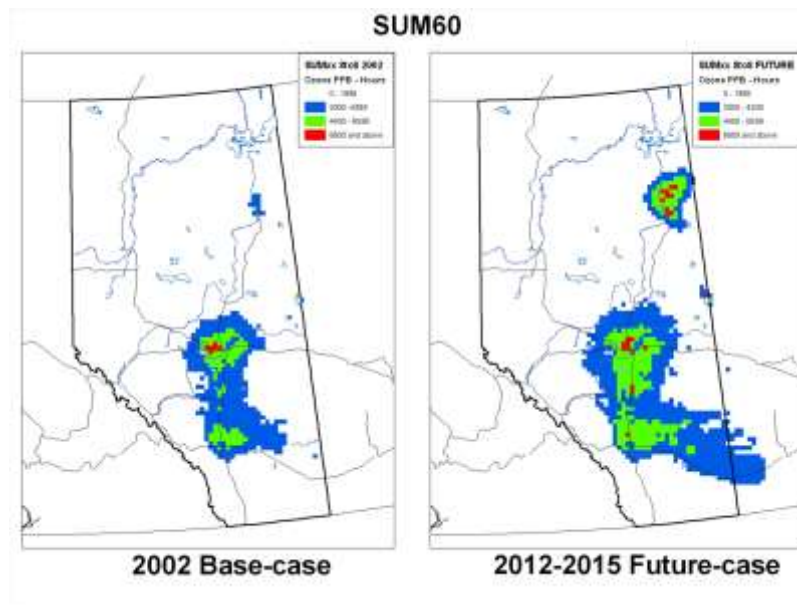


Figure 10.4 Model predicted SUM60 in Alberta for the 2002 base-case (left) and a future scenario (right).

The SUM60 values for Alberta, presented in Figure 10.4, were calculated by summing the hourly modelled O₃ concentrations that were greater than or equal to 60 ppb, occurring during daylight hours (08:00-20:00), for the months of June, July and August. In the base-case scenario, SUM60 levels of between 2,000 and 4,400 ppb-hours are observed in the area around the oil sands in Fort McMurray and in the Edmonton-Calgary corridor. Smaller areas around

Calgary and Edmonton have levels greater than 4,400 ppb-hours, and a small area west of Edmonton has levels above 6,600 ppb-hours. In the future-case scenario, the areas with elevated SUM60 levels increased especially around Fort McMurray, where SUM60 values greater than 6,600 ppb-hours are projected, and in southeast Alberta.

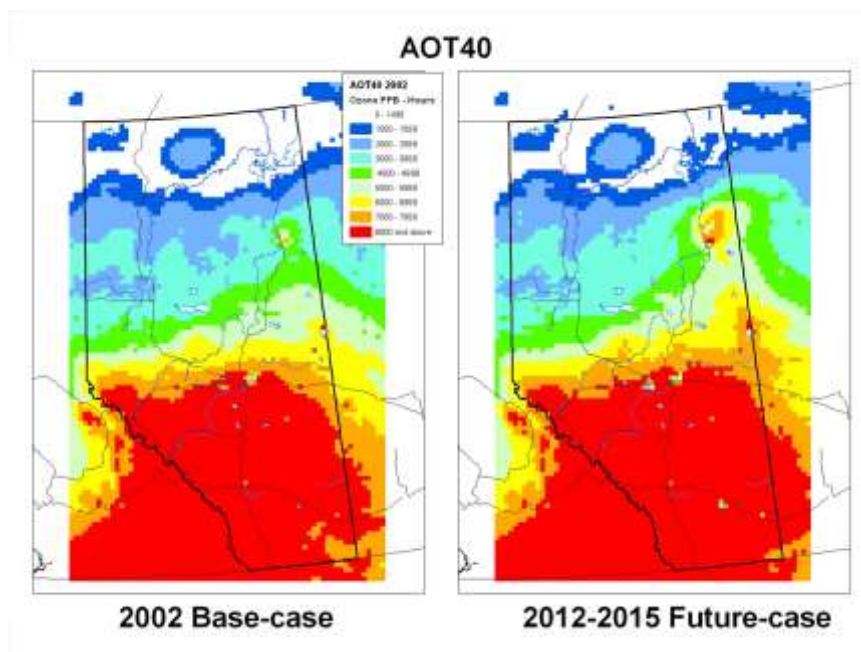


Figure 10.5 Model predicted AOT40 levels in Alberta for the 2002 base-case (left) and a future scenario (right).

The AOT40 values for Alberta seen in Figure 10.5, were calculated by summing the positive differences between hourly O_3 concentrations and a threshold value, 40 ppb, during daylight hours (when solar radiation $> 50 \text{ W m}^{-2}$), over the months of June, July and August. The spatial distribution of the AOT40 values for both the base-case and future-case scenarios is very similar, with higher levels in southern Alberta and decreasing northwards. In the future-case scenario, AOT40 values are elevated around the Fort McMurray and Cold Lake areas in comparison to the base-case (refer to Chapter 7 for a detailed map of the region).

The AOT40 follows a similar spatial pattern to the predicted mean O_3 concentrations (presented in Chapter 6, Figure 6.11), which are higher in the south and west of the province, and correspond to known latitudinal and elevation gradients in O_3 . The similarity between the patterns of AOT40 and mean daytime O_3 suggest that the AOT40 metric is more sensitive than the SUM60 to broad geographic patterns of O_3 distribution, and less sensitive to episodes of local O_3 production. Given that the SUM60 metric is more influenced by anthropogenic emissions than the AOT40 metric, this may suggest that the SUM60 metric is more useful for managing the anthropogenic portion of vegetation exposure to O_3 in Alberta.

10.3 Summary of Previous Assessments

10.3.1 Ozone Impacts on Vegetation

The Federal-Provincial Working Group on Air Quality Objectives and Guidelines undertook a science assessment on the effects of O₃ on vegetation in 1999 (WGAQOG, 1999a). The 1999 Science Assessment Document (SAD) recommended that O₃ exposure be expressed as a cumulative 8-hour index (SUM60) in order to protect vegetation, based on the Lowest Observable Adverse Effect Level (LOAEL). The SUM60 was based on hourly measurements of O₃ between 08:00-19:59 hours for a defined period (i.e. days or months). For every hour with a concentration over 60 ppb the reported concentration was added to the running total to derive an ultimate total in ppb-hour. The literature review determined a LOAEL range could be established for agricultural crops and tree species in order to protect vegetation from chronic effects of O₃ on yield and productivity. In addition, a short-term LOAEL range was also identified for acute impacts (foliar injury) to agricultural species.

The Canadian Council of Ministers of the Environment (CCME, 2003a) undertook an update of the 1999 SAD to assess the recent literature and determine whether new findings would change the conclusions of the 1999 SAD. The Update in Support of the Canada-Wide Standards for Particulate Matter and Ozone (2003 CWS Update) document provided a summary of the considerable volume of research undertaken in Europe between 1999 and 2003. The focus of the European research was the relationship of the AOT40, a cumulative index (ppb-hour) based on summing the positive difference between hourly O₃ measurement and 40 ppb within a specified time window, and vegetation response.

The 2003 CWS Update acknowledged that recent literature published between 1999 and 2003 suggested further refinements to the 1999 SAD recommendation of the SUM60 as a secondary standard to protect vegetation where possible, but the means by which to improve it were not clear. Considerable work had been completed in Europe focussing on the AOT40 index, but the 2003 CWS Update concluded the AOT40 would not provide a significant improvement over the SUM60 index in ascertaining the relationship between O₃ exposure and plant response. While literature regarding the incorporation of O₃ flux into the plant, or effective dose, into a secondary or level 2 air quality standard was prevalent at the time of the writing of the 2003 CWS Update, it was recognized that while the approach was preferred, there were many more data required to assess the methods by which such an approach could be incorporated into an air quality standard for the protection of vegetation.

The United States Environmental Protection Agency's Air Quality Criteria for Ozone and Related Photochemical Oxidants (USEPA AQCD) (USEPA, 2006) discussed a large body of new research that emerged between 1996 and 2003, largely from Europe, which examined the relationship between effective dose and plant response. The literature was reviewed in the

USEPA AQCD, but it was concluded that there was insufficient information to identify a flux-based model that incorporated all the complexities that can occur across space, time and species. In particular, this literature pointed out the potential disconnect between peak O₃ events and maximum stomatal conductance due to the closure of stomates during water stress. In addition, the new literature demonstrated that O₃ could still enter plants during the evening and night hours, and not just during daylight hours as previous O₃ metrics had assumed.

The USEPA AQCD cautiously noted that not all stomatal uptake of O₃ results in yield reduction, as it depends on the amount of internal detoxification that occurs within individual plant species. The USEPA noted that as of 2003, there was a relative paucity of data concerning O₃ flux and growth response, in comparison to the large body of literature that had been used in the United States (U.S.) to establish exposure-response relationships.

The USEPA AQCD suggested more data concerning the relationship between stomatal conductance, O₃ concentration, and defence and repair mechanisms will allow for better precision and predictability in the use of flux based critical O₃ values in the setting of standards. The USEPA AQCD therefore suggested that the best approach toward a secondary standard to protect vegetation in the U.S. continues to be a cumulative exposure index that differentially weights higher O₃ concentrations, but also includes the mid-level values. The differential weighting of the higher concentrations incorporates the premise that plants' defence and repair mechanisms are eventually overwhelmed when exposed to higher concentrations. The W126, a sigmoid function weighting of all hourly concentrations for the growing season was supported by the USEPA Office of Air Quality Planning and Standards (OAQPS) Staff Paper (USEPA, 2007) as the preferred approach for a secondary air quality standard of O₃ for the protection of vegetation.

10.3.2 Ozone Impacts on Materials

The 1999 SAD for O₃ (WGAQOG, 1999a) concluded significant O₃ effects were realized on elastomeric materials (natural rubber, general purpose rubber and synthetic polymers of polyisoprene, polybutadiene, acrylonile-butadiene and styrene-butadiene) due to the potential for O₃ to break the long chain of unsaturated organic molecules that create these types of material. Materials that consist of saturated organic molecules (i.e. silicones, and butyl rubber) are more resistant to O₃ damage.

Some effects of O₃ were noted on textiles, dyes and surface coatings. Although not well quantified, the contribution of O₃ to the degradation of textiles is generally considered insignificant. The cellulose fibers in textiles such as cotton and silk can be degraded by O₃ exposure; however, sunlight, heat, alternate wetting and drying, and micro-organisms cause greater degradation. The lowest concentration at which effects were observed was on wet cotton cloth exposed to 0.02 ppm O₃.

Exposure to O₃ can also cause fading or degradation in textile dyes and artists' pigments in paintings and other cultural assets. The lowest exposure to O₃ where effects were realized was 0.4 ppm over 95 days (which was also the lowest experimental concentration used in the study). Effects of pigment on watercolour paper were also realized after 7 days exposure to 0.4 ppm O₃.

Surface coatings, such as paint, varnish or lacquer can be affected by O₃ exposure. Both the binding of the coating to the substrate and the pigment can be affected, causing erosion over time. Various studies were reviewed and the lowest concentration at which a response to surface coatings was observed was 0.05 ppm.

The 1999 SAD concluded modest effects were realized on inorganic building materials such as metals, where corrosion occurred only in the presence of sulphur dioxide. It was also noted that O₃ effects on metals and stone are influenced by environmental factors and other chemicals in the atmosphere.

The 2003 CWS Update of the effect of O₃ on materials (CCME, 2003b) focused on the review of published literature that would contribute to the scientific basis for the establishment of an air quality standard for O₃. Literature published between 1999 and 2003 focused on the mechanisms of effects but contributed little to the further understanding of dose-response relationships. The United Nations Economic Commission for Europe (UN ECE) International Co-operative Programme on Effects on Materials (ICP Materials) provided more recent data that did not support synergistic effects of O₃ observed in previous studies.

The 2003 CWS Update concluded that in recent years, very little basic work on the effect of O₃ on materials that could contribute to dose-response understanding was completed. There was insufficient new information on O₃ effects on materials to suggest any changes to the CWS for O₃.

The USEPA AQCD (USEPA, 2006) came to the same conclusion as the 2003 CWS Update that very little new information on the impact of O₃ on materials had been published, and therefore, a summary of the discussion contained in the 1996 air quality criteria document (USEPA, 1996) for O₃ was provided.

10.3.3 Particulate Matter

Vegetation

The Federal-Provincial Working Group on Air Quality Objectives and Guidelines completed a science assessment on the impact of PM in 1997, which was revised in 1999 (WGAQOG, 1999b) The Addendum to the SAD for PM included the following paragraph on vegetation impacts:

“The primary effects of particulate matter on vegetation are reduced growth and productivity, due to interference with photosynthesis, and phytotoxic impacts as a result of particle composition. The mechanisms of action include smothering of the leaf, physical blocking of the stomata, biochemical interactions, and indirect effects through soil. Particles make contact with vegetation surfaces in three ways: sedimentation, impaction and deposition. The relative efficiency of these methods depends upon the plant or soil surface, the microclimate and ambient conditions (temperature and humidity).

Given the limited amount of information available, specifically the lack of quantitative dose-effect information, it is not possible to define a Reference Level for vegetation.”

The USEPA undertook a review of the current state of knowledge of PM and vegetation effects in 2004 (USEPA, 2004). This review points to the complexity of PM, which is not a single pollutant, but rather a heterogeneous mixture of particles differing in origin, size, and chemical constituents. The ambient concentration of PM, which is the reported parameter, can vary widely in terms of chemical constituents, which will control the phytotoxic response of plants.

The USEPA review concluded the PM constituents of greatest environmental significance are particulate nitrates and sulphates, whose indirect effects occur primarily via their deposition onto the soil. Upon entering the soil environment, they can alter the ecological processes of energy flow and nutrient cycling, inhibit nutrient uptake, change ecosystem structure, and affect ecosystem biodiversity.

The deposition of heavy metal PM can also change soil chemistry and result in plant exposure. Exposures to metals are highly variable, depending on whether deposition is by wet or dry processes. Few metals (e.g., Cu, Ni, Zn) have been documented to have direct phytotoxicity under field conditions. Exposure to coarse particles of natural origin and elements such as Fe and Mg are more likely to occur via dry deposition, while fine particles formed through atmospheric processes are more likely to contain elements such as Ca, Cr, Pb, N, and V. Ecosystems immediately downwind of major emissions sources such as power generating, industrial, or urban complexes can receive locally heavy inputs.

Key conclusions and findings from the USEPA document regarding PM-related effects on vegetation and ecosystems include the following:

- “A number of ecosystem-level conditions (e.g., nitrogen saturation, terrestrial and aquatic acidification, coastal eutrophication) that can lead to negative impacts on human health and welfare have been associated with chronic, long-term exposure of ecosystems to elevated inputs of compounds containing Nr (reactive nitrogen), sulphur and/or associated hydrogen ions.
- Some percentage of total ecosystem inputs of these chemicals is contributed by deposition of atmospheric particles, although the percentage greatly varies temporally and geographically and has not generally been well quantified.
- Unfortunately, our ability to relate ambient concentrations of PM to ecosystem response is hampered by the following significant data gaps and uncertainties:
 - a. *The lack of a long-term, historic database of annual speciated PM deposition rates in sensitive ecosystems precludes establishing relationships between PM deposition (exposure) and ecosystem response at this time.*
 - b. *Modelled deposition rates, used in the absence of monitored data, can be highly uncertain, since there are a multitude of factors that influence the amounts of PM that get deposited from the air onto sensitive receptors. These factors include the mode of deposition (wet, dry, occult), wind speed, surface roughness/stickiness, elevation, particle characteristics (e.g., size, shape, chemical composition, etc.), and relative humidity.*
 - c. *Each ecosystem is unique from all others, since each has developed within a context framed by the topography, underlying bedrock, soils, climate, meteorology, hydrologic regime, natural and land use history, species associations that co-occur at that location (i.e., soil organisms, plants, etc.), and successional stage. Because of this variety, and insufficient baseline data on each of these features for most ecosystems, it is currently impossible to extrapolate with much confidence any effect from one ecosystem to another, or to predict an appropriate “critical load.” Thus, a given PM deposition rate or load of nitrates in one ecosystem may produce entirely different responses than the same deposition rate at another location.*
 - d. *There remain large uncertainties associated with the length of residence time of Nr (reactive Nitrogen) in a particular ecosystem component or reservoir, and thus, its impact on the ecosystem as it moves through the various levels of the N cascade.*
- *As additional PM speciated air quality and deposition monitoring data become available, there is much room for fruitful research into the areas of uncertainty identified above.”*

Contrary to the U.S. position presented above in (c.), Canada has utilized an ecosystem critical load approach for more than 20 years to set targets for acid deposition as part of emissions reduction strategies. Since the mid-to-late 1980s, European countries have similarly worked towards the development of critical loads to guide continent-wide emission control programs. The early Canadian critical loads were developed in the 1980s and only considered sulphur-based acidification of aquatic systems in eastern Canada. Over the years, the critical loads approach has been refined to take into account both the sulphur and nitrogen components of acid deposition and the ecosystem effects on both lakes and upland forest soils. The 2004 Canadian Acid Deposition Science Assessment (Environment Canada, 2005) provides the most recent scientific summary of acid deposition levels in Canada, the associated ecosystem effects and presented the first combined aquatic-terrestrial critical loads in North America. Since the 2004 Canadian Acid Deposition Science Assessment, efforts have continued to refine critical loads in eastern Canada and expand the evaluation to western Canada (Carou *et al.*, 2008). Although a critical loads approach was not recommended in the USEPA Assessment document, research and interest in the development and potential implementation of critical loads approach in the U.S. continues (Fisher *et al.*, 2007).

10.3.4 PM Impacts on Materials

The Addendum to the SAD for Particulate Matter (WGAQOG, 1999b) included only the following paragraph on materials impacts:

“The deposition of particulate matter on materials can reduce their aesthetic appearance, as well as increase the rate of physical and chemical degradation. The primary effects of particulate matter on materials are to accelerate the rates of corrosion and erosion, and soiling and discolouration. Particles may act as catalysts for the conversion of SO₂ and NO_x to sulphuric acid and nitric acid which accelerate the chemical degradation of susceptible material surfaces on which they are deposited. Most information available is on the effects of particle exposure in combination with SO₂.

Given the limited amount of information available and specifically the lack of quantitative dose-effect information, it is not possible to define a Reference Level for materials.”

The USEPA Air Quality Criteria document for PM concluded there are insufficient data available in the scientific literature to determine a threshold level at which the effects of PM on materials are perceived, either visually or physically (USEPA, 2004). The USEPA concluded a dose-response function or threshold definition by which to set air quality criteria for PM based on effects on materials was not possible at the time of the writing of the criteria document.

10.4 Recent Literature on Ozone Effects

10.4.1 Vegetation

10.4.1.1 Individual Plant Effects

The 2003 CWS Update for O₃ and PM (CCME, 2003a) summarized a number of uncertainties or data gaps that limited the conclusions drawn from the literature on the effect of O₃ at the individual plant level, namely:

- few recently published data on important Canadian crops that are likely to be grown in regions of Canada that experience elevated O₃ concentrations (examples of which are soybean, corn, wheat, flax, hay);
- scant data on belowground effects of O₃ exposure, particularly in woody plants, and as a result of multi-year exposures; and
- few linkages between the occurrence of visible injury on plants as a result of O₃ exposure, its importance to the value of some plant communities, and its absence from consideration as an endpoint for most exposure indices (such as SUM60 or W126).

Because the number of new papers addressing the effects of O₃ on individual plant species published since 2003 is quite extensive, those papers addressing these deficiencies/data gaps are extensively reviewed in this section, with the key points of the remaining papers summarized in tabular form. Additionally, papers addressing forest tree species (of potential relevance to Canada), and any papers that provide additional knowledge of dose-response that can be related to economic variables such as yield, health of forest trees were also extensively reviewed in this section.

All studies discussed in this section are summarized in Tables 10.2 and 10.3.

Table 10.2 Recent studies that contributed to the advancement of understanding of the impact of O₃ on individual plant species

Citation	Species	Endpoint	Conclusion
Bassin <i>et al.</i> 2004b	Brown Knapweed	Visible Injury	Populations varied in response to ozone, thus use as bioindicator depends on origin of population; dose response not calculated per se, but easily could be
Braun <i>et al.</i> 2007	European Beech	Reduction in shoot growth	7.4% reduction in shoot growth / 10 ppm-hr AOT40
Braun <i>et al.</i> 2007	Norway Spruce	Reduction in shoot growth	-0.3 to +1.0% reduction in shoot growth / 10 ppm-hr AOT40
Cano <i>et al.</i> 2007.	Elder Species (Dwarf elderberry, Red Elderberry, Black Elderberry)	Visible injury, chlorophyll; function	Dwarf elderberry more sensitive than Red Elderberry and Black Elderberry; some plants of all three were injured below AOT40 of 10000 ppm-hr
Chappelka <i>et al.</i> 2003	Cutleaf Coneflower and Crown-beard	Visible injury	First observation of injury in these species, in the field (Great Smoky Mountain Park)
Chappelka <i>et al.</i> 2007	Tall milkweed	Visible injury	Over 5 y, incidence of injury on same populations varied between 44% and 90%, not consistent with ambient O ₃ concentrations; microsite influences very important modifiers
Christ <i>et al.</i> 2006.	Soybean	Agricultural yield	Agricultural yield is preserved under moderate ozone exposure (1.2 x ambient) at the expense of leaf growth using FACE, when open-top chamber studies would predict yield loss
Davis and Orendovici, 2006.	European Beech	Stem increment and may parameters at the whole leaf and cellular level	Despite many endpoints demonstrating sensitivity to ozone, the reduction in stem increment from 2 x ambient ozone was not statistically separable from 1 x ambient
Davis and Orendovici, 2006.	Norway Spruce	Stem increment and may parameters at the whole leaf and cellular level	Despite many endpoints demonstrating sensitivity to ozone, the reduction in stem increment from 2 x ambient ozone was not statistically separable from 1 x ambient
Grebenc and Kraigher, 2007.	European Beech and Norway Spruce	Mycorrhizal colonization	Greater in roots from ozone exposed plants
Hayes <i>et al.</i> 2007.	Many semi-natural species	Sensitivity	Derived linear exposure-response functions for numerous species; these e-r relationships were not presented, but were used to calculate relative sensitivity index
Jones <i>et al.</i> 2007.	Many species	Sensitivity	Developed predictive equation for ozone sensitivity based on Ellenberg Indicator values for salinity and light
Kohut 2007.	Many ozone sensitive species	Visible injury	Framework for estimating risk of visible injury to ozone sensitive plants in protected areas, based on known sensitive species, ambient ozone and soil moisture: ~25% of 244 parks were at "high" risk
Morgan <i>et al.</i> 2003.	Soybean (meta-analysis of existing studies)	Marketable yield	24% reduction in marketable yield results from 70 ppb; yield loss even results from chronic average ozone concentrations <60 ppb

Citation	Species	Endpoint	Conclusion
Novak <i>et al.</i> 2007.	Lombardy Poplar European Poplar Wayfaring Viburnum	Annual growth ring width	~ 50% reduction in growth ring width in <i>P. nigra</i> after two years of exposure, to AOT40 ~ 20 ppm-hr
Oksanen 2003.	Birch (Clones)	Basal diameter, Stem height and gas exchange parameters	Reduction in basal diameter in both tolerant and sensitive clones after five years exposure to elevated ozone compared to ambient air
Pleijel <i>et al.</i> 2007.	Wheat	1000 seed weight, harvest index, ear weight + qualitative parameters	AOT40 ~ 9 - 9.7 micromol mol ⁻¹ h reduced harvest index and 1000 seed yield relative to control
Schlöter <i>et al.</i> 2005.	European Beech (in lysimeters)	Plant development, biochemical parameters rhizosphere physiology	No stastically significant effects on plant performance, including litter decomposition despite the fact that microbial diversity of rhizosphere soil reduced
Smith <i>et al.</i> 2003.	A large number of naturally occurring species in protected forests	Visible injury on foliage	Under dry conditions, ozone does not cause foliar injury to indicator species; only when soil moisture is above normal is ambient ozone related to appearance of foliar injury
Soja <i>et al.</i> 2004.	Cultivated Grape	Yield and carbohydrate concentration in fruit	Exposure in prior two years was best predictor of yield, and modelling on basis of uptake (CU06) was better than AOT40
Yamaji <i>et al.</i> 2003.	Birch	Root and shoot masses, physiological parameters	Shoot/root ratio lower for ozone fumigated plants because of greater INCREASE in root mass than increase in shoot mass, in response to AOT40 over two years of 27 ppm-hr

Table 10.3 Recent studies on the impact of O₃ on individual species that included dose response relationships

Citation	Species	Endpoint	Conclusion
Bender <i>et al.</i> 2006a.	Common Mallow	Leaf Dry Matter	$y = -0.1189(8 \text{ h mean})^2 + 7.391(8 \text{ h mean}) - 5.31$ ($R^2 = 0.79426$); $y = -4.662(\text{AOT40 (ppm-hr)}) + 106.38$ ($R^2 = 0.4645$)
Bender <i>et al.</i> 2006a.	Pineapple weed	Leaf Dry Matter	$y = -0.149(8 \text{ h mean})^2 + 10.711(8 \text{ h mean}) - 68.52$ ($R^2 = 0.6992$); $y = -2.075(\text{AOT40 (ppm-hr)}) + 109.89$ ($R^2 = 0.1482$)
Bender <i>et al.</i> 2006a.	Common Sorrel	Leaf Dry Matter	$y = -0.0332(8 \text{ h mean})^2 + 1.152(8 \text{ h mean}) + 95.62$ ($R^2 = 0.7320$); $y = -4.7546(\text{AOT40 (ppm-hr)}) + 101.84$ ($R^2 = 0.6113$)
Bender <i>et al.</i> 2006a.	German Chamomile	Leaf Dry Matter	$y = -0.0970(8 \text{ h mean})^2 + 5.6905(8 \text{ h mean}) + 24.60$ ($R^2 = 0.8182$); $y = -5.083(\text{AOT40 (ppm-hr)}) + 105.51$ ($R^2 = 0.6744$)
Bender <i>et al.</i> 2006a	Blindeyes	Leaf Dry Matter	$y = -0.01522(8 \text{ h mean})^2 + 0.4784(8 \text{ h mean}) + 96.76$ ($R^2 = 0.8120$); $y = -4.070(\text{AOT40 (ppm-hr)}) + 98.08$ ($R^2 = 0.7987$)

Citation	Species	Endpoint	Conclusion
Bennett <i>et al.</i> 2006.	Black Cherry	% injured trees (in the landscape)	% injured trees (in the landscape) = 24.6 + 0.43(SUM06) R ² = 0.44
Davis and Orendovici, 2006.	Common Milkweed	Foliar injury in the field	log (injury/1-injury) = -4.63 - 5.48(Drought Index) - 0.015(W126) + 0.215(N100) + 0.0244(DI x W126) + 0.035(DI x N100) + B, where B=3.44
Davis and Orendovici, 2006.	Tree-of-Heaven	Foliar injury in the field	log (injury/1-injury) = -4.63 - 5.48(Drought Index) - 0.015(W126) + 0.215(N100) + 0.0244(DI x W126) + 0.035(DI x N100) + B, where B=3.01
Davis and Orendovici, 2006.	Virginia Creeper	Foliar injury in the field	log (injury/1-injury) = -4.63 - 5.48(Drought Index) - 0.015(W126) + 0.215(N100) + 0.0244(DI x W126) + 0.035(DI x N100) + B, where B=2.03
Davis and Orendovici, 2006.	Winged Sumac	Foliar injury in the field	log (injury/1-injury) = -4.63 - 5.48(Drought Index) - 0.015(W126) + 0.215(N100) + 0.0244(DI x W126) + 0.035(DI x N100) + B, where B=1.44
Davis and Orendovici, 2006.	Black Cherry	Foliar injury in the field	Relationship not significant
Davis and Orendovici, 2006.	Sassafras	Foliar injury in the field	Relationship not significant
Davis and Orendovici, 2006.	Wild Grape	Foliar injury in the field	log (injury/1-injury) = -4.63 - 5.48(Drought Index) - 0.015(W126) + 0.215(N100) + 0.0244(DI x W126) + 0.035(DI x N100) + B, where B=3.6
Ferretti <i>et al.</i> 2007a.	European Beech	Crown defoliation in field survey plots	%crown defoliation = -9.17(foliar P, mg g ⁻¹) - 0.019(Asspect, degrees) - 0.40(organic soil N, g kg ⁻¹) + 0.00009(AOT40, ppb h) + 0.76(foliar K, mg g ⁻¹)
Fumagalli <i>et al.</i> 2003.	Clover (sensitive and resistant clones)	Dry mass, ratio of sensitive : resistant; current year and following year measured	ratio (following year growth, site 1) = -7 x 10 ⁻⁵ (AOT40) + 1.037 (R ² = .62); ratio (following year growth, site 2) = -1 x 10 ⁻⁴ (AOT40) + 1.38 (R ² = .91)
Karlsson <i>et al.</i> 2003.	Subterranean Clover	Visible injury	% Visible injury = 0.0326(AOT30) + 7.5, where AOT30 is for 10 days prior to measurement, not including a 3d lag time
Karlsson <i>et al.</i> 2006.	Norway Spruce	Basal Area	Relative Annual Basal Area Increment = -3.9 + 1.161(stand BA, m ² ha ⁻¹) + 0.0047(Temp_Sum, degree days) - 0.0459 (SWP<1, days) - 0.00012 (AOT40, nmol mol ⁻¹ + 5.82 (VPD, kPa - .0031(Prec_Sum, mm) - 0.00009(Radiation_sum, mJ m ⁻²)
Nali <i>et al.</i> 2006.	White Clover (resistant and tolerant lines)	Dry mass of sensitive line relative to tolerant line	Epigeous biomass (Sensitive/Tolerant) = 0.928 - 2.83e ⁻⁵ (cumulative AOT40), measured over eight years
Wipfler <i>et al.</i> 2005.	Norway Spruce	Radial growth	Diameter Increment = 0.112 + 0.041(Initial Diameter) - 0.0001(SUM00, ppb-hr) for Norway spruce; Fagus not significant
Wipfler, <i>et al.</i> 2005.	European Beech	Radial growth	European Beech not significant

Table 10.4 Recent studies on the impact of O₃ on individual species that confirmed previous results

Citation	Species	Endpoint	Conclusion
Anderson 2003.	Review: No primary data	Below ground effects of ozone	Physiologically based, can include effects on symbionts, and the interaction between effects on host plants and symbionts is complex
Braun <i>et al.</i> 2004.	Norway Spruce European Beech (in pots outside)	Carbohydrate content	May be an indicator of ozone exposure
Burkey <i>et al.</i> 2005	Snap Bean	Final pod weight	Reduced by ozone and there was a range in genotype sensitivity
Bussotti <i>et al.</i> 2006.	Many native European species	Ozone injury observed in monitoring plots	Not definitively related to ozone, and much variation due to genotype and edaphic factors
Calatayud <i>et al.</i> 2007.	Bel-W3 Tobacco	Visible Injury	Ozone indices explained ~one half of variation in foliar injury, for 24h or 12h mean, or AOT20 or AOT40 cumulative indices
Coulston <i>et al.</i> 2003.	Sweet Gum	Visible Injury	Significant proportions of populations identified as "at high risk" for ozone impacts
Coulston <i>et al.</i> 2003.	Black Cherry	Visible Injury	Significant proportions of populations identified as "at high risk" for ozone impacts
Coulston <i>et al.</i> 2003.	Loblolly Pine	Visible Injury	Significant proportions of populations identified as "at high risk" for ozone impacts
Crous <i>et al.</i> 2006.	White Clover (two lines)	Physiological endpoints (including dose response relationships) indicative of photosynthesis	Attributes physiological effects of ozone to flux, suggesting that this is superior to using external cumulative dose
Elagoz and Manning 2005.	Bush Beans	Growth and agriculture yield	Plants treated with EDU had greater yield than non-EDU treated plants, grown outside with ambient air; demonstration of chamberless exclusion of ozone
Fagnano <i>et al.</i> 2004.	White Clover (two lines)	Growth and water use	Evaluation of CSTR chambers to estimate ozone effects on plants: greater water use and air temperature in chambers influenced resistant/sensitive ratio, but both ambient air and chambered ratios demonstrated significant effect of ozone
Gombert <i>et al.</i> 2006.	Lichen	Distribution and N content	Identification of ozone sensitive lichens based on their absence in areas with elevated ozone concentrations
Gombert <i>et al.</i> 2006.	Bel-W3 Tobacco	Distribution and N content	Bel W3 tobacco is good bioindicator
Hayes <i>et al.</i> 2006.	33 upland grassland species	Above-ground biomass	Following year effects on growth more closely related to ozone exposure than current year
Keutgen <i>et al.</i> 2005.	Cultivated strawberry	Above and below ground biomass; tissue carbohydrate levels	One variety more sensitive than another; roots more reduced in growth and carbohydrate than shoots
Lorenzini <i>et al.</i> 2003.	Bel-W3 Tobacco	Visible injury and epiphytic lichen biodiversity	Bel W3 tobacco sensitive to ozone
Lorenzini <i>et al.</i> 2003.	Lichen	Visible injury and epiphytic lichen biodiversity	No correlation with lichen biodiversity

Citation	Species	Endpoint	Conclusion
Manning <i>et al.</i> 2003.	Review: no primary data	Effects	Abiotic measurement of ozone concentrations do not capture local environmental/edaphic factors that influence flux to leaves, thus effect
Piikki <i>et al.</i> 2004.	Potato (Bintje and Kardal variations)	Leaf number duration and tuber yield	Excluding ozone from OTC increased tuber yield ~30%, but was not statistically detectable; Early variety (Bintje) more sensitive than late maturing variety
Ranford and Reiling 2007.	European Holly	Leaf duration	Ozone exposure has carry-over effects on leaves produced after fumigation
Souza <i>et al.</i> 2006.	Tall Milkweed	Leaf injury	Milkweed is sensitive; there has been no selection for tolerance over 7 years
Timonen <i>et al.</i> 2004	Many European native species	Sensitivity	Lots of species are sensitive, and sensitivity is not predictable based on genetic relationships among species
Tiwari <i>et al.</i> 2005.	Wheat cultivars	Growth, agricultural yield	Varieties are differently sensitive, to ozone, chamberless control plants created with EDU; no positive control
Uddling <i>et al.</i> 2006.	Birch	Leaf N	Nitrogen not resorbed from leaves into tree prior to abscission, thus potentially reducing available nutrients for following growing season
Wang <i>et al.</i> 2007.	Rice	Growth, agricultural yield	Rice not sensitive at all; chamberless control plants created with EDU; no positive control
Wang <i>et al.</i> 2007.	Wheat	Growth, agricultural yield	species are differently sensitive, to ozone, chamberless control plants created with EDU; no positive control
Woo and Hinckley, 2005.	Poplar Hybrid	Growth and gas exchange parameters	Variation among clones in sensitivity; early leaf-fall not necessarily correlated with growth reduction; stomatal closure as a result of ozone not related to growth reduction

Table 10.4 provides a list of recently published literature that confirmed what was previously known about individual plant response to O₃ and is therefore not discussed in the following section.

Table 10.2 provides a summary of recently published studies that contributed to the advancement of understanding of the impact of O₃ on individual plant species. Christ *et al.* (2006) found that agronomic yield (pod weight) of field-grown soybean in response to elevated O₃ was preserved at the cost of leaf growth. The O₃ concentrations used were ambient compared to 1.2x ambient, and the plants (a known sensitive variety) were exposed using free air concentration enrichment (FACE). The O₃ exposures were characterized as daily maximum (a few peaks greater than 80 ppb), seasonal AOT40 (approximately 20 ppm-hr in the elevated O₃ treatment) and seasonal SUM06 (approximately 32 ppm-hr in the elevated O₃ treatment). Although this study did not identify dose response relationships, these values could be considered as NOAELs (No Observable Adverse Effects Levels) for soybean yield (although not vegetative growth), an important field crop in Canada. Importantly, these NOAELs were established using FACE, which is considered to be a more realistic predictor of field plant response than open top chambers. In brief, FACE has no enclosure around the plants, whereas

open top chambers do; thus, the microclimate around the plants grown and exposed to O₃ in FACE are not considered to cause modification of the plant's response to O₃ thus is a better predictor of field response.

A meta-analysis of published studies of soybean suggested that chronic exposure to 70 ppb results in an approximately 24% yield reduction, and that even chronic exposure <60 ppb results in some yield loss (Morgan *et al.*, 2003). Open top chambers were used to compare two varieties of wheat. Seasonal AOT40 of between 9 and 9.7 ppm-h⁻¹ was sufficient to reduce ear dry weight and 1000 grain weight by approximately 20%. Harvest index was also reduced, and overall, the older, lower yielding variety was less sensitive than the modern variety (Pleijel *et al.*, 2007). In conclusion, soybean yield in many parts of Canada is likely to be reduced by chronic exposure to O₃.

Effects on commercial grape yield were better related to the prior two years of O₃ exposure, suggesting that carry-over effects in perennial crops must be considered (Soja *et al.*, 2004). As well, this study demonstrated a better fit of the yield data to dose expressed as uptake (CU06: cumulative uptake when concentration exceeds 6 ppb) rather than AOT40.

The potential for belowground effects of O₃ on plant health primarily results from weakened production of carbohydrates due to reduced photosynthesis, which reduces the amount of carbon that is available for export to plant sinks, including roots (Anderson, 2003). The effect on roots may be partially mitigated by demands by mycorrhizal colonists for carbon. The growth of mycorrhizal colonists may in turn be stimulated by O₃ exposure through the loss of plant carbon into the rhizosphere. This paper also details the potential for below ground effects of O₃ through changed carbon addition to soils, as well as altered element composition of plant litter deposited to soils. This remains speculative, although based on observed effects of O₃ on plants.

A study of beech trees grown in lysimeters and fumigated with O₃ (ambient and 2 x ambient, up to 150 ppb) for one growing season demonstrated no significant effects on plant physiology or senescence (aging) of leaves, but, the microbial diversity of the rhizosphere soil was reduced (Schloter *et al.*, 2005). There was no effect on litter decomposition suggesting that although diversity was affected by O₃, the soil microbial community retained its functionality.

Yamaji *et al.* (2003) exposed clones of hybrid poplar to O₃ over two seasons, for a total AOT40 of 27 ppm-hr. Averaged over all the clones, shoot/root (s/r) dry mass ratio slightly decreased as a result of, on average, a greater increase in root dry weight (DW) than in shoot DW, in response to O₃. This stands in sharp contrast to one of the "truisms" of plant response to O₃, which is that dry weight of roots is more reduced than that of shoots. However, the hybrid poplar were grown in pots, and therefore the function of the roots as a sink may have been limited allocation to the shoots. The authors of this work divided the clones into three

groups, namely shoot/root ratio decreased, increased or unchanged. Those clones with unchanged s/r dry mass ratio had high constitutive concentrations of phenolics (which detoxify the products of O₃ dissolution), and lower stomatal flux of O₃ to foliage.

Mixed forest stands of *Picea abies* and *Fagus sylvatica* were exposed to 1 or 2 x ambient O₃ using FACE; numerous cellular and leaf parameters were measured, as was stem increment, over 2 years (Matyssek *et al.* 2007). Despite numerous changes at the leaf or sub-leaf level, there was no detectable effect on stem increment; this was attributed to a combination of variability in the data, which reduced the precision of the experiment, and plant accommodation of chronic O₃ exposure. While dose response relationships were not determined in this study, the SUM00 (300 and 440 ppm-hr) and AOT40 (61 and 124 ppm-hr) for each of the two years of the study could be considered as NOAELs.

Populus nigra, *Viburnum lantana* and *Fraxinus excelsior* were subjected to two seasons of ambient O₃ or filtered air in open top chambers (OTCs). In response to AOT40 cumulative doses of 20-25 ppm-hr (year 1) and 15-20 ppm-hr (year 2), mean growth ring width was reduced by 52% (ambient air) and 46% (non-filtered chambers) in *P. nigra*, but not in the other two species (Novak *et al.*, 2007).

A 5-year cumulative AOT40 of 87 ppm-hr was associated with reduced (approximately 25%) basal diameter of *Betula pendula*, both sensitive and tolerant clones, compared to plants grown with a 5-year cumulative AOT40 of approximately 3 ppm-hr (Oksanen, 2003). This multi year study demonstrated well the need for long-term observations, as the differences between the O₃ regimes were not measurable until after three years.

Smith *et al.* (2003) demonstrated that visible foliar injury could not be related to O₃ concentration under low soil moisture conditions in a wide variety of species in protected areas of the US. However, when soil moisture was above normal, then ambient O₃ concentrations could be related to appearance of injury, thus supporting the importance of the flux approach to estimating dose. The species studied included milkweed, black cherry, sassafras, and yellow poplar, all of which can be found in areas of Canada that receive elevated ambient O₃.

Wipfler *et al.* (2005) exposed mixed stands of Norway spruce and beech to O₃ using FACE, for one season, with the goal of identifying the effect of O₃ on the increase in diameter at breast height (DBH) relative to O₃ exposure and DBH at the start of the fumigation. Ozone had no effect on seasonal increase in DBH of beech, and had a very minor effect in Norway spruce. In the same type of exposure system, Grebenc and Kraigher (2007) measured mycorrhizal colonization of roots in mixed beech/spruce stands that had either been fumigated with O₃, or not. Mycorrhizal colonization of the roots is beneficial to plants, as mycorrhizae are a symbiotic fungi that aid in nutrient uptake. Colonization was greater in fumigated plants, and

some mycorrhizal species were present only at the O₃ fumigated plots. The authors suggest that mycorrhizal species abundance could be used as a bioindicator of O₃ exposure, particularly as an indicator of below-ground effects.

In conclusion, there is a lot of evidence that realistic multi-year exposures of perennial plants lead to changes in biomass that would not otherwise be detected in shorter studies. These longer-term studies typically capture the effects of O₃ on health of below-ground processes, the degradation of which result from feedback from changes to health of above-ground organs.

Biomonitoring for O₃ effects on plants has a very long history, and the usefulness of a number of “new” species has been documented since the 2003 CWS Update (CCME, 2003a). Progress in this area was included in this review as biomonitors can be a method of field-validating effects of O₃ on plants predicted from air quality measurements. *Centaurea jacea* (brown knotweed; Bassin *et al.*, 2004b) and *Sambucus* sp. (Cano *et al.*, 2007) have been described as sensitive; beyond these, the number of studies using clover clones differing in O₃ tolerance has increased since the 2003 CWS review. Ozone sensitive clover clones have been widely used in Europe, one of the advantages being that it is a perennial species, thus is a reasonable surrogate with which to study carry-over effects of O₃. Chappelka *et al.* (2003) identified cutleaf coneflower and crown beard as sensitive species with the potential to be considered indicator plants. In contrast, Chappelka *et al.* (2007) reported visible injury ratings for the same populations of tall milkweed for five consecutive years. The incidence of injury varied between 44% and 90% depending on the year, but most importantly, the incidence was not highly correlated with ambient O₃ concentrations, or with other topographic features known to influence plant response to O₃, such as slope, aspect or elevation. The authors concluded that microsite conditions (rainfall, temperature) must have influenced the expression of injury in this species, and that further use of populations as indicators should be accompanied by the installation of a weather station at each site.

Predicting which species will be sensitive to O₃ on the basis of known characteristics rather than on primary studies exposing those species to O₃ would be useful as a screening tool for individual plant effects. Hayes *et al.* (2007) used meta-analysis to determine the linear exposure-response relationship between O₃ exposure and relative biomass for a large number of species. The study does not present the exposure-response relationships per se, but uses the slopes to calculate a relative sensitivity index (ranging in value between <1 and >1) for each species, which could be used to estimate a threshold which would protect x% of species from a growth reduction of y%. In this study,, this relative sensitivity index was used to explore the hypothesis that sensitivity was associated with particular plant ecology strategies, either Grime’s C-S-R(Competitive-Stress Tolerator-Ruderal) , or Ellenberg score, numeric ratings of a plant species’ ecological strategy. They concluded that in contrast to the earlier hypotheses that earlier flowering species were more sensitive to O₃, some mid- and late-flowering species were also sensitive. Fabaceae and therophytes (one of the Raunkiarian life forms) species contained, as previously known, the most sensitive species. Their policy conclusion was that

previous European practice to set O₃ criteria to emphasize spring exposures as more important in the protection of vegetation was not supported by the results of this species sensitivity survey. Although such sensitivity indices do not capture the complexity of plant response to O₃ in competition with other species, aggregate sensitivity ratings for existing plant communities have the potential to be useful in risk assessment, providing that the plant communities are representative of real-world ozone impacts on Canadian ecosystems. To ensure that Canadian ecosystems are adequately protected, further research on the relationships between exposure (several metrics) and impacts (several indicators) in important Canadian species or – possibly – ecosystems is recommended. The research must be based on realistic experiments, i.e. long-term (>3 years) free air exposure and correlative studies at the landscape scale that would validate the controlled experiments.

On the principle that visible injury to plants in national parks is an undesirable human and ecosystem welfare effect, an assessment framework for risk of visible injury to plant species in protected areas was applied to over 200 parks in the US (Kohut, 2007). If a park was assessed as having O₃ sensitive species, elevated O₃ concentrations, and high soil moisture during the periods of elevated ambient O₃, the risk of visible injury was estimated as “high”. Of the 244 parks assessed, 65 were deemed to be at high risk of occurrence of visible injury from O₃. A similar assessment framework might be applicable to Canada, although the list of known sensitive species presented in this paper would need to be expanded as many are not occurring (or widely occurring) in Canada. Applying a similar assessment framework to Canada may be accomplished through modelling, as demonstrated by Jones *et al.* (2007), who used Ellenberg Indicator values (Ellenberg *et al.*, 1991) for light and salinity to predict relative sensitivity to O₃ ($RS = 1.805 - 0.118\text{Light} - 0.135\sqrt{\text{Salinity}}$). Clearly, response to light and salinity are not likely to be good surrogates for response to O₃, but the Ellenberg Indicators represent gradients in sensitivity so species that are tolerant of difficult conditions might be approximately ranked similarly. Because this model under-predicted actual sensitivity and more importantly, focuses on individual species, it was used to develop two further indices of O₃ sensitivity. The first of these is prediction of the net change in community biomass (ORI%_{cw}) from a list of species present; this index can be weighted by the relative abundance of each species (‘cover-weighted’). The second is community ozone response index (CORI) which addresses the fact that changes in biomass do not necessarily tell the entire story of effects at the ecosystem level, as a plant community might consist of species that react oppositely to O₃, thus their individual changes in biomass leading to a net change that is very small. Both indices were more accurate predictors of species response to O₃, although more actual data on community response using mixtures of species are required in order to confirm the usefulness of these additional indices.

In conclusion, ecological rationalization of species sensitivity for the purposes of either predicting sensitivity or identifying biomonitors continues to be a research priority in parallel with studies of effects. It remains uncertain, however, whether such classifications or rankings would be reliable indicators of larger plant community response under varied conditions of other environmental inputs, such as soil moisture, etc.

Table 10.3 provides a summary of dose-response functions that were included in the recent literature. Dose response functions were calculated for a number of wild species and for a number of response endpoints. The goals were to compare the goodness of fit of reduction in dry matter to either the 8-h mean O₃ concentration (better) or the AOT40 sum (not as good) of O₃ concentration (Bender *et al.*, 2006a). The studies also concluded that reproductive endpoints were not necessarily well predicted by vegetative endpoints. For instance, for all species reproduction was impaired even when vegetative growth was enhanced.

The occurrence of visible injury on wild plants, and its link to the value of those wild plants through loss of yield is addressed in Bennett *et al.* (2006), who found no relationship between foliar injury and growth in black cherry in the field. The authors agreed with previous investigators that >10 year exposure was needed in order to see growth effects. However, they did suggest a dose-response relationship between SUM06 O₃ exposure and percentage of landscape trees likely to show injury.

For established *Fagus sylvatica*, shoot growth was reduced by 7% for each 10 ppm-hr (AOT40) O₃ (ranging from 15 – 23 ppm-hr), whereas for *Picea abies* in the same forest, shoot growth for this dose interval was approximately zero (Braun *et al.*, 2007). Davis and Orendovici (2006) determined exposure response functions for a number of wild species, both herbaceous and woody, for injury. These exposure-response functions fit best when both chronic (W126) and acute (N100) cumulative O₃ exposures were used as predictors. As well, their exposure-response function includes “drought index”, to account for the observation that injury was reduced in dry years; however, the paper does not explain how to calculate the “drought index” other than to indicate that it is linked to soil moisture. (Edwards *et al.* (2004) describe more fully the calculation of O₃ exposure including Drought Index, which is a unit-less scale ranging from -4 (extreme drought) to +4 (extremely moist). The exposure-response relationships for wild grape, black cherry, Virginia creeper, and common milkweed would be particularly applicable to many parts of Canada and could form a basis for predicting the potential for local effects of O₃ on other species from observation of these bioindicators. Exposure-response functions for crown defoliation of beech trees at long-term monitoring sites in Europe were determined, incorporating other soil and plant health factors known either to cause or contribute to crown defoliation or to plant response to O₃ (Ferretti *et al.*, 2007a). The best exposure-response function included foliar phosphorous (P) and potassium (K), as well as aspect of the site, organic soil nitrogen (N), and AOT40.

Fumagalli *et al.* (2003) developed exposure-response functions for re-growth of two clones of clover in the year following initial exposure to ambient O₃. At neither of the two sites in Italy was the sensitive:resistant ratio of shoot dry mass significantly related to O₃ in the current year, but re-growth in the following year was strongly and negatively related to cumulative O₃ exposure (AOT40). Above-ground biomass loss of a sensitive clone of clover (relative to a tolerant clone) was linked to cumulative AOT40 over 9 years of study, using an exposure-response relationship, thus capturing the cumulative effect of O₃ on perennial species (Nali *et*

al., 2006). While it is unlikely that the clover grown in hay fields is a sensitive clone, this study does identify the maximum likely yield loss to clover as an agronomic crop that would occur as a result of O₃ exposure. Injury to clover (*T. subterraneum*) was better related to AOT30 for the ten-day period prior to observation, not including a 3 day lag period, than was AOT40 in the same construct using an exposure-response regression (Karlsson *et al.*, 2003).

An exposure-response function for relative basal area (RBA, annual increment) of Norway spruce was determined from 9 years of observation (Karlsson *et al.*, 2006). The inclusion of other factors such as precipitation, air temperature, soil moisture, radiation and vapour pressure deficit with AOT40 explained over 90% of the variation in annual increment of basal area. Within the range of AOT40 found in this study, the annual basal area increment change attributable to O₃, alone, was -0.8%, in comparison to an overall change in RBA of +4.6% over the period of the study.

In conclusion, all of the exposure response functions in the preceding text are from field studies, many of which were multi-year and observed naturally occurring plant communities, in response to ambient O₃. Many of these studies were able to detect modification of plant response to O₃ as a result of edaphic or climatic factors known to influence plant response to O₃ and thus are likely to be the more accurate tools for developing or validating toxicity thresholds. Even if the dose-response relationships are the same as would be derived from controlled experiments, the fact that they have been determined under less- or non-controlled studies makes them a more credible basis for identification of toxicity thresholds that will protect plant communities.

10.4.1.2 Ecosystem Responses

The 2003 CWS Update for O₃ and PM (CCME, 2003a) summarized a number of uncertainties or data gaps that limited the conclusions drawn from the literature on the effect of O₃ on individual plants (described in the previous section), which also apply to consideration of O₃ effects on ecosystems. There were few data that allowed scaling of effects on individual seedlings to forest level impacts. The USEPA's OAQPS Staff paper (USEPA, 2007) also identified that there were few data that allowed assessment of impact on ecosystem services.

Table 10.5 Recent studies that contributed to the advancement of understanding of the impact of O₃ on ecosystems

Citation	Species	Endpoint	Conclusion
Ashmore 2005.	Review paper	Ecosystem Health	Need to characterize exposure as uptake flux; need to consider ozone, climate, and nutrient and water availability, with individual plant effects, species interactions and ecosystem effects
Bassin <i>et al.</i> 2007.	Meta-analysis/review	Grassland health	Grassland communities can be separated into categories of ozone sensitivity; current knowledge of ozone effects is applicable to intensively managed, high productivity grasslands - those with lower productivity not as sensitive
Felzer <i>et al.</i> 2004.	Hardwood and pine trees and crops across conterminous United States	C Budget	C sequestration since '50's has been reduced by 18-38 Tg y ⁻¹ , and reduction in Net Primary Production due to ozone 2.6 - 6.8% per year
Fuhrer and Booker 2003.	Agro-ecosystems	Productivity	Need to characterize exposure as uptake flux; need to consider initial toxicity events; need to scale up from cell to whole plant: need to consider crop quality, C sequestration, nutrient cycling and ecosystem effects
Karnosky <i>et al.</i> 2007	Forests	Productivity	effects demonstrated at seedling stage of growth in controlled ozone exposures remain difficult to identify in the field due to interacting factors; suggest that "effects" are likely to increase
Laurence and Andersen, 2003.	Review paper	Natural ecosystem health	Ozone effects on natural ecosystems must include soil food webs, landscape water budgets, wildlife and recreational values, cycling of nutrients
Percy and Karnosky, 2007.	Natural Areas	Health	Policy to protect natural areas needs exposure-based indices to protect against change in relevant endpoints, supported by exposure-response relationships developed in ambient air
Shrestha and Grantz, 2005	Tomato and Yellow Nutsedge	Growth of the two species when cultivated together	Yellow nutsedge is more sensitive to competition, but tomato is more sensitive to ozone, thus under conditions of moderately increasing ozone concentration, yellow nutsedge could be more of a weed problem
Thwaites <i>et al.</i> , 2006	Calcareous grassland communities	Species composition	Species composition changed over three years of ozone exposure, but, ozone explained only 4.6% of the variation

Table 10.6 Recent studies on the impact of O₃ on ecosystems that confirmed previous results

Citation	Species	Endpoint	Conclusion
Bytnerowicz <i>et al.</i> 2003	Carpathian mountain Norway spruce forests	Forest Health	Norway spruce only species demonstrating "decline" and that could be due to bark beetle infestation

Accordingly, the published studies since 2003 that add new information to these areas were extensively reviewed, with the remaining papers summarized in tabular form. All studies discussed in this section are summarized in Table 10.5. Papers which confirmed what was

already known about ecosystem responses to O₃ but did not contribute significantly new information are summarized in Table 10.6. There were no dose response functions cited in any of the studies.

The need to consider ecosystem effects is summarized by Ashmore (2005), who suggests the need to consider O₃ in the context of climate change, including nutrient and water availability. More importantly, the net effect needs to be considered beyond the individual plant level to include species interaction and ecosystem function. Ashmore's position is that global O₃ distribution patterns and exposure concentrations need to be included in the predicted effects of climate change, as there is potential for increased O₃ to have an important, negative effect on global food supply. Fuhrer and Booker (2003) similarly summarized the need to apply an ecosystems approach to considering the effects of O₃ on agricultural production, particularly in regions of the world with growing populations and the need for a secure food supply. They prioritized the "data gaps" were identified as: need to characterize exposure as uptake flux; consideration of initial toxicity events; scaling up from cell to whole plant; including crop quality, carbon sequestration, nutrient cycling; and ecosystem effects as endpoints.

Karnosky *et al.* (2007) reviewed documented effects of O₃ on forests in the last 50 years, and concluded that while effects observed for seedlings in controlled environments are difficult to identify in the field, these effects are likely to become greater in future scenarios of greater population and climate change. Laurence and Andersen (2003) similarly concluded that in order to protect natural ecosystem health from O₃, endpoints must include effects on the soil food web, the contribution of those ecosystems to the landscape water budget, landscape and recreational values, and the cycling of elements, both macro and micro nutrients. As well, these must be understood in the context of climate change scenarios and other stresses that may fragment the landscape, including invasive species.

Percy and Karnosky (2007) recommended that the protection of natural areas from O₃ effects requires exposure-based indices that protect endpoints that are socially, ecologically as well as economically relevant, and which are supported by exposure-response relationships determined from ambient air studies. While this recommendation may seem obvious, the authors see it as an urgent need, because natural areas in Canada and the US attract hundreds of millions of visitors per year. Their selection criteria for response endpoints are:

1. Is the endpoint a final point in a key ecosystem process?
2. Can the endpoint be measured with accuracy and, importantly, with precision over time?
3. Is the endpoint supported by published exposure response science completed within the ambient air context?
4. If the endpoint's status changes, does this provide feedback to tree productivity or some other ecosystem value of social, economic or ecological importance?
5. If positive or negative feedback is demonstrated, is the estimate of change in a form that can be understood and used by air-quality regulators?

6. If it can be used by regulators, can it be used in the short-term to support decisions on air quality management (prevention), or in the longer term to provide scientific input to a criterion setting process (protection)?

Bassin *et al.* (2007) demonstrated this “ecosystem-centric” principle with a meta-analysis of O₃ effects on grasslands. They suggested that communities where most species are stress tolerators are more resistant to O₃ effects than those communities populated with ruderal or competitor species, both of which are faster growing than stress tolerators. As most experimental data are gathered from newly sown communities dominated by ruderal or competitive species, these studies may overestimate the potential for O₃ effects on mature grassland communities.

Thwaites *et al.* (2006) demonstrated altered species composition of calcareous grassland turf transplanted intact to open top chambers, and fumigated with O₃ for three consecutive summers. *Festuca rubra* decreased in percent cover with time in the highest O₃ treatment, and *Campanula rotundifolia* disappeared entirely in all O₃ treatments. The frequency of *Galium verum* and *Plantago lanceolata* increased with O₃ exposure. While O₃ is a significant factor in community compositional change, it accounted for slightly less than 5% of the total change. The remainder of change in species composition was attributed to the transplantation to the open top chambers. The lack of large response to O₃ was partially attributed to the fact that the plant communities under study did not have Fabaceae (well-known to be sensitive to O₃) among their species, thus the study identified tolerance of a plant community.

The context into which O₃ effects on net primary productivity (NPP) and carbon sequestration fit was demonstrated for hardwood, pine trees, and agricultural crops using the Terrestrial Ecosystem Model (Felzer *et al.*, 2004). This model used data developed by Reich (1987) through meta-analysis of many studies by different investigators. The study found that since the 1950's NPP has been reduced by 2.6 – 6.8 % per year due to O₃, and carbon sequestration (which includes the effect of O₃ on vegetation) has been reduced by 18 - 38 Tg/year . The effects of O₃ on NPP were similar in value to those of CO₂ fertilization and climate variability, but smaller than the effect of land-use changes and agricultural management on NPP. Changes in carbon sequestration as a result of O₃ were similar to the negative change predicted to result from land use, and would offset the effect of fertilization from N and CO₂, as well as from climate variability. The results of this modelling study did include the reduction of stomatal conductance as a result of O₃ fumigation, and the resulting reduction in internal dose to the plant, which would offset or enhance (or both, for net “no change”) some of the predicted change in NPP. As well, the authors acknowledged that the consideration of agricultural practice in this model was not finely tuned, and could have a substantial effect on the predictions. For example, irrigation and nitrogen fertilization will influence the growth of crops, thus the uptake of O₃ and the effect of O₃ on NPP.

In conclusion, ecosystems as a whole must be protected by the CWS for O₃, and in order to do that, an “ecosystem approach” must be taken to determine its sensitivity to O₃. The endpoints that must be considered for protection include species composition of identifiable plant communities, as well as the role of plant communities in the global carbon cycle.

10.4.1.3 Ozone Combined with Other Stressors and Mixtures

The 2003 CWS Update document (CCME, 2003a) noted that most of the co-contaminant studies up to that date were for O₃ and CO₂, and that the exposure dose as presented was not in a form usable for quantitative analysis. In consequence, the papers published since 2003 that measure mixture effects of CO₂ and O₃ expressed as quantitative doses/exposures were extensively reviewed and the remainder were tabulated. The 2003 CWS Update was quite silent on other environmental biotic and abiotic factors that could influence plant response to O₃, something that the OAQPS Staff paper (USEPA, 2007) noted as a conclusion from their review of literature up to 2004. Thus, these studies are extensively reviewed in this section, as this area seemed largely unexplored.

Table 10.7 Recent studies that contributed to the advancement of understanding on the impact of O₃ combined with other stressors or mixtures on vegetation

Citation	Species	Mixture with O ₃	Endpoint	Conclusion
Bender <i>et al.</i> 2006b	Kentucky Bluegrass with four other competitive species	Other species	Biomass and nutritive quality	Ozone fumigation in the spring of three consecutive years affected nutritive quality of Kentucky Bluegrass harvested each fall, but competition did not affect response to ozone
Holton and Lindroth, 2003.	Quaking aspen	CO ₂	Tent caterpillar infestation and parasitization	Enriched CO ₂ and O ₃ reduced tent caterpillar performance, depending on aspen genotype
Jones and Paine 2006.	Oak, pine, fern forests of San Bernardino Mountains, CA	N	Herbivore species richness, diversity, and community characterization	Leaf chewers more prevalent in plant communities growing with elevated O ₃ /N pollution, although richness and diversity indices were similar in high and low pollution
Karnosky <i>et al.</i> 2003	Trembling Aspen, Paper Birch, Sugar Maple	CO ₂	Leaf to Ecosystem Level Endpoints	Increased production from increased CO ₂ can be somewhat offset by negative effect of O ₃ .
Karnosky <i>et al.</i> 2005.	Trembling Aspen, Paper Birch, Sugar Maple	CO ₂	Carbon flow through ecosystem	CO ₂ largely ameliorated O ₃ effects, except for paper birch, in which the negative effect of O ₃ was greatest under elevated CO ₂ ; effects of O ₃ on sugar maple not noted until after 3y exposure
King <i>et al.</i> 2005	Trembling Aspen, Paper Birch, Sugar Maple	CO ₂	Net Primary Productivity	O ₃ had negative effects on NPP, while CO ₂ had positive effects, generally speaking; even moderate exposure to ozone reduces the response of these species to CO ₂ .
Kozovits <i>et al.</i> 2005.	European Beech and Norway Spruce	CO ₂ , inter/intra-specific competition	Leaf gas exchange, biomass, crown volume	Growth responses to O ₃ or CO ₂ (spruce benefited from elevated CO ₂ , and beech was sensitive to O ₃) was greater with inter-specific competition, than intra-specific competition
Kubiske <i>et al.</i> 2006a.	Trembling Aspen, Paper Birch, Sugar	CO ₂	Species importance	Elevated O ₃ hastened conversion of stands to paper birch, whereas the presence of

Citation	Species	Mixture with O ₃	Endpoint	Conclusion
	Maple			elevated CO ₂ delayed it. Elevated O ₃ slightly increases the rate of conversion of aspen stands to sugar maple, but maple is placed at a competitive disadvantage to aspen under elevated CO ₂ .
Kubiske <i>et al.</i> 2006b.	Model Aspen	CO ₂ , inter-annual variation in climate	Growth	Years with higher PPFD were associated with greater positive effect of CO ₂ and greater negative effect of O ₃ on biomass production of aspen
Kull <i>et al.</i> 2005.	Birch	CO ₂	Crown structure (leaf area index)	Extrapolation of field experiment data (see Kull <i>et al.</i> 2003, in "Confirmation") to the canopy scale using a model demonstrates the influence of radiation on the outcome
Liu <i>et al.</i> 2004	European beech and Norway spruce	CO ₂ , inter/intra specific competition	carbohydrate, biomass	No detectable biomass effects (large variability), but positive effects of CO ₂ on carbohydrate content counteracted by O ₃ ; effects of CO ₂ on beech disappeared in co-culture with spruce, the stronger competitor
Long <i>et al.</i> 2006.	Crops meta-analysis	CO ₂	Yield	Examined the "CO ₂ and O ₃ will cancel each other out" theory, comparing FACE and OTC determinations of yield gain/loss: FACE with soybean 20% loss from O ₃ , vs. 8% loss using OTC; simultaneous exposure to O ₃ and CO ₂ using FACE are needed for food crops
Luedemann <i>et al.</i> 2005.	European beech and Norway spruce	<i>Phytophthora citricola</i>	Infection and belowground competitiveness	Spruce less sensitive to ozone than beech, which is less sensitive to Phytophthora after ozone fumigation than is spruce - so, effect of O ₃ on plant communities is complex
McLaughlin <i>et al.</i> 2007b.	Southern Appalachian forest	Climate	Water use, soil moisture content, streamflow	Increases in whole-tree canopy conductance, depletion of soil moisture in the rooting zone, and reduced late-season streamflow in forested watersheds were detected in response to increasing ambient ozone levels.
McLaughlin <i>et al.</i> 2007a.	Southern Appalachian forest	Climate	Stem increment and sap flow	Ozone can increase water use in trees, thus future elevated ozone and reduced water supply (due to increased global temperature) could synergistically limit forest tree productivity
Muzika <i>et al.</i> 2004.	Norway Spruce and European Beech	SO ₂ and NO ₂	Basal Area Increment (BAI)	Average SO ₂ and NO ₂ inversely related to BAI of trees; highest O ₃ concentration also negatively related to BAI; a combined variable of the three pollutants also calculated and correlated
Plessl <i>et al.</i> 2007.	Potato (Indira variation)	CO ₂	Infection and biomass	Potato susceptibility to Phytophthora is enhanced by ozone, and reduced by CO ₂ , independent of the effects of these gases on growth
Rämö <i>et al.</i> 2006.	Lowland hay meadow	CO ₂	Biomass	Ozone reduced biomass in four of seven species, and this was not restored by elevated CO ₂ ; although no functional groups were lost, biggest reductions were seen in least frequently occurring species, suggesting O ₃ -induced suppression of the weakest competitors
Rämö <i>et al.</i> 2007.	Species typical of lowland hay meadow	CO ₂	Growth onset, flowering, biomass	ozone reduced flowering and early season coverage in some species, and this was not recovered by CO ₂ fumigation; negative implications for community reproduction are suggested

Citation	Species	Mixture with O ₃	Endpoint	Conclusion
Ren <i>et al.</i> 2007.	Grassland	CO ₂ plus other climate changes	C sequestration and net primary productivity (NPP)	In last 40 years, slight increase in NPP and C sequestration in soil and vegetation of grasslands in China; O ₃ is predicted to have reduced the max increase in NPP and C sequestration that would have been seen if O ₃ hadn't increased during this period
Shrestha and Grantz, 2005	Tomato and brown nutsedge	Interspecific competition	Growth of the two species when cultivated together	Yellow nutsedge is more sensitive to competition, but tomato is more sensitive to ozone, thus under conditions of moderately increasing ozone concentration, yellow nutsedge could be more of a weed problem
Tonneijck <i>et al.</i> 2004.	Species typical of wet grasslands	Interspecific competition	Biomass, senescence, visible foliar injury	Interspecific competition between plants from wet grasslands does not alter effects of early season ozone on plant growth in a three-year experiment.
Van Oijen <i>et al.</i> 2004.	Spring Wheat	CO ₂	Growth	Modelling exercise, where effects of CO ₂ and O ₃ on wheat growth are integrated into a well-parameterized model for wheat growth in absence of O ₃
Zeleznik <i>et al.</i> 2007.	Beech	Light	Root parameters and ectomycorrhizae	O ₃ didn't affect mycorrhization, but light regime did; O ₃ generally depressed root growth relative to control plants, suggesting potential for altered nutrient cycling in soil

Table 10.8 Recent studies on the impact of O₃ combined with other stressors or in mixtures that included dose response relationships

Citation	Species	Mixture with O ₃	Endpoint	Conclusion
Khan and Soja 2003.	Winter wheat	Water stress	Grain yield	Grain yield (g plant ⁻¹) = 1.147 - 1095/x ² - 0.03656y ^{0.5} , where x = soil water capacity (%) and y = AOT40 (micromol mol ⁻¹ k ⁻¹) (exposure response functions for other yield parameters in paper)

Table 10.9 Recent studies on the impact of O₃ combined with other stressors or in mixtures that confirmed previous results

Citation	Species	Mixture with O ₃	Endpoint	Conclusion
Ambasht and Agrawal 2003/4.	Wheat	UV-B	Yield	Combination of UV-B and O ₃ has additive effects on plant yield
Awmack <i>et al.</i> 2007	Clover	CO ₂	Biomass	No response to ozone, with or without CO ₂
Booker <i>et al.</i> 2005	Soybean	CO ₂	Biomass and photosynthesis	Ozone inhibits both biomass production and photosynthesis; CO ₂ enhances both; responses of pot-grown plants were similar to those for soil-grown
Darbah <i>et al.</i> 2007	Paper Birch	CO ₂	Flowering and reproduction	Elevated CO ₂ largely has a negative effect on reproduction, while elevated O ₃ largely has a negative effect. The combination is likely to have a mixed effect.

Citation	Species	Mixture with O ₃	Endpoint	Conclusion
Darbah <i>et al.</i> 2008	Paper Birch	CO ₂	Flowering and reproduction	Elevated CO ₂ largely has a negative effect on reproduction, while elevated O ₃ largely has a negative effect. The combination is likely to have a mixed effect.
Dittmar <i>et al.</i> 2003.	Beech	Other environmental stressors	Radial growth	Beech growth is enhanced at lower altitudes, but impaired at higher altitudes, where elevated ozone (among other environmental changes) occurs
Heagle <i>et al.</i> 2003.	Potato	CO ₂	Yield	Increased production from increased CO ₂ somewhat offset by negative effect of O ₃
Kull <i>et al.</i> 2003	Silver Birch	CO ₂	Crown structure	O ₃ decreases leaf area index (LAI, m ² m ⁻²) CO ₂ increases LAI - so, if both increase in the future, their effects will likely ameliorate each other
Loya <i>et al.</i> 2003.	Birch and Aspen	CO ₂	Soil C	Raising ambient CO ₂ and O ₃ by 50% reduces input of C to soil by half relative to that from raising CO ₂ alone
Maggio <i>et al.</i> 2007.	Tomato	Salt	Biomass	Salinity can influence stomatal aperture, thus effective ozone dose - however, study is complicated by effects of salinity alone; conclusion is that ozone criteria need to be environment specific, in this example, if salinity and ozone co-occur
Matyssek <i>et al.</i> 2006.	Forests	Drought	Productivity	Trade-off between benefits of drought on plants growing in ozone (reduction of ozone influx) and negatives (reduction of CO ₂ influx, thus growth)
Percy and Ferretti 2004.	Forests	Other pollutants and stresses	Health	To protect forest health, consideration of ozone, CO ₂ , acidification have to be integrated into a model which can be used to assess forest health, upon which environmental criteria can be based; conclusions are largely supported, and sometimes not, in the work that has been subsequently published and is described in this document
Persson <i>et al.</i> 2003.	Potato (Bintje variation)	CO ₂	Yield	Potato growth more sensitive to these pollutants than tuber yield, which was sparingly sensitive to either; however, large unattributable variation limited the detection of effects
Rämö <i>et al.</i> 2006.	Brown Knapweed ecotypes	CO ₂	Visible injury, dry mass production	All ecotypes were sensitive to ozone; response to CO ₂ varied among ecotypes, and elevated CO ₂ increased ozone sensitivity of most tolerant ecotype, presumably due to increased stomatal conductance? Brown knapweed is not a suitable bioindicator of ozone, because of variability
Riikonen <i>et al.</i> 2004.	Silver Birch	CO ₂	Growth and carbon allocation	Net total effect of O ₃ (negative) and CO ₂ (positive) on growth and carbon allocation depends on clone
Sanz <i>et al.</i> 2005.	Subterranean Clover	N	Growth and nutritive quality	Ozone reduced yield and nutritive value of above-ground material; this was enhanced if N was supplemented, also, due to increased production of acid detergent fibre
Schaub <i>et al.</i> 2003.	Black cherry, Red maple, American ash	Water stress	Visible injury	High soil water availability favours ozone uptake, increases foliar injury, and exacerbates the negative ozone effect on gas exchange of seedlings of deciduous tree species.
Shimizu and Feng 2007.	Gold Birch	Water stress	Biomass, gas exchange, leaf biochemistry	No interaction between ozone and water stress, in the reduction in plant growth noted as a response to each; effects on dry matter

Citation	Species	Mixture with O ₃	Endpoint	Conclusion
				production are additive
Smidt and Herman 2004.	Austrian forests	Other pollutants	Forest health	Reduction in industrial emissions has converted "atmospheric pollution" from acidic to oxidative, and ozone (particularly at elevation) and Pb deposition are likely most important determinants of forest health in Austria
Thomas <i>et al.</i> 2005	Norway Spruce	Nitrogen in soil	Biomass and carbohydrates	N enhanced growth, and O ₃ depressed growth, and only interaction between the two was alleviation by N of O ₃ effect (negative) on root starch content
Thomas <i>et al.</i> 2006	European Beech	Nitrogen in soil	Biomass, carbohydrates and macronutrient composition of foliage	N enhanced growth (except at highest load), and O ₃ depressed growth; combined effects largely additive except at highest N where effects were synergistic

Recently published studies that contribute to the advancement of the understanding of O₃ combined with other stressors and mixtures are summarized in Table 10.7. Where exposure- or dose-response functions were provided in the recent literature, they are summarized in Table 10.8. Recent papers which confirmed what was already known about O₃ in combination with other stressors and in mixtures, but did not contribute significantly new information are summarized in Table 10.9.

Ozone and competition with other species can interact if the species in the community are differentially sensitive to O₃. This topic was addressed to some degree in section 10.4.1.2 on ecosystem responses. Bender *et al.* (2006b) exposed *Poa pratensis* to O₃ in common culture with four other competitive species to assess biomass production and nutritive quality. The O₃ fumigations took place in the spring, for three consecutive years. In addition to foliar injury as a response to O₃, there was a decline in nutritive quality of *Poa* at the fall harvests, but competition with other species did not modify this effect. The ability of tomato to compete with yellow nut sedge (weed) was tested under O₃ fumigation. Nut sedge was more sensitive to competition than tomato, which was more sensitive to O₃ (Shrestha and Grantz, 2005). The authors suggest that under a scenario of moderately increased O₃, nut sedge could become more of a weed problem than it currently is. Kozovits *et al.* (2005) demonstrated that beech was more sensitive to O₃ than Norway spruce, which benefited from elevated CO₂ more than beech. If these species were grown together, these effects were enhanced, demonstrating very clearly that scaling up of experimental data to predict landscape effects would require data for the mixed species communities that occur and that scaling up from single species data could underestimate effects on the more sensitive species in a plant community. Kull *et al.* (2005) predicted crown structure of birch at the canopy scale from short-term experimental plots in response to elevated CO₂ and O₃. Although this was a single species study, these authors make

the point that changes in crown structure manifested as altered leaf area index (LAI) vary among species and could have profound implications for competition among species since LAI is the key controller of light penetration to lower layers of forest community.

Luedemann *et al.* (2005) studied the susceptibility of Norway spruce and European beech to Phytophthora (a plant pathogen) relative to previous O₃ exposure. This study investigated how these two stresses affected the competitive relationship between the two tree species. Acclimation to O₃ enhanced susceptibility of spruce to Phytophthora, but reduced susceptibility of beech; this was balanced against the greater sensitivity of beech to O₃, expressed as reduced biomass gain. Thus, in co-culture, spruce would gain a competitive advantage over beech under elevated O₃, an advantage that might be reduced under conditions of Phytophthora infection. Susceptibility of other species to Phytophthora has also been investigated relative to O₃ and CO₂ fumigation. Leaves of potato (var Indira) were slightly more susceptible to Phytophthora inoculation after O₃ exposure, and less susceptible after CO₂ exposure, a difference the authors link to altered biochemistry of the foliage (Pleschl *et al.*, 2007).

Liu *et al.* (2004) confirmed the strength of spruce in competition with beech by demonstrating that the positive effects of CO₂ on carbohydrate content in both species (counteracted by exposure to O₃) disappeared for beech, but not spruce, when grown in co-culture with spruce. The sensitivity of the species composing a hay meadow to very low concentrations of O₃ varied, with four of the seven species experiencing biomass loss after a two year exposure to 40 ppb O₃ (Rämö *et al.*, 2006). This biomass loss was not relieved by fumigation with elevated CO₂ likely because nitrogen was limiting to growth stimulation, suggesting that the expectation that elevated CO₂ will counteract the negative effect of O₃ will not be fulfilled in all ecosystems. Using the same set of species grown in mesocosms, Rämö *et al.* (2007) demonstrated that O₃ reduced flowering and early season coverage in a few species - and this was not recovered by CO₂ fumigation - suggesting negative implications for community reproduction. Tonneijck *et al.* (2004) grew wet grassland species either alone or in combination, for three consecutive years with O₃ treatments (AOT40) reaching as high as 18 ppm-h, exceeding the proposed critical level for the adverse effects of O₃ on semi-natural vegetation. Except for the first year, however, O₃ effects were generally absent throughout the three-year experiment and there was no clear evidence that inter-specific competition between plant species from wet grasslands altered the phytotoxicity of early season O₃ on biomass production.

In conclusion, most plant communities consist of species (including pests and pathogens) with varied growth habits. Differential sensitivity to O₃ among these species can alter inter-specific relationships, possibly in ways that change the fundamental structure of the plant community. Studies of O₃ sensitivity of plants in competitive situations is an important advance in addressing this data gap.

Elevated O₃ and moisture stress are studied in combination because of the potential for water stress to reduce influx of O₃, thus reduce plant response. Khan and Soja (2003) developed exposure response functions for winter wheat grain yield parameters, in response to O₃ under various degrees of soil moisture stress (Table 10.8). (As they also measured stomatal conductance, they were able to express the response in terms of actual dose to the plant; these results are also presented in the paper.) Their conclusion is not new, i.e. that water stress reduces the impact of O₃ on plants by reducing the flux of O₃ into the leaves, but the presentation of both exposure- and dose-response functions, for marketable yield, is notable. McLaughlin *et al.* (2007a; 2007b) studied the interaction between water use and O₃ exposure in situ, in southern Appalachian forests which were instrumented to measure daily stem increment of trees, transpiration, streamflow, and soil moisture. Their conclusion was that overall, O₃ exposure increased water movement through the trees from soil to the atmosphere, and as a result, streamflow in the forest was reduced and tree growth was less than what would occur in the absence of O₃.

Elevated O₃ and CO₂ are often studied in combination because under climate change scenarios, elevated temperature accompanying elevated CO₂ will enhance O₃ production. Exposure-response functions are not typically generated in these studies, as most are conducted using exposure systems (such as FACE) that are not available in enough multiples at most research facilities. While many of the CO₂/O₃ studies are short-term, and conclude that the effects of these two gases largely cancel each other out, there is a series of papers that report the results of a seven-year study of trees using FACE exposure systems. The duration of these studies make them a significant advancement.

Percy and Karnosky (2007) discussed the current North American air quality standards in the context of new experimental data and made recommendations for policy-relevant scientific experiments. In particular, they suggest free-air experiments are necessary to develop a better understanding of how O₃ and environmental factors interact to cause plant response.

Karnosky *et al.* (2003, 2005) studied trembling aspen, paper birch and sugar maple responses to elevated CO₂ and O₃ over seven years using a FACE system. They demonstrated that contrary to many other observations, the negative effect of O₃ on paper birch was greatest in combination with elevated CO₂. As well, the effect of O₃ on sugar maple was not detectable until after three exposure-years. They were able to demonstrate changes to above ground growth and physiology in the saplings, and because they continued the study for seven years, they were also able to demonstrate changes to carbon flow below-ground, hypothetically caused by O₃-mediated changes in leaf chemistry which influenced the activity of soil microbes. For seven years, using the FACE system, aspen, birch and maple communities were exposed to CO₂ and O₃; relative to control, elevated CO₂ increased total biomass 25, 45 and 60% in the aspen, aspen–birch and aspen–maple communities, respectively (King *et al.*, 2005). Elevated ozone caused 23, 13 and 14% reductions in total biomass relative to the control in the respective communities. Combined fumigation resulted in total biomass response of -7.8, +8.4

and +24.3% relative to the control in the aspen, aspen–birch and aspen–sugar maple communities, respectively. These results indicate that exposure to even moderate levels of O₃ significantly reduce the capacity of NPP to respond to elevated CO₂ in some forests. Successional studies of the same plant communities, as part of the FACE experiments, some clones of aspen grew better under O₃ fumigation (Kubiske *et al.*, 2006a). For the mixed aspen–birch community, importance of aspen and birch decreased and increased, respectively, in the controls. In the treatments, the change in importance was in the same direction, but to a greater degree in elevated O₃, and to a lesser degree in elevated CO₂. Thus, the presence of elevated O₃ hastened conversion of stands to paper birch, whereas the presence of elevated CO₂ delayed it. Relative importance of aspen and maple decreased and increased, slightly, respectively, in the control treatments. But elevated O₃ slightly increased the rate of conversion of aspen stands to sugar maple, and maple was placed at a competitive disadvantage to aspen under elevated CO₂.

Many of the studies of CO₂ and O₃ in combination measure endpoints that are not typically considered in regulatory standard setting, in addition to measuring growth and productivity which are more typically used in regulatory settings. While they are known to influence ecosystem function, critical changes in these processes that will lead to detectable changes in some measure of productivity (such as forest growth, or agricultural yield) are not well established. An example is the study by Holton and Lindroth (2003) who measured decreased “performance” of tent caterpillar on aspen, under conditions of elevated CO₂ and O₃. “Performance” was enhanced by ambient CO₂ and elevated O₃, and depressed when both CO₂ and O₃ were elevated, results that depended on the genotype of aspen. Zeleznik *et al.* (2007) measured the effects of O₃ on root growth and mycorrhizal colonization in beech, in sun versus shade. While the amount of light altered the mycorrhizal symbiont on the beech roots, O₃ fumigation did not, and overall, O₃ fumigation reduced root vigour (i.e. number of root tips, root length density per volume of soil, Zn concentration, Ca/Al ratio). On a large scale, this would have implications for nutrient cycling in forests fumigated with O₃, but the subsequent relationship to a productivity measure was not well established. Integrated studies, such as AspenFACE, attempts to do that by measuring many endpoints on the same plant communities. These studies are discussed further in this document, under consideration of multi-factor experiments, as AspenFACE focused as much on elevated CO₂ as it did on elevated O₃.

In contrast with the effort to establish the effect of combined CO₂/O₃ on forest species, much less is known about the effect of this mixture on food crops, although individually, these gases have been extensively studied. Long *et al.* (2006) conducted a meta-analysis of crop response to CO₂ or O₃ measured using FACE versus field chambers, and concluded that for soybean, it would be more realistic to project a 5% decrease in yield in response to the two gases at projected future concentrations rather than the 23% increase in yield currently being used in modelling exercises. This suggested correction largely arises from the comparison of FACE and chamber data for soybean yield reduction in response to O₃: 20% loss versus 8% loss,

respectively. The authors conclude that it is vital for global food security to study the effects of mixtures of CO₂ and O₃ on food crop yield using FACE installations. Van Oijen *et al.* (2004) describe “simple” equations to predict the joint effects of elevated O₃ and CO₂ on wheat growth by re-parameterizing a well-characterized growth model to include the effects of these gases on all plant processes. Their model predicts a 25% increase in biomass at low O₃ concentrations (< 0.025 ml l⁻¹) when ambient CO₂ concentration is doubled, versus a 45% decrease in biomass at higher O₃ concentrations (~ 0.09 ml l⁻¹) under conditions of ambient CO₂. When both gases are elevated the net change in biomass is -14%, indicating that elevated CO₂ does offset the effect of O₃. While their definition of “simple” is not typical, their study does demonstrate the potential for modifying well-known growth models for major agricultural crops with data generated from various studies of O₃ and CO₂, none of which on their own lead to landscape-scale predictions. Ren *et al.* (2007) used the Dynamic Land Ecosystem Model (DLEM) to calculate the changes in net primary productivity (NPP) and carbon (C) sequestration in Chinese grasslands over the previous 40 years as a result of climate change, including increased O₃ concentrations. Their conclusion was that from all causes, over the last 40 years, the grasslands have been a weak C sink with predicted increases in NPP by 14 Tg C yr⁻¹ and 0.11 Pg C stored over the same period; this is if O₃ had not increased during the 40 years. Including the effect of O₃, these numbers dropped to 0.30 Tg C yr⁻¹ and 0.07 Pg C stored. Regionally, both increases and decreases in NPP were calculated depending on the local climate. The conclusion is that the primary productivity of the grasslands is substantially compromised by elevation in O₃ concentration, with the reduction in C sink strength a potential contributor to climate change.

In conclusion, these results demonstrate that O₃ is an important part of climate, and that increases in ambient O₃ concentrations as a result of global warming or anthropogenic activity will contribute to the changes in global C cycling and water budgets that are predicted to accompany climate change.

Jones and Paine (2006) measured herbivore richness and diversity, as well as herbivore community organization, along a well-characterized gradient of N and O₃ pollution in the San Bernardino Mountains (CA, USA). While there was no change in richness or diversity, the authors detected increased numbers of leaf-chewing herbivores at the higher pollution sites relative to the greater predominance of sucking insects at the cleaner sites. Acknowledging that other factors may be changing along with the gradient in pollution concentrations that could partially explain their observations, the authors supported their conclusions by reference to earlier studies that demonstrate enhanced activity of leaf-chewing species on O₃-fumigated vegetation, likely a result of alterations in leaf biochemistry. While this study calculated separate contrasts of high versus low pollution for N and O₃, the “high” and “low” sites were mostly the same, so attribution of the effect to one or the other pollutant was difficult.

Ozone in combination with SO₂ and/or NO₂ could have positive or negative effects, depending on the concentrations of the latter two pollutants. Muzika *et al.* (2004) demonstrated a negative correlation between average SO₂ and NO₂ concentrations, and basal area increment (BAI) of spruce and beech trees growing along a gradient of pollution in the Carpathian Mountains. As well, there was a negative correlation between BAI and the highest O₃ concentration: when the three pollutants were combined into a single index of exposure, the negative correlation with BAI was greater than 60%, although O₃ was not the strongest of the three pollutants in terms of explaining reduced BAI.

10.4.1.3 Ozone Dose Expression

The 2003 CWS Update (CCME, 2003a) and the USEPA AQCD (2006) extensively discussed the various dose metrics for vegetation O₃ exposure. These discussions of dose metrics were focused on the development of an appropriate air quality standard to ensure the protection of vegetation.

This present review of scientific literature published between 2003 and 2007 has focused on the gaps identified by both the 2003 CWS Update (CCME, 2003) and the USEPA AQCD (2006), as well as by the OAQPS Staff Paper (USEPA, 2007), in terms of the development of an air quality standard for the protection of vegetation. In particular, while these documents recognized the biological rationale of a flux-based approach to the establishment of air quality standards in North America and critical levels in Europe, the data required to confirm the approach were lacking.

Ashmore *et al.* (2004) suggested flux-based critical levels for the protection of vegetation in Europe is preferred because they will provide a stronger mechanistic basis for O₃ risk assessment. Ashmore *et al.* further noted the application of flux-based critical levels requires a large amount of data, which were not presently available. The authors promoted the undertaking of investigations, which will provide further insight into the link between stomatal flux and variable rates of O₃ detoxification. Karlsson *et al.* (2004a) suggested that critical level protection in Europe should be modified to include a simple model for stomatal conductance, which includes vapour pressure deficit, solar radiation and air temperature.

In further support of the flux-based approach, Matyssek *et al.* (2007) determined the AOT_x (where x is the dosage threshold, e.g. exposure threshold of 40 ppb is AOT₄₀) exposure type concept is appropriate to consider potential risk to vegetation under high water and nutrient availability conditions only. Therefore, risk to vegetation in Europe can be misjudged. In dry conditions, such as Mediterranean climates, risk to vegetation can be overestimated because of low humidity and soil moisture, which limit the amount of O₃ uptake. Where low humidity and soil moisture are not limiting, the estimated risk to vegetation may be appropriate.

Table 10.10 Recent studies contributing to the advancement of understanding of O₃ dose expression.

Citation	Species	Endpoint	Conclusion
Wieser <i>et al.</i> 2003.	Norway Spruce, Cembra pine, European larch	Ozone uptake	Sap-flow based measurements were used to estimate O ₃ uptake at the whole-tree and stand levels
Grunhage and Jager, 2003.	Spring wheat (Europe)	Ozone deposition	Introduction of a new model to ascertain O ₃ flux-effect relationships in consideration of background deposition, deposition rates and vegetation responses
Nussbaum <i>et al.</i> 2003.	Wheat (Switzerland)	Stomatal ozone fluxes	Introduction of the new Ozone Deposition Model (ODEM) to ascertain O ₃ flux-effect relationships in consideration of O ₃ concentration at 3 - 5 m; wind speed, precipitation and soil moisture content
Gerosa <i>et al.</i> , 2003.	Wheat (Northern Italy)	Stomatal ozone fluxes	Direct measurements of O ₃ depositional fluxes over a wheat field; on average, stomatal flux was 50 - 60% of total flux but changed during the life cycle of the wheat
Simpson <i>et al.</i> 2003.	Temperate coniferous forest, temperate cereals (Europe)	Stomatal ozone fluxes	Development of the European Monitoring and Evaluation Programme (EMEP) O ₃ deposition model and testing of environmental factors that affect the sensitivity of the model
Nikolov and Zeller, 2003.	N/A	Gas exchange model	Introduction of FORFLUX, a new biophysical model to ascertain the simultaneous exchange of O ₃ , CO ₂ and water vapour between terrestrial ecosystems and the atmosphere
Massman 2004.	Grapes – vineyard (United States)	Plant injury	Simple model for estimating effective dose by combining canopy's rate of stomatal O ₃ uptake and the plant's defence to O ₃ uptake
Uddling <i>et al.</i> 2004.	Birch (Roth Europe)	Biomass reduction	Biomass reduction in juvenile birch more strongly related to stomatal uptake of O ₃ rather than external exposure
Karlsson <i>et al.</i> 2004a.	Subterranean Clover (Europe)	Visual injury	Critical level protection in Europe should be modified to include a simple model for stomatal conductance, which included vapour pressure deficit, solar radiation and air temperature
Karlsson <i>et al.</i> 2004b.	Norway Spruce (Europe)	Biomass reduction	Cumulative O ₃ uptake was significantly related to biomass reduction in saplings; 1% reduction in total biomass per 10 mmol m ⁻² cumulated O ₃ uptake on a needle area basis
Karlsson <i>et al.</i> 2004c.	Various young coniferous and deciduous tree species Europe	Biomass reduction	Cumulative leaf uptake of O ₃ was significantly related to biomass reduction in young trees; proposal of an hourly flux threshold of 1.6 nmol m ⁻² s ⁻¹ the "Accumulated stomatal flux above a threshold Y" Index
Matyssek <i>et al.</i> 2004.	Various ages of coniferous and deciduous tree species Europe	N/A	Recommend future air quality standards incorporate flux and defence capacity; sap flow measurements are a useful tool for estimating O ₃ uptake at the tree and canopy level
Elvira <i>et al.</i> 2004.	Kermes Oak (Spain)	Relative growth rate, photosynthesis, stomatal conductance	Differences noted between ecotypes of Kermes Oak in stomatal conductance response to O ₃ exposure
Wieser and Emberson, 2004.	Norway Spruce (Europe)	Stomatal conductance	Factors important in controlling stomatal conductance in Norway spruce were investigated
Bassin <i>et al.</i> 2004a.	Grasslands, wheat (Europe)	N/A	Field testing of the Ozone Deposition Model for Europe; conclusion that quality of the model results is dependent upon an extensive set of biological, climatic and edaphic input data
Grulke <i>et al.</i> 2004.	Ponderosa pine (California, U.S.A.)	Stomatal conductance	Lack of stomatal closure at night in mature and pole-sized Ponderosa pine; nighttime stomatal conductance 10 -20% of maximum daytime values

Citation	Species	Endpoint	Conclusion
Mikkelsen <i>et al.</i> 2004.	Norway Spruce - dominated coniferous forest (Europe)	N/A	Field measurements of O ₃ concentrations and fluxes to quantify diurnal, seasonal and yearly fluxes to estimate non-stomatal and stomatal removal
Tuovinen <i>et al.</i> 2004.	Coniferous forest, moorland, wetland, wheat field and grassland (Europe)	N/A	Assessment of the performance of the EMEP photochemical transport model and suggested improvements
Altimir <i>et al.</i> 2004.	Scots pine (Finland)	Stomatal conductance	Assessment of O ₃ deposition to pine shoots; non-stomatal contribution to total conductance was approximately 50% of total; revised EMEP model incorporated relative humidity
Cieslik 2004.	Various vegetation types (Europe)	Stomatal conductance	Non-stomatal contribution to O ₃ deposition is the dominant portion of deposition; water supply is a key variable in influencing stomatal uptake of O ₃ in Mediterranean climate
Gerosa <i>et al.</i> 2004.	Barley (Northern Italy)	Stomatal ozone fluxes	Direct measurements of O ₃ flux are difficult to obtain; method for calculating O ₃ exposure using O ₃ concentrations and meteorological observations is provided
Finkelstein <i>et al.</i> 2004.	Cutleaf Coneflower (North Carolina, U.S.)	Deposition model	Meyers and Paw U model to predict O ₃ deposition within a canopy was used and field verification measurements recorded
Utiyama <i>et al.</i> 2004.	Red Pine (Japan)	Ozone vertical profile	Forest is not always a sink for O ₃ , but also can be a source of O ₃ during sunlit conditions in the presence of NO _x
Panek, 2004.	Ponderosa pine (California, U.S.A.)	CO ₂ uptake	Seasonal measurements of peak ozone and CO ₂ uptake did not correspond to periods of peak ozone concentration, supporting the inappropriateness of exposure-based metrics
Nunn <i>et al.</i> 2005.	Beech (Germany)	Leaf injury	Differences in response between adult and young beech trees at least partially due to a lower detoxification capacity of young trees
Emberson <i>et al.</i> 2007.	Scots pine, Beech, Holm Oak (Europe)	Stomatal ozone fluxes	Application of the "Accumulated stomatal flux above a Threshold Y" index shows significant differences between species predominantly due to differences in timing and length of growing season, the impact of soil moisture deficit on stomatal conductance and soil moisture stress
Percy <i>et al.</i> 2007b.	Trembling Aspen (United States)	Tree diameter converted to cross sectional area	4th highest daily maximum O ₃ concentration, growing degree days and growing season average wind speed was well correlated with 5 year growth
Blumenrother <i>et al.</i> 2007.	Beech (Germany)	Sucrose and starch in adult tree leaves	O ₃ flux influenced sucrose and starch levels in adult beech tree leaves, sugar synthesis decreased with increased exposure
Low <i>et al.</i> 2007.	Beech (Germany)	Photosynthesis, respiration and stomatal conductance	No clear relationship between cumulated O ₃ uptake and plant gas exchange (photosynthesis and respiration)
Ferretti <i>et al.</i> 2007a.	Beech (Italy)	Defoliation and visible injury	AOT40 was significantly related to defoliation in beech, but not visible foliar injury in native vegetation
Ferretti <i>et al.</i> 2007b.	Crops and Forests (Italy)	N/A	A flux-based approach is preferred, but a number of factors limit its applicability for routine monitoring
Simpson <i>et al.</i> 2007.	Wheat, Beech (Europe)	N/A	EMEP chemical transport model used to map Accumulated exposure over threshold of X ppb and Accumulated stomatal flux above threshold of X ppb
Alonso <i>et al.</i> 2007.	Clover species (Spain)	Stomatal conductance	Differential O ₃ sensitivity among species was not related to differential maximum stomatal conductance values

Citation	Species	Endpoint	Conclusion
Ashmore <i>et al.</i> 2007.	Grassland (Europe)	Stomatal ozone flux and deposition	use of DO ₃ SE ozone deposition model shows spatial and temporal variation and modification by management and soil water status
Bassin <i>et al.</i> 2007.	Temperate grasslands (Europe)	Various	initial indications are that grassland communities may be able to be classified into ozone sensitivity based on physiological or ecological principles but more data is needed
Buker <i>et al.</i> 2007.	Wheat, Grape, Beech, Birch (Europe)	Stomatal ozone fluxes	Measured values of stomatal conductance compared to predicted values from a 1987 model on an hourly and daily basis
Elvira <i>et al.</i> 2007.	Aleppo pine (Spain)	Stomatal conductance	EMEP stomatal conductance model modified to account for maximum stomatal conductance, air temperature, vapour pressure deficit and phenological changes
Karlsson <i>et al.</i> 2007.	Various young tree species (Europe)	Biomass reduction	AF _{st} Y1.6 (accumulated stomatal ozone flux) was superior to AOTX in predicting biomass reduction in young trees known to be sensitive to ozone
Keller <i>et al.</i> 2007.	Wheat and Grasslands (Switzerland)	Yield	AF _{st} Y was superior to AOT40 in estimating yield losses during a dry year using the ODEM model
Matyssek <i>et al.</i> 2007.	Forest trees (Europe)	Various	promotion of the flux-based approach in assessing O ₃ risk; however, effective O ₃ dose is preferred, whereby inherent defence and tolerance mechanisms are accounted for
Tuovinen <i>et al.</i> 2007.	Wheat, Beech (Europe)	Various	testing of the robustness of the AOTX and the AF _{st} Y indices
Pleijel <i>et al.</i> 2007.	Wheat, Potato (Europe)	Relative yield	calibration of flux based model using primary data and values from the literature (AF _{st} 6 for winter wheat); flux based models are now sufficiently well calibrated to be used in Europe
Nunn <i>et al.</i> 2007.	Norway Spruce, Beech, Larch (Austria)	Ozone uptake	validation of flux based O ₃ uptake models can be validated using sap flow measurements
Grulke <i>et al.</i> 2007a.	Snapbean, Black oak and Blue oak seedlings	Stomatal ozone fluxes	comparison of calculated and measured stomatal ozone fluxes - calculated tended to overestimate direct measurements
Grulke <i>et al.</i> 2007b.	Cutleaf Coneflower (North Carolina, U.S.)	Stomatal behaviour	greater ozone uptake occurred in sensitive plants due physiological differences (i.e. response of stomates to light and vapour pressure deficit) rather than morphological differences
Goumenaki <i>et al.</i> 2007.	Paris Island Lettuce (Greece)	Yield	AF _{st} Y4 (accumulated stomatal ozone flux) was superior to AOTX in predicting yield reduction in Mediterranean climate
Gerosa <i>et al.</i> 2007.	Onion (Italy)	Stomatal ozone fluxes	Comparison of two models for calculating water vapour pressure deficit as input to algorithms to determine stomatal ozone fluxes
Harmens <i>et al.</i> 2007.	Winter Wheat (Europe)	Stomatal ozone fluxes	Climate change will likely result in a reduction in stomatal ozone fluxes despite increasing tropospheric ozone levels
Schaub <i>et al.</i> 2007.	Beech (Europe)	Stomatal ozone fluxes	Comparison of AOT40 and AF _{st} Y at standard research plots in Europe but completeness and availability of data is of concern

Table 10.10 provides a summary of the recent literature that contributed to the advancement of relating O₃ exposure to plant response (dose expression) and the major findings of the studies. In the intervening years, a vast majority of the scientific literature has focused on the refinement of the flux-based approach for the setting of Critical Levels in Europe.

Simpson *et al.* (2003) undertook further development of the European Monitoring and Evaluation Programme (EMEP) O₃ deposition model and tested environmental factors that affect the sensitivity of the model. The EMEP model simulates emissions, transport, transformation and removal of pollutants. Various authors further calibrated the model for a variety of plant species and landcover types and provided an assessment of its performance (Tuovinen *et al.*, 2004; Altimir *et al.* 2004; Simpson *et al.*, 2007; Elvira *et al.*, 2007). Simpson *et al.* (2007) modified the model to allow for the calculation of O₃ fluxes to vegetation communities.

Nussbaum *et al.* (2003) introduced the new Ozone Deposition Model (ODEM) to ascertain O₃ flux-effect relationships in winter wheat, in consideration of O₃ concentration at 3 - 5 m, wind speed, precipitation and soil moisture content. Bassin *et al.* (2004a) noted during field verification of the ODEM that the quality of the model results is dependent upon an extensive set of biological, climatic and edaphic (soil) input data, which is expensive and labour intensive to collect and analyse.

Karlsson *et al.* (2004c), through their investigations of cumulative leaf uptake of O₃ and biomass reduction in young trees, introduced the "Accumulated stomatal flux above a threshold Y" (AF_{st}Y) Index, which incorporates factors such as species types, phenology and environmental conditions, as a flux-based alternative to the AOT40 approach to risk assessment that was previously promoted in Europe. An hourly threshold value of 1.6 nmol m⁻² s⁻¹ was promoted for various young coniferous and deciduous tree species. Several authors examined the AF_{st}Y index for a variety of species, and generally concluded its performance was superior to the AOTx (Emberson *et al.*, 2007; Karlsson *et al.*, 2007; Keller *et al.*, 2007; Tuovinen *et al.*, 2007; Pleijel *et al.*, 2007; Goumenaki *et al.*, 2007; Schaub *et al.*, 2007).

Several European studies examining impact of O₃ on tree species suggest that sap-flow based measurements can be used to estimate O₃ uptake at the whole-tree and stand levels (Wieser *et al.* 2003; Matyssek *et al.*, 2004) and that flux based O₃ uptake models can be validated using sap flow measurements (Nunn *et al.*, 2007).

Kubiske *et al.* (2006b) monitored inter-annual climatic variation for the same seven years, in the same aspen community and demonstrated that much of the year-to-year variation in plant response to elevated O₃ or CO₂ could be explained by variation in photosynthetic photon flux density (PPFD) – the greater the PPFD, the greater the (negative and positive, respectively)

response to elevated O₃ or CO₂. As both of these gases mediate their effect through stomatal uptake, this study confirmed the usefulness of an air quality criterion for O₃ based on flux rather than ambient concentration.

Table 10.11 Recent studies summarizing O₃ dose expression issues.

Citation	Main Findings
Ashmore <i>et al.</i> 2004	Flux approach is preferred in the establishment of critical levels to protect vegetation in Europe, but further information regarding detoxification under variable stomatal flux scenarios
Grunhage <i>et al.</i> 2004.	Discussion of differences between the European "critical level" approach and the US and Canadian approach of exposure indices
Musselman <i>et al.</i> 2006.	Overall critical review and analysis of the use of exposure-and flux-based ozone indices for the prediction of vegetation effects
Paoletti and De Marco 2007.	Adequate flux models are not yet available, so until they are exposure-based O ₃ metrics are the only practical measure available to relate plant response to ambient air quality; all exposure metrics are highly correlated, so it is recommended the most biologically meaningful metric be employed
Percy and Ferretti, 2004.	Despite extensive monitoring that has occurred in forests, cause and effect relationships cannot be ascertained; there is a need to re-examine our monitoring strategies
Percy and Karnosky, 2007.	The current air quality standards in North America are discussed in the context of new experimental data and recommendations are made for policy-relevant scientific experiments

Very few experiments that contributed to the understanding of O₃ uptake and O₃ dose expression were completed in North America in recent years (Table 10.11). Panek (2004) noted that seasonal measurements of peak O₃ and CO₂ uptake in Ponderosa pine in California did not correspond to periods of peak O₃ concentration, supporting the inappropriateness of exposure-based metrics. Grulke *et al.* (2004) confirmed the lack of stomatal closure at night in mature and pole-sized Ponderosa pine and found that night time stomatal conductance was 10 - 20% of maximum daytime values.

Massman (2004) provided a plant injury model for grapevines in California with the intention of further developing the relationship of injury to flux-based metrics. Two studies were completed on cutleaf coneflower (*Rudbeckia laciniata* var. *digitata*) in North Carolina (Finkelstein *et al.* 2004; Grulke *et al.*, 2007b). Finkelstein *et al.* (2004) employed a model developed by Meyers and Paw U (Meyers and Paw U, 1986, 1987) to predict O₃ deposition within a canopy and field verification measurements were recorded. Grulke *et al.* (2007b) determined greater O₃ uptake occurred in sensitive plants due to physiological differences (i.e. response of stomates to light and vapour pressure deficit) rather than morphological differences. Grulke *et al.* (2007a) compared calculated and measured stomatal O₃ fluxes of *Phaseolus vulgaris* (snapbean), *Quercus kelloggii* (black oak) and *Quercus douglasii* (blue oak) seedlings in a greenhouse experiment in California and found calculated fluxes tended to overestimate stomatal O₃ fluxes.

Percy *et al.* (2007b) determined the air quality attainment level for O₃ in the US and Canada (the 4th highest daily maximum eight hour average O₃ concentration), growing degree days and growing season average wind speed were well correlated with 5 year growth of trembling aspen (*Populus tremuloides*) in the United States. The authors suggest this metric of the O₃ air quality attainment level performed better than SUM06, AOT40 or maximum one hour average O₃ concentration metrics.

Ferretti *et al.* (2007a) noted that the AOT40 metric was significantly related to defoliation in beech, but not visible foliar injury in native vegetation in Italy.

In Japan, Utiyama *et al.* (2004) recorded direct measurements of the O₃ profile within a stand of red pine and found that O₃ immediately above the canopy and at the trunk level may be a result of O₃ being created during sunlit conditions in the presence of NO_x and therefore the interpretation of O₃ fluxes must be undertaken with caution. This study points to the creation of O₃ from volatile organic carbon (VOC) released by the forest trees themselves, rather than O₃ precursors that were formed as a result of industrial or vehicular air pollution.

Harmens *et al.* (2007) considered the implications of climate change variables, such as elevated CO₂ concentrations, warming and changes in precipitation will impact the stomatal flux of O₃ into leaves. In particular, these climate change variables will impact stomatal conductance, atmospheric O₃ concentrations, frequency and extent of pollution episodes and alterations to length of growing seasons. Stomatal fluxes of O₃ to winter wheat in Europe are predicted to be reduced in the future.

A few studies in recent years undertook validation of the results of modelling of stomatal conductance, flux or cumulative O₃ uptake (Gerosa *et al.*, 2003; Mikkelsen *et al.*, 2004; Finkelstein *et al.*, 2004; Grulke *et al.*, 2007a; Buker *et al.*, 2007). Gerosa *et al.*, 2004 point out direct measurements of O₃ flux are difficult to obtain and they therefore provided a method for calculating O₃ exposure using O₃ concentrations and meteorological observations.

Pleijel *et al.* (2007) concluded that flux based models are now sufficiently well calibrated to be used in Europe and, in contrast, Paoletti and De Marco (2007) suggested adequate flux models are not yet available. Similarly, Karlsson *et al.* (2007) agreed that the flux concept cannot be applied to all forest species across Europe due to an incomplete understanding of the internal exposure-response relationships and parameterization issues with the stomatal conductance model.

Matyssek *et al.* (2007) stated that while a flux-based metric is preferred, the modelling of stomatal O₃ flux requires extensive data that are not often routinely collected simultaneously with O₃ exposure data. It is Matyssek *et al.*'s opinion that eventually a flux metric will have to be simplified, as it is not practical to parameterize the model for each species or genotype across all environments. Their suggestion is to focus on the most ecological or economically

relevant species under prevailing stand conditions (in the case of forest trees) rather than a vegetation type and that there is a strong need to also consider defence capacity of the species in order to examine “effective O₃ uptake” in vegetation.

Table 10.11 provides a brief summary of recent literature that examined the overall issue of O₃ dose expression and response of vegetation. Grunhage *et al.* (2004) provided a discussion of differences between the European "critical level" approach and the US and Canadian approach to setting air quality standards. While the flux based approach is accepted by North American scientists, there has not been nearly the extent of research on O₃ flux and vegetation response compared to that which has occurred in Europe.

Percy and Ferretti (2004) note that despite extensive environmental monitoring that has occurred in European and North American forests, cause and effect relationships cannot be ascertained between environmental factors, such as O₃ exposure, and forest health. Percy and Ferretti suggest there is a need to re-examine our monitoring strategies to ensure appropriate scientific questions are being addressed through monitoring programs.

Musselman *et al.* (2006) provided an extensive review of various O₃ exposure metrics and the flux based approach to assessing plant response. They note the complexities of the biological processes that affect plant response to O₃ and the potential for their modification due to physical factors such as environmental conditions, soil moisture and nutrient conditions. The authors suggest that current O₃ uptake models do not effectively identify and quantify defence mechanisms and their relationship to O₃ uptake and as such, models based solely on O₃ flux will overestimate the effects on vegetation. They conclude that until models are based on “effective dose”, exposure based O₃ metrics are the most appropriate method by which to relate air quality standards to vegetation response.

Percy *et al.* (2007a) similarly concluded that at this time in North America, the only practical method for relating vegetation response to air quality standards is to use exposure-based metrics. Their study incorporated measurements of wind speed and growing degree days into an exposure based metric and found it improved the statistical relationship with trembling aspen growth over a five year period.

Further, Paoletti and De Marco (2007) recommend that until appropriate flux models are available, exposure-based O₃ metrics are the only practical measure available to relate plant response to ambient air quality. They further conclude that all exposure metrics are highly correlated, so it is recommended that the most biologically meaningful metric be employed.

In conclusion, significant progress has been made by European scientists in the flux based approach to improve our understanding of the relationship between O₃ exposure and vegetation response in the past five years. Regardless, the complexity of biological response to

physical factors and the weak understanding of the implication of the plant's defence mechanisms mean that further work is required before we can relate use to concept of flux to refine air quality standards.

In the interim, it is appropriate to use exposure based metrics to set air quality standards and the literature generally supports the current approach of use of the 4th highest daily maximum to calculate the Canada Wide Standard for ozone.

10.4.2 Materials

A search of the recent literature revealed a scant number of new studies on the impact of O₃ on materials. The recent few studies are almost entirely related to the use of O₃ as a biocide or to biodegrade tannins and remove colour in commercial textile dyeing. Aoki and Tanabe (2007) exposed various building materials [polystyrene, rubber adhesive, cedar board, Japanese Cypress board, silver fir board, d-limonene (contained in certain woods or cleaning products), and waxed or unwaxed plastic tiles] to O₃. The researchers found that O₃ exposure to d-limonene, cedar board or cypress board produced sub-micron particles. They further discovered plastic tiles exposure to O₃ produced sub-micron and secondary organic compounds. The findings have potential implications for human exposure to indoor air quality.

The United Nations Economic Commission for Europe (UNECE) International Cooperative Programme on Effects on Materials (ICP Materials) continues to be the only apparent program that addresses air quality effects on materials, such as steel, bronze, metals, limestone, etc. Kucera *et al.* (2007) conducted a multi-pollutant assessment program examining the impacts of a variety of air pollutants on carbon steel, zinc, copper, bronze and limestone at various international test sites from 1997 to 2003. Other related variables included measures of precipitation acidity such as H⁺ and Cl⁻. Dose-response functions of corrosion damage were developed, but O₃, while measured at all sites, was only included in the dose response function for copper corrosion, along with SO₂, annual rainfall, and relative humidity.

Overall, however, there are few data on the impact of O₃ on materials and the results and conclusions of the 2003 CWS Update continue to be upheld, mainly that there is no new information that suggests changes to the Canada Wide Standard for O₃ in order to protect materials.

10.5 Recent Literature on Particulate Matter Effects

10.5.1 Vegetation

Grantz *et al.* (2003) provided a very comprehensive review of the ecological effects of PM. The main challenge in addressing the effects of PM on vegetation is that the effect will depend on the speciation of the PM, i.e. particles which are alkaline (e.g. cement dust) are likely to have quite different ecological effects than those which are acidic (e.g. sulphate (SO_4^{2-}) aerosols), or metallic. As well, the size of the particles influences their residence time on vegetation (thus exposure to the particles) and few of the studies have fractionated the particles for mass. Except for very localized areas of impact there is little evidence of widespread direct effects on vegetation, and indirect effects on vegetation through deposition to soils is considered to be largely outside the scope of this review. Many of the studies published between 2003 and 2007 focus on the use of vegetation as biomarkers for particulate deposition to ecosystems, rather than the ecological effects.

Grantz *et al.* (2003) considered the potential for PM to affect vegetation by first reviewing what was known about deposition itself (e.g. particle size, mode of deposition, magnitude of deposition relative to various species of PM). They then described the direct effects of PM (on ecosystem and individual plants through surface injury) as well as the indirect effects (on rhizosphere functions such as nutrient cycling, soil pH and metal accumulation) and the effect on atmospheric turbidity, which will influence the potential for photosynthesis. Finally, these authors described the critical load approach to determining threshold levels for regulatory purposes. The number of studies published since 2003 that make new contributions to these topics are scant, but are described below using the framework of Grantz *et al.* (2003). Not considered in this discussion are effects of sulphate or nitrate aerosols (extensively reviewed by Grantz *et al.*, 2003) as these are covered as part of the 2004 Canadian Acid Deposition Science Assessment (Environment Canada, 2005). Also not discussed are particulates from Cu/Zn smelters, as these have been considered as part of the Canadian Environmental Protection Act Assessment (Environment Canada/Health Canada, 2001).

Table 10.12 Recent studies on the impact of PM on vegetation that confirmed previous results

Citation	Species	PM Type	Endpoint	Conclusion
Mandre and Korsjukov 2007.	Scots Pine	Alkaline cement dust	Tissue composition	Doubling of soil pH resulted in more lignin less hemicellulose and similar cellulose
Sardans and Peñuelas 2006.	Evergreen Oak and Moss	Urban	Enrichment factors for tissue concentration	Concentrations of many elements in plant tissues enriched in urban environment compared to pristine, b/c of deposition and absorption of elements to foliage
Trimbacher and Weiss 2004.	Norway Spruce	Various emission sources	Epicuticular wax	damage to wax results from particles themselves, as well as wind abrasion; damage not correlated to concentrations of metals in dust particles, although elevated elemental concentration is related to that of deposited dust
van Heerden <i>et al.</i> 2007.	Dollar Bush	Limestone dust	Photosynthetic parameters	Deposition of dust reduces plant's photosynthetic capacity evidenced by all measured parameters; recovery after rainfall or cessation of quarry activities
Wang <i>et al.</i> 2006.	Numerous	Urban	Deposition velocity and composition	Deposition to leaves dependent on aerodynamics of plant and microroughness of leaf surfaces; mostly PM ₁₀ and PM _{2.5} collected on foliage

Recently published scientific literature did not contribute new understanding to the impact of PM on vegetation. Recent papers which confirmed what was already known about the impact of PM on vegetation are summarized in Table 10.12.

The characteristics of PM deposition (e.g. particle size, mode of deposition, magnitude of deposition of various species) are not discussed extensively here; however, Wang *et al.* (2006) did characterize the size of particles that adhered to various plant species, demonstrating that nearly 100% of the particles were PM₁₀, and of that, approximately 60% were PM_{2.5}. The density of particles on the leaf surface increased as microroughness of the leaf surface also increased.

The direct effects of PM were described by Grantz *et al.* (2003) as including damage to the leaf epicuticular wax through abrasion, which was confirmed in the Austrian study by Trimbacher and Weiss (2004) of Norway spruce. Despite a wide range in the deposited particles, damage to the surface of the needles was not correlated with contaminant concentration; however, concentration of several trace elements in needle tissue was related to concentrations in the PM deposited to the needle surface. Direct effects of PM can also include reduction in photosynthesis through shading, as noted by van Heerden *et al.* (2007), an effect that was reversed by rainfall. As well, tissues can accumulate elevated concentrations of trace elements through foliar absorption, as noted by Sardans and Peñuelas (2006). Although this study doesn't implicate toxicity as a result, it is considered possible if the elemental concentrations are high enough.

The indirect effects of PM were noted by Grantz *et al.* (2003) to include changes in soil quality as a result of deposition, such as alkaline dust from cement or quarry operations which increase soil pH and subsequently affect nutrient availability and cycling. Mandre and Korsjuko (2007) studied Scots pine growing in soils that had pH levels of 12.3 – 12.6 as a result of deposition of cement dust. There were changes in wood quality (more lignin, less hemicellulose), and, although K, Mg and Ca were all elevated in high pH soils, the changes in levels in plant tissues were more subtle (only K was higher at the contaminated site), likely because these elements are essential and thus regulated by the organism.

10.5.2 Materials

A search of the recent literature revealed almost no studies that included the impact of PM on materials. The exception was the Kucera *et al.* (2007) paper discussed above, which showed that PM₁₀ was a significant regressor in dose response functions for deterioration of carbon steel, bronze and limestone. This study defined PM in terms of SO₄²⁻, NO₃⁻, Cl⁻, NH₄⁺, Na⁺, Ca²⁺, Mg²⁺ and K⁺. It omitted the metallic elements that are not major soil cations, and are likely a significant deposition only in relatively well-defined footprints of smelters or other metal mining or metallurgical operations.

The USEPA (2004) assessment concluded that it is not possible to determine the visual or physical threshold level where PM effects on materials are apparent and therefore air quality criteria on this basis are not achievable.

10.6 Uncertainties

10.6.1 Ozone

10.6.1.1 Vegetation

There continues to be a scarcity of studies examining the impact of O₃ to agricultural species that are relevant to Canada, specifically soybean, corn, wheat, flax and hay. Similarly, studies on species that are dominant in the Canadian natural landscape and of economic importance for the forestry industry, such as black spruce, jack pine, balsam poplar, and sugar maple are lacking.

In addition, there is a lack of information on the O₃ dose-response relationships for Canada-relevant species. Further information is required regarding the incorporation of factors that influence O₃ dose to vegetation into exposure metrics. This would aid in the creation of biologically relevant air quality standards for the protection of vegetation.

The bulk of the recent research examining O₃ flux into plants and the development and verification of models has been undertaken in European environments, with the exception of a few studies in California under greenhouse conditions. While researchers in North America have confirmed stomatal opening at night and the disconnection between maximal O₃ concentrations and maximum stomatal conductance in a few species, little advancement has occurred in quantifying or ascertaining effective dose and vegetation response. The contribution of detoxification or repair mechanisms into models of stomatal conductance requires further study before models of effective O₃ dose and plant response can be developed.

The literature does not contain significant information of relevance to ecosystem responses of Canadian specific ecosystem types such as wetlands, grasslands and forests. The exception is recent studies on trembling aspen, which is the most widely distributed tree species in North America, and the most abundant deciduous tree species in the Canadian boreal forest.

There continue to be uncertainties regarding the relative O₃ sensitivity of ecological significant species, such as rare, threatened or endangered species, and the potential impact of O₃ on the vegetation in protected areas.

10.6.1.2 Materials

There has been little new information published on O₃ and its impact to materials due to the fact that materials are relatively tolerant of O₃ exposure. Vegetation and humans continue to be more sensitive and significant receptors to O₃. Further development of dose-response models for materials would aid in ascertaining the potential economic impact of O₃.

10.6.2 Particulate Matter

10.6.2.1 Vegetation

The impact of PM on vegetation is dependent upon the speciation of the PM, which makes defining a threshold value for PM in its entirety very difficult. Information on speciation of PM and vegetation response is lacking in the scientific literature. The greatest impact to plants occurs due to the modification of soil chemistry by the deposition of the PM. While the impact on soil chemistry by metal PM is fairly well understood, the impact of other cations and anions is not as well known.

10.6.2.2 Materials

Impacts of PM to materials are also dependent on the speciation of the PM; therefore, more information on the speciation of PM in the environment is needed. Studies that develop dose-response relationships for the impact of various species of PM on materials are not frequent in the literature. In addition, the threshold levels where visual or physical effects on materials occur are not well understood.

10.7 Summary and Conclusions

The main findings of the review of the recent literature are included in the following section. In addition, conclusions regarding the potential impact of the findings on the setting of air quality standards for the protection of vegetation or materials are provided.

10.7.1 Ozone

10.7.1.1 Vegetation

Many new studies of plant responses to O₃ have been completed since the previous assessments, with the majority of these studies confirming what is already generally known: that O₃ has negative effects on plant health, and that the response varies with species (and genotype within species) and can be modified by external environmental factors. The most significant conclusions have arisen from the multi-year studies of woody species, particularly those using some version of the FACE exposure system, which is regarded as generating data that are most likely to represent what would happen in the field. In addition, many of the recent studies have shown that realistic, multi-year exposures of perennial plants lead to changes in biomass that would not be otherwise detected in shorter studies.

Highlights of the recent studies on individual plant species relevant to Canada and on ecosystems are summarized below.

Agriculture Plant Species

A number of recent studies revealed some important observations of specific impacts to agricultural plant species:

- NOAELs for soybean yield (AOT40 \approx 20 ppm-h or SUM06 \approx 32 ppm-h), an important field crop in Canada, were established using FACE.

- A meta-analysis of published studies of soybean suggested that chronic exposure to 70 ppb results in approximately 24% yield reduction, and that even chronic exposure to <60 ppb results in some yield loss.
- Seasonal AOT40 of between 9 and 9.7 ppm-hr was sufficient to reduce wheat yield by approximately 20%, and the older, lower yielding variety was less sensitive than the modern variety.
- If the effect of future elevated CO₂ with O₃ is projected from FACE data for soybean, it is more realistic to project a 5% decrease in yield in response to the two gases rather than the 23% increase in yield that is currently used in modelling exercises. This suggested correction largely arises from the comparison of FACE and chamber data for soybean yield reduction in response to O₃: 20% loss versus 8% loss, respectively. These authors conclude that for global food security it is vital to study the effects of mixtures of CO₂ and O₃ on food crop yield, using FACE installations.
- Another study demonstrated the potential for modifying well-known growth models for major agricultural crops with data generated from various studies of O₃ and CO₂ (none of which on their own lead to landscape-scale predictions) to achieve this goal.

Forest Plant Species

Recent literature has shown that for tree species, O₃ impacts are often only evident in longer term studies lasting several years. For example, a 5-year cumulative AOT40 of 87 ppm-h was associated with a 25% reduction in basal diameter of *Betula pendula* compared to plants grown with AOT40 of approximately 3 ppm-h, a change that was noted only after three years of exposure.

Trembling aspen, paper birch and sugar maple responses to elevated CO₂ and O₃ over seven years using a FACE system, demonstrated that contrary to many other observations, the negative effect of O₃ on paper birch was greatest in combination with elevated CO₂. Also, the effect of O₃ on sugar maple was not detectable until after three exposure-years. Changes to above ground growth and physiology in the saplings were detected, and because they continued the study for seven years; changes to C flow below-ground were also measurable.

Ecosystem or Ecological Responses

Several studies in the recent literature provide further insight into ecosystem or ecological level responses of plants and vegetation communities to O₃ exposure. For example, the application an assessment framework to determine the risk of visible injury to plants from O₃ in US National Parks was demonstrated and may be applicable to Canada, with appropriate expansion of the list of known sensitive species to include a wider range of species that occur in Canada.

European scientists have explored the hypothesis that O₃ sensitivity was associated with particular plant ecology strategies, either Grime's C-S-R, or Ellenberg score. There is evidence that "stress tolerators" (the "S" in C-S-R) are more tolerant of O₃ exposure. However, in contrast to a hypothesis that earlier flowering species were more sensitive to O₃, some mid- and late-flowering species have demonstrated sensitivity to O₃. The conclusion was that a previous European consideration to set O₃ criteria to emphasize spring exposures as more important to protection of vegetation was not supported by the results of this species sensitivity survey.

The sink strength of grasslands for carbon over the last 40 years was modelled, with the conclusion that the primary productivity is substantially compromised by elevation in O₃ concentration, with the reduction in carbon sink strength a potential contributor to climate change. These results demonstrate that O₃ is an important part of climate, and that increases in ambient O₃ concentrations as a result of global warming or anthropogenic activity will contribute to the changes in global C cycling and water budgets that are predicted to accompany climate change. This implication should be considered when developing and applying a Canada Wide Standard for ozone.

10.7.1.2 Secondary Standard for Ozone

The 2003 CWS Update (CCME, 2003a) assessment acknowledged that recent literature published between 1999 and 2003 suggested further refinements to the 1999 SAD recommendation of the SUM60 as a secondary standard to protect vegetation were possible, but the means by which to improve it were not clear.

Significant research has occurred in Europe with respect to quantifying and refining the flux based approach to the assessment of risk to vegetation from O₃ in recent years. However, the application of the flux-based approach continues to require further refinement with respect to the internal exposure-response relationships and there are parameterization issues with the stomatal conductance models. In addition, internal repair and detoxification mechanisms have generally not been incorporated into dose expressions. The modelling of stomatal O₃ flux requires extensive data that are not often routinely collected simultaneously with O₃ exposure data.

The USPEA UAQPS Staff Paper (USEPA, 2007) supports the use of the W126, a sigmoid functional weighting of all hourly concentrations (8 a.m. to 8 p.m.) for the growing season, as a secondary air quality standard of O₃ for the protection of vegetation. It also indicates this exposure metric provided the best statistical fit to plant response for North American vegetation impact data. However, recent research has shown that maximum daily stomatal uptake does not necessarily correspond with daily maximum O₃ concentrations and therefore plant response could be overestimated. In addition, the W126 does not account for potential O₃ uptake during night time hours, which would underestimate plant response.

As stated by Musselman *et al.* (2006), at this time, exposure-based metrics are the only practical method for relating plant response to air quality in North America. There is no clear indication from the recent literature as to the best metric to use for a secondary standard, although further refinements to include meteorological variables that influence stomatal uptake are helpful in improving the relationship between O₃ exposure and plant response (i.e. Percy *et al.*, 2007a).

The question posed by this assessment, as well as those previous, is whether there is recent scientific evidence to suggest that the current Canada Wide Standard for O₃ is insufficient to protect vegetation. This question is becoming increasingly difficult to answer, as with each science assessment, there are fewer plant-effects studies that describe plant response to standard air quality data. Most studies published in the last five years use one of these integrative descriptions of exposure (i.e. flux), as it is now accepted that these may offer an improvement in explaining the relationship between air quality data and plant response. There is an extremely urgent need for the development of exposure data in areas of known elevated O₃ occurrence across Canada in the form of cumulative indices (i.e. AOT40, SUM60, W126 etc) against which vegetation harm thresholds identified by current literature studies and future studies can be compared.

10.7.1.3 Materials

Limited recent investigations regarding the impact of O₃ on materials have occurred since the 2003 CWS Update (CCME, 2003b). Consequently, the results and conclusions of the 2003 CWS Update and the USEPA AQCD (2006) continue to be upheld; mainly that there is no new information that suggests changes to the Canada Wide Standard for O₃ in order to protect materials.

10.7.2 Particulate Matter

10.7.2.1 Vegetation

The assessment of the recent literature revealed no new significant findings regarding the effect of PM on vegetation. It should be noted that soil changes by PM were not considered in this assessment as these were addressed in the 2004 Canadian Acid Deposition Science Assessment (Environment Canada, 2005). However, previous studies have concluded that PM impacts on vegetation are highly dependent on PM chemical constituent, which can have impacts on soil chemistry. The number of influencing factors with their associated uncertainties along with the general lack of dose-response data increases the difficulty in defining a critical level for vegetation as a result of PM exposure.

10.7.2.1 Materials

The assessment of the recent literature revealed no new significant findings and therefore it is recommended that the conclusions of the 2003 CWS Update and 2004 USEPA assessments of PM continue to be appropriate. “There is insufficient data available in the scientific literature to determine a threshold level at which the effects of PM on materials are perceived, either visually or physically. Therefore, a dose-response function or threshold definition by which to set air quality criteria for PM based on effects on materials is not possible at this time.” (USEPA, 2004)

10.8 Effects of Ozone and PM on Wildlife – An Emerging Issue

In order to consider the larger ecosystem impacts of O₃ and PM, consideration should also be given to their associated effects on wildlife. Limited research is available to assess the impacts of PM and O₃ on animals and wildlife species. Research has generally focused on the indirect effects of PM and O₃ on wildlife through the influences on vegetation, soil conditions and changes to the ecosystem’s habitat and not on the direct health effects of exposure or inhalation of PM and O₃.

Animal exposure studies, most often using rats, have been geared towards extrapolating the results to assess the potential effects of O₃ and PM exposure to humans rather than to wildlife. Rats and humans respond differently to exposure to PM and O₃ both in terms of dose (i.e. the amount of PM that is deposited in the lungs) and the associated health response (e.g. lung inflammation) from a given dose of PM or O₃ (USEPA, 2004). Ozone animal exposure studies on species including mice, rats, guinea pigs, and rhesus monkeys have demonstrated that there is the potential for significant interspecies sensitivity to O₃ exposure (USEPA, 2006). It is reasonable to assume that this variation in sensitivity to direct O₃ and PM exposure can be extended to wildlife species: different species will receive different effective doses of PM and O₃ because of variances in anatomical lung structure, respiration rates, and the varying capacities to clear the pollutants from the lungs will influence the health effects observed among species. There is no research currently available to directly extend the health effect results of exposure studies in humans or rats to assess the impacts to wildlife species or to identify which wildlife species are more sensitive to exposure than others.

The indirect effects of O₃ exposure on ecosystems occur mainly through the influence of O₃ on vegetation. As discussed thoroughly in this chapter, exposure of plants and trees to O₃ has been shown to be a significant ecosystem stressor with documented impacts on the biotic condition, ecological processes, and chemical and/or physical nature of natural ecosystems. These impacts to vegetation may result in changes to ecosystem biodiversity, which in turn adversely influence the wildlife species that are dependent on these plants as part of their habitat.

The indirect terrestrial ecosystem effects of PM include changes to soil nutrient levels and the presence of acidifying compounds, which in turn may result in unintended changes to the natural ecosystem through adverse impacts on essential ecological attributes including species shifts, loss of species richness and diversity, and impacts on threatened and endangered species. For example, as sensitive vegetation species affected by the influences of PM are lost, wildlife species that depend on these plants are adversely affected. In the U.S., the impacts of PM on vegetation are contributing to a shift in the prevalence of native grasses to invasive grass species which in turn has been shown to adversely influence the populations of threatened species such as the the bay checkerspot butterfly (*Euphydryas editha bayensis*) and the desert tortoise (Fenn *et al.*, 2003; Brooks, 2003).

Aquatic ecosystems are also negatively influenced by the effects of PM, and these effects were discussed thoroughly in the 2004 Acid Deposition Science Assessment (Environment Canada, 2005). Inputs of acidic PM deposition may result in the acidification of groundwater, streams and lakes which causes a lowering of pH and changes to aquatic chemistry that are toxic to fish and other aquatic animals. Deposition of nitrate containing PM can also influence the nutrient loadings of aquatic ecosystems. Although eutrophication is not currently an issue in Canada, excess nitrogen deposition into a waterway can cause conditions of severe water oxygen content depletion and the formation of algal blooms which can cause extensive fish kills.

10.9 Recommendations for Future Research

The review of studies published between 2003 and 2007 demonstrated a significant increase in the availability of experimental response data expressed relative to a cumulative O₃ exposure. This is a significant advance on the previous reviews, where the studies more typically reported O₃ exposure in terms of number of hours at a target concentration, or, exposure to some multiple of O₃ concentration in ambient air with limited summary statistics. Because it was difficult to reduce these various expressions of exposure into a single index, these studies tend to stand alone as point estimates. Exposure-response (continuous) functions are still in somewhat short supply in the published literature, and are of the greatest use to regulators. It is therefore recommended that the potential for a meta-analysis of existing data from multiple studies to generate exposure-response functions be explored, with a cumulative dose as the independent variable, and some normalized value for vegetation response (relative yield loss, for example) as the dependent variable. Meta-analysis is defined below, and the website goes on to describe the cautions that must be considered in its construction, the most important of which is quality, quantity and potential bias of published studies.

“Meta-analysis is the combination of data from several studies to produce a single estimate. From the statistical point of view, meta-analysis is a straightforward application of multifactorial methods. We have several studies of the same thing, which might be clinical

trials or epidemiological studies, perhaps carried out in different countries. Each trial gives us an estimate of an effect. We assume that these are estimates of the same global population value. We check the assumptions of the analysis, and, if these assumptions are satisfied, we combine the separate study estimates to make a common estimate. This is a multifactorial analysis, where the treatment or risk factor is one predictor variable and the study is another, categorical, predictor variable.”

(<http://www-users.york.ac.uk/~mb55/intro/meta.htm>)

Further research on the O₃ dose-response relationships for Canada-relevant species is also recommended, ideally using FACE (free air concentration enrichment)-type exposures. In addition, it is apparent the quantification and field validation of O₃ flux modelling and in particular, the quantification of plant defences to O₃ damage, is required for North American species and environments.

In the context of primary effects on forest growth and productivity, as well as the potential for forests to respond to, and/or mitigate, increasing atmospheric CO₂ concentrations, Paoletti *et al.* (2007) listed the following priorities for further work on O₃ and forest ecosystems: understanding the disruption of metabolic pathways (ascorbate and ethylene); quantifying plant detoxification processes in the flux models; quantifying stomatal and nonstomatal O₃ fluxes in many plant species; translating stomatal O₃ flux to biological effects; using long-term experiments that utilize free-air O₃ release systems; and making O₃ standards more biologically based, statistically sound, yet practical for wide use by air quality regulators.

Research conducted regarding the creation and application of predictive indices of O₃ sensitivity for plants show that predictive indices might allow for the prediction of dose-response functions for plant species that have not been directly investigated. Thus, further work to create and apply such indices is recommended.

Percy *et al.* (2007a) point to a reasonable approach to the incorporation of meteorological or edaphic variables into exposure metrics that represent the factors that could influence O₃ dose to vegetation. Further studies to ascertain reasonable approaches to creating metrics that can be used to establish biologically relevant air quality standards for the protection of vegetation are recommended.

Future research should contribute to the development of exposure data in areas of known elevated O₃ occurrence across Canada in the form of cumulative indices (i.e. AOT40, SUM60, W126 etc) against which vegetation harm thresholds identified by current literature studies and future studies can be compared.

There is a clear paucity of research available on the effects of PM and O₃ on an ecosystem level, especially with respect to the direct effects of exposure on wildlife species. Research in this area is recommended as it would be beneficial to better evaluate the broader ecosystem risks associated with O₃ and PM exposure to sensitive or endangered species.

References

- Alonso, R., Bermejo, V., Sanz, J., Valls, B., Elvira, S., Gimeno, B.S., 2007. Stomatal conductance of semi-natural Mediterranean grasslands: implications for the development of ozone critical levels. *Environmental Pollution* 146, 692-698.
- Altimir, N., Tuovien, J.-P., Vesala, T., Kulmala, M., Hari, P., 2004. Measurements of ozone removal by Scots pine shoots: calibration of a stomatal uptake model including the non-stomatal component. *Atmospheric Environment* 38, 2387-2398.
- Ambasht, N.K., Agrawal, M., 2003/4. Effects of enhanced UV-B radiation and tropospheric ozone on physiological and biochemical characteristics of field grown wheat. *Biologia Plantarum* 47, 625-628.
- Anderson, C.P., 2003. Source-sink balance and carbon allocation below ground in plants exposed to ozone. *New Phytologist* 157, 213-228.
- Aoki, T., Tanabe, S. 2007. Generation of sub-micron particles and secondary pollutants from building materials by ozone reaction. *Atmospheric Environment* 41: 3139-3150.
- Ashmore, P., Emberson, L., Karlsson, P., E., Pleijel, H., 2004. New Directions: A new generation of ozone critical levels for protection of vegetation in Europe. *Atmospheric Environment* 38, 2213-2214.
- Ashmore, M.R., 2005. Assessing the future global impacts of ozone on vegetation. *Plant, Cell and Environment* 28, 949-964.
- Ashmore, M.R., Buker, P., Emberson, L.D., Terry, A.C., Toet, S., 2007. Modelling stomatal ozone flux and deposition to grassland communities across Europe. *Environmental Pollution* 146, 659-670.
- Awmack, C.S., Mondor, E.B., and Lindroth, R.L., 2007. Forest understory clover populations in enriched CO₂ and O₃ atmospheres: Interspecific, intraspecific, and indirect effects. *Environmental and Experimental Botany* 59, 340-346.

Bassin, S., Calanca, P., Weidinger, T., Gerosa, G., Fuhrer, J., 2004a. Modelling seasonal ozone fluxes to grassland and wheat: model improvement, testing and application. *Atmospheric Environment* 38, 2349-2359.

Bassin, S., Kolliker, R., Cretton, C., Bertossa, M., Widmer, F., Bunger, P., Fuhrer, J., 2004b. Intra-specific variability of ozone sensitivity in *Centaurea jacea* L., a potential bioindicator, for evaluated ozone concentrations. *Environmental Pollution* 131, 1-12.

Bassin, S., Volk, M., Fuhrer, J., 2007. Factors affecting the ozone of temperate European grasslands: An overview. *Environmental Pollution* 146, 678-691.

Bender, J., Bergmann, E., and Weigel, H.J., 2006a. Responses of biomass production and reproductive development to ozone exposure differ between European wild plant species. *Water, Air, and Soil* 176, 253-267.

Bender, J., Muntifering, R.B., Lin, J.C., Weigel, H.J., 2006b. Growth and nutritive quality of *Poa pratensis* as influenced by ozone and competition. *Environmental Pollution* 142, 109-115.

Bennett, J.P., Jespen, E.A., Roth, J.A., 2006. Field response of *Prunus serotina* and *Asclepias syriaca* to ozone around southern Lake Michigan. *Environmental Pollution* 142, 354-366.

Blumenrother, M.C., Low, M., Matyssek, R., Obwald, W., 2007. Flux-based response of sucrose and starch in leaves of adult beech trees (*Fagus sylvatica* L.) under chronic free-air O₃ fumigation. *Plant Biology* 9, 207-214.

Booker, F.L., Miller, J.E., Fiscuc, E.L., Pursley, W.A., Stefanski, L.A., 2005. Competitive responses of container- versus ground-grown soybean to elevated carbon dioxide and ozone. *Crop Science* 45, 883-895.

Braun, S., Zugmaier, U., Thomas, V., Fluckiger, W., 2004. Carbohydrate concentrations in different plant parts of young beech and spruce along a gradient of ozone pollution. *Atmospheric Environment* 38, 2399-2407.

Braun, S., Schindler, C., Rihm, B., Fluckiger, W., 2007. Shoot growth of mature *Fagus sylvatica* and *Picea abies* in relation to ozone. *Environmental Pollution* 146, 624-628.

Brooks, M.L. 2003. Effects of increased soil nitrogen on the dominance of alien annual plants in the Mojave Desert. *Journal of Applied Ecology*. 40:344-353.

Buker, P., Emberson, L.D., Ashmore, M.R., Cambridge, H.M., Jacobs, C.M.J., Massman, W.J., Muller, J., Nikolov, N., Novak, K., Oksanen, E., Schaub, M., de la Torre, D. 2007. Comparison of different stomatal conductance algorithms for ozone flux modelling. *Environmental Pollution* 146, 726-735

Burkey, K.O., Miller, J.E., Fiscus, E.L., 2005. Assessment of ambient ozone effects on vegetation using snap bean as a bioindicator species. *Journal of Environmental Quality* 34, 1081-1086.

Bytnerowicz, A., Badae, O., Barbu, I., Fleischer, P., Fraczek, W., Gancz., V., Godzik, B., Grodzinska, K., Grodzki, W., Karnosky, D., Koren, M., McManus, M., Musselman, R.C., Novotny, J., Popescu, F., Postelnicu, D., Prus-Glowacki, W., Skawinski, P., Skiba, S., Szaro, R., Tamas, S., Vasile, C., 2003. New international long-term ecological research on air pollution effects on the Carpathian Mountain forests, Central Europe. *Environmental International* 29, 367-376.

Bussotti, F., Cozzi, A., Ferretti, M., 2006. Field surveys of ozone symptoms on spontaneous vegetation. Limitations and potentialities of the European programme. *Environmental Monitoring and Assessment* 115, 335-348.

Calatayud, V., Sanz, M.J., Calvo, E., Cervero, J., Ansel, W., Klumpp., 2007. Ozone biomonitoring with Bel-W3 tobacco plants in the city of Valencia (Spain). *Water, Air and Soil Pollution*.

Cano, V., Calatayud, J., Sanz, M.J., 2007. Ozone effects on three *Sambucus* species. *Environmental Monitoring and Assessment* 128, 83-91.

Carou, S., Dennis, I., Aherne, J., Ouimet, R., Arp, P.A., Watmough, S.A., DeMerchant, I., Shaw, M., Vet, R., Bouchet, V., and M. Moral, 2008. A National Picture of Acid Deposition Critical Loads for Forest Soils in Canada, Report Prepared by Environment Canada for the Canadian Council of Ministers of the Environment.

CCME (Canadian Council of Ministers of the Environment) 2003a. Effects of Ozone on Vegetation: Update in Support of the Canada-Wide Standards for Particulate Matter and Ozone.

CCME (Canadian Council of Ministers of the Environment) 2003b. Effects of Ozone on Materials: Update in Support of the Canada-Wide Standards for Particulate Matter and Ozone.

Chappelka, A.H., Neufeld, H.S., Davison, A.W., Somers, G.L., Renfro, J.R., 2003. Ozone injury on cutleaf coneflower (*Rudbeckia laciniata*) and crown-beard (*Verbesina occidentalis*) in Great Smoky Mountains National Park. *Environmental Pollution* 125, 53-59.

Chappelka, A.H., Somers, G.L., Renfro, J.R., 2007. Temporal patterns of foliar ozone symptoms on tall milkweed (*Asclepias exaltata* L.) in Great Smoky Mountains National Park. *Environmental Pollution* 149, 358-365.

Christ, M.A., Ainsworth, E.A., Nelson, R., Schurr, U., Walter, A., 2006. Anticipated yield loss in field-grown soybean under elevated ozone can be avoided at the expense of leaf growth during early reproductive growth stages in favourable environmental conditions. *Journal of Experimental Botany*, 57, 2267-2275.

Cieslik, S.A., 2004. Ozone uptake by various surface types; a comparison between dose and exposure. *Atmospheric Environment* 38, 2409-2420.

Coulston, J.W., Smith, G.C., Smith, W.D., 2003. Regional assessment of ozone sensitive tree species using bioindicator plants. *Environmental Monitoring and Assessment* 83c, 113-127.

Crous, K.Y., Vandermeiren, K., Ceulemans, R., 2006. Physiological responses to cumulative ozone uptake in two white clover (*Trifolium repens* L. cv. Regal) clones with different ozone sensitivity. *Environmental and Experimental Botany* 58, 169-179.

Darbah, J.N.T., Kubiske, M.E., Nelson, N., Oksanen, E., Vaapavuori, E. and Karnosky, D.F., 2007. Impacts of Elevated Atmospheric CO₂ and O₃ on Paper Birch (*Betula papyrifera*): Reproductive Fitness. *The Scientific World Journal*. 7(S1), 240-246.

Darbah, J.N.T., Kubiske, M.E., Nelson, N., Oksanen, E., Vaapavuori, E. and Karnosky, D.F., 2008. Effects of Decadal Exposure to Interacting Elevated CO₂ and/or O₃ on Paper Birch (*Betula papyrifera*) Reproduction, *Environmental Pollution*, 155, 446-452

Davis, D.D., Orendovici, T., 2006. Incidence of ozone symptoms on vegetation within a National Wildlife Refuge in New Jersey, USA. *Environmental Pollution* 143, 555-564.

Dittmar, C., Zech, W., Elling, W., 2003. Growth variations of common beech (*Fragus sylvatica* L.) under different climatic and environmental conditions in Europe – a dendroecological study. *Forest Ecology and Management* 173, 63-78.

Edwards, P., Huber, C., Wood, F., 2004. Ozone exposures and implications for vegetation in rural areas of the central Appalachian mountains, U.S.A. *Environmental Monitoring and Assessment* 98, 157-174.

Elagoz, V., Manning, W.J., 2005. Field affecting the effects of EDU on growth and yield of field-grown bush beans (*Phaseolus vulgaris* L.) with varying degrees of sensitivity to ozone. *Environmental Pollution* 136, 385-395.

Ellenberg, H., Weber, H.E., Du`ll, R., Wirth, V., Werner, W., Paulissen, D., 1991. Zeigerwerte von Pflanzen in Mitteleuropa. *Scripta Geobotanica* 18, 1-248.

Elvira, S., Bermejo, V., Manrique, E., Gimeno, B.S., 2004. On the response of two populations of *Quercus coccifera* to ozone and its relationship with ozone uptake. *Atmospheric Environment* 38, 2305 – 2311.

Elvira, S., Alonso, R., Gimeno, B.S. 2007. Simulation of stomatal conductance for Aleppo pine to estimate its ozone uptake. *Environmental Pollution* 146, 617-623.

Emberson, L.D., Buker, P., Ashmore, M.R. 2007. Assessing the risk caused by ground level ozone to European forest trees: A case study in pine, beech and oak across different climate regions. *Environmental Pollution* 147, 454-466.

Environment Canada / Health Canada. 2001. Priority substances list assessment report for releases from primary and secondary copper smelters and copper refineries – releases from primary and secondary zinc smelters and zinc refineries. EN 40-215/62E.

Environment Canada, 2005. 2004 Acid Deposition Science Assessment. ISBN 0-662-38754-6. Available at: http://www.msc-smc.ec.gc.ca/saib/acid/assessment2004/index_e.html

Fagnano, M., Merola, G., Forlani, A., Postiglione, L., Fuhrer, J., 2004. Monitoring yield loss from ozone pollution in a Mediterranean environment: a comparison of methods. *Water, Air, and Soil Pollution* 155, 383-398.

Felzer, B., Kicklighter, D., Melillo, J., Wang, C., Zhuang, Q., Prinn, R., 2004. Effects of ozone on net primary production and carbon sequestration in the conterminous United State using a biogeochemistry model. *Tellus* 56B, 230-248.

Fenn, M. E.; Baron, J. S.; Allen, E. B.; Rueth, H. M.; Nydick, K. R.; Geiser, L.; Bowman, W. D.; Sickman, J. O.; Meixner, T.; Johnson, D. W.; Neitlich, P. 2003. Ecological effects of nitrogen deposition in the western United States. *BioScience* 53: 404-420.

Ferretti, M., Calderisi, M., Bussotti, F., 2007a. Ozone exposure, defoliation of beech (*Fagus sylvatica* L.) and visible foliar symptoms on native plants in selected plots of South-Western Europe. *Environmental Pollution* 145, 644-651.

Ferretti, M., Fagnano, M., Amoriello, T., Badiani, M., Ballarin-Denti, A., Buffoni, A., Bussotti, F., Castagna, A., Cieslik, S., Costantini, A., De Marco, A., Gerosa, G., Lorenzini, G., Manes, F., Merola, G., Nali, C., Paoletti, E., Petriccione, B., Racalbutto, S., Rana, G., Ranieri, A., Tagliaferri, A., Vialetto, G., Vitale, M. 2007b. Measuring, modelling and testing ozone exposure, flux and effects on vegetation in southern European conditions – What does not work? A review from Italy. *Environmental Pollution* 146, 648-658.

- Finkelstein, P.L., Davison, A.W., Neufeld, H.S., Meyers, T.P., Chappelka, A.H., 2004. Sub-canopy deposition of ozone in a stand of cutleaf coneflower. *Environmental Pollution* 131, 295-303.
- Fisher, L.S., Mays, P.A., and Wylie, C.L., 2007. An Overview of Nitrogen Critical Loads for Policy Makers, Stakeholders, and Industries in the United States. *Water, Air & Soil Pollution*. 179(1-4): 3-18.
- Fuhrer, J., Booker, F., 2003. Ecological issues related to ozone: agricultural issues. *Environmental International* 29, 141-154.
- Fumagalli, I., Mignanego, L., Mills, G., 2003. Ozone biomonitoring with clover: yield loss and carryover effect under high ambient ozone levels in northern Italy. *Agriculture, Ecosystems and Environment* 95, 119-128.
- Gerosa, G., Cieslik, S., Ballarin-Denti, A., 2003. Micrometeorological determination of time-integrated stomatal ozone fluxes over wheat: a case study in Northern Italy. *Atmospheric Environment* 37, 777-788.
- Gerosa, G., Marzuoli, R., Cieslik, S., Ballarin-Dent, A., 2004. Stomatal ozone fluxes over a barley field in Italy. "Effective exposure" as a possible link between exposure- and flux-based approaches. *Atmospheric Environment* 38, 2421-2432.
- Gerosa, G. Derghi, F. Cieslik, S. 2007. Comparison of different algorithms for stomatal ozone flux determination from micrometeorological measurements. *Water, Air and Soil Pollution* 179, 309-321.
- Gombert, S., Asta, J., Seaward, M.R.D., 2006. Lichens and tobacco plants as complementary biomonitors of air pollution in the Grenoble area (Isère, southeast France). *Ecological Indicators* 6, 429-443.
- Goumenaki, E., Fernandez, I.G., Papanikolaou, A., Papadopoulou, D., Askianakis, C., Kouvarakis, G., Barnes, J. 2007. Derivation of ozone flux-yield relationships for lettuce: A key horticultural crop. *Environmental Pollution* 146, 699-706.
- Grantz, D.A., Garner, J.H.B., Johnson, D.W. 2003. Ecological effects of particulate matter. *Environmental Pollution* 129, 213-235.
- Grenbenc, T., Kraigher, H., 2007. Types of Ectomycorrhiza of mature beech and spruce at ozone-fumigated and control forest plots. *Environmental Monitoring and Assessment* 128, 47-59.

- Grulke, N.E., Alonso, R., Nguyen, T., Cascio, C., Dobrowolski, W., 2004. Stomatal open at night in pole-sized and mature ponderosa pine: implications for O₃ exposure metrics. *Tree Physiology* 24, 1001-1010.
- Grulke, N.E., Paoletti, E., Heath, R.L. 2007a. Comparison of calculated and measured foliar O₃ flux in crop and forest species. *Environmental Pollution* 146, 640-647.
- Grulke, N.E., Neufeld, H.S., Davison, A.W., Roberts, M., Chappelka, A.H. 2007b. Stomatal behaviour of ozone-sensitive and -insensitive coneflowers (*Rudbeckia laciniata* var. *digitata*) in Great Smoky Mountains National Park. *New Phytologist* 173, 100-109.
- Grunhage, L., and Jager, H-J., 2003. From critical levels to critical loads for ozone: a discussion of a new experimental and modelling approach for establishing flux-response relationships for agricultural crops and native plant species. *Environmental Pollution* 125, 99-110.
- Grunhage, L. S.V. Krupa, A.H. Legge, Jager, H.-J., 2004. Ambient flux-based critical values for ozone for protecting vegetation: differing spatial scales and uncertainties in risk assessment. *Atmospheric Environment* 38, 2433-2437.
- Harmens, H., Mills, G., Emberson, L.D, Ashmore, M.R. 2007. Implications of climate change for the stomatal flux of ozone: A case study for winter wheat. *Environmental Pollution* 146, 763-770.
- Hayes, F., Mills, G., Williams, P., Harmens, H., Buker., 2006. Impacts of summer ozone exposure on the growth and overwintering of UK upland vegetation. *Atmospheric Environment* 40, 4088-4097.
- Hayes, F., Jones, M.L.M., Mills, G., Ashmore, M., 2007. Meta-analysis of the relative sensitivity of semi-natural vegetation species to ozone. *Environmental Pollution* 146, 754-762.
- Heagle, A.S., Miller, J.E., Pursley, W.A., 2003. Growth and yield response of potato to mixtures of carbon dioxide and ozone. *Journal of Environmental Quality* 32, 1603-1610.
- Holton, M.K., Lindroth, R.L., 2003. Foliar quality influences tree-herbivore-parasitoid interactions: effects of elevated CO₂, O₃, and plant genotype. *Oecologia* 137, 233-244.
- Jones, M.L.M., Hayes, F., Mills, G., Sparks, T.H., Fuhrer, J., 2007. Predicting community sensitivity to ozone, using Ellenberg Indicator values. *Environmental Pollution* 146, 744-753.
- Jones, M.E., Paine, T.D., 2006. Detecting changes in insect herbivore communities along a pollution gradient. *Environmental Pollution* 143, 377-387.

Karlsson, G.P., Karlsson, P.E., Danielsson, H., Pleijel, H., 2003. Clover as a tool for bioindication of phytotoxic ozone – 5 years of experience from southern Sweden – consequences for the short-term critical levels. *The Science of the Total Environment* 301, 205-215.

Karlsson, G.P., Karlsson, P.E., Soja, G., Vandermeiren, K., Pleijel, H., 2004a. Test of the short-term critical levels for acute ozone injury on plants – improvements by ozone uptake modelling and the use of an effect threshold. *Atmospheric Environment* 38, 2237-2245.

Karlsson, P.E., Medin, E.L., Ottosson, S., Sellden, G., Wallin, G., Pleijel, H., Skarby, L., 2004b. A cumulative ozone uptake-response relationship for the growth of Norway spruce saplings. *Environmental Pollution* 128, 405-417.

Karlsson, P.E., Uddling, J., Braun, S., Broadmeadow, M., Elvira, S., Gimeno, B.S., Le Thiec, D., Oksanen, E., Vandermeiren, K., Wilkinson, M., Emberson, L., 2004c. New critical levels for ozone effects on young trees based on AOT40 and simulated cumulative leaf uptake of ozone. *Atmospheric Environment* 38, 2283-2294.

Karlsson, P.K., Orlander, G., Lanvall, O., Uddling, J., Hjorth, U., Wiklander, K., Areskoug, B., Grennfelt, P., 2006. Negative impact of ozone on the stem basal area increment of mature Norway spruce in south Sweden. *Forest Ecology and Management* 232, 146-151.

Karlsson, P.E., Braun, S., Broadmeadow, M., Elvira, S., Emberson, L., Gimeno, B.S., Le Thiec, D., Novak, K., Oksanen, E., Schaub, M., Uddling, J., Wilkinson, M., 2007. Risk assessments for forest trees: The performance of the ozone flux versus the AOT concepts. *Environmental Pollution* 146, 608-616.

Karnosky, D.F., Zak, D.R., Pregitzer, K.S., Awmack, C.S., Bockheim, J.G., Dickson, R.E., Hendrey, G.R., Host, G.E., King, J.S., Kopper, B.J., Kruger, E.L., Kubiske, M.E., Lindroth, R.L., Mattson, W.J., McDonald, E.P., Noormets, A., Oksanen, E., Parsons, W.F.J., Percy, K.E., Podila, G.K., Riemenschneider, D.E., Sharma, P., Thakur, R.C., Sober, A., Sober, J., Jones, W.S., Anttonen, S., Vapaavuori, E., Mankovska, B., Heilman, W.E. and Isebrands, J.G., 2003. Tropospheric O₃ moderates responses of temperate hardwood forests to elevated CO₂: A synthesis of molecular to ecosystem results from the Aspen FACE project. *Functional Ecology* 17,289-304.

Karnosky, D.F., Pregitzer, K.S., Zak, D.R., Kubiske, M.E., Hendrey, G.R., Weinstein, D., Nosal, M., Percy, K.E., 2005. Scaling ozone responses of forest trees to the ecosystem level in a changing climate. *Plant, Cell and Environment* 28, 965-981.

- Karnosky, D.F., Skelly, J.M., Percy, K.E., Chappelka, A.H., 2007. Perspectives regarding 50 years of research on effects of tropospheric ozone air pollution on US forests. *Environmental Pollution* 147, 489-506.
- Keutgen, A.J., Noga, G., Pawelzik, E., 2005. Cultivar-specific impairment of strawberry growth, photosynthesis, carbohydrate and nitrogen accumulation by ozone. *Environmental and Experimental Botany* 53, 271-280.
- Keller, F., Bassin, S., Ammann, C., Fuhrer, J. 2007. High-resolution modelling of AOT40 and stomatal uptake in wheat and grassland: A comparison between 2000 and the hot summer of 2003 in Switzerland. *Environmental Pollution* 146, 671-677.
- Khan, S., Soja, G., 2003. Yield responses of wheat to ozone exposure as modified by drought-induced difference in ozone uptake. *Water, Air, and Soil Pollution* 147, 299-315.
- King, J.S., Kubiske, M.E., Pregitzer, K.S., Hendrey, G.R., McDonald, E.P., Giardina, C.P., Quinn, V.S. and Karnosky, D.F., 2005. Tropospheric O₃ compromises net primary production in young stands of trembling aspen, paper birch and sugar maple in response to elevated atmospheric CO₂. *New Phytologist* 168,623-636.
- Kohut, R., 2007. Assessing the risk of foliar injury from ozone on vegetation in parks in the U.S. National Park Service's Vital Signs Network. *Environmental Pollution* 149, 348-357.
- Kozovits, A.R., Matyssek, R., Blaschke, H., Gottlein, A., Grams, T.E.E., 2005. Competition increasingly dominates the responsiveness of juvenile beech and spruce to elevated CO₂ and/or O₃ concentrations throughout two subsequent growing seasons. *Global Change biology* 11, 1387-1401.
- Kubiske, M.E., Quinn, V.S., Marquardt, P.E. and Karnosky, D.F., 2006a. Effects of Elevated Atmospheric CO₂ and/or O₃ on Intra- and Interspecific Competitive Ability of Aspen. *Plant Biology* 9, 342-355.
- Kubiske, M.E., Quinn, V.S., Heilman, W.E., McDonald, E.P., Marquardt, P.E., Teclaw, R.M., Friend, A.L., Karnosky, D.F., 2006b. Interannual climatic variation mediated elevated CO₂ and O₃ effects on forest growth. *Global Change Biology* 12, 1054-1068.
- Kucera, V., Tidblad, J., Kreislova, K., Knotkova, D., Faller, M., Reiss, D., Sneathlge, R., Yates, T., Henriksen, J., Schreiner, M., Melcher, M., Ferm, M., Lefevre, R-A., Kobus, J. 2007. UN/ECE ICP materials dose-response functions for the multi-pollutant situation. *Water Air and Soil Pollution* 7, 249-258.

- Kull, O., Tulva, I., Vapaavuori, E., 2003. Influence of elevated CO₂ and O₃ on *Betula pendula* Roth crown structure. *Annals of Botany* 91, 559-569.
- Kull, O., Tulva, I., Vapaavuori, E., 2005. Consequences of elevated CO₂ and O₃ on birch canopy structure: Implementation of a canopy growth model. *Forest Ecology and Management* 212, 1-13.
- Laurence, L.A., Andersen, C.P., 2003. Ozone and natural systems: understanding exposure, response and risk. *Environmental International* 29, 155-160.
- Lefohn, A.S., J.A. Laurence and R.J. Kohut. 1988. A comparison of indices that describe the relationship between exposure to ozone and reduction in the yield of agricultural crops. *Atmospheric Environment* 22: 1229-1240.
- Liu, X., Kozovits, A.R., Grams, T.E.E., Blaschke, H., Rennenberg, H., Matyssek, R., 2004. Competition modifies effects of enhanced ozone/carbon dioxide concentrations on carbohydrate and biomass accumulation in juvenile norway spruce and european beech. *Tree Physiology* 24, 1045-1055.
- Long, S.P., Ainsworth, E.A., Leakey, A.B., Nosberger, J., Ort, D.R., 2006. Food for thought: lower-than-expected crop yield stimulation with rising CO₂ concentrations. *Science* 312, 1918-1921.
- Lorenzini, G., Landi, U., Loppi, S., Nali, C., 2003. Lichen distribution and bioindicator tobacco plants give discordant response: a case study from Italy. *Environmental Monitoring and Assessment* 82, 243-264.
- Low, M. Haberle, K.-H., Warren, C., Matyssek, R., 2007. O₃ Flux- related responsiveness of photosynthesis, respiration and stomatal conductance of adult *Fagus sylvatica* to experimentally enhanced free-air O₃ exposure. *Plant Biology* 9, 197-206.
- Loya, W.M., Pregitzer, K.S., Karberg, N.J., King, J.S., Giardina, C.P., 2003. Reduction of soil carbon formation by tropospheric ozone under increased carbon dioxide levels. *Nature* 425, 705-707.
- Luedemann, G., Matyssek, R., Fleischmann, F., Grams, T.E.E., 2005. Acclimation to ozone affects host/pathogen interaction and competitiveness for nitrogen in juvenile *Fagus sylvatica* and *Picea abies* trees infected with *Phytophthora citricola*. *Plant Biology* 7, 640-649.
- Maggio, A., De Pascale, S., Fagnano, M., Barbieri, G., 2007. Can salt stress-induced physiology responses protect tomato crops from ozone damages in Mediterranean environments? *European Journal of Agronomy* 26, 454-461.

- Manning, W.J., Flager, R.B., Frenkel, M.A., 2003. Assessing plant response to ambient ozone: growth of ozone-sensitive loblolly pine seedlings treated with ethylenediurea or sodium erythorbate. *Environmental Pollution* 126, 73-81.
- Mandre, M., Korsjukov, R., 2007. The quality of stemwood of *Pinus sylvestris* in an alkalisied environment. *Water, Air and Soil Pollution* 182, 163-172.
- Massman, W.J., 2004. Toward an ozone standard to protect vegetation based on effective dose: a review of deposition resistances and a possible metric. *Atmospheric Environment* 38, 2323-2337.
- Matyssek, R., Wieser, G., Nunn, A.J., Kozovits, A.R., Reiter, I.M., Heerd, C., Winkler, J.B., Baumgarten, M., Haberle, K.-H., Grams, T.E.E., Werner, H., Fabian, P., Havranek, W.M., 2004. Comparison between AOT40 and ozone uptake in forest trees of different species, age and site conditions. *Atmospheric Environment* 38, 2271 – 2281.
- Matyssek, R., Le Thiec, D., Low, M., Dizengremel, P., Nunn, A.J., Haberle, K.-H., 2006. Interactions between drought and O₃ stress in forest trees. *Plant Biology* 8, 11-17.
- Matyssek, R., Bytnerowicz, A., Karlsson, P.-E., Paoletti, E., Sanz, M., Schaub, M., Wieser, G. 2007. Promoting the O₃ flux concept for European forest trees. *Environmental Pollution* 146, 587-607.
- McLaughlin, S.B., Nosel, M., Wullschleger, S.D., Sun, G., 2007a. Interactive effects of ozone and climate on tree growth and water use in a southern Appalachian forest in the USA. *New Phytologist* 174, 109-124.
- McLaughlin, S.B., Wullschleger, S.D., Sun, G., Nosal, M., 2007b. Interactive effects of ozone and climate on water use, soil moisture content and streamflow in a southern Appalachian forest in the USA. *New Phytologist* 174, 125-136.
- Meyers, T.P., Paw U, K.T., 1986. Testing of a higher-order closure model for modelling airflow within and above plant canopies. *Boundary-Layer Meteorology*, 37, 297-311.
- Meyers, T.P., Paw U, K.T., 1987. Modelling the plant canopy micrometeorology with higher-order closure principles. *Agricultural and Forest Meteorology*, 41, 143-163.
- Mikkelsen, T.N., Ro-Poulsen, H., Hovmand, M.F., Jensen, N.O., Pilegaard, K., Egelov, A.H., 2004. Five-year measurements of ozone fluxes to a Danish Norway spruce canopy. *Atmospheric Environment* 38, 2361-2371.
- Morgan, P.B., Ainsworth, E.A., Long, S.P., 2003. How does elevated ozone impact soybean? A meta-analysis of photosynthesis, growth and yield. *Plant Cell and Environment* 26, 1317-1328.

- Musselman, R.C., Lefohn, A.S., Massman, W.J., Heath, R.L., 2006. A critical review and analysis of the use of exposure-and flux-based ozone indices for predicting vegetation effects. *Atmospheric Environment* 40, 1869-1888.
- Muzika, R.M., Guyette, R.P., Zielonka, T., Liebhold, A.M., 2004. The influence of O₃, NO₂, and SO₂ on growth of *Picea abies* and *Fagus sylvatica* in the Carpathian Mountains. *Environmental Pollution* 1320, 65-71.
- Nali, C., Francini, A., Lorenzini, G., 2006. Biological monitoring of ozone: the twenty-year Italian experience. *Journal of Environmental Monitoring* 8, 25-32.
- Nikolov, N. and Zeller, K.F., 2003. Modelling coupled interactions of carbon, water, and ozone exchange between terrestrial ecosystems and the atmosphere. I. Model description. *Environmental Pollution* 124, 231-246.
- Novak, K., Cherunini, P., Saurer, M., Fuhrere, J., Skelly, J.M., Krauchi, N., Schaub, M., 2007. Ozone air pollution effects on tree-ring growth \square ¹³C, visible foliar injury and leaf gas exchange in three ozone-sensitive woody plant species. *Tree Physiology* 27, 941-949.
- Nunn, A.J., Kozovits, A.R. Reiter, I.M., Heerdt, C., Leuchner, M., Lutz, C., Liu, X., Low, M., Winkler, J.B., Grams, T.E.E., Haberle, H-H., Werner, H., Fabian, P., Rennenber, H., Matyssek, R., 2005. Comparison of ozone uptake and sensitivity between a phytotron study with young beech and a field experiment with adult beech (*Fagus sylvatica*). *Environmental Pollution* 137, 494-506.
- Nunn, A.J., Wieser, G., Metzger, U., Low, M., Wipfler, P., Haberle, K-H., Matyssek, R. 2007. Exemplifying whole-plant ozone uptake in adult forest trees of contrasting species and site conditions. *Environmental Pollution* 146, 629-639.
- Nussbaum, S., Remund, J., Rihm, B., Miegliitz, K., Gurtz, J., Fuhrer, J., 2003. High-resolution spatial analysis of stomatal ozone uptake in arable crops and pastures. *Environmental International* 29, 385-392.
- Oksanen, K., 2003. Response of selected birch (*Betula pendula* Roth) clones to ozone change over time. *Plant, Cell and Environment* 26, 875-886.
- Panek, J. A. 2004. Ozone uptake, water loss and carbon exchange dynamics in annually drought-stressed *Pinus ponderosa* forests: measured trends and parameters for uptake modelling. *Tree Physiology* 24, 277-290.

Paoletti, E., De Marco, A., 2007. Why should we calculate complex indices of ozone exposure? Results from Mediterranean background sites. *Environmental Monitoring and Assessment* 128, 19-30.

Paoletti, E., Bytnerowicz, A., Anderson, C., Augustaitis, A., Ferretti, M., Grulke, N., Gunthardt-Goerg, M.S., Innes, J., Johnson, D., Karnosky, D.F., Luangjame, J., Matyssek, R., McNulty, S., Muller-Starck, G., Musselman, R. and Percy, K., 2007. Impacts of Air Pollution and Climate Change on Forest Ecosystems - Emerging Research Needs. *The Scientific World Journal* 7(S1), 1-8.

Percy, K.E., Ferretti, M., 2004. Air pollution and forest health: toward new monitoring concepts. *Environmental Pollution* 130, 113-126.

Percy, K.E., Karnosky, D.F., 2007. Air quality in natural areas, interface between the public, science and regulation. *Environmental Pollution* 149, 256-267.

Percy, K.E., Nosal, M. Heilman, W., Dann, T. Sober, J., Legge, A.H., Karnosky, D.F., 2007. New exposure-based metric approach for evaluating O₃ risk to North American aspen forests. *Environmental Pollution* 147, 554-566.

Persson, K., Danielsson, H., Sellden, G., Pleijel, H., 2003. The effects of tropospheric ozone and elevated carbon dioxide on potato (*Solanum tuberosum* L. cv. Bintje) growth and yield. *The Science of the Total Environment* 310, 191-201.

Piikki, K., Sellden, G., Pleijel, H., 2004. The impact of tropospheric O₃ on leaf number duration and tuber yield of the potato (*Solanum tuberosum* L.) cultivars Bintje and Kardal. *Agriculture, Ecosystems and Environment* 104, 483-492.

Pleijel, H., Berglen Eriksen, A., Danielsson, H., Bondesson, N., Sellden, G., 2006. Differential ozone sensitivity in an old and a modern Swedish wheat cultivar – grain yield and quality, leaf chlorophyll and stomatal conductance. *Environmental and Experimental Botany* 56, 63-71.

Pleijel, H., Danielsson, H., Emberson, L., Ashmore M.R., Mills, G. 2007. Ozone risk assessment for agricultural crops in Europe: Further development of stomatal flux and flux-response relationships for European wheat and potato. *Atmospheric Environment* 41, 3022-3040.

Plessl, M., Elstner, E.F., Rennenberg, H., Habermeyer, J., Heiser, I., 2007. Influence of elevated CO₂ and ozone concentrations on late blight resistance and growth of potato plants. *Environmental and Experimental Botany* 60, 447-457.

- Rämö, K., Slotte, H., Kanerva, T., Ojanpera, K., Manninen, S., 2006. Growth and visible injuries for four *Centaurea jacea* L. ecotypes exposed to elevated ozone and carbon dioxide. *Environmental and Experimental Botany* 58, 287-298.
- Rämö, K., Kanerva, T., Ojanpera, K., Manninen, S., 2007. Growth onset, senescence, and reproductive development of meadow species in mesocosms exposed to elevated O₃ and CO₂. *Environmental and Experimental Botany* 145, 850-860.
- Ranford, J., Reiling, K., 2007. Ozone induced leaf loss and decreased leaf production of European Holly (*Ilex aquifolium* L.) over multiple seasons. *Environmental Pollution* 145, 355-364.
- Reich P.B. 1987. Quantifying plant response to ozone: a unifying theory. *Tree Physiology* 3:63-91.
- Ren, W., Tian, H., Chen, G., Liu, M., Zhang, C., Chappelka, A.H., Pan, S., 2007. Influence of ozone pollution and climate variability on net primary productivity and carbon storage in China's grassland ecosystems from 1961 to 2000. *Environmental Pollution* 149, 327-335.
- Riikonen, J., Lindsberg, M.-M., Holopainen, T., Oksanen, E., Lappi, J., Peltonen, P., Vapaavuori, E., 2004. Silver birch and climate change: variable growth and carbon allocation responses to elevated concentrations of carbon dioxide and ozone. *Tree Physiology* 24, 1227-1237.
- Sanz, J., Muntifering, R.B., Bermejo, V., Gimeno, B.S., Elvira, S., 2005. Ozone and increased nitrogen supply effects on the yield and nutritive quality of *Trifolium subterraneum*. *Atmospheric Environment* 39, 5899-5907.
- Sardans, J., Penuelas, J., 2006. Introduction of the factor of partitioning in the lithogenic enrichment factors of the trace element bioaccumulation in plant tissues. *Environmental Monitoring and Assessment* 115, 473-498.
- Schaub, M., Skelly, J.M., Steiner, K.C., Davis, D.D., Pennypacker, S.P., Zhang, J., Ferdinand, J.A., Savage, J.E., Stevenson, R.E., 2003. Physiological and foliar injury responses of *Prunus serotina* and *Fraxinus americana*, and *Acer rubrum* seedlings to varying soil moisture and ozone. *Environmental Pollution* 124, 307-320.
- Schaub, M., Emberson, L., Buker, P., Karuchi, N. 2007. Preliminary results of modelled ozone uptake for *Fagus sylvatica* L. trees at selected EU/UN-ECE intensive monitoring plots. *Environmental Pollution* 145, 636-643.

Schlöter, M., Winkler, J.B., Aneja, M., Koch, N., Fleischmann, F., Pritsch, K., Heller, W., Stich, S., Grams, T.E.E., Gottlen, A., Matyssek, R., Munch, J.C., 2005. Short term effects of ozone on the plant-rhizosphere-bulk soil system of young beech trees. *Plant Biology* 7, 728-736.

Shimizu, H., Feng, Y.W., 2007. Ozone and/or water stress could have influenced the *Betula ermanii* Cham. Forest decline observed at Oku-Nikko, Japan. *Environmental Monitoring and Assessment* 128, 109-119.

Shrestha, A., Grantz, D.A., 2005. Ozone impacts on competition between tomato and yellow nutsedge above- and below-ground effects. *Crop Science* 45, 1587-1595.

Simpson, D., Tuovinen, J.-P., Emberson, L., Ashmore, M.R., 2003. Characteristics of an ozone deposition module II: sensitivity analysis. *Water, Air and Soil Pollution* 143, 123-137.

Simpson, D., Ashmore, M.R., Emberson, L., Tuovinen, J.-P. 2007. A comparison of two different approaches for mapping potential ozone damage to vegetation. A model study. *Environmental Pollution* 146, 715-725.

Smidt, S., Herman, F., 2004. Evaluation of air pollution-related risks for Austrian mountain forests. *Environmental Pollution* 130, 99-112.

Smith, G., Coulston, J., Jepsen, E., Prichard, T., 2003. A national ozone biomonitoring program – results from field surveys of ozone sensitive plants in northeastern plants in northeastern forests (1994-2000). *Environmental Monitoring and Assessment* 87, 271-291.

Soja, G., Reichenauer, T.G., Eid, M., Soja, A.-M., Schaber, R., Gangl, H., 2004. Long-term ozone exposure and ozone uptake of grapevines in open-top chambers. *Atmospheric Environment* 38, 2313-2321.

Souza, L., Neufeld, H.S., Chappelka, A.H., Burkey, K.O., Davison, A.W., 2006. Seasonal development of ozone-induced foliar injury on tall milkweed (*Asclepias exaltata*) in Great Smokey Mountains National Park. *Environmental Pollution* 141, 175-183.

Thomas, V.F.D., Braun, S., Fluckiger, W., 2005. Effects of simultaneous ozone exposure and nitrogen loads on carbohydrate concentrations, biomass, and growth of young spruce trees (*Picea abies*). *Environmental Pollution* 137, 507-516.

Thomas, V.F.D., Braun, S., Fluckiger, W., 2006. Effects of simultaneous ozone exposure and nitrogen loads on carbohydrate concentrations, biomass, growth. *Environmental Pollution* 143, 341-354

Thwaites, R.H., Ashmore, M.R., Morton, A.J., Pakeman, R.J., 2006. The effects of tropospheric ozone on the species dynamics of calcareous grassland. *Environmental Pollution* 144, 500-509.

Timonen, U., Huttunen, S., Manninen, S., 2004. Ozone sensitivity of wild field layer plant species of northern Europe: A Review. *Plan Ecology* 172, 27-39.

Tiwari, S., Agrawal, M., Manning, W.J., 2005. Assessing the impact of ambient ozone on growth and productivity of two cultivars of wheat in India using three rates of application of ethylenediurea (EDU). *Environmental Pollution* 138, 153-160.

Tonneijck, A.E.G., Franzaring, J., Brouwer, G., Metselaar, K., Dueck, Th.A., 2004. Does interspecific competition alter effects of early season ozone exposure on plants from wet grasslands? Results of a three-year experiment in open-top chambers. *Environmental Pollution* 131, 205-213.

Trimbacher, C., Weiss, P., 2004. Norway Spruce: a novel method using surface characteristics and heavy metal concentrations of needles for a large-scale monitoring survey in Austria. *Water, Air, and Soil Pollution* 152, 363-386.

Tuovinen, J.-P., Ashmore, M.R., Emberson, L.D., Simpson, D., 2004. Testing and improving the EMEP ozone deposition module. *Atmospheric Environment* 38, 2372-2385.

Tuovinen, J.-P., Simpson, D., Emberson, L., Ashmore, M., Gerosa, G. 2007. Robustness of modelled ozone exposure and doses. *Environmental Pollution* 146, 578-586.

Uddling, J., Karlsson, P.E., Glorvigen, A., Sellden, G., 2006. Ozone impairs autumnal resorption of nitrogen from birch (*Betula pendula*) leaves, causing an increase on whole-tree nitrogen loss through litter fall. *Tree Physiology* 26, 113-120.

Uddling, J., Gunthardt-Goerg, M.S., Matyssek, R., Oksanen, E., Pleijel, H., Sellden, G., Karlsson, P.E., 2004. Biomass reduction of juvenile birch is more strongly related to stomatal uptake of ozone than to indices based on external exposure. *Atmospheric Environment* 38, 4709-4719.

USEPA (United States Environmental Protection Agency) 2007. Review of the National Ambient Air Quality Standards for Ozone: Policy Assessment of Scientific and Technical Information. Office of Air Quality Planning and Standards (OAQPS) Staff Paper

USEPA (United States Environmental Protection Agency), 2006. Air Quality Criteria for Ozone and Related Photochemical Oxidants.

USEPA (United States Environmental Protection Agency), 2004. Air Quality Criteria for Particulate Matter.

USEPA (United States Environmental Protection Agency), 1996. Air Quality Criteria for Ozone and Related Photochemical Oxidants.

Utiyama, M., Fukuyama, T., Maruo, Y.Y., Ichino, T., Izumi, K., Hara, H., Takano, K., Suzuki, H., Aoki, M., 2004. Formation and deposition of ozone in a red pine forest. *Water, Air and Soil Pollution* 151, 53-70.

Van Heerden, P.D.R., Kruger, G.H.J., Kilbourn Louw, M., 2007. Dynamic responses of photosystem II in the Namib Desert shrub, *Zygophyllum prismatocarpum*, during and after foliar deposition of limestone dust. *Environmental Pollution* 146, 34-35.

Van Oijen, M., Dreccer, M.F., Firsching, K.-H., Schnieders, B.J., 2004. Simple equations for dynamic models of the growth effects of CO₂ and O₃ on light-use efficiency and growth of crops. *Ecological Modelling* 179, 39-60.

Wang, L., Liu, L.-y., Gao, S.-y., Hasi, E., Wang, Z., 2006. Physicochemical characteristics of ambient particles settling upon leaf surfaces of urban plants in Beijing. *Journal of Environmental Sciences* 18, 921-926.

Wang, X., Zheng, Q., Yao, F., Chen, Z., Feng, A., Manning, W.J., 2007. Assessing the impact of ambient ozone on growth and yield of a rice (*Oryza sativa* L.) and a wheat (*Triticum aestivum* L.) cultivar grown in the Yangtze Delta, China, using three rates of application of ethylenediurea (EDU). *Environmental Pollution* 148, 390-395.

WGAQOG, 1999a. National Ambient Air Quality Objectives for Ground-Level Ozone. Science Assessment Document.

WGAQOG, 1999b. Addendum to Science Assessment Document for Particulate Matter.

Wieser, G., Matyssek, R., Kostner, B., Oberhuber, W., 2003. Quantifying ozone uptake at the canopy level of spruce, pine and larch trees at the alpine timberline: an approach based on sap flow measurement. *Environmental Pollution* 126, 5-8.

Wieser, G., Emberson, L.D., 2004. Evaluation of the stomatal conductance formulation in EMEP ozone deposition model for *Picea abies*. *Atmospheric Environment* 38, 2339-2348.

Wipfler, P., Seifert, T., Heerdt, C., Werner, H., Pretzsch, H., 2005. Growth of adult Norway Spruce (*Picea abies* [L.] karst.) and European Beech (*Fagus sylvatica* L.) under free-air ozone fumigation. *Plant Biology* 7, 611-618.

Woo, S.Y., Hinckley, T.M., 2005. The effects of ozone on growth and stomal response in the F2 generation of hybrid poplar (*Populus trichocarpa* x *Populus deltoids*). *Biologia Plantarum* 43, 395-404.

Yamaji, K., Julkunen-Tiitto, R., Rousi, M., Freiwald, V., Oksanen, E., 2003. Ozone exposure over two growing seasons alters root-to-shoot ratio and chemical composition of birch (*Betula pendula* Roth). *Global Change Biology* 9, 1363-1377.

Zeleznik, P., Hrenko, M., Then, C., Koch, N., Grebenc, T., Levanic, T., Kraigher, H., 2007. CASIROZ: Root parameters and types of ectomycorrhiza of young beech plants exposed to different ozone and light regimes. *Plant Biology* 9, 298-308.

CHAPTER 11: Impact of Smog on Visibility in Developed Regions of Canada

Karen McDonald

KEY MESSAGES AND IMPLICATIONS

- The expansion of the Canadian National Air Pollution Surveillance (NAPS) network to include particulate matter (PM) speciation at 11 urban and impacted rural sites starting in 2003, has enhanced the ability to understand how fine mass and its chemical components influence visibility in Canada. Data from primarily urban locations does not indicate how well visibility in Canadian parks and wilderness areas is being protected.
- Algorithms from the Interagency Monitoring of Protected Visual Environments (IMPROVE) program of the United States can be applied to NAPS observations from urban and impacted rural sites to estimate light extinction and visual range. Following a pattern similar to PM mass, visibility is best on the coasts (e.g. Vancouver mean = 20 dv) and worst in the more urbanized central points of Canada (e.g. Windsor mean = 27 dv).
- Model predictions show an overall improvement in visibility across eastern Canada but a decrease in visibility for some areas in western Canada by 2015 once legislated SO₂ and NO_x emission controls are achieved. Additional improvements in visibility are projected to occur in western Canada with further emission reductions proposed under Canada's Clean Air Regulatory Agenda.
- The Canada Wide Standard for PM_{2.5} does not have the capacity to preserve visual air quality.

11.1 Context and Issue

Visibility is a secondary measure of the impacts of atmospheric particulate matter (PM) and one of the most obvious indicators of poor air quality to the public. An observed change in visibility is recognized as change in air pollution especially in our national parks and wilderness areas, but also in our urban environments. In addition, those particles responsible for impeding the ability to see through the atmosphere are the same ones that can affect respiratory health in the human population.

The development of the Canada Wide Standards (CWS) for $PM_{2.5}$ (CCME, 2000) required a national review of PM measurements and science, which was undertaken in 2003 and included in a trans-boundary assessment of PM science (EC, 2004). Review of the progress towards the implementation of the CWS for $PM_{2.5}$ was published in 2007 (CCME, 2007). During this time frame, the United States (US) has completed its update of the National Ambient Air Quality Standards (NAAQS) for $PM_{2.5}$ in 2006 (USEPA, 2006) following a substantive review process, and took steps toward the implementation of the Regional Haze Rule since 1999 (USEPA, 1999). It is important to assess the updated information on visibility in these reviews in the Canadian context.

This chapter reviews literature on visibility since the 2003 CWS science assessment (EC, 2004) until 2007. Any appropriate advances to investigate the relationship of $PM_{2.5}$ to visibility were applied in selected regions of Canada for which there are data available (sections 11.4 and 11.5). The enhanced monitoring efforts for PM speciation will be used to identify PM species that contribute to visibility degradation. In its on-going processes, the United States EPA has initiated further reviews of the PM standards and readers are encouraged to access the most recent (post -2007) documents through that agency directly.

Although PM speciation measurements in Canada have not been designed for visibility characterization explicitly, they can be used for this purpose through a targeted data analysis effort. Both the National Air Pollution Surveillance (NAPS) network and the Canadian Air and Precipitation Monitoring Network (CAPMoN) have undertaken PM speciation measurements over the past few years, but only a limited number of sites have data sufficient to support the visibility characterization algorithm from the Interagency Monitoring of Protected Visual Environments (IMPROVE) program of the US. The NAPS sites are in urban impacted rural areas. At the time of writing, no CAPMoN data were available for review, but this data may provide insights into regional scale visibility when available.

11.2 Relationship between Ambient PM and Visibility

The ability to see through the atmosphere depends fundamentally upon concentrations, and the light scattering and absorption properties of gases and particles found between the observer and the vista. Gases in the atmosphere scatter light creating the blue sky; particles that are about the same diameter as the wavelengths of visible light (0.4-0.7 μm) are the most efficient at scattering that light. Some gases and particles are able to absorb light directly. The angle of the sun with the horizon, weather phenomena such as fog, precipitation, humidity, light pollution, and the perception ability of the observer, for example, also play a part in determining overall visibility.

The theories behind visual extinction have been covered well in previous reviews (Malm, 2000); however, a brief summary is presented here for completeness. The reduction of visibility by contributing physical processes is described through the Beer-Lambert Law. The extinction of light along a path between the observer and the vista is characterized by the extinction coefficient (b_{ext}) relating change in intensity of the light (dI) to the length of the path travelled (dx) by that light in units of inverse distance.

$$dI / I = b_{\text{ext}} dx$$

This extinction coefficient can be broken into the contributing components of scattering (scat or s) and absorption (abs or a) by either gases (g) or particles (p) such that each individual physical process is described by its own coefficient.

$$b_{\text{ext}} = b_{\text{scat}} + b_{\text{abs}} = b_{\text{sg}} + b_{\text{sp}} + b_{\text{ag}} + b_{\text{ap}}$$

In a very clean atmosphere with low particle and gaseous pollutant concentrations, gas or Rayleigh scattering dominates and total light extinction can be approximated by the scattering due to gases alone $b_{\text{ext}} \sim b_{\text{scat}} \sim b_{\text{sg}}$. This value is between 8 and 12 Mm^{-1} (inverse megameters). As particle concentration increases, for example with increasing use of fossil fuels and/or the release of gaseous precursor emissions such as sulphur dioxide (SO_2) and ammonia (NH_3), particle scattering will also increase so that $b_{\text{sp}} > b_{\text{sg}}$ and $b_{\text{ext}} \sim b_{\text{sp}} + b_{\text{sg}}$. In an atmosphere affected by higher nitrogen oxide (NO_2) emissions (e.g. in an urban centre or from the plume of a fossil fuel-using industrial facility), the so-called “brown cloud” may be observed due to the absorption of the shorter wavelengths of visible light by $\text{NO}_2(\text{g})$; then, $b_{\text{ext}} \sim b_{\text{scat}} + b_{\text{ag}}$. Particles that are able to directly absorb light are generally composed of black carbon from fuel combustion and forest fires. In turn, the size of b_{ap} will depend on the concentration of black carbon in the PM. In pristine areas unaffected by fossil fuel use, $b_{\text{abs}} \ll b_{\text{scat}}$ and b_{ag} can be assumed to be negligible. For most urban centres, however, all four coefficients should be considered in the measurement, management and assessment of the reduction of visibility due to PM.

Visual Range (VR) is the measure of atmospheric visibility used by meteorologists to identify visibility concerns for aircraft safety. VR is related to the visual extinction represented through the Koschmeider equation, which relates the ability to see an object at a distance with its contrast against the background.

$$\text{VR (km)} = 3910 / b_{\text{ext}}(\text{Mm}^{-1})$$

Because human perception of changes in visibility depends on relative, rather than absolute, changes in light extinction, the unit of deciview (dv) has been developed to account for this relationship (Pitchford and Malm, 1994).

$$dv = 10 \ln (b_{\text{ext}}(\text{Mm}^{-1})/ 10)$$

A change of one deciview is equivalent to a 10% change in the light extinction and this amount has been described as a “just-noticeable-change” although this has not been validated through human perception studies (Watson, 2002). It is important to note that the deciview does not vary directly with the change in PM concentration. For instance, similar differences in deciview will be related to a smaller change in particulate mass concentration in a cleaner atmosphere than in a more polluted one.

11.3 Literature Review of Visibility Research Post-2003

This brief review of the literature summarizes substantive assessments specifically related to the visibility issue covering the period 2003 to 2007. The intent of this section is to introduce recent sources of information and to provide the Canadian context.

Review of the 2004 US-EPA Criteria Documents for PM National Ambient Air Quality Standards (NAAQS) Assessment

The United States Environmental Protection Agency’s (EPA) PM NAAQS Assessment in 2006 was supported by the 2004 US Air Quality Criteria for PM document (USEPA, 2004), in which section 4.3 of Volume 1 covers the issue of airborne particle effects on visibility. The criteria document reiterates the importance of some references referred to in the 2001 U.S. PM Criteria Document (USEPA, 2001) and also introduces many materials published prior to 2000 but not included in the 2001 document. A review of the 2001 U.S. PM Criteria Document along with the new information up to 2002 is available in other publications (McDonald, 2002; EC, 2004). Below is a review of new information (2002 through 2004) reviewed in the 2004 Criteria Document.

The Interagency Monitoring of Protected Visual Environments (IMPROVE) program provides the US with data and analysis needed for national assessments of visibility in parks and wilderness areas. The method of using speciated PM mass measurements to reconstruct extinction and, thus, visual range is explained in IMPROVE (2002). This method is used for national assessments of visibility in the US, and was the basis for the Transboundary PM Science Assessment (EC, 2004). The appropriate selection of scattering efficiencies (representing how well each chemical species is able to scatter light) is critical to this approach. As such, many of the more recent publications provide updated estimates of scattering efficiencies for dry (Chow *et al.*, 2002) and wet (Malm *et al.*, 2000a, b) particles. Particular attention has been given to the water-absorbing properties of organic species

(Hemming and Seinfeld, 2001; Cocker *et al.*, 2001) with the resulting conclusion that ambient organic aerosol are, at most, weak moisture absorbers (weakly hygroscopic), and are often hydrophobic.

With regard to regional variability, McMurray (2000) concluded that the geographic variation in the ratio of dry scattering coefficient to dry fine particle mass concentration was small, but concurrent ambient relative humidity measurements were critical to accurately estimate the relationship between fine particles and light extinction.

Visibility monitoring in the US, continues to be performed by the IMPROVE network producing long-term quality data for PM speciation in rural and Class I areas. Other organizations have taken up the measurement of visibility. Of particular note are the Northeast States for Coordinated Air Use Management (NESCAUM), the Arizona Department of Environmental Quality, the State of Virginia, and the Midwest Regional Planning Organization who are employing digital photographic imaging in urban locations.

Watson (2002) provided a critical review of national visibility impairment that was included as part of the Transboundary PM science assessment (EC, 2004) and emphasized the application needs of the Regional Haze Rule in order to achieve the goal of returning 156 national parks and wilderness areas to their natural visibility conditions within 65 years. Some further work has been conducted employing statistical analysis to find trends in data (Schichtel *et al.*, 2001; Hess *et al.*, 2001). The results indicate that haziness has declined across the US between 1980 and 1995 with the greatest improvement in visibility in the southeast. There remains some concern with the Shenandoah and Great Smoky Mountain Class I areas as summer sulphate concentrations were shown to be increasing (Iyer *et al.*, 2000). In southern California, visibility conditions have improved between 1970 and 1990 (Kleeman *et al.*, 2001) while the Denver, Colorado region continues to exceed their visibility standard 50 to 80 days per year (Lloyd, 2002).

The 2004 US EPA PM Criteria Document (USEPA, 2004) cites the same fundamental works on economic valuation of visibility impairment as the 2001 report (USEPA, 2001). One relevant new study in the literature focuses on regional haze in the east (Smith *et al.*, 2005). Based on willingness-to-pay, the results suggest that the distribution in response is highly skewed and dependent upon the context in which questions are posed. The implication is that a haze reduction policy with costs per person equal to the average willingness-to-pay would be rejected by 70-80% of the public if given the choice. From that survey, respondents were more open to paying for improvements on the worst of days, but not on the days with near-average regional haze.

Review of the 1999 US Regional Haze Rule and updates in the IMPROVE network

The Regional Haze Rule (RHR) was enacted in 1999 to protect and improve visibility in Class I national parks and wilderness areas of the US. The RHR makes use of the IMPROVE data network for assessing changes in visibility over time in deciview (dv) units. The RHR calls for the evaluation of the mean of the annual best and worst 20% of days in each protected area. Over the next 60 years, states are required to manage emissions to improve the worst haze days to the natural conditions without resulting in a degradation of those days with the least haze. As a result of the implications of this RHR, the use of the IMPROVE data and algorithm has been critically reviewed recently (Lowenthal and Kumar, 2003; Ryan, *et al.*, 2005) and resulted in the review (Hand and Malm, 2007) and introduction of a new algorithm to be applied to the IMPROVE network data (Pitchford *et al.*, 2007).

The IMPROVE network measures 24-hour mass concentrations for PM₁₀ and PM_{2.5} as well as the chemical constituents of the PM_{2.5} fraction. Given these data are used to assess visibility levels as part of the 1999 RHR, the application of an algorithm for estimating light extinction from the aerosol and relative humidity data is required. Some of the coefficients of scattering for specific chemical constituents have changed due to the research over the past 5 years as discussed in the USEPA criteria documents. The original formula was employed in the CWS science review of visibility (McDonald, 2002), but it is necessary to update the algorithm in Canada to match that change in the US for consistency and because the basis of the theory behind the change applies to Canada as well.

The algorithm is based on the concept that the coefficient of extinction (b_{ext}) can be estimated by summing the contributions of the major chemical components of the PM_{2.5} mass. The original formula included factors for sulphate, nitrate, organic mass, elemental carbon, fine soil and coarse mass plus a constant factor for Rayleigh scattering of 10 Mm^{-1} . The revised algorithm incorporates an additional term for sea salt that will be important in coastal regions. A new term is added for the presence of atmospheric NO₂(g) absorption that may be important in urban regions. The Rayleigh scattering term is made to vary with the regional conditions between about 12 Mm^{-1} at sea level to 8 Mm^{-1} or less at higher elevations. The sulphate, nitrate and organic carbon terms are changed to reflect the difference in scattering efficiency between small and large size fractions of particles, which becomes most important at lower particle loads ($<20 \mu\text{g m}^{-3}$).

This new algorithm was demonstrated to reduce biases in light extinction as compared to direct measures of visibility such as with a nephelometer (a field instrument that draws in air samples and provides a measure of extinction). In addition, the new algorithm better estimated the extreme conditions needed to apply the RHR except in the haziest of days when the original algorithm performed best. It was determined that the largest reduction of bias is associated with the splitting of the extinction efficiencies for sulphate, nitrate and organic carbon. It

should be noted, however, that this distinction between small and large particles is only engaged in regions below $20 \mu\text{g m}^{-3}$ $\text{PM}_{2.5}$ particle species concentrations meaning that it could be influence the estimated extinction in many regions of Canada. Through the International Joint Commission Air Quality Advisory Board, Environment Canada is participating in an IMPROVE comparison project at Egbert, ON. The objective of this work is to facilitate comparability of data between the two countries. At the time of writing, no data were yet available for review.

Review of New Information in the Literature (2003-2007)

Since 2003, much of the literature specific to visibility issues reports on special studies focused on implementing the Regional Haze Rule in Class I Areas of the US where multiple sources contribute to a reduced visual air quality. With the national acceptance of the IMPROVE algorithm, some work has been done on validating algorithms and understanding source apportionment. Routine monitoring data through IMPROVE support much of this need. For instance, Copeland (2005) performed a statistical analysis of national IMPROVE data to demonstrate that all Class I Areas in the contiguous US are significantly impaired by sulphate aerosols with respect to a natural background visibility. Special studies were done where needed to enhance the air quality, meteorological, and emission data and identify the sources, their frequency, duration, and contribution to visibility impairment. As a result, recent papers bring attention to two specific case studies of interest.

The Big Bend Regional Aerosol and Visibility Observation (BRAVO) study was designed to investigate the causes of haze at Big Bend National Park located in Texas near the US-Mexican border. The network operated from July to October 1999 measuring fine aerosol mass and its constituents, atmospheric optical properties, gaseous air pollutants and meteorology at Big Bend. New papers continue to come from this substantial program.

A recent comparison between visibility monitoring methods (Hand *et al.*, 2004) demonstrated that surface visibility was a good indicator of the column aerosol optical depth implying that remote sensing data can be used to extend the spatial coverage of ground-based visibility monitoring. Due to the intensity of the monitoring and tracer activities in BRAVO, model evaluation and analyses were possible. Schichtel *et al.* (2005a) identified dispersion characteristics in the regional modelling system for aerosols and deposition (REMSAD) Eulerian and the Center for Air Pollution and Trend Analysis (CAPITA) Monte Carlo Lagrangian models. Barna *et al.* (2006) quantified concerns with the use of spatially invariant boundary conditions in the application of REMSAD recommending a varying boundary condition approach. Schichtel *et al.* (2005b, 2006) were able to recently reconcile and improve the source apportionment estimates for PM at Big Bend National Park. High particulate sulphur concentrations were associated with low-level and low-speed air mass transport from the eastern US, eastern Texas, and northeastern Mexico, while low particulate sulphur concentrations coincided with low-level but high-speed air mass transport from the Gulf of

Mexico and along the Mexico–Texas border. The Carbón power plants, located 225 km southeast of Big Bend in Mexico, contributed 19% of the sulphate making them the largest single contributing facility to the PM load and hence visibility degradation in the region.

The Yosemite Aerosol Characterization Study (YACS) was an intensive field measurement campaign including several US research groups running from July 15 to September 4, 2002, at Yosemite National Park, California. Particular focus was placed on the measurement, analysis and behaviour of organic aerosols (Carrico *et al.*, 2005; Malm *et al.*, 2005a; Engling *et al.*, 2005) enhancing knowledge of how those particles affect visibility (Malm *et al.*, 2005b). The results indicate that ambient organic mass aerosols may be only weakly hygroscopic even at higher relative humidities. Opportunity arose in the monitoring period to include study of smoke aerosols. (McMeeking *et al.*, 2005a, 2005b, 2006) Observations suggest that emissions from wild fires can have strong and sustained regional impacts on aerosol concentrations, air quality, and visibility.

11.4 Reconstructed Particulate Matter Levels and Visibility in Canada

Due to the scarcity of direct measurements of visibility in Canada, a national assessment of visibility requires that temporal and spatial patterns of visual light extinction be derived either from atmospheric modelling or by reconstructing light extinction by combining measurements of aerosol species with the light scattering, absorption and hygroscopic growth characteristics of those aerosol species. Reconstructed aerosol concentrations and light extinctions are developed according to the updated method described in Pitchford *et al.* (2005). The revised algorithm equation is:

$$\begin{aligned}
 b_{\text{ext}} &\approx 2.2 f_{\text{S}}(\text{RH}) [\text{ASO4}]_{\text{S}} + 4.8 f_{\text{L}}(\text{RH}) [\text{ASO4}]_{\text{L}} \\
 &+ 2.4 f_{\text{S}}(\text{RH}) [\text{ANO}_3]_{\text{S}} + 5.1 f_{\text{L}}(\text{RH}) [\text{ANO}_3]_{\text{L}} \\
 &+ 2.8 f_{\text{S}}(\text{RH}) [\text{OM}]_{\text{S}} + 6.1 f_{\text{L}}(\text{RH}) [\text{OM}]_{\text{L}} \\
 &+ 10 [\text{EC}] + [\text{Fine Soil}] + 0.6 [\text{CM}] + 1.7 f_{\text{SS}}(\text{RH}) [\text{Sea Salt}] \\
 &+ 0.33 [\text{NO}_2 \text{ (ppb)}] + \text{Rayleigh Scattering (site specific)}
 \end{aligned}$$

By comparison with the earlier algorithm, this revised algorithm takes into account more site specific conditions including the influence of sea salt, NO₂(g) and regional Rayleigh scattering. The terms for coarse mass (PM₁₀-PM_{2.5}) [CM], elemental carbon [EC], and fine soil have not changed in the revised algorithm. Total (T) ammonium sulphate [ASO4], ammonium nitrate [ANO₃], and organic matter [OM] concentrations are split into small (S) and large (L)

size distributions with varying relationships to daily-averaged concurrent relative humidity represented by $f_S(\text{RH})$ and $f_L(\text{RH})$, respectively. All three of these species are apportioned according to the following equations:

$$[\text{ASO4}]_L = [\text{ASO4}]_T / 20 \mu\text{g m}^{-3} \times [\text{ASO4}]_T \quad \text{if } [\text{ASO4}]_T < 20 \mu\text{g m}^{-3}$$

$$[\text{ASO4}]_L = [\text{ASO4}]_T \quad \text{if } [\text{ASO4}]_T \geq 20 \mu\text{g m}^{-3}$$

$$[\text{ASO4}]_S = [\text{ASO4}]_T - [\text{ASO4}]_L$$

Within the equation, the organic mass concentration used in this new algorithm is 1.8 times the measured organic carbon mass concentration, changed from 1.4 times carbon mass concentration as used for input for the prior IMPROVE algorithm. Because the Canadian NAPS stations are in a mixture of urban and agricultural environments with none in pristine areas, a value of 1.6 will be employed throughout as suggested for urban aerosols (Turpin and Lim, 2001). Sea salt is calculated as $1.8 \times [\text{Chloride}]$, or $1.8 \times [\text{Chlorine}]$ if the chloride measurement is below detection limits, missing or invalid. The algorithm uses three water growth adjustment terms: $f_S(\text{RH})$, $f_L(\text{RH})$, and $f_{SS}(\text{RH})$ as described in Pitchford *et al.* (2007).

Table 11.1 Site specific Rayleigh scattering values for Canadian NAPS particle speciation monitoring locations.

NAPS #	Site Name	Rayleigh Estimation (Mm^{-1})
100119	Vancouver BC	12
101004	Abbotsford BC	12
103202	Golden BC	10
90132	Edmonton AB	11
60211	Windsor ON	12
62601	Simcoe ON	11
61902	Wallaceburg ON	12
60427	Toronto ON	12
54401	St. Anicet PQ	12
50104	Montreal PQ	12
40801	Canterbury NB	12

Rayleigh scattering is the scattering of light by gas molecules in the air. A constant value of 10 Mm^{-1} was used in the prior IMPROVE algorithm; however, Rayleigh scattering depends on the density of the air and thus varies with temperature and pressure. The IMPROVE network now applies a site-specific Rayleigh scattering estimate based on the standard atmospheric pressure corresponding to the monitoring site elevation, and an estimated annual mean temperature

from the nearest climate station. These estimates are rounded to the nearest integer and vary from 12 Mm^{-1} for sites near sea level to 8 Mm^{-1} for sites at the highest elevations. For the purposes of this assessment, a Rayleigh scattering value was estimated for each monitoring station in Canada. The stations were evaluated with respect to the site elevation and average temperatures as recorded at the station for a Rayleigh scattering value to be used in the algorithm. To be consistent with the IMPROVE program, only integer values of Rayleigh scattering are employed. A listing of the estimated Rayleigh scattering values used within the calculations for the NAPS speciation sampling sites is given in Table 11.1.

To be consistent with the IMPROVE program and include the substantive scientific advances included in the algorithm, the revised form of the equation and the associated relative humidity functions will be used for the following calculations. Some compromises are required to be able to use the data from the NAPS stations. Most calculations will be based on $\text{PM}_{2.5}$ data only and the algorithm will only include the $0.6 \cdot [\text{CM}]$ term if coarse mass is available at the site. Similarly, those sites with $\text{NO}_2(\text{g})$ measurements will have that term included. Elemental carbon is directly available at the NAPS PM speciated monitoring stations. Soil data is determined from the IMPROVE algorithm for those sites with the metal element measurements.

11.4.1 Data Availability for the Assessment

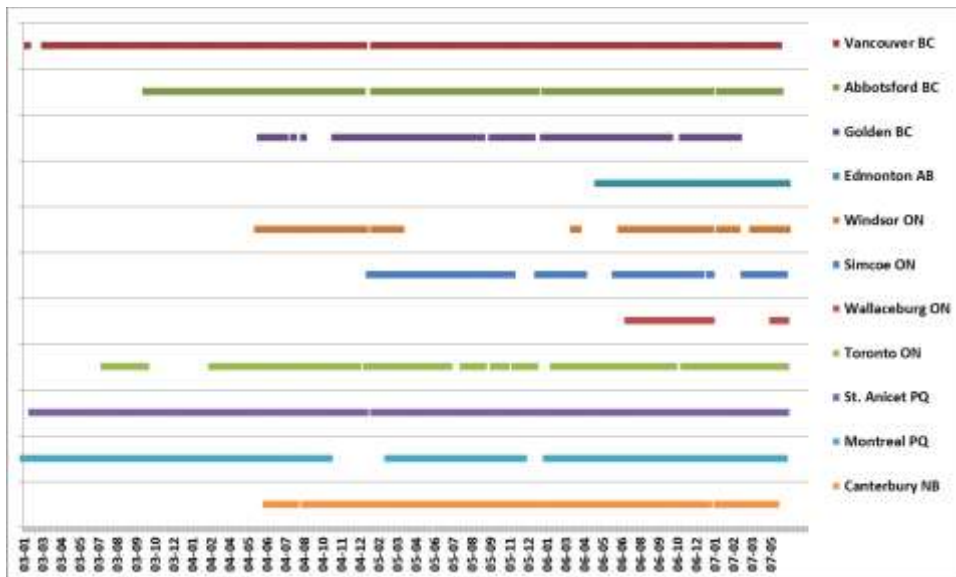


Figure 11.1 Summary of NAPS monitoring stations and data availability used in the assessment of visibility over the period 2003-2007.

The NAPS PM speciation sampling program began in 2003 and data to support this analysis is available for 11 sites across Canada. Because NAPS runs on a 6-day sampling schedule, the evaluation is based on about 15% of the total days in the record period. Figure 11.1 presents the stations used ordered from west to east with the date range of available data from the speciation program running from January 2003 through June 2007. Gaps in the data record are shown. Data from applicable monitoring performed by CAPMoN (Canadian Air and Precipitation Monitoring Network) was not available at the time of writing.

At the 11 NAPS sites, all the dominant chemical species are measured, but the selection of other available species and the period of record vary. The number in parenthesis provides the total number of data points available at each site: Vancouver (445) and Abbotsford (358) in BC, Windsor (151) and Toronto (353) in ON, and Montreal, PQ (417) each include data for sulphate, nitrate, organic carbon and elemental carbon species as well as sea salt, soil, coarse mass and $\text{NO}_2(\text{g})$. Note that in all these sites $\text{NO}_2(\text{g})$ was not available after January 2007 and was included as zero in the calculations after that date. Golden BC (229) includes all PM components but has only one-half year of $\text{NO}_2(\text{g})$ measurements taken in 2005. Edmonton AB (119) has neither soil nor coarse mass available. Simcoe (176) and Wallaceburg (53) in ON have no $\text{NO}_2(\text{g})$ measurements. St. Anicet PQ (441) and Canterbury NB (294) have no $\text{NO}_2(\text{g})$ nor coarse mass measurements. As these missing components can be relatively small contributors to light extinction, they are included where possible and noted as missing when necessary.

11.4.2 Spatial Distributions of Reconstructed Aerosol Concentrations

The aerosol component concentrations used in the IMPROVE algorithm presented above are reconstructed from the measured concentrations at each monitoring site with PM speciated data available. Due to variations in the selection of measured species and monitoring methods, the reconstructed mass is separated into the “SNC mass”, which includes only the ammonium sulphate, ammonium nitrate, organic matter and elemental carbon, and the “Total mass”, which includes soils and sea salt, where available. Coarse mass is not included in this mass comparison as it is not in the measured $\text{PM}_{2.5}$ mass value.

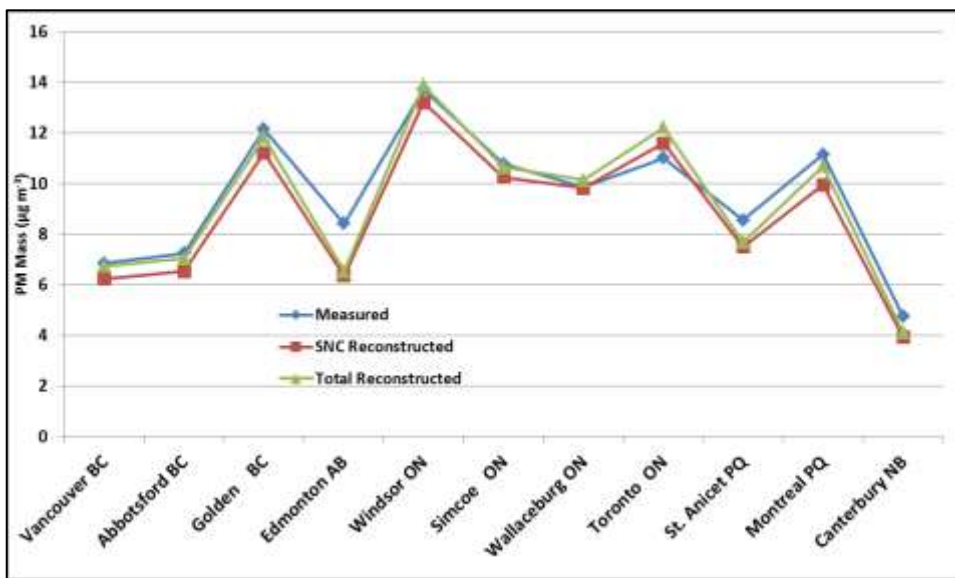


Figure 11.2 Comparison of means of measured and reconstructed fine mass at NAPS speciation sampling sites. Note that the SNC Reconstructed mass includes only ammonium sulphate, ammonium nitrate, and carbon species. The Total Reconstructed mass includes soils and sea salt where available.

Figure 11.2 shows that the SNC reconstructed fine PM mass is less than the values measured at each site except where it over-predicts in Toronto ON. The reasons for this are not clear, but could be due to the loss of ammonium nitrate or volatile organics during the mass measurements. The overall pattern shows that the sites in the heavily populated and industrialized Windsor – Montreal corridor have higher concentrations of particulate mass as compared to the Maritimes and the western sites. Notably, Golden BC demonstrates a relatively high particulate concentration due predominantly to periodic high-carbon events likely from natural fires, prescribed burns, or the use of wood for heating. Within the Windsor – Montreal corridor, it is evident that the less urbanized sites (Simcoe, Wallaceburg and St. Anicet) have lower overall concentrations than Windsor, Toronto and Montreal. The inclusion of the other PM species in the reconstructed mass does create a difference between the stations. Of particular note in the west is Edmonton AB where it is probable that including the fine soil component could improve the comparability between the measured and reconstructed values. This could also be the case in St. Anicet QC. However, while contributing to the total mass, the soil and sea salt components are on average small contributors to light extinction as evident from their small scattering efficiencies in the IMPROVE equation.

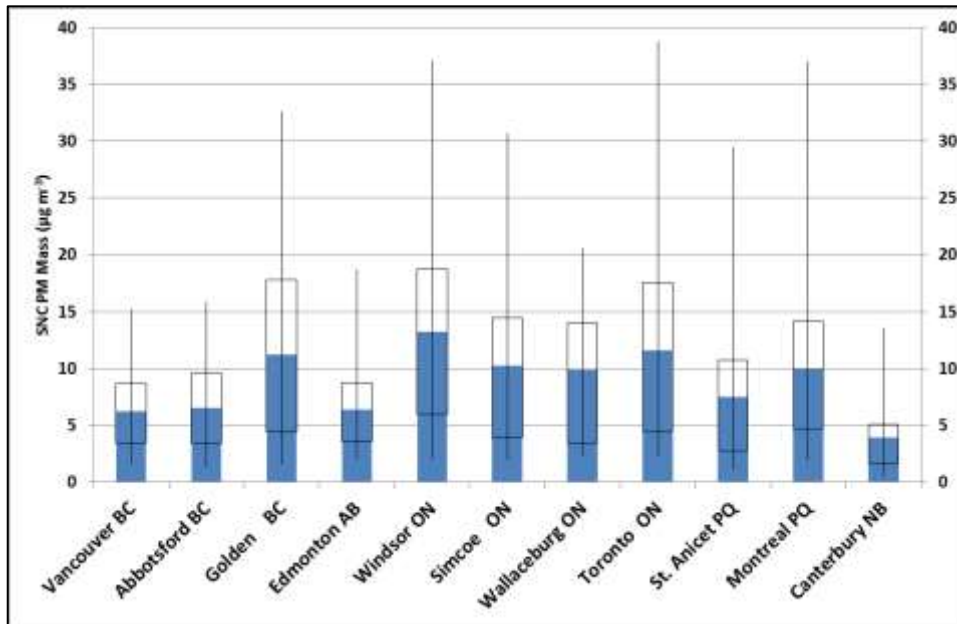


Figure 11.3 Statistical representation of reconstructed fine mass ($\mu\text{g m}^{-3}$) with ammonium sulphate, ammonium nitrate, and carbon species only at NAPS speciation stations. Tops of the blue bars represent the mean values. The outlined box represents the 20th to 80th percentile range. Whiskers represent the 2nd to 98th percentile range.

Figure 11.3 provides a statistical comparison of the mean, 20th to 80th percentile range and 2nd to 98th percentile range for the fine reconstructed mass (SNC only) at each NAPS speciation station. While the mean is an indicator of the typical concentrations, it is the extremes that are most obvious to human observers. The ranges were selected according to the regulatory framework requirements since the Canada Wide Standard employs a 98th percentile value and the US Regional Haze Rule focuses on maintaining the best and improving the worst 20% of days.

In Canada, as in the measured fine mass, the reconstructed mass shows greater concentrations in the central regions of the country while each coast experiences lower concentrations. In addition, the central regions demonstrate a wider spread in the extreme percentiles than either the east or west. This can be due to either local source variability or the influence of transboundary air pollution. Interestingly, Golden BC in a non-urban area demonstrates a similar pattern to the highly urbanized locations (Windsor ON, Toronto ON, and Montreal QC). This community is affected by episodic high carbon events due to woodsmoke in a way similar to the eastern sites with the episodic high sulphate events.

Table 11.2 Canadian total reconstructed fine particle mass statistics for the period 2003-2007 as available. Note that these values are determined by applying the IMPROVE reconstruction procedure to mass and chemical concentration measurements taken at the NAPS stations.

RCFM ($\mu\text{g m}^{-3}$)	2% ile	20% ile	Median	80% ile	98% ile	Mean	Std Dev	Correlation
Vancouver BC	1.88	3.71	5.99	9.28	16.18	6.74	4.02	0.88
Abbotsford BC	1.63	3.71	6.22	10.03	17.05	7.04	3.88	0.85
Golden BC	2.05	4.80	8.83	18.86	34.58	11.83	8.94	0.93
Edmonton AB	2.06	3.62	5.56	8.84	18.90	6.53	3.83	0.75
Windsor ON	2.92	6.54	11.27	19.13	40.54	13.90	9.93	0.84
Simcoe ON	2.11	4.27	9.14	14.90	31.84	10.64	7.18	0.96
Wallaceburg ON	2.40	3.55	8.24	14.47	20.86	10.14	8.71	0.86
Toronto ON	2.40	5.00	9.39	18.67	38.98	12.22	9.32	0.93
St. Anicet PQ	1.14	2.86	5.66	11.09	30.49	7.69	7.36	0.96
Montreal PQ	2.42	5.20	8.46	15.14	38.72	10.69	8.43	0.94
Canterbury NB	0.72	1.81	3.13	5.33	13.86	4.12	3.46	0.77

For completeness, the numerical values for Total reconstructed fine mass (RCFM) including sea salt and soil are provided in Table 11.2. The correlations (r^2) between measured and reconstructed PM mass are also provided and range from 0.75 to 0.96. Those sites with the lowest correlations also have the fewest data points for analysis as given in Section 11.4.1 above, and so correlations should improve with the period of record. Therefore, given the comparability of the reconstructed mass with observations, the updated IMPROVE formula will be used to reconstruct the associated visibility with an effort to be as consistent as possible across the country.

11.4.2.1 Spatial Distributions of Calculated Light Extinction

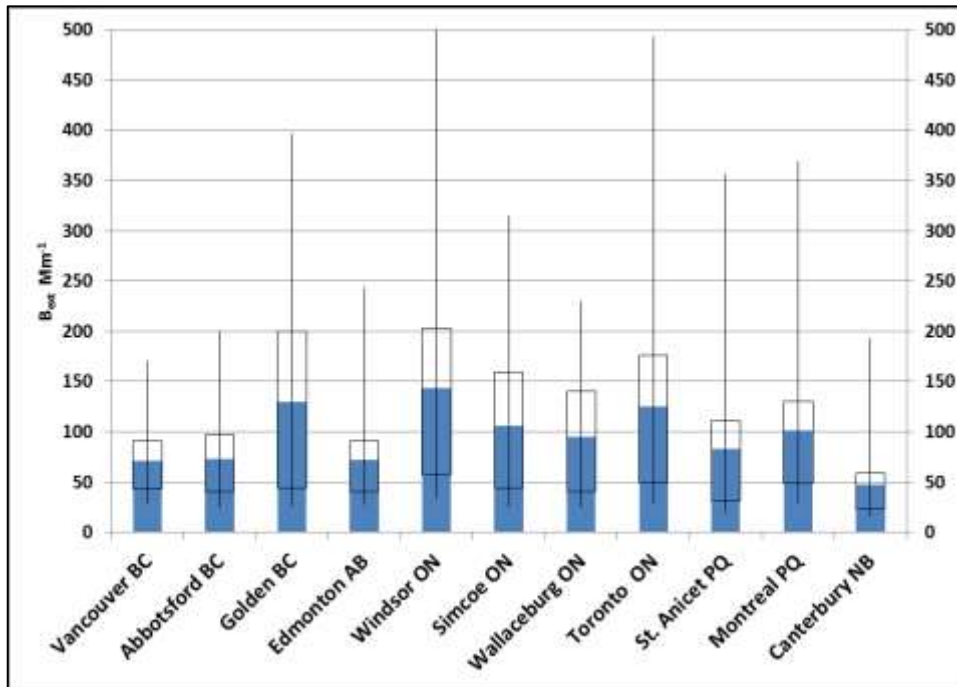


Figure 11.4 Reconstructed extinction coefficient (Mm^{-1}) statistical ranges for PM species and $NO_2(g)$ at NAPS speciation sites where available. Tops of the blue bars represent the mean values. The outlined box represents the 20th to 80th percentile range. Whiskers represent the 2nd to 98th percentile range.

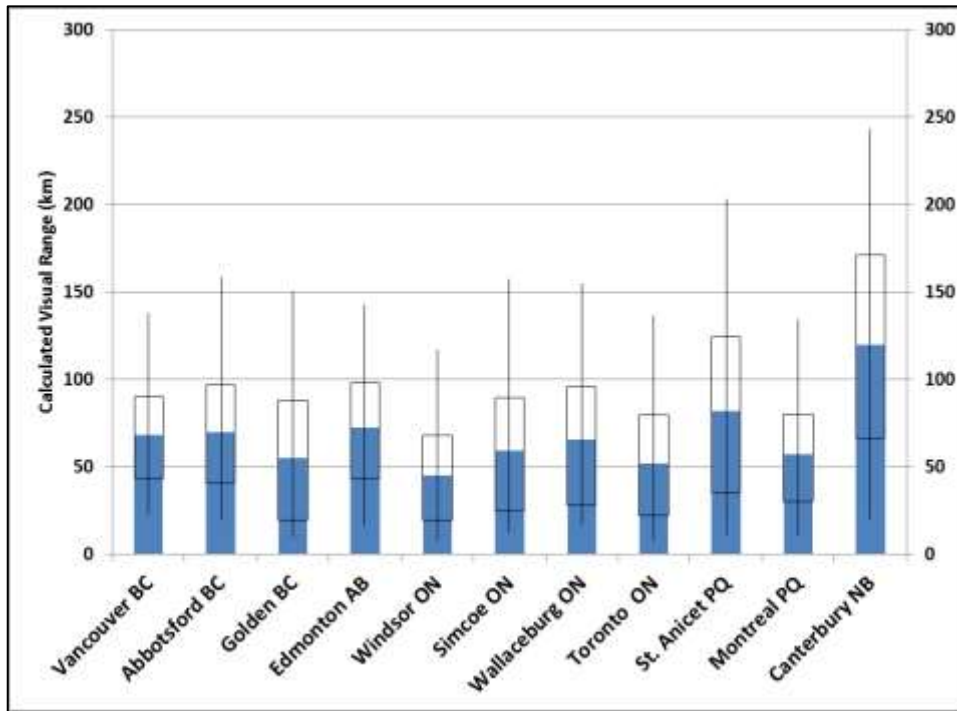


Figure 11.5 Reconstructed visual range (km) statistical ranges for PM species and NO₂(g) at NAPS speciation sites where available. Tops of the blue bars represent the mean values. The outlined box represents the 20th to 80th percentile range. Whiskers represent the 2nd to 98th percentile range.

Table 11.3 Total reconstructed fine particle mass statistics for the period 2003-2007 as available. Note that these values are determined by applying the IMPROVE reconstruction procedure to mass and chemical concentration measurements taken at the NAPS stations. Correlation with measured fine mass is shown.

Total Visual Range (km)	2% ile	20% ile	Median	80% ile	98% ile	Mean	Std Dev
Vancouver BC	23	43	64	90	138	68	30
Abbotsford BC	20	40	61	97	159	70	36
Golden BC	10	20	46	88	150	55	39
Edmonton AB	16	43	71	98	142	73	32
Windsor ON	8	19	37	68	186	45	30
Simcoe ON	12	25	47	89	158	59	40
Wallaceburg ON	17	28	53	96	155	66	46
Toronto ON	8	22	44	79	136	52	33
St. Anicet PQ	11	35	73	124	203	82	51
Montreal PQ	11	30	51	80	134	57	32
Canterbury NB	20	66	120	171	243	120	58

The equation used in IMPROVE to estimate particle scattering from the chemical reconstruction of aerosol measurements is based on the multiplication of the fine mass chemical components by dry scattering efficiencies and a correction function for the relative humidity. The calculated b_{ext} is in units of inverse megameters (Mm^{-1}). Figure 11.4 displays the light extinction corresponding to the reconstructed fine mass including all constituents as available at each site. A more recognizable unit for presentation is shown in Figure 11.5 where the b_{ext} is converted into visual range in kilometres (km). Therefore, b_{ext} will follow the same general pattern as the mass reconstruction while the visual range will appear as the inverse. That is, the central parts of Canada demonstrate higher extinctions and lower visual ranges in comparison to either coast. The numerical visual ranges are provided in Table 11.3.

The variability at the highest extinction levels is more obvious in Figure 11.4 where Windsor and Toronto ON are shown to have some extreme days of haze shown by the top ends of the whisker plots. Yet, to recognize those sites with the clearest days, Figure 11.5 is the better depiction as it presents visual range such that the tops of the whisker plots here indicate the clearest days. Consider Golden BC that has clear conditions similar to the rest of western Canada while at times, compared to Figure 11.3, this community experiences a relatively high particle load. Golden is periodically affected by good and poor air quality.

The contributions of the additional PM components (soil, sea salt, and coarse mass) and $\text{NO}_2(\text{g})$ to the light extinction are generally small and few sites in Canada currently possess all measurements. Since these additional species are not very controllable aspects of the particle load, and therefore of extinction, it is reasonable to be aware of them but exclude them from the discussions of visibility management perhaps until such time as they are consistently measured at sites in Canada.

11.4.3 Characteristics of Calculated Fine Particle Scattering

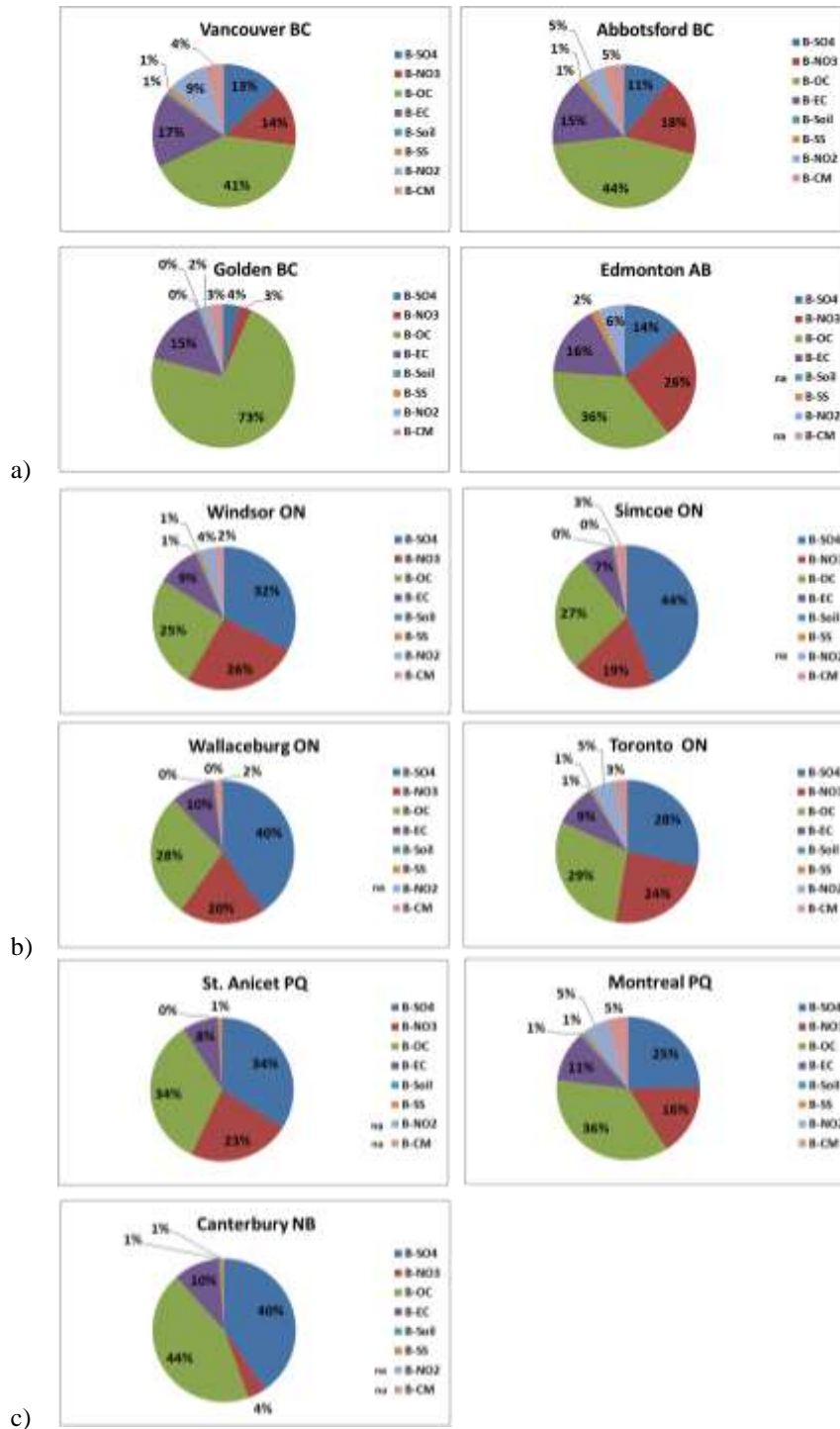


Figure 11.6 a) Proportion of mean particle extinction contributions at Western Canada NAPS sites. b) Proportion of mean particle extinction contributions at Ontario NAPS sites. c) Proportion of mean particle extinction contributions at Eastern Canada NAPS sites.

Table 11.4 Mean scattering contributions by chemical component for NAPS sites across Canada for the period 2003-2007. Note that the B_{ext} columns include the site specific Rayleigh scattering term.

Extinction Mm ⁻¹)	B(ASO ₄)	B(ANO ₃)	B(OC)	B(EC)	B _{ext} (SNC)
Vancouver BC	7.79	8.23	24.14	9.97	62.14
Abbotsford BC	6.66	11.14	27.04	9.34	66.17
Golden BC	7.22	9.68	25.59	9.66	122.40
Edmonton AB	4.29	3.43	86.75	17.93	66.94
Windsor ON	8.29	15.73	22.11	9.81	134.85
Simcoe ON	41.53	18.14	25.63	6.74	103.04
Wallaceburg ON	33.41	16.28	23.31	8.13	93.12
Toronto ON	42.59	34.49	33.44	12.33	114.66
St. Anicet PQ	31.91	27.50	32.80	10.45	82.02
Montreal PQ	37.25	31.00	33.12	11.39	91.20
Canterbury NB	23.98	16.38	23.99	5.67	46.54
Extinction (Mm ⁻¹)	B(Soil)	B(sea salt)	B(NO ₂)	B(CM)	B _{ext} (Total)
Vancouver BC	0.38	0.75	5.25	2.62	71.13
Abbotsford BC	0.37	0.88	2.79	3.11	73.32
Golden BC	0.38	0.82	4.02	2.86	129.46
Edmonton AB	0.53	0.41	2.41	3.70	71.67
Windsor ON	na	1.00	3.73	na	143.76
Simcoe ON	0.35	0.31	na	2.52	106.21
Wallaceburg ON	0.26	0.34	na	1.21	94.94
Toronto ON	0.52	1.12	4.70	2.56	124.79
St. Anicet PQ	0.50	0.66	5.74	3.24	82.73
Montreal PQ	0.51	0.89	5.22	2.90	101.77
Canterbury NB	0.09	0.63	na	na	47.00

As in the US, Canada experiences an east-west difference in the PM characteristics and, therefore, will also experience differences in the species contribution to visibility impairment. Figures 11.6a, 11.6b and 11.6c display charts of the mean particle species contributions to the extinction coefficient as a percentage of the total extinction at the western sites, Ontario sites, and eastern sites, respectively. Table 11.4 provides the numerical values separated into the SNC and Total extinction components. Refer also to Table 11.1 for the site-specific Rayleigh scattering components.

In the Vancouver BC area, carbon species account for about 60% of the particle extinction on average whereas ammonium sulphate and ammonium nitrate account for less than a third. Vancouver has the highest contribution of $\text{NO}_2(\text{g})$ in the country at 9%. In the British Columbia mountains, Golden experiences almost 90% of its extinction from carbon species, but less than 10% due to ammonium sulphate and ammonium nitrate. Combined with the high light extinction, this suggests that fire (wildfire, prescribed burns, or domestic wood burning) plays a large role in the visibility in Golden. In Edmonton, Alberta the distribution is more balanced where about 50% is due to carbon species and 40% due to ammonium sulphate and ammonium nitrate species. This location has a relatively high contribution of $\text{NO}_2(\text{g})$ and is likely missing some contribution of soil and coarse mass since these are not measured at this site. By contrast, extinction at the Ontario sites is dominated by ammonium sulphate and ammonium nitrate on the order of 60% with a slightly lower proportion in the urban centres. Extinction at the Quebec sites is more balanced between the acidifying and carbonaceous species. Montreal, Quebec has a relatively high contribution from coarse mass. On the east coast, Canterbury, New Brunswick shows much of its extinction is due to carbon and ammonium sulphate but not ammonium nitrate. It is notable, however, that the Rayleigh scattering at 12 Mm^{-1} represents approximately 25% of the total extinction on average at that relatively clean location.

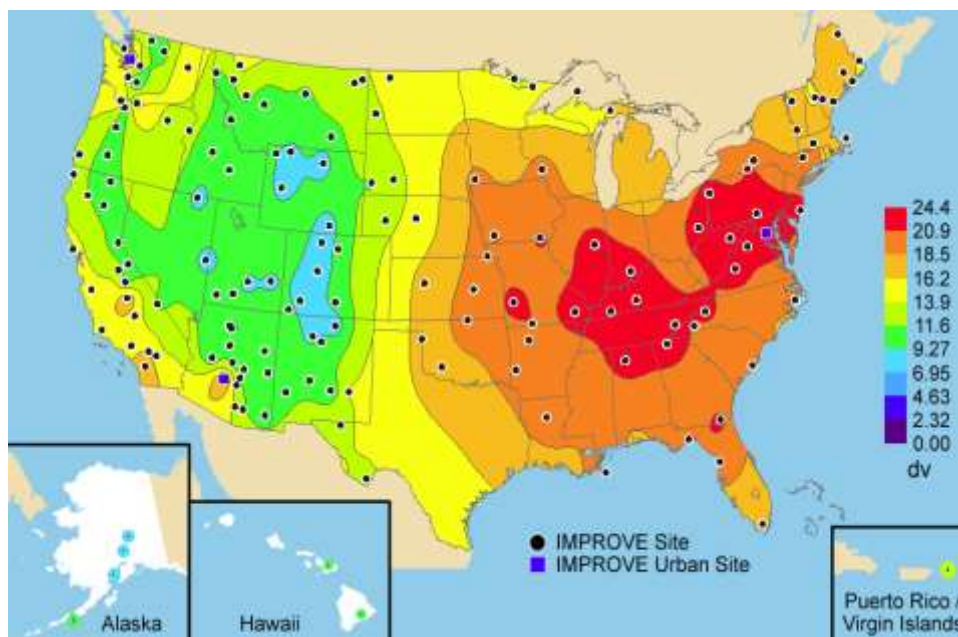


Figure 11.7 Five-year average (2000–2004) deciview (DV) using only IMPROVE data from IMPROVE (2006).

Table 11.5 Mean deciview visibility at Canadian NAPS stations (2003-2007).

	$B_{ext}(\text{Total})$	Deciview (dv)	IMPROVE range for comparison (dv)
Vancouver BC	71.1	19.6	16.2-18.5
Abbotsford BC	73.3	19.9	16.2-18.5
Golden BC	129.5	25.6	13.9-16.2
Edmonton AB	71.7	19.7	13.9-16.2
Windsor ON	143.8	26.7	18.5-20.9
Simcoe ON	106.2	23.6	18.5-20.9
Wallaceburg ON	94.9	22.5	18.5-20.9
Toronto ON	124.8	25.2	18.5-20.9
St. Anicet PQ	82.7	21.1	16.2-18.5
Montreal PQ	101.8	23.2	16.2-18.5
Canterbury NB	47.0	15.5	13.9-16.2

In an attempt to demonstrate a comparison across the US border, the deciview unit has been employed. Figure 11.7 is the 2000-2004 average deciview visibility map from the IMPROVE report IV (2006) for comparison to the NAPS mean values in Table 11.5. Higher deciview levels are associated with lower visual ranges; therefore, due to the more developed urban and agricultural nature of the NAPS stations, the values are expected to be somewhat higher than measured at the more pristine Class I locations in the IMPROVE network. The Vancouver and Abbotsford BC locations could be best compared geographically with the IMPROVE locations in the Northwest US region that show a range of 16.2-18.5 dv. It is very difficult to assign an IMPROVE region to either Golden BC or Edmonton AB due to the distance from the border, but potentially the Northern Rocky Mountains and the Northern Great Plains could be relatively comparable at 13.9-16.2 dv. The Ontario sites can best be compared with the Ohio River Valley regional sites (18.5-20.9 dv) and the Quebec sites with the IMPROVE Northeast US region (16.2-18.5 dv). On the east coast, Canterbury NB could lie in the 13.9-16.2 dv contour in the far northeast US.

11.5 Predicted Visibility from Air Quality Modelling Applications

In addition to the use of monitoring site data, the output of air quality model simulations has been used to estimate visibility in Canada with the regional air quality model AURAMS (refer to Chapter 5 for a detailed description of AURAMS, and Chapter 6 for a discussion of the model scenarios presented in this section). Since the fall of 2006, the calculation of visibility from the modelled PM speciation concentrations has been included as an output for all annual

AURAMS model simulations. This provides a new opportunity to explore the specific impacts of current or future emissions on visibility. Utilizing the model-predicted ambient pollutant concentrations, visibility levels were derived from a slightly modified and simpler version of the mathematical relationship presented in Section 11.4 suited to the AURAMS outputs.

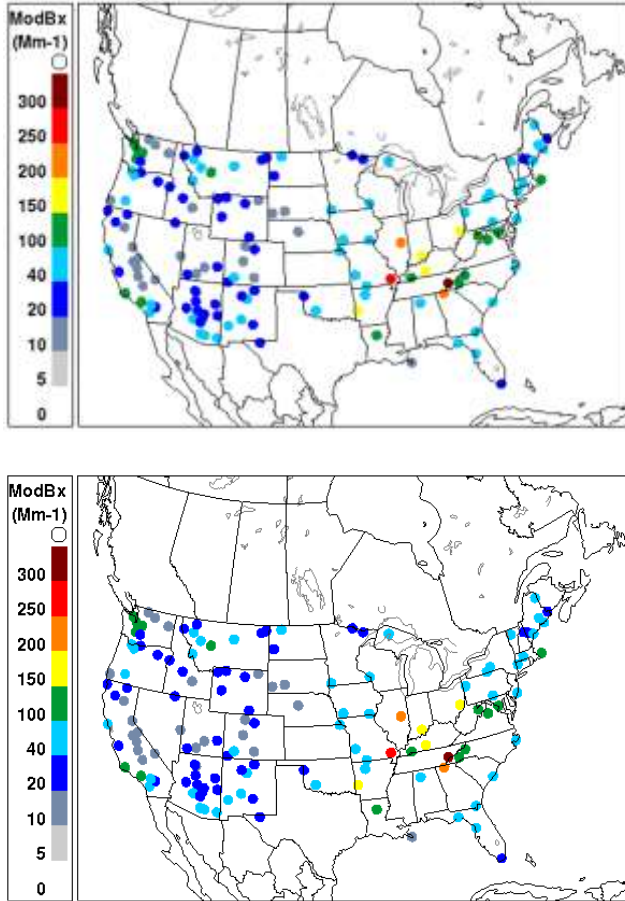


Figure 11.8 Comparison of AURAMS modelled visibility calculations (top) and measurement data collected from the IMPROVE network (bottom) for July 16th, 2006 produced using the same extinction reconstruction algorithm.

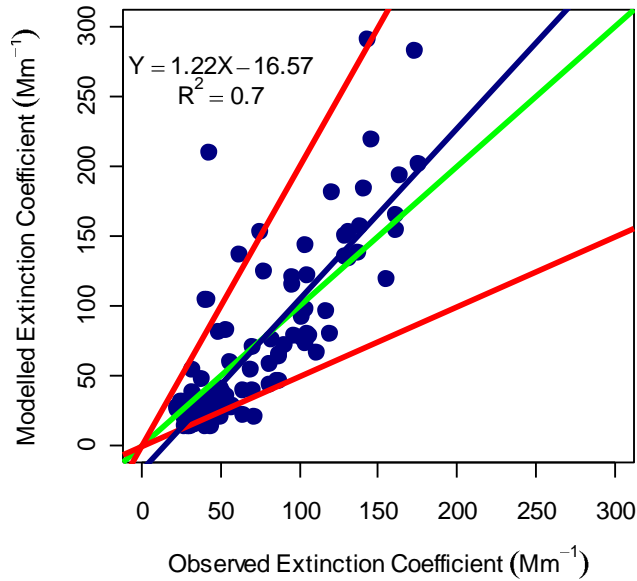


Figure 11.9 Comparison of AURAMS predicted visibility calculations (y-axis) against IMPROVE measurement site data (x-axis) for July 2002.

The visibility output calculated from AURAMS-modelled PM speciation concentrations is evaluated against measurement data collected from the US IMPROVE network to assess the performance of the model and the results for the extinction coefficient (b_{ext}) for July 16th, 2002 (Figure 11.8) and for the month of July 2002 (Figure 11.9). Visibility measurement data from urban sites in the US Speciation Trends Network (STN) were also compared with the AURAMS visibility output (not shown). The predictive ability of the model was lower for urban measurements from the STN sites ($r^2=0.58$) than for the rural IMPROVE sites ($r^2=0.71$) likely due to the differences in the monitoring and data reporting protocols between the networks. The model also exhibits a tendency to underpredict visual range in comparison to the measurement data and this discrepancy is more pronounced in urban areas given the regional grid scale of the AURAMS model. However, there is overall good agreement between the modelled and measured data.

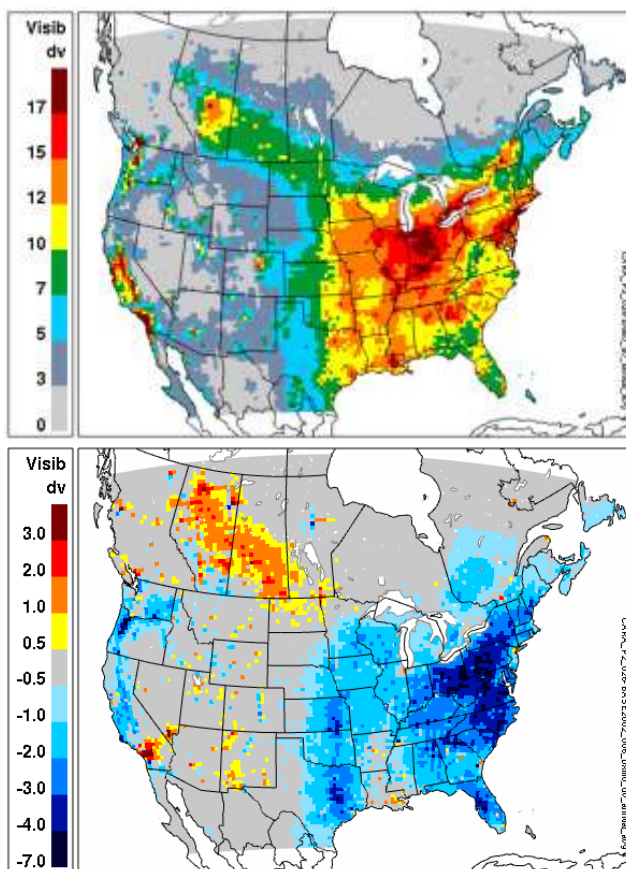


Figure 11.10 Projected annual average levels of visibility in 2015 BAU modelling scenario (top), and the difference in annual average visibility between the 2015 BAU and the 2002 base-case scenarios (bottom).

The output from the regional air quality model AURAMS has been used to predict visibility for the year 2015. The model estimates of visibility from the 2015 business-as-usual (BAU) scenario are compared to a 2002 base-case (refer to Chapter 6 for a complete scenario description) to estimate the potential changes in visibility occurring in the year 2015 (Figure 11.10). The 2015 BAU scenario incorporates emissions projections that are based on Canadian and US official projections and take into account growth and the implementation of regulations that have been promulgated and will be in place by 2015, including the US Clean Air Interstate Rule (CAIR) but not the proposed Clean Air Regulatory Agenda (CARA) for Canada. The results show an overall improvement in visibility across eastern Canada, but a decrease in visibility for some areas within western Canada, including parts of Manitoba, Saskatchewan, northern Alberta and British Columbia. This trend in visibility is the results of emissions changes which are anticipated as part of the 2015 BAU scenario, including large reductions in SO₂ and NO_x emissions due to the implementation of the US CAIR and significant average reductions in Canadian SO₂ and NO_x emissions. Decreases in visibility in western parts of Canada seem to be associated with the occurrence in the model of higher levels of PM_{2.5} in the winter (refer to Chapter 6 for a complete discussion).

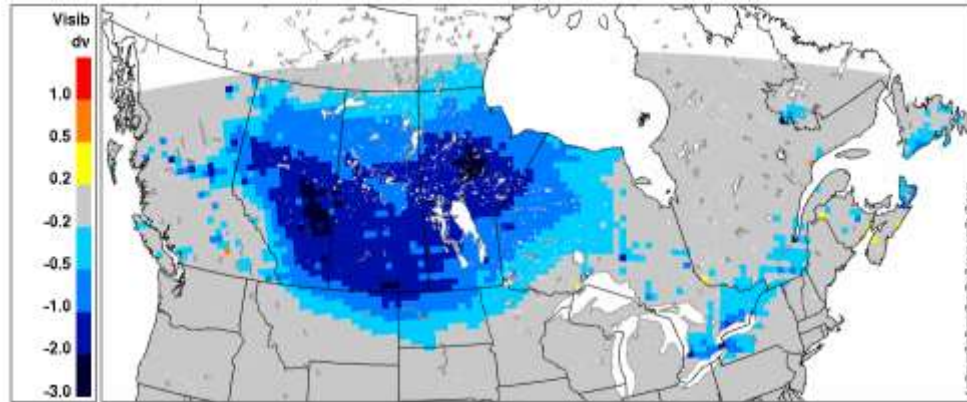


Figure 11.11 Projected difference in the annual average visibility between the 2015 CARA and 2015 BAU emissions scenarios.

The influence on visibility of Canada's proposed Clean Air Regulatory Agenda (CARA), which will result in emission reductions of NO_x , SO_2 , VOCs and primary $\text{PM}_{2.5}$ from industrial sources (see Chapter 6), have also been modelled using AURAMS. Figure 11.11 below presents the difference in annual average visibility between the CARA 2015 and the BAU 2015 emissions projection scenarios. The model results project an improvement in visibility over central and western Canada under the CARA 2015 scenario, relative to the BAU 2015 scenario, which is largely driven by emission reductions in the electricity generation and base-metal smelting sectors. As compared to the 2002 base-case, the industrial sector emission reductions under the CARA 2015 scenario have the potential to offset the predicted decrease in visibility in western Canada that is projected under the BAU 2015 scenario.

Visibility is of particular public interest in the Lower Fraser Valley region of British Columbia. A number of high-resolution model scenario runs have investigated the impact of various emission projections on visibility in this area (RWDI, 2005, 2006). The CMAQ modelling system (see Chapter 5 for a description) was used to simulate a summer (Aug. 9-31, 2001) and winter (Dec. 1-13, 2002) base-cases, which were then compared to the results of a series of emission scenario modelling runs. The results of the base-case model simulations were also compared to visibility measurement data collected with monitoring cameras installed along lines of sight to key landmarks and vistas during the summer and winter base-case periods. An analysis of the base-cases indicates that visibility in the summer ranges from 5 to 45 deciviews with episodic spikes mirroring the $\text{PM}_{2.5}$ concentrations. Visibility in the winter appears more stable with values up to 40 deciviews, but typically varying between 20-30 deciviews. The projected visibility in 2015 was variable in comparison to the base-case, between -6 Dv to +4 Dv during the summer and -8 to +4 Dv during the winter, depending on the day and the line of sight. Further model scenario runs have indicated the importance of the agricultural sector on visibility in the region, and the relatively high influence on regional visibility of Canadian emissions in comparison to US emissions sources.

11.6 Conclusions and Recommendations for Future Research

The NAPS PM speciation measurements were initiated in 2003 and the number of stations has steadily grown. This NAPS network has added greatly to the ability to understand how fine mass and its chemical components behave across specific developed regions of Canada. As a surrogate for direct visibility measurements, these monitors produce quality data for the reconstruction of fine mass. Using the IMPROVE algorithm, reconstructed fine mass demonstrates patterns akin to measured $PM_{2.5}$ at the NAPS stations. Thus, the calculated extinction coefficients and hence, visual range values will demonstrate patterns appropriate for those developed areas being measured.

IMPROVE program scientists parameterized, evaluated, and revised the IMPROVE algorithm using field measurements with specified monitoring protocols and comparisons between direct visibility measurements and PM analyses. In Canada, only the Georgia Basin in British Columbia employs direct visibility measurements for comparison with concurrent PM data; therefore, there is no mechanism possible at present to evaluate the formulae for use in the Canadian context and within the NAPS monitoring protocols. Measures of direct visibility at other NAPS stations would enhance this comparability for the developed areas in Canada. The inclusion of CAPMoN sites will provide some rural regionally representative comparisons. Cross-border comparative studies of technologies and methodology would support knowledge exchange.

Within the NAPS network, measurements at each site include all dominant species, but the minor species are not consistent across the locations. The NAPS PM speciation measurements were not implemented with the intention of measuring and understanding changes in visibility. Using the data from these developed locations to evaluate how well Canadian parks and wilderness areas are being protected is not possible. The variety of ecosystems and range of spectacular scenic vistas associated with the Parks Canada sites of nationally significant Canadian natural and cultural heritage are not covered as the 156 Class I sites are by the IMPROVE sites in the US. The inclusion of optical measurements or scene monitoring (with automated camera systems) could provide information as well as enhance the awareness of visibility in these special areas. In addition, the valuation of visibility in urban centres and wilderness areas could be assessed for more of the country.

The development of visibility modules in regional scale models is a great step forward in providing a national picture of visibility. Modelling is especially useful as a way to estimate visibility in areas currently without a visibility monitoring capacity and as a means to evaluate the impact of potential emission scenarios on visibility. The capability to model visibility for various emission scenarios facilitates the consideration of visibility, along with other air

quality parameters, in policy decision-making processes. Improvements are still needed, however, to address some of the biases in modelled visibility values. Satellite remote sensing may provide some data by which to extend such studies into the remote regions of Canada.



Figure 11.12 Photographs of Toronto featuring a day with $6 \mu\text{g m}^{-3}$ (top panel) and $33 \mu\text{g m}^{-3}$ (bottom panel) (TEOM measurement).

Lastly, the Canada-Wide Standard for $\text{PM}_{2.5}$ is not protective of visibility in pristine environments. This is contrary to the concept of “keeping clean areas clean” as described in the Canada-wide Standard, and which is further demonstrated by projected deterioration of visibility especially in western Canada. Figure 11.12 illustrates photographically the impact of achieving the numerical level of the national standard ($30 \mu\text{g m}^{-3}$) on the vista of Toronto and clearly, the CWS is not capable of preserving visual air quality particularly in pristine environments. Canada has not developed a network explicitly for the characterization of visibility, but data now exist and more are forthcoming that will be able to provide regional and urban characteristics of visibility. The current measurement programs do not provide this information automatically; thus, it will be necessary to establish a mechanism for on-going analyses of data to provide visibility information.

References

- Barna, M.G., Knipping, Eladio M., 2006. Insights from the BRAVO study on nesting global models to specify boundary conditions in regional air quality modelling simulations. *Atmospheric Environment*, 40, 574-582.
- Carrico, C.M., Kreidenweis, S.M., Malm, W.C., Day, D.E., Lee, T., Carrillo, J., McMeeking, G.R., Collett, J.L., 2005. Hygroscopic growth behavior of a carbon-dominated aerosol in Yosemite National Park. *Atmospheric Environment*, 39, 1393-1404.
- Canadian Council of Ministers of the Environment (CCME), 2000. Canada-Wide Standards for Particulate Matter (PM) and Ozone, endorsed June 5-6, 2000, Quebec City. Available online at: http://www.ccme.ca/ourwork/air.html?category_id=99
- Canadian Council of Ministers of the Environment (CCME), 2003. Effects of Ozone on Vegetation: Update in Support of the Canada-Wide Standards for Particulate Matter and Ozone.
- Canadian Council of Ministers of the Environment (CCME), 2007. Government of Canada, Five Year Progress Report, Canada-Wide Standards for Particulate Matter and Ozone, January 2007,
- Available online at: http://www.ec.gc.ca/cleanair-airpur/Reports_and_Publications-WSC9B6CBBA-1_En.htm
- Chow, J.C., Watson, J.G., Lowenthal, D.H., Richards, L.W., 2002. Comparability between $PM_{2.5}$ and particle light scattering measurements. *Environmental Monitoring and Assessment*, 79, 29-45.
- Cocker, D. R., III, Whitlock, N. E., Flagen, R. C., Seinfeld, J. H., 2001. Hygroscopic properties of Pasadena, California aerosol. *Aerosol Science and Technology*, 35, 637-647.
- Copeland, S.A., 2005. A Statistical Analysis of Visibility-Impairing Particles in Federal Class I Areas. *Journal of the Air & Waste Management Association*, 55, 1621-1635.
- Environment Canada (EC), 2004. Canada-United States Transboundary PM Science Assessment: A report by the Canada-U.S. Air Quality Committee, Subcommittee 2: Scientific Cooperation, December 2004, ISBN 0-662-38678-7. Report available online at http://www.msc-smc.ec.gc.ca/saib/smog/smog_e.html

Engling, G., Herckes, P., Kreidenweis, S.M., Malm, W.C., Collett Jr., J.L., 2005. Composition of the fine organic aerosol in Yosemite National Park during the 2002 Yosemite Aerosol Characterization Study, *Atmospheric Environment*, 40, 2959-2972.

Hand, J.L., Kreidenweis, S.M., Slusser, J., Scott, G., 2004. Comparisons of aerosol optical properties derived from Sun photometry to estimates inferred from surface measurements in Big Bend National Park, Texas. *Atmospheric Environment*, 38, 6813-6821.

Hand, J.L., Malm, W.C., 2007. Review of the IMPROVE equation for estimating ambient light extinction coefficients. *Journal of Geophysical Research*, 112, D16203, doi:10.1029/2007JD008484. Also available at: http://vista.cira.colostate.edu/improve/Publications/GrayLit/gray_literature.htm

Hemming, B. L., Seinfeld, J. H., 2001. On the hygroscopic behavior of atmospheric organic aerosols. *Industrial & Engineering Chemical Research*, 40, 4162-4171.

Hess, A., Iyer, H., Malm, W., 2001. Linear trend analysis: a comparison of methods. *Atmospheric Environment*, 35, 5211-5222.

IMPROVE, 2002. Interagency Monitoring of Protected Visual Environments, National Park Service, Fort Collins CO (<http://vista.cira.colostate.edu/IMPROVE>).

IMPROVE, 2006. Spatial and Seasonal Patterns and Temporal Variability of Haze and its Constituents in the United States: Report IV, November 2006, Debell, L.J., Gebhart, K.A., Malm, W.C., Pitchford, M.L., Schichtel, B.A., and White, W.H. Available at: <http://vista.cira.colostate.edu/improve/Publications/Reports/2006/2006.htm>

Iyer, H., Patterson, P., Malm, W. C., 2000. Trends in the extremes of sulphur concentration distributions. *Journal of the Air & Waste Management Association*, 50, 802-808.

Kleeman M., A. Eldering, J. Hall, G. Cass, 2001. Effect of emissions control programs on visibility in southern California. *Environmental Science & Technology*, 35, 4668.

Lloyd, J., 2002. After years of smog, a shroud lifts. *The Christian Science Monitor*. June 4: 1(s. 1).

Lowenthal, D.H., Kumar, N., 2003. PM_{2.5} mass and light extinction reconstruction in IMPROVE. *Journal of the Air & Waste Management Association*, 53, 1109-1120.

Malm W.C., 2000. Introduction to Visibility. Cooperative Institute for Research in the Atmosphere (CIRA), Ft. Collins, Colorado. pp. 70

Malm, W. C., Day, D. E., Kreidenweis, S. M., 2000a. Light scattering characteristics of aerosols as a function of relative humidity: part I—a comparison of measured scattering and aerosol concentrations using the theoretical models. *Journal of the Air and Waste Management Association*, 50, 686-700.

Malm, W. C., Day, D. E., Kreidenweis, S. M., 2000b. Light scattering characteristics of aerosols as a function of relative humidity: part II—a comparison of measured scattering and aerosol concentrations using the statistical models. *Journal of the Air and Waste Management Association*, 50, 701-709.

Malm, W.C., Day, D.E., Kreidenweis, S.M., Collett, J.L., Carrico, C., McMeeking, G., Lee, T., 2005a. Hygroscopic properties of an organic-laden aerosol. *Atmospheric Environment*, 39, 4969-4982.

Malm, W.C., Day, D.E., Carrico, C.M., Kreidenweis, S.M., Collett Jr., J.L., McMeeking, G., Lee, T., Carrillo, J., Schictel, B.A., 2005b. Inter-comparison and closure calculations using measurements of aerosol species and optical properties during the Yosemite Aerosol Characterization Study, *Journal of Geophysical Research*, 110, D14302, doi:10.1029/2004JD005494.

McDonald, K., 2002. Review and Characterization of Visibility Impacts Related to Particulate Matter in Canada, En40-773/2002E-IN, ISBN 0-662-33118-4.

McMeeking, G.R., Kreidenweis, S.M., Carrico, C.M., Lee, T., Collett Jr., J.L., Day, D.E., Malm, W.C., 2005a. Observations of smoke influenced aerosol during the Yosemite Aerosol Characterization Study: 1. Size distributions and chemical composition. *Journal of Geophysical Research*, 110, D09206, doi:10.1029/2004JD005389.

McMeeking, G.R., Kreidenweis, S.M., Carrico, C.M., Lee, T., Collett Jr., J.L., Day, D.E., Malm, W.C., 2005b. Observations of smoke influenced aerosol during the Yosemite Aerosol Characterization Study: 2. Aerosol scattering and absorbing properties, *Journal of Geophysical Research*, 110, D18209, doi:10.1029/2004JD005624.

McMeeking, G.R., Kreidenweis, S.M., Lunden, M., Carrillo, J., Carrico, C.M., Lee, T., Herckes, P., Engling, G., Day, D.E., Hand, J., Brown, N., Malm, W.C., Collett, J.L., 2006. Smoke-impacted regional haze in California during the summer of 2002. *Agricultural & Forest Meteorology*, 137, 25-42.

McMurray, P.H., 2000. A review of atmospheric aerosol measurements. *Atmospheric Environment*, 34, 1959-1999.

Pitchford, M., Malm, W., 1994. Development and applications of a standard visual index, *Atmospheric Environment*, 28, 1049-1054.

Pitchford, J., Malm, W., Schichtel, B., Kumar, N., Lownethal, D., Hand, J., 2007. Revised algorithm for estimating light extinction from IMPROVE particle speciation data. *Journal of the Air & Waste Management Association*, 57, 1337-1350. Also available at: http://vista.cira.colostate.edu/improve/Publications/GrayLit/gray_literature.htm

Ryan, P.A., Lowenthal, D., Kumar, N., 2005. Improved light extinction reconstruction in Interagency Monitoring of Protected Visual Environments. *Journal of the Air & Waste Management Association*, 55, 1751-1759.

RWDI, 2005. The Pacific Northwest Air Quality Scenarios Modelling PNW CMAQ Scenarios Report, Project Number W04-227, Environment Canada – Pacific & Yukon Region, prepared by RWDI Air Inc., May 20, 2005.

RWDI, 2006. The Pacific Northwest Air Quality Scenarios Modelling PNW CMAQ Scenarios 2 Report, Project Number W06-5097A, Environment Canada – Pacific & Yukon Region, prepared by RWDI Air Inc., June 13, 2006.

Schichtel, B., Husar, R., Falke, S., Wilson, W., 2001. Haze trends over the United States, 1980-1995. *Atmospheric Environment*, 35, 5205.

Schichtel, B.A., Barna, Michael G., Gebhart, Kristi A., Malm, William C. (2005a) Evaluation of a Eulerian and Lagrangian air quality model using perfluorocarbon tracers released in Texas for the BRAVO haze study. *Atmospheric Environment*, 39, 7044-7062.

Schichtel, B.A., Gebhart, K.A., Malm, W.C., Barna, M.G., Pitchford, M.L., Knipping, E.M., Tombach, I.H., 2005b. Reconciliation and Interpretation of Big Bend National Park Particulate Sulphur Source Apportionment: Results from the Big Bend Regional Aerosol and Visibility Observational Study--Part I. *Journal of the Air & Waste Management Association*, 55, 1709-1725.

Schichtel, B.A., Gebhart, K.A., Barna, M.G., Malm, W.C., 2006. Association of air mass transport patterns and particulate sulphur concentrations at Big Bend National Park, Texas. *Atmospheric Environment*, 40, 992-1006.

Smith, A. E., Kemp, M.A., Savage, T.H., and Taylor, C.L., 2005. Methods and results from a new survey of values of eastern regional haze improvements. *Journal of the Air & Waste Management Association*, 55, 1767-1779.

Turpin, B.J., Lim, H.-J., 2001. Contributions to PM_{2.5} mass concentrations: revisiting common assumptions for estimating organic mass. *Aerosol Science & Technology*, 35, 602-610.

USEPA, 1999. Federal Register, 40 CFR Part 51, Regional Haze Regulations, Final Rule, July 1, 1999. <http://www.epa.gov/air/visibility/actions.html#1999rule>

USEPA, 2001. Air Quality Criteria for Particulate Matter, U.S. Environmental Protection Agency, Report Number: EPA 600/P-99/002aB.

USEPA, 2004. United States Environmental Protection Agency, Air Quality Criteria for Particulate Matter, Volume I, EPA/600/P-99/002aF, October 2004.

http://www.epa.gov/ttn/naaqs/standards/pm/s_pm_cr_cd.html

Staff Paper: http://www.epa.gov/ttn/naaqs/standards/pm/s_pm_cr_sp.html

Technical Documents: http://www.epa.gov/ttn/naaqs/standards/pm/s_pm_cr_td.html

USEPA, 2006. Federal Register, 40 CFR Part 50, National Ambient Air Quality Standards for Particulate Matter: Proposed Rule, January 17, 2006.

http://www.epa.gov/ttn/naaqs/standards/pm/s_pm_cr_fr.html

Watson, J.G., 2002. Visibility: Science and Regulation. *Journal of the Air & Waste Management Association*, 52, 628-713.

CHAPTER 12: Quantification of Social and Economic Impacts of Smog

Timothy Folkins

Contributing Authors: Yves Bourassa, Michael Donohue, Jean-Sébastien Landry, Robyn Rittmaster, and Dave Stieb

KEY MESSAGES AND IMPLICATIONS

- Economic valuation permits quantification of different environmental and human health impacts using a common scale that reflects the preferences of Canadians, in turn helping to develop programs that strike an efficient balance between different social, economic, and environmental concerns.
- The negative socio-economic impacts of smog are wide-ranging. In the past, most of the attention has been focused on how smog impacts the health of Canadians. Impacts can be quantified based on factors such as medical treatment costs, lost worker productivity, and the willingness of individuals to pay to reduce the risks they face, such as increased risks of premature mortality and other health effects that decrease the quality of life for Canadians.
- Smog also decreases the welfare of Canadians in non-health-related areas. These include reduced growth of crops and trees, impaired visibility, increased cleaning costs and material damages, as well as impacts on ecosystem services.
- Only a portion of the total impact of smog has currently been quantified through economic valuation. Methodologies for valuation continue to be developed and are becoming more standardized. Further research into both the scientific basis underlying physical drivers of smog's impacts and how these impacts are valued by Canadians will deepen our understanding of how to formulate effective and efficient smog abatement policies.

12.1 Introduction

12.1.1 The Role of Valuation of Socio-Economic Impacts in Smog Abatement Strategies

While we know that smog-causing pollutants have a negative influence on our lives, reducing their levels to zero may not be realistic. There may be significant trade-offs involved with the removal of all negative impacts of smog. For example, the abatement of emissions that cause

smog often comes at a cost of lost production and income, offsetting some of the benefits of improved environmental quality. The crucial policy question then is not “how do we stop pollution?” or even “what pollution level will avoid all damages?”, but rather “how can environmental, social, and economic priorities be best balanced, in order to benefit Canadians?” It is into this question that economics and valuation are particularly well suited to provide insight.

While some believe that economics is the study of business and money, at its core economics is actually a study of decision making, about how to best meet the seemingly unlimited needs and wants of a society living in a world with limited resources. In the context of smog policy, these decisions often involve trade-offs between what is considered to be the natural condition of the environment⁴¹ and the costs of restricting activities that cause air pollution. While humankind’s very existence necessarily affects the environment to some degree, environmental economics recognizes that people should act in such a way that balance is achieved. This balance upholds the three pillars of sustainable development comprising the environment, the society, and the economy. These form the base on which long-term improvements in quality of life are built, ensuring that the needs of the present generation are met without compromising the ability of future generations to meet their own needs (World Commission on Environment and Development (Brundtland Commission), 1987).

To attain the balance required to achieve sustainable development, we need a scale on which to weigh the costs and benefits of a decision. Only by having a means to measure the impacts of our decisions can we determine whether limited resources are being used in an optimal manner. While economics is not about money *per se*, it uses money as its scale, with currency acting as a proxy measurement of welfare and value. Because not all things of value are bought and sold on markets, economics makes use of special valuation techniques to assign a monetary value to things that do not have a market value in a way that is meaningful and allows for comparisons.

It is in this way, using standardized methodologies supported by sound scientific research to gauge impacts through a common scale, that economic valuation can play a key role in smog abatement policy. It provides guidance and allows for a more thorough appreciation of the benefits of controlling smog-causing emissions, which can then be compared to the costs of

41 Throughout this chapter, unless otherwise noted, the word “environment” is used to mean the natural environment and the man-made infrastructure.

such control. Comparing benefits and costs in this way allows for the development of policies that are economically efficient, that is, policies which achieve the largest net benefit. However, net benefits are not the only input to decision making. Issues such as the fairness or equity of a policy also need to be considered in policy development. Identifying and quantifying benefits and costs is critical for both achieving economic efficiency and uncovering possible equity concerns.

12.1.2 Organization of Chapter

The chapter outline is as follows: an overview of economic valuation — what it is, why it is needed, and the techniques commonly used to estimate economic value (section 12.2); a discussion on valuation of smog's environmental impacts, including effects on agriculture, forestry, visibility, and others (section 12.3); a section on the valuation of the health impacts of smog (section 12.4); and, finally, conclusions and recommendations (section 12.5).

12.2 Overview of Economic Valuation

The economic value of an item, service, or preferred outcome (in this chapter collectively referred to as a “good”) is associated with the benefit, or utility, derived from it. Value is measured in terms of exchange, meaning that the value of a good is signified by what someone is willing to give up to acquire it. Because currency is a universal unit of exchange, it is useful to measure value in dollars.

Although economic value is measured in dollars, it is not analogous to price. People who purchase a good do so because they expect its value to exceed its price, or at least equal it. In general, economics assumes that each successive purchase of a good provides less value than the previous ones. For instance, people receive more value from the purchase of their first television than they do from their second, than from their third, and so on. Subject to income limitations, a person will buy more of a good until its expected added value is less than its price.

The surplus to the consumer is the difference between the value of the good for the consumer and the (usually lower) market price at which he bought it. Similarly, the surplus to the producer is the difference between the price at which the producer would have accepted to sell the good and its (usually higher) market price. All consumers and producers surpluses together represent the net social welfare (*i.e.* total social benefits minus total social costs of consumption and production in a society). In a properly behaving market, the net social value is maximized. When market exchanges of a good produces environmental degradation that negatively impacts third parties and that is not accounted for in the market price of the good, an externality (market failure) is said to exist. If the externality was accounted for in the price

of the good (*i.e.* if an amount was added to the price of the good that compensated those negatively impacted by the environmental degradation), there would be less of the polluting good produced and an overall increase in net social value would result.

In a properly behaving market, price thus not only acts as an indicator of value, but it also limits wasteful overconsumption. However, there is often no market for and thus no price signal assigned to environmental degradation. This means that, without government intervention, industries and individuals will engage in activities that cause environmental degradation, such as air pollution, well past the point that is optimal. When this arises because of people using a shared resource for which ownership is not defined, such as air, then the resulting inefficient overexploitation of resources is commonly referred to as the tragedy of the commons, a concept popularized by Garret Hardin (1968).

The goal of economic valuation is to estimate in dollar terms, often in the absence of a market, the net value of the benefits gained or lost from a particular choice. These values can be used as a means to assess and compare the trade-offs that occur when implementing available options. For example, suppose a government is considering a pollution abatement policy that would reduce smog, thereby improving the health of Canadians and the overall productivity of ecosystems; however, as a result of the policy, a doubling of the price of electricity would occur, lowering disposable income and increasing production costs. Given this trade-off, how would a policy maker decide whether to adopt the policy or not? Even if it was thought to be a beneficial policy, how would one compare it to other policies that might achieve a similar outcome? By using economic valuation techniques, the aforementioned outcomes could be put into dollar terms, making the costs and benefits of policies easier to compare and assess.

The total economic value (TEV) is a key concept to understanding changes in well-being due to a project or policy targeted at lowering smog. Essentially, this concept recognizes that people can derive value in many different ways, and it applies equally to both market and non-market goods. For instance, a person who purchases a famous sports car receives value above the ability to be transported from point (a) to point (b) at posted speeds. While a car is mostly associated with providing a means of transportation, if this was the sole source of value then other lower priced options would be preferred. So why are some people willing to pay more for a sports car? There are many reasons, mainly to do with the fact that a car is valued for benefits other than transportation. Even if the person is a law-abiding citizen and never drives the car to its maximum speed, simply knowing that he could go 300 kph has value. The owner may also value a branded luxury item because it conveys a message that he is wealthy and successful.

While the price of a market good usually captures many of the different sources of values contained within the total economic value, valuation of non-market goods is more complex. For instance, if a sports car were not a market good, we might be tempted to estimate its value as a means of transport alone and equate its value to that of an economy-class car. When

estimating economic value of non-market goods, one must consider all the sources of value. For instance, how does a hiker value a tree compared to a bird watcher, a logger, or a parent? The hiker may value the aesthetics of the tree, the bird watcher the habitat it provides that attracts birds, the logger the timber from the tree, and a parent the future enjoyment that it will provide for a child. Accounting for only one or two of these different types of value may result in a less than optimal outcome. However, it should be understood that all the different values cannot always all be added together. For example, the logging value of a specific tree should not be considered at the same time as its habitat for birds' value.

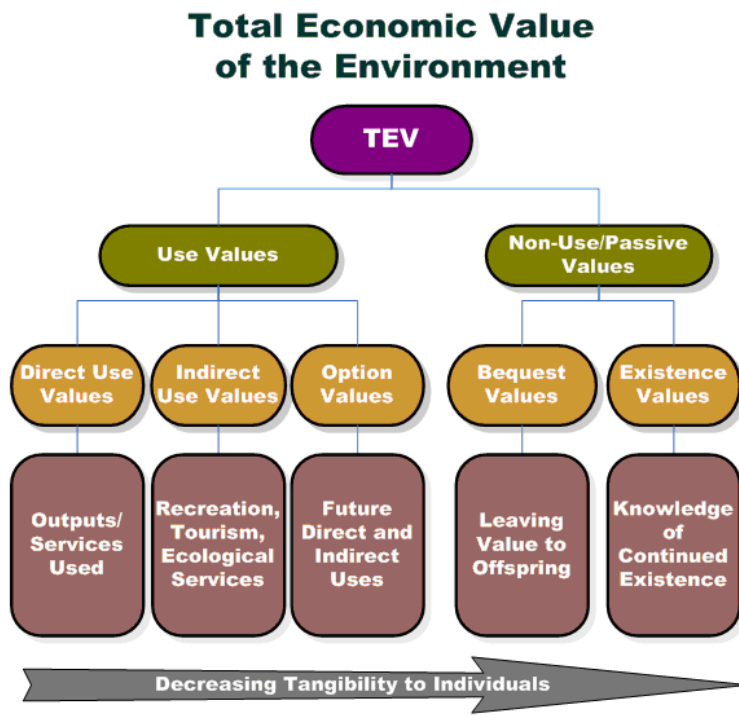


Figure 12.1 Values that comprise the total economic value, or TEV, of the environment.

Figure 12.1 shows how total economic value can be broken down. The total economic value of a resource comprises use values and non-use values (or passive use values). Use values include direct use, indirect use, and option value. Direct use involves the consumption of a resource, as occurs in logging or mining. Indirect use is the non-consumptive use of a resource, such as some tourism activities and ecosystem services. Option value exists when people do not currently use a resource, but wish to be able to use it in the future either directly or indirectly; this concept can be useful in decision making that involves irreversible conditions. Non-use values are subdivided into bequest value and pure existence value. Bequest value means that people want to leave the environment for the enjoyment of future generations. Pure existence value occurs when individuals value the environment for its own sake, irrespective of any present or future use by human beings. Note that there are other common ways to classify environmental values, each one with its own strengths and weaknesses. The point of these visualization tools is to help analysts identify all the sources of value.

The economic concepts of value and total economic value have precedents in law within Canada, as verified by the Supreme Court.⁴² On June 11, 2004, the Supreme Court made a ruling that recognized that environmental assets can have a value greater than their market value. It also recognized that a number of economic methods could be used to establish non-market values for the purpose of estimating damages. The *Canadian Cost-Benefit Analysis Guide* provides information about such economic methods to federal departments and agencies to help them perform cost-benefit analysis in support of regulatory decisions (Treasury Board of Canada Secretariat, 2007). In the United States, federal agencies have been using non-market valuation for three decades to provide economic advice, the Environmental Protection Agency is required to perform cost-benefit analysis of environmental regulation, and courts have recognized the use of environmental valuation, including for existence value (Loomis, 2005).

12.2.1 Willingness to Pay

A measure that underpins the economic theory of value is the willingness to pay (WTP). It is defined as the maximum amount an individual is willing to pay to acquire some good.⁴³ It is essentially a measure of the value of particular attributes of the total economic value of a good. The key idea is that if something has value to people, then people should be prepared to make

⁴² The precedent-setting case concerned a 1992 fire that destroyed an Environmentally Sensitive Area in northern British Columbia. The B.C. Government sued the company responsible for the damages and the lower court awarded one third of the market price of the timber. The B.C. Government appealed the case to the Supreme Court of Canada, and the case was heard in October 2003. The Government of Canada was asked by the B.C. Government to intervene, and Environment Canada collaborated with the Department of Justice to prepare a factum that was presented during the hearing. Environment Canada's input used the total economic value framework and suggested that the Environmentally Sensitive Area should be valued using modern economic valuation techniques, approaches, and theory, which ascribe values beyond commercial or market value.

⁴³ There is considerable research on valuation that also deals with the concept of willingness to accept and how it differs from willingness to pay. Willingness to pay attempts to measure how much a person would pay to receive a beneficial outcome, whereas willingness to accept measures how much a person would accept in compensation for a negative outcome. For instance, revealed preference based on wage-risk studies, to be discussed later in this chapter, is based on willingness to accept and not willingness to pay. While theoretically the two concepts are distinct, in this chapter the term "willingness to pay" will be used to refer to both. However, the two can be perceived very differently as has been revealed by empirical analysis, especially when changes are extreme or when a given state of the environment has come to be considered as an entitlement. When possible, the literature recommends the use of the willingness to pay in order to present conservative estimates (Arrow *et al.*, 1993).

sacrifices or trade-offs to obtain it. This idea applies both to environmental resources like air quality and to market goods. It is important to recognize that willingness to pay as a measure of value is anthropogenic: its use assumes that environmental resources only have value from the point of view of humans. If an outcome is not considered to affect humans in some way, by this measure, its value is zero. Now, the impact does not need to be physical and can be an emotion, like the one coming from a beautiful sunset.

Willingness to pay is the approach to defining the value of a particular trait of a good, but not the method itself. The methods that are used to measure value, often as represented by willingness to pay, are discussed in further detail in the following section and are called “valuation techniques”.

12.2.2 Valuation Techniques

A variety of techniques can be used to value pollution’s effects on environmental (health and non-health) endpoints (*e.g.* the amount of wheat produced in a given region). As noted earlier, price and value are generally not exactly equivalent; however, price can be a good indicator of marginal changes in value. Therefore, when smog results in damage to a good sold on the market, an estimate of marginal damages can be based on observed market changes, such as changes in prices and quantities. Typical approaches include measuring changes in productivity and in net income of an industry, the cost of illness, as well as estimating replacement costs. These techniques all rely on market observations directly related to the marketed environmental good.

When pollution affects non-traded environmental endpoints, economic valuation can be more challenging. The absence of a market means that prices are not readily available as a proxy of marginal changes in value. Without such information, alternative methods are required to infer value. The two main approaches used by economists to accomplish this are revealed preferences and stated preferences.

12.2.2.1 Revealed Preferences

The revealed preferences approach looks at the market choices that people make and infers from those choices a value that consumers place on some other non-marketed attribute. For instance, the additional money a buyer will pay for an equivalent house with a nicer view can be used as an indication of the value a buyer places on visibility. While the revealed preferences approach has drawbacks, its main advantage is that it is based on actual behaviour rather than on hypothetical activities or scenarios.

Techniques to assess revealed preferences include the travel cost method, hedonic wage method, and averting behaviour. For example, the hedonic wage method evaluates the additional compensation required for individuals to work in riskier jobs. Each of these methods is based on a different theory and has advantages and disadvantages that may make one more appropriate than others in the valuation of a specific environmental good. However, all these approaches use market information and/or observed behaviour to assign a value to an associated non-market outcome.

To many economists, the fact that they are based on actual behaviour makes revealed preferences preferable to stated preferences. In reality, the relative merit of these methods depends on the specific application because the revealed preferences approach has several drawbacks. First, it can be challenging to isolate a particular attribute of interest, such as visibility, from a behaviour that is based on a number of characteristics. Second, it is extremely difficult to rely upon revealed preferences to estimate the non-use values that people attach to certain environmental goods.

12.2.2.2 Stated Preferences

The difficulties of the revealed preferences approach to estimate non-use value is one of the main reasons why the stated preferences approach has become a common technique for estimating the value of non-market environmental endpoints. At the most basic level, the stated preferences approach involves simply asking people how much they value a change in a particular environmental good, through a survey. The two basic stated preferences methods, which are the contingent valuation and the contingent choice, are among the most popular survey techniques, and have been widely used according to the environmental valuation literature. Contingent valuation surveys ask respondents to value an environmental good, whereas contingent choice surveys ask respondents to choose which of several scenarios they prefer.

Although the stated preferences approach is considered by some to be controversial, it continues to gain acceptance as a valid approach for estimating the value of non-market impacts (OECD, 2006). Some of the basis for the movement towards acceptance of this approach came from the special panel appointed by the U.S. National Oceanic and Atmospheric Administration (NOAA) in 1993 (Arrow *et al.*, 1993) following the *Exxon Valdez* oil spill in Alaska in 1989. The panel concluded that stated preferences studies could produce estimates reliable enough to be used in a judicial process of natural resource damage assessment.

On the whole, developments in stated preferences research overwhelmingly point to the conclusion that studies using a sound methodology provide results that are both valid and reliable. However, the fact that a wide variety of methods are used in such studies, not all of

information from several studies to develop a more complete picture of values to apply in benefits transfer (see section 12.2.2.3), contributing to a more consistent body of research in the future. Despite improvements, the main drawback of the stated preferences approach still holds, *i.e.* it is less certain that responses reflect actual behaviour in comparison to the revealed preferences approach.

12.2.2.3 Benefits Transfer

The benefits transfer method is the procedure of transferring value estimates of non-market goods derived from primary valuation studies to estimate the value of other non-market goods in a different but similar context. Since the costs of primary valuation studies are typically high in terms of data, expertise, and time needed, the benefits transfer method has been developed to take advantage of existing results.

Benefits transfer is based on the creation of an analogy between the study case, or the conditions under which the data were obtained, and the policy case, where the data are to be applied to a new valuation. The unadjusted willingness to pay transfer assumes perfect analogy between the study and the new valuation. In the unadjusted benefits transfer, the average per capita or per household measure of willingness to pay from the primary study is multiplied by the relevant population size at the policy case, leading to an estimate of aggregated benefits. If there are divergences between the study case and the policy case, such as socio-economic differences or differences in the possibility of recovering lost uses, the unadjusted benefit transfer will result in a biased view of the true value of the benefits in the policy case.

Although making use of more sophisticated transfer techniques leads to more accurate benefits estimates, their reliability will always be bounded by the accuracy and adequacy of the original estimates. Hence, the first step in conducting a benefits transfer is to review all existing primary studies to appraise the valuation methodology used and to analyze the information regarding the baseline and the change expected with regard to the non-market good, as well as the study characteristics. The cost of searching for primary valuation studies has been reduced with the creation of the Environmental Valuation Reference Inventory (EVRI)⁴⁴ database, which stemmed from an international initiative to facilitate the use of benefits transfer.

⁴⁴ The Environmental Valuation Reference Inventory is an online database available at <http://www.evri.ca>. Free access is provided to all member countries' residents, including Canadians.

12.2.3 From Emissions to Economic Valuation

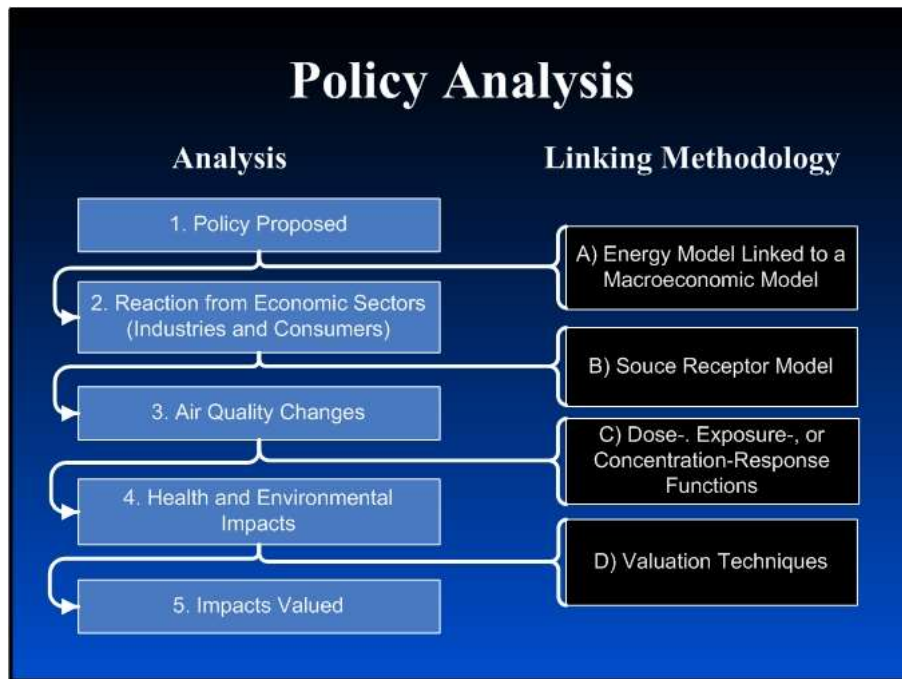


Figure 12.2 Steps in the damage function approach to policy analysis.

Most environmental valuation studies of smog-related outcomes closely follow the analytical steps of the generic damage function approach, as illustrated in Figure 12.2. The damage function approach has been used for many types of air pollution policy assessments and is generally regarded as the preferred approach for computing benefits where the required literature and data are available and can be cost-effectively applied (Freeman *et al.*, 1994). While the damage function approach is the most commonly used and conducive to assess marginal changes between air quality scenarios, other approaches also exist. For example, the defensive expenditures approach would consider the costs of mitigating the impacts of pollution rather than the direct damages resulting from it.

In order to do a policy assessment, the damage function approach must consider at least two scenarios. The first scenario, often referred to as the business-as-usual scenario, considers conditions that will exist under current or fully anticipated policies only and forms the standard of comparison. This scenario is then compared to at least one other policy scenario in which the government takes new action to influence activities in such a way as to reduce pollution that contributes to the formation of smog.

In order to estimate how a policy will change emissions, the way industries and consumers respond needs to be modelled. This is a complex process that is usually accomplished by using models of the economy and energy use. The next step in the analysis is to determine the air quality conditions that result from emissions, using an air quality model.

Then, in order to estimate the impact of air quality on some environmental endpoint, a clear relationship between the two needs to be identified and defined based on scientific research. For example, impacts on health are usually verified and estimated based on statistically derived epidemiological studies. These relationships are referred to as dose-response functions, exposure-response functions, or concentration-response functions.⁴⁵ Concentration-response functions for health outcomes are based on risk assessment and relate increases in concentration of an air pollutant to increases in the probability of a specific health outcome, such as an asthma attack. Once these functions are combined with air quality levels and exposed populations, estimates of expected impacts can be made. A similar process is also used for non-health impacts, such as the effect of ozone on plants.

The final step of the damage function approach is to value the actual impacts using the methods already described. While health impacts directly influence human welfare, impacts on the environment require further consideration to discern in what ways these changes affect human welfare. After these impacts have been valued for both the business-as-usual scenario and the policy scenario, the two cases are compared to determine the net benefit of the policy. If this information is to be used as part of a cost-benefit analysis, the benefits will need to be aggregated in a common metric across the relevant areas and time frame, in a similar way as the costs have been aggregated.

12.2.4 A Common Scale — Adjusting for Time, Risk, and Uncertainty

As mentioned, economic value is measured using currency in order to allow for aggregation and comparison of various outcomes. To have a truly equal scale requires that we adjust for outcomes by time scale and degree of certainty.

⁴⁵ Although those three expressions have a similar meaning and are often used interchangeably, there is in fact a conceptual difference between them. “Dose” refers to the level of pollutant that is actually absorbed by an organism, “exposure” refers to the level of pollutant to which an organism is actually exposed, and “concentration” refers to the ambient level of pollutant in a given environment.

12.2.4.1 Adjusting for Time

According to the investment theory, receiving a benefit today is considered better than receiving the same benefit next year, which is better than receiving it ten years from now. In order to compare different benefits that spread over many years, we thus need to know *how much* better it is to receive a benefit today, rather than in one or ten years. The concept of present value represents today's value of a benefit or a series of benefits occurring in the future. The same concept also applies to costs, and the difference between the present value of benefits and the present value of costs gives the net present value.

Discounting is the procedure that is used to estimate future values in today's terms. Discounting, in its simplest form, applies a percentage reduction (usually expressed as an annual rate) to the value of the benefit or cost for every time period in the future in which it occurs. This percentage reduction is termed the discount rate.

The discount rate can be one of the primary variables that determine the economic viability of a policy. Discount rates are especially important for projects with high upfront costs and where benefits occur in the future. For example, to use a 10% discount rate in a cost-benefit analysis is to assume that it is not worth investing more than ~\$150,000 on smog abatement today to avoid \$1 million in damages 20 years in the future.

Now, the concept of net present value is particularly useful and appropriate from the perspective of an investor trying to find the best way to use his limited resources, but the extent to which it should be used in public policy is debatable. Some people, including some economists, argue that present generations have the moral obligation to protect the interests of future generations and that significantly discounting the needs of future generations is inappropriate. These arguments are often used to support very low discounting rates or even negative discount rates. This view can be seen in recent reports such as the Stern (2006) review on the *Economics of Climate Change*, which used a discount rate of 0.1%. While there are some compelling ethical arguments against discounting, the opportunity cost of capital suggests that a positive discount rate better reflects societal preferences. In fact, the implication of a non-positive discount rate is that each successive generation should impoverish itself for the benefit of future generations (Koopmans, 1965). As this is inconsistent with what we would consider a realistic policy objective, it is recommended that all discount rates used in smog valuation be positive. For long-term social or environmental analyses, it is nevertheless common to use discount rates substantially lower than those used for short-term financial analyses.

12.2.4.2 Adjusting for Risk and Uncertainty

It is often necessary to adjust and/or qualify values that are of a risky or uncertain nature to properly communicate a range of possible outcomes. The notions of risk and uncertainty relate to a probabilistic conception of the future and can be used to refer to both beneficial and harmful events. Risk is the combination of probability that a given event will occur and the consequences of that event. Uncertainty refers to the quality of our knowledge about the risk (Jones *et al.*, 2004).

There are a number of ways to represent risk and uncertainty in a valuation assessment. Uncertainty can be characterized by sensitivity analysis, in which key variables are given a number of values to see how they impact the result. Sensitivity analysis is often used to express uncertainty about the proper discount rate to apply. Using the interval analysis method, extreme values of all relevant parameters are used to define extreme upper and lower limits.

Valuation based on various possible outcomes can be reported as an expected outcome. Here, all possible outcomes are combined into a weighted average determined by their probability of occurrence. Expected outcomes are often a good way to represent a central value, but can be deceptive on their own as the expected outcome reported may itself have a zero probability of occurrence.

Another common method used to assess the impacts of parameters that have an element of uncertainty is the Monte Carlo simulation. The Monte Carlo simulation generates values for the uncertain parameters of a model by making iterative random draws from series of probability distributions. Solving the objective function for each iteration then yields a set of data points that exemplify the range and likelihood of possible outcomes.

12.3 Valuation of Environmental Smog Impacts on the Welfare of Canadians

Smog has a range of effects on Canadians. Although reduced well-being caused by smog-induced health impacts is important and will be discussed later on in this chapter, it should not overshadow the significant impacts that smog has on our environment. Smog reduces the growth of crops and trees, decreases our enjoyment of picturesque views, and soils our homes and places of work. Valuation of these impacts presents unique challenges and requires the use of all of the methodologies and concepts discussed in the previous section.

12.3.1 Ozone Impacts on Crops

As discussed in the chapter on smog impacts on vegetation (Chapter 10), it has been well documented that some crops are very sensitive to elevated levels of tropospheric ozone (O_3). Various scientific research programs, such as the U.S. Environmental Protection Agency's National Crop Loss Assessment Network (NCLAN) (Heck *et al.*, 1984), have established negative relationships between elevated levels of O_3 and crop yields, which have formed the basis for O_3 exposure-response functions. These have been estimated and derived from regressions in which the dependent variable is associated with yield, and one of the independent variables is a metric of O_3 exposure.

12.3.1.1 Valuation of Ozone Impacts on Crops

The agriculture and agri-food system as a whole is a significant contributor to the Canadian economy, accounting in 2004 for 8.1% of total GDP and 13% of employment (Agriculture and Agri-Food Canada, 2006). Crop production makes up a considerable portion of this contribution.

In a valuation of the damage to Canadian crops due to O_3 , the starting point is the relationships contained within the exposure-response functions. However, before these can be applied, several more pieces of information are required. In order to estimate the actual reduction in crop production, information is needed on the number of hectares planted for each crop and on the tonnes of crop produced when a hectare of crop is seeded (the yield). Finally, a methodology to assign a dollar amount to marginal changes in crop damages is required.

Combining the above information and using prices to estimate marginal damages can give an indication of possible benefits of reduced damage from O_3 . However, for more precise estimates, one must consider that O_3 primarily impacts crop productivity, which may or may not increase long-term production levels. Actual crop output is determined by a number of inputs in addition to clean air, such as land, fertilizers, agrochemicals, and climatological factors. A decrease in O_3 levels is equivalent to an increased endowment of one factor of production for farmers. In response to this increased endowment, farmers are likely to vary the amount and proportion of other factors of production to maximize their expected returns, given market conditions. Fundamentally, this increased endowment of clean air shifts the supply curves of crops. Depending on an individual crop's relationship between its price and its availability on the market, this can also imply a price change. For crops that are sold internationally, prices are likely to be fixed based on international rates and are not likely to change in response to small variations in domestic production. However, for locally marketed crops, increases in supply may result in price decreases. While a producer's revenues may increase or decrease as a result of the combination of increased production and lower prices, consumers will unambiguously benefit. Overall, the effect on Canadians' net social welfare would be positive.

To estimate how a policy introduced to lower O₃ will reduce damage to crops in Canada, the Value of Ozone Impacts on Canadian Crops Estimator (VOICCE) model has been developed by Environment Canada (Environment Canada, 2007). The model works by using various measures of O₃ levels applied to available exposure-response functions and historical information from the 82 census agricultural regions of Canada to estimate resulting changes in yields of major crops. This information is then used to estimate the value of damages compared to a business-as-usual case. To further refine the VOICCE methodology, Environment Canada has been exploring options that would link changes in productivity to a more comprehensive Canadian agricultural model. Linking to such a model would allow better understanding of direct impacts of increased supplies of crops on consumer and producer surpluses and indirect cross-industry impacts.

12.3.1.2 Illustrative Valuations

There have been many studies of the economic effects of reduced agricultural production due to O₃ air pollution (Spash, 1997). However, most of those estimated regional impacts and relatively few estimated national impacts for Canada.

In an Ontario study, Pearson and Donnan (1989) estimated that, if its levels were to increase by 40 parts per billion, O₃ would cause damage to major crops such as wheat, corn, soybeans, and vegetables, estimated at an average annual value of \$44.5 million. Another study (Ontario Ministry of the Environment, 2005) estimated that smog created through human activity causes \$201 million in damages annually in Ontario for select crops. A recent analysis using the VOICCE model (Environment Canada, 2007) indicated that reduced levels of O₃ from a proposed regulatory framework for air emissions would reduce damages to key agricultural crops by an estimated \$123 million. This included substantial reductions in damages to soybeans within the southern and western agricultural regions of Ontario (~\$20 million) and to spring wheat throughout the Prairie provinces (~\$60 million).

Outside Canada, some national models also exist for the United States (Kopp *et al.*, 1985, Adams *et al.*, 1986, and Adams and Crocker, 1989). These national studies generally have found that a 25% reduction in ambient O₃ would provide benefits of at least 1 – 2 billion USD annually (Adams and Crocker, 1989). A similar study (Murphy *et al.*, 1999) estimated that in 1990, smog was responsible for 2.8 to 5.8 billion USD in damages to eight major crops in the United States. This same study estimated that emissions from motor vehicles alone contributed to about 2 – 3 billion USD of this damage. Holland *et al.* (2002) estimated smog damages to European crops at £4.3 billion. France was estimated to experience the greatest losses at £1.1 billion, followed by Germany, Ukraine, Italy, and Poland.

No studies have been found that assess the impacts of smog on producer or consumer surplus; this may be an important area for further research. Another possible future direction for research would be the development of computable general equilibrium (CGE) models, which would help to better evaluate the provincial and national economic consequences of changes to crop harvests due to O₃ exposure in Canada.

12.3.2 Ozone Impacts on Forests

The physical impacts of O₃ on trees start at the chemical level with negative effects on the photosynthetic process, which contribute to decreased growth in tree volume and biomass (Karnosky *et al.*, 2005). The correlation between decreased biomass and O₃ exposure has been demonstrated in both open-forest experiments (Kubiske *et al.*, 2006) and in laboratory settings. Recent experiments involving open-faced chambers of aspen trees resulted in a decrease of 10–15% when the trees were exposed to O₃ levels 1.5 times greater than background levels (Karnosky *et al.*, 2005). Chapter 10 of this assessment provides a more detailed discussion of the impacts of O₃ on forests.

The extrapolation of results from a laboratory setting to a forest ecosystem poses challenges for scientists and policy makers, because natural ecosystems are dynamic and have many interactions. Not only do different species of trees have different tolerances for O₃, it is also likely that trees of the same species also differ in their tolerances to O₃ according to genotype. Therefore, while one tree by itself may show signs of damage during an experiment, it is difficult to predict how this will impact a forest or a particular species within that forest. Furthermore, elevated levels of O₃ may cause more tolerant species to overtake less tolerant species, as they fill the ecological niche created by less competition for moisture and nutrients. Trees also have longer life spans than agricultural crops and are thus exposed to a significant variation in the levels of O₃, which impact may vary depending on the age of the tree (Herbinger *et al.*, 2005). All of these factors combine to make it difficult to predict the change in total biomass in a forest, as well as which species will be present in the long term. As different species have different values (among others, to the forestry industry), this further complicates the valuation of O₃ impacts.

12.3.1.1 Valuation of Ozone Impacts on Forests

Table 12.1 Examples of values that comprise the total economic value, or TEV, of trees in forest ecosystems

Function and Use	Description	Examples of Valuation Methodology	Type of Value
Timber values	The value of timber felled for commercial uses, such as paper manufacture and home construction	Market price of timber	Direct use
Non-timber values	All functions of forests not related to commercial uses		
a) Non-timber forest products	Use of wild species for mostly local purposes, such as fuel wood, food (e.g. nuts and wild meat), and as pharmaceuticals	Market prices or approximations of those prices	Direct use
b) Carbon storage	Carbon sequestration functions	Price of carbon	Indirect use
c) Recreation	Hiking, nature viewing, and other outdoor activities	Travel cost method, contingent valuation	Indirect use
d) Ecological functions	Watershed protection, erosion and sedimentation control, maintenance of biodiversity	Contingent valuation	Indirect use

Determining the marginal change in total economic value caused by O₃-induced damage to a tree or a forest is a difficult task. Much of what is valued from a standing tree is not part of a market. As can be seen in **Error! Reference source not found.**, in the context of total economic value, only a single part of the value of the tree is associated with the timber harvested by the forestry industry. Unfortunately, impacts on non-market values such as forest recreation and ecological functions are difficult to quantify.

Focusing on the timber value of trees, damages from O₃ can be valued on the basis that the production of biomass will decline and therefore there will be less quantity of wood available. The benefit from controlling O₃ arises from the additional forest products that can be manufactured as a result of increased harvest volumes and the spin-off economic activity associated with these increased volumes. In addition, increased harvests will augment stumpage revenue to the government and have other downstream forestry impacts.

Stumpage charges are payments made to the Crown for timber harvested, usually based on a rate per cubic metre of timber harvested (Canadian Council of Forest Ministers, 2008). Total revenues to the Canadian provincial and territorial governments in 2006 were over \$1.0 billion (Canadian Council of Forest Ministers, 2007). Assuming that an increase in biomass would result in an increase in harvest and given that the stumpage rates are not modified, stumpage revenues would then also increase.

Downstream production and resulting economic activity would also be affected by a change in harvest levels. It is estimated the forest industry contributed approximately \$30 billion to the GDP (2.9%) and provided 339,900 direct jobs in 2005. Revenues from value-added wood products (*e.g.* doors, windows, and other prefabricated building material) totalled \$4.9 billion in 2006 (Canadian Council of Forest Ministers, 2007). These values are substantial, and any change to the biomass and harvest could cause impacts to the forest industry, as well as to other sectors that depend on forestry.

When performing a more complex dynamic analysis, economists consider further complications. For instance, in reality, logging companies cannot, nor would it necessarily be desirable for them to, automatically cut down all the increase in biomass resulting from a reduction in O₃ levels. On Crown lands, forestry companies are limited in how much they can harvest by the annual allowable cut. In theory, the annual allowable cut will be adjusted when the amount of timber available for harvest changes. Assuming the annual allowable cut is fully harvested, an increase in biomass will thus cause an increase in harvest. However, a time lag is likely to happen between increased biomass production and a change in the annual allowable cut.

Further considerations may also be of importance. As it was the case with crops, increased production of forest biomass may or may not cause a shift in price. An eventual price decrease may cause overall revenues to fall or increase depending on its magnitude in relation to the increased production. Besides, as a large portion of the forestry products in Canada is exported and sold on international markets, small increases in production are likely to provide limited benefits to Canadian consumers in terms of lower prices and higher consumer surplus.

12.3.1.2 Illustrative Valuations

A recent study in Sweden estimated that current O₃ levels reduced the economic return from the sale of timber and pulpwood by 2.6% (Karlsson *et al.*, 2005). A similar analysis in the European Union in 1998 suggested that a reduction in O₃ would increase annual timber harvest value by €140 million – €190 million (European Commission, 1998).

Environment Canada has been working toward estimating the biophysical impacts on forest resulting from O₃ exposure and a first analysis should be completed in the near future. The development of CGE or other economic models that would translate the timber part of these biophysical impacts into economic terms would also be valuable. Finally, more work on assessing non-timber-related benefits such as ecosystem services is needed to better capture the total economic impacts of O₃ on forests.

12.3.3 Particulate Matter Impacts on Visibility

Visibility refers to how distinctly people are able to see objects through the atmosphere. Reductions in visibility are one of the most noticeable effects of smog, as the associated haze is easy for people to observe. Particularly in major cities, smog is considered a major problem by a large number of Canadians, and economic analysis indicates that the visibility benefits of pollution control can be substantial.

Factors that affect visibility in a particular area include humidity, position of the sun, and light pollution. Particulate matter (PM) in the air can also have an effect, which depends greatly on the size and composition of the PM. Fine PM is a particularly efficient scatterer of light, whereas coarser PM, dark and soot-like in nature, is more apt to absorb light. Chapter 11 of this assessment specifically addresses the impacts of PM on visibility and can be referenced for additional details on this topic.

12.3.3.1 Economic Valuation of Visibility

Economic assessments of the value of changes in visibility are challenging to make, since there are a number of ways to define and measure visibility itself. The value of visibility depends on people's perception, and this includes not only how far and how clearly one can see, but also what can be seen and when it can be seen. Visibility is not a directly marketed commodity such as agricultural or forest products. Valuation of visibility effects must therefore be based on revealed preferences through real behaviour or stated preferences through surveys. While values of visibility are less tangible than values of market goods, there is no question that a portion of the price of commodities like condos and hotel rooms is associated with the value derived from attributes such as unobstructed views of scenic landscapes.

Valuation of visibility is further complicated by the fact that many individuals mentally link air clarity with overall air quality. There is a common perception that if the air is clear, then the air is clean. Therefore, people who value clean air are likely to derive a lower utility from reduced visibility, because they will assume the air is less clean and less healthy. The linkages between visibility and human activities need to be further developed for a better understanding of how visibility affects Canadians' welfare.

Currently available studies of the value of visibility comprise two groups, residential and recreational. Residential value refers to the enjoyment that people get from the view they have at home and at work on a day-to-day basis. Recreational value is associated with the enjoyment derived when people visit scenic locations for vacation or on an outing.

12.3.3.2 Illustrative Valuations

One of the most influential visibility studies was a contingent valuation survey to determine residential visibility valuation in Chicago and Atlanta (McClelland *et al.*, 1991). Although the methodology used for this study, commonly referred to as the two-cities study, has been criticized (U.S. Environmental Protection Agency, 1999), it has formed the basis for much of the work that has since been done on visibility valuation.

The U.S. Environmental Protection Agency (1999) estimated visibility valuation in a logarithmic model. Like most other multi-regional studies, it derived values for residential visibility and recreational visibility separately. The agency found that, while both residential and recreational values are significant, residential visibility has a greater impact on overall welfare than visibility in scenic areas. The agency's 1999 study was aimed primarily at assessing the economic impacts of the 1990 *Clean Air Act*, and it found that the value of the associated visibility improvements ranged from 40 to 137 USD per household, depending on location.

However, a study focusing on regional haze in the east (Smith *et al.*, 2005) suggests that willingness to pay is highly dependent upon the context in which the questions are asked. The study showed that 70 to 80% of the survey respondents would reject a haze reduction policy with per capita costs equal to the average willingness to pay, but would be more open to paying for improvements on bad air quality days rather than on days with near-average regional haze.

In Canada, there has been some similar research into the valuation of residential visibility. Haider *et al.* (2002) used a contingent choice survey to estimate economic value of improved summer visibility in the lower mainland of British Columbia. Although confined to that region, the study was constructed in a way to facilitate benefits transfers to other parts of Canada. The final estimates for the welfare benefits ranged from \$29.38 for a 5% improvement in visual range to \$48.55 for a 20% increase. Although not completely inconsistent with earlier U.S. studies, these were lower than most U.S. estimates. This, the authors argued, could be attributed to the generally superior air clarity in lower mainland British Columbia compared to many U.S. cities.

To partially offset the problem of valuation of differing visibility baselines, it is useful to use deciviews⁴⁶ as a measure of visibility for multi-region assessments. The deciview index is analogous to the decibel index for sound. The deciview scale is set at zero for pristine conditions and the rating increases as visibility degrades. Each deciview change represents a perceptible change in visual air quality to the average person. Expressed as value per deciview, Haider *et al.*'s (2002) results were \$14.40 per household per deciview. Recent analysis done by the U.S. Environmental Protection Agency on the National Ambient Air Quality Standards (NAAQS) quoted a similar value of 14 USD per household per deciview, where the residential visibility valuation estimate was derived from the results of McClelland *et al.* (1991).

While little is known about the impact of visibility on recreational values in Canada, initial indications suggest it could be significant. A study conducted in the Greater Vancouver Regional District and the Fraser Valley surveyed tourists on whether or not visibility affected their decision to recommend the region to others or to return for additional visits (McNeill and Roberge, 2000). The study suggested that future drops in tourist revenues (not the same as welfare losses, although the two are related) will occur because a proportion of visitors who experience an episode of poor visibility will not return or will not recommend the area to others. For a single extreme visibility event, revenue losses are estimated to be about \$7.45 million in the Vancouver area and \$1.32 million in the Fraser Valley. These estimates do not represent the annual mean revenue losses from reduced visibility, which could be much higher.

There is still a great deal of research to be done on estimating the value that Canadians place on residential visibility. Much of this value is derived to a large extent from their surroundings. Both the scenic quality and the current visibility level at that location will influence the value that a person places on a change in visibility. While value proxies of visibility can be transferred between locations, doing so introduces a large degree of uncertainty. Further research through the stated preferences approach is required in order to conduct a more reliable national assessment of the impacts of reduced visibility. Also, more work needs to be done to understand the effect of visibility on recreational values within Canada and how this may, in turn, impact the tourism industry.

⁴⁶ Deciviews = $10 * \ln(\text{Light Extinction Coefficient}/10)$.

12.3.4 Other Environmental Smog Impacts

There are a number of other welfare-reducing effects of smog on Canadians. Pollution-induced elevated levels of O₃ and PM likely impact the health of wildlife, and just as O₃ impacts agricultural crops and trees, it is likely to negatively affect other vegetation types as well. These impacts can be expected to have a negative influence on ecosystem services and could add further stress to areas and species already at risk from habitat loss and overexploitation.

Unfortunately, there is currently little scientific information on which to base an economic valuation of such impacts. Exposure-response functions for individual species of a non-commercial nature are virtually non-existent. Even if they existed, however, the complex interactions that occur within an ecosystem would make it difficult to evaluate how varying levels of air quality would interact with other factors to form an overall outcome.

Also, smog negatively affects our day-to-day lives in marginal ways that often go unnoticed or are not commonly associated with smog. For instance, increased levels of PM often necessitate increases in cleaning costs. PM emitted from human sources ends up settling on all surfaces (buildings, vehicles, etc.) in forms such as dust, in a process more formally referred to as soiling. This has a dual negative impact in that it increases the required frequency of cleaning of these surfaces and decreases the aesthetic quality of associated soiled surfaces. Cummings *et al.*, 1981, Manuel *et al.*, 1982, Watson and Jaksch, 1982, Gilbert, 1985, and McClelland *et al.*, 1991, attempted to value the former, but few studies exist that try to value the latter.

Studies have demonstrated that, in addition to soiling of exposed surfaces, a number of other types of damage are caused by elevated levels of PM and O₃. These impacts can take a number of forms, such as surface erosion, blistering, and discolouration of paint; corrosion and tarnishing of structural metals and electronic components; fading and reduction of the tensile strength of fabrics; and spalling of stone building materials and monuments. The extent of damages depends on natural environmental conditions, such as moisture, temperature, wind fluctuations, atmospheric oxygen concentrations, sunlight, and the activity of microorganisms. Air pollutants aggravate or accelerate these harmful processes. These damages are often valued based on changes in repair frequencies caused by air pollution. While replacement of infrastructure, due to factors such as obsolescence, often occurs at a rate much higher than would be required to repair damage caused by air pollution, this ignores the loss in utility from reduced aesthetics (*e.g.* infrastructure that is still functional may be an eyesore) and damages from marginal losses in infrastructure performance as opposed to damages that induces complete failure. Very few studies have been done on valuation in these areas, and there is still considerable work needed to increase our understanding of such impacts.

12.4 Valuation of the Impacts of Smog on Health

In the context of the effect of smog, although the valuation of health impacts is a subset of all impacts, it is the one that is often considered the most important, and the one that receives the most attention. Empirical estimates of the health benefits relative to the total benefits of a policy action, as documented through a comparison of different air pollution valuation studies, indicate that health benefits are more than 80% of the total, and often much more (OECD, 2007). While this is, in part, due to a scientific knowledge gap on non-health impacts, it highlights the fact that to date, most smog-related policies have been primarily justified on the grounds of improvements to human health.

12.4.1 Health Valuation Methods

Because of the relative importance of health valuation and its applicability to a wide range of topics, there has been much research and technical development in this area. While the basic concepts for valuation of health-related and non-health-related endpoints are essentially the same and subject to similar principles, there are terms and methodologies that are unique to the field of health valuation. The breadth of topic of health valuation makes it difficult to cover its entire scope within the limits of this chapter. For this reason, this section can only give a general overview of some of the most common methods, recent developments, and important concepts.

Because of the importance that is often placed on health concerns, the idea of “putting a value” on health benefits has in the past been seen as controversial. However, this is often a result of a misunderstanding regarding the nature of what is being valued. Health valuation is not so much about measuring the value of an individual’s health, as it is about comparing low levels of risks with other factors that impact the quality of life. Health valuation has become an accepted and critical element in the development of smog-related policies and programs. For the same reasons discussed previously, valuation is needed in order to compare alternative outcomes objectively. This is true for health impacts as much as for other impacts, if not more.

Economic health valuation is used to express in dollars outcomes of premature mortality (loss of life) and morbidity (deterioration of health) as a result of chronic (long term) or acute (short term) causes. Health values are typically estimated through one of two general approaches. The cost of illness approach relies on estimates of medical costs and lost productivity associated with poor health, and focuses mainly on financial costs. The alternative approach focuses more on society’s wide costs, including the social value of pain and suffering, to estimate a net social willingness to pay for reduced risks of health problems.

12.4.1.1 Cost of Illness

Cost of illness measures include the savings related to avoided medical treatment and income losses, often referred to respectively as direct and indirect costs of medical treatment. These measures exclude the benefits derived from less pain and suffering associated with improved health. Therefore, cost of illness alone does not reflect the total value of an adverse health effect and is an understatement of the value of avoiding negative health impacts. However, cost of illness measures have the practical advantage of being easily understood and often more readily available, because they are based on market expenditure data and medical statistics.

12.4.1.2 Willingness to Pay for Reduced Risks to Health

The benefits associated with reductions of pain and suffering caused by smog-induced health-related impacts is a non-market good, and thus prices are not directly available. Many inferences on their value can be made through revealed and stated preferences studies.

Many valuation studies have tried to measure willingness to pay of individuals to avoid health risks, including those associated with pain and suffering. These studies usually observe wage differences between occupations with high and low risks of negative health outcomes (the hedonic wage method previously referred to). Depending on the studies' methodology, such willingness to pay estimates may exclude the medical costs associated with the treatment of chronic or acute outcomes due to air pollution exposure. For instance, individuals living in a country with a universal health care system, such as Canada, would not be expected to account for direct cost of illness in either their revealed or stated preferences.

In all cases, it is important not to count the same benefits twice. Sometimes, an individual's willingness to pay for an avoided health problem may include that individual's calculations of how much money he will lose by missing work, or how much he will have to spend on medication. In such a case, the person's willingness to pay includes more than just the value of pain and suffering. Adding this result to a cost of illness estimate would result in the same values being counted twice.

Also, in cases where altruism is a large factor, the sum of the willingness to pay of individuals to avoid personal health impacts across a group could result in a total that is less than the willingness to pay of the group as a whole to avoid negative impacts on everyone. A good example is that of parents and children. While there may be difficulties in having children express their willingness to pay to avoid an asthma symptom, the children's parents can express a willingness to pay to avoid having to witness their children's pain and suffering. There is evidence that parents may be willing to pay more to avoid an acute morbidity impact on their children than they would to avoid an impact on themselves (Dickie and Messman, 2004). This example also points to an important consideration for indirect costs of illness. In

these situations, not only do ill people have reduced productivity, but guardians may also need to take time off work to provide care. This results in the reduced productivity, or reduced human capital acquisition, of both the ill people and the guardians.

12.4.2 Mortality Risk Valuation

As noted previously, exposure to smog increases the risk of premature death. In order to measure the value of these risks on the quality of life of Canadians, there are a number of methods that can be used. Generally, these methods rely on estimates of how much an average person would be willing to pay for a very minor reduction in his annual risk of death. By aggregating the willingness to pay for small changes in risks over a large population, it is possible to estimate the net social value of a reduction in national mortality risks. These measures include the value of a statistical life and the value of a statistical life-year. The way in which these values are calculated and applied will be discussed in further detail in the following sections, along with related issues.

Note that for both the value of a statistical life and the value of a statistical life-year, many estimates come from the hedonic wage method. There are reservations about the appropriateness of transferring estimates from studies based largely on workplace accidents, which typically represent healthy, middle-aged adults, to an environmental context. Someone with 35 years of expected life remaining who faces an immediate risk would probably tend to value time differently than an older individual with less expected life remaining who faces a more diffuse risk.

12.4.2.1 Value of a Statistical Life

At the level of an individual, air pollution increases *the risk* of premature mortality, whereas from the perspective of society as a whole, air pollution does in fact increase *the number* of deaths occurring. The value of a statistical life is a concept used by economists to approximate the social benefits of small reductions in risks of premature death at the individual level, applied to a large population. The value of a statistical life does not estimate the impacts of an individual's death for this individual. It is rather the change in his *risk* of premature mortality that is valued; the values of these individual risks changes can then be aggregated over a population to come up with a value per mortality.

As a simplistic example of how the value of a statistical life is calculated, suppose that a given reduction in pollution confers on each exposed individual a decrease in risk of mortality of 1/1,000. This implies that among 1,000 such individuals, one fewer individual can be expected to die prematurely. If the average individual's willingness to pay for that risk reduction is \$1,000, then the implied value of a statistically premature death avoided is $\$1,000 \times 1,000$, or \$1 million, for that group of people.

There are many factors that can influence an individual's willingness to pay for risk reductions. There is evidence that variables such as income (Viscusi and Aldy, 2003), age, and level of risk (Hammit and Graham, 1999) can all impact on willingness to pay for reductions in risks related to premature mortality. It can be very hard to fully account and correct for all of these different influences. Also, some studies may account for some of these factors, while other studies account for different factors. As a result, comparisons of results between different studies can be quite difficult. When willingness to pay for the value of a statistical life is applied to an entire population in a different context than the original, this is a benefits transfer. As already mentioned, bias can occur with benefits transfer if there are socio-economic, demographic, risk-level, or other differences that are not accounted for between the study case and the policy case to which it is applied.

While there is an argument in the literature that age should play an important factor in the value of a statistical life, the evidence from cross-study meta-analysis is somewhat inconclusive (OECD, 2006). It seems sensible that the more years of expected life remaining, the more a person should value those remaining years. The theoretical rationale for supposing that willingness to pay varies with life expectancy is based on the lifetime consumption model. In the lifetime consumption model, willingness to pay to reduce the probability of dying is equal to the present value of expected utility of consumption for the remaining years of life. If the lifetime consumption model is correct, we would expect willingness to pay to avoid increased probabilities of premature mortality to vary inversely with age. However, only some studies actually observe this relationship. One possible explanation is that this model ignores the influence of scarcity. When scarcity is considered, there is an inverse relationship between the value of a single year of life and the number of years of life remaining. As a person ages, the expected number of life-years decreases but the value of each remaining year increases, meaning the results of a comparison between the values of a statistical life based on age can be somewhat ambiguous.

For risk level, the common assumption used when applying the value of a statistical life to a policy case is that willingness to pay varies directly with the policy-induced risks reduction. For example, if the willingness to pay for a reduction in risks of 1/1,000 chance of mortality is valued at \$1,000, then a reduction in risks of 2/1,000 should be valued at \$2,000. However, this may not be the case and willingness to pay for mortality risk reductions may be subject to decreasing marginal valuation. This means that, while each additional reduction in risk would be valued positively, it would be worth less than the previous reduction. This would imply that a population at high risk compared to one at low risk would have a higher willingness to pay for an equivalent absolute risk reduction. Other studies indicate that the nature of the risk may matter as well.

In terms of income, there are good reasons to believe that as income increases, willingness to pay to avoid mortality risks is also likely to increase. Viscusi and Aldy (2003) found that a 1% increase in income, all else remaining equal, would result in an increase in the willingness to

pay for reductions in mortality risks by 0.5–0.6%. If studies based on measuring the willingness to pay for a reduction in risks of mortality are based on a sample of individuals with a lower or higher per capita income than the population to which it is being applied, it may be justifiable to adjust for this difference. For instance, a study performed 10 years ago being applied today may need to be adjusted to account for changes in real incomes over that period of time, if any.

12.4.2.2 Value of a Statistical Life-Year

It has been suggested that while the value of a statistical life is relevant for acute deaths, for mortality as a result of chronic health effects the value of a statistical life-year may be more relevant (OECD, 2006).

To account for this, the method used for valuing a statistical life-year values life-years that would be lost if an individual were to die prematurely. In its simplest form, the method derives estimates of the value of a statistical life-year from the value of a statistical life. The underlying premise is that a value of a statistical life is the aggregation of a stream of constant annual values for the remaining expected years of life of an individual. In this interpretation, the estimate of the value of a statistical life-year depends on three factors: the underlying estimate of the value of a statistical life, a discount rate, and the number of years of life remaining. It has been suggested that many wage-risk studies are based on individuals with an average life expectancy of an additional 35 years (Moore and Viscusi, 1988). Using a 35-year life expectancy, an estimate of \$5 million as the value of a statistical life, and a zero discount rate, this approach yields an estimate of ~\$143,000 per life-year. If a discount rate of 5% is used, then it translates into a value of a statistical life-year of ~\$305,000. In this method, the estimated value of a statistical life is assumed to already be a discounted value, and thus the higher the discount rate underlying the value of a statistical life, the higher the derived value of a statistical life-year. Although the process described here is one of the most common to estimate the value of a statistical life-year, other approaches do exist (see National Research Council, 2008).

12.4.2.3 Illustrative Valuations

The U.S. Environmental Protection Agency's (2000) *Guidelines for Preparing Economic Analyses* advises analysts to use a central value of a statistical life estimate of 4.8 million in 1990 USD. This value is the result of a meta-analysis of 26 estimates assembled for the agency's first retrospective analysis of the *Clean Air Act* (U.S. Environmental Protection Agency, 1997). Each of the 26 estimates is from a unique study, with 21 of the estimates from hedonic wage studies and the remaining five from contingent valuation studies. The valuations vary from 0.9 million to 20.9 million in 2002 USD, and the studies were published between 1976 and 1991. These studies were then fitted to a distribution to arrive at a central estimate.

In Canada, the Air Quality Benefits Assessment Tool (AQBAT) is a model designed by Health Canada to facilitate analysis of the health impacts of air pollution. It makes use of defined concentration-response functions to predict how ambient air quality changes will affect per capita mortality and morbidity risks. Changes in per capita risks are then multiplied by an exposed population to determine the net increase or decrease in adverse health outcomes. Finally, changes in adverse health outcomes are assigned socio-economic values, so that they can be aggregated into a single estimate.

The federally recommended value of a statistical life in Canada is approximately \$6 million. This recommendation is based on a number of literature reviews that looked at results from both domestic and international research. The studies included in the reviews also resorted to both revealed and stated preferences. These literature reviews have formed the basis of the values recommended by the Treasury Board of Canada Secretariat for use in cost-benefit analysis, and have also been used by Health Canada for assessment of air quality benefits using AQBAT. Recently, the study of Chestnut and De Civita (2009) updated the previous literature reviews, including some of the more recent research, and recommended that the value of a statistical life be \$6.5 million. For use in sensitivity analysis, the authors recommended using a value of \$3.5 million and \$9.5 million for the low and high end range respectively. These values, it is suggested, represent the lower and higher end of values in the literature that are still fairly robust. It is also important to note that the federal government does not currently reduce the value of a statistical life as age increases. In previous analyses conducted by Health Canada, it was standard procedure to adjust the value of a statistical life numbers downward slightly as age increases. However, since the recent literature is inconclusive to this end, Health Canada no longer recommends adjusting the value of a statistical life for age.

12.4.3 Morbidity Risk Valuation

Most science assessments of morbidity risks resulting from smog exposure are based on information on cardiovascular and respiratory impacts. Many of the issues that surround the application of willingness to pay for reductions in risks of mortality are also important when dealing with morbidity impacts; however, there are some additional issues that will be discussed in more depth in this section.

First, the distinction between acute and chronic is of great importance when discussing morbidity impacts. In general, acute illness can be more easily accommodated into a person's life, as it involves only temporary changes in lifestyle. Chronic morbidity, however, is associated with permanent changes, which are more disruptive to a person's overall long-term lifestyle. Because of such impacts, it has been considered more difficult to value chronic morbidity as compared to acute morbidity. Also, care must be taken to avoid double counting when valuing both chronic and acute morbidity impacts in a single policy valuation.

Second, there is evidence to suggest that baseline health can play an important role in the willingness to pay of individuals to avoid morbidity impacts. Studies have long shown that people who are in worse health are generally willing to pay more to prevent additional morbidity or to reduce current morbidity (Loehman *et al.*, 1979 and Rowe and Chestnut, 1984). This finding is of importance for valuation of smog morbidity impacts because it is usually people who already have poor health who are most at risk of experiencing further negative morbidity impacts.

12.4.3.1 Illustrative Valuations

AQBAT employs valuation estimates for acute morbidity that are based on willingness to pay measures (in some cases, these measures are drawn from cost of illness data). These estimates were derived from an analysis that integrated data from studies on the quality of life and economic impacts of acute episodes of cardiac and respiratory disease (Stieb *et al.*, 2002).

Table 12.2 Valuation estimates^a (in 1997 dollars) and ratio of total value to cost of illness, by endpoint and component

Endpoint	Cost of treatment (\$)	Lost productivity (\$)	Pain, suffering, and averting expenditures (\$)		Total (\$)		Ratio of total value/(cost of treatment + lost productivity)
			In hospital	Out of hospital	Point estimate	95% CI	
Hospital admission, respiratory	2,800	300	670	410	4,200	(3,400, 5,000)	1.3
Hospital admission, cardiac	3,800	270	760	340	5,200	(4,000, 6,400)	1.3
Emergency department visit, respiratory	930	160	430	520	2,000	(1,700, 2,500)	1.9
Emergency department visit, cardiac	3,200	210	680	330	4,400	(3,300, 5,600)	1.3
Restricted activity day		25		23	48	(13, 82)	1.9
Asthma symptom day		12		16	28	(11, 71)	2.3
Acute respiratory symptom day		12		1	13	(0, 28)	1.1

^aRounded to two significant figures.

Source: Stieb *et al.*, 2002

In one of these studies, data were collected prospectively on individuals visiting emergency departments for cardiac and respiratory conditions, as part of an epidemiological study on air pollution (Stieb *et al.*, 2000). Information was collected on the duration of the disease episode that prompted their visit, disposition of their visit (*i.e.* whether they were admitted or

discharged), and the occurrence of various outcomes from the onset of their earliest symptoms until the follow-up interview. These outcomes included restricted-activity days; days of missed work for the patient, parent, or other caregiver; health-care utilization; and illness-related expenses. Data were also abstracted from the clinical records of randomly selected patients, and cost of illness estimates were generated which included fully allocated costs related to hospital utilization and emergency department visits, as well as costs of physician visits, medication use, equipment, and out-of-pocket expenses (Anis *et al.*, 2000). Compared to other literature in this area, this study had the advantage of having been designed specifically to prospectively quantify the broad impacts on the quality of life and the cost of illness associated with episodes of cardiac and respiratory disease, thus ensuring that the required data elements were collected in a consistent, coordinated fashion. The associated results are presented in Table 12.2.

Cost of treatment accounted for most of the overall value in the case of hospital admissions for respiratory and cardiac illnesses, as well as cardiac emergency department visits. In the case of emergency department visits for respiratory illness, cost of treatment accounted for approximately 45% of the overall value. Lost productivity costs represented a small proportion of the overall value, although the proportion was greater for those endpoints that do not include a cost of treatment component. For both hospital admissions and emergency department visits, the overall value was larger for cardiac than for respiratory conditions. This is primarily attributable to the higher cost of treatment for cardiac versus respiratory conditions.

12.4.4 Alternative Measures

In the health literature, there are several measures that attempt to combine morbidity and mortality impacts into one metric, independent of money-based valuation. These are referred to as health-adjusted life-years, and represent an alternative approach to using willingness to pay to reflect preferences between loss of quantity and loss of quality of life. Health-adjusted life-years measures are based on health status indexes, which were developed in 1970 (Fanshel and Bush, 1970). Health status indexes involve a subjective rating of different states of health based on their perceived disutility. These indexes are sometimes based on surveys of patients who are asked to rank or score alternative states of health. Consequently, health status indexes are actually calculated in a similar manner to stated preferences estimations of willingness to pay. Survey methodologies commonly used to calculate health status indexes are visual analogue scale, time trade-off, person trade-off, and standard gamble (Robberstad, 2005). Alternatively, some health status indexes are based on expert opinion.

The first and most commonly used type of health-adjusted life-year is the quality-adjusted life-year, which was first used by Zeckhauser and Shepard (1976) to specify a health outcome unit of measurement that combines both duration and quality of life. The quality-adjusted life-year

is essentially a year of life that is then weighted based on a health status index with a range of zero to one. A perfectly healthy year of life has an associated health status index of one, and one associated with death would be measured as zero. Quality-adjusted life-years can then be summed over time and across populations and even be subjected to discount rates (Sassi, 2006). The benefits of an action are then measured in terms of quality-adjusted life-years gained compared to no action or an alternative action.

Another, more recently developed type of health-adjusted life-year is the disability-adjusted life-year. Originally developed by the World Health Organization (Murray, 1994), it has become common in the fields of public health and health impact assessment. The disability-adjusted life-year, as opposed to the quality-adjusted life-year, measures the burden of disease. Thus, while more quality-adjusted life-years are a desirable outcome, more disability-adjusted life-year implies a reduced level of well-being. Consequently, actions that benefit health are measured in disability-adjusted life-years saved and quality-adjusted life-years gained. A disability-adjusted life-year is the aggregate of two separate measures: years of life lost and years lived with disability. Years of life lost essentially corresponds to the number of deaths multiplied by the standard life expectancy at the age at which death occurs. Years lived with disability for a particular cause in a particular time period corresponds to the number of incident cases in that period multiplied by the average duration of the disease and a health quality index where zero is perfect health and one is death (World Health Organization, 2007).

While health-adjusted life-years are useful for comparing alternative outcomes and assessing cost effectiveness within the health realm, they are, on their own, of limited use for a comprehensive smog abatement policy assessment (Miller *et al.*, 2006). Since health-adjusted life-years are not measured in dollars, they cannot be directly aggregated with non-health benefits based on willingness to pay or on cost of illness. In addition, they cannot be compared to costs, as would typically be done in a cost-benefit analysis. While threshold values of cost-effectiveness for medical procedures for a quality-adjusted life-year gained are often quoted at values such as 50,000 USD (Eichler *et al.*, 2004), methodologically such values are not equivalent to willingness to pay and are questionable when incorporated into a policy assessment framework. The reasons for this mainly stem from the fact that health-adjusted life-years are based on health status indexes, which are built relative to other health outcomes, whereas willingness to pay measures the value of an outcome relative to other consumption choices. In other words, because health-adjusted life-years and willingness to pay are based on different measures, they are not comparable.

12.5 Conclusion

The field of economics provides a very important set of tools for aiding decision making in smog abatement policy. Sustainable development is one of the key objectives of any policy, and this requires us to balance environmental, social, and economic concerns on behalf of

current and future generations. To achieve this balance, a scale is required to weigh the costs and benefits resulting from a decision, which helps to determine whether our limited resources are being used in an optimal manner. Economic valuation uses standardized methodologies supported by sound scientific research to gauge impacts through a common scale (dollars). It facilitates a more thorough appreciation of the extent of impacts caused by smog, and it converts the effects to dollars so that they can be compared with the costs of controlling smog-causing emissions.

The impacts of smog derive their value from a number of sources. The concept of total economic value recognizes that any environmental outcome that impacts humans does so both through use and non-use values. The concept has become more common in economic and political discussions. Many people place real and personal value on goods they will never themselves experience. To account fully for the benefits of a policy to society, policy makers must include estimates of the changes to total economic value of both environmental and health endpoints in their cost-benefit analyses.

The value and price of market goods are not equivalent; however, in many instances, price can provide an indication of marginal changes in value. Smog also affects non-market goods for which no price exists to act as a proxy for the value. In these cases, special techniques have been developed to estimate willingness to pay for reductions in these impacts and the resulting estimates act as a price surrogate. These techniques fall into two major categories: revealed and stated preferences. The results of such studies for a particular set of circumstances are often applied to new situations under slightly different circumstances; economists call this a benefits transfer. While it is a useful tool, benefits transfer must be applied with proper attention to possible differences between the circumstances of the primary study and of the studied case.

Smog significantly affects outcomes that Canadians value, through a number of health-related and non-health-related impacts. However, only a portion of the impacts of smog has been quantified through economic valuation, and much of the work is based on results coming from Europe or the United States.

Non-health-related impacts are significant. Smog can impact the output of Canadian farms and forestry operations by lowering the productivity of crops and forests. Smog also decreases visibility, which lowers the enjoyment Canadians receive from being able to see their surroundings and that of tourists visiting scenic locations within Canada. Smog dirties our buildings, vehicles, and clothes, and increases the rate at which materials break down. Smog can also negatively impact ecosystems in various ways, possibly increasing the stress on areas and species that are already under pressure.

The value of reductions in harmful impacts on health has been the major rationale used for increased restrictions of smog-inducing emissions, and, in all cases, accounted for more than 80% of associated benefits. Benefits from smog reduction are measured in terms of lower costs of illness and reduced pain and suffering, as measured by willingness to pay. Lower cost of illness includes reductions in the cost to treat illness (direct costs) and less lost productivity of workers and caregivers (indirect costs). A large portion of the value from reduced smog impacts comes from associated reductions in risk of premature mortality, but reductions in the risk of cardiopulmonary-related morbidity impacts are also of significance.

As knowledge of how smog impacts our health and our surroundings increases, the techniques used to value these effects also continue to develop. It is likely that current methods only capture a portion of the true value Canadians receive from smog-reducing policies. It is important that this work continues and that new methods are put to use in the Canadian context to help guide future smog-related policies towards the best possible outcome to the benefit of all Canadians.

12.5.1 Recommendation for Future Research and Initiatives

There is a clear need for more primary valuation research on the impacts of smog in Canada. The majority of valuation studies related to smog impacts come from Europe or the United States. Much of the valuation work done on smog impacts in Canada has focused on replicating or applying the results of these studies for the purpose of policy assessments. While this tactic provides useful insights, it is a second best approach that leaves many knowledge gaps in areas that are important in the Canadian context. Application of studies from other countries can also result in biased valuation in areas where Canadian preferences are unique. To improve this situation, a research network could be created in tandem with enhanced funding. Such a program already exists in the United States under the U.S. Environmental Protection Agency's Science to Achieve Results research grants program, which could serve as a model for Canada. Support for primary research in Canada on valuation of smog impacts would also help to develop a domestic capacity of skilled valuation practitioners.

Progress has been made in Canada over the last few years in applying research to the development of new and enhanced applications that provide insight into the benefits of smog-reducing policies. For example, the Air Quality Benefits Assessment Tool is used to value health impacts of smog, while the Value of Ozone Impacts on Canadian Crops Estimator has been used to estimate revenue losses resulting from the exposure of crops to ozone. However, these and other models need to be improved, particularly the non-health valuation tools, to take advantage of the latest analytical techniques. A primary example of this will be making use of geographic information systems (GIS) to allow for better analysis and smoother integration of air quality, ecosystem, demographic, and economic data sets. In addition to improving existing tools, Canadians need new tools to help assess the values of other smog impacts. Large holes

still exist in our knowledge of how smog affects the welfare of Canadians through impacts on ecosystem services. Also, very little is known about how multiple stressors such as smog, climate change, acid deposition, and habitat destruction combine to reduce our well-being.

Next, the traditional damage function approach, which is one of the most widely used methods for analysing policy benefits, needs to be expanded beyond a linear process toward a more integrated feedback model. The linear process of relating industrial emissions to negative effects on air quality, and relating the poor air quality, in turn, to damages to humans and the environment ignores feedback impacts. These may take the form of positive feedback loops, which amplify damages. For example, natural services damaged by smog-inducing pollution may need to be replaced by artificial services requiring more energy and more resources, creating more pollution. The current approach is not able to capture such dynamics. To develop a framework capable of capturing such impacts will require an integrated assessment approach, with much greater coordination between the various fields of expertise involved in the damage function approach chain of analysis.

Also, it would be of use to augment current environmental sustainability indicators with information from valuation of smog and other damages. The current Canadian Environmental Sustainability Indicators (CESI) for air quality include both ozone and fine particulate matter exposure indicators, which are population-weighted average concentrations observed at monitoring stations across Canada during the warm season (Canadian Environmental Sustainability Indicators, 2007). While the CESI are useful because they are weighted according to human health population, they do not account for ecosystem impacts, and the unique qualities measured by the CESI cannot be combined for a more quantitative evaluation.

Finally, here is a list of other possible areas for future research:

- Study stated preferences values over multiple locations within Canada, in order to identify attributes that have universal applicability and those that are place- or population-based;
- Estimate changes in producer and consumer surpluses resulting from smog pollution;
- Perform additional research on elements related to the impacts of smog pollution on health, including the variation of the value of a statistical life among age categories and possibly other variables, as well as the willingness to pay of parents for reducing health risks in their children; and
- Consider alternatives to the traditional damage function approach, especially when some information is missing in order to rigorously quantify all the steps of the damage function.

Many of these recommendations will be challenging to implement, and implementation would require significant additional resources, including experts from fields other than economics. However, the additional insight such programs would provide could revolutionize the way we measure progress and set goals as a country. This would provide guidance not only in how smog-related policies are set, but also in how all policies act together to create a more sustainable Canada.

References

Agriculture and Agri-Food Canada, 2006. The Agriculture and Agri-Food Sector. In: Report on long term challenges and opportunities for future competitiveness and prosperity of the agriculture and agri-food industry, Chapter 1: Primary Agriculture.

Adams, R.M. and Crocker, T.D., 1989. The agricultural economics of environmental change: Some lessons from air pollution. *Journal of Environmental Management* 28, 295–307.

Adams, R.M., Hamilton, S.A. and McCarl, B.A., 1986. The benefits of pollution control: The case of ozone and U.S. agriculture. *American Journal of Agricultural Economics* 68, 886–889.

Anis, A.H., Guh, D., Stieb, D., Leon, H., Beveridge, R.C., Burnett, R.T. and Dales, R.E., 2000. The costs of cardiorespiratory disease episodes in a study of emergency department use. *Canadian Journal of Public Health* 91, 103–106.

Arrow, K., Solow, R., Portney, P., Leamer, E., Radner, R. and Schuman, H., 1993. Report of the NOAA Panel on Contingent Valuation. *Federal Register* 58, 4016–4064.

Bateman, I., Carson, R.T., Day, B., Hanemann, M., Hanley, N., Hett, T., Jones-Lee, M., Loomes, G., Mourato, S., Ozdemiroglu, E., Pearce, D.W., Sugden, R. and Swanson, J., 2002. *Economic valuation with stated preference techniques: A manual*, Edward Elgar Publishing Ltd., Cheltenham, U.K.

Canadian Council of Forest Ministers, 2007 [cited on September 10, 2007]. National Forestry Database Program [online]. Available from <http://nfdp.ccfm.org/>.

Canadian Council of Forest Ministers, 2008 [cited in April 2008]. Revenues and economic profile terminology [online]. Last updated: June 25, 2004. Available from http://nfdp.ccfm.org/compendium/profile/terminology_e.php.

Canadian Environmental Sustainability Indicators, 2007 [cited on September 10, 2007]. Highlights [online]. Available from <http://www.environmentandresources.ca>.

Champ, P.A., Boyle, K.J. and Brown, T.C. (Eds.), 2003. A primer on non-market valuation, Kluwer, Dordrecht.

Chestnut, L.G. and De Civita, P., 2009. Economic Valuation of Mortality Risk Reduction: Review and Recommendations for Policy and Regulatory Analysis. Research Paper, Policy Research Initiative, Ottawa.

Cummings, R., Burness, H. and Norton, R. 1981. Methods development for environmental control benefits assessment. In: Measuring household soiling damages from suspended air particulates: A methodological inquiry, Volume V. Report prepared for the U.S. Environmental Protection Agency, Washington, D.C.

Dickie, M. and Messman, V.L., 2004. Parental altruism and the value of avoiding acute illness: Are kids worth more than parents? *Journal of Environmental Economics and Management* 48, 1146–1174.

Eichler, H.G., Kong, S.X., Gerth, W.C., Mavros, P. and Jönsson, B., 2004. Use of cost-effectiveness analysis in health-care resource allocation decision-making: How are cost-effectiveness thresholds expected to emerge? *Value in Health* 7, 518–528.

Environment Canada, 2007 [cited on September 20, 2007]. Benefits and costs of the regulatory framework for air emissions [online]. Available from <http://www.ec.gc.ca/default.asp?lang=En&n=714D9AAE-1&news=C33CCDD9-3186-4A43-875A-A1D88135164F>.

European Commission, DG XI, 1998. Economic evaluation of air quality targets for tropospheric ozone, Part C, Economic benefit assessment, Final report. International Institute for Applied Systems Analysis (IIASA), Laxenburg, Austria; AEA Technology, Culham, U.K.; Norwegian Meteorological Institute (DNMI), Oslo, Norway; National Institute of Public Health and the Environment (RIVM), Bilthoven, The Netherlands.

Fanshel S. and Bush J.W., 1970. A health-status index and its application to health-services outcomes. *Operations Research* 18, 1021–1066.

Freeman, A., Rowe, R.D. and Thayer, M., 1994. Economic issues in the application of externalities to electricity resource selection. In: Technical review of externalities, EPRI TR-104813, Electric Power Research Institute, Palo Alto, CA.

Gilbert, C., 1985. Household adjustment and the measurement of benefits from environmental quality improvements. Doctoral Dissertation, Department of Economics, University of North Carolina, Chapel Hill.

- Haider, W., Moore, J., Knowler, D. and Anderson, D., 2002. Estimating visibility aesthetics damages for AQVM. Unpublished report prepared for Environmental Economics Branch, Environment Canada, Ottawa.
- Hammitt, J. and Graham J., 1999. Willingness to pay for health protection: Inadequate sensitivity to probability. *Journal of Risk and Uncertainty* 18, 33–62.
- Hardin, G., 1968. The tragedy of the commons. *Science* 162, 1243–1248.
- Heck, W.W., Cure, J.O., Rawlings, L.J., Zaragoza, A.S., Heagle, H.E., Heggstad, R.J., Kohut, L.W. and Kress, P.J., 1984. Assessing impacts of ozone on agricultural crops, I, Overview. *Journal of Air Pollution Control Association* 34, 729–735.
- Herbinger, K., Then, Ch., Low, M., Haberer, K., Alexous, M., Koch, N., Remele, K., Heerdt, C., Grill, D., Rennenberg, H., Haberle, K.-H., Matyssek, R., Tausz, M. and Wieser, G., 2005. Tree age dependence and within-canopy variation of leaf gas exchange and antioxidative defence in *Fagus sylvatica* under experimental free-air ozone exposure, Issue 3, Forests under changing climate, enhanced UV and air pollution. *Environmental Pollution* 137, 476–482.
- Holland, M., Mills, G., Hayes, F., Buse, A., Emberson, L., Cambridge, H., Cinderby, S., Terry, A. and Ashmore, M., 2002. Economic assessment of crop yield losses from ozone exposure. Centre for Ecology and Hydrology: Natural Environment Research Council; U.K. Department for Environment, Food and Rural Affairs; Centre for Ecology and Hydrology: Natural Environment Research Council.
- Jones, R., Boer, R., Magezi, S. and Mearns, L., 2004. Assessing Current Climate Risk. Technical paper for Adaptation Policy Framework, United Nations Development Program. Available from http://www.undp.org/cc/apf_outline.htm.
- Karlsson, E., Pleijel, H., Belhaj, M., Danielsson, H., Dahlin, B., Andersson, M., Hansson, M., Munthe J. and Grennfelt, P., 2005. Economic Assessment of the Negative Impacts of Ozone on Crop Yields and Forest Production. A Case Study of the Estate Östads Säteri in Southwestern Sweden. *A Journal of the Human Environment* 34, 32–40.
- Karnosky, D.F., Pregitzer, K.S., Zak, D.R., Kubiske, M.E., Hendrey, G.R., Weinstein, D., Nosal, M. and Percy, K.E., 2005. Scaling ozone responses of forest trees to the ecosystem level in a changing climate. *Plant, Cell and Environment* 28, 965–981.
- Koopmans, T.C., 1965. On the concept of optimal economic growth. *Pontificae Academiae Scientiarum, Scripta Varia* 28, 225–300.

- Kopp, R.J., Vaughan, W.J., Hazilla, M. and Carson, R., 1985. Implications of environmental policy for U.S. agriculture: The case of ambient ozone standards. *Journal of Environmental Management* 20, 321–331.
- Kubiske, E.M., Quinn, V.S., Heilman, W.E., McDonald, E.P., Marquardt, P.E., Teclaw, R.M., Friend, A.L. and Karnosky, D.F., 2006. Interannual climatic variation mediates elevated CO₂ and O₃ effects on forest growth. *Global Change Biology* 12, 1054–1068.
- Loehman, E.T., Berg, S.V., Arroyo, A.A., Hedinger, R.A., Schwartz, J.M., Shaw, M.E., Fahien, R.W., De, V.H., Fische, R.P., Rio, D.E., Rossley, W.F. and Green, A.E.S., 1979. Distribution analysis of regional benefits and cost of air quality control. *Journal of Environmental Economics and Management* 6, 222–243.
- Loomis, J., 2005. Economic Values Without Prices: The Importance of Nonmarket Values and Valuation for Informing Public Policy Debates. *Choices* 20, 179-182.
- Manuel Jr, E., Horst Jr, R.L., Brennan, K., Lanen, W., Duff, M.C. and Tapiero, J.K., 1982. Benefits analysis of alternative secondary National Ambient Air Quality Standards for sulphur dioxide and total suspended particulates, Volume II. Prepared by the U.S. Environmental Protection Agency, Office of Air Quality Planning and Standards, Research Triangle Park, North Carolina.
- McClelland, G., Schulze, W., Waldman, D., Irwin, J., Schenk, D., Stewart, T., Deck, L. and Thayer, M., 1991. Valuing eastern visibility: A field test of the contingent valuation (draft). Prepared for the U.S. Environmental Protection Agency, Washington, D.C.
- McNeill, R. and Roberge, A., 2000. The impact of visual air quality on tourism revenues in Greater Vancouver and the Lower Fraser Valley. Prepared for Environment Canada, Georgia Basin Ecosystem Initiative, Vancouver, B.C.
- Miller, W., Robinson, L.A. and Lawrence, L.S., Eds., 2006. Valuing Health for Regulatory Cost-Effectiveness Analysis. National Academy Press, Washington, D.C.
- Moore, M.J. and Viscusi, W.K., 1988. The quantity-adjusted value of life. *Economic Inquiry* 26, 369–388.
- Murphy, J.J., Delucchi, M. A., McCubbin, D.R. and Kim, H. J., 1999. The cost of crop damage caused by ozone air pollution from motor vehicles. *Journal of Environmental Management* 55, 273–289.
- Murray C., 1994. Quantifying the burden of disease: The technical basis for disability-adjusted life years. *Bulletin of the World Health Organization* 72, 429–445.

National Research Council (Committee on Estimating Mortality Risk Reduction Benefits from Decreasing Tropospheric Ozone Exposure), 2008. *Estimating Mortality Risk Reduction and Economic Benefits from Controlling Ozone Air Pollution*. National Academy Press, Washington, D.C.

OECD, 2006. *Cost-benefit analysis and the environment: Recent developments*. Prepared by Pearce, D., Atkinson, G. and Mourato, S. for the Organisation for Economic Co-operation and Development, Paris.

OECD, 2007. *Costs of environmental policy inaction: Technical report*. Prepared by Johnstone, N. and Hascic, I. for the Organisation for Economic Co-operation and Development, Paris.

Ontario Ministry of the Environment, 2005 [cited on November 28, 2006]. *Transboundary air pollution in Ontario* [online]. Available from <http://www.ene.gov.on.ca/envision/techdocs/5158e.pdf>.

Pearson, R.G. and Donnan, J.A., 1989. *Impact of ozone exposure on vegetation in Ontario*. Report Number ARB-179-89-Phyto, Air Resources Branch, Ontario Ministry of Environment, Toronto, Ontario.

Robberstad, B., 2005. QALYs vs DALYs vs LYs gained: What are the differences, and what difference do they make for health care priority setting? *Norsk Epidemiologi* 15, 183–191.

Rowe, R.D. and L.G. Chestnut, 1984. *Valuing Changes in Morbidity: WTP versus CPI Measures*. Energy and Resource Consultants Inc.

Sassi, F., 2006. Calculating QALYs, comparing QALY and DALY calculations. *Health Policy and Planning* 21, 402–408. Oxford University Press in association with The London School of Hygiene and Tropical Medicine. [Advance access originally published on line on 28 July 2006. Available at <http://heapol.oxfordjournals.org/cgi/content/abstract/21/5/402>.]

Smith, A.E., Kemp, M.A., Savage, T.H., and Taylor, C.L., 2005. Methods and results from a new survey of values of eastern regional haze improvements, *Journal of the Air and Waste Management Association*, 55, 1767-1779.

Spash, C. L., 1997. Assessing the economic benefits to agriculture from air pollution control. *Journal of Economic Surveys* 11, 47–70.

Stern, N. 2006. *The economics of climate change: The Stern review*. Cabinet Office, HM Treasury, London, U.K. Available from Cambridge University Press, Cambridge, U.K.

Stieb, D., Civita, P.D., Johnson, F.R., Manary, M.P., Anis, A.H., Beveridge R.C. and Judek, S., 2002. Economic evaluation of the benefits of reducing acute cardiorespiratory morbidity associated with air pollution. *Environmental Health: A Global Access Science Source* 1, 7. Available from <http://www.ehjournal.net/content/1/1/7>.

Stieb, D.M., Beveridge, R.C., Smith-Doiron, M., Burnett, R.T., Judek, S., Dales, R.E. and Anis, A.H., 2000. Beyond administrative data: Characterizing cardiorespiratory disease episodes among patients visiting the emergency department. *Canadian Journal of Public Health* 91, 107–112.

Treasury Board of Canada Secretariat, 2007 [cited on December 16, 2009]. *Canadian Cost-Benefit Analysis Guide: Regulatory Proposals* [online]. Available from <http://www.tbs-sct.gc.ca/ri-qr/documents/gl-ld/analys/analystb-eng.asp>.

U.S. Environmental Protection Agency, 1997. *The benefits and costs of the Clean Air Act, 1970 to 1990*. Office of Administration and Resources Management and Office of Policy, Planning and Evaluation.

U.S. Environmental Protection Agency, 1999. *The benefits and costs of the Clean Air Act, 1990 to 2010*. EPA, Office of Air and Radiation, Pennsylvania.

U.S. Environmental Protection Agency, 2000. *Guidelines for preparing economic analyses*. EPA 240-R-00-003, Office of the Administrator.

Viscusi, W.K. and Aldy, J., 2003. The value of statistical life: A critical review of market estimates throughout the world. *Journal of Risk and Uncertainty* 27, 5–76.

Watson, W. and Jaksch, J., 1982. Air pollution: Household soiling and consumer welfare losses. *Journal of Environmental Economics and Management* 9, 248–262.

World Commission on Environment and Development (Brundtland Commission), 1987. *Our common future*, Oxford University Press, Oxford, U.K.

World Health Organization, 2007 [cited on June 6, 2007]. *Health statistics and health information systems*. Available from <http://www.who.int/healthinfo/bodday/en/index.html>.

Zeckhauser, R. and Shepard, D.S., 1976. Where now for saving lives? *Law and Contemporary Problems* 40, 5–45.

WWW.ec.gc.ca

Additional information can be obtained at:

Environment Canada
Inquiry Centre
351 St. Joseph Boulevard
Place Vincent Massey, 8th Floor
Gatineau, Quebec K1A 0H3
Telephone: 1-800-668-6767 (in Canada only)
or 819-997-2800
Fax: 819-994-1412
TTY: 819-994-0736
Email: enviroinfo@ec.gc.ca

WWW.hc-sc.gc.ca

Additional information can be obtained at:

Health Canada
Address Locator 0900C2
Ottawa, Ontario K1A 0K9
Telephone: 1-866-225-0709 (in Canada only)
or 613-957-2991
Fax: 613-941-5366
TTY: 1-800-267-1245
Email: Info@hc-sc.gc.ca